

POLYMER

*The Chemistry, Physics and Technology of
High Polymers*

Editorial Board

C. H. BAMFORD, PH.D., SC.D.

*Director of Research,
Courtaulds Research Laboratory, Maidenhead*

C. E. H. BAWN, C.B.E., F.R.S.

*Professor of Inorganic and Physical Chemistry,
University of Liverpool*

GEOFFREY GEE, C.B.E., F.R.S.

*Sir Samuel Hall Professor of Chemistry,
University of Manchester*

ROWLAND HILL, PH.D.

*Director of Research,
I.C.I. Fibres Division, Harrogate*

REPRINTED 1972 FOR

Wm. DAWSON & SONS Ltd., FOLKESTONE

WITH THE PERMISSION OF

IPC SCIENCE AND TECHNOLOGY PRESS, LTD.

Carbonization of Polymers I— Thermogravimetric Analysis

J. B. GILBERT, J. J. KIPLING, B. MCENANEY and J. N. SHERWOOD

The pyrolysis of a number of vinyl and related polymers in an inert atmosphere has been followed by means of a specially modified thermo-recording balance. In simple cases, the loss of the side-chain together with a hydrogen atom is completed as a separate stage before extensive breakdown of the carbon structure, resulting in evolution of tar and other volatiles, commences as a second stage. For a series of chloro-polymers there is a sharp fall in the loss of weight during the second stage as the chlorine content is increased from polyvinyl chloride to polyvinylidene chloride. The different effects of the stable ether link in a polyvinyl ether and the triple bond in polyacrylonitrile are discussed.

THE THERMAL decomposition of linear high polymers usually involves considerable degradation of the chain. In some cases (e.g. polymethyl methacrylate, polystyrene) this is so extensive as to result in the formation only of the monomer or other simple volatile products. In other cases, part of the material suffers condensation to leave a solid residue which can loosely be described as a carbon. The former processes have been extensively investigated¹. The processes of carbonization, however, are more complex and have received less attention over a wide range of temperature, although much work has been published on the very early stages of decomposition.

After papers had appeared on the carbonization of polyvinylidene chloride²⁻⁴, polyvinyl chloride⁴, and divinylbenzene polymers⁵, a general survey⁶ showed that a wide range of polymers could be carbonized. A more detailed examination of a small group of polymers has now been undertaken by several techniques. A number of interesting conclusions can be drawn from thermogravimetric analysis.

EXPERIMENTAL

Materials

Most of the polymers were obtained as commercial products free from plasticizers etc., and in the form of powders. Before carbonization the powders were briquetted in a 10-ton laboratory press (polyvinyl butyrate, ethyl ether, and the laboratory sample of polyvinyl acetate were not compressed in this way).

Polyvinyl chloride—This was a sample of Corvic D65/1 from Imperial Chemical Industries Ltd, Plastics Division.

Polyvinylidene chloride—This was prepared in the laboratory by bulk polymerization of the monomer using benzoyl peroxide as initiator.

Polyvinyl acetate—Two samples were used. One was a sample of Gelva 7, from Shawinigan Ltd. The other was prepared in this laboratory by bead

polymerization (with benzoyl peroxide as initiator) of vinyl acetate from The Distillers Co. Ltd.

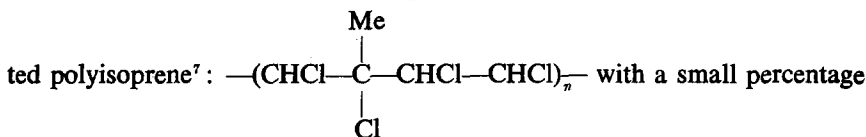
Polyvinyl butyrate—This was prepared by bead polymerization in the laboratory of vinyl butyrate from Union Carbide Ltd.

Polyvinyl alcohol—A laboratory sample from Vinyl Products Ltd.

Polyacrylonitrile—A laboratory sample from Imperial Chemical Industries Ltd, Dyestuffs Division.

Chlorinated polyvinyl chloride—A sample of Rhenoflex from Dynamit Aktien Gesellschaft. The chlorine content of the polymer was 61.3 per cent, corresponding to an average monomer unit of $C_2H_{2.81}Cl_{1.19}$.

Chlorinated rubber—A sample of Parlon S 20 from Hercules Powder Co. The chlorine content was 66 to 68 per cent, corresponding to tetrachlorina-



of the monomer units only trichlorinated.

Polyvinyl pyrrolidone—A sample (NP K30) made by Antara Chemicals.

Polyvinyl ethyl ether—A sample (EDBM) supplied by Bakelite Ltd.

Polyacrylamide—A sample (PAM 100) produced by Cyanamid.

Procedure

In most of the thermogravimetric analyses the samples were heated to a final temperature of 900° in a thermo-recording balance (Stanton Instruments Ltd) modified so that carbonization could be carried out in an inert atmosphere. The modification is shown in *Figure 1*. The crucible containing the sample is enclosed within a silica sheath (supplied by the manufacturers of the balance) which rests in a circular groove cut in an asbestos plate attached to the under-side of the furnace. A small central hole is cut in the

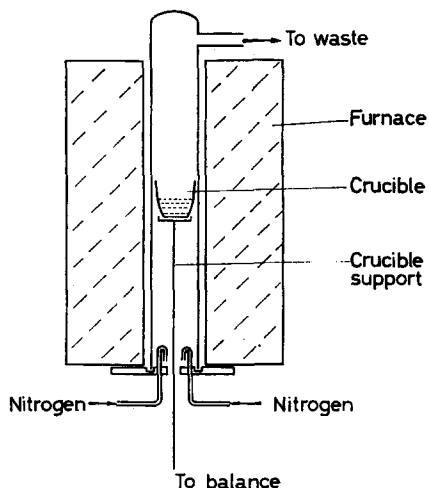


Figure 1—Modified thermobalance

plate so that the stem carrying the crucible can be attached to the balance. The plate is divided centrally and the two halves can be moved apart in the slide which supports them.

As the silica sheath must remain open (at the point where the stem supporting the crucible passes through the asbestos plate), it is necessary to exclude atmospheric oxygen by maintaining a flow of an inert gas outwards through the hole in the plate. At the same time, gaseous products of carbonization must be removed. It was therefore arranged to pass nitrogen (dry, oxygen-free) into the sheath through two small brass tubes, of *ca.* $\frac{1}{4}$ in. diameter carried by the asbestos plate, and to remove waste gases through the side-arm at the top of the sheath. The flow of gas into and out of the sheath was metered, and maintained at 1.5 l./min and 0.3 l./min, respectively. These rates were found, empirically, to be adequate to prevent oxidation of a carbon black (Spheron 6) held in the furnace at 900°C. The instrument was re-calibrated to give the correct temperature of the sample under these conditions of use. After making these modifications to the balance, we found that a rather more elaborate system had been devised by Stonhill for work with corrosive materials⁸. In general, the samples were heated at approximately 2°/min. In some analyses, however, the rate was about 6°/min, but the sample was held at a given temperature to investigate whether a particular stage of decomposition could be completed at that temperature, given sufficient time.

RESULTS AND DISCUSSION

Thermograms for a number of vinyl and related polymers are shown in *Figures 2 to 6*.

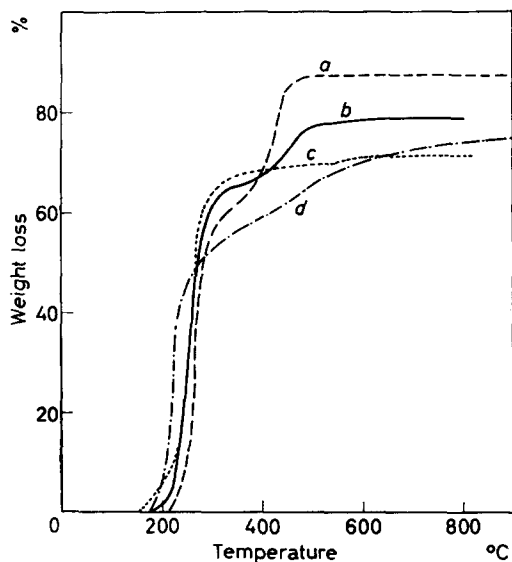


Figure 2—Thermograms for chloro-polymers heated at 2°/minute: (a) polyvinyl chloride, (b) chlorinated polyvinyl chloride, (c) chlorinated rubber, (d) polyvinylidene chloride

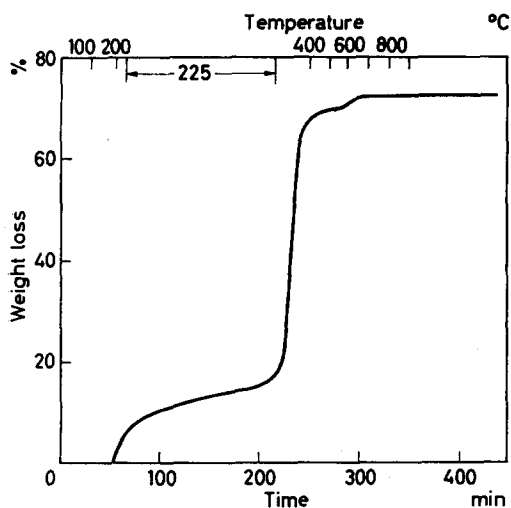
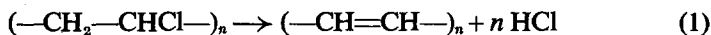


Figure 3—Thermogram for chlorinated rubber heated at 6°/minute

(1) *Polyvinyl chloride and related chloro polymers*

The simplest form of degradation for a vinyl polymer is typified by polyvinyl chloride and is depicted in *Figure 2*. It occurs in two readily distinguishable stages. The first, which is complete at about 250°C, consists solely of loss of hydrogen chloride, which can be represented formally as



If the material is held at 250°C until loss of weight ceases, chemical analysis

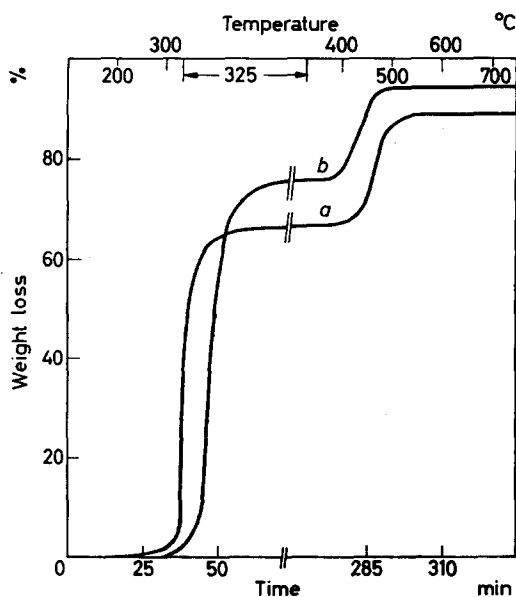
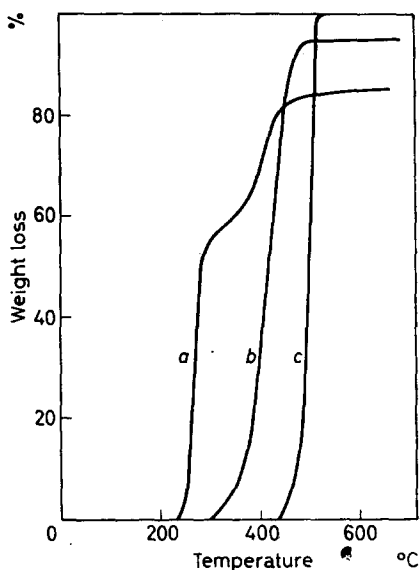


Figure 4—Thermograms for (a) polyvinyl acetate and (b) polyvinyl butyrate heated at 6°/minute, with a break at 325°

Figure 5 — Thermograms for (a) polyvinyl alcohol, (b) polyvinyl ethyl ether, (c) polyethylene, heated at 2°/minute



of the product shows that elimination of chlorine is almost quantitative (Table I). The second stage, which occurs mainly between 300° and 500°C, is similar to the carbonization of coal, although it is much simpler. Tar and simple gases (hydrogen, methane) are evolved, and a carbon remains which loses very little weight between 500° and 900°C. The complete thermogram is very similar to that published by Winslow⁴.

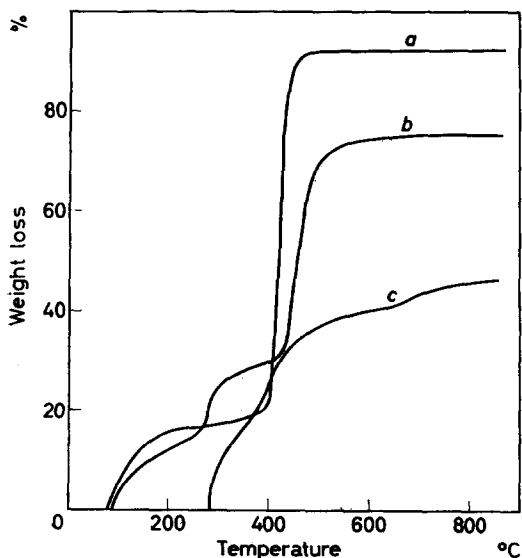


Figure 6—Thermograms for (a) polyvinyl pyrrolidone, (b) polyacrylamide, (c) polyacrylonitrile, heated at 2°/minute

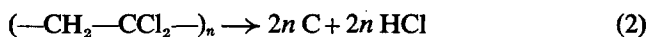
Table 1. Analyses (dry mineral matter free) of polymer carbons

| Sample | Temp. °C | Percentage composition | | | | | Ratio H/C |
|--------------------------------|-------------|------------------------|-----|------|------|----------|--------------|
| | | C | H | Cl | N | O+errors | |
| Polyvinyl chloride | 250 | 84.3 | 6.9 | 0.6 | — | 8.3 | 0.98 |
| | 700 | 99.1 | 0.6 | 0.0 | — | 0.3 | 0.07 |
| Polyvinyl acetate | 250 | 82.2 | 6.9 | — | — | 10.9 | 1.00 |
| | 700 | 96.9 | 1.4 | — | — | 1.7 | 0.17 |
| Polyvinyl alcohol | 300 | 84.5 | 7.8 | — | — | 7.7 | 1.09 |
| | 700 | 89.7 | 1.3 | — | — | 9.0 | 0.17 |
| Polyacrylonitrile | 250 | 72.9 | 4.5 | — | 22.1 | 0.5 | 0.74 |
| | 700 | 78.9 | 1.0 | — | 18.4 | 1.7 | 0.15 |
| Chlorinated polyvinyl chloride | 250 | 77.4 | 5.7 | 15.9 | — | 1.0 | 0.88 |
| | 700 | 96.2 | 1.4 | 0.1 | — | 2.3 | 0.17 |
| Chlorinated rubber | 250 | 81.3 | 3.8 | 9.8 | — | 5.1 | 0.56 |
| | 700 | 96.3 | 1.1 | 0.5 | — | 2.1 | 0.14 |

The effect of increasing the chlorine content of the polymer is very interesting. The three other chlorine-containing polymers which we have investigated (chlorinated polyvinyl chloride, chlorinated rubber, and polyvinylidene chloride) also decompose in two stages, the first being loss of hydrogen chloride only. The onset of dehydrochlorination occurs at a lower temperature for these polymers than for polyvinyl chloride, implying that the groupings $-\text{CHCl}-\text{CHCl}-$ and $-\text{CH}_2-\text{CCl}_2-$ are less stable than $-\text{CH}_2-\text{CHCl}-$.

In the second stage, the two polymers of intermediate chlorine content give decreasing yields of tar with increasing chlorine content of the polymer. At 250°C a substantial amount of chlorine remains in the residue, in contrast to the situation with polyvinyl chloride (*Table 1*). This chlorine is able to remove hydrogen which would otherwise be used in the compounds forming the tar. As a consequence of the lower H/C ratio, the potentially tarry material has a higher molecular weight and a greater proportion of it suffers condensation before a high enough temperature is reached for its release by distillation.

The limiting case is polyvinylidene chloride, which contains equal numbers of atoms of chlorine and hydrogen. Dacey and Thomas² showed that it gave a quantitative yield of carbon and hydrogen chloride



i.e. there is no evolution of tar or of other volatile matter usually encountered in carbonization.

The increase in chlorine content has a very marked effect on the percentage of carbon atoms from the original polymer which remain in the final

CARBONIZATION OF POLYMERS I—THERMOGRAVIMETRIC ANALYSIS

Table 2. Effect of chlorine content of polymer on carbon yield at 900°C
 Rate of heating: 2°/min Atmosphere: nitrogen

| Sample | Chlorine content of polymer (%) | Carbon yield (%) | Nature of carbon | Relative carbon yield* (%) |
|--------------------------------|---------------------------------|------------------|------------------|----------------------------|
| Polyvinyl chloride | 56.8 | 11.5 | Coke | 30 |
| Chlorinated polyvinyl chloride | 61.3 | 22.3 | Char | 64 |
| Chlorinated rubber | 66 to 68 | 28.0 | Char | 97 |
| Polyvinylidene chloride | 73.2 | 25.9 | Char | 104† |

*Yield of residue relative to carbon content of original polymer.

†The yield is over 100 per cent because the residue had absorbed some oxygen.

residue, instead of being lost as tar or volatiles. This is shown as the relative carbon yield at 900° in Table 2. Even a small degree of chlorination of polyvinyl chloride doubles the relative carbon yield. In the carbonization of chlorinated rubber, only three per cent of the carbon in the polymer is lost as volatile matter.

A further effect is also evident during the second stage of decomposition. The polyvinyl chloride residue fuses during this stage (giving a coke, as defined by Davis⁹), whereas the polymers of higher chlorine content decompose without fusion (thus giving a char). The more extensive the removal of hydrogen, the greater is the chance of condensation of the residue, both by crosslinking between chains, and by cyclization of individual chains. (The Diels–Alder type of condensation which Winslow⁴ has proposed for the decomposition of polyvinylidene chloride may occur.) If these processes occurred extensively, the physical mobility of the system would be considerably reduced because large molecular units would be formed and these would be too big to break away as volatile fragments even at the higher temperatures.

The effect of specific groupings is also apparent from the thermograms. Chlorinated rubber loses chlorine at a lower temperature than any of the other polymers, but only to the extent of one chlorine atom per monomer unit (Figure 3). This may be presumed to be the chlorine atom in the tertiary position. The remaining three chlorine atoms are equivalent to one another and are removed in one stage. This is presumably because they are attached to separate and equivalent carbon atoms. The initial temperature of breakdown of chlorinated polyvinyl chloride is about the same as that at which the three chlorine atoms of chlorinated rubber are lost. This suggests that chlorination of polyvinyl chloride tends to produce polyvinylene chloride rather than polyvinylidene chloride.

The loss of the second chlorine atom from polyvinylidene chloride takes

place over a wide range of temperature. At this stage the residue must be undergoing considerable cyclization and aromatization, so that successive chlorine atoms are lost from changing molecular environments.

(2) Polyvinyl esters

The thermogram for polyvinyl acetate shows two well-defined stages (*Figure 4*) analogous to those for polyvinyl chloride. In the first stage, acetic acid is lost quantitatively, though much less readily than hydrogen chloride is lost from polyvinyl chloride. Although the mechanisms for the removal of hydrogen chloride and acetic acid are believed to differ¹, the stoichiometric effects are the same; compare equations (1) and (3).



These equations represent the formal composition of the low-temperature residue; it will be shown in subsequent publications that the poly-ene chain suffers rearrangement even at low temperatures.

The low-temperature residues are thus formally identical, and behave very similarly in the second stage of decomposition. Thus the chemical analyses are very similar (*Table I*).

The thermogram for polyvinyl butyrate (*Figure 4*) closely resembles that for polyvinyl acetate, showing a quantitative loss of butyric acid in the first stage. This seems likely to be a common mechanism for degradation of simple polyvinyl esters.

(3) Polyvinyl alcohol and ether

By analogy with polyvinyl chloride and polyvinyl esters, the initial decomposition of polyvinyl alcohol would be expected to accord with the equation



In one instance this has been reported, though the reaction did not go to completion¹⁰. Its maximum rate was at 160°C, which is considerably below the temperature of decomposition of other vinyl polymers. The implication of other published work, however (e.g. ref. 11), is that such a definite stage is not observed separately from a more general decomposition. Our results (*Figure 5*) show no substantial decomposition below 200°C. Moreover, decomposition which occurs between 200° and 300°C involves a greater loss in weight than accords solely with equation (4), and the yield of carbon at 900°C is correspondingly low. It has been established¹¹ that, besides water, other simple degradation products, such as acetaldehyde, are produced. This points to a greater degree of chain scission than occurs with the chloro-polymers. The formation of a solid residue is then only likely to occur if some inter-chain dehydration takes place in addition to the intra-chain dehydration of equation (4).

The different modes of decomposition call for further investigation. At present it is not clear whether they arise from different conditions of pyrolysis (Kaesche-Krischer and Heinrich used a low vacuum, whereas we used a stream of nitrogen) or from differences in the samples of polymer.

The decomposition of polyvinyl ethyl ether occurs essentially in one stage, giving a very low yield of solid residue. The decomposition occurs at an appreciably higher temperature than is found for other vinyl polymers. The temperature of maximum decomposition is higher than that of polyethylene oxide and polypropylene oxide¹², but lower than that of polyethylene (Figure 5), which also gives a negligible yield of carbon. The decomposition is thus governed by the thermal stability of the ether link, and appears to occur essentially by chain scission. Further work is needed to show whether this is initiated by rupture of the ether link or of a C—C bond in the main chain, weakened by the presence of the side chain.

(4) Nitrogen-containing polymers

The interest in these polymers is in the specific effect of the nitrogen on their decomposition, and in particular in the possibility of its retention in the carbon residue. Polyacrylamide (Figure 6) decomposes in three stages, corresponding to loss of water, of ammonia, and of tar and volatiles, respectively. The second stage appears to be inter- and intra-molecular imidization, as the thermal analogue of the reactions which can be induced at lower temperatures by acid catalysis¹³.

The carbonization stage involves an extensive loss of material, which is, however, as a proportion of the low-temperature residue, slightly less than with polyvinyl chloride and polyvinyl acetate.

Polyvinyl pyrrolidone undergoes such extensive degradation that most of the nitrogen must be lost in the process.

The degradation of polyacrylonitrile presents features which are, so far, unique. In the first two stages, volatiles (mainly ammonia) and then tars are eliminated. A large percentage of nitrogen is, however, retained in the residue (Table I). From 600°C upwards, however, there is a third stage in which weight is lost only slowly, although the carbon yield is very high.

It has been established^{1, 14} that only very small amounts of hydrogen cyanide are removed thermally from this polymer. There is, however, evidence from infra-red spectra that the triple bond of the cyanide group can open, with resultant formation of crosslinks inter-molecularly and of 6-membered heterocyclic rings intra-molecularly¹⁴. Nitrogen retained in this form has very considerable thermal stability, and the 700°C carbon still contains 18.4 per cent. This stability would not be expected to persist indefinitely with rise in temperature, and the loss of weight in the third stage (which continues up to about 1500°C) is due to elimination of nitrogen from the heterocyclic groupings.

These results suggest that for the conditions which we have used, nitrogen is only likely to be retained in any considerable proportion if present in an unsaturated group in the polymer. Nitrogen present in the other polymers might well be retained if carbonization were carried out under pressure to prevent the escape of volatile nitrogen compounds. Thus Riley *et al.*¹⁵ found that nitrogen was retained in the carbon formed from hexamethylene tetramine under these conditions.

(5) General comments

The results quoted above for the decomposition of polyvinyl alcohol show

the importance of the conditions used for carbonizing polymers. The source of a given sample may also be important. We hope to publish further data on these aspects of carbonization in due course.

We are indebted to the United Kingdom Atomic Energy Authority, the National Coal Board, and the British Coke Research Association for their support of this work and for their awards, respectively of a Post-Doctoral Fellowship (to J.N.S.), a research grant (to B. McE.) and a Coke Research Fellowship (to J.B.G.). The views expressed are those of the authors and not necessarily those of the organizations supporting the work.

We are also grateful to the firms mentioned in the experimental section for the gift of polymers, and to the National Coal Board, Scientific Department (Coal Survey), Sheffield for the chemical analyses.

*The University,
Hull*

(Received June 1961)

REFERENCES

- ¹ GRASSIE, N. *Chemistry of High Polymer Degradation Processes*. Butterworths: London, 1956
- ² DACEY, J. R. and THOMAS, D. G. *Trans. Faraday Soc.* 1954, **50**, 740
- ³ PIERCE, C., WILEY, J. W. and SMITH, R. N. *J. phys. Chem.* 1949, **53**, 669
- ⁴ WINSLOW, F. H., BAKER, W. O. and YAGER, W. A. *Proceedings of the Conferences on Carbon*, p 93. University of Buffalo: Buffalo, N.Y., 1956
- ⁵ WINSLOW, F. H., MATREYEK, W. and YAGER, W. A. *Industrial Carbon and Graphite*, p 190. Society of Chemical Industry: London, 1958
- ⁶ KIPLING, J. J. and WILSON, R. B. *Proceedings of Residential Conference on Science in the Use of Coal* (Sheffield, April 1958), p C6. Institute of Fuel: London
- ⁷ GIDVANI, B. S. *Paint Manuf.* 1949, **29**, 419
- ⁸ STONHILL, L. G. *J. inorg. nucl. Chem.* 1959, **10**, 153
- ⁹ DAVIS, J. E. *Proceedings of Residential Conference on Science in the Use of Coal* (Sheffield, April 1958), p C1. Institute of Fuel: London
- ¹⁰ KAESCHE-KRISCHER, B. and HEINRICH, H. J. *Z. phys. Chem. (N.S.)*, 1960, **23**, 297
- ¹¹ FUTAMA, H. and TANAKA, H. *J. phys. Soc. Japan*, 1957, **12**, 433
- ¹² MADORSKY, S. L. and STRAUS, S. J. *Polym. Sci.* 1959, **36**, 183
- ¹³ MINSK, L. M. and KENYON, W. O. *U.S. Pat. No. 2486192, Chem. Abstr.* 1950, **44**, 1750
- ¹⁴ BURLANT, W. J. and PARSONS, J. L. *J. Polym. Sci.* 1956, **22**, 249
- ¹⁵ BARANIECKI, C., RILEY, H. L. and STREETER, E. *Industrial Carbon and Graphite*, p 283. Society of Chemical Industry: London, 1958

Shear Viscosities of Polyisobutene Systems —A Study of Polymer Entanglement*

R. S. PORTER and J. F. JOHNSON

Viscosity/shear effects have been evaluated for cetane and tetralin solutions of polyisobutene. Eleven polymers, molecular weights 224 to 71000, were studied at temperatures from 100° to 135°C. Systems from pure solvent to 100 per cent polymer were tested with capillaries and with two types of rotational viscometers. The results yield concepts from which conditions and magnitudes for non-Newtonian flow may be predicted. The onset of non-Newtonian flow occurs above the transition in a plot of log low-shear viscosity versus log polyisobutene molecular weight. The transition occurs at a critical polymer concentration and molecular weight corresponding to the conditions for extensive polymer chain entanglement.

THE FLOW properties of polyisobutene have probably been studied more widely than those of any other polymer. Non-Newtonian aspects, however, have been touched upon only lightly. Recently, the conditions and magnitudes for non-Newtonian flow of polyisobutene have been broadly defined¹⁻³. In the present work, these postulates are extended and related to the concept of polymer chain entanglement. The polyisobutenes and the cetane and tetralin which were used have been previously described^{1, 2}. They represent eleven polymers with viscosity average molecular weights up to 71 000. For the six low molecular weight polymers, number average molecular weights were also measured with the values of M_v exceeding M_n by less than 50 per cent. The instrumentation used for these studies has also been previously described¹⁻⁵. It includes low-shear, crossarm capillary viscometers, a low-shear concentric cylinder viscometer, and a thin-film, double-thermostated, high-shear concentric cylinder viscometer. All measurements were made in equilibrium steady-state flow.

RESULTS AND DISCUSSION

The viscosity transition

Viscosity changes with polymer molecular weight commonly exhibit an abrupt transition⁶. This transition occurs at polymer molecular weights sufficient for polymer entanglements to dominate the flow process⁶⁻⁸. For polymer solutions, the viscosity transition and polymer entanglement are reported to occur above a critical polymer molecular weight and volume fraction. In recent studies, the viscosity/molecular weight transition has also been related to the onset of non-Newtonian flow^{1, 3, 9}.

The way in which the viscosity/molecular weight transition depends on temperature, shear, and solution variables is just now starting to be understood^{1, 3, 6, 9}. *Figure 1* shows an interpretation of this transition in terms of

*Part VII of a series on the 'Flow properties of polymeric systems'. Presented in part before the 137th National Meeting of the American Chemical Society, Cleveland, April 1960.

reduced variables^{6, 10}. As for other systems, the transitions are shown as the intersection of lines⁶. The molecular weight for the entanglement transition has been previously reported to be 1.7×10^4 for bulk polyisobutene⁶. This is in good agreement with the common transition in *Figure 1* at 1.6×10^4 . This agreement of bulk and solution transitions for polyisobutene is closer than previously supposed⁶, although the choice of solvent may be influential.

Below the transition in *Figure 1*, viscosity/molecular weight correlations depend on concentration and temperature with slopes approaching a lower limit of one at higher temperatures⁷. Where the slope drops below one, at the lowest molecular weights and concentrations, the plots show notable curvature. Above the transition polymer systems are commonly characterized by a temperature independent and high, about 3.4, power dependence of low-shear viscosity on polymer molecular weight⁶. Solutions of higher molecular weight polyisobutenes than used here conclusively yield a 3.4 dependence⁶.

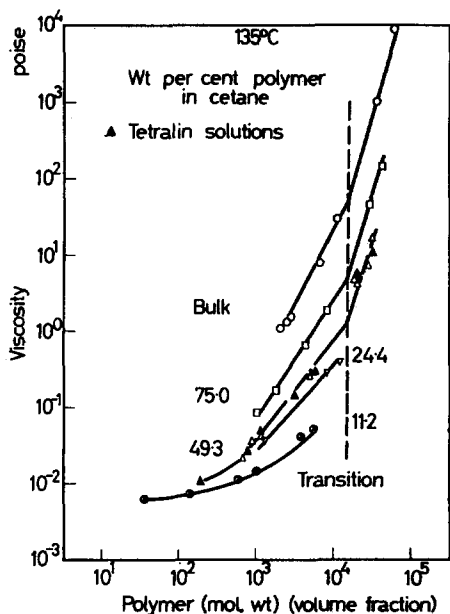


Figure 1—Solution viscosities of polyisobutenes: reduced variable correlation

Shear tests on systems below the transition in *Figure 1* indicate essentially Newtonian flow for stresses to about 2×10^5 dyne/cm². In contrast, above the transition, viscosity becomes abruptly and markedly non-Newtonian at stresses above only 10^3 dyne/cm². Typical shear tests leading to these conclusions are shown in *Figure 2*. The highest viscosity slope, obtained at low shear, is drawn to a 3.4 slope. The lower limit, approached at high shear, has been defined by a slope of one, the limiting theoretical value below the transition⁷. These shear measurements are entirely reversible with no observation of hysteresis or permanent viscosity loss.

SHEAR VISCOSITIES OF POLYISOBUTENE SYSTEMS

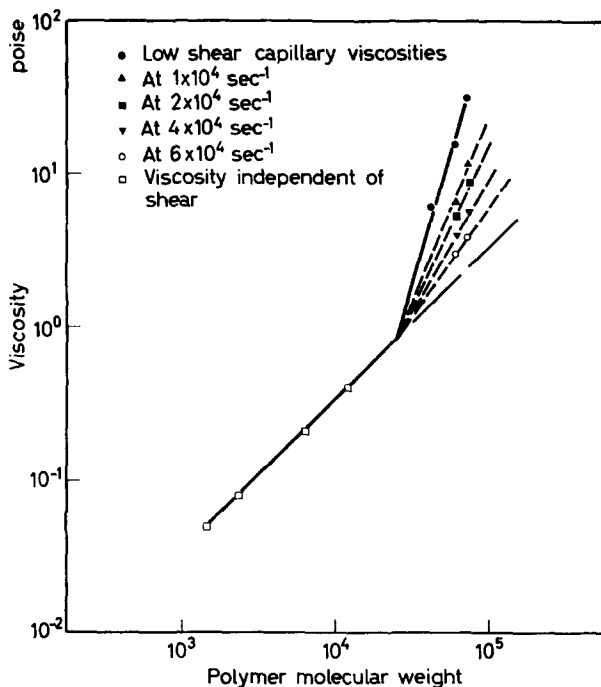


Figure 2—Solution viscosities of polyisobutenes: 49.3 wt per cent polymer in cetane at 100°C: dependence on rate of shear

The conditions above the transitions in *Figures 1* and *2* appear to be a necessary and sufficient provision for non-Newtonian flow in low molecular weight polymer systems^{1, 3, 9, 11}. Bueche has developed a two-term equation which treats the low-shear viscosity transition as the polymer entanglement point^{7, 8}. The first term dominates at low molecular weights and represents simple frictional forces between molecules. The second term applies above the transition and incorporates a slippage factor for intermolecular entanglements. This second term may vary with shear and represent non-Newtonian flow through changes in the slippage factor and/or the number or importance of polymer entanglements due to network deformation.

Reduced variables

Non-Newtonian data on polymer systems are known to superimpose by several reduced variable correlations¹²⁻¹⁴. These polyisobutene data are found to superimpose on a plot of fractional viscosity loss versus shear stress/ $T^\circ\text{K} \times C$, where C is polymer volume concentration³. This correlation is convertible to the reduced coordinates and master curve developed by Bueche for other polymer systems¹⁴. From this it is evident that certain polystyrenes, polymethyl methacrylates, rubber solutions, as well as polyisobutene data, show similar non-Newtonian behaviour and probably exhibit a common flow mechanism. Deviations from this non-Newtonian correlation are observed here only at the lowest polymer molecular weights

and concentrations. This corresponds to conditions below the transitions in *Figures 1* and *2*. In this region abnormally high shear is required to induce non-Newtonian effects³. A successful reduced variable correlation has previously been reported for polyisobutene systems below the transition². The reduced variables for non-Newtonian flow above and below the transition differ only in the concentration term. For dilute polyisobutene solutions, the reduced variables contain no concentration term; and the fractional viscosity losses with shear are relatively small². This indicates that non-Newtonian flow below the transition may be due to deformation of individual polymer molecules rather than due to network deformation which contributes to non-Newtonian flow above the transition.

Temperature effects

Viscosity/temperature data on polyisobutene systems, over limited ranges, are essentially linear on plots of log viscosity versus $1/T^{\circ}\text{K}$ ¹⁵⁻²³. From the slope of this correlation, an apparent activation energy for viscous flow, ΔE^* , may be obtained. The definition used here is $\Delta E^* = R(d \ln \eta / 1/T^{\circ}\text{K})$, where η is absolute viscosity; R , the gas constant with ΔE^* in kcal/mole. Activation energy and activation heat for flow have frequently been considered equivalent.

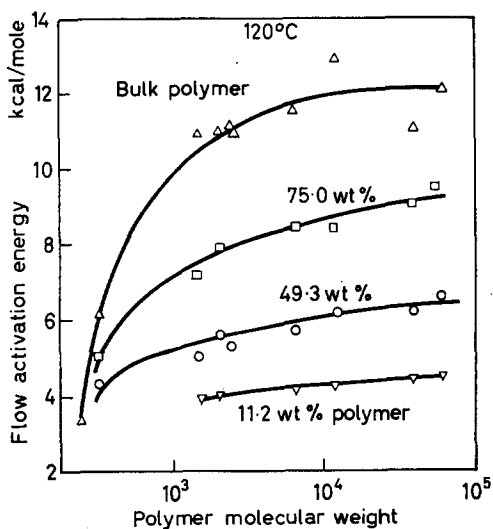


Figure 3—Flow activation energies for polyisobutene in cetane

Figure 3 gives new values of ΔE^* for polyisobutene solutions as a function of polymer concentration and molecular weight. Values for bulk polymer are in accord with the data of Fox in both magnitude and molecular weight dependence²³. The curvature in plots of log viscosity versus $1/T^{\circ}\text{K}$ leads to a higher ΔE^* at lower temperatures²³. This may be associated with an increase in the number of polymer entanglements at reduced temperature¹¹.

Flow activation energies have also been evaluated as a function of the reduced ordinate used in *Figure 1*. This interpretation merges the curves of

Figure 3 at the lowest values. Consistent with the concepts of Hirai¹⁰, at higher values of reduced ordinate, the ΔE^* curves show the type of spread in Figure 3. The onset of the plateau in ΔE^* , see Figure 3, is closely associated with the viscosity transitions in Figures 1 and 2. Changes in ΔE^* below the plateau lead to the temperature dependence of log viscosity/log molecular weight slopes below the transition. Conversely, the plateau regions for ΔE^* lead to a viscosity/molecular weight slope which is independent of temperature above the transition.

Figure 4—Flow activation energies for polyisobutenes in cetane

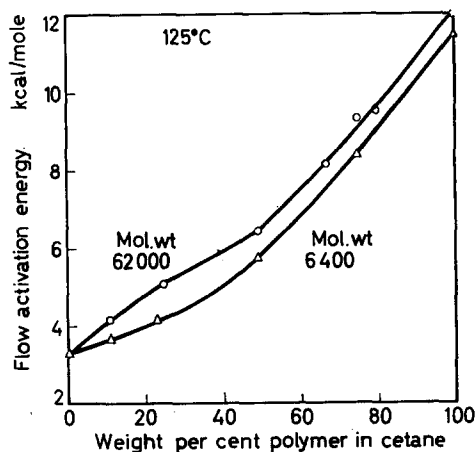


Figure 4 is a cross plot of Figure 3, containing additional data. The lower molecular weight polymer in Figure 4 is below entanglement conditions at all concentrations. Solutions of the higher molecular weight polymer show a change in dependence near the composition for the entanglement transition given by Figure 1. This may be the result of two contributions to flow activation, that for simple viscous flow and also that for activation of entanglement deformation. By the method of Hirai¹⁰, the point of inflection in Figure 4 indicates a small energy of formation, 1 kcal or less, for formation of the entangled state. This energy of formation is consistent with a small, but apparently real, increase in the molecular weight for the entanglement transition with increasing temperature.

For solutions of low polyisobutene molecular weight and concentration, ΔE^* is constant from low shear to above 2×10^5 dyne/cm². At higher polymer molecular weights and concentrations, notably for entanglement conditions, ΔE^* depends markedly on rate of shear. Shear, just as temperature, may reduce the contribution of polymer entanglements, leading¹¹ to a lower ΔE^* . In some cases, limiting values of ΔE^* , measured at constant shear rate, have been approached at both high and low rates of shear^{2, 3}. In accord with theory, ΔE^* at constant shear rate for these polyisobutene systems is equal to or lower than ΔE^* evaluated at constant shear stress²⁴. Indeed, activation energies measured at constant stress for these and for many other polymer systems are only slightly reduced by stress up to attainable limits.

The inflection in ΔE^* in *Figure 4*, the onset of plateaux in ΔE^* in *Figure 3*, the onset of non-Newtonian flow in *Figure 2*, the viscosity transition in *Figure 1*, and a change in the form of reduced variables are thus ramifications of the same phenomenon, the onset at higher molecular weights of a flow mechanism dominated by the slippage of polymer entanglements.

The authors express appreciation to Mr A. R. Bruzzone for aid in obtaining experimental measurements.

California Research Corporation,
Richmond, Calif.

(Received July 1961)

REFERENCES

- ¹ PORTER, R. S. and JOHNSON, J. F. *J. Polym. Sci.* 1961, **50**, 379
- ² PORTER, R. S. and JOHNSON, J. F. *J. appl. Polym. Sci.* 1960, **3**, 107
- ³ PORTER, R. S. and JOHNSON, J. F. *J. appl. Phys.* 1961, **32**, 2326
- ⁴ PORTER, R. S. and JOHNSON, J. F. *J. phys. Chem.* 1959, **63**, 202
- ⁵ BARBER, E. M., MUENGER, J. R. and VILLFORTH, F. J., Jr. *Analyt. Chem.* 1955, **27**, 425
- ⁶ FOX, T. G. and LOSHAEK, S. *J. appl. Phys.* 1955, **26**, 1080
- ⁷ BUECHE, F. *J. chem. Phys.* 1952, **20**, 1959
- ⁸ BUECHE, F. *J. chem. Phys.* 1956, **25**, 599
- ⁹ BAGLEY, E. B. and WEST, D. C. *J. appl. Phys.* 1958, **29**, 1511
- ¹⁰ HIRAI, N. *J. Polym. Sci.* 1959, **39**, 435
- ¹¹ MERKER, R. L. *J. Polym. Sci.* 1956, **22**, 353
- ¹² HOROWITZ, H. H. *Industr. Engng Chem. (Industr.)*, 1958, **50**, 1089
- ¹³ PADDEN, F. J. and DEWITT, T. W. *J. appl. Phys.* 1954, **25**, 1086
- ¹⁴ BUECHE, F. and HARDING, S. W. *J. Polym. Sci.* 1958, **32**, 177
- ¹⁵ OEHLE, R., DAVIS, J. H. and KINMONTH, R. A. *J. Amer. Leath. Chem. Ass.* 1955, **50**, 16
- ¹⁶ JOHNSON, M. F., EVANS, W. W., JORDAN, I. and FERRY, J. D. *J. Colloid Sci.* 1952, **7**, 498
- ¹⁷ DEWITT, T. W., MARKOVITZ, H., PADDEN, F. J., Jr and ZAPAS, L. J. *J. Colloid Sci.* 1955, **10**, 174
- ¹⁸ FERRY, J. D. and PARKS, G. S. *Physics*, 1935, **6**, 356
- ¹⁹ FOX, T. G., Jr and FLORY, P. J. *J. Amer. chem. Soc.* 1948, **70**, 2384
- ²⁰ LOWER, G. W., WALKER, W. C. and ZETTMLOYER, A. C. *J. Colloid Sci.* 1953, **8**, 116
- ²¹ LEADERMAN, H., SMITH, R. G. and JONES, R. W. *J. Polym. Sci.* 1954, **14**, 47
- ²² JORDAN, I. *Ann. Ass. quim. Brasil*, 1952, **11**, 11
- ²³ FOX, T. G., Jr and FLORY, P. J. *J. phys. Colloid Chem.* 1951, **55**, 221
- ²⁴ BESTUL, A. B. and BELCHER, H. V. *J. appl. Phys.* 1953, **24**, 696

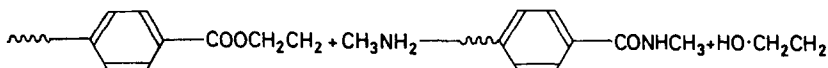
The Degradation of Polyethylene Terephthalate by Methylamine— A Study by Infra-red and X-ray Methods

G. FARROW, D. A. S. RAVENS and I. M. WARD

The physical changes taking place during the degradation of polyethylene terephthalate with aqueous methylamine at room temperature have been followed by chemical, X-ray and infra-red methods and it is concluded that although there is a rapid initial degradation of the amorphous regions, extensive degradation leads to attack of both crystalline and amorphous regions.

PREVIOUS studies of the chemical degradation of polyethylene terephthalate (PET) have been concerned with the chemical nature of the degradation and little consideration has been given to the physical changes taking place. Previous work has also shown that initially the reaction depends on the solution of the reagent in the amorphous regions of the polymer and that therefore attack is principally confined to these regions¹. It was thought that it would be possible, by choice of a suitable reagent, to degrade PET extensively and leave a highly crystalline, slowly reacting residue in a way similar to the hydrolysis of cellulose². This would mean that a detailed study of the effect of orientation and crystallinity could be made by various physical methods which would give information about the nature of the crystalline regions.

Aqueous methylamine was chosen because it reacts rapidly with PET at room temperature thus minimizing side effects due to high temperatures and also the reaction of methylamine with esters has been studied previously³. The reaction is



EXPERIMENTAL

Sample preparation

500 g of PET polymer free from delustrant was spun to give small diameter filaments ($\sim 5 \times 10^{-4}$ in.) of low orientation and from this fibre, samples with different structures were prepared. These were

- | | |
|--|---------------------------|
| (a) Amorphous, spun fibre | 0 per cent crystallinity |
| (b) Crystalline, unoriented fibre by heating (a) at 200°C for 30 min | 47 per cent crystallinity |
| (c) Drawn fibre of high orientation | 18 per cent crystallinity |
| (d) Drawn fibre of high orientation and heat crystallized | 48 per cent crystallinity |
| (e) A sample of commercial 'Terylene' yarn containing delustrant | 28 per cent crystallinity |

Degradation of the samples

Samples (3g) were degraded for various times in 20 per cent w/v aqueous methylamine at room temperature, the samples being shaken throughout the reaction. After the reaction the fibre was extracted to constant weight with ethylene glycol at 60°C, it having been previously shown that undrawn amorphous film was not crystallized by this treatment. The washings and the insoluble fraction were retained and the loss in weight measured.

Infra-red measurements

Measurements of hydroxyl end-group concentrations were made. The samples were examined by a modification for PET of the standard technique of incorporation in potassium bromide discs⁴.

About 25 mg of the sample were mixed with 0.4 g potassium bromide, the degraded fibre being finely powdered at solid carbon dioxide temperatures. The optical density of the —OH stretching vibration absorption at 3 543 cm^{-1} was measured and a calibration was obtained by making similar measurements on the series of samples A to L used in the original end-group calibration⁵. In each sample the intensity of the carbonyl absorption at 3 430 cm^{-1} was used as a measure of the concentration of polymer in the potassium bromide disc. This calibration is shown in *Figure 1*.

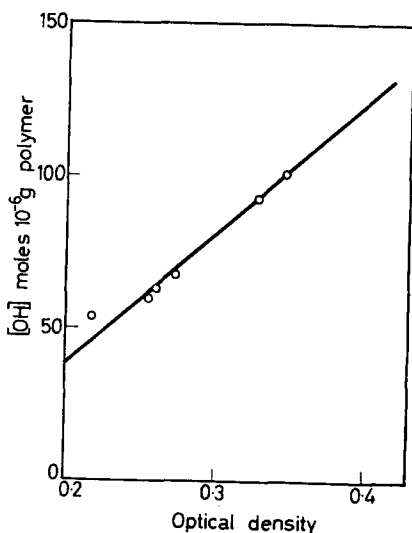


Figure 1—Calibration curve for hydroxyl end-group measurements

X-ray measurements

(i) *Crystallinity*—The method used for untreated and degraded samples has been previously described⁶. It consists, in principle, of a comparison between the integrated intensity of the crystalline reflections and those of the non-crystalline background, considerable refinements of X-ray technique being necessary to make this comparison quantitatively valid.

(ii) *Low-angle scattering*—Specimens were also examined by this method. They were made up as random samples of approximately 1 mm diameter by compression in a suitable mould⁶. This method was used because after

degradation the samples of fibre invariably consisted of small particles which were too small to be examined individually.

The low-angle camera consisted essentially of a small film cassette 1 in. in diameter, mounted on a graduated track rail and with a movable platinum backstop placed directly in front of the X-ray film. Copper K_{α} (nickel filtered) X-ray radiation was used to irradiate the specimen which was mounted directly behind a second set of slits with both horizontal and vertical movements. These slits, which were placed between the collimator (a stainless steel tube of 0.1 mm diameter) and the low-angle camera, limited the secondary X-ray radiation striking the film. The whole assembly was evacuated to eliminate air scatter which is prevalent at low angles. Exposure times were about 16 hours and a specimen to film distance of 135 mm was used which gave a resolution of about 250Å. The exposed X-ray films (Ilford G) were developed and dried under standard conditions. X-ray photographs were also taken without samples so that the necessary adjustments could be made to the low-angle photographs to account for any scatter from the slit system. The exposure times were adjusted to account for the absorption of the X-ray beam when the specimen was in position. Finally the low-angle photographs were scanned by a microdensitometer and resulting traces normalized and corrected for any background radiation.

Intrinsic viscosity values

These were obtained by measuring the specific viscosities of one per cent solutions in *o*-chlorophenol and the intrinsic viscosity was calculated from the value of the Huggins viscosity slope constant determined by Todd⁷.

RESULTS

Degradation experiments

The degradation results for the five types of fibre are given in *Tables 1* to *5*, where percentage weight loss and percentage crystallinity results are compared. In the cases of amorphous yarn and heat crystallized unoriented yarn intrinsic viscosity results are also included.

In addition to the insoluble fraction whose weight was determined, a glycol-soluble material was obtained whose infra-red spectrum showed clearly that this compound is an aromatic secondary amide. The evidence

Table 1. Amorphous fibre, sample (a)

| <i>Time, h</i> | <i>% loss in weight</i> | <i>X-ray % crystallinity</i> | <i>I.V.</i> |
|----------------|-------------------------|----------------------------------|-------------|
| 0 | 0 | 0 | 0.55 |
| 1 | 0.3 | — | 0.43 |
| 2 | 7.9 | — | 0.33 |
| 2.5 | — | 0 | 0.34 |
| 3 | 27.5 | — | 0.24 |
| 4 | 51.3 | — | 0.17 |
| 5 | 58 | 20 | 0.09 |
| 6 | 63 | — | 0.09 |

Table 2. Heat crystallized fibre, sample (b)

| <i>Time, h</i> | <i>% loss in weight</i> | <i>X-ray % crystallinity</i> | <i>I.V.</i> |
|----------------|-------------------------|----------------------------------|-------------|
| 0 | 0 | 47 | 0.55 |
| 3 | 0.2 | 48 | 0.45 |
| 5 | 0.4 | 51 | 0.43 |
| 16 | 32.5 | 59 | 0.20 |
| 30 | 79.2 | 72 | 0.10 |
| 40 | 89.6 | 65 | — |

Table 3. Drawn fibre, high orientation, sample (c)

| <i>Time, h</i> | <i>% loss in weight</i> | <i>X-ray % crystallinity</i> |
|----------------|-------------------------|----------------------------------|
| 0 | 0 | 18 |
| 5 | 0 | 20 |
| 8 | 2.7 | 26 |
| 16 | 44 | 56 |
| 24 | 93 | 60 |

Table 4. Drawn and heat crystallized fibre, sample (d)

| <i>Time, h</i> | <i>% loss in weight</i> | <i>X-ray % crystallinity</i> |
|----------------|-------------------------|----------------------------------|
| 0 | 0 | 48 |
| 16 | 0 | 50 |
| 24 | 33 | 60 |
| 48 | 74 | 66 |

Table 5. Commercial 'Terylene', sample (e)

| <i>Time, h</i> | <i>% loss in weight</i> | <i>X-ray % crystallinity</i> |
|----------------|-------------------------|----------------------------------|
| 0 | 0 | 20 |
| 6 | 0.3 | 31 |
| 16 | 44 | 65 |
| 24 | 89 | 61 |

for this is as follows. There were several absorptions which are typical of the terephthalate residue, viz. C—H out of the plane deformation absorption at 730 cm^{-1} and C—H deformation vibrations at 872 and $1\,025\text{ cm}^{-1}$. Also absorptions occurred at $1\,630$ and $1\,543\text{ cm}^{-1}$ which can be assigned to the C=O stretching vibration and the N—H deformation of a secondary amide.

DEGRADATION of POLYETHYLENE TEREPHTHALATE by METHYLAMINE

This together with elementary analysis of the recrystallized material (m.pt 325°C) shows that it is *NN'* dimethyl terephthalamide. For $C_{10}H_{12}N_2O_2$:

| | C | H | N |
|-------|------|-----|---------------|
| Calc. | 62.6 | 6.3 | 14.6 per cent |
| Found | 62.1 | 6.6 | 15.3 per cent |

Molecular weight of degraded fragments

Independent estimates of the molecular weight were obtained from viscosity and infra-red measurements on the insoluble fractions.

In the normal molecular weight range ($\bar{M}_n = 1$ to 3×10^4) intrinsic viscosity measurements are used, and converted to values of \bar{M}_n using the relationship established by infra-red end-group techniques⁸, although it is appreciated that \bar{M}_n is particularly susceptible to the smaller molecular weight fraction most of which is removed by extraction where degradation is extensive.

A more direct value of \bar{M}_n was calculated from the infra-red hydroxyl end-group concentrations, assuming that each chain split produces a hydroxyl and a methylamide end. Thus the final end-group concentration is the initial one plus twice the number of additional hydroxyl end groups. Values obtained by these methods are given in *Table 6*.

Table 6

| Sample | Duration of reaction h | Molecular weights $\times 10^3$ | |
|--------|---------------------------|------------------------------------|------|
| | | Infra-red | I.V. |
| b | 16 | 8.3 | 5.0 |
| b | 40 | 7.6 | — |
| c | 16 | 8.1 | — |
| c | 24 | 9.2 | — |
| d | 24 | 8.2 | 1.1 |
| d | 48 | 8.3 | — |

Low-angle scattering

The normalized low-angle curves for the samples [except the amorphous sample (a) which showed no low-angle scattering for such exposure times] are given in *Figure 2*. The degraded samples all show a continuous scattering pattern. The peak observed at $\sim 200\text{\AA}$ for these samples is an instrumental effect and represents the limits of resolution of the low-angle camera. Two low-angle photographs [sample (d), original and degraded for 48 hours] taken for us at the National Physical Laboratory on a high-resolution low-angle camera, based on a design by Franks⁹, when analysed gave curves almost identical with the corresponding ones in *Figure 2*. The continuous scattering from the degraded specimen was also a maximum at the limits of resolution of this camera ($\sim 450\text{\AA}$ under the set conditions).

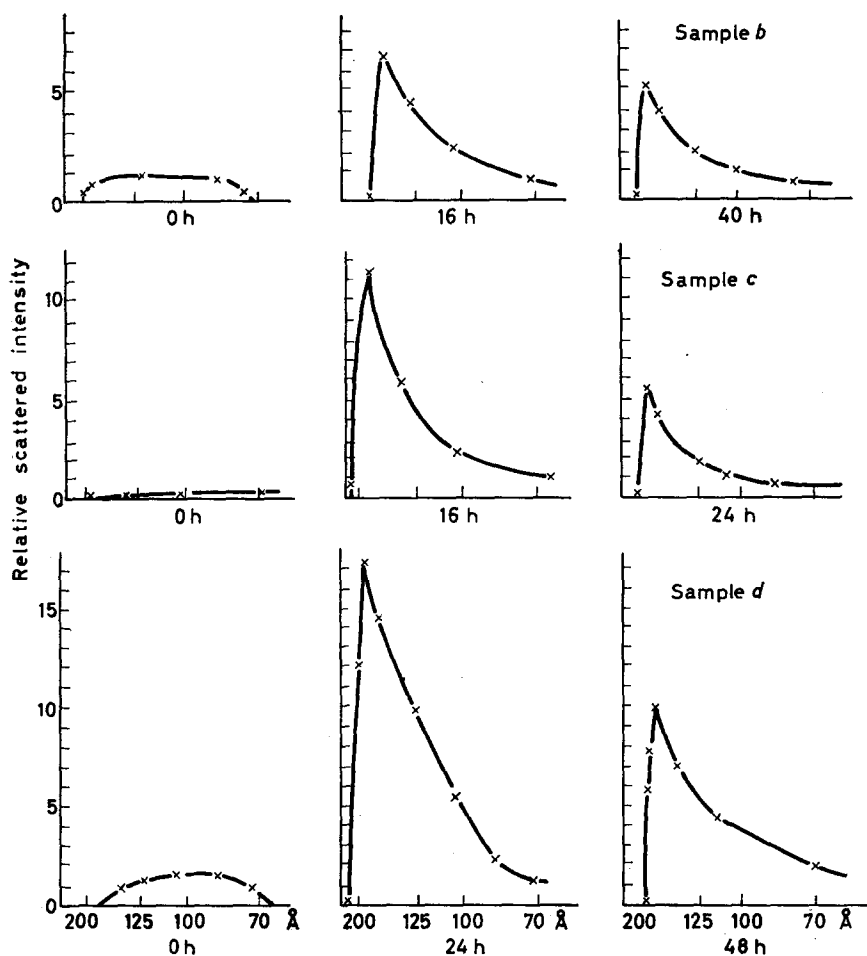


Figure 2—Normalized curves showing low-angle scattering of X-rays by various PET samples

DISCUSSION

Nature of the degradation

Examination of Figure 3 together with results in Tables 1 and 2 shows that initially some reduction in molecular weight occurs in the first stages of the reaction with little loss of weight. This suggests that there is a rapid fall in the molecular weight due to attack in the amorphous regions but little low molecular weight material is formed and hence the sample weight and crystallinity are almost unchanged. In the second stage chain scission now produces a much larger amount of extractable (low molecular weight) material and there is a rapid fall in sample weight and a rise in the degree of crystallinity. During the third stage there is a gradual decrease in the reaction rate and this may be attributed to a much slower attack on both amorphous and crystalline regions in the sample. This is suggested

DEGRADATION of POLYETHYLENE TEREPHTHALATE by METHYLAMINE

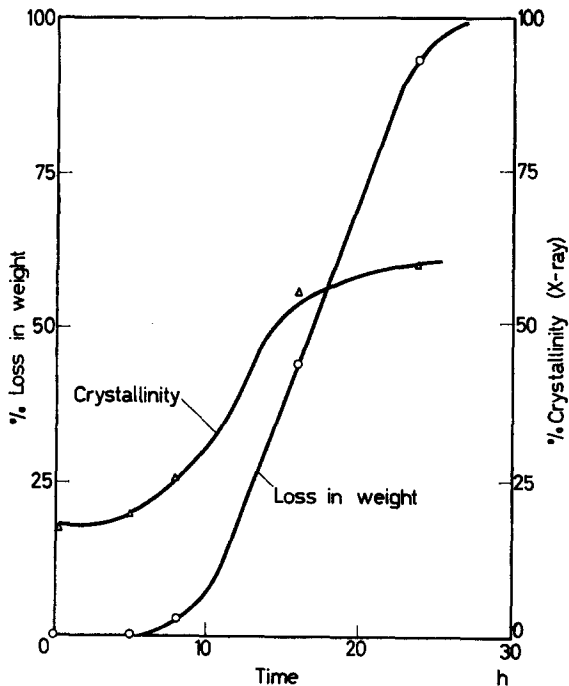


Figure 3—Loss in weight and increase in crystallinity of sample c during degradation

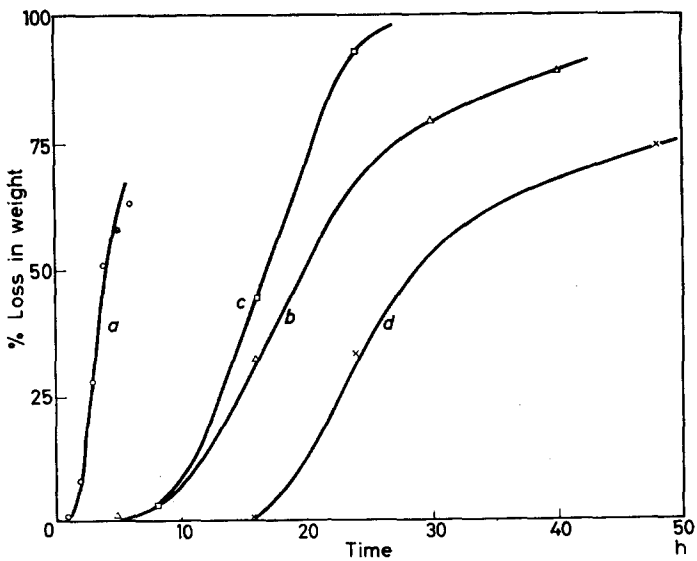


Figure 4—Loss in weight curves for samples a, b, c, d during degradation

by the fact that the loss in weight for all the samples is much greater than would be expected if only the amorphous regions were attacked and this evidence together with the fact that no crystallinity higher than 72 per cent could be obtained confirms that in the later stages both regions are attacked.

These results show that it is not possible to separate crystalline and amorphous phases in PET by degradation as has been suggested for cellulose². A further complication is the induced crystallization occurring during degradation which is shown by the presence of crystallinity in degraded amorphous fibre (*Table 1*).

Comparison of the rates of weight loss for samples with various physical structures (*Figure 4*) shows that when weight loss becomes appreciable there are only small differences between the reaction rates but there is the expected trend to lower rates at higher crystallinities and orientation. However, there are much larger differences in the time taken for loss in weight to become appreciable due to the large variations in the rates of chain scission. Thus the order of reactivity; unoriented amorphous: unoriented crystalline: oriented crystalline, is similar to that found for the hydrochloric acid hydrolysis of PET¹, where the decrease in rate with increasing crystallinity was found to be due to lower solubility but the decrease with orientation is due to changes in the rate constant.

Low-angle scattering

PET fibres of high crystallinity produce discrete X-ray reflections at low angles¹⁰. In *Figure 2*, the untreated, heat crystallized samples [(b) and (d)] show a definite broad band of intensity. It is considered that this is principally composed of two discrete reflections from the randomized samples of PET—one from spacings parallel to the fibre axis occurring at $\sim 120\text{\AA}$ and the other from spacings normal to the fibre axis which give a ring¹⁰ at $\sim 60\text{\AA}$. On degradation these discrete reflections apparently disappear and are overlapped or replaced by a continuous scattering pattern the interpretation of which is complicated and controversial. It is possible that the continuous scattering on the low-angle patterns arises from the dimensions of the degraded particles themselves or that these particles, because of the action of methylamine, contain holes of molecular dimensions which in themselves would give rise to such scattering¹¹. Beyond this the low-angle X-ray patterns do not give any further structural information.

We wish to thank Mr P. E. Knapp for supervising the preparation of the yarns, also Miss J. Bagley and Mrs J. A. Watson for experimental assistance.

*Fibres Division of I.C.I. Ltd,
Hookstone Road, Harrogate, Yorkshire*

(Received August 1961)

REFERENCES

- ¹ RAVENS, D. A. S. *Polymer, Lond.* 1960, **1**, 375
- ² SHARPLES, A. *Trans. Faraday Soc.* 1957, **53**, 1003; 1958, **54**, 913
- ³ ARNETT, E. M., MILLER, J. G. and DAY, A. R. *J. Amer. chem. Soc.* 1950, **72**, 5634
- ⁴ STIMSON, M. M. and O'DONNELL, M. J. *Amer. chem. Soc.* 1952, **74**, 1805
- ⁵ WARD, I. M. *Trans. Faraday Soc.* 1957, **53**, 1406
- ⁶ FARROW, G. and PRESTON, D. *Brit. J. appl. Phys.* 1960, **11**, 353
- ⁷ TODD, A. *Nature, Lond.* 1954, **174**, 613
- ⁸ RAVENS, D. A. S. and WARD, I. M. *Trans. Faraday Soc.* 1961, **57**, 150
- ⁹ FRANKS, A. *Brit. J. appl. Phys.* 1958, **9**, 349
- ¹⁰ STATTON, W. O. and GODARD, G. M. *J. appl. Phys.* 1957, **28**, 1111
- ¹¹ GUINIER, A. *X-ray Crystallographic Technology*, Chap. 12. HILGER and WATTS: London, 1952

A Kinetic Study of the Benzene-induced Crystallization of Polyethylene Terephthalate

R. P. SHELDON

A study has been made into some of the factors associated with the kinetics of the benzene-induced crystallization of polyethylene terephthalate. Four thicknesses of the film were used at temperatures of 25°, 30°, 35° and 40°C and in one case at 55°C. The rate was found to increase with increase of temperature and within the restricted range studied no tendency towards a maximum was detected. Making the usual assumptions between density and crystallinity the mathematical expression relating to the major part of the rate curves was found to have the form

$$A' - V/A' = C \exp [-(C'/x^3) (e^{-\Delta E/RT}) t]$$

where A' and V are the volume fractions of crystallinity at equilibrium and after time t respectively, C and C' are constants, x is the specimen thickness, T is the temperature on the absolute scale, R the gas constant and E , which has the value of 10.3 kcal/mole, is identified with an activation energy term. It is believed that the crystallization process is diffusion controlled in that it probably occurs along a progressive front accompanying liquid diffusion.

IT HAS recently been shown that a number of organic liquids will induce substantial degrees of crystallization in amorphous polyethylene terephthalate (PET) at temperatures well below those at which appreciable air or normal crystallization occurs¹. For example, a 50 per cent degree is achieved within a few minutes by immersion of an 8 mil thick specimen in dioxan at 25°C, whereas in the absence of organic liquids a temperature of the order of 100°C higher would be necessary for a comparable effect. It is probable that this property is by no means restricted to PET but is one characteristic of those crystallizable polymers which may, by suitable treatment, be obtained in the amorphous form since cellulose triacetate appears to show the same behaviour² whilst stereoregular polymethyl methacrylate, like PET, may only be crystallized with liquids whose solubility parameters lie within a certain range³.

From the previous work¹ it was seen that the rates and extent of crystallization may vary widely from one system to another and since no information is available, so far as the author is aware, upon the kinetics of such induced crystallization an investigation has been made using one liquid, benzene, preliminary studies having shown that at ambient temperatures this system produced changes at a rate convenient for measurement. It is proposed at a later date to extend the work to other liquids.

In normal thermal treatment extensive investigations have been carried out⁴ and it has been shown that crystallization occurs within a range of temperatures intermediate between the glass temperature and the melting point as may be expected and the rate curves have the typical sigmoidal

characteristics to be expected on the basis of the Avrami treatment which considers growth concomitant with nucleation⁵. It may also be noted that the time exponents of the experimentally derived Avrami equations have the values of 2, 3 or 4.

With the present system, however, the behaviour may be more difficult to predict owing to lack of adequate theory but it appears reasonable to assume that the factors which might exert an influence will include such parameters as are determined by the nature of the liquid, thickness of sample, temperature and previous history of the polymer, e.g. temperature of the melt prior to extrusion, dwell-time, etc. Some information is already available upon the first of these points, as previously mentioned¹, in that the density at equilibrium may be interpolated from a knowledge of the solubility parameter of the liquid. The contribution due to the history of the polymer has largely been ignored, although this aspect is intended to be the basis of some future work.

EXPERIMENTAL

Materials

The PET used in these studies was in the form of transparent film of low density (1.340 g/cm^3) corresponding to a calculated crystallinity of 4.2 per cent by volume. It was also unoriented showing no evidence of birefringence under a polarizing microscope. Four thicknesses were taken, each being measured with a micrometer and were found to be 2.1, 2.7, 3.4 and 4.1×10^{-2} cm, subsequently referred to as A, B, C and D.

The benzene used as immersion liquid was of A.R. quality and was dried and fractionally distilled before use, as were also the carbon tetrachloride and ethyl alcohol for the density measurements.

Procedure

The experimental procedure was similar to that previously described¹. Samples of polymer of the various thicknesses were cut into small pieces of approximately 1 cm^2 in surface area. Four pieces from the four samples were weighed on a balance capable of reading to 0.01 mg and introduced into test-tubes containing benzene, each tube itself being immersed in a thermostatically controlled bath, at a temperature of $25 \pm 0.01^\circ\text{C}$. After predetermined intervals of time the pieces were removed, surface dried and transferred to an evacuated desiccator where they remained for at least 48 hours before being reweighed. The apparent density was determined by a flotation method in which alcohol is run in from a microburette to 10 ml of carbon tetrachloride until the polymer sample is on the point of sinking. Allowance was made for the residual benzene to convert the apparent density to a corrected value, the former being interpolated from a calibration curve of various mixtures of the flotation liquids and their densities.

The procedure was repeated at 30° , 35° and 40°C and in the case of sample B, at 55°C . The temperature control at this latter temperature was of the order of $\pm 0.1^\circ\text{C}$.

RESULTS

The rate curves showing the increase of density as a function of time are shown in *Figure 1*. Investigation shows that, within experimental error, in

CRYSTALLIZATION OF POLYETHYLENE TEREPHTHALATE

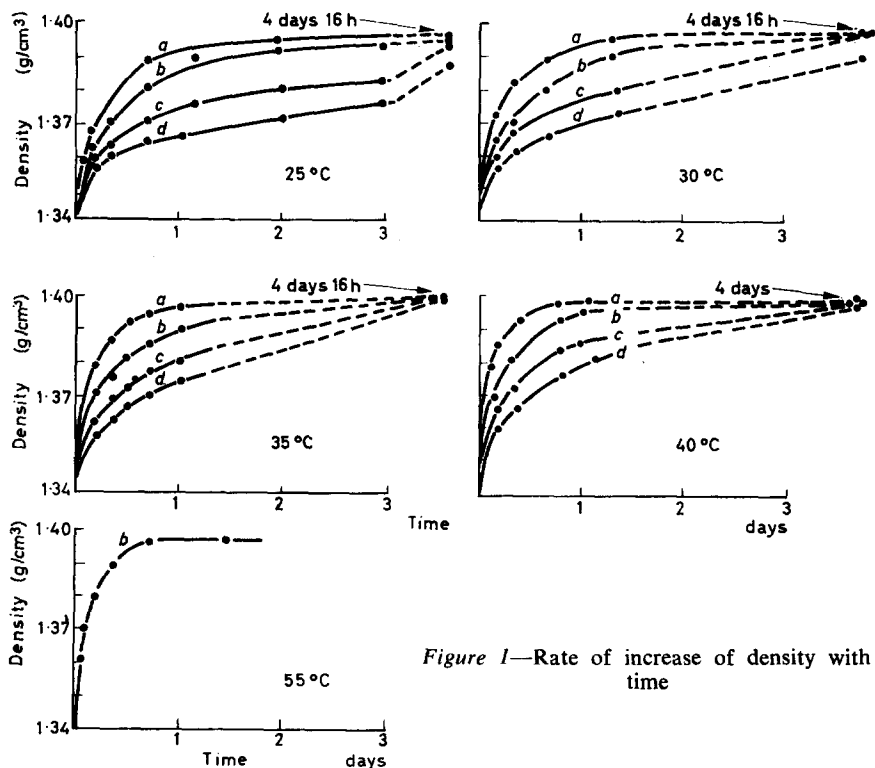


Figure 1—Rate of increase of density with time

those cases where equilibrium has apparently been reached the equilibrium density has the value 1.396 g/cm^3 , independently of sample thickness and temperature. Taking this to be the value for all cases a plot is made of $\log(d_\infty - d_t)$ versus time where d_∞ and d_t are the density values at equilibrium and after time t respectively (Figure 2). The magnitudes of the slopes of the straight lines obtained are measures of the rates of attainment of equilibrium and thus may be identified with rate constants (Table 1). Following the usual kinetic procedure the dependence of rate constant upon temperature is obtained by means of a plot of $\log k$ versus T^{-1} where k is the rate constant at a particular temperature T (Figure 3). Again by analogy with normal kinetic procedure, where an Arrhenius relationship is usually valid, an activation energy term and a temperature-independent term may be evaluated (Table 2). The relationship between rate constant and sample thickness is obtained from a plot of $\log k$ versus \log (thickness), the thickness being measured in centimetres (Figure 4). The corresponding slopes and ordinate intercept values are given in Table 3.

It may be relevant at this stage to point out that in view of the similarities in the slopes in Figure 3, and yet where a small divergence can have a significant effect upon ordinate intercept value, in order to obtain the values quoted (Table 2), an average was taken of the slopes followed by extrapolation from the value of $\log k$ at $T^{-1} = 0.0030^\circ \text{K}^{-1}$. In Figure 4 the slopes were found to be identical and thus a similar treatment was unnecessary.

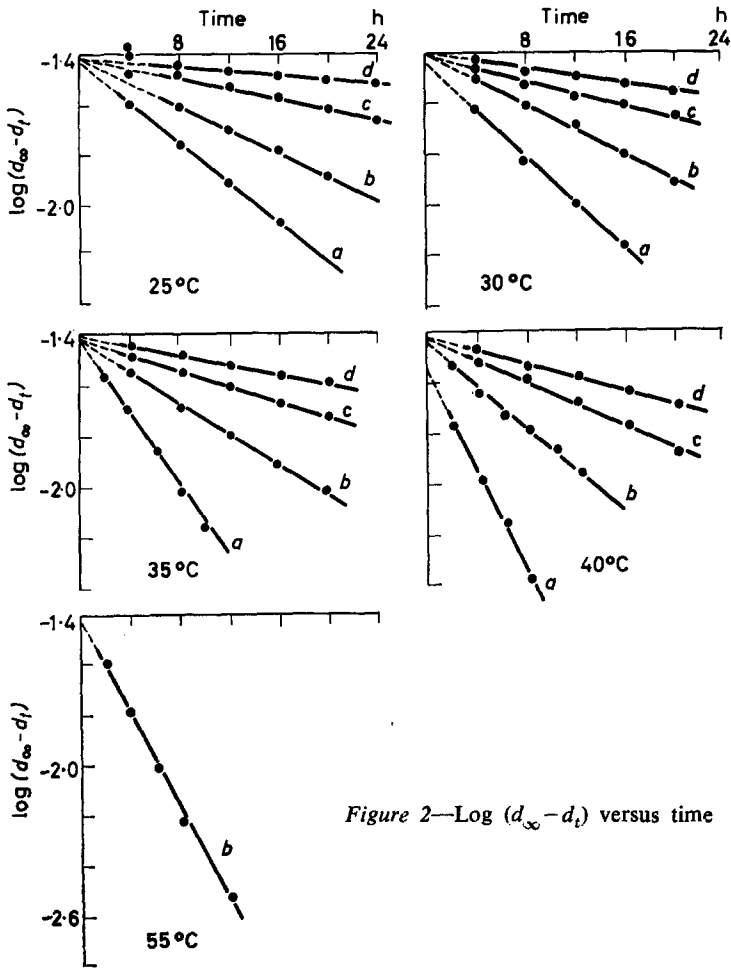


Figure 2— $\log(d_{\infty} - d_t)$ versus time

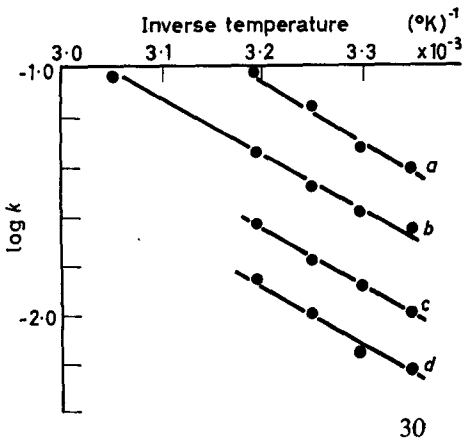


Figure 3— $\log k$ versus inverse temperature

CRYSTALLIZATION OF POLYETHYLENE TEREPHTHALATE

Table 1. Rate constants of induced crystallization

| Sample | Temp. (°C) | k (h^{-1}) | Sample | Temp. (°C) | k (h^{-1}) |
|--------|------------|------------------|--------|------------|--------------------|
| A | 25 | 0.039 | C | 25 | 0.010 |
| | 30 | 0.046 | | 30 | 0.012 ₅ |
| | 35 | 0.068 | | 35 | 0.016 |
| | 40 | 0.096 | | 40 | 0.023 |
| B | 25 | 0.022 | D | 25 | 0.006 |
| | 30 | 0.025 | | 30 | 0.007 |
| | 35 | 0.032 | | 35 | 0.010 |
| | 40 | 0.044 | | 40 | 0.014 |
| | 55 | 0.092 | | | |

Table 2. Activation energies and frequency factors of crystallization ($k = Ae^{-\Delta E/RT}$)

| Sample | ΔE (kcal/mole) | A (h^{-1}) |
|--------|------------------------|--------------------|
| A | 10.6 | 10.5×10^5 |
| B | 9.7 | 5.6×10^5 |
| C | 10.4 | 2.8×10^5 |
| D | 10.4 | 1.7×10^5 |

Table 3. Slopes and ordinate intercept values from the relationship $\log k = x \log(\text{thickness}) + \log K$

| Temp. (°C) | Slope (x) | Ordinate intercept (log K) | K |
|------------|-----------|----------------------------|-----------------------|
| 25 | 3.0 | -6.31 | 4.90×10^{-7} |
| 30 | 3.0 | -6.22 | 6.03×10^{-7} |
| 35 | 3.0 | -6.10 | 7.94×10^{-7} |
| 40 | 3.0 | -5.96 | 1.10×10^{-6} |

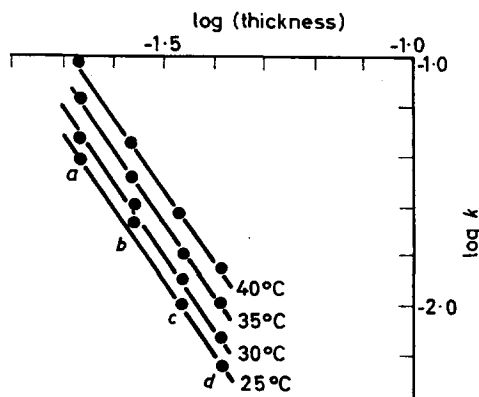


Figure 4—Log k versus log (thickness)

DISCUSSION

The first noticeable feature of the results is that the crystallization rate is dependent upon sample thickness, the rate at any one temperature decreasing with increase of thickness. Also attention is drawn to the apparent absence of the sigmoidal type rate curve characteristic of normal crystallization; this appears to be a facet of a more general phenomenon in liquid-induced crystallization. If it occurs at all, it must be in a time interval too small for normal measurement. Moreover, the curves are of a regular shape with no superimposition of one curve seemingly on top of another, indicative of a secondary process found in normal crystallizations^{4, 6}. These features alone immediately suggest a different mechanism as might of course be expected on other grounds.

It is interesting to note, as mentioned previously, that at least in the temperature range studied, the equilibrium density, and hence presumably the equilibrium crystallinity, is independent of temperature. This is useful in that it gives a more reliable value for d_∞ at 25°C which slightly modifies the value previously quoted but without prejudicing the conclusions¹. This result implies that the maximum degree of crystallinity at these temperatures is the same independent of temperature suggesting that the previous history of the polymer has some bearing upon the crystallization process. (Preliminary results on samples recently received indicate visual confirmation of this hypothesis in that the samples, which were prepared under different melt conditions, showed different degrees of brittleness after identical treatment with liquid and subsequent vacuum.)

The results also indicate that the rate increases with increase of temperature and that if a situation obtains such as occurs in normal crystallization where the overall rate increases to a maximum and then decreases as the melting point is approached then in the present case the system must be well below the maximum. On the other hand, as discussed below, if a different type of mechanism applies then the variation of rate with temperature will not be simply described as above.

It is shown in *Figure 2* that $\log(d_\infty - d_t)$ is a rectilinear function of the time which enables a kinetic study to be made since the slope is a measure of the rate at which equilibrium is attained. Careful inspection, however, shows that this statement is not entirely true in that, although the derived rate equation holds over the major part of the curve, the initial rate occurring over the first five per cent or so of the effective time interval is greater than would be expected from the equation, since the extrapolated zero-time density is greater than the measured value. *Figure 3* shows another rectilinear relationship, this time between $\log k$ and T^{-1} . This relationship may be expressed mathematically as $k = Ae^{-\Delta E/RT}$ where ΔE is identified as an activation energy term although the final equilibrium state does not correspond to one usually considered in kinetic studies, and A is substantially a temperature-independent constant. The value of the activation energy, to which reference will be made later, is roughly the same irrespective of sample thickness, and this factor has been utilized in the extrapolations for the A values. *Figure 4* shows that there is a relationship between k and sample thickness (x), of the form $k = K/x^3$ where K is a constant which, for the sake of a physical picture, may be regarded as a

rate constant for a sample 1 cm thick. To obtain the combined effect of the two equations upon the rate of density increase and at the same time substituting experimental numerical values we can write

$$d_{\infty} - d_t = 2.63 \times 10^{-2} \times \exp [-(23.03/x^3) \times e^{-\Delta E/RT} \cdot t]$$

Comparison may be made with the form of the equation obtained from the Avrami treatment which can be expressed⁷ as

$$A' - V/A' = e^{-Bt^n}$$

where A' , which should not be confused with the A of the Arrhenius type equation, is the limiting volume fraction of crystallinity, V is the volume fraction after time t , B is a constant and n is an integer having theoretical values of 1, 2, 3 or 4 depending on the mode of nucleation and crystallization. Making the usual assumptions between density and crystallinity it may easily be shown that

$$A = \frac{d_{\infty} - d_{A'}}{d_c - d_{A'}} \quad \text{and} \quad V = \frac{d_t - d_{A'}}{d_c - d_{A'}}$$

and that

$$A' - V/A' = \frac{d_{\infty} - d_t}{d_{\infty} - d_{A'}}$$

where d_c and $d_{A'}$ are the densities of completely crystalline and amorphous PET respectively and have the values^{8, 9} 1.455 and 1.335 g/cm³. The equation may now be written

$$A' - V/A' = C \exp [-(C'/x^3)(e^{-\Delta E/RT}) \cdot t]$$

where C and C' are constants having values of 0.44 and 23.03 respectively. There appears to be a superficial similarity between the two equations but the situations are not considered to be strictly analogous since in the present case crystallization presumably occurs on a progressive front accompanying liquid diffusion whereas the Avrami treatment is based on random heterogeneous or homogeneous nucleation with subsequent crystallite growth. However, the time exponent of unity is, on the latter treatment, indicative of diffusion controlled crystallization following heterogeneous nucleation, which may well be the behaviour in the present example.

Perhaps a more reasonable comparison may be made with diffusion and for this purpose we can consider the equation for diffusion into a plane slab¹⁰

$$C_{\infty} - C_t/C_{\infty} = A''e^{-a''Dt/x^2} + B''e^{-b''Dt/x^2} + \dots$$

where C_{∞} and C_t are the concentrations of diffusing substance at equilibrium and after time t , respectively, A'' , B'' , ... and a'' , b'' , ... are constants peculiar to the system (not to be confused with any previous constants), and D is the diffusion coefficient. Ignoring the less significant secondary terms on the RHS, the form of the equation bears a striking resemblance to the experimental equation particularly when it is remembered that the diffusion equation is derived on the basis of Flick's law type of diffusion with constancy of diffusion coefficient, an assumption not always valid for polymers¹¹, and although no evidence is available to contradict this assumption at the low concentration end of the scale for diffusing substances such

as dyes in PET¹², the same may not be true for the relatively high concentrations (~ 10 per cent) encountered in these studies. Because of this the theoretical equation may have to be modified, the modification perhaps accounting for the discrepancy in the thickness indices, and at the same time suggesting a better plot for the experimental equation which may thus include the initial part of the curves.

On the basis of this the picture is now possibly one in which the benzene presumably induces some relaxation which enables suitable juxtaposition of polymer chain units for crystallization to occur. It is not clear at this stage to what extent established crystallization will affect further diffusion, nor at higher temperatures with suitable diffusing liquid what would be the influence of temperature alone. In the present case the activation energy mentioned will be associated with diffusion, the value of 10.3 kcal/mole perhaps not being an unreasonable one for this system. It is imagined that the value of ΔE for any diffusing substance will be strongly dependent upon the size and nature of the substance¹².

The extension of this work to include a wider range of liquids might confirm these postulates and at the same time throw more light on the mechanism of liquid-induced crystallization.

The author wishes to thank I.C.I. Ltd, Plastics Division for their generous gift of the polyethylene terephthalate film used in these studies.

*Polymer Research Laboratories,
Department of Chemical Technology,
Institute of Technology, Bradford, Yorkshire*

(Received August 1961)

REFERENCES

- ¹ MOORE, W. R. and SHELDON, R. P. *Polymer, Lond.* 1961, **2**, 315
- ^{2a} SPENCE, J. J. *phys. Chem.* 1941, **45**, 401
- ^b BAKER, W. O., FULLER, C. S. and PAPE, N. R. *J. Amer. chem Soc.* 1942, **64**, 776
- ³ *Aus. Pat. No. 36 684*
- ^{4a} KELLER, A., LESTER, G. R. and MORGAN, L. B. *Phil. Trans.* 1954, **247**, 1
- ^b MORGAN, L. B. *Phil. Trans.* 1954, **247**, 13
- ^c HARTLEY, F. D., LORD, F. W. and MORGAN, L. B. *Phil. Trans.* 1954, **247**, 23
- ⁵ AVRAMI, M. *J. chem. Phys.* 1939, **7**, 1103; 1940, **8**, 212
- ⁶ HARTLEY, F. D., LORD, F. W. and MORGAN, L. B. *Ric. sci. (Suppl. A)*, 1955, **25**, 577
- ⁷ COBBS, W. H., Jr and BURTON, R. L. *J. Polym. Sci.* 1953, **10**, 275
- ⁸ THOMPSON, A. B. and WOODS, D. W. *Nature, Lond.* 1955, **176**, 78
- ⁹ BUNN, C. W. in *Fibres from Synthetic Polymers*, edited by R. HILL. Elsevier: Amsterdam, 1953
- ¹⁰ See e.g. VICKERSTAFF, T. *The Physical Chemistry of Dyeing*. Oliver and Boyd: London, 1954
- ¹¹ KOKES, R. J., LONG, F. A. and HOARD, J. L. *J. chem. Phys.* 1952, **20**, 1711
- ¹² See e.g. PATTERSON, D. and SHELDON, R. P. *Trans. Faraday Soc.* 1959, **55**, 1254

A New Technique for Following Rapid Rates of Crystallization II

Isotactic Polypropylene

J. H. MAGILL

The depolarized light intensity technique has been used to follow the crystallization of isotactic polypropylene. Crystallization rate constants of the same magnitude as recently published literature values derived from dilatometer measurements have been obtained. A maximum in the crystallization rate is believed to occur in the region of 60° to 70°C. Induction times were derived from the rate data. The generation of nuclei is simultaneous or predetermined and the morphology spherulitic above about 115°C. Below this temperature nuclei are sporadically formed (in time) and the geometry of the crystallized specimen ranges from spherulitic to unidentifiable shapes.

CONSIDERABLE attention has been focused recently on the crystallization behaviour of isotactic polypropylene because of its novel nature and possibilities in the fibre and moulding fields. Several papers on the isothermal crystallization of this polymer have appeared in the literature. Dilatometric techniques¹⁻⁴ have been used to study the kinetics of crystallization in the temperature range 120° to 160°C¹⁻³, but these methods are limited to temperatures where the rate constant is less than 10⁻³ minutes⁻³. Spherulite growth measurements are restricted to a similar temperature range because of a transition in morphology which occurs not far below 120°C. The lowest temperature where spherulite growth rates have been measured⁵ is about 112°C. A higher temperature⁴ (117°C) for this transition was deduced from induction times of the onset of nucleation in films of fused polymer isothermally crystallized in a thermostated silicone oil bath. A recent publication¹⁴ which appeared after the completion of this present study of isotactic polypropylene outlined the utility of the depolarized light intensity or birefringence method for determination of melting points and crystallization rates in polyolefins, but no detailed measurements were presented.

The present paper is concerned especially with measurement of isothermal crystallization of isotactic polypropylene using the depolarized light intensity technique described in earlier communications⁹⁻¹¹. The method embraces a wider crystallization range than has hitherto been mentioned in the literature. The rate measurements are discussed together with some observations on polymer texture produced on crystallization.

EXPERIMENTAL

Polymer

Shell Carlon White isotactic polypropylene was used throughout these experiments. The polymer had an initial inherent viscosity of 2.7 dl/g measured at 135°C in 0.2 per cent (w/v) solution of tetralin containing 0.05 per cent (w/v) α -naphthol as an anti-oxidant. On melting this polymer,

mounted between cover slips in silicone oil for $\frac{1}{2}$ h at 270°C, the inherent viscosity fell rapidly in the initial stages of heating but showed a gradual levelling off at the end of the melt period. The final polymer had an inherent viscosity of 1.5 dl/g corresponding to a \bar{M}_w of 1.96×10^5 which characterizes the polymer in the crystallization experiments described below. The ash content of the polymer was 0.16 per cent.

Apparatus

The apparatus used consisted of a stabilized light source used to illuminate the specimen on the Köfler hot stage of the polarizing microscope. A photomultiplier was placed over the ocular tube of the microscope so that the depolarized light from the crystallizing specimen fell on the photocathode. The cathode ray oscilloscope-camera arrangement which recorded the output from the photomultiplier was used to follow the fast rates of crystallization. This was replaced by a variable chart-speed Honeywell Brown recorder when making measurements at the higher crystallization temperatures where the rates were comparatively slow. A more detailed account is given in an earlier publication⁹.

Procedure

Dried sections (*ca.* 150 to 200 μ) of polymer chip were mounted between microscope slide cover slips of $\frac{5}{8}$ in. diameter. M.S. 550 silicone oil was used as an immersion medium to reduce oxidation of the sample during melting. Samples were melted on the Gallenkamp hot stage at $270 \pm 3^\circ\text{C}$ for 30 minutes followed by rapid transfer to the Köfler hot stage of the polarizing microscope which was maintained to within $\pm 0.5^\circ\text{C}$ of the desired crystallization temperature. The rate of depolarization of the light by the sample measured during the isothermal crystallization corresponds to the rate of development of crystallinity during the phase change when macrocrystalline structures are formed. All measurements were made within the linear operating range of the apparatus.

RESULTS

Depolarized light intensity/time curves (I/t)

Typical depolarized light intensity/time curves for a range of isothermals where crystallization is spherulitic are illustrated in *Figure 1*. Most of these results were obtained using the Honeywell Brown recorder. Photographic recordings are similar at the corresponding crystallization temperatures.

Induction time of crystallisation τ

Values of τ defined as the time interval which elapses during which no depolarization of the light occurred for a given crystallization temperature were derived from I/t curves. The induction time/temperature relationship for isotactic polypropylene is given in *Figure 2*. The results cover a wide temperature range and show a transition in the region of 115° to 120°C. This transition is more clearly depicted when the results are analysed using the Kantrovitz equation⁸

$$\tau^* = k(\Delta T)^{-n}$$

A TECHNIQUE FOR FOLLOWING RAPID RATES OF CRYSTALLIZATION

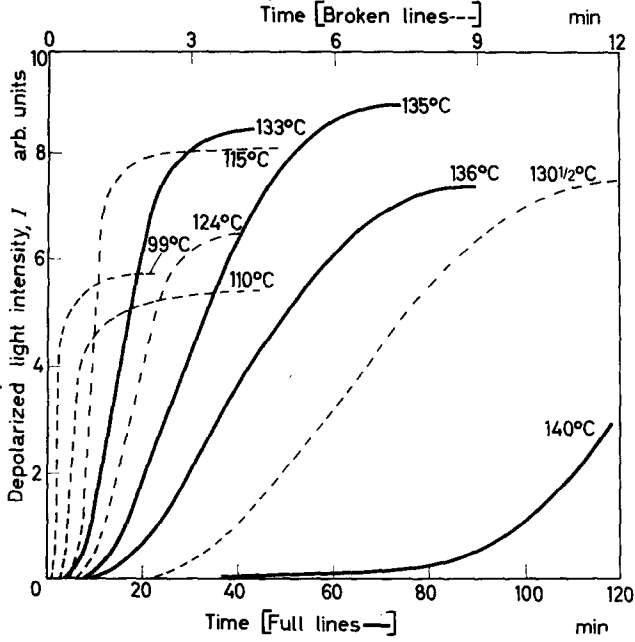


Figure 1—Light depolarization versus time curves for various crystallization temperatures of isotactic polypropylene

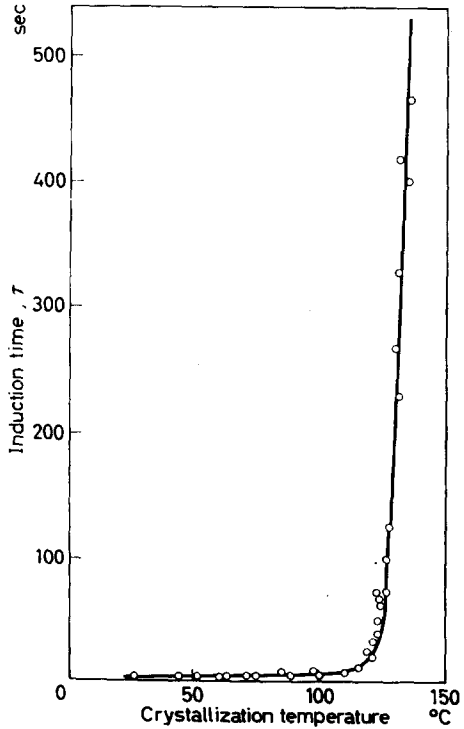


Figure 2—Induction time versus crystallization temperature for isotactic polypropylene

where τ^* is the incubation period and $\Delta T = T_m - T_c$; T_m being the 'melting point' and T_c the crystallization temperature. The identification of τ with the incubation period provides a useful empiricism for the determination of morphological transitions as reflected in the change of the exponent n . When $\log(\Delta T)$ is plotted against $\log \tau$, results on either side of the transition lie on straight lines intersecting at a temperature corresponding to 115°C.

Avrami plots

The depolarized light intensity versus time plots are readily transformed to fit the Avrami equation

$$\theta = e^{-kt^n}$$

where θ is put equal to $(I_c - I_t)/(I_c - I_0)$ which is obtained from the I/t plots of Figure 1. I_0 , I_t and I_c are the light intensities corresponding to the initial, intermediate and final stages of the isothermal crystallization process as detailed in previous papers⁹⁻¹¹. The Avrami θ in Figure 3 represents the

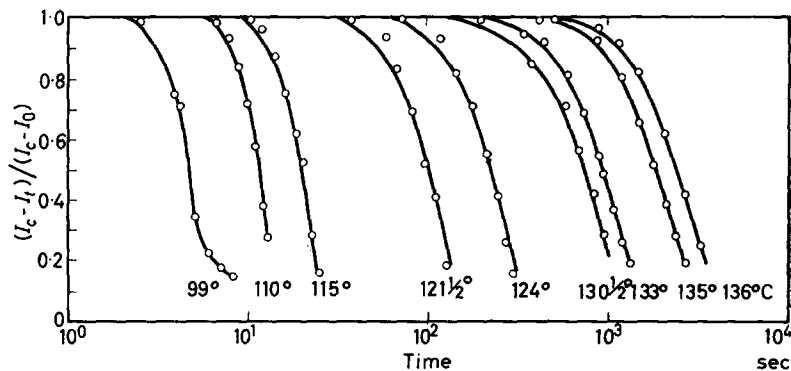


Figure 3—Light depolarization versus time plots for isotactic polypropylene at various crystallization temperatures

fraction of unchanged material remaining after a time t . The parameters k and n in the expression describe the rate and mechanism of crystallization respectively.

Figure 4 shows typical plots of $\ln [-\ln(I_c - I_t)/(I_c - I_0)]$ versus $\ln t$. Some results were also analysed by plotting $\ln(I_c - I_t)/(I_c - I_0)$ versus t^n where the first portion of the plot (Figure 5) was best fitted to an Avrami n of 3 in that region where the nucleation was predetermined and subsequent crystal growth spherulitic.

Morphology

Microscopical examination of samples crystallized above 115°C reveal that spherulitic growth occurs from nuclei which are formed simultaneously. The number of spherulites per unit volume decreases while their sizes increase, as the isothermal crystallization temperature is raised. The precise morphology of structures which grow in specimens crystallized below 115°C cannot be completely resolved even when the growth process is arrested at an early stage by rapid quenching of crystallizing samples to -65°C.

A TECHNIQUE FOR FOLLOWING RAPID RATES OF CRYSTALLIZATION

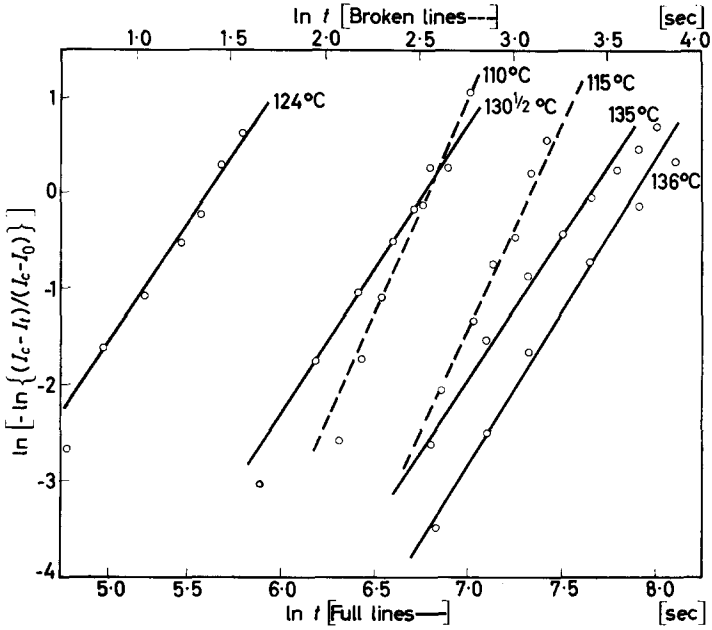


Figure 4—Avrami crystallization isotherms for isotactic polypropylene

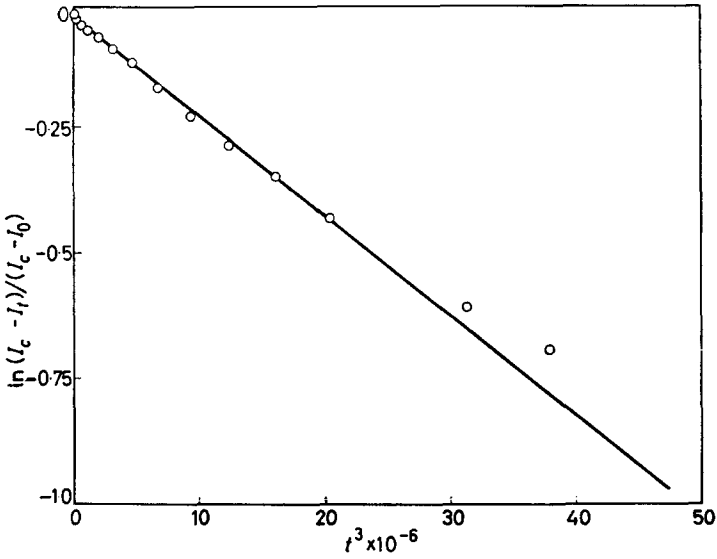


Figure 5—Avrami plot for crystallization isothermal, 127°C (t sec)

X-ray diffraction of crystallized films

Some X-ray measurements by Dr T. C. Tranter (using a 100 μ collimator) on spherulites (ca. 1 500 μ) grown at 145°C show that there is a high degree

of orientation within these spherulites compared with zero orientation in the surrounding quenched material.

Ordinary X-ray diffraction patterns of samples crystallized on the Köfler hot stage at 129°C, 108°C and 62°C respectively have the same spacings and relative intensities. There is no preferred overall orientation as assessed visually—the patterns appear identical in all respects.

DISCUSSION

Crystallization kinetics

The typical crystallization isothermals illustrated in *Figures 1, 3 and 4* are representative of results obtained by this method. Where the growth is spherulitic the kinetics are governed by a predetermined nucleation mechanism with an Avrami $n=3$ in agreement with microscope observations and the results of other workers^{1, 2, 4}. The rate constants calculated using the equation

$$(I_c - I_t)/(I_c - I_0) = e^{-kt^3}$$

agree with results obtained from dilatometric data in the literature². Rate values are plotted in *Figure 6* together with the corresponding half-times of crystallization.

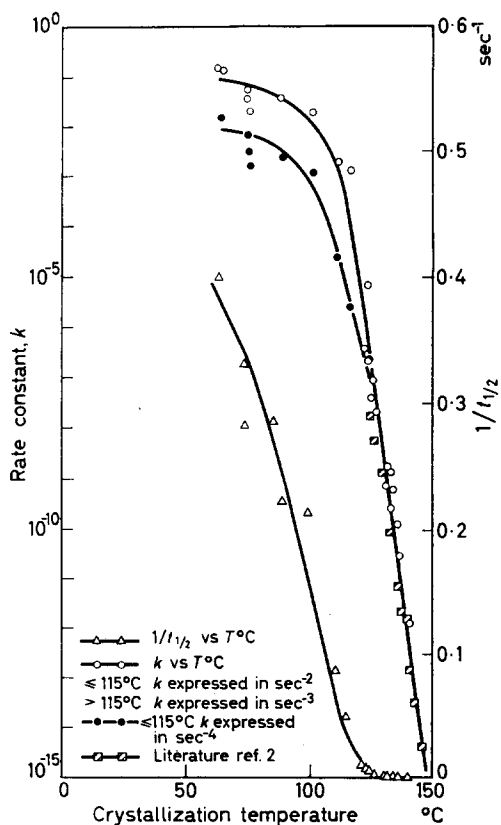


Figure 6—Rate parameters for isotactic polypropylene

An unexpected result in the rate measurements is the change in shape of the normalized plots of *Figure 3* which gives rise to an Avrami parameter of $n=4$ on lowering the crystallization temperature. No satisfactory explanation can be put forward for this behaviour, but the effects of internal stress and rate of equilibration of the specimen to the crystallization temperature at large degrees of supercooling probably introduce uncertainties in the type of nucleation. Because the morphological structures produced below this transition temperature are not unambiguously defined by microscope observations, calculations of rate parameters were made using both $n=4$ and $n=2$ in the transformed Avrami equation

$$k = \ln 2 / (t_{\frac{1}{2}})^n$$

since both these n values can be identified with changes which are sporadic in time¹³. In this equation the parameters k and n have their usual significance and $t_{\frac{1}{2}}$ is the half-time of the rate process equivalent to the light depolarization change. On the basis of these calculations isotactic polypropylene has a maximum crystallization rate in the region of 60° to 70°C which means that this polymer must crystallize at an appreciable rate at room temperature. The maximum in the rate curve has its origin in classical theory⁶ and arises because of competing factors contributing to the crystallization process. The effect of viscosity becomes increasingly important exerting a retarding and finally a controlling influence over the growth of crystallizing birefringent structures as the temperature is lowered. To date, no other experimental technique has given any indication of the position of this maximum rate although its existence has been postulated³.

Other workers² have found that when their rate data are analysed according to the relationship

$$\log k = A - (B/T) - (C/T)(T_m/\Delta T)^2$$

(where T , T_m and ΔT are respectively the crystallization temperature, thermodynamic melting point and supercooling; A , B and C are parameters peculiar to the given polymer) positive deviations of the rate measurements occur at the higher crystallization temperatures ($> 135^\circ\text{C}$). The higher values of the measured over the calculated rates can be explained by impurities associated with the high ash content of isotactic polypropylene. Any increase in the number of nucleation sites will accelerate the overall crystallization rate⁷. Such effects will be more obvious the higher the crystallization temperature as found experimentally.

The morphological transition temperature

An analysis of induction times interpolated from the I/t curves of *Figure 1* shows that the change in mechanism of crystal growth occurs about 115°C. The change in shape of the normalized isothermals (*Figure 3*) together with the microscopical examination of the texture of samples crystallized at temperatures around 115°C are in agreement with the conclusion of the induction time experiments. Isothermal crystallizations carried out on the Köfler hot stage will differ slightly from those made in silicone oil baths⁴ because of different equilibration rates at lower crystallization temperatures. However, this difference is not more than a few

degrees centigrade in the transition region. The minor disagreement between the 115°C found in this investigation and the results of earlier workers^{4, 5} may also arise because of differences on the degrees of polymerization of the samples and conditions of fusion¹².

Thanks are due to Dr T. C. Tranter for the X-ray diffraction measurements and to Mr C. Mumford for assistance with the experimental work.

*Research Department,
British Nylon Spinners Ltd,
Pontypool, Mon.*

(Received August 1961)

REFERENCES

- ¹ VON FALKAI, B. and STUART, H. A. *Kolloidzshr.* 1959, **162**, 138
- ² MARKER, L., HAY, P. M., TILLEY, G. P., EARLY, R. M. and SWEETING, O. J. *J. Polym. Sci.* 1959, **38**, 33
- ³ GRIFFITH, J. H. and RÄNBY, B. G. *J. Polym. Sci.* 1959, **38**, 107
- ⁴ DYER, J. Unpublished work
- ⁵ PADDEN, F. J., Jr and KEITH, H. D. *J. appl. Phys.* 1959, **30**, 1479
- ⁶ MANDELKERN, L. *Chem. Rev.* 1956, **56**, 903
- ⁷ FLORY, P. J. and McINTYRE, A. D. *J. Polym. Sci.* 1955, **18**, 592
- ⁸ KANTROVITZ, A. *J. chem. Phys.* 1951, **19**, 1097
- ⁹ MAGILL, J. H. *Polymer, Lond.* 1961, **2**, 221
- ¹⁰ MAGILL, J. H. *Nature, Lond.* 1961, **191**, 1092
- ¹¹ MAGILL, J. H. *Nature, Lond.* 1960, **187**, 770
- ¹² HARTLEY, F. D., LORD, F. W. and MORGAN, L. B. *International Symposium on Macromolecular Chemistry*, p 577. Milano-Torino, September-October 1954
- ¹³ MORGAN, L. B. *Phil. Trans. A*, 1954, **247**, 13
- ¹⁴ HOCK, C. W. and ARBOGAST, J. F. *Analyt. Chem.* 1961, **33**, No. 3, 462

Melting Behaviour and Spherulitic Crystallization of Polycaproamide (Nylon 6)

J. H. MAGILL

The effect of fusion conditions, moisture and polymer relative viscosity on the crystallization behaviour of nylon 6 polymer has been obtained from induction time measurements which reflect the rate of appearance of birefringent structures during isothermal crystallization. These results are discussed in relation to other relevant data on 'order in polyamide melts'. Brief mention is also made of the morphology of nylon 6 spherulitic structures.

DURING the past decade considerable attention has been focused on crystallization processes in high polymers suitable for extrusion and/or moulding purposes. Until recently, however, there was a dearth of literature information especially for those polymers of technological interest in the polyamide field. The influence of important factors such as melt conditions, adventitious impurities, 'crystallite' stability and molecular weight are not completely understood even though these factors have profound effects on crystallization behaviour and subsequent polymer texture and properties.

The measurement of induction times (τ) for crystallization is a simple technique which can be used to study the influence of melt temperature and melt time on the crystallization behaviour and morphology of polymers^{1, 2}. The value obtained for τ depends on the sensitivity of the experimental method for the detection of crystallinity. For microscope methods it is that period which elapses between cooling the polymer melt film to the crystallization temperature and the first observation of a birefringent sheaf when the specimen is viewed between crossed polars.

For a given experimental technique, factors which influence τ will also affect the half-time of crystallization and hence the crystallization rate constant. McIntyre³ has shown that the limit of the microscope method for studying spherulitic formation occurs at a time corresponding to about five per cent of the total dilatometric change occurring at the same crystallization temperature.

Kantrovitz⁴ on theoretical grounds predicts that the incubation time, for the development of spherical nuclei in a condensed system, varies inversely as $(\Delta T)^4$, where ΔT is the extent of the supercooling. More generally, induction time = $k(\Delta T)^{-n}$ where k and n are constants.

EXPERIMENTAL

Materials

The polymers used were unstabilized commercial and laboratory preparations. They were initially free from lactam, contained no titanium dioxide and had the average chain length characteristics shown in *Table 1*.

Table 1

| | | | | |
|--------------------|--------|--------|--------|--------|
| Relative viscosity | 9.3 | 16.1 | 45.6 | 51.9 |
| M_n ~ | 5 000 | 9 180 | 17 900 | 19 300 |
| Relative viscosity | 70.8 | 73.0 | 81.0 | 100 |
| M_n ~ | 24 100 | 24 700 | 26 000 | 29 000 |

Relative viscosity (RV) measurements were made on 8.4 per cent (w/w) polymer in 90 per cent formic acid solution.

With the exception of the RV/τ measurements, the polymer used in the other experiments was RV 70.8 which had a previous known melt history. It had an optical melting of 226°C.

Temperature control

The melt bath temperature was controlled to $\pm 0.5^\circ\text{C}$ using a Sunvic Control Type TS1. The crystallization bath was kept to $\pm 0.2^\circ\text{C}$ using a mercury regulator with a Sunvic electronic controller Type EA3 and proportionating head. The thermometers were calibrated against Baird and Tatlock N.P.L. standardized thermometers.

Method

Cross sections of polymer chip, 50μ thickness, were mounted between cover slips using MS. 550 silicone oil. After a specified time in the melt bath they were rapidly transferred (< 1 sec) to the crystallization bath for the required crystallization period after which the samples were quickly quenched in acetone-solid carbon dioxide at -65°C . In this way the crystallization was arrested and the induction time was ascertained by microscope examination between crossed polars (at $\times 340$). The induction time was taken as the crystallization time required just to produce a birefringent sheaf in the quenched sample. The measurements were repeated two or more times for each set of experimental conditions.

A similar experimental procedure was used for polymer sections dried at 160°C for 3 h at 10^{-3} mm of mercury pressure. These specimens were stored over phosphorus pentoxide and later mounted between cover slips using dried MS. 550 silicone oil when required.

All induction time results are accurate to about ± 10 per cent.

RESULTS

Effect of melt temperature on induction time

Figure 1 shows the dependence of induction time of crystallization on crystallization temperature and illustrates the effect of melt temperature, for 30 minutes melt time, on the value of τ for various crystallization temperatures in the range 170° to 210°C .

When these results are plotted in the form $\log \tau$ versus $\log (\Delta T)$ (Figure 2) a transition is noted in the region of 190°C for the higher melt temperatures. Above this temperature the slope n is 7; below it $n=3$. This transition temperature moves to higher values as the melt temperature is lowered towards the optical melting point. At crystallization temperatures on the

MELTING BEHAVIOUR AND CRYSTALLIZATION OF POLYCAPROAMIDE

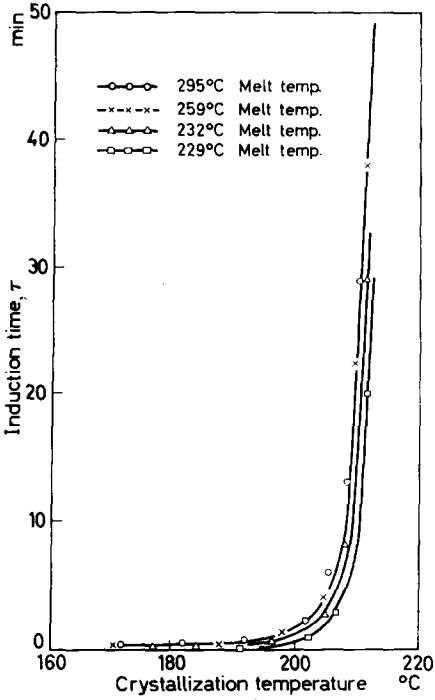
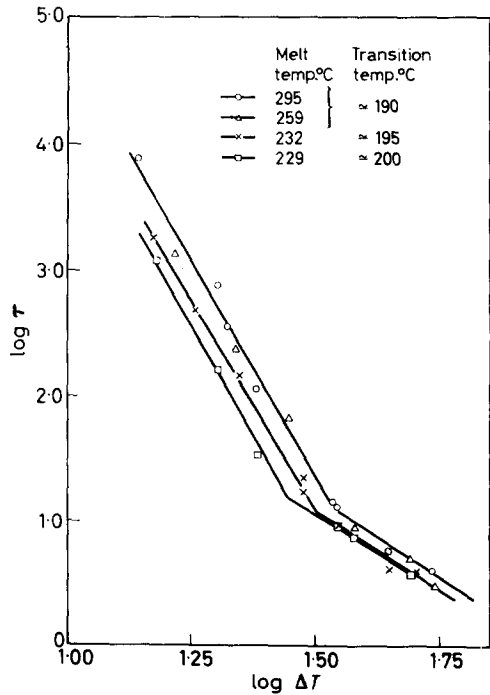


Figure 1—Dependence of induction time of crystallization of nylon 6 on crystallization temperature for various melt temperatures

Figure 2—Log (induction time) versus log (supercooling) for various melt and crystallization temperatures



higher side of this observed transition, nucleation of spherulites is sporadic in time; below it, the spherulitic nucleation is simultaneous or predetermined in time. This change in mechanism was verified by microscope observation of crystallized films.

Influence of melt time on induction time of crystallization

Figure 3 illustrates the dependence of τ on melt time (minutes), for a

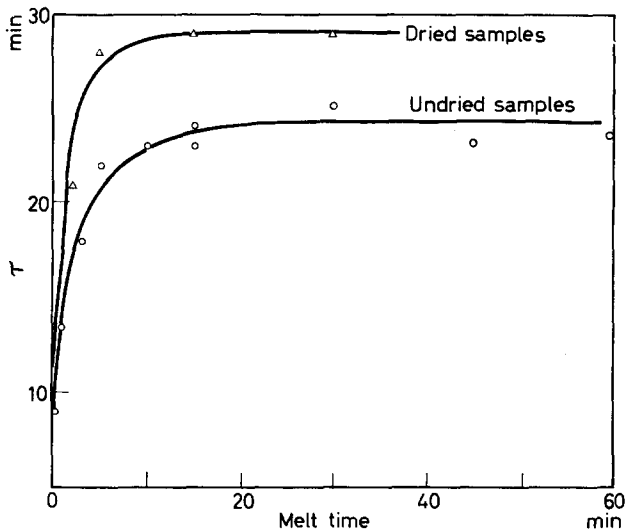


Figure 3—Induction time versus melt time plots for unstabilized nylon 6 polymer (dried and undried) for crystallization at 211°C (melt temperature 259°C)

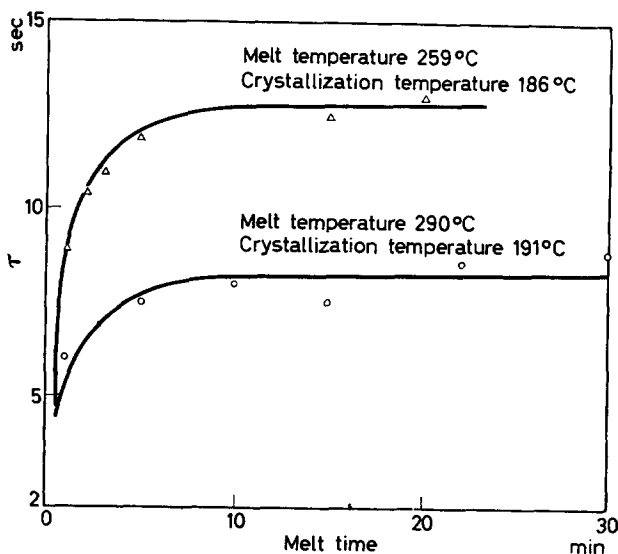


Figure 4—Induction time versus melt time plots for unstabilized nylon 6 polymer

crystallization temperature where the growth occurs from sporadically formed nuclei. A similar trend is shown in *Figure 4* where the nucleation is simultaneous in nature.

Influence of moisture and melt time on τ

The τ /melt time relationships for both dried and undried polymer sections are illustrated in *Figure 3*. All samples were crystallized at 211°C after fusion at 259°C.

When undried spherulitic samples were placed in the crystallization bath at 210°C and upwards, the positively birefringent spherulites were readily transformed, within 5 to 10 sec, to a granular highly birefringent matrix not unlike that associated with the formation of negative spherulites⁵ in nylon 6.6. If the samples and MS. 550 silicone oil are carefully dried beforehand, spherulites persist and the visual structure remains unchanged.

X-ray diffraction patterns (by Dr T. Tranter) of randomized samples treated in this way revealed that the crystalline perfection in the heated dried specimens was significantly higher than that in the heated undried samples. The unheated undried polymer (used as a control) showed a perfection similar to that of the heated dried material.

Dependence of induction time on relative viscosity

The RV/τ relationship for unstabilized nylon 6 (*Figure 5*) indicates a

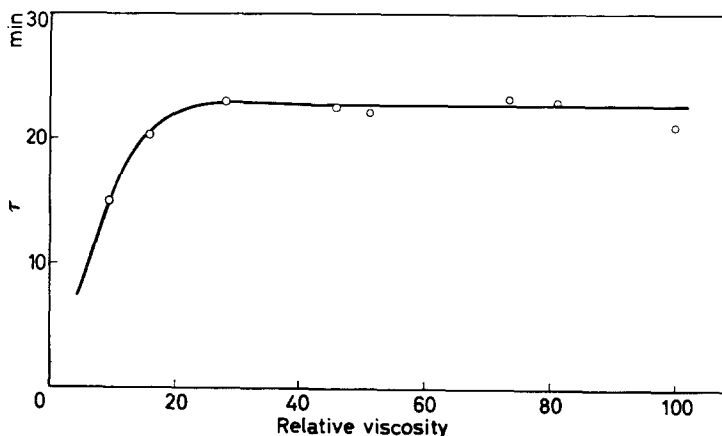


Figure 5— RV/τ relationship for unstabilized nylon 6 polymer (melt temperature 259°C, crystallization temperature 211°C)

distinct levelling off for the higher RV polymers for the range studied. This plot was obtained for the sporadic nucleation region (211°C), after melting at 259°C for 30 minutes. Under these fusion conditions the high RV polymers show a downward trend while the low RV polymers show an upward movement towards an equilibrium RV level commensurate with these fusion conditions. However, the RV changes involved on melting are not of sufficient magnitude to alter significantly the general trend observed in *Figure 5*.

Attempts to grow negatively birefringent spherulites

All attempts to grow negatively birefringent spherulites from crystallized samples containing positively birefringent spherulites failed. Experiments using melted films for crystallization temperatures in the same range, 205° to 225°C, have also proved unsuccessful, but birefringent entities of the type illustrated in *Figure 6* were obtained. In these structures the refractive index



Figure 6—Birefringent structures formed at 218°C.
Magnification $\times 300$: reduced 8/10 on reproduction

for light polarized parallel to the smaller dimension of these 'arc-like' structures is greater than that polarized at right angles to this direction.

DISCUSSION

Effect of fusion conditions on course of crystallization

Figure 1 shows an enormous temperature dependence of the induction time for the higher crystallization temperatures where nucleation is sporadic. For a particular melt temperature this dependence is considerably less pronounced at lower crystallization temperatures where the nucleation process is simultaneous (verified by microscope examination). The induction time versus melt temperature relationships indicate that after 30 minutes fusion at temperatures above 260° 'melting' is substantially completed. Below about 260°C there is a definite dependence of the nucleation rate on melt conditions. The induction time decreases in magnitude and the incidence of nuclei increases as the fusion temperature is lowered. The marked dependence of morphological structures on experimental melt conditions have also been found by Heckelhammer⁸ but the results are not detailed.

Increasing the fusion temperature results in a lowering of the temperature of the transition from predetermined to sporadic nucleation^{7, 8}. For nylon 6

this behaviour is reflected in the change of slope in *Figure 2*. The experimentally determined value of 7 for sporadic nucleation is not in agreement with the theoretical estimate of 4 for spherical nuclei⁴. According to Mandelkern *et al.*¹⁰ this apparent discrepancy is explicable on the basis that the measured induction time cannot be identified with the incubation period necessary to produce stable nuclei. However, a relationship between the two quantities is likely to exist and the substitution of the measured induction time for the incubation period does indicate that lowering of the fusion temperature is accompanied by an increase in the temperature of the transition from sporadic to simultaneous or non-random nuclei formation. This treatment of results is also helpful in depicting changes in the mechanism of nucleation and gives answers in substantial agreement with microscope observations on crystallized structures obtained at the same crystallization temperatures.

The position of the transition temperature in the above analysis is dependent on the value for the thermodynamic melting point T_m , assigned to the polymer. The value of 226°C used in this work is in reasonable agreement with that determined elsewhere¹¹⁻¹³.

Influence of melt time on course of crystallization

The results in *Figure 1* refer to melt times of 30 minutes but shorter melt times are important and can give rise to heterogeneous nucleation. *Figures 3* and *4* show the induction time versus melt time relationships corresponding to sporadic (211°C) and simultaneous (186°C) nucleation respectively. As expected, there is a considerable difference in magnitude of the τ values for these two temperatures, but the trend in τ is the same in both instances. It is only after melt periods of some five minutes that τ becomes insensitive to the time of melting and that such conditions of fusion are conducive to homogeneous nucleation. On the basis of these results, the heterogeneous nucleation noted by Burnett and McDevit¹¹ in their study of the kinetics of spherulitic growth is immediately explicable since they only melted their samples at 300°C for 30 seconds.

Influence of moisture on nylon 6 crystallization

Moisture is a prime factor affecting the crystallization behaviour of condensation polymers and recently considerable attention has been devoted to transition and crystallization phenomena in polyamides¹³⁻¹⁵. The onset of nucleation in primary spherulitic crystallization from the melt is accelerated by moisture as shown in *Figure 3*. The unpublished results of McLaren and Palmer¹⁶ on the kinetics of spherulitic crystallization in polyhexamethylene adipamide show a similar trend.

Secondary crystallization processes and molecular re-arrangements in these polyamides are also facilitated by moisture^{14, 17, 18}. Annealing in water promotes the crystal transition which occurs in the crystalline state¹⁴. In the present work moisture has been found to accelerate the rate of secondary processes in films of quenched nylon 6.

On the contrary, rapid heating of undried crystalline spherulitic samples of nylon 6 involves the fast effusion of moisture from within the structures and causes disordering on the macroscale (disruption of spherulites) and

microscale (decreases in crystalline perfection). Such a process has not been mentioned previously in the literature.

Effect of molecular weight on induction time for crystallization

The \bar{M}_n or RV/τ relationship for nylon 6 polymer (Figure 5) shows a similar trend to that noted earlier for 6.6 nylon¹. For crystallization at equal degrees of supercooling, limiting τ values are reached at \bar{M}_n s of 11 500 and 13 000 for nylon 6 and 6.6 polymers respectively.

Spherulitic growth rate dependence on molecular weight has been noted for polyamides^{11, 16, 19}. In these polymers, measurements cannot be made on narrow molecular weight fractions because of segment interchange and the re-equilibration processes which occur in the melt. For this reason, results can only be correlated with corresponding \bar{M}_n , relative viscosity or melt viscosity data. The viscosity of the respective supercooled polymer melts will assume a very important role at low crystallization temperatures. Strong amide-amide dipole interactions will also exert a controlling influence over the configurations adopted by molecules in the melt prior to the onset of crystallization^{20, 21}.

Morphology of nylon 6 spherulites

All known experiments in the literature^{11, 30, 31} and in this work show that only positively birefringent spherulites are found in the crystallization of nylon 6.

Order in polyamide melts

An analysis of viscosity data of melts of non-polymeric hydrocarbon molecules^{22, 23} suggests that cybotactic groups or clusters persist far above the melting point in the molten state. Although a wide variety of states of aggregation is possible only a limited number will be conducive to crystal formation. For unbranched chain substances such as paraffins and polymers, crystallization is facilitated by the segmental behaviour of the molecules.

The application of numerous techniques has been instrumental in acquiring information about both solid and liquid phases in polyamides^{12, 20, 21, 24, 25}. The magnitude of the volume change on fusion or crystallization of polymers²⁶ (ca. 10 to 15 per cent) suggests that molecular configurations in the solid cannot be greatly extended in the liquid phase. Furthermore, that crystalline platelets having the optical and structural properties of single crystals have been grown directly from the melts of several polyamides²⁷ gives further support to this concept.

Although the origin of the nucleation process in the formation of spherulites is not clearly understood, it is believed to stem from suitable molecular orientations prevalent in the melt. It is conceivable that this order will be reflected in the incubation times for crystallization or in the observed τ results.

It would appear that the now discarded theories of Tammann²⁸, revised by Morgan⁹ and by Stuart²⁹, on the persistence of some states of aggregation in the melts, should be re-introduced to explain the intricate behaviour of these polyamides in the liquid and supercooled states. Such order will have its origin in molecular chain folding or coiling as well as in chain alignment in melts of nylon 6 and 6.6.

MELTING BEHAVIOUR AND CRYSTALLIZATION OF POLYCAPROAMIDE

Elucidation of the more precise nature of this state of aggregation may come from a study of the melt using X-ray diffraction techniques.

The author thanks Mr C. Mumford and Mr J. A. Nixon for assistance with the experimental details. He is also indebted to colleagues at British Nylon Spinners Limited for helpful discussion.

Research Department,
British Nylon Spinners Ltd,
Pontypool, Mon.

(Received September 1961)

REFERENCES

- ¹ McLAREN, J. V. Unpublished work
- ² MAGILL, J. H. In course of publication
- ³ McINTYRE, A. D. *Ph.D. Thesis*. Cornell University, 1956. University Microfilm No. 16 256
- ⁴ KANTROVITZ, A. *J. chem. Phys.* 1951, **19**, 1097
- ⁵ KHOURY, F. J. *Polym. Sci.* 1958, **33**, 389
- ⁶ HECKELHAMMER, W. *Kunststoffe*, 1955, **45** (10), 414
- ⁷ HARTLEY, F. D., LORD, F. W. and MORGAN, L. B. *Symposium on Macromolecular Chemistry*, p 577. Milan-Turin, September-October 1954
- ⁸ ALLEN, P. W. *Trans. Faraday Soc.* 1952, **48**, 1178
- ⁹ MORGAN, L. B. *Phil. Trans. A*, 1954, **247**, 13
- ¹⁰ MANDELKERN, L., QUINN, F. A. and FLORY, P. J. *J. appl. Phys.* 1954, **25**, 830
- ¹¹ BURNETT, B. B. and McDEVIT, W. F. *J. appl. Phys.* 1957, **28**, 1101
- ¹² DOLE, M. and WUNDERLICH, B. *Makromol. Chem.* 1959, **34**, 29
- ¹³ HENDUS, H., SCHMIEDER, K., SCHNELL, G. and WOLF, K. A. 'Molecular arrangement in polycaprolactam' (from B.A.S.F. volume, prepared in honour of 60th birthday of their President, pp 291-319)
- ¹⁴ DECHANT, J. *Faserforschung u. Textiltechnik*, 1955, **6** (9), 422
- ¹⁵ ZIABICKI, A. *Kolloidzshr.* 1959, **167**(2), 132
- ¹⁶ McLAREN, J. V. and PALMER, H. J. Unpublished work
- ¹⁷ FRUNZE, T. M., KORSHAK, V. V. and MAKANKIN, V. A. *High Molecular Weight Compounds*, 1959, **1**, 342
- ¹⁸ CANNON, C. G. and CHAPPELL, F. P. Unpublished work
- ¹⁹ LINDEGREN, C. R. *J. Polym. Sci.* 1961, **50**, 181
- ²⁰ TRIFAN, D. S. and TEREZI, J. F. *J. Polym. Sci.* 1958, **28**, 443
- ²¹ CANNON, C. G. *Spectrochim. Acta*, 1960, **16**, 302
- ²² MAGILL, J. H. and UBBELOHDE, A. R. *Trans. Faraday Soc.* 1958, **54**, 1811
- ²³ McLAUGHLIN, E. and UBBELOHDE, A. R. *Trans. Faraday Soc.* 1958, **54**, 1804
- ²⁴ SLICHTER, W. A. *J. Polym. Sci.* 1959, **36**, 259
- ²⁵ HYBART, F. J. and WHITE, T. R. *J. appl. Polym. Sci.* 1960, **3**, 118
- ²⁶ MANDELKERN, L. *Chem. Rev.* 1956, **56**, 903
- ²⁷ MAGILL, J. H. and HARRIS, P. H. To be published
- ²⁸ TAMMANN, G. *The States of Aggregation*. Constable: London, 1926
- ²⁹ STUART, H. A. *Kolloidzshr.* 1959, **165**, 3
- ³⁰ HARRIS, P. H. and MAGILL, J. H. *J. Polym. Sci.* 1961, **54**, S47
- ³¹ MASUZAWA, K. *Kobunshi Kagaku*, 1958, **15**, 14

Thermodynamic Properties of Dilute Solutions of Polymethyl Methacrylate in Butanone and in Nitroethane

EDWARD F. CASASSA* and WALTER H. STOCKMAYER†

Solutions of methyl methacrylate polymers, fractionated and unfractionated, in the two good solvents butanone and nitroethane have been studied by light scattering. The experimental molecular weight dependence of the second virial coefficient A_2 is compared in considerable detail with theoretical treatments. A rough qualitative test is also obtained of a relation between the second coefficient and the third. Ternary systems composed of two polymer fractions of far different molecular weight in butanone do not show a maximum in the second coefficient as a function of solute composition—a result contrary to the prediction of the only pertinent theory.

DURING the last two decades much effort has been devoted to the development of a quantitatively adequate statistical mechanical theory of the large deviations found in polymer solutions from the ideal thermodynamic behaviour represented by Raoult's law. Despite the considerable successes achieved by the lattice theory of Flory¹ and of Huggins², by treatments based on molecular distribution functions³, and by various combinations, refinements, and simplifications of both approaches, the inherent complexity of the problem has so far prevented the achievement of a rigorous and complete treatment for sufficiently detailed models. For this reason, the comparison of theory and experiment is still a matter of importance in appraising the adequacy of approximations made in the various derivations.

In this paper we describe a study by the light scattering method of the thermodynamic properties of dilute poly-(methyl methacrylate)—PMMA—solutions in two good solvents, butanone and nitroethane. Specifically, we have measured the second and third virial coefficients for a number of fractionated and unfractionated polymers covering a hundredfold molecular weight range. In addition we have determined the dependence of the second coefficient upon composition for a heterogeneous solute obtained by mixing in various proportions two polymer fractions of widely differing molecular weights.

MATERIALS, APPARATUS, AND EXPERIMENTAL PROCEDURES

Polymers

The methyl methacrylate polymers used in this work were of diverse origins identified as follows: (a) Polymers 5, 7, 8 from the Rohm and Haas Co., unfractionated high conversion products prepared with a chain transfer

*Present address: Mellon Institute, Pittsburgh, Pennsylvania, U.S.A.

†Present address: Dartmouth College, Hanover, New Hampshire, U.S.A.

agent; (b) Fractions 2-3, 9-3, separated by conventional precipitation techniques from other members of the series of Rohm and Haas polymers and supplied to us by the M.I.T. Plastics Laboratory; (c) Sharpened fractions 2-3S, 5-3S, 5-5S, prepared by us from fractions of series (b) by fractional precipitation with hexane or methanol from butanone solutions, the upper and lower ends of the distribution being rejected; (d) Polymer D, unfractionated high conversion polymer from E. I. du Pont de Nemours and Co., prepared by 'pearl polymerization' with lauryl mercaptan as a chain transfer agent; (e) Polymers I, II, III, unfractionated, low conversion (9 to 12 per cent) polymers prepared by us with lauryl mercaptan.

Solvents

Butanone and nitroethane were obtained in the purest grades commercially available. Both solvents were dried and distilled before use. The butanone boiled at 80°C and the nitroethane at 112° to 114°C. Butanone was stored in the dark at about 5°C until used since samples left on the laboratory shelves developed a slight yellow colour and fluoresced red upon irradiation with green light.

The photometer

Since the light scattering photometer used in this work was closely modelled after a design published by Zimm⁴; it is only necessary to mention a few modifications made by Stanley⁵. As in Zimm's apparatus, the light source was a mercury arc operated from a 60 c/s a.c. source. Scattered light was detected by a photomultiplier tube (1P21), and a portion of the incident beam, by an ordinary phototube (929). The two photocurrents, necessarily consisting of 120 c/s pulses from the mode of operation of the arc, were compared in a potentiometer circuit, and the out-of-balance current was amplified by a tuned a.c. amplifier and then registered by a suitable null detector. The 'magic eye' valve originally specified as the null detector was, however, found to be much too insensitive and was replaced by an oscilloscope. With this change it became evident that because of capacitance effects in leads, the two photocurrents were not combined exactly out of phase in the potentiometer and a null reading was not obtained. A phase shifting network was therefore incorporated into the circuit and adjusted to make a true balance possible.

The conical sample cell used by Zimm was replaced by a similar but much larger one of about 25 ml capacity. The advantage of this cell lay in the fact that the photomultiplier could view scattering only from an illuminated volume at the centre of the cell, to the exclusion of light refracted from the glass surfaces as the beam entered and left the cell. The outer jacket containing thermostating fluid surrounding the cell, which was also of conical form in Zimm's design, was replaced with a crystallizing dish. The cylindrical symmetry of this new arrangement eliminated downward refraction of the incident beam in passing through the thermostat and cell and thus obviated the need for a prism to keep the beam direction horizontal.

Preparation of solutions

The ordinary procedure in making light scattering measurements was to use a series of five solutions increasing in concentration by factors of about

two, with the most dilute chosen to have a turbidity roughly double that of the solvent alone.

The essential removal of dust from polymer solutions and solvent was accomplished by filtration under nitrogen pressure through an 'ultra-fine' sintered glass filter, directly into a light scattering cell, which had previously been thoroughly rinsed with portions of the same solution. There was no evidence, even for the polymer of highest molecular weight, that solution concentration was changed by the filtration: after repeated filtration the turbidity of the solution had not decreased, and the filter showed no sign of plugging.

Light scattering measurements

All light scattering determinations were made at $25^\circ \pm 0.5^\circ\text{C}$ with unpolarized 5461 Å light. Since solvent and solutions were all run at the same time, six cells were needed. Before use, cells were checked by measuring the fluorescence scattering from fluorescein solutions in order to ensure that all were optically equivalent and did not have flaws producing spurious asymmetry in the angular dependence of scattered intensity.

In order to compensate for drifts in signal intensity, measurements were always carried out by a method of repeated comparison between samples or between a sample and a standard. Measurements repeated on three successive days, with one series of polymer solutions, showed that the relative scattering determined in this way at the 90° angle on the same solution in the same cell could be reproduced to at least ± 0.25 per cent over the range of turbidities encountered in this work. At angles of 45° and 135° precision was somewhat lower, presumably owing to greater and more erratic contributions from stray light; but it appears that the dissymmetry, the ratio of 45° to 135° scattering, could ordinarily be reproduced with an error of one per cent at most.

Since the photometer does not measure absolute light intensity directly, it is necessary to compare unknown solutions with a standard. For this purpose purified dust-free benzene in a sealed cell was used; and its scattering power at right angles to the incident beam (Rayleigh's ratio) was assumed to be 16.3×10^{-6} , the value determined by Carr and Zimm⁶. In treating data, solvent scattering was always subtracted from the solution scattering; thus the effects, presumed constant, of stray light were automatically eliminated. With the turbidity standard, however, for which the total intensity was required, an estimate of stray light had to be made. By comparing the apparent ratio of transverse scattering from water and from benzene with the correct value, assumed to be 0.054, it was determined that 4.06 per cent of the total measured intensity from benzene was due to stray light.

In principle, data must also be corrected for the depolarization of scattered light induced by the anisotropic polarizability characteristic of most molecules. Appreciable depolarizations were found in this work; but an analysis of the geometry of the photometer optical system and comparison of the observed depolarization of benzene with the published values indicated that the effect was entirely spurious, arising largely from the slightly divergent form of the incident beam. Consequently no correction

was required. It seems likely that the depolarization is similarly negligible for most polymers; hence the all too common uncritical application of corrections for measured depolarization probably introduces much larger errors in measured molecular weights than would the complete neglect of the effect.

Finally, two other sources of experimental error that were also taken into account must be mentioned. The photomultiplier was found to be more sensitive to horizontally than to vertically polarized light by a factor of 1.025 at 5461 Å. This fact introduces a small error in the comparison of the scarcely depolarized scattering at right angles due to the polymer solution with the scattering of benzene, which shows a larger depolarization effect. Another source of difficulty in the comparison of solutions with the standard lies in the fact that benzene has a considerably higher refractive index than the polymer solutions studied in this work. Since the cell and the liquid filling the thermostat around it act as a lens, the illuminated volume observed by the photomultiplier depends on the refractive indices of the sample and of the outer bath. Moore⁷ has worked out the correction to be made when the thermostat fluid has a refractive index of about 1.4 (a value close enough to the indices of butanone and ethyl acetate, the liquids actually used). Because the incident beam leaving the sample cell was intercepted by a piece of absorbing glass immersed in the thermostat liquid, no correction was required for the effect of the considerable back-reflection of light from a glass/air interface⁸.

Refractive index increment

The refractive index increment (the derivative of refractive index with respect to solute concentration) was determined by comparison of solutions with solvent in a Brice-Phoenix differential refractometer^{9,10}. Measurements made with polymer concentrations of about 0.01 and 0.02 g ml⁻¹ indicated, as expected, a value independent of concentration. For the PMMA-butanone system an average of several determinations gave 0.111 ml g⁻¹ at 25°C for the green line of the mercury arc, 5461 Å, with uncertainty estimated at no more than ±0.002. The same refractive increment was found by Cohn and Schuele¹¹ under identical conditions and by Bischoff and Desreux¹² at 28°C and 4880 Å. A value of 0.109 at the same temperature and 5461 Å, apparently in agreement within experimental uncertainty, was determined by Jose and Biswas¹³. A few other values both somewhat higher and lower have also been reported¹³. A result of Bhatnagar and Biswas¹⁴, lower by an order of magnitude, has now been explained by an experimental error¹³.

A refractive increment of 0.094 was used for solutions in nitroethane. This value was not determined independently but was chosen so as to make molecular weights of the polymers best agree in the two solvent systems.

Intrinsic viscosity

Values of the intrinsic viscosity of some of the polymers in nitroethane are cited below in *Table 2*. They were determined in conventional Ostwald-Fenske viscometers at 25.0°C. Kinetic energy corrections were applied.

The data for two fractions and six unfractionated polymers ranging in weight average molecular weight M_w from about 1×10^5 to 2×10^6 obey the relation

$$[\eta] = 5.70 \times 10^{-5} M_w^{0.74}$$

Two results at lower molecular weight indicate a smaller exponent. If this is assumed to become 0.50 in a sharp transition¹⁵⁻¹⁸ the critical point lies at a molecular weight of about 60 000.

DISCUSSION AND INTERPRETATION OF THE
EXPERIMENTS

Analysis of light scattering data

For the purposes of the present treatment we write the virial expansion of the equation of state relating to Rayleigh scattering from a solution of a heterogeneous solute in the form

$$\frac{Kc}{R(\theta)} = \frac{1}{\sum_i M_i P_i(\theta) w_i} + 2A_2 c + 3A_3 c^2 + \dots \quad (1)$$

$$A_2 = M_w^{-2} \sum_i \sum_j B_{ij} M_i M_j w_i w_j$$

$$K = 2\pi^2 n^2 (dn/dc)^2 / N\lambda^4$$

where M_i is the molecular weight of the polymer species i comprising a weight fraction w_i of the solute. The total polymer concentration c is in units of mass per unit solution volume. The excess scattering (reduced intensity for solution less contribution from solvent) at an angle θ from the direction of the incident beam is denoted by $R(\theta)$; and the intensity distribution normalized to unity at $\theta=0$, for an isolated molecule of species i is given by $P_i(\theta)$. The second and third terms of equation (1) in which we identify A_2 , A_3 with the second and third virial coefficients, respectively, are in general only approximate¹⁹, but become exact subject to either of the sufficient conditions that the dimensions of the solute molecule be small compared with the wavelength of light or that the angle θ approach zero. In the constant K , N is Avogadro's number; λ the wavelength of the incident light *in vacuo*; and n , the refractive index of the solution. The assumption is implicit that all solute species have the same refractive index increment dn/dc , an approximation certainly acceptable for high polymers differing only in molecular weight.

In this investigation, measurements of scattered radiation were made at only three angles: 45°, 90° and 135°. Since this information does not provide an adequate basis for completely empirical extrapolation of the data to $\theta=0$, the determination of the weight average molecular weight is probably best carried out with the aid of assumptions concerning the form of $P(\theta)$ and of the molecular weight distribution. We assume that $P(\theta)$ for each polymer species is given by²⁰

$$P(\theta) = 1 - \frac{1}{3}u + \frac{1}{15}u^2 + \dots$$

$$u = (16\pi^2 n^2 / \lambda^2) \langle s^2 \rangle \sin^2(\frac{1}{2}\theta)$$

which is the correct form for a strictly random-flight chain with mean square radius of gyration $\langle s^2 \rangle$. Integrating this $P(\theta)$ over an assumed

molecular weight distribution^{4, 21} such that the weight fraction of polymer of molecular weight in the range dM is given by

$$f(M) dM = \left(\frac{Z+1}{M_w}\right)^{Z+1} \frac{M^Z}{Z!} \exp[-(Z+1)M/M_w] dM \quad (2)$$

we obtain an averaged $P(\theta)$ at 90°

$$P_z^{-1}(90) = \left(\frac{1}{M_w} \int P(90) M f(M) dM\right)^{-1} \\ = 1 + \frac{q}{2 \cos \phi} + \frac{q^2}{2 \cos^2 \phi} \left[1 - \cos^2(\frac{1}{2}\phi) - \frac{Z-1}{8(Z+2)}\right] + \dots$$

where the dissymmetry $q+1$ is defined by

$$q+1 = [R(\phi)/R(\pi-\phi)]$$

with ϕ in this work always 45° . The parameter Z characterizes the dispersity of the molecular weight distribution. For $Z=1$ equation (2) reduces to the polyester type distribution¹, which also applies to vinyl polymerization at low degrees of conversion with termination by chain transfer to solvent²; while for $Z=\infty$, the polymer is homogeneous.

In treating experimental data, the series forms for Kc/R and P_z^{-1} were approximated by their first three terms:

$$\frac{Kc}{R(90)} = A_1 + 2A_2c + 3A_3c^2 \quad (3)$$

$$A_1^{-1} = P_z(90) M_w$$

$$P_1^{-1}(90) = 1 + 0.7071q + Aq^2 \quad (4)$$

where $A=0.146$ when $Z=1$; 0.075 when $Z=5$; and 0.038 when $Z=20$.

Table 1. Light scattering measurements for PMMA in butanone at 25°C

| Polymer code | $A_1 \times 10^6$ | $A_2 \times 10^6$ $ml\ g^{-2}$ | $A_3 \times 10^8$ $ml^2\ g^{-3}$ | $P_z^{-1}(90)$ | $M_w \times 10^{-5}$ | $A_2 M_w / [\eta]^*$ |
|-------------------------|-------------------|-----------------------------------|-------------------------------------|----------------|----------------------|----------------------|
| Unfractionated polymers | | | | | | |
| I | 48.5 | 4.02 | 1.4 | 1.00 | 0.206 | 95 |
| III | 24.4 | 3.78 | 1.3 | 1.00 | 0.411 | 108 |
| D | 7.67 | 2.39 | 1.9 | 1.04 | 1.36 | 96 |
| II | 4.42 | 2.22 | 2.8 | 1.06 | 2.41 | 104 |
| S | 2.77 | 2.09 | 2.4 | 1.16 | 4.19 | 115 |
| 7 | 1.71 | 1.77 | 2.9 | 1.27 | 7.42 | 114 |
| 8 | 0.963 | 1.39 | 6.1 | 1.67 | 17.3 | 114 |
| Fractions | | | | | | |
| 2-3 | 7.91 | 3.04 | — | 1.03 | 1.30 | 120 |
| 2-3 | 8.23 | 2.82 | 1.8 | 1.01 | 1.22 | 110 |
| 9-3 | 0.679 | 1.07 | 17 | 1.87 | 27.6 | 100 |
| 9-3 | 0.712 | 1.10 | 9.0 | 1.78 | 25.1 | 100 |
| Sharpened fractions | | | | | | |
| 2-3S | 7.38 | 2.83 | 1.7 | 1.01 | 1.37 | 114 |
| 5-5S | 5.06 | 1.98 | 2.2 | 1.02 | 2.02 | 89 |
| 5-3S | 2.13 | 1.57 | 8.6 | 1.15 | 5.37 | 92 |

*The intrinsic viscosity was calculated by equation (13).

Rather arbitrarily, these values of Z were assumed, respectively, for the unfractionated samples, for the ordinary fractions, and for the sharpened fractions. The experimental values of $c/R(90)$, obtained ordinarily at five different concentrations, were fitted by a quadratic expression in c . Since the least-squares method for determining the quadratic coefficients is laborious and, although completely objective, involves the arbitrary assumption of a normal distribution of errors, it seemed just as well to use the somewhat simpler trial and error procedure of adjusting parameters until no trend was discernible in a plot of the deviations from the trial function. Greater weight was given subjectively to data at the higher concentrations, in accordance with experimental precision. From the three parameters of the quadratic function, A_2 , A_3 and $M_w P_z(90)$ were obtained. The value of $P_z(90)$ at infinite dilution was determined by extrapolation of a plot of $1/q$ versus concentration to infinite dilution since this relation is nearly linear⁴.

Table 2. PMMA in nitroethane at 25°C

| Polymer code | $A_1 \times 10^6$ | $A_2 \times 10^4$ | $A_3 \times 10^3$ | $P_z^{-1}(90)$ | $M_w \times 10^{-5}$ | $[\eta]$ 100 ml g ⁻¹ | $\frac{A_2 M_w}{[\eta]}$ |
|--------------|-------------------|-------------------|-------------------|----------------|----------------------|------------------------------------|--------------------------|
| I | 45.4 | 5.51 | 2.4 | 1.00 | 0.220 | 0.116 | 104 |
| III | 24.8 | 4.38 | 3.2 | 1.01 | 0.410 | 0.170 | 106 |
| D | 7.44 | 3.09 | 3.9 | 1.05 | 1.42 | 0.379 | 116 |
| II | 4.28 | 2.72 | 6.7 | 1.05 | 2.45 | 0.573 | 116 |
| 7 | 1.79 | 2.05 | 10.1 | 1.28 | 7.16 | 1.28 | 115 |
| 8 | 1.04 | 1.68 | 14.7 | 1.78 | 17.1 | 2.39 | 120 |
| 2-3S | 9.09 | 3.38 | 3.9 | 1.04 | 1.14 | 0.322 | 120 |
| 5-3S | 2.06 | 1.73 | 18.8 | 1.16 | 5.64 | 1.06 | 92 |

The assumptions involved in equations (3) and (4), while not satisfactory generally, are completely acceptable if the dissymmetry is not too much greater than unity. For all the polymers studied here of molecular weight less than 10^6 , experimental errors are probably greater than any inaccuracy in these expressions. For the three polymers of highest molecular weight, the adequacy of the treatment may be less certain, but the conclusions to be drawn from the results could scarcely be changed. Furthermore, since the molecular weight distribution of the samples is not known, a more elaborate and more accurate treatment of the data does not appear worthwhile. The use of 90° measurements alone to determine A_2 seems justified since no significant difference was found when, with the highest molecular weight polymers, 45° measurements were tried instead. We have not calculated molecular radii of gyration from our angular scattering data since readings at many angles are needed to provide reliable values.

The second virial coefficient for fractionated and unfractionated polymers

Results obtained by the foregoing analysis are given in Tables 1 and 2, and the second virial coefficients are shown plotted in Figure 1.

For both butanone and nitroethane as solvents, the familiar decrease in A_2 with increasing molecular weight is apparent, the experimental results for unfractionated polymers in both cases being fairly well fitted by $A_2 \propto M^{-0.25}$. More precisely, least-squares fitting of the results for whole

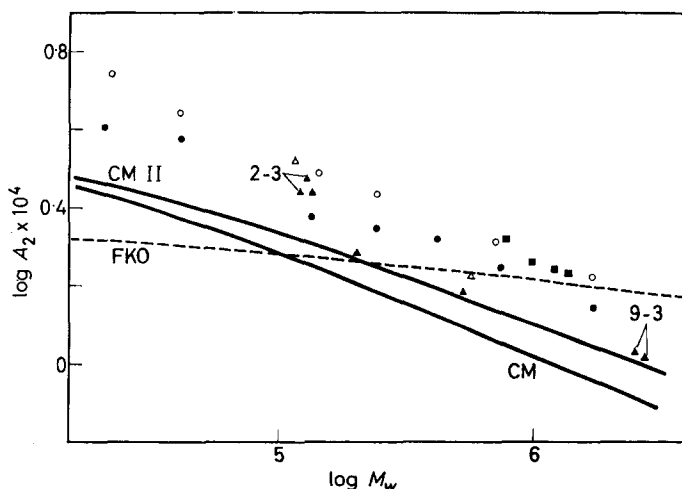


Figure 1—Second virial coefficient for polymethyl methacrylate in butanone ●▲ and in nitroethane ○△. Circles indicate whole polymers; triangles, fractions. Results of Bischoff and Desreux on four fractions in butanone ■. Computation of the three theoretical relations (for the butanone system) shown is described in the text: for the Flory-Krigbaum-Orofino (FKO) curve, f is unity; for the others, 0.4913. Duplicate measurements on fractions 2-3 and 9-3 are indicated

polymers in butanone gives an exponent of -0.242 and the corresponding value for nitroethane (with the point at lowest molecular weight not included) is -0.257 . Empirically an expression of this form has been found to hold in a variety of systems over a wide molecular weight range. The magnitude of the negative exponent parallels roughly the solvent power, and in the present cases is nearly as large as one ever finds. It appears qualitatively from Figure 1 that the apparently random errors are distinctly larger for solutions in butanone than for those in nitroethane and that the nine points for fractions follow a much more erratic course than do the results on whole polymers. The first effect may very well be due to absorption of small amounts of atmospheric moisture by butanone and the latter suggests that some of the fractionations may have given products of peculiar molecular weight distribution. It has been observed before that PMMA is difficult to fractionate effectively^{12, 17, 22, 23} and it has been suggested that incipient crystallization is responsible. It is even conceivable that fractionation may effect separation with regard to variation in stereospecific structure as well as in molecular weight. It definitely seems that the experimental uncertainties are larger than errors of measurement inherent in the apparatus and must reflect real differences in the solutions under study. It is not possible to conclude from the present data whether A_2 differs for fractions and whole polymers of the same weight average molecular weight; but if one speculates that fraction 2-3, and fraction 2-3S derived from it, are abnormal, the other fractions would appear to give lower values than the unfractionated samples. It should be recalled, however, that the second

virial coefficient from osmotic pressure for acetone solutions of PMMA has been found the same for fractions as for whole polymers at a given number average molecular weight¹⁶. We have also entered on *Figure 1*, four points obtained by Bischoff and Desreux¹² for high molecular weight PMMA fractions in butanone. These virial coefficients appear higher than ours, considerably so in comparison with our fractions of similar molecular weight.

Although comparison between experiments on unfractionated polymers and theoretical predictions for homogeneous species must be taken with considerable reserve, they are still of interest in view of the lack of an adequate treatment of the effect of a distribution in molecular weight. In *Figure 1* we show curves computed according to three theories: that of Flory and Krigbaum^{24, 25} as expressed in an approximate closed mathematical expression by Orofino and Flory²⁶ (FKO), a rather different development by Casassa and Markovitz (CM)²⁷, and a refinement of the latter method by Casassa (CMII)²⁷. All the theories in question give A_2 in the form

$$A_2 = YF(X) \quad (5)$$

The common 'single contact' factor Y , invariant to molecular weight but temperature dependent, is multiplied by a function F , which decreases monotonically from unity with increasing molecular weight to approach zero asymptotically. The theories are concerned essentially with the prediction of a form for F .

The parameters necessary for determining the theoretical curves exhibited in *Figure 1* were derived from viscosity measurements treated according to the method of Flory and Fox^{1, 29}. Specifically the characteristic temperature Θ and the entropy of mixing parameter ψ_1 (to use the symbolism adopted by these investigators) were obtained from viscosity/temperature data and the relation

$$\alpha^5 - \alpha^3 = 2C_m f \psi_1 (1 - \Theta/T) M^{1/2} \quad (6)$$

from Flory's theory^{1, 30} of chain configuration. The molecular expansion factor α at temperature T was found from

$$\alpha^3 = [\eta]/[\eta]_\theta \quad (7)$$

where $[\eta]_\theta$ represents the intrinsic viscosity in a solvent for which $\theta \approx T$. The molar volume of solvent and the partial specific volume of solute are denoted by V_1 and \bar{v} respectively. The constant C_m was also obtained from viscosity data and assumed to be independent of solvent, thus a quantity characteristic of the polymer and temperature. In the original derivations of Flory and Fox the factor f is always unity; but Stockmayer³¹ has more recently suggested on theoretical grounds that a value of 0.4913 should be preferred.

For PMMA in butanone, the actual numerical values we utilized are as given by Fox³²:

$$\begin{array}{lll} \Theta = 175^\circ \text{K} & f\psi_1 = 0.075 & C_m = 0.0457 \\ V_1 = 90 \text{ ml} & \bar{v} = 0.821 \text{ g ml}^{-1} & \end{array}$$

Curves are shown in *Figure 1* for this system only, since the necessary information does not exist for PMMA-nitroethane.

In terms of these thermodynamic and configurational constants, the single contact term in A_2 is written

$$Y = \psi_1 (1 - \Theta/T) (\bar{v}^2/V_1)$$

No additional information is needed for determining the function F . In the FKO treatment this is given by²⁶

$$F(X)_{\text{FKO}} \approx (4/\pi^{1/2}X) \ln(1 + \pi^{1/2}X/4) \quad (8)$$

where

$$X \equiv (4C_m\psi_1/\alpha^3) (1 - \Theta/T) M^{1/2} = (2/f) (\alpha^2 - 1) \quad (9)$$

the last equality implying acceptance of equation (6). Then with X related to M through α and equation (6), the same constants being used as in computing Y , one can evaluate A_2 according to equation (5). For the CM theory the procedure is the same except that now $F(X)$ is given by²⁷

$$F(X)_{\text{CM}} \approx [1 - \exp(-1.093X)]/1.093X \quad (10)$$

For statistical mechanical treatments, it is usually convenient and it has more or less become standard to use a variable z , which may be defined in terms of Flory's thermodynamic parameters by

$$z \equiv (4/3^{3/2}) C_m\psi_1 (1 - \Theta/T) M^{1/2}$$

hence

$$X = 3^{3/2}z/\alpha^3$$

In the CM II modification²⁷ of the CM theory, the function of equation (10) is retained but a different variable X' is introduced

$$X' = 1.507 (\alpha_2^2 - 1)$$

The expansion factor α_2 used here refers to a cluster of two interacting molecules and is related to the experimentally accessible quantity α by

$$\alpha^5 - \alpha^3 = (134/105)z$$

and

$$\alpha_2^5 - \alpha_2^3 = 2.043z$$

In this last derivation of the molecular weight dependent part of A_2 , the choice of $f=0.4913$ is implied; hence, for the sake of consistency, this value is used in calculating the other factor Y .

The FKO theory with $f=1$ predicts quite well the magnitude of A_2 but the slope is not negative enough. The FKO curve for $f=0.4913$, which we have not shown, would give a much less satisfactory result: a value of A_2 much too large at molecular weights above 50 000 with the slope only slightly improved. The CM theory, on the other hand, gives an A_2 decidedly too small but a molecular weight dependence which is fairly realistic for $f=0.4913$. The use of the larger f with this theory would worsen the agreement with experiment, giving A_2 smaller than that shown and a decrease with molecular weight somewhat too slow. The best representation is given by the CM II theory: the virial coefficient is still predicted to be too small, perhaps by some twenty per cent, but the molecular weight dependence is fairly well reproduced. Although we regard the fact as of little significance, this theory does agree almost precisely with the data

on the three fractions of highest molecular weight. Qualitatively our results are in agreement with findings reported on other good solvent systems studied osmotically: polystyrene in toluene^{27,28,33}, polyisobutene in cyclohexane^{27,28,33}, and PMMA in acetone¹⁶. Light scattering studies¹⁷ on the system last named have given results exhibiting the same general character. The major apparent defect of the FKO treatment is always the prediction of an insufficient molecular weight dependence while the CM and CMII theories give A_2 in some degree too small. Again, the FKO theory always gives reasonable results only with f as unity while the other treatments strongly favour 0.4913.

It should perhaps be emphasized that this agreement of theory with experiment, such as it is, has been obtained by methods completely independent of the thermodynamic measurements. No adjustable parameters have been introduced to impose agreement at any particular point. By inserting an arbitrary scale factor in equation (9), and thus requiring merely a proportionality between X and $\alpha^2 - 1$ in the FKO theory, it is sometimes possible to rectify the inadequate molecular weight dependence³³ of A_2 ; but for both the systems discussed here, this procedure would require very large, physically meaningless values of X . For the other theories, relatively modest adjustments of this kind would serve the purpose. Our method of deducing the theoretical A_2 is open to the objection that the results do depend on both the theory of intrinsic viscosity and on the configuration theory through equation (6) and therefore do not indicate unambiguously the adequacy of the various forms for F . The most questionable of our assumptions is perhaps the form of equation (6) linear in $M^{1/2}$, as in fact $(\alpha^5 - \alpha^3)/M^{1/2}$ is usually found to increase somewhat with M and perhaps to go through a maximum^{1,34,35}.

Although the theories examined above do not exhaust pertinent derivations concerning the second virial coefficient³⁶⁻⁴⁰; we choose to limit the present discussion to these possibilities except for a few comments *passim* on some of the others. Krigbaum *et al.*⁴⁰ have developed a theory capable of reproducing the full range of behaviour from the FKO theory to the CMII theory through variation of a parameter appearing in the molecular-weight dependent function in addition to X . Another of the thermodynamic theories, by Isihara and Koyama³⁷, is practically equivalent to the FKO treatment even though the formalism is quite different. Their replacement of a simple Gaussian segment density distribution about the molecular centre of mass by a more correct sum of Gaussians (one for each chain segment) makes only insignificant changes numerically over the normal range of physical applicability. A recent assertion⁴¹ that the Isihara-Koyama theory is in good accord with experimental data on PMMA in a number of solvents while the FKO theory fails by comparison, hangs upon two rather infelicitous assumptions: that f is best taken as 0.4913 in the FKO theory and that the variable X in the Isihara-Koyama theory is proportional to z rather than to z/α^3 as in the FKO treatment. It is quite true that the molecular expansion is not mentioned explicitly in the Isihara-Koyama derivation; but the logical necessity of including it implicitly has been pointed out⁴².

Recently Kurata, Stockmayer and Roig⁴³ have developed a new theory of chain configuration. Since they propose a different relation in place of equation (6) and a smaller exponent⁴² in equation (7), the evaluation of thermodynamic parameters from viscosity measurements would be affected although the structure of the FKO and CM theories would not be altered *per se*. On the other hand, in relating α_2 of the CM II theory to α , we did assume the form of equation (6).

In the final column of *Table 2* are shown values of the dimensionless ratio $A_2M_w/[\eta]$ for PMMA in nitroethane. If only the unfractionated polymers are considered, this quantity appears to be nearly constant, probably increasing slowly with molecular weight. Empirically, of course, this fact merely reflects the approximate dependence of A_2 and $[\eta]$ on $M^{-0.25}$ and $M^{0.75}$ respectively. It is interesting that constancy of this ratio would be predicted for the asymptotic behaviour of A_2 at high molecular weight according to all the theories discussed above and also to an earlier one developed by Flory³⁶ on the basis of a very simple model, a representation of a polymer molecule as a sphere containing chain segments uniformly distributed. In the CM theory, for example

$$F(X)_{\text{CM}} \sim 0.914/X = \frac{0.228\alpha^3}{C_m\psi_1(1-\Theta/T)M^{1/2}} \quad (11)$$

Then, with the relation

$$[\eta] = K_1M^{1/2}\alpha^3$$

and equation (5), this leads to

$$A_2M/[\eta] \sim 0.228\bar{v}^2/K_1C_mV_1 \quad (12)$$

a result which, it is to be noted, is not affected by uncertainty about the proper value of f in equation (6). The CM function F attains essentially asymptotic behaviour at rather small values of X —equation (11) is in error by less than two per cent for $X > 4$ —in contrast to the FKO function which attains a similar dependence only in a much higher range of the variable^{26, 27}.

Since we have made no intrinsic viscosity measurements in butanone on the polymers studied here, a direct determination of $A_2M_w/[\eta]$ cannot be presented. However, to calculate the values given in the last column of *Table 1*, we have used a relation (for fractions at 30°C) established by Cohn-Ginsberg *et al.*¹⁷

$$[\eta] = 6.83 \times 10^{-5}M^{0.72} \quad (13)$$

which agrees very well with other published work^{23, 44}. The results obviously resemble closely those for PMMA–nitroethane. Lest it be thought that these systems necessarily exhibit almost asymptotic behaviour, we note that putting K_1 from equation (13) into equation (12) gives $A_2M/[\eta] \sim 550$. The CM II theory requires merely the replacement of α^3 in equation (11) by $\alpha_2^3 \sim \alpha^3(1.60)^{0.6}$; hence the numerical constant in equation (12) is increased by a factor of 1.33. In the analogous form of the FKO theory the constant is also somewhat increased, by a similar factor 1.38.

The third virial coefficient

Empirical values of the coefficient A_3 , determined by fitting the quadratic expression, equation (3), to 90° light scattering data are shown in *Tables*

THERMODYNAMIC PROPERTIES OF POLYMETHYL METHACRYLATE

Table 3. The third virial coefficient

| Polymer | <i>g</i> in butanone | | <i>g</i> in nitroethane | |
|---------|----------------------|--------|-------------------------|--------|
| | Experiment | Theory | Experiment | Theory |
| I | 0.42 | 0.10 | 0.36 | 0.16 |
| III | 0.22 | 0.12 | 0.41 | 0.19 |
| D | 0.24 | 0.18 | 0.29 | 0.24 |
| II | 0.24 | 0.20 | 0.37 | 0.26 |
| 5 | 0.13 | 0.22 | | |
| 7 | 0.12 | 0.25 | 0.34 | 0.30 |
| 8 | 0.18 | 0.29 | 0.30 | 0.33 |
| 2-3 | 0.19 | 0.17 | | |
| 2-3S | 0.15 | 0.18 | 0.30 | 0.23 |
| 5-5S | 0.28 | 0.20 | | |
| 5-3S | 0.65 | 0.23 | 1.1 | 0.29 |
| 9-3 | 0.54 | 0.21 | | |
| 9-3 | 0.30 | 0.21 | | |

1 and 2. For comparison with theory an appropriate quantity is $g = A_3/A_2^2M$, which is listed in Table 3 for the polymer samples studied in this work. The theoretical values for butanone solutions were obtained from a relation between g and α developed by us⁴⁵ some years ago with α from equation (6) and the constants given by Fox³². The same method was used for the PMMA-nitroethane solutions except that the relation

$$\alpha^5 - \alpha^3 = 4.4 \times 10^{-3}M^{1/2}$$

for this system was derived from direct light scattering measurements of molecular radii of gyration by Moore⁷. Since this equation depends on but two somewhat discordant observations, it is to be regarded as only an approximation.

As an aid in extrapolating thermodynamic measurements to infinite dilution, Flory *et al.*^{25, 46} originally suggested that g be assigned the value 5/8, correct for hard sphere molecules. For 'soft' spheres, however, the ratio must be less than this. With the aid of a probably unrealistic but mathematically tractable intermolecular potential function and an approximate graphical method of matching its parameters to those of the Flory-Krigbaum model, we found g to increase slowly from zero for $\alpha=1$ to approach the asymptotic hard sphere value only for α of somewhat larger magnitude than one would expect to find even for very high molecular weight (uncharged) polymers in good solvents. Another theory by Koyama³⁸ gives practically indistinguishable results. The present experiments agree with the theory in indicating that the hard sphere model is altogether inadequate, but at low molecular weights the theoretical g seems too small. It must be remembered that this comparison is of necessity very crude: not only does the theory itself very obviously lack in rigour, but the apparent A_3 has been used without regard to the effects of a distribution of molecular weight, of dependence on scattering angle, and of the possible inadequacy of a virial expansion cut off at the c^2 term.

In fitting light scattering data for good solvents by a quadratic expression, as in equation (3), Flory¹ has proposed to set g equal to 1/3 as an improvement over the hard sphere value. If this arbitrary g is sufficiently accurate, a plot of $[Kc/R(\theta)]^{1/2}$ against c (with intercept $M^{-1/2}$ and slope

$A_2/[M^3P_z(\theta)]^{1/2}$ can be fitted by a linear relation to higher concentrations than can the more conventional plot with $Kc/R(\theta)$ as the ordinate. The present experimental results support this suggestion as a g of 1/3 appears to lie within the considerable experimental uncertainty in the majority of cases.

Mixtures of two fractions

Although a useful theoretical derivation of the second virial coefficient for heterogeneous polymers appears as a difficult (and still largely unrealized) task, the simplest example of a mixture of two polymer species differing only in molecular weight in a single solvent has been worked out for the FKO theory²⁵. The theory predicts, perhaps surprisingly, that under some conditions A_2 may pass through a maximum as the relative proportions of the two solute species are varied. (The rigorous statistical method of Zimm³, carried to the approximation of double intermolecular contacts, reveals no maximum in A_2 but the result is applicable only in the neighbourhood of the Θ point⁴⁷.) Considerable interest attaches, therefore, to evaluation of this aspect of the theory by comparison with experiment. Only a very few measurements on such mixtures have been reported: polyisobutene-cyclohexane and polystyrene-toluene systems investigated osmotically showed maxima as expected³³; but PMMA fractions in acetone, studied both by osmotic pressure and light scattering, yielded data, which on close analysis proved indecisive for assessing the reality of the predicted maximum^{48,49}. In the present study we have made measurements on three mixtures of

Table 4. Mixtures of fractions 2-3 and 9-3 in butanone

| w_4 | $A_1(90) \times 10^6$ | | $A_2(90) \times 10^4$ | $B_{24} \times 10^4$ |
|--------|-----------------------|--------------|-----------------------|----------------------|
| | <i>Expt</i> | <i>Calc.</i> | | |
| 0 | 8.07* | | 2.93* | |
| 0.0588 | 5.25 | 4.98 | 1.91 | 1.50 |
| 0.0597 | 4.91 | 4.95 | 2.09 | 1.90 |
| 0.177 | 2.88 | 2.81 | 1.47 | 1.68 |
| 1 | 0.696* | | 1.08* | |

*Averages from two determinations: see Table 1.

fractions 2-3 and 9-3 in butanone to obtain the results given in Table 4 and also presented graphically in Figure 2 together with theoretical relations, the evaluation of which is described below.

Before discussing our results, it is necessary to remark that the variation of apparent A_2 with scattering angle cannot generally be ignored if angular dissymmetry is large and the two polymer components are of widely different molecular weight. Denoting the lower molecular weight polymer by subscript 2 and the higher by subscript 4, we write

$$A_2(\theta) = \frac{B_{22}M_2^2P_2^2(\theta)w_2^2 + 2B_{24}M_2P_2(\theta)M_4P_4(\theta)w_2w_4 + B_{44}M_4^2P_4^2(\theta)w_4^2}{[M_2P_2(\theta)w_2 + M_4P_4(\theta)w_4]^2} \quad (14)$$

where w_2 and w_4 represent the weight fractions of components 2 and 4 in the solute so that $w_2 + w_4 = 1$. This relation is a generalization of the single contact approximation¹⁹ to a polymer mixture^{5,50}. The apparent virial coefficient $A_2(\theta)$ converges at $\theta=0$ to the purely thermodynamic expression for $A_2 = A_2(0)$ in a mixture of two solutes.

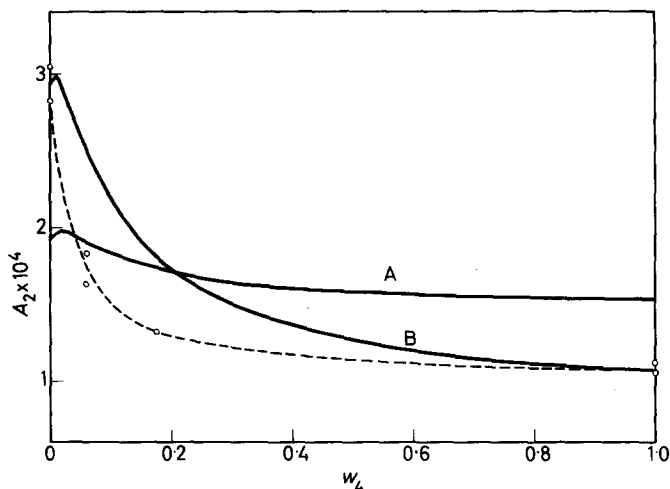


Figure 2—Second virial coefficient for mixtures of fractions 2-3 and 9-3 in butanone. Curve A is for the FKO theory with $f=1$; curve B for the same theory forced to fit the experimental data for the binary systems and with $f=0.4913$. The dashed line is determined by experimental parameters B_{22} , B_{24} , B_{44} , respectively 2.93×10^{-4} , 1.69×10^{-4} , 1.08×10^{-4}

The three coefficients B_{22} , B_{44} and B_{24} characterizing the thermodynamic interactions among components may be obtained from measurements with three solute compositions. Most simply, measurements on the two binary systems of polymers 2 and 4 in the solvent yield $M_2P_2(\theta)$, $M_4P_4(\theta)$, B_{22} and B_{44} , from intercepts and slopes of $Kc/R(\theta)$ versus c ; and then measurements on any one ternary system give the remaining unknown, the cross-coefficient B_{24} . The values of B_{24} given in Table 4 were determined in this way, the properties of each of the two binary solutions being taken as the average of two determinations. A partial check is possible since the intercept $[M_2P_2(\theta)w_2 + M_4P_4(\theta)w_4]^{-1}$ for a ternary system can be calculated from the binary system intercepts. It is a quite simple matter to show⁴⁹ that the condition for the appearance of a maximum in A_2 is that B_{24} be larger than both B_{22} and B_{44} . For B_{24} intermediate between B_{22} and B_{44} , A_2 is a monotone function of w . The interpretation of measurements representing various compositions to evaluate B_{24} according to equation (14) provides a much more sensitive means of establishing the reality of the maximum, which, if it exists at all, is not usually very marked, than does a completely empirical examination of data. In other words, the imposition upon the experimental data of a definite analytical form that can be accepted as correct reduces the uncertainty of interpretation.

The calculated values of B_{24} give an average value of 1.7×10^{-4} and thus indicate that a maximum in A_2 cannot exist in this system. This result is interesting in that the Flory-Krigbaum theory predicts B_{24} to be greater than B_{22} . In the present case the theory is unequivocal since a sufficient condition is merely that M_4/M_2 be greater than 4.24 with B_{22} and B_{44} positive, irrespective of particular values of the thermodynamic parameters

contained in X . For the two fractions used here, however, this ratio is 21. Aside from the sparsity of our data and the possibility of a difference in stereoregularity of the two polymers, the only doubtful consideration remaining is the effect of heterogeneity of the individual fractions. We have no way of determining this, but it is easy to show that the *form* of equation (14) is unaffected. If the fractions are in fact heterogeneous, the quantities $MP(\theta)$ and B determined experimentally actually represent averages over the values for the individual species present.

The two solid curves presented in *Figure 2* show theoretical relations based on the FKO theory. In one instance (curve *A*) with Fox's³² constants and f as unity, we made a completely independent evaluation generalizing the FKO variable X in equation (9) to the case of interaction between unlike polymers by the expression²⁵

$$\left(\frac{M_2 M_4}{X_{24}}\right)^{2/3} = \frac{1}{2} \left[\left(\frac{M_2^2}{X_{22}}\right)^{2/3} + \left(\frac{M_4^2}{X_{44}}\right)^{2/3} \right] \quad (15)$$

and then using $B_{24} = YF(X_{24})$ in equation (14). Repeating this treatment with f as 0.4913 led to a similar curve lying above the one shown but gave no better semblance of conformity with the empirical results.

To calculate the other curve we again adopted Fox's constants to determine Y but forced the theory to fit the experiments for the binary systems by letting $F(X)$ equal A_2/Y for these. Then making use of equations (8) and (15) to find X_{22} , X_{44} , and thence X_{24} and $F(X_{24})$, we again invoked equation (8) to obtain B_{24} . This last scheme failed with $f=1$ for then $F(X_{22})$ was found to be greater than unity and consequently X_{22} was negative, a physically meaningless result for a system in a good solvent. With f as 0.4913, however, this difficulty was avoided, and curve *B* of *Figure 2* refers to this case. For the calculations of X_{24} , average molecular weights $M_2 = 1.26 \times 10^5$ and $M_4 = 2.64 \times 10^6$ were used.

The theoretical interaction coefficients determining curve *A* are $B_{22} = 1.90 \times 10^{-6}$, $B_{24} = 2.16 \times 10^{-4}$, $B_{44} = 1.54 \times 10^{-4}$; and for curve *B* the calculated cross-coefficient is $B_{24} = 3.30 \times 10^{-4}$. These plots illustrate, as we indicated above, that sufficient experimental precision to permit direct unambiguous observance of a maximum in graphs of A_2 against w would often be difficult to attain. For the virial coefficient from osmotic pressure the situation is somewhat different: the equivalent function is parabolic in form with a broader maximum less compressed toward low concentrations of component 4 and thus probably easier to discern empirically²⁵ from a limited number of experimental points.

Part of the experimental work described herein was supported by the Office of Ordnance Research.

*Department of Chemistry,
Massachusetts Institute of Technology,
Cambridge, Massachusetts, U.S.A.*

*and
Mellon Institute,
Pittsburgh, Pa, U.S.A.*

(Received September 1961)

REFERENCES

- ¹ FLORY, P. J. *Principles of Polymer Chemistry*. Cornell University Press: Ithaca, N.Y., 1953
- ² HUGGINS, M. L. *Physical Chemistry of High Polymers*. Wiley: New York, 1958
- ³ ZIMM, B. H. *J. chem. Phys.* 1946, **14**, 164
- ⁴ ZIMM, B. H. *J. chem. Phys.* 1948, **16**, 1099
- ⁵ STANLEY, H. E. *Thesis*. Massachusetts Institute of Technology, 1949
- ⁶ CARR, C. I. and ZIMM, B. H. *J. chem. Phys.* 1950, **18**, 1616
- ⁷ MOORE, L. D. *Thesis*. Massachusetts Institute of Technology, 1951
- ⁸ SHEFFER, H. and HYDE, J. C. *Canad. J. Chem.* 1952, **30**, 817
- ⁹ BRICE, B. A. and SPEISER, R. *J. opt. Soc. Amer.* 1946, **36**, 363A
- ¹⁰ BRICE, B. A. and HALWER, M. *J. opt. Soc. Amer.* 1951, **41**, 1033
- ¹¹ COHN, E. S. and SCHUELE, E. *J. Polym. Sci.* 1954, **14**, 309
- ¹² BISCHOFF, J. and DESREUX, V. *Bull. Soc. chim. Belg.* 1952, **61**, 10
- ¹³ JOSE, C. I. and BISWAS, A. B. *J. Polym. Sci.* 1958, **27**, 575
- ¹⁴ BHATNAGAR, H. L. and BISWAS, A. B. *J. Polym. Sci.* 1954, **13**, 461
- ¹⁵ ROSSI, C., BIANCHI, V. and BIANCHI, E. *Makromol. Chem.* 1960, **41**, 31
- ¹⁶ FOX, T. G., KINSINGER, J. B., MASON, H. F. and SCHUELE, E. M. *Polymer, Lond.* 1962, **3**, 71
- ¹⁷ COHN-GINSBERG, E. S., FOX, T. G. and MASON, H. F. *Polymer, Lond.* 1962, **3**, 97
- ¹⁸ FOX, T. G. and OROFINO, T. A. To be published
- ¹⁹ ZIMM, B. H. *J. chem. Phys.* 1948, **16**, 1093
- ²⁰ DEBYE, P. J. *phys. Colloid Chem.* 1947, **51**, 18
- ²¹ SCHULZ, G. V. *Z. phys. Chem. B*, 1939, **43**, 25
- ²² MEYERHOFF, G. and SCHULZ, G. V. *Makromol. Chem.* 1952, **7**, 294
- ²³ BISCHOFF, J. and DESREUX, V. *J. Polym. Sci.* 1953, **10**, 437
- ²⁴ FLORY, P. J. *J. chem. Phys.* 1949, **17**, 1347
- ²⁵ FLORY, P. J. and KRIGBAUM, W. R. *J. chem. Phys.* 1950, **18**, 1086
- ²⁶ OROFINO, T. A. and FLORY, P. J. *J. chem. Phys.* 1957, **26**, 1067
- ²⁷ CASASSA, E. F. and MARKOVITZ, H. *J. chem. Phys.* 1958, **29**, 493
- ²⁸ CASASSA, E. F. *J. chem. Phys.* 1959, **31**, 800
- ²⁹ FLORY, P. J. and FOX, T. G. *J. Amer. chem. Soc.* 1951, **73**, 1904
- ³⁰ FLORY, P. J. *J. chem. Phys.* 1949, **17**, 303
- ³¹ STOCKMAYER, W. H. *J. Polym. Sci.* 1955, **15**, 595
- ³² FOX, T. G. *Polymer, Lond.* 1962, **3**, P48/61
- ³³ KRIGBAUM, W. R. and FLORY, P. J. *J. Amer. chem. Soc.* 1953, **75**, 1775
- ³⁴ KRIGBAUM, W. R. and FLORY, P. J. *J. Polym. Sci.* 1953, **11**, 37
- ³⁵ NOTLEY, N. T. and DEBYE, P. J. *Polym. Sci.* 1957, **24**, 275
- ³⁶ FLORY, P. J. *J. chem. Phys.* 1945, **13**, 453
- ³⁷ ISIHARA, A. and KOYAMA, R. *J. chem. Phys.* 1956, **25**, 712
- ³⁸ KOYAMA, R. *J. chem. Phys.* 1957, **27**, 234
- ³⁹ PTITSYN, O. B. and ÉIZNER, YU. E. *Vyosokomol. Soed.* 1959, **1**, 1200
- ⁴⁰ KRIGBAUM, W. R., CARPENTER, D. K., KANEKO, M. and ROIG, A. *J. chem. Phys.* 1960, **33**, 921
- ⁴¹ KIRSTE, R. and SCHULZ, G. V. *Z. phys. Chem. (N.S.)*, 1961, **27**, 20
- ⁴² KURATA, M. and YAMAKAWA, H. *J. chem. Phys.* 1958, **29**, 311
- ⁴³ KURATA, M., STOCKMAYER, W. H. and ROIG, A. *J. chem. Phys.* 1960, **33**, 151
- ⁴⁴ BILLMEYER, F. W. and DEIHAN, C. B. *J. Amer. chem. Soc.* 1955, **77**, 4763
- ⁴⁵ STOCKMAYER, W. H. and CASASSA, E. F. *J. chem. Phys.* 1952, **20**, 1560
- ⁴⁶ FOX, T. G., FLORY, P. J. and BUECHE, A. M. *J. Amer. chem. Soc.* 1951, **73**, 285
- ⁴⁷ YAMAKAWA, H. and KURATA, M. *J. chem. Phys.* 1960, **32**, 1852
- ⁴⁸ CHIEN J.-Y., SHIH L.-H. and YU S.-C. *J. Polym. Sci.* 1958, **29**, 117
- ⁴⁹ CASASSA, E. F. *Polymer, Lond.* 1960, **1**, 169
- ⁵⁰ BLUM, J. J. and MORALES, M. F. *J. chem. Phys.* 1953, **20**, 1822

Properties of Dilute Polymer Solutions I—Osmotic and Viscometric Properties of Solutions of Conventional Polymethyl Methacrylate

T. G. FOX*, J. B. KINSINGER†, H. F. MASON and E. M. SCHUELE

This is the first report of a series on the properties of dilute solutions of conventional polymethyl methacrylate designed to characterize the chain length and its distribution, the intramolecular chain interactions and the thermodynamic interactions with solvent and their effects on the chain dimensions, and to establish the accuracy and reproducibility of such data. Herein $[\eta]/\bar{M}_n$ relations in benzene at 30° are established for both fractionated and unfractionated polymers from ebulliometric determinations in benzene for \bar{M}_n from 200 to 6×10^3 and from osmotic pressure measurements in two or more solvents for \bar{M}_n from 10^4 to 7×10^5 . Evidence is presented that the values of \bar{M}_n so obtained are generally accurate and reproducible within an uncertainty of three per cent. The observed curvature and its molecular weight dependence in osmotic pressure/concentration relations is in general accord with theoretical expectation. The identity of $[\eta]/\bar{M}_n$ relationships found for unfractionated polymers prepared both with and without added chain transfer agent indicates that both have the same molecular weight distribution and that disproportionation is the predominant mode of termination of methyl methacrylate radicals at 60°.

INVESTIGATIONS of the properties of dilute polymer solutions can provide data on the polymer chain structure, average degree of polymerization, and average chain conformation. The data on chain length and structure generally provide information on certain vital details of the polymerization mechanism. The data on chain conformation contribute to the characterization of intrachain interactions and of the thermodynamic interactions of segments of the polymer chains with their surroundings. Such knowledge is useful in the interpretation of the hydrodynamic, thermodynamic, and mechanical properties in bulk and in solution. Consequently it is important to obtain precise measurements of dilute solution properties of well-characterized polymers over wide ranges in the pertinent variables.

In view of the difficulties in duplicating the results of such measurements in different laboratories¹, it is of particular importance to demonstrate the validity and reliability of the data. It was with these objectives in mind that the work reported in this and in subsequent communications was initiated several years ago. Polymethyl methacrylate, chosen as the first polymer for investigation in this and in the two companion papers² was prepared by conventional free radical polymerizations in bulk or in benzene at 50° or

*Present address: Mellon Institute, Pittsburgh, Pennsylvania.

†Present address: Department of Chemistry, Michigan State University, East Lansing, Michigan.

60° carried to low conversions (generally 8 to 32 per cent). The results are therefore characteristic of 'conventional polymethyl methacrylate', believed to consist of monomer units united head-to-tail in random sequence of syndiotactic and isotactic placements of nearest neighbours occurring with probabilities of *ca.* 0.77 and 0.23, respectively³. It should not be assumed that the parameters obtained in these investigations will necessarily be characteristic of other stereochemical forms of this polymer^{3a}.

Extensive osmotic measurements at 30° with different osmometers, membranes and solvents on eight well-fractionated polymethyl methacrylate samples ranging in number average molecular weight, \bar{M}_n , from 12 000 to 725 000 provide a rigorous test of the validity of the osmotic techniques. Ebulliometric molecular weight determinations were made on seven other fractions of \bar{M}_n from 200 to 6 100. These data, together with intrinsic viscosity data on the fractions, establish over a wide range for fractionated polymethyl methacrylate the molecular weight dependence of both the intrinsic viscosity, $[\eta]$, and the second virial coefficient, Γ_2 . Comparison of the molecular weights with the results of light scattering measurements² provides information on the efficiency of the fractionation procedures.

Similar data were obtained on two series of whole polymers ranging in \bar{M}_n from 160 000 to 650 000, prepared to low conversion in bulk polymerizations at 60° with 2,2'-azobisisobutyronitrile (AIBN) as the initiator. Comparison of the data on the whole polymers with those on the fractions yields information on the effect of molecular weight heterogeneity on $[\eta]$ and on Γ_2 .

The whole polymers in one series were polymerized with various amounts of the chain transfer agent *n*-butyl mercaptan, such that the chain transfer reaction was the predominant mode of chain termination. For such polymers, the expected molecular weight distribution is known⁴, e.g. the ratio of $\bar{M}_w/\bar{M}_n=2$, where \bar{M}_w is the weight average molecular weight. In the other series of polymerizations no mercaptan had been added, so that the molecules were terminated chiefly by a biradical reaction, either disproportionation or combination. Since termination exclusively by combination yields a narrower distribution⁴, i.e. $\bar{M}_w/\bar{M}_n=1.5$, comparison of the osmotic-intrinsic viscosity data on the two series provides a basis for choice between the alternate possible modes of biradical termination. Confirmation of this choice is afforded by comparison of these data with the $[\eta]/\bar{M}_w$ relationship for polymethyl methacrylate² as well as comparison of the osmotic data with light scattering data on six of these whole polymers.

The present results are discussed in relation to the existing related experimental and theoretical relationships in the literature.

EXPERIMENTAL

Preparation of polymers

Twenty polymers were prepared by polymerization (*Table 1*) of methyl methacrylate with AIBN or (in two cases) benzoyl peroxide as initiator. Polymers prepared as materials to be fractionated were generally isolated from reactions carried to low conversion (8 to 32 per cent) by dropwise

PROPERTIES OF DILUTE POLYMER SOLUTIONS I

addition to a five- to ten-fold excess of rapidly stirred precipitant, either methanol or Skellysolve B (a commercially available mixture of low boiling paraffinic hydrocarbons), and dried *in vacuo* at 110°. The four lowest molecular weight polymers prepared in reactions carried to high conversions were not precipitated; instead, the solvent benzene and/or residual monomer were evaporated under vacuum. The large excess of AIBN employed in two cases was precipitated by cooling the concentrated solutions and was then filtered out.

The second and third sets of polymers (*Table 1*) prepared as materials for molecular weight distribution studies were polymerized to low conversion (*ca.* 10 per cent) and were isolated in such a manner (*cf. seq.*) that the lower molecular weight polymer species would not be lost. Polymerization conditions were chosen such that the molecular weight would not be too high for accurate osmotic molecular weight determinations, and not so small that an appreciable fraction of the shorter polymer chains would diffuse through the osmotic membranes.

Dimethyl α -methylene- α' -methyladipate (methyl methacrylate dimer) was prepared by a modification of the method described by Albisetti *et al.*⁵. Methyl methacrylate containing 0.1 per cent hydroquinone was pumped

Table 1. Details of polymerizations

| Designation | AIBN conc. $m/l \times 10^2$ | Solvent conc. | Reaction time, h, and temp., °C | Conv. % | $\bar{M}_v \times 10^{-3}$ | Precipitant [§] |
|---|------------------------------|---------------|---------------------------------|---------|----------------------------|--------------------------|
| Polymers for fractionation | | | | | | |
| MMA 2 | 1 (BPO)* | — | 3 /50° | 8 | (700) | MeOH |
| MMA 4 | 1.2 | — | 4 /50° | 15 | 660 | MeOH |
| MMA 1 | 4 (BPO)* | 0.85† | 5.5/50° | 27 | 200 | MeOH |
| MMA 3 | 4 | 0.85† | 3 /50° | 32 | 120 | MeOH |
| JK 14 | 0.10 | 63 ‡ | 24 /60° | 95 | 28 | None |
| JK 41 | 0.17 | 215 ‡ | 48 /60° | 95 | 15 | None |
| JK 16 | 3.0 | 9.4 † | 2.3/60° | 80 | — | None |
| JK 17 | 4.6 | 20 † | 3.5/60° | — | 1.28 | None |
| Whole polymers polymerized without chain transfer agent | | | | | | |
| AIN 2 | 0.26 | — | — /60° | 11.0 | 1260 | MeOH |
| JK 4 | 0.34 | — | 1.0 /60° | 7.4 | 1000 | SS |
| AIN 4 | 0.47 | — | — /60° | 11.6 | 891 | MeOH |
| AIN 5 | 0.61 | — | — /60° | 11.9 | 870 | MeOH |
| JK 3 | 0.76 | — | 0.65/60° | 6.8 | 690 | SS |
| AIN A' | 2.8 | — | — /60° | 10.3 | 363 | MeOH |
| JK 5 | 3.0 | — | 0.5 /60° | 9.8 | 316 | SS |
| Whole polymers polymerized with <i>n</i> -butyl mercaptan | | | | | | |
| JK 8 | 0.04 | 2.3‡ | 4.5/60° | 9.2 | 800 | SS |
| NBM 1 | 0.0026 | 2.4‡ | 4 /60° | 7.4 | 690 | SS |
| JK 7 | 0.04 | 3.9‡ | 4 /60° | 7.7 | 562 | SS |
| NBM 2 | 0.026 | 5.0‡ | 4 /60° | 7.4 | 385 | SS |
| JK 6 | 0.04 | 6.3‡ | 5 /60° | 10.2 | 355 | SS |

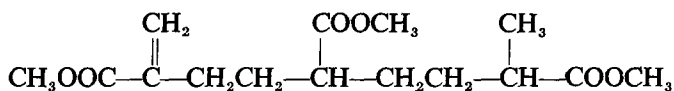
*Benzoyl peroxide (BPO) was used as initiator in these preparations.

†Molar ratio, benzene: MMA.

‡Butyl mercaptan, $m/l \times 10^2$.

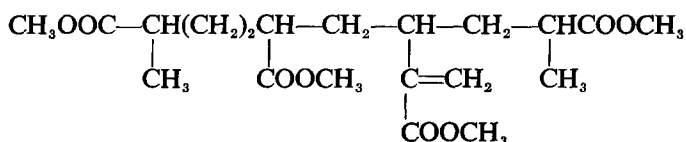
§MeOH designates methanol; SS, Skellysolve.

under pressure through a coil held at 325°C. The pressure was maintained at 1 500 lb/in² and the average holding time in the coil was 4.5 min. The conversion of methacrylate to high boiling products was 26.5 per cent of which 80.8 per cent was dimer, 15.1 per cent trimer, and the remaining 4 per cent unidentified high boiling products. Tentatively the trimer has been assigned the structure⁵



The methacrylate dimer was hydrogenated to the saturated analogue whose properties have already been described⁵.

The tetramer of methyl methacrylate was prepared by refluxing methyl methacrylate dimer containing 0.1 per cent hydroquinone for four hours at 245° to 250°C under a blanket of nitrogen. Conversion of dimer was 45 per cent of which 74.5 per cent was tetramer and 25 per cent higher polymers of methyl methacrylate. The tetramer of methyl methacrylate boils at 199° to 202°C/0.4 mm, n_D^{25} 1.4649. A probable structure is



The viscosity average molecular weights, \overline{M}_v , listed in *Table 1* were calculated from the intrinsic viscosities (in dl/g) at 30° in benzene by the relationship

$$\log \overline{M}_v = (\log [\eta] + 4.28) / 0.76 \quad (1)$$

established in the companion paper^{2a}.

Isolation of whole polymers

The following considerations indicate that the present whole polymers can be isolated satisfactorily without appreciable loss of low molecular weight species by precipitation at room temperature by the addition of a dilute acetone solution of the polymer to a tenfold excess of Skellysolve B.

At room temperature approximately ten per cent by weight of a low conversion unfractionated polymethyl methacrylate of \overline{M}_v of 20 000 was found to be soluble in a 10:1 ratio of Skellysolve/acetone, when from 4 to 40 g of this polymer was equilibrated with 1 l. of the mixed solvent. Assuming the polymer had the expected 'random' chain distribution for vinyl polymerizations propagated by monoradicals and terminated by a transfer reaction⁴, and assuming the number average degree of polymerization of the polymer to be 100, it can be shown by a method illustrated most recently by Valentine⁶ that the chains of $n \leq 50$, where n is the degree of polymerization, constitute nearly ten per cent by weight of the mixture. If as a first approximation we assume from this that only chains of $n \leq 60$ are soluble in this mixed solvent, we can again employ Valentine's method to estimate the fraction of chains soluble in the precipitation in this medium

of an MMA polymer of known distribution. Thus for polymers having the 'random' distribution and having \bar{M}_n of 150 000 to 600 000 the error in \bar{M}_n introduced by the solubility of the shorter molecules ($n < 60$) is estimated to range from four to one per cent respectively. Such errors are not serious in the present instance.

Four of the whole polymers were isolated with a tenfold amount of methanol as the precipitant. Assuming (on the basis of the observed solubility of fractions) that chains of $n \leq 200$ are soluble in this mixture, the error in \bar{M}_n due to this preferential solubility is between three and ten per cent for 'random' polymers of \bar{M}_n from 650 000 to 200 000. Thus methanol should *not* be used in isolating the whole polymers of methyl methacrylate in the low molecular weight range.

Since the osmotic membranes used proved to be sufficiently impermeable to polymer chains to permit accurate molecular weight measurements of a fraction with \bar{M}_n as low as 12 000, clearly such membranes can be used to determine the \bar{M}_n values of the present whole polymers of $\bar{M}_n \geq 167 000$ with negligible error from the diffusion of the small species.

Fractionation

Seven polymers were fractionally precipitated by successive addition of non-solvents to their solutions at 30° according to the general technique described earlier⁷. Certain of the separated fractions were redissolved and then refractionated. In the high molecular weight range, third fractionations were generally carried out. In three cases the yield of polymer was so small that two similar fractions were mixed to provide a sample for the dilute solution studies. Usually the whole polymers were first fractionated from solutions of initial concentration of *ca.* 0.1 per cent into three to five sub-fractions. The solvent employed for the higher molecular weight polymers ($\bar{M}_v \geq 55 000$) was generally acetone with either methanol or 1:1 mixtures of methanol and water as the precipitant. In the low molecular weight range the most effective solvent-precipitant combination found was carbon tetrachloride-Skellysolve, although acetone-Skellysolve, acetone-water, and benzene-Skellysolve combinations were also employed in the moderate molecular weight range.

Out of some sixty fractions prepared in this way eleven 'best' fractions were chosen for this study. The details of the fractionations are available on request.

Intrinsic viscosities

Solution viscosity measurements made at several concentrations were extrapolated by plotting versus the concentration c both the reduced specific viscosity η_{sp}/c and the corresponding value of $(\ln \eta_r)/c$, where $\eta_r = 1 + \eta_{sp}$ is the relative viscosity. The common intercept at $c=0$ was taken as $[\eta]$. Ubbelohde viscometers having flow times for benzene at 30° of *ca.* 70 sec or 250 sec employed for the high and low molecular weight polymers, respectively, were calibrated and used in the manner described previously⁷. The kinetic energy correction was always applied. Concentrations were so

chosen that the specific viscosities generally ranged from 0.2 to 0.8. In the range studied here ($[\eta] \leq 2.5$), the correction for non-Newtonian behaviour was found to be negligible^{2b}. Temperature control of ± 0.02 °C was achieved with a water bath and a thyatron relay.

Osmotic techniques

The osmometer, a modification of the Schulz-Wagner type⁸ (Figure 1),

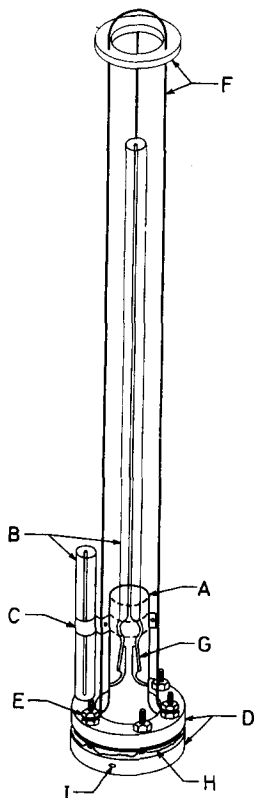


Figure 1—Diagram of osmometer: A, 28/15 spherical socket joint, ground optically flat on bottom; B, 9 in. precision bore (1 mm.) capillary; C, steel shim stock band; D, stainless steel plates; E, 6 bolts; F, Nichrome wire and stainless steel suspension hanger; G, 7/15 joint; H, membrane; I, vent for air trapped under cell

consists of a glass cell (A) and capillary containing the solution in contact with the membrane (H). The assembly is suspended in a large glass tube containing enough solvent to immerse the cell almost completely. A matched reference capillary tube (B) is employed to correct for the capillary rise of the solution. Two stainless steel plates (D) pulled together by six bolts (E) hold the membrane against the polished flat bottom surface of the cell. The upper plate rests against the outer wall of the cell; the base of the lower plate has six concentric circles cut into its upper side, with 28 holes punched through the troughs to provide access to the solvent. A thin disc of porous filter paper inserted between the membrane and the lower plate protects the surface of the membrane from any sharp edges on the latter. The membrane acts as its own gasket in sealing the cell. A glass joint (G) permits removal of the capillary for filling or emptying the osmotic cell.

After filling the cell and putting the capillary in place, the joint G is sealed by mercury poured into the space about it, provided first that no air bubbles are visible in the cell. The cell was always rinsed several times with the solution before filling, and the concentration was determined by method of residue *after* the osmotic pressure measurement was complete. Temperature control was obtained by immersing the tube containing the solvent and cell into a large water bath whose temperature was held with the aid of a thyatron relay at $30.5^\circ \pm 0.003^\circ\text{C}$ for short periods, and to $\pm 0.01^\circ$ over a period of months. The osmotic pressure, expressed here as cm of solution, represents the difference in height of the liquid levels in the two capillary tubes, measured with a cathetometer reading directly to ± 0.01 cm.

The basic premise of osmometry is that the membrane is permeable to the solvent but not to the solute. It is necessary to demonstrate that this condition is met for the given polymer-solvent-membrane system. With truly semi-permeable membranes the molecular weight calculated from the limiting equilibrium osmotic pressure extrapolated to infinite dilution should be a characteristic of the polymer independent of time, of the membrane, and of the solvent. Consequently confidence in the validity of the results is heightened if the same molecular weight is obtained with different membrane-solvent combinations. For this reason with few exceptions we adopted the procedure of employing at least two different solvent-membrane combinations on every polymer sample studied.

The membranes investigated in our preliminary work included these types: polyvinyl alcohol⁹, Carter-Record¹⁰, bacterial cellulose¹¹, Ultracella Filters¹², and wet regenerated cellulose treated according to the method described by Flory¹³. Of these, the latter two were found most convenient and suitable for this investigation. The Ultracella membranes are available in three grades, 'dense', 'very dense', and 'super dense', which we will designate as UC-d, UC-vd, and UC-sd. The wet regenerated cellulose

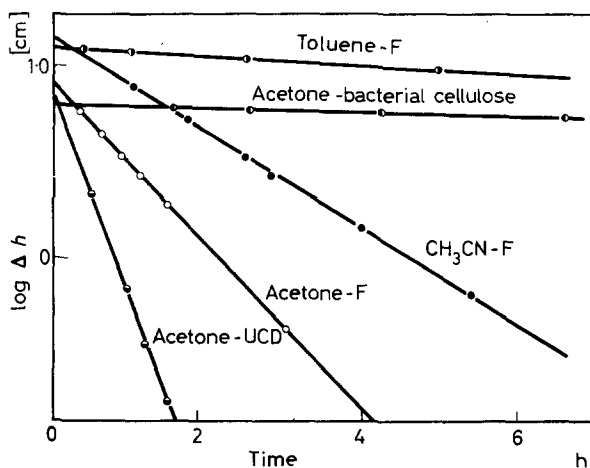


Figure 2—Equilibration curves at 30° for various solvent-membrane pairs

membrane (obtained from the Sylvania Division of American Viscose and designated as No. 300) is referred to as type F. Since the rate of penetration of solvent depends on the membrane-solvent pair (Figure 2) we shall always prefix the name of the solvent to the membrane designation.

A measure of membrane permeability to solvent is obtained by filling the osmometer with solvent and determining the rate of approach of the driving head to zero height. This qualitative test is used to screen membrane and osmometer assemblies for leaks. The permeability to the polymer may be characterized by plotting the osmotic height versus time when the osmometer is charged with solution to a level below the equilibrium osmotic height. Ideally, the liquid should rise to its equilibrium position and thereafter remain constant. Actually, diffusion of low molecular weight polymer through the membrane will cause a decrease in height versus time. Thus the rate of decrease of osmotic height versus time for a standard polymer concentration (Figures 3 and 4) is a measure of the permeability of the

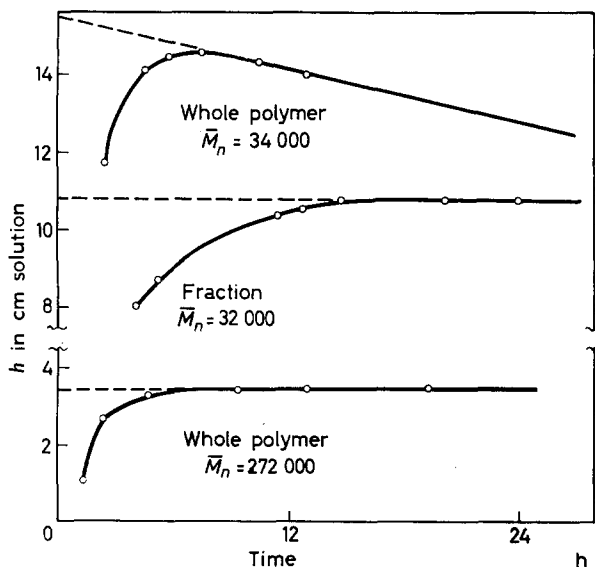


Figure 3—Osmotic equilibration curve at 30° for poly-methyl methacrylate with acetone-F membranes. Concentrations from top to bottom are 1.5, 1.3 and 2.0 g/100 ml

membrane to the low molecular weight components of the sample. This rate is dependent on the membrane-solvent pair and on the molecular weight and molecular weight distribution of the polymer. In the present instance, the toluene-F membranes were suitable for polymer fractions of \bar{M}_n as low as ca. 10 000, whereas the acetone-F membranes were suitable for whole polymers of \bar{M}_n at least as low as 50 000. It was observed that although the super dense Ultracella membranes were less permeable to toluene than the F membranes, they were more permeable to the low molecular weight polymers.

In practice, curves such as those shown in *Figures 3 and 4* were obtained and the osmotic height extrapolated linearly to zero time (the time of charging of the osmometer). The data were reported here only if the slope of this line was ≤ 0.4 per cent per hour. This criterion of acceptability is such that the error introduced by the linear extrapolation will be small in the present case.

Ebulliometric \bar{M}_n determinations

The Hansen-Bowman¹⁴ modification of the Menzies-Wright ebulliometer was used with a highly sensitive thermocouple in the place of the water-filled differential thermometer. Copper-constantan thermocouples (e.m.f. of about

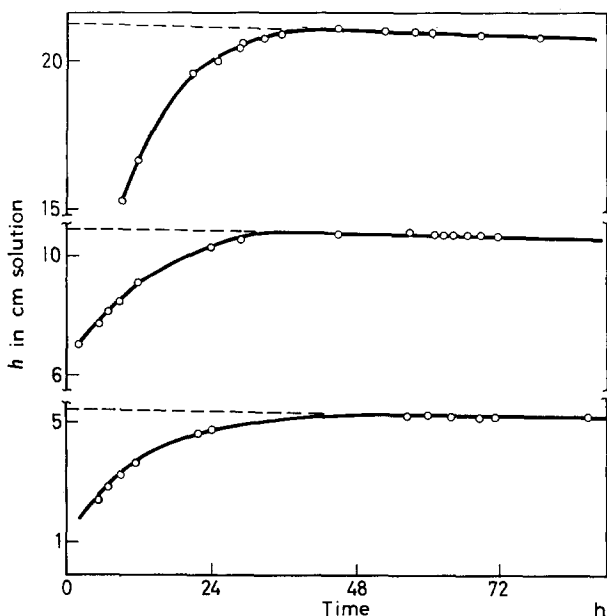


Figure 4—Osmotic equilibration curves at 30° for a fraction of polymethyl methacrylate of $\bar{M}_n = 15\,700$ with toluene-F membranes. Concentrations from top to bottom are 1.18, 0.64 and 0.32 wt %

0.05 mV per degree) were made from 3 mil wires and mounted in a glass tube of 4 mm outside diameter bent at the base similar to the Menzies differential thermometer. A Liston-Becker amplifier, capable of amplifying the output of this thermocouple to permit detection of differences of as little as 0.0002°C between the solution and vapour junctions of the couple, was employed. An Esterline-Angus graphic milliammeter was used to record the amplified output.

The ebulliometric technique used was the external standard method involving a comparison of the boiling point elevation produced by the addition of equal molar quantities of the sample being studied and the

standard to equal volumes of the same solvent. Benzil ($M=210$) was most commonly used as the standard. The number average molecular weight was calculated from the following relationship

$$\bar{M}_n \text{ sample} = \frac{\text{g sample} \times M_n \text{ standard} \times \text{change due to addition of standard (in chart units)}}{\text{g standard} \times \text{change due to addition of sample (in chart units)}}$$

It was not necessary to extrapolate the concentration versus Δt data to zero concentration since the extreme sensitivity of the instrument allowed us to work with solutions of sufficiently low concentrations to approach ideality. This method made possible the measurement of molecular weights in the range of 1 000 to 10 000 with ± 5 per cent accuracy.

Solvents

The solvents used were redistilled at a high reflux ratio in a 60 in. column packed with stainless steel helices. The first and last sixths of the distillate were discarded.

RESULTS

Osmotic data

Osmotic measurements (Appendix) were obtained on eight fractions and twelve low conversion whole polymers, generally at five or more concentrations in each of two solvents, acetone and acetonitrile. Often different osmometers were employed in measurements at the different concentrations in a series. Data were obtained in a third solvent, toluene, in one instance. Since toluene-F membranes proved to be least permeable to low molecular weight polymer, measurements on the three fractions of lowest molecular weight ($\bar{M}_n < 20\,000$) were made exclusively in this system.

Plots of π/c versus c (Figure 5) are best represented by curved lines in accord with the theoretical relationship¹⁵

$$\pi/c = RT/\bar{M}_n(1 + \Gamma_2 c + \Gamma_3 c^2 + \dots) \quad (2)$$

Here $\pi = h\rho$ is the osmotic pressure at polymer concentration c (g/ml of solution), h is the corresponding height (cm of solution), R is the gas constant (8.4783×10^4 g cm mole⁻¹ deg⁻¹), T is the absolute temperature, ρ is the solution density (g/ml), and Γ_2 and Γ_3 are virial coefficients. It is apparent that the data covering the widest range in concentration must be represented by curved lines. On first inspection it appears that those data covering relatively narrow concentration bands may be represented by either straight or curved lines. However, the values of \bar{M}_n obtained for a given fraction by linear extrapolations to infinite dilution are different for different solvents, indicating that such linear representations are not reliable for the precise evaluation of \bar{M}_n and of the virial coefficients.

Guidance in extrapolating properly data on π versus c is provided by theoretical considerations relating the virial coefficients in equation (2)¹⁵⁻¹⁷. Thus it is expected¹⁷ that $\Gamma_3 = g\Gamma_2^2$ where the coefficient g is a slowly

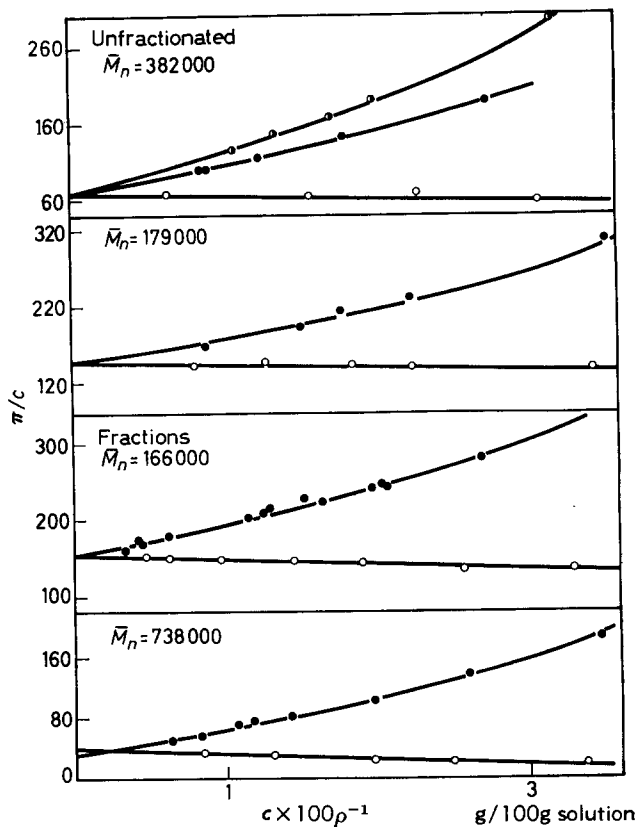


Figure 5— π/c versus c at 30° for polymethyl methacrylate solutions in toluene (○), acetone (●), or acetonitrile (○). The curves are drawn according to equation (3) with the parameters of Tables 2 and 3. Here $\pi = h\rho$ where h is in cm of solution, ρ is solution density in g/ml, and c is g polymer/ml of solution

increasing function of Γ_2 —one that is about $\frac{1}{4}$ in a good solvent and vanishes as Γ_2 goes to zero. Since the third term is important here only as it aids in the accurate evaluation of the preceding terms, and since it makes a negligible contribution to the poor solvents throughout the concentration range covered osmotically, it suffices to take for g its appropriate value in a good solvent¹⁷, i.e. 0.25, and to treat it as a constant. Neglecting higher terms, equation (2) can be reduced to

$$\left(\frac{\pi}{c}\right)^{1/2} = \left(\frac{RT}{\bar{M}_n}\right)^{1/2} \left(1 + \frac{1}{2}\Gamma_2 c\right) \quad \frac{\pi}{c} \leq 3 \frac{RT}{\bar{M}_n} \quad (3)$$

Thus, as suggested by Berglund-Larsson¹⁸ and illustrated subsequently¹⁹, plots of $(\pi/c)^{1/2}$ versus c should be linear, with values of \bar{M}_n and Γ_2 obtainable from the intercept and slope of the line.

Table 2. Data on polymethyl methacrylate fractions

| Designation | $[\eta]$ in benzene at 30°, dl/g | $\bar{M}_n \times 10^{-3}$ | Osmotic | | \bar{M}_w/\bar{M}_n |
|------------------|-------------------------------------|----------------------------|--|--|-----------------------|
| | | | Γ_2 in acetone, cm ³ /g | $\bar{M}_w \times 10^{-3}$ from light scattering ^{2a} | |
| Osmotic | | | | | |
| XF 1B+F2 | 1.80 | 726 | 95 | 865±7 | 1.19±0.01 |
| 3F1D | 0.89 | 278 | 46 | 360±5 | 1.30±0.02 |
| 3F5B & C | 0.58 | 166 | 33 | 223±2 | 1.34±0.01 |
| 3M1 | 0.278 | 66 | 15 | 81±1 | 1.23±0.02 |
| JK14M2B | 0.281 | 64 | 12.3 | 76±5 | 1.19±0.08 |
| JK14M4C | 0.145 | 20.2 | | | |
| JK 41 F2 | 0.121 | 15.6 | | 22±1 | 1.41±0.07 |
| JK 14 M5C & D | 0.111 | 12.3 | | | |
| Ebulliometric | | | | | |
| JK 16 F4 | 0.089 | 6.10 | | | |
| JK 16 F5 | 0.074 | 5.25 | | | |
| JK 16 F8 & 9 | 0.058 | 3.43 | | | |
| JK 16 F11 & 12 | 0.053 | 2.53 | | | |
| JK 17 | 0.039 | 1.28 | | | |
| Tetramer* | 0.022 | 0.393 | | | |
| Trimer* | 0.019 | 0.300 | | | |
| Dimer* | 0.011 | 0.199 | | | |
| Saturated dimer* | 0.011 | 0.194 | | | |

*Strictly speaking these do not represent members of the homologous series since their structures do not correspond to the head-to-tail arrangements of monomer units characteristic of the macromolecular species.

Table 3. Data on unfractionated polymethyl methacrylate

| Designation | $[\eta]$ at 30° in C ₆ H ₆ , dl/g | Osmotic | | $\bar{M}_w \times 10^{-3}$ from light scattering ^{2a} | \bar{M}_w/\bar{M}_n | 1.05 \bar{M}_w/\bar{M}_n |
|--|--|---|---------------------------------------|--|-----------------------|----------------------------|
| | | Γ_2 in acetone, cm ³ /g | $\bar{M}_n \times 10^{-3}$ osmotic | | | |
| Polymerized with <i>n</i> -butyl mercaptan | | | | | | |
| JK 8 | 1.63 | 61 | 402 | 880±10 | 2.19±0.03 | 2.09 |
| NBM 1 | 1.45 | 61 | 382 | | | 1.90 |
| JK 7 | 1.22 | 49 | 285 | (492) | (1.73) | 2.07 |
| NBM 2 | 0.91 | 35 | 209 | | | 1.94 |
| JK 6 | 0.86 | 37 | 179 | 370±20 | 2.06±0.12 | 2.08 |
| Polymerized without transfer agent | | | | | | |
| AIN 2 | 2.27 | 88 | 647 | | | 2.05 |
| JK 4 | 1.86 | 77.5 | 517 | 1 100±100 | 2.13±0.20 | 2.04 |
| AIN 4 | 1.80 | 65 | 457 | | | 2.05 |
| AIN 5 | 1.71 | 68 | 434 | | | 2.10 |
| JK 3 | 1.40 | 51.3 | 332 | 750±30 | 2.26±0.09 | 2.18 |
| AIN A' | 0.88 | 35.0 | 201 | | | 1.90 |
| JK 5 | 0.80 | 28.8 | 162 | 370±20 | 2.28±0.12 | 2.05 |
| Av. 2.11±0.14 | | | | | | |

Plots of $(\pi/c)^{1/2}$ versus c for the present data are in all cases linear, as illustrated in Figure 6, and for a given polymer yield values of \bar{M}_n which are independent of the solvent within an experimental uncertainty of ± 3 per cent. Thus, we have employed such square root plots and equation (3) to determine all of the values of \bar{M}_n and Γ_2 given here (Tables 2 and 3).

Viscosity/molecular weight data on fractions

The solution viscosity and ebulliometric data were obtained by well-established techniques and normal concentration dependence was always observed². The resulting values of $[\eta]$ in benzene at 30° for \bar{M}_n obtained either osmotically or ebulliometrically, and for Γ_2 , are tabulated (Table 2) for fractions of polymethyl methacrylate. Values of light scattering molecular weights (\bar{M}_w) obtained elsewhere^{2a} are also given.

A log-log plot of $[\eta]$ versus \bar{M}_n [Figure 7(a)] is represented by two straight lines intersecting at $\bar{M}_n = 44\,000$ corresponding to the relations

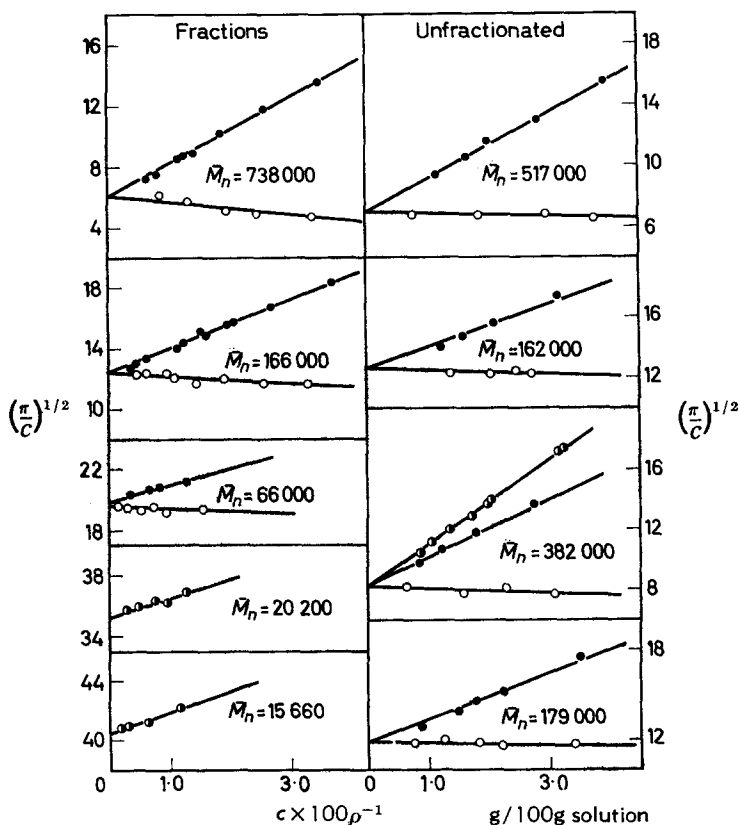


Figure 6— $(\pi/c)^{1/2}$ versus c at 30° for polymethyl methacrylate in toluene \bullet , acetone \bullet , or acetonitrile \circ

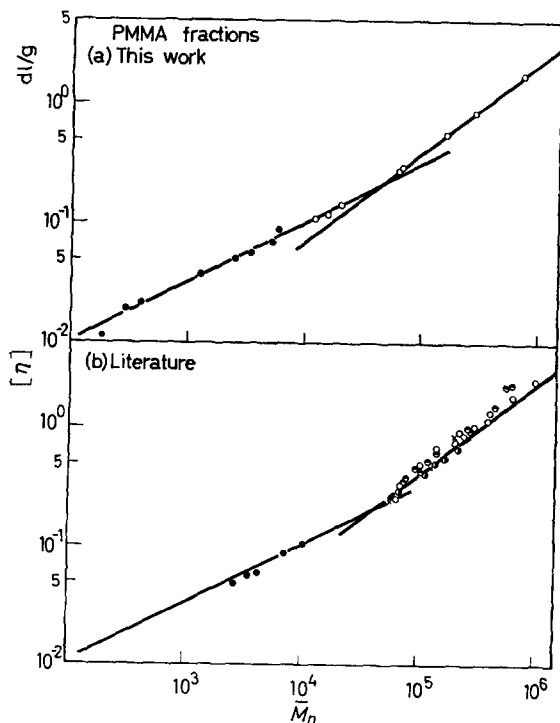


Figure 7(a)—Log-log plot of observed values of $[\eta]$ versus \bar{M}_n for polymethyl methacrylate fractions in benzene at 30° . \circ , osmotic and \bullet , ebulliometric determinations of \bar{M}_n

Figure 7(b)—Comparison of literature values of $[\eta]$ versus \bar{M}_n (points) for polymethyl methacrylate fractions in benzene at 30° with the present results (full line): \bullet Schön and Schulz²¹, \circ Baxendale *et al.*²³, \odot Schulz and Dinglinger²⁴, \ominus Bischoff and Desreux²⁰, and \times Doll²²

$$[\eta] = 6.27 \times 10^{-5} \bar{M}_n^{0.76} \quad \bar{M}_n \geq 44\,000 \quad (4-1)$$

and

PMMA fractions in benzene
at 30°

$$[\eta] = 10.4 \times 10^{-4} \bar{M}_n^{0.50} \quad \bar{M}_n \leq 44\,000 \quad (4-2)$$

Deviation from the linear approximation of equation (4-2) occurs at the lowest molecular weight investigated (200); the data for the trimer and tetramer are adequately represented by equation (4-2) even though their structures are not truly representative of the higher members of the homologous series.

Comparison of the present results with comparable results of earlier workers is afforded by Figure 7(b). The excellent agreement with the most

recent work²⁰⁻²² and the observation that the present data on low molecular weight polymers may be represented by a single line independent of whether the values of \bar{M}_n were obtained osmotically or ebulliometrically provide evidence for the validity of the number average molecular weight values. The deviations of the results of the very early work of Baxendale *et al.*²³ and of Schulz and Dinglinger²⁴ from the present findings is not unexpected in view of the greater molecular weight heterogeneity which doubtless

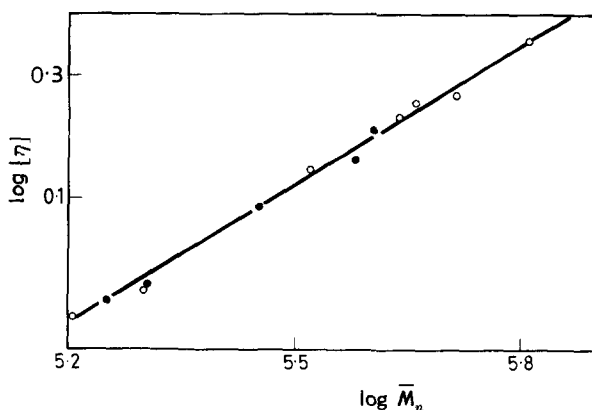


Figure 8—Log-log plot of observed values of $[\eta]$ versus \bar{M}_n in benzene at 30° for whole polymers of methyl methacrylate, prepared with ● and without ○ added chain transfer agent

obtained in their less extensive fractionations. Even in the repeated fractionations carried out here, the ratio (Table 2) of \bar{M}_w (from light scattering to \bar{M}_n is generally 1.2 to 1.4, in accord with the results obtained by others^{20, 25} who have also attempted careful and repeated fractionations. Evidently it is more difficult to get fractions of $\bar{M}_w/\bar{M}_n \leq 1.1$ with polymethyl methacrylate than for less polar polymers such as polystyrene and polyisobutylene²⁶.

Viscosity/molecular weight data on whole polymers

The results of the viscometric, osmotic and light scattering studies on the twelve low conversion whole polymers prepared both with and without *n*-butyl mercaptan are summarized in Table 3. Data for both series plotted as $\log [\eta]$ versus $\log \bar{M}_n$ fall on the same straight line (Figure 8) corresponding to the relationship

$$[\eta] = 8.69 \times 10^{-5} \bar{M}_n^{0.76} \quad \text{unfractionated polymethyl methacrylate in benzene at } 30^\circ \quad (5)$$

In such a relationship for a series of polymers of a given molecular weight distribution the value of the exponent will be independent of the heterogeneity in chain length, but the value of the coefficient will be a characteristic of the distribution²⁷. Since a single value of the coefficient is

observed to apply to both series of whole polymers prepared with and without a chain transfer agent, *it follows that the two series undoubtedly have similar molecular weight distributions*. This will be so if biradical termination at 60° occurs predominantly by disproportionation, when \bar{M}_w/\bar{M}_n for both series of polymers will be 2.0, and the ratio of the coefficient in equation (5) to the coefficient for a series of polymers homogeneous in molecular weight should be 1.64^{27, 28}. Thus the ratio of the coefficients in equations (5) and (1) should be approximately 1.64; in accord with this the ratio found is 1.67. Similarly the ratio of 1.05 \bar{M}_v/\bar{M}_n should be 2.0; correspondence to this within ± 5 per cent is observed for eleven of the twelve whole polymers studied (*Table 3*). The ratio of \bar{M}_w/\bar{M}_n obtained in six cases by direct comparison of light scattering and osmotic data (*Table 3*) averages 2.11, in satisfactory agreement with the above findings within the wider fluctuations inherent in the light scattering measurements^{2b}.

In summary, the coincidence of the $[\eta]/\bar{M}_n$ data for the two series of polymethyl methacrylates indicates that they have the same molecular weight distribution such that $\bar{M}_w/\bar{M}_n = 2.0$. The fact that observed values of \bar{M}_w/\bar{M}_n (or of the related ratio 1.05 \bar{M}_v/\bar{M}_n) based on light scattering and osmotic measurements are 2.0 within experimental error, is indicative of the accuracy of the absolute molecular weight scales which rest on the experimental techniques described here and in the companion paper^{2b}.

Molecular weight dependence of the virial coefficient

Values of Γ_2 in acetone versus \bar{M}_n for the whole polymers and for the fractions are given on a log-log plot in *Figure 9*. They may be represented by a single line corresponding to the linear relationship

$$\Gamma_2(\text{dl/g}) = A_2 \bar{M}_n = 2.63 \times 10^{-5} \bar{M}_n^{0.78} \quad \text{PMMA in acetone at } 30^\circ \quad (6)$$

Data on Γ_2 reported by others^{20, 22, 29} for polymethyl methacrylate in acetone (*Figure 9*) are generally ten to twenty per cent higher than given by equation (6). In all of the prior investigations values of A_2 were obtained from linear representation of π/c versus c plots, whereas the present results require that a non-linear relationship such as equation (2) must apply. It is readily shown that use of a linear relationship, although it may present adequately data covering a limited concentration range, leads to erroneously high values of Γ_2 and of \bar{M}_n . The errors thereby introduced in Γ_2 are appreciable (*ca.* 5 to 20 per cent) even at concentrations sufficiently low that only negligible errors in \bar{M}_n arise. Precise determinations of Γ_2 require even more care in choosing a proper extrapolation procedure than does the precise determination of \bar{M}_n .

DISCUSSION

Biradical termination mechanism

The conclusion that disproportionation is the predominant mode of biradical termination in the free radical bulk polymerization of methyl methacrylate at 60° is in agreement with the findings of Bevington, Melville

and Taylor³⁰ who report that polymethyl methacrylate formed at 60° by the action of AIBN labelled with ¹⁴C in the methyl group contains an average of 1.08 initiator fragments per molecule, i.e. that disproportionation occurs about six times as frequently as combination. It is also in accord with the findings of kinetic and molecular weight studies^{31a}, as discussed by O'Brien and Gornick^{31b}.

Allen and co-workers³² working with unfractionated polymethyl methacrylate prepared at 60° with ¹⁴C labelled AIBN or benzoyl peroxide report $[\eta]/\bar{M}_n$ values which almost exactly fit equation (5), thereby supporting the present results which indicate that biradical termination occurs predominantly by disproportionation. However, their finding of between 1.24 and 1.27 initiator fragments per molecule, corresponding to disproportionation occurring only 1.5 times as often as combination, is in only fair agreement with this conclusion. This apparent inconsistency could be explained easily for initiation by benzoyl peroxide, wherein initiator fragments may be incorporated in the polymer directly by termination, and

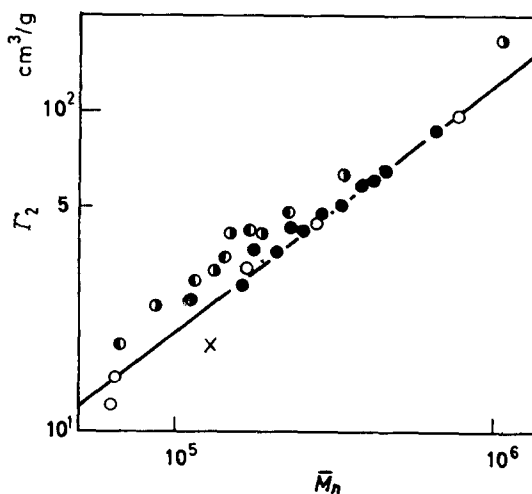


Figure 9—Log-log plot of Γ_2 versus \bar{M}_n obtained from the present osmotic data for polymethyl methacrylate fractions \circ and whole polymers \bullet in acetone at 30°. The other points represent similar data from the literature: \bullet Bischoff and Desreux²⁰, \times Schulz and Doll²², \bullet Chien *et al.*²⁹

not just by initiation. Thus their data^{32b} indicate that phenyl radicals represent about 40 per cent of all the initiator fragments in the polymer, while Bevington³³ concludes that phenyl radicals are extremely inefficient in initiating polymethyl methacrylate chains. A high rate of cross-termination between phenyl radicals and polymeric methyl methacrylate radicals would not be unexpected in view of the results of copolymerization

studies³⁴. The above-mentioned inconsistency may not exist when the initiator is AIBN, since the results of Allen and co-workers³² employing tagged AIBN agree within experimental error with those of Bevington *et al.*³⁰ for the higher molecular weight samples, at least if only the direct evidence based on comparison of osmotic molecular weight determinations with radioactive counts is considered. The single discrepancy is in the case of a rather low molecular weight sample, where diffusion of polymer through the membrane in the osmometer could have been the source of an error.

It is not clear why Allen and co-workers regard the agreement between their $[\eta]/\bar{M}_n$ data and the previously quoted^{31b} findings of the present work as 'fortuitous'. Their criticism of osmotic data as being 'incorrect' when curved π/c versus c plots obtain is obviously not justified. The linearity evidenced in such plots of their own data, obtained at very low concentrations (0.3 to 1.0 g/100 g) where curvature is so slight that its neglect will not measurably affect the extrapolated values of \bar{M}_n is, of course, no certain guide to the concentration dependence expected for more concentrated solutions.

Baysal and Tobolsky²⁸ using the method employed here for determining the mode of biradical termination from viscosity-molecular weight data in chloroform on unfractionated and fractionated polymers concluded that radical combination is the predominant termination mechanism at 60°. However, four out of five of their polymers were of such relatively low molecular weight (*ca.* 10^5 to 2.5×10^5) that an appreciable number fraction of the lower molecular weight species would have been lost in their isolation by precipitation in acetone-methanol mixtures, and/or by diffusion through the osmotic membranes. Their fifth sample was of relatively high molecular weight (*ca.* 9×10^5) where precise determination of the low osmotic pressure is difficult.

The second virial coefficient

Theoretical equations for the molecular weight dependence of the second virial coefficient A_2 are compared in *Figure 10* with the experimental data. Viscometric information was interpreted according to a method described previously³⁵ to obtain the parameters needed in numerical evaluation of the parameters occurring in three different theoretical treatments by Flory, Krigbaum and Orofino (FKO)^{15, 16, 36}, by Casassa and Markovitz (CM)³⁷, and by Casassa (CM II)³⁸. The theories agree in requiring that A_2 be given by a molecular weight-independent factor—in fact, the virial coefficient according to the familiar Flory-Huggins lattice theory¹⁵—multiplied by a function which decreases slowly from unity to approach zero asymptotically as the molecular weight becomes indefinitely large: the only difference is in the form of this function. Thus

$$A_2 = YF(X) \quad (7)$$

where Y is the constant factor, and $F(X)$ is the molecular weight-dependent function.

First to evaluate the constant factor

$$Y = \psi_1 \left(1 - \frac{\Theta}{T}\right) \frac{\bar{v}^2}{V_1} \quad (8)$$

we use the viscometrically derived values of the entropy parameter ψ_1 and the theta temperature together with the partial specific volume of polymer \bar{v} and the molar volume of solvent. These are obtained in the third paper^{2b} of this series from the equation

$$\psi_1 \left(1 - \frac{\Theta}{T}\right) = \frac{\alpha^5 - \alpha^3}{2C_m f M^{1/2}} \quad (9)$$

where the expansion factor α has been evaluated from the experimental ratio

$$\alpha^3 = [\eta]/[\eta]_0 \quad (10)$$

Here $[\eta]$ is the viscosity for a polymer of molecular weight M in the solvent of interest, and $[\eta]_0$ is the viscosity in a solvent at the critical miscibility temperature Θ . In practice the experimental values of $(\alpha^5 - \alpha^3)/M^{1/2}$ are not quite constant and independent of M as equation (9) requires; consequently, the 'best value' for this ratio has been chosen in evaluating the constants on the LHS of this equation. The factor f is usually taken as unity but we include it here to show the effect of using a value of 0.4913 suggested on theoretical grounds by Stockmayer³⁹ [this is equivalent to multiplying the apparent value of ψ_1 in equation (9) by 2.036].

The FKO and CM theories then require respectively evaluation of the functions

$$F(X)_{\text{FKO}} = \frac{4}{\pi^{1/2} X} \ln \left(1 + \frac{\pi^{1/2}}{4} X\right) \quad (11)$$

and

$$F(X)_{\text{CM}} = \frac{1 - e^{-1.093X}}{1.093X} \quad (12)$$

Here

$$X = \frac{4C_m \psi_1 (1 - \Theta/T) M^{1/2}}{\alpha^3} \quad (13)$$

where the constant C_m is given in a subsequent paper^{2b} and the value of α^3 is obtained by solution of equation (9). Alternatively one could use equation (10) to obtain α^3 , and by combining equations (13) and (9) $X = (2/f)(\alpha^2 - 1)$. Numerically the two methods would give almost the same result, the differences arising from the fact that the ratio $(\alpha^5 - \alpha^3)/M^{1/2}$ determined experimentally as described above is not quite constant. We have consistently used equation (9) in the theoretical calculation of the A_2/M curves of *Figure 10*.

In a modification (CM II) of the earlier theory, Casassa³⁸ suggested that Y be obtained as before, but that the expansion factor used to determine the molecular weight dependence should be α_2 , that deduced theoretically for

a cluster of two molecules from α . A given α related to molecular weight as above determines α_2 by

$$\alpha_2^5 - \alpha_2^3 = 1.601(\alpha^5 - \alpha^3) \quad (14)$$

The variable X is now given by

$$X = 1.507(\alpha_2^2 - 1) \quad (15)$$

but $F(X)$ is still expressed by equation (12).

Examination of *Figure 10* indicates that taking f as 0.4913 instead of unity improves agreement with experiment except in the case of the FKO theory where A_2 is made much too large. The CM theory gives a value

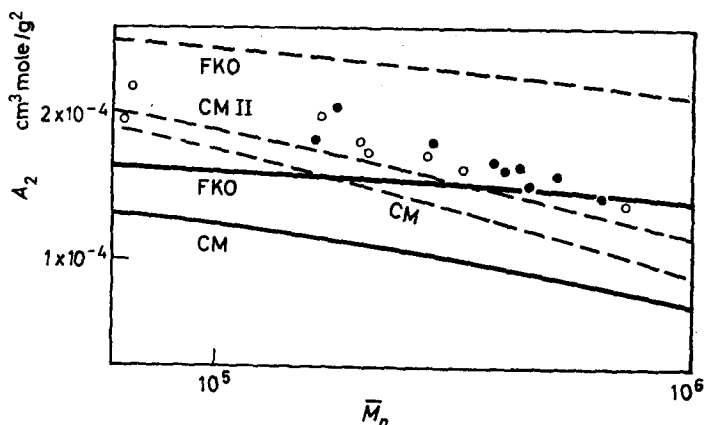


Figure 10—Comparison of log-log plot A_2 versus \bar{M}_n observed for heterogeneous whole polymers ● and fractions ○ of polymethyl methacrylate in acetone at 30° with theoretical curves calculated as described in the text for $f=1$ (solid lines) and for $f=0.4913$ (dashed lines). Values of the parameters used in the calculation of the theoretical curves are: $\Theta=218^\circ\text{K}$, $\psi_1=0.069$, $C_m=5.63 \times 10^{-2}$, $V_1=73$ ml, and $\bar{v}=0.84$ g/ml^{2b}

which is always too low, very much so for $f=1$. The CM II theory probably affords the most satisfactory agreement both in magnitude and slope of A_2 , though it too falls below the experimental points.

The insistence on a linear dependence of $\alpha^5 - \alpha^3$ on $M^{1/2}$ is a rather arbitrary feature of the evaluation we have just described, but it does serve the purpose of making Y invariant with respect to M as is required by the thermodynamic theory. Eliminating $\psi_1(1 - \Theta/T)$ from Y by using equation (9) we can write

$$Y = \frac{(\alpha^5 - \alpha^3)\bar{v}^2}{2V_1 C_m f M^{1/2}} \quad (16)$$

Use of the empirical α determined by^{2b}

$$[\eta] = KM^{1/2}\alpha^3 \quad (17)$$

then gives a value of Y (hence of ψ_1) generally dependent on molecular

weight. In the present case the empirical relations for the polymer fractions in acetone^{2a}

$$[\eta] = 7.7 \times 10^{-5} M^{0.70} \quad (18)$$

and in a Θ solvent^{2b}

$$[\eta]_{\theta} = 4.8 \times 10^{-4} M^{0.50} \quad (19)$$

lead to a value of Y which increases slightly with the molecular weight. At high molecular weights (10^6), the resulting virial coefficients, with the same α used in the function $F(X)$, do not differ much from the FKO and CM curves shown in *Figure 10*; but at low molecular weights the values are much smaller and actually pass through a broad maximum. The agreement with experiment is therefore definitely poorer than that indicated in *Figure 10*.

It should be recalled that the theoretical treatments for A_2 all refer to homogeneous polymers for lack of any adequate formulation for heterogeneous solutes. Our conclusions therefore must surely be regarded with some reservations in connection with whole polymers, but the fact that A_2 is found to be essentially the same for the whole polymers and fractions is encouraging.

We are indebted to Mr O. Kohler and Mrs Sorensen for the ebulliometric data, to Mrs H. Desman for the fractionations and the intrinsic viscosity measurements, to Mr G. Agnew and Dr C. H. McKeever who prepared the methyl methacrylate dimer, trimer and tetramer, and hydrogenated the dimer, and to Mrs E. Cohn-Ginsberg for assistance in the preparation of this manuscript. We are grateful to Dr E. F. Casassa for his suggestions which have been incorporated in the discussion of the second virial coefficient.

Rohm and Haas Company,
Philadelphia, Pennsylvania, U.S.A.

(Received September 1961)

REFERENCES

- ¹ FRANK, H. P. and MARK, H. F. *J. Polym. Sci.* 1951, **6**, 243; 1955, **17**, 1
- ^{2a} COHN-GINSBERG, E., FOX, T. G and MASON, H. F. *Polymer, Lond.* 1962, **3**, 97
- ^b FOX, T. G. *Polymer, Lond.* 1962, **3**, 111
- ^{3a} FOX, T. G., GOODE, W. E., GRATCH, SERGE, HUGGETT, C. R., KINCAID, J. F., SPELL, A. and STROUPE, J. D. *J. Polym. Sci.* 1958, **31**, 73
- ^b COLEMAN, B. D. *J. Polym. Sci.* 1958, **31**, 1955
- ^c BOVEY, F. A. *J. Polym. Sci.* 1961, **46**, 59
- ⁴ FLORY, P. J. *Principles of Polymer Chemistry*, Chap. VIII. Cornell University Press: Ithaca, N.Y., 1953
- ⁵ ALBISETTI, C. J., ENGLAND, D. C., HOGSED, M. J. and JOYCE, R. M. *J. Amer. chem. Soc.* 1956, **78**, 472
- ⁶ VALENTINE, L. J. *Polym. Sci.* 1955, **17**, 263
- ⁷ FOX, T. G and FLORY, P. J. *J. Amer. chem. Soc.* 1948, **70**, 2384
- ⁸ WAGNER, R. H. *Industr. Engng Chem. (Anal.)* 1944, **16**, 520
- ⁹ HOOKWAY, H. T. and TOWNSEND, R. *J. chem. Soc.* 1952, 3190
- ¹⁰ CARTER, S. R. and RECORD, B. R. *J. chem. Soc.* 1939, 660
- ¹¹ MASSON, C. R., MENZIES, R. F., CRUICKSHANK, J. and MELVILLE, H. W. *Nature, Lond.* 1946, **157**, 74
- MASSON, C. R. and MELVILLE, H. W. *J. Polym. Sci.* 1949, **4**, 337

- ¹² MÜNSTER, A. *Z. phys. Chem.* 1951, **197**, 17
- ¹³ FLORY, P. J. *J. Amer. chem. Soc.* 1943, **65**, 372
- ¹⁴ HANSON, W. E. and BOWMAN, J. R. *Industr. Engng Chem. (Anal.)* 1939, **11**, 440
- ¹⁵ FLORY, P. J. *Principles of Polymer Chemistry*, p 533. Cornell University Press: Ithaca, N.Y., 1953
- ¹⁶ FLORY, P. J. and KRIGBAUM, W. R. *J. chem. Phys.* 1950, **18**, 1086
FLORY, P. J. *J. chem. Phys.* 1949, **17**, 1347
- ¹⁷ STOCKMAYER, W. H. and CASASSA, E. F. *J. chem. Phys.* 1952, **20**, 1560.
- ¹⁸ BERGLUND-LARSSON, U., quoted by: FLORY, P. J. *Principles of Polymer Chemistry*, p 280. Cornell University Press: Ithaca, N.Y., 1953
- ¹⁹ KRIGBAUM, W. R. *J. Amer. chem. Soc.* 1954, **76**, 3758
KRIGBAUM, W. R. and FLORY, P. J. *J. Polym. Sci.* 1952, **9**, 503
- ²⁰ BISCHOFF, J. and DESREUX, V. *Bull. Soc. chim. Belg.* 1952, **61**, 10
- ²¹ SCHÖN, K. G. and SCHULZ, G. V. *Z. phys. Chem. (N.S.)*, 1954, **2**, 197
- ²² DOLL, H., quoted by: MEYERHOFF, G. and SCHULZ, G. V. *Makromol. Chem.* 1952, **7**, 294
SCHULZ, G. V. and DOLL, H. *Z. Elektrochem.* 1952, **56**, 248; 1953, **57**, 841
- ²³ BAXENDALE, J. H., BYWATER, S. and EVANS, M. G. *J. Polym. Sci.* 1946, **1**, 237
- ²⁴ SCHULZ, G. V. and DINGLINGER, A. *J. prakt. Chem.* 1941, **158**, 136
- ²⁵ MEYERHOFF, G. and SCHULZ, G. V. *Makromol. Chem.* 1952, **7**, 294
- ²⁶ KRIGBAUM, W. R. and FLORY, P. J. *J. Amer. chem. Soc.* 1953, **75**, 1775
- ²⁷ BAMFORD, C. H. and DEWAR, M. J. *Proc. Roy. Soc. A*, 1948, **192**, 329; 1949, **197**, 356
- ²⁸ BAYSAL, B. and TOBOLSKY, A. V. *J. Polym. Sci.* 1952, **9**, 171
- ²⁹ CHIEN, J.-Y., SHIH, L.-H. and YU, S.-C. *J. Polym. Sci.* 1958, **29**, 117
- ³⁰ BEVINGTON, J. C., MELVILLE, H. W. and TAYLOR, R. P. *J. Polym. Sci.* 1954, **14**, 463
- ^{31a} ARNETT, L. M. *J. Amer. chem. Soc.* 1952, **74**, 2031
^b O'BRIEN, J. L. and GORNICK, F. *J. Amer. chem. Soc.* 1955, **77**, 4757.
- ^{32a} ALLEN, P. W., AYREY, G., MERRETT, F. M. and MOORE, C. G. *J. Polym. Sci.* 1956, **22**, 549
^b AYREY, G. and MOORE, C. G. *J. Polym. Sci.* 1959, **36**, 41
- ³³ BEVINGTON, J. *J. Polym. Sci.* 1958, **29**, 235
- ³⁴ FLORY, P. J. *Principles of Polymer Chemistry*, p 202. Cornell University Press: Ithaca, N.Y., 1953
- ³⁵ FLORY, P. J. and FOX, T. G. *J. Amer. chem. Soc.* 1951, **73**, 1904
- ³⁶ OROFINO, T. A. and FLORY, P. J. *J. chem. Phys.* 1957, **26**, 1067
- ³⁷ CASASSA, E. F. and MARKOVITZ, H. *J. chem. Phys.* 1958, **29**, 493
- ³⁸ CASASSA, E. F. *J. chem. Phys.* 1959, **31**, 800
- ³⁹ STOCKMAYER, W. H. *J. Polym. Sci.* 1955, **15**, 595

PROPERTIES OF DILUTE POLYMER SOLUTIONS I

APPENDIX

Detailed osmotic data on solutions of polymers of methyl methacrylate

| Sample designation and result | 100 $c\rho^{-1}$ g sample | | π/c^* | Sample designation and result | 100 $c\rho^{-1}$ g sample | | π/c^* |
|--------------------------------------|------------------------------|-------|-----------|-------------------------------------|------------------------------|-------|-----------|
| | 100 g soln | | | | 100 g soln | | |
| Fractionated polymethyl methacrylate | | | | | | | |
| XF ₁ B+F ₂ | 0.625±0.004 | 49.6 | | 3F ₅ B&C | | | |
| in acetone | 0.649±0.003 | 51.1 | | in acetone | 0.353±0.003 | 161.5 | |
| $\bar{M}_n=738\ 000$ | 0.660±0.003 | 49.9 | | $\bar{M}_n=166\ 000$ | 0.353±0.003 | 161.5 | |
| $\Gamma_2=95\ \text{cm}^3/\text{g}$ | 0.830±0.002 | 56.6 | | $\Gamma_2=33$ | 0.433±0.002 | 175.1 | |
| | 1.174±0.003 | 71.5 | | | 0.441±0.006 | 177.0 | |
| | 1.264±0.005 | 74.3 | | | 0.443±0.006 | 169.5 | |
| | 1.424±0.003 | 80.8 | | | 0.623±0.01 | 178.3 | |
| | 1.960±0.004 | 102.5 | | | 1.149±0.003 | 196.0 | |
| | 2.600±0.001 | 137.3 | | | 1.241±0.007 | 207.5 | |
| | 2.614±0.006 | 138.2 | | | 1.29 ±0.06 | 208.5 | |
| | 3.485±0.01 | 184.4 | | | 1.537±0.003 | 226.0 | |
| in acetonitrile | 0.867±0.002 | 36.9 | | | 1.619±0.003 | 221.3 | |
| $\bar{M}_n=714\ 000$ | 1.315±0.003 | 32.7 | | | 1.969±0.003 | 242.5 | |
| $\Gamma_2=15$ | 1.977±0.004 | 25.3 | | | 2.057±0.02 | 248.0 | |
| | 2.477±0.003 | 24.65 | | | 2.702±0.006 | 280.8 | |
| | 2.49 ±0.04 | 23.7 | | | 3.69 ±0.03 | 337.5 | |
| | 3.377±0.009 | 22.5 | | | 3.74 ±0.02 | 344.0 | |
| 3F ₁ D | 0.912±0.005 | 126.0 | | in acetonitrile | 0.483±0.001 | 151.3 | |
| in acetone | 0.914±0.01 | 125.9 | | $\bar{M}_n=166\ 000$ | 0.630±0.002 | 152.3 | |
| $\bar{M}_n=278\ 000$ | 1.969±0.002 | 171.0 | | $\Gamma_2=5$ | 0.975±0.004 | 152.8 | |
| $\Gamma_2=46$ | 1.978±0.01 | 170.5 | | | 1.072±0.004 | 143.5 | |
| | 2.65 ±0.01 | 208.8 | | | 1.459±0.001 | 135.9 | |
| | 2.710±0.002 | 210.0 | | | 1.900±0.003 | 144.7 | |
| | 5.98 ±0.04 | 397.0 | | | 2.568±0.01 | 136.2 | |
| in acetonitrile | 0.606±0.001 | 86.7 | | | 3.300±0.003 | 137.5 | |
| $\bar{M}_n=278\ 000$ | 1.162±0.002 | 85.1 | | JK ₁₄ M ₄ C | | | |
| $\Gamma_2=-6$ | 2.08 ±0.001 | 81.5 | | in toluene | 0.278±0.001 | 1263 | |
| | 3.26 ±0.02 | 77.9 | | $\bar{M}_n=20\ 000$ | 0.328±0.001 | 1278 | |
| | | | | $\Gamma_2=8.5$ | 0.490±0.003 | 1287 | |
| 3M ₁ | | | | | 0.771±0.002 | 1323 | |
| in acetone | 0.339±0.003 | 413.0 | | | 0.950±0.01 | 1305 | |
| $\bar{M}_n=65\ 000$ | 0.681±0.006 | 428.0 | | | 1.296±0.003 | 1357 | |
| $\Gamma_2=15$ | 0.828±0.003 | 435.0 | | JK ₄₁ F ₂ | | | |
| | 1.279±0.001 | 448.0 | | in toluene | 0.204±0.002 | 1657 | |
| in acetonitrile | 0.152±0.002 | 381.8 | | $\bar{M}_n=15\ 660$ | 0.315±0.001 | 1680 | |
| $\bar{M}_n=67\ 000$ | 0.311±0.005 | 379.5 | | $\Gamma_2=8.1$ | 0.322±0.001 | 1690 | |
| $\Gamma_2=-4$ | 0.519±0.002 | 378.0 | | | 0.638±0.001 | 1705 | |
| | 0.723±0.004 | 382.0 | | | 1.178±0.001 | 1798 | |
| | 1.06 ±0.02 | 367.0 | | JK ₁₄ M ₅ C&D | | | |
| | 1.536±0.006 | 377.0 | | in toluene | 0.340±0.001 | 2103 | |
| JK ₁₄ M ₂ B | | | | $\bar{M}_n=12\ 300$ | 0.440±0.003 | 2178 | |
| in acetone | 0.483±0.006 | 414.0 | | $\Gamma_2=5.7$ | 0.572±0.001 | 2150 | |
| $\bar{M}_n=64\ 000$ | 0.716±0.004 | 427.2 | | | 0.736±0.002 | 2159 | |
| $\Gamma_2=12.3$ | 0.866±0.005 | 434.2 | | | | | |
| | 1.297±0.05 | 447.8 | | | | | |
| in acetonitrile | 0.760±0.02 | 411.0 | | | | | |
| $\bar{M}_n=63\ 000$ | 0.766±0.001 | 405.0 | | | | | |
| $\Gamma_2=-8$ | 1.009±0.001 | 408.3 | | | | | |
| | 1.484±0.001 | 404.0 | | | | | |

Continued Overleaf

 *Here $\pi = h\rho$ where h is the osmotic height in cm of solution and ρ is the density in g/ml; c is in g/ml.

Appendix—continued

| Sample designation and result | $100 c\rho^{-1}$ g sample | | π/c^* | Sample designation and result | $100 c\rho^{-1}$ g sample | |
|---|------------------------------|--------|------------------------|-------------------------------|------------------------------|--|
| | 100 g soln | | | | 100 g soln | |
| Whole polymers | | | | | | |
| Unfractionated polymethyl methacrylate polymerized with butyl mercaptan | | | | | | |
| JK8 | | | NBM No. 1 | | | |
| in acetone | 1.369 ± 0.002 | 105.6 | in acetone | 0.861 ± 0.001 | 97.6 | |
| $\bar{M}_n = 402\ 000$ | 1.949 ± 0.003 | 135.5 | $\bar{M}_n = 382\ 000$ | 1.236 ± 0.002 | 113.2 | |
| $\Gamma_2 = 61$ | 2.026 ± 0.001 | 141.7 | $\Gamma_2 = 61$ | 1.800 ± 0.004 | 140.6 | |
| | 2.298 ± 0.004 | 152.3 | | 2.753 ± 0.006 | 186.6 | |
| | 3.839 ± 0.001 | 238.2 | | | | |
| in acetonitrile | 1.180 ± 0.001 | 61.0 | in acetonitrile | 0.642 ± 0.005 | 68.6 | |
| $\bar{M}_n = 402\ 000$ | 1.572 ± 0.001 | 55.95 | $\bar{M}_n = 382\ 000$ | 1.582 ± 0.001 | 63.3 | |
| $\Gamma_2 = -5$ | 2.233 ± 0.001 | 56.85 | $\Gamma_2 = -1.7$ | 2.286 ± 0.01 | 68.3 | |
| | 3.296 ± 0.01 | 52.95 | | 3.094 ± 0.001 | 59.5 | |
| JK7 | | | in toluene | | | |
| in acetone | 0.900 ± 0.007 | 112.25 | $\bar{M}_n = 382\ 000$ | 3.184 ± 0.005 | 297.4 | |
| $\bar{M}_n = 285\ 000$ | 1.068 ± 0.002 | 126.3 | | 3.179 ± 0.004 | 295.8 | |
| $\Gamma_2 = 49$ | 1.816 ± 0.000 | 160.2 | | 2.052 ± 0.004 | 198.3 | |
| | 2.528 ± 0.004 | 197.1 | | 1.998 ± 0.004 | 191.7 | |
| | 3.752 ± 0.002 | 265.6 | | 1.72 ± 0.02 | 167.1 | |
| in acetonitrile | 1.242 ± 0.004 | 88.6 | | 1.348 ± 0.002 | 145.4 | |
| $\bar{M}_n = 285\ 000$ | 1.308 ± 0.004 | 90.2 | | 1.075 ± 0.001 | 125.6 | |
| $\Gamma_2 = -2$ | 2.471 ± 0.001 | 84.6 | | 0.893 ± 0.005 | 108.4 | |
| | 2.794 ± 0.004 | 85.5 | NBM No. 2 | | | |
| | 4.052 ± 0.002 | 83.9 | in acetone | 0.574 ± 0.001 | 142.1 | |
| JK6 | | | $\bar{M}_n = 208\ 600$ | 0.655 ± 0.002 | 143.0 | |
| in acetone | 0.892 ± 0.004 | 168.2 | $\Gamma_2 = 35$ | 1.093 ± 0.001 | 160.2 | |
| $\bar{M}_n = 179\ 000$ | 1.513 ± 0.004 | 195.0 | | 1.190 ± 0.004 | 165.6 | |
| $\Gamma_2 = 37$ | 1.785 ± 0.007 | 214.6 | | 2.275 ± 0.003 | 216.2 | |
| | 2.227 ± 0.004 | 229.8 | in acetonitrile | 0.634 ± 0.002 | 123.0 | |
| | 3.518 ± 0.001 | 308.0 | $\bar{M}_n = 208\ 600$ | 1.35 ± 0.01 | 117.7 | |
| | 3.524 ± 0.005 | 307.2 | $\Gamma_2 = -3$ | 1.402 ± 0.001 | 117.6 | |
| in acetonitrile | 0.804 ± 0.002 | 141.7 | | 1.66 ± 0.01 | 117.8 | |
| $\bar{M}_n = 179\ 000$ | 1.282 ± 0.002 | 144.3 | | 2.774 ± 0.001 | 115.3 | |
| $\Gamma_2 = -1.3$ | 1.846 ± 0.003 | 142.5 | | | | |
| | 2.246 ± 0.009 | 140.7 | | | | |
| | 3.44 ± 0.04 | 139.8 | | | | |

Continued Overleaf

*See footnote, page 93.

PROPERTIES OF DILUTE POLYMER SOLUTIONS I

Appendix—continued

| Sample designation and result | 100 cp^{-1} g sample 100 g soln | | π/c^* | Sample designation and result | 100 cp^{-1} g sample 100 g soln | | π/c^* |
|---|---|-------|-----------|-------------------------------|---|-------|-----------|
| | | | | | | | |
| Unfractionated polymethyl methacrylate polymerized without transfer agent | | | | | | | |
| AIN No. 2 | | | | JK3 | | | |
| in acetone | 0.409 ± 0.001 | 49.2 | | in acetone | 0.857 ± 0.001 | 94.5 | |
| $\bar{M}_n = 647\ 000$ | 1.768 ± 0.008 | 104.1 | | $\bar{M}_n = 332\ 000$ | 0.948 ± 0.005 | 108.7 | |
| $\Gamma_2 = 88$ | 1.837 ± 0.003 | 111.0 | | $\Gamma_2 = 51.3$ | 1.93 ± 0.05 | 144.6 | |
| | 3.08 ± 0.02 | 172.0 | | | 2.10 ± 0.02 | 155.5 | |
| | | | | | 3.56 ± 0.03 | 236.2 | |
| in acetonitrile | 0.674 ± 0.001 | 38.58 | | in acetonitrile | 1.019 ± 0.003 | 76.5 | |
| $\bar{M}_n = 647\ 000$ | 1.26 ± 0.03 | 34.05 | | $\bar{M}_n = 317\ 000$ | 1.675 ± 0.003 | 65.1 | |
| $\Gamma_2 = -9$ | | | | $\Gamma_2 = -36$ | 2.08 ± 0.01 | 66.8 | |
| | | | | | 2.08 ± 0.06 | 65.4 | |
| | | | | | 5.00 ± 0.05 | 46.0 | |
| JK4 | | | | AIN A' | | | |
| in acetone | 1.163 ± 0.001 | 87.7 | | in acetone | 0.724 ± 0.002 | 150.8 | |
| $\bar{M}_n = 517\ 000$ | 1.67 ± 0.02 | 113.2 | | $\bar{M}_n = 201\ 000$ | 1.691 ± 0.001 | 192.0 | |
| $\Gamma_2 = 77.5$ | 2.02 ± 0.03 | 133.7 | | $\Gamma_2 = 35$ | 2.347 ± 0.003 | 222.0 | |
| | 2.849 ± 0.003 | 170.7 | | | 2.580 ± 0.005 | 237.4 | |
| | 3.975 ± 0.003 | 243.7 | | | | | |
| | 4.08 ± 0.02 | 245.3 | | | | | |
| in acetonitrile | 0.882 ± 0.001 | 48.75 | | in acetonitrile | 0.736 ± 0.001 | 126.3 | |
| $\bar{M}_n = 517\ 000$ | 1.873 ± 0.001 | 46.45 | | $\bar{M}_n = 201\ 000$ | 1.597 ± 0.004 | 114.7 | |
| $\Gamma_2 = -4$ | 2.99 ± 0.007 | 48.17 | | $\Gamma_2 = -4$ | 2.591 ± 0.004 | 112.0 | |
| | 3.81 ± 0.02 | 45.12 | | | | | |
| AIN No. 4 | | | | JK5 | | | |
| in acetone | 0.669 ± 0.001 | 74.7 | | in acetone | 1.244 ± 0.002 | 197.8 | |
| $\bar{M}_n = 457\ 000$ | 1.172 ± 0.005 | 94.7 | | $\bar{M}_n = 162\ 000$ | 1.610 ± 0.001 | 218.1 | |
| $\Gamma_2 = 65$ | 2.352 ± 0.003 | 146.7 | | $\Gamma_2 = 28.8$ | 2.101 ± 0.001 | 242.8 | |
| in acetonitrile | 0.72 ± 0.02 | 52.8 | | | 3.148 ± 0.002 | 299.0 | |
| $\bar{M}_n = 457\ 000$ | 1.11 ± 0.01 | 49.50 | | | 3.162 ± 0.001 | 309.0 | |
| $\Gamma_2 = -10$ | 2.25 ± 0.03 | 45.33 | | | | | |
| | | | | | | | |
| AIN No. 5 | | | | in acetonitrile | 1.399 ± 0.003 | 151.6 | |
| in acetone | 0.731 ± 0.001 | 80.7 | | $\bar{M}_n = 162\ 000$ | 2.071 ± 0.001 | 151.6 | |
| $\bar{M}_n = 434\ 000$ | 1.288 ± 0.003 | 104.1 | | $\Gamma_2 = -1.4$ | 2.504 ± 0.002 | 156.9 | |
| $\Gamma_2 = 68$ | 2.112 ± 0.001 | 142.0 | | | 3.730 ± 0.006 | 149.6 | |
| | | | | | 3.760 ± 0.008 | 155.6 | |
| in acetonitrile | 0.769 ± 0.004 | 59.85 | | | | | |
| $\bar{M}_n = 434\ 000$ | 1.342 ± 0.002 | 55.9 | | | | | |
| $\Gamma_2 = -4$ | 1.997 ± 0.002 | 53.08 | | | | | |

*See footnote, page 93.

Properties of Dilute Polymer Solutions II

Light Scattering and Viscometric Properties of Solutions of Conventional Polymethyl Methacrylate

E. COHN-GINSBERG, T. G FOX* and H. F. MASON

Light scattering determinations of molecular weight and coil size made at room temperature with three different cells at two wavelengths of incident light and in two solvents (acetone and acetonitrile) on fourteen fractions and six whole polymers of polymethyl methacrylate ranging in molecular weight from 2.7×10^3 to 2.5×10^6 provide a basis for estimation of the validity and reliability of such measurements. It is concluded that the absolute scale for \bar{M}_w may be high by a factor of 1.05 ± 0.05 . Values of $\Phi \times 10^{-21}$ of 2.3 ± 0.2 and 2.6 ± 0.4 obtained in acetone and acetonitrile, respectively, agree with the 'best value' of 2.1 suggested earlier, within the uncertainty (ca. 15 to 20 per cent) arising from the experimental uncertainty in $[\eta]$, M and $(\bar{r}^2)^{3/2}$. The close agreement between $[\eta]/\bar{M}_w$ relationships established herein for conventional polymethyl methacrylate fractions at 30° in benzene, for M from 200 to 2.5×10^6 , and in eight other solvents, with similar results from other laboratories demonstrates that reliable and reproducible dilute solution measurements of $[\eta]$ and of \bar{M}_w are indeed possible.

IN THE preceding paper¹ the validity of techniques for determining the number average molecular weight, \bar{M}_n , by osmotic pressure measurements on dilute solutions of conventional polymethyl methacrylate was investigated. In the present work it is intended to put to similar test determinations of the weight average molecular weight, \bar{M}_w , by light scattering measurements on dilute solutions of these same polymers.

Herein are described light scattering measurements at room temperature, made with three different cells at two different wavelengths of incident light and in two different solvents, on fourteen fractions and six unfractionated polymers ranging in weight average molecular weight (\bar{M}_w) from 2.7×10^3 to 2.5×10^6 . The consistency of these data obtained under different conditions affords a measure of their reliability and reproducibility. Comparison of the ratio of \bar{M}_w/\bar{M}_n for six unfractionated polymers with the value expected from kinetic considerations provides an indication of the validity of the absolute molecular weight scale in the present work. Intrinsic viscosity-molecular weight relations at 30° are also established for polymethyl methacrylate fractions in benzene and in eight other solvents. Comparison with published $[\eta]/\bar{M}_w$ relationships based on other methods for determining \bar{M}_w provides further test of the significance of the present absolute molecular weight determinations.

*Present address: Mellon Institute, Pittsburgh, Pennsylvania.

EXPERIMENTAL

Preparation of polymers and fractionation

The preparation of conventional polymethyl methacrylate samples employed in this study and their isolation and fractionation has been described in the preceding communication¹. Two additional polymers were prepared and fractionated by similar techniques for this study.

Intrinsic viscosity measurements

Data were obtained at four or five concentrations in each case, with the viscometers and by techniques described previously¹. The data are represented satisfactorily by the Huggins equations²

$$\left. \begin{aligned} (\eta_{sp}/c) &= [\eta] + k[\eta]^2c \\ \ln \eta_{rel}/c &= [\eta] - k'[\eta]^2c \end{aligned} \right\} \quad (1)$$

where the parameters $k + k' = 0.5$. The mean value of $k = 0.36 \pm 0.05$ found for polymethyl methacrylate in benzene and in other solvents studied here is in agreement with values obtained previously³ for other polymers in thermodynamically good solvents.

Light scattering measurements

Light scattering measurements were made in a Brice-Phoenix light scattering photometer⁴, with three different light scattering cells, the Brice dissymmetry cell⁴, the Cornell cell⁵ and the Witnauer cell⁶. The photometer-cell combinations were calibrated with the Cornell Turbidity Standard⁷ (the Debye Polystyrene Standard) in toluene and methylethyl ketone.

The Brice-Phoenix differential refractometer⁸ was used to measure the incremental change of refractive index of the solute with concentration. The refractive index increment, dn/dc , for polymethyl methacrylate in acetone at 25°C was 0.136 and 0.134 at wavelengths of 436 m μ and of 546 m μ respectively⁹. Corresponding values of 0.140 and 0.137, respectively, were found for dn/dc in acetonitrile at the same temperature. Values of dn/dc for polymethyl methacrylate in acetone at 546 m μ ranging from 0.107 to 0.134 have been reported¹⁰. However, different workers using different values of dn/dc obtain similar $[\eta]/\bar{M}_w$ relationships, indicating that there may exist differences in the purity of the solvents and/or polymers employed in the different laboratories.

In each case light scattering measurements were made at four or more concentrations. Both the solvent and solutions were clarified by filtration through ultrafine sintered glass filters under positive pressure of dry nitrogen. Unpolarized light was used at two wavelengths, 436 m μ (blue) and 546 m μ (green), for all measurements. In the Brice dissymmetry cell, the scattering ratio (intensity of light scattered at angle θ /intensity of incident light) was obtained at $\theta = 45^\circ$, 90° and 135° . Values of the excess scattering ratio at 90° , S_{90° , over that of the solvent, and of the dissymmetry ratio, $Z_{45^\circ} = S_{45^\circ}/S_{135^\circ}$, were obtained for each concentration. With the Cornell cell and the Witnauer cell the scattering ratio was obtained at five degree intervals from 45° to 135° relative to the direction of the incident light.

The quantity c/S_θ , where c = concentration in g/dl, was plotted versus $\sin^2 \frac{1}{2}\theta$ and extrapolated to zero angle, in order to obtain the value of c/S_0 .

Treatment of light scattering data

Values of the weight average molecular weight were calculated from the equations

$$\left. \begin{aligned} K^* (c/S_0)_{c \rightarrow 0} &= 1/\bar{M}_w \\ K^* &= [2\pi^2 n (dn^2/dc)^2 / \lambda_0^4 N] K_\theta \end{aligned} \right\} \quad (2)$$

where K_θ is a function of θ and may be considered as an instrument calibration constant, N is Avogadro's number, λ_0 is the wavelength of the incident light in air, and n is the refractive index of the solution. Theoretical considerations employed in the extrapolation of osmotic data to infinite dilution^{1, 11} suggest that

$$(c/S_\theta) = [(c/S_0)_{c \rightarrow 0} P^{-1}(\theta)] [1 + 2\Gamma_2 P(\theta)c + 3g\Gamma_2^2 P(\theta)c^2 + \dots] \quad (3-1)$$

where $P(\theta)$ is a correction factor interpolated from a plot of tabulated values of $1/P(\theta)$ and dissymmetries at infinite dilution. Previously we assumed that $g=0.25$. Here it is convenient to assume that $g=P(\theta)/3$. Then

$$(c/S_\theta)^{1/2} = [(c/S_0)_{c \rightarrow 0} P^{-1}(\theta)]^{1/2} [1 + P(\theta)\Gamma_2 c] \quad (c/S_\theta) \leq 4 (c/S_\theta)_{c \rightarrow 0} \quad (3-2)$$

It is expected that plots of $(c/S_\theta)^{1/2}$ versus c should be linear and in accord with equation (3-2) should yield an accurate measure of $(c/S_0)_{c \rightarrow 0} P^{-1}(\theta)$ and an approximation to Γ_2 which does not differ significantly from that obtained from the previous treatment of osmotic pressure data, provided that the limits specified in equation (3-2) are observed and also that the dimensions of the polymer chain are not too large, i.e. provided $P(\theta)$ is not too far from unity.

Values of $(c/S_0)_{c \rightarrow 0}$ obtained by application of equation (3-2) for the extrapolation of $(c/S_0)^{1/2}$ observed at different concentrations in the Cornell or Witnauer cells were inserted directly into equation (2) in the calculation of \bar{M}_w . With the Brice cell, values of $(c/S_0)_{c \rightarrow 0}$ employed in equation (2) were computed from the $(c/S_0)(1/P_{90^\circ})$ obtained as the intercept of plots of $(c/S_{90^\circ})^{1/2}$ and from the tabulated values⁷ of $1/P_{90^\circ}$ corresponding to the dissymmetry at infinite dilution. Values of the latter were obtained from plots of Z_{45° versus c for low values of Z_{45° . At higher values of Z_{45° more linear plots were obtained by plotting $1/(Z_{45^\circ} - 1)$ versus c .

For the Cornell cell, the values of $(c/S_0)_{c \rightarrow 0}$ were multiplied by a factor of 1.25 to correct for attenuation in the incident and scattered light (see discussion in Appendix.)

Values of the mean square radius of gyration, \bar{s}^2 , and of the corresponding mean square end-to-end distance, $\bar{r}^2 = \bar{s}^2/6$, were obtained for $Z_{45^\circ} \geq 1.05$ from tabulated values⁷ for randomly coiled polymer chains corresponding to the observed dissymmetry ratio at infinite dilution. The Zimm method was used to calculate values of \bar{s}^2 and \bar{r}^2 from angular scattering measurements in the Cornell and Witnauer cells. The values thus obtained were in reasonable agreement with those obtained by the dissymmetry method outlined above in the several instances in which checks were made.

RESULTS

Determination of molecular weight

Light scattering measurements were made at room temperature in the Brice dissymmetry cell on fourteen fractions of polymethyl methacrylate in acetone (Tables 1 and 2) and on six of these fractions in acetonitrile (Table 2). Similar determinations (Table 3) were made on five whole polymers in

Table 1. Results on polymethyl methacrylate fractions

| Designation | [η], dl/g, in benzene at 30° | Light scattering data in acetone (Brice cell) | | | | | Osmotic ¹ $\bar{M}_n \times 10^{-5}$ | \bar{M}_w/\bar{M}_n |
|-------------|---|---|--------|-----------------------------|-------|--------------------|--|-----------------------|
| | | $\bar{M}_w \times 10^{-5}$ | | $(r^2)^{1/2}$ in Å | | Γ_2 dl/g | | |
| | | Blue | Green | Blue | Green | | | |
| 4M2B | 3.6 | 24.8 | 25.2 | 1400 | — | 3.90 | — | |
| 23F2 | 3.10 | 20.1 | 20.8 | 1256 | — | 1.79 | — | |
| 4M1A-A | 2.40 | 13.9 | 14.5 | 938 | 937 | — | — | |
| XF1B+F2 | 1.80 | 8.62 | 8.72 | 741 | 757 | 1.03 | 7.26 | |
| 3F1D | 0.89 | 3.62 | 3.56 | — | — | 0.49 | 2.78 | |
| 3F5B+C | 0.58 | 2.25 | 2.21 | — | — | 0.35 | 1.66 | |
| 3M1 | 0.278 | 0.822 | 0.795 | — | — | 0.156 | 0.66 | |
| 14M2B | 0.281 | 0.713 | 0.811 | — | — | 0.110 | 0.64 | |
| 14M2C | 0.246 | 0.683 | 0.570 | — | — | 0.11 | — | |
| 41F2 | 0.122 | 0.210 | 0.229 | — | — | 0.038 | 0.156 | |
| 41F6 | 0.038 | 0.0932 | 0.098 | — | — | 0.026 | — | |
| 42F2 | 0.064 | 0.0505 | 0.0491 | — | — | 0.020 | — | |
| 42F3 | 0.059 | 0.0381 | 0.0428 | — | — | 0.015 | — | |
| 42F10 | 0.050 | 0.0265 | 0.0273 | — | — | 0.0097 | — | |

Table 2. Comparison of light scattering data obtained on acetone and acetonitrile solutions of polymethyl methacrylate fractions

| Designation | [η], dl/g, at 30° | Acetone (Brice cell) | | | Acetonitrile (Brice cell) | | | |
|-------------|-----------------------------|----------------------------|--------------------------------|------------------------|------------------------------|----------------------------|--------------------------------|------------------------|
| | | $\bar{M}_w \times 10^{-5}$ | $(r^2)^{1/2}$ in Å | $\Phi \times 10^{-21}$ | [η], dl/g, at 30°* | $\bar{M}_w \times 10^{-5}$ | $(r^2)^{1/2}$ in Å | $\Phi \times 10^{-21}$ |
| 4M2B | 2.31 | 25.0 | 1400 | 2.14 | 0.62 | 24.2 | 706 | 4.23 |
| 23F2 | 2.01 | 20.5 | 1256 | 2.06 | — | — | — | — |
| 4M1A-A | 1.55 | 14.2 | 938 | 2.66 | 0.47 | 14.6 | 608 | 3.05 |
| XF1B+F2 | 1.11 | 8.65 | 749 | 2.26 | 0.369 | 9.44 | 545 | 2.15 |
| 3F1D | — | 3.60 | — | — | — | 4.05 | — | — |
| 3F5B+C | — | 2.23 | — | — | — | 2.33 | — | — |
| 3M1 | — | 0.81 | — | — | — | 0.825 | — | — |

*Calculated from \bar{M}_w and equations in Table 5.

Table 3. Results on whole polymers of methyl methacrylate

| Designation | [η], dl/g, in benzene at 30° | Light scattering data in acetone (Cornell or Witnauer cell) | | | | $\Phi_{\text{corr.}}^*$ $\times 10^{-21}$ | Osmotic ¹ $\bar{M}_n \times 10^{-5}$ | \bar{M}_w/\bar{M}_n |
|-------------|---|--|-------|-----------------------------|-------|--|--|-----------------------|
| | | $\bar{M}_w \times 10^{-5}$ | | $(r^2)^{1/2}$ in Å | | | | |
| | | Blue | Green | Blue | Green | | | |
| JK 4 | 1.86 | 10.9 | 11.0 | 1 210 | 1 200 | 1.72 | 5.17 | 2.13 |
| JK 3 | 1.40 | 7.85 | 7.26 | 1 080 | 906 | 1.73 | 3.32 | 2.26 |
| JK 5 | 0.80 | 3.89 | 3.64 | — | — | — | 1.62 | 2.28 |
| JK 8 | 1.63 | 8.79 | 8.93 | 634 | 600 | — | 4.02 | 2.19 |
| JK 7 | 1.22 | 4.92 | — | — | — | — | 2.85 | 1.73 |
| JK 6 | 0.857 | 3.84 | 3.49 | — | — | — | 1.79 | 2.07 |

$$^*\Phi_{\text{corr.}} = \frac{[\eta]\bar{M}_w}{(r^2)^{3/2}} \cdot \frac{1}{\gamma}$$

$$\gamma = (Z+1)\Gamma(Z+1.5+3E) \left[\frac{\Gamma(Z+2)}{\Gamma(Z+3+2E)} \right]^{3/2} \frac{1}{\Gamma(Z+1)}$$

$$\frac{Z+1}{Z} = \frac{\bar{M}_w}{\bar{M}_n}; \quad E = \frac{1}{2}(a-1) = 0.066$$

$a = 0.70$ for acetone, cf. Table 5.

[η] in acetone calculated from [η] in benzene from respective equations in Table 5.

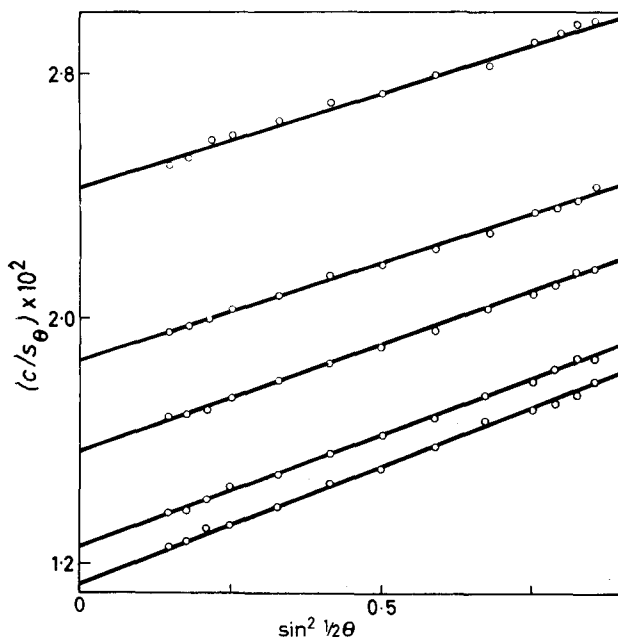


Figure 1—Extrapolation to $\theta=0^\circ$ for the scattering of blue light in the Cornell cell by unfractionated polymethyl methacrylate of $\bar{M}_w=1.1 \times 10^6$ in acetone at 25° at various concentrations (cf. Figure 2)

the Cornell cell and on one whole polymer in the Witnauer cell. Typical plots showing extrapolation of data to zero angle and to infinite dilution are shown in Figures 1 and 2.

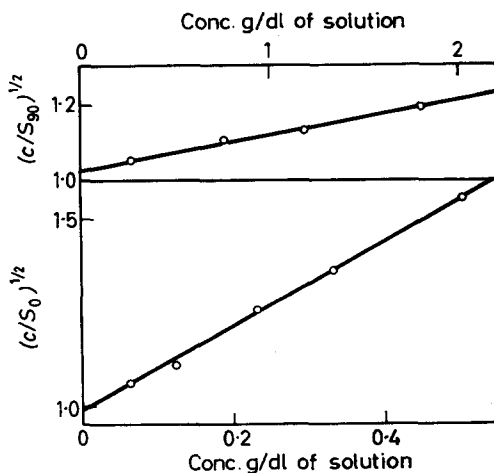


Figure 2—Extrapolation of scattering data from the Brice cell (upper plot) and from the Cornell cell to infinite dilution. Data given for the scattering at 25° of blue light by acetone solutions of a fraction of polymethyl methacrylate of $\bar{M}_w=8.5 \times 10^5$ (upper curve) and of a similar whole polymer of $\bar{M}_w=1.1 \times 10^6$

As indicated in *Figure 1*, plots of (c/S_θ) versus $\sin^2 \frac{1}{2} \theta$ were adequately represented by straight lines, although occasionally the data suggested curvature toward lower values at low angles. In all cases, plots of $(c/S_0)^{1/2}$ or $(c/S_{90})^{1/2}$ versus c were linear, in accord with equation (3-2). Molecular weight values determined on a given sample with blue and with green light agree within four per cent. Larger deviations (ca. 5 to 10 per cent) occur with measurements on unfractionated polymers and polymer fractions of $M < 80\,000$. Comparison of molecular weights determined on the same sample in acetonitrile and in acetone yields an average ratio of 1.04 ± 0.04 . These results indicate an uncertainty of about ± 4 per cent in the present values of \bar{M}_w , with somewhat greater uncertainty (± 5 to 10 per cent) for values of $\bar{M}_w < 80\,000$.

In the preceding paper¹ it was shown that the two series of unfractionated polymers investigated here have the same $[\eta]/\bar{M}_n$ relationship, and it was concluded that the expected value of the ratio of \bar{M}_w/\bar{M}_n is 2.0. The average value of this ratio for the six samples in *Table 3* is 2.11 ± 0.14 . Assuming that the actual ratio is as expected and that the absolute molecular weight scale for osmometry is correct, it appears that the present absolute weight average molecular weight scale may be high by a factor of ca. 1.05 ± 0.07 .

Values of \bar{M}_w/\bar{M}_n range from 1.2 to 1.4 for six of the fractions in *Table 1*. We have commented previously¹ on the difficulty experienced by several investigators in obtaining fractions of conventional polymethyl methacrylate which have $\bar{M}_w/\bar{M}_n < 1.1$. The discovery¹² that conventional polymethyl methacrylate prepared by free radical polymerizations under conditions such as those employed with the present polymers is almost stereoregular enough to crystallize from a moderately concentrated solution in a thermodynamically borderline solvent may provide a clue to the difficulty encountered in obtaining sharp fractions. Conceivably some partial and imperfect crystallization may be induced in the polymeric gel precipitated from the mother liquor thus preventing the escape by diffusion of the occluded soluble low molecular weight species and the attainment of true liquid-liquid equilibrium on which the isolation of sharp fractions depends.

The significance of the Γ_2 values obtained from the slopes of plots of $(c/S_{90})^{1/2}$ versus c is not altogether certain, since no wholly satisfactory theoretical treatment exists for the effect of large dissymmetry on the apparent value of Γ_2 at angles other than 0° . Nevertheless, it is noted that the values in acetone at 30° (in dl/g) are adequately represented by the relation $\Gamma_2 = 2.16 \times 10^{-5} \bar{M}_w^{0.78}$. The Γ_2 values from light scattering measurements are about 20 per cent lower than those calculated from osmotic pressure measurements¹ for fractions of the corresponding number average molecular weight, and are generally 20 per cent or more lower than similar data reported in the literature. Comparison of the observed values of A_2 versus M with the predictions of the theoretical treatment of Casassa¹³ (designated CM II in the preceding paper¹) is shown in *Figure 3*. Agreement of the theory for $f = 0.4913$ with the present data is excellent.

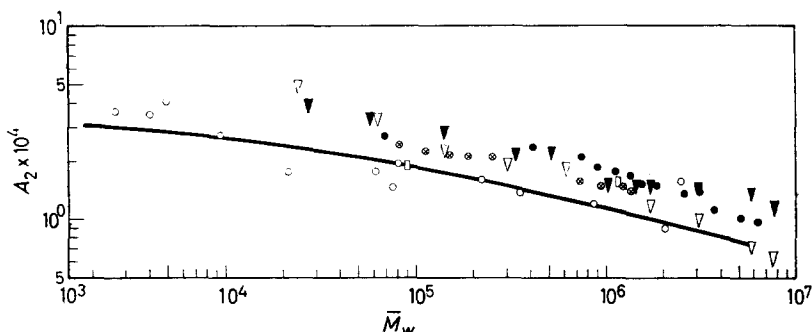


Figure 3—Log-log plot of A_2 versus \bar{M}_w from light scattering data on solutions of polymethyl methacrylate fractions in acetone at 30°: ○ present data; ● Fattakhov *et al.*¹⁵; ⊗ Bischoff and Desreux¹⁶; □ Chien *et al.*¹⁷; ▼ Cantow and Schulz¹⁸; ▽ Cantow and Schulz¹⁸ (sedimentation-diffusion). The solid line was computed by the theory of Casassa¹³ employing the procedure and parameters described in the preceding paper, with $f=0.4913$

Determination of coil size

Values of \bar{r}^2 determined from the dissymmetry ratios in blue and green light appear to be in somewhat better agreement for the fractions (*Table 1*) than for the whole polymers (*Table 2*). For the latter, values of $(\bar{r}^2)^{1/2}$ average about five per cent higher in blue light than in green light, which is within the apparent uncertainty of ± 5 per cent in these data. Values in *Table 2* of the 'universal' factor $\Phi \times 10^{-21}$ defined^{3, 11} as

$$\Phi = [\eta] M / (\bar{r}^2)^{3/2} \quad (4)$$

average 2.3 ± 0.2 in acetone and 3.1 ± 0.7 in acetonitrile. The former is in good accord with the 'best value' of 2.1 established in studies of other systems^{3, 11}. The Φ value in acetonitrile is reminiscent of Krigbaum's observation that the value of Φ is higher in thermodynamically 'borderline' solvents¹⁴. For two of the present samples the values of Φ obtained in the two solvents agree within ten per cent, whereas for the third they differ by a factor of nearly two. If the latter value is disregarded, the average value for Φ in acetonitrile $(2.6 \pm 0.45) \times 10^{21}$ agrees with that for acetone within the previously mentioned uncertainties of five per cent in $(\bar{r}^2)^{1/2}$ and four per cent in \bar{M}_w . Clearly the uncertainties in the experimentally determined values involved in the calculation of Φ are such that the reproducibility in the determination of the value of Φ by the present techniques is no better than ± 15 or 20 per cent. Values of Φ in acetone computed from the data on unfractionated polymers (*Table 3*) corrected for heterogeneity are somewhat lower (*ca.* 1.7×10^{21}) than the corresponding result for the fractions.

Intrinsic viscosity relationship in benzene at 30°

A log-log plot of the values of $[\eta]$ determined on fourteen fractions in benzene at 30° versus the corresponding values of \bar{M}_w determined above (*Table 1*) may be represented (*Figure 4*) by two intersecting straight lines

corresponding to the equations

$$[\eta] = 5.2 \times 10^{-5} \bar{M}_w^{0.76}, \quad \bar{M}_w \geq 35\,000 \quad (5-1)$$

Polymethyl methacrylate
fractions in benzene at 30°

$$[\eta] = 19.5 \times 10^{-4} \bar{M}_w^{0.41}, \quad \bar{M}_w \leq 35\,000 \quad (5-2)$$

Deviations from the lines average less than two per cent in \bar{M}_w . Furthermore, use of equation (5-1) to calculate the viscosity average molecular weight \bar{M}_v from the intrinsic viscosities in benzene observed for the whole polymers (Table 3) yields an average value of $\bar{M}_w/\bar{M}_v = 1.05$ as expected on the basis of their molecular weight distribution. The good agreement of the present result of equation (5-1) with earlier work^{16, 19} is also illustrated in Figure 4. The agreement between the molecular weight over a 100-fold

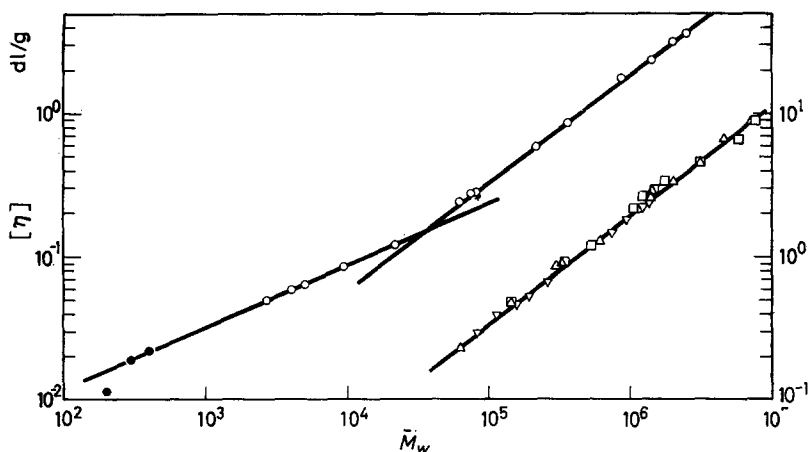


Figure 4—The $[\eta]/\bar{M}_w$ relation of equation (5) (full lines) for fractions of conventional polymethyl methacrylate in benzene at 30°. In this work (upper curve, left ordinate) the molecular weights were obtained by light scattering, \circ , or (for the dimer, trimer and tetramer) ebulliometrically¹, \bullet . Data (lower curve, right ordinate) of Bischoff and Desreux¹⁶, ∇ , and of Cantow and Schulz¹⁹, \square by light scattering and of Meyerhoff and Schulz^{20, 21}, \triangle , from sedimentation-diffusion measurements

range based on light scattering investigations in three laboratories and on the ultracentrifugal determinations of Meyerhoff and Schulz^{20, 21} provides further strong evidence for the reliability and accuracy of the weight average molecular weight values obtained by the present techniques. The $[\eta]/\bar{M}_w$ relationship for conventional polymethyl methacrylate in benzene at 30° has now been investigated for values of M from 200 (the dimer) to nearly 8 000 000.

Intrinsic viscosity-molecular weight relationships at 30° in other solvents

Molecular weight values ranging from 63 000 to 2 600 000 of twenty one fractions of polymethyl methacrylate were calculated by equation (5-1) from

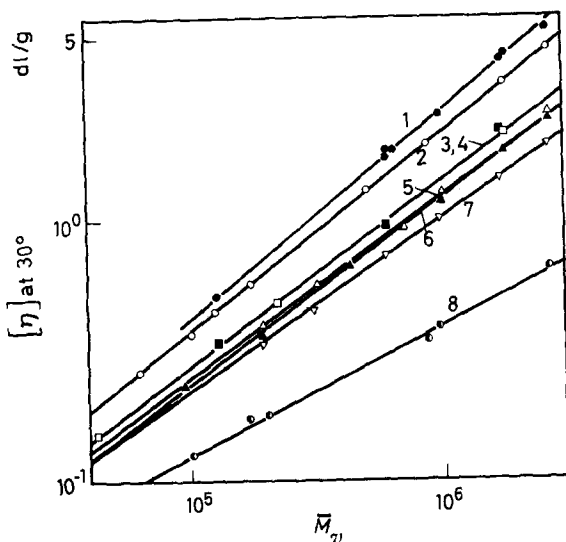


Figure 5—Log-log plot of $[\eta]$ versus \bar{M}_w for conventional polymethyl methacrylate fractions in various solvents at 30°. For curves 1 to 8, respectively, the solvents for the $[\eta]$ measurements are chloroform, dichloroethane, methylethyl ketone, methyl methacrylate, toluene, acetone, methyl isobutyrate and acetonitrile

observed values of $[\eta]$ in benzene at 30°. Intrinsic viscosities of various of these fractions were determined in eight other solvents (*Table 4*). Plots of $[\eta]$ versus \bar{M}_w on a log-log scale (*Figure 5*) are represented by straight lines conforming to the relation

$$[\eta] = K_1 \bar{M}_w^a \quad (6)$$

Values of the parameters K_1 and a corresponding to these straight lines are given in *Table 5* together with corresponding data from the literature. With one or two exceptions, the agreement between the $[\eta]/\bar{M}_w$ relationships determined for a given system in different laboratories is gratifying evidence that reliable and reproducible dilute solution measurements of $[\eta]$ and of \bar{M}_w of polymethyl methacrylate at least are indeed possible if carried out with reasonable care and appropriate techniques.

The present viscosity data were not corrected to zero shear rate, consequently the parameters in equation (5) and in *Table 5* refer to viscosities obtained at the shear rates (3 000 to 6 000 sec^{-1}) which prevail in the Ubbelohde viscometer used here. This shear range is typical of viscometers commonly employed in viscosity measurements of dilute polymer solutions. Correction to zero shear rate would usually yield slightly larger values of a and lower values of K_1 in *Table 5*. Such corrections, which are appreciable (≥ 2 per cent) for $[\eta] \geq 2$, are made in the subsequent papers where the results are compared with theory.

Table 4. Intrinsic viscosity data at 30° in various solvents

| Designation | $M_w \times 10^{-6}$ calc'd from $[\eta]$ in benzene | Benzene | Chloro- form | Dichloro- ethane | Aceto- nitrile | Acetone | Toluene | Methyl- iso- butyrate | Methyl- meth- acrylate | Methyl- ethyl- ketone |
|-------------|---|---------|-----------------|---------------------|-------------------|---------|---------|-----------------------------|------------------------------|-----------------------------|
| 3F10 | 0.063 | 0.233 | — | 0.262 | — | — | — | — | — | — |
| 1F7 | 0.094 | 0.32 | — | — | — | 0.235 | — | — | — | — |
| 3F8 | 0.103 | 0.337 | — | 0.362 | 0.124 | — | — | — | — | — |
| 3F7 | 0.127 | 0.393 | 0.51 | 0.438 | — | — | — | — | 0.335 | — |
| 3F5D | 0.175 | 0.504 | — | 0.567 | 0.17 | — | — | — | — | — |
| 1F5 | 0.192 | 0.542 | — | — | — | 0.35 | 0.405 | 0.35 | — | — |
| 3F4 | 0.200 | 0.556 | — | — | 0.18 | — | — | — | — | — |
| 3F2 | 0.221 | 0.598 | — | — | — | — | — | — | — | 0.470 |
| 1F4 | 0.307 | 0.769 | — | — | — | — | 0.57 | 0.45 | — | — |
| 14M2D | 0.043 | 0.975 | — | — | — | — | — | — | — | 0.149 |
| 1F3D | 0.433 | 1.00 | — | — | — | 0.685 | — | — | — | — |
| 3F1C | 0.5 | 1.12 | — | — | — | — | — | — | — | — |
| 4F3D | 0.590 | 1.27 | 1.71 | — | — | — | — | — | — | — |
| 1F3B | 0.603 | 1.29 | 1.87 | — | — | — | 0.92 | — | 0.93 | — |
| 2F5A | 0.63 | 1.32 | 1.86 | — | — | — | — | 0.74 | — | — |
| 4F3A1 | 0.864 | 1.69 | — | 1.94 | — | — | — | — | — | — |
| 2F4 | 0.98 | 1.86 | 2.53 | — | 0.33 | — | 1.32 | — | — | — |
| 4F1C | 1.1 | 2.03 | — | — | 0.38 | 1.19 | — | 1.00 | — | — |
| 2F3 | 1.73 | 2.86 | 4.17 | 3.30 | — | — | 2.00 | — | — | — |
| 4F1A-E | 1.75 | 2.88 | 4.27 | — | — | 1.86 | — | 1.42 | 2.19 | — |
| 2F2A | 2.63 | 3.94 | 5.40 | 4.54 | 0.65 | 2.40 | 2.62 | 1.98 | — | 2.19 |

PROPERTIES OF DILUTE POLYMER SOLUTIONS II

 Table 5. Parameters of viscosity/molecular weight relations for polymethyl methacrylate in various solvents at 30°: $[\eta] = K_1 M^a$

| Solvent | Present work | | Literature | | | |
|-------------------------------|--------------|-------------------|------------|-------------------|------|----------------------------|
| | <i>a</i> | $K_1 \times 10^5$ | <i>a</i> | $K_1 \times 10^5$ | Ref. | $\bar{M}_w \times 10^{-5}$ |
| Chloroform | 0.80 | 4.3 | 0.82 | 4.88 | 22 | 0.6 -10 |
| | | | 0.80 | 4.8 | 16 | 0.6 -2 |
| | | | 0.80 | 4.85 | 20 | 0.75-70 |
| | | | 0.83 | 3.4 | 23 | 4 -30 |
| Dichloroethane | 0.77 | 5.3 | 0.68 | 17 | 24 | 0.3 -100 |
| Benzene | 0.76 | 195 † | 0.73 | 8.35 | 20 | 0.75-70 |
| | | | 0.76 | 7.24 | 22 | 0.6 -10 |
| | | | 0.76 | 5.5 | 21 | 0.25-70 |
| | | | | | 19 | 0.25-70 |
| Methyl-ethyl ketone | 0.72 | 6.83 | 0.72 | 6.8 | 24 | 0.3 -100 |
| | | | 0.72 | 6.8 | 16 | 7.6 -14 |
| Methyl methacrylate (monomer) | 0.72 | 6.75 | 0.72 | 7.1 | 23 | 4 -30 |
| | | | | | | |
| Acetone | 0.70 | 7.7 | 0.76 | 3.90 | 20 | 0.7 -70 |
| | | | 0.70 | 7.50 | 24 | 0.3 -100 |
| | | | 0.73 | 5.15 | 21 | 0.25-70 |
| | | | 0.70 | 7.5 | 16 | 0.6 -14 |
| Toluene | 0.71 | 7.0 | 0.69 | 9.6 | 23 | 18 -35 |
| | | | 0.73 | 7.1 | 23 | 4 -30 |
| Methyl isobutyrate | 0.67 | 9.9 | | | | |
| Acetonitrile | 0.50 | 39.3 | | | | |

 $^* \bar{M}_w \geq 35\,000$
 $^\dagger \bar{M}_w \leq 35\,000$

Comparison of the present experimental data on the $[\eta]/M$ relationships for polymethyl methacrylate in various solvents with the prediction of an approximate theoretical treatment presented earlier³ is made in the third paper of this series²⁵. A further discussion of this comparison, and particularly of the difference in the $[\eta]/M$ relationships found for low and high molecular weight polymethyl methacrylate in benzene [cf. equations (5) above and equations (4) of the preceding paper], will be given elsewhere²⁶.

We are indebted to H. W. Desman, M. Rich and Dr J. B. Kinsinger for assistance in the preparation and fractionation of the polymers and for the intrinsic viscosity measurements. We are grateful to D. Conlon and to Dr J. F. Woodman for helpful comments offered during the early stages of this work.

Rohm and Haas Company,
Philadelphia, Pennsylvania, U.S.A.

(Received September 1961)

APPENDIX²⁷

The galvanometer deflection g_θ corresponding to scattered light of intensity i_θ reaching the photomultiplier tube when incident light of intensity I_0 traverses a cell containing a solution of turbidity τ is

$$g_\theta \sim I_0 \tau e^{-\tau(l_1+l_2)}$$

where the last factor expresses the attenuation of the incident and scattered light travelling the paths l_1 and l_2 , respectively. Normally I_0 is also measured by sampling some portion of the incident light passing directly through the cell, where

$$g_0 \sim I_0 e^{-\tau(l_1+l_2)}$$

For symmetrical cells such as are usually employed, $l_1 + l_2 = l_1 + l_3$ and $\tau \sim g_\theta/g_0$ directly, i.e. the attenuations which obtain in measuring both I_θ and I_0 being identical cancel out of the calculation of τ_θ .

For a Cornell cell of relatively large dimensions, the attenuation factor may be large. Furthermore, because of the light trap, it is not possible to sample the incident light passing directly through the cell. Instead, the cell is removed and a galvanometer reading g_0 is obtained on a portion of the incident light passing directly through an opal filter. Thus

$$\tau = k_1 (g_\theta/g_0) e^{\tau(l_1+l_2)}$$

The proportionality constant, k_1 , is obtained from the observed value of $(g_\theta/g_0)_s$ for a standard solution of known turbidity τ_s , so that

$$\tau = [(g_\theta/g_0)/(g_\theta/g_0)_s] \cdot \tau_s \cdot e^{-(\tau_s-\tau)(l_1+l_2)}$$

In the limit of infinite dilution for the solute, $\tau=0$ and

$$(c/\tau)_0 = (c/\tau)_0^* e^{\tau_s(l_1+l_2)}$$

where $(c/\tau)_0^* = [(g_\theta/g_0)^{-1} \cdot (g_\theta/g_0)_s \cdot c/\tau_s]_0$ is the 'apparent' value for the turbidity ratios uncorrected for attenuation. The Cornell cell used occasionally in the present work had dimensions of $l_1 = 6.1$ cm and $l_2 = 2.8$ cm. The correction factor, $e^{\tau_s(l_1+l_2)}$, would therefore be about 1.25. Since $(c/S_\theta)_{c \rightarrow 0}$ is proportional to $(c/\tau)_{c \rightarrow 0}$, the 'apparent' values of $(c/S_\theta)_{c \rightarrow 0}$ were multiplied by 1.25. Experimental verification of this was obtained by direct comparison of molecular weight on polymethyl methacrylate fractions and on other polymers measured in both the Cornell and Brice cells.

REFERENCES

- ¹ FOX, T. G., KINSINGER, J. B., MASON, H. F. and SCHUELE, E. M. *Polymer, Lond.* 1962, **3**, P46/61
- ² HUGGINS, M. L. *J. Amer. chem. Soc.* 1942, **64**, 2716
- ³ FOX, T. G. and FLORY, P. J. *J. Amer. chem. Soc.* 1951, **73**, 1909, 1915
- ⁴ BRICE, B. A., HALWER, M. and SPEISER, R. J. *opt. Soc. Amer.* 1950, **40**, 768
- ⁵ DEBYE, P. and ANACKER, E. W. *J. phys. Colloid Chem.* 1951, **55**, 644
- ⁶ WITNAUER, L. P. and SCHERR, H. J. *Rev. sci. Instrum.* 1952, **23**, 99
- ⁷ DOTY, P. and STEINER, R. F. *J. chem. Phys.* 1950, **18**, 1211
- ⁸ BRICE, B. A. and SPEISER, R. J. *opt. Soc. Amer.* 1946, **36**, 363
- ⁹ COHN, E. S. and SCHUELE, E. M. *J. Polym. Sci.* 1954, **14**, 309
- ¹⁰ JOSE, C. I. and BISWAS, A. B. *J. Polym. Sci.* 1958, **27**, 575

PROPERTIES OF DILUTE POLYMER SOLUTIONS II

- ¹¹ FLORY, P. J. *Principles of Polymer Chemistry*. Cornell University Press: Ithaca, N.Y., 1953
- ¹² FOX, T. G., GOODE, W. E., GRATCH, S., HUGGETT, C. R., KINCAID, J. F., SPELL, A. and STROUPE, J. D. *J. Polym. Sci.* 1958, **31**, 173
- ¹³ CASASSA, E. F. *J. chem. Phys.* 1959, **31**, 800
- ¹⁴ KRIGBAUM, W. R. and CARPENTER, D. K. *J. phys. Chem.* 1955, **59**, 1166
- ¹⁵ FATTAKHOV, K. Z., TSVEITKOV, V. N. and KALLISTOV, O. V. *J. exp. theor. Phys., Moscow*, 1954, **26**, 345, 351
- ¹⁶ BISCHOFF, J. and DESREUX, V. *Bull. Soc. chim. Belg.* 1952, **61**, 10
- ¹⁷ CHIEN J.-Y., SHIH L.-H. and YU S.-C. *J. Polym. Sci.* 1958, **29**, 117
- ¹⁸ CANTOW, H. J. and SCHULZ, G. V. *Z. phys. Chem. (N.S.)*, 1954, **2**, 9
- ¹⁹ CANTOW, H. J. and SCHULZ, G. V. *Z. phys. Chem. (N.S.)*, 1954, **1**, 365
- ²⁰ MEYERHOFF, G. and SCHULZ, G. V. *Makromol. Chem.* 1952, **7**, 294
- ²¹ SCHULZ, G. V. and MEYERHOFF, G. *Z. Elektrochem.* 1952, **56**, 904
- ²² BAXENDALE, J. H., BYWATER, S. and EVANS, M. G. *J. Polym. Sci.* 1946, **1**, 237
- ²³ CHINAI, S. N., MATLACK, J. D., RESNICK, A. L. and SAMUELS, R. J. *J. Polym. Sci.* 1955, **17**, 391
- ²⁴ BILLMEYER, F. W. and DE THAN, C. B. *J. Amer. chem. Soc.* 1955, **77**, 4763
- ²⁵ FOX, T. G. *Polymer, Lond.* 1962, **3**, 111
- ²⁶ FOX, T. G. and OROFINO, T. A. To be published
- ²⁷ MASON, H. F. and GARRETT, B. S. Unpublished results presented at the 128th National Meeting of the American Chemical Society, Minneapolis, Minnesota, September 1955

Properties of Dilute Polymer Solutions III

Intrinsic Viscosity/Temperature Relationships for Conventional Polymethyl Methacrylate

T. G Fox

Intrinsic viscosity/temperature relationships from 0° to 120°C determined in a variety of solvents on sixteen fractions of conventional polymethyl methacrylate ranging in molecular weight from 10⁵ to 2.6 × 10⁶ yield, through comparison with existing theory, information on both the intrachain forces and the thermodynamic interactions with the solvent, and their effect on the average dimensions of the polymer coil. The observation that the viscosity at the critical miscibility temperature Θ is $4.8 \times 10^{-4} M^{1/2}$ independent of temperature, from 30° to 70° at least, indicates an average linear dimension for the polymer coil twice that expected for free rotation about the chain bonds; the observed temperature independence indicates that the trans and gauche minima in the potential energy profile on rotation have the same energy. The heat of mixing and the Θ -temperature for polyisobutylene, polystyrene, and polymethyl methacrylate in different solvents are shown to be generally related to (and to increase with) the difference between the Hildebrand solubility parameters for the polymer and the solvent, and other unknown factors which in specific instances play a dominant role. The abnormally low entropy of mixing observed for these solutions indicates a high degree of local order in the packing of solvent molecules and polymer segments as a result of specific interactions dependent on the chemical and geometrical structure of the polymer-solvent pair.

THE RESULTS of an approximate theoretical treatment of the effects of intramolecular interactions of polymer chains in infinitely dilute solutions on their conformation and intrinsic viscosity are summarized in the equations¹⁻³:

$$[\eta] = KM^{1/2}\alpha^3 \quad (1-1)$$

$$\alpha^5 - \alpha^3 = 2C_m\psi_1(1 - \Theta/T)M^{1/2} \quad (1-2)$$

$$K = \Phi(\bar{r}_0^2/M)^{3/2} \quad (1-3)$$

$$\Phi = [\eta]M/(\bar{r}^2)^{3/2} \quad (1-4)$$

$$C_m = 1.4 \times 10^{-24} (\bar{v}^2/V_1) \Phi/K \quad (1-5)$$

Here $[\eta]$ is the intrinsic viscosity in the given solvent of molar volume V_1 at temperature T for a flexible chain molecule of molecular weight M and partial specific volume \bar{v} , and α represents the ratio of $(\bar{r}^2)^{1/2}$, the root-mean-square end-to-end distance for the polymer coil in the given solvent to $(\bar{r}_0^2)^{1/2}$, the corresponding dimension in a solvent at the temperature $T = \Theta$ where the net thermodynamic interaction between the solvent and the polymer segments is zero. Values of the entropy parameter ψ_1 , the critical miscibility temperature Θ , and the constant C_m are, as illustrated by

*Present address: Mellon Institute, Pittsburgh, Pennsylvania.

application of these equations to extensive $[\eta]-T-M$ data for a variety of polymers³, specific for the solvent-polymer pair. Such data indicate K to be a constant characteristic of the polymer and of the temperature, while Φ appears to be a universal constant, of 'best value' 2.1×10^{21} , for long flexible chains.

Herein it is intended to establish $[\eta]-T-M$ relationships for conventional polymethyl methacrylate fractions in various solvents, and to test the applicability of the above equations to these data and to the $[\eta]/\bar{M}$ relationships of the preceding paper⁴. Intrinsic viscosities were measured on polymer fractions in sixteen solvents at temperatures ranging from 0° to 120° and in three solvents at their respective theta (Θ) temperatures (ranging from 31° to 71°C) determined from critical miscibility studies. Application of the procedure outlined earlier^{2,3} for fitting the above equations to such data provides both a test of the adequacy of the relationships and an evaluation of the parameters therein characterizing the unperturbed size of the polymer coil (\bar{r}_0^2/M) and the thermodynamic interaction of the chain segments with various solvents. Comparison with similar parameters obtained for other polymers and solvents and a consideration of the applicability of certain revisions suggested recently in the above theoretical relations will be presented.

EXPERIMENTAL AND RESULTS

Materials

Two polymers in addition to those already mentioned^{4,5} were prepared and fractionated under conditions similar to those described previously⁵.

The solvents employed were of high purity, obtained commercially or prepared in these laboratories and freshly distilled before use.

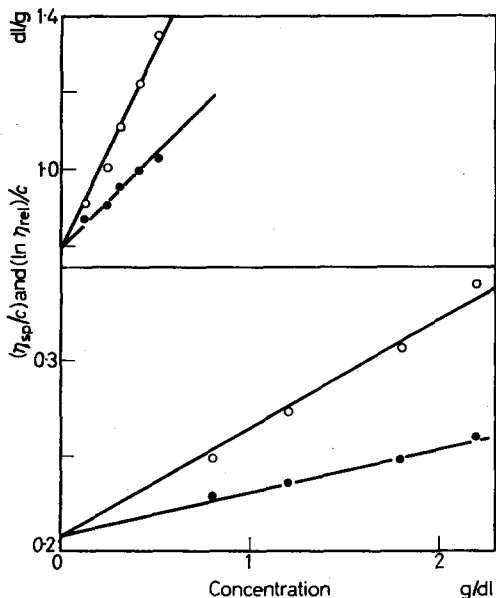


Figure 1—Reduced viscosity/concentration plots for solutions of polymethyl methacrylate fractions for $M=2.6 \times 10^5$ in 4-heptanone at $T=\Theta=35^\circ$ (top) and for $M=2 \times 10^5$ in acetonitrile at $T=42^\circ$, where $\Theta=45^\circ\text{C}$

PROPERTIES OF DILUTE POLYMER SOLUTIONS III

Intrinsic viscosities

Intrinsic viscosities were determined with the viscometers and techniques described earlier^{4,5}. In good solvents the reduced viscosity plots of the data are linear with values of the Huggins constant k of about 0.34 to 0.40 depending on the solvent. The accuracy estimated for $[\eta]$ determined in these solvents is ± 1 per cent. In poor solvents (*Figure 1*) at temperatures at or near Θ , the plots may be non-linear and the Huggins equation does not apply, as was noted earlier for similar data for other polymers^{6,7}. The accuracy estimated for $[\eta]$ determined in these poor solvents is ca. ± 4 per cent.

Measurement of the dependence on the rate of shear γ of the dilute solution viscosity at 30° of polymethyl methacrylate fractions in six solvents were made with the Ostwald viscometer and techniques applied previously to solutions of polyisobutylene⁸. The results were approximately represented by the equations

$$\ln \eta_{sp} = \ln \eta_{sp}^0 - \phi\gamma/100 \quad (2-1)$$

$$\phi = 5 \times 10^{-4} [\eta]^2 / [\eta]_{\text{CHCl}_3} \quad (2-2)$$

Here η_{sp} is the specific viscosity at the rate of shear γ (sec⁻¹); η_{sp}^0 is the corresponding value extrapolated to $\gamma=0$; $[\eta]$ and $[\eta]_{\text{CHCl}_3}$ are the intrinsic

Table 1. Data on the shear dependent viscosities of solutions of fractions of conventional polymethyl methacrylate at 30°C in various solvents

| Designation | $\bar{M}_v \times 10^{-6}$ | Solvent | [η] at zero shear (dl/g) | $\phi \times 10^3$ | |
|-----------------------------------|----------------------------|---------------|---------------------------------------|--------------------|---------------------|
| | | | | Obs. | Calc. by eq. (2) |
| MMA ₂ F ₃ | 1.72 | Chloroform | 4.17 | 2.00 | 2.00 |
| MMA ₂ F ₃ | 1.72 | Dichlorethane | 3.34 | 1.32 | 1.29 |
| MMA ₂ F ₃ | 1.72 | Benzene | 2.89 | 0.87 | 0.95 |
| MMA ₂ F ₃ | 1.72 | Toluene | 2.09 | 0.55 | 0.50 |
| MMA ₂ F ₃ | 1.72 | Acetone | 1.70 | 0.30 | 0.34 |
| MMA ₄ F ₁ C | 1.1 | Chloroform | 3.54 | 1.38 | 1.70 |
| MMA ₂ F ₅ A | 0.62 | Chloroform | 1.86 | 0.90 | 0.90 |
| MMA ₁ F ₃ B | 0.60 | Chloroform | 1.87 | 0.67 | 0.89 |

Table 2. Intrinsic viscosities of fractions of conventional polymethyl methacrylate in benzene at 30°C

| Polymer | [η] (dl/g) | Calc.* $\bar{M}_v \times 10^{-3}$ | Polymer | [η] (dl/g) | Calc.* $\bar{M}_v \times 10^{-3}$ |
|-------------------|----------------------|--------------------------------------|-------------------|----------------------|--------------------------------------|
| 2F ₂ A | 3.91 | 2 610 | 3F ₅ A | 0.622 | 232 |
| 2F ₂ B | 3.04 | 1 940 | 3F ₂ | 0.584 | 227 |
| 2F ₃ | 2.84 | 1 720 | 3F ₄ | 0.556 | 200 |
| HD2F ₂ | 1.66 | 1 680 | 1F ₅ | 0.542 | 192 |
| HD2 | 1.04 | 1 060 | 3F ₅ D | 0.514 | 181 |
| 2F ₄ | 1.86 | 970 | 3F ₇ | 0.393 | 127 |
| 2F ₃ A | 1.69 | 864 | 3F ₈ | 0.337 | 102 |
| 1F ₃ | 1.29 | 600 | 1F ₇ | 0.32 | 94 |
| 4F ₃ D | 1.27 | 590 | 3F ₁₀ | 0.233 | 63 |
| 3F ₁ C | 1.12 | 500 | 11F ₇ | 0.096 | 13.4 |
| 1F ₃ D | 1.00 | 433 | 11F ₆ | 0.103 | 15.9 |
| 1F ₄ | 0.769 | 308 | 11F ₉ | 0.079 | 8.33 |

*Calculated from $[\eta]$ and equations (5) of ref. 4.

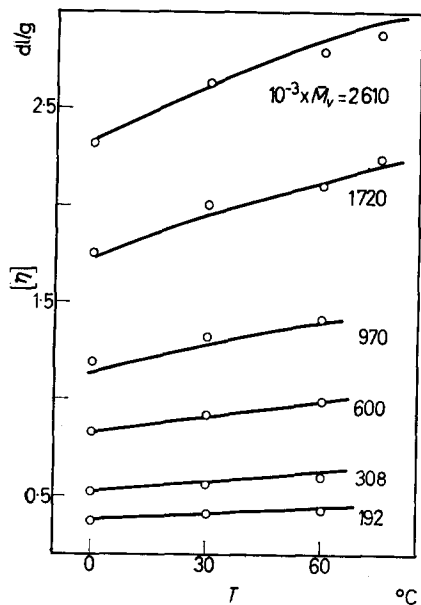


Figure 2— $[\eta]$ - T - M data for poly-methyl methacrylate fractions in toluene. The solid lines were computed by equations (1) with the parameters of Table 7

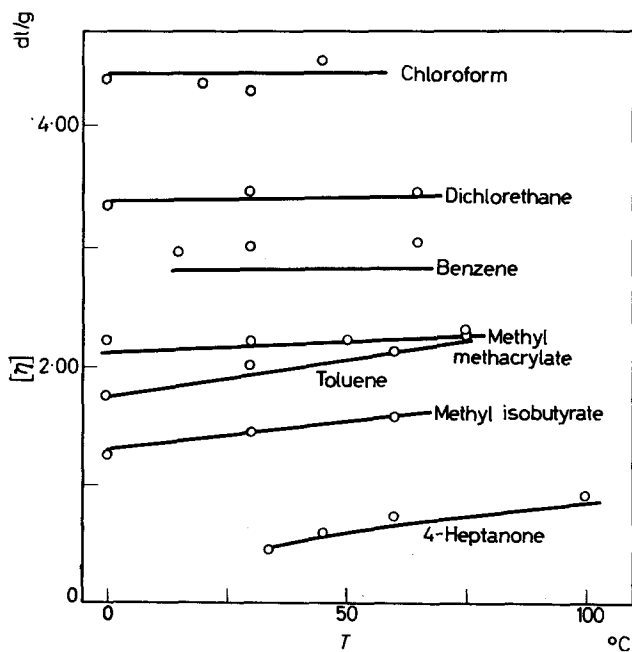


Figure 3— $[\eta]/T$ data in various solvents for polymethyl methacrylate fractions of $10^{-3} M$ of 970 (lowest curve) and of 1720 (others). All curves were computed by equations (1) with the parameters of Table 7

PROPERTIES OF DILUTE POLYMER SOLUTIONS III

 Table 3. $[\eta]$ - T - M data for polymethyl methacrylate fractions in various solvents

| Fraction | $\bar{M}_v \times 10^{-3}$ | $T, ^\circ\text{C}$ | Obs. $[\eta], \text{dl/g}$ | Calc.* $[\eta], \text{dl/g}$ | Fraction | $\bar{M}_v \times 10^{-3}$ | $T, ^\circ\text{C}$ | Obs. $[\eta], \text{dl/g}$ | Calc.* $[\eta], \text{dl/g}$ |
|--------------------------------|----------------------------|---------------------|----------------------------|------------------------------|---------------------------|----------------------------|---------------------|----------------------------|------------------------------|
| Toluene | | | | | Methyl isobutyrate | | | | |
| 2F ₂ A | 2 610 | 0 | 2.32 | 2.32 | 2F ₂ A | 2 610 | 0 | 1.70 | 1.69 |
| | | 30 | 2.62 | 2.62 | | | 30 | 1.98 | 1.93 |
| | | 60 | 2.79 | 2.84 | | | 60 | 2.12 | 2.11 |
| | | 75 | 2.88 | 2.94 | 2F ₃ | 1 720 | 0 | 1.26 | 1.28 |
| 2F ₃ | 1 720 | 0 | 1.75 | 1.73 | | | 30 | 1.42 | 1.45 |
| | | 30 | 2.00 | 1.95 | | | 60 | 1.56 | 1.57 |
| | | 60 | 2.10 | 2.10 | 2F ₄ | 970 | 0 | 0.86 | 0.87 |
| | | 75 | 2.24 | 2.20 | | | 30 | 1.00 | 0.98 |
| 2F ₄ | 970 | 0 | 1.19 | 1.15 | | | 60 | 1.06 | 1.06 |
| | | 30 | 1.32 | 1.29 | 1F ₃ B | 600 | 0 | 0.65 | 0.63 |
| | | 60 | 1.41 | 1.40 | | | 30 | 0.74 | 0.71 |
| 1F ₃ B | 600 | 0 | 0.83 | 0.82 | | | 60 | 0.75 | 0.76 |
| | | 30 | 0.92 | 0.92 | 1F ₄ | 308 | 0 | 0.41 | 0.41 |
| | | 60 | 0.99 | 0.99 | | | 30 | 0.45 | 0.455 |
| 1F ₄ | 308 | 0 | 0.525 | 0.523 | | | 60 | 0.47 | 0.486 |
| | | 30 | 0.57 | 0.58 | 1F ₅ | 192 | 0 | 0.32 | 0.304 |
| | | 60 | 0.60 | 0.62 | | | 30 | 0.35 | 0.332 |
| 1F ₅ | 192 | 0 | 0.37 | 0.382 | | | 60 | 0.38 | 0.355 |
| | | 30 | 0.405 | 0.418 | Benzene | | | | |
| | | 60 | 0.43 | 0.445 | 2F ₃ | 1 720 | 15 | 2.94† | 2.79 |
| Chloroform | | | | | | | 30 | 2.99† | 2.80 |
| 2F ₂ A | 2 610 | 0 | 6.14† | 6.05 | | | 65 | 3.03† | 2.83 |
| | | 30 | 6.25† | 6.05 | 1F ₃ B | 600 | 10 | 1.22 | 1.28 |
| | | 45 | 6.44† | 6.05 | | | 30 | 1.29 | 1.29 |
| 2F ₃ | 1 720 | 0 | 4.37† | 4.42 | | | 60 | 1.29 | 1.29 |
| | | 20 | 4.35† | 4.42 | 1F ₄ | 308 | 10 | 0.726 | 0.79 |
| | | 30 | 4.28† | 4.42 | | | 30 | 0.764 | 0.795 |
| | | 45 | 4.54† | 4.42 | 1F ₅ | 192 | 30 | 0.550 | 0.565 |
| 2F ₄ | 970 | 0 | 2.80† | 2.86 | | | 60 | 0.542 | 0.565 |
| | | 20 | 2.78† | 2.86 | | | 60 | 0.542 | 0.570 |
| | | 30 | 2.72† | 2.86 | Acetonitrile | | | | |
| | | 45 | 2.77† | 2.86 | 2F ₂ A | 2 610 | 0 | 0.29 | — |
| 3F ₇ | 127 | 0 | 0.554 | 0.626 | | | 30 | 0.67 | — |
| | | 20 | 0.53 | 0.626 | | | 42 | 0.83 | 0.675 |
| | | 30 | 0.51 | 0.626 | | | 45 | 0.93 | 0.776 |
| | | 45 | 0.53 | 0.626 | | | 45 | 0.98 | 0.776 |
| Dichlorethane | | | | | | | 50 | 0.90 | 0.895 |
| 2F ₃ | 1 720 | 0 | 3.32† | 3.36 | | | 65 | 1.27 | 1.13 |
| | | 30 | 3.45† | 3.39 | 2F ₄ | 970 | 30 | 0.38 | — |
| | | 65 | 3.44† | 3.42 | | | 45 | 0.50 | 0.473 |
| 4F ₃ A | 864 | 0 | 1.96† | 2.02 | | | 50 | 0.54 | 0.52 |
| | | 30 | 1.99† | 2.03 | 4F ₃ A | 864 | 30 | 0.33 | — |
| | | 65 | 1.99† | 2.04 | | | 42 | 0.43 | 0.41 |
| 3F ₈ | 102 | 0 | 0.37 | 0.42 | | | 50 | 0.425 | 0.485 |
| | | 30 | 0.36 | 0.43 | | | 65 | 0.59 | 0.58 |
| Methyl methacrylate | | | | | | | 30 | 0.17 | 0.183 |
| 2F ₃ | 1 720 | 0 | 2.20 | 2.12 | | | 42 | 0.19 | 0.221 |
| | | 30 | 2.19 | 2.18 | | | 50 | 0.20 | 0.24 |
| | | 50 | 2.22 | 2.22 | | | 65 | 0.21 | 0.27 |
| | | 75 | 2.31 | 2.25 | 3F ₄ | 200 | 30 | 0.196 | 0.174 |
| 4F ₃ D | 590 | 30 | 0.93 | 1.01 | | | 42 | 0.208 | 0.207 |
| | | 50 | 0.97 | 1.02 | | | 50 | 0.22 | 0.223 |
| 3F ₇ | 127 | 30 | 0.335 | 0.347 | | | 65 | 0.25 | 0.248 |
| | | 50 | 0.33 | 0.350 | 3F ₈ | 102 | 30 | 0.124 | 0.134 |
| Acetone | | | | | | | 42 | 0.14 | 0.15 |
| 2F ₂ A | 2 610 | 0 | 2.21 | 2.07 | | | 50 | 0.146 | 0.158 |
| | | 30 | 2.44 | 2.40 | | | 65 | 0.163 | 0.173 |
| | | 30 | 2.40 | 2.40 | 4-Heptanone | | | | |
| | | 46 | 2.60 | 2.53 | 2F ₄ | 970 | 33.8 | 0.45 | 0.47 |
| HD ₂ F ₂ | 1 680 | 20 | 1.63 | 1.69 | | | 45 | 0.585 | 0.57 |
| | | 30 | 1.72 | 1.76 | | | 60 | 0.72 | 0.66 |
| | | 40 | 1.79 | 1.82 | | | 100 | 0.90 | 0.84 |
| Acetone | | | | | | | 33.8 | 0.26 | 0.266 |
| | | 0 | 2.21 | 2.07 | | | 45 | 0.297 | 0.30 |
| | | 30 | 2.44 | 2.40 | 1F ₄ | 308 | 60 | 0.333 | 0.335 |
| | | 30 | 2.40 | 2.40 | | | 60 | 0.333 | 0.335 |
| | | 46 | 2.60 | 2.53 | 11F ₆ | 159 | 33.8 | 0.065 | 0.060 |
| | | 20 | 1.63 | 1.69 | | | 45 | 0.073 | 0.062 |
| | | 30 | 1.72 | 1.76 | | | 60 | 0.078 | 0.064 |
| | | 40 | 1.79 | 1.82 | 4-Heptanone | | | | |

Continued overleaf

Table 3. Continued

| Fraction | \bar{M}_w $\times 10^{-3}$ | T, °C | Obs. $[\eta]$, dl/g | Calc.* | Fraction | \bar{M}_w $\times 10^{-3}$ | T, °C | Obs. $[\eta]$, dl/g | Calc.* | | |
|---|---------------------------------|-------|----------------------|--------|--------------------|---------------------------------|-------|----------------------|--------|-------|------|
| Tentative results from preliminary measurements | | | | | | | | | | | |
| Methylethyl ketone | | | | | 2-Octanone | | | | | | |
| HD ₂ F2 | 1 680 | 20 | 1.95 | 1.97 | HD ₂ F2 | 1 680 | 80 | 1.02 | 1.01 | | |
| | | 30 | 2.02 | 2.00 | | | 100 | 1.25 | 1.24 | | |
| | | 35 | 2.06 | 2.02 | | | 120 | 1.37 | 1.42 | | |
| | | 40 | 2.06 | 2.04 | | | HD2 | 1 060 | 80 | 0.764 | 0.75 |
| | | 50 | 2.07 | 2.07 | | | | | 100 | 0.66 | 0.91 |
| | | 50 | 2.09 | 2.07 | | | | | 120 | 1.01 | 1.04 |
| 60 | 2.10 | 2.11 | | | | | | | | | |
| Amyl acetate | | | | | 3-Heptanone | | | | | | |
| HD ₂ F2 | 1 680 | 50 | 0.85 | 0.86 | HD ₂ F2 | 1 680 | 30 | 0.80 | 0.74 | | |
| | | 70 | 1.14 | 1.15 | | | 70 | 1.28 | 1.30 | | |
| | | 80 | 1.25 | 1.26 | | | 100 | 1.46 | 1.53 | | |

*Calculated by equations (1) with the parameters of Table 7.

†Corrected to zero shear rate by equation (2).

viscosities in the chosen solvent and in chloroform, respectively, and ϕ is the percentage decrease in η_{sp} per unit increase in γ . The agreement between the calculated and observed values of ϕ is illustrated in Table 1. Corrections to zero shear rate of the viscosity data on the high molecular weight fractions in the three solvents (chloroform, dichlorethane and benzene) yielding the highest correction (ca. 3 to 18 per cent) were made in a manner analogous to that described previously⁸. Conceivably the additional uncertainty in $[\eta]$ for the corrected data may be ca. 1 or 2 per cent. Corrections in the other solvents were not made since for these generally $\phi < 5 \times 10^{-4}$ and the corresponding corrections were small (< 3 per cent).

Equations (2) are approximate, and additional studies would be needed if more precise knowledge of the viscosity/shear rate dependence is desired. We note, however, that for the molecular weight range investigated (ca. 10^5 to 10^6) the magnitudes of the effect for polymethyl methacrylate and polyisobutylene at the same molecular weight and $[\eta]$ are similar, although the values of ϕ are higher for the latter polymer when compared at the same $[\eta]$ and chain length.

Molecular weights for all of the fractions were calculated from the observed values of $[\eta]$ in benzene at 30° (Table 2) employing equations (5) of the preceding study⁴.

Intrinsic viscosity data obtained at several temperatures are presented in Table 3 and illustrated in plots of $[\eta]/T$ in Figures 2 and 3.

Determination of precipitation temperatures

The critical precipitation temperature for a polymethyl methacrylate fraction in a chosen solvent was determined by preparing several solutions at concentrations in the vicinity of the theoretical critical volume fraction v_c of the polymer⁹. The temperature T_p at which the stirred solution became turbid on slow cooling was recorded for each concentration. The maximum temperature T_c for the coexistence of two phases was obtained with adequate precision (0.3°C) from measurements at four or five concentrations. The critical temperature T_c and critical volume fraction of polymer v_c for

complete miscibility in a given solvent should depend on M as

$$T_c \approx \Theta (1 - b/M^{1/2}) \tag{3-1}$$

$$b = (V_1/\bar{v})^{1/2} \psi_1^{-1} \tag{3-2}$$

$$v_c \approx (V_1/\bar{v})^{1/2} / M^{1/2} \tag{3-3}$$

The desired quantity Θ is obtained as the intercept in the plot of T_c versus $M^{-1/2}$, whereas the value of ψ_1 is calculated from the slope and intercept of this line.

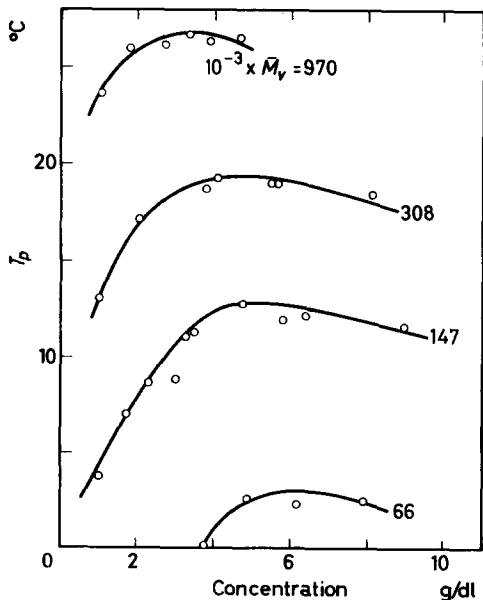
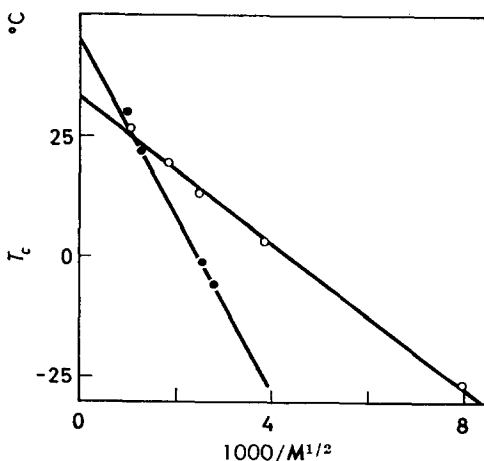


Figure 4 — Precipitation temperatures versus concentration for polymethyl methacrylate fractions in 4-heptanone

Figure 5 — $T_c/M^{-1/2}$ for polymethyl methacrylate fractions in 4-heptanone (○) and in acetonitrile (●)



Precipitation temperatures T_p were obtained on seventeen fractions and in seven different solvents. Values of T_c and v_c obtained from these maxima in the observed T_p/v curves (Figure 4) are summarized in Table 4. Values

Table 4. Critical precipitation data on fractions of conventional polymethyl methacrylate in various solvents

| Solvent and parameters | Fraction | $\bar{M}_v \times 10^{-3}$ | T_c (°C) | $v_c \times 10^2$ |
|---|---------------------|----------------------------|------------|-------------------|
| 3-Octanone $\Theta = 72^\circ\text{C}$ $b = 29$ $\psi_1 = 0.48$ | 2F ₄ | 970 | 61 | 2.3 |
| | 4F ₃ 1-A | 860 | 60 | 3.0 |
| | 1F ₄ | 308 | 52.5 | 4.0 |
| | 3F ₆ | 147 | 46.5 | 5.5 |
| | 3F ₇ | 127 | 42.4 | 5.0 |
| 2-Octanone $\Theta = 52^\circ\text{C}$ $b = 25$ $\psi_1 = 0.55$ | — | 1 400 | 48 | 2.6 |
| | 2F ₄ | 970 | 44.5 | — |
| | 3F ₁ G | 135 | 26 | 5.7 |
| | — | 55 | 18 | 6.7 |
| Diisopropyl ketone $\Theta = 46^\circ\text{C}$ $b = 32$ $\psi_1 = 0.41$ | 2F ₄ | 970 | 35.0 | (1) |
| | 1F ₄ | 308 | 26.7 | (1) |
| | 3F ₇ | 127 | 17.0 | (1.8) |
| | — | — | — | — |
| Acetonitrile $\Theta = 45^\circ\text{C}$ $b = 56.5$ $\psi_1 = 0.145$ | 2F ₄ | 970 | 30.0 | 3.5 |
| | 4F ₃ D | 590 | 21.5 | 5.0 |
| | 3F ₆ | 147 | -1.5 | 6.0 |
| | 3F ₇ | 127 | -6.0 | 9.0 |
| Methyl neopentyl ketone $\Theta \approx 35^\circ\text{C}$ | 2F ₄ | 970 | 28.4 | 4.45 |
| | — | — | — | — |
| 4-Heptanone $\Theta = 33.8^\circ\text{C}$ $b = 23.6$ $\psi_1 = 0.50$ | 2F ₄ | 970 | 26.8 | 3.0 |
| | 1F ₄ | 308 | 19.4 | 4.8 |
| | 3F ₆ | 147 | 13.0 | 5.0 |
| | 5F1-A | 66.4 | 3.2 | 6.5 |
| | 11F ₆ | 15.9 | -27.0 | (22) |
| 2-Ethyl butyraldehyde $\Theta = 22^\circ\text{C}$ $b = 38.6$ $\psi_1 = 0.32$ | 2F ₄ | 970 | 11.7 | — |
| | 4F ₃ D | 590 | 7.7 | 4.2 |
| | 3F ₇ | 127 | (-8.5) | — |
| | — | — | — | — |

of Θ , b and ψ_1 determined according to equations (3-1) from linear plots of $T_c/\bar{M}^{-1/2}$ (Figure 5) are also summarized in Table 4.

CALCULATION AND DISCUSSION

Evaluation of K

Values of $K \times 10^4$ (Table 5) were computed by equation (1-1) from intrinsic viscosities measured at the observed Θ -temperature (where $\alpha = 1$) in 3-octanone at 72° , in acetonitrile at 45° , and in three samples of 4-heptanone (evidently differing in purity) at their respective Θ -temperatures of 31.5° , 33.8° and 35.0° , employing sixteen different fractions of polymethyl methacrylate. Although the K/T coefficient indicated from the data in different solvents is slightly positive, contrary to the behaviour observed for other polymers^{6,7}, the small increase (ca. 6 per cent in 40°) is within the experimental uncertainty in these determinations. Thus, in seventeen of nineteen instances for fractions ranging in \bar{M}_v from 1.3×10^4 to 2.6×10^6 the average value of $K \times 10^4$ is 4.8 ± 0.2 , i.e.

$$[\eta]_0 = 4.8 \times 10^{-4} (\bar{M}_v)^{1/2} \quad (4)$$

PROPERTIES OF DILUTE POLYMER SOLUTIONS III

 Table 5. Values of K determined for various solutions of fractions of conventional polymethyl methacrylate at $T = \Theta$

| Solvent | Θ (°C) | Fraction | \bar{M}_v $\times 10^{-3}$ | $[\eta]$ in dl/g at $T = \Theta$ | $K \times 10^4$ |
|-------------------------|------------------|--------------------|---------------------------------|--|-----------------|
| 4-Heptanone Sample 1 | 31.5* | 2F ₂ B | 1 940 | 0.64 | 4.7 |
| | | 1F ₃ D | 433 | 0.28 | 4.3 |
| 4-Heptanone Sample 2 | 35.0* | 2F ₂ A | 2 610 | 0.80 | 4.9 |
| | | 2F ₄ | 970 | 0.48 | 4.8 |
| | | 3F ₈ | 102 | 0.148 | 4.6 |
| 4-Heptanone Sample 3 | 33.8* | 2F ₃ | 1 720 | 0.57 | 4.3 |
| | | 2F ₄ | 970 | 0.45 | 4.6 |
| | | 1F ₄ | 308 | 0.26 | 4.7 |
| | | 11F ₆ | 15.9 | 0.065 | 5.1 |
| | | 11F ₇ | 13.4 | 0.056 | 4.8 |
| | | 11F ₉ | 8.33 | 0.061 | 6.7 |
| | | Trimer | 0.30 | 0.0176 | 10 |
| | | Dimer | 0.20 | 0.0097 | 6.9 |
| Acetonitrile | 45.0 | 2F ₂ A | 2 610 | 0.92 | 5.7 |
| | | 2F ₄ | 970 | 0.50 | 5.1 |
| | | 4F ₃ A1 | 864 | 0.45 | 4.8 |
| | | 3F ₄ | 200 | 0.215 | 4.8 |
| | | 3F ₅ A | 232 | 0.20 | 4.2 |
| | | 3F ₈ | 102 | 0.15 | 4.7 |
| 3-Octanone | 72.0 | 2F ₂ A | 2 610 | 0.785 | 4.8 |
| | | 2F ₄ | 970 | 0.525 | 5.3 |
| | | 3F ₇ | 127 | 0.176 | 4.9 |

*Data on solvent samples 1, 2 and 3 were determined independently on different occasions (1950, 1952 and 1953).

for $\bar{M}_v \geq 10^4$, $70^\circ \geq \Theta \geq 31^\circ$. Deviations from equation (4) occur at lower chain lengths. An appreciably higher value of $K = 5.92 \times 10^{-4}$ in a 50:50 mixture of butanone and isopropanol at 25° was reported earlier¹⁰.

Unperturbed coil dimensions

Values of $(\bar{r}_0^2/Z)^{1/2}$ computed for a variety of polymers by equation (1-3) from the observed values of K and by assuming $\Phi = 2.1 \times 10^{21}$ are given in Table 6. Here Z is the number of chain atoms in the polymer molecule. The corresponding ratio $(\bar{r}_0^2/\bar{r}_{00}^2)^{1/2}$ (Table 6) computed from the corresponding values of (\bar{r}_{00}^2/Z) , with free rotation and the usual values for bond lengths and angles, characterizes the expansion in the equilibrium dimensions of the polymer coil arising from the intramolecular hindrances to rotations within the chain.

The present data indicate for the coil expansion factor of conventional polymethyl methacrylate a value (2.0) intermediate between the extremes (1.4 and 2.5) observed for other polymers, with an apparent uncertainty of about 0.1 unit in the relative value of this ratio. The constancy of K/T found here implies that \bar{r}_0^2 for this polymer is independent of temperature, and therefore that in the potential energy profile versus rotational angle the minima occurring at the trans and gauche positions have the same energy.

Table 6. Unperturbed end-to-end distances computed from K values

| Polymer | T (°C) | $K \times 10^4$ | $(\bar{r}_0^2/M)^{1/2}$ | $(\bar{r}_0^2/Z)^{1/2}$ | $(\bar{r}_0^2/\bar{r}_{0f}^2)^{1/2}$ |
|--|-------------|-----------------|-------------------------|-------------------------|--------------------------------------|
| | | | $\times 10^{11}$ | $\times 10^8$ | |
| Poly- <i>n</i> -hexyl methacrylate ¹¹ | 32.6 | 4.30 | 595 | 5.50 | 2.51* |
| Polystyrene ¹² | ca. 25 | 8.3 | 735 | 5.30 | 2.42 |
| Poly- <i>n</i> -octyl methacrylate ¹³ | 16.8 | 2.68 | 503 | 5.01 | 2.31* |
| Polyvinyl acetate ^{14, 15} | 0 | 9.2 | 760 | 5.00 | 2.29 |
| Polyethyl methacrylate ¹⁶ | 23.0 | 4.73 | 609 | 4.60 | 2.10* |
| Poly- <i>n</i> -butyl methacrylate ¹⁷ | 4.5 | 2.95 | 520 | 4.38 | 2.00* |
| Polymethyl methacrylate ¹⁰ | 25 | 5.92 | 656 | 4.65 | 2.10* |
| Present work | 30 to 70 | 4.8 | 612 | 4.34 | 1.98 |
| Polyacrylic acid ¹² | 30.0 | 7.6 | 710 | 4.26 | 1.95 |
| Polyisobutylene ¹² | 24 | 10.6 | 795 | 4.20 | 1.92 |
| Polyethylene ¹⁸ | 140 | — | 1 070† | 4.00† | 1.83† |
| Natural rubber ¹² | 0 to 60 | 11.9 | 830 | 3.42 | 1.71 |
| Polydimethyl siloxane ¹² | 20 | 8.1 | 730 | 4.45 | 1.60 |
| Gutta percha ¹² | 60 | 23.2 | 1 030 | 4.25 | 1.46 |

*These values of \bar{r}_0^2 calculated from K differ somewhat from those given in the original references by Chinai and co-workers since the latter are based on light scattering data which do not always correspond to the 'best value' of $\Phi = 2.1 \times 10^{21}$ used here.

† (\bar{r}_0^2/M) was computed in ref. 18 by combining viscosity/molecular weight data and virial coefficient data for polyethylene in α -chloronaphthalene at 135°C.

Attempts to correlate the values of $(\bar{r}_0^2/\bar{r}_{0f}^2)^{1/2}$ for different polymers with the structure of the monomer unit may be of limited significance, since the coil dimensions may also depend on the unknown stereochemical and/or geometrical arrangement of the units relative to each other in the chain. Thus the fact that this ratio for the methacrylate ester series does not increase in a regular fashion with increasing length of the side chain conceivably might reflect differences in stereochemical structures that are dependent on differences in the condition chosen for the polymerizations. The data of Table 6 do illustrate clearly that this 'coil expansion ratio' cannot be taken as a measure of 'stiffness' insofar as the mobility of the polymer segment is concerned, since there is no correlation between values of $(\bar{r}_0^2/\bar{r}_{0f}^2)^{1/2}$ for various polymers and their corresponding glass temperatures. Thus 'rubbers' with low glass temperatures such as polydimethyl siloxane, polyethylene, and polyhexyl methacrylate appear at the bottom, middle and top of Table 6, and polystyrene and polymethyl methacrylate possessing nearly the same high glass temperature are widely separated on this scale. Similarly, there appears to be no unique relation between the glass temperature, T_g , and the difference, ΔE_0 , in energy of the two minima in the potential energy curve on rotation about the valence bond. Thus polyisobutylene¹⁹ and polymethyl methacrylate having small values for

PROPERTIES OF DILUTE POLYMER SOLUTIONS III

ΔE_0 differ greatly in T_g , whereas polyethylene¹⁹ with a relatively high value of ΔE_0 exhibits a low T_g .

Evaluation of thermodynamic parameters

For the polymethyl methacrylate fractions, the thermodynamic parameters in equations (1) were evaluated by the scheme used previously^{2,3} based on the assumption that K is a constant characteristic of the polymer and unaffected by specific interactions with the solvent. Thus, values of $\alpha^3 = [\eta]/KM^{1/2}$ and of $(\alpha^5 - \alpha^3)/M^{1/2}$ were computed in each case from the measured value of $[\eta]$ and of M , and the values of θ and of $2C_m\psi_1\theta$ were determined for each solvent for the polymer from the slope and intercept, respectively, of the best straight line representing plots of $(\alpha^5 - \alpha^3)/M^{1/2}$ versus T^{-1} . Recognizing that C_m is to a sufficient approximation independent of temperature and given by $4.11V_1^{-1}$ (where V_1 is the molar volume of the solvent at 27°C) and using the numerical values, $\bar{v} = 0.821^{20}$, $K = 4.8 \times 10^{-4}$, $\Phi = 2.1 \times 10^{21}$, one can deduce ψ_1 from the above results. Values of Θ and of ψ_1 so obtained, and of the heat of mixing parameter $\kappa_1 = \psi_1\Theta/T$, are summarized in Table 7.

Table 7. Approximate values for the thermodynamic parameters for polymethyl methacrylate from $[\eta]$ - T - M data in various solvents

| Solvent | *Best values | | $T = 300^\circ K$ | |
|---|--------------------|----------|-------------------|----------|
| | $\Theta, ^\circ K$ | ψ_1 | κ_1 | χ_1 |
| Chloroform | 0* | 0.136† | 0† | 0.364 |
| Dichlorethane | 40* | 0.093† | 0.0124† | 0.419 |
| Benzene | 50* | 0.076† | 0.0127 | 0.437 |
| Methyl methacrylate | 110* | 0.070† | 0.026† | 0.466 |
| Toluene | 208 ± 10 | 0.110† | 0.076† | 0.466 |
| Acetone | 218 ± 10 | 0.069‡ | 0.050‡ | 0.481 |
| Methyl isobutyrate | 220 ± 10 | 0.067‡ | 0.049‡ | 0.482 |
| 4-Heptanone | 307 ± 10 | 0.08† | 0.0815† | 0.5015 |
| Acetonitrile | 318 ± 10 | 0.030‡ | 0.0318‡ | 0.5018 |
| Tentative results from preliminary data | | | | |
| 2-Butanone | 175 | 0.075 | 0.0437 | 0.469 |
| Ethyl acetate§ | 175 | 0.051 | 0.029 | 0.478 |
| 2-Heptanone§ | 284 | 0.133 | 0.126 | 0.493 |
| 3-Heptanone | 298 | 0.13 | 0.129 | 0.499 |
| Carbon tetrachloride§ | 300 | 0.066 | 0.066 | 0.500 |
| Amyl acetate | 314 | 0.155 | 0.162 | 0.507 |
| 2-Octanone | 333 | 0.160 | 0.178 | 0.518 |

*Generally ca. ± 50°.

†Generally ca. ± 0.015.

‡Uncertainty < 0.01.

§The parameters for these solvents were calculated from a few rough measurements of intrinsic viscosities not recorded in Table 3.

According to equation (1-2), the plots of $(\alpha^5 - \alpha^3)/M^{1/2}$ versus $1/T$ should be linear and independent of M . Linear representations within the scatter of the experimental data were indeed possible for a given polymer fraction in a particular solvent at different temperatures. Values of $(\alpha^5 - \alpha^3)/M^{1/2}$ at a given temperature, however, tended to increase with increasing M . This departure from the requirement of the approximate theory would be worsened by the use, suggested recently²¹, of a lower power of α in equation

(1-1), and would not be eliminated by the use of the amended form of equation (1-2) recently advanced²², since the percentage increase in $(\alpha^5 - \alpha^3)/M^{1/2}$ found here with increasing M is very small in some solvents, such as toluene and methyl isobutyrate, and larger in others. The latter observation also weighs against the supposition that the deviations from theory arise from a possible systematic dependence on chain length of a structural feature of the polymer chain (such as end group content²³ or stereoregularity²⁴) and suggests instead that in certain instances specific solvent-polymer interactions influence the value of K . Such a possibility, which may be more likely for polymethyl methacrylate, containing polar groups, than for polystyrene or polyisobutylene studied previously, will be explored more thoroughly elsewhere²⁵.

Despite the emphasis in the foregoing on the failings of equations (1), intrinsic viscosities covering a wide range in temperature, molecular weight and solvent-polymer type may actually be represented to a good approximation through their use. In the present instance for $M \geq 3 \times 10^5$ the average deviation in most solvents between the observed and computed viscosity (*Table 3*) is only two to three per cent. Larger deviations (averaging *ca.* 5 per cent) occur at lower M , where assumption of a cloud distribution of segments made in the development of equation (1-2) may not be justified, and in the poorer solvents, especially near $T = \Theta$, where the experimental scatter in the data is more marked. These deviations are generally within the estimated experimental errors discussed in the experimental section.

Aware of both the success and limitations of the present simple application of the approximate theory to $[\eta]-T-M$ data, we shall explore in the following section the relation of the thermodynamic parameters obtained to values determined by other measurements, and the dependence of these parameters on the nature of the solvent-polymer pair.

Correlations of the thermodynamic parameters

Values of Θ obtained from $[\eta]-T-M$ measurements in many polymer-solvent systems are in good agreement with those obtained directly by critical miscibility studies, where such comparison is possible. However, as pointed out earlier²⁶ by Krigbaum, values of ψ_1 and of κ_1 obtained from observed T_c/M relationships are five to ten times greater than the corresponding values obtained from $[\eta]-T-M$ data (*Table 8*). Closer agreement obtains (*Table 8*) between the latter parameters and those computed as $\psi_1 = \Delta\bar{S}_1/Rv_2^2$ and $\kappa_1 = \Delta\bar{H}_1/RTv_2^2$ where $\Delta\bar{S}_1$ and $\Delta\bar{H}_1$ are the partial entropy and heat of dilution²⁷ from osmotic pressure/temperature measurements²⁷ at fixed volume fraction v_2 of polymer, except that negative values for κ_1 are often given by the osmotic data. As reported earlier by Orofino and Flory²⁸, values of the dimensionless thermodynamic parameters χ_1 computed as $\frac{1}{2} - \psi_1(1 - \Theta/T)$ from the $[\eta]-T-M$ data on polymethyl methacrylate solutions (*Table 7*) agree well with corresponding values from osmotic pressure/concentration measurements at fixed temperature in acetone or in methylethyl ketone, although in chloroform the latter method yields a result (0.426) appreciably higher than that (0.364) determined from the viscosity.

PROPERTIES OF DILUTE POLYMER SOLUTIONS III

Table 8. Comparison of thermodynamic parameters determined by different methods

| Polymer | Solvent | ψ_1 from [η]- M - T data* | ψ_1/ψ_1 | κ'_1/κ_1 |
|-------------------------|--|--|-----------------|----------------------|
| | ψ_1 from $T_c/M^{-1/2}$ plots† | | | |
| Natural rubber | 4-Heptanone | 0.085 | 9.4 | |
| Polystyrene | Cyclohexane | 0.13 | 8.1 | |
| Polymethyl methacrylate | 4-Heptanone | 0.08 | 6.3 | |
| | Acetonitrile | 0.03 | 4.8 | |
| | 2-Octanone | 0.16 | 3.4 | |
| Polydimethyl siloxane | Butanone | 0.08 | 5.4 | |
| Polysisobutylene | Ethylbenzene: phenyl ether (3:1) | 0.17 | 5.0 | |
| | Benzene | 0.15 | 4.3 | |
| | ψ_1 from temperature dependence of osmotic pressure ²⁷ | | | |
| Polymethyl methacrylate | Benzene | 0.076 | 1.2 | Negative |
| | Acetone | 0.069 | 1.1 | 0.5 |
| | Toluene | 0.11 | 1.1 | 0.4 |
| | Chloroform | 0.136 | 0.7 | Negative |
| Polystyrene | Cyclohexane | 0.13 | 1.5 | 1.3 |
| | Butanone | 0.006 | 1.2 | Negative |
| | Benzene | 0.09 | 0.3 | Negative |
| | Toluene | 0.11 | 0.3 | Negative |

*From refs. 3, 7, 26 and present work.

†From ref. 26, and from present work for polymethyl methacrylate.

Approximate correlations of κ_1 and of Θ with the solubility parameters²⁹⁻³¹ of the solvent and polymer, and of ψ_1 with the chain length of the solvent in a homologous series are presented in Figures 6, 7 and 8, on the basis of values (Table 9) computed by equations (1) from [η]- T - M data on poly-

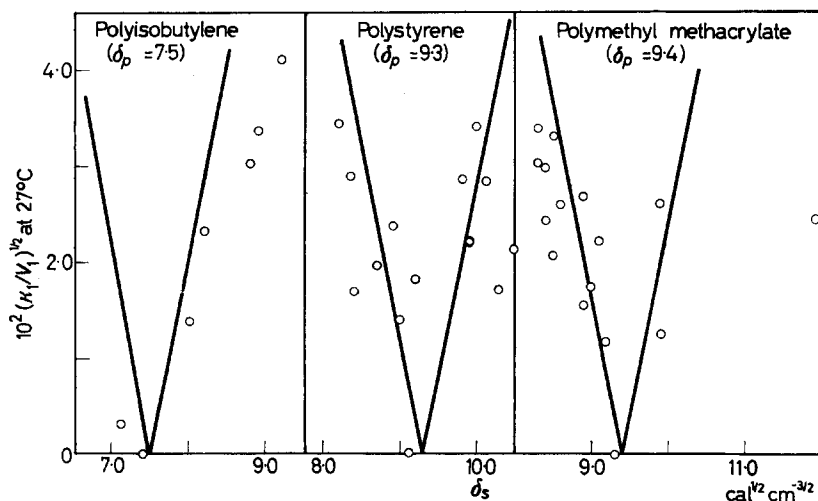


Figure 6— $(\kappa_1/V_1)^{1/2}$ at 27° from [η]/ T data versus δ_s for three polymers in various solvents. The lines are drawn in accord with equation (5) and the indicated values of δ_p

Table 9. Thermodynamic parameters for various polymer-solvent pairs from $[\eta]$ - T - M data*

| Solvent | δ_s | V_1 | $100 \psi_1$ | | | $\theta, ^\circ K$ | | | $(10^4 \kappa_1/V_1)$ at 27°C | | | |
|---------------------------|------------|-------|--------------|-----|-----|--------------------|------|-----|-------------------------------|----|-----|---|
| | | | PMMA | PS | PIB | PMMA | PS | PIB | PMMA | PS | PIB | |
| <i>o</i> -Dichlorobenzene | 10.0 | 113 | — | 18 | — | — | — | — | — | — | — | — |
| Chloroform | 9.3 | 80 | 13.6 | 13 | — | 0 | 220 | — | — | — | — | — |
| Cyclohexane | 8.2 | 109 | — | 14 | — | — | 307 | — | — | — | — | — |
| Toluene | 8.9 | 107 | 11 | 11 | — | 208 | 160 | — | — | — | — | — |
| Ethyl benzene | 8.8 | 127 | — | 11 | — | — | 156 | — | — | — | — | — |
| Benzene | 9.2 | 89 | 7.6 | 9 | — | 50 | 100 | — | — | — | — | — |
| 1, 4-Dioxan | 9.3 | 86 | — | 10 | — | — | 198 | — | — | — | — | — |
| Bromobenzene | (10.3) | 103 | — | 9 | — | — | 115 | — | — | — | — | — |
| 2, 5-Dimethylfuran | (8.7) | 106 | — | 9 | — | — | 145 | — | — | — | — | — |
| Cyclohexanone | 9.9 | 103 | — | 8 | — | — | 170 | — | — | — | — | — |
| Pyridine | 10.9 | 80 | — | 8 | — | — | 161 | — | — | — | — | — |
| Carbon tetrachloride | 8.6 | 96 | 6.6 | — | — | 300 | — | — | — | — | — | — |
| Methyl cyclohexane | 7.8 | 128 | — | — | — | — | 344† | — | — | — | — | — |
| Ethyl cyclohexane | (7.9) | 143 | — | — | — | — | 343† | — | — | — | — | — |
| Phenetole | (9.2) | 126 | — | — | — | — | — | — | — | — | — | — |
| Anisole | (9.4) | 108 | — | — | — | — | — | — | — | — | — | — |
| Phenyl ether | (9.7) | 159 | — | — | — | — | — | — | — | — | — | — |
| 2-Octanone | (8.3) | 156 | 16 | — | — | 333 | — | — | — | — | — | — |
| Amyl acetate | 8.5 | 148 | 15.5 | — | — | 314 | — | — | — | — | — | — |
| 2-Heptanone | 8.4 | 141 | 13.3 | 5 | — | 284 | 210 | — | — | — | — | — |
| 3-Heptanone | (8.3) | 139 | 13 | — | — | 298 | — | — | — | — | — | — |
| <i>n</i> -Hexadecane | 8.0 | 294 | — | — | 9.4 | — | — | — | — | — | — | — |
| Ethyl chloroacetate | (10.1) | 105 | — | 8 | — | — | 255 | — | — | — | — | — |
| 5-Dichloroethane | 9.9 | 79 | 9.3 | 6 | — | 40 | 190 | — | — | — | — | — |
| 4-Heptanone | 8.4 | 139 | 8 | — | — | 307 | — | — | — | — | — | — |
| 2-Butanone | 9.1 | 90 | 7.5 | 0.6 | — | 175 | 0 | — | — | — | — | — |
| Methyl methacrylate | (8.9) | 107 | 7.0 | — | — | 110 | — | — | — | — | — | — |
| Acetone | 9.9 | 73 | 6.7 | — | — | 218 | — | — | — | — | — | — |
| Methyl isobutylate | 8.5 | 115 | — | — | — | 220 | — | — | — | — | — | — |
| Diisobutylene | (7.1) | 158 | — | — | — | — | — | — | — | — | — | — |
| Nitropropane | 10.4 | 89 | — | — | — | — | — | — | — | — | — | — |
| Ethyl acetate | 9.0 | 98 | — | — | — | — | — | — | — | — | — | — |
| 2, 2, 3-Trimethylbutane | (6.9) | 160 | 5.1 | 3 | — | 175 | 272 | — | — | — | — | — |
| <i>n</i> -Heptane | 7.4 | 148 | — | — | — | — | 222 | — | — | — | — | — |
| Acetonitrile | 11.9 | 53 | 3.0 | — | — | — | — | — | — | — | — | — |
| 2-Ethylbutyraldehyde | (8.3) | 123 | — | — | — | 318 | — | — | — | — | — | — |
| Methylisopentyl ketone | (8.3) | 139 | — | — | — | 295† | — | — | — | — | — | — |
| Diisopropyl ketone | 8.1 | 141 | — | — | — | 308† | — | — | — | — | — | — |
| 3-Octanone | (8.3) | 156 | — | — | — | 319† | — | — | — | — | — | — |
| | | | | | | 345† | — | — | — | — | — | — |

*Data for polyisobutylene (PIB) from ref. 6; for polystyrene (PS) from ref. 7; for polymethyl methacrylate (PMMA) from present work, cf. ref. 3.
† θ from critical precipitation data.

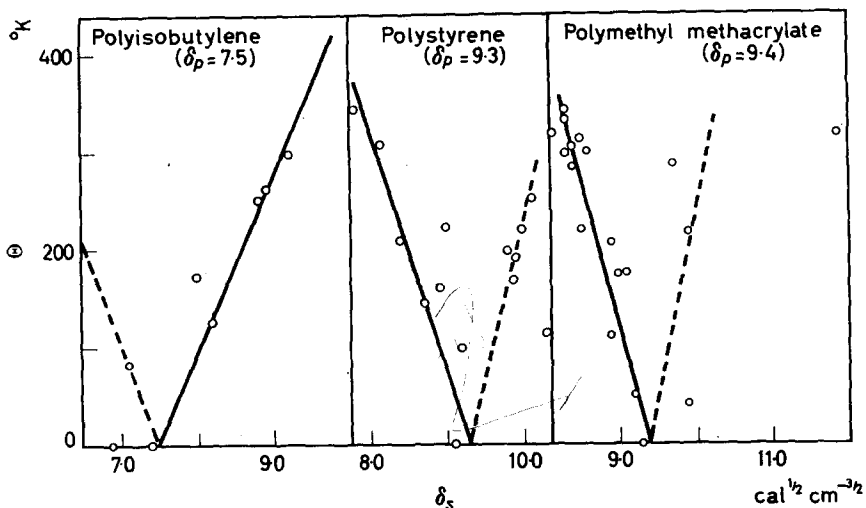


Figure 7—An empirical correlation of Θ/δ_p for three polymers in various solvents. Here for polyisobutylene, polystyrene and polymethyl methacrylate, respectively, in equations (6) β is 206, 250 and 307, and β' is 184, 330 and 400

isobutylene^{3,6}, on polystyrene^{3,7}, and on polymethyl methacrylate in a variety of solvents.

These data are generally in rough accord with Hildebrand's precept²⁹ that the heat of mixing of two liquids is related to their relative cohesive energy densities, but indicate also the existence in some cases of wide discrepancies. Thus plots of $(\kappa_1/V_1)^{1/2}$ derived from the viscosity measurements versus δ_s (Figure 6) frequently but not invariably agree within the large experimental uncertainty in κ_1 with the prediction of Hildebrand's expression

$$(\kappa_1/V_1) = (\delta_s - \delta_p)^2 / RT \quad (5)$$

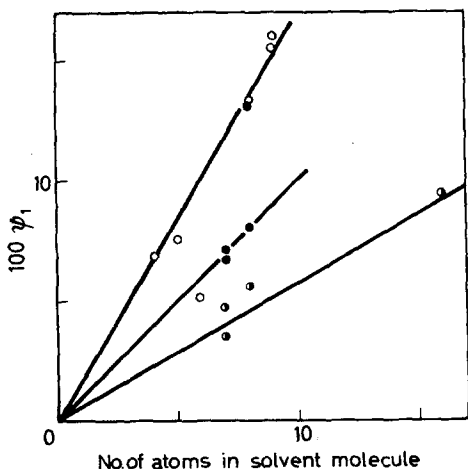


Figure 8—An empirical correlation of ψ_1 computed from $[\eta]/T$ data with the number of atoms (other than hydrogen) in the solvent molecule. Polymethyl methacrylate in aliphatic ketones or esters with C=O in the 2-position (\circ , upper curve) or in the 3- or 4-position (\bullet , middle curve), polyisobutylene in aliphatic hydrocarbon solvents (\odot). The slopes of the three curves are 0.17, 0.10 and 0.058, respectively

Here the solubility parameter of the solvent $\delta_s = (\Delta E_1/V_1)^{1/2}$, where ΔE_1 is the molar energy of vaporization, δ_p is a corresponding parameter for the polymer, and R is the gas constant. Negative deviations from equation (5) appear to be the rule for $|\delta_s - \delta_p| > 0.7$, which suggests that complete mixing of solvent molecules and of polymer segments is less likely for such 'unlike' components. Variations in the magnitude of such deviations, and in the positive and negative deviations observed in some cases even when δ_p and δ_s do not differ greatly, suggest that other, more specific, interaction factors may also play an important role.

The values of δ_p of 7.5, 9.3 and 9.4 respectively, for polyisobutylene, polystyrene, and polymethyl methacrylate obtained by fitting the data in *Figure 6* with the form of equation (5), are in good agreement with corresponding values of 7.3, 9.25 and 9.4 calculated from the 'molar attractive constants'³¹ and the specific volumes in the liquid state²⁰. Somewhat different values (7.8, 8.56 or 8.73, and 9.1, respectively) were determined recently³² by a method which rests on the assumptions that equation (5) is rigorously applicable and that ψ_1 is a constant for a given polymer structure. Neither of these was found to apply to the present data.

Approximate empirical correlation of Θ with $(\delta_p - \delta_s)$ in *Figure 7* corresponding to the equations :

$$\Theta = \beta (\delta_p - \delta_s) \quad \delta_p > \delta_s \quad (6-1)$$

$$\Theta = \beta' (\delta_s - \delta_p) \quad \delta_p < \delta_s \quad (6-2)$$

provides at least a useful guide in a search for polymer-solvent pairs possessing Θ in a certain range. The results suggest that the polymer-solvent interactions are more marked the greater the difference in the solubility parameters, and the more polar the system, but that other factors exist which make quantitative predictions hazardous.

The observed values of ψ_1 are all appreciably lower than the 'ideal' value of 0.5 and vary over 20-fold for different polymer-solvent pairs. No consistent relationship between ψ_1 and $(\delta_s - \delta_p)$ or between ψ_1 and κ_1 was found although such a dependence would be required if both equations (5) and (6) were precisely obeyed. Instead, the geometry and chemical nature of the solvent molecule and of the repeating unit in the polymer appear to be important in determining ψ_1 . For a given homologous series of solvent molecules of similar structure, the value of ψ_1 increases (*Figure 8*) in proportion to chain length at a rate that seems to be specific for the polymer and the class of solvents considered. It may be that in certain instances a specific locus on the solvent molecule, such as the carbonyl group or a chain end, is attracted to some particular point on the repeat unit of the polymer chain, thereby introducing a degree of local order in the solution. On this basis, we should expect, as observed, that ψ_1 would increase as the length of the non-complexing hydrocarbon portion of the solvent molecule; moreover, as observed, for isomeric solvents containing a single complexing carbonyl group, the degree of order should be greater and ψ_1 should be smaller the more symmetrical the isomer. If, for the polyisobutylene-paraffin chain pairs, the end of the solvent packs preferentially adjacent to the polymer chain, then, as observed, the average order should decrease (and ψ_1 increase) for longer chains and for branched

isomers with many distinguishable possible points of attachment. Preferred orientation of this sort may be less likely for highly symmetrical, non-polar ring compounds, thereby accounting for the larger ψ_1 values (generally ≥ 0.10) observed in such instances.

The writer is pleased to acknowledge the assistance of Mrs Helen Desman who performed most of the experimental work reported here and of Mrs Elizabeth Cohn-Ginsberg, who assisted with the calculations and with the preparation of the manuscript. I am also indebted to Dr E. F. Casassa for his suggestions in revision of earlier drafts of this paper. The support by the Rohm and Haas Company of the investigations reported here and in the two companion papers in this series is appreciated.

Rohm and Haas Company,
Philadelphia, Pennsylvania, U.S.A.

(Received September 1961)

REFERENCES

- ¹ FLORY, P. J. *J. chem. Phys.* 1949, **17**, 303
- ² FLORY, P. J. and FOX, T. G. *J. Amer. chem. Soc.* 1951, **23**, 1904
- ³ FLORY, P. J. *Principles of Polymer Chemistry*, Chap. XIV. Cornell University Press: Ithaca, N.Y., 1953
- ⁴ COHN-GINSBERG, E. S., FOX, T. G. and MASON, H. F. *Polymer, Lond.* 1962, **3**, 97
- ⁵ FOX, T. G., KINSINGER, J. F., MASON, H. F. and SCHUELE, E. M. *Polymer, Lond.* 1962, **3**, 71
- ⁶ FOX, T. G. and FLORY, P. J. *J. Amer. chem. Soc.* 1951, **73**, 1909; *J. phys. Colloid Chem.* 1949, **53**, 197
- ^{7a} FOX, T. G. and FLORY, P. J. *J. Amer. chem. Soc.* 1951, **73**, 1915
- ^b CRAGG, L. H., DUMITRU, E. T. and SIMKINS, J. E. *J. Amer. chem. Soc.* 1952, **74**, 1977
- ⁸ FOX, T. G., FOX, J. C. and FLORY, P. J. *J. Amer. chem. Soc.* 1951, **73**, 1901
- ^{9a} FLORY, P. J. *J. chem. Phys.* 1942, **10**, 51
- ^b HUGGINS, M. L. *J. Amer. chem. Soc.* 1942, **64**, 2716
- ¹⁰ CHINAI, S. N. and BONDURANT, C. W., Jr. *J. Polym. Sci.* 1956, **22**, 555
- ¹¹ CHINAI, S. N. *J. Polym. Sci.* 1957, **25**, 413
- ¹² See ref. 3, page 618, Table XXXIX
- ¹³ CHINAI, S. N., RESNICK, A. L. and LEE, H. T. *J. Polym. Sci.* 1958, **33**, 471
- ¹⁴ MATSUMOTO, M. *J. Polym. Sci.* 1960, **46**, 441
- ¹⁵ SHULTZ, A. *J. Amer. chem. Soc.* 1954, **76**, 3422
- ¹⁶ CHINAI, S. N. and SAMUELS, R. J. *J. Polym. Sci.* 1956, **19**, 463
- ¹⁷ CHINAI, S. N. and GUZZI, R. A. *J. Polym. Sci.* 1956, **21**, 417
- ¹⁸ FLORY, P. J., CIFFERI, A. and CHIANG, R. J. *J. Amer. chem. Soc.* 1961, **83**, 1023
- ¹⁹ CIPERRI, A., HOEVE, C. A. J. and FLORY, P. J. *J. Amer. chem. Soc.* 1961, **83**, 1015
- ²⁰ FOX, T. G. and LOSHAEK, S. J. *J. Polym. Sci.* 1955, **15**, 371
- ^{21a} YAMAKAWA, H. and KURATA, M. *J. phys. Soc. Japan*, 1958, **13**, 94
- ^b KURATA, M. and YAMAKAWA, H. *J. chem. Phys.* 1958, **29**, 311
- ^c KURATA, M., YAMAKAWA, H. and UTIYAMA, H. *Makromol. Chem.* 1959, **34**, 139
- ^d PTITSYN, O. B. and ÉIZNER, YU. E. *Zh. fiz. Khim., Mosk.* 1958, **32**, 2464
- ²² KURATA, M., STOCKMAYER, W. H. and ROIG, A. *J. chem. Phys.* 1960, **33**, 151
- ²³ MCINTYRE, D., O'MARA, J. H. and KONOUCK, B. C. *J. Amer. chem. Soc.* 1959, **81**, 3498
- ^{24a} COLEMAN, B. D. *J. Polym. Sci.* 1958, **31**, 155
- ^b FOX, T. G., GOODE, W. E., GRATCH, S., HUGGETT, C. M., KINCAID, J. F., SPELL, A. and STROUPE, J. D. *J. Polym. Sci.* 1958, **31**, 173

- ²⁵ FOX, T. G and OROFINO, T. A. To be published
- ²⁶ KRIGBAUM, W. R. *J. Amer. chem. Soc.* 1954, **76**, 3758
- ^{27^a} SCHULZ, G. V. and DOLL, H. *Z. Elektrochem.* 1952, **56**, 248
- ^b SCHULZ, G. V. and HELLFRITZ, H. *Z. Elektrochem.* 1953, **57**, 835
- ²⁸ OROFINO, T. A. and FLORY, P. J. *J. chem. Phys.* 1957, **26**, 1067
- ^{29^a} HILDEBRAND, J. *Chem. Revs.* 1949, **44**, 37
- ^b HILDEBRAND, J. and SCOTT, R. *The Solubility of Nonelectrolytes*, 3rd ed. Reinhold: New York, 1949
- ^{30^a} WALKER, E. E. *J. appl. Chem.* 1953, **24**, 70
- ^b KRIGBAUM, W. R. Private communication
- ^c SMALL, P. A. *J. appl. Chem.* 1953, **3**, 71
- ^d ALLEN, G., GEE, G. and WILSON, G. J. *Polymer, Lond.* 1960, **1**, 456
- ³¹ BURRELL, J. *Interchemical Reviews*, 1955, **14**, 1, 31
- ^{32^a} BRISTOW, G. M. and WATSON, W. F. *Trans. Faraday Soc.* 1958, **54**, 1731, 1742
- ^b GREEN, J. H. S. *Nature, Lond.* 1959, **183**, 818

The Solution Properties of Olefin Polysulphones I—Hexene-1 Polysulphone

K. J. IVIN*, H. A. ENDE† and G. MEYERHOFF‡

The solubility of twelve olefin polysulphones in about twenty five solvents has been investigated. Pure theta solvents have been found for several polysulphones. Refractive index increments have been measured for five polysulphones in chloroform and for hexene-1 polysulphone in n-hexyl chloride ($\theta=13^{\circ}\text{C}$) and in two theta-solvent mixtures of methylethyl ketone and isopropanol.

Light scattering, viscosity, sedimentation and diffusion measurements on fractions of hexene-1 polysulphone (m.wt 47000 to 695000) have been used to determine molecular weights and coil dimensions in three different theta solvents. The value of $(r_v^2)_z$ in n-hexyl chloride is about 2.1 times the value for a freely rotating chain, but in methylethyl ketone-isopropanol it is only about 1.6 times as big. This difference is discussed.

THE solution properties of olefin polysulphones have not previously been investigated in any detail. A study of these polymers offers interesting possibilities. One can, for example, investigate the effect of substituents on the dimensions of the chains in theta (θ) solvents. An interesting comparison would be between the polysulphones of hexene-1, hexene-2 and 2-methyl pentene-1 which are α -, $\alpha\beta$ - and $\alpha\alpha$ -substituted, respectively. In these three polymers the repeat units are isomeric, all having the formula $\text{C}_6\text{H}_{12}\text{SO}_2$. No comparisons have previously been made between the polymers made from differently substituted but isomeric repeat units.

A further point of interest lies in the highly polar backbone of the polysulphone chains and the question arises as to whether it will have the same dimensions in θ -solvents which are respectively more and less polar than the polymer. In previous investigations no distinction has been made between θ -solvents which are less polar and θ -solvents which are more polar than the polymer, though such a division is clearly implied by solubility relations^{1, 2}.

In the present paper we report a preliminary survey of the general solubility properties of a number of olefin polysulphones, some refractive index increment measurements on five polysulphones and a detailed investigation of hexene-1 polysulphone fractions by light scattering, viscosity, sedimentation and diffusion measurements.

EXPERIMENTAL

Fractionation of hexene-1 polysulphone

20 g of polymer, kindly supplied by Phillips Petroleum Co., was dissolved in 4 l. of distilled acetone. The solution was somewhat hazy but

*Department of Physical Chemistry, University of Leeds.

†Chemstrand Research Center Inc., Durham, N. Carolina.

‡Institut für physikalische Chemie der Universität Mainz.

cleared after a few days throwing out a white deposit. This deposit was about 0.1 per cent of the original weight and probably originated from the emulsion catalyst system. The clear solution was decanted, the temperature raised to 40°C and distilled methanol added until the turbidity point was reached. This required about 1.2 times the volume of acetone. The temperature was raised slightly until the turbidity disappeared, then allowed to fall by three degrees and held at this temperature overnight. Next morning the first fraction had collected as a gel and the supernatant liquid was easily decanted. Seven fractions (A1 to A7) were collected in this way by lowering the temperature in stages to 15°C. The temperature was then raised to 40°C, more methanol added and three more fractions obtained by successive cooling (A8 to A10). The residual solution was evaporated in a stream of air to obtain a final fraction. Each fraction was dissolved in acetone to give a one per cent solution and reprecipitated by addition to methanol containing a small amount of concentrated hydrochloric acid. After one to two days the polymer had settled to a fine cake which could easily be broken up, filtered and washed with water. Washing with methanol was found inadvisable since it caused swelling and agglomeration of the polymer which subsequently led to coloration (yellow-red-brown) of the polymer on vacuum-drying at 50°C, though not to degradation as judged by viscosity measurements.

The intrinsic viscosities of the fractions in chloroform at 20°C ranged from 207 to 12 ml/g and the weighted average agreed well with the intrinsic viscosity of the original polymer (73 ml/g) indicating that no degradation had occurred during the first fractionation. The following pairs of fractions were combined and refractionated:

| | $[\eta]_{av.}$, ml/g | Wt, g |
|----------|-----------------------|-------|
| A2 + A3 | 132 | 2.9 |
| A5 + A6 | 74 | 3.7 |
| A9 + A10 | 35 | 2.7 |

A2 + A3 were taken first and refractionated from 0.1 per cent solution with the intention of removing a head and a tail fraction. However, the average intrinsic viscosity of the resulting fractions was somewhat less than 75 ml/g indicating considerable degradation during the second fractionation. The reason for this is not clear. It seems that the original polymer contained a stabilizing impurity which was removed in the first fractionation. Some tests were made to determine the importance of the pH value, since the poly-sulphones are stable in acid solution, but unstable to alkali³. The presence of acid certainly reduced the rate of degradation at 50° to 60°C, but not to the extent found for the original polymer. The fractions from A2 + A3 were rejected and a fresh batch of 20 g of polymer fractionated to obtain a fraction (B1) corresponding to A1 + A2 + A3 + part of A4. This had an intrinsic viscosity of 143 ml/g and weighed 6.6 g. This and the aforementioned A5 + A6 and A9 + A10 were subjected to two further fractionations and degradation was minimized by working with 0.2 per cent solutions in an attempt to speed up deposition of the gels, and at temperatures not exceeding 30°C. The final fractions used in the light scattering work and their

limiting viscosity numbers in chloroform at 20°C were: G2, 119 ml/g; E2, 67 ml/g; F2, 31.5 ml/g. Slight degradation occurred during the second and third fractionations. Sedimentation and diffusion measurements were made on G2 and on two large tail fractions from the third fractionation, G3, 57 ml/g and F3, 18 ml/g. Shortage of material prevented us from using the same fractions for all measurements.

Materials

The olefin polysulphones were obtained from Phillips Petroleum Co. and from previous work⁴.

All solvents used for physical measurements were the best available grades and were finally distilled through a 3 ft column. Before distillation acetone was dried over sodium sulphate, chloroform was washed with water and dried, while *n*-hexyl chloride (from Schuchardt, Munich), was washed with sodium carbonate solution and water, dried over calcium chloride and sodium sulphate and the fraction distilling at 133.7° to 134.0°C collected.

Viscosity measurements

These were made in Ubbelohde suspended-level viscometers, with 0.3 or 0.4 mm capillaries, and flow times in excess of 100 sec. No shear corrections were made; they would be very small for the molecular weights used here.

Light scattering measurements

These were made on a Cantow-type apparatus⁵ using vertically polarized 436 m μ radiation. The instrument was calibrated by means of benzene using the value $R_{90,v} = 62.4 \times 10^{-6}$ for the absolute scattering power of benzene at 90°, as determined by Cantow and Schulz⁵. The solutions were centrifuged for one hour at 12 000 rev/min to remove dust before measurement.

Diffusion measurements

These were made using a free diffusion cell⁶. One fraction was also studied with a thermal diffusion cell as described elsewhere⁷.

Sedimentation measurements

These were made in a Spinco analytical ultracentrifuge operating at 42 040, 50 740 and 59 780 rev/min for F3, G3 and G2 respectively. Acetone was used as solvent because its compressibility was known, and because the apparent molar volume of the polymer in acetone was also known⁸.

Refractive index increments

These were measured in chloroform using Bodmann's apparatus⁹. dn/dc values at 20°C in ml/g were as follows for 436 m μ (polymer has the higher n): polysulphone of butene-1, 0.0970; hexene-1, 0.0790; octene-1, 0.0732; dodecene-1, 0.0695; cyclohexene, 0.1133. The corresponding values for 578 m μ were 0.0949, 0.0782, 0.0718, 0.0581 and 0.1104 respectively. As the alkyl group is lengthened dn/dc tends towards the value for a long chain paraffin. The difference between the values for 1-hexene and cyclohexene polysulphones (0.032) may be compared with the difference in refractive indices of hexane and cyclohexane (0.054).

Table 1. Refractive index increments for hexene-1 polysulphone (436 m μ)

| Solvent | T(°C) | dn/dc (ml/g) |
|---------------------------------|-------|--------------|
| <i>n</i> -Hexyl chloride | 7 | 0.0796 |
| | 20 | 0.0834 |
| Methylethyl ketone- | 20 | 0.1229 |
| isopropanol (37-63 by vol.) | 27 | 0.1242 |
| | 37 | 0.1261 |
| Methylethyl ketone- | 7 | 0.1208 |
| isopropanol (41.5-58.5 by vol.) | 20 | 0.1233 |

The increments for hexene-1 polysulphone in the θ -solvents are shown in Table 1. Methylethyl ketone (MEK) and isopropanol (isoPrOH) were chosen as components of the mixed θ -solvent since their refractive indices are very close together and effects due to selective adsorption are thereby avoided¹⁰.

RESULTS

Solubility of polysulphones and search for θ -solvents

The solubility of twelve olefin polysulphones in a number of solvents is summarized in Table 2. The solvents are arranged in order of increasing

Table 2. Solubility of olefin polysulphones

+ soluble, - insoluble, \pm soluble above a certain temperature,
 \mp soluble below a certain temperature (see text).

| Olefin | δ_{85}° * | Solvents (in order of δ_{85}°) | | | | | | | | | | | |
|--------------------------|-------------------------|---|---------------|---------------------|-----------|--------------|----------|-------------|----------|----------|----------------|----------|------------|
| | | Isobutene | 3-Me butene-1 | 4, 4-diMe pentene-1 | Propylene | Cyclopentene | Butene-2 | Cyclohexene | Butene-1 | Hexene-1 | 2-Me pentene-1 | Octene-1 | Dodecene-1 |
| Hexane | 7.24 | - | - | - | - | - | - | - | - | - | - | - | - |
| Diethyl ether | 7.74 | - | - | - | - | - | - | - | - | - | - | - | - |
| Cyclohexane | 8.18 | - | - | - | - | - | - | - | - | - | - | - | - |
| <i>n</i> -Hexyl chloride | 8.21 | - | - | - | - | - | - | - | - | - | - | - | - |
| Butyl acetate | 8.28 | - | - | - | - | - | - | - | - | - | - | - | - |
| Cyclohexene | 8.55 | - | - | - | - | - | - | - | - | - | - | - | - |
| Carbon tetrachloride | 8.58 | - | - | - | - | - | - | - | - | - | - | - | - |
| Ethyl benzene | 8.80 | - | - | - | - | - | - | - | - | - | - | - | - |
| <i>m</i> -Xylene | 8.80 | - | - | - | - | - | - | - | - | - | - | - | - |
| Mesitylene | 8.80 | - | - | - | - | - | - | - | - | - | - | - | - |
| Toluene | 8.91 | - | - | - | - | - | - | - | - | - | - | - | - |
| <i>o</i> -Xylene | 9.00 | - | - | - | - | - | - | - | - | - | - | - | - |
| Ethyl acetate | 9.04 | - | - | - | - | - | - | - | - | - | - | - | - |
| Diethyl ketone | 9.05 | - | - | - | - | - | - | - | - | - | - | - | - |
| Benzene | 9.15 | - | - | - | - | - | - | - | - | - | - | - | - |
| Chloroform | 9.24 | - | - | - | - | - | - | - | - | - | - | - | - |
| Cyclohexanone | 9.26 | - | - | - | - | - | - | - | - | - | - | - | - |
| Tetrachlorethylene | 9.31 | - | - | - | - | - | - | - | - | - | - | - | - |
| Tetrahydrofuran | 9.32 | - | - | - | - | - | - | - | - | - | - | - | - |
| Chlorobenzene | 9.51 | - | - | - | - | - | - | - | - | - | - | - | - |
| Methylethyl ketone | 9.52 | - | - | - | - | - | - | - | - | - | - | - | - |
| Acetone | 9.71 | - | - | - | - | - | - | - | - | - | - | - | - |
| Tetrachlorethane | 9.72 | - | - | - | - | - | - | - | - | - | - | - | - |
| Dioxan | 9.73 | - | - | - | - | - | - | - | - | - | - | - | - |
| Sulphur dioxide | 10.3 | - | - | - | - | - | - | - | - | - | - | - | - |
| Isopropanol | 11.35 | - | - | - | - | - | - | - | - | - | - | - | - |
| Allyl alcohol | 12.30 | - | - | - | - | - | - | - | - | - | - | - | - |
| Dimethyl sulphoxide | 13.00 | - | - | - | - | - | - | - | - | - | - | - | - |

* δ values have been taken from refs. 11, 12 and 2. Those not available were calculated.

solubility parameter δ at 25°C (see footnote to *Table 2*) and the polymers in approximate order of increasing solubility. A borderline between solubility and insolubility runs very roughly diagonally across the table, and θ -solvents are to be expected in the borderline region. Such θ -solvents are less polar than the polymer. A second borderline exists at the bottom right hand corner of *Table 2* and θ -solvents in this region will be more polar than the polymer. If the solubility parameter were the only factor determining solubility one would expect in going down a given column a region of insolubility followed by a region of solubility followed by another region of insolubility. This pattern is followed almost perfectly by the polysulphones of hexene-1, 2-methyl pentene-1 and dodecene-1. Some of the other polysulphones show a less regular pattern due no doubt to other influences. In particular it is apparent that chloroform is a better solvent than would be expected from its δ value and this is attributable to hydrogen bonding of the acidic hydrogen in chloroform to the oxygen atoms of the sulphone groups (cf. Small²). Tetrachlorethylene is also somewhat anomalous. Some additional effect is also apparent with ethyl acetate and butyl acetate since butene-1 polysulphone shows a *lower* critical solution temperature. The exceptionally insoluble nature of the first three polysulphones in *Table 2* suggests that they have very high δ values probably arising from relatively high densities. In this connection we may note that the apparent solution densities of the polysulphones of butene-1 and butene-2 are 1.45 and 1.54 g/ml respectively⁸.

A number of 'boundary' systems were investigated in more detail and the following θ -solvents were found. The temperatures indicate turbidity points obtained with dilute solutions (about one per cent) of polymer (mol. wt about 10^5 to 10^6) and serve to indicate the general region of the θ -point, which may be up to 30° different from the temperature quoted. Butene-1 polysulphone: butyl acetate 23°C, ethyl acetate 65°C; these are exceptional in being *lower* solution temperatures, i.e. solutions turbid *above* the temperatures quoted. Hexene-1 polysulphone: *n*-amyl chloride -10°C, *n*-hexyl chloride 5°C ($\theta=13^\circ\text{C}$, see below), tetrachlorethylene 15°C (slow degradation), *n*-heptyl chloride 50°C, cyclohexanol 72°C, allyl alcohol 75°C, sec-octyl alcohol 86°C, *n*-amyl alcohol 92°C, *n*-hexyl alcohol 94°C, *n*-octyl chloride 113°C (isopropanol $> 82^\circ\text{C}$). Dodecene-1 polysulphone: methyl-ethyl ketone -10°C, *n*-hexane 0°C, acetone 52°C, isopropanol 82°C. Octene-1 polysulphone: isopropanol 82°C, allyl alcohol 72°C.

The degradation of hexene-1 polysulphone in tetrachlorethylene is surprising and possibly caused by impurities. The small variation of the turbidity points for the alcohols suggests that their δ values decrease strongly with increasing temperature on account of the loss of hydrogen bonding.

Hexene-1 polysulphone was chosen for detailed investigation because of the possibility of later comparison with isomeric or near-isomeric polysulphones and because a pure, less polar, solvent with a θ -point in the region of room temperature had been found, *n*-hexyl chloride. Mixtures of methyl-ethyl ketone and isopropanol were used as θ -solvents which were more polar than the polymer.

Molecular weights by light scattering

Plots of Kc/R_θ against $\sin^2(\frac{1}{2}\theta)$ were extrapolated to zero angle, and the values of $(Kc/R_\theta)_{\theta=0}$ are plotted against the concentration c in Figure 1. The

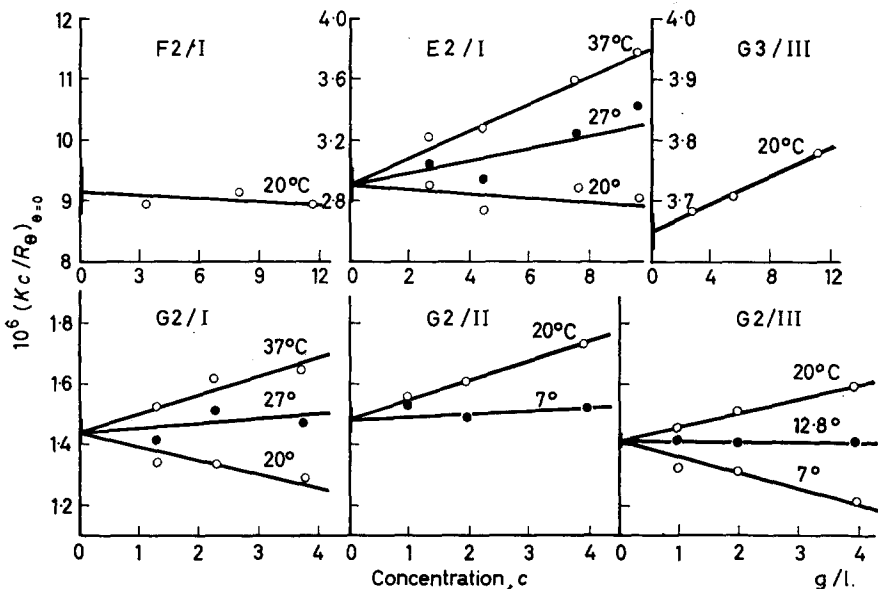


Figure 1—Light scattering results for four fractions in θ -solvents: I 37/63 MEK/isoPrOH; II 41.5/58.5 MEK/isoPrOH; III *n*-hexyl chloride. Limits of error in intercepts are indicated. Ordinates: $10^6 (Kc/R_\theta)_{\theta=0}$. Abscissae: c (g litre⁻¹)

resulting intercepts and errors are shown in Table 3. The molecular weights in different solvents agree within the experimental error of about ± 3 per cent and average values have been taken.

Table 3. Molecular weights by light scattering, M_{LS}

| Fraction | Solvent | 10^6 Intercept = $10^6/M_{LS}$ | Average M_{LS} |
|----------|--------------------------|----------------------------------|------------------------|
| G2 | 37/63 MEK/isoPrOH | 1.44 ± 0.04 | $695\ 000 \pm 20\ 000$ |
| | 41.5/58.5 MEK/isoPrOH | 1.48 ± 0.04 | |
| | <i>n</i> -Hexyl chloride | 1.42 ± 0.02 | |
| E2 | 37/63 MEK/isoPrOH | 2.91 ± 0.10 | $345\ 000 \pm 12\ 000$ |
| | <i>n</i> -Hexyl chloride | 2.87 ± 0.10 | |
| G3 | <i>n</i> -Hexyl chloride | 3.65 ± 0.03 | $274\ 000 \pm 3\ 000$ |
| F2 | 37/63 MEK/isoPrOH | 9.15 ± 0.4 | $109\ 000 \pm 4\ 000$ |

Molecular weights by sedimentation and diffusion

Figures 2 and 3 show the results of the sedimentation and diffusion measurements on three fractions in acetone at 20°C. The difference in the values of the diffusion constant D for G3 at finite concentrations as deter-

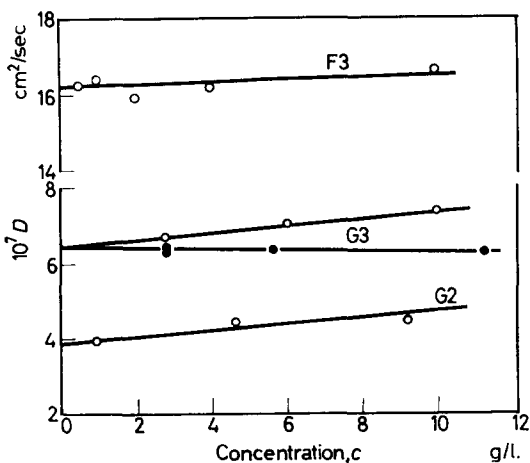
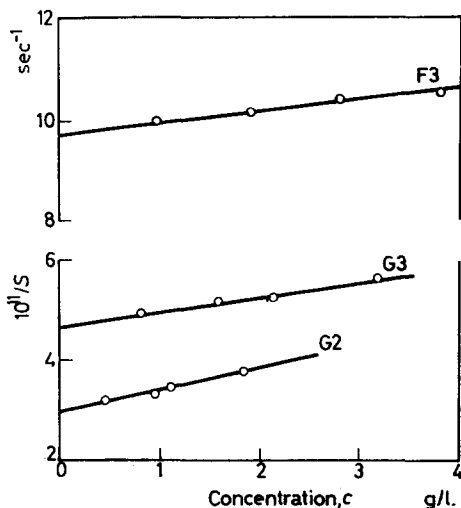


Figure 2—Diffusion constant measurements (acetone, 20°). Open circles, free diffusion method. Filled circles, thermal diffusion method.

Figure 3—Sedimentation constant measurements (acetone, 20°).



mined by the two methods suggests that this fraction is not very sharp; it was in fact a large tail fraction from the third fractionation. However, the D_0 values are the same. The molecular weights calculated from the limiting values D_0 and S_0 using the equation

$$M = RTS_0 / D_0 (1 - \bar{v}\rho)$$

are shown in Table 4. The partial specific volume of the polymer \bar{v} has been taken as equal to its apparent specific volume in acetone³, 0.793 ml/g, and the density of acetone ρ as 0.792 g/ml. These results give $D_0 \propto M_{SD}^{-0.57}$, $S_0 \propto M_{SD}^{0.43}$. The molecular weights of G2 and G3 are somewhat lower than those found by light scattering (cf. ref. 13), but the difference is rather greater than would be expected from the different averaging of M_{SD} and M_{LS} .

Table 4. Molecular weights by sedimentation and diffusion (acetone, 20°C)

| Fraction | $[\eta]$ (ml/g) (In acetone) | $10^{13} S_0$ (sec) | $10^7 D_0$ (cm ² /sec) | M_{SD} |
|----------|---------------------------------|------------------------|--------------------------------------|----------|
| G2 | 117 | 33.8 | 3.9 | 571 000 |
| G3 | 57.1 | 21.5 | 6.4 | 222 000 |
| F3 | 18.05 | 11.5 | 16.2 | 46 800 |

 θ -points

The following values for the θ -points are estimated from the temperatures at which the slopes in Figure 1 are equal to zero, i.e. the second virial coefficient is zero.

Table 5. Interpolated θ -points

| Solvent | Fraction | θ -point (°C) |
|------------------------------|----------|----------------------|
| I 37/63 MEK/isoPrOH | G2 | 26 ± 3 |
| | E2 | 22 ± 2 |
| | F2 | 23 ± 5 |
| II 41.5/58.5 MEK/isoPrOH | G2 | 4 ± 5 |
| III <i>n</i> -Hexyl chloride | G2 | 13 ± 2 |

For solvents I and III measurements of the turbidity point were also used to obtain approximate θ -points before the light scattering measurements were performed. These fit in fairly well with the values given above, as shown in Figure 4. For *n*-hexyl chloride the critical solution temperature is

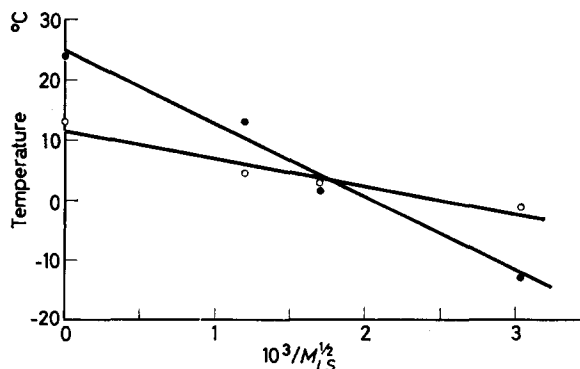


Figure 4—Turbidity point measurements. Open circles, critical solution temperatures in *n*-hexyl chloride. Filled circles, turbidity points in 37/63 MEK/isoPrOH, extrapolated to zero concentration. Points on the ordinate are the average values in Table 4.

plotted against M_{LS}^{-1} in accordance with Flory's method of extrapolation for single solvent systems¹⁴. For mixed θ -solvents it is necessary to extrapolate to infinite molecular weight *and* to zero concentration¹⁵.

In the present system the values of θ determined from the second virial coefficient are more reliable than those which would have been obtained from turbidity points alone, although in other systems, when more fractions have been used, the reverse has usually applied¹⁵.

Viscosity/molecular weight relations

The limiting viscosity numbers of the various fractions in acetone (20°C), *n*-hexyl chloride (13°C) and 37/63 MEK/isoPrOH (27°C) are shown in Figure 5 as a function of M . The values in chloroform (20°C) are almost

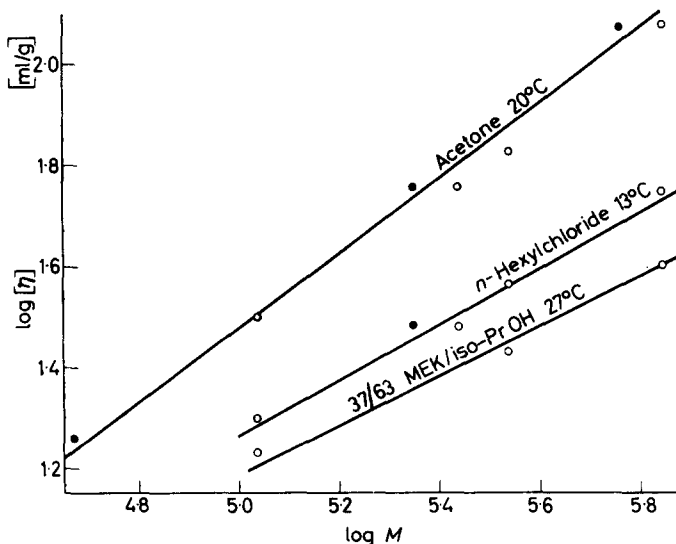


Figure 5—Viscosity measurements. Filled circles, M_{SD} values; open circles, M_{LS} values.

identical with those in acetone (20°C). Molecular weights determined from sedimentation and diffusion measurements are indicated by the filled circles; the others are the light scattering values. The best straight lines for the three solvents (giving M_{SD} and M_{LS} points equal weight) are given by:

| | |
|------------------------------------|--|
| I 37/63 MEK/isoPrOH 27°C, | $[\eta] = 4.8 \times 10^{-2} M^{0.50}$ ml/g |
| III <i>n</i> -Hexyl chloride 13°C, | $[\eta] = 3.3 \times 10^{-2} M^{0.55}$ ml/g |
| Acetone (or chloroform) 20°C, | $[\eta] = 5.9 \times 10^{-3} M^{0.74}$ ml/g. |

Although the number of points on each graph is rather small it is clear that the lines for solvents I and III have slopes close to the value of 0.50 expected for a θ -solvent, while acetone and chloroform are to be classed as good solvents. It may be questioned from the viscosity relation whether

Table 6. Dissymmetry measurements on G2

| Solvent | Temp. (°C) | Conc. (g/l.) | z | Slope Intercept | $\left(\frac{r_0^-}{r_0^+}\right)^{1/2} \frac{n/\lambda}{z}$ from slope int. | $\left(\frac{r_0^-}{r_0^+}\right)^{1/2} \frac{A}{\text{int.}}$ | |
|---|--|-----------------|-------------------------|-------------------------|--|--|-----------------|
| I 37/63 MEK/isoPROH $\lambda=436 \text{ m}\mu$ $n=1.38$ $\theta=23.5^\circ\text{C}$ | 20 | 1.31 | 1.145 1.125 1.135 | 0.21 | Av. =0.19 ± 0.02 | 464 ± 47 | |
| | | 2.29 | | 0.18 | | | |
| | | 3.78 | | 0.19 | | | |
| | 27 | 1.30 | 1.165 1.105 1.13 | 0.24 | 0.19 ± 0.04 | 0.147 ± 0.019 | 464 ± 47 |
| | | 2.27 | | 0.15 | | | |
| | | 3.75 | | 0.17 | | | |
| | 37 | 1.28 | 1.155 1.115 1.165 | 0.23 | 0.21 ± 0.04 | 0.142 ± 0.008 | 490 ± 22 |
| | | 2.24 | | 0.16 | | | |
| | | 3.70 | | 0.25 | | | |
| | II 41.5/58.5 MEK/isoPROH $\lambda=436 \text{ m}\mu$ $n=1.38$ $\theta=4^\circ\text{C}$ | 7 | 0.99 | 1.115 1.135 1.115 | 0.185 | 0.21 ± 0.02 | 490 ± 22 |
| | | | 2.00 | | 0.22 | | |
| | | | 3.98 | | 0.215 | | |
| 20 | | 0.98 | 1.135 1.145 1.13 | 0.205 | 0.22 ± 0.015 | 0.155 ± 0.007 | 490 ± 22 |
| | | 1.96 | | 0.230 | | | |
| | | 3.92 | | 0.220 | | | |
| III <i>n</i> -Hexyl chloride $\lambda=436 \text{ m}\mu$ $n=1.42$ $\theta=13^\circ\text{C}$ | 7 | 0.99 | 1.235 1.21 1.215 | 0.339 | Extrap. =0.34 ± 0.02 | 604 ± 19 | |
| | | 1.99 | | 0.304 | | | |
| | | 3.97 | | 0.316 | | | |
| | 13 | 0.99 | 1.235 1.205 1.19 | 0.344 | 0.34 ± 0.02 | 0.197 ± 0.006 | 604 ± 19 |
| | | 1.98 | | 0.304 | | | |
| | | 3.95 | | 0.284 | | | |
| | 20 | 0.98 | 1.22 1.20 1.18 | 0.320 | 0.34 ± 0.02 | 0.190 ± 0.008 | 604 ± 19 |
| | | 1.96 | | 0.282 | | | |
| | | 3.92 | | 0.251 | | | |

the θ -point for *n*-hexyl chloride is not somewhat lower than 13°C. However, the light scattering plot (*Figure 1*) leaves no doubt that the θ -point is 13°C and this is supported by the turbidity point measurements (*Figure 4*). The deviation of the exponent from 0.50 is largely due to experimental error. Furthermore we have found that the temperature coefficient of $[\eta]$ is only 0.15 per cent per degree for G2 in *n*-hexyl chloride, so that even if the θ -point were ten degrees lower the points plotted in *Figure 5* for *n*-hexyl chloride would be very little affected. Temperature also has a very small effect on the dissymmetry, see *Table 6*.

Coil dimensions from dissymmetry and viscosity measurements

We may either take the $z = i_{45^\circ}/i_{135^\circ}$ values, extrapolate to zero concentration and then use Doty and Steiner's theoretical relation for random monodisperse coils with Gaussian density distribution¹⁶, or we may plot Kc/R_θ against $\sin^2(\frac{1}{2}\theta)$ and equate the limiting value of slope/intercept at zero concentration to $(8\pi^2/9)(\bar{r}_0^2/\lambda^2)n^2$, where n is the refractive index for the wavelength λ , and \bar{r}_0^2 is the mean square end-to-end distance of the polymer coils at the θ -point¹⁷. Fairly good straight lines were obtained for the $\sin^2(\frac{1}{2}\theta)$ plots but the slope/intercept and the z values did not always vary systematically with concentration. The values for G2 are shown in *Table 6* at θ -temperatures and at other temperatures for comparison of internal consistency.

The relative values of $(\bar{r}_0^2)^{\frac{1}{2}}$ in solvents I and III are supported by the viscosity measurements as may be seen directly from *Figure 5*. A given fraction in *n*-hexyl chloride at 13°C has a value of $[\eta]$ some 30 to 40 per cent higher than that for 37/63 MEK/isoPrOH at 27°C.

The Flory constant Φ , which equals $[\eta]_0 M/(\bar{r}_0^2)^{3/2}$, is calculated from the light scattering results as $(2.6 \pm 0.9) \times 10^{23}$ for 37/63 MEK/isoPrOH and $(1.8 \pm 0.2) \times 10^{23}$ for *n*-hexyl chloride. The latter is somewhat low for a θ -solvent and is more in keeping with a good solvent, as may be seen from the collection of values by Krigbaum and Carpenter¹⁹. Theoretically Φ has the value 2.84×10^{23} for θ -solvents and decreases with increasing solvent power (cf. Meyerhoff²⁰). However, the experimental error in Φ values is rather large partly because of errors of measurement and partly because $(\bar{r}^2)^{\frac{1}{2}}$ as measured by light scattering is a 'z' average while M is a weight average; these vary to different extents with the dispersity of the polymer fractions. Hence it is difficult to decide from the Φ value whether *n*-hexyl chloride at 13°C is really a θ -solvent because the value $(1.8 \pm 0.2) \times 10^{23}$ lies within the experimental spread of Φ values for θ -solvents.

The end-to-end distance $(\bar{r}_{fr}^2)^{\frac{1}{2}}$ for a chain in which the bonds are completely free to rotate may be calculated using C—C=1.54Å, C—S=1.82Å, and taking the valence angles as tetrahedral²¹. For G2 we find $(\bar{r}_{fr}^2)^{\frac{1}{2}} = 291 \pm 4\text{Å}$ so that $(\bar{r}_0^2/\bar{r}_{fr}^2)^{\frac{1}{2}}$ is 1.6 for the MEK-isoPrOH mixture and 2.1 for *n*-hexyl chloride. These values are similar to those usually found.

Effect of temperature on second virial coefficient A_2

The variation of temperature in these experiments was too limited to

provide any sort of test of the theory of the variation of A_2 with M or T . Table 7 shows the values of B_H defined by²²

$$B_H = -RT^2 dA_2/dT$$

Table 7. B_H values for hexene-1 polysulphone

| Fraction | Solvent | Av. temp. (°C) | Av. $10^{-6} B_H$ (J ml/g ²) |
|----------|--------------------------|-------------------|---|
| G2 | <i>n</i> -Hexyl chloride | 13.5 | -2.6 ± 0.7 |
| G2 | 37/63 MEK/isoPrOH | 28.5 | -2.4 ± 0.6 |
| E2 | 37/63 MEK/isoPrOH | 28.5 | -2.3 ± 0.9 |
| G2 | 41.5/58.5 MEK/isoPrOH | 13.5 | -1.5 ± 1.1 |

DISCUSSION

The most surprising feature of the present results is the large difference in coil dimensions in θ -solvents consisting of MEK-isoPrOH mixtures on the one hand, and *n*-hexyl chloride on the other. It is possible that this difference may be associated with the fact that the MEK-isoPrOH mixtures are more polar, i.e. have higher δ -values, than the polymer, while *n*-hexyl chloride is less polar (cf. Table 1). This would mean that there are two sets of stable configurations of the polymer chains, a more compact set, stabilized by a more polar environment, the other, less compact set, stabilized by a less polar environment. Put another way it appears possible that, for polymers having strongly polar groups in the main chain, the polarity of the medium may have an important effect on the potential energy curve for rotation about the main chain bonds. Thus in a less polar θ -solvent more extended configurations may be preferred if these lead to a greater partial cancellation of the dipoles of adjacent sulphone groups.

In previous investigations of polymer coil dimensions at the θ -point, no attention has been paid to whether the θ -solvent has been less polar or more polar than the polymer. Kirste and Schulz's data²³ on $[\eta]_0$ for polymethyl methacrylate in various θ -solvents show no evidence for any systematic difference between the two types of θ -solvent. The same is also true of polystyrene data²⁴, although Bianchi *et al.* report some variation of $[\eta]_0$ according to the nature of the mixed θ -solvents, all more polar than polystyrene²⁵. However, the θ -values and hence the $[\eta]_0$ values may not be too accurate since the θ -points were only determined as the temperatures at which the exponent in the viscosity equation was equal to 0.5. θ -solvents for polyisobutene are all more polar than the polymer and provide no test.

The work described here is exploratory in nature, representing as it does the first investigation of the solution properties of the polysulphones. Further work is needed to test the ideas which have emerged, particularly with other polymers having polar groups in the backbone. Vinyl polymers with polar *side* groups presumably will not exhibit the effects so strongly because the polar groups are relatively free to rotate, independently of the main chain.

K.J.I. thanks the Leverhulme Trustees for a Research Award, Professor G. V. Schulz for laboratory facilities and stimulating discussion, and the University of Leeds for granting leave of absence. We thank the Phillips Petroleum Co. for supplies of polysulphones. We also thank Herr M. Bendix, Frl. U. Kirsten and Frl. Blum for technical assistance and Mr J. Biggins for calculating some of the solubility parameters.

*Institut für physikalische Chemie
der Universität Mainz*

(Received August 1961)

REFERENCES

- ¹ WALKER, E. E. in *Fibres from Synthetic Polymers*, p 355. Edited by R. HILL. Elsevier: Amsterdam, 1953
- ² SMALL, P. A. *J. appl. Chem.* 1953, **3**, 71
- ³ HUNT, M. and MARVEL, C. S. *J. Amer. chem. Soc.* 1935, **57**, 1691
- ⁴ COOK, R. E., DAINTON, F. S. and IVIN, K. J. *J. Polym. Sci.* 1957, **26**, 351
- ⁵ CANTOW, H-J. and SCHULZ, G. V. *Z. phys. Chem. (N.F.)*, 1954, **1**, 366
- ⁶ MEYERHOFF, G. *Makromol. Chem.* 1951, **6**, 197
- ⁷ NACHTIGALL, K. and MEYERHOFF, G. *Makromol. Chem.* 1959, **33**, 85
- ⁸ IVIN, K. J. *J. Polym. Sci.* 1957, **25**, 228
- ⁹ BODMANN, O. *Chem.-Ing.-Tech.* 1957, **29**, 468
- ¹⁰ EWART, R. H., ROE, C. P., DEBYE, P. and MCCARTNEY, J. R. *J. chem. Phys.* 1946, **14**, 687
- ¹¹ ALLEN, G., GEE, G. and WILSON, G. J. *Polymer, Lond.* 1960, **1**, 456
- ¹² BRISTOW, G. M. and WATSON, W. F. *Trans. Faraday Soc.* 1958, **54**, 1731
- ¹³ MEYERHOFF, G. *Makromol. Chem.* 1954, **12**, 45, 61
- ¹⁴ MANDELKERN, L. and FLORY, P. J. *J. Amer. chem. Soc.* 1952, **74**, 2517
- ¹⁵ KRIGBAUM, W. R. and SPERLING, L. H. *J. phys. Chem.* 1960, **64**, 99
- ¹⁶ DOTY, P. and STEINER, R. F. *J. chem. Phys.* 1950, **18**, 1211
- ¹⁷ PEAKER, F. W. in *Techniques of Polymer Characterization*, p 142. Edited by P. W. ALLEN. Butterworths: London, 1959
- ^{18a} KIRKWOOD, J. G. and RISEMAN, J. *J. chem. Phys.* 1948, **16**, 565
- ^b ZIMM, B. H. *J. chem. Phys.* 1956, **24**, 269
- ¹⁹ KRIGBAUM, W. R. and CARPENTER, D. K. *J. phys. Chem.* 1955, **59**, 1166
- ²⁰ MEYERHOFF, G. *J. Polym. Sci.* 1960, **43**, 269
- ²¹ ALLEN, P. W. and SUTTON, L. E. *Acta cryst., Camb.* 1950, **3**, 46
- ²² SCHULZ, G. V. and CANTOW, H-J. *Z. Elektrochem.* 1956, **60**, 517
- ²³ KIRSTE, R. and SCHULZ, G. V. *Z. phys. Chem. (N.F.)*, 1961, **30**, 171
- ²⁴ OUTER, P., CARR, C. I. and ZIMM, B. H. *J. chem. Phys.* 1950, **18**, 830
- ²⁵ BIANCHI, U., MAGNASCO, V. and ROSSI, C. *Chim. e Industr.* 1958, **40**, 263

A Treatment of Static and Dynamic Birefringence in Linear Amorphous Polymers by an Extension of the Molecular Theory of Viscoelasticity

B. E. READ

Calculations are made of the time and frequency dependence of the birefringence of a linear amorphous polymer held at constant extension and subjected to an oscillating extension (or compression) respectively. The method involves an extension of Mooney's version of the molecular theory of viscoelasticity. The birefringence is expressed in terms of a discrete number of relaxation times each of which is related to a normal mode of molecular motion. At constant strain the stress-optical coefficient is predicted to be independent of time. For a sinusoidally imposed strain the birefringence and stress should be in phase and the ratio of birefringence amplitude to stress amplitude should be independent of frequency and equal to the stress-optical coefficient. The frequency and temperature limits of applicability of the analysis are briefly discussed.

MOST molecular theories of the viscoelastic properties of polymers relate the time or frequency dependence of their mechanical properties to the rates of configurational changes of their chain molecules¹. The theories assume that when the equilibrium distribution of molecular configurations is disturbed upon deforming a sample, the new configurations are not initially at equilibrium and move toward equilibrium at rates dependent on the mobility of the individual chain links and on the lengths of chain involved in the motion. In the theory of Rouse² the polymer chains are divided into a number of 'submolecules' of equal length, and the motion of each chain is described (with the aid of the normal coordinate method of analysis) as a sum of cooperative movements of the ends of each submolecule. Although the Rouse theory concerns mainly polymer solutions, Mooney³ has recently modified it in a form more suitable to the treatment of bulk polymers, and in addition has extended it to the region of finite deformations.

The birefringence exhibited by a deformed polymer is also related to the orientation or configurational states of the molecules, and under equilibrium conditions, this phenomenon has received a satisfactory molecular interpretation^{4, 5}. Since birefringence measurements may also provide useful information regarding the rates of configurational changes responsible for the viscoelastic behaviour of polymers, it is of interest to consider an extension of the molecular theories to this problem. In particular it would be interesting to predict the optical properties of a polymer which is subjected to a small oscillating strain. An experimental study of this problem is at present being undertaken in this laboratory. Also, a

preliminary investigation on polyethylene has very recently been reported by Onogi, Keedy and Stein⁶.

In the subsequent analysis Mooney's treatment is briefly summarized and extended to calculate the time dependence of the birefringence for a polymer sample held at constant extension (i.e. stress-relaxation conditions). Further an expression is derived for the frequency dependence of the birefringence for a sample subjected to a small sinusoidal extension or compression. The birefringence is expressed in terms of a discrete distribution of relaxation times in which each relaxation time characterizes the motion of a given configuration mode of the molecule and is related to molecular parameters by means of the viscoelastic theory.

CONFIGURATIONS OF THE MOLECULES

Following the procedure of Rouse², each polymer chain is arbitrarily divided into ν submolecules, each just long enough so that its end-to-end distance obeys the Gaussian probability distribution. Each submolecule is assumed to contain z statistical freely jointed links, each link of length a . If one end of submolecule i is placed at the origin of a private coordinate system $OXYZ$, then, at equilibrium, the probability that the other end will lie at the point x_i, y_i, z_i , in the volume element dx_i, dy_i, dz_i , is

$$P_i(x_i, y_i, z_i) dx_i dy_i dz_i = (b/\pi)^{3/2} \exp[-b(x_i^2 + y_i^2 + z_i^2)] dx_i dy_i dz_i \quad (1)$$

where $b = 3/2za^2$.

We may now represent the configuration probability of the entire molecule by a representative point in 3ν dimensional space. The probability that this point lies in the volume element $dx_1 \dots dz_\nu$ at the point $x_1 \dots z_\nu$ is given by

$$\begin{aligned} P_\nu dx_1 \dots dz_\nu &= \prod_{i=1}^{\nu} P_i(x_i, y_i, z_i) dx_i dy_i dz_i \\ &= (b/\pi)^{3\nu/2} \exp[-b \sum_{i=1}^{\nu} (x_i^2 + y_i^2 + z_i^2)] dx_1 \dots dz_\nu \end{aligned} \quad (2)$$

MOTIONS OF THE MOLECULES

If a polymer is suddenly extended, the submolecule end-to-end distances will initially be displaced from their equilibrium values to a less probable distribution of configurations. This will result in an overall decrease in entropy (ΔS) and hence an increase in Helmholtz free energy (ΔF). Assuming that all configurations have the same internal energy then $\Delta F = -T\Delta S$. The tendency of the free energy of the system to seek a minimum value causes the configurations to change gradually toward a new equilibrium distribution.

A diffusion of the end of each submolecule will take place along each space coordinate. The velocity of flow along a particular coordinate is proportional to the product of the mobility, μ , of a junction point and the negative gradient of free energy with respect to that coordinate. A set of 3ν partial differential equations follows for the net rate of change of each

component of each submolecule end-to-end distance. For example, the net rate of change of length x_i is given by

$$\frac{\partial x_i}{\partial t} = \mu T \left(-\frac{\partial S_v}{\partial x_{i-1}} + \frac{2\partial S_v}{\partial x_i} - \frac{\partial S_v}{\partial x_{i+1}} \right) \quad (3)$$

where S_v , the entropy of a molecule of given configuration $x_1 \dots z_v$, is equal to $k \ln P_v$, where k is Boltzmann's constant. In order to solve these equations they are each reduced to a *single configurational variable* by transforming the original Cartesian coordinates to a system of normal coordinates. Representing the normal coordinates by $u_1, v_1, w_1, \dots, u_v, v_v, w_v$, the transformation is effected by an orthogonal matrix such that:

$$\sum_{n=1}^v u_n^2 = \sum_{i=1}^v x_i^2, \quad \sum_{n=1}^v v_n^2 = \sum_{i=1}^v y_i^2 \quad \text{and} \quad \sum_{n=1}^v w_n^2 = \sum_{i=1}^v z_i^2 \quad (4)$$

The expression for P_v in the new coordinates is, therefore,

$$P_v du_1 \dots dw_v = (b/\pi)^{3v/2} \exp \left[-b \sum_{n=1}^v (u_n^2 + v_n^2 + w_n^2) \right] du_1 \dots dw_v \quad (5)$$

which may be expressed as a product of probabilities each involving an individual variable

$$P_v = \prod_{n=1}^v \rho_n(u_n) \rho_n(v_n) \rho_n(w_n) \quad (6)$$

The velocity of flow along each normal coordinate is given by the time derivative of ρ_n . From equations (3), after transforming coordinates, and the equation of continuity Mooney obtains the following expression

$$\frac{\partial \rho_n}{\partial t} = -D_n \frac{\partial}{\partial u_n} \left(\frac{\partial \rho_n}{\partial u_n} + 2b \bar{u}_n \rho_n \right) \quad (7)$$

which contains only the u_n configuration variable. D_n , the diffusion coefficient governing motions of the n th mode, is given by

$$D_n = 4kT\mu \frac{\sin^2 n\pi}{2(v+1)} \quad (n=1, 2, \dots, v) \quad (8)$$

Since the diffusion of each mode of configuration is characterized by a separate diffusion coefficient, it is clear that the motion of the complete molecule will be described by a discrete distribution of relaxation rates.

A basic physical assumption underlying the theory is that when the specimen undergoes a rapid deformation with principal extension ratios λ_x, λ_y and λ_z , parallel to the X, Y and Z axes respectively, the components of the vectors joining the ends of each submolecule *initially* undergo a change in the same ratio (i.e. an affine deformation). On account of the linear transformation of coordinates the normal coordinates also undergo the same relative change. For example, the u_n, v_n, w_n coordinates change instantaneously to $\lambda_x u_n, \lambda_y v_n$ and $\lambda_z w_n$. During the subsequent relaxation process the coordinates move to their new equilibrium values. If β_{xn} denotes the

time-dependent deformation of the u_n coordinate, then Mooney has shown that an exact solution of equation (7) exists in the form

$$\rho_n = \frac{1}{\beta_{zn}} \left(\frac{b}{\pi} \right)^{\dagger} \exp \left(\frac{-bu_n^2}{\beta_{zn}^2} \right) \quad (9)$$

Substituting (9) into (7), we obtain*,

$$\frac{d\beta_{zn}}{dt} = -2D_n b \left(\beta_{zn} - \frac{1}{\beta_{zn}} \right) \quad (10)$$

The solution of equation (10) is

$$\beta_{zn}^2 = 1 + (\lambda_x^2 - 1) \exp(-t/\tau_n) \quad (11)$$

where the relaxation time τ_n , which characterizes the diffusion rate of the n th mode, is equal to $(4bD_n)^{-1}$.

Thus when $t=0$, $\beta_{zn}=\lambda_x$, and when $t=\infty$, $\beta_{zn}=1$, its equilibrium value. Corresponding expressions exist for β_{yn} and β_{zn} . From equations (11) and (8) we obtain

$$\tau_n = z\alpha^2 [24 k\mu T \sin^2 \{n\pi/2(\nu+1)\}]^{-1} \quad (12)$$

which is identical with the equation of Rouse².

THE TIME DEPENDENCE OF THE BIREFRINGENCE AND OF THE STRESS FOR A SAMPLE HELD AT CONSTANT DEFORMATION

Birefringence

We require to calculate first the contribution of a single polymer molecule, as a function of its configuration, to the total polarizability anisotropy of the bulk sample. We first consider a submolecule whose Cartesian coordinates are given by x_i, y_i, z_i . Let each freely jointed link within the submolecule have polarizabilities α_{01} and α_{02} for light with electric vector parallel and perpendicular respectively to the link direction. By analogy with the treatment of Kuhn and Grün⁵ and of Treloar^{4, 7} for a complete molecule, the polarizability anisotropy of a submolecule with ends fixed at a distance l apart may be written (for small l)

$$\begin{aligned} \alpha_{1s} - \alpha_{2s} &= \frac{3}{5} \cdot \frac{l^2}{za^2} (\alpha_{01} - \alpha_{02}) \\ &= \frac{3}{5} \cdot \frac{(x_i^2 + y_i^2 + z_i^2)}{za^2} (\alpha_{01} - \alpha_{02}) \end{aligned} \quad (13)$$

where α_{1s} and α_{2s} are respectively the polarizabilities of a submolecule along and perpendicular to the vector joining its ends. Equation (13) was derived from the *equilibrium* distribution of angles between each link and chain end-to-end vector. In the present application it is assumed that the rate of change of l is slow compared with Brownian motions of the submolecule so

*Note: Mooney's equation 35 [equivalent to (10) above] appears to contain a numerical error, containing a factor $\frac{1}{2}$ instead of 2. Furthermore, a factor 4 seems to have been lost between equations 37 and 38. The relaxation time given by Mooney's equation 38 therefore differs by a factor of 16 from that given by Rouse.

that the submolecule can instantaneously assume all available configurations for any change of l .

It is convenient to consider an elongation or compression in the OX direction. If the vector \mathbf{l} makes an angle θ_i with OX , then the contribution of the submolecule to the polarizability anisotropy of the sample, referred to directions along and perpendicular to the stretching direction, is given by⁷

$$(\alpha_{1s} - \alpha_{2s})(\cos^2 \theta_i - \frac{1}{2} \sin^2 \theta_i) \quad (14)$$

If P_l and P_t are the polarizabilities of the entire molecule for light with electric vector along and at right angles to the direction of stretch, then

$$\begin{aligned} P_l - P_t &= \sum_{i=1}^v (\alpha_{1s} - \alpha_{2s}) (\cos^2 \theta_i - \frac{1}{2} \sin^2 \theta_i) \\ &= \frac{3}{5Za^2} (\alpha_{01} - \alpha_{02}) \sum_{i=1}^v [x_i^2 - \frac{1}{2} (y_i^2 + z_i^2)] \end{aligned} \quad (15)$$

Transforming to normal coordinates by means of equation (4), we have

$$P_l - P_t = \frac{3}{5Za^2} (\alpha_{01} - \alpha_{02}) \sum_{n=1}^v [u_n^2 - \frac{1}{2} (v_n^2 + w_n^2)] \quad (16)$$

We may now calculate the total polarizability anisotropy of the bulk sample in the unstrained state. If N is the number of molecules per unit volume, then the number of molecules with representative points in the volume element $du_1 \dots dw_v$ at the point $u_1 \dots w_v$ is given by

$$dN = NP_v du_1 \dots dw_v = N (b/\pi)^{3v/2} \exp [-b \sum_{n=1}^v (u_n^2 + v_n^2 + w_n^2)] du_1 \dots dw_v \quad (17)$$

The polarizability anisotropy per unit volume is given by

$$P_1 - P_2 = \int_{-\infty}^{+\infty} \dots \int_{-\infty}^{+\infty} (P_l - P_t) NP_v du_1 \dots dw_v \quad (18)$$

Substituting (16) and (17) into (18) and evaluating the integral we find, as expected, that $P_1 - P_2$ is zero.

At any instant after an imposed deformation and partial relaxation the dN molecules (equation 17) will now have representative points in the volume element $\beta_{x1} du_1 \dots \beta_{zv} dw_v$ at the point $\beta_{x1} u_1 \dots \beta_{zv} w_v$. The contribution of each of these molecules to the total polarizability anisotropy is now

$$P_l - P_t = \frac{3}{5Za^2} (\alpha_{01} - \alpha_{02}) \sum_{n=1}^v [\beta_{xn}^2 u_n^2 - \frac{1}{2} (\beta_{yn}^2 v_n^2 + \beta_{zn}^2 w_n^2)] \quad (19)$$

For an elongation or compression in the OX direction at constant volume

$\beta_{yn}^2 = \beta_{zn}^2 = 1 + (\lambda_x^{-1} - 1) e^{-l/\tau_n}$, and hence,

$$\begin{aligned} P_1 - P_2 &= \frac{3}{5Za^2} (\alpha_{01} - \alpha_{02}) N (b/\pi)^{3v/2} \int_{-\infty}^{+\infty} \dots \int_{-\infty}^{+\infty} \exp [-b \sum_{n=1}^v (u_n^2 + v_n^2 + w_n^2)] \times \\ &\quad \sum_{n=1}^v [\beta_{xn}^2 u_n^2 - \frac{1}{2} \beta_{yn}^2 (v_n^2 + w_n^2)] du_1 \dots dw_v \end{aligned} \quad (20)$$

$$= \frac{N}{5} (\alpha_{01} - \alpha_{02}) \sum_{n=1}^{\nu} (\beta_{zn}^2 - \beta_{yn}^2) \quad (21)$$

The birefringence, Δn , is obtained from $P_1 - P_2$ via the Lorentz-Lorenz equation⁴. Thus

$$\Delta n = \frac{(\bar{n}^2 + 2)^2}{\bar{n}} \cdot \frac{2\pi}{45} N (\alpha_{01} - \alpha_{02}) \sum_{n=1}^{\nu} (\beta_{zn}^2 - \beta_{yn}^2) \quad (22)$$

where \bar{n} is the mean refractive index.

The contribution to the total birefringence due to a single configuration mode is clearly

$$\Delta n_n = \frac{(\bar{n}^2 + 2)^2}{\bar{n}} \cdot \frac{2\pi}{45} N (\alpha_{01} - \alpha_{02}) (\beta_{zn}^2 - \beta_{yn}^2) \quad (23)$$

Equation (22) may be rewritten in the form

$$\Delta n = \frac{(\bar{n}^2 + 2)^2}{\bar{n}} \cdot \frac{2\pi}{45} N (\alpha_{01} - \alpha_{02}) (\lambda_x^2 - \lambda_x^{-1}) \sum_{n=1}^{\nu} e^{-t/\tau_n} \quad (24)$$

At short times the discrete distribution of relaxation times may be replaced approximately by a continuous spectrum¹. In the limit of very small strains, equation (24) can then be reduced to

$$\Delta n/\varepsilon = K(t) = K\nu \int_0^{\infty} H(\tau) e^{-t/\tau} d\tau \quad (25)$$

where

$$K = \frac{(\bar{n}^2 + 2)^2}{\bar{n}} \cdot \frac{6\pi}{45} N (\alpha_{01} - \alpha_{02})$$

and the strain $\varepsilon = \lambda_x - 1 \ll 1$. $K(t)$ is the time-dependent strain-optical coefficient, and $H(\tau)$ the conventional distribution of relaxation times.

Stresses

The stress in a deformed material is obtained from the derivative of free energy ($\Delta F = -T\Delta S$) with respect to strain. ΔS , the difference between the total entropy of the deformed polymer at any instant and the entropy in the unstrained state, may be evaluated from the configurational probabilities of the individual molecules. For a simple extension or compression at constant volume, we obtain from Mooney's equation (51) the following expression for the observed stress f in the stretching (OX) direction

$$f = NkT(\lambda_x^2 - \lambda_x^{-1}) \sum_{n=1}^{\nu} e^{-t/\tau_n} \quad (26)$$

In the limit of very small strains and at short times, we have

$$E(t) = f/\varepsilon = 3\nu NkT \int_0^{\infty} H(\tau) e^{-t/\tau} d\tau \quad (27)$$

where $E(t)$ is the time-dependent Young's modulus.

The constant $3NkT$ is equivalent to the equilibrium Young's modulus of a crosslinked network containing N chains per unit volume between cross-

links⁴. $3\nu NkT$ is the total instantaneous modulus of the viscoelastic material. Although permanent crosslinks are absent from linear polymers, it is envisaged that the stress is initially transmitted by temporary physical junction points (such as secondary forces or entanglements) located at the ends of each submolecule. As the temporary junctions break down, the molecules diffuse back to equilibrium at rates dependent on the various normal modes of motion. After a certain time, determined by the magnitudes of the τ_n , the stress will decay to zero.

According to equations (24) and (26) both the birefringence and the stress are predicted to have a similar non-linear dependence on λ_x , as is found for a crosslinked polymer at equilibrium⁴. In addition they are both predicted to have a similar time dependence, which is observed experimentally for linear polymers held at constant elongation except in the 'glassy' region of the relaxation spectrum⁸. The stress-optical coefficient, C , should therefore be independent of time

$$C = \frac{\Delta n(t)}{f(t)} = \frac{(\bar{n}^2 + 2)^2}{\bar{n}} \cdot \frac{2\pi}{45kT} (\alpha_{01} - \alpha_{02}) \quad (28)$$

Equation (28) complies with the more general result of Lodge⁹ who has treated the flow behaviour of a polymeric network subjected to any three-dimensional strain history*. The experiments of Saunders¹⁰ on the creep of unvulcanized rubber show that C is also time-independent when the stress is held constant as opposed to the strain. Under these conditions, however, the theory is more complicated⁸.

SINUSOIDALLY IMPOSED STRAIN

Birefringence

In calculating the frequency dependence of the birefringence for a polymer sample subjected to a small oscillating elongation or compression we first consider the behaviour of a single configuration mode of all N molecules. The variations of β_{zn} and β_{yn} due to a continuously imposed deformation are given by

$$\frac{1}{\beta_{zn}} \frac{d\beta_{zn}}{dt} = -\frac{1}{2\tau_n} \left(1 - \frac{1}{\beta_{zn}^2}\right) + \frac{1}{\lambda_x} \cdot \frac{d\lambda_x}{dt} \quad (29)$$

$$\frac{1}{\beta_{yn}} \frac{d\beta_{yn}}{dt} = -\frac{1}{2\tau_n} \left(1 - \frac{1}{\beta_{yn}^2}\right) + \frac{1}{\lambda_y} \cdot \frac{d\lambda_y}{dt} \quad (30)$$

The second terms on the right express the rate of change of the β s due to the applied deformation. The first terms represent the relaxation [cf. equation (10)]. If $\epsilon \ll 1$ subtraction of (30) from (29) and elimination of β_{zn} and β_{yn} by means of equation (23) yields

$$K \frac{d\epsilon}{dt} = \frac{\Delta n_n}{\tau_n} + \frac{d\Delta n_n}{dt} \quad (31)$$

*Note: The equations derived here for the relaxation of birefringence also follow from Lodge's analysis if two of the three normal components of refractive index are made equal and the tangential component put equal to zero. In the latter treatment the relaxation is specifically attributed to the breaking and reforming of temporary network junctions. Several relaxation times are arbitrarily introduced but they are not individually defined.

Therefore, in the linear region ($\varepsilon \ll 1$), the behaviour of *each mode* is equivalent to that of a single Maxwell element comprising a spring and a dashpot in series¹¹. K is the strain-optical coefficient of the spring (analogous to the modulus) and $K\tau_n$ the ratio of birefringence to rate of strain for the dashpot (analogous to viscosity coefficient).

For a sinusoidal strain $\varepsilon = \varepsilon_0 \sin \omega t$, in which ε_0 is the strain amplitude and ω the applied frequency, from equation (31) we obtain, after summing over all configurations,

$$\Delta n = \sum_{n=1}^{\nu} \Delta n_n = \varepsilon_0 [K'(\omega) \sin \omega t + K''(\omega) \cos \omega t] \quad (32)$$

where

$$K'(\omega) = K \sum_{n=1}^{\nu} \frac{\omega^2 \tau_n^2}{1 + \omega^2 \tau_n^2} \quad \text{and} \quad K''(\omega) = K \sum_{n=1}^{\nu} \frac{\omega \tau_n}{1 + \omega^2 \tau_n^2} \quad (33)$$

Approximating the discrete spectra by continuous spectra we have

$$\left. \begin{aligned} K'(\omega) &= K \nu \int_0^{\infty} H(\tau) \frac{\omega^2 \tau^2}{1 + \omega^2 \tau^2} d\tau \\ \text{and} \\ K''(\omega) &= K \nu \int_0^{\infty} H(\tau) \frac{\omega \tau}{1 + \omega^2 \tau^2} d\tau \end{aligned} \right\} \quad (34)$$

Stress

Substitution of β_{xn} and β_{yn} in equations (29) and (30) by σ_{xn} and σ_{yn} , the principal partial stresses in the OX and OY directions respectively³, leads readily to an equation analogous to (31) but with Δn_n replaced by $\sigma_{xn} - \sigma_{yn}$ and K replaced by $3NkT$. We obtain finally

$$f = \varepsilon_0 [E'(\omega) \sin \omega t + E''(\omega) \cos \omega t] \quad (35)$$

where

$$E'(\omega) = 3NkT \sum_{n=1}^{\nu} \frac{\omega^2 \tau_n^2}{1 + \omega^2 \tau_n^2} \quad \text{and} \quad E''(\omega) = 3NkT \sum_{n=1}^{\nu} \frac{\omega \tau_n}{1 + \omega^2 \tau_n^2} \quad (36)$$

Equations (35) and (32) may be written in the form

$$f = f_0 \sin(\omega t + \delta) \quad (37)$$

and

$$\Delta n = \Delta n_0 \sin(\omega t + \delta') \quad (38)$$

where δ and δ' are the phase angles by which the stress and birefringence, respectively, lead the applied strain, and f_0 and Δn_0 the amplitudes of stress and birefringence respectively. According to equations (33) and (36) we have

$$\tan \delta = \frac{E''}{E'} = \frac{K''}{K'} = \tan \delta' \quad (39)$$

so that the birefringence and the stress are predicted to be in phase with each other. It follows that

$$\frac{K''(\omega)}{E''(\omega)} = \frac{\Delta n_0 \sin \delta'}{f_0 \sin \delta} = \frac{\Delta n_0}{f_0} = C \quad (40)$$

Similarly

$$\frac{K'(\omega)}{E'(\omega)} = \frac{\Delta n_o \cos \delta'}{f_o \cos \delta} = \frac{\Delta n_o}{f_o} = C \quad (41)$$

Therefore the ratio of the birefringence amplitude to the stress amplitude should be independent of frequency and equal to the stress-optical coefficient C .

It is important to realize that the assumptions underlying this analysis will only be valid at sufficiently low frequencies and high temperatures where the polymer behaviour is approaching that of a rubber. Only under these conditions will the molecules behave as long flexible chains capable of assuming many configurations. In this region the same distribution function $H(\tau)$ probably characterizes the behaviour of both $E(t)$ and $K(t)$. Rouse² has discussed fully the upper frequency limit at which the theory should hold, and has shown that the shortest relaxation time ($n = \nu$) is determined by the length of the submolecule. Shorter relaxation times than accounted for by the theory would involve configurational changes *within* each submolecule, and Gaussian statistics would no longer be adequate. Furthermore, in the very short time or high frequency range, or at low temperatures, where the behaviour is tending toward that of a glass, internal energy changes would have to be considered. Also, since glassy materials generally have a Poisson ratio of about a third, the constant volume assumption would no longer be valid. In the rubber-glass transition region it is often observed that the change of birefringence with time or temperature exhibits an abrupt reversal⁸. It is probable that distortional mechanisms are here replacing the orientational effects, and it is possible that a study of the phase relationship between birefringence and stress in this region may aid in a further understanding of the mechanism of viscoelastic response.

The work described above has been carried out as part of the research programme of the National Physical Laboratory, and this paper is published by permission of the Director of the Laboratory.

Basic Physics Division,
National Physical Laboratory,
Teddington, Middlesex

(Received September 1961)

REFERENCES

- ¹ FERRY, J. D. *Viscoelastic Properties of Polymers*. Wiley: New York, 1961
- ² ROUSE, P. E. *J. chem. Phys.* 1953, **21**, 1272
ROUSE, P. E. *J. chem. Phys. Japan*, 1955, **10**, 804
- ³ MOONEY, M. J. *Polym. Sci.* 1959, **34**, 599
- ⁴ TRELOAR, L. R. G. *The Physics of Rubber Elasticity*. Oxford University Press: London, 1958
- ⁵ KUHN, W. and GRÜN, F. *Kolloidzshr.* 1942, **101**, 248
- ⁶ ONOGI, S., KEEDY, D. A. and STEIN, R. S. *J. Polym. Sci.* 1961, **50**, S15

- ⁷ TRELOAR, L. R. G. in *Die Physik der Hochpolymeren*, Vol. IV (edited by H. A. STUART), Chapter 5, p 337, Springer: Berlin, 1956
- ⁸ STEIN, R. S. in *Die Physik der Hochpolymeren*, Vol. IV (edited by H. A. STUART), Chapter 1, p 110. Springer: Berlin, 1956
- ⁹ LODGE, A. S. *Trans. Faraday Soc.* 1956, **52**, 120
LODGE, A. S. *Flow Properties of Blood*. Pergamon: London, 1960
- ¹⁰ SAUNDERS, D. W. *Trans. Faraday Soc.* 1956, **52**, 1414
- ¹¹ ALFREY, T. and GURNEE, E. F. *Rheology*, Vol. I (edited by F. R. EIRICH), Chapter 11, p 387. Academic Press: New York, 1956

Development of an Elution Chromatography Technique for *cis*-1,4-Polybutadiene*

J. M. HULME and L. A. McLEOD

Experiments are described to show that cis-1,4-polybutadiene can be fractionated using the elution chromatography technique of Baker and Williams. Changes have been made to the equipment to give easier and more reliable operation. A method of selecting solvents and precipitants is described and it is shown that by proper selection of solvent and precipitant, the resolution of the higher molecular weight fractions may be improved. The influence on the fractionation of temperature, concentration of polymer in the eluant and column loading are investigated. It is concluded that column loading is the most important factor in explaining reversals of limiting viscosity number in the fractionation results.

ESTABLISHED methods of determining the molecular weight distribution of high polymers by fractional precipitation are generally tedious and require considerable quantities of polymer. Recently attention has been focused on separations effected by techniques employing packed columns from which the polymer is eluted in fractions by solvents of increasing solvent power or by combinations of solvent and precipitant¹⁻³. One of these methods² employs a column packed with small glass beads (0.1 mm diameter). A temperature differential is maintained along the length of the column by means of a large aluminium jacket which is heated at the top and cooled at the bottom. The polymer is eluted from the column by an eluant which is continuously enriched in solvent power by the progressive addition of a solvent to a precipitant. This method is claimed to produce results superior to those from the more conventional 'batch' technique and offers advantages in speed of operation and in the size of the polymer sample required for characterization.

There have been few publications describing the use of this technique; the originators of the method³ describe the separation of polystyrene as do Pepper and Rutherford⁴, and Schneider *et al.*⁵ A recent paper by Jungnickel and Weiss⁶ deals with polystyrene and polyolefins. Caplan⁷ has used a slightly modified version for the separation of polysarcosine dimethylamide. None of these methods involves the separation of elastomers. The work presented here describes the development of this technique for the fractionation of stereoregular polybutadiene.

EQUIPMENT

The original equipment described by Baker and Williams was duplicated in this laboratory but it was found that ice water flowing through the copper

*Presented in part at the Tenth Canadian High Polymer Forum, Sainte Marguerite, Quebec, September 1960.

cooling coil at the bottom of the jacket was not adequate to give a sufficiently large temperature differential along the length of the column. The cooling coil was therefore replaced by a jacket (D, *Figure 1*), through which was pumped a temperature controlled refrigerant. The top of the column jacket was heated by an electrical heating element wound directly on the jacket and controlled by an autotransformer in series with a voltage stabilizer. The whole of the column jacket assembly was insulated by a 1 in. layer of glass wool. With these modifications it was found possible to establish a temperature gradient of 50°C along the length of the column with a maximum variation of $\pm 0.1^{\circ}\text{C}$.

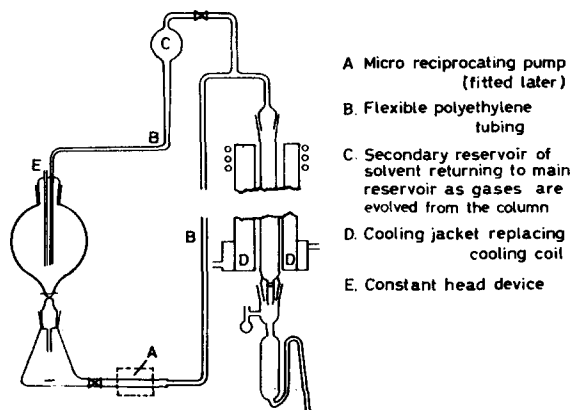


Figure 1—Equipment after modification

After several trial runs using polystyrene, it was evident that control of flow rate through the column by means of a capillary jet fitted to the outlet was variable and troublesome. Frequent blockages and marked changes in the flow rate occurred, particularly towards the end of the experiment when the viscosity of the column effluent was high due to high molecular weight polymer in solution. This difficulty was minimized by the use of a syphoning technique which permitted ready control of flow rate by simply raising and lowering the whole of the eluant mixing assembly. The relatively small driving head eliminated the need for a capillary constriction. It was also found that the evolution of dissolved gases from the eluant components on entering the heated zone of the column interfered with smooth operation and changed the pre-set volume in the mixing vessel controlling the solvent gradient. These gases were allowed to escape through a suitable arrangement at the highest point of the syphon (C, *Figure 1*).

This method of operation was found to be more reliable than the original apparatus but has been still further improved by the use of a micro reciprocating pump (A, *Figure 1*), with a variable stroke, fitted between the mixing vessel and the column.

Fractions were collected by volume in a syphon arrangement similar to that described by Baker and Williams. The fraction collector turntable was operated by a relay actuated by the change in dielectric constant

between the plates of a condenser fitted to the discharge arm of the collecting syphon. The polymer fractions were isolated by transferring a suitable volume of the column effluent to a tared volumetric flask. The excess eluant was then evaporated in a current of nitrogen by a warm water bath.

SAMPLE PREPARATION

Baker and Williams describe a method in which the polymer is coated on to the surface of a portion of the glass beads used for column packing. This was found to be impracticable with elastomers since the mixture tended to ball together rather than to form discrete particles as with polystyrene. Instead, the polymer, as a solution in a volatile solvent, was mixed with about 5 g of a calcined diatomaceous aggregate sold commercially under the name of 'Chromosorb' (Canadian Johns-Manville Co. Ltd, Celite Division). It has been found possible to impregnate this material with polymer using the method described by Baker and Williams. When dealing with polybutadiene, nitrogen was used to drive off the excess solvent in order to prevent oxidative degradation. However, Chromosorb is a powerful adsorbent and it has been found that an appreciable quantity of polymer is retained even under severe extraction conditions. To overcome this difficulty the Chromosorb is impregnated as described above with *cis*-1,4-polybutadiene with a limiting viscosity number of about 4.5. The impregnated Chromosorb is extracted in the column by carrying out a blank run in which the eluant is discarded after it has passed through the column. The recovered Chromosorb may then be used many times until the amount becomes depleted by losses or accidentally contaminated with gelled polymer. There are possible objections to this practice but experience has shown that recovery of subsequent polymer samples is usually 97 to 100 per cent and that the results are quite reproducible.

Another technique was tried in an attempt to eliminate the use of Chromosorb. The polymer was charged to the column in a solvent-precipitant mixture which just maintained solution at the highest temperature of the column. The lower temperatures encountered as the solution passed down the column caused progressive precipitation of polymer along the length of the column. However, it was found difficult to arrange for a solvent-precipitant mixture which would give complete precipitation of the polymer over the 50°C temperature gradient. The method was rejected in favour of the Chromosorb technique described earlier.

SELECTION OF THE SOLVENT GRADIENT

Examination of the eluant mixing technique shows that an exponential gradient will be produced which can be defined by the expression

$$V = I \ln (C - x_1) / (C - x_2) \quad (1)$$

where V is the total volume of eluant passing through the system, I is the volume in the mixing vessel, C is the concentration of the enriching solvent vessel, and x_1 and x_2 are the concentrations of solvent in the eluant at the beginning and end of the experiment.

It was found during trial runs that the use of a solvent gradient where $x_1=0$ and $C=100$ (corresponding to pure precipitant and pure solvent) is inefficient and causes elution of most of the sample in a small volume. For maximum efficiency the values of x_1 and x_2 should be adjusted so that at concentration x_1 the polymer is just completely insoluble at the high temperature of the column and at concentration x_2 the polymer is just completely soluble at the low temperature of the column. The value of C should be set slightly higher than x_2 .

For a given average concentration of polymer in the eluant, defined as

$$\frac{\text{Weight of polymer charged, } Wg \times 100}{\text{Total volume of eluant which contains polymer, } V \text{ ml}}$$

the size of the charge defines the elution volume V . The values x_1 and x_2 are fixed by the solubility characteristics of the polymer in the solvent-precipitant pair and C is set slightly higher than x_2 . Substituting these values in the expression (1) gives the volume l to be used in the mixing vessel.

The size of the sample to be fractionated and the average concentration of polymer in the eluant cannot be chosen so readily. For columns of comparable diameter Baker and Williams³ have used 0.3 g of polymer on a 30 cm column and Pepper and Rutherford have used 8 g on a 90 cm column. A charge of 0.6 g on a 30 cm column was initially used in this laboratory and allowed the collection of 12 to 14 samples of a size suitable for the measurement of limiting viscosity number. Baker and Williams do not quote the average concentration in their experiments but from the results shown it is judged to be about 0.2 g/100 ml. Pepper and Rutherford arbitrarily fix 0.5 g/100 ml as the *maximum* average concentration to be used. We chose initially to use an average concentration of 0.2 g/100 ml. The choice of 0.6 g as the size of the sample to be fractionated and 0.2 g/100 ml as the average concentration therefore fixes the eluant volume V at 300 ml. Experiments will be described which show that 0.3 g of polymer is a more suitable charge to use.

SOLVENT SELECTION

The arguments of the previous paragraphs, and those of Pepper and Rutherford, indicate that the choice of eluant components is restricted only by properties such as boiling point and chemical stability. However, it has been found that the use of 'good' solvents and vigorous precipitants allows only a small change in composition of the eluant from complete insolubility to complete solubility of the polymer. Combinations which would effect solution of the different molecular species over a large range of concentrations would simplify the make-up of eluants, and it was thought that the sensitivity of the method might be improved. Jungnickel and Weiss⁶ have selected solvents for polystyrene fractionation using the same premise. After the fractionation technique had been developed to give reliable data the question of choosing a solvent-precipitant pair was reviewed. Four experiments were carried out using combinations of 'good' and 'poor' solvent (toluene and di-isobutylene), with vigorous and mild precipitants (*n*-propanol and iso-octane). The *average* concentration of polymer in the

eluant was comparable in each experiment (0.085 to 0.09 per cent), and did not exceed 0.15 per cent at any stage. *Figure 2* shows the result when the limiting viscosity number of a given fraction is plotted against the concentration of solvent in the eluant at which the fraction was eluted. It is seen that the change in limiting viscosity number for a given change in solvent concentration is much lower in the experiment where di-isobutylene and iso-octane were used.

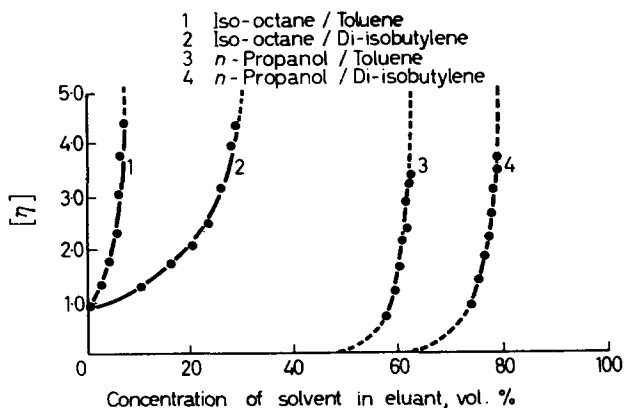


Figure 2—Solubility curves for polybutadiene in various solvent-precipitant systems

It should be mentioned that the resolution was poor above a limiting viscosity number of about 3.0 in the two experiments where *n*-propanol was used and only when iso-octane and di-isobutylene were used was the fractionation completely free of reversals of limiting viscosity number at the higher molecular weights.

It is concluded from these results that, for a given set of conditions, the fractionation is much less sensitive to random imperfections in the solvent gradient and is probably capable of higher resolution at higher molecular weights when a suitable solvent-precipitant pair is used. This may be compensated by increasing the mixing volume *I* when an unsuitable solvent-precipitant combination is used. Then, for a given flow rate through the column, the elution volume *V* and the residence time of the polymer in the column will be increased proportionately. With heat sensitive polymers this could result in serious thermal degradation.

A simple method has been devised to select a suitable solvent-precipitant pair: the polymer is dissolved in a known 'good' solvent to give a concentration of about 0.5 g/100 ml and portions of this solution are then titrated to the cloud-point at room temperature with a selection of precipitants. That precipitant which gives the highest titre to induce precipitation is considered the mildest and most desirable. For the choice of solvent the polymer is dissolved in a selection of solvents, again at about 0.5 g/100 ml, and each solution is titrated with a known vigorous precipitant to the cloud-point.

That solvent which requires least precipitant to induce precipitation is considered the poorest and most desirable.

A dilute solution of the polymer in the selected solvent is then titrated with the selected precipitant to the cloud-point at the high and low temperatures of the column. The difference found in the compositions of the mixture at which precipitation occurs then gives an arbitrary measure of the range over which a given pair will effect solution of the polymer. The concentration of incipient precipitation at the low temperature of the column fixes the value of x_2 referred to in equation (1). The value of x_1 is determined from a precipitation curve carried out at the high temperature of the column.

STABILITY OF THE POLYMERS

Polystyrene and polyisobutylene were used for trial runs on the equipment and it was considered that these polymers were sufficiently stable to give a positive indication of fractionation without the use of antioxidant. Because of its structure polybutadiene was expected to be more sensitive to attack by oxygen dissolved in the solvents especially at the higher temperatures encountered in the column.

An experiment was carried out in which a sample of polybutadiene was dissolved in di-isobutylene to give a concentration of about 0.45 g/100 ml. The solution was divided into three parts, A, B and C. Phenyl- β -naphthylamine was added to solution A to give a concentration of 0.02 g/100 ml; an antioxidant of the bis-phenol type was added to solution B to the same concentration and solution C was left unprotected. Aliquot portions of these solutions were heated in lightly corked test tubes at $60^\circ \pm 1^\circ\text{C}$. Table 1 shows the limiting viscosity numbers of the samples after heating for various times.

Table 1. Stability at 60°C of polybutadiene, $[\eta]=2.93$

| Sample | Antioxidant | Hours at 60°C | $[\eta]$ |
|------------|-------------|---------------|----------|
| Solution A | PBNA | 16 | 2.73 |
| | | 40 | 2.67 |
| | | 88 | 2.36 |
| Solution B | Bis-phenol | 42 | 2.86 |
| | | 66 | 2.79 |
| | | 138 | 2.76 |
| Solution C | Nil | 16 | 2.13 |
| | | 40 | 1.53 |
| | | 88 | 0.74 |

Since the fractionations were expected to be completed within 40 hours the protection afforded by the antioxidant used in solution B was thought to be adequate. Experience showed that the fractionations were completed in 3 to 5 hours.

In a similar series of stability tests using high and low molecular weight fractions the solutions were heated in the presence of the bis-phenol anti-oxidant at 80°C. The limiting viscosity number of the high molecular weight fraction fell from 4.18 to 4.15 after heating for 7 hours and to 4.03 after 16 hours. No change could be detected in the limiting viscosity number of the low molecular weight fraction ($[\eta]=0.71$), after 88 hours at 80°C.

From these experiments it was concluded that the polymer could be protected by the addition of a suitable antioxidant to the eluant at the rate of 0.02 g/100 ml. In this way the polymer would be protected at all times in the column and during the evaporation of the eluants prior to measuring the limiting viscosity numbers of the fractions. Corrections to the weight of the fraction used for measurement of the limiting viscosity number could be made by measuring the volume of eluant collected for each fraction.

RESULTS

Materials and analytical techniques

The following materials were used in this work:

Polystyrene— $[\eta]=1.73$ (in toluene at 30.2°C).

Polyisobutylene— $[\eta]=1.22$ (in di-isobutylene at 30.2°C).

Polybutadiene—Two polymers were used for this work. Each was prepared in solution in a hydrocarbon solvent with a titanium tetraiodide-aluminium alkyl complex catalyst.

Sample A $[\eta]=2.40$ (in toluene at 30.2°C)

Sample B $[\eta]=2.31$ (in toluene at 30.2°C)

Both samples were analysed by infra-red spectroscopy and were found to have 92 to 94 per cent *cis*-1,4-; 2 to 3 per cent *trans*-1,4- and 4 to 5 per cent 1,2- configuration.

Solvents—

Methylethyl ketone, technical grade

Ethyl alcohol, technical grade

Iso-octane, Phillips Petroleum Co., pure grade

n-Propanol, technical grade

Di-isobutylene, technical grade, re-distilled in these laboratories

All solvents were checked for the presence of non-volatile components which would interfere with the recovery of the polymer fractions.

Limiting viscosity number—Limiting viscosity numbers were determined by measuring $\eta_{sp.}/c$ at a concentration between 0.1 and 0.2 g/100 ml and calculating $[\eta]$ from the equation of Schulz and Sing⁹.

$$[\eta](1 + k\eta_{sp.}) = \eta_{sp.}/c$$

A value of 0.28 was adopted for k in all cases and was shown to give results accurate to ± 0.05 when compared with results determined by plotting $\ln(\eta_r/c)$ versus c at four concentrations and extrapolating to $c=0$.

Flow times were measured in an Ubbelohde suspended level viscometer at 30.2°C using toluene as the solvent for polybutadiene and polystyrene and di-isobutylene as the solvent for polyisobutylene. The concentrations of the polybutadiene solutions were corrected for the antioxidant included from

the fractionation when measuring the flow times of the fractions. Flow times of antioxidant solutions in toluene in excess of those encountered during the experimental work were found to be within 0.1 second of the flow time of the pure toluene.

The distribution curves were plotted in the form $[\eta]$ versus $W_n + \frac{1}{2} W_{n+1}$ where W_n is the sum of the weight per cent of all the fractions to the n th and $\frac{1}{2}W_{n+1}$ is half the weight per cent of the $(n+1)$ th fraction.

Preliminary experiments were carried out with polystyrene using the techniques described by Baker and Williams, unmodified except for the changes made to improve control of the temperature gradient. A few runs sufficed to show that the polymer was being separated but that there were deficiencies in the equipment. With the equipment modified as illustrated in *Figure 1*, fractionations were undertaken of a polystyrene sample and of a polyisobutylene sample. Typical results of the fractionations are shown in *Figure 3*.

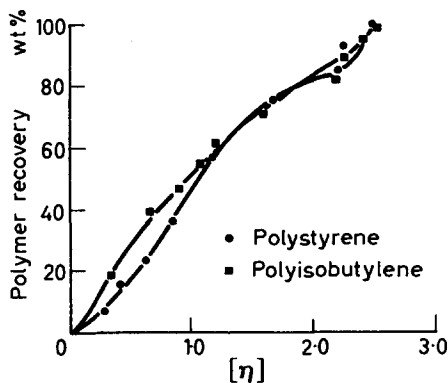


Figure 3—Results of polystyrene and polyisobutylene fractionation

It is evident that a molecular weight separation has been achieved in both cases and that the technique is applicable to an elastomer such as polyisobutylene as well as for a plastic as originally claimed. Attention is drawn to the curvature of the integral curve at the higher molecular weight end. This effect was initially regarded as spurious since most of the high molecular weight samples were quite small in total weight and the accuracy of the determinations of the limiting viscosity number was doubtful. The effect was recognized as real when fractionations of polybutadiene gave integral curves of reversed slope at the high molecular weight end. Other workers² have observed a similar behaviour for polyethylene and attributed it to degradation. A typical reversal of this type, for polybutadiene sample A, is illustrated in *Figure 4*.

It was thought that the reversal was due to degradation of the high molecular weight fragments of the polymer. The stability tests on high and low molecular weight fractions described earlier were carried out at this

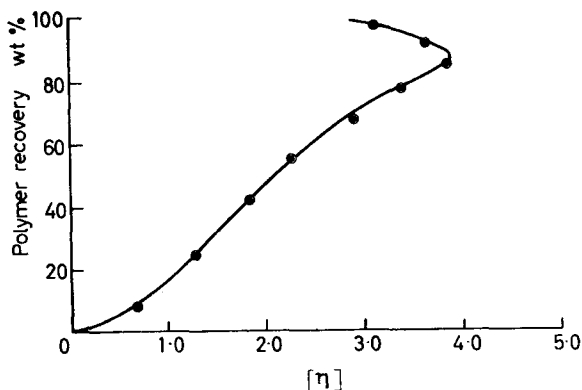


Figure 4—Typical reversal of limiting viscosity number

time and showed that the high molecular weight fractions were not appreciably affected by heating at column temperatures for periods longer than the duration of the experiments.

Other sources of the reversal effect were investigated including the removal of catalyst residues from the sample, the use of eluants free of dissolved oxygen, various types and sizes of column packing, and changes in the temperatures of the column. Most of these changes did not appear to influence the results. The result of one run in which the column was packed with washed sand graded to 840 to 1410 microns gave results which indicated severe degradation and crosslinking of the polymer despite the presence of antioxidant. A second run in which the column was packed with glass beads of 420 microns diameter, compared with 120 microns for the usual packing and giving about one sixth of the surface area, gave a result similar to that shown in *Figure 4*. It was found that a temperature gradient of 31° to -17°C gave worse resolution of the higher molecular weight fractions than did a similar gradient at higher temperatures (75° to 25°C). This suggested that adsorption may be the cause of the reversal since adsorption effects should be more severe at lower temperatures. Krigbaum and Kurz⁸ investigated this phenomenon and have shown that adsorption of the high molecular weight fractions on to the column packing can influence the results. If adsorption were contributing to reversals in this case, then a low charge of polymer should show more severe reversal than a high charge because of the greater ratio of packing surface to polymer. To test this theory a series of runs was carried out at 90° to 40°C , the highest practicable temperatures when using iso-octane as precipitant and diisobutylene as solvent. Runs were made with 0.3 g, 0.6 g and 1.1 g of polybutadiene sample A. The results, illustrated in *Figure 5*, showed that the low charge gave the best result and the high charge the poorest. From this it was concluded that adsorption did not interfere with fractionation at these temperatures but that the size of the polymer charge was critical.

At lower temperatures with 0.3 g of polymer charged to the column the problem of reversal was again evident as shown by the fractionations of

sample A illustrated in *Figure 6*. Overloading the column, adsorption, or poor equilibrium between the static and moving phases may be the cause but the investigation of these effects was not pursued.

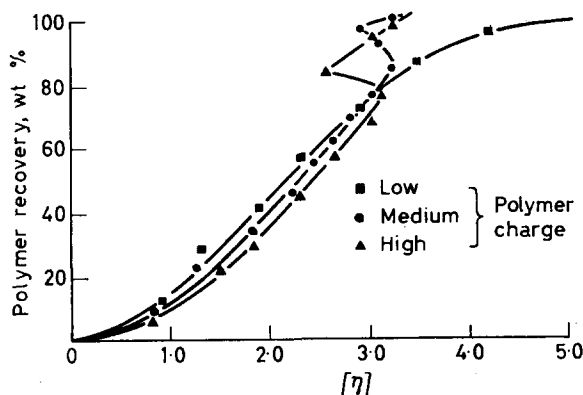


Figure 5—Effect of varying the charge of polymer to the column

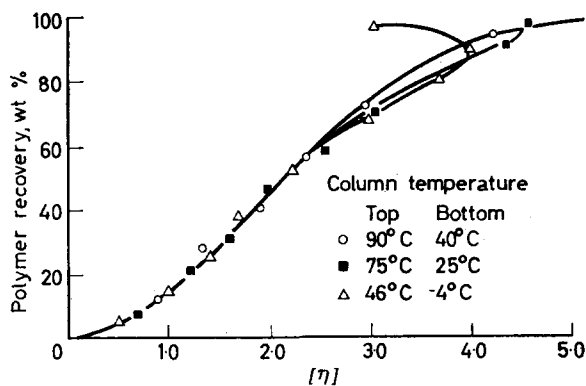


Figure 6—Effect of varying the temperatures of the column

The results of Pepper and Rutherford⁴, and of Schneider *et al.*⁵, show that high concentrations of polymer in the eluant can also contribute to reversal. A series of experiments was conducted in which the concentration of polymer in the eluant was varied while the rate of elution of the polymer remained substantially the same. This was done by changing the mixing volume and the flow rate so that the rate of elution was approximately 0.1 g/h. The average concentration of polymer was varied from a low of 0.096 g/100 ml in which the maximum concentration was 0.105 g/100 ml to 0.147 g/100 ml in which the maximum was 0.288 g/100 ml. The temperature gradient was 90° to 40°C. Polybutadiene sample B was used

for this work. The results, illustrated in *Figure 7*, showed that the concentration of polymer in the eluant was not critical over the range investigated.

Experiments in which the flow rate was varied were not exhaustive but eluant flow rates up to 125 ml/h and polymer elution rates approaching 0.3 g/h were employed successfully. An eluant flow rate of 125 ml/h with a total residence time of three to five hours has been adopted for routine fractionations.

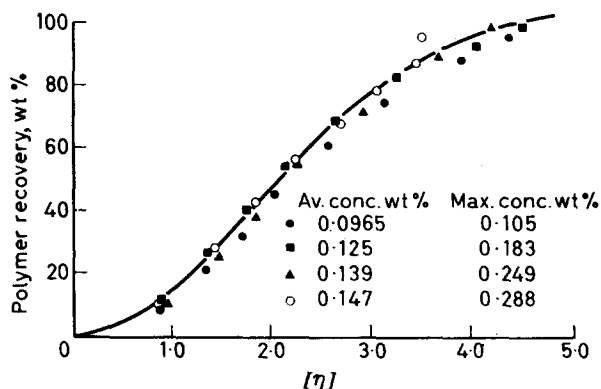


Figure 7—Effect of varying the concentration of polymer in the eluant

The efficiency of the fractionation technique was tested by refractionation of polymer fractions. A series of identical runs was carried out. Fractions of about 10 per cent by weight of the polymer charged were taken at the same stage in each run and combined until about 0.5 g of each fraction was available. The polymer fractions were recovered by evaporating the excess eluants to a volume of about 25 ml in a hot water bath by a stream of nitrogen. The approximate concentration of the polymer at this stage was 2 g/100 ml. 100 ml of ethanol was added to this solution slowly with

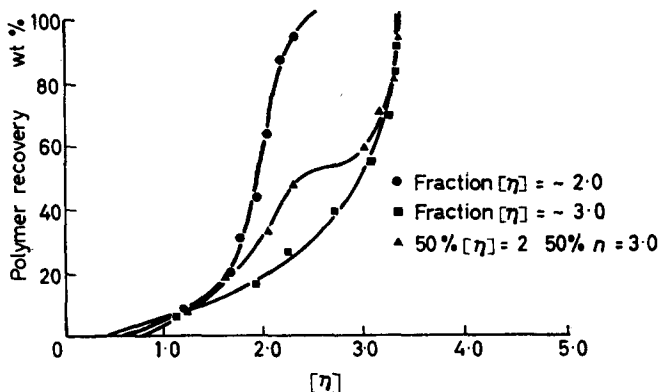


Figure 8—Refractionation of fractionated samples

stirring. The coagulated polymer was recovered by decantation, washed with a small amount of fresh alcohol and dried in a vacuum oven at 35°C. A test conducted separately showed that about 95 per cent of the antioxidant was removed by this treatment leaving not more than 1 to 2 mg/100 mg in the polymer. This treatment was necessary to remove the large quantity of antioxidant from the fractions. Two fractions and a mixture containing 50 per cent by weight of each of these fractions were refractionated. The results of these experiments are shown in *Figure 8*.

Typical results from fractionations of other polybutadiene samples listed in *Table 2* are shown in *Figure 9*.

Table 2. Polybutadiene samples fractionated by this technique

| | <i>Sample description</i> | $[\eta]$ | % <i>cis</i> - 1,4 | % <i>trans</i> - 1,4 | % 1,2- vinyl |
|----------|---|----------|-----------------------|-------------------------|-----------------|
| Sample C | Polybutadiene catalysed with a Li butyl catalyst | 2.44 | 35.4 | 53.6 | 11.0 |
| Sample D | Polybutadiene catalysed with a cobalt/aluminium alkyl complex | 2.31 | 96.7 | 1.4 | 2.0 |
| Sample E | Polybutadiene catalysed with a titanium/aluminium alkyl complex | 2.58 | 94 | 2 | 4 |

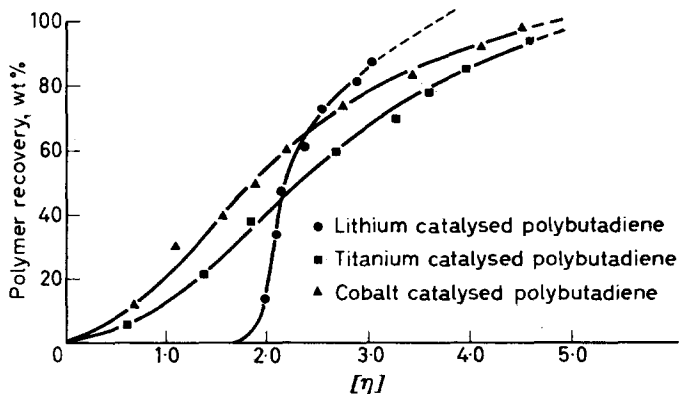


Figure 9—Typical distribution curves for polybutadiene

CONCLUSIONS

Polybutadiene can be fractionated by the chromatographic technique of Baker and Williams. The following general conditions should be used in order to achieve the best fractionations:

- (a) The solvent gradient should be adjusted to give an elution volume which will not allow concentrations of polymer of more than 0.3 g/100 ml.

- (b) The column temperatures should be as high as possible for the eluant components employed and the polymer should be protected against thermal degradation.
- (c) The solvent and precipitant should be selected to give as large a difference as possible between concentration at which the polymer is not soluble to that at which the polymer is completely soluble.
- (d) With a temperature gradient from 90° to 40°C there is no evidence that adsorption of polymer on the column packing interferes with successful fractionation. It has been clearly established that overloading the column with polymer is responsible for reversals of limiting viscosity number in the fractionation results. The optimum charge to a column of the dimensions used in this work (30 cm long \times 2.4 cm internal diameter), lies between 0.3 g and 0.6 g of polymer. At lower operating temperatures a charge of 0.3 g of polymer gave reversals. Whether this effect is due to a change in the tolerable charge of polymer at lower temperatures or to other effects has not been established.

The authors wish to acknowledge the cooperation of Mr W. A. Congdon of this laboratory for determining the limiting viscosity numbers and of Polymer Corporation Limited for permission to publish this work.

*Research and Development Division,
Polymer Corporation Ltd,
Sarnia, Ontario, Canada*

(Received October 1961)

REFERENCES

- ¹ DESREUX, V. *Rec. Trav. chim. Pays-Bas*, 1949, **68**, 789
- ² FRANCIS, P. S., COOKE, R. C., Jr and ELLIOTT, J. H. *J. Polym. Sci.* 1958, **31**, 453
- ³ BAKER, C. A. and WILLIAMS, R. J. P. *J. chem. Soc.* **1956**, 2352
- ⁴ PEPPER, D. C. and RUTHERFORD, P. P. *J. appl. Polym. Sci.* 1959, **2**, No. 4, 100
- ⁵ SCHNEIDER, N. S., HOLMES, L. G., MJAL, C. F. and LOCONTI, J. D. *J. Polym. Sci.* 1959, **37**, 551
- ⁶ JUNGnickel, J. L. and WEISS, F. T. *J. Polym. Sci.* 1961, **49**, 437
- ⁷ CAPLAN, S. R. *J. Polym. Sci.* 1959, **35**, 409
- ⁸ KRIGBAUM, W. R. and KURZ, J. E. *J. Polym. Sci.* 1959, **41**, 275
- ⁹ SCHULZ, G. V. and SING, G. *J. prakt. Chim.* 1942, **161**, 161

The Reactivity of the Growing Ion in Ionic Polymerization

T. HIGASHIMURA, Y. IMANISHI, T. YONEZAWA, K. FUKUI and S. OKAMURA

In order to discuss reactivity in the propagation reaction of ionic polymerization, the reactivities of both vinyl monomers and growing ions were investigated. In this paper, three methods of comparing the reactivities of ions were proposed: (1) direct measurement of the propagation rate constant, (2) comparison between the chain transfer constant ratios, and (3) a molecular orbital approach. From these experimental and theoretical investigations, it was found that the ion produced from the more reactive monomer was stable and less reactive, analogous to radical polymerization.

IN ORDER to discuss reactivity in the propagation reaction of a vinyl monomer, both the reactivity of monomer and the reactivity of the growing ion must be considered. There have been many investigations on the reactivity of a monomer towards a radical or an ion in copolymerization. In radical copolymerization the reactivity may be considered in terms of Q/e values. Alfrey and Price¹ showed that the propagation rate constant can be expressed as

$$k_p = P Q \exp(-e, e_m) \quad (1)$$

where Q and e_m are the values representing the reactivity and the electrostatic character of the monomer, respectively; P and e_r relate to the adduct radical. Okamura *et al.*² reconsidered the experimental results so far reported and found that the following relation held between P and Q

$$\log P = k Q + a \quad k < 0 \quad (2)$$

In equation (2), it is seen that the reactivity of the radical produced from the monomer with greater reactivity is generally smaller.

On the other hand there have been few discussions on the reactivities of growing ions produced from the various kinds of monomers. Since the monomer reactivity ratio, γ_1 , is approximately equal to $1/\gamma_2$ in ionic copolymerization, it has been considered that the relative reactivities of the two monomers towards different growing ions are about the same³. The difference in reactivity of the different kinds of ions has not been discussed.

In the present paper, the relation between the reactivity of the monomer and of the growing ion is investigated theoretically. Further, we discuss the outline of procedures to determine the reactivity of a growing ion.

PROPAGATION RATE CONSTANTS AND THE REACTIVITIES OF POLYMER IONS

Cationic polymerization

In order to determine the reactivity of growing ion, we have to decide upon the propagation rate constant (k_p) and the monomer reactivity ratio

(γ_1, γ_2) as in radical polymerization. In ionic polymerization, however, there have been no methods to determine k_p . Recently we found a method of determining k_p in the iodine catalysed system⁴. In this investigation, k_p and (γ_1, γ_2) were determined for vinyl isobutyl ether (VIBE) and vinyl 2-chloroethyl ether (VCEE). The polymerization in dichloroethane by iodine at 30°C gave the following results: $\gamma_1 = 2.0 \pm 0.1$, $\gamma_2 = 0.5 \pm 0.1$ (M_1 is VIBE and M_2 is VCEE). On the other hand, k_{11} and k_{22} are considered to be equal to the values of k_p of the respective monomers under the same polymerization conditions. Thus we obtained $k_{11} = 390$ and $k_{22} = 260$ l./mol min. Substituting these values into γ_1 and γ_2 we can obtain k_{12} and k_{21} . The results are shown in Table 1. (All these values have been reported⁴. The results appear here for convenience.)

Table 1. Propagation rate constants (l./mol min) in the copolymerization of vinyl isobutyl ether (M_1) and vinyl 2-chloroethyl ether (M_2)

| k_{11} | k_{12} | k_{21} | k_{22} |
|----------|----------|----------|----------|
| 390 | 195 | 520 | 260 |

Catalyst: iodine. Solvent: dichloroethane. Polymerization temperature: 30°C.

It is seen in Table 1 that the reaction rate constants in ionic copolymerization decrease in the order:

$$k_{21} > k_{11} > k_{22} > k_{12}$$

This order obviously indicates that a possible set of conditions, $k_{11} = k_{21}$ and $k_{22} = k_{12}$, to make $\gamma_1 = 1/\gamma_2$, is not satisfied. This order also means that the addition is easiest between the more reactive monomer (M_1) and the growing ion produced from the less reactive monomer (M_2) and is most difficult between the less reactive monomer and the ion from the more reactive monomer. Hence it may be concluded that the ion from the reactive monomer is not so reactive as that from the less reactive monomer.

In order to obtain quantitatively the relative reactivity of the two ions in ionic polymerization, we tentatively assume that the rate constant k_{ij} in the propagation step may be represented as

$$k_{ij} = R_{I_i} \times R_{M_j} \quad (3)^*$$

where R_{I_i} is characteristic of the i th growing ion and R_{M_j} is the mean reactivity of the j th monomer.

Using equation (3), the following relations are easily derived.

$$k_{11}/k_{12} = k_{21}/k_{22} = R_{M_1}/R_{M_2}$$

$$k_{11}/k_{21} = k_{12}/k_{22} = R_{I_1}/R_{I_2}$$

*The equation (3) may reasonably be applied to treat the rate constant in ionic copolymerization where the relation $\gamma_1 = 1/\gamma_2$ holds. This equation, however, is open to criticism. At the present stage, it is doubtful whether $\gamma_1 = 1/\gamma_2$ always holds, and there is no definite explanation why the intermolecular term can be ignored in the rate constant.

Inserting the rate constants from *Table 1*, we obtain

$$R_{M_1}/R_{M_2}=2.0 \quad R_{I_1}/R_{I_2}=1/1.3$$

Thus monomer 1 is twice as reactive as monomer 2, but ion 2 is 1.3 times as reactive as ion 1. This tendency is the same as in radical polymerization², and it was expected from the reaction mechanism.

Anionic polymerization

It has been reported for styrene-methyl methacrylate copolymerization that the growing anion produced from styrene which is the less reactive monomer can initiate the polymerization of styrene and methyl methacrylate, and that the growing anion produced from the more reactive monomer, methyl methacrylate, cannot initiate the polymerization of styrene⁵. This result may indicate that the reactivity of the anion produced from the more reactive monomer is smaller, as in cationic polymerization.

A MOLECULAR ORBITAL TREATMENT

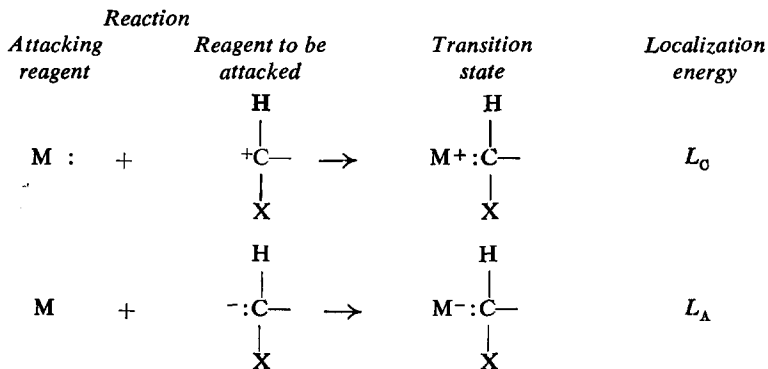
In the foregoing, experimental evidence was chosen to show that the growing ion produced from the reactive monomer is not so reactive in cationic polymerization or in anionic polymerization. However, it is not clear whether this tendency is found with other substances, since available experimental results are few. In these circumstances, a molecular orbital approach to clarify this point is presented below.

On radical polymerizations, the present authors⁶ discussed the reactivity of a monomer and a radical in terms of the radical localization energy of a monomer L_M^R and the localization energy of a radical L_R . From this investigation it was found, as a general trend, that the radical produced from the more reactive monomer is less reactive. Similarly, L_M^C and L_M^A , the cationic and the anionic localization energies of the monomer, respectively, are calculated, based on the model of the transition state* shown below.

| Type of reaction | Reagent monomer | Transition state | Localization energy |
|------------------------|---|--|---------------------|
| Electrophilic addition | $R^+ + CH_2=CH$ $\quad \quad \quad $ $\quad \quad \quad X$ | \rightarrow $\begin{array}{c} H \quad H \\ \quad \\ R : C - C^+ \\ \quad \\ H \quad X \end{array}$ | L_M^C |
| Nucleophilic addition | $R^- + CH_2=CH$ $\quad \quad \quad $ $\quad \quad \quad X$ | \rightarrow $\begin{array}{c} H \quad H \\ \quad \\ R : C - C^- \\ \quad \\ H \quad X \end{array}$ | L_M^A |

L_C and L_A , the localization energies of cation and anion respectively, are calculated by a similar procedure.

*The effect of the gegenion is neglected here. The gegenion has an electrostatic effect on the reaction site. This effect will shortly be discussed.



Parameters (Coulomb integral and resonance integral) used in these calculations are the same as those in the previous paper. In regard to the methyl group in isobutene and propylene, however, we use the parameters which are approximately equal to the values given by Coulson⁷, who treated the methyl group as $-\overset{a}{\text{C}}\equiv\overset{b}{\text{H}}_3$.

$$\alpha_a = \alpha - 0.1\beta$$

$$\alpha_b = \alpha - 0.5\beta$$

$$\beta_{\text{C}\equiv\text{H}_3} = 2.5\beta$$

where α and β are the values of the Coulomb integral of the carbon atom and of the resonance integral of the C—C double bond in benzene.

From the definition of the localization energy⁸, we can consider that a low value of the localization energy indicates a low value of the activation energy, that is, the larger reactivity in an addition reaction*. In *Figure 1*, L_M^0 and L_O are shown as ordinate and abscissa, respectively, and calculated values of L_M^0 and L_O are plotted against each other.

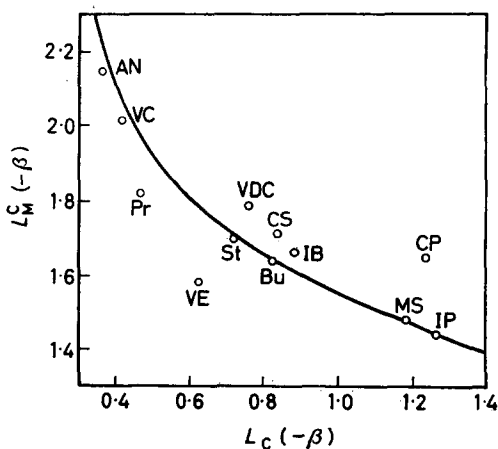


Figure 1—Relation between the reactivity of a monomer and the reactivity of the cation produced from the monomer, calculated from the localization energies

AN is acrylonitrile, VC vinyl chloride, Pr propylene, VDC vinylidene chloride, VE vinyl ether, St styrene, Bu butadiene, CS chlorostyrene, IB isobutene, MS α -methylstyrene, CP chloroprene, IP isoprene

*Solvents have an effect on the propagation reaction, but this is neglected here.

From *Figure 1*, it is shown that the easily polymerizable monomers (α -methylstyrene, etc.) have the smaller values of L_M^c and the larger values of L_c , and that the less easily polymerizable monomers (acrylonitrile, etc.) have the larger values of L_M^c and the smaller values of L_c . We can therefore understand that the carbonium ion of the more reactive monomer has a small reactivity in accordance with the experiments.

The localization energies of monomers and ions in anionic polymerization are calculated and the results are plotted in *Figure 2*. Again, it can be shown

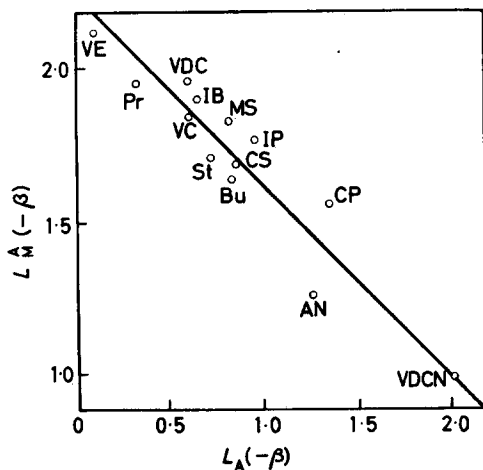


Figure 2—The relation between the reactivity of the anion produced from the monomer, calculated from the localization energies. VDCN: Vinylidene cyanide, other symbols as used in *Figure 1*

that the reactive monomer produces the unreactive adduct anion in anionic polymerization.

REACTIVITIES OF IONS ESTIMATED BY CHAIN TRANSFER CONSTANT

It is pointed out above that satisfactory information on which to discuss the reactivities of growing ions can be supplied when the values of propagation rate constants and monomer reactivity ratios are available. Unfortunately, however, there are only a few cases in which k_p is determined. It is attempted next to determine the range of the reactivity ratios of two polymer ions by obtaining both the chain transfer constant ratio and the monomer reactivity ratio, which can be measured.

Method of estimation

If the reactivity of a chain transfer reagent towards different kinds of ions is constant, the magnitude of the chain transfer constant (k_t) of growing ions towards a certain substance indicates the magnitude of the reactivity of growing ions. Bamford *et al.*⁹ investigated radical reactivity by this procedure.

Two kinds of monomers are named as M_1 and M_2 , respectively, and it is assumed that M_1 is more reactive than M_2 . In the foregoing, the inverse proportionality of the ion reactivity to the monomer reactivity was found, and we can deduce that the reactivity of an ion produced from M_2 is not less than that of M_1 . So equation (4) may be valid.

$$k_{11}/k_{22} \leq k_{21}/k_{12} \quad (4)$$

According to the definition of γ_1 and γ_2 , together with equation (4), equation (5) is derived.

$$\begin{aligned} (\gamma_1/\gamma_2)^{\frac{1}{2}} &= (k_{11}/k_{12})^{\frac{1}{2}} \times (k_{21}/k_{22})^{\frac{1}{2}} \\ &\geq k_{11}/k_{22} \end{aligned} \quad (5)$$

Thus $(\gamma_1/\gamma_2)^{\frac{1}{2}}$ is considered to be slightly greater than k_{11}/k_{22}^* .

If a is the ratio of the chain transfer constant ratio measured, it is given by equation (6)

$$a = (k_{t_2}/k_{22})/(k_{t_1}/k_{11}) = (k_{t_2}/k_{t_1}) \times (k_{11}/k_{22}) \quad (6)$$

We obtained equation (7) using the reactivity ratio of the ions from equations (5) and (6).

The reactivity ratio of the ions $\simeq k_{t_2}/k_{t_1}$

$$= a \times k_{22}/k_{11} \geq a \times (\gamma_2/\gamma_1)^{\frac{1}{2}} \quad (7)$$

Under the same polymerization conditions, if we obtain the chain transfer constant ratios for more than two monomers and the monomer reactivity ratios for these monomer pairs, we may determine the lowest limit of the ratio of the ion reactivity according to equation (7). In the next section the experimental results will be discussed, using equation (7).

Comparison with experimental results

We can hardly find reports which determine the chain transfer constant ratios of more than two monomers towards a certain transfer reagent under the same conditions. The only example is the report by Haas *et al.*¹⁰, who measured the chain transfer constant ratios of styrene and para-methoxystyrene towards para-methylanisole. Both monomers were polymerized by stannic chloride at 0°C. The chain transfer constant ratios towards para-methylanisole in styrene polymerization (k_t/k_p)_{st} and in para-methoxystyrene polymerization (k_t/k_p)_{PMS} were 1.08 and 2.7×10^{-3} , respectively.

Inserting these values into equation (7), we calculated the ratio of the ion reactivity, and the results are tabulated together with related data. However, as the monomer reactivity ratio is not accurately determined, the value of $(\gamma_1/\gamma_2)^{\frac{1}{2}}$ is not certain. Therefore, the lower limit of the relative reactivities of two ions, 4.0, is only an approximate value.

To check the validity of equation (7), we conducted an experiment choosing styrene and para-chlorostyrene as a monomer pair. The details of the experimental results will be published in the succeeding paper¹¹.

*With VIBE and VCEE, $(\gamma_1/\gamma_2)^{\frac{1}{2}}$ is equal to 2.0 and k_{11}/k_{22} is equal to 1.5. Therefore equation (5) holds.

THE REACTIVITY OF THE GROWING ION IN IONIC POLYMERIZATION

Table 2. Reactivities of ions estimated by chain transfer constant

| Monomer | Transfer reagent, polymerization temp., catalyst | Chain transfer constant ratio (k_t/k_p) | Ratio of (k_t/k_p), (k_t/k_p) ₂ /(k_t/k_p) ₁ |
|---|--|---|---|
| Styrene (M_2) | <i>p</i> -Methyl anisole | 1.08 | 400 |
| <i>p</i> -Methoxy- styrene (M_1) | 0°C SnCl ₄ | 2.7×10^{-3} | |
| <i>p</i> -Chloro- styrene (M_2) | Toluene | 4.0×10^{-2} | 14.3 |
| Styrene (M_1) | 30°C SnCl ₄ -CCl ₃ COOH | 2.8×10^{-3} | |

Table 2—continued

| Monomer | Monomer reactivity ratio (γ_1, γ_2) | (γ_2/γ_1) ² or (R_{M_2}/R_{M_1}) | Lower limit of (k_t) ₂ /(k_t) ₁ or (R_{I_2}/R_{I_1}) |
|---|--|---|---|
| Styrene (M_2) | $\gamma_1 = 100$ | 0.01 | 4.0 |
| <i>p</i> -Methoxy- styrene (M_1) | $\gamma_2 = 0.01$ | | |
| <i>p</i> -Chloro- styrene (M_2) | $\gamma_1 = 2.5 \pm 0.4$ | 0.35 | 5.0 |
| Styrene (M_1) | $\gamma_2 = 0.3 \pm 0.03$ | | |

Para-chlorostyrene was synthesized from para-chlorobenzaldehyde ($n_{\text{obs}}^{22^\circ\text{C}} = 1.5643$, $n_{\text{lit}}^{20^\circ\text{C}} = 1.5648$)¹². It was polymerized by SnCl₄-CCl₃COOH at 30°C, and the chain transfer constant ratio towards toluene was determined. To determine this, the same method was used as for styrene polymerization, in which the polymerization was carried out by changing the mole ratio of monomer to toluene, and the chain transfer constant ratio was calculated by measuring the degree of the polymer produced¹³. A lot of reports concerning the monomer reactivity ratio were published for the styrene-para-chlorostyrene system. We used $\gamma_1 = 2.5 \pm 0.4$, $\gamma_2 = 0.3 \pm 0.03$ ¹⁴, where styrene was M_1 and para-chlorostyrene was M_2 . The ratios of the ion reactivities are listed in Table 2 with some related values.

Values in the last column in Table 2 show the lowest limit of the ion reactivity calculated from equation (7). The true value of the ratio of the ion reactivity is considered to be larger than that in Table 2. For the styrene-para-methoxystyrene pair, the monomer reactivity of para-methoxystyrene is 100 times as large as that of styrene, while the ion reactivity of styrene is 4 times as large as that of para-methoxystyrene. Moreover, the ion reactivity of para-chlorostyrene is about 5 times as large as that of styrene, while the monomer reactivity of styrene is larger than that of para-chloro-

styrene. In either case $(k_i)_2/(k_i)_1$, which is considered to show the ratio of the ion reactivity, is considerably greater than unity, where monomer 1 has the greater reactivity. We were interested in this fact and are now investigating other kinds of monomer pairs. The results will be published later.

Faculty of Engineering,
Kyoto University,
Kyoto, Japan

(Received October 1961)

REFERENCES

- ¹ ALFREY, T. and PRICE, C. C. *J. Polym. Sci.* 1947, **2**, 101
- ² OKAMURA, S., KATAGIRI, K. and YONEZAWA, T. *J. Polym. Sci.* 1960, **42**, 535
- ³ PEPPER, D. C. *Quart. Rev. chem. Soc., Lond.* 1954, **8**, 88
- ⁴ OKAMURA, S., HIGASHIMURA, T. and KANO, N. *Makromol. Chem.* 1961, **47**, 19, 35
- ⁵ GRAHAM, R. K., DUNKELBERGER, D. L. and GOODE, W. E. *J. Amer. chem. Soc.* 1960, **82**, 400
- ⁶ YONEZAWA, T., HIGASHIMURA, T., KATAGIRI, K., OKAMURA, S. and FUKUI, K. *Kobunshi Kagaku*, 1957, **14**, 533
- ⁷ COULSON, C. A. and CROMFORD, U. A. *J. chem. Soc.* 1953, 2052
- ⁸ WHELAND, G. W. *J. Amer. chem. Soc.* 1942, **64**, 900
- ⁹ BAMFORD, C. H., JENKINS, A. D. and JOHNSTON, R. *Trans. Faraday Soc.* 1959, **55**, 418
- ¹⁰ KAMATH, P. M. and HAAS, H. C. *J. Polym. Sci.* 1957, **24**, 143
- ¹¹ OKAMURA, S., HIGASHIMURA, T., IMANISHI, Y. and MIZOTE, A. Part II in this series
- ¹² BROOKS, L. A. *J. Amer. chem. Soc.* 1944, **66**, 1295
- ¹³ OKAMURA, S. and HIGASHIMURA, T. *Chem. High Polymer Japan*, 1956, **13**, 262
- ¹⁴ OVERBERGER, C. G., ARNOLD, L. H. and TAYLOR, J. J. *J. Amer. chem. Soc.* 1951, **73**, 5541

The Butyllithium-initiated Polymerization of Methyl Methacrylate

D. M. WILES and S. BYWATER

*The kinetics of the polymerization of methyl methacrylate initiated by *n*-butyllithium in toluene solution have been studied at -30°C and to a lesser extent at -5°C . Measurements were made to determine the effect of monomer and initiator concentrations on the rate of polymerization, on the quantity of low molecular weight product, and on the molecular weight and microstructure of the high molecular weight polymer. A complete explanation of the results has not been possible but it seems that the differences between initiation by butyllithium and by other organometallic compounds may be due in part to a side reaction of butyllithium with ester groups.*

INTEREST in the kinetics of the homogeneous anionic polymerization of vinyl monomers has led to the recent publication of data for several, including styrene¹⁻³, α -methyl styrene⁴, and methyl methacrylate^{5, 6}. The only kinetic data available for the polymerization of methyl methacrylate initiated by *n*-butyllithium, however, are those of Korotkov *et al.*⁷. Their results are not given in sufficient detail for the establishment of a comprehensive kinetic scheme but they indicate complexities which were not found for other anionic initiators.

This paper presents kinetic data for the methyl methacrylate-*n*-butyllithium-toluene system at low temperatures. An attempt has been made to correlate the results with those obtained by other workers using different organometallic initiators to polymerize this monomer. The apparent differences and additional complications reported here do not seem to be explicable in terms of the mechanisms proposed previously.

EXPERIMENTAL

Materials

Methyl methacrylate (Rohm and Haas Co.) was degassed, distilled on to calcium hydride in a vacuum system and stirred for 24 hours. This was followed by stirring on a freshly-formed sodium mirror for 1 hour at -10°C . Approximately one third of the monomer polymerized and the remainder was distilled on to additional calcium hydride where it was stirred for 48 hours and then stored in a connected bulb at 0°C in the dark. No impurities could be detected with analysis by gas chromatography, the monomer polymerized readily on exposure to sunlight, and successive batches gave the same kinetic results.

Toluene (Merck and Co., reagent grade) was dried with calcium hydride and fractionally distilled through a 3 ft column containing Podbielniak Heli-Pak packing. The middle portion was degassed and distilled *in vacuo* into a storage vessel containing calcium hydride.

Other organic liquids used in the experiments were reagent grade, whenever possible, and were dried before use with appropriate drying agents.

n-Butyllithium (Foote Mineral Co.) was obtained as a dilute solution in mixed pentane–heptane solvent. Aliquot portions were withdrawn with a syringe in a dry box containing an atmosphere of high purity nitrogen. The concentration was periodically checked using the double titration method described by Gilman and Haubein⁸.

Lithium methoxide was synthesized by reacting butyllithium with a slight excess of methanol in a petroleum ether medium. The precautions taken to remove unreacted methanol were similar to those described by Goode *et al.*⁹.

Apparatus and procedure

The manipulation of the reagents and apparatus during the course of the experiments will be given in some detail because the results are strongly influenced by the success with which reactive impurities have been excluded.

Weighed quantities of monomer were distilled immediately before use into Pyrex tubes with a thin, breakable glass membrane at one end. Until its addition to the initiator solution the methyl methacrylate was kept below 0°C and protected from strong light as much as possible.

Aliquot portions of butyllithium solution, varying in size from 0.1 to 0.3 ml, were injected in a dry box through a self-sealing serum cap into a small, thin-walled Pyrex bulb connected to a stopcock. The bulb had previously been evacuated to a pressure of 10^{-5} mm of mercury and re-opened in the dry box. After the injection of butyllithium the bulb was pumped to remove some of the pentane–heptane solvent, and sealed off.

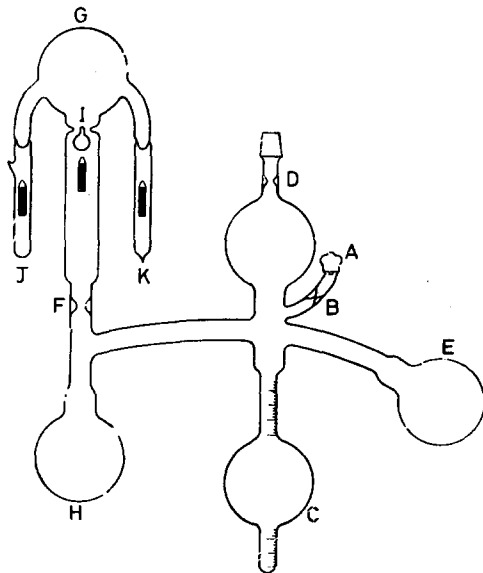


Figure 1—Apparatus for kinetic experiments

The apparatus used for the kinetic experiments (*Figure 1*) was evacuated and approximately 3 ml of stock butyllithium solution was injected through the serum cap at A. The side tube was sealed at B and most of the solvent was pumped away. Toluene was distilled into bulb C and the apparatus was sealed off under vacuum at D. The inside surfaces were washed with butyllithium solution which was then poured back into C and E. The polymerization vessel (F to G) was washed several times with pure toluene collected in H by distillation and finally, the wash butyllithium being left in C, the required volume of toluene was collected in G. The polymerization vessel was sealed off at F, the bulb I containing initiator was broken, and the resulting butyllithium solution was brought to the desired temperature by stirring in the low temperature bath, controlled to $\pm 0.1^\circ\text{C}$. Monomer at the same temperature was admitted rapidly by breaking the thin membrane in J; the reaction was stopped rapidly by adding methanol from K. This procedure was repeated for various polymerization times at different concentrations of butyllithium and methyl methacrylate.

After termination by methanol the vessel G was rapidly brought to room temperature, opened, and the contents plus chloroform washings were slowly added to ten times the volume of either methanol or petroleum ether (boiling range 30° to 90°C). The polymer was collected by filtration, washed repeatedly with precipitant and dried at 50°C to a constant weight in a vacuum desiccator. The filtrate was evaporated slowly to dryness and the residue taken to constant weight under the same conditions.

The lithium from the initiator appeared in the products as a mixture of lithium hydroxide and lithium carbonate, soluble in methanol but insoluble in petroleum ether. The proportions of these lithium salts in the mixture were established in blank experiments and the weights of the appropriate parts of the products were corrected accordingly.

In some cases, after the complete conversion of methyl methacrylate to polymer, a second portion of monomer was added and allowed to polymerize for various times to different degrees of conversion.

Characterization of products

Molecular weights of many of the polymers insoluble in the precipitant were calculated from viscosities measured in chloroform solution at 25°C in a Cannon-Ubbelohde dilution viscometer. The viscosity/molecular weight relationship used was $[\eta] = 3.4 \times 10^{-5} M_w^{0.83}$, derived by Chinai and co-workers¹⁰. It seems reasonable that this equation, established for more random poly(methyl methacrylate), should be applicable to the stereoregular polymer obtained in this work (cf. ref. 11). In a few cases the molecular weights of precipitant-soluble products were measured using a Mechrolab vapour pressure osmometer.

The microstructure of a selected number of polymers in chloroform solution was examined with a proton magnetic resonance apparatus under conditions similar to those described by Bovey and Tiers¹². The amounts of the three types of sequences were calculated, as percentages, from simple measurements of relative peak areas.

RESULTS

The experimental results showing total conversion of monomer as a function of time are given in *Figures 2 to 5*, for a variety of reaction conditions. At higher monomer/initiator ratios (≥ 26) there appear to be two reaction stages for which the overall rate is externally of first order in

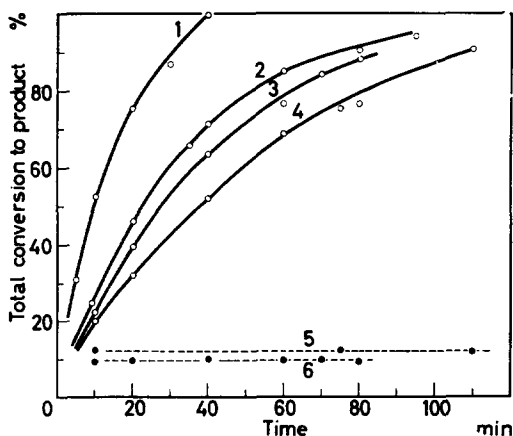


Figure 2—Per cent conversion of monomer as a function of [butyllithium] and temperature
[Methyl methacrylate]=0.125 mole/l.

| Curve | 1 | 2 | 3 | 4 | 5 | 6 |
|------------------------------|-------|-------|-------|-------|----------------------------|----------------------------|
| [BuLi] mole/l. $\times 10^3$ | 11.5 | 7.6 | 5.7 | 5.7 | 5.7 | 5.7 |
| Temp. °C | -30 | -30 | -5 | -30 | -30 | -5 |
| Product | total | total | total | total | soluble in petroleum ether | soluble in petroleum ether |

monomer concentration. At lower monomer/initiator ratios the first stage is apparently missing, possibly because it is obscured by a much more rapid second stage and because of the progressive shortening of this initial part with increasing butyllithium concentration. Although the later stages of the reactions are approximately internally of first order in monomer concentration over the whole initiator range, *Figure 4* shows the behaviour typical of the three highest butyllithium concentrations where the rate varies inversely with initial monomer concentration. Experiments at all concentrations indicate the rapid formation of low molecular weight products, for none of the curves in *Figures 2, 3 and 4* can be extrapolated smoothly to the origin. The experiments at -5°C indicate a low activation energy for propagation, approximately 1 kcal/mole.

The first order rates of monomer consumption in both stages of the two part curves in *Figure 5(a)* vary considerably for a small change in initiator concentration. *Figure 5(b)* indicates the apparently simpler situation at higher butyllithium concentrations. For the two butyllithium concentrations

THE POLYMERIZATION OF METHYL METHACRYLATE

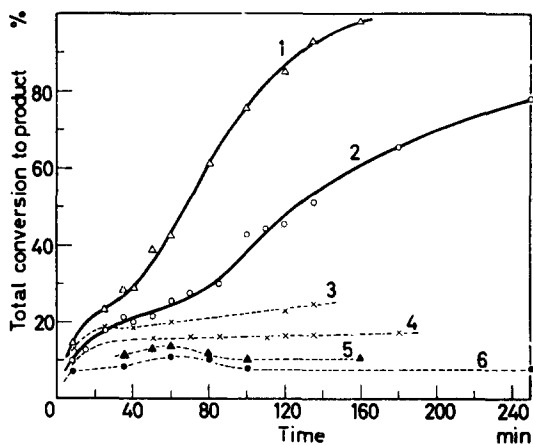


Figure 3—Per cent conversion of monomer as a function of [butyllithium]. [Methyl methacrylate]=0.125 mole/l. Temp.= -30°C

| Curve | 1 | 2 | 3 | 4 | 5 | 6 |
|------------------------------|------------------|------------------|---------------------|---------------------|----------------------------|----------------------------|
| [BuLi] mole/l. $\times 10^3$ | 4.7 ₅ | 3.8 ₅ | 4.7 ₅ | 3.8 ₅ | 4.7 ₅ | 3.8 ₅ |
| Product | total | total | soluble in methanol | soluble in methanol | soluble in petroleum ether | soluble in petroleum ether |

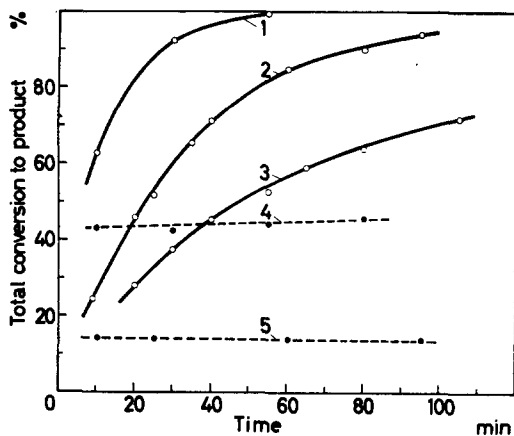


Figure 4—Per cent conversion of monomer as a function of [monomer]. [Butyllithium]= 7.6×10^{-3} mole/l. Temp.= -30°C

| Curve | 1 | 2 | 3 | 4 | 5 |
|-------------------|--------------------|-------|-------|---------------------|----------------------------|
| [Monomer] mole/l. | 0.062 ₅ | 0.125 | 0.250 | 0.062 ₅ | 0.125 |
| Product | total | total | total | soluble in methanol | soluble in petroleum ether |

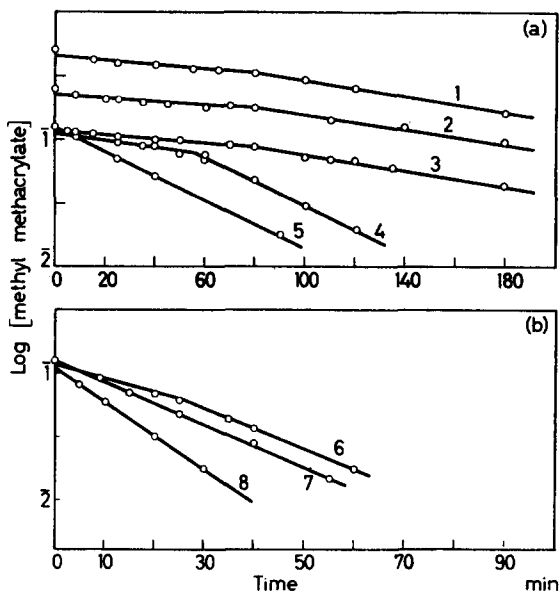


Figure 5—Logarithmic plot of experimental data. Temp. = -30°C

(a)

| Curve | 1 | 2 | 3 | 4 | 5 |
|------------------------------|------------------|------------------|------------------|------------------|------------------|
| [BuLi] mole/l. $\times 10^3$ | 3.8 ₅ | 3.8 ₅ | 3.8 ₅ | 4.7 ₅ | 4.7 ₅ |
| [Monomer] mole/l. | 0.125 | 0.250 | 0.500 | 0.125 | 1.125* |

(b)

| Curve | 6 | 7 | 8 |
|------------------------------|-------|--------|-------|
| [BuLi] mole/l. $\times 10^3$ | 7.6 | 7.6 | 11.5 |
| [Monomer] mole/l. | 0.125 | 0.125* | 0.125 |

*0.125 mole/l. monomer polymerized completely, then an additional 0.125 mole/l. monomer added.

where a second equal quantity of monomer was added, *Figure 5* shows a rapid polymerization with a first order rate equal to that established in the final part of the original reaction. The first order plots in this case can be extrapolated directly to the original added monomer concentration. There was in fact, no change, during the polymerization of the second portion, in the amount of low molecular weight product formed in the polymerization of the first part. These results indicate that no chain termination occurs in the final part of a normal polymerization and that many of the complexities associated with initiation by butyllithium are absent when poly(methyl methacrylate) anions initiate polymerization.

Figure 6 shows typical results of viscosity-average molecular weight determinations for experiments at two monomer/initiator ratios. These

THE POLYMERIZATION OF METHYL METHACRYLATE

results indicate that the two stage behaviour shows up in the molecular weight of the polymer. While it is difficult to exclude the effects of a changing molecular weight distribution during the polymerization, the two stage curve does not seem to be due to changes in the number of growing chains. The number-average molecular weight of the petroleum ether-soluble product was determined for curve 1 and found to be about 600 at all stages of reaction. The methanol-soluble product for the same system appears to have an \bar{M}_n value of 900.

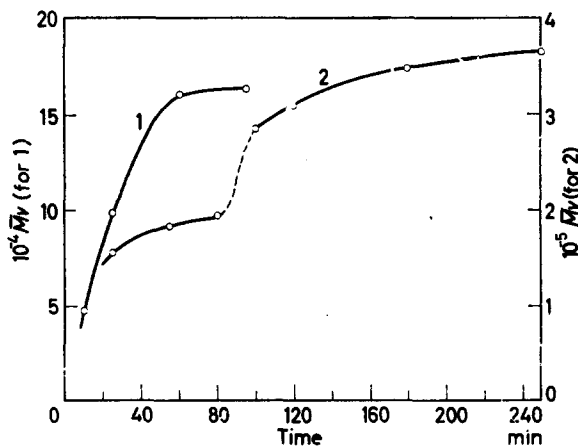


Figure 6—Typical changes in viscosity-average molecular weight as a function of polymerization time. Polymerization temp. = -30°C

| Curve | [Butyllithium] mole/l. $\times 10^3$ | [Methyl methacrylate] mole/l. |
|-------|---|----------------------------------|
| 1 | 7.6 | 0.125 |
| 2 | 3.8 ₅ | 0.500 |

It is possible that methoxide ions could be present in the polymerizing systems as a result of attack by butyllithium on the ester group¹³. In order to determine its effect if any, lithium methoxide was added alone or with butyllithium to monomer-solvent mixtures. Its solubility in toluene being very low, it was added as a suspension in toluene. These experiments show that lithium methoxide neither initiates polymerization at a measurable rate nor affects the butyllithium-initiated polymerization.

Figure 7 illustrates the effect of the initial methyl methacrylate/butyllithium ratio on the proportion of monomer converted to precipitant-soluble products. The percentage of soluble polymer increases markedly with increasing initiator concentration, but the overall trend is governed largely by the ratio and not by the individual concentrations of either component. Variations in the quantity of soluble material during a reaction at one set of concentrations are usually small, presumably within experimental

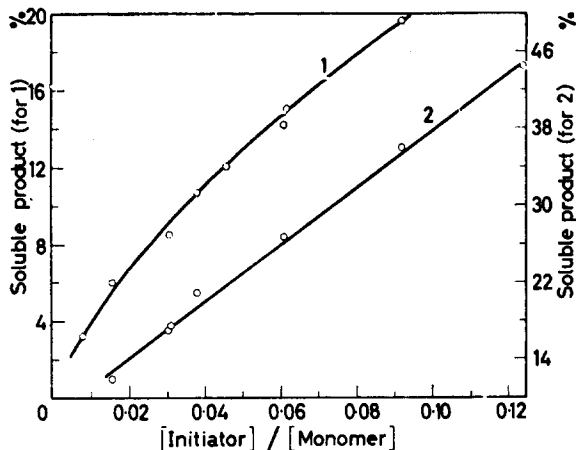


Figure 7—Change in per cent initial [monomer] converted to precipitant-soluble product as a function of [butyllithium]/[monomer] ratio. Temp. = -30°C . Curve 1—soluble in petroleum ether; Curve 2—soluble in methanol

error. The larger fluctuations in the amounts of product soluble in petroleum ether shown in *Figure 3* correspond roughly to the points of inflection between the two stages of the total conversion curves. If similar fluctuations occur at higher butyllithium concentrations they may be less noticeable for the same reasons that no inflection points are observed.

Table 1. Proton magnetic resonance measurements

| Sample* | [Monomer] mole/l. | [Butyl- lithium] mole/l. $\times 10^3$ | Conversion % | Sequences % | | |
|---------|----------------------|---|-----------------|----------------|-------------------|-------------------|
| | | | | Iso- tactic | Hetero- tactic | Syndio- tactic |
| F.R.† | — | — | — | 11 | 42 | 47 |
| SK100 | 0.125 | 7.6 | 52 | 74 | 16 | 10 |
| BSK4 | 0.125 | 7.6 | 94 | 82 | 10 | 8 |
| SK109‡ | 0.125 | 7.6 | 100 | 86 | 8 | 6 |
| SK32 | 0.500 | 3.85 | 32 | 52 | 29 | 19 |
| SK125 | 0.500 | 3.85 | 34 | 52 | 31 | 17 |
| SK121 | 0.500 | 3.85 | 73 | 72 | 18 | 10 |
| SK121§ | 0.500 | 3.85 | 73 | 80 | 12 | 8 |

*Methanol-soluble products removed from sample SK32. Petroleum ether-soluble products removed from all other samples.

†Polymer made at 60°C by initiation with 2,2'-azo-bis-isobutyronitrile. Results included for comparison.

‡Polymerized completely under the same conditions as BSK4. Then the same amount of monomer was added again and polymerized completely.

§Approximately a quarter of Sample SK121 removed by extraction with 4-heptanone.

Typical results of proton magnetic resonance measurements are shown in *Table 1* for polymers prepared under a variety of conditions. A trend toward greater isotacticity is apparent at higher butyllithium concentration as well as at higher conversion. A polymer formed by the addition of monomer in two portions has a higher degree of isotacticity at the end of the second polymerization than at the end of the first. The isotactic content

of a polymer appears to be slightly enhanced on extraction with 4-heptanone but non-isotactic sequences are not removed completely so they must be incorporated in longer chains as well.

DISCUSSION

The scope of the experiments has been restricted to rather low monomer/initiator ratios because at lower butyllithium concentrations the rates would be very low and at higher methyl methacrylate concentrations the resulting toluene solutions of polymer would be extremely viscous. In some cases the small quantity of methanol added to terminate the reaction caused the solution to become cloudy, indicating how close the systems were to incipient precipitation.

A complete explanation of the results does not appear to be possible owing to their complexity. Much of the butyllithium is accounted for in the initial rapid formation of very low molecular weight polymer and only a small fraction of the initiator is responsible for the consumption of most of the monomer. At the highest monomer/initiator ratio used (130) about 70 per cent of the butyllithium results in petroleum ether-soluble material. If it is assumed that one insoluble polymer molecule accounts for one butyllithium molecule then the number-average molecular weight would have to be 50 000, i.e. $\bar{M}_v/\bar{M}_n \approx 7$. This ratio is about that generally found in the anionic polymerization of methyl methacrylate. At the lowest monomer/initiator ratio (10.9) petroleum ether-soluble products arise from 35 per cent of the butyllithium molecules. To account for the remaining initiator one would have to assume that \bar{M}_n for the insoluble polymer is 1 350. This result ($\bar{M}_v/\bar{M}_n \sim 90$) seems unreasonable because an appreciable quantity of such a polymer would have been soluble in petroleum ether. Although it is possible that there is a broadening of molecular weight distribution associated with an increase in initiator concentration it is more likely that some butyllithium is consumed under these conditions in one or more side reactions. Butyllithium is more reactive than fluorenyllithium which has been used in a previous study^{5a, b}; butyllithium will correspond more closely to but may be even more reactive than Grignard reagents in toluene solution^{6a, b}. It has been shown that polystyryl anions react with polymer ester groups¹⁴ and it is likely that butyllithium reacts with ester groups on the monomer¹³ and polymer. Attack on polymer ester groups would be restricted to short chains formed in the early stages of reaction since it is probable that butyllithium is rapidly consumed in at least as short a time as that found for fluorenyllithium^{5a}.

Figure 3 shows that at low initiator concentrations the initial fast consumption of monomer is followed by a period of slower growth, which leads to a final fast reaction internally of first order in monomer concentration. This latter stage appears to represent the establishment of a steady concentration of reactive centres, as shown by the results obtained on the addition of a second portion of monomer [Figure 5(a)]. At high butyllithium concentrations only the second fast polymerization, internally of first order in monomer concentration, is observed, there being no apparent period of

slow growth (*Figure 2*). The first order rate constants, calculated for the systems after steady state conditions appear to have been reached, increase more rapidly than the increase in added initiator concentration and at high values are a function of the added monomer concentration (*Figure 4*). The number of active centres which lead to high polymer depends therefore in a complex manner on initial butyllithium and monomer concentrations. This also suggests multiple attack of initiator on monomer and polymer.

The slow growth period is associated with a lower degree of isotacticity in the insoluble polymer whereas the faster reaction stages produce polymer of nearly 90 per cent isotactic structure in both normal experiments and when additional monomer is added. The slow period could be due to failure to produce an isotactic helix until quite large polymer molecules are formed, or it could be the result of inhibition by products of butyllithium side reactions. Glusker has suggested^{5b} that a polymer molecule must be eight or nine monomer units in length before a rapidly propagating helix is formed. However, in the present work the molecular weight of the polymer formed during the slow period changes with experimental conditions and can reach large values. There does not seem to be any sound reason for increasing the chain length associated with the transition to a helix to very high values. The inhibition theory suffers from the disadvantage that the temporary period of slower conversion is most readily observed at low initiator concentrations for which the butyllithium balance is reasonably good and reaction with ester groups is least likely. At the highest added initiator concentrations, where the butyllithium balance is least satisfactory, the highest terminal rates are found. This might suggest that the effective chains arise from other than simple attack of butyllithium on the monomer carbon-carbon double bond. Glusker's hypothesis^{5b} for the fluorenyllithium-initiated system supposes that the source of the chains growing to high molecular weight is a part of the low molecular weight soluble material formed early in the reaction. In the present work at two low butyllithium concentrations there was, in fact, a temporary increase in the petroleum ether-soluble fraction during the slow period (*Figure 3*). At all concentrations the quantity of material soluble in methanol tended to rise slightly during the polymerizations. Nevertheless there does not seem to be a correlation between the terminal rate and the quantity of soluble material, which for the most part does not apparently change appreciably throughout a reaction. It should be remembered, however, that a small number of short chains growing to high molecular weight can account for a large consumption of monomer, and that in the present work the errors in the measurement of small amounts of soluble material are appreciable.

There is some recent evidence in the literature that spontaneous termination in rigorously purified anionic initiator-methyl methacrylate systems is not rapid at low temperature. This evidence is, in fact, only a qualitative indication that some polymeric anions survive for many hours. However, it has now been shown that, at least for initiation by butyllithium, only a small proportion of the active centres formed initially is responsible for most of the monomer consumption but that the amount of spontaneous termination of these growing polymer chains is sufficiently small to have no effect on the kinetics of polymerization of a second portion of monomer.

The authors wish to thank Dr S. K. Brownstein for measuring the proton magnetic resonance spectra, and Dr D. J. Worsfold for helpful discussions.

*Division of Applied Chemistry,
National Research Council,
Ottawa, Canada*

(Received November 1961)

REFERENCES

- ¹ WELCH, F. J. *J. Amer. chem. Soc.* 1959, **81**, 1345
- ² O'DRISCOLL, K. F. and TOBOLSKY, A. V. *J. Polym. Sci.* 1959, **35**, 259
- ³ WORSFOLD, D. J. and BYWATER, S. *Canad. J. Chem.* 1960, **38**, 1891
- ⁴ WORSFOLD, D. J. and BYWATER, S. *Canad. J. Chem.* 1958, **36**, 1141
- ^{5a} GLUSKER, D. L., STILES, E. and YONCOSKIE, B. *J. Polym. Sci.* 1961, **49**, 297
- ^b GLUSKER, D. L., LYSLOFF, I. and STILES, E. *J. Polym. Sci.* 1961, **49**, 315
- ^{6a} GOODE, W. E., OWENS, F. H., FELLMANN, R. P., SNYDER, W. H. and MOORE, J. E. *J. Polym. Sci.* 1960, **46**, 317
- ^b GOODE, W. E., OWENS, F. H. and MYERS, W. L. *J. Polym. Sci.* 1960, **47**, 75
- ⁷ KOROTKOV, A. A., MITSSENGENDLER, S. P. and KRASULINA, V. N. *Proceedings of the International Symposium on Macromolecular Chemistry, Moscow, 14th to 18th June 1960*. Section 2, p 208
- ⁸ GILMAN, H. and HAUBEIN, A. H. *J. Amer. chem. Soc.* 1944, **66**, 1515
- ⁹ GOODE, W. E., SNYDER, W. H. and FETTES, R. C. *J. Polym. Sci.* 1960, **42**, 367
- ¹⁰ CHINAI, S. N., MATLACK, J. D., RESNICK, A. L. and SAMUELS, R. J. *J. Polym. Sci.* 1955, **17**, 391
- ¹¹ TSVETKOV, V. N., SKAZKA, V. S. and KRIVORUCHKO, N. M. *Vysokomol. Soedineniya*, **1960**, No. 2, 1045
- ¹² BOVEY, F. A. and TIERS, G. V. D. *J. Polym. Sci.* 1960, **44**, 173
- ¹³ BYWATER, S. *International Symposium on Macromolecular Chemistry, Montreal, 27th July to 1st August 1961*. Paper D5
- ¹⁴ REMPP, P., VOLKOV, V. I., PARROD, J. and SADRON, CH. *Bull. Soc. chim. Fr.* **1960**, 919

The Action of Ethylamine on Cellulose

Part I—The Acetylation of Ethylamine-treated Cotton

T. P. NEVELL* and S. H. ZERONIAN*

The hygroscopicity of cotton that has been acetylated in pyridine after it has been treated with ethylamine, washed with water, and solvent-exchanged with pyridine, has been compared with that of cotton acetylated without pre-treatment. The results show that the acetylation does not cause decrystallization additional to that due to the ethylamine treatment until substitution in the amorphous regions is virtually complete. The influence of the type of solvent used to remove ethylamine from cotton on the ease of acetylation of the treated material has also been studied. Pyridine gives the most reactive product, n-hexane the least, and water a product of intermediate reactivity. These facts are interpreted in terms of the relative hydrogen-bonding capacity of the three solvents. X-ray photographs of equally acetylated products obtained from cotton, cotton treated with ethylamine and water, and cotton treated with ethylamine and pyridine, show progressively increasing proportions of crystalline cellulose acetate. The hygroscopicity of the products also increases in the same order.

DURING the last ten years the decrystallization of cotton cellulose by means of ethylamine has been the subject of numerous investigations at the Southern Regional Research Laboratory of the United States Department of Agriculture. In one of these investigations Loeb and Segal¹ have shown that the enhanced reactivity of the decrystallized cotton towards acetylation is largely lost if the material is allowed to dry between the processes of ethylamine extraction and acetylation. They have also concluded that ethylamine is more effective than sodium hydroxide of mercerizing strength in increasing the reactivity of cotton towards acetylation, but this conclusion is not necessarily correct because different solvents were used to remove the ethylamine and the sodium hydroxide from the treated cotton. The present paper describes experiments that were carried out to determine the combined effect of decrystallization and acetylation on the affinity of cotton for water vapour, and the influence of the nature of the solvent used to remove the swelling agent on the reactivity of the cotton and on the fine structure of the final products.

EXPERIMENTAL PROCEDURE

Materials

An unspun Texas cotton that had been mechanically cleaned and boiled under pressure (35 lb/in²) for three hours with 2 per cent sodium hydroxide was used as starting material.

*Present address: Department of Textile Chemistry, Manchester College of Science and Technology, Manchester 1.

Ethylamine was purified by distillation from solid potassium hydroxide in an apparatus from which the air had been pumped off and which had a receiver cooled in a mixture of solid carbon dioxide and acetone.

Pyridine and *n*-hexane, which were used for extracting the ethylamine from the treated cotton, were dried over solid potassium hydroxide and fractionated before use. The boiling ranges of the fractions collected were: pyridine 115° to 116°C, *n*-hexane 67° to 69°C, both at a pressure of 760 mm of mercury.

The acetylating reagent described in Procedure I in Loeb and Segal's paper¹ was used in the present work. It consisted of a mixture of equal volumes of acetic anhydride (analytical reagent grade) and pyridine (purified as described above).

Methods of treatment

Treatment with ethylamine—Cotton was treated with ethylamine in a vessel that could be closed with a ground-glass stopper carrying two tubes. One tube was used to remove the air in the vessel and the water adsorbed on the cotton by evacuation; the other was used to introduce the required amount of ethylamine into the evacuated vessel. Both tubes were fitted with taps, which were closed during the treatment. Usually about 10 g of cotton was immersed in 350 to 400 ml of ethylamine for four hours at 0°C, as recommended by Segal, Nelson and Conrad². After treatment the cotton was removed from the ethylamine and extracted with water, *n*-hexane, or pyridine, as follows.

Extraction with water—The sample was stirred vigorously with several successive portions of ice-cold water and then steeped in water for about 18 hours, the water being changed from time to time. The product was kept in cold water until required for further treatment, or, when required for the measurement of hygroscopicity, freed from as much liquid water as possible by centrifuging and dried in a vacuum over phosphorus pentoxide.

Extraction with n-hexane—The sample was stirred with three successive portions of *n*-hexane and then extracted with the same solvent in a Soxhlet apparatus for eight hours. A little syrupy phosphoric acid was added to the boiling flask to prevent recycling of the ethylamine. The product was kept wet with solvent until required for further treatment.

Extraction with pyridine—The sample was stirred with five successive portions of pyridine at room temperature during 18 hours and preserved in pyridine for acetylation.

Treatment with sodium hydroxide—Cotton was immersed in 16 per cent sodium hydroxide solution for 30 min at 20°C. The product was washed successively with saturated sodium chloride solution, 10 per cent acetic acid, and water, the water being changed periodically until a neutral extract was obtained. It was kept in cold water until required.

Acetylation—Samples (2 g) of material to be acetylated were suspended in 50 ml of dry pyridine. Air-dry samples were washed with four, and samples wet with water or *n*-hexane with five, successive portions of pyridine, the final portion being adjusted to 50 ml (roughly 50 g) by weighing. Acetic anhydride (50 ml) was added and the mixture was shaken well and kept at 25°C for the required length of time. The acetylating mixture

was then poured off and the product was washed with numerous changes of distilled water until free from acid. Half was dried in a vacuum over phosphorus pentoxide and used for the measurement of hygroscopicity. The other half was dried by exposure to the air.

Characterization of products

Acetyl content—A modification of the third method of Howlett and Martin³ was used for the determination of acetyl contents. The sample (0.2 to 0.4 g) was dried at 110°C, weighed, and transferred to a stoppered conical flask containing 0.4N potassium hydroxide in 50 per cent aqueous alcohol (25 ml) at room temperature. After 18 hours sulphuric acid of concentration slightly greater than 0.4N (25 ml) was added, and after a further half hour the solution was titrated with 0.1N sodium hydroxide, phenolphthalein being used as indicator.

Hygroscopicity—Moisture regains were determined by drying duplicate 0.5 g samples of material in a vacuum desiccator over phosphorus pentoxide and exposing them to an atmosphere of 66 per cent r.h. at 20°C (obtained by means of a saturated solution of sodium nitrite) until they reached a constant weight.

X-ray diagrams—Fibre photographs were taken with 25 mg bundles of parallel fibres and nickel-filtered copper K_{α} radiation.

HYGROSCOPICITY OF ACETYLATED MATERIALS

One of the most remarkable claims made for the use of ethylamine for decrystallizing cotton was that recrystallization does not readily occur⁴. Non-aqueous solvents were at first recommended for removing the ethylamine, chloroform being suggested, but subsequently it appeared that ice-cold water was equally satisfactory⁵. This has now been confirmed by hygroscopicity measurements: chloroform-washed and water-washed materials both adsorbed 30 per cent more water vapour than the original cotton at 66 per cent r.h. and 20°C. It is possible, however, that some collapse of structure may occur during the drying of decrystallized materials and it was thought that such collapse might be prevented by the introduction of 'blocking groups'. A comparison was therefore made of the affinity for water vapour of cotton and never-dried decrystallized cotton after they had been acetylated to various extents in fibrous form and dried. The results are illustrated in *Figure 1*, which shows the relation between the moisture regain and the degree of acetylation of cotton and of cotton that had been treated with ethylamine, washed with water, and solvent-exchanged with pyridine.

The curve for cotton (Curve 1) will be considered first. It falls into two parts: an initial linear portion representing products with acetyl contents between 2.5 per cent and 14 per cent, and a second portion of markedly lower slope at higher degrees of acetylation. When the initial portion is extrapolated back to zero acetyl content it strikes the moisture-regain axis at a higher value than the moisture regain of the original cotton. This suggests that a small increase in hygroscopicity occurs during the very early stages of acetylation (up to an acetyl content of about four per cent); similar results were obtained by Aiken⁶ with slightly acetylated rag stock. The

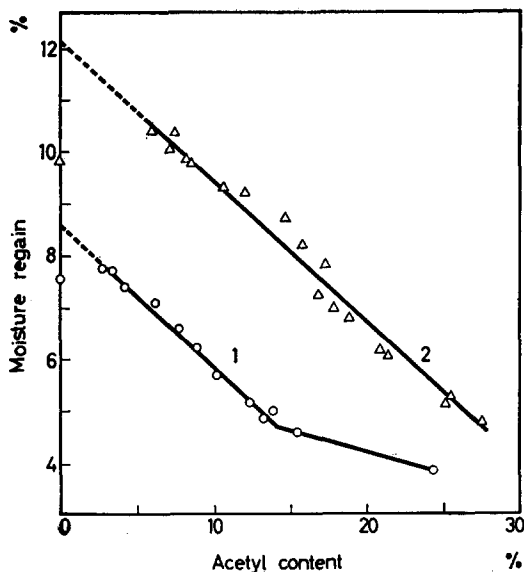


Figure 1—Relation between hygroscopicity and acetyl content of acetylated cellulose. Curve 1—cotton; Curve 2—ethylamine-treated cotton that had been washed with water

increase in hygroscopicity must be due to an increase in the number of hydroxyl groups accessible to water vapour in the amorphous regions of the material. This could arise from the partial acetylation of a number of hydroxyl groups initially bound together too strongly by hydrogen bonds to permit them to adsorb water. The linear fall of hygroscopicity between acetyl contents of 2.5 per cent and 14 per cent represents the substitution of accessible hydroxyl groups in the amorphous regions by acetyl groups, which are less hydrophilic; the subsequent lower rate of fall of hygroscopicity with increasing acetyl content represents the opening up and acetylation of the crystalline regions. A change in the rate of fall of moisture regain with degree of acetylation at an acetyl content of about 15 per cent was observed previously by Honold, Keating and Skau⁷, and was interpreted by Bailey, Honold and Skau⁸ as an indication of the extension of acetylation from the amorphous to the crystalline regions. They did not have sufficient results, however, to enable them to detect the small increase in moisture regain in the very early stages of acetylation.

The hygroscopicity of acetylated decrystallized cotton has been measured only over a range of acetyl contents corresponding to acetylation of the amorphous regions. The maximum degree of substitution attainable in these regions is, of course, much higher than with the original cotton. Once again, the initial rise in moisture regain at very low acetyl contents is evident, and this is followed by the linear fall characteristic of the replacement of hydroxyl by acetyl groups in amorphous regions (Curve 2). The slopes of the linear portions of the two curves relating to acetylation in the amorphous regions are identical, which shows that the difference in the affinity of hydroxyl and acetyl groups for water vapour is the sole cause of the fall of hygroscopicity in both cases. The linearity of the relation between moisture regain and acetyl content shows that the amount of inter-chain

hydrogen-bonding is not altered during acetylation, but is in fact fixed by this process at whatever level it may be when the acetylation is begun. It also follows that the acetylation of ethylamine-treated cotton does not cause any additional decrystallization until substitution in the amorphous regions is virtually complete.

The moisture regains of unacetylated cotton and decrystallized cotton obtained by extrapolating Curves 1 and 2 back to the ordinate axis are higher than the corresponding directly-determined values, for the reason already given. In addition it is significant that, of the extrapolated values, that for the decrystallized cotton is about 42 per cent greater than that for cotton, whereas of the directly-determined values, that for the decrystallized cotton is only 30 per cent greater than that for cotton. Thus the potential accessibility of the hydroxyl groups in cotton to water vapour is increased by 42 per cent by treatment with ethylamine followed by washing with water, but some of this increased accessibility is lost when the material is dried before its moisture regain is determined. This loss is avoided if the formation of inter-chain hydrogen bonds in the amorphous regions is prevented by the introduction of a small number of acetyl groups. The extrapolated value of the moisture regain for the decrystallized cotton is about 12 per cent whereas completely decrystallized cotton would be expected⁹ to have a moisture regain of about 17 per cent. It is thus clear that the treatment of cotton with ethylamine followed by washing with water leads to a partial decrystallization only.

REACTIVITY OF COTTON SWOLLEN WITH ETHYLAMINE AND WITH SODIUM HYDROXIDE

Loeb and Segal¹ showed that ethylamine-treated cotton from which the amine had been removed by successive portions of pyridine and which had not been allowed to dry was much more readily acetylated in pyridine than material that had been air-dried after treatment. It was also more readily acetylated than cotton that had been mercerized and, without drying, solvent-exchanged with pyridine. On the other hand never-dried material from which the ethylamine had been removed with *n*-hexane was hardly acetylated at all in this solvent unless it was further activated by means of acetic acid. These observations are not easy to reconcile with one another, because they are not strictly comparable owing to the use of significantly different experimental conditions in the two cases. For this reason three different methods of removing the amine from ethylamine-treated cotton have been compared by measuring the degree of acetylation attained in 24 hours under the conditions stated in the experimental section. The solvents used to remove ethylamine were water, *n*-hexane, and pyridine; the first two were subsequently replaced by pyridine and in each case the material was acetylated in pyridine without being allowed to dry. The degree of substitution of cotton that had been swollen with 16 per cent sodium hydroxide, washed with water, solvent-exchanged with pyridine, and acetylated in the same way was also measured. The results, given in *Table 1*, show that the reactivity of ethylamine-treated cotton that has been extracted with *n*-hexane is little greater than that of the original cotton, but the reactivity of the pyridine-extracted material is very much greater.

Table 1. Effect of acetylating cotton for 24 hours after various swelling and washing treatments

| Swelling agent | Solvent used to remove swelling agent | Acetyl content % |
|----------------------|---------------------------------------|------------------|
| None* | None* | 7.7 |
| Ethylamine | <i>n</i> -Hexane | 9.4 |
| Ethylamine | Water | 14.7 |
| Ethylamine | Pyridine | 25.4 |
| 16% sodium hydroxide | Water | 17.4 |

*Original cotton.

The reactivity of the water-extracted material is intermediate between those of the other two. It is this material that should be considered when comparing the relative effectiveness of ethylamine and sodium hydroxide, since only water can be used to wash out the latter. It is clear that when this is done cotton swollen with sodium hydroxide is more readily acetylated than ethylamine-treated cotton.

The relative effectiveness of *n*-hexane, water and pyridine, in maintaining ethylamine-treated cotton in a reactive state may be explained in terms of their hydrogen-bonding capacity. Since a high degree of decrystallization is maintained whatever the solvent used for extracting the ethylamine, loss of reactivity must be due to the formation of hydrogen bonds between adjacent chain-molecules in the amorphous regions of the material. This involves small lateral movements of some of the chains—insufficient to constitute recrystallization, but sufficient to form a crosslinked network capable of blocking the entry of the acetylating reagent. *n*-Hexane has no affinity for the hydroxyl groups of the cellulose and assists this process by acting as a lubricant. Pyridine, on the other hand, forms hydrogen bonds with the free hydroxyl groups in the amorphous regions¹⁰, thus preventing the cellulose chains from coming close enough together to be able to form hydrogen-bonded crosslinks. The intermediate effect of water is due to its ability to form more than one hydrogen bond per molecule. Since a water molecule may be attached to hydroxyl groups in adjacent chains, this has the effect of drawing the chains close enough together for them to become linked directly by hydrogen bonds between hydroxyl groups at neighbouring sites. Thus water prevents formation of inter-chain hydrogen bonds in some parts of decrystallized regions of cotton but assists it in other parts. The resulting material is therefore acetylated more slowly than material washed with pyridine but more rapidly than that washed with *n*-hexane.

The ability of pyridine to maintain ethylamine-treated cotton in a highly disordered (and therefore highly reactive) state is illustrated by the hygroscopicity measurements given in Table 2. This table compares the moisture regain of cotton with that of acetylated cotton, cotton acetylated after treatment with ethylamine and cold water, and cotton acetylated after treatment with ethylamine and pyridine, the degree of substitution being roughly the same in each case. The affinity of the acetylated pyridine-extracted material for water vapour is double that of acetylated cotton and 50 per cent greater than that of the acetylated water-washed material.

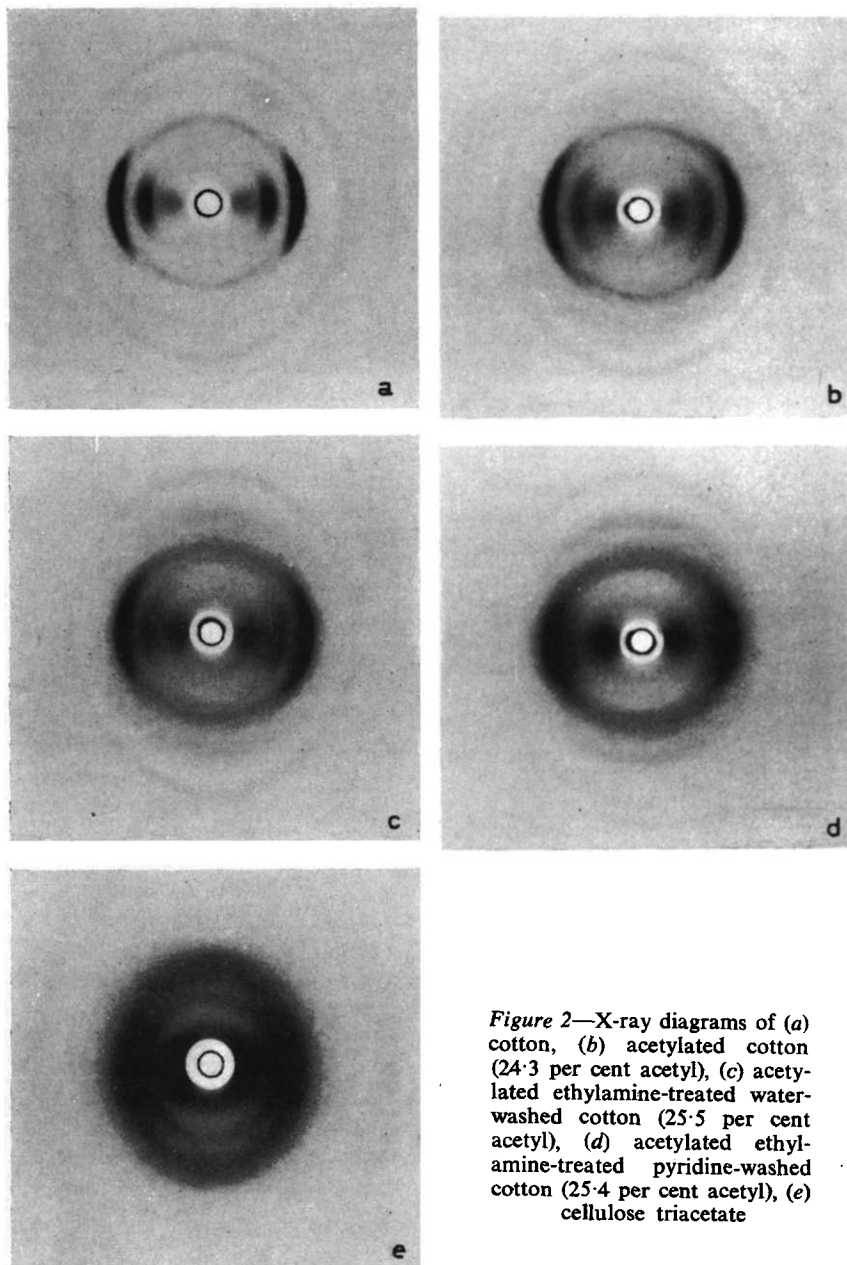


Figure 2—X-ray diagrams of (a) cotton, (b) acetylated cotton (24.3 per cent acetyl), (c) acetylated ethylamine-treated water-washed cotton (25.5 per cent acetyl), (d) acetylated ethylamine-treated pyridine-washed cotton (25.4 per cent acetyl), (e) cellulose triacetate

Table 2. Moisture regain of acetylated cotton at 66% r.h. and 20°C

| Starting material | Acetyl content % | Moisture regain |
|---|---------------------|-----------------|
| Cotton | 0 | 7.58 |
| Cotton | 24.3 | 3.89 |
| Ethylamine-treated cotton washed with water | 25.5 | 5.27 |
| Ethylamine-treated cotton washed with pyridine | 25.4 | 7.80 |

The X-ray fibre diagrams of the three acetylated products in Table 2 are shown in Figure 2, which also contains the diagrams of cotton and cellulose triacetate for comparison. The diagram of cotton acetylated without pre-treatment consists of the normal cellulose I pattern with a feeble cellulose acetate pattern superimposed, while that of acetylated cotton that had been pre-treated with ethylamine and washed with water shows a cellulose acetate pattern superimposed on a pattern characteristic of a distorted cellulose I lattice. It thus appears that when ethylamine-swollen cotton is washed with water some re-formation of cellulose I occurs at once and that, when the remaining decrystallized regions are acetylated to a sufficient extent, some of the cellulose acetate formed also crystallizes. The diagram of the material obtained by acetylating the pyridine-extracted decrystallized cotton consists mainly of the pattern of cellulose acetate together with a feeble pattern characteristic of a distorted cellulose I lattice. From this it would appear that the treatment of cotton with ethylamine followed by extraction with pyridine leads to a completely decrystallized product. On acetylation to a sufficiently high degree, however, some crystallization of the cellulose acetate can occur.

The authors thank Dr J. O. Warwicker for taking the X-ray photographs and Miss Beryl Johnson for much of the analytical work.

The Shirley Institute,
Didsbury,
Manchester 20

(Received December 1961)

REFERENCES

- 1 LOEB, L. and SEGAL, L. *Text. Res. (J.)* 1954, **24**, 654
- 2 SEGAL, L., NELSON, M. L. and CONRAD, C. M. *Text. Res. (J.)* 1953, **23**, 428
- 3 HOWLETT, F. and MARTIN, E. *J. Text. Inst.* 1944, **35**, T 1
- 4 SEGAL, L., NELSON, M. L. and CONRAD, C. M. *J. phys. Colloid Chem.* 1951, **55**, 325
- 5 JANSSEN, H. J., HAYDEL, C. H., SEAL, J. F. and VIX, H. L. E. *Text. Res. (J.)* 1957, **27**, 622
- 6 AIKEN, W. H. *Industr. Engng Chem. (Industr.)* 1943, **35**, 1206
- 7 HONOLD, E., KEATING, E. J. and SKAU, E. L. *Text. Res. (J.)* 1957, **27**, 400
- 8 BAILEY, A. V., HONOLD, E. and SKAU, E. L. *Text. Res. (J.)* 1958, **28**, 861
- 9 URQUHART, A. R. *Recent Advances in the Chemistry of Cellulose and Starch*, Ed. HONEYMAN, J., p 262. Heywood: London, 1959
- 10 SPEDDING, H. *Polymer, Lond.* 1962, **3**, 195

The Action of Ethylamine on Cellulose

Part II—Solvent Extraction of Ethylamine-treated Bacterial Cellulose: Changes in the Hydroxyl-absorption Region of the Infra-red Spectrum

H. SPEDDING

Dry bacterial cellulose films were treated with anhydrous ethylamine. The ethylamine was removed by one or more solvents and the films examined in the hydroxyl-stretching region of the infra-red spectrum (a) while still immersed, (b) after pumping-off the immersion liquid, (c) after exposure of the films to air, and (d) after heating the films in boiling water. Some films, kept wet after the ethylamine treatment, were acetylated to a small extent. It was found that the effect of anhydrous ethylamine on bacterial cellulose films was partly preserved even when the ethylamine was washed out. Solvent extraction with pyridine alone preserved this effect in cellulose in the wet state to a larger extent than when chloroform, n-hexane, cyclohexane, dimethyl formamide, water, methanol, or glacial acetic acid was used. There was generally a change, consistent with an increase in the strength of the intra-cellulosic hydrogen bonds on exposing the films to moist air, or heating them in boiling water, but this could be reduced and even reversed by acetylation to a small extent before such exposure to water vapour or hot water. Consequently the ethylamine-treated film washed with pyridine only and acetylated was the most weakly hydrogen-bonded of all the films in the dry state.

THE work to be described concerns the changes in hydrogen bonding of the hydroxyl groups in bacterial cellulose that are produced by treatment with ethylamine and subsequent solvent extraction with various liquids. Such changes have been investigated by examination of changes in the shape and frequency of the hydroxyl-stretching bands.

Ethylamine is known to swell cellulose and penetrate into the crystal lattice¹. In this process the state of hydrogen bonding throughout the whole sample must be drastically altered and it is very probable that, in the presence of excess of amine, a large proportion of the cellulose hydroxyl groups are hydrogen-bonded to ethylamine molecules and not to each other¹. The interest lies in what happens when the ethylamine is removed; whether the original structure is re-formed or whether a modified structure, whose nature depends on the liquid used for removing the amine, is obtained instead. Published results of previous experiments on cotton and bacterial cellulose show that ethylamine treatment brings about a reduction in crystallinity²⁻⁵; the crystal lattice can also be changed from cellulose I to III under certain conditions of removal of the amine^{5, 6}. Formation of cellulose III after this treatment can be detected by its characteristic X-ray diagram⁴, or by the presence in the hydroxyl-stretching region of the infra-red (i.r.) spectrum of a sharp peak at $3\,484\text{ cm}^{-1}$ that is absent from the spectrum of cellulose I⁷. The presence of cellulose III complicates the interpretation of

the hydroxyl-absorption region, and for the purposes of the present work it has been avoided in the way described later.

In the present work, separation, by deuteration, of the absorption of the hydroxyl groups in the amorphous regions from those in the crystalline regions⁸ was either impossible or undesirable. Many of the measurements were made on immersed films that could not be deuterated, and others on samples whose state might very well have been affected by exposure to deuterium oxide vapour. (The experiments, to be described below, that involved exposure of films to atmospheric water vapour support this hypothesis.) The hydroxyl absorption in each sample was therefore due to all the hydroxyl groups present.

The shape and position of the hydroxyl absorption region are dependent on the amount and the nature of both the amorphous and the crystalline phases, and would be affected by a change in any of these factors. In principle, any one, or all, of them may change in any particular treatment given to the sample; there is evidence from deuteration studies on dry, ethylamine-treated bacterial cellulose that even the nature of the crystalline phase may be modified, although cellulose III is not formed⁹. Thus a decrease in the prominence of 'crystalline' peaks could be due to (i) a decrease in the percentage-crystallinity, or (ii) a broadening of the 'crystalline' absorption bands caused by a modification of the molecular packing of the crystalline phase, or perhaps (iii) a narrowing of the amorphous absorption region caused by a decrease in the range of hydrogen-bond strengths of the amorphous phase. Consequently it is difficult to be specific about the change in each factor separately and this has not been attempted.

RESULTS AND DISCUSSION

Untreated films; band parameters

The hydroxyl-stretching region in untreated, dry, bacterial cellulose is composed of several overlapping bands and is markedly asymmetrical (*Figure 1*). The main peak is a fairly sharp one at $3\,355\text{ cm}^{-1}$. On the low-frequency side (LFS) there is a shoulder at *ca.* $3\,250\text{ cm}^{-1}$ and two others, poorly defined, at *ca.* $3\,280\text{ cm}^{-1}$ and *ca.* $3\,315\text{ cm}^{-1}$, while on the high-frequency side (HFS) there are weak shoulders at *ca.* $3\,375$ and *ca.* $3\,405\text{ cm}^{-1}$. The shape is similar to that of the hydroxyl-absorption region in the spectrum of the crystalline phase alone⁵, as might be expected from the high crystallinity of bacterial cellulose. Because of the very irregular shape found here and in other, ethylamine-treated, samples a much better idea of the asymmetry is given by the ratio of the absorption area on the HFS to that on the LFS than by the ratio of the half-band widths of the two sides; this is referred to hereinafter as the Area Ratio. To permit comparison of hydroxyl-absorption regions with different peak frequencies another parameter has been derived. This is the frequency of the Centre of Absorption, ν_c , which is defined in the experimental section and which is taken to represent the frequency of the 'centre of gravity' of the hydroxyl-absorption region. In the determination of ν_c it was impossible to allow for the well-known fact that the absorption coefficient of any hydroxyl group varies across the absorption region, since its value depends on the strength with

which the group is hydrogen-bonded. In spite of the inevitable simplification, ν_c values so determined are affected by changes in the overall strength of hydrogen bonding and can be used as a measure of such changes since no other factor is likely to have an effect comparable to that of hydrogen bonding. An increase (decrease) in ν_c implies a decrease (increase) in the

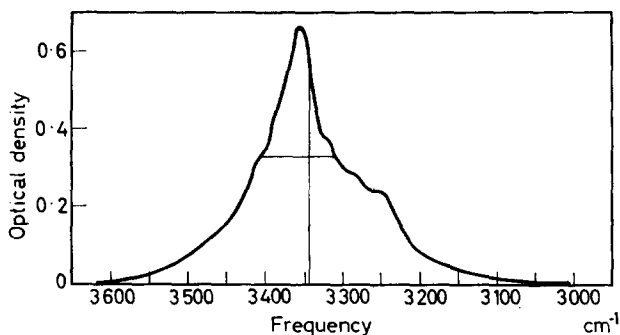


Figure 1—Hydroxyl-stretching region in dry bacterial cellulose film. (The horizontal line indicates the half-band width, and the vertical line the position of ν_c . This applies to each figure.)

strength of bonding. Although it is possible for ν_c to coincide with the Peak Frequency, ν_{\max} , without the Area Ratio being unity, there was only one instance of this. Otherwise, when the Area Ratio was greater (less) than unity, ν_c lay on the HFS (LFS) of the peak. Table 1 lists Area Ratio and ν_c in untreated films and ethylamine-treated films. In three dry, untreated films the Area Ratio was 0.86 ± 0.02 and ν_c was $3345 \pm 1 \text{ cm}^{-1}$, i.e. it lay on the LFS of ν_{\max} , which was at $3355 \pm 1 \text{ cm}^{-1}$.

Ethylamine-treated films

(a) *Immersed in solvents*—The bacterial cellulose films were treated with ethylamine and the amine exchanged, generally after an intermediate wash in pyridine (see below), for the liquid whose effect was to be examined. Spectra in the region 3000 to 3650 cm^{-1} were recorded with the films immersed after being kept wet with solvent during the entire solvent-extraction process. The liquids investigated differ considerably in their polarity, dielectric constant, and hydrogen-bonding capacity. Eight were examined: water, dimethyl formamide (DMF), cyclohexane, *n*-hexane, chloroform, pyridine, glacial acetic acid, and methanol.

It was discovered early in this work that, when pyridine alone was used to remove the ethylamine, the appearance of the cellulose hydroxyl region changed completely from that in the original untreated film. A peak now appeared at *ca.* 3430 cm^{-1} , and at 3365 cm^{-1} there was either a weaker peak or just a shoulder [Figure 2(i)]. The value of 3430 cm^{-1} is very similar to the frequency of the absorption band of water when dissolved in pyridine¹⁰, and it is very likely that the absorption peak at *ca.* 3430 cm^{-1} corresponds to cellulose hydroxyl groups hydrogen-bonded to the

H. SPEDDING

Table 1. Results of measurements of hydroxyl-absorption region in bacterial cellulose films. Area Ratio (A.R.), and Centre of Absorption (ν_c cm⁻¹)

| Type of film | Wet films | | Dry films (P ₂ O ₅ ; vac.) | | Acetylated films, Dry (P ₂ O ₅ ; vac.) | | | |
|------------------------------------|-----------|---------|---|---------|--|---------|------------------------------|---------|
| | | | | | Acetylated same extent, ca. 5% | | Acetylated same time, 30 min | |
| | A.R. | ν_c | A.R. | ν_c | A.R. | ν_c | A.R. | ν_c |
| Untreated | | | 0.86 | 3 345 | 0.90 | 3 344 | | |
| — | | | | | (0.93 | 3 346) | | |
| DMF | 0.78 | 3 347 | | | | | | |
| pyridine | | | 0.87† | 3 342 | | | | |
| Never-dried water/pyridine | | | 0.85† | 3 342 | | | | |
| Ethylamine-treated pyr./water/pyr. | 0.93 | 3 341 | 1.12 | 3 357 | | | | |
| | | | (1.10 | 3 357) | | | | |
| | 0.97 | 3 350 | 1.12* | 3 357 | | | | |
| | | | (0.82 | 3 337) | | | | |
| | | | 1.03† | 3 351 | 1.14† | 3 359 | | |
| | | | (1.07 | 3 352) | (1.09 | 3 353) | | |
| pyr./cyclohexane | 1.21 | 3 365 | 1.33 | 3 370 | | | | |
| | | | (1.15 | 3 359) | | | | |
| pyr./n-hexane | 1.22 | 3 366 | 1.30 | 3 369 | | | | |
| | | | (1.08 | 3 353) | | | | |
| | | | 1.18† | 3 356 | 1.17† | 3 359 | | |
| | | | (1.07 | 3 350) | (1.17 | 3 359) | | |
| | | | 1.13† | 3 359 | | | 1.41† | 3 374 |
| DMF | 1.11 | 3 365 | 1.25 | 3 367 | | | | |
| | [1.33] | | [1.35]§ | | | | | |
| | | | (1.18 | 3 359) | | | | |
| pyr./chloroform | 1.21 | 3 364 | 1.31§ | 3 368 | | | | |
| | | | (1.03 | 3 352) | | | | |
| | | | 1.18† | 3 358 | 1.31† | 3 365 | | |
| | | | (1.11 | 3 354) | (1.31 | 3 364) | | |
| pyridine | | 3 355 | 1.38 | 3 375 | | | | |
| | | | [1.53] | | | | | |
| | | | (0.91 | 3 343) | | | | |
| | | | 1.29† | 3 367 | | | 1.75† | 3 387 |
| | | | 1.17† | 3 363 | (1.49† | 3 375 | | |
| | | | (1.10 | 3 351) | (1.51 | 3 377) | | |

For ethylamine-treated films, entries on the same line refer to same film when one is wet and the other dry, and to films treated together when one is unacetylated and the other acetylated.

*Film unavoidably exposed to air for 5 min during drying.

†Film exposed to air when taken from liquid, but dried over phosphorus pentoxide *in vacuo* before measuring.

‡Film measured air-dry.

§Other regions show presence of traces of solvent.

() denotes values after film boiled in distilled water 2 h.

[] denotes values measured relative to 3 355 cm⁻¹ instead of peak frequency.

pyridine (O—H---N) and prevented to a considerable extent by the pyridine from hydrogen bonding to each other. Whatever the reason, the hydrogen bonding of these particular hydroxyl groups was significantly weaker than originally, as is shown by the shift in peak frequency to $3\,430\text{ cm}^{-1}$.

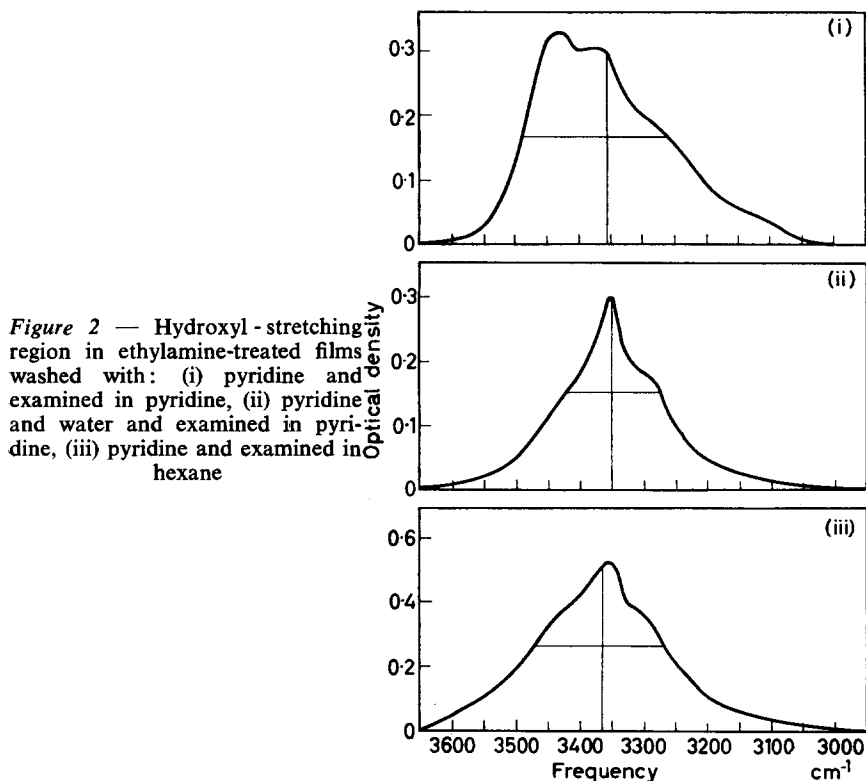


Figure 2 — Hydroxyl-stretching region in ethylamine-treated films washed with: (i) pyridine and examined in pyridine, (ii) pyridine and water and examined in pyridine, (iii) pyridine and examined in hexane

It is this property of pyridine that made it possible to measure the effects of those liquids that, when used alone, resulted in the formation¹¹ of cellulose III; the ethylamine was first removed with pyridine, the film examined in pyridine to check that the peak frequency was *ca.* $3\,430\text{ cm}^{-1}$, and the pyridine replaced by the other liquid in which the film could then be examined. The same property also afforded a method of examining the effects of water, methanol, and glacial acetic acid—liquids whose absorption in the 3μ region would have completely masked the hydroxyl absorption of the immersed cellulose film. This was avoided by exchanging these liquids for pyridine and examining the films in the pyridine. The six liquids examined in these ways, *viz.* glacial acetic acid, methanol, water, hexane, cyclohexane, and chloroform, gave a hydroxyl band whose peak was within a few cm^{-1} of $3\,355\text{ cm}^{-1}$ —the value in the original untreated film—showing that the hydrogen bonding as a whole was stronger (and the cellulose structure more 'collapsed') than with pyridine alone. Otherwise, pyridine could not have been used in conjunction with these other liquids.

The only liquid apart from pyridine that did not possess either of the disadvantages of the other liquids (i.e. formation of cellulose III or masking of 3μ region) was DMF.

The peak frequency of the band in seven of the eight immersed ethylamine-treated films (hereinafter referred to simply as 'treated films') was near $3\ 355\text{ cm}^{-1}$ (within 10 cm^{-1}); the exception was the film washed in pyridine only. The band shapes in the same seven films were similar to one another, though detailed measurement of the bands in five of these films (see *Table 1*) showed that the band in the water-washed film was considerably more symmetrical and had a markedly lower ν_c than the other four. The effect of DMF on band shape compared to that of the two hydrocarbons and chloroform was the same (if measured by the ν_c values) or greater (if measured by Area Ratio values). All the eight liquids gave a hydroxyl band with a much smoother contour than that in the untreated film; *Figures 2(ii) and 2(iii)* show the spectra of films washed with water and with hexane, as examples of this. In the six spectra measured in detail, the central peak and the shoulders were not nearly so pronounced or sharp as in the original, the decrease in the relative intensity of the peak being accompanied by a large increase in the half-band width. Both sides of the peak were affected in every case, but while the half-band width of the HFS varied widely, that of the LFS was fairly constant; also the shape of the LFS was very similar. (The film washed with pyridine only is not included in these remarks on band widths since ν_{max} was so very different.) The increases in ν_c and Area Ratio indicate that there was a decrease in the strength of hydrogen bonding in the samples as a whole. The values of ν_c and Area Ratio, in the film washed with pyridine only, were surprisingly low in view of the high value of ν_{max} , but this fact may be due to the difficulty encountered in estimating the correct shape of the absorption curve in the $3\ 200$ to $3\ 000\text{ cm}^{-1}$ region; see experimental section. This uncertainty would seem to be the reason, judging by the much higher values of these parameters in the same film when dried; see *Table 1*.

The similarity in measured band shape and peak frequency in five instances, where the liquids concerned differ considerably in hydrogen-bonding capacity (e.g. DMF and *n*-hexane) suggests that, for the films immersed in these five liquids, all, or nearly all, the cellulose hydroxyl groups were hydrogen-bonded to one another. By contrast, for the film washed with pyridine only, some at least of the cellulose hydroxyl groups were probably hydrogen-bonded to liquid molecules.

In no instance is there any evidence of free (i.e. not hydrogen-bonded) hydroxyl groups. The hydroxyl-absorption intensity in all samples decreased smoothly above *ca.* $3\ 450\text{ cm}^{-1}$ which is well below the frequency of free alcoholic hydroxyl groups in solution¹² and, almost certainly, in the solid state too, in spite of the fact that the effect of the change of state on the frequency is uncertain. (It has been suggested¹³ that free hydroxyl groups in a primary cellulose acetate absorbed at *ca.* $3\ 560\text{ cm}^{-1}$.) The intra-cellulosic hydrogen bonds are unlikely to be between a hydroxyl group and an oxygen atom (hydroxyl or acetal) within the same

chain unit, for, on the basis of comparison with intramolecular hydrogen bonding in solutions of cyclohexane diols and simple sugar derivatives¹⁴, such hydrogen-bonded hydroxyl groups would be expected to absorb at a higher frequency than observed. It is very probable that they are between different units in the one chain and/or between different chains. They are certainly not of the former type exclusively, for the three hydroxyl groups of each chain unit could not all be hydrogen-bonded to adjacent units of the same chain, as some of the distances involved are too great. This conclusion is contrary to the view of Staudinger *et al.*¹⁵ that there is no intermolecular hydrogen bonding between cellulose chains in 'inclusion celluloses' produced by swelling cellulose fibres in water and exchanging the water for non-polar liquids, for the systems concerned are similar.

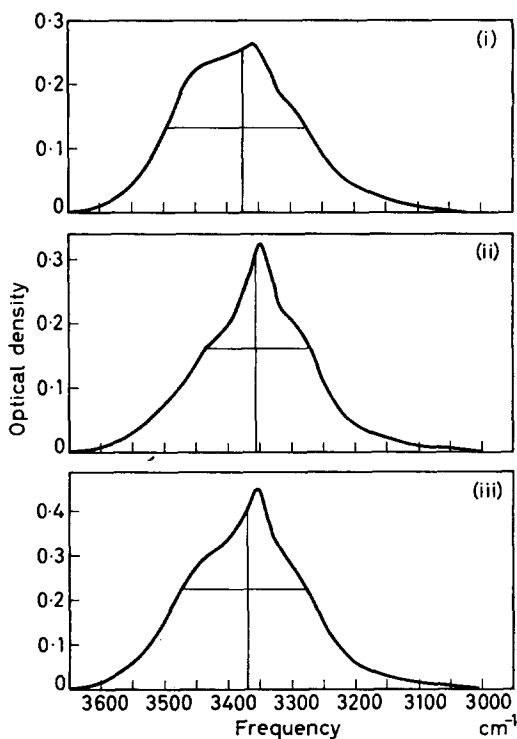
The present experiments show that DMF has no outstanding ability to break hydrogen bonds in cellulose, which was one explanation offered for the effect of DMF on the rate of acetylation of cellulose¹⁶. Thus with the treated film $\nu_{\max.}$ ($= 3365 \text{ cm}^{-1}$) was only 10 cm^{-1} different from its value in the untreated film, while ν_c was no different from its value in the films immersed in hexane, cyclohexane, and chloroform. This conclusion is confirmed by the examination of a dry, untreated film immersed in DMF; apart from the same shift of $+10 \text{ cm}^{-1}$ in peak frequency as in the treated film, the other parameters were very similar to those in the dry, untreated film itself.

The small effect of immersion liquids alone on the hydroxyl-absorption region was demonstrated with pyridine (as well as DMF—see above), the liquid in which the treated films differed most from the untreated ones. Thus the hydroxyl band in an untreated film immersed in pyridine was at 3353 cm^{-1} , and the band had the same appearance as in the film before immersion with the exception that the shoulders at *ca.* 3250 , 3375 and 3405 cm^{-1} were rather more pronounced, the last-named now being a weak peak. (These same small differences were even more pronounced in the hydroxyl band in a never-dried bacterial cellulose film examined in pyridine.) In the untreated film immersed in DMF it was noticeable there too that the shoulders were more distinct than before immersion. The lack of effect was further shown in a treated film that had been washed and examined in pyridine (peak at 3430 cm^{-1}), dried in the air and *in vacuo* and re-immersed in pyridine for re-examination; the peak was now at 3351 cm^{-1} .

(b) *Dried films*—When the treated films washed with pyridine only were taken out of the liquid and dried *in vacuo* over phosphorus pentoxide without exposure to the air at any time, the peak frequency decreased to 3361 cm^{-1} —nearly the same value as in the untreated film—and there was a marked change in the appearance of the hydroxyl-absorption region [Figure 3(i)]. There was now more resemblance to the same region in the five other films similarly dried (the films immersed in methanol and glacial acetic acid were not examined in the dry state), where the changes on drying were less pronounced; Figures 3(ii) and 3(iii) show the spectra of two such films. The similarity in ν_c and Area Ratio values for the films treated with the liquids cyclohexane, hexane, DMF,

and chloroform is particularly noticeable, with the film washed with pyridine only having rather greater values for these parameters. As with the wet films, the water-treated film is again somewhat in a class of its own. In all six films, drying produced a surprising increase in all the values of ν_c and Area Ratio; the changes in half-band width were less consistent but

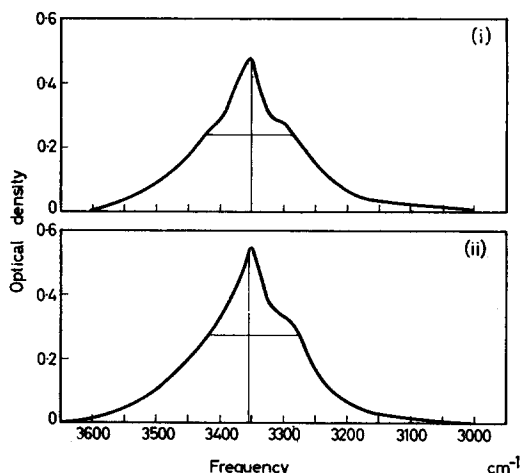
Figure 3—Hydroxyl-stretching region in ethylamine-treated films washed with: (i) pyridine, (ii) pyridine, water, and pyridine, (iii) pyridine and hexane; all dried and examined *in vacuo* over phosphorus pentoxide



were generally small. This increase is difficult to understand, even though it is fairly certain that there were still traces of liquids present in all these dried films. In those dried from DMF and chloroform, particularly the former, liquid absorption bands were apparent in the spectra. Moreover fibres of 'inclusion cellulose' retain *ca.* 5 per cent of liquid after being heated to 60° *in vacuo* for days¹⁵. As in the immersed films, the hydroxyl groups are all hydrogen-bonded, and again some at least of the bonds must be between different chains. There is, however, no direct evidence from the hydroxyl-absorption region as to whether some hydroxyl groups in the film dried from pyridine are still hydrogen-bonded to any residual pyridine molecules. In a separate experiment a film of regenerated cellulose was treated with ethylamine, washed with pyridine and heated *in vacuo* at 100°C for four hours. (This film was chosen because it was thicker than the bacterial cellulose films and thus facilitated detection of 'included' pyridine bands in the dry, treated film.) Bands due to pyridine were found at 707, 750 and 1 597 cm^{-1} . The point of interest is that these

frequencies are slightly different from the values for pure pyridine; similar shifts were found in the i.r. spectra of pyridine-water mixtures, where they were ascribed to hydrogen bonding between the water and the pyridine molecules¹⁷. Thus there is indirect evidence to suggest that hydrogen bonding to pyridine molecules, of which there were very probably some still present, occurred.

Figure 4—Hydroxyl-stretching region in ethylamine-treated films washed with: (i) pyridine, (ii) pyridine and hexane; both dried, heated in boiling water, dried and examined *in vacuo* over phosphorus pentoxide



If the films were dried in the air prior to being dried *in vacuo* over phosphorus pentoxide the ν_c and Area Ratio values decreased, and this decrease was accentuated, with one exception, if the films were boiled in water for two hours before being re-examined in the rigorously dry state. The exception concerned the water-treated cellulose. (Although in one of the three water-treated films boiling produced a large decrease in these parameters, in the other two films they changed very little, and it is considered that generally there would be little change as one would expect the effect to be small after a prior immersion in water.) Thus, exposure of the treated films to water vapour or liquid water caused a reversion towards the original band shape, and the characteristics of the films, other than the water-treated one, after boiling-water treatment and final drying were intermediate between those of the original untreated film and those of the solvent-included, treated films whether wet or 'dry'. (Figure 4 shows two examples of films heated in boiling water.) This reversion involved the release of the liquid molecules previously retained in the treated films as was shown by the disappearance of the liquid absorption bands after boiling the films. A similar release occurs on exposure of 'inclusion celluloses' to moist air¹⁸. It was also noted that when the films were heated in boiling water the half-band width always decreased, often to a considerable extent. Further, this decrease affected the HFS almost exclusively, while the LFS changed little and, unlike the HFS, had virtually the same final value each time.

(c) *Acetylated films*—After suggestions that acetylation of the treated films to a small extent might decrease the reversion that occurred on

removal of the ethylamine (see Part I), the effect of such acetylation on the hydroxyl-absorption region was examined. In the first of two experiments a batch of four pairs of films was treated with ethylamine and each pair was washed with a different liquid. One film in each pair was acetylated while still wet and then all the eight films were dried in the air and *in*

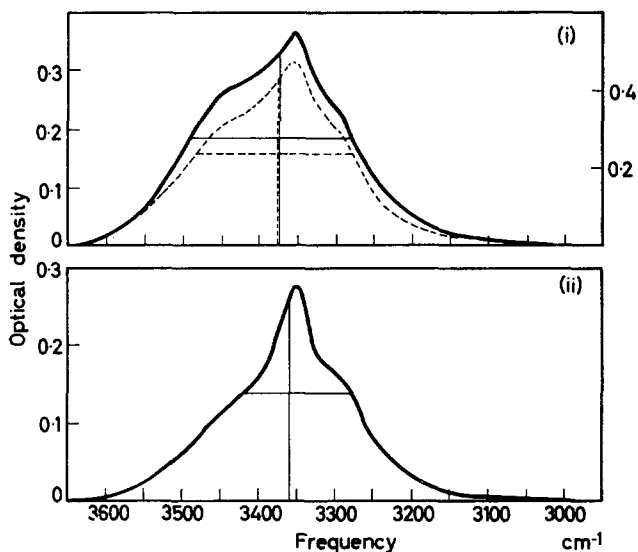


Figure 5—Hydroxyl-stretching region in ethylamine-treated films washed with: (i) pyridine, (ii) pyridine, water, and pyridine; both acetylated to *ca.* 5 per cent while still wet, dried in air and examined *in vacuo* over phosphorus pentoxide. [Broken curve and RH scale in (i) are Figure 7 (i) for comparison]

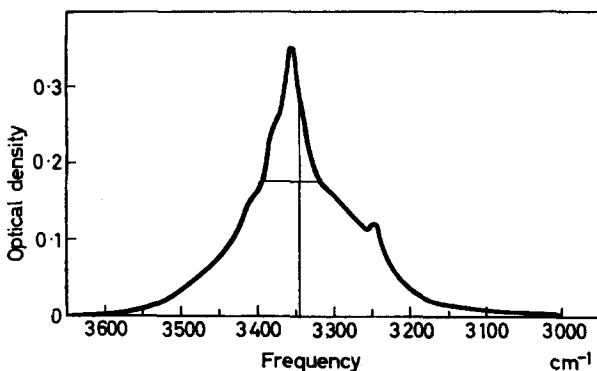


Figure 6—Hydroxyl-stretching region in acetylated, untreated film, examined *in vacuo* over phosphorus pentoxide

vacuo over phosphorus pentoxide. The hydroxyl region of each film was measured at this stage and again after the films had been heated for two hours in boiling water and rigorously dried a second time. (Figures 5 and 7 show the spectra of two of the acetylated films at these two stages.) The acetyl content was not known exactly but was probably about five per cent

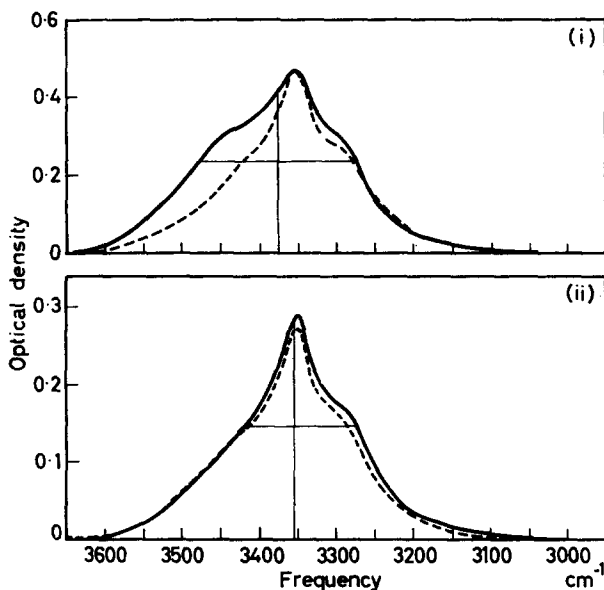


Figure 7—Hydroxyl-stretching region in ethylamine-treated films washed with: (i) pyridine, (ii) pyridine, water, and pyridine; both acetylated (ca. 5 per cent), dried, heated in boiling water, dried and examined *in vacuo* over phosphorus pentoxide. [Broken curve in (i) is Figure 4 (i); broken curve in (ii) is Figure 5 (ii), for comparison]

in all four films. The time of reaction was varied in order to achieve approximately the same extent of acetylation in each film, but even so there was a twofold variation between the extreme intensities of the ester (C=O) band. (These intensities were measured relative to that of the 1430 cm^{-1} band whose intensity appeared hardly affected at these low degrees of acetylation.)

This variation largely prevented comparison of the effects of different washing liquids, but there is some indication that washing with pyridine followed by acetylation produced a sample with weaker hydrogen bonding than did washing with chloroform followed by acetylation to the same extent. However, it is quite clear from the results given in Table 1 that a small degree of acetylation can have quite an appreciable effect on the hydroxyl-absorption region, particularly in films heated in boiling water [compare Figures 4(i) and 7(i)]. It is interesting to note also that in some instances the ν_c and Area Ratio values of the acetylated, treated films, even after exposure of the films to moist air or hot water, were greater than

they were in any of the treated films, however examined, that had not been acetylated. Little effect was apparent when the water-washed film and one of the two films that had been washed with *n*-hexane were acetylated, but there the degrees of acetylation were lower than in any other films. Acetylation of untreated films did not result in any similar change; *Figure 6* shows a typical example. Instead, the band shape remained very much the same even when the degree of acetylation was greater than in all the treated films, other than the one that had been washed with pyridine only and acetylated for 30 min. The shoulders at *ca.* 3 250 and *ca.* 3 405 cm^{-1} were as distinct as in the original film and the Area Ratio was still less than unity. The structure of the acetylated, treated films was maintained to a much larger extent on heating the films in boiling water for two hours than when unacetylated, treated films were similarly heated. This is apparent from the results in *Table 1* and *Figures 5(i)* and *7(i)* even though the effect of boiling was measured relative to films that had been exposed to air. The rate of acetylation of films increased according to whether they had been washed with hexane, water, chloroform, or pyridine (only), in that order. There was a two- to three-fold variation between the extreme rates. The order of these reactivities is somewhat different from that expected from a consideration of the shapes of the hydroxyl-absorption regions in the wet films, inasmuch that the hexane-washed film was expected to be more reactive than the water-washed film and to be about as reactive as the chloroform-washed one. (In these particular samples, however, the absorption bands concerned were very weak and their intensities could not be measured accurately.) The order of reactivity of the films apart from the hexane-washed one was as expected.

The half-band widths in the acetylated films varied widely on the HFS but were virtually constant, and approximately the same as before acetylation, on the LFS. Similar phenomena were noticed at each stage in the subsequent treatment of ethylamine-treated films; it was always on the HFS that changes in the half-band width and shape occurred. This indicates that although the *proportion* of the stronger hydrogen bonds changed (as denoted by changes in Area Ratio), the *distribution* of strengths of these stronger hydrogen bonds, i.e. those concerned with absorption on the LFS, remained approximately constant.

EXPERIMENTAL

Preparation of bacterial cellulose films

The films were grown from *Acetobacter acetigenum* and *Acetobacter xylinum* on Henneburg's medium. They were purified by washing with water, cold normal caustic soda (air excluded), and boiling 1 per cent caustic soda under nitrogen; then they were washed in distilled water followed by 0.5 per cent acetic acid, and finally in distilled water again. By this treatment the nitrogen content, determined on each batch of films, was reduced to less than 0.5 per cent generally and less than 1 per cent always.

Ethylamine treatment

This followed the method described in Part I and the same apparatus

was used. Each film was mounted in an aluminium holder for ease of handling. The films were dried *in situ* for 15 to 30 min before ethylamine was introduced into the evacuated reaction vessel. B.D.H. anhydrous ethylamine was always used and was taken directly from the sealed ampoule. All the results in *Table 1* were obtained on films treated together with ethylamine for 5½ h, except for one water-washed film (treated for 4½ h) and the films used in experiments concerned with the effects of acetylation. In these latter experiments the time of treatment in one series (where acetylation was *ca.* 5 per cent) was 3½ h, and 2 h in the other series.

Solvent extraction

Of the organic liquids used, glacial acetic acid, *n*-hexane, cyclohexane, DMF, and chloroform were of reagent quality. The last two, being hygroscopic, were examined for the presence of water. The 3 μ water absorption (0.1 mm thickness) showed that the water content of each was negligible. The methanol and pyridine were of analytical reagent quality. The pyridine was dried rigorously by distillation under anhydrous conditions without the addition of any entrainer¹⁰. The absorption in the 3 400 to 3 450 cm⁻¹ region was less than 4 per cent (0.1 mm thickness), which corresponded to a water content less than 0.01 per cent v/v. A guide as to the amount of water picked up during the washing treatments was obtained by examination of each final wash liquid (see below), and was extremely small (estimated as less than 0.05 per cent v/v) even in the hygroscopic liquids. Since water was shown by the present experiments to have a 'collapsing' effect, it was always necessary to work with liquids as dry as possible. These precautions were more necessary with pyridine than with other washing liquids because, in addition to its hygroscopicity, it was the only liquid used where there was any absorption due to water at the same frequency as the cellulose hydroxyl peak. Such absorption, if appreciable and not fully compensated, would have distorted the recorded band shape. Each film was always kept wet with solvent during the entire solvent extraction process and never allowed to dry until required. If more than one liquid was used for the extraction, films were given four or five thorough washes when it was necessary to remove all traces of the previous solvent.

Acetylation

The film to be acetylated was transferred into 10 ml pyridine and the whole added to a mixture of 50 ml acetic anhydride and 40 ml pyridine that had been kept thermostatted at 25°C. After the desired time the film was quickly transferred into pyridine to stop the reaction. It was washed two or three times with pyridine and then dried in air and *in vacuo* over phosphorus pentoxide in the sample compartment of the spectrometer.

Cell

The cell used was constructed so that films could be inserted and examined in the wet state; it was in two parts. The film to be examined was placed in one part and then the other part was screwed into position

with the cell immersed in the final wash liquid. An outlet, which was later stoppered, was provided to allow excess of liquid to escape as the two parts were screwed together. The windows were circular microscope cover glasses fastened with Tenasitine. The transmittance in the region of interest was perfectly adequate, but a pair of similar cover glasses was placed in the reference beam for compensation. Cover glasses that did not show interference fringes were selected. During the entire experiment each film was sandwiched in a folded spacer made from aluminium foil; this considerably facilitated handling of the films, particularly during the insertion of wet ones into the cell. The liquid path-length with such a spacer was *ca.* 0.07 mm, and all the liquids used in the cell were sufficiently transparent, except for pyridine in the region below *ca.* $3\ 100\text{ cm}^{-1}$. A variable-thickness cell with sodium chloride windows was used in the reference beam to compensate for absorption by the liquid in the sample beam. This reference cell was filled with the overflow from the sample cell as it was screwed up in the final wash liquid. This provided the best way of cancelling out absorption in the sample beam due to absorption by any traces of water in the sample-cell liquid. With pyridine, where it became essential to exclude the possibility that water was responsible for the altered band shape (see earlier), additional confirmation was obtained by examining two films, one untreated and the other treated and dried, immersed in pyridine; there was no similar alteration in either of the two spectra.

Drying of ethylamine-treated films

Apart from the films used in the acetylation experiments all the other treated films were dried in the cell. The cell-stopper was removed and the immersion liquid was pumped off by means of a rotary oil-pump with phosphorus pentoxide in the cell-well and an acetone-carbon dioxide trap in the pumping system. During this process the cell was in position in the sample cell-well of the spectrometer, and both the cell and cell-well remained evacuated during the spectroscopic measurements. The hydroxyl-absorption region assumed a constant shape within a few minutes, but pumping was continued for 15 to 35 min, depending on the volatility of the liquid, before the spectrum was finally recorded. The films were then taken out of the cell in order that the region below $2\ 000\text{ cm}^{-1}$, where the cell windows were opaque, could be examined for the presence of liquid-absorption bands in the dry films. They were replaced in the sample compartment as quickly as possible (less than 5 min) to minimize the time of exposure to air and immediately examined again *in vacuo* over phosphorus pentoxide. (When taken out of the cell all the films appeared to be dry.)

Spectroscopic measurements

Spectra were measured on a Unicam SP.100 spectrometer thermostatted at 30°C . The region $3\ 000$ to $3\ 650\text{ cm}^{-1}$ was measured with a 3 000 lines-per-inch grating and frequencies were checked against water-vapour and ammonia bands. A sodium chloride prism was used for measurements

below 2000 cm^{-1} . All the dried films were examined *in vacuo* over phosphorus pentoxide except for one untreated film (noted in *Table I*).

Band parameters were determined by dividing the hydroxyl-absorption region, each side of the peak, into 20 cm^{-1} intervals from 3000 to 3650 cm^{-1} and measuring the optical density (D) at the centre of each interval. Optical densities were measured from a baseline intercepting the absorption curve at 3000 and 3650 cm^{-1} . In the films immersed in pyridine the shape of the curve below *ca.* 3200 cm^{-1} was estimated graphically as it proved impossible, for some unknown reason, to obtain adequate compensation for liquid absorption below 3200 cm^{-1} , even though pyridine absorption was not intense above 3100 cm^{-1} . This method is considered to be sufficiently good for the present purpose, bearing in mind that the choice of baseline is somewhat arbitrary and that the parameters are required for comparison purposes only.

The Centre of Absorption, ν_c , is then defined as $\Sigma \nu D / \Sigma D$, and Area Ratio as $\Sigma D_{\text{HFS}} / \Sigma D_{\text{LFS}}$.

The author is indebted to Miss S. Burgess for her assistance in carrying out most of the experimental work.

*The Shirley Institute,
Didsbury, Manchester 20*

(Received December 1961)

REFERENCES

- ¹ DAVIS, W. E., BARRY, A. J., PETERSON, F. C. and KING, A. J. *J. Amer. chem. Soc.* 1943, **65**, 1294
- ² SEGAL, L., NELSON, M. L. and CONRAD, C. M. *J. phys. Colloid Chem.* 1951, **55**, 325
- ³ SEGAL, L., NELSON, M. L. and CONRAD, C. M. *Text. Res. (J.)* 1953, **23**, 428
- ⁴ SEGAL, L., LOEB, L. and CREELY, J. J. *J. Polym. Sci.* 1954, **13**, 193
- ⁵ MARRINAN, H. J. and MANN, J. J. *J. Polym. Sci.* 1956, **21**, 301
- ⁶ SEGAL, L. *Text. Res. (J.)* 1954, **24**, 861
- ⁷ MANN, J. and MARRINAN, H. J. *Chem. & Ind.* 1953, 1092
- ⁸ MARRINAN, H. J. and MANN, J. J. *appl. Chem., Lond.* 1954, **4**, 204
- ⁹ JEFFRIES, R. Private communication
- ¹⁰ COULSON, E. A., HALES, J. L. and HERINGTON, E. F. G. *J. chem. Soc.* 1951, 2125
- ¹¹ See this Journal, page 211
- ¹² BELLAMY, L. J. *The Infra-red Spectra of Complex Molecules.* Methuen: London, 1958
- ¹³ BROWN, L., HOLLIDAY, P. and TROTTER, I. F. *J. chem. Soc.* 1951, 1532
- ¹⁴ SPEDDING, H. *J. chem. Soc.* 1961, 3617 and references therein
- ¹⁵ STAUDINGER, H., IN DEN BIRKEN, K.-H. and STAUDINGER, M. *Makromol. Chem.* 1953, **9**, 148
- ¹⁶ BLUME, R. C. and SWEZEY, F. H. *TAPPI*, 1954, **37**, 481
- ¹⁷ SIDOROV, A. N. *Optics and Spectroscopy*, 1960, **8**, 24
- ¹⁸ STAUDINGER, H. and DOHLE, W. *J. prakt. Chem.* 1942, **161**, 219

The Action of Ethylamine on Cellulose

Part III—The Formation of Cellulose III and Its Infra-red Spectrum between 1500 and 650 cm^{-1}

H. SPEDDING

When the amine is removed from ethylamine-treated bacterial cellulose films by washing with hexane or chloroform, formation of cellulose III can occur even before the films are allowed to dry. The formation of cellulose III from cellulose I is accompanied by some changes in band frequencies in the infra-red spectrum between 1 400 and 1 000 cm^{-1} , and these show up more clearly in the spectra of films than in those of fibres.

FORMATION OF CELLULOSE III

THE existence of at least four crystalline modifications of cellulose, each with its own characteristic X-ray diffraction pattern and unit cell, is now well established. Of these cellulose III can be obtained by treatment of native or regenerated cellulose with liquid ammonia¹ or dry ethylamine², followed by removal of the liquid under certain conditions. In the ethylamine treatment there has been some confusion as to what these conditions are^{3, 4}, but it is clear from the literature and from the present work that, when solvent extraction is employed, the chances of obtaining cellulose III are greater with hexane or chloroform as solvent than with pyridine, water or dimethylformamide.

The experiments to be described have been mainly concerned with the ethylamine treatment of bacterial cellulose films. When the amine was removed with hexane or chloroform at room temperature, formation of cellulose III occurred even before the films were dry. This was shown by measurement of the infra-red (i.r.) spectra of the films immersed in the final wash liquids which revealed the presence of a sharp peak at 3 484 cm^{-1} that is characteristic of cellulose III prepared⁵ from cellulose I. In three other experiments the ethylamine was again washed off with hexane, under various conditions, and the hexane exchanged for pyridine—a liquid that never gave cellulose III when used alone, even when the films were finally dried. Cellulose III was formed in each immersed film. (The proportion present—as judged by the relative prominence of the peak at 3 484 cm^{-1} —varied. It was greatest when the hexane was used at room temperature; slightly less when a similar hexane washing was supplemented by extraction with hot hexane; and very much less when ice-cold hexane was used.) These experiments showed that prolonged extraction did not prevent the formation of cellulose III, and that the formation of cellulose III is not necessarily due to incomplete washing, as was suggested previously^{3, 6}.

INFRA-RED SPECTRUM OF CELLULOSE III

The first evidence cited for the identification by i.r. spectroscopy of cellulose III formed from cellulose I was the characteristic band at $3\,484\text{ cm}^{-1}$ in the hydroxyl-stretching region⁵. Since then this region has been investigated in detail^{3, 7}, but there does not appear to be any definite information available on characteristic differences in band frequencies between this polymorphic form and cellulose I in the $1\,500$ to 650 cm^{-1} region where cellulose I shows so many absorption bands. Spectra of celluloses incorporated into potassium bromide discs have been measured^{4, 6} without yielding any satisfactory differentiation between cellulose I and III (and II also) throughout the entire region of $4\,000$ to 670 cm^{-1} . A sample of ethylamine-treated cotton containing a large proportion of cellulose III (as shown by X-ray diffraction) was examined over this range as a fibre-film¹⁰; this form has the advantage over a potassium bromide disc that no grinding is required. Close inspection showed some minor differences in the $1\,400$ to $1\,100\text{ cm}^{-1}$ region between this film and fibre-films of cottons containing the cellulose I lattice only, but it really required evidence from bacterial cellulose films (see below), where the same differences were much more noticeable, to confirm them. These differences consisted of a weak band at *ca.* $1\,228\text{ cm}^{-1}$ and a shift in the absorption maximum near $1\,110\text{ cm}^{-1}$ from $1\,111\text{ cm}^{-1}$ to $1\,103\text{ cm}^{-1}$. Contrary to expectation there was no peak at $3\,484\text{ cm}^{-1}$ but a broad absorption region centred at *ca.* $3\,410\text{ cm}^{-1}$, as was also found in the spectrum of the same sample measured as a potassium bromide disc. (In the latter there was a suggestion of a shoulder at *ca.* $3\,484\text{ cm}^{-1}$.) This is probably due to the fact that the intrinsic absorption in the hydroxyl-stretching region of cellulose is too great for much detail to show within this region in the spectra of samples examined as fibres without their being severely ground, and such grinding would destroy their crystallinity.

By contrast, an ethylamine-treated bacterial cellulose film, whose crystalline fraction contained at least 50 per cent cellulose III as estimated from its X-ray diffraction pattern, showed several distinguishing features in addition to the $3\,484\text{ cm}^{-1}$ peak. There was a band at $1\,363\text{ cm}^{-1}$ that may be a synthesis of the bands at $1\,370$ and *ca.* $1\,357\text{ cm}^{-1}$ which occur in bacterial cellulose both untreated and decrystallized (i.e. ethylamine-treated but containing no cellulose III); this would account for the relatively increased intensity of the $1\,363\text{ cm}^{-1}$ band. There were also two weak bands at $1\,264$ and $1\,224\text{ cm}^{-1}$, and two strong ones at $1\,103$ and $1\,073\text{ cm}^{-1}$, all of which were characteristic. Finally the weak band at 900 cm^{-1} appears to be sharper than in the spectrum of the decrystallized specimen. *Figure 1* shows the spectrum of the film containing cellulose III, together with those of untreated and of decrystallized bacterial cellulose films. (The ordinate origins have been shifted for ease of comparison.) By comparison with the absorption bands in native cellulose¹¹ the band found at $1\,363\text{ cm}^{-1}$ is probably due to a C—H bending mode, while those at $1\,103$ and $1\,073\text{ cm}^{-1}$ are most likely due to single-bond stretching modes; the origin of the bands at $1\,264$ and $1\,224\text{ cm}^{-1}$ is uncertain.

Ethylamine treatment, followed by pyridine washing, of a film containing cellulose III resulted in the disappearance of the strong peak at $3\,484\text{ cm}^{-1}$.

THE ACTION OF ETHYLAMINE ON CELLULOSE

The spectrum of the dried film showed a band with a flat top from 3 440 to 3 360 cm^{-1} instead. A similar reversion was found by Barry *et al.* on treatment of a cellulose III sample with liquid ammonia¹.

EXPERIMENTAL

All the films were about 5μ thick. Their preparation, the method of ethylamine treatment, and the spectroscopic measurements were as described in Part II.

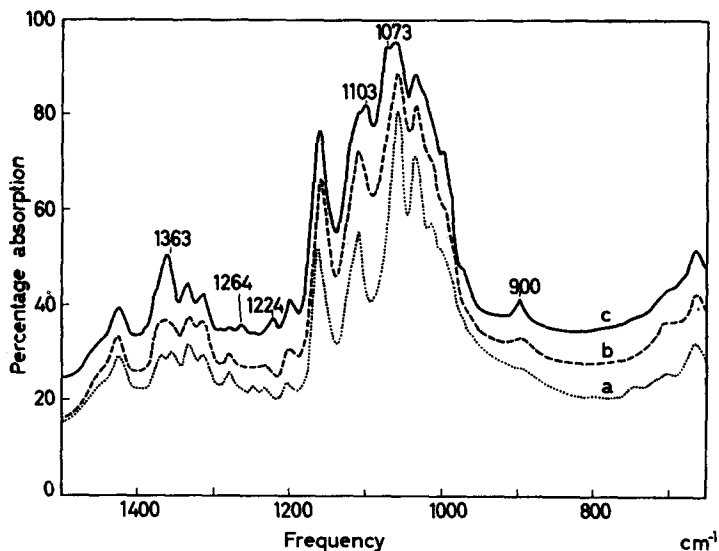


Figure 1—Infra-red spectrum 1 500 to 650 cm^{-1} of (a) untreated bacterial cellulose film, (b) ethylamine-treated bacterial cellulose film containing no cellulose III, and (c) ethylamine-treated bacterial cellulose film containing cellulose III

The film washed with *n*-hexane alone was given ten washes and that washed with chloroform alone four washes, all washings being at room temperature. Each film was examined in the region 3 650 to 3 000 cm^{-1} in the final wash liquids. Of the samples whose spectra are recorded in Figure 1, the film containing a large proportion of cellulose III and the one that had been decrystallized had been treated together with ethylamine: the former was washed with *n*-hexane and then with pyridine, and the latter in pyridine only, always at room temperature. Two other films were washed with both *n*-hexane and pyridine. One of these was washed three times with hexane at room temperature, then in a Soxhlet with hot hexane for six hours (with phosphoric acid in the distillation flask to prevent recycling of amine⁶), and finally three times with pyridine at room temperature. The other was washed five times with ice-cold hexane and then twice with ice-cold pyridine before being transferred to pyridine at room temperature.

The potassium bromide disc of the ethylamine-treated cotton was prepared by cutting the fibres fine with a Hardy microtome, adding

potassium bromide, and grinding the mixture in a vibration mill for a very short time (3 min).

The author thanks Dr J. O. Warwicker for measuring the X-ray diffraction patterns of samples and Miss S. Burgess for experimental assistance.

*The Shirley Institute,
Didsbury, Manchester 20*

(Received December 1961)

REFERENCES

- ¹ BARRY, A. J., PETERSON, F. C. and KING, A. J. *J. Amer. chem. Soc.* 1936, **58**, 333
- ² SEGAL, L., LOEB, L. and CREELY, J. J. *J. Polym. Sci.* 1954, **13**, 193
- ³ MARRINAN, H. J. and MANN, J. *J. Polym. Sci.* 1956, **21**, 301
- ⁴ HAYDEL, C. H., SEAL, J. F., JANSSEN, H. J. and VIX, H. L. E. *Industr. Engng Chem. (Industr.)*, 1958, **50**, 74
- ⁵ MANN, J. and MARRINAN, H. J. *Chem. & Ind.* 1953, 1092
- ⁶ SEGAL, L. *Text. Res. (J.)* 1954, **24**, 861
- ⁷ MANN, J. and MARRINAN, H. J. *J. Polym. Sci.* 1958, **32**, 357
- ⁸ O'CONNOR, R. T., DUPRÉ, E. F. and MITCHAM, D. *Text. Res. (J.)* 1958, **28**, 382
- ⁹ SEGAL, L. and CREELY, J. J. *J. Polym. Sci.* 1961, **50**, 451
- ¹⁰ BURGESS, S. and SPEDDING, H. *Chem. & Ind.* 1961, 1166
- ¹¹ LIANG, C. Y. and MARCHESSAULT, R. H. *J. Polym. Sci.* 1959, **39**, 269

A Study of the Thermodynamic Properties and Phase Equilibria of Solutions of Polyisobutene in n-Pentane

C. H. BAKER, W. B. BROWN, G. GEE, J. S. ROWLINSON, D. STUBLEY
and R. E. YEADON

The thermodynamic properties and phase equilibria have been studied for samples of polyisobutene of mean molecular weights from 250 to 2 250 000 in solution in n-pentane. The following properties have been measured for solutions of one or more samples; volumes of mixing at 25°C, free energies of dilution of the solvent from 25° to 55°C (from which heats and entropies of dilution are derived by differentiation), the temperatures of phase separation and the relative volumes of the resulting phases on heating above 70°C, and the critical end-points. Polymers of low molecular weight are not precipitated until the solution is heated to temperatures near the gas-liquid critical point of pure solvent, and the thermodynamic properties of the solution at room temperature are given approximately by the Flory-Huggins equation with a positive heat of dilution. Polymers of high molecular weight are precipitated at temperatures little above the normal boiling point of the solvent. Their thermodynamic properties at room temperature are incompatible with the Flory-Huggins equation since both heat and entropy of dilution are negative. The volume of mixing at 25°C is negative for all molecular weights.

AN ALKANE polymer that is above its melting point is generally miscible in all proportions with a paraffin solvent. The heat of mixing is very small and positive. The polymer is often incompletely miscible with aromatic and polar solvents in which the heat of mixing is always large and positive. The polymer becomes more soluble in these poor solvents as the temperature is raised, until complete miscibility is attained at an upper critical solution temperature (UCST). However, it has been shown recently¹ that hydrocarbon polymers can also be precipitated from all hydrocarbon solvents, whether aliphatic or aromatic, by raising the temperature sufficiently far above the normal boiling point of the solvent. The minimum temperature at which immiscibility occurs is a lower critical solution temperature (LCST). The heat of mixing must be negative at such a point to satisfy the well-known thermodynamic inequalities that hold at critical points². The occurrence of LCST in solutions of non-polar polymers, although established only recently, is apparently a very widespread, if not universal, phenomenon. This paper reports an extended study of the phase equilibria and thermodynamic properties of one system of this type, polyisobutene in *n*-pentane, in which it has already been established¹ that the LCST is as low as 75°C for polymers of long chain length.

MATERIALS

Five samples of polyisobutene were used. Four were viscous liquids of mean molecular weights 250, 1 170, 14 000 and 62 000, which for convenience are

denoted Polymer I to IV respectively. These were maintained *in vacuo* for several days to remove traces of monomer and dissolved air, but were otherwise untreated.

Polymer V was a rubbery material whose mean molecular weight was initially about 1 400 000. 20 g of this sample was dissolved in 2 l. of carbon tetrachloride and the solution was filtered through glass wool to remove any crosslinked material. The polymer was recovered by precipitation with acetone, filtered, and freed from solvent by heating *in vacuo* at 80°C until the pressure did not rise above 10^{-5} mm of mercury on standing overnight. This material is called VA and had a mean molecular weight of 1 400 000. A second sample of 50 g of V was dissolved in 4.5 l. of benzene and fractionated by the addition of acetone, as recommended by Fox and Flory³. 30 g of the precipitated polymer was dissolved in cyclohexane and the viscous solution was poured on to water. The cyclohexane was removed by evaporation in a dust-free atmosphere to leave a clear film of polymer which was free of air bubbles and which evolved no more residual gas or vapour after several hours evacuation at 90°C. The mean molecular weight of this sample, VB, was 2 250 000.

The densities of I and II were approximately 0.82 and 0.875 g cm⁻³. These values were obtained in the course of measurements of volumes of mixing and of vapour pressure respectively. The density of VB was measured carefully at 25°C by finding the density of aqueous alcohol in which pieces of the clear polymer film neither floated nor sank. The mean of three concordant results was 0.914₁ g cm⁻³. This density is 3 per cent lower than that of 0.9437 reported by Bawn and Patel⁴ for material of molecular weight 45 000 to 100 000, but agrees with the value of 0.915 g cm⁻³ found by Allen, Gee and Nicholson⁵ for a sample from the same stock as V which was probably almost identical with polymer VA. The low density agrees with the value of 0.913 g cm⁻³ obtained for material of this molecular weight by an extrapolation (possibly unjustified) of an equation, proposed by Fox and Flory⁶ to represent their result at higher temperatures.

The samples used were, therefore, as follows:

| Polymer 10 ⁻³ M | I | II | III | IV | VA | VB |
|-----------------------------------|------|-------|-----|----|----|-------|
| Density (g cm ⁻³ 25°C) | 0.82 | 0.875 | — | — | — | 0.914 |

The molecular weights of I and II are those quoted by the suppliers; other molecular weights were determined from the intrinsic viscosity of solutions in carbon tetrachloride at 25°C by using the equation⁷

$$[\eta] = 3.20 \times 10^{-4} M^{0.674}$$

The *n*-pentane that was used for measurements of vapour pressure was obtained from the National Chemical Laboratory and had a quoted purity of not less than 99.98 per cent. Other measurements were made with pentane that was obtained by careful fractionation of a commercial product. The principal impurity was isopentane, and gas chromatograms of the final product showed that all but 0.5 per cent had been removed. The physical properties of the purified material were as follows:

A STUDY OF THE THERMODYNAMIC PROPERTIES OF POLYISOBUTENE

| | | |
|--|---------------------|-----------|
| normal boiling point (°C) | 35.95 to 36.10 | (36.074) |
| density (g ml ⁻¹ , 25°C) | 0.6212 ₁ | (0.62139) |
| refractive index n_{20}^D | 1.3573 | (1.35748) |
| critical temperature (°C) | 196.6 ₃ | (196.62) |

The values in parentheses are those recommended by the American Petroleum Institute⁸. The triple point of this sample was within 0.1°C of that supplied by the National Chemical Laboratory.

EXPERIMENTAL

(1) *Volumes of mixing*

The approximate volume of mixing of polymer I with *n*-pentane was measured by introducing weighed amounts of each (1 to 2 g) into a precision-bore tube of 5 mm internal diameter, with as little mixing as possible. The height of the meniscus was observed, the tube was stirred without loss of solvent, and the new height of the meniscus was observed.

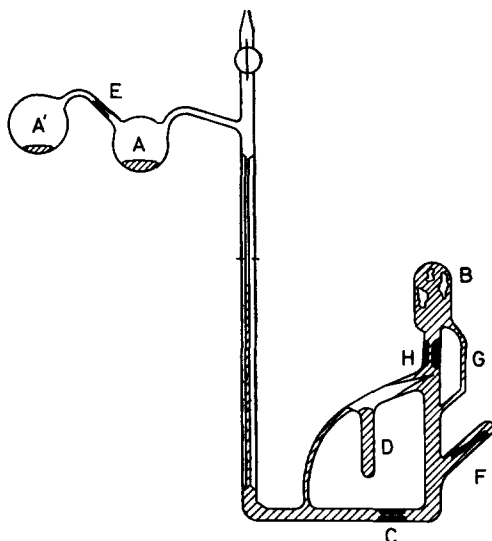


Figure 1—Apparatus for measurement of mixing volume

The volume change on dissolving the 'solid' polymer VB in the volatile solvent, *n*-pentane, was measured directly in the apparatus shown in *Figure 1*. This was set up initially with all the mercury in bulb A' and a weighed amount of polymer in bulb B, whose volume was about 3 cm³. The apparatus was evacuated to 10⁻⁶ mm of mercury for several days during which the mercury was occasionally boiled gently under total reflux. About 35 cm³ of mercury was then distilled into A, and bulb A' removed by sealing at the constriction E. A weighed amount of *n*-pentane, previously sealed *in vacuo*, was now distilled into tube D. The mercury was cooled to prevent the too rapid warming of the solvent, and poured down the capillary to fill

B and D and to trap an iron rod, sealed in glass, in the pocket F. The constriction C was necessary to prevent the rush of mercury from snapping the break-seal. Air was now admitted through the tap to prevent the pentane forcing its way back up the capillary under its own vapour pressure as it warmed up to room temperature. The apparatus was now immersed in a

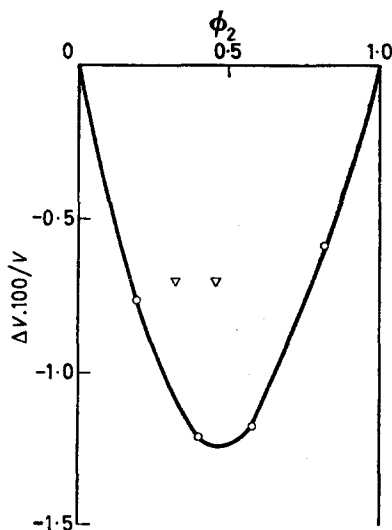


Figure 2—Volume changes on mixing:
○ Polymer VB, ▽ Polymer I

thermostat at $25.00 \pm 0.01^\circ\text{C}$ and the break-seal below H was broken with the iron rod. The pentane rose into B, displaced the excess mercury through G, and dissolved the polymer. The change of volume was measured by observing the change of height of mercury in the precision-bore capillary, whose diameter was 1 mm. The height became steady after a lapse of time of from several hours to ten days, according to the concentration of the final solution. The results are shown in *Figure 2*.

(2) Vapour pressures

The vapour pressures of dilute solutions of polymer are almost indistinguishable from those of the pure solvent, and therefore the lowering of the vapour pressure in these solutions was measured indirectly by using the isothermal still described by Gee and Orr⁹. A known weight of polymer VA was placed in one compartment of the still and a known weight of α -lupene ($\text{C}_{30}\text{H}_{50}$) in the other. The still was evacuated to 10^{-5} mm of mercury and solvent added by distillation on to the α -lupene. The weight of solvent was found both by weighing the sealed still and by observing the decrease in the volume remaining in the reservoir from which it was distilled. The two weights agreed well. The solvent distributed itself between the two solutes by isothermal distillation. The weight of solvent that remained in the solution of α -lupene was found by measuring the volume of this solution

in a precision-bore tube attached to the still, under standard conditions of temperature and time of drainage. The weight in the polymer solution was found by difference after allowance for the amount in the vapour. The difference in chemical potential between pure pentane and the pentane in either solution was found by assuming that the solution of α -lupene was ideally dilute. This assumption was justified since the mole fraction of solute never exceeded 0.02. Measurements above 40°C could not be made by this method because of the large correction for the amount of solvent in the vapour phase at temperatures above its normal boiling point.

The vapour pressures of solutions in which the weight fraction of polymer exceeded 0.4 were measured directly for polymers II and VB at 25°, 35°, 45° and 55°C. The apparatus was essentially that of Baxendale, Enustun and Stern¹⁰, with the modifications of Rowlinson and Thacker¹¹ to eliminate any contact between the mercury in the null-manometer and the rubber tubing. A further small change was the replacement of the conventional tap at the base of the null-manometer by a greaseless tap with a key of solid polytetrafluoroethylene. An additional sample tube was attached to the space above the null-manometer to allow the simultaneous measurement of the vapour pressure of the solvent. All pressures were reduced to mm of mercury at 0°C and standard gravity.

The vapour pressures of *n*-pentane at 25°, 35°, 45° and 55°C were respectively 512.3, 732.2, 1 021.4 and 1 389.8 mm of mercury. These differ from those recommended by the American Petroleum Institute⁸ by -0.2, -0.3, +0.7 and +0.8 mm of mercury respectively. The maximum difference is 0.07 per cent. The difference of chemical potential ($\mu_1 - \mu_1^0$) between the pentane in solution and the pure pentane was calculated from the ratio (p_1/p_1^0) after correction to the perfect-gas state with the second virial coefficients measured by Beattie, Levine and Douslin¹². The volume fractions at 25°C were calculated from the densities quoted above without any correction for the volume change on mixing. The volume fractions at higher temperatures were calculated from densities of the polymers derived from the measurements of the coefficients of thermal expansion of Fox and Flory⁶. The parameter χ of the Flory-Huggins equation was obtained from the chemical potentials and volume fractions

$$(\mu_1 - \mu_1^0)/RT = \ln \phi_1 + \phi_2(1 - r^{-1}) + \chi\phi_2^2 \quad (1)$$

where r is taken to be the ratio of the molar volumes of solute and solvent. The results for polymer II are given in *Table 1*; those from the isothermal distillations for polymer VA, and of the direct measurements for polymer VB are collected in *Table 2*.

The isothermal distillation data are shown in *Figure 3*, from which it is concluded that χ varies linearly with ϕ_2 , up to $\phi_2 = 0.4$. The equations to the straight lines drawn are:

$$\begin{aligned} 25^\circ\text{C}, \chi &= 0.485 + 0.220 \phi_2 \\ 40^\circ\text{C}, \chi &= 0.488 + 0.212 \phi_2 \end{aligned}$$

It appears from *Figure 3* that the vapour pressure data at 25°C do not fit this pattern, the three highest of the four observed points indicating rather

Table 1. The partial pressure of solvent (p_1), the chemical potential $\mu_1 - \mu_1^\circ (= \Delta\mu_1)$, and the Flory-Huggins parameter χ , as functions of the weight and volume fractions of polymer, w_2 and ϕ_2

| <i>Polymer II:</i> | | | |
|--------------------|----------|----------------|-------------------|
| w_2 | ϕ_2 | p_1 mm Hg | $-\Delta\mu_1/RT$ |
| <i>25°C</i> | | | |
| 0.413 | 0.333 | 500.4 | 0.023 |
| 0.500 | 0.415 | 488.1 | 0.047 |
| 0.596 | 0.512 | 460.9 | 0.103 |
| 0.680 | 0.601 | 429.4 | 0.173 |
| 0.785 | 0.722 | 387.2 | 0.274 |
| 0.902 | 0.868 | 223.3 | 0.817 |
| <i>35°C</i> | | | |
| 0.415 | 0.333 | 710.0 | 0.030 |
| 0.501 | 0.414 | 694.0 | 0.052 |
| 0.598 | 0.511 | 655.0 | 0.108 |
| 0.682 | 0.601 | 609.2 | 0.179 |
| 0.786 | 0.720 | 541.1 | 0.295 |
| 0.903 | 0.867 | 313.7 | 0.830 |
| <i>45°C</i> | | | |
| 0.418 | 0.334 | 983.4 | 0.036 |
| 0.600 | 0.511 | 907.7 | 0.114 |
| 0.685 | 0.602 | 844.9 | 0.183 |
| 0.787 | 0.720 | 741.6 | 0.309 |
| 0.905 | 0.869 | 428.8 | 0.845 |
| <i>55°C</i> | | | |
| 0.422 | 0.336 | 1333.0 | 0.040 |
| 0.603 | 0.512 | 1230.5 | 0.116 |
| 0.688 | 0.604 | 1141.8 | 0.189 |
| 0.788 | 0.720 | 944.8 | 0.320 |
| 0.907 | 0.871 | 571.4 | 0.860 |

that $\chi=0.63$, independent of ϕ_2 . This is in agreement with the observations of Prager, Bagley and Long¹³, who obtained $\chi=0.62 \pm 0.04$ for the range $\phi_2 > 0.5$. This high value of χ cannot persist below $\phi_2=0.3$, for *Figure 3* also shows the limiting values of χ for which $\Delta\mu_1=0$ (for $r \rightarrow \infty$). The most likely explanation of the apparent discrepancy between the two lines of evidence appears to be that the vapour pressure measurements were much less precise than had been hoped. It must be borne in mind that the calculation of χ imposes a severe test on the reliability of free energy data. We consider it to be well established that χ increases with ϕ_2 up to at least $\phi_2=0.5$. The behaviour at higher concentrations merits further investigation, but the balance of present evidence suggests that χ tends to level off to a value of *ca.* 0.65.

The results for polymer II are even less satisfactory, and we have judged it best to use a less exacting method of evaluation. In *Figure 4*, $\chi\phi_2^2$ is

A STUDY OF THE THERMODYNAMIC PROPERTIES OF POLYISOBUTENE

Table 2. Polymer V

| w_2 | ϕ_2 | p_1 mm Hg | $-\Delta\mu_1/RT$ | χ |
|-------------|----------|----------------|-------------------|--------|
| <i>25°C</i> | | | | |
| 0.112 | 0.0789 | — | 0.00016 | 0.498 |
| 0.174 | 0.125 | — | 0.00055 | 0.513 |
| 0.241 | 0.178 | — | 0.00135 | 0.528 |
| 0.285 | 0.213 | — | 0.00241 | 0.532 |
| 0.383 | 0.297 | — | 0.00596 | 0.550 |
| 0.414 | 0.324 | — | 0.00987 | 0.549 |
| 0.438 | 0.346 | — | 0.0110 | 0.565 |
| 0.457 | 0.364 | — | 0.0135 | 0.566 |
| 0.476 | 0.380 | 504.5 | 0.0150 | 0.575 |
| 0.594 | 0.496 | 496.2 | 0.0310 | 0.637 |
| 0.700 | 0.612 | 462.2 | 0.1004 | 0.627 |
| 0.811 | 0.744 | 388.7 | 0.270 | 0.630 |
| <i>35°C</i> | | | | |
| 0.477 | 0.379 | 721.2 | 0.0147 | 0.577 |
| 0.594 | 0.495 | 707.2 | 0.0336 | 0.631 |
| 0.701 | 0.611 | 660.9 | 0.0994 | 0.627 |
| 0.812 | 0.743 | 554.3 | 0.271 | 0.630 |
| <i>40°C</i> | | | | |
| 0.123 | 0.0860 | — | 0.00016 | 0.507 |
| 0.188 | 0.134 | — | 0.00057 | 0.516 |
| 0.266 | 0.196 | — | 0.00153 | 0.533 |
| 0.308 | 0.230 | — | 0.00274 | 0.537 |
| 0.373 | 0.285 | — | 0.00541 | 0.550 |
| 0.402 | 0.311 | — | 0.00757 | 0.552 |
| 0.435 | 0.341 | — | 0.0111 | 0.554 |
| 0.471 | 0.374 | — | 0.0136 | 0.571 |
| 0.489 | 0.391 | — | 0.0167 | 0.570 |
| <i>45°C</i> | | | | |
| 0.477 | 0.379 | 1002.8 | 0.0174 | 0.558 |
| 0.596 | 0.495 | 986.0 | 0.0339 | 0.630 |
| 0.703 | 0.610 | 920.1 | 0.1007 | 0.621 |
| 0.815 | 0.745 | 769.6 | 0.273 | 0.628 |
| <i>55°C</i> | | | | |
| 0.482 | 0.381 | 1368.8 | 0.0151 | 0.576 |
| 0.597 | 0.495 | 1342.8 | 0.0329 | 0.634 |
| 0.706 | 0.613 | 1250.3 | 0.1007 | 0.627 |
| 0.818 | 0.748 | 1041.3 | 0.277 | 0.633 |

plotted against ϕ_2^2 , and the best straight line drawn to give mean values of χ over the range of measurement. The lines drawn give:

| | | | | | | |
|-------------------|-----|-----|------|------|------|------|
| $t^\circ\text{C}$ | ... | ... | 25 | 35 | 45 | 55 |
| χ | ... | ... | 0.59 | 0.56 | 0.55 | 0.51 |

Having regard to the low molecular weight of this polymer, these values of χ could persist down to $\phi_2=0$, without producing phase separation. They are therefore taken as the best available representation of our data for this polymer.

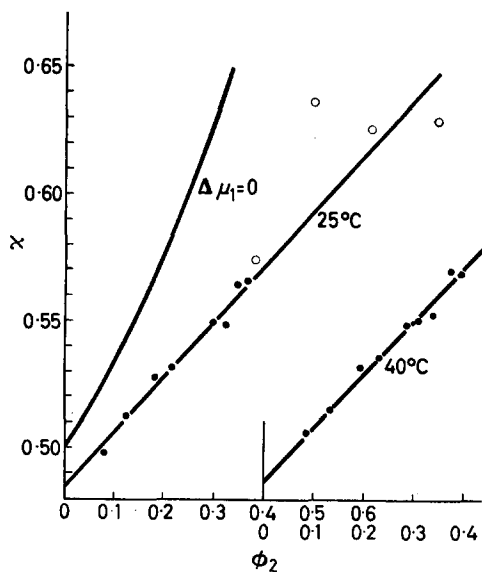


Figure 3— χ versus ϕ_2 for polymer V (● Isothermal distillation, ○ Vapour pressure). Curve $\Delta\mu_1=0$ calculated from Flory-Huggins equation

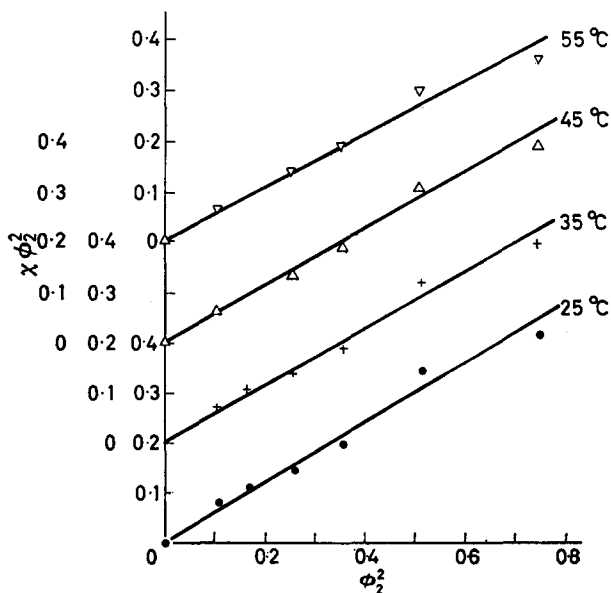


Figure 4— $\chi\phi_2^2$ versus ϕ_2^2 from vapour pressure data on Polymer II

(3) *Heats and entropies of dilution*

Three different methods have been used to derive heats of dilution from the relationship

$$\Delta h_1 = -RT^2[\partial(\Delta\mu_1/RT)/\partial T]_{w_2}$$

(1) The isothermal distillation data on polymer V were plotted in the form $\Delta\mu_1/RT$ versus w_2 at 25°C and 40°C, and smoothed curves used to read off $\Delta\mu_1/RT$ at $w_2=0.15$ to 0.45 for each temperature.

(2) The data for polymer II have been represented by plots of χ versus ϕ_2 at each of four temperatures. It is easily shown that

$$\frac{1}{\phi_2^2} \left(\frac{\partial(\Delta\mu_1/RT)}{\partial T} \right)_{w_2} = \left(\frac{\partial\chi}{\partial T} \right)_{\phi_2} + (\alpha_1 - \alpha_2) \left[1 - \frac{1}{r} - 2\chi\phi_1 - \phi_1\phi_2 \left(\frac{\partial\chi}{\partial\phi_2} \right)_T \right]$$

This equation has been used, with $(\partial\chi/\partial T)_{\phi_2} = -2.7 \times 10^{-3} \text{ deg}^{-1}$,

$$(\partial\chi/\partial\phi_2)_T = 0, \quad \alpha_1 - \alpha_2 = 8.0 \times 10^{-4} \text{ deg}^{-1}$$

(3) The vapour pressure data can be seen from *Tables 1* and *2* to fall into groups. Once the apparatus had been filled, measurements were made at a series of temperatures. Within this group w_2 changes only by reason of evaporation of more solvent as the temperature is raised. Correction of $\Delta\mu_1/RT'$ for the small increase δw_2 is readily calculated, since

$$[\partial(\Delta\mu_1/RT)/\partial w_2]_T = -\frac{\rho_2}{\rho_1} \left(\phi_2 + \phi_1 \frac{\rho_1}{\rho_2} \right)^2 (\phi_2/\phi_1 + 1/r - 2\chi\phi_2)$$

In this equation χ has been assumed independent of ϕ_2 as suggested by the vapour pressure data. This comparison of the measurements in groups greatly reduces the experimental scatter which has been mentioned above,

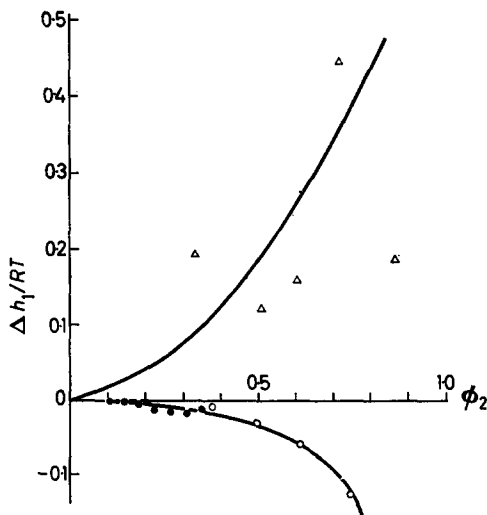


Figure 5—Calculated heats of dilution: Δ II at 40°C (method 2), \bullet V at 32.5°C (method 1), \circ V at 40°C (method 3)

and shows that the latter must arise from irreproducibility in our procedure for setting up the system. Most probably, with polymer II (where the scatter is most marked), the different systems contained slightly variable proportions of low polymer.

As shown in *Figure 5*, the methods 1 and 3 give results in satisfactory agreement, bearing in mind the difficulties inherent in the determination of heats by differentiation of free energies. There can be no doubt that Δh_1 is positive in solutions of polymer II and negative in solutions of polymer V.

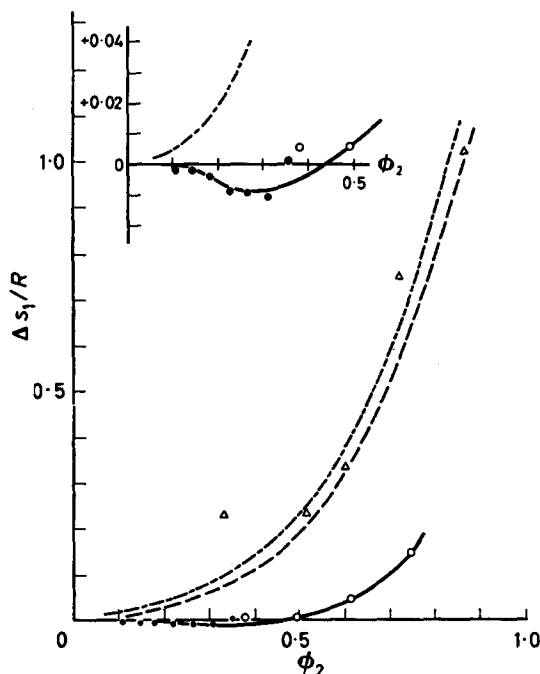


Figure 6—Derived entropies of dilution: Δ Polymer II, \bullet \circ V. Dashed curve—Theoretical (Pol. II). Chain-dotted curve—Theoretical (V)

The entropies of dilution are no more accurate than the heats. However, *Figure 6* shows that the entropy of dilution in polymer II conforms to the Flory-Huggins expression

$$\Delta s_1/R = -\ln \phi_1 - (1-r^{-1})\phi_2 \quad (2)$$

within the experimental error. This equation is consistent with equation (1) if the term in χ is purely a heat of dilution; that is, if χ is inversely proportional to the temperature.

The entropy of dilution of the solution of polymer V is small, and is definitely negative at low concentrations.

(4) Phase equilibria

Polymers II, III, IV and VB could be precipitated from *n*-pentane by

heating the solutions above 70°C. The lower phase was either a viscous liquid or a gel according to the concentration and molecular weight of the polymer.

Weighed amounts of polymer and solvent were mixed *in vacuo* in glass tubes which were then sealed. The concentrated mixtures were stirred gently at 60°C until solution was complete. The tubes were heated in a stirred bath

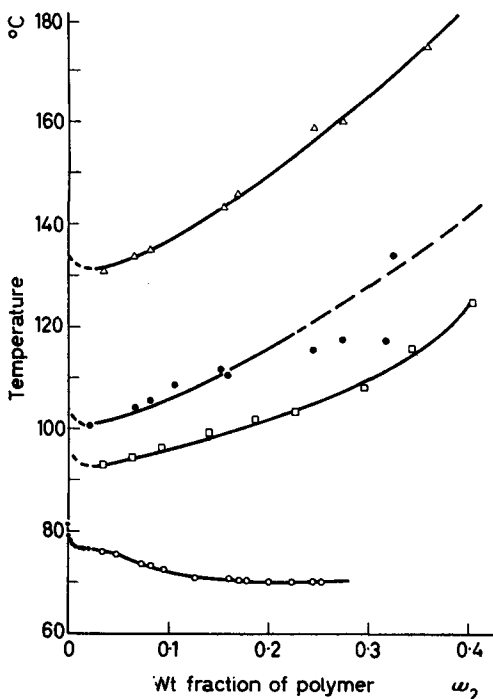


Figure 7—Phase boundary curves: Δ II, \bullet III, \square IV, \circ VB

of 1 l. of a silicone oil whose temperature was controlled by a vapour jacket and manostat. The temperature of phase separation was found by heating the bath very slowly, usually at 0.2°C per hour, until a strong opalescence or a second phase could be seen. The results for all four polymers are shown in Figure 7. Those for polymer VB, which extend over a wide range of compositions, are also shown in Table 3. Unfortunately weight fractions above 0.25 could not be studied for this system because of the high viscosity of the solutions. The accuracy of the results at this upper limit is only $\pm 0.3^\circ\text{C}$. The point of inflection at a weight fraction of 0.07 appears to be well-established since the reproducibility of the results in this region was $\pm 0.1^\circ\text{C}$. It may, of course, be a peculiarity of this sample of polymer.

The ratios of the volumes of the two phases at temperatures just above the point of separation were estimated by measuring the lengths of tube occupied by each. These are shown in Figure 8.

Some very dilute solutions of polymer VB were prepared in order to find the critical end-point¹ of this system. This is the temperature and composition at which the liquid phase that is poorer in polymer becomes identical with the vapour phase. Sealed tubes which contained from 0.9×10^{-5} to 20×10^{-5} weight fraction of polymer were prepared by successive dilution

Table 3. Temperatures of phase separation for solutions of polymer VB in *n*-pentane

| w_2 | T (°C) | w_2 | T (°C) | w_2 | T (°C) |
|----------|-------------|--------|-------------|-------|-------------|
| 0.000953 | 82.70 | 0.0202 | 76.50 | 0.162 | 70.7 |
| 0.00178 | 79.60 | 0.0282 | 76.18 | 0.171 | 70.6 |
| 0.00209 | 78.60 | 0.0341 | 76.00 | 0.179 | 70.4 |
| 0.00273 | 78.00 | 0.0495 | 75.40 | 0.201 | 70.2 |
| 0.00530 | 77.35 | 0.0754 | 73.90 | 0.225 | 70.3 |
| 0.00783 | 76.88 | 0.0830 | 73.20 | 0.246 | 70.1 |
| 0.0125 | 76.80 | 0.0982 | 72.5 | 0.254 | 70.1 |
| 0.0195 | 76.35 | 0.128 | 71.1 | | |

of a stock solution made up by weight. Great care was taken to exclude both air and grease. All tubes had the same critical temperature of 197.05°C, within the reproducibility of the results, $\pm 0.05^\circ\text{C}$. This temperature is 0.42°C above that of the pure solvent. The difference shows that some of the polymer is soluble in pentane at its critical point. However, the observed

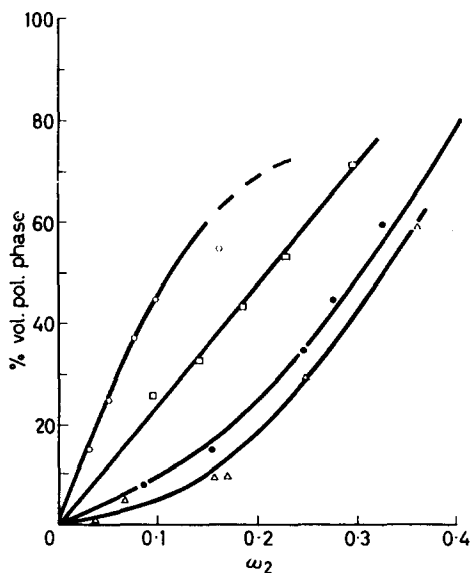


Figure 8—Relative phase volumes: \triangle II, \bullet III, \square IV, \circ VB

critical temperatures were independent of w_2 and so excess polymer must be present in each tube. The solubility, therefore, must be less than a weight fraction of 10^{-5} .

Polymer VA, which contains some material of comparatively low molecular weight, had a critical end-point of 197.33°C, or 0.70°C above the critical temperature of pure solvent. Clearly the material of lower molecular weight must be more soluble. The critical end-point of polymer II was at 205.33°C.

DISCUSSION

A comparison of results obtained with polymer II with those obtained with V shows that the properties of polyisobutene change profoundly as the chain length of the polymer increases. A solution of a polymer of low molecular weight is a long way below its critical solution point at room temperature. It dissolves with a small positive heat of mixing and with a change of entropy that is represented adequately by the Flory-Huggins equation. This result accords with that of der Minassian and Magat¹⁴ who found that polyisobutene (of unspecified molecular weight) conformed to the Flory-Huggins equation in solutions of cyclohexane. It accords also with the results of Bawn and Patel⁴ who found that polyisobutene ($\bar{M}=45\,000$) in cyclohexane was in reasonable agreement with the Flory-Huggins equation from 25° to 60°C, although χ increased with ϕ_2 for volume fractions above 0.7. At room temperature these solutions in cyclohexane are also a long way below their critical temperatures¹.

The solutions of polymer V are, however, quite incompatible with the Flory-Huggins equation. The parameter χ depends strongly on concentration, as is shown in *Figure 3*. The entropy of dilution at 40°C is very small and is, in fact, negative at low concentrations. The heat of dilution at 40°C is also small and is negative at all concentrations. Negative heats and entropies are thermodynamic necessities in a binary solution that is close to a LCST.

The general pattern of the thermodynamics of solutions of hydrocarbon polymers becomes clear after a comparison of these results and the measurements of LCST previously reported¹. An amorphous polymer of low molecular weight, say 10^3 to 10^4 , dissolves in all paraffins at room temperature with a small positive heat of solution and an entropy of solution that is given approximately by the Flory-Huggins equation. It can be precipitated from these solutions at a LCST that is within 10° to 50°C of the critical temperature of the pure solvent. At these high temperatures it is necessary that the heat and entropy have become negative (insofar as these can be defined satisfactorily at high vapour pressures). As the chain length of the polymer increases, this region of negative heats and entropies, and the associated LCST moves to lower temperatures relative to the critical point of the pure solvent. Thus polypropylene of $\bar{M}=2 \times 10^4$ can be precipitated from *n*-pentane at 152°C (i.e. 44° below the critical temperature of the solvent) but polypropylene of $\bar{M}=2 \times 10^6$ can be precipitated at 105°C (that is, 91° below the critical temperature). The results above show that polyisobutene behaves similarly, and imply that the regions of temperature where the heat and entropy are negative have also moved to lower temperatures at the higher molecular weights. For a polymer of given molecular weight

the temperature range of negative heat and entropy is determined primarily by the critical temperature of the pure solvent. If this is as low at 200°C as for *n*-pentane, then the region will extend to room temperature for polymers of $\bar{M}=10^5$ and above. This applies with polymer V, and also with natural rubber in *n*-pentane¹⁵.

This general pattern of behaviour can be re-expressed in terms of an equation of the Flory-Huggins type, where the parameter χ is in general dependent on both temperature and composition, to be determined experimentally. In the region where polymer and liquid are infinitely miscible Δh_1 is generally positive, and χ therefore decreases with rise of temperature. If Δh_1 is temperature dependent, $\chi T = \text{constant}$. This is approximately true for our measurements on polymer II.

| | | | | | | |
|-----------------------|-----|-----|-----|-----|-----|-----|
| $T(^{\circ}\text{K})$ | ... | ... | 298 | 308 | 318 | 328 |
| χT | ... | ... | 176 | 172 | 175 | 167 |

If the temperature is lowered sufficiently, χ becomes large enough for phase separation to be observed.

The separation observed on heating means that at sufficiently high temperatures χ has again become large. It is evident then that (with rise of T) χ passes through a minimum beyond which $\partial\chi/\partial T$ becomes positive, and Δh_1 negative. An approximate estimate of χ at the LCST can be obtained by solving the equations $(\partial\mu_1/\partial\phi_1)_T = (\partial^2\mu_1/\partial\phi_1^2)_T = 0$. This gives $\chi \approx 0.85$ for polymer II, $\chi \approx 0.53$ for polymer V; these values apply at the respective LCSTs, 130°C and 71°C. It may be noted that UCSTs should occur at the same χ as the LCSTs. If χT remains constant for polymer II the expected

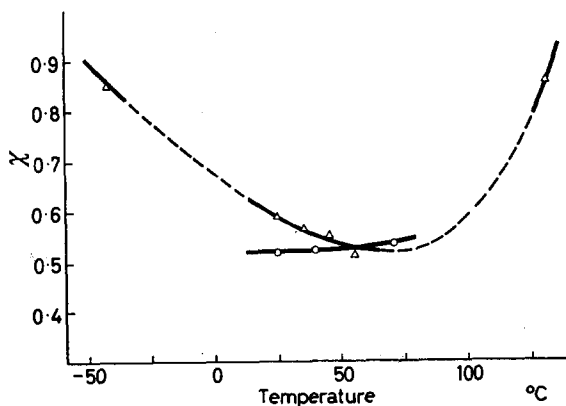


Figure 9—Temperature dependence of χ : Δ II, \circ V

UCST is at *ca.* 200°K; no prediction can be made for polymer V. Experimentally, UCST for II is found at *ca.* 230°K: its determination for V has not been found possible owing to the high viscosity of the solutions. Figure 9 summarizes our rather fragmentary data on the temperature dependence of χ .

This analysis in terms of χ only reformulates the problem of the physical origin of the phenomena observed. This kind of variation of χ with T could, however, be foreseen in relation to the dependence of χ on the solubility parameters ∂_1 and ∂_2 of liquid and polymer. There is a good deal of evidence that, over a range of liquids, χ increases with $(\partial_1 - \partial_2)^2$. A similar dependence might therefore be expected for a single liquid over a range of T . Now as the critical temperature of the liquid is approached ∂_1 falls rapidly and χ would therefore be expected to increase rapidly. This is essentially a more sophisticated way of saying that at high temperatures the liquid becomes more gas-like and therefore a poorer solvent.

This view of the origin of the LCST also suggests that as this temperature is approached negative mixing volumes might be expected, as the liquid is transferred from a highly expanded liquid structure to one much more condensed.

The volume of mixing is indeed negative for solutions of both polymer I and polymer V at 25°C. Negative volumes of mixing near the critical temperature are the rule for all systems² which are known to have LCSTs, and the solution of polymer V is no exception. Nevertheless it does not appear that the occurrence of such a contraction is necessarily related to the occurrence of a LCST. It is a much more common phenomenon in non-polar systems; for example, contractions are often found in mixtures of aliphatic hydrocarbons of widely different chain lengths. There is a contraction on dissolving so low a 'polymer' as *n*-hexadecane ($M=226$) in *n*-pentane, *n*-hexane, *n*-heptane or *n*-octane¹⁶, as well as on dissolving polymers I and V in *n*-pentane.

We conclude, therefore, that contraction occurs whenever two aliphatic hydrocarbons of widely different chain lengths are mixed. This is attributed to a reduction in the mean molecular volume that occurs when a molecule of the lighter component is transferred from a liquid of very low internal energy to a mixture of much higher average internal energy. This transfer is a process that is similar to, but much less drastic than, the transfer of a molecule from a pure vapour to a pure liquid. Both are accompanied by a very large reduction of the mean molecular volume and by decreases in the mean molecular heat and entropy. The results above show, however, that the difference between the components must be greater for there to be negative heat and entropy of dilution than for there to be a negative volume of mixing.

A final point which calls for a comment is the shape of the phase-boundary curves and their relation to the relative volumes of the two phases just above the phase boundary. At UCSTs it is found that the critical concentration of polymer decreases as the molecular weight increases. This is in accord with the Flory-Huggins equation. However, the minima of the curves in *Figure 6* are all very close to the boundary except for that of polymer V which appears to be at about a weight fraction of 0.25. On the other hand, the composition at which the system divides into two phases of equal volume does behave regularly, and moves monotonically to lower concentrations of polymer as the molecular weight increases (*Figure 8*). The lack of concordance of the results in *Figures 7* and *8* shows that the

polymer-solvent system cannot be treated as a binary system and that some fractionation of the polymer is occurring between the two phases. This point is to be studied further.

*Department of Chemistry,
University of Manchester*

(Received February 1962)

REFERENCES

- ¹ FREEMAN, P. I. and ROWLINSON, J. S. *Polymer, Lond.* 1960, **1**, 20
- ² ROWLINSON, J. S. *Liquids and Liquid Mixtures*, Chap. 5. Butterworths: London, 1959
- ³ FOX, T. G and FLORY, P. J. *J. Amer. chem. Soc.* 1948, **70**, 2384
- ⁴ BAWN, C. E. H. and PATEL, R. D. *Trans. Faraday Soc.* 1956, **52**, 1664
- ⁵ ALLEN, G., GEE, G. and NICHOLSON, J. P. *Polymer, Lond.* 1960, **1**, 56
- ⁶ FOX, T. G and FLORY, P. J. *J. phys. Chem.* 1951, **55**, 221
- ⁷ FOX, T. G and FLORY, P. J. *J. phys. Chem.* 1949, **53**, 197
- ⁸ American Petroleum Institute, *Research Project 44*. Carnegie Press: Pittsburgh, 1953
- ⁹ GEE, G. and ORR, W. J. C. *Trans. Faraday Soc.* 1946, **42**, 507
- ¹⁰ BAXENDALE, J. H., ENUSTUN, B. V. and STERN, J. *Phil. Trans.* 1951, **243**, 169
- ¹¹ ROWLINSON, J. S. and THACKER, T. *Trans. Faraday Soc.* 1957, **53**, 1
- ¹² BEATTIE, J. A., LEVINE, S. W. and DOUSLIN, D. R. *J. Amer. chem. Soc.* 1952, **74**, 4778
- ¹³ PRAGER, S., BAGLEY, E. and LONG, F. A. *J. Amer. chem. Soc.* 1953, **75**, 2742
- ¹⁴ DER MINASSIAN, L. and MAGAT, M. *J. Chim. phys.* 1951, **48**, 574
- ¹⁵ GEE, G. *Trans. Faraday Soc. B*, 1946, **42**, 33
- ¹⁶ DESMYTER, A. and VAN DER WAALS, J. H. *Rec. Trav. chim. Pays-Bas*, 1958, **77**, 53

Polymerization of Epoxides Part IV (1)

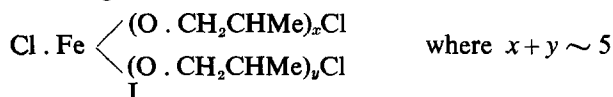
Polymerization of Propylene Oxide and Ethylene Oxide with Ferric Chloride Catalyst

G. GEE, W. C. E. HIGGINSON and J. B. JACKSON

Ferric chloride reacts rapidly with propylene oxide at room temperature giving a product analysing approximately $\text{FeCl}_3(\text{C}_3\text{H}_6\text{O})_4$. This product has been employed as catalyst in the polymerization of propylene oxide and ethylene oxide at higher temperatures. Kinetic studies have shown that ethylene oxide polymerizes at a rate proportional to catalyst and epoxide concentrations. A period of acceleration observed in the initial stages of propylene oxide polymerization is attributed to a unimolecular change in the catalyst.

Addition of water accelerates both polymerizations and greatly increases the yield of crystalline polymer obtained from propylene oxide. This behaviour is attributed to partial hydrolysis of the catalyst followed by condensation to structures containing Fe—O—Fe bridges.

PRICE² observed that propylene oxide can be polymerized with ferric chloride to give a partially crystalline product, and the reaction has two clearly defined stages. The first stage occurs at or below room temperature and the product of the reaction appears^{2, 3} to have the structure I. Virtually no further reaction takes place until mixtures of this product and the monomer are heated in the range 70° to 100°C.



The present kinetic investigation employed the initial reaction product as catalyst in excess propylene oxide (the solution being stored at 0°C) to polymerize both ethylene oxide and propylene oxide. Kinetic measurements were made dilatometrically, the method having previously been shown valid⁴. Most of the data reported here relate to measurements at 91.6°C.

EXPERIMENTAL

Materials

Ethylene oxide was first treated with sodium in polyglycol 400, then distilled *in vacuo* on to calcium hydride for final drying and storage (b. pt 10.5°C/760). Propylene oxide was dried over calcium hydride, decanted and then fractionated from fresh calcium hydride. A vacuum-jacketed column (25 cm × 2 cm) packed with Dixon rings was used in conjunction with a total condensation variable take-off head and a reflux ratio of 30:1 (b. pt 33.0°C/760). Methylene chloride was dried and fractionated in the same way (b. pt 39.5°C/755). All these liquids were stored over calcium hydride, in absence of air.

Ferric chloride was made by burning pure, dry iron wire in dry chlorine and distilling the product from a side arm into the main vessel. The side arm was sealed off and any non-volatile impurities removed. The catalyst solution was made by distilling a measured volume of propylene oxide on to the anhydrous ferric chloride. The two were allowed to react, control being

achieved by occasional chilling of the reaction flask, and on completion the pressure was adjusted to atmospheric by addition of dry gaseous nitrogen. The stock solution was stored at 0°C.

Procedure

A vacuum line technique was used for filling dilatometers, which consisted of 25 cm lengths of tubing, accurately 8 mm bore, sealed at the bottom, constricted at the top and joined to a B14 cone. Dilatometers used later for polymerizations in solvent consisted of a 20 ml bulb sealed to a 20 cm length of 4 mm bore Veridia tubing, constricted and joined to a B14 cone. All dilatometers were pumped on the vacuum line for 24 hours before use. Transfer of catalyst solution was from a second side arm via a self-sealing vaccine cap and small tap with an Agla micrometer syringe (claimed accuracy ± 0.5 per cent). The syringe was dried in an oven at 150°C for several hours before use. A 7 in. stainless steel needle was used to pass through a second vaccine cap and small vacuum tap on the vacuum line and past the constriction on the dilatometer. The dilatometer was flushed with dry nitrogen to equalize pressures before inserting the needle. After transferring the requisite volume of catalyst solution, a measured volume of monomer was distilled under vacuum into the dilatometer chilled with liquid nitrogen, and the dilatometer sealed at the constriction. Shaking of the mixture after warming to room temperature ensured homogeneity of the solution before placing in the high temperature bath.

The effect of water added to the catalyst during the filling of the dilatometer was investigated. Various runs were made with a small added quantity of water, which was measured in the vapour phase and then condensed into the dilatometer. A few preliminary polymerizations in solvent (methylene chloride) were carried out, the procedure being similar to that for bulk runs. Methylene chloride was condensed, however, under acetone-carbon dioxide mixtures before sealing, due to a tendency to crack the dilatometer on warming if liquid nitrogen was used.

Purification of polymers

Propylene oxide polymerization products were dissolved in boiling methanol and the ensuing solution acidified with one drop of concentrated nitric acid. The colour of the solution changed slowly from brown to a yellow-green characteristic of free iron (III) in methanol. This ion was removed by passing the solution through an ion-exchange column Amberlite IR-120 and the solution was passed through a second column containing Amberlite IRA-400 to remove acid. Both columns were flushed with methanol before use. Methanol was removed by evaporation in a vacuum oven (30°C and $\frac{1}{2}$ mm) before re-dissolving the polymer in acetone in order to fractionate the product.

The polymer was split into two fractions by chilling the acetone solution to -30°C for at least two days. The precipitate (described below as the crystalline fraction) was rapidly filtered from the cold solution, and dissolved in benzene. The bulk of this solvent was removed by freeze-drying at -75°, followed by final drying at 40° and $\frac{1}{2}$ mm for several hours. Polymeric material present in the filtrate was recovered by drying at 40° and $\frac{1}{2}$ mm.

The products of ethylene oxide polymerization experiments were dissolved in boiling methanol and a drop of concentrated nitric acid was added. The bulk of the polymeric material crystallized on holding this solution at 0° for several days. This material was dissolved in benzene and freeze-dried as described for the propylene oxide polymer. The methanolic filtrate obtained at 0°C contained only a small amount of material of low molecular weight and iron (III).

Characterization of polymers

Molecular weights were determined viscometrically in Fitzsimons viscometers in benzene solution at 25°C. The values of K and α used in the Houwink equation were those determined by Price and Osgan² for polypropylene oxide and by Price and Miller⁵ for polyethylene oxide.

RESULTS

Kinetic data

Typical dilatometric plots for the bulk polymerization of ethylene oxide and propylene oxide at 91.6°C are shown in *Figure 1* and the corresponding logarithmic plots in *Figure 2*. Polymerization of ethylene oxide under

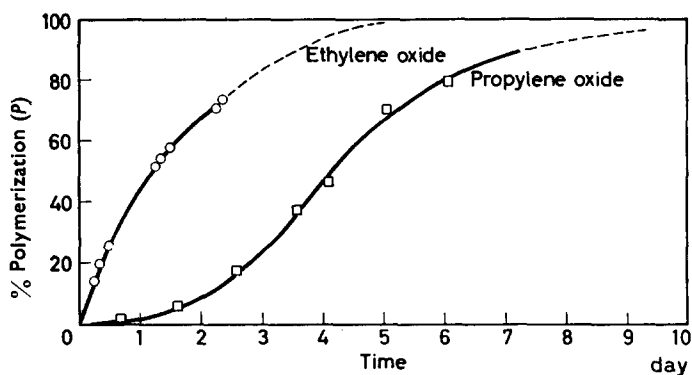


Figure 1—Bulk polymerization at 91.6°C

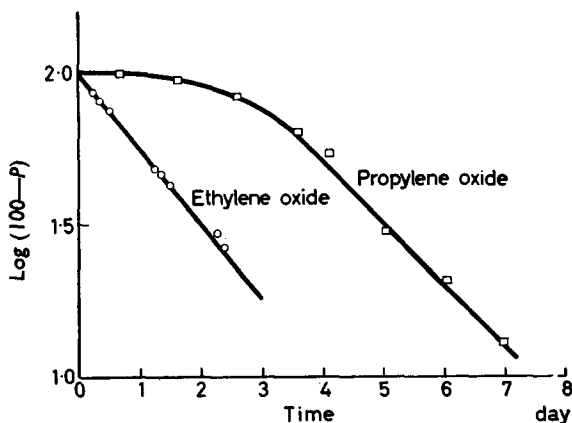
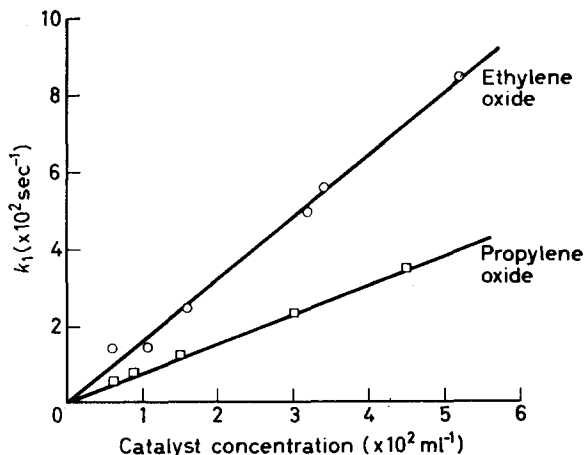


Figure 2—Determination of k_1

Figure 3—Effect of catalyst concentration on k_1

these conditions is seen to follow a first order law, whereas with propylene oxide the polymerization obeys a first order rate law in the later stages of the reaction only. This behaviour was observed in all experiments with propylene oxide using the stock catalyst solution in the absence of added water; about three days elapsed before the onset of first order kinetics, irrespective of the concentration of catalyst. The significance of this period of acceleration is discussed below; for our present purpose the first order constant calculated from the later stages of the reaction is used as a measure of rate. This procedure is supported by the results of a few measurements in methylene chloride solution. Ethylene oxide again showed first order plots, with constants (for a fixed catalyst concentration) independent of monomer

Table 1. Velocity constants for polymerization in bulk and in methylene chloride (at 91.6°C)

| $[M]_0$ moles l^{-1} | Ethylene oxide | | $[M]_0$ | Propylene oxide | |
|---------------------------|-------------------------------|---|---------|-----------------|------------------|
| | $10^3[C]_0$ moles l^{-1} | 10^4k_2 $l \text{ mole}^{-1} \text{ sec}^{-1}$ | | $10^3[C]_0$ | 10^4k_2 |
| 17.3* | 6.3 to 52† | 2.9 | 13* | 6.3 to 45† | 1.8 ₁ |
| 6.0 | 1.75 | 2.6 | 4.07 | 1.61 | 1.3 ₃ |
| 3.61 | 1.70 | 2.5 ₅ | 3.61 | 1.68 | 1.4 ₂ |
| 2.68 | 1.66 | 2.8 ₅ | 2.26 | 1.65 | 1.4 ₅ |
| 1.64 | 1.64 | 2.9 | 1.45 | 1.57 | 1.4 ₂ |

*Undiluted; †Figure 3. $[M]_0$ is initial monomer concentration; $[C]_0$ is catalyst concentration.

concentration. A similar conclusion is reached with propylene oxide (ignoring again the period of acceleration). In Figure 3, values of $k_1 = -d \ln [\text{monomer}]/dt$ are plotted against catalyst concentration, and it is evident that, for both monomers, the reaction is first order in catalyst. Table 1 records second order constants $k_2 = -[\text{catalyst}]^{-1} d \ln [\text{monomer}]/dt$ from Figure 3 and from experiments in methylene chloride solution. All of these have been corrected⁴ for the volume change accompanying polymerization.

A few bulk polymerizations were carried out at considerably lower temperatures. Ethylene oxide again showed simple first order behaviour

with respect to both monomer and catalyst, giving a mean second order constant at 25°C of 2.1×10^{-5} l. mole⁻¹ sec⁻¹. Propylene oxide at 30°C also polymerized according to the simple rate equation, i.e. no period of acceleration was observed. Polymerization was extremely slow, the rate constant being 0.56×10^{-5} l. mole⁻¹ sec⁻¹.

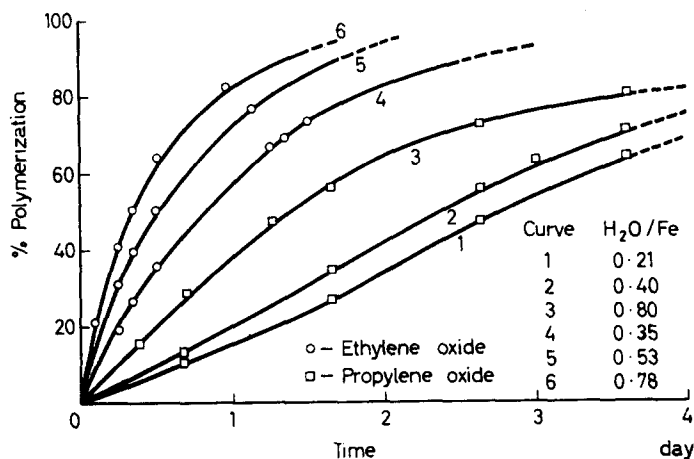


Figure 4—Bulk polymerization in presence of water

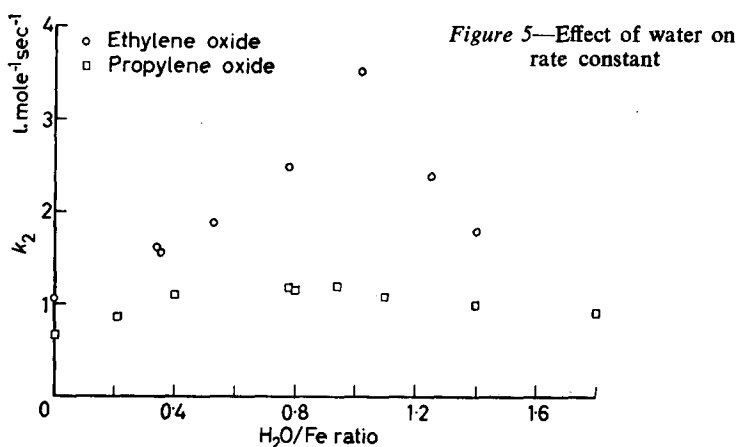
Effect of water

The effect of adding water to the reaction mixture was studied for both monomers, and typical curves are shown in *Figure 4*. The polymerization of ethylene oxide remained first order in monomer concentration and up to values of the ratio $[H_2O]/[catalyst]$ of approximately unity the value of k_2 increased with increase in this ratio. When the reaction solutions were made up at room temperature precipitation of part of the catalyst occurred for values of $[H_2O]/[catalyst]$ in excess of unity, although the precipitate apparently re-dissolved on warming to 91.6°C for values not exceeding 1.4. This observation suggests that the fall in the value of k_2 as the ratio $[H_2O]/[catalyst]$ is increased above unity is due to precipitation of catalyst in an inactive form.

In the propylene oxide system an increase in k_2 was observed with $[H_2O]/[catalyst]$ followed by a decrease as this ratio exceeded 0.9. Again precipitation occurred at room temperature for values of the ratio $[H_2O]/[catalyst]$ exceeding the value corresponding to the maximum in k_2 . A further effect of adding water to this system was that the deviation of the logarithmic plots from linearity was reduced and for values of the ratio $[H_2O]/[catalyst]$ of 0.8 or greater these plots were linear throughout the reaction. The effect of water on the second order rate constant is shown in *Figure 5*.

Supplementary observations

Two additional experiments were carried out to try to throw further light on the reaction. In the first, a small volume of the stock catalyst solution (which contained excess propylene oxide) was heated at 90°C for two days, cooled, and further propylene oxide distilled in. Polymerization was then



followed at 91.6°C in the usual way and gave substantially the normal rate constant, but monomer disappearance followed a first order law from the start. Thus the induction period had been eliminated, for the quantity of polymer formed during the pre-heating period was very much less than is normally formed during the period of acceleration.

In the second experiment, a propylene oxide polymerization was carried substantially to completion, cooled, and a second quantity of monomer distilled in. After the first reaction product had dissolved in the new monomer, the temperature was raised to 91.6°C, when the additional monomer was observed to polymerize at a normal rate.

Study of the polymer

The polymers have not been exhaustively examined. The only fractionation undertaken was the crude separation of the propylene oxide polymers into two fractions. The less soluble of these was always solid at room temperature; comparable samples have been shown by X-ray examination to be partially crystalline. The more soluble fraction varied from liquid to rubber according to its molecular weight, and was evidently substantially or completely amorphous. The ratio crystalline/amorphous did not change significantly during the course of a polymerization. All the ethylene oxide polymers were solid (crystalline) at room temperature.

There is a very striking effect of water on the relative proportions of the two fractions obtained in the polymerization of propylene oxide (*Figure 6*). It is believed that the limiting value of *ca.* 0.12 for the crystalline/amorphous ratio in absence of water is a true result, and not simply a measure of our failure to dry the system. Very similar ratios were found in experiments in dry methylene chloride solution.

The only molecular weight measurements were based on intrinsic viscosities and, in the absence of distribution curves, are of only semi-quantitative

POLYMERIZATION OF EPOXIDES PART IV (1)

Table 2. Typical molecular weight data*

| [C] ₀ | H ₂ O/Fe | 10 ⁻³ MW | Moles polymer/atom Fe | | |
|------------------------------|---------------------|---------------------------------|-----------------------|----------------|--------------|
| (a) Ethylene oxide polymers | | | | | |
| 0.63 | 0 | 28 | 4.9 | | |
| 1.6 | 0 | 11 | 4.9 | | |
| 3.2 | 0 | 6 | 4.9 | | |
| 5.4 | 0 | 3.7 | 4.6 | | |
| 1.7 | 0.34 | 100 | 0.53 | | |
| 1.7 | 0.78 | 65 | 0.77 | | |
| 1.7 | 1.02 | 47 | 1.10 | | |
| 1.7 | 1.25 | 58 | 0.88 | | |
| (b) Propylene oxide polymers | | | | | |
| [C] ₀ | H ₂ O/Fe | <i>Cryst.</i> <i>Amorph.</i> | <i>Cryst.</i> | <i>Amorph.</i> | <i>Total</i> |
| 0.63 | 0 | 0.12 | 0.6 | 6.4 | 7.0 |
| 1.5 | 0 | 0.10 | 0.3 | 5.3 | 5.6 |
| 4.5 | 0 | 0.12 | 0.2 | 3.1 | 3.3 |
| 1.5 | 0.21 | 0.28 | 0.9 | 5.0 | 5.9 |
| 1.5 | 0.78 | 0.45 | 0.3 | 1.3 | 1.6 |
| 1.5 | 0.94 | 0.50 | 0.2 | 1.0 | 1.2 |

*All polymerizations in bulk at 91.6°C carried to completion.

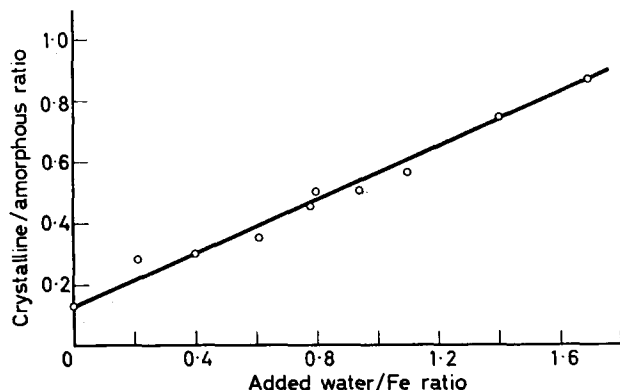


Figure 6—Effect of water on yield of crystalline polymer from propylene oxide

significance. For both polymers they ranged from a few thousand to 10⁵, and in Table 2 have been used to calculate the number of moles of polymer produced per atom of iron in the catalyst employed. Most of the data refer to polymerization carried to completion, and it will be seen that in the absence of water several polymer molecules are formed per atom of iron, average numbers being four for ethylene oxide and six for propylene oxide. The higher molecular weights found in 'wet' systems are reflected in a reduction in this ratio to approximately unity for either monomer. In the

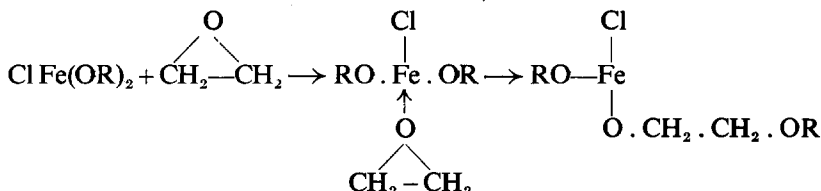
few cases where molecular weight was determined as a function of conversion the number of polymer molecules in the system was found to increase with conversion.

In the purification of polymer samples for investigation, our normal procedure involved acidification to remove combined iron. When this step was omitted the polymer was of higher intrinsic viscosity. Calculation showed that in runs without added water there was approximately one less polymer molecule per iron atom. It is therefore concluded that in the reaction mixture each iron atom is associated with two polymer chains.

Infra-red examination of polymers from both monomers revealed the presence of small concentrations of both —OH groups and unsaturation.

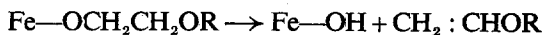
DISCUSSION

We begin by considering the polymerization of ethylene oxide, which is kinetically straightforward. Earlier discussions have supported a mechanism termed by Price and Miller⁵ 'coordinate complex polymerization', which can be written, for this system :



The product of this pair of reactions is kinetically equivalent to the original catalyst so that the total concentration of all growing centres will remain constant, and equal to that of the catalyst originally added. The significance of the observed second order constant will depend on the rate of the second step relative to dissociation of the complex into its original components. The observed rate constant will only measure directly the rate of the first reaction if this is the slow step. As previously pointed out, the actual process will be more complicated than is represented here, since a coordination number of 4 is doubtless retained throughout by all the iron atoms, by association and/or chelation. The rate constants reported above lead to Arrhenius parameters of $E=9.4$ kcal, $A=1.5 \times 10^2$ l. mole⁻¹ sec⁻¹. These very low values appear to be superficially consistent with the suggested mechanism.

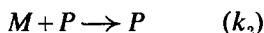
Two other predictions of this interpretation can be readily tested. In the absence of a termination reaction, growth should re-start if fresh monomer is admitted at the end of a reaction: this has been reported above. The second prediction is that two polymer chains should be formed per catalyst molecule and that both should remain attached to Fe. Experimentally we find the two attached chains, but also some others. There must therefore be some kind of transfer process and this is no doubt concerned with the production of the unsaturation already reported; e.g. Price has plausibly suggested



Turning now to propylene oxide, polymerization at 30°C appears to follow exactly the same pattern. The overall rate is about a quarter of that

of ethylene oxide at the same temperature. At 90°C more complicated behaviour is observed. Our tentative interpretation is that the initial rate refers to the process which at 30°C continued throughout the reaction. This initial rate is difficult to estimate, but is probably not more than one tenth of that of ethylene oxide at the same temperature. At 30°C the reactivities are of the same order but the ratio is about four. If this interpretation is correct, the Arrhenius parameters for the two monomers are comparable, E being somewhat lower for propylene oxide. We must then attribute the acceleration to some process which occurs in propylene oxide polymerization at 91.6°C but not at 30°C, and does not occur in ethylene oxide at either temperature. The nature of this process is by no means fully understood, but the following evidence leads us to attribute it to a change in the nature of the catalyst.

Two observations already reported suggest that this process is independent of both catalyst and monomer concentrations. (a) The time required to establish first order disappearance of monomer is essentially independent of catalyst concentration. (b) The acceleration period can be eliminated by pre-heating the catalyst (effectively a highly concentrated catalyst solution in monomer) for the same length of time. Further supporting evidence comes from a kinetic analysis of the complete polymerization curve. Denoting the initial catalyst by C and an actively growing centre by P , we assume a unimolecular rearrangement of C to P , followed by growth:



If $[C]_0$ is the initial catalyst concentration

$$-d[C]dt = d[P]/dt = k_1\{[C]_0 - [C]\}$$

whence

$$[P] = [C]_0(1 - e^{-k_1 t})$$

If, to a first approximation, we ignore polymerization induced by unchanged catalyst ($M + C \rightarrow C$), we have

$$-d[M]/dt = k_2[M][C]_0(1 - e^{-k_1 t})$$

It is easily shown that if this equation holds, the linear section of the log plot in *Figure 2* can be extrapolated to

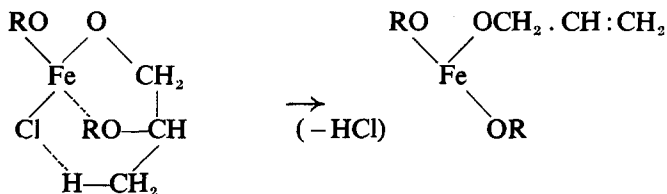
$$t_0 = 1/k_1 \text{ at } \ln[M]_0/[M] = 0$$

Using the value of k_1 obtained in this way, with k_2 from the linear slope, the full curve of *Figure 1* was calculated, and is seen to represent the observed behaviour very well, with $k_1 = 3.0_s \times 10^{-6} \text{ sec}^{-1}$. A further check was made by carrying out* an additional series of runs in methylene chloride at 101.1°C, in which initial monomer concentrations ranged from 0.73 to 4.3 moles l^{-1} . These gave an average value of $k_2 = 2.7 \times 10^{-4} \text{ l. mole}^{-1} \text{ sec}^{-1}$, while k_1 decreased from 13.6×10^{-6} to $9.7 \times 10^{-6} \text{ sec}^{-1}$ with increasing $[M]_0$.

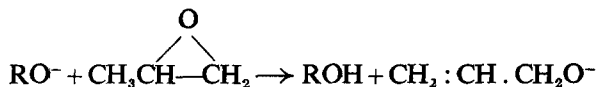
*This work was done by J. R. Atkinson, to whom our thanks are due.

Comparison of the k_1 values at 91.6°C and 101.1°C indicates an activation energy of roughly 30 kcal, and shows that this process would be far too slow to observe under our experimental conditions at 30°C.

The kinetic evidence for a unimolecular process appears compelling, but the chemistry involved is far from clear. A tentative suggestion identifies the process with the replacement of the third Cl atom on the iron, e.g.



In support of this suggestion is the observation that the base-catalysed polymerization of propylene oxide is limited by a reaction believed to be



No comparable reaction has been reported for ethylene oxide. Further support comes from polymerization rate studies with ferric tri(*n*-butoxide) as catalyst⁶: the *initial* polymerization rate was comparable with the *maximum* rates reported here, and increased only slightly as polymerization proceeded*.

An alternative hypothesis as to the chemical changes occurring in the catalyst would relate these with condensation reactions similar to those discussed in the next section.

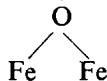
Effects of water

The addition of water in quantities less than a molecular equivalent of the iron produces the following effects: (a) an increase in the overall rate; (b) reduction and eventual elimination of the acceleration period observed with dry propylene oxide at 90°C; (c) reduction in the number of polymer molecules produced; (d) increase in the crystalline/amorphous ratio for propylene oxide polymers.

(b) We shall discuss first point (b), because it appears to be closely related to the preceding section. The primary reaction of water must be hydrolytic, and there are independent lines of evidence suggesting the removal of both alkoxide and —Cl. Borkovec³ has isolated the first reaction product (I) of ferric chloride with propylene oxide, dissolved it in carbon tetrachloride plus hexane, and slowly added 0.7 mole H₂O (per Fe) dissolved in propylene oxide. His analysis of the resulting precipitate (which was an active catalyst) shows it to be very nearly ClFe(OH)₂. Our own observation is that

*The overall polymerization showed further complicating features, possibly due to the progressive replacement of the 3 —OBu groups by polymer chains.

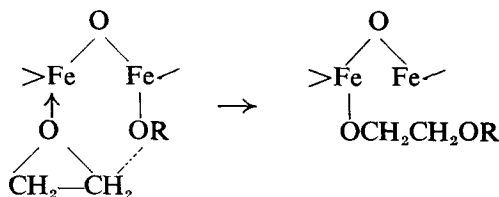
when polymerization has been carried out at 90°C in presence of water, no ionic chlorine remains. We therefore regard the effect of water as being essentially parallel with that of heating the dry catalyst, in that structural changes are produced. Hydroxyl groups are unlikely to survive under the polymerization conditions. Unless first incorporated (as terminal OH) in a growing chain, they must be expected to condense, giving



structures. Catalyst precipitation which eventually occurs at high water contents gives visual evidence of the extension of these condensation products.

(c) The observed reduction in the number of polymer chains implies that only a fraction of the iron atoms remains catalytically active. The obvious interpretation is that in a condensed polymeric catalyst only the peripheral atoms are sterically accessible for reaction. The considerable scatter in the last column of *Table 2* is not surprising in view of the difficulty of ensuring that the condensation occurs uniformly. In particular, when catalyst separation is observed at room temperature, there must be doubts as to the state of aggregation in the apparently homogeneous solution obtained on heating.

(a) Despite this loss of catalyst, the overall polymerization rate is increased, which can only mean that new types of site of enhanced specific activity have been produced. At present we can only speculate as to their nature, but it is tempting to identify them with oxygen-bridged iron, which make possible a two-centre propagation process, involving a six-membered cyclic transition complex, instead of four-membered.



(d) The remaining problem is the origin of crystalline polymer, from a monomer which is a mixture of two optical isomers. Crystallinity implies the presence of stereoregularity, and X-ray evidence has shown these crystalline propylene oxide polymers to be isotactic⁷. Growth of an isotactic chain could occur in two different ways: (i) by preferential incorporation of one of the optical isomers, with retention (or complete reversal) of configuration, or (ii) by random selection of monomer, with control of configuration in the ring-opening reaction. Our evidence would not distinguish between these, for either appears to depend on steric restrictions. It is entirely in line with the views expressed above that the condensed catalyst structures produced by partial hydrolysis should possess a greater proportion of suitably hindered sites than is present in the original catalyst.

*Department of Chemistry,
University of Manchester*

(Received February 1962)

REFERENCES

- ¹ Parts I to III, *J. chem. Soc.* **1959**, 1338, 1345; **1961**, 4298
- ² PRICE, C. C. and OSGAN, M. J. *Amer. chem. Soc.* 1956, **78**, 4787
- ³ BORKOVEC, A. B. *U.S. Patent No. 2 873 258*, 1959
- ⁴ Part II
- ⁵ MILLER, R. A. and PRICE, C. C. *J. Polym. Sci.* 1959, **34**, 161
- ⁶ COLCLOUGH, R. O. and LANGRISH, J. Unpublished
- ⁷ NATTA, G. *et al. Atti. Accad. Lincei*, 1956, **20**, 408
- STANLEY, E. and LITT, M. *J. Polym. Sci.* 1960, **43**, 453

Book Reviews

Glass Reinforced Plastics

Ed. PHILLIP MORGAN

Iliffe: London; Interscience: New York; for *British Plastics*, 1961.
(xvi+340 pp.; 6 in. by 9½ in.), 50s.

IN THE preface to the third edition the editor notes that there have been few major technical developments in the four years since the last edition of this book appeared but draws attention to the increased usage of glass reinforced plastics. It is indeed significant to compare the data, on page 296, for the annual production of polyester and epoxide resins used for laminates in the U.K. since this book was first published in 1954. The quantities given are 430 tons and 8 550 tons for 1954 and 1960 respectively. These data certainly illustrate the need for a revised text on a subject such as this.

The treatment remains unaltered; a comprehensive account of glass reinforced plastics is given in 21 chapters, each chapter being written by a specialist on that particular subject. The first seven chapters describe briefly, but adequately, the various raw materials used in the manufacture of these substances and the next five chapters deal with the methods used for moulding various products. The chapter dealing with commercial moulding processes has been improved by splitting it into three sections to cover separately hand lay-up and contact moulding, spray techniques, and matched die moulding. The section dealing with polyester dough moulding compounds has been expanded from 3 to 18 pages and this now forms a chapter by itself. The remaining 8 chapters describe the specialized applications of glass reinforced plastics, and here new chapters have been added which deal with reinforced sheeting and pressure vessels. Additional data are becoming available for the design of structures, although it is evident that much remains to be done in this field.

The very interesting chapter on miscellaneous applications has doubled in size and the increasing number of end-uses for these materials is illustrated by the additional 200 references given in this edition. Some interesting tables give production data and the proportional usage of glass reinforced plastics is included in this edition but these are not indexed very clearly.

The book is essentially a practical guide to glass reinforced plastics. It is easy to read and the convenient arrangement of the varied topics covered enables one readily to attain an up-to-date basic knowledge of this rapidly expanding field. Useful references to literature and patents are given for most subjects for anyone with a particular interest.

A. G. TURNER

Die hochpolymeren organischen Verbindungen-Kautschuk und Cellulose

H. STAUDINGER

Springer-Verlag: New Impression, Berlin, 1960.
(xvi+540 pp.; 6½ in. by 10 in.), DM 59.00.

"*Vier Tage hintereinander kam ich nicht aus der Wohnung. Denn STAUDINGER hat mich befangen. Und alles andere ruhte.*"* Thus wrote LIESEGANG when reviewing this book in the *Kolloid Zeitschrift* on its first appearance in 1932.

*'For four days on end I have not left my house. For Staudinger had made me a prisoner. And all else had to wait'.

The quotation may help to recall something of the force of its impact on colloid chemists at the time, resulting, after considerable resistance, in a revolutionary change in the concept of 'lyophilic colloids'. Its reappearance, reprinted in its original form, after almost thirty years, stimulates reflections on a remarkable turning point in the history of science.

Colloid chemistry in its early days had been a descriptive science. Largely as the result of the invention of the ultramicroscope, considerable advances were made in the first two decades of the century in the understanding of lyophobic colloids. A more difficult problem was presented by many natural products which were classified as lyophilic colloids. The complexity of their large sub-microscopic particles, as for instance in proteins, seemed to present the organic chemist with insurmountable difficulties or, in cases where the chemistry was simpler, the large and variable particle size was attributed to micelle formation and it was strongly held that these 'sols' could not be treated as dispersions of single molecules.

Attempts were therefore made, not without qualitative success, to explain their properties in terms of the size, shape and surface characteristics of the particles and by supposing that, unlike lyophobic colloids, they were surrounded by an envelope of 'bound' solvent which considerably increased the effective size of the particle and so accounted for the viscosity being much greater than would have been expected from the Einstein equation which held for lyophobic colloids.

In a few years of intensive research STAUDINGER (with his many collaborators) radically changed the situation by concentrating his researches on a few synthetic polymers, particularly polystyrene, polyoxymethylene, polyethylene oxide and polyacrylic acid. As early as 1922 he was able to establish formulae for polystyrene and to show that there were simple long-chain molecules of varying chain length. STAUDINGER called polymers having molecular weights between 10^2 and 10^4 *Hemikolloide* and those having molecular weights between 10^4 and 10^6 *Eukolloide*, the former range being those whose molecular weights could be determined by cryoscopic methods or end-group determinations. Well established information was obtained correlating the physical properties with the chemical nature and chain length of the first group and this was skilfully used to establish, with the help of other observations, at least the principle of the correlation in the second group.

The most characteristic property of high polymers and lyophilic colloids is their unique ability to give highly viscous solutions even at great dilution. Viscosity is also a property which is easily measured and it was chosen by STAUDINGER as the main tool of his research other than the methods of organic chemistry. The original Staudinger equation expressed a linear relationship between viscosity and molecular weight. This of course was an over-simplification and was inaccurate, but was a great advance on previous ideas since it showed the chain length to be the essential factor in determining the viscosity of unassociated linear polymers and in STAUDINGER'S hands it proved remarkably fruitful in explaining the nature of the synthetic linear polymer and the essential similarity of certain natural organic colloids (cellulose and rubber), their derivatives and their degradation products.

That STAUDINGER'S simple conception of the nature of linear molecules could be applied to many natural polymers was still being strongly resisted when this book appeared. MEYER and MARK, who in 1928 were attributing the high viscosity of rubber in benzol to 'very strong solvation of the micelles', were doubting (*Der Aufbau der hochpolymeren organischen Naturstoffe*, 1930) the evidence that linear molecules could be longer than the crystallites they form. FREUNDLICH, in the fourth edition of *Kapillarchemie*, which appeared in 1932,

remained faithful to the old approach and failed to appreciate the wide applicability of STAUDINGER'S conception. KRUYT'S *Colloids*, second edition 1930, did not even mention STAUDINGER'S work. But although it was still some time before his point of view was generally accepted (as late as 1939 it was still possible for WEISER to publish his *Colloid Chemistry* without referring to STAUDINGER) the romantic age of colloid chemistry had come to an end and the modern science of polymers had been born as the work of CAROTHERS and others in the next few years made clear.

In reading the book now one is impressed by the extraordinary simplicity of his approach, the clearness of thought and the skill shown in choosing and attaining his limited objectives. It is also remarkable how many conceptions are introduced which need little modification today. The monotonous repetition of his theme and the amount of space given to detail were perhaps justified at the time when defending an unpopular theme. The almost naïve character of some of his theories probably prejudiced some physical chemists against his point of view. But it was his insight into what was essential for his purpose that led to his success.

C. ROBINSON

Polymeric Materials

C. C. WINDING and G. D. HIATT

McGraw-Hill Publishing Co. Ltd: London, 1961.

(x+406 pp.; 6½ in. by 9¼ in.), 93s.

DR WINDING, who is Chairman of the Education Committee of the Society of Plastics Engineers, and Dr HIATT have evidently seen the need for a volume which would provide a general technical introduction to polymers. *Polymeric Materials* is aimed at engineers and scientists who are not actively engaged in the field but wish to become conversant with the general principles used in the manufacture and fabrication of polymers. Within this framework the authors have been successful.

The book opens with a satisfactory description of the basic chemical principles involved in polymerization. This is followed by a rather less satisfactory discussion of the factors affecting the physical properties of polymers. Two important omissions were noticed in this section. The effect on physical properties of changing the crystalline/amorphous ratio of a polymer is inadequately described and there is no reference to the effect of rate of testing on mechanical properties.

The third section of the book is devoted to a general description of the fabrication of films, fibres, mouldings, laminates, etc. from polymers. Here the American origin of the book becomes apparent. For instance, in the description of the injection moulding process, screw preplasticizing machines, which are widely used in Europe, are not mentioned.

The final chapters set out to describe the methods of production and the fields of application of all the commercially important polymers. The treatment of the older polymers such as the thermosets, the cellulose derivatives, polyvinyl chloride, polystyrene, polythene and nylon is most successful. However, when the authors come to the more recent developments such as the polycarbonates, polypropylene, and polyformaldehyde, the information is not available and they have to be content with a few lines of general description gleaned from the patent literature.

Like all McGraw-Hill publications, the book is a joy to handle. The line diagrams and formulae are very clear and the reviewer did not notice any printing errors. Unfortunately one has to pay a high price for one's pleasure.

B. E. JENNINGS

Book Reviews

Glass Reinforced Plastics

Ed. PHILLIP MORGAN

Iliffe: London; Interscience: New York; for *British Plastics*, 1961.
(xvi+340 pp.; 6 in. by 9½ in.), 50s.

IN THE preface to the third edition the editor notes that there have been few major technical developments in the four years since the last edition of this book appeared but draws attention to the increased usage of glass reinforced plastics. It is indeed significant to compare the data, on page 296, for the annual production of polyester and epoxide resins used for laminates in the U.K. since this book was first published in 1954. The quantities given are 430 tons and 8 550 tons for 1954 and 1960 respectively. These data certainly illustrate the need for a revised text on a subject such as this.

The treatment remains unaltered; a comprehensive account of glass reinforced plastics is given in 21 chapters, each chapter being written by a specialist on that particular subject. The first seven chapters describe briefly, but adequately, the various raw materials used in the manufacture of these substances and the next five chapters deal with the methods used for moulding various products. The chapter dealing with commercial moulding processes has been improved by splitting it into three sections to cover separately hand lay-up and contact moulding, spray techniques, and matched die moulding. The section dealing with polyester dough moulding compounds has been expanded from 3 to 18 pages and this now forms a chapter by itself. The remaining 8 chapters describe the specialized applications of glass reinforced plastics, and here new chapters have been added which deal with reinforced sheeting and pressure vessels. Additional data are becoming available for the design of structures, although it is evident that much remains to be done in this field.

The very interesting chapter on miscellaneous applications has doubled in size and the increasing number of end-uses for these materials is illustrated by the additional 200 references given in this edition. Some interesting tables give production data and the proportional usage of glass reinforced plastics is included in this edition but these are not indexed very clearly.

The book is essentially a practical guide to glass reinforced plastics. It is easy to read and the convenient arrangement of the varied topics covered enables one readily to attain an up-to-date basic knowledge of this rapidly expanding field. Useful references to literature and patents are given for most subjects for anyone with a particular interest.

A. G. TURNER

Die hochpolymeren organischen Verbindungen-Kautschuk und Cellulose

H. STAUDINGER

Springer-Verlag: New Impression, Berlin, 1960.
(xvi+540 pp.; 6½ in. by 10 in.), DM 59.00.

"*Vier Tage hintereinander kam ich nicht aus der Wohnung. Denn STAUDINGER hat mich befangen. Und alles andere ruhte.*"* Thus wrote LIESEGANG when reviewing this book in the *Kolloid Zeitschrift* on its first appearance in 1932.

*'For four days on end I have not left my house. For Staudinger had made me a prisoner. And all else had to wait'.

remained faithful to the old approach and failed to appreciate the wide applicability of STAUDINGER'S conception. KRUYT'S *Colloids*, second edition 1930, did not even mention STAUDINGER'S work. But although it was still some time before his point of view was generally accepted (as late as 1939 it was still possible for WEISER to publish his *Colloid Chemistry* without referring to STAUDINGER) the romantic age of colloid chemistry had come to an end and the modern science of polymers had been born as the work of CAROTHERS and others in the next few years made clear.

In reading the book now one is impressed by the extraordinary simplicity of his approach, the clearness of thought and the skill shown in choosing and attaining his limited objectives. It is also remarkable how many conceptions are introduced which need little modification today. The monotonous repetition of his theme and the amount of space given to detail were perhaps justified at the time when defending an unpopular theme. The almost naïve character of some of his theories probably prejudiced some physical chemists against his point of view. But it was his insight into what was essential for his purpose that led to his success.

C. ROBINSON

Polymeric Materials

C. C. WINDING and G. D. HIATT

McGraw-Hill Publishing Co. Ltd: London, 1961.

(x+406 pp.; 6½ in. by 9¼ in.), 93s.

DR WINDING, who is Chairman of the Education Committee of the Society of Plastics Engineers, and Dr HIATT have evidently seen the need for a volume which would provide a general technical introduction to polymers. *Polymeric Materials* is aimed at engineers and scientists who are not actively engaged in the field but wish to become conversant with the general principles used in the manufacture and fabrication of polymers. Within this framework the authors have been successful.

The book opens with a satisfactory description of the basic chemical principles involved in polymerization. This is followed by a rather less satisfactory discussion of the factors affecting the physical properties of polymers. Two important omissions were noticed in this section. The effect on physical properties of changing the crystalline/amorphous ratio of a polymer is inadequately described and there is no reference to the effect of rate of testing on mechanical properties.

The third section of the book is devoted to a general description of the fabrication of films, fibres, mouldings, laminates, etc. from polymers. Here the American origin of the book becomes apparent. For instance, in the description of the injection moulding process, screw preplasticizing machines, which are widely used in Europe, are not mentioned.

The final chapters set out to describe the methods of production and the fields of application of all the commercially important polymers. The treatment of the older polymers such as the thermosets, the cellulose derivatives, polyvinyl chloride, polystyrene, polythene and nylon is most successful. However, when the authors come to the more recent developments such as the polycarbonates, polypropylene, and polyformaldehyde, the information is not available and they have to be content with a few lines of general description gleaned from the patent literature.

Like all McGraw-Hill publications, the book is a joy to handle. The line diagrams and formulae are very clear and the reviewer did not notice any printing errors. Unfortunately one has to pay a high price for one's pleasure.

B. E. JENNINGS

Notes

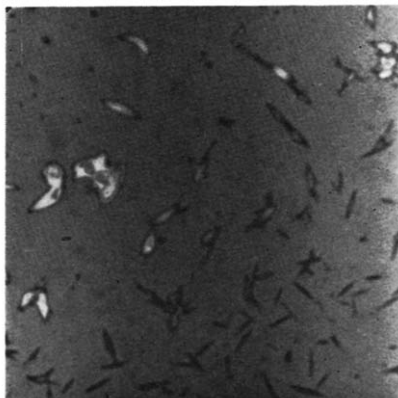
Interference Microscopy of Solution-grown Polyethylene Single Crystals

DURING the course of our investigation of the thermodynamics of the crystalline state of polyethylene^{1, 2}, it became necessary to acquire information about the different possible growth habits of solution-grown crystals. To observe the habit, as well as measure length, width, and thickness, an interference microscope³ was used. Its main features are the ability to detect vertical thickness of polyethylene down to 20Å and to measure it with a precision of $\pm 6\text{Å}$ in favourable cases³. In this note three new growth habits of polyethylene will be described: needles, six-ended single crystals, and right angle crystal clusters.

A. NEEDLES

Figure 1 shows a large number of typical needles of polyethylene. The needles were grown from a solution of 0.1 per cent linear polyethylene in chlorobenzene over which pure toluene was layered. The growth occurred isothermally at the interface at 89.7°C.

Figure 1—Interference micrograph of polyethylene needles. Air mounted, 40× shearing interference objective, the long diagonal of the figure is 0.15 mm



The needles look similar to those found for paraffins by Rhodes, Mason and Sutton⁴. The paraffin needles were proved to be rolled up platelets⁴. There is some evidence which indicates a similar mechanism for the polyethylene. The polyethylene needles were found in a preparation which also contained large amounts of single crystal platelets. Under the polarizing microscope the thickest needles show a weak line of birefringence on each of the two sides, but little or none in the middle, which is actually thicker. Estimation of the birefringence from measurements of the retardation with

a Berek compensator and values of the thickness of identical regions measured with the interference microscope⁵ resulted in an approximate order of magnitude of 10^{-2} . Light vibrating parallel to the long axis has the low refractive index. This is in accord with the assumption of rolled crystals, which would show a side view of the curved single crystal along the edges. Thus the *c* axis (chain axis) would be only along the sides at right angles to the needle direction. The birefringence⁶ for light vibrating parallel to *c* and *a* or *b* is 0.062. Light vibrating parallel to *a* and *b* has a weak birefringence⁵ of 3×10^{-3} and could account for the unrecognizable birefringence in the centre of the needles. The sizes of the needles varied. Typical dimensions are: 10 to 20×10^{-4} cm long, 0.5 to 2×10^{-4} cm wide, and a thickness at the centre of 0.1 to 0.5×10^{-4} cm.

B. SIX-ENDED SINGLE CRYSTALS

Figure 2 shows two single crystals with considerable overgrowth at right angles to the long dimension. These crystals exhibit the only habit found for slow crystallization of a 0.052 per cent linear polyethylene solution in toluene at 129°C under a pressure of 2 600 atm. Reducing the pressure to 2 300 atm, approximating equilibrium conditions at a somewhat lower temperature, yields normal orthorhombic single crystals⁷ with four (110) growth faces. Increasing the pressure to 3 000 atm or more renders the solution strongly supersaturated at 129°C and six-ended dendrites arise, which are fully described in ref. 5.

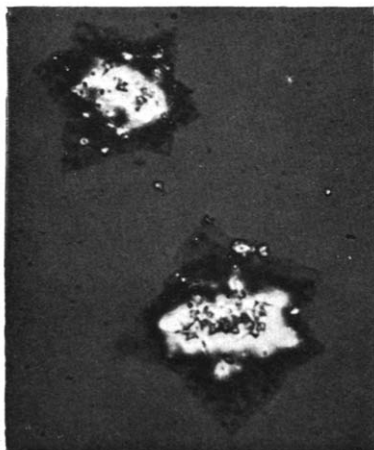


Figure 2—Interference micrograph of six-ended polyethylene single crystals. Air mounted, 40× shearing interference objective, the long diagonal of the figure is 0.12 mm

Quenching more concentrated solutions of polyethylene under a room temperature gradient at atmospheric pressure also gives six-ended dendrites. Crystallographically, it is possible to describe six-ended growth, assuming two(110)twin planes and one(120)twin plane. The theoretical angle between the *a* axes of 67°40' is closely approximated by the crystals of Figure 2. The average of ten crystals measured was $70 \pm 2^\circ$. Dendrites have been

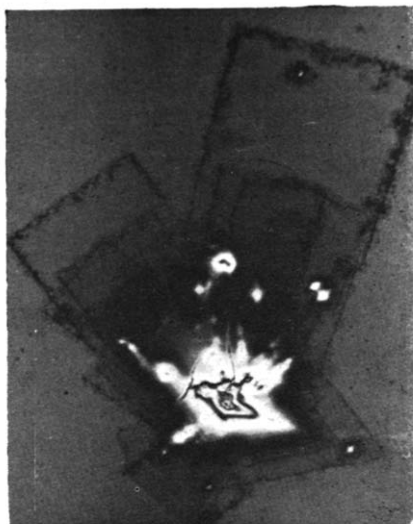
NOTES

reported to show the same angle⁵. The thickening across the long dimensions is similar to the thickening of analogous branches in the corresponding dendrites.

C. RIGHT ANGLE CRYSTAL CLUSTERS

Figures 3 and 4 show clusters of polyethylene crystals grown from a common centre with almost right angle boundaries. The growing conditions were identical to those described in part A. The isolated growth spirals on

Figure 3—Interference micrograph of a right angle polyethylene crystal cluster. Air mounted, 40× shearing interference objective, the long diagonal of the figure is 0.25 mm



the right angle baseplates and the large growth spiral at the bottom of Figure 3 indicate that the long faces are (110) planes. A careful measurement of the 'right angles' shows that they are 87.5°. This is close to the

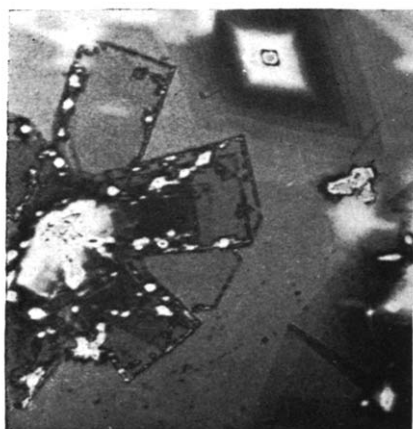


Figure 4—Interference micrograph of a right angle polyethylene crystal cluster. Air mounted, 10× shearing interference objective, the long diagonal of the figure is 0.40 mm

theoretical angle between a (110) and a (210) face ($86^{\circ} 45'$). The cut-off corner in *Figure 4* shows an angle of 142° with the (210) face and 124° with the (110) face which agrees with the assignment of a (100) plane for the cut-off face (theoretical angles 143° and $123^{\circ} 40'$). The right angle clusters are thus made up of (110)-twin crystals. The thickness of the baseplate is approximately 95\AA and the large number of small growth spirals at the edges reach as high as $3\,000\text{\AA}$.

This research has been supported in part by the Advanced Research Projects Agency and the Office of Naval Research. Their support is gratefully acknowledged.

B. WUNDERLICH
P. SULLIVAN

*Department of Chemistry,
Cornell University,
Ithaca, New York*

(Received September 1961)

REFERENCES

- ¹ WUNDERLICH, B. and KASHDAN, W. H. *J. Polym. Sci.* 1961, **50**, 71
- ² WUNDERLICH, B. and POLAND, D. *J. Polym. Sci.* In press
- ³ WUNDERLICH, B. and SULLIVAN, P. *J. Polym. Sci.* 1962, **56**, 19
- ⁴ RHODES, F. H., MASON, C. W. and SUTTON, W. R. *Industr. Engng Chem. (Industr.)* 1927, **19**, 935
- ⁵ WUNDERLICH, B. and SULLIVAN, P. *J. Polym. Sci.* In press
- ⁶ BRYANT, W. M. D. *J. Polym. Sci.* 1947, **2**, 547
- ⁷ For a recent review see for example: KELLER, A. in *Growth and Perfection of Crystals*. Editors: R. H. DOREMUS, B. W. ROBERTS and D. TURNBULL; Wiley, New York, 1958 or *Makromol. Chem.* 1959, **34**, 1

The Formation of Nuclei in Crystallizing Polymers

DURING an investigation into the crystallization of poly(decamethylene terephthalate) an effect was observed which is likely to be of importance in relation to crystallization mechanism. The picture normally proposed to account for the formation of crystallinity in a polymer cooled from the melt is that nuclei form at random positions in the supercooled liquid, and grow at a constant linear rate in one, two or three dimensions, to form rods, discs or spheres^{1, 2}. The nuclei are postulated to appear either instantaneously at the start of the process, in which case they are assumed to be derived from pre-existing heterogeneities; or sporadically, with a linear dependence on time, as a result of random fluctuations in a homogeneous material. The present observations suggest that these may be two special cases of a more general relationship.

Samples of polymer, prepared by the method of Flory and Leutner³, were pressed between cover slips at various temperatures above the melting point (137.5°C) to give films approximately 10μ thick. The behaviour of the material was very much dependent on the method of film preparation, a point which is discussed in a separate publication⁴, but was reproducible

theoretical angle between a (110) and a (210) face ($86^{\circ} 45'$). The cut-off corner in *Figure 4* shows an angle of 142° with the (210) face and 124° with the (110) face which agrees with the assignment of a (100) plane for the cut-off face (theoretical angles 143° and $123^{\circ} 40'$). The right angle clusters are thus made up of (110)-twin crystals. The thickness of the baseplate is approximately 95\AA and the large number of small growth spirals at the edges reach as high as $3\,000\text{\AA}$.

This research has been supported in part by the Advanced Research Projects Agency and the Office of Naval Research. Their support is gratefully acknowledged.

B. WUNDERLICH
P. SULLIVAN

*Department of Chemistry,
Cornell University,
Ithaca, New York*

(Received September 1961)

REFERENCES

- ¹ WUNDERLICH, B. and KASHDAN, W. H. *J. Polym. Sci.* 1961, **50**, 71
- ² WUNDERLICH, B. and POLAND, D. *J. Polym. Sci.* In press
- ³ WUNDERLICH, B. and SULLIVAN, P. *J. Polym. Sci.* 1962, **56**, 19
- ⁴ RHODES, F. H., MASON, C. W. and SUTTON, W. R. *Industr. Engng Chem. (Industr.)* 1927, **19**, 935
- ⁵ WUNDERLICH, B. and SULLIVAN, P. *J. Polym. Sci.* In press
- ⁶ BRYANT, W. M. D. *J. Polym. Sci.* 1947, **2**, 547
- ⁷ For a recent review see for example: KELLER, A. in *Growth and Perfection of Crystals*. Editors: R. H. DOREMUS, B. W. ROBERTS and D. TURNBULL; Wiley, New York, 1958 or *Makromol. Chem.* 1959, **34**, 1

The Formation of Nuclei in Crystallizing Polymers

DURING an investigation into the crystallization of poly(decamethylene terephthalate) an effect was observed which is likely to be of importance in relation to crystallization mechanism. The picture normally proposed to account for the formation of crystallinity in a polymer cooled from the melt is that nuclei form at random positions in the supercooled liquid, and grow at a constant linear rate in one, two or three dimensions, to form rods, discs or spheres^{1, 2}. The nuclei are postulated to appear either instantaneously at the start of the process, in which case they are assumed to be derived from pre-existing heterogeneities; or sporadically, with a linear dependence on time, as a result of random fluctuations in a homogeneous material. The present observations suggest that these may be two special cases of a more general relationship.

Samples of polymer, prepared by the method of Flory and Leutner³, were pressed between cover slips at various temperatures above the melting point (137.5°C) to give films approximately 10μ thick. The behaviour of the material was very much dependent on the method of film preparation, a point which is discussed in a separate publication⁴, but was reproducible

once the film had been formed. In the present case, *ca.* 1 mg was heated *in vacuo* at 170°C for 15 min prior to covering with a glass slip and heating

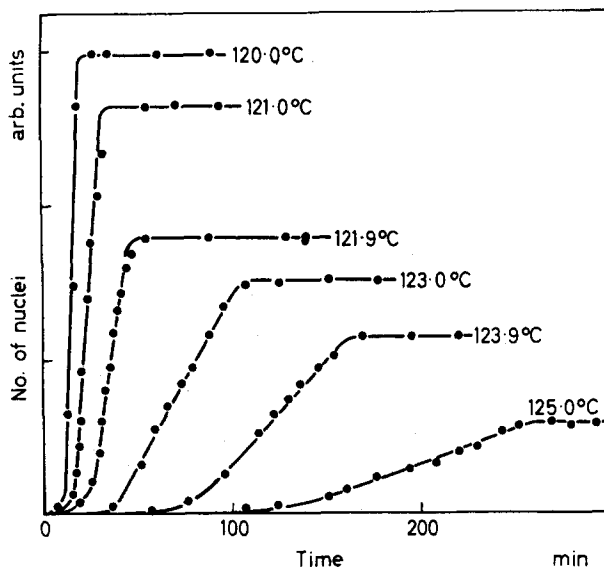


Figure 1—Nucleus formation in poly(decamethylene terephthalate)

for a further 30 min at 200°C. Nucleus formation was observed microscopically between crossed polaroids, using a thermostatted hot-stage controlled to $\pm 0.1^\circ\text{C}$, and in general the sample was raised to 160°C for 5 min prior to crystallizing at a fixed temperature below the melting point. It was established, however, that melting at 140°C, and at 300°C, produced results identical with those at 160°C.

Figure 1 indicates the relationship between number of nuclei and time, observed for a range of crystallization temperatures. It takes the form of a constant rate of increase terminating sharply after a period of time characteristic of the temperature of crystallization, to leave a number which remains constant throughout the subsequent crystallization. Slight deviations from linearity during the initial stages were considered to be due to the arbitrary, but reproducible, size at which a nucleus becomes visible. The maximum area covered by the birefringent spherulitic structures grown from the nuclei was estimated to be approximately 5 per cent, so that reduction in the space available for nucleation was not considered to be a relevant factor in causing the cessation. It was established that the nuclei reappeared in the same positions, although not necessarily in the same order in time. The possibility that they might result from undissociated remnants of previous structures was considered unlikely in view of the fact that although memory effects could be observed under appropriate conditions, they disappeared at temperatures greater than 1°C above the melting point.

The following points arise from these observations:

(1) In general, 'predetermined' nucleation will be apparently operative when the time at which the nuclei cease to be formed is short compared with the overall time of crystallization.

(2) 'Sporadic' nucleation will be the relevant process when crystallization is complete before the cessation point is reached.

(3) Nucleation may sometimes appear to change from 'sporadic' to 'predetermined' during the course of crystallization. The kinetics of the process will in consequence be more complicated, a point considered by Price and his colleagues in connection with some recent work on polyethylene oxide⁶.

(4) The most important implication is that all nucleation processes, whether 'predetermined' or 'sporadic', arise from heterogeneities, and as such can be controlled by varying the number of centres present, once their nature is known.

The first three factors considered above are only relevant provided that the point at which nucleation stops t_s can be varied relative to the time of crystallization. A consideration of some dilatometric data, obtained for the same polymer⁵, showed that temperature of crystallization was not an important factor in this connection, as the ratio t_s/t_1 varied by only 20 per cent over the range of temperature covered in *Figure 1*. It was observed, however, to be affected by variations in specimen preparation, a feature which does not seem unreasonable in view of the fact that nucleation appears to depend on heterogeneities. In addition, preliminary results on a range of polymers (polyethylene oxide, polyoxymethylene, polypropylene and polyethylene) indicated that the relationship observed in *Figure 1* is of general application. Consequently the nature of the polymer itself is likely to be an important factor in deciding whether the nucleation process is apparently 'predetermined' or 'sporadic'.

A. SHARPLES

Arthur D. Little Research Institute,
Inveresk, Musselburgh, Midlothian

(Received February 1962)

REFERENCES

- ¹ MORGAN, L. B. *Phil. Trans.* 1954, **247**, 13
- ² MANDELKERN, L. *Chem. Rev.* 1956, **56**, 903
- ³ FLORY, P. J. and LEUTNER, F. S. *U.S. Patent No. 2 589 688*, 1952
- ⁴ BANKS, W., HAY, J. N., SHARPLES, A. and THOMSON, G. To be published
- ⁵ SHARPLES, A. and SWINTON, F. L. To be published
- ⁶ BARNES, W. J., LUETZEL, W. G. and PRICE, F. P. *J. phys. Chem.* 1961, **65**, 1742

Single Crystals from Polyamide Melts

SINGLE crystals of a number of polymers have been obtained by crystallization from dilute solutions in various solvents^{1, 2}. In particular, polyamide crystals have been grown in this manner^{3, 4}. Crystallization from polymer

The following points arise from these observations:

(1) In general, 'predetermined' nucleation will be apparently operative when the time at which the nuclei cease to be formed is short compared with the overall time of crystallization.

(2) 'Sporadic' nucleation will be the relevant process when crystallization is complete before the cessation point is reached.

(3) Nucleation may sometimes appear to change from 'sporadic' to 'predetermined' during the course of crystallization. The kinetics of the process will in consequence be more complicated, a point considered by Price and his colleagues in connection with some recent work on polyethylene oxide⁶.

(4) The most important implication is that all nucleation processes, whether 'predetermined' or 'sporadic', arise from heterogeneities, and as such can be controlled by varying the number of centres present, once their nature is known.

The first three factors considered above are only relevant provided that the point at which nucleation stops t_s can be varied relative to the time of crystallization. A consideration of some dilatometric data, obtained for the same polymer⁵, showed that temperature of crystallization was not an important factor in this connection, as the ratio t_s/t_1 varied by only 20 per cent over the range of temperature covered in *Figure 1*. It was observed, however, to be affected by variations in specimen preparation, a feature which does not seem unreasonable in view of the fact that nucleation appears to depend on heterogeneities. In addition, preliminary results on a range of polymers (polyethylene oxide, polyoxymethylene, polypropylene and polyethylene) indicated that the relationship observed in *Figure 1* is of general application. Consequently the nature of the polymer itself is likely to be an important factor in deciding whether the nucleation process is apparently 'predetermined' or 'sporadic'.

A. SHARPLES

Arthur D. Little Research Institute,
Inveresk, Musselburgh, Midlothian

(Received February 1962)

REFERENCES

- ¹ MORGAN, L. B. *Phil. Trans.* 1954, **247**, 13
- ² MANDELKERN, L. *Chem. Rev.* 1956, **56**, 903
- ³ FLORY, P. J. and LEUTNER, F. S. *U.S. Patent No. 2 589 688*, 1952
- ⁴ BANKS, W., HAY, J. N., SHARPLES, A. and THOMSON, G. To be published
- ⁵ SHARPLES, A. and SWINTON, F. L. To be published
- ⁶ BARNES, W. J., LUETZEL, W. G. and PRICE, F. P. *J. phys. Chem.* 1961, **65**, 1742

Single Crystals from Polyamide Melts

SINGLE crystals of a number of polymers have been obtained by crystallization from dilute solutions in various solvents^{1, 2}. In particular, polyamide crystals have been grown in this manner^{3, 4}. Crystallization from polymer

melts normally results in spherulitic forms, the most crystalline of these being the aggregates^{5, 6} of nylon 6.6 and the hedrites of polyoxymethylene⁷.

Recent work in these laboratories¹⁰ has shown that single crystals can be obtained from polyamide melts when crystallization is carried out isothermally in thin films for long periods (upwards of several hours) at small degrees of supercooling. Birefringent aggregates are formed in thick films crystallized under these conditions suggesting that such structures are composed of single crystal platelets. Optical micrographs of structures grown in thin films are shown in *Figures 1* and *2* for nylons 5.6 and 5.7 respectively.

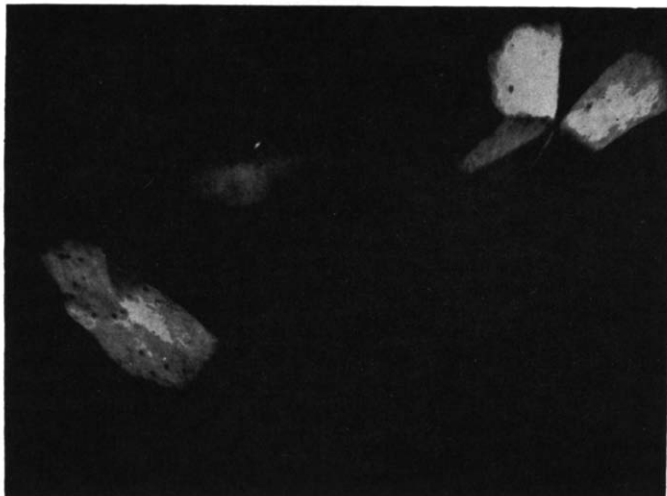


Figure 1



Figure 2

Rotation of these specimens between crossed polars showed uniform extinction of individual platelets, many of which appear in the extinction position in the completely crystallized film in *Figure 2*. This behaviour was observed in films of different thicknesses down to less than 0.1μ .

The electron microscope was used to obtain selected area electron diffraction patterns of these thin films. Using an aperture corresponding to a specimen area of approximately 40μ square, the patterns shown in *Figures 3* and *4* were obtained from nylons 5.6 and 5.7 respectively. These patterns

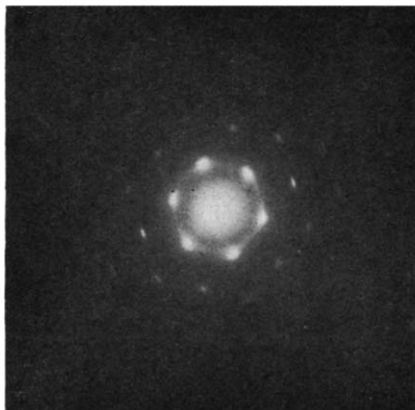


Figure 3

confirm the single crystal nature of the platelets observed optically. Normal beam intensities rapidly destroyed the crystalline structure giving rise to the diffuse diffraction pattern. In these patterns the diffraction spots are pseudo-hexagonally arranged and in some instances extend out to five orders on the photographic negative. A detailed analysis of the diffraction patterns has

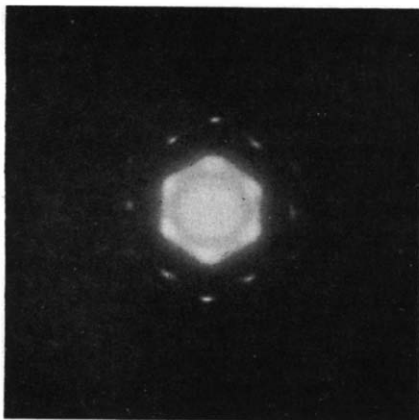


Figure 4

yet to be made, but their observed symmetry is in agreement with the unit cells proposed by Kinoshita⁸ for 'odd-odd' and 'odd-even' polyamides where it is assumed that the molecular chains are lying normal to the film plane.

Figure 5 shows a dark field electron micrograph obtained by using one of the inner reflections. To obtain the most favourable conditions for diffraction this specimen was thinned by negative ion bombardment for 15 minutes

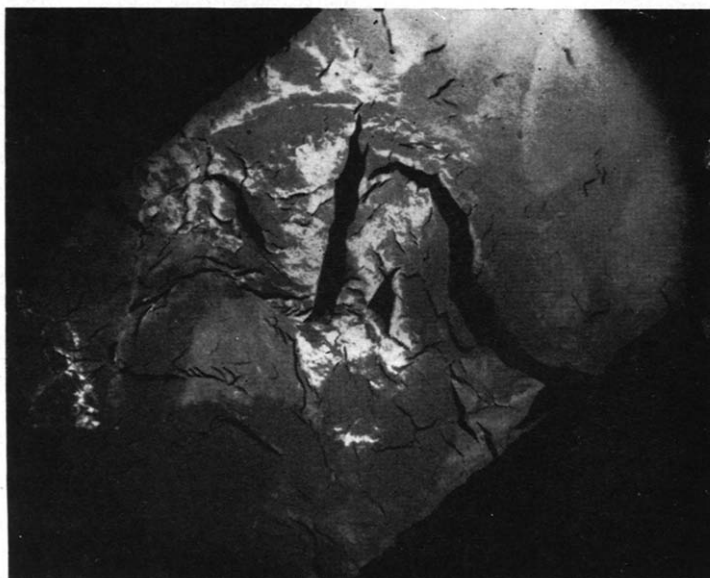


Figure 5

using a discharge in pure oxygen under the conditions described by Spit⁹. No evidence of any change in internal structure has been observed when this etching technique is used. The extent of suitably oriented diffracting areas is consistent with the single crystal nature of the platelets observed optically (Figure 2).

Uniformly extinguishing platelets similar to those shown in Figures 1 and 2 have been found in nylon 5.5, nylon 6.6, nylon 8 and nylon 10.10 and are under investigation. Results will be described in more detail later.

Thanks are due to Professor M. H. L. Pryce, F.R.S., H. H. Wills Physics Laboratories, University of Bristol, for kindly providing electron microscope facilities.

British Nylon Spinners Ltd,
Research Department,
Pontypool, Mon.

J. H. MAGILL*
P. H. HARRIS

(Received October 1961)

*Present address of J. H. M.: Mellon Institute, 4400 Fifth Ave., Pittsburgh 13, Pa, U.S.A.

NOTES

REFERENCES

- ¹ KELLER, A. *Makromol. Chem.* 1959, **34**, 1
- ² TRILLAT, J. J. and SELLA, CL. *Bull. Inst. text. Fr.* 1961, **92**, 35
- ³ BADAMI, D. V. and HARRIS, P. H. *J. Polym. Sci.* 1959, **41**, 540
- ⁴ GEIL, P. H. *J. Polym. Sci.* 1960, **44**, 449
- ⁵ KHOURY, F. *J. Polym. Sci.* 1958, **33**, 389
- ⁶ MANN, J. and ROLDAN, L. 'Conference on Physics of High Polymers, Bristol, January 1961'
- ⁷ GEIL, P. H. in *Growth and Perfection of Crystals*, pp 579-585. (Ed. DOREMUS, R. H., ROBERTS, B. W. and TURNBULL, D.) Wiley: New York, 1958
- ⁸ KINOSHITA, Y. *Makromol. Chem.* 1959, **33**, 1 and 21
- ⁹ SPIT, B. J. *Proceedings of the European Regional Conference on Electron Microscopy, Delft 1960*, Vol. I, p 564
- ¹⁰ MAGILL, J. H. *Chem. & Ind.* **1962**, No. 1, 33

The Kinetics of the Polycondensation of 12-Hydroxystearic Acid

C. E. H. BAWN and M. B. HUGLIN

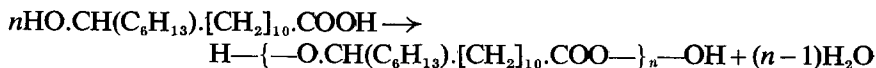
The polycondensation of 12-hydroxystearic acid, catalysed by p-toluenesulphonic acid, obeys simple second order kinetics for about 85 per cent of the reaction. Thereafter a tailing-off in degree of polymerization obtains. The constants K_0 and α in the Staudinger viscosity/molecular weight relationship are derived for poly 12-hydroxystearates.

THE mechanism of condensation polymerization between dibasic acids $\text{HOOC} \cdot [\text{CH}_2]_m \cdot \text{COOH}$ and dihydric alcohols $\text{HO} \cdot [\text{CH}_2]_n \cdot \text{OH}$ as well as that of hydroxyacids $\text{HOOC} \cdot [\text{CH}_2]_n \cdot \text{OH}$ is well established, although a complete kinetic analysis of the latter type of reaction has not yet been reported. For all such reactions the degree of polymerization varies with time in accord with equation (1).

$$1/(1-p) = \gamma C_0 K t + 1 \quad (1)$$

in which p denotes the extent of reaction, $1/(1-p)$ is the degree of polymerization, K is the specific velocity constant, C_0 is the initial concentration of functional groups, γ is the concentration of acid catalyst, and t is the time of reaction.

For the reaction between adipic acid and diethylene glycol, Flory¹ has shown that equation (1) is obeyed except for the initial stage of reaction. More recently Pope and Williams² have corroborated this on the same system. The purposes of the present study were twofold: first, to re-investigate the early stages of reaction on a new system and secondly, to utilize a branched hydroxy acid in order to observe any steric effect of the side chain on the kinetic behaviour. 12-Hydroxystearic acid was used as monomer and the reaction, which was performed in the melt to prevent any ring formation, can be represented thus



EXPERIMENTAL

Materials

The monomer was crystallized five times from ethanol. Removal of stearic acid was effected by repeated refluxing with petroleum ether in which this impurity is soluble. Three crystallizations from ethylacetate yielded the monomer of m.pt 81.0°C. The catalyst, *p*-toluenesulphonic acid of B.D.H. 'micro-analytical reagent' grade, was used without further purification and was stored as a solution in AR chloroform.

APPARATUS AND METHOD

3 to 4 g of monomer were weighed out in pellet form for convenience of handling. The volume of catalyst solution necessary for the requisite value of γ was pipetted into the round-bottomed reaction vessel and the solvent was pumped off. After addition of the monomer the vessel was placed in the thermostat and opened to a vacuum system (10^{-2} mm). Boiling *n*-butanol, chlorobenzene, bromoform and cyclohexanol afforded temperatures in the thermostat of 116.6, 133.5, 152.5 and 160.5°C respectively, constant to $\pm 0.1^\circ$. At convenient intervals of time the reaction vessel was isolated from the pumping line and dry air was admitted. The molten polymer was stirred, a sample withdrawn into a tared flask, and quickly chilled to quench the reaction. After the aliquots had attained room temperature in a desiccator, they were weighed, dissolved in chloroform and titrated against alcoholic sodium hydroxide solution, using phenolphthalein as indicator. Where necessary, neutralized ethanol was added to homogenize the solutions during titration. The degree of polymerization was calculated from³

$$1/(1-p) = (w - 18t) / [(S + 190\gamma)t - \gamma w] \quad (2)$$

in which w is the weight of sample in grammes, t is the titre in moles of caustic soda, S is the molecular weight of one segment = 282, and

$$\gamma = \frac{\text{moles of } p\text{-toluenesulphonic acid monohydrate}}{\text{total moles of segments}}$$

Kinetics

In *Figure 1* the degree of polymerization is plotted against time for a fourfold range in γ at 160.5°C. Equation (1) is obeyed from $p=0$ to about $p=85$ per cent reaction. Thereafter the chain length fails to increase at

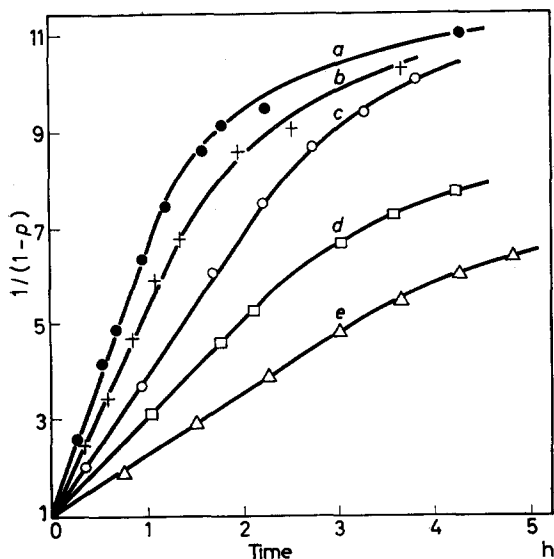


Figure 1—Variation of degree of polymerization with time at 160.5°C:

- (a) $\gamma=0.02$, (b) $\gamma=0.015$,
(c) $\gamma=0.01$, (d) $\gamma=0.0075$,
(e) $\gamma=0.005$

the same uniform rate. Similar behaviour is exhibited in *Figure 2* in which the course of the reaction at constant γ of 0.01 is shown at different temperatures. For any particular constant time of reaction, a plot of the corresponding value of $1/(1-p)$ versus γ (equation 1) is linear and the direct dependence of rate on catalyst concentration is thus confirmed.

In *Figures 1* and *2* the commencement of curvature appears to be related to the extent of reaction solely. γ and T are significant only insofar as they affect the time taken to reach this point. This phenomenon has already been noted by Davies⁴ in an acid-catalysed esterification and by Flory⁵

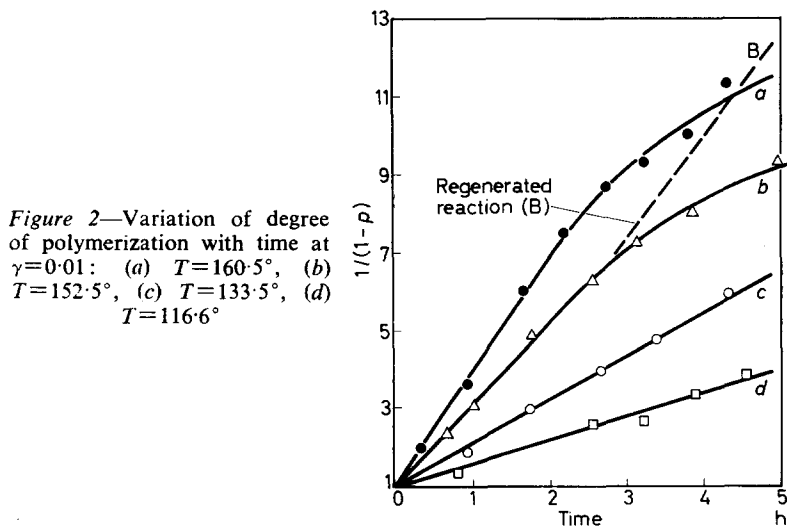


Figure 2—Variation of degree of polymerization with time at $\gamma=0.01$: (a) $T=160.5^\circ$, (b) $T=152.5^\circ$, (c) $T=133.5^\circ$, (d) $T=116.6^\circ$

and Ivanoff⁶ in polyesterifications, and was attributed to consumption of the catalyst. Assuming this to be a feasible explanation in this case a test was made by carrying out a reaction at 152.5°C with $\gamma=0.01$ until the start of curvature on the $1/(1-p)$ versus t plot, when the reaction was quenched by chilling. After removal of unused catalyst (vide section on viscosity) and addition of fresh catalyst at the same initial concentration, the regenerated polycondensation proceeded linearly at a rather higher rate and its course was observed up to 95 per cent reaction, corresponding to $1/(1-p)$ of 20 (*Figure 2B*).

Tables 1 and *2* give the dependence of K^1 on catalyst and temperature. The mean value of K at 160.5° is $6.32 \times 10^{-3} \text{ mole}^{-2} \text{ l}^2 \text{ sec}^{-1}$. An overall energy of activation of $11.45 \text{ kcal mole}^{-1}$ and a pre-exponential factor $A = kT/h \exp(S/R)$ of $3.65 \times 10^{-3} \text{ sec}^{-1}$ are found.

VISCOSITY OF POLYMER SOLUTIONS

Polymers of molecular weights M_n were obtained by withdrawing samples at different intervals of time from a reaction at 160.5° , with $C_{\text{cat.}}=0.0354 \text{ mole l}^{-1}$. They were dissolved in chloroform, shaken with ice-cold water to remove the catalyst and the chloroform layers were dried with magnesium

Table 1—Specific velocity constants K at 160.5°C for different catalyst concentrations
$$K^1 = K C_0 C_{\text{cat.}}^* ; C_0 = 1000/282 \text{ mole l}^{-1}; C_{\text{cat.}} = 1000 \gamma / 282 \text{ mole l}^{-1}$$

| $10^2 C_{\text{cat.}}$ mole l^{-1} | $10^4 K^1$ sec $^{-1}$ | $10^3 K$ mole $^{-2}$ l 2 sec $^{-1}$ |
|--------------------------------------|------------------------|--|
| 1.77 | 3.75 | 5.96 |
| 2.65 | 5.83 | 6.20 |
| 3.54 | 8.17 | 6.50 |
| 5.31 | 12.1 | 6.42 |
| 7.08 | 16.4 | 6.53 |

*Whilst it is convenient to have used γ as defined in equation (2) for the calculation of $1/(1-p)$ from experimentally measured quantities, the catalyst concentration C_{cat} is in units of mole l^{-1} , where C_{cat} is simply $1000\gamma/282$. C_0 and K will also involve these standard units. Flory's work on the negligible departure of the density of molten polyesters from unity when the chain length and temperature (in this region) are altered justifies the use of the molarities instead of molalities, although the weights and not volumes are actually measured.

Table 2. Specific velocity constants K at constant catalyst concentration
$$C_{\text{cat.}} = 0.0354 \text{ mole l}^{-1} \text{ for different temperatures } T$$

$$K^1 = K C_0 C_{\text{cat.}} = K \times 1000/282 \times 0.0354$$

| T | $10^4 K^1$ sec $^{-1}$ | $10^3 K$ mole $^{-2}$ l 2 sec $^{-1}$ |
|--------|------------------------|--|
| 116.6° | 1.80 | 1.44 |
| 133.5 | 3.28 | 2.61 |
| 152.5 | 6.17 | 4.91 |
| 160.5 | 8.17 | 6.50 |

sulphate. The solvent was removed by gentle heating under vacuum. Viscosities in the concentration range 0.1 to 1.0 g/100 ml solution were measured in chloroform at $25^\circ \pm 0.02^\circ\text{C}$. The values of M_n were determined then by titration of these solutions against alcoholic sodium hydroxide.

$$M_n = 282 \times 1/(1-p) + 18$$

For the relatively small range of M_n studied, the viscosities of the solutions, including that of the monomer, follow the relation

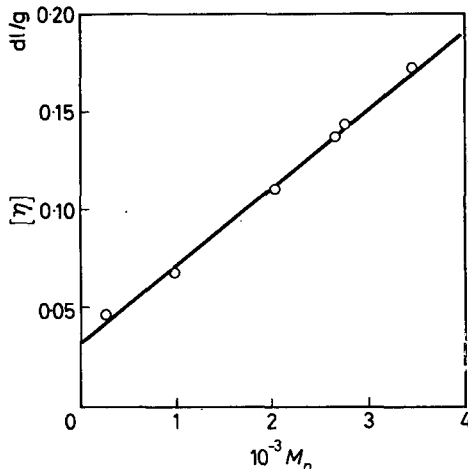
$$[\eta] = K_v M_n^\alpha + I_v$$

in which $\alpha = 1$, $K_v = 0.41 \times 10^{-4} \text{ dl g}^{-1}$ and $I_v = 0.032 \text{ dl g}^{-1}$. These values of K_v and I_v are of the same order as those reported for other polyesters⁷⁻⁹.

NATURE OF POLYMER

The following evidence supports the conclusion that the reaction product consists entirely of open-chain polyesters and not ring compounds: (a) the viscosity exponent $\alpha = 1$, which is typical for polyester solutions; (b) absence of any volatile product (e.g. lactone) other than water in the cold trap; (c) determination of the number of hydroxyl and carboxyl groups in a polymer sample by acetylation for the former and direct titration for the latter yielded 0.308×10^{-3} and 0.304×10^{-3} groups per gramme respectively. Further a reaction in the melt favours intermolecular reaction and not intramolecular condensation, which can occur in dilute solution. A lactone of the size required would, in any case, be most unstable.

Figure 3—Dependence of intrinsic viscosity on molecular weight for poly 12-hydroxystearates in chloroform at 25°C



The polymers are very viscous colourless compounds, the amorphous nature of which is attributed to the *n*-hexyl group attached to each segment. The random presence of these groups on either side of the polyester backbone chain prevents parallel alignment for crystallinity. Comparable compounds without any branching, e.g. poly 11-hydroxyundecanoates even of low molecular weight have considerable crystallinity.

DISCUSSION

It seems reasonable to assume that the failure of the kinetics to obey equation (1) in the later stages of reaction is caused by participation of the catalyst in the esterification. Since, to obtain convenient reaction times, the values of C_{cat} were some two to three times greater than those normally employed, the effective concentrations of $-\text{SO}_3\text{H}$, $-\text{CO}_2\text{H}$ and $-\text{OH}$ become comparable towards the end of reaction. Hence, at this point, the *p*-toluenesulphonic acid is tantamount to a monofunctional impurity.

More fundamentally, the accurate adherence of the kinetics to the equation $1/(1-p) = KC_0 C_{\text{cat}} t + 1$ over the early stages of reaction does not accord with the findings of Flory and others. His postulate, that the changes in kinetics are due to the pronounced changes in the characteristics of the medium in this region, is untenable in this particular reaction and cannot be universally true.

It is of interest to compare the kinetic data with some published ones. All values of K have been interpolated to 100°. In this work K_{100° , activation energy E , pre-exponential factor $A = kT/h \exp(S/R)$ and entropy of activation S are respectively $7.3 \times 10^{-4} \text{ mole}^{-2} \text{ l}^2 \text{ sec}^{-1}$, $11.45 \text{ kcal mole}^{-1}$, $3.65 \times 10^{-3} \text{ sec}^{-1}$ and $-42.8 \text{ cal mole}^{-1} \text{ deg}^{-1}$. Corresponding values for the unbranched system adipic acid–diethylene glycol are 293×10^{-4} , 11.15 , 97.4×10^{-3} and -36.2 . E is therefore sensibly constant, the decrease in K_{100° for the branched system being reflected in A and may be attributed to the larger negative value of S which increases the free energy of activation.

Department of Inorganic, Physical and Industrial Chemistry,
University of Liverpool

(Received February 1962)

REFERENCES

- ¹ FLORY, P. J. *J. Amer. chem. Soc.* 1939, **61**, 3334
- ² POPE, M. T. and WILLIAMS, R. J. P. *J. chem. Soc.* **1959**, 3579
- ³ FLORY, P. J. *J. Amer. chem. Soc.* 1940, **62**, 1057
- ⁴ DAVIES, M. M. *Trans. Faraday Soc.* 1937, **33**, 331; 1938, **34**, 410
- ⁵ FLORY, P. J. *J. Amer. chem. Soc.* 1940, **62**, 2261
- ⁶ IVANOFF, N. *Bull. Soc. chim. Fr.* **1950**, 347
- ⁷ FORDYCE, R. and HIBBERT, H. *J. Amer. chem. Soc.* 1939, **61**, 1912
- ⁸ KRAEMER, E. O. and VAN NATTA, F. J. *J. phys. Chem.* 1932, **36**, 3175
- ⁹ BAKER, W. O., FULLER, C. S. and HEISS, J. H. *J. Amer. chem. Soc.* 1941, **63**, 2142

Thermodynamic Functions of Linear High Polymers

Part I—Polyoxymethylene

F. S. DAINTON, D. M. EVANS, F. E. HOARE and T. P. MELIA

An adiabatic, vacuum calorimeter has been used to determine the heat capacity of two samples of polyoxymethylene (prepared by different routes) in the temperature range 20° to 300°K. Entropy and enthalpy values have been derived for the two polymers and are listed at ten degree intervals. The entropy of polymerization, ΔS_{pc}^0 has been calculated as -41.8 ± 0.2 cal. deg.⁻¹ per CH₂O unit whereas that obtained from equilibrium pressure measurements of gaseous formaldehyde over solid polyoxymethylene is -30.7 cal. deg.⁻¹ per CH₂O unit. Possible reasons for this discrepancy are examined and suggestions are made for further work to resolve it.

VALUES of the heat capacity of linear high polymers over a temperature range extending from room temperature down to as close to absolute zero as may be attained have considerable topical interest. In the first place they may serve to indicate the temperature regions of second order transitions. Secondly, in certain cases, polymers can now be made with varying degrees of crystallinity and therefore some estimate might become possible of the relation between residual entropy and crystallinity and hence, subsequently, heat capacity data might be used to indicate configurational or other changes induced by mechanical working or other polymer treatments. Thirdly, non-calorimetric methods based on the Second Law, such as 'ceiling temperature studies', have become increasingly available¹ (The reference list follows Part VIII.) and the standard entropies of many monomers are either known or readily calculable so that a comparison of the Second Law entropy of polymerization with the Third Law value becomes possible.

Some years ago we decided to construct an adiabatic, vacuum calorimeter for measurement of heat capacities in the range 20° to 300°K and much preliminary work was carried out by T. R. E. Devlin and D. R. Hulbert whose help we gratefully acknowledge. In this series of papers we describe the data concerning the heat capacities of some linear high polymers obtained with this calorimeter and the values of certain derived thermodynamic functions. In this paper we are concerned with polyoxymethylene which can be made by the polymerization of either formaldehyde (H.CHO) or its cyclic trimer (C₃H₆O₃) and which is thought to be a simple unbranched polymer in which the repeat unit is —CH₂—O—.

EXPERIMENTAL

Calorimeter

The calorimeter is of the adiabatic, vacuum type closely resembling that of Scott *et al.*² Temperature measurements were made with a platinum

resistance thermometer ($R_0=92$ ohms) calibrated above 90°K at fixed points on the International Temperature Scale³. Below 90°K the thermometer was calibrated at numerous temperatures against a thermometer C3 kindly lent to us by Dr L. A. K. Staveley, which had been calibrated against one owned by Dr J. G. Aston of Pennsylvania State University.

Heat capacity measurements

Before sealing the calorimeter each sample was degassed for two days to remove air and moisture. A small quantity of helium gas, sufficient to give a pressure of 100 mm of mercury at room temperature, was sealed in the calorimeter and served to accelerate thermal equilibration during the experiments. Heat capacity measurements were made over the range 20° to 300°K , the temperature increments being varied from 2° at the lowest temperatures to about 12° at room temperature. The rate of temperature rise was varied from 0.2° to 2° per minute. This did not appear to affect the heat capacity value. At the end of a heating period the temperature was generally recorded six to seven minutes after the calorimeter heater had been switched off (this being the time taken by simple compounds such as benzoic acid to reach temperature equilibrium). Although this procedure will lead to a decrease in the precision of the measurements over the temperature ranges in which temperature drifts occur, the general nature of the heat capacity curve is believed to be preserved. Except in the region of the glass transition temperature, curvature corrections⁴ were negligible.

Reliability of the heat capacity measurements

To assess the accuracy of the experimental method measurements were made on a sample of thermochemically pure benzoic acid (B.D.H.). The heat capacity of this substance has been accurately measured by Furukawa, McCoskey and King⁵. Over most of the temperature range from 20° to 300°K the difference between our smoothed values and those of Furukawa *et al.* did not exceed 0.3 per cent. Between 273° and 300°K our values were about 0.5 per cent larger than theirs. This increased discrepancy may be associated with the slight deterioration in the vacuum which occurred at temperatures above 273°K .

Materials

A commercial research sample of Delrin, coded B-5622, was kindly given by E. I. Du Pont de Nemours, U.S.A. It is a thermally stable, high molecular weight polyoxymethylene ($DP=1500$) thermally stabilized by ester groups. More detailed information concerning polymers of this type can be found in refs. 6 to 11. The sample was used in the form of small, cylindrical pellets about 2 mm^3 (as supplied). The weight of the sample used was 46.032 g.

Trioxan copolymer was a stabilized commercial sample prepared by the polymerization of trioxan and was in the form of a fine powder. The weight of sample used was 22.198 g.

RESULTS

The observed values of the heat capacity (shown in *Figures 1* and *2*) were smoothed graphically and the smoothed values, together with the derived

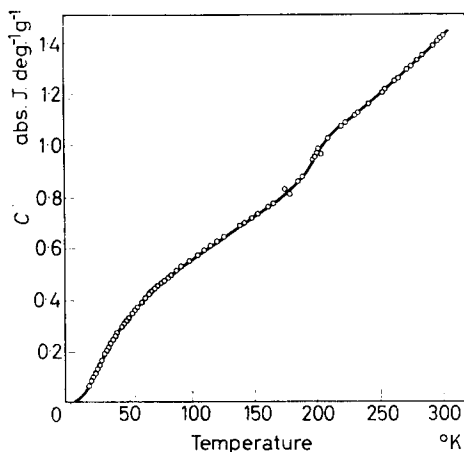


Figure 1—Observed heat capacities of Delrin

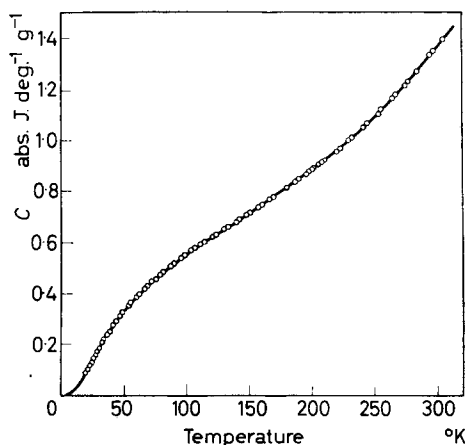


Figure 2—Observed heat capacities of trioxan copolymer

values of the entropy and enthalpy, are given in *Tables 1* and *2*. For both samples the heat capacity values below 22°K were obtained by fitting a Debye function of the form

$$C = Af_D(\theta_D/T)^*$$

where C is the heat capacity, and A and θ_D are constants for each polymer, to the data at 22°, 24° and 26°K. This function which can be evaluated from the tables of Debye functions prepared by Beattie¹², was then used

*This equation has no significance except for the extrapolation of heat capacity data.

Table 1. Smoothed values of the heat capacity, enthalpy and entropy of Delrin

| Temp. °K | C (abs.J.deg. ⁻¹ g ⁻¹) | $H_T^0 - H_0^0$ (abs.J.g ⁻¹) | $S_T^0 - S_0^0$ (abs.J.deg. ⁻¹ g ⁻¹) |
|-------------|--|---|--|
| 0 | 0 | 0 | 0 |
| 10 | 0·0120 | 0·0372 | 0·0045 |
| 20 | 0·0806 | 0·4434 | 0·0300 |
| 30 | 0·1783 | 1·748 | 0·0810 |
| 40 | 0·2608 | 3·942 | 0·1439 |
| 50 | 0·3310 | 6·909 | 0·2097 |
| 60 | 0·3902 | 10·52 | 0·2755 |
| 70 | 0·4393 | 14·68 | 0·3394 |
| 80 | 0·4810 | 19·29 | 0·4009 |
| 90 | 0·5208 | 24·30 | 0·4599 |
| 100 | 0·5558 | 29·69 | 0·5167 |
| 110 | 0·5882 | 35·41 | 0·5712 |
| 120 | 0·6197 | 41·45 | 0·6237 |
| 130 | 0·6530 | 47·81 | 0·6746 |
| 140 | 0·6892 | 54·52 | 0·7243 |
| 150 | 0·7227 | 60·98 | 0·7730 |
| 160 | 0·7547 | 68·97 | 0·8207 |
| 170 | 0·7891 | 76·69 | 0·8674 |
| 180 | 0·8325 | 84·79 | 0·9137 |
| 190 | 0·8856 | 93·36 | 0·9601 |
| 200 | 0·9598 | 102·6 | 1·007 |
| 210 | 1·025 | 112·5 | 1·056 |
| 220 | 1·069 | 123·0 | 1·104 |
| 230 | 1·112 | 133·9 | 1·153 |
| 240 | 1·156 | 143·6 | 1·201 |
| 250 | 1·199 | 157·0 | 1·249 |
| 260 | 1·242 | 169·2 | 1·297 |
| 270 | 1·285 | 181·9 | 1·345 |
| 280 | 1·330 | 194·9 | 1·392 |
| 290 | 1·377 | 208·5 | 1·440 |
| 300 | 1·425 | 222·5 | 1·487 |

to evaluate the heat capacity at lower temperatures. The values assigned to A and θ_D are shown in *Table 3*.

DISCUSSION

Figure 1 shows a pronounced change in the slope of the C/T curve in the 190°K region. This is probably related to the much more pronounced break in the heat capacity curves observed with rubber¹³, polybutadiene¹⁴ and other polymers in the temperature range of the glass transition. Further evidence in favour of this interpretation is provided by brittle point⁶ and internal friction⁶ measurements which indicate the presence of a glass transition in this region.

Rather surprisingly *Figure 2* which relates to the trioxan copolymer shows no evidence for the existence of a glass transition in the 200°K region. Since the glass transition in semicrystalline polymers is characteristic of the amorphous phase we are led to the conclusion that the polyoxymethylene formed from trioxan has a higher degree of crystallinity than Delrin. This

THERMODYNAMIC FUNCTIONS OF LINEAR HIGH POLYMERS—I

Table 2. Smoothed values of the heat capacity, enthalpy and entropy of trioxan copolymer

| Temp. °K | C (<i>abs. J. deg.⁻¹ g⁻¹</i>) | $H_T^0 - H_0^0$ (<i>abs. J. g⁻¹</i>) | $S_T^0 - S_0^0$ (<i>abs. J. deg.⁻¹ g⁻¹</i>) |
|-------------|--|--|--|
| 0 | 0 | 0 | 0 |
| 10 | 0.0134 | 0.0348 | 0.0047 |
| 20 | 0.0847 | 0.4827 | 0.0327 |
| 30 | 0.1749 | 1.794 | 0.0842 |
| 40 | 0.2601 | 3.964 | 0.1463 |
| 50 | 0.3320 | 6.948 | 0.2123 |
| 60 | 0.3890 | 10.55 | 0.2780 |
| 70 | 0.4334 | 14.67 | 0.3414 |
| 80 | 0.4723 | 19.20 | 0.4019 |
| 90 | 0.5105 | 24.12 | 0.4597 |
| 100 | 0.5461 | 29.40 | 0.5153 |
| 110 | 0.5809 | 35.04 | 0.5690 |
| 120 | 0.6152 | 41.02 | 0.6211 |
| 130 | 0.6483 | 47.33 | 0.6716 |
| 140 | 0.6815 | 53.98 | 0.7209 |
| 150 | 0.7139 | 60.96 | 0.7690 |
| 160 | 0.7472 | 68.26 | 0.8161 |
| 170 | 0.7805 | 75.90 | 0.8624 |
| 180 | 0.8141 | 83.87 | 0.9080 |
| 190 | 0.8493 | 92.19 | 0.9529 |
| 200 | 0.8846 | 100.9 | 0.9974 |
| 210 | 0.9230 | 109.9 | 1.041 |
| 220 | 0.9629 | 119.3 | 1.085 |
| 230 | 1.005 | 129.2 | 1.129 |
| 240 | 1.049 | 139.4 | 1.173 |
| 250 | 1.094 | 150.1 | 1.216 |
| 260 | 1.144 | 161.3 | 1.260 |
| 270 | 1.196 | 173.0 | 1.304 |
| 280 | 1.250 | 185.2 | 1.349 |
| 290 | 1.308 | 198.0 | 1.394 |
| 300 | 1.369 | 211.4 | 1.439 |

interpretation is supported by the internal friction measurements of McCrum and Sinnott (see ref. 6) on polyoxymethylenes of differing degrees of crystallinity. They observed a pronounced lowering of the 'glass peak' as the crystallinity of the polymer was increased from 65 to 80 per cent.

The values obtained for the entropies of the two semicrystalline, solid polymers at 25°C are 10.61 (Delrin) and 10.27 (trioxan copolymer) cal. deg.⁻¹ per CH₂O unit. The entropy of polymerization ΔS_{ur}^0 can be obtained by subtracting the entropy of the gaseous monomer at 25°C¹⁵ (52.26 cal. deg.⁻¹ mole⁻¹) from the entropy of the solid polymer at the same temperature. The values obtained are -41.65 (Delrin) and -41.99

Table 3

| Sample | A | θ_D |
|-------------------|-------|------------|
| Delrin | 0.422 | 140 |
| Trioxan copolymer | 0.370 | 129 |

(trioxan copolymer) cal. deg.⁻¹ per CH₂O unit. There is a serious discrepancy between these values and that of -30.66 cal. deg.⁻¹ per CH₂O unit obtained from equilibrium pressure measurements by Dainton, Ivin and Walmsley¹⁶. The entropy of the solid polymer based on the Dainton, Ivin and Walmsley value is 21.60 cal. deg.⁻¹ per CH₂O unit.

In an attempt to decide which of these two values for ΔS_{oc}^0 is correct a number of semi-empirical methods have been used to estimate this quantity. The methods employed are discussed below.

Comparison of the heat capacity and Third Law entropy of a number of polymers at 25°C (Table 4) shows that they are almost equal. On this basis and taking C (25°C) as determined either by us or by Dainton, Ivin and Walmsley¹⁶ the entropy of the solid polymer is clearly more likely to be the calorimetric than the equilibrium pressure value.

Table 4. Comparison of heat capacity and entropy at 25°C

| Polymer | $C_{p, 298}^0$ (cal. deg. ⁻¹ g ⁻¹) | S_{298}^0 (cal. deg. ⁻¹ g ⁻¹) | $\frac{S}{C}$ |
|--------------------------------|--|---|---------------|
| Polystyrene | 0.293 | 0.310 | 1.06 |
| Buta-1,3-diene | 0.467 | 0.488 | 1.04 |
| Natural rubber | 0.450 | 0.452 | 1.00 |
| Butadiene-styrene copolymer | 0.462 | 0.470 | 1.02 |
| Hycar. O.R. rubber | 0.471 | 0.417 | 0.88 |
| Polyethylene (79% crystalline) | 0.443 | 0.418 | 0.94 |
| Polyoxymethylene (Delrin) | 0.338 | 0.353 | 1.04 |
| (Trioxan copolymer) | 0.326 | 0.342 | 1.05 |
| Polypropylene | 0.441 | 0.398 | 0.90 |
| Propene polysulphone | 0.277 | 0.303 | 1.09 |
| But-1-ene polysulphone | 0.292 | 0.310 | 1.06 |
| Hex-1-ene polysulphone | 0.338 | 0.356 | 1.05 |
| Penton | 0.276 | 0.293 | 1.06 |

Dainton and Ivin¹ have analysed ΔS_{oo}^0 in terms of the component entropy changes, translational, internal and external rotational, and vibrational. For simple monomers, e.g. ethylene, S_{tr}^0 , S_v^0 , S_{ir}^0 and S_r^0 may be calculated from standard formulae. For polymers it is found that $S_v^0 + S_{tr}^0 \gg S_{ir}^0 + S_r^0$ regardless of molecular shape, therefore $S_{tr}^0 + S_r^0$ may be neglected. Calculations for ethylene, isobutene and styrene¹ show that on polymerization the loss of external rotational entropy mainly balances the gain in vibrational and internal rotational entropy so that $-\Delta S_{oo}^0$ has a value quite close to the translational entropy of the monomer.

For gaseous formaldehyde at 25°C the translational entropy¹⁷ is 36.13 cal. deg.⁻¹ mole⁻¹ and $-\Delta S_{oo}^0$ is probably close to this. The value in which we are interested is ΔS_{oc}^0 ; the two values are related by the equation

$$\Delta S_{oc}^0 = \Delta S_{oo}^0 - \Delta S_v - \Delta S_f$$

where ΔS_f and ΔS_v represent the entropies of fusion and vaporization respectively. For polythene¹ $\Delta S_v + \Delta S_f = 7$ cal. deg.⁻¹ per C₂H₄ unit, and assuming the sum of the two entropy changes is the same for polyoxymethylene we obtain a value of -43.1 cal. deg.⁻¹ per CH₂O unit for ΔS_{oc}^0 , again in good agreement with the calorimetric value.

We have also measured the heat capacity of low-pressure semicrystalline polythene in the range 20° to 300°K¹⁸. The value obtained for the entropy of solid polythene at 25°C is 11.80 cal. deg.⁻¹ per C₂H₄ unit. For the replacement of CH₂ by O, Small¹⁹ has compared the entropies of ten ethers, esters, aldehydes and ketones, for which reliable data exist, with those of the parent hydrocarbon. He finds that in general the entropy of the parent hydrocarbon exceeds that of the corresponding oxygen-containing compound by approximately 1 cal. deg.⁻¹ mole⁻¹. If we regard polythene as the parent hydrocarbon from which polyoxymethylene is derived, a value of 10.8 cal. deg.⁻¹ per CH₂O unit is predicted for the entropy of the solid polymer at 25°C.

The above considerations lead us to the conclusion that the value obtained for ΔS_{gr}^0 by combining the Third Law entropy of the polymer with the spectroscopic entropy of the monomer is essentially correct, whilst that obtained from the equilibrium pressure measurements is not.

Several possible explanations of the discrepancy can be suggested:

(1) The vapour phase in equilibrium with the solid polyoxymethylene does not consist of just monomeric formaldehyde but a complex mixture of polymers of low molecular weight, e.g. dimer, trimer, etc. and water. Some preliminary mass spectrometric investigations of the vapour phase over solid polymers, by Lauder²⁰, indicate the presence of molecules of mass number up to 90 in the vapour phase. In addition, vapour density measurements on formaldehyde vapour at 135°C²¹ give values at least ten per cent higher than the ideal value for CH₂O, i.e. 30. Both these experiments indicate that the vapour phase in equilibrium with polyoxymethylene is not so simple and straightforward as Dainton, Ivin and Walmsley and many other investigators have supposed it to be.

(2) The vapour phase may contain a considerable amount of water due to the high reversibility of the first step of the reaction scheme shown below:



This interpretation has been used by Illiceto and Bezzi²² to explain their data on the equilibrium pressure of formaldehyde and water over aqueous solutions of formaldehyde. A formally similar problem has been treated by Tobolsky and Eisenberg²³. This concerns the polymerization of caprolactam (M) in the presence of initiator (X). Tobolsky and Eisenberg are able to interpret existing data for this polymerization in terms of the equilibria (3) and (4):



They attribute the high concentration of free initiator in the system at equilibrium to the high reversibility of the first step (3) in comparison with subsequent steps. The absence of peaks at or around mass number 18 in the mass spectrometric scan of the vapour phase by Lauder contradicts the above explanation.

(3) A first order transition may occur between 25°C, the temperature of the calorimetric value, and 80°C, the mean temperature of the equilibrium measurements. Such a transition would have to involve an improbably large entropy change to account for the major part of the discrepancy. However, it is worth noting that internal friction⁶, dynamic mechanical²⁴ and dielectric loss²⁴ measurements all indicate the occurrence of a crystal disordering process in this temperature range.

Further work is obviously needed to resolve the discrepancy which the present work has revealed. In particular the equilibrium pressure measurements should be repeated with the aid of some instrument such as the mass spectrometer thereby allowing the composition as well as the pressure of the gaseous phase to be measured at a particular temperature. In addition, in view of the greater accuracy now demanded of thermochemical data, the heat of formation of formaldehyde should be re-determined.

Part II—Thermodynamic Functions of Penton

F. S. DAINTON, D. M. EVANS, F. E. HOARE and T. P. MELIA

The heat capacity of 3,3-bis(chloromethyl)oxacyclobutane and its polymer have been measured in the temperature range 20° to 310°K. Entropy and enthalpy values have been derived for the monomer and polymer and are listed at ten degree intervals. The melting of 3,3-bis(chloromethyl)oxacyclobutane has also been studied under equilibrium conditions and values for the heat and entropy of fusion, the purity, and the melting temperature have been determined. The glass transition temperature of the polymer was found to be 278°K, the melting point of the monomer is 19°C and at 25°C $\Delta S_{lc}^0 = 19.85 \pm 0.24$ cal. deg.⁻¹ mole⁻¹, S^0 (monomer) = 65.25 ± 0.12 and S^0 (polymer) = 45.40 ± 0.12 cal. deg.⁻¹ mole⁻¹.

CONSIDERABLE interest and importance are attached to the effects of monomer structure on heats and entropies of polymerization¹. 3,3-Bis(chloromethyl)oxacyclobutane is a readily polymerizable cyclic ether forming a semicrystalline polymer²⁵.

The present work was undertaken with three aims: (1) to determine the Third Law entropy of polymerization from heat capacity measurements on the monomer and polymer, and to use this value in conjunction with the measured heat of polymerization²⁶ to evaluate the free energy of polymerization, (2) to study the glass transition which occurs in the polymer and compare the value obtained for the glass transition temperature (T_g) with that obtained by other methods²⁷, (3) to measure the heat and entropy of fusion of the monomer.

EXPERIMENTAL

Heat capacity measurements

The apparatus and method used were the same as those described previously²⁸.

Materials

Both monomer and polymer used in the present work were given by I.C.I. (Plastics Division). The monomer had the following physical properties: melting point 18.9°C; d_{25}^{25} 1.2951; n^{20} 1.4858. The weight of sample used was 64.655 g.

The polymer (trade name 'Penton'), made by the Hercules Powder Co., U.S.A. was used as supplied in the form of small pellets about 3 mm³. The weight of sample used was 42.361 g.

RESULTS

The observed values of the heat capacity are plotted against temperature in *Figures 3* and *4*. The smoothed values of the heat capacity together with the derived entropy and enthalpy values are recorded in *Tables 5* and *6*. The

extrapolated values of the heat capacity below 22°K were obtained by the method described previously²⁸.

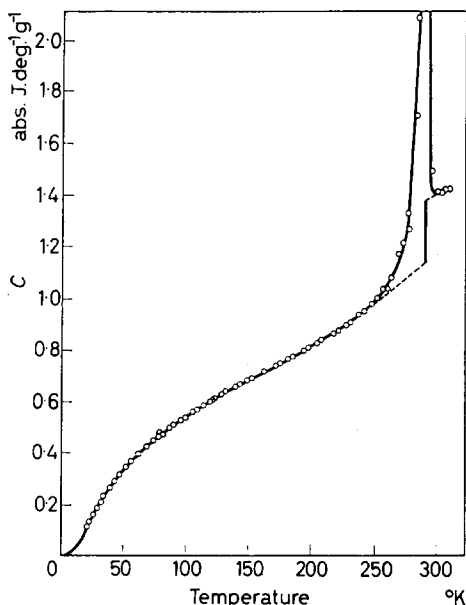


Figure 3—Observed heat capacities of 3,3-bis-(chloromethyl)oxacyclobutane

Since a considerable amount of pre-melting occurs in the monomer at temperatures above 250°K the smoothed values of the heat capacity shown in *Table 5* were corrected for pre-melting by extrapolating the data for the

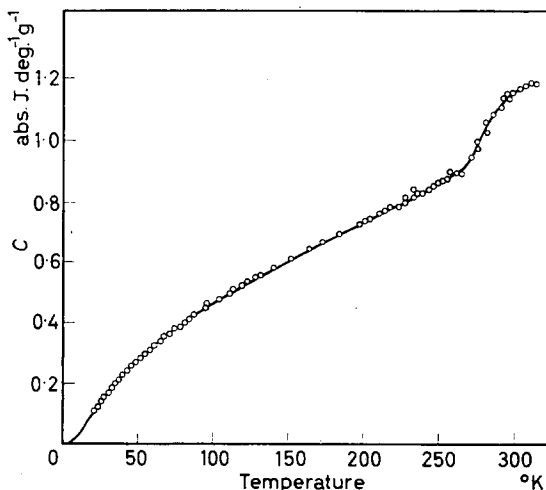


Figure 4—Observed heat capacities of Penton

THERMODYNAMIC FUNCTIONS OF LINEAR HIGH POLYMERS—II

Table 5. Smoothed values of the heat capacity, enthalpy and entropy of 3,3-bis(chloromethyl)oxacyclobutane

| Temp. °K | C (abs.J.deg. ⁻¹ g ⁻¹) | S _T ⁰ - S ₀ ⁰ (abs.J.deg. ⁻¹ g ⁻¹) | H _T ⁰ - H ₀ ⁰ (abs.J.g ⁻¹) |
|-----------------------------|--|--|---|
| 0 | 0 | 0 | 0 |
| 10 | 0·0160 | 0·0054 | 0·0412 |
| 20 | 0·0975 | 0·0382 | 0·5639 |
| 30 | 0·1910 | 0·0960 | 2·033 |
| 40 | 0·2691 | 0·1619 | 4·331 |
| 50 | 0·3351 | 0·2294 | 7·362 |
| 60 | 0·3876 | 0·2953 | 10·99 |
| 70 | 0·4307 | 0·3584 | 15·09 |
| 80 | 0·4695 | 0·4182 | 19·59 |
| 90 | 0·5069 | 0·4759 | 24·47 |
| 100 | 0·5415 | 0·5312 | 29·72 |
| 110 | 0·5722 | 0·5842 | 35·29 |
| 120 | 0·6010 | 0·6353 | 41·15 |
| 130 | 0·6292 | 0·6845 | 47·31 |
| 140 | 0·6558 | 0·7321 | 53·73 |
| 150 | 0·6825 | 0·7783 | 60·43 |
| 160 | 0·7090 | 0·8232 | 67·38 |
| 170 | 0·7356 | 0·8669 | 74·60 |
| 180 | 0·7628 | 0·9098 | 82·10 |
| 190 | 0·7905 | 0·9517 | 89·86 |
| 200 | 0·8174 | 0·9930 | 97·91 |
| 210 | 0·8461 | 1·034 | 106·2 |
| 220 | 0·8758 | 1·074 | 114·8 |
| 230 | 0·9085 | 1·113 | 123·8 |
| 240 | 0·9446 | 1·153 | 133·0 |
| 250 | 0·9858 | 1·192 | 142·7 |
| Extrapolated data for solid | | | |
| 260 | 1·027 | 1·232 | 152·7 |
| 270 | 1·066 | 1·271 | 163·2 |
| 280 | 1·106 | 1·311 | 174·1 |
| 290 | 1·145 | 1·350 | 185·3 |
| Liquid | | | |
| 300 | 1·411 | 1·770 | 308·1 |
| 310 | 1·435 | 1·816 | 322·3 |

solid from 250°K to the melting point. For this purpose the gross heat capacity of the monomer, calculated by means of the equation

$$C = (C_s - C_e + E) / (M_s - M_e)$$

where C_s is the gross heat capacity of the calorimeter plus sample, C_e is the heat capacity of the empty calorimeter, M_s and M_e are the weights respectively of the calorimeter full and empty, and E is a small correction term for the different weights of grease and Wood's metal used in the two sets of measurements, should be converted to the quantity $C_{\text{sat.}}$, in order to allow for the fact that the gross heat capacity, C , includes some heat of vaporization. This correction can be carried out by means of the equation²⁹

$$C_{\text{sat.}} = C - \frac{T}{M} \frac{d}{dT} \left\{ (V - Mv_0) \frac{dP}{dT} \right\}$$

Table 6. Smoothed values of the heat capacity, enthalpy and entropy of Penton

| Temp. °K | C (abs.J.deg. ⁻¹ g ⁻¹) | S _T ⁰ - S ₀ ⁰ (abs.J.deg. ⁻¹ g ⁻¹) | H _T ⁰ - H ₀ ⁰ (abs.J.g ⁻¹) |
|-------------|--|--|---|
| 0 | 0 | 0 | 0 |
| 10 | 0.0206 | 0.0078 | 0.0641 |
| 20 | 0.1016 | 0.0448 | 0.6445 |
| 30 | 0.1718 | 0.1001 | 2.042 |
| 40 | 0.2273 | 0.1573 | 4.034 |
| 50 | 0.2756 | 0.2132 | 6.561 |
| 60 | 0.3194 | 0.2674 | 9.528 |
| 70 | 0.3589 | 0.3196 | 12.92 |
| 80 | 0.3960 | 0.3700 | 16.70 |
| 90 | 0.4309 | 0.4187 | 20.83 |
| 100 | 0.4643 | 0.4656 | 25.31 |
| 110 | 0.4961 | 0.5116 | 30.12 |
| 120 | 0.5261 | 0.5561 | 35.23 |
| 130 | 0.5542 | 0.5993 | 40.63 |
| 140 | 0.5810 | 0.6414 | 46.31 |
| 150 | 0.6063 | 0.6823 | 52.25 |
| 160 | 0.6317 | 0.7223 | 58.44 |
| 170 | 0.6562 | 0.7613 | 64.88 |
| 180 | 0.6818 | 0.7995 | 71.57 |
| 190 | 0.7070 | 0.8370 | 78.51 |
| 200 | 0.7342 | 0.8740 | 85.72 |
| 210 | 0.7602 | 0.9104 | 93.19 |
| 220 | 0.7863 | 0.9464 | 100.9 |
| 230 | 0.8133 | 0.9820 | 108.9 |
| 240 | 0.8359 | 1.017 | 117.2 |
| 250 | 0.8608 | 1.052 | 125.6 |
| 260 | 0.8866 | 1.086 | 134.4 |
| 270 | 0.9347 | 1.120 | 143.5 |
| 280 | 1.037 | 1.156 | 153.3 |
| 290 | 1.115 | 1.194 | 164.1 |
| 300 | 1.160 | 1.232 | 175.5 |
| 310 | 1.182 | 1.271 | 187.2 |

where $C_{\text{sat.}}$ is the heat capacity of unit mass of condensed monomer in equilibrium with its own vapour, M is the mass of the sample contained in the calorimeter, V is the total volume of the calorimeter, v_c is the specific volume of the condensed phase and P is the vapour pressure. However, the last term on the RHS is negligible for the solid and liquid (just above the melting point) because the vapour pressure is low. No attempt has been made, therefore, to apply this correction and we have assumed that $C_{\text{sat.}} = C$.

Heat of fusion of 3,3-bis(chloromethyl)oxacyclobutane

The heat of fusion of the sample was determined by measuring the energy required to heat the calorimeter and its contents from a temperature below the melting point to a temperature above it. The initial temperature was chosen so as to be below the pre-melting region. The heat of fusion was then obtained by substitution of the measured quantities in the equation

$$\Delta H_f = \Delta Q_1 - \Delta Q_2 - \Delta Q_3$$

where ΔH_f is the heat of fusion of the mass of sample contained in the calorimeter, ΔQ_1 is the total energy supplied to the calorimeter during the experiment, ΔQ_2 is the energy required to heat the calorimeter and its solid contents from the initial temperature to the melting point, and ΔQ_3 is the energy required to heat the calorimeter plus its liquid contents from the melting point to the final temperature. In computing ΔQ_2 the heat capacity data for the calorimeter plus solid contents were extrapolated from below the pre-melting region to the melting point. In this way the heat of pre-melting is included in the value obtained for the heat of fusion and errors due to pre-melting are avoided.

The results of three determinations of the heat of fusion are as follows: 109.22, 109.27, 109.28 abs.J.g⁻¹. Assigning a reasonable probable error the heat of fusion may be given as 109.3 ± 0.3 abs.J.g⁻¹.

Purity of the sample and melting point of pure 3,3-bis(chloromethyl)-oxacyclobutane

We have studied the melting of 3,3-bis(chloromethyl)oxacyclobutane under equilibrium conditions in order to determine its true melting temperature and to assess its purity. The melting point of the pure sample was determined by the method used by Douslin and Huffmann³⁰ to measure the melting point of cyclopentene and some of its alkyl substitution products. In this method the temperatures corresponding to given fractions of material in the liquid form are observed (*Table 7*). The observed temperatures are

Table 7

| % melted | 1/F | T _{obs.} °K | ΔT | N ₂ | N _{total} |
|----------|-------|----------------------|-------|----------------|--------------------|
| 36.22 | 2.761 | 291.897 | 0.263 | 0.00629 | 0.00228 |
| 51.59 | 1.938 | 291.976 | 0.184 | 0.00440 | 0.00227 |
| 66.99 | 1.493 | 292.030 | 0.130 | 0.00311 | 0.00208 |
| 82.37 | 1.214 | 292.043 | 0.117 | 0.00280 | 0.00230 |
| 97.76 | 1.023 | 292.064 | 0.096 | 0.00229 | 0.00224 |

Melting point of pure sample 292.16 ± 0.05°K
 Impurity in sample 0.22 ± 0.05 mole %
 $N_2 = 0.0239 \Delta T$

then plotted against 1/F, where F is the fraction melted, and the graph is extrapolated to 1/F = 0 to obtain the melting point of the pure sample. The value obtained is 292.16 ± 0.05°K.

Mair, Glasgow and Rossini³¹ have shown that if the impurity present in a sample is soluble in the liquid phase but insoluble in the solid phase the thermodynamic relation between the temperature of equilibrium and the impurity present in the liquid phase is (when N₂ and ΔT are small)

$$N_2 = (\Delta H_f / RT_f^2) \Delta T = K \Delta T \quad (5)$$

where N₂ denotes the mole fraction of impurity corresponding to a given fraction melted, T_f is the melting point of the pure substance in °K, ΔH_f is the heat of fusion of the major component in the pure state, ΔT = T_f - T,

where T is the given equilibrium temperature, and $K = \Delta H_f / RT^2$. The results of these calculations are shown in columns 5 and 6 of *Table 7*. The N_2 values of column 5 are those calculated using equation (5) and represent the amount of impurity present in the liquid phase. The total impurity present, obtained from the relation

$$N_{\text{total}} = K\Delta T F$$

is shown in column 6.

DISCUSSION

The heat capacity versus temperature curve for Penton shows a pronounced upward sweep in the 260°K region. This is probably associated with the onset of the glass transition which has been located in this region by other methods. In the glass transition range persistent temperature drifts were obtained of about 0.0003 deg. min⁻¹, but no attempt was made to follow them to completion, since, experience on other polymers has shown³², they are likely to persist for days and even weeks. The glass temperature reported by Sandiford²⁷ (280°K) is essentially the same as that (278°K) estimated from the present measurements, taking T_g as the half-height of the upward sweep in the heat capacity versus temperature curve.

The entropy change, ΔS_{ic}^0 , associated with the polymerization of 1 mole of liquid 3,3-bis(chloromethyl)oxacyclobutane to the solid polymer at 25°C is -19.85 ± 0.24 cal. deg.⁻¹ mole⁻¹. Substitution of this value and that obtained by Dainton, Ivin and Walmsley²⁶ for ΔH_{ic}^0 (-20.2 ± 0.2 kcal. mole⁻¹) in the equation

$$\Delta G_{ic}^0 = \Delta H_{ic}^0 - T\Delta S_{ic}^0$$

leads to a value of -14.3 ± 0.3 kcal. mole⁻¹ for the free energy of polymerization, ΔG_{ic}^0 , at 25°C. This agrees quite well with the value of -14 kcal. mole⁻¹ estimated by Dainton, Devlin and Small^{33, 19} for the free energy of polymerization of 1,1-dimethyl-substituted oxacyclobutanes. This indicates that the substitution of one hydrogen atom on each methyl group by a chlorine atom has very little effect on ΔG_{ic}^0 .

Part III—Polyethylene

F. S. DANTON, D. M. EVANS, F. E. HOARE and T. P. MELIA

Heat capacity measurements have been made on two samples of low-pressure polythene in the temperature range 20° to 300°K and on a sample of high-pressure polythene in the range 90° to 300°K. The following values have been derived for the entropies of the solid polymers at 25°C

Low-pressure $11.8 \pm 0.1 \text{ cal. deg.}^{-1} \text{ per C}_2\text{H}_4 \text{ unit}$

High-pressure $12.4 \pm 0.6 \text{ cal. deg.}^{-1} \text{ per C}_2\text{H}_4 \text{ unit}$

and these in conjunction with published heat capacity data for low-pressure polythene and values for the X-ray crystallinity of the two samples used lead to the value $11.0 \pm 0.1 \text{ cal. deg.}^{-1} \text{ per C}_2\text{H}_4 \text{ unit}$ for the entropy of 100 per cent crystalline polythene at 25°C.

POLYTHENE is a particularly suitable polymer for a thermodynamic investigation of the solid state because of the relative simplicity of its chemical constitution and the wide range of well characterized samples which are available. Although polythene from the high-pressure process is branched and of low crystallinity, new methods for synthesizing polythene at low pressures³⁴ give products which are highly crystalline and approach crystalline polymethylene in properties. This discovery, coupled with the more reliable methods now available of estimating the crystallinity of polymers, has opened up possibilities of reliable estimates of the thermodynamic properties of 100 per cent crystalline polythenes. In addition, low-pressure polythene provides a convenient starting point at which to begin our investigations of the thermal properties of stereospecific, vinyl-type polymers.

Sochava³⁵, with Trapeznikova³⁶, measured the heat capacity of polythene in the range 17° to 273°K. The sample which they used was not well characterized, the only information given being that it was a 'typical commercial product'. Since they used a glass calorimeter (in which heat transfer would be slow) and relatively small quantities of sample, their results, especially at the lowest temperatures of measurement, cannot be expected to be too accurate. They make no attempt to assess the absolute accuracy of their heat capacity data but they do point out that above 58°K the spread of the experimental values does not exceed 1.5 per cent. No indication is given of the precision of their data below this temperature. Dole *et al.*^{37, 38} have measured the heat capacity of different samples of polythene from 250°K to temperatures above the melting point. Their results are presented in *Figure 8*.

In the present work heat capacity measurements have been made in the range 20° to 310°K on polythenes of known crystallinity (X-ray) and the derived entropies of the solid polymers have been used to obtain reliable estimates of the entropies of 100 per cent crystalline polythenes.

EXPERIMENTAL

Heat capacity measurements

The apparatus and method used have been described previously²⁸.

Materials

The 'Rigidex 50' and 'W.N.C.18' polythene samples were kindly given by I.C.I. (Plastics Division) and the 'Marlex 50' by the General Electric Co. Research Laboratory.

'Rigidex 50' is a low-pressure polythene of density 0.964, melt flow index 5.11, X-ray crystallinity 79 per cent and ash content < 0.01 per cent. Spectrographic analysis showed the ash consists essentially of titanium and calcium with traces of lead, chromium and aluminium.

'W.N.C.18' is a high-pressure polythene of density 0.921, melt flow index 6.87 and X-ray crystallinity 58 per cent. The material contains about 0.1 to 0.2 per cent risella oil, a hydrocarbon about C₂₀ with one double bond, which is indistinguishable from low molecular weight polythene and therefore no attempt was made to remove it.

'Marlex 50' is a low-pressure polythene manufactured by the Phillips Petroleum Co., U.S.A. It consists mainly of unbranched polymethylene chains terminated at one end in a vinyl group and at the other in a methyl group. The X-ray crystallinity is 79 per cent and the infra-red crystallinity 78 per cent.

The samples were used in the form of small pellets about 3 mm³ (as supplied). The masses of samples investigated were: 'Rigidex 50' 31.571g; 'Marlex 50' 31.912 g; 'W.N.C. 18' 20.765 g.

RESULTS

The observed values of the heat capacity are plotted against temperature in *Figures 5, 6 and 7*. The smoothed values of the heat capacity, together with the derived values of the entropy and enthalpy for 'Rigidex 50' and 'Marlex 50', are given in *Tables 8, 9 and 10*. For 'Rigidex 50' and 'Marlex 50' the values of the heat capacity below 22°K were obtained by extrapolation, using the Debye functions²⁸:

$$\begin{aligned} C &= 0.415 f_D(155/T) && \text{'Rigidex 50'} \\ C &= 0.328 f_D(136/T) && \text{'Marlex 50'} \end{aligned}$$

Since the heat capacity measurements on 'W.N.C. 18' were only made in the range 90° to 310°K it was necessary to extrapolate the heat capacity data below 90°K in order to evaluate the entropy relative to 0°K. This was accomplished using the Kelley, Parks and Huffmann method³⁹. The value obtained for the entropy at 25°C is 12.4 ± 0.6 cal. deg.⁻¹ per C₂H₄ unit.

DISCUSSION

In *Table 11* are shown some of the values quoted by Sochava and Trapeznikova for the heat capacity of the polythene sample which they studied. Our data for 'Marlex 50', 'Rigidex 50' and 'W.N.C. 18', at the same temperatures, are shown for comparison.

The earlier comments on the work of Sochava and Trapeznikova make discussion of the discrepancies, which occur at the lower temperatures, unnecessary. Those which occur at higher temperatures probably arise from the different crystallinities and thermal histories of the polymer specimens.

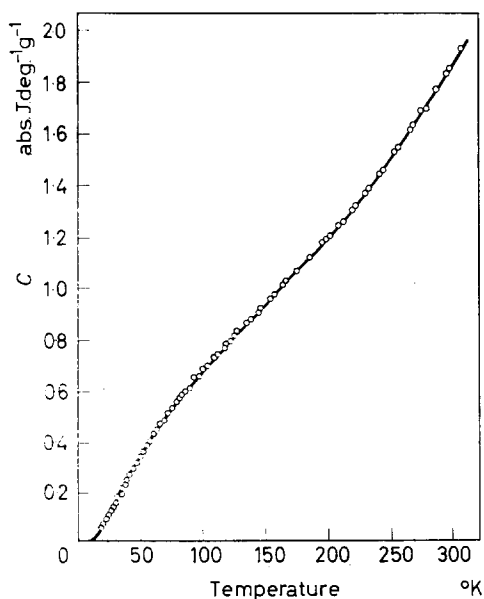
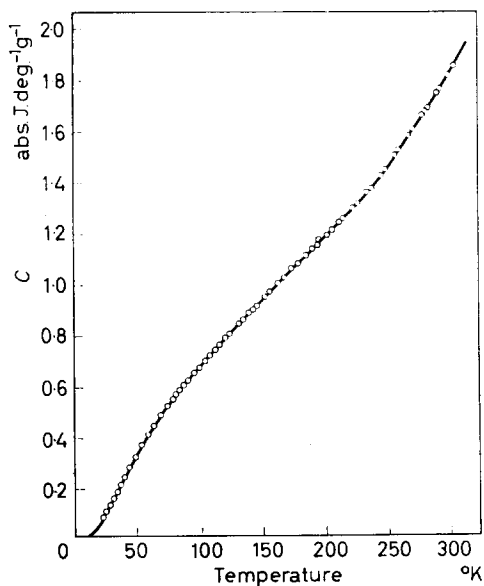


Figure 5—Observed heat capacities of 'Marlex 50' polythene

Figure 6—Observed heat capacities of 'Rigidex 50' polythene



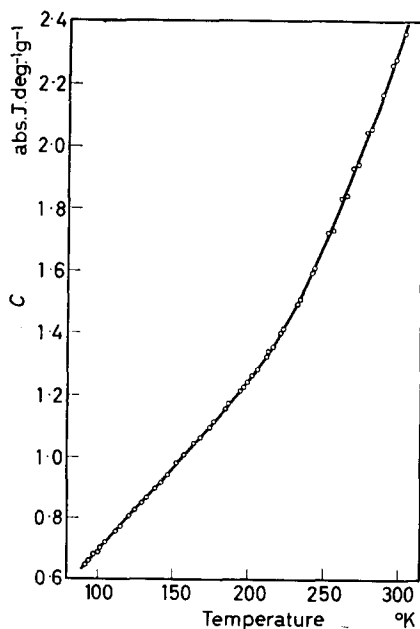


Figure 7—Observed heat capacities of 'W.N.C. 18' polythene

Dole *et al.*^{37, 38} have measured the heat capacity of both high-pressure and low-pressure polythene in the range 250° to 410°K. The various heat capacity versus temperature curves obtained by these workers together with those obtained in this work are compared in Figure 8. The small differences

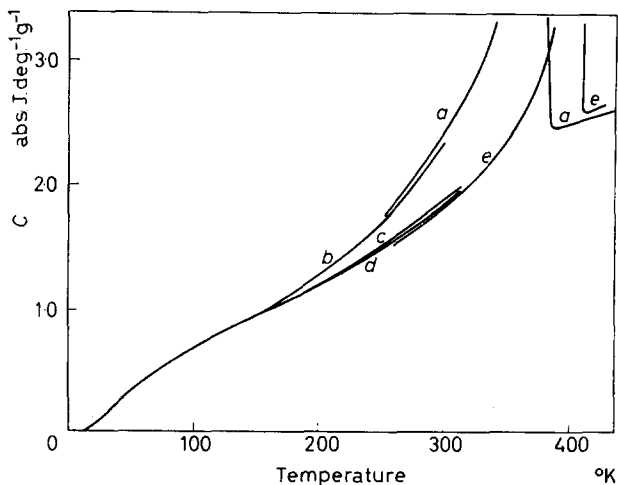


Figure 8—Comparison of heat capacity versus temperature curves for various polythene samples: (a) 'Alkathene' (Dole and Wethington³⁷), (b) 'W.N.C.18' (this work), (c) 'Marlex 50' (this work), (d) 'Rigidex 50' (this work), (e) 'Marlex 50' (Wunderlich and Dole³⁸)

THERMODYNAMIC FUNCTIONS OF LINEAR HIGH POLYMERS—III

which exist between samples prepared by similar methods, i.e. the low-pressure polythenes on the one hand and those prepared by the high-pressure process on the other, can again be considered to arise from crystal-

Table 8. Smoothed values of the heat capacity, entropy and enthalpy for 'Rigidex 50' polythene

| Temp. °K | C (abs.J.deg. ⁻¹ g ⁻¹) | $S_T^0 - S_0^0$ (abs.J.deg. ⁻¹ g ⁻¹) | $H_T^0 - H_0^0$ (abs.J.g ⁻¹) |
|-------------|--|--|---|
| 0 | 0 | 0 | 0 |
| 10 | 0.0087 | 0.0030 | 0.0224 |
| 20 | 0.0621 | 0.0223 | 0.3334 |
| 30 | 0.1462 | 0.0634 | 1.384 |
| 40 | 0.2371 | 0.1175 | 3.278 |
| 50 | 0.3328 | 0.1808 | 6.130 |
| 60 | 0.4192 | 0.2492 | 9.898 |
| 70 | 0.4939 | 0.3196 | 14.47 |
| 80 | 0.5610 | 0.3899 | 19.75 |
| 90 | 0.6240 | 0.4597 | 25.68 |
| 100 | 0.6820 | 0.5285 | 32.22 |
| 110 | 0.7356 | 0.5960 | 39.31 |
| 120 | 0.7876 | 0.6623 | 46.92 |
| 130 | 0.8394 | 0.7274 | 55.06 |
| 140 | 0.8905 | 0.7915 | 63.71 |
| 150 | 0.9423 | 0.8547 | 72.87 |
| 160 | 0.9952 | 0.9172 | 82.56 |
| 170 | 1.046 | 0.9790 | 92.77 |
| 180 | 1.096 | 1.040 | 103.5 |
| 190 | 1.145 | 1.101 | 114.7 |
| 200 | 1.195 | 1.161 | 126.4 |
| 210 | 1.247 | 1.220 | 138.6 |
| 220 | 1.300 | 1.280 | 151.3 |
| 230 | 1.355 | 1.339 | 164.6 |
| 240 | 1.415 | 1.397 | 178.4 |
| 250 | 1.484 | 1.457 | 192.9 |
| 260 | 1.560 | 1.516 | 208.2 |
| 270 | 1.636 | 1.577 | 224.1 |
| 273.15 | 1.660 | 1.596 | 229.3 |
| 280 | 1.713 | 1.637 | 240.9 |
| 290 | 1.791 | 1.699 | 258.4 |
| 298.15 | 1.855 | 1.749 | 273.3 |
| 300 | 1.869 | 1.761 | 276.7 |
| 310 | 1.950 | 1.824 | 295.8 |

linity and thermal history effects. The correlation between thermal properties and crystallinity is emphasized by the data of Table 12.

For both the low-pressure and high-pressure polythenes the more crystalline polymers are seen to have both a lower heat capacity and a lower entropy. This is expected since the heat capacity of the amorphous polythene (and hence the entropy) would be expected to be greater than that of the crystalline solid. It can also be seen from Figure 8 that the heat capacity versus temperature curves converge as the temperature falls. This tendency is so pronounced that below 140°K the curves for the different

polythenes are virtually indistinguishable. Whether or not they remain so down to the very lowest temperatures is open to question. Unfortunately, the measurements on 'W.N.C. 18' were not extended below 90°K, so the trend shown by the results of Sochava and Trapeznikova cannot be checked.

Table 9. Smoothed values of the heat capacity, entropy and enthalpy for 'Marlex 50' polythene

| Temp. °K | C (<i>abs.J.deg.⁻¹g⁻¹</i>) | $S_T^0 - S_0^0$ (<i>abs.J.deg.⁻¹g⁻¹</i>) | $H_T^0 - H_0^0$ (<i>abs.J.g⁻¹</i>) |
|-------------|---|---|--|
| 0 | 0 | 0 | 0 |
| 10 | 0.0101 | 0.0035 | 0.0264 |
| 20 | 0.0668 | 0.0252 | 0.3730 |
| 30 | 0.1470 | 0.0672 | 1.446 |
| 40 | 0.2385 | 0.1216 | 3.351 |
| 50 | 0.3329 | 0.1853 | 6.234 |
| 60 | 0.4183 | 0.2534 | 9.975 |
| 70 | 0.4921 | 0.3235 | 14.54 |
| 80 | 0.5606 | 0.3938 | 19.80 |
| 90 | 0.6254 | 0.4636 | 25.74 |
| 100 | 0.6828 | 0.5325 | 32.29 |
| 110 | 0.7347 | 0.6000 | 39.37 |
| 120 | 0.7868 | 0.6662 | 46.98 |
| 130 | 0.8390 | 0.7312 | 55.11 |
| 140 | 0.8918 | 0.7953 | 63.76 |
| 150 | 0.9434 | 0.8586 | 72.94 |
| 160 | 0.9941 | 0.9211 | 82.62 |
| 170 | 1.046 | 0.9829 | 92.83 |
| 180 | 1.099 | 1.044 | 103.6 |
| 190 | 1.149 | 1.105 | 114.8 |
| 200 | 1.199 | 1.165 | 126.5 |
| 210 | 1.253 | 1.225 | 138.8 |
| 220 | 1.312 | 1.285 | 151.6 |
| 230 | 1.375 | 1.344 | 165.0 |
| 240 | 1.442 | 1.404 | 179.1 |
| 250 | 1.511 | 1.464 | 193.9 |
| 260 | 1.584 | 1.525 | 209.4 |
| 270 | 1.660 | 1.586 | 225.6 |
| 273.15 | 1.683 | 1.606 | 230.9 |
| 280 | 1.735 | 1.648 | 242.6 |
| 290 | 1.812 | 1.710 | 260.3 |
| 298.15 | 1.874 | 1.762 | 275.3 |
| 300 | 1.888 | 1.773 | 278.8 |
| 310 | 1.966 | 1.836 | 298.1 |

A particularly interesting feature of the present measurements lies in the fact that from them one can calculate an exact value for the entropy of a 100 per cent crystalline, low-pressure polythene at 25°C. In order to perform this calculation it is necessary to know both the crystallinity and entropy of fusion at 25°C. For the 'Rigidex 50' and 'Marlex 50' samples used in the present investigation the weight fraction crystallinity was estimated by a standard X-ray method.

THERMODYNAMIC FUNCTIONS OF LINEAR HIGH POLYMERS—III

The entropy of fusion was calculated as follows: Wunderlich and Dole³⁸ have represented the temperature variation of the heat of fusion and heat capacities of 'Marlex 50' by the equations:

$$\Delta H_f = 54.6 + 0.1716t - 6.36 \times 10^{-4} t^2 \text{ cal. g}^{-1} \quad (6)$$

$$C_A = 0.5455 + 5.38 \times 10^{-4} t \text{ cal. deg.}^{-1} \text{ g}^{-1} \quad (7)$$

$$C_C = 0.3739 + 1.81 \times 10^{-3} t \text{ cal. deg.}^{-1} \text{ g}^{-1} \quad (8)$$

where t is temperature ($^{\circ}\text{C}$), ΔH_f is the heat of fusion of 100 per cent crystalline 'Marlex 50', and C_A and C_C represent the heat capacities of the

Table 10. Smoothed values of the heat capacity for 'W.N.C.18' polythene

| Temp. $^{\circ}\text{K}$ | C (abs.J.deg. $^{-1}\text{g}^{-1}$) | Temp. $^{\circ}\text{K}$ | C (abs.J.deg. $^{-1}\text{g}^{-1}$) |
|-----------------------------|---|-----------------------------|---|
| 100 | 0.6840 | 210 | 1.310 |
| 110 | 0.7410 | 220 | 1.389 |
| 120 | 0.7955 | 230 | 1.479 |
| 130 | 0.8511 | 240 | 1.582 |
| 140 | 0.9055 | 250 | 1.693 |
| 150 | 0.9591 | 260 | 1.810 |
| 160 | 1.014 | 270 | 1.932 |
| 170 | 1.069 | 273.15 | 1.973 |
| 180 | 1.125 | 280 | 2.063 |
| 190 | 1.181 | 290 | 2.198 |
| 200 | 1.242 | 298.15 | 2.315 |
| | | 300 | 2.342 |

completely amorphous and 100 per cent crystalline forms, respectively. The temperature of zero enthalpy for the purpose of their calculations was arbitrarily chosen as 140°C . The entropy of fusion at 25°C , ΔS_f , can be calculated by substituting the relevant data of equations (6), (7) and (8) into equation (9)

$$\Delta S_f = \frac{\Delta H_f}{413.15} + \int_{298.15}^{413.15} \frac{(C_C - C_A)}{T} dT \quad (9)$$

The value obtained is $3.83 \text{ cal. deg.}^{-1}$ per C_2H_4 unit. For a polythene

Table 11

| Temp. $^{\circ}\text{K}$ | S.T. 35, 36 | 'Rigidex 50' | 'Marlex 50' | 'W.N.C. 18' |
|-----------------------------|-------------|--------------|-------------|-------------|
| 20 | 0.071 | 0.0621* | 0.0668* | — |
| 30 | 0.159 | 0.1462 | 0.1470 | — |
| 50 | 0.335 | 0.3328 | 0.3329 | — |
| 100 | 0.674 | 0.6820 | 0.6828 | 0.684 |
| 200 | 1.167 | 1.195 | 1.199 | 1.242 |
| 250 | 1.523 | 1.484 | 1.511 | 1.693 |

Specific heats are expressed in abs.J.deg. $^{-1}\text{g}^{-1}$.

*Extrapolated value.

sample of weight fraction crystallinity, W_c , the entropy of the 100 per cent crystalline form, $S_{100\%}$ is related to that of the semicrystalline form, S_{W_c} , by the expression

$$S_{100\%} = S_{W_c} - (1 - W_c) \Delta S_f$$

The results of these calculations for 'Rigidex 50' and 'Marlex 50' are summarized in *Table 13*. In the last column of the same table values of $-\Delta S_{oc}^0$, which were obtained by subtracting the entropy of gaseous ethylene at 25°C from that of the 100 per cent crystalline polymer, are given. The two values for $-\Delta S_{oc}^0$ compare favourably with that of 41.1 cal. deg.⁻¹ per C₂H₄ unit estimated by Dainton and Ivin¹ by the extrapolation of data for the lower members of the *n*-alkane series.

Table 12

| Sample | X-ray crystallinity % | $C_{p, 25^\circ\text{C}}$ | $S_{25^\circ\text{C}}^0$ |
|-----------------------------------|-----------------------|---------------------------|--------------------------|
| High-pressure polythene | | | |
| 'W.N.C.18' | 58 | 2.315 | 12.44 |
| 'Alkathene' | 50 | 2.352 | — |
| Low-pressure polythene | | | |
| 'Rigidex 50' | 79 | 1.855 | 11.73 |
| 'Marlex 50' (This work) | 79 | 1.874 | 11.81 |
| 'Marlex 50' (Dole <i>et al.</i>) | 92 | 1.815 | — |

Recorded values of the glass transition temperature for polythene vary widely. Early dielectric constant⁴⁰ and dilatometric⁴¹ measurements located the glass transition for samples of high-pressure polythene at -65°C and -80°C, respectively. More recent dilatometric measurements by Danusso *et al.*⁴² and Quinn and Mandelkern⁴³ place it at -21°C and these authors conclude that the earlier values were applicable only to the particular sample under investigation. In support of this view Danusso *et al.*⁴² point out that such transitions show a distinct dependence on the previous history of the sample and they quote the values -43°, -47°, -21°, -28°, -25°, -20°, -17°C which they obtained for T_g for a particular sample in a series of runs. For well annealed samples they invariably obtained reproducible results for which $T_g = -21^\circ\text{C}$.

Table 13

| Polymer | W_c | $S_{W_c, 25^\circ\text{C}}^0$ | $S_{100\%}^0$ | $-\Delta S_{oc}^0$ |
|--------------|-------|-------------------------------|---------------|--------------------|
| 'Marlex 50' | 0.79 | 11.81 | 11.01 | 41.44 |
| 'Rigidex 50' | 0.79 | 11.73 | 10.93 | 41.52 |

T_g is usually obtained from heat capacity data by finding the intersection of straight lines drawn through the derived points on an enthalpy/temperature plot above and below T_g . Unfortunately enthalpy/temperature lines show a definite curvature and with highly-crystalline polymers the magnitude of the glass transition is so small that the change in slope of the

enthalpy/temperature curve is barely detectable. A more sensitive method of locating T_g , which has been employed successfully by Dole⁴⁴, is to plot C/T as a function of temperature and take T_g as the temperature at which the rise in C/T is half the total rise.

With polythene neither of these procedures is successful, the enthalpy/temperature plot for the reason given above and the C/T versus temperature plot because it is impossible to locate a midpoint since the curve rises continuously above about 240°K.

It would appear that for highly crystalline polymers static methods are not suitable for locating the glass transition temperature and other methods, such as dynamic-mechanical or dielectric loss experiments, are preferable. For example, both dynamic mechanical⁴⁵ and n.m.r.⁴⁵ methods indicate the occurrence in polythene of a transition in the vicinity of -100°C as well as one at -20°C . The transition occurring at -100°C supposedly corresponds to either side-chain rotation (the side chains arising from chain branching effects) or the rotation of small segments of the main chain and that at -20°C to the onset of segmental motion in the main polymer chain. Whilst our specific heat measurements indicate some form of continuous devitrification above 240°K, they give no indication whatsoever concerning the transition at -100°C .

Part IV—Stereospecific Poly- α -Olefines

F. S. DAINTON, D. M. EVANS, F. E. HOARE and T. P. MELIA

The heat capacities of four stereospecific poly- α -olefines have been measured in the range 20° to 310°K. The heat capacity data yield the following values for the Third Law entropy at 25°C:

| | |
|---------------------------|---|
| Isotactic polypropylene | 17.22 ± 0.06 cal. deg. ⁻¹ mole ⁻¹ |
| Atactic polypropylene | 18.88 ± 0.19 cal. deg. ⁻¹ mole ⁻¹ |
| Isotactic poly(but-1-ene) | 24.61 ± 0.09 cal. deg. ⁻¹ mole ⁻¹ |
| Isotactic polystyrene | 31.40 ± 0.10 cal. deg. ⁻¹ mole ⁻¹ |

The entropies of the 100 per cent crystalline forms at 25°C estimated from these and X-ray crystallinity data are:

| | |
|---------------------------|---|
| Isotactic polypropylene | 14.8 ± 0.3 cal. deg. ⁻¹ mole ⁻¹ |
| Atactic polypropylene | 15.0 ± 0.4 cal. deg. ⁻¹ mole ⁻¹ |
| Isotactic poly(but-1-ene) | 20.7 ± 0.3 cal. deg. ⁻¹ mole ⁻¹ |
| Isotactic polystyrene | 30.7 ± 0.2 cal. deg. ⁻¹ mole ⁻¹ |

Isotactic and atactic polypropylene and poly(but-1-ene) exhibit glass transitions at 260°, 249° and 249°K, respectively.

FOLLOWING the discovery of stereospecific catalysts by Natta⁴⁶ a wide range of stereoregular, solid poly- α -olefines has become available. The possibility therefore exists of attempting to detect trends in thermal properties as the nature of the α -substituent and its steric configuration is changed. However, only a few of the poly- α -olefines which have been reported are available as well characterized samples large enough for our purposes.

In the series chosen as the subject of the present investigation, polypropylene, poly(but-1-ene) and polystyrene, the first two members exhibit a glass transition in the range covered by these measurements. Hence, in addition to detecting trends in thermal properties as the tacticity, crystallinity and nature of the α -substituent are changed, the effects of these different factors on the glass transition can also be studied.

EXPERIMENTAL

Heat capacity measurements

The method used has been described previously²⁸.

Materials

All the samples used in the present investigation were given by I.C.I. (Plastics Division), who also supplied the following information concerning the samples.

Isotactic polypropylene was an unstabilized sample containing no ether-soluble material. On combustion it gave 0.02 per cent ash and had an X-ray crystallinity of 48 per cent. The atactic polypropylene sample was not completely atactic. The atactic content by the infra-red (i.r.) method is 57 per cent, but this value may be slightly low, as it is based on a reference standard which is not itself completely atactic. Attempts have been made to

extract this sample with cold ether and other solvents in order to get completely atactic material, but no appreciable increase in atactic content was obtained. The crystallinity of this sample as determined by X-rays is 16 ± 4 per cent. Determinations are not very accurate at this level of crystallinity. At least half of this crystallinity is due to the isotactic polymer. Three crystalline forms of poly(but-1-ene) exist^{47, 48}. The two principal ones, Types I and II, are those described originally by Natta *et al.*⁴⁷. Type I, maximum melting point 132.5°C , is stable at room temperature and Type II, maximum melting point 118.5°C , is metastable at room temperature and changes to Type I. The powder used in the present investigations was approximately 44 per cent crystalline (X-rays) and at the date measured (15.11.1960) contained 37 per cent Type I and 7 per cent Type II and was probably still converting slowly during the measurements (completed 14.12.1960), although no evidence for this was found from the heat capacity measurements. The crystallinity measurements are not highly accurate because of the mixture of forms present. The atactic content of the sample of isotactic polystyrene as measured by an i.r. method was less than 5 per cent and probably nearer 1 per cent. It had an X-ray crystallinity of 43 per cent.

The isotactic polypropylene (small pellets, approximately 3 mm^3), poly(but-1-ene) (fine powder), and polystyrene (fine powder) samples were used as supplied. The atactic polypropylene was supplied in the form of a large block. This material was rubbery and tacky and proved difficult to cut. This difficulty was overcome by cooling the block of material in liquid nitrogen, thus taking the polymer below its glass transition temperature, and then it was shattered with a hammer. Irregular shaped pieces varying in size from about 1 mm^3 to 10 mm^3 were then used to pack the calorimeter. Many workers have commented on the difficulty experienced in removing rubbery polymers from the calorimeter at the conclusion of the measurements. However, we have found that no such difficulty presents itself if the polymer is cooled below its glass transition temperature before removal.

The weights of the samples used were: isotactic polypropylene, 29.524 g; atactic polypropylene, 23.667 g; isotactic poly(but-1-ene), 20.497 g; isotactic polystyrene, 16.145 g.

RESULTS

The measurements on the three isotactic polymers were made after they had been shock cooled to the lowest temperature attainable with the particular refrigerant. No pronounced temperature drifts were observed during the experiments on these three samples. With atactic polypropylene persistent temperature drifts were observed over long temperature ranges and consequently it was decided to subject this polymer to different cooling rates to assess the effect of this treatment on the heat capacity. The experimental details of heat treatment, temperature range of measurements, and temperature drifts are summarized in *Table 14*.

The upward temperature drifts in the region of the glass transition are similar to those observed with other amorphous polymers^{14, 50}. Their origin can be explained readily if we assume that during the cooling process some

polymer molecules fail to make the transition to the lower energy states. When the temperature reaches a certain value during the heat capacity measurements these molecules acquire sufficient thermal energy for transition to the lower energy states with the consequent liberation of heat. However, the persistent downward temperature drifts which were observed

Table 14. Heat treatments and observations with atactic polypropylene

| Run | Sample treatment | Range of temperature measurement °K | Temperature drift observations |
|-----|--|-------------------------------------|--|
| 1 | Cooled rapidly to 20°K | 20 to 45 | No drift |
| 2 | Cooled rapidly to 80°K | 80 to 200 | Downward drifts throughout |
| 3 | Cooled rapidly to 195°K | 195 to 295 | Downward drift from 195° to 230°K, upward drift from 230° to 295°K |
| 4 | Cooled rapidly to 80°K | 80 to 200 | Downward drifts throughout |
| 5 | Cooled rapidly to 195°K | 195 to 258 | Downward drift from 195° to 240°K, upward drift from 240° to 258°K |
| 6 | Cooled rapidly to 20°K | 20 to 80 | Downward drift from 40° to 80°K |
| 7 | Warmed to room temperature overnight | 295 to 314 | Downward drift from 294° to 314°K |
| 8 | Cooled slowly to 216°K overnight | 216 to 284 | Downward drift from 216° to 267°K, upward drift from 267° to 284°K |
| 9 | Cooled slowly to 211°K overnight, then rapidly to 94°K | 94 to 136 | Downward drift from 94° to 136°K |
| 10 | Cooled rapidly to 273°K | 273 to 303 | Downward drift from 273° to 303°K |

in the range 40° to 240°K, and which appeared to be independent of the rate of cooling, are more difficult to explain and are most probably associated with a heat transfer effect arising from the presence in the calorimeter of quite large pieces of sample (some were about 10 mm³). If this is so the effect has no theoretical significance and should be much reduced by the use of smaller pieces of sample. During the initial measurements the temperature drifts were followed for at least an hour. The results indicated that tempera-

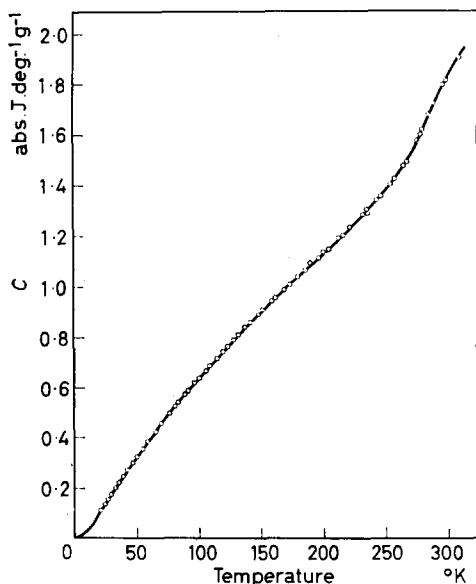


Figure 9—Observed heat capacities of isotactic polypropylene

ture equilibrium could not be attained within a reasonable length of time. Similar observations have been made on other polymers³². In subsequent measurements no attempt was made to reach temperature equilibrium (the temperature being taken seven minutes after the end of the heating period) and this did not appear to alter the general nature of the heat capacity results obtained.

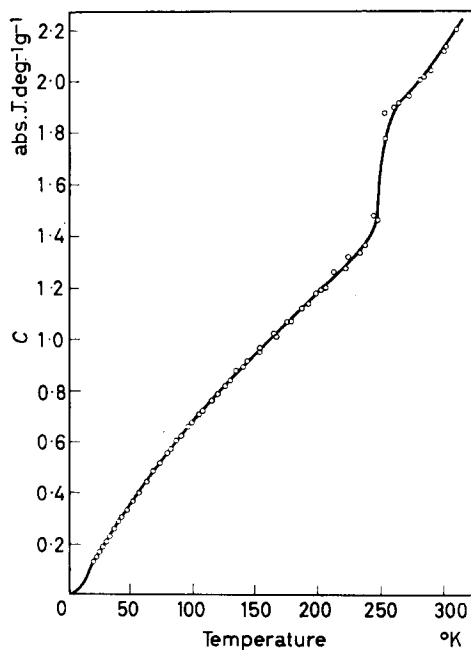


Figure 10—Observed heat capacities of atactic polypropylene

The observed values of the heat capacity are shown in *Figures 9 to 12*. These results were used to obtain the smoothed values, shown in *Tables 15 to 18*, from which were computed the enthalpy and entropy values shown in the same tables. The values of the heat capacity below 22°K were obtained using a Debye function of the form²⁸

$$C = Af_D(\theta_D/T)$$

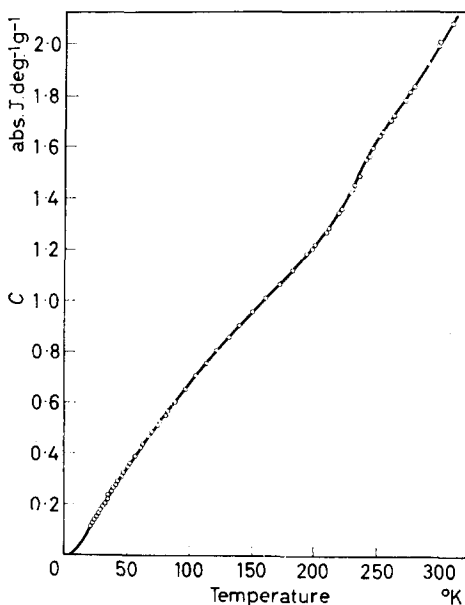
The values of the constants A and θ_D are shown in *Table 19*.

DISCUSSION

The entropy (and any other thermal property) of a polymer shows a marked dependence on the crystallinity of the samples. Hence, if the entropies of a series of polymers are to be compared it is necessary to correct them to a standard state. The standard state generally chosen is either the completely amorphous or completely crystalline form at a particular temperature. In order to apply this correction the crystallinity and entropy of fusion of the polymer must be known at the temperature in question, in this case, 25°C. For the present series of polymers the crystallinities have been determined by standard X-ray techniques. However, lack of the necessary heat capacity

data prevents the calculation of an exact value for the entropy of fusion at 25°C. This problem has been overcome by assuming that the percentage decrease in the entropy of fusion in going from the melting point to 25°C is the same as that observed for polythene⁵¹, i.e. about 20 per cent. This

Figure 11—Observed heat capacities of isotactic poly(but-1-ene)



assumption is unlikely to introduce any large errors since it involves a correction of only 1 to 2 cal. deg.⁻¹ mole⁻¹. The results of these calculations are summarized in *Table 20*. The data for 'Rigidex 50' polythene are included for comparison.

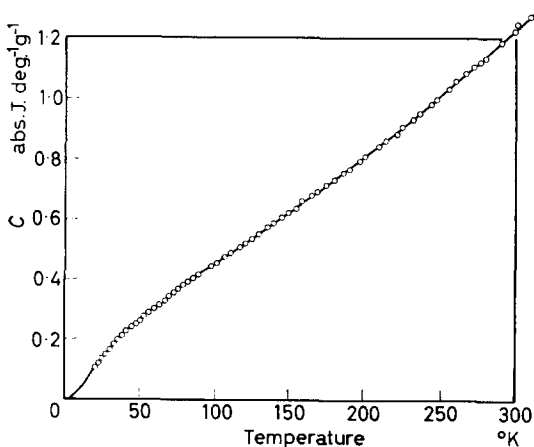


Figure 12—Observed heat capacities of isotactic polystyrene

THERMODYNAMIC FUNCTIONS OF LINEAR HIGH POLYMERS—IV

Table 15. Smoothed values of the heat capacity, entropy and enthalpy for isotactic polypropylene

| Temp. °K | C (abs.J.deg. ⁻¹ g ⁻¹) | $S_T^0 - S_0^0$ (abs.J.deg. ⁻¹ g ⁻¹) | $H_T^0 - H_0^0$ (abs.J.g ⁻¹) |
|-------------|--|--|---|
| 0 | 0 | 0 | 0 |
| 10 | 0.0175 | 0.0059 | 0.0453 |
| 20 | 0.0975 | 0.0402 | 0.5878 |
| 30 | 0.1813 | 0.0959 | 2.002 |
| 40 | 0.2568 | 0.1584 | 4.180 |
| 50 | 0.3275 | 0.2234 | 7.105 |
| 60 | 0.3935 | 0.2890 | 10.71 |
| 70 | 0.4565 | 0.3544 | 14.96 |
| 80 | 0.5190 | 0.4194 | 19.84 |
| 90 | 0.5797 | 0.4840 | 25.33 |
| 100 | 0.6397 | 0.5482 | 31.43 |
| 110 | 0.6972 | 0.6119 | 38.12 |
| 120 | 0.7520 | 0.6749 | 45.36 |
| 130 | 0.8044 | 0.7372 | 53.15 |
| 140 | 0.8541 | 0.7987 | 61.45 |
| 150 | 0.9029 | 0.8593 | 70.23 |
| 160 | 0.9507 | 0.9191 | 79.50 |
| 170 | 0.9993 | 0.9782 | 89.25 |
| 180 | 1.046 | 1.037 | 99.48 |
| 190 | 1.093 | 1.094 | 110.2 |
| 200 | 1.140 | 1.152 | 121.3 |
| 210 | 1.188 | 1.208 | 133.0 |
| 220 | 1.237 | 1.265 | 145.1 |
| 230 | 1.287 | 1.321 | 157.7 |
| 240 | 1.338 | 1.377 | 170.8 |
| 250 | 1.392 | 1.433 | 184.5 |
| 260 | 1.452 | 1.488 | 198.7 |
| 270 | 1.535 | 1.544 | 213.6 |
| 273.15 | 1.570 | 1.563 | 218.5 |
| 280 | 1.646 | 1.602 | 229.5 |
| 290 | 1.752 | 1.662 | 246.5 |
| 298.15 | 1.834 | 1.712 | 261.2 |
| 300 | 1.851 | 1.723 | 264.5 |
| 310 | 1.931 | 1.785 | 283.5 |

The experimental values of ΔS_{ic}^0 compare favourably with those estimated by Dainton and Ivin¹ using a semi-empirical method, and lend added support to their general conclusion that structure has very little effect on $-\Delta S_{ic}^0$. It is interesting to note that for both polypropylene and polystyrene the entropy ($S_{298}^0 - S_0^0$) difference between the isotactic and atactic forms, after correction for crystallinity effects, is only 0.2 cal. deg.⁻¹ mole⁻¹. This suggests that the major cause of the difference between the thermal properties of an isotactic and atactic polymer is crystallinity, rather than molecular configuration, effects.

The values estimated for the glass transition temperatures for the present series of polymers are shown in Table 21. The value for polystyrene is that obtained by Brickwedde *et al.* (see ref. 55). In all cases the T_g values were

Table 16. Smoothed values of the heat capacity, entropy and enthalpy for atactic polypropylene

| Temp. °K | C (<i>abs.J.deg.⁻¹g⁻¹</i>) | $S_T^0 - S_0^0$ (<i>abs.J.deg.⁻¹g⁻¹</i>) | $H_T^0 - H_0^0$ (<i>abs.J.g⁻¹</i>) |
|-------------|---|---|--|
| 0 | 0 | 0 | 0 |
| 10 | 0·0243 | 0·0084 | 0·0637 |
| 20 | 0·1180 | 0·0524 | 0·7552 |
| 30 | 0·2003 | 0·1164 | 2·373 |
| 40 | 0·2798 | 0·1847 | 4·755 |
| 50 | 0·3564 | 0·2554 | 7·939 |
| 60 | 0·4267 | 0·3267 | 11·86 |
| 70 | 0·4929 | 0·3975 | 16·46 |
| 80 | 0·5566 | 0·4675 | 21·71 |
| 90 | 0·6182 | 0·5366 | 27·59 |
| 100 | 0·6778 | 0·6048 | 34·07 |
| 110 | 0·7349 | 0·6721 | 41·13 |
| 120 | 0·7909 | 0·7385 | 48·76 |
| 130 | 0·8451 | 0·8040 | 56·95 |
| 140 | 0·8974 | 0·8685 | 65·66 |
| 150 | 0·9477 | 0·9322 | 74·88 |
| 160 | 0·9965 | 0·9949 | 84·61 |
| 170 | 1·044 | 1·057 | 94·81 |
| 180 | 1·091 | 1·118 | 105·5 |
| 190 | 1·137 | 1·178 | 116·6 |
| 200 | 1·184 | 1·237 | 128·2 |
| 210 | 1·231 | 1·296 | 140·3 |
| 220 | 1·279 | 1·355 | 152·8 |
| 230 | 1·327 | 1·413 | 165·9 |
| 240 | 1·385 | 1·470 | 179·4 |
| 250 | 1·708 | — | — |
| 260 | 1·901 | 1·604 | 212·8 |
| 270 | 1·952 | 1·676 | 232·1 |
| 273·15 | 1·968 | 1·699 | 238·3 |
| 280 | 2·004 | 1·748 | 251·8 |
| 290 | 2·068 | 1·819 | 272·2 |
| 298·15 | 2·129 | 1·878 | 289·3 |
| 300 | 2·145 | 1·891 | 293·3 |
| 310 | 2·229 | 1·963 | 315·1 |

THERMODYNAMIC FUNCTIONS OF LINEAR HIGH POLYMERS—IV

Table 17. Smoothed values of the heat capacity, entropy and enthalpy for isotactic poly(but-1-ene)

| Temp. °K | C (<i>abs.</i> J.deg. ⁻¹ g ⁻¹) | $S_T^0 - S_0^0$ (<i>abs.</i> J.deg. ⁻¹ g ⁻¹) | $H_T^0 - H_0^0$ (<i>abs.</i> J.g ⁻¹) |
|-------------|---|---|--|
| 0 | 0 | 0 | 0 |
| 10 | 0·0171 | 0·0059 | 0·0447 |
| 20 | 0·0965 | 0·0397 | 0·5797 |
| 30 | 0·1817 | 0·0951 | 1·988 |
| 40 | 0·2649 | 0·1587 | 4·208 |
| 50 | 0·3433 | 0·2263 | 7·268 |
| 60 | 0·4147 | 0·2954 | 11·05 |
| 70 | 0·4813 | 0·3643 | 15·53 |
| 80 | 0·5470 | 0·4329 | 20·67 |
| 90 | 0·6113 | 0·5011 | 26·47 |
| 100 | 0·6734 | 0·5687 | 32·90 |
| 110 | 0·7335 | 0·6357 | 39·93 |
| 120 | 0·7904 | 0·7020 | 47·55 |
| 130 | 0·8460 | 0·7675 | 55·74 |
| 140 | 0·8996 | 0·8322 | 64·47 |
| 150 | 0·9513 | 0·8960 | 73·73 |
| 160 | 1·002 | 0·9590 | 83·49 |
| 170 | 1·053 | 1·021 | 93·77 |
| 180 | 1·106 | 1·083 | 104·6 |
| 190 | 1·161 | 1·144 | 115·9 |
| 200 | 1·219 | 1·205 | 137·8 |
| 210 | 1·281 | 1·266 | 140·3 |
| 220 | 1·349 | 1·327 | 153·4 |
| 230 | 1·437 | 1·389 | 167·3 |
| 240 | 1·540 | 1·452 | 182·2 |
| 250 | 1·629 | 1·517 | 198·1 |
| 260 | 1·703 | 1·583 | 214·7 |
| 270 | 1·777 | 1·648 | 232·1 |
| 273·15 | 1·801 | 1·669 | 237·8 |
| 280 | 1·854 | 1·714 | 250·3 |
| 290 | 1·933 | 1·781 | 269·2 |
| 298·15 | 2·000 | 1·835 | 285·3 |
| 300 | 2·016 | 1·848 | 289·0 |
| 310 | 2·101 | 1·915 | 309·6 |

Table 18. Smoothed values of the heat capacity, entropy and enthalpy for isotactic polystyrene

| Temp. °K | C (<i>abs.J.deg.⁻¹g⁻¹</i>) | $S_T^0 - S_0^0$ (<i>abs.J.deg.⁻¹g⁻¹</i>) | $H_T^0 - H_0^0$ (<i>abs.J.deg.⁻¹g⁻¹</i>) |
|-------------|---|---|---|
| 0 | 0 | 0 | 0 |
| 10 | 0·0223 | 0·0078 | 0·0590 |
| 20 | 0·0976 | 0·0458 | 0·6531 |
| 30 | 0·1569 | 0·0970 | 1·944 |
| 40 | 0·2108 | 0·1496 | 3·775 |
| 50 | 0·2597 | 0·2019 | 6·131 |
| 60 | 0·3029 | 0·2531 | 8·949 |
| 70 | 0·3417 | 0·3027 | 12·17 |
| 80 | 0·3789 | 0·3508 | 15·78 |
| 90 | 0·4149 | 0·3975 | 19·75 |
| 100 | 0·4501 | 0·4431 | 24·07 |
| 110 | 0·4855 | 0·4876 | 28·75 |
| 120 | 0·5206 | 0·5314 | 33·78 |
| 130 | 0·5552 | 0·5744 | 39·16 |
| 140 | 0·5901 | 0·6168 | 44·89 |
| 150 | 0·6254 | 0·6587 | 50·96 |
| 160 | 0·6608 | 0·7002 | 57·39 |
| 170 | 0·6970 | 0·7414 | 64·18 |
| 180 | 0·7324 | 0·7822 | 71·32 |
| 190 | 0·7689 | 0·8228 | 78·83 |
| 200 | 0·8066 | 0·8632 | 86·71 |
| 210 | 0·8457 | 0·9035 | 94·97 |
| 220 | 0·8853 | 0·9437 | 103·6 |
| 230 | 0·9267 | 0·9840 | 112·7 |
| 240 | 0·9698 | 1·024 | 122·2 |
| 250 | 1·013 | 1·065 | 132·1 |
| 260 | 1·056 | 1·105 | 142·4 |
| 270 | 1·100 | 1·146 | 153·2 |
| 273·15 | 1·114 | 1·159 | 156·7 |
| 280 | 1·145 | 1·187 | 164·4 |
| 290 | 1·189 | 1·228 | 176·1 |
| 298·15 | 1·225 | 1·261 | 186·0 |
| 300 | 1·233 | 1·269 | 188·2 |
| 310 | 1·277 | 1·310 | 200·8 |

Table 19

| Polymer | A | θ_D |
|---------------------------|-------|------------|
| Isotactic polypropylene | 0·327 | 113 |
| Atactic polypropylene | 0·320 | 100 |
| Isotactic poly(but-1-ene) | 0·329 | 114 |
| Isotactic polystyrene | 0·233 | 92 |

THERMODYNAMIC FUNCTIONS OF LINEAR HIGH POLYMERS—IV

Table 20

| Polymer | W_c^* | $S_{25^\circ C}^0$ | $\Delta S_{f, 25^\circ C}^0$ | S_A^0 | $S_{100\%}^0$ |
|---------------------------|---------|--------------------|------------------------------|---------|---------------|
| Polythene ('Rigidex 50') | 0.79 | 11.73 | 3.8 | 14.8 | 10.9 |
| Isotactic polypropylene | 0.48 | 17.22 | 4.6 ⁵² | 19.4 | 14.8 |
| Atactic polypropylene | 0.16 | 18.88 | — | 19.6 | 15.0 |
| Isotactic poly(but-1-ene) | 0.44 | 24.61 | 6.9 ⁵³ | 27.6 | 20.7 |
| Isotactic polystyrene | 0.43 | 31.40 | 1.3 ⁵⁴ | 32.0 | 30.7 |
| Atactic polystyrene | 0 | 32.23 | — | 32.2 | 30.9 |

| Polymer | $-\Delta S_{nc}^0$ | $-\Delta S_{uc}^0$ | $-\Delta S_{lc}^0$ | $-\Delta S_{lc'}^0$ | $-\Delta S_{:c}^0 \dagger$ |
|---------------------------|--------------------|--------------------|--------------------|---------------------|----------------------------|
| Polythene ('Rigidex 50') | 37.7 | 41.5 | — | — | — |
| Isotactic polypropylene | 44.4 | 49.0 | 27.8 | 32.4 | 27.0 |
| Atactic polypropylene | 44.2 | — | 27.6 | — | — |
| Isotactic poly(but-1-ene) | 45.4 | 52.3 | 26.8 | 33.7 | 26.9 |
| Isotactic polystyrene | — | — | 25.2 | 26.5 | — |
| Atactic polystyrene | — | — | 24.9 | — | — |

* W_c denotes weight fraction crystallinity.

†Values of $-\Delta S_{:c}^0$ estimated by Dainton and Ivin¹ using semi-empirical methods. S_A^0 and $S_{100\%}^0$ are the entropies of amorphous and wholly crystalline polymers respectively. All entropy values in cal. deg.⁻¹.

estimated from the change in slope of the enthalpy/temperature curves. It has previously been pointed out⁵¹ that the enthalpy/temperature method of detecting T_g is not very sensitive when applied to semi-crystalline polymers. Hence, the T_g values assigned to isotactic polypropylene and isotactic poly(but-1-ene) must be treated with some reserve.

The glass transition temperatures shown in Table 21 correspond fairly closely with the temperatures at which n.m.r.⁴⁵ and dynamic-mechanical measurements⁴⁵ locate the onset of segmental motion in the main polymer chain. These methods also indicate the occurrence of side chain rotation in poly- α -olefines at temperatures well below T_g . The present heat capacity studies have failed to reveal this effect, probably because the energy involved is too small to cause a detectable anomaly in the heat capacity/temperature curve.

The following are some general conclusions which can be drawn from the data of Table 21.

(1) For the first three members of the series, polythene, polypropylene and poly(but-1-ene), structure has very little effect on T_g . With polystyrene, however, the more bulky phenyl side group tends to inhibit the rotation of the skeletal structure and this leads to a marked increase in T_g .

Table 21

| Polymer | T_g °K | T_m °K | T_g/T_m |
|---------------------------|----------|----------|-----------|
| Polythene ('Rigidex 50') | 246 | 410 | 0.60 |
| Isotactic polypropylene | 260 | 449 | 0.58 |
| Atactic polypropylene | 249 | — | — |
| Isotactic poly(but-1-ene) | 249 | 405 | 0.61 |
| Atactic polystyrene | 355 | — | — |

(2) The change from an isotactic to an atactic structure (polypropylene) causes an apparent lowering of T_g . The explanation of this decrease could be that the chain segments rotate more easily in the amorphous, atactic material than in the semi-crystalline, isotactic material. However, the 11° difference between the T_g values for the two polymers is rather small and could possibly be caused by other effects such as the previous thermal histories of the polymer specimens.

(3) The empirical rule^{5,6} that the ratio of the glass temperature, T_g , to the melting temperature, T_m , is approximately equal to 0.66 holds for the poly- α -olefine series.

Part V—*cis*- and *trans*-1,4-Polybutadiene

F. S. DAINTON, D. M. EVANS, F. E. HOARE and T. P. MELIA

The heat capacity of cis-1,4-polybutadiene has been measured in the temperature range 20° to 310°K and that of trans-1,4-polybutadiene in the range 20° to 345°K. The data were used to obtain a table of smoothed values of heat capacity, enthalpy and entropy. The glass transition temperature, melting point and heat of fusion of cis-1,4-polybutadiene were found to be 165°, 262°K and 72.6 ± 7.3 abs. J. g⁻¹, respectively. The trans-1,4-polybutadiene undergoes a first order transition at 317°K which has associated with it a heat of transition of 63.1 ± 6.0 abs. J. g⁻¹.

Cis- and *trans*-1,4-polybutadiene, despite their chemical similarity, show widely different physical properties. For example, *cis*-1,4-polybutadiene is a rubber which melts at about 273°K³⁴ and has a glass transition at 165°K, whilst the *trans* form exists in two crystalline modifications with a transition point at about 60°C and a melting point of the high temperature form at 130°C³⁴.

Some recent heat capacity measurements have been reported¹⁴ for polybutadiene but the results are difficult to interpret because the samples used were not stereochemically pure. In view of the fact that certain anomalies were observed in the heat capacity versus temperature curve it was decided to repeat these measurements using stereochemically pure (or nearly so) polybutadiene samples. It was also felt that useful thermal data could be obtained concerning the various transitions which have been observed in the *cis* and *trans* isomers by other methods³⁴.

EXPERIMENTAL

Heat capacity measurements

The method used has been described previously²⁸.

Materials

The *cis*-1,4-polybutadiene was kindly given by I.C.I. (Plastics Division). Its composition, as obtained by infra-red analysis, was 94 per cent *cis*-1,4-; 3 per cent *trans*-1,4- and 3 per cent 1,2-polybutadiene. The weight of sample used was 22.612 g. *Trans*-1,4-polybutadiene was kindly given by Dr Lloyd McCleod of the Polymer Corporation, Canada. His analysis shows 96.2 per cent *trans*-1,4- and 3.8 per cent 1,2-polybutadiene. The material was soluble in toluene, had an intrinsic viscosity of 2.1 and was stabilized with 2,3-di-*t*-butyl *p*-cresol. The weight of sample used was 27.318 g.

RESULTS

(a) *cis*-1,4-Polybutadiene

The experimental details of the heat treatment, range of temperature measurements and temperature drifts are summarized in Table 22. The

Table 22. Heat treatments and observations with *cis*-1,4-polybutadiene

| Run | Sample treatment | Range of temperature measurement °K | Temperature drift observations |
|-----|--------------------------------------|-------------------------------------|--|
| 1 | Cooled rapidly to 78°K | 78 to 217 | Upward drift from 160° to 217°K. Excessive upward drifts of approx. 0·1° per minute from 180° to 217°K |
| 2 | Cooled rapidly to 195°K | 195 to 252 | Upward drift from 195° to 252°K |
| 3 | Cooled rapidly to 20°K | 20 to 84 | No drift |
| 4 | Cooled rapidly to 78°K | 78 to 235 | Upward drift from 150° to 235°K. Excessive upward drift from 195° to 235°K |
| 5 | Cooled rapidly to 190°K | 190 to 290 | Upward drift from 190° to 265°K, small downward drift from 265° to 290°K |
| 6 | Cooled rapidly to 20°K | 20 to 83 | No drift. |
| 7 | Cooled rapidly to 273°K | 273 to 305 | Downward drift from 295° to 305°K |
| 8 | Cooled slowly over 5 days to 145°K | 145 to 233 | Downward drift from 150° to 233°K |
| 9 | Cooled overnight to 208°K | 212 to 294 | Upward drift from 235° to 262°K. Downward drift from 262° to 294°K |
| 10 | Cooled slowly over 6 days to 135°K | 135 to 185 | Downward drift from 158° to 185°K |
| 11 | Cooled overnight to 145°K | 145 to 299* | — |
| 12 | Cooled to 216°K over 3 days | 216 to 270 | Upward drift from 230° to 262°K, downward drift from 262° to 270°K |
| 13 | Warmed to room temperature overnight | 296 to 311 | Downward drift from 296° to 311°K |
| 14 | Cooled rapidly to 145°K | 145 to 300* | — |

*Continuous heating.

observed values of the heat capacity are given in *Table 23* and the general pattern of these results is shown in the plots of *Figures 13* and *14*.

During the course of the heat capacity measurements both upward and downward temperature drifts were observed at temperatures above 150°K. The upward drifts generally, but not invariably, occurred after the polymer had been shock-cooled. These drifts may originate in the possibility that when the polymer was cooled a certain fraction of the polymer molecules failed to make the transition to states of lower energy. As the temperature was raised during the heat capacity measurements, these molecules acquired enough thermal energy (in the region of the glass transition) to make this transition. The resultant heat release thus caused upward temperature drifts. Similarly, the downward drifts of runs 8 and 10 arose from the fact that in the slowly cooled polymer, molecules were 'frozen' into the lower energy states. The excessive upward temperature drifts (approximately 0·1°K per minute) which were observed in the range 180° to 220°K, after the polymer had been shock-cooled to liquid nitrogen temperature (runs 1 and 4), are attributed to the occurrence of a large amount of crystallization ('cold crystallization'⁵⁷) just above the glass transition temperature. This crystallization, with its subsequent liberation of latent heat, caused the apparent heat capacity to be relatively low and gave rise to the *N*-like shape of the heat capacity versus temperature curve in this region (see *Figure 14*). The downward drifts observed above the melting point probably arose from the slow thermal equilibration in the liquid state.

THERMODYNAMIC FUNCTIONS OF LINEAR HIGH POLYMERS—V

 Table 23. Observed values of the heat capacity for *cis*-1,4-polybutadiene

| Temp. (°K) | $C(\text{abs. J. deg.}^{-1} \text{g}^{-1})$ | Temp. (°K) | $C(\text{abs. J. deg.}^{-1} \text{g}^{-1})$ |
|------------|---|------------|---|
| Run 1 | | Run 4 | |
| 81·85 | 0·5426 | 84·20 | 0·5391 |
| 89·95 | 0·5939 | 93·66 | 0·6077 |
| 99·31 | 0·6368 | 104·85 | 0·6651 |
| 109·74 | 0·6899 | 115·97 | 0·7213 |
| 120·60 | 0·7452 | 127·03 | 0·7779 |
| 130·75 | 0·7983 | 138·78 | 0·8385 |
| 141·11 | 0·8522 | 150·51 | 0·9004 |
| 152·41 | 0·9110 | 161·91 | 1·068 |
| 163·22 | 1·203 | 172·52 | 1·359 |
| 173·12 | 1·457 | 183·00 | 1·272 |
| 184·64 | 1·043 | 194·80 | 1·008 |
| 199·07 | 0·6957 | 206·09 | 1·466 |
| 212·32 | 1·440 | 217·52 | 1·565 |
| | | 230·01 | 1·673 |
| Run 2 | | Run 5 | |
| 196·81 | 1·484 | 194·99 | 1·446 |
| 207·03 | 1·535 | 206·13 | 1·523 |
| 217·51 | 1·657 | 217·58 | 1·648 |
| 228·04 | 1·789 | 228·41 | 1·788 |
| 238·52 | 2·008 | 239·22 | 2·005 |
| 248·53 | 2·357 | 249·18 | 2·416 |
| Run 3 | | 257·07 | 3·722 |
| 21·46 | 0·1398 | 265·40 | 3·027 |
| 24·16 | 0·1654 | 274·95 | 1·790 |
| 27·09 | 0·1928 | 283·88 | 1·836 |
| 30·12 | 0·2198 | Run 6 | |
| 33·30 | 0·2465 | 21·20 | 0·1336 |
| 36·56 | 0·2707 | 23·79 | 0·1597 |
| 39·95 | 0·2963 | 26·99 | 0·1906 |
| 43·44 | 0·3242 | 30·06 | 0·2171 |
| 47·63 | 0·3538 | 33·14 | 0·2446 |
| 52·63 | 0·3865 | 37·22 | 0·2766 |
| 57·89 | 0·4131 | 41·07 | 0·3065 |
| 63·31 | 0·4493 | 45·20 | 0·3388 |
| 69·15 | 0·4776 | 49·97 | 0·3697 |
| 75·13 | 0·5055 | 55·29 | 0·4024 |
| 80·70 | 0·5440 | | |

Continued overleaf.

Table 23—continued

| Temp. (°K) | C(abs.J.deg. ⁻¹ g ⁻¹) | Temp. (°K) | C(abs.J.deg. ⁻¹ g ⁻¹) |
|---------------|--|---------------|--|
| Run 6 (Contd) | | Run 9 (Contd) | |
| 60·89 | 0·4361 | 271·20 | 1·774 |
| 67·05 | 0·4683 | 279·09 | 1·791 |
| 73·37 | 0·5004 | 289·04 | 1·843 |
| 79·70 | 0·5307 | | |
| Run 7 | | Run 10 | |
| 278·07 | 1·758 | 138·54 | 0·8319 |
| 289·51 | 1·849 | 146·88 | 0·8739 |
| 300·57 | 1·857 | 155·59 | 0·9216 |
| | | 161·87 | 0·9906 |
| | | 165·76 | 1·139 |
| | | 169·39 | 1·273 |
| | | 173·19 | 1·327 |
| | | 177·25 | 1·348 |
| | | 181·60 | 1·367 |
| Run 8 | | Run 12 | |
| 149·73 | 0·8823 | 223·65 | 1·723 |
| 156·51 | 0·9323 | 237·95 | 2·065 |
| 166·52 | 1·186 | 250·02 | 2·806 |
| 175·63 | 1·321 | 256·54 | 3·066 |
| 182·81 | 1·361 | 258·62 | 3·858 |
| 190·53 | 1·393 | 260·33 | 5·148 |
| 199·41 | 1·452 | 261·49 | 5·794 |
| 209·30 | 1·539 | 262·26 | 6·717 |
| 219·38 | 1·664 | 263·02 | 6·014 |
| 228·81 | 1·870 | 263·89 | 4·806 |
| | | 265·80 | 2·196 |
| | | 268·88 | 1·781 |
| Run 9 | | Run 13 | |
| 212·65 | 1·621 | 299·72 | 1·842 |
| 222·69 | 1·713 | 307·21 | 1·875 |
| 232·86 | 1·928 | | |
| 242·06 | 2·280 | | |
| 248·61 | 2·663 | | |
| 252·82 | 3·051 | | |
| 256·51 | 3·802 | | |
| 259·51 | 5·218 | | |
| 261·85 | 6·908 | | |
| 265·60 | 1·963 | | |

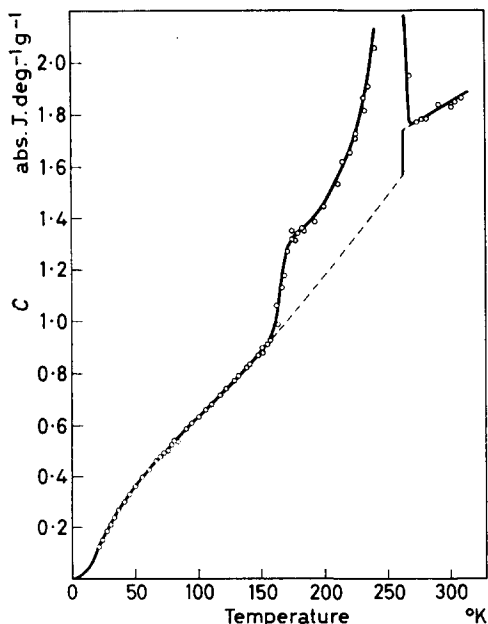


Figure 13—Observed heat capacities of *cis*-1,4-polybutadiene. The broken line represents the 'corrected' heat capacity curve used in the heat of fusion calculations

The smoothed heat capacities given in *Table 24* were obtained from the results of those experiments in which the polymer was slowly cooled (above 150°K that is). The heat capacity data below 20°K were obtained by extrapolation using the Debye function²⁸

$$C = 0.398 f_D(112/T)$$

The enthalpy and entropy of *cis*-1,4-polybutadiene were obtained by

Figure 14—Observed heat capacities of *cis*-1,4-polybutadiene (runs 1 and 4) showing the *N*-like shape of the heat capacity versus temperature curve. The broken line represents the smoothed curve values of *Figure 13*

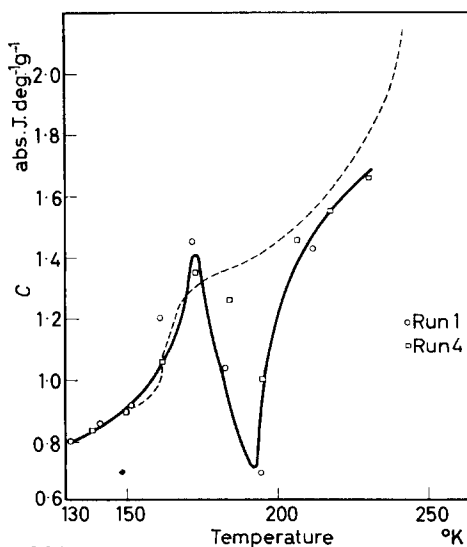


Table 24. Smoothed values of the thermodynamic functions for *cis*-1,4-polybutadiene

| Temp. °K | C (<i>abs.J.deg.⁻¹g⁻¹</i>) | $H_T^0 - H_0^0$ (<i>abs.J.g⁻¹</i>) | $S_T^0 - S_0^0$ (<i>abs.J.deg.⁻¹g⁻¹</i>) |
|-------------|---|--|---|
| 0 | 0 | 0 | 0 |
| 10 | 0·0218 | 0·0569 | 0·0075 |
| 20 | 0·1206 | 0·7306 | 0·0501 |
| 30 | 0·2179 | 2·461 | 0·1184 |
| 40 | 0·2985 | 5·032 | 0·1921 |
| 50 | 0·3693 | 8·383 | 0·2665 |
| 60 | 0·4286 | 12·38 | 0·3392 |
| 70 | 0·4837 | 16·94 | 0·4094 |
| 80 | 0·5374 | 22·05 | 0·4776 |
| 90 | 0·5892 | 27·68 | 0·5439 |
| 100 | 0·6402 | 33·83 | 0·6077 |
| 110 | 0·6904 | 40·48 | 0·6720 |
| 120 | 0·7404 | 47·64 | 0·7342 |
| 130 | 0·7916 | 55·30 | 0·7955 |
| 140 | 0·8434 | 63·47 | 0·8560 |
| 150 | 0·8967 | 72·17 | 0·9160 |
| 160 | 0·997 | — | — |
| 170 | 1·289 | — | — |
| 180 | 1·364 | — | — |
| 190 | 1·402 | — | — |
| 200 | 1·472 | — | — |
| 210 | 1·562 | — | — |
| 220 | 1·679 | — | — |
| 230 | 1·826 | — | — |
| 240 | 2·126 | — | — |
| 250 | 2·693 | — | — |
| | LIQUID | | |
| 262 | 1·745 | 282·3 | 1·892 |
| 270 | 1·771 | 296·4 | 1·945 |
| 273·15 | 1·782 | 302·0 | 1·965 |
| 280 | 1·803 | 314·3 | 2·010 |
| 290 | 1·832 | 332·4 | 2·073 |
| 298·15 | 1·854 | 347·5 | 2·124 |
| 300 | 1·859 | 350·9 | 2·136 |
| 310 | 1·882 | 369·6 | 2·197 |

evaluating the thermodynamic relations

$$H_T^0 - H_0^0 = \int_0^T C dT$$

and

$$S_T^0 - S_0^0 = \int_0^T (C/T) dT$$

respectively. Except below 20°K and above 145°K these integrals were evaluated using Simpson's rule. Below 20°K the Debye function was evaluated graphically. Between 145° and 300°K the enthalpy was obtained by two methods. First, by summing the energy input of runs 8 and 9 in

which the experiments were made from 147.48° to 293.90°K (allowance being made for the overlap of the two runs). The enthalpy change was then corrected to the temperature interval 145° to 300°K. Secondly, by heating the polymer continuously from 144.73° to 299.27°K (run 11) and again correcting to the temperature interval 145° to 300°K. The entropy change was obtained by summing similarly the various $C\Delta T/T_m$ terms of runs 8 and 9, where $C\Delta T$ is the enthalpy change of the interval, ΔT , and T_m is the mid-temperature of the interval (allowance was again made for the overlap of the two runs). The entropy change was corrected to the 145° to 300°K temperature interval. The results of these various calculations, together with the data for the enthalpy change over the same temperature interval when the polymer was rapidly cooled (run 14) are shown in Table 25.

Table 25. The enthalpy and entropy changes of *cis*-1,4-polybutadiene from 145° to 300°K

| Treatment | ${}_{145}^{300}H - H_{145}^0$ (abs. J. g ⁻¹) | $S_{300}^0 - S_{145}^0$ (abs. J. deg. ⁻¹ g ⁻¹) |
|--|---|--|
| Slow-cooled (runs 8 and 9) | 282.9 | 1.250 |
| Slow-cooled, continuous heating (run 11) | 283.1 | — |
| Shock-cooled (run 14) | 264.1 | — |

The glass transition temperature of this particular specimen is found to be about 165°K. The melting point, which was taken to be that temperature at which the heat capacity reached a maximum value, is 262° ± 1°K.

From the heat capacity data a value was estimated for the heat of fusion of the *cis*-1,4-polybutadiene sample by means of the equation

$$\Delta H_f = \Delta Q_1 - \Delta Q_2 - \Delta Q_3$$

where ΔH_f is the heat of fusion of 1 g of *cis*-1,4-polybutadiene, ΔQ_1 is the increase in enthalpy of 1 g of polymer in going from a temperature (145°K) below the glass transition temperature to one (300°K) above the melting point, ΔQ_2 is the energy required to heat 1 g of solid polymer from 145°K to the melting point (262°K), and ΔQ_3 is the energy required to heat 1 g of liquid polymer from 262° to 300°K. In computing ΔQ_2 it was necessary to extrapolate the heat capacity data for the solid polymer from 145° to 262°K in order to avoid errors which may be caused by the glass transformation and pre-melting effects. For this purpose the equation

$$C = 0.222 + 3.6 \times 10^{-3}T + 6.0 \times 10^{-6}T^2 \text{ abs. J. deg.}^{-1} \text{ g}^{-1}$$

which fitted the smoothed heat capacity data in the range 120° to 150°K was used. Such a long extrapolation is open to obvious objections but is the only procedure available.

The results of the above calculations are summarized in Table 26.

Table 26

| | |
|--------------|--|
| ΔQ_1 | 283.0 ± 0.1 abs. J. g ⁻¹ |
| ΔQ_2 | 141.8 ± 7.0 abs. J. g ⁻¹ (estimated probable error) |
| ΔQ_3 | 68.6 ± 0.2 abs. J. g ⁻¹ |
| ΔH_f | 72.6 ± 7.3 abs. J. g ⁻¹ |

(b) *trans-1,4-Polybutadiene*

The experimental details concerning the different runs are summarized in *Table 27*. The observed values of the heat capacity are given in *Table 28* and are plotted against temperature in *Figure 15*.

Table 27. Heat treatments and observations with *trans-1,4-polybutadiene*

| Run | Sample treatment | Range of temperature measurement °K | Temperature drift observations |
|-----|---|-------------------------------------|--|
| 1 | Cooled rapidly to 78°K | 78 to 220 | Upward drift from 190 to 220°K |
| 2 | Cooled rapidly to 193°K | 193 to 282 | Upward drift from 193 to 275°K |
| 3 | Warmed to room temperature overnight | 297 to 313 | No drift |
| 4 | Cooled rapidly to 273°K | 273 to 307 | Upward drift from 273 to 307°K |
| 5 | Cooled rapidly to 20°K | 20 to 86 | No drift |
| 6 | Cooled slowly over 3 days to 145°K | 145 to 224 | Downward drift from 175 to 224°K |
| 7 | Left overnight at 220°K then warmed to room temperature. Cooled slowly to 224°K | 224 to 289 | Downward drift from 224 to 289°K |
| 8 | Left at room temperature overnight | 297 to 341 | Both upward and downward drifts observed but these may be due to deterioration of the vacuum |
| 9 | Cooled to room temperature overnight | 297 to 338 | |
| 10 | Cooled to 224°K overnight | 224 to 329* | |

*Continuous heating.

During the heat capacity measurements both upward and downward temperature drifts were observed at temperatures above 175°K. The explanation of these drifts is presumed to be the same as that already given for similar drifts observed with the *cis* isomer.

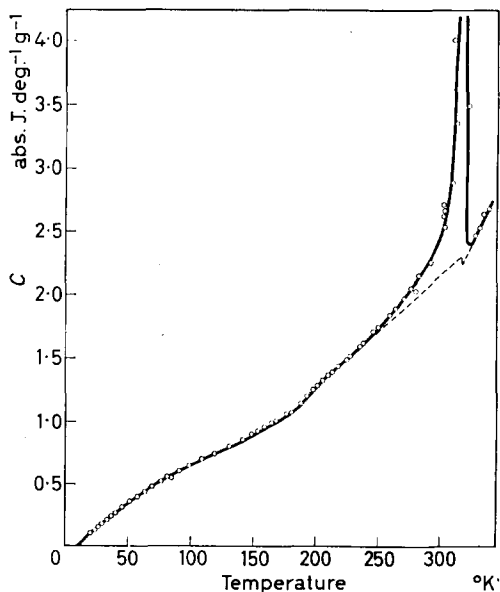


Figure 15 — Observed heat capacities of *trans-1,4-polybutadiene*. The broken line represents the 'corrected' heat capacity curve used in the heat of transition calculations

The heat capacity results indicate the occurrence of two transitions in *trans-1,4-polybutadiene*. The first, which can be recognized by the sudden change in slope of the heat capacity versus temperature curve at about

190°K, probably corresponds to the glass-rubber transition for this material. The second, for which the transition temperature is $317 \pm 1^\circ\text{K}$ (i.e. that temperature at which the heat capacity reaches a maximum value), is probably associated with the change in chain configuration from linear to helical, which Natta⁵⁸ has located, by X-ray diffraction, at 333°K.

Table 28. Observed values of the heat capacity for *trans*-1,4-polybutadiene

| Temp. (°K) | $C(\text{abs. J. deg.}^{-1} \text{g}^{-1})$ | Temp. (°K) | $C(\text{abs. J. deg.}^{-1} \text{g}^{-1})$ |
|------------|---|---------------|---|
| Run 1 | | Run 5 (Contd) | |
| 82.04 | 0.5440 | 51.64 | 0.3591 |
| 90.10 | 0.5934 | 57.28 | 0.3964 |
| 99.38 | 0.6439 | 63.38 | 0.4400 |
| 109.11 | 0.6962 | 69.86 | 0.4755 |
| 119.60 | 0.7519 | 76.38 | 0.5125 |
| 130.30 | 0.8068 | 82.93 | 0.5524 |
| 141.18 | 0.8635 | Run 6 | |
| 153.03 | 0.9269 | 149.39 | 0.8994 |
| 165.02 | 0.9887 | 158.76 | 0.9496 |
| 177.11 | 1.058 | 169.36 | 1.005 |
| 189.23 | 1.151 | 181.02 | 1.073 |
| 201.22 | 1.272 | 193.41 | 1.208 |
| 213.06 | 1.391 | 205.57 | 1.348 |
| Run 2 | | 217.57 | 1.451 |
| 199.26 | 1.270 | Run 7 | |
| 212.06 | 1.383 | 227.66 | 1.515 |
| 224.95 | 1.498 | 236.81 | 1.613 |
| 237.87 | 1.615 | 247.74 | 1.716 |
| 250.82 | 1.743 | 258.83 | 1.849 |
| 263.69 | 1.892 | 270.62 | 1.984 |
| 276.43 | 2.072 | 283.00 | 2.164 |
| Run 3 | | Run 8 | |
| 301.54 | 2.704 | 301.72 | 2.674 |
| 309.38 | 2.888 | 311.06 | 3.358 |
| Run 4 | | 317.83 | 7.775 |
| 279.56 | 2.034 | 324.06 | 4.944 |
| 291.39 | 2.274 | 331.44 | 2.526 |
| 302.27 | 2.540 | 338.13 | 2.680 |
| Run 5 | | Run 9 | |
| 21.42 | 0.1036 | 301.97 | 2.638 |
| 24.10 | 0.1248 | 310.66 | 4.070 |
| 26.97 | 0.1512 | 315.35 | 7.424 |
| 29.95 | 0.1794 | 317.28 | 9.692 |
| 32.95 | 0.2054 | 319.15 | 7.972 |
| 36.35 | 0.2346 | 322.20 | 3.482 |
| 40.23 | 0.2672 | 327.96 | 2.462 |
| 45.56 | 0.3137 | 335.18 | 2.644 |

In order to obtain the heat capacity of the sample above 310°K the smoothed values of the empty calorimeter were extrapolated from 310° to 345°K. Although it is believed that the error in this extrapolation is quite small the rapid deterioration in the vacuum which occurred above 310°K may introduce an error in the experimental heat capacities above this temperature of perhaps two per cent.

The experimental values of the heat capacity were smoothed graphically and the smoothed values, together with the derived values of the entropy

Table 29. Smoothed values of the thermodynamic functions for *trans*-1,4-polybutadiene

| Temp. °K | C (<i>abs.J.deg.⁻¹g⁻¹</i>) | $H_T^0 - H_0^0$ (<i>abs.J.g⁻¹</i>) | $S_T^0 - S_0^0$ (<i>abs.J.deg.⁻¹g⁻¹</i>) |
|--------------|---|--|---|
| 0 | 0 | 0 | 0 |
| 10 | 0.0148 | 0.0381 | 0.0050 |
| 20 | 0.0891 | 0.5194 | 0.0353 |
| 30 | 0.1794 | 1.872 | 0.0884 |
| 40 | 0.2660 | 4.088 | 0.1518 |
| 50 | 0.3465 | 7.151 | 0.2199 |
| 60 | 0.4171 | 10.98 | 0.2895 |
| 70 | 0.4787 | 15.46 | 0.3585 |
| 80 | 0.5362 | 20.54 | 0.4262 |
| 90 | 0.5919 | 26.18 | 0.4926 |
| 100 | 0.6467 | 32.38 | 0.5578 |
| 110 | 0.6999 | 39.11 | 0.6220 |
| 120 | 0.7525 | 46.38 | 0.6852 |
| 130 | 0.8047 | 54.17 | 0.7475 |
| 140 | 0.8553 | 62.47 | 0.8089 |
| 150 | 0.9057 | 71.27 | 0.8697 |
| 160 | 0.9560 | 80.58 | 0.9297 |
| 170 | 1.008 | 90.40 | 0.9893 |
| 180 | 1.070 | 100.8 | 1.049 |
| 190 | 1.157 | 111.9 | 1.109 |
| 200 | 1.272 | 124.0 | 1.171 |
| 210 | 1.372 | 137.3 | 1.235 |
| 220 | 1.456 | 151.4 | 1.301 |
| 230 | 1.543 | 166.4 | 1.368 |
| 240 | 1.638 | — | — |
| 250 | 1.745 | — | — |
| 260 | 1.859 | — | — |
| 270 | 1.982 | — | — |
| 273.15 | 2.023 | — | — |
| 280 | 2.113 | — | — |
| 290 | 2.253 | — | — |
| 298.15 | 2.402 | — | — |
| 300 | 2.458 | — | — |
| 310 | 3.370 | — | — |
| 317 | — | 334.9 | 1.986 |
| HELICAL FORM | | | |
| 317 | 2.232 | 398.0 | 2.185 |
| 320 | 2.294 | 404.8 | 2.207 |
| 330 | 2.505 | 428.8 | 2.280 |
| 340 | 2.726 | 445.0 | 2.359 |

and enthalpy are given in *Table 29*. Below 20°K the heat capacity values were obtained by extrapolation using the Debye function

$$C = 0.347 f_D (122/T)$$

The entropy and enthalpy values, in the range 0° to 230°K, were obtained in the usual manner. Between 230° and 330°K methods similar to those described for *cis*-1,4-polybutadiene in the range 145° to 300°K, were used to evaluate the enthalpy and entropy. The results of these calculations are shown in *Table 30*. The difference between the two enthalpy values shown in *Table 30* may be due to errors introduced by the deterioration in the vacuum which occurred above 310°K.

Table 30

| Run | $H_{330}^0 - H_{230}^0$ (abs. J. g ⁻¹) | $S_{330}^0 - S_{230}^0$ (abs. J. deg. ⁻¹ g ⁻¹) |
|-----------------------------|---|--|
| Runs 4, 7 and 8 | 262.5 | 0.9126 |
| Run 10 (continuous heating) | 268.2 | — |

The enthalpy change accompanying the transformation from a linear (Form I) to a helical (Form II) crystal structure in *trans*-1,4-polybutadiene was estimated by means of the equation

$$\Delta H_{tr} = \Delta Q_1 - \Delta Q_2 - \Delta Q_3$$

where ΔH_{tr} is the heat of transition, ΔQ_1 is the increase in enthalpy of 1 g of the solid polymer in going from a temperature (230°K) below the transition to one (330°K) above it, ΔQ_2 is the energy required to raise 1 g of solid polymer (I) from 230°K to the transition temperature (317°K), and ΔQ_3 is the energy required to heat 1 g of the solid polymer (II) from 317° to 330°K. Even though the major part of the change from one crystalline form to the other is concentrated in a small temperature range around 317°K, the transformation cannot be said to take place sharply (some forewarning of the impending change is given even at 230°K when the heat capacity versus temperature curve begins to show a steady upward trend). In order to make some allowance for this 'smearing' effect the heat capacity values used in the calculation of ΔQ_2 were obtained by a linear extrapolation of the heat capacity versus temperature curve in the range 230° to 317°K. This extrapolated curve (shown by the broken line in *Figure 15*) in effect represents that which the hypothetical solid polymer would probably follow if it remained in Form I right up to the transition temperature.

Table 31 summarizes the heat of transition calculations.

Table 31

| | | |
|-----------------|---------------|--|
| ΔQ_1 | 262.4 | abs. J. g ⁻¹ |
| ΔQ_2 | 168.5 | abs. J. g ⁻¹ |
| ΔQ_3 | 30.8 | abs. J. g ⁻¹ |
| ΔH_{tr} | 63.1 ± 6.0 | abs. J. g ⁻¹ |
| ΔS_{tr} | 0.199 ± 0.002 | abs. J. deg. ⁻¹ g ⁻¹ |

DISCUSSION

These results add to the significance of those of Furukawa and McCoskey¹⁴ on samples described by them as 41°F and 122°F polybutadienes. For example, the anomalous *N*-like shape of the heat capacity versus temperature curve which they detected for the 122°F polybutadiene has been shown to be a property of the shock-cooled *cis*-1,4-polybutadiene. The absence of this anomaly in the 41°F polymer indicates that this had a much lower *cis*-1,4 content than the 122°F polymer. Furthermore, the diffuse peak in the heat capacity versus temperature curve which was observed for both the 41°F and 122°F polymers in the 270°K region has been shown to be due to the melting of the *cis*-1,4 isomer. It is rather strange that their results show no positive evidence for the solid \rightleftharpoons solid transition in *trans*-1,4-polybutadiene which has been observed in the present work. The most probable explanation is that it has been shifted to lower temperatures, e.g. in the 41°F polymer (which is expected to contain the greater proportion of the *trans*-1,4 isomer) the diffuse peak extends up to about 300°K, and it is quite likely that the solid \rightleftharpoons solid transition is masked by the melting of the *cis*-1,4 isomer.

The value obtained for the heat of fusion of the *cis*-1,4-polybutadiene specimen used in the present work (940 ± 90 cal. mole⁻¹) is much smaller than that obtained by Natta⁵⁸ (2000 cal. mole⁻¹). Natta's method of measurement is not given so one can only speculate as to the cause of the difference. The most probable reason is that his sample was more crystalline than the one used in the present investigation. This interpretation is borne out by the fact that the melting point of the sample used by Natta (said to contain a percentage of *cis*-1,4 units greater than 99) was 274°K (compare the present value of 262°K). Natta also points out that the melting temperature is determined primarily by the way in which the steric impurities are distributed rather than by the steric impurity itself. For example, some catalytic systems, such as titanium tetraiodide and aluminium triethyl, give random copolymers of monomeric units with different steric configurations. Such polymers, even with a *cis*-1,4 content as high as 93 per cent, have rather low melting points in the range 262° to 266°K. Other catalytic systems prepared from different titanium halides give mixtures of macromolecules. From such mixtures, which are very rich in *cis*-1,4 units, macromolecules may be separated which melt at about 273°K. In such polymers the steric impurities are not statistically distributed along the chain and this allows the existence in the macromolecules of sections containing *cis*-1,4 units sufficiently long to have a melting point very close to that of the sterically pure polymer. It would appear from this that the *cis*-1,4-polybutadiene specimen used in the present work is of the former type.

The temperature at which the transition occurs between the two crystalline forms of *trans*-1,4-polybutadiene has been located by Natta, Corradini and Porri^{59, 60}, using X-ray diffraction techniques, at 333°K and by Baccaredda and Butta⁶¹, using a dynamic mechanical method, in the range 309° to 329°K. The present heat capacity measurements locate this first order transition at $317^\circ \pm 1^\circ$ K. Baccaredda and Butta⁶¹ also located a change of

slope in the sound velocity versus temperature curve at 225°K which they attribute to the glass transition in the amorphous areas of the polymer. The difference between their value for the glass transition temperature and that found in this work (approximately 195°K) is typical of the agreement to be expected between the two methods⁵⁸.

The entropy change which occurs when 1 mole of 1,3-polybutadiene is polymerized to *cis*-1,4-polybutadiene at 25°C is 20.12 cal. deg.⁻¹ mole⁻¹. This value is quite close to that obtained from the results of Furukawa and McCoskey¹⁴ (21.2 cal. deg.⁻¹ mole⁻¹).

Part VI—Polysulphones

F. S. DAINTON, D. M. EVANS, F. E. HOARE and T. P. MELIA

Heat capacity measurements have been made on two polysulphones (propene and hex-1-ene) in the range 20° to 300°K and on another (but-1-ene) in the range 90° to 300°K. The heat capacity data yield the following values for the entropy of the solid polymers at 25°C:

| | |
|-------------------------------|---|
| <i>Propene polysulphone</i> | $32.08 \pm 0.15 \text{ cal. deg.}^{-1} \text{ mole}^{-1}$ |
| <i>But-1-ene polysulphone</i> | $37.2 \pm 1.0 \text{ cal. deg.}^{-1} \text{ mole}^{-1}$ |
| <i>Hex-1-ene polysulphone</i> | $52.83 \pm 0.25 \text{ cal. deg.}^{-1} \text{ mole}^{-1}$ |

KINETIC studies on olefine polysulphone systems⁶² have revealed the existence of a ceiling temperature above which the polymer is thermodynamically unstable with respect to the co-monomers under the prevailing experimental conditions. Values for the heat and entropy changes associated with the copolymerization process may be obtained from kinetic data alone. Lack of the necessary heat capacity data for the polymers and activity data for the monomer and polymer solutions has prevented a comparison being made between the entropies of polymerization obtained by the ceiling temperature method and those obtained from heat capacity measurements on the monomers and polymers by the application of the Third Law of Thermodynamics. The present work was undertaken as part of a programme to obtain the thermodynamic data necessary to allow this comparison to be made.

EXPERIMENTAL

Heat capacity measurements

The method used has been described previously²⁸.

Materials

All the samples used in the present work were kindly given by Dr F. E. Frey of the Phillips Petroleum Co., U.S.A., who furnished the following information concerning the polymers: Propene polysulphone was prepared by mass polymerization of propene and sulphur dioxide at 100°F to a conversion of 95 per cent using lithium nitrate as the polymerization initiator. But-1-ene polysulphone was prepared by the polymerization of but-1-ene with sulphur dioxide in an emulsion recipe in which a small amount of ammonium nitrate was used as the initiator. The polymerization temperature was 100°F; olefine conversion was 95 per cent by weight. The hydrocarbon used in preparing the polymer was shown by infra-red analysis to consist of 95.8 mole per cent but-1-ene; 3.5 mole per cent *trans*-but-2-ene; 0.6 mole per cent *cis*-but-2-ene and 0.1 mole per cent 1,3-butadiene. The principal impurity in the polymer was residual emulsifier, sodium lauryl sulphate. Hex-1-ene polysulphone was prepared by polymerization in emulsion to greater than 90 per cent conversion at 100°F.

THERMODYNAMIC FUNCTIONS OF LINEAR HIGH POLYMERS—VI

Table 32. Smoothed values of the heat capacity, entropy and enthalpy for propene polysulphone

| Temp. °K | C (abs.J.deg. ⁻¹ g ⁻¹) | S _T ⁰ - S ₀ ⁰ (abs.J.deg. ⁻¹ g ⁻¹) | H _T ⁰ - H ₀ ⁰ (abs.J.g. ⁻¹) |
|-------------|--|--|--|
| 0 | 0 | 0 | 0 |
| 10 | 0·0158 | 0·0059 | 0·0490 |
| 20 | 0·0770 | 0·0341 | 0·4913 |
| 30 | 0·1319 | 0·0760 | 1·552 |
| 40 | 0·1893 | 0·1217 | 3·144 |
| 50 | 0·2459 | 0·1701 | 5·336 |
| 60 | 0·2980 | 0·2194 | 8·043 |
| 70 | 0·3477 | 0·2691 | 11·27 |
| 80 | 0·3963 | 0·3187 | 14·99 |
| 90 | 0·4444 | 0·3682 | 19·20 |
| 100 | 0·4870 | 0·4172 | 23·85 |
| 110 | 0·5272 | 0·4655 | 28·93 |
| 120 | 0·5666 | 0·5131 | 34·40 |
| 130 | 0·6052 | 0·5600 | 40·26 |
| 140 | 0·6422 | 0·6062 | 46·50 |
| 150 | 0·6776 | 0·6519 | 53·10 |
| 160 | 0·7118 | 0·6968 | 60·04 |
| 170 | 0·7458 | 0·7409 | 67·33 |
| 180 | 0·7810 | 0·7846 | 74·97 |
| 190 | 0·8155 | 0·8277 | 82·95 |
| 200 | 0·8506 | 0·8704 | 91·28 |
| 210 | 0·8858 | 0·9128 | 99·96 |
| 220 | 0·9198 | 0·9548 | 109·0 |
| 230 | 0·9540 | 0·9965 | 118·4 |
| 240 | 0·9818 | 1·038 | 128·0 |
| 250 | 1·012 | 1·078 | 138·0 |
| 260 | 1·040 | 1·119 | 148·3 |
| 270 | 1·067 | 1·159 | 158·8 |
| 273·15 | 1·076 | 1·171 | 162·2 |
| 280 | 1·098 | 1·198 | 169·6 |
| 290 | 1·130 | 1·237 | 180·8 |
| 298·15 | 1·159 | 1·269 | 190·1 |
| 300 | 1·165 | 1·276 | 192·3 |

The samples were stored for several years, i.e. received in 1954, measurements carried out in 1959–60, but no apparent change occurred in this period. The samples were used as supplied; but-1-ene and hex-1-ene polysulphones in the form of fine powders; propene polysulphone in the form of small pellets about 4 mm³. The masses of the samples investigated were: propene polysulphone 35·166 g, but-1-ene polysulphone 27·695 g, hex-1-ene polysulphone 18·297 g.

RESULTS

The observed heat capacities are plotted against temperature in *Figures 16, 17 and 18*. These were smoothed graphically and the smoothed values of the heat capacity, from which were derived the values, relative to 0°K, of the enthalpy and entropy, are given in *Tables 32, 33 and 34*.

Table 33. Smoothed values of the heat capacity, entropy and enthalpy of hex-1-ene polysulphone

| Temp. °K | C (<i>abs.J.deg.⁻¹g⁻¹</i>) | $S_T^0 - S_0^0$ (<i>abs.J.deg.⁻¹g⁻¹</i>) | $H_T^0 - H_0^0$ (<i>abs.J.g⁻¹</i>) |
|-------------|---|---|--|
| 0 | 0 | 0 | 0 |
| 10 | 0·0186 | 0·0064 | 0·0488 |
| 20 | 0·0903 | 0·0401 | 0·5783 |
| 30 | 0·1551 | 0·0891 | 1·820 |
| 40 | 0·2225 | 0·1428 | 3·694 |
| 50 | 0·2876 | 0·1996 | 6·260 |
| 60 | 0·3454 | 0·2572 | 9·421 |
| 70 | 0·4005 | 0·3146 | 13·15 |
| 80 | 0·4542 | 0·3717 | 17·43 |
| 90 | 0·5065 | 0·4282 | 22·23 |
| 100 | 0·5591 | 0·4843 | 27·56 |
| 110 | 0·6102 | 0·5400 | 33·41 |
| 120 | 0·6599 | 0·5952 | 39·76 |
| 130 | 0·7081 | 0·6499 | 46·60 |
| 140 | 0·7538 | 0·7041 | 53·91 |
| 150 | 0·7982 | 0·7576 | 61·67 |
| 160 | 0·8402 | 0·8105 | 69·87 |
| 170 | 0·8796 | 0·8626 | 78·47 |
| 180 | 0·9194 | 0·9141 | 87·47 |
| 190 | 0·9587 | 0·9648 | 96·86 |
| 200 | 0·9982 | 1·015 | 106·6 |
| 210 | 1·039 | 1·065 | 116·8 |
| 220 | 1·081 | 1·114 | 127·4 |
| 230 | 1·125 | 1·163 | 138·4 |
| 240 | 1·166 | 1·212 | 149·9 |
| 250 | 1·208 | 1·260 | 161·8 |
| 260 | 1·250 | 1·308 | 174·1 |
| 270 | 1·292 | 1·356 | 186·8 |
| 273·15 | 1·306 | 1·371 | 190·9 |
| 280 | 1·335 | 1·404 | 199·9 |
| 290 | 1·377 | 1·452 | 213·5 |
| 298·15 | 1·413 | 1·490 | 224·9 |
| 300 | 1·420 | 1·499 | 227·5 |
| 310 | 1·464 | 1·546 | 241·9 |

Table 34. Smoothed values of the heat capacity for but-1-ene polysulphone

| Temp. °K | C (abs.J.deg. ⁻¹ g ⁻¹) | Temp. °K | C (abs.J.deg. ⁻¹ g ⁻¹) |
|-------------|--|-------------|--|
| 100 | 0.4912 | 220 | 0.9636 |
| 110 | 0.5368 | 230 | 0.9989 |
| 120 | 0.5812 | 240 | 1.034 |
| 130 | 0.6250 | 250 | 1.067 |
| 140 | 0.6679 | 260 | 1.101 |
| 150 | 0.7100 | 270 | 1.134 |
| 160 | 0.7491 | 273.15 | 1.143 |
| 170 | 0.7873 | 280 | 1.165 |
| 180 | 0.8240 | 290 | 1.195 |
| 190 | 0.8594 | 298.15 | 1.219 |
| 200 | 0.8942 | 300 | 1.225 |
| 210 | 0.9288 | | |

For propene and hex-1-ene polysulphones the values of the heat capacity below 20°K were obtained by extrapolation, using the Debye functions²⁸

$$C = 0.209 f_D(100/T) \quad \text{propene polysulphone}$$

and

$$C = 0.245 f_D(100/T) \quad \text{hex-1-ene polysulphone}$$

The heat capacity data for but-1-ene polysulphone were extrapolated below 90°K using the Kelley, Parks and Huffmann method³⁹ and the value thus obtained for the entropy relative to 0°K is 37.2 ± 1.0 cal. deg.⁻¹ mole⁻¹.

The following entropies of the liquid monomers at 25°C have been used in deriving ΔS_{ic}^0 values: propene³³, 47.2; but-1-ene⁶³, 54.41; hex-1-ene⁶⁴, 70.55; sulphur dioxide, 37.88 cal. deg.⁻¹ mole⁻¹. The sulphur dioxide value has been estimated from the data of Giauque and Stephenson⁶⁵ as follows: Since sulphur dioxide boils at 263.08°K it is necessary to extrapolate the heat capacity data for the liquid state above the boiling point to 298.15°K.

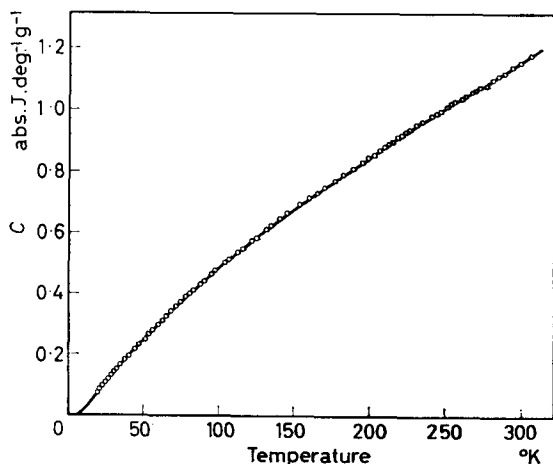


Figure 16—Observed heat capacities of propene polysulphone

Table 35. Comparison of the Second and Third Law entropies of polysulphones

| Polysulphone | $-\Delta S_{10}(\text{cal. deg.}^{-1}\text{mole}^{-1})$ | |
|--------------|---|-----------|
| | Second Law | Third Law |
| Propene | 55.7 | 53.0 |
| But-1-ene | 63.0 | 55.1 |
| Hex-1-ene | 62.6 | 55.6 |

In the range 200° to 260°K the heat capacity of sulphur dioxide may be represented by the equation

$$C = 22.62 - 1.075 \times 10^{-2}T + 1.250 \times 10^{-5}T^2 \text{ cal. deg.}^{-1} \text{ mole}^{-1}$$

This equation has been used to evaluate the entropy increase of the liquid in going from 263.08° to 298.15°K. The value 2.57 cal. deg.⁻¹ mole⁻¹ is ob-

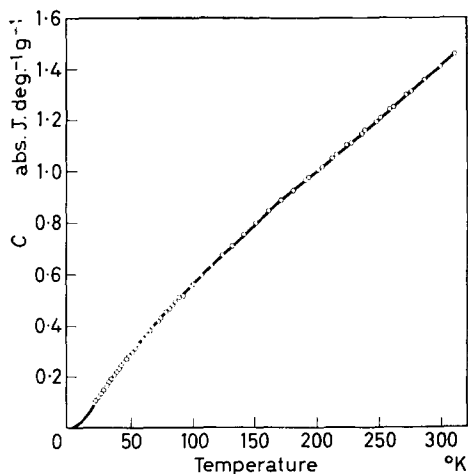
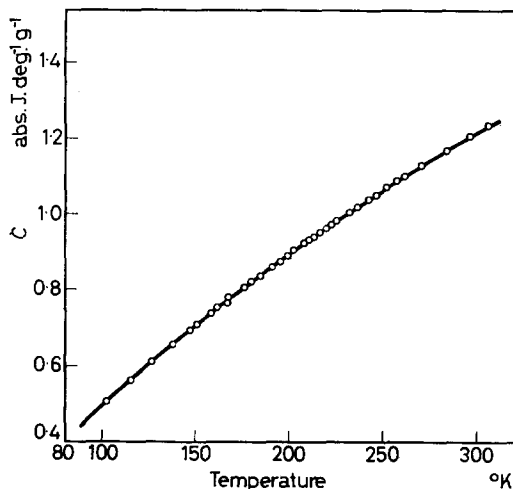


Figure 17—Observed heat capacities of hex-1-ene polysulphone

Figure 18—Observed heat capacities of but-1-ene polysulphone



tained, which, in conjunction with the Giaque and Stephenson value for the entropy of liquid sulphur dioxide at 263.08°K, leads to a value of 37.88 cal. deg.⁻¹ mole⁻¹ for the entropy of liquid sulphur dioxide at 25°C.

DISCUSSION

The formation of propene, but-1-ene and hex-1-ene polysulphones from the liquid monomers has been studied kinetically in the region of the ceiling temperature and the entropy of polymerization for each of these processes evaluated. The Second Law entropies of polymerization, referred to a standard concentration product $[M][S]$ of 27 mole² litre⁻², together with those obtained by applying the Third Law of Thermodynamics to the heat capacity data on the monomers and polymers are shown in *Table 35*.

It would be of interest to obtain a direct comparison between the Second and Third Law entropies for the polysulphones which are the subject of the present work. However, since the Second Law value for the entropy of polymerization is dependent on both (1) the percentage conversion of co-monomers to polymer (see, for example, the variation of the heat of polymerization for but-1-ene polysulphone⁶⁶ as the percentage conversion is varied), and (2) the activities of the monomers and polymers in the reaction mixture, a direct comparison cannot at present be made because the relevant activity data are not available.

Part VII—Lexan

F. S. DAINTON, D. M. EVANS, F. E. HOARE and T. P. MELIA

LEXAN is a polycarbonate formed by the condensation of phosgene and 4,4'-dihydroxydiphenyl-2,2-propane in the presence of alkali⁶⁷. The present communication reports a series of heat capacity measurements which were made on this polymer in the range 20° to 300°K. The smoothed heat

Table 36. Smoothed values of the heat capacity, entropy and enthalpy for Lexan

| Temp. °K | <i>C</i> (abs.J.deg. ⁻¹ g ⁻¹) | <i>S_T^u - S₀⁰</i> (abs.J.g ⁻¹) | <i>H_T^u - H₀^u</i> (abs.J.deg. ⁻¹ g ⁻¹) |
|-------------|---|--|---|
| 0 | 0 | 0 | 0 |
| 10 | 0.0234 | 0.0089 | 0.0730 |
| 20 | 0.0998 | 0.0475 | 0.6738 |
| 30 | 0.1567 | 0.0993 | 1.982 |
| 40 | 0.2063 | 0.1512 | 3.792 |
| 50 | 0.2507 | 0.2022 | 6.090 |
| 60 | 0.2899 | 0.2514 | 8.786 |
| 70 | 0.3249 | 0.2988 | 11.86 |
| 80 | 0.3594 | 0.3444 | 15.28 |
| 90 | 0.3950 | 0.3887 | 19.05 |
| 100 | 0.4315 | 0.4322 | 23.18 |
| 110 | 0.4673 | 0.4750 | 27.68 |
| 120 | 0.5038 | 0.5172 | 32.53 |
| 130 | 0.5411 | 0.5590 | 37.75 |
| 140 | 0.5796 | 0.6005 | 43.36 |
| 150 | 0.6180 | 0.6418 | 49.34 |
| 160 | 0.6566 | 0.6829 | 55.72 |
| 170 | 0.6953 | 0.7238 | 62.48 |
| 180 | 0.7328 | 0.7647 | 69.62 |
| 190 | 0.7716 | 0.8054 | 77.14 |
| 200 | 0.8106 | 0.8460 | 85.06 |
| 210 | 0.8501 | 0.8865 | 93.36 |
| 220 | 0.8890 | 0.9269 | 102.0 |
| 230 | 0.9281 | 0.9673 | 111.1 |
| 240 | 0.9636 | 1.007 | 120.6 |
| 250 | 0.9995 | 1.048 | 130.4 |
| 260 | 1.037 | 1.087 | 140.6 |
| 270 | 1.074 | 1.127 | 151.1 |
| 273.15 | 1.085 | 1.140 | 154.6 |
| 280 | 1.112 | 1.167 | 162.1 |
| 290 | 1.150 | 1.207 | 173.4 |
| 298.15 | 1.181 | 1.239 | 182.9 |
| 300 | 1.188 | 1.246 | 185.1 |
| 310 | 1.224 | 1.286 | 197.1 |

capacity values together with the derived values of the entropy and enthalpy, relative to 0°K, are shown in Table 36. The measurements were carried out in an adiabatic, vacuum calorimeter which has been described previously²⁸.

Part VIII—Methylmethacrylate and Polymethylmethacrylate

T. P. MELIA

THE HEAT capacity of polymethylmethacrylate has been measured from 16° to 60°K by Sochava⁶⁸ and from 60° to 260°K by Sochava and Trapeznikova⁶⁹. The heat capacity of methylmethacrylate has also been determined⁶⁹ between 60° and 210°K, and by Erdős, Jäger and Pouchly⁷⁰ over the temperature range 293° to 323°K.

The smoothed values of the heat capacity of polymethylmethacrylate, together with the derived values of the enthalpy and entropy, are listed at ten degree intervals in Table 37. The values of the heat capacity below

Table 37. Heat capacity, enthalpy and entropy of polymethylmethacrylate

| Temp. °K | C (cal.deg. ⁻¹ g ⁻¹) | $H_T^0 - H_0^0$ (cal.g ⁻¹) | $S_T^0 - S_0^0$ (cal.deg. ⁻¹ g ⁻¹) |
|-------------|--|---|--|
| 10 | 0.004 | 0.01 | 0.002 |
| 20 | 0.019 | 0.15 | 0.009 |
| 30 | 0.035 | 0.40 | 0.019 |
| 40 | 0.051 | 0.83 | 0.032 |
| 50 | 0.066 | 1.41 | 0.045 |
| 60 | 0.083 | 2.16 | 0.059 |
| 70 | 0.098 | 3.06 | 0.073 |
| 80 | 0.111 | 4.11 | 0.087 |
| 90 | 0.126 | 5.30 | 0.101 |
| 100 | 0.139 | 6.63 | 0.115 |
| 110 | 0.148 | 8.07 | 0.129 |
| 120 | 0.157 | 9.59 | 0.142 |
| 130 | 0.166 | 11.21 | 0.155 |
| 140 | 0.175 | 12.92 | 0.168 |
| 150 | 0.186 | 14.73 | 0.180 |
| 160 | 0.194 | 16.63 | 0.193 |
| 170 | 0.202 | 18.61 | 0.205 |
| 180 | 0.210 | 20.67 | 0.216 |
| 190 | 0.218 | 22.80 | 0.228 |
| 200 | 0.225 | 25.01 | 0.239 |
| 210 | 0.235 | 27.32 | 0.250 |
| 220 | 0.243 | 29.71 | 0.262 |
| 230 | 0.250 | 32.18 | 0.273 |
| 240 | 0.255 | 34.71 | 0.283 |
| 250 | 0.261 | 37.30 | 0.294 |
| 260 | 0.266 | 39.93 | 0.304 |
| 270 | 0.271 | 42.62 | 0.314 |
| 273.15 | 0.273 | 43.48 | 0.317 |
| 280 | 0.276 | 45.36 | 0.324 |
| 290 | 0.281 | 48.14 | 0.334 |
| 298.15 | 0.284 | 50.45 | 0.342 |
| 300 | 0.285 | 50.98 | 0.344 |

16°K were obtained by extrapolation using the Debye function²⁸

$$C = 0.0436 f_D(90/T)$$

In the range 260° to 300°K the heat capacity was evaluated using the equation

$$C = 4.37 \times 10^{-2} + 1.18 \times 10^{-3}T - 1.25 \times 10^{-6}T^2 \text{ cal. deg.}^{-1} \text{ g}^{-1}$$

which fits the heat capacity data between 200° and 260°K. The heat capacity values of methylmethacrylate between 0° and 60°K were obtained

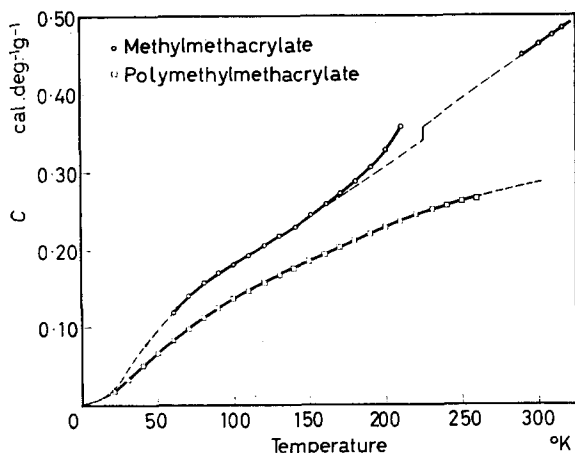


Figure 19—Heat capacities of methylmethacrylate and polymethylmethacrylate. The broken lines represent extrapolated and interpolated values

Table 38. Smoothed values of the heat capacity of methylmethacrylate

| Temp. °K | C (cal.deg. ⁻¹ g ⁻¹) | | Temp. °K | C (cal.deg. ⁻¹ g ⁻¹) | |
|-------------|--|-------|-------------|--|-------|
| | Exptl | Calcd | | Exptl | Calcd |
| 0 | 0 | 0 | 190 | 0.305 | 0.292 |
| 10 | — | 0.008 | 200 | 0.328 | 0.304 |
| 20 | — | 0.016 | 210 | 0.358 | 0.316 |
| 30 | — | 0.048 | 220 | — | 0.328 |
| 40 | — | 0.073 | 225 | — | 0.334 |
| 50 | — | 0.097 | LIQUID | | |
| 60 | 0.117 | — | 225 | — | 0.355 |
| 70 | 0.141 | — | 230 | — | 0.362 |
| 80 | 0.157 | — | 240 | — | 0.376 |
| 90 | 0.170 | — | 250 | — | 0.390 |
| 100 | 0.180 | — | 260 | — | 0.404 |
| 110 | 0.191 | — | 270 | — | 0.418 |
| 120 | 0.203 | — | 273.15 | — | 0.422 |
| 130 | 0.216 | — | 280 | — | 0.432 |
| 140 | 0.229 | — | 290 | — | 0.446 |
| 150 | 0.244 | — | 298.15 | 0.457 | — |
| 160 | 0.256 | — | 300 | 0.460 | — |
| 170 | 0.268 | — | | | |
| 180 | 0.285 | 0.280 | | | |

by a freehand graphical extrapolation of the C/T data above 60°K and those between the melting point⁷¹ (225°K) and 290°K were evaluated using the equation

$$C = 0.040 + 0.0014 T \text{ cal. deg.}^{-1} \text{ g}^{-1}$$

which approximately fits the data of Erdős *et al.* in the range 293° to 323°K (Figure 19). Since a considerable amount of pre-melting appears to occur in methylmethacrylate at temperatures above 170°K the smoothed values of the heat capacity were corrected for pre-melting. This was achieved by extrapolating the data for the solid from 170°K to the melting point. These values, which are given in column 3 of Table 38, were used to derive the entropy changes given in Table 39. Such long extrapolations are open to obvious objections but are the only procedures available.

Table 39. Entropy changes on heating methylmethacrylate

| | |
|--------------------------------------|---|
| $\int_0^{60} \frac{C}{T} dt$ | 0.085 cal. deg. ⁻¹ g ⁻¹ |
| $\int_{60}^{225} \frac{C}{T} dt$ | 0.278 cal. deg. ⁻¹ g ⁻¹ |
| $\int_{225}^{298.15} \frac{C}{T} dt$ | 0.113 cal. deg. ⁻¹ g ⁻¹ |

There are several lines of evidence^{13, 72} that the residual entropy of polymers is less than 2 cal. deg.⁻¹ mole⁻¹ and hence the absolute entropy of polymethylmethacrylate at 25°C lies in the range 34.4 to 36.4 cal. deg.⁻¹ mole⁻¹. Combining this with Ivin's⁷³ and Small's⁷⁴ value of ΔS_{ic}^0 we obtain $S_i^0(25^\circ\text{C}) = 60.6 \pm 3.0$ cal. deg.⁻¹ mole⁻¹ which should exceed the sum of the three quantities given in Table 39 by the entropy of fusion of methylmethacrylate which is therefore 13.0 ± 4.5 cal. deg.⁻¹ mole⁻¹. This compares with the value of 13.8 cal. deg.⁻¹ mole⁻¹ obtained by subtracting the entropy of vaporization⁷⁵ from the entropy of sublimation⁷⁵.

D. M. Evans thanks the Department of Scientific and Industrial Research for the award of a maintenance grant and T. P. Melia thanks his employers, I.C.I. Ltd, Alkali Division, who seconded him to the University of Leeds during the period in which this work was carried out. We are greatly indebted to Messrs Devlin and Hulbert for their earlier work, to Dr L. A. K. Staveley for the loan of thermometer C3, and to the following who kindly supplied the polymer samples used: Dr F. E. Frey of the Phillips Petroleum Company, U.S.A.; I.C.I. Ltd, Plastics Division; E. I. Du Pont De Nemours, U.S.A.; General Electric Research Laboratory, U.S.A. We are also indebted to the D.S.I.R. for a grant in aid of this investigation.

Part VIII reports results obtained in part at the Research Dept, I.C.I. Ltd (Alkali Division), Northwich, Cheshire.

*Schools of Chemistry and Physics,
University of Leeds*

(Received January 1962)

REFERENCES

- ¹ DAINTON, F. S. and IVIN, K. J. *Quart. Rev. chem. Soc., Lond.* 1958, **12**, 61
- ² SCOTT, R. B., MEYERS, C. H., RANDS, R. D., BRICKWEDDE, F. D. and BEKKEDAHL, N. *J. Res. Nat. Bur. Stand.* 1945, **35**, 39
- ³ STIMSON, H. F. *J. Res. Nat. Bur. Stand.* 1949, **42**, 209
- ⁴ OSBORNE, N. S., STIMSON, H. F., SLIGH, T. S. and CRAGOE, C. S. *Sci. Pap. U.S. Bur. Stand.* 1925, **20**, 65, 5501.
- ⁵ FURUKAWA, G. T., MCCOSKEY, R. E. and KING, G. J. *J. Res. Nat. Bur. Stand.* 1951, **47**, 256
- ⁶ LINTON, W. H. *Trans. Plast. Inst., Lond.* 1960, **28**, 131
- ⁷ SCHWEITZER, C. E., MACDONALD, R. N. and PUNDERSON, J. O. *J. appl. Polym. Sci.* 1959, **1**, 158
- ⁸ KOCH, T. A. and LINDVIG, P. E. *J. appl. Polym. Sci.* 1959, **1**, 164
- ⁹ HAMMER, C. F., KOCH, T. A. and WHITNEY, J. F. *J. appl. Polym. Sci.* 1959, **1**, 169
- ¹⁰ LINTON, W. H. and GOODMANN, H. H. *J. appl. Polym. Sci.* 1959, **1**, 179
- ¹¹ ALSUP, R. G., PUNDERSON, J. O. and LEVERETT, G. F. *J. appl. Polym. Sci.* 1959, **1**, 185
- ¹² BEATTIE, J. A. *J. Math. Phys.* 1926, **6**, 1
- ¹³ BEKKEDAHL, N. and MATHESON, H. *J. Res. Nat. Bur. Stand.* 1935, **15**, 503
- ¹⁴ FURUKAWA, G. T. and MCCOSKEY, R. E. *J. Res. Nat. Bur. Stand.* 1953, **51**, 321
- ¹⁵ ROSSINI, F. D. 'Selected values of chemical thermodynamic properties'. *Circ. U.S. Nat. Bur. Stand. No. 500*, 1952
- ¹⁶ DAINTON, F. S., IVIN, K. J. and WALMSLEY, D. A. G. *Trans. Faraday Soc.* 1959, **55**, 61
- ¹⁷ Calculated in this work by means of the standard equation given in ref. 15
- ¹⁸ DAINTON, F. S., EVANS, D. M., HOARE, F. E. and MELIA, T. P. Part III of this Series, page 277
- ¹⁹ SMALL, P. A. *Trans. Faraday Soc.* 1955, **51**, 1717
- ²⁰ LAUDER, I. Private communication
- ²¹ WALKER, J. F. *Formaldehyde*. Reinhold: New York, 1953
- ²² ILICETO, A. and BEZZI, S. *Chim. e Industr.* 1960, **42**, 728
- ²³ TEBOLSKY, A. V. and EISENBERG, A. *J. Amer. chem. Soc.* 1959, **81**, 2302
- ²⁴ ISHIDA, Y., MASATO, M., HIDEO, I., MASATSUGU, Y., FUJIO, I. and MOTOWO, T. *Kolloidzshr.* 1961, **174**, 162

From Part II

- ²⁵ FARTHING, A. C. *J. chem. Soc.* 1955, 3648
- ²⁶ DAINTON, F. S., IVIN, K. J. and WALMSLEY, D. A. G. *Trans. Faraday Soc.* 1960, **56**, 1784
- ²⁷ SANDIFORD, D. J. H. *J. appl. Chem.* 1958, **8**, 188
- ²⁸ Part I of this series, p 263
- ²⁹ HOGE, H. J. *J. Res. Nat. Bur. Stand.* 1946, **36**, 111
- ³⁰ DOUSLIN, D. R. and HUFFMANN, H. M. *J. Amer. chem. Soc.* 1946, **68**, 173
- ³¹ MAIR, B. J., GLASGOW, A. R. and ROSSINI, F. D. *J. Res. Nat. Bur. Stand.* 1941, **26**, 591
- ³² FURUKAWA, G. T. and REILLY, M. L. *J. Res. Nat. Bur. Stand.* 1956, **56**, 285
- ³³ DAINTON, F. S., DEVLIN, T. R. E. and SMALL, P. A. *Trans. Faraday Soc.* 1955, **51**, 1710

From Part III

- ³⁴ GAYLORD, N. G. and MARK, H. F. *Linear and Stereoregular Addition Polymers Interscience*: New York, 1959
- ³⁵ SOCHAVA, I. V. *Dokl. Akad. Nauk S.S.S.R.* 1960, **130**, 126
- ³⁶ SOCHAVA, I. V. and TRAPEZNIKOVA, O. N. *Dokl. Akad. Nauk S.S.S.R.* 1957, **113**, 784
- ³⁷ DOLE, M. and WETHINGTON, W. P. *J. chem. Phys.* 1952, **20**, 781

- ³⁸ WUNDERLICH, B. and DOLE, M. *J. Polym. Sci.* 1957, **24**, 201
³⁹ KELLEY, K. K., PARKS, G. S. and HUFFMANN, H. M. *J. Phys. Chem.* 1929, **33**, 1802
⁴⁰ WURSTLIN, F. *Kunststoffe*, 1950, **40**, 158
⁴¹ HUNTER, E. and OAKES, W. E. *Trans. Faraday Soc.* 1945, **41**, 49
⁴² DANUSSO, F., MORAGLIO, G. and TALAMINI, G. *J. Polym. Sci.* 1956, **21**, 139
⁴³ QUINN, F. A. and MANDELKERN, L. *J. Amer. chem. Soc.* 1958, **80**, 3178
⁴⁴ DOLE, M. *Kolloidzshr.* 1959, **165**, 40
⁴⁵ SAUER, J. A. and WOODWARD, A. E. *Rev. mod. Phys.* 1960, **32**, 88

From Part IV

- ⁴⁶ NATTA, G. *J. Polym. Sci.* 1955, **16**, 143
⁴⁷ NATTA, G., CORRADINI, P., BASSI, I. W. and PASQUON, I. *R.C. Accad. Lincei*, 1955, **19**, 404 and 453
⁴⁸ NATTA, G., CORRADINI, P. and BASSI, I. W. *Makromol. Chem.* 1956, **21**, 240
⁴⁹ TURNER-JONES, A. Private communication
⁵⁰ FURUKAWA, G. T., MCCOSKEY, R. E. and KING, G. J. *J. Res. Nat. Bur. Stand.* 1953, **50**, 357
⁵¹ Part III of this series, p 277
⁵² DANUSSO, F., MORAGLIO, G. and FLORES, E. *R.C. Accad. Lincei*, 1958, **25**, 520
⁵³ SCHAEFGEN, J. R. *J. Polym. Sci.* 1959, **38**, 549
⁵⁴ GEE, G. *Proc. chem. Soc.* 1957, 105
⁵⁵ BOUNDY, R. H. and BOYER, R. *Styrene*, p 67. Reinhold: New York, 1952
⁵⁶ KAUZMANN, W. *Chem. Rev.* 1948, **43**, 219

From Part V

- ⁵⁷ DOLE, M. *Fortschritte der Hochpolymeren-Forschung*, 1960, **2**, 221
⁵⁸ NATTA, G. *Makromol. Chem.* 1960, **35**, 94
⁵⁹ NATTA, G., CORRADINI, P. and PORRI, L. *R.C. Accad. Lincei*, 1955, **20**, 728
⁶⁰ PORRI, L., CORRADINI, P. and MORERO, D. *Chim. e Industr.* 1958, **40**, 362
⁶¹ BACCAREDDA, M. and BUTTA, E. *J. Polym. Sci.* 1961, **51**, 539

From Part VI

- ⁶² DAINTON, F. S. and IVIN, K. J. *Trans. Faraday Soc.* 1950, **46**, 331
⁶³ ASHTON, J. G., FINKE, H. L., BESTUL, A. B., PACE, E. L. and SZASZ, G. J. *J. Amer. chem. Soc.* 1946, **68**, 52
⁶⁴ MCCULLOCH, J. P., FINKE, H. L., CROSSE, M. E., MESSERLY, J. F. and WADDINGTON, G. *J. phys. Chem.* 1957, **61**, 289
⁶⁵ GIAUQUE, W. F. and STEPHENSON, C. C. *J. Amer. chem. Soc.* 1938, **60**, 1389
⁶⁶ DAINTON, F. S., DIAPER, J., IVIN, K. J. and SHEARD, D. R. *Trans. Faraday Soc.* 1957, **53**, 1269

From Part VII

- ⁶⁷ SCHNELL, H. *Trans. Plast. Inst., Lond.* 1960, **28**, 143

From Part VIII

- ⁶⁸ SOCHAVA, I. V. *Vestnik Leningrad Univ.* 1961, **2**, 70
⁶⁹ SOCHAVA, I. V. and TRAPEZNIKOVA, O. D. *Vestnik Leningrad Univ., Ser. Fiz. i Khim.* 1958, **13**, 65
⁷⁰ ERDÖS, E., JÄGER, L. and POUCHLY, J. *Chem. Listy*, 1952, **46**, 770; *Chem. Abst.* 1953, **47**, 4183
⁷¹ BLOUT, E. R. and MARK, H. *Monomers*. Interscience: New York, 1951
⁷² TEMPERLEY, H. N. V. *J. Res. Nat. Bur. Stand.* 1956, **56**, 55
⁷³ IVIN, K. J. *Trans. Faraday Soc.* 1955, **51**, 1273
⁷⁴ SMALL, P. *Trans. Faraday Soc.* 1953, **49**, 441
⁷⁵ BYWATER, S. *J. Polym. Sci.* 1952, **9**, 417

Radiation-induced Solid State Polymerization

P. G. GARRATT

One of the more recent advances in the field of polymer radiation has been the polymerization of solid monomers. This can occur even when the monomer is frozen down to liquid nitrogen temperature. Indeed some of the monomers can only be polymerized by exposure to gamma radiation when in the solid state, and in the majority of cases investigated more rapid polymerization was observed in the crystalline state than in the liquid state. This field is attracting growing interest and the following review attempts to outline many of the results already obtained.

MOST of the previous work on radiation-induced polymerization has been mainly concerned with the irradiation of vinyl monomers in the liquid state or in solution. The absorbed energy produces ionization and excitation, this resulting in the formation of radicals which can initiate or terminate the growing polymer chains. The kinetics of the reaction indicate that the initiating radicals are distributed at random throughout the system. The propagation reaction is independent of the radiation process, and is identical with that found in chemical initiation. For many monomers, irradiated at low intensities, the number of chains is dependent only on the dose absorbed, although their average length decreases as the radiation intensity rises (more radicals are available to terminate the growing chains)*. Under these conditions the rate of polymerization varies as the half power of the radiation intensity ($I^{1/2}$). This, however, is not found with acrylonitrile for example, when due to the insolubility of the polymer in the monomer the growing chains fold occlude the radical ends.

More recently evidence has been produced to account for polymerization occurring by ionic mechanisms, these usually being favoured at low temperatures. The polymerization yield (conversion per unit dose) is found to be independent of the intensity indicating that termination is not due to radiation-induced radicals. In this instance the polymerization rate varies with the intensity (I). Further, greatly increased yields are obtained when polymerization occurs in the presence of certain inorganic additives. This is probably due to the stabilization of the initial charged species. There is not so much information available on ionic polymerizations as on radical polymerizations. One of the major difficulties encountered in solid state polymerization is the accurate determination of true polymer yields. These yields are one of the predominant factors involved in elucidating the mechanisms operative in this type of polymerization.

In the solid state polymerization it is often necessary to destroy the frozen monomer phase after irradiation to determine the polymer yield.

*This is assuming no chain transfer.

Evidence (discussed later) has been produced to show that a large contribution to the polymerization reaction may occur during the warming of the frozen mixture. During this period it is visualized that reactive species may be released, thereupon producing additional polymerization. It is possible, however, to follow the course of solid state polymerization by the following techniques: X-ray diffraction, optical methods and electron spin resonance (e.s.r.) studies. These later methods do not involve the destruction of the crystalline solid phase.

For the purpose of this review, the work already carried out in this field is described under the headings of various monomer groups.

ACRYLAMIDE

One of the first reports on solid state polymerization by ionizing radiations was published as early as 1954, when acrylamide was polymerized using gamma radiation¹. At low temperatures an extremely long induction period was observed and on warming a violent polymerization reaction occurred. The polymer was subsequently isolated using methanol as precipitant.

Much of the detailed work on solid state polymerization has been carried out using acrylamide as monomer, this being crystalline at room temperature (m. pt 84°C)²⁻¹⁷. By measuring the polymer formed after various periods of standing, it has been observed that polymerization continues for several months after removal from the source²⁻⁶. When the monomer is exposed to gamma rays at -78°C, a temperature at which there is no appreciable polymerization, subsequent warming to higher temperatures showed polymerization to continue for six months, there being no indication of an approach to a limiting conversion². The kinetics of such a system has been reported to be consistent with a bimolecular termination. The dependence of yield on radiation intensity and radical concentration is intermediate between that expected from a uniform radical distribution and that expected from the radical growth in isolated tracks of gamma rays²⁻⁵. The kinetic data obtained from the study of the polymerization of acrylamide in the temperature range 0° to 60°C may be expressed in the form

$$Y = A \log(1 + Bt)$$

where Y is the fractional yield of polymer in time t , and A and B are constants, A being essentially temperature independent^{4, 7}. The time dependence of the polymerization is characterized by the lack of an induction period and by a rapid decay in rate with monomer conversion. It is important to note, however, that during the period of polymerization the radical concentrations measured by electron spin resonance were found to remain almost constant. This indicates that the characteristic bimolecular termination step observed in liquid state polymerization is not involved in solid state polymerization. The observed radical concentrations were in good agreement with the number of polymer chains obtained from the polymer yield and molecular weight data, which is an indication that all the radicals initiate chains and that chain transfer is negligible.

In solid solutions of acrylamide and propionamide (which are isomorphous) the polymer chain length was determined by chain transfer to

the propionamide. The high value of the chain transfer coefficient was ascribed to the directing influence of the crystal lattice. The chain transfer behaviour of the propionamide points to the importance of lattice control in solid state polymerization. It is suggested that the polymer chains grow at the monomer/polymer interface with the growing end anchored in the crystal lattice of the monomer. There is no appreciable chain transfer in solid solutions of acrylamide containing acetamide²⁻⁵, which is not isomorphous with the crystalline acrylamide.

As there would appear to be no free radical termination involved, the usual steady state assumptions were found inadequate⁶. The results obtained were consistent with the view that polymerization is a heterogeneous reaction, there being a nucleation mechanism in which the free radicals are probably trapped by overlapping of the growing polymer chains. Favourable sites for nucleation of reaction are crystal imperfections. As the reaction proceeds from the imperfect regions, additional strains can then release the dormant trapped radicals by creating an environment favourable for propagation. This latter release is termed 'enhanced nucleation'. This theory is supported by the results of experiments with mixed crystals. The addition of diluent propionamide, even though isomorphous with acrylamide, introduces more imperfections, these resulting in a higher rate of reaction than pure acrylamide. Evidence that polymerization occurs at crystal imperfections is shown by the fact that if the crystal is scratched, the polymerization proceeds rapidly along the scratch. X-ray diffraction studies demonstrate that during the entire course of reaction both the crystalline monomer and amorphous polymer are present, this being further proof of a two-phase mechanism⁸.

Electron spin resonance and various microscopic studies of the solid state polymerization of acrylamide confirm that the reaction involves free radicals which do not terminate in the normal manner because they are trapped when the growing polymer regions overlap⁹. It is concluded that the rates of polymerization are governed at least in part by local build up and release of compressive and tensile stresses. Evidence is given for the polymer nuclei being non-uniformly distributed, these falling into lines believed to be dislocations or other defects.

Further microscopic studies of initially crystalline acrylamide at doses when the acrylamide was completely polymerized showed no evidence of birefringence. X-ray diffraction diagrams showed only a broad diffuse ring characteristic of unoriented and non-crystalline polymers¹⁰. This shows that the initial orientation present in the monomer crystal has been completely lost in the course of polymerization. Taken in conjunction with the earlier work, these results are consistent with polymerization occurring in the vicinity of definite sites, probably dislocations or regions of high strain.

On the other hand, it has been concluded that the irradiation of an acrylamide crystal with X-rays yields a polymer which has the same external form as the monomer and is still double refracting. Since the polymer shows no sharp X-ray lines, the optical effects observed must arise from a strain or anisotropic arrangement produced by the 'fixing' of monomer molecules whilst the polymerization occurs¹¹. These birefringent optical properties have been confirmed in this laboratory¹².

It was concluded from electron spin resonance data that the continued polymerization of acrylamide after removal from the source is probably due to long-lived free radicals. An attempt to utilize these radicals to initiate the polymerization of methylmethacrylate by dissolving irradiated acrylamide in it, proved unsuccessful. However, with irradiated *N-t*-butyl acrylamide (which is a monomer that reacts only slowly with itself due to steric hindrance) immersion in styrene produced a polymer containing polystyrene and *N-t*-butyl acrylamide. This result indicates that free radicals may be stored in some kinds of irradiated crystals and that they may be used to initiate further polymerizations at a later date¹³.

CARBOXYLIC ACID MONOMERS

Further work with the salts of carboxylic acid monomers, mainly acrylic and methacrylic acid, allowed the arrangement of the reactive monomer in the crystal lattice to be varied by altering the cation and the degree of hydration in some of the salts^{7,18}. A study of the potassium, sodium and lithium salts of acrylic acid exposed to gamma rays at -78°C showed the reactivity of the salts to be in the order potassium > sodium > lithium, from which it was concluded that the polyacrylate chain propagates more easily in the lattice of the potassium salt. Evidence for the chain length being determined by chain transfer is shown by the fact that the molecular weight of the polymer increases only slightly with polymer yield.

More recently it has been found that the solid state polymerization of methacrylic acid in samples following irradiation with gamma rays at -78°C leads to a polymer which is less syndiotactic than that obtained from the monomer in the liquid phase¹⁹. Further, it has been shown that for alkali methacrylates the sodium salt is more reactive than the potassium salt, while lithium methacrylate does not polymerize. This is the opposite order to that found for the alkali acrylates.

ACRYLONITRILE AND METHACRYLONITRILE

It has been established that the polymerization of acrylonitrile at room temperature proceeds by a radical mechanism. It appears that in its own monomer the termination step is retarded by poor solvent conditions, giving a long lifetime to the growing radicals. The dependence of the polymerization rate on radiation intensity I is, therefore, approximately $I^{0.8}$ instead of the normal dependence as $I^{0.5}$. Marked post-irradiation steps have also been observed with acrylonitrile, due to these trapped radicals.

In the solid state the irradiation of acrylonitrile gives rather unexpected results. Even on continuous irradiation of the monomer at liquid nitrogen temperature it appears impossible to polymerize the monomer beyond a conversion of approximately five per cent²⁰⁻²². To discover whether any reaction occurs during the warming of the frozen monomer-polymer phase, the effect of slow and fast melting of the reaction mixture has been investigated. Experimental results have shown that on slow melting the mixture yields twice as much polymer as it yields on fast melting, although conversion for slow melting still only yields five per cent polymer²⁰. If, however, the reaction mixture is allowed to melt and then recrystallize a much

higher conversion is obtained on further irradiation. This would point to the increased polymerization being due to defects in crystal structure around polymer chains.

It has also been reported that if acrylonitrile is irradiated at -196°C to a dose of 7.8×10^5 rads, subsequent warming to room temperature caused the acrylonitrile to polymerize explosively before the solid began to melt, giving large quantities of polymer²³.

It has been found that during the polymerization the reaction vessels became electronically charged, and subsequent discharging with a grounded electrode causes polymerization to proceed further²⁴. A linear conversion up to twenty three per cent was achieved when the solid monomer was irradiated with X-rays in a grounded steel vessel²⁰. This phenomenon was interpreted as indicating that some electronically charged species are the precursors of the active centres responsible for the initiation of polymerization. Recent work in our laboratory has shown that the application of high voltages to the monomer at -196°C during irradiation with gamma rays has little or no effect on the yield of polymer²⁵.

The infra-red spectra of polyacrylonitrile polymerized by irradiation has shown that a reaction which gives the C:N linkage to the polymer occurs at low temperatures²⁶.

It has recently been shown that acrylonitrile can polymerize by two different mechanisms, one radical and one probably ionic when initiated by ionizing radiations in different temperature regions^{21,27}. The following evidence can be forwarded to support this claim that the mechanism in the solid state is almost certainly ionic:

- (a) Acrylonitrile was found to polymerize easily at -196°C even in the presence of radical inhibitors such as diphenyl picryl hydrazyl and benzoquinone which affect the polymerization at room temperature.
- (b) The induction period observed at room temperature was absent at low temperatures.
- (c) The initial polymerization rate was found to be proportional to the intensity of radiation, this being characteristic of ionic polymerizations, although the rate for acrylonitrile at room temperature was dependent on the intensity to the power 0.8 (which is higher than for normal radical polymerization due to lack of the usual termination reaction).
- (d) Very low activation energies are observed (approximately 0.4 kcal/mole) at low temperatures, as against about 5 kcal/mole for typical radical reactions.

Similar observations have been made for methacrylonitrile in the solid state, it being concluded that the reaction is probably ionic at low temperatures²⁸.

NON-VINYL MONOMERS

Several non-vinyl monomers can also polymerize in the crystalline state and the polymerization of one of these, formaldehyde, initiated by ionizing radiations has been reported^{23,29}. The irradiation in the solid state at -196°C induces a rapid, almost explosive polymerization reaction, which can be initiated on warming the irradiated solid formaldehyde or by

mechanical shock. A very high G value for conversion 5.4×10^6 is obtained for a conversion of 52 per cent which is not normally obtained in radiation polymerization. In view of this very high G value it was considered that the initiation mechanism of the radiation polymerization in this case is different from the free radical or a simple ionic mechanism. It is conceivable that ionizing radiation brings formaldehyde to highly excited states including a polar state $\text{H}_2\text{C}^+ - \text{O}^-$, which will presumably initiate an ionic polymerization reaction. It is possible to regard the highly excited molecule as trapped active centres at low temperatures, which initiate polymerization as soon as the temperature of the irradiated solid monomer is partly raised²³. This polymerization has also been interpreted in terms of an internal warming up due to the exotherm of growing chains²⁹. The solid state polymerization of formaldehyde by gamma radiation has been described in a recent patents report³⁰. The polymer obtained from the solid state polymerization of formaldehyde was found to have a fibrous bulky appearance. From observations of birefringence or X-ray diffraction photographs, the orientation of polymer molecules was observed to be rather perpendicular than parallel to the fibre axis.

Acetaldehyde has also been found to polymerize in the solid state³¹ and further investigations³² by X-ray diffraction methods showed polymerization occurring at -140°C .

RING COMPOUNDS

The radiation-induced solid state polymerization of ring compounds which are known to have strained structures has been intensively investigated. Trioxan^{33,34}, diketene^{34,35}, β -propiolactane^{34,36} and 3,3-bis-chloromethyl-oxacyclobutane^{34,37} have been found to polymerize only in the solid state by the irradiation of gamma rays or electrons. It was assumed that the ions produced by radiation have prolonged activities in the solid state which are sufficient to cause polymerization, and that the monomer molecules are suitably arranged in the crystalline state to initiate polymerization efficiently. The polymerization rate is approximately proportional to the first order of radiation intensity and the apparent activation energy is observed to be negative.

With diketene, β -propiolactane and 3,3-bis-chloromethyl-oxacyclobutane a maximum conversion was obtained at relatively low yields, the conversion of trioxan being linear up to high values. The saturation phenomenon observed has been ascribed to the fact that at high conversions polymer molecules aggregate with each other to form bunches of polymer. Unreacted monomer is squeezed out and loses its crystalline orientation to the extent of hindering further polymerization³⁸. A kinetic scheme has been developed to account for both the kinetic data obtained and the saturation phenomena. The rate of polymerization is given by the equation

$$dY/dt = A(1 - ZY)$$

where

$$A = k_i k_p I / k_t$$

I being the radiation intensity, $k_i k_p k_t$ the rate constants for initiation, propagation and termination, and Y the polymer yield. It is assumed that

the effective monomer fraction for polymerization is $(1 - ZY)$. From investigations of polymerization kinetics and analysis of the polymer structure it was concluded that the polymerization takes place by an ionic mechanism in the monomer crystalline lattice.

A study of the structure of these polymers shows them to have good crystallinity as well as orientation³⁹. The polymers obtained from the monomer in the large single crystals have higher melting points and better orientation than those obtained from suddenly cooled monomers. In general the polymers obtained from such large monomer crystals have the outward appearances of large crystals. It was noted that the orientation observed for polytrioxan obtained from large crystalline monomer was greater than that of stretched polyoxymethylene film or fibre obtained from formaldehyde. This illustrates the fact that the monomer arrangement in crystals greatly influences the mechanism of the propagation reaction in the solid state, and that with trioxan the propagation reaction takes place along a crystallographic axis.

It was observed that the rate of polymerization was remarkably reduced in the presence of solvent or co-monomer⁴⁰. These results suggested that the molecules of the solvent or co-monomer may be able to invade the crystal of the monomer and disorder its lattice so that polymerization no longer occurs.

MISCELLANEOUS MONOMERS

The polymerization of various other vinyl monomers has been investigated in detail. The radiochemical polymerization of styrene and 2,4-dimethyl styrene is considered to proceed by a predominantly cationic mechanism at low temperatures and mainly by a radical mechanism at high temperatures⁴¹. The effects of the change of phase and heterogeneity on the polymerization of these monomers have also been studied⁴². It was found that in the pure solid monomers the rate of polymerization increases with temperature up to a maximum value at the melting point where the system is heterogeneous. The rate then falls rapidly above the melting point to a minimum value, and then rises in the customary manner for radical polymerization. Another report on the polymerization of styrene in the solid state, interprets the results as indicating that reaction at low temperatures probably proceeds by an anionic mechanism⁴³. A twofold increase in yield (per hour) was obtained in the presence of benzoquinone. It was later observed that freshly sublimated benzoquinone (present in concentrations below one per cent) does not have any effect on the polymerization²⁰.

It is interesting to note that methyl methacrylate does not polymerize in the solid state^{20,44}. However, a rapid polymerization was observed when frozen mixtures of the monomer with paraffin wax or mineral oil were treated with radiation²⁰. This may be due to a different crystalline or amorphous environment.

In the polymerization of vinyl stearate by 1 MV electrons, a discontinuity of reaction rate and molecular weight with respect to temperature was noted in the vicinity of the monomer melting point, and it was suggested that in this region the diffusion constant for propagation is easily affected⁴⁵.

The polymerization of vinyl stearate has also been reported by other workers^{10,14}.

The solid state polymerization of butadiene⁴⁶ has been shown to proceed by an ionic mechanism at low temperatures. The polymerization of various other monomers in the solid state initiated by ionizing radiations has been reported from time to time. These include hexamethylcyclotrisiloxane^{47,48}, isobutylene⁴⁹, ethensulphonamide⁵⁰, methacrylamide^{14,15}, methylene bisacrylamide^{10,14,15}, acrylic and methacrylic acid¹⁴, the metallic acrylates^{10,14} and tetraethylene-glycoldimethacrylate⁵¹.

PHOTOCHEMICALLY INITIATED POLYMERIZATION

The photochemical polymerization of crystalline methacrylic acid by ultraviolet light has been investigated either with or without azobisisobutyronitrile as photosensitizer⁵². Because of the low energy of each photon, it is assumed that such reactions proceed through a radical mechanism, there being no ionic contribution. Results indicate that the radicals formed on the surface of the crystal are immobile at -196°C , but they become progressively more mobile as the temperature increases. It was suggested that the reaction is probably initiated by radicals formed near the surface of crystals or cracks. Micrographs show boundaries travelling inwards from surfaces with the gradual establishment of the reaction zone; this accounts for the autocatalytic character of the unsensitized reaction in the early stages.

Further investigation of the photochemical polymerization of crystalline monomers has been reported⁵³. A study of the crystal birefringence of crystalline acrylic and methacrylic acid was followed by optical methods. A remarkable effect is found if a small stress is mechanically applied to the monomer during the polymerization. The reaction is immediately halted or retarded, and on removal of the stress the polymerization restarts. With methacrylic acid the polymerization restarts immediately, but with acrylic acid the reaction only resumes after an induction period similar to the one initially observed.

It is now assumed that dislocations within the crystals are suitable sites for radical formation⁵⁴. When the stress is applied it is thought that the dislocations move away from the polymer chains, preventing the growth of these chains. It is possible that with methacrylic acid the dislocations move under stress elastically, whilst in acrylic acid the dislocations move non-elastically, accounting for the further induction period.

MISCELLANEOUS REPORTS

Discussions on the possible mechanisms of solid state polymerization have been published^{55,56}. A summary of solid state polymerization was included in a review of radiation polymerization⁵⁷. More recently a hypothesis explaining the mechanism of low temperature polymerization has appeared⁵⁸.

DISCUSSION

One of the major problems is to interpret the mechanism involved in these solid state reactions. It is plausible that both ionic and radical mechanisms exist in the polymerization of various monomers. This is illustrated for a

large number of monomers including acrylonitrile²⁷, methacrylonitrile²⁸, butadiene⁴⁶, styrene⁴¹, and 2,4-dimethylstyrene⁴¹, different polymerization mechanisms existing in polymerization under identical conditions but for temperature. At a certain transition temperature which varies for each monomer both these mechanisms occur to some extent.

It is apparent that ionic mechanisms are favoured at low temperatures. This view is supported by an accumulation of evidence, i.e. the lack of induction period, very low activation energies, initial polymerization rates and the absence of any inhibition of polymerization in the presence of radical scavengers. Further evidence is found in strained ring compounds which have only been effectively polymerized with ionic initiators^{34,38}. In addition it has been established that during the polymerization of acrylonitrile at low temperatures, the reaction vessel became electronically charged, this also being attributed to an ionic species²⁴. It has been suggested that styrene and 2,4-dimethylstyrene react by a predominantly cationic mechanism⁴¹, but with acrylonitrile and methacrylonitrile it may be argued that the reaction is mainly anionic, as these monomers are known not to polymerize in the presence of cationic initiators.

In the liquid state the majority of polymerizations proceed by a radical mechanism. However, evidence can be produced to support radical mechanisms in the solid state, although as it will be seen later in this discussion, part of this evidence is open to question. It is noticeable that this evidence relates mainly to monomers which are crystalline at higher temperatures. Electron spin resonance measurements on acrylamide have shown that the radical concentration was approximately equal to the number of polymer chains calculated from kinetic evidence^{3,4}. Further, the photochemically initiated polymerization of methacrylic acid and acrylic acid is found to proceed in the presence of the free radical initiator azobisisobutyronitrile⁵². It has been shown that acrylamide can polymerize at 80°C in the presence of this initiator¹⁶, which would certainly appear to support a radical mechanism.

It cannot, however, be assumed that if a radical mechanism does operate in the solid state then it is of a similar nature to that observed in liquids. It has already been mentioned that there is no characteristic bimolecular termination in the polymerization of acrylamide⁶. Also in the polymerization of various acrylate salts, where the polymerizing species is the anion, different polymerization rates have been observed for the varying cations^{7,18}. Chemically similar monomers, i.e. acrylamide, methacrylamide and methylene bisacrylamide, which have similar reactivities in the liquids, are described as having markedly dissimilar polymerization rates in the solid state⁷.

In the e.s.r. studies it has usually been assumed that the radical concentrations observed are the species responsible for the propagation of polymerization. This assumption may be questioned. The free radicals observed in irradiated acrylamide at room temperature are confirmed to be only those formed in the polymer portion of the crystal⁵⁹. The radical concentrations derived from e.s.r. techniques with acrylamide^{3,4,7,9} and methacrylic acid⁵⁴ are almost constant despite a marked increase in polymerization. If

indeed it is a radical mechanism, this type of polymerization could be attributed to the formation of two types of radicals, one short-lived (somewhat similar to that encountered in the liquid state) and one long-lived encountered in the solid state. In this concept the short-lived radicals would be mainly responsible for polymerization. It is the long-lived species which is observed by electron spin resonance and which remains in the irradiated crystal. These crystals have induced polymerization in other monomers after some considerable time¹³.

The number of trapped radicals observed by electron spin resonance could still equal the number of chains obtained if an ionic propagation mechanism prevails; the ionic part of a radical anion or cation would be the initiating species, the radical anion or cation being fixed during chain growth⁶⁰. Alternatively, the ejected electron may be recaptured at the end of polymerization, to give a radical species.

Electron spin resonance, X-ray diffraction and microscope techniques would appear to confirm the view that the polymer nuclei are non-randomly distributed, the reaction occurring in definite regions associated with areas of high strain⁹. There would appear to be areas which involve the buildup and release of strain. Indeed, the polymerization is found to proceed along scratches marked on the crystal⁸, and the addition of diluent propionamide to acrylamide systems produces a higher rate of reaction²⁻⁵ due to the introduction of more imperfections. Even more remarkable evidence is the fact that the application of small pressures during the polymerization of acrylic and methacrylic acid halts or retards the reaction⁵³.

Associated with the view that the polymerization proceeds at areas of high strain is the idea that the reaction is of a heterogeneous nature, the monomer and polymer coexisting in different phases (crystalline and amorphous) throughout the reaction. This is found to be so with acrylamide¹⁰. A maximum value for polymerization rate has been observed with styrene and 2,4-dimethylstyrene at the melting point where the system is obviously heterogeneous⁴².

One of the conflicting aspects of these polymerizations is concerned with the structure of the polymer. Polyacrylamide and several related compounds exhibit no birefringence and appear to be unoriented and amorphous¹⁰. These investigations led to the conclusion that the formation of amorphous polymer was probably universal in solid state polymerization, the crystal symmetry not imposing order and orientation on the polymer.

In opposition to this concept polymers obtained from heterocyclic compounds are found to have the appearance of a uniaxial fibril and to possess better orientation than those obtained from suddenly cooled monomer^{38,39}. Optical birefringence is obtained with all these materials. In these latter materials, it was presumed that the crystalline monomer structure directly imposes order on the polymer and that propagation occurs along a crystallographic axis.

Several more arguments can be put forward to extend the theory that the crystal lattice may impose control on the polymerization. The rate of polymerization would seem to depend on the purity of the crystal and on the rate of strain. Chemically similar compounds are found to give differing

reactivities in the solid state as previously mentioned, despite having similar reactivities in the liquid state⁷. Different polymerization rates are observed with various metallic acrylates^{7,18}. Finally, the high chain transfer of propionamide with acrylamide illustrates this argument, particularly the negative temperature coefficient of the chain transfer efficiency which is again contrary to the behaviour of chain transfer agents in the liquid state^{2-5, 7}.

Although no final conclusions can be expressed, it would appear that ionic mechanisms can account certainly for many polymerizations at low temperatures. While this extent of polymerization is associated with areas of high strain, the method of control by the crystal lattice is still uncertain. The field of solid state polymerization presents an intriguing problem to all radiation workers and its elucidation will provide much novel information on the nature of reactions in the solid state.

The author wishes to acknowledge the helpful advice and criticism given by Professor A. Charlesby.

Physics Branch,
Royal Military College of Science,
Shrivenham, Nr Swindon,
Wiltshire

(Received May 1962)

REFERENCES

- ¹ MESROBIAN, R. B., ANDER, P., BALLANTINE, D. S. and DIENES, G. J. *J. chem. Phys.* 1954, **22**, 565
- ² FADNER, T. A., RUBIN, I. and MORAWETZ, H. *J. Polym. Sci.* 1959, **37**, 549
- ³ MORAWETZ, H. and FADNER, T. A. *Makromol. Chem.* 1959, **34**, 162
- ⁴ FADNER, T. A. and MORAWETZ, H. *J. Polym. Sci.* 1960, **45**, 475
- ⁵ MORAWETZ, H. *Chem. Listy*, 1959, **9/34**, 41
- ⁶ BAYSAL, B., ADLER, G., BALLANTINE, D. S. and COLOMBO, P. *J. Polym. Sci.* 1960, **44**, 117
- ⁷ MORAWETZ, H. *Proceedings of the Fourth International Symposium on Reactivity of Solids, Amsterdam, 1960*
- ⁸ ADLER, G. and REAMS, W. *J. chem. Phys.* 1960, **32**, 1698
- ⁹ ADLER, G., BALLANTINE, D. S. and BAYSAL, B. *J. Polym. Sci.* 1960, **48**, 195
- ¹⁰ ADLER, G. *J. chem. Phys.* 1959, **31**, 848
- ¹¹ SCHULZ, R., HENGLEIN, A., STEINWEHR, H. and BAMBAUER, H. *Angew. Chem.* 1955, **67**, 232
- ¹² LENHAM, A. P. and ORMEROD, M. G. Private communication
- ¹³ ADLER, G. and COLOMBO, P. *J. Polym. Sci.* 1959, **37**, 309
- ¹⁴ RESTAINO, A. J., MESROBIAN, R. B., MORAWETZ, H., BALLANTINE, D. S., DIENES, G. J. and METZ, D. J. *J. Amer. chem. Soc.* 1956, **78**, 2939
- ¹⁵ RESTAINO, A. J., MESROBIAN, R. B., BALLANTINE, D. S. and DIENES, G. J. *Ric. Sci.* 1955, **25A**, 178
- ¹⁶ SCHULZ, R., RENNER, G., HENGLEIN, A. and KERN, W. *Makromol. Chem.* 1954, **12**, 20
- ¹⁷ HENGLEIN, A. and SCHULZ, R. *Z. Naturf.* 1954, **9b**, 617
- ¹⁸ MORAWETZ, H. Unpublished report
- ¹⁹ MORAWETZ, H. and RUBIN, I. *International Symposium on Macromolecular Chemistry, Montreal, 1961*
- ²⁰ CHAPIRO, A. To be published

- ²¹ BENSASSON, R. and MARZ, R. *J. Polym. Sci.* 1960, **48**, 53
- ²² CHARLESBY, A., GARRATT, P. and MORRIS, J. Unpublished results
- ²³ TSUDA, Y. *J. Polym. Sci.* 1960, **49**, 369
- ²⁴ SOBUE, H., TABATA, Y. and SHIBANO, H. *Annual Meeting on Radiation Chemistry, Japan, 1960*, Vol. III, p 67
- ²⁵ CHARLESBY, A., GARRATT, P. and MORRIS, J. To be published
- ²⁶ TSUDA, Y. *Bull. chem. Soc. Japan*, 1961, **34**, 1046
- ²⁷ TABATA, Y. and SOBUE, H. *J. Polym. Sci.* 1960, **43**, 459
- ²⁸ TABATA, Y., ODA, E. and SOBUE, H. *J. Polym. Sci.* 1960, **45**, 469
- ²⁹ CHACHATY, C., MAGAT, M. and TER MINASSIAN, L. *J. Polym. Sci.* 1960, **48**, 139
- ³⁰ *Belgian Patent No. 580 839* (1959)
Delwent Belgian Patents Report 59B, A3 (1959)
- ³¹ CHACHATY, C. *C. R. Acad. Sci., Paris*, 1960, **251**, 385
- ³² LETORT, M. and RICHARD, A. *J. Chim. phys.* 1960, **57**, 752
- ³³ OKAMURA, S., HAYASHI, K. and NAKAMURA, Y. *Isotopes and Radiation, Japan, 1960*, **3**, 416
- ³⁴ HAYASHI, K. and OKAMURA, S. *Makromol. Chem.* 1961, **47**, 230
- ³⁵ OKAMURA, S., HAYASHI, K. and KITANISHI, Y. *Isotopes and Radiation, Japan, 1960*, **3**, 346
- ³⁶ OKAMURA, S., HAYASHI, K., KITANISHI, Y. and NISHII, M. *Isotopes and Radiation, Japan, 1960*, **3**, 510
- ³⁷ OKAMURA, S., HAYASHI, K. and WATANABE, H. *Isotopes and Radiation, Japan, 1961*, **4**, 73
- ³⁸ OKAMURA, S., HAYASHI, K. and KITANISHI, Y. *International Symposium on Macromolecular Chemistry, Montreal, 1961*
- ³⁹ HAYASHI, K., KITANISHI, Y., NISHII, M. and OKAMURA, S. *Makromol. Chem.* 1961, **47**, 237
- ⁴⁰ OKAMURA, S. and HAYASHI, K. *Symposium on the Effects of Ionizing Radiations on Organic and Biological Solids, Paris, 1961*
- ⁴¹ CHEN, C. S. H. and STAMM, R. F. *International Symposium on Macromolecular Chemistry, Montreal, 1961*
- ⁴² CHEN, C. S. H. *International Symposium on Macromolecular Chemistry, Montreal, 1961*
- ⁴³ CHAPIRO, A. and STANNETT, V. *J. Chim. phys.* 1960, **57**, 35
- ⁴⁴ MAJURY, T. *J. Polym. Sci.* 1955, **15**, 297
- ⁴⁵ BURLANT, W. and ADICOFF, A. *J. Polym. Sci.* 1958, **27**, 269
- ⁴⁶ SOBUE, H., TABATA, Y. and ODA, E. *J. phys. Chem.* 1961, **65**, 1645
- ⁴⁷ LAWTON, E. J., GRUBB, W. T. and BALWIT, J. S. *J. Polym. Sci.* 1956, **19**, 455
- ⁴⁸ BURLANT, W. and TAYLOR, C. *J. Polym. Sci.* 1959, **41**, 547
- ⁴⁹ HOFFMAN, A. S. *J. Polym. Sci.* 1959, **34**, 241
- ⁵⁰ WILEY, R. H. and GRENSHEIMER, D. E. *J. Polym. Sci.* 1960, **42**, 119
- ⁵¹ SCHMITZ, J. V. and LAWTON, E. *J. Science*, 1951, **113**, 718
- ⁵² BAMFORD, C. H., JENKINS, A. D. and WARD, J. C. *J. Polym. Sci.* 1960, **48**, 37
- ⁵³ BAMFORD, C. H., EASTWOOD, G. C. and WARD, J. C. *Nature, Lond.* 1961, **192**, 1036
- ⁵⁴ BAMFORD, C. H. *Chemical Society Meeting, Reading, England, 1961*
- ⁵⁵ MAGAT, M. *J. Polym. Sci.* 1960, **48**, 379
- ⁵⁶ MAGAT, M. *Makromol. Chem.* 1960, **35**, 159
- ⁵⁷ CHAPIRO, A. *Nucleonics*, 1961, **19**, No. 10
- ⁵⁸ SEMENOV, N. N. *J. Polym. Sci.* 1961, **35**, 159
- ⁵⁹ CHARLESBY, A. and ORMEROD, M. *Fifth International Symposium on Free Radicals, Uppsala, Sweden, July 1961*
- ⁶⁰ VON DER HEIJDE, H. B. Discussion on paper by H. MORAWETZ in *Fourth International Symposium on Reactivity of Solids, Amsterdam, 1960*

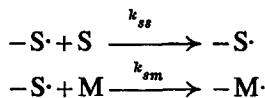
Notes

The Reactivity Ratio in Styrene Maleic Anhydride Copolymerization

IN THE course of other work¹ on branched polymers derived from styrene (*S*) and maleic anhydride (*M*), a series of copolymers of varying composition was prepared at 50°C in acetone with 0.014% w/v azo-bis-[isobutyronitrile] as catalyst after the reactants had been outgassed and the tubes sealed off. Polymerizations were carried out to less than 15 per cent conversion. The molar concentrations of monomers in the feed S_f and M_f were determined by weighing and those in the resultant copolymers S_p and M_p by the titrimetric estimation of their maleic anhydride content, following the method of Fritz and Lisicki².

| | | | | | | |
|-----------|-------|-------|------|------|------|------|
| S_f/M_f | 0.594 | 0.709 | 2.86 | 3.91 | 8.98 | 20.5 |
| S_p/M_p | 1.05 | 1.07 | 1.28 | 1.38 | 1.85 | 3.02 |

The reactivity ratio r_s represents the ratio of the velocity constants k_{ss}/k_{sm} for the two radical additions



The corresponding ratio r_m is zero and r_s is given directly by

$$S_p/M_p = 1 + r_s \cdot S_f/M_f$$

Utilizing the data above, r_s is found to be 0.097. If no assumption about r_m is made, adoption of the standard graphical intersection method³ to the full copolymerization-composition equation yields values for r_m and r_s of 0 ± 0.002 and 0.097 ± 0.002 respectively.

Bamford and Barb⁴ have reported r_s values of 0.01, 0.022, 0.023 and 0.029 for this reaction in different pure and mixed solvents at 60°C and Alfrey and Lavin⁵ have found $r_s = 0.04$ at 80°C in benzene. The system in acetone was homogeneous throughout the copolymerization, whereas the polymer precipitated during those quoted above. Further differences lie in the temperature and in the polarity of the solvent. As the latter should not affect such a radical reaction and the value of r_s at 50° might if anything be expected to be somewhat lower than at 60°C, the new value is reported without explanatory comment.

It is, however, noteworthy that a higher value than 0.04 for r_s would be more in keeping with the linear relation between $\log 1/r_s$ and $\log k_{\text{methyl}}/k_{\text{styryl}}$ found by Leavitt, Stannett and Szwarc⁶ in their comparison of methyl and styryl affinities towards vinyl substrates. Here k_{methyl} and k_{styryl} are, respectively, the rate constants for addition of methyl and styryl

radicals to the monomers. Their point [utilizing $r_s=0.04$] for addition to maleic anhydride lies considerably off the line but is brought into coincidence with it if the value of $r_s=0.097$ is employed.

M. B. HUGLIN

*Department of Inorganic and Physical Chemistry,
University of Liverpool*

(Received February 1962)

REFERENCES

- ¹ BAWN, C. E. H. and HUGLIN, M. B. To be published
- ² FRITZ, J. S. and LISICKI, N. M. *Analyt. Chem.* 1951, **23**, 589
- ³ MAYO, F. R. and LEWIS, F. M. *J. Amer. chem. Soc.* 1944, **66**, 1594
- ⁴ BAMFORD, C. H. and BARB, W. G. *Disc. Faraday Soc.* 1953, **14**, 208
- ⁵ ALFREY, T., Jr and LAVIN, E. *J. Amer. chem. Soc.* 1945, **67**, 2044
- ⁶ LEAVITT, F., STANNETT, V. and SZWARC, M. *J. Polym. Sci.* 1958, **31**, 193

*Molecular Motion in Polymethylmethacrylate by Proton
Spin-Lattice Relaxation*

WE REPORT the proton spin-lattice relaxation time, T_1 , in a sample of polymethylmethacrylate* over a wide temperature range. The apparatus will be described elsewhere¹ but we remark here that T_1 was measured directly and not by saturation techniques by means of a 90° , τ , 90° pulse sequence at variable τ . The 90° pulses used had a length $t_w=1$ microsecond and the Bloch decay after the pulse could be observed from 4 microseconds from the beginning of the pulse. Since in most of the temperature range the line width δH is about 5 gauss rising to 18 gauss at the lowest temperatures the pulse condition $T_2 \approx 1/\gamma \delta H \gg t_w$ is well satisfied. Further, the reading of the decays after only 4 microseconds is sufficiently less than T_2 . We compare our results with those of Kawai². He has $t_w=5$ microseconds and is able to read from 20 microseconds after the beginning of his pulse and claims a rather low accuracy. We consider this dangerous and feel that at least some of the discrepancy between our results and his in the intermediate temperature region in *Figure 1* may be due to this. Single exponential recoveries were observed in all cases.

The higher temperature minimum in T_1 in *Figure 1* we regard, with Kawai, as due to reorientation of substantial parts of the polymer chain. The variation of T_1 with the correlation frequency ν_c of the motion which modulates the interaction giving the relaxation is of the form^{3,4}

$$\frac{1}{T_1} = \frac{1}{1.41 T_{1,\text{min.}}} \left[\frac{\nu_r/\nu_c}{1 + (\nu_r/\nu_c)^2} + \frac{4\nu_r/\nu_c}{1 + (2\nu_r/\nu_c)^2} \right]$$

where ν_r is the resonant frequency (here 21.5 Mc/s). T_1 has a minimum when $\nu_c=1.62 \nu_r$, the difference between our and Kawai's frequency (25 Mc/s) is not important. The experimental curve is quite well represented by the sum of three terms of the above form. The ν_c for the high temperature T_1 minimum, point A, correlates quite well with extrapolated

*The sample is from the same batch to which some of the mechanical measurements of *Figure 2* refer. It is 'Perspex' sheet treated to reduce monomer content to about 0.1 per cent. Vicat softening point 123.6°C, molecular weight $>10^6$, molecular weight distribution gaussian.

radicals to the monomers. Their point [utilizing $r_s=0.04$] for addition to maleic anhydride lies considerably off the line but is brought into coincidence with it if the value of $r_s=0.097$ is employed.

M. B. HUGLIN

*Department of Inorganic and Physical Chemistry,
University of Liverpool*

(Received February 1962)

REFERENCES

- ¹ BAWN, C. E. H. and HUGLIN, M. B. To be published
- ² FRITZ, J. S. and LISICKI, N. M. *Analyt. Chem.* 1951, **23**, 589
- ³ MAYO, F. R. and LEWIS, F. M. *J. Amer. chem. Soc.* 1944, **66**, 1594
- ⁴ BAMFORD, C. H. and BARB, W. G. *Disc. Faraday Soc.* 1953, **14**, 208
- ⁵ ALFREY, T., Jr and LAVIN, E. *J. Amer. chem. Soc.* 1945, **67**, 2044
- ⁶ LEAVITT, F., STANNETT, V. and SZWARC, M. *J. Polym. Sci.* 1958, **31**, 193

*Molecular Motion in Polymethylmethacrylate by Proton
Spin-Lattice Relaxation*

WE REPORT the proton spin-lattice relaxation time, T_1 , in a sample of polymethylmethacrylate* over a wide temperature range. The apparatus will be described elsewhere¹ but we remark here that T_1 was measured directly and not by saturation techniques by means of a 90° , τ , 90° pulse sequence at variable τ . The 90° pulses used had a length $t_w=1$ microsecond and the Bloch decay after the pulse could be observed from 4 microseconds from the beginning of the pulse. Since in most of the temperature range the line width δH is about 5 gauss rising to 18 gauss at the lowest temperatures the pulse condition $T_2 \approx 1/\gamma \delta H \gg t_w$ is well satisfied. Further, the reading of the decays after only 4 microseconds is sufficiently less than T_2 . We compare our results with those of Kawai². He has $t_w=5$ microseconds and is able to read from 20 microseconds after the beginning of his pulse and claims a rather low accuracy. We consider this dangerous and feel that at least some of the discrepancy between our results and his in the intermediate temperature region in *Figure 1* may be due to this. Single exponential recoveries were observed in all cases.

The higher temperature minimum in T_1 in *Figure 1* we regard, with Kawai, as due to reorientation of substantial parts of the polymer chain. The variation of T_1 with the correlation frequency ν_c of the motion which modulates the interaction giving the relaxation is of the form^{3,4}

$$\frac{1}{T_1} = \frac{1}{1.41 T_{1,\min.}} \left[\frac{\nu_r/\nu_c}{1 + (\nu_r/\nu_c)^2} + \frac{4\nu_r/\nu_c}{1 + (2\nu_r/\nu_c)^2} \right]$$

where ν_r is the resonant frequency (here 21.5 Mc/s). T_1 has a minimum when $\nu_c=1.62 \nu_r$, the difference between our and Kawai's frequency (25 Mc/s) is not important. The experimental curve is quite well represented by the sum of three terms of the above form. The ν_c for the high temperature T_1 minimum, point A, correlates quite well with extrapolated

*The sample is from the same batch to which some of the mechanical measurements of *Figure 2* refer. It is 'Perspex' sheet treated to reduce monomer content to about 0.1 per cent. Vicat softening point 123.6°C, molecular weight $>10^6$, molecular weight distribution gaussian.

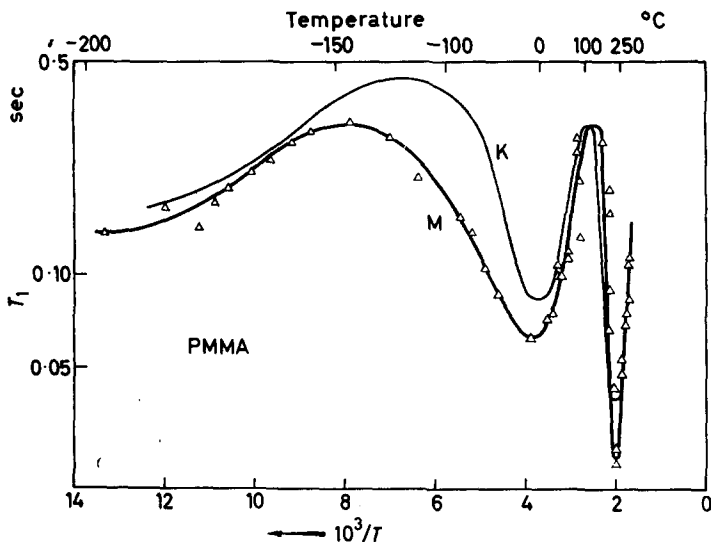


Figure 1—Proton spin-lattice relaxation times as a function of temperature from this paper (M) and from Kawai²(K)

mechanical absorption measurements (G), sometimes called the α process, in the same sample as shown in the correlation frequency map of Figure 2. It is known⁶ that the apparent activation energy is lower in the presence of a distribution of correlation frequencies and this could explain the slightly smaller slope. The difference in T_1 at the minimum between us and Kawai is probably due to variations in sample and apparatus.

The lower temperature minimum in T_1 is interpreted by Kawai, by a comparison with results for PMA, PEA, PEMA, etc., as due to the α -methyl (main chain) proton reorientation in PMMA rather than the ester methyl proton motion. We find a minimum at almost the same temperature but ours is a little lower and shows a less rapid variation of T_1 with temperature. In fact our apparent activation energy is 2.5 kcal/mole as compared with Kawai's 3.6 kcal/mole. This curve passing through point B is also shown in Figure 2.

The points D and D' are from measurements of proton line width variation^{7,8}, although the existence of two falls has been disputed⁹, and fix ν_c at about 10^4 c/s.

All measurements^{7,8,10,11} also agree to a line narrowing centred at about -110°C with an apparent activation energy of order 3.1 kcal/mole which gives the curve through the point E. The point F corresponds to a small peak in mechanical loss observed at low temperatures by Sinnott¹² and associated by him⁹ with the main chain methyl group reorientation. Since B is also very probably due to the main chain methyl we are encouraged to draw in the curve FEB. This gives the variation of the correlation frequency of the main chain methyl with temperature and we suppose that the lower slopes of the lines through E and B from n.m.r. to be due to distributions of correlation times⁶ or other secondary matters. This then supports Sinnott's⁹ assignment of point E to main chain methyl rather than

NOTES

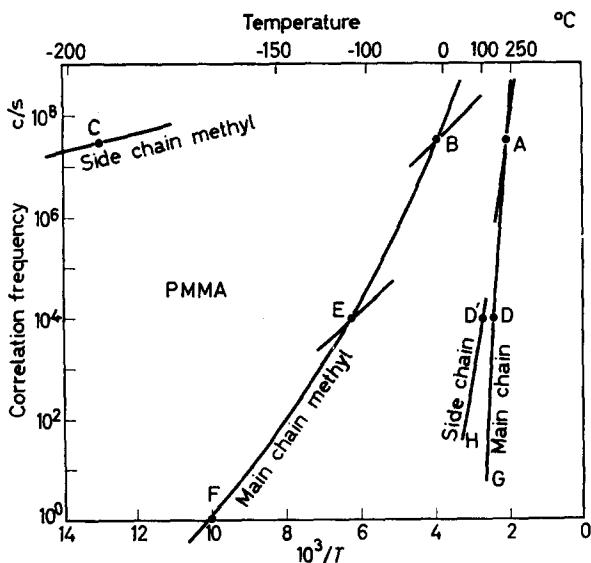


Figure 2—Correlation frequencies as a function of temperature from proton magnetic resonance (A–E), mechanical (F,G) and dielectric (H) measurements. The tentative assignment of the moving entity for the four bands is discussed in the text

Powles's⁷ earlier indecision, both of which depended on values of second moments which are difficult to measure and interpret.

The T_1 curve shows signs of a third rather shallow minimum at low temperature which leads to the point C in Figure 2 and the line through it with slope 0.7₅ kcal/mole, although this result is rather uncertain. We suggest, with Kawai, that point C is associated with side chain methyl group motion. It is possible that this correlates with Sinnott's suggestion¹³, from mechanical loss measurements, that this methyl reorientation has a correlation frequency of order 10 c/s below 4.2°K since the curve through C can be extrapolated back to about 15°K for 10 c/s. However, some care is required in the analysis of methyl group reorientation with very low apparent activation energies in view of possible tunnelling^{14,15}. It is, however, consistent as is the complete transition map, with the general rule that processes have lower activation energies the farther they are from the main one.

The interpretation of the $T_{1,\text{min}}$ values and of the T_1 curve in detail will be discussed together with T_1 measurements on a series of acrylic polymers at present in hand in a later publication.

The samples used were kindly supplied by D. J. H. Sandiford of I.C.I. Plastics Division.

Physics Department,
Queen Mary College,
Mile End Road, London E1

J. G. POWLES
P. MANSFIELD

(Received June 1962)

REFERENCES

- ¹ MANSFIELD, P. To be published
- ² KAWAI, T. *J. phys. Soc. Japan*, 1961, **16**, 1220
- ³ BLOEMBERGEN, N., PURCELL, E. M. and POUND, R. V. *Phys. Rev.* 1948, **73**, 679
- ⁴ KUBO, R. and TOMITA, K. *J. phys. Soc. Japan*, 1954, **9**, 888
- ⁵ DEUTSCH, K., HOFF, E. A. W. and REDDISH, W. *J. Polym. Sci.* 1954, **13**, 565
- ⁶ POWLES, J. G. IUPAC Symposium Report, Wiesbaden, October 1959
- ⁷ POWLES, J. G. *J. Polym. Sci.* 1956, **22**, 79
- ⁸ ODAJIMA, A., SOHMA, J. and KOIKE, M. *J. chem. Phys.* 1955, **23**, 1959
- ⁹ SINNOTT, K. M. *J. Polym. Sci.* 1960, **42**, 3
- ¹⁰ SLICHTER, W. P. and MANDELL, E. R. *J. appl. Phys.* 1959, **30**, 1473
- ¹¹ ODAJIMA, A., WOODWARD, A. E. and SAUER, J. A. *J. Polym. Sci.* 1961, **55**, 181
- ¹² SINNOTT, K. M. Results quoted in ref. 9
- ¹³ SINNOTT, K. M. *J. Polym. Sci.* 1959, **35**, 273
- ¹⁴ POWLES, J. G. and GUTOWSKY, H. S. *J. chem. Phys.* 1953, **21**, 1695
- ¹⁵ STEJSKAL, E. O. and GUTOWSKY, H. S. *J. chem. Phys.* 1958, **28**, 388

Molecular Motion in Polypropylene by Proton Spin-Lattice Relaxation

WE REPORT measurements of the proton spin-lattice relaxation time, T_1 , at a resonant frequency of 21.5 Mc/s as a function of temperature for polypropylene (PP) and for poly(3,3,3-d₃-propylene), [P(3DP)]* in *Figure 1*. Also given in *Figure 1* are some measurements on PP (K) due to Hirai and Kawai² which are generally similar to ours but differ substantially in the important intermediate temperature region. This is probably due to apparatus and sample differences as discussed in the accompanying 'Note' on polymethylmethacrylate³.

The transient method of measuring T_1 is described briefly in the accompanying 'Note'³ and will be described in detail elsewhere⁴.

In comparing the T_1 curves for the normal polypropylene and for the polypropylene with all methyl groups deuterated it is striking that the higher temperature minimum is hardly affected but that the lower temperature one is very much shallower. The higher temperature minimum is thought to be connected with motion of substantial portions of the chains, as discussed below. It is plausible that the lower temperature minimum is connected with reorientation of the methyl group as has already been suggested² from measurements on polypropylene. It should be borne in mind that we observe in this temperature region simple exponential recovery of the magnetization and so presumably the T_1 values given refer to all the protons in the sample, namely the methyl, methylene and CH protons in polypropylene and to the methylene and CH protons in the deuterated polypropylene. We note that on deuteration the T_1 minimum is less marked

*The sample of polypropylene is an isotactic polymer from Hercules Powder Co., Profax Batch 6501. The sample of poly(3,3,3-d₃-propylene) was prepared by A. D. Caunt of I.C.I. Plastics Division. The PP sample was moulded at 85°C and the P(3DP) at 175°C. Both samples were kindly loaned to us by Dr M. P. McDonald of I.C.I. Fibres Division and are the same ones for which broad line proton resonance measurements are quoted in this paper and which are published in detail elsewhere¹.

REFERENCES

- ¹ MANSFIELD, P. To be published
- ² KAWAI, T. *J. phys. Soc. Japan*, 1961, **16**, 1220
- ³ BLOEMBERGEN, N., PURCELL, E. M. and POUND, R. V. *Phys. Rev.* 1948, **73**, 679
- ⁴ KUBO, R. and TOMITA, K. *J. phys. Soc. Japan*, 1954, **9**, 888
- ⁵ DEUTSCH, K., HOFF, E. A. W. and REDDISH, W. *J. Polym. Sci.* 1954, **13**, 565
- ⁶ POWLES, J. G. IUPAC Symposium Report, Wiesbaden, October 1959
- ⁷ POWLES, J. G. *J. Polym. Sci.* 1956, **22**, 79
- ⁸ ODAJIMA, A., SOHMA, J. and KOIKE, M. *J. chem. Phys.* 1955, **23**, 1959
- ⁹ SINNOTT, K. M. *J. Polym. Sci.* 1960, **42**, 3
- ¹⁰ SLICHTER, W. P. and MANDELL, E. R. *J. appl. Phys.* 1959, **30**, 1473
- ¹¹ ODAJIMA, A., WOODWARD, A. E. and SAUER, J. A. *J. Polym. Sci.* 1961, **55**, 181
- ¹² SINNOTT, K. M. Results quoted in ref. 9
- ¹³ SINNOTT, K. M. *J. Polym. Sci.* 1959, **35**, 273
- ¹⁴ POWLES, J. G. and GUTOWSKY, H. S. *J. chem. Phys.* 1953, **21**, 1695
- ¹⁵ STEJSKAL, E. O. and GUTOWSKY, H. S. *J. chem. Phys.* 1958, **28**, 388

Molecular Motion in Polypropylene by Proton Spin-Lattice Relaxation

WE REPORT measurements of the proton spin-lattice relaxation time, T_1 , at a resonant frequency of 21.5 Mc/s as a function of temperature for polypropylene (PP) and for poly(3,3,3-d₃-propylene), [P(3DP)]* in *Figure 1*. Also given in *Figure 1* are some measurements on PP (K) due to Hirai and Kawai² which are generally similar to ours but differ substantially in the important intermediate temperature region. This is probably due to apparatus and sample differences as discussed in the accompanying 'Note' on polymethylmethacrylate³.

The transient method of measuring T_1 is described briefly in the accompanying 'Note'³ and will be described in detail elsewhere⁴.

In comparing the T_1 curves for the normal polypropylene and for the polypropylene with all methyl groups deuterated it is striking that the higher temperature minimum is hardly affected but that the lower temperature one is very much shallower. The higher temperature minimum is thought to be connected with motion of substantial portions of the chains, as discussed below. It is plausible that the lower temperature minimum is connected with reorientation of the methyl group as has already been suggested² from measurements on polypropylene. It should be borne in mind that we observe in this temperature region simple exponential recovery of the magnetization and so presumably the T_1 values given refer to all the protons in the sample, namely the methyl, methylene and CH protons in polypropylene and to the methylene and CH protons in the deuterated polypropylene. We note that on deuteration the T_1 minimum is less marked

*The sample of polypropylene is an isotactic polymer from Hercules Powder Co., Profax Batch 6501. The sample of poly(3,3,3-d₃-propylene) was prepared by A. D. Caunt of I.C.I. Plastics Division. The PP sample was moulded at 85°C and the P(3DP) at 175°C. Both samples were kindly loaned to us by Dr M. P. McDonald of I.C.I. Fibres Division and are the same ones for which broad line proton resonance measurements are quoted in this paper and which are published in detail elsewhere¹.

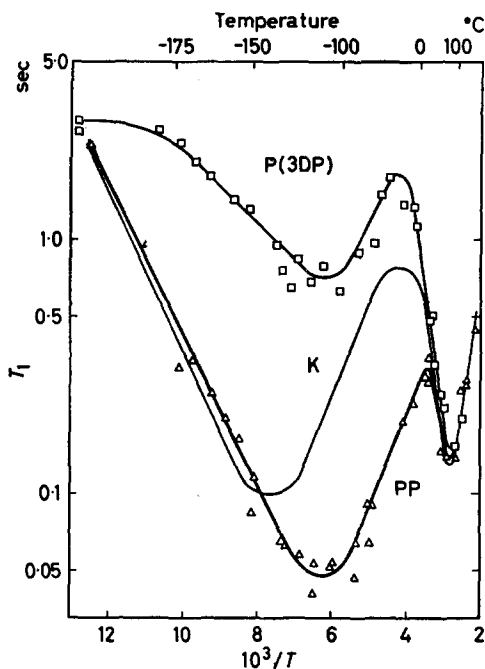


Figure 1—Proton spin-lattice relaxation times as a function of temperature for polypropylene (PP) and poly(3,3,3-d₃-propylene) [P(3DP)]. The curve K is for polypropylene from the data of Hirai and Kawai²

but is not removed. We suggest, as is very plausible, that the CD₃ group in poly(3,3,3-d₃-propylene) performs much the same reorientational motion as the CH₃ group in polypropylene. Since the minimum occurs at the same temperature in both cases we presume that it is in both cases caused by the same motion. However, in polypropylene we are concerned with the direct dipolar interactions between protons both within the methyl group and between the methyl and the methylene and CH protons. The T_1 minimum in this case depends in first approximation on the quantity $(\mu_H^2/d^3)^2$ where μ_H is the classical proton dipole moment and d is a characteristic separation. On the other hand in the poly(3,3,3-d₃-propylene) the protons in the CH₂ and CH groups are being relaxed by the deuterons in the CD₃ groups which are in effective motion. The T_1 minimum is now therefore expected to depend on $(\mu_H\mu_D/d^3)^2$ where μ_D is the classical magnetic moment of the deuteron. Hence we expect

$$\frac{T_{1,\min.} \text{ for P(3DP)}}{T_{1,\min.} \text{ for PP}} \approx \left(\frac{\mu_H^2}{d^3}\right)^2 / \left(\frac{\mu_H\mu_D}{d^3}\right)^2 = \left(\frac{\mu_H}{\mu_D}\right)^2 = 16$$

In fact the observed ratio in Figure 1 is 13 and so our interpretation of the mechanism is strongly supported.

We believe the levelling off of the T_1 curve for P(3DP) at the lowest temperatures is due to impurity since the sample was slightly coloured. Paramagnetic impurities are expected to be important in reducing T_1 when the intrinsic T_1 rises substantially above one second.

The T_1 results for polypropylene can be well represented by

$$\frac{1}{T_1} = \frac{1}{1.42} \sum_{i=1}^2 \frac{1}{T_{1,\min,i}} \left[\frac{\nu_r/\nu_{ci}}{1 + (\nu_r/\nu_{ci})^2} + \frac{4\nu_r/\nu_{ci}}{1 + (2\nu_r/\nu_{ci})^2} \right]$$

with

$$T_{1,\min,1} = 0.13 \text{ sec}, \nu_{c1} = 3.5 \times 10^7 \exp \frac{6.5}{R} (2.8 - 10^3/T)$$

$$T_{1,\min,2} = 0.048 \text{ sec}, \nu_{c2} = 3.5 \times 10^7 \exp \frac{1.5}{R} (6.2 - 10^3/T)$$

where ν_r is the resonant frequency (here 21.5 Mc/s) and $R = 1.98 \text{ cal/mole } ^\circ\text{C}$. This formula is a slight generalization of current theory^{5,6}. $\nu_{c1}(T)$ and $\nu_{c2}(T)$ are the curves through the points A and B (for $T_{1,\min}$) in Figure 2. The points D and E in Figure 2 correspond to the centres of line narrowing from line width measurements in proton magnetic resonance in polypropylene^{1,7-9} which determine the temperature at which the correlation frequency is approximately 10^4 c/s . The point X corresponds to a peak in mechanical loss at approximately 100 c/s in a similar sample of polypropylene¹⁰. Y is also a mechanical loss result due to Sauer *et al.*⁷.

We have tentatively drawn in the curve XYDA and so extend, in effect, knowledge of the behaviour of the mechanical softening process to frequencies of order 10^8 c/s which has not so far been done directly. In Figure 2 this curve is identified as Chain since it is clear that this frequency is associated with motion of substantial portions of the chain, probably in the amorphous regions of the sample. The lower slope of the curve through A deduced from T_1 may be due to distributions of correlation times or other disturbing effects as discussed in the accompanying 'Note'³.

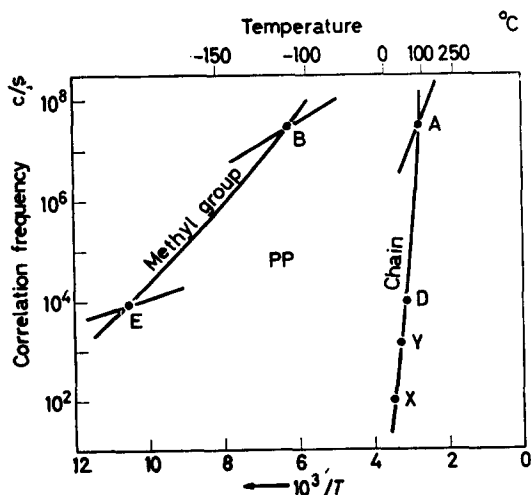


Figure 2—Correlation frequency as a function of temperature for polypropylene incorporating nuclear resonance and mechanical loss measurements

We have also tentatively passed a curve through the points E and B to suggest that this is the way the rate of reorientation of the methyl groups in polypropylene varies with temperature. The lower slopes of the curves through B and E from magnetic resonance are explained as above. This curve suggests that one should look for a mechanical loss peak in polypropylene due to the methyl groups in the region of -200°C for 100 c/s.

If our analysis is accepted it is clear that the rather complicated subsidiary mechanical processes at frequencies of order 2 kc/s and temperatures of order -45°C have little to do directly with the reorientation of the methyl groups.

A more detailed discussion of the magnitude of the T_1 values and their variation with temperature—a more difficult matter—will be given elsewhere when measurements on a series of other polypropylenes and deuterated samples are completed.

J. G. POWLES
P. MANSFIELD

*Physics Department,
Queen Mary College,
Mile End Road, London E1*

(Received June 1962)

REFERENCES

- ¹ McDONALD, M. P. and WARD, I. M. To be published
- ² HIRAI, A. and KAWAI, T. *Mem. Coll. Sci. Univ. Tokyo*, 1961, **29**, No. 3
- ³ POWLES, J. G. and MANSFIELD, P. *Polymer, Lond.* 1962, **3**, 339
- ⁴ MANSFIELD, P. To be published
- ⁵ BLOEMBERGEN, N., PURCELL, E. M. and POUND, R. V. *Phys. Rev.* 1948, **73**, 679
- ⁶ KUBO, R. and TOMITA, K. *Proc. phys. Soc. Japan*, 1954, **9**, 888
- ⁷ SAUER, J. A., WALL, R. A., FUSCHILLO, N. and WOODWARD, A. E. *J. appl. Phys.* 1958, **29**, 1385
- ⁸ SLICHTER, W. P. and MANDELL, E. R. *J. appl. Phys.* 1958, **29**, 1438
- ⁹ NISHIOKA, A. *et al. J. phys. Soc. Japan*, 1960, **15**, 416
- ¹⁰ SANDIFORD, D. J. H. Private communication

Contributions to Polymer

Papers accepted for future issues of POLYMER include the following:

- Mechanical Relaxation in Some Oxide Polymers*—B. E. READ
The Melting Point of Polyethylene Terephthalate—G. W. TAYLOR
X-ray Measurements of the Elastic Modulus of Cellulose Crystals—
J. MANN and L. ROLDAN-GONZALEZ
The Gelation of Aqueous Solutions of Polymethacrylic Acid—J. ELIASSAF
and A. SILBERBERG
*Dilute Solution Properties of Tactic Polymethyl Methacrylates I—Intrinsic
Viscosities of Isotactic Fractions*—SONJA KRAUSE and ELIZABETH COHN-
GINSBERG
*The Effect of Temperature, Conversion and Solvent on the Stereospecificity
of the Free Radical Polymerization of Methyl Methacrylate*—T. G
FOX and H. W. SCHNECKO
*Tracer Studies of 2-Cyano-2-propylazofornamide I—Use of the Compound
as a Sensitizer for the Polymerization of Styrene*—J. C. BEVINGTON
and ABDUL WAHID
Ceiling Temperature and Low Temperature Polymerization—D. HEIKENS
and H. GEELEN
Solution and Diffusion in Silicone Rubber, Parts I, II—R. M. BARRER,
J. A. BARRIE and N. K. RAMAN
Viscosity of Branched Styrene—Maleic Anhydride Copolymers—C. E. H.
BAWN and M. B. HUGLIN
*Effect of Heterogeneity in Molecular Weight on the Second Virial Coefficient
of Polymers in Good Solvents*—E. F. CASASSA
Heterogeneous Radical Polymerization of Ethylene—B. L. ERUSSALIMSKY,
S. G. LYUBETZKY, W. W. MAZUREK, S. YA. FRENKEL and L. G.
SHALTYKO
Crystallization Kinetics Study of Nylon 6—J. H. MAGILL
Some Properties of Poly-(2-vinylpyridine) in Solution—A. J. HYDE and
R. B. TAYLOR
*The Dependence of the Viscosity on the Concentration of Sodium
Carboxymethylcellulose in Aqueous Solutions*—D. A. I. GORING and
G. SITARAMAIAH
*Radiochemical Investigation of Polymer Unsaturation. Reaction of Butyl
Rubber with Radiochlorine*—I. C. MCNEILL
*The Low Frequency Dielectric Relaxation of Polyoxymethylene (Delrin)
using a Direct Current Technique*—G. WILLIAMS
Viscosity/Temperature Relationships for Dilute Solutions of High Polymers
—R. J. FORT, R. J. HUTCHINSON, W. R. MOORE and Miss M. MURPHY
Rubber Elasticity in a Highly Crosslinked Epoxy System—D. KATZ and
A. V. TOBOLSKY
*Infra-red Spectra and Chain Arrangement in Some Polyamides, Polypeptides
and Fibrous Proteins*—E. M. BRADBURY and A. ELLIOTT

CONTRIBUTIONS

- The Crystallization of Polyethylene, Part I*—W. BANKS, M. GORDON, R.-J. ROE and A. SHARPLES
- The Radiation Chemistry of Some Polyamides. An Electron Spin Resonance Study*—C. T. GRAVES and M. G. ORMEROD
- Proton Magnetic Relaxation in Polyamides*—D. W. MCCALL and E. W. ANDERSON
- Intermolecular Forces and Chain Flexibilities IV—Internal Pressures of Polyethylene Glycol in the Region of Its Melting Point*—G. ALLEN and D. SIMS
- The Crystallization of Poly(decamethylene terephthalate)*—A. SHARPLES and F. L. SWINTON
- Stress Relaxation of Vulcanized Rubbers I—Theoretical Study*—S. BAXTER and H. A. VODDEN
- Stress Relaxation of Vulcanized Rubbers II—Mathematical Analysis of Observations*—L. A. EDELSTEIN, H. A. VODDEN and M. A. A. WILSON
- Stress Relaxation of Vulcanized Rubbers III—Experimental Study*—S. BAXTER and M. A. A. WILSON
- A Kinetic Study of the Isothermal Spherulitic Crystallization of Poly (hexamethylene adipamide)*—J. V. MCLAREN
- The Influence of Particle Size and Distortions upon the X-ray Diffraction Patterns of Polymers*—R. BONART, R. HOSEMANN and R. L. MCCULLOUGH

CONTRIBUTIONS should be addressed to the Editors, *Polymer*, 4-5 Bell Yard, London, W.C.2.

Authors are solely responsible for the factual accuracy of their papers. All papers will be read by one or more referees, whose names will not normally be disclosed to authors. On acceptance for publication papers are subject to editorial amendment.

If any tables or illustrations have been published elsewhere, the editors must be informed so that they can obtain the necessary permission from the original publishers.

All communications should be expressed in clear and direct English, using the minimum number of words consistent with clarity. Papers in other languages can only be accepted in very exceptional circumstances.

A leaflet of instructions to contributors is available on application to the editorial office.

Crystallinity in High Polymers, especially Fibres

R. HOSEMANN

The structure of real fibres is examined in relation to the crystallinity of some idealized models of substances and the distortions which they may undergo. Sections of the treatment deal in order with fundamental theory, distortions of the first kind and degree of crystallinity, the concept of a paracrystal and distortions of the second kind, paracrystalline macrolattices, paracrystals in atomic dimensions, the amorphous lattice, and the structure of linear polyethylene including results of some recent work in the laboratory.

IN 1950 we published two theories, the one of the paracrystal and the other of the so-called colloidal polydisperse system of particles. These two theories are more general than the better known theories. As you know, in 1912, nearly 50 years ago, Max von Laue, Friedrich and Klipping¹ made their famous discovery of the interferences of X-rays by single crystals. A new branch of science, X-ray crystallography, developed in the following years and when about 1925 it was found that even fibres gave rise to some reflections, the first rough approximation was to speak about a crystalline fraction or a crystalline phase in these substances. However, one must be very careful and first study the meaning of the word 'crystalline' and the concept of a crystal. This is the central problem I would like to write about and to show that there is a more general idea, the concept of a paracrystal² which can degenerate to the form of a crystal. We then have more structural parameters which can be adapted to the problem.

In 1915, the theory of the gaseous state was developed by Debye which is related to the theory of Lord Rayleigh on the diffuse scattering of amorphous phases. Guinier³ published a similar theory of the continuous small-angle scattering of X-rays. This theory we have generalized somewhat to polydisperse colloids and introduced a so-called interference correction term⁴. Now, the next theory we have is very predominant in the structure analysis of liquids, glasses, etc. It was given by Debye⁵ and by Zernike and Prins⁶. We can show that the paracrystalline theory for special combinations of structure parameters can degenerate both to the theory of liquids and to that of crystals. We shall see that natural fibres and man-made fibres cannot be substances which contain real crystallites. The only people who had clothes of crystalline material were the old knights in the middle ages with their iron and bronze armour. We are sure that these materials consisted of single small crystallites. The most predominant and interesting macroscopic properties of the fibres depend, we believe, upon properties which are beyond the conventional crystal-like state.

To determine the structure of real fibres I will deal first with some

This paper was presented at a Polymer Science Conference, held in conjunction with the Second World Congress of Man-made Fibres, at the Connaught Rooms, Holborn, London W.C.2, 2nd and 3rd May 1962.

fundamentals of structure analysis, with the help of diagrams and using some idealized models of substances. Then I shall define distortions of the first kind in a crystal and discuss the physical definition of the degree of crystallinity. The third section deals with the concept of a paracrystal and distortion of the second kind. Then in the next section I shall describe a real paracrystal, and indicate where such real paracrystals occur in nature. We must distinguish two possibilities. The first one is that such a paracrystalline lattice can be found in macrostructures such as collagen or β -keratin. Hence this section will deal with some real paracrystalline macrolattices. In the following section we may discover in nature a real paracrystal in atomic dimensions. I will give some ideas as to where such paracrystals might be found. In the sixth section we will discuss the amorphous lattice. This is the most randomly distributed irregular structure and corresponds to the theories of Rayleigh and Debye. The last section contributes some practical examples of polyethylene which we have investigated in recent years in our laboratory.

I. FUNDAMENTALS

The intensity function $I(\mathbf{b})$ is nothing more than the time ξ -average of the squared scattered amplitude $R(\mathbf{b})$. [See ref. 7 for details.]

$$I(\mathbf{b}) = \overline{R(\mathbf{b}) R^*(\mathbf{b})} \quad (1)$$

The scattered amplitude R can be calculated for X-rays both as electrons and neutrons or light-scattering on screens by a Fourier integral (symbol \mathcal{F}) of the density distribution $\rho(\mathbf{x})$ inside the irradiated sample.

$$R(\mathbf{b}) = \mathcal{F}(\rho) \quad (2)$$

$$\mathcal{F} = \int \exp \{ -2\pi i(\mathbf{b}\mathbf{x}) \} dv_x \quad (3)$$

This density distribution $\rho(\mathbf{x})$ is a three-dimensional distribution function of the radius vector \mathbf{x} which expands the physical space. dv_x is a volume element of \mathbf{x} space. For X-rays $\rho(\mathbf{x})$ is given by the density of the electron clouds, for electron radiation by the density distribution of the electrons and protons and for neutrons by the distribution of the nuclei and spinning electrons. We get direct information not of the amplitude but of the squared amplitude (see equation 1), which is the Fourier transform of the so-called Q function

$$I(\mathbf{b}) = \mathcal{F}(Q) \quad (4)$$

This Q function is nothing more than the so-called folding square of the unknown density distribution

$$Q(\mathbf{x}) = \int \rho(\mathbf{y}) \rho(\mathbf{y} - \mathbf{x}) dv_y \quad (5)$$

It is important to emphasize that this Q function for unbounded ideal crystals degenerates to the Patterson function or for statistical structures consisting of point-like single particles to the correlation function of

statistical mechanics. In other cases the Q function is much more general and contains all observable details of the unknown structure $\rho(\mathbf{x})$ †.

The folding square is a special folding product of the function $\rho(\mathbf{x})$ with $\rho(-\mathbf{x})$. The folding (or convolution) product of a function $g_1(\mathbf{x})$ with $g_2(\mathbf{x})$ is defined by

$$\overline{g_1 g_2} = \int g_1(\mathbf{y}) g_2(\mathbf{x} - \mathbf{y}) d\mathbf{v}_y \quad (6)$$

Again it is a function in physical space, depending upon \mathbf{x} as $\rho(\mathbf{x})$. The three-dimensional \mathbf{y} integration must be carried out over the whole physical space and $d\mathbf{v}_y$ is again a volume element in physical space.

Such a folding integral is well known in the one-dimensional case from the theory of Laplace transformations. Ewald⁸ was the first to introduce special three-dimensional folding products to analyse the electron density distribution of ideal bounded crystals. J. J. Hermans⁹ was the first to use one-dimensional convolution integrals in calculating statistical problems in liquids. It will be shown how powerful these operations are for structure analysis. The three-dimensional reciprocal vector \mathbf{b} in the Fourier integrals (1) to (3) is connected with the unit vectors \mathbf{s}_1 , \mathbf{s}_0 in the direction of the scattered and primary intensity and the wavelength λ of the primary beam by the so-called Ewald construction

$$\mathbf{b} = (\mathbf{s} - \mathbf{s}_0) / \lambda; \quad |\mathbf{b}| = u = 2 \sin \vartheta / \lambda \quad (7)$$

The equations (1) to (7) give in a condensed form the whole mathematical background of structure analysis. 2ϑ is the scattering angle.

The question is how to get information on $\rho(\mathbf{x})$ from $I(\mathbf{b})$. The step from $I(\mathbf{b})$ to $Q(\mathbf{x})$ is given by a Fourier transformation (equation 4) which can always be calculated uniquely. The step from ρ to Q (equation 5) can be illustrated by the following folding machine (Figure 1). It consists of a

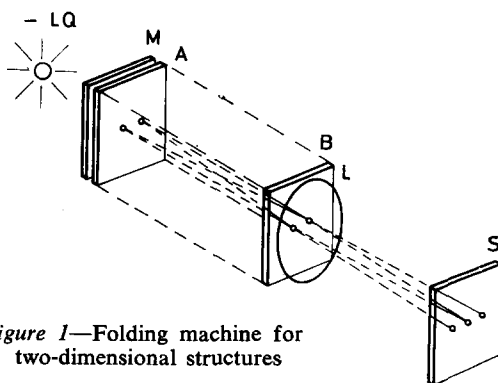


Figure 1—Folding machine for two-dimensional structures

ground glass screen M which scatters diffuse light from the source LQ and two identical transparent models A and B of the structure of interest. In Figure 1 these identical models consist of two points. In the focal plane S of the lens L one will find the folding square (or Q function) of the two-point

†For details see ref. 7.

structure which according to equation (5) consists of three points. The problem is to go back from Q to ρ , which implies solution of the integral equation (5) of the second degree, a new task not yet to be found in mathematical literature (the so-called folding root).

Some years ago we found the general solution for all bounded structures which have a centre of symmetry or antisymmetry. This solution is defined by a convolution polynomial (see ref. 10) of the Q function which must be known exactly in all its details. That means one must have very high experimental precision.

It is very good to know from the theoretical standpoint, that if we could measure with higher precision we could get much more information than we now have. *Figure 2* gives the black and white structure of a chair and its folding square. Here $\rho(\mathbf{x})$ has no centre of symmetry and a convolution polynomial does not exist. Nevertheless I think it will be possible to return from $Q(\mathbf{x})$ to the structure $\rho(\mathbf{x})$ of the chair.

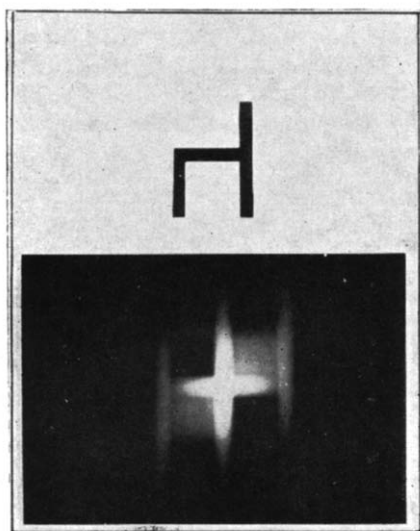


Figure 2—A chair and its folding square

Figure 3 gives a special point structure, a paracrystalline lattice, where all the single points have a certain freedom in the horizontal direction. The Q function below shows some spotlike points and, as $|\mathbf{x}|$ increases, more and more diffuse humps. They are smeared out only in the horizontal direction. Here we have a short domain of small-range order which is shorter in the horizontal than in the vertical direction. With respect to the vertical width of the humps we have an unbounded long-range order in all directions. So very complicated correlation functions, more complicated than those defined and to be found in the literature, are introduced.

II. DISTORTIONS OF THE FIRST KIND. DEGREE OF CRYSTALLINITY

Let us summarize very briefly the idea of a crystal. In *Figure 4* we have single point-like atoms. They are very regularly arranged. It makes no

difference that here we have only two-dimensional crystals because one can prove that most of the interesting geometrical problems arise if one goes from one to two dimensions. The step from the second to the third,

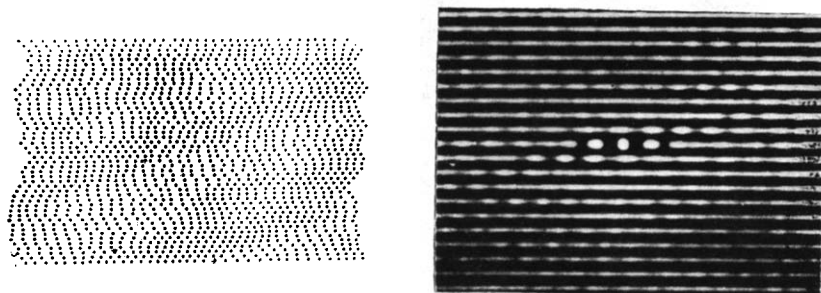


Figure 3—Paracrystalline point structure (lattice) and its folding square (distance statistics)

fourth or fifth dimension is not so essential although the geometrical possibilities certainly become more complicated. Nevertheless in two-dimensional models we find nearly all the essential features. The diffraction pattern of Figure 4, a so-called Fraunhofer pattern, shows many Bragg reflections. It is well known that each reflection has the same shape. In Figure 4 the central reflections seem to be thicker. This is solely due to the fact that they have a higher intensity. The half-widths are the same for all

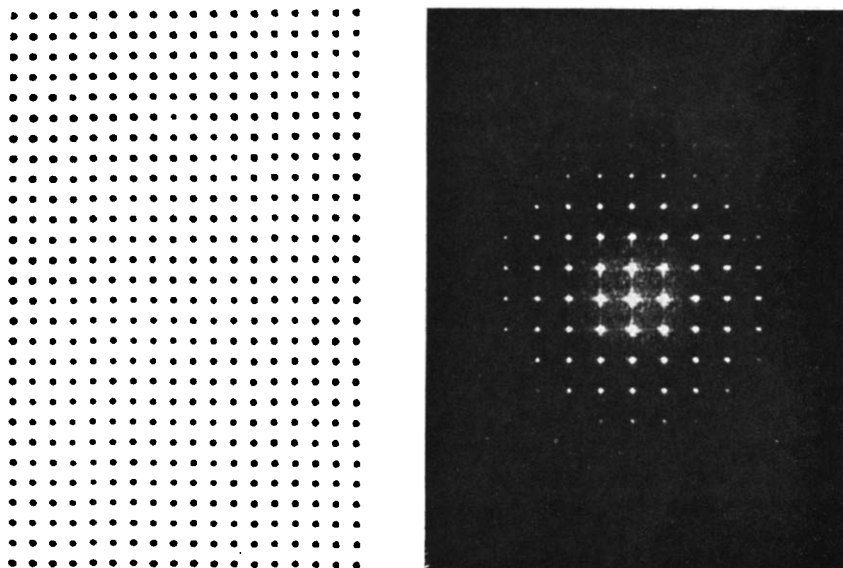


Figure 4—Two-dimensional crystalline lattice and its Fraunhofer pattern

reflections. We can use any of these reflections and get the same information about the size and shape of the crystal. Only a weak background appears. From the intensities of the reflections a Fourier synthesis gives information on the shape and size of the single point-like atoms.

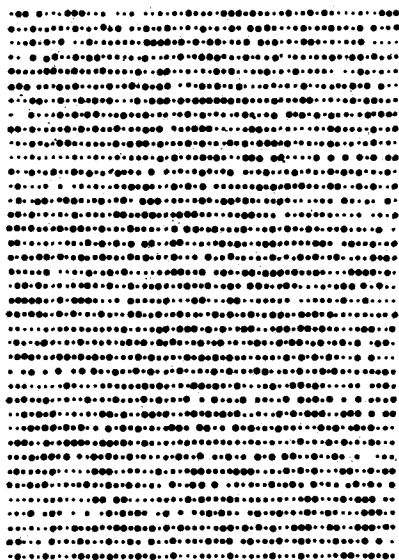


Figure 5(a)

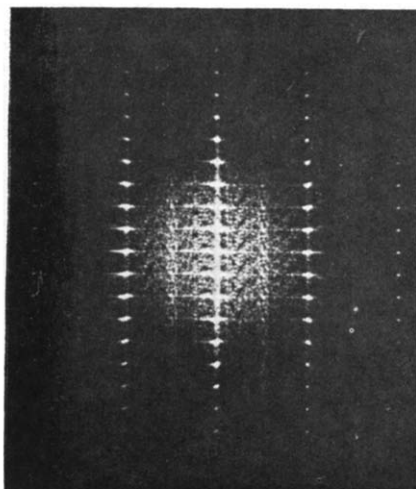


Figure 5(b)

Figure 5—(a) Ideal mixed crystal. (b) Fraunhofer pattern with high resolution. Ghosts appear. (c) Fraunhofer pattern with low resolution. Ghosts are smeared out

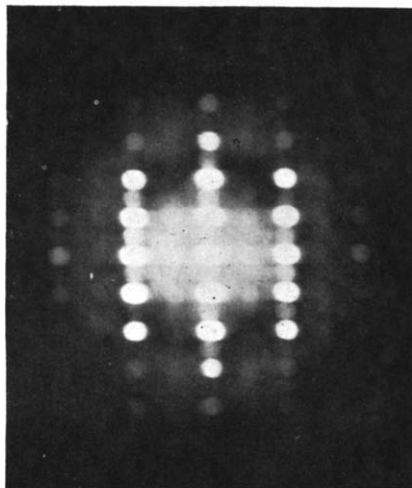


Figure 5(c)

In Figure 5 we have a crystal with different kinds of atoms, the so-called ideal mixed crystal. Here there are 'chemical distortions' and there is also a strong background. It is interesting to note that in real crystals we have

found such a background even if there is only one sort of atom and if the absolute temperature is not small enough compared with the characteristic temperature¹¹. In this case each atom has at each moment another individual shape of its electron cloud, although they all are chemically identical. If, for instance, in the model of *Figure 5* each point represents a pyranose ring in cellulose and if each pyranose ring has a different shape this produces the same kind of background. All these different sorts of distortions we call distortions of the first kind. The atoms or molecules lie in the right positions but each atom has a different shape.

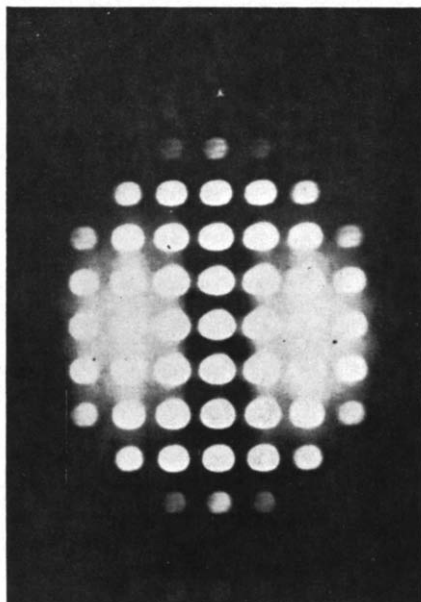


Figure 6—Bragg reflections and anisotropic background

The Fraunhofer picture of *Figure 6* shows a strong background also and it is interesting to see where this background comes from. The model is given in *Figure 7*. All atoms now have the same shape, but suffer a small horizontal displacement from their ideal positions. This is another kind of distortion of the first kind, which can be produced by micromechanical strains or thermal oscillations. *Figure 7* is the frozen structure of linear (highly anisotropic) thermal vibrations. This distortion is so small that one can hardly see it in the model. The standard displacement of the atoms has a magnitude of only ten per cent of the mean distance between neighbouring atoms. Nevertheless this gives rise to a very strong background. So it is seen that diffraction patterns are quite sensitive to distortions.

Furthermore, it is very interesting to note that at the same time as distortions of the first kind appear, the Bragg reflections lose some of their intensity and transfer it quantitatively to the background. The same thing happens in Fourier space as if one wanted to place a small piece of butter on a hot potato. The mound of butter melts and gives quantitatively liquid

butter to the background on the potato. If there are no overlapping effects of single atoms one can prove that no intensity is lost. It goes quantitatively from the Bragg peaks to the background. Conversely, if one has such a background on the X-ray diagram, this means that peaks have transferred some of their intensity quantitatively to it. One can then introduce an artificial Debye factor D^2 and give the lost intensity from the background

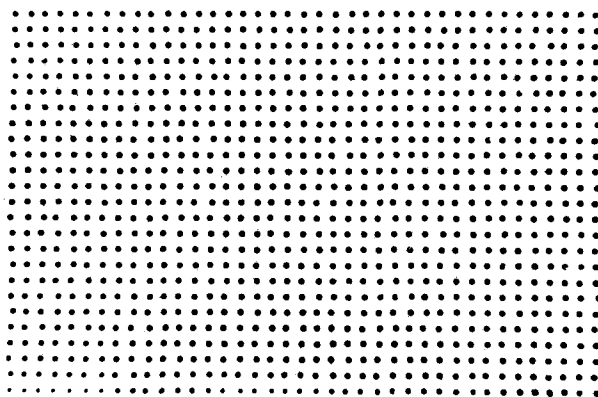


Figure 7—Model to Figure 6 with horizontal frozen thermal vibrations

back to the reflections to eliminate the effects of the distortions. Such a method was developed by Ruland¹². What he did was to measure in different u_1 - u_2 intervals (cf. equation 7) in Fourier space the intensity in the peaks compared with the intensity in the background. Table 1 shows in the columns $D_i^2=1$ (no Debye factor) according to Figure 6 the integral intensity in the peaks relative to the background. This quotient decreases at larger scattering angles or u values. Now instead of $D_i^2=1$ we introduce an adapted Debye factor D^2_{apt} . We multiply the measured integral intensities of the reflections by $1/D^2_{\text{apt}}$ and the measured integral intensity of the background by $(1-D^2_{\text{apt}})$. In this way one can use any adapted Debye factor. It always systematically raises the outer reflections more than the inner ones. The exact factor D^2_{apt} is found, when the quotient of the corrected peak intensity and total intensity is independent of the u interval. This quotient then is the correct degree of crystallinity (D.C.) As Table 1 shows in the case of polypropylene, one can use the same adapted Debye factor

$$D^2_{\text{apt}} = \exp(-4u^2) \quad (8)$$

for isotactic material or material annealed at 105°C or 160°C or amorphous material. Calculating the standard deviation of the centres of the single bricks in the lattice one gets for all four materials the same

fluctuation of 0.3 Å. All these very different substances with different degrees of crystallinity have the same mean amplitudes of displacement. This is very interesting and proves that in polypropylene the crystalline

Table 1. Degree of crystallinity (D.C.) in polypropylene after Ruland¹².

$$D_{\text{apt}}^2 = \exp(-4u^2)$$

| Interval in u (Å ⁻¹) | Isotactic, quenched | | Annealed at 105°C | | Annealed at 160°C | | 'Amorphous' | |
|---------------------------------------|------------------------|--------------------|----------------------|--------------------|----------------------|--------------------|----------------------|--------------------|
| | $\overline{D_i^2} =$ | | $\overline{D_i^2} =$ | | $\overline{D_i^2} =$ | | $\overline{D_i^2} =$ | |
| | 1 | D_{apt}^2 | 1 | D_{apt}^2 | 1 | D_{apt}^2 | 1 | D_{apt}^2 |
| 0.1–0.3 | 0.27 | 0.33 | 0.35 | 0.43 | 0.55 | 0.66 | 0.12 | 0.15 |
| 0.1–0.6 | 0.16 | 0.29 | 0.22 | 0.41 | 0.33 | 0.61 | 0.08 | 0.14 |
| 0.1–0.9 | 0.11 | 0.31 | 0.15 | 0.42 | 0.22 | 0.64 | 0.04 | 0.13 |
| 0.1–1.3 | 0.07 | 0.32 | 0.09 | 0.44 | 0.15 | 0.68 | 0.03 | 0.14 |
| D.C. (averaged): | 0.31 | | 0.43 | | 0.65 | | 0.14 | |

phase always has the same amount of distortions, whether the D.C. is 0.65 or 0.43 or 0.3 or 0.14. Dr P. H. Hermans has informed me that these values agree very well with those he calculated by his method.

Figure 8 gives an example of the method of Hermans and Weidinger¹³ for mercerized cotton linters. The intensity function is divided by a dotted line into peaks and into a background without recourse to an adapted Debye factor. If a totally amorphous substance (D.C.=0) gives rise to an

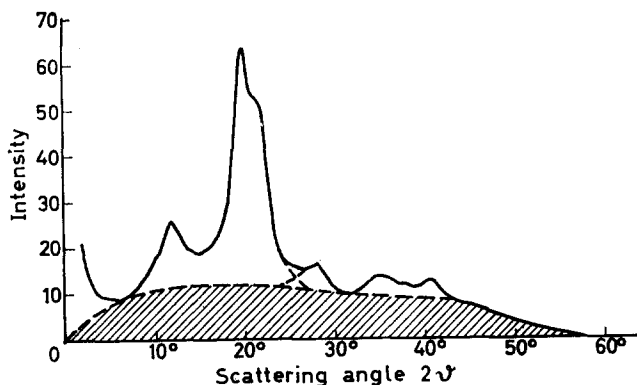


Figure 8—X-ray diagram of mercerized cotton linters ($\lambda=1.54\text{Å}$). Background construction according to P. H. Hermans. D.C.=40.9%

intensity proportional to the background scattering of Figure 8, one obtains from Figure 8 by linear extrapolation procedures a degree of crystallinity D.C.=40.9.

However, one must be very careful in other practical examples. The above-mentioned construction by Hermans can give correct values or nearly correct values or interesting values which characterize the fibre. But some-

times, something unexpected can occur and then this method fails and the following may happen. In *Figure 9* for instance we have single crystals. All have the same orientation; there are voids between them. All crystallites produce the same Laue reflections and we can calculate a mean size and size

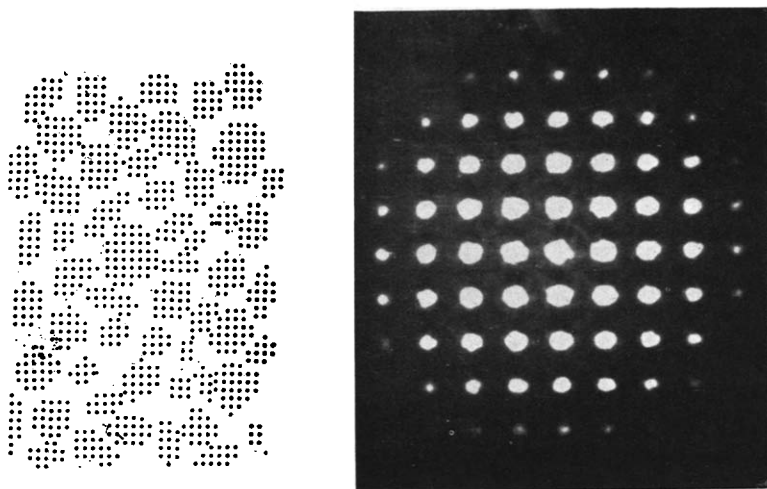


Figure 9—Single crystals with voids and their Fraunhofer pattern. No background

distribution of the crystallites from a quantitative study of the peaks. Each reflection can be used. Since no background exists, we obtain D.C.=100 per cent.

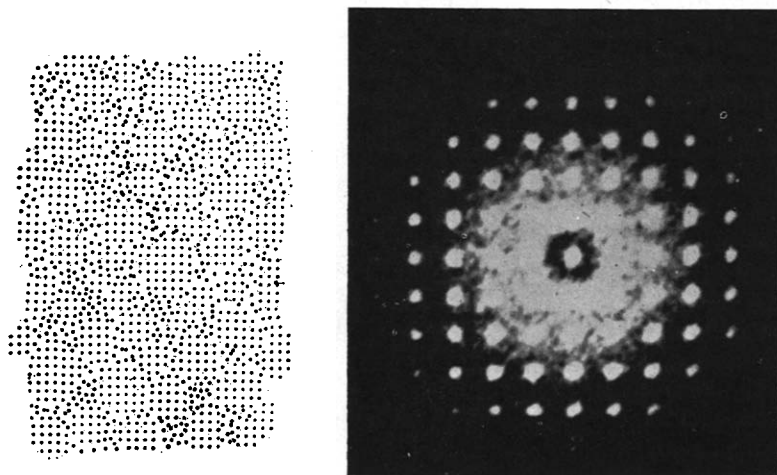


Figure 10—Single crystals and an amorphous phase. Fraunhofer pattern with background scattering from this phase

In *Figure 10* there is a lattice with an amorphous phase embedded in the voids. We now observe the appearance of a large background. We are sure that now the Hermans method will work well and we can calculate the degree of crystallinity exactly.

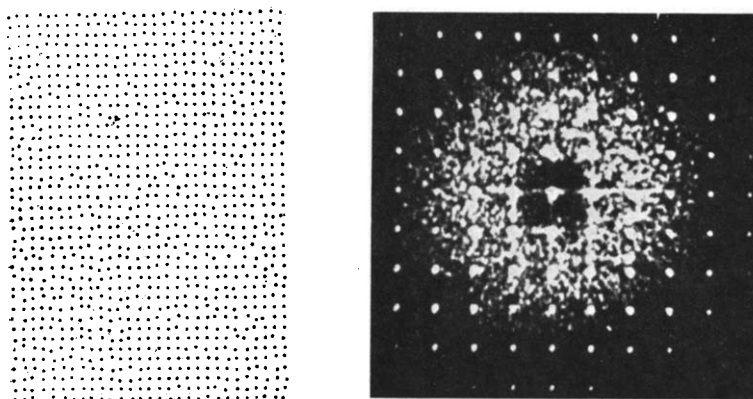


Figure 11—One single crystal with an inhomogeneous displacement statistic. Fraunhofer pattern with background, produced by the lattice distortions

By contrast, in *Figure 11* things have become a little more complicated. Here we have one single crystal and only dislocations of a special type. They are so-called inhomogeneous statistics. That means that a point-like statistic of perhaps 50 per cent of weight is superimposed upon a distance statistic of large width. Now 50 per cent of the atoms lie exactly in the right position while the rest have large deviations. A heavy diffuse background arises which has nothing to do with an amorphous phase. Here one must use Ruland's method.

III. THE CONCEPT OF A PARACRYSTAL. DISTORTIONS OF THE SECOND KIND

Figure 12 shows a point structure with a new type of distortion which gives rise to background scattering which again has nothing to do with an amorphous phase. It is a paracrystalline lattice. The long-range order is lost now and the atoms no longer know exactly their ideal position. Now each atom is very 'stupid'. It only knows its distance statistics to its next neighbour and the neighbour reacts only to its neighbour. Thus the neighbour of the neighbour has a larger distance fluctuation from the first atom than the nearest neighbour and the long-range order of the crystalline lattice with distortions of the first kind is lost.

The diffraction pattern of *Figure 12* has now a new character. Only the reflection at the zero point alone depends upon the size of the single paracrystal. All the other reflections depend both upon the size of this paracrystal as well as upon the new kind of distortions. Analysing two or three such reflections, one can calculate both the size of the lattices and the magnitude of the distortions.

Now there are many types of lattices which depend only on the shape of the distance statistics of neighbours. In a Gaussian approximation each of the three distance statistics of the edge-vectors of a paracrystalline lattice cell can be described by a symmetric tensor, hence six components, altogether 18 new structure parameters. In *Figure 13* an orthogonal para-

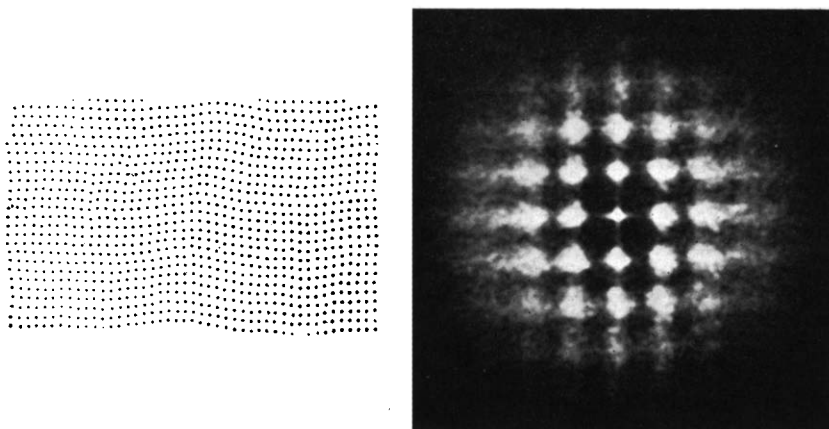


Figure 12—One single paracrystal and its Fraunhofer pattern

crystalline cell is drawn, whereby the principal axes of these tensors lie parallel to the mean directions of the three cell edges. Here we have $3 \times 3 = 9$ statistical parameters. But in general one can turn these principal axes into other general directions. This gives rise to $3 \times 3 = 9$ more statistical parameters. With the help of these 18 new parameters a large variety of new kinds of diffraction patterns arises. The task, and our main interest, is

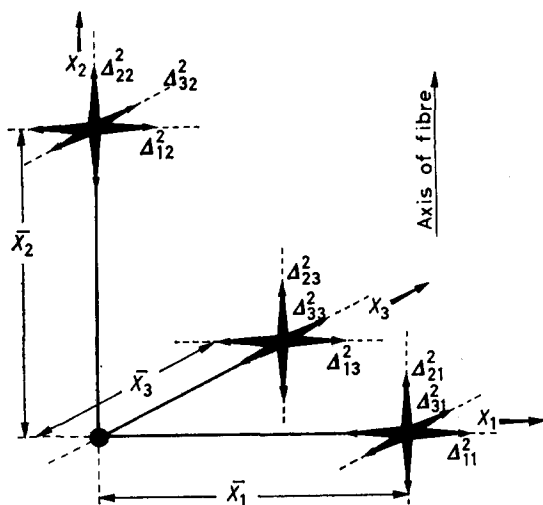


Figure 13—Principal axes of the coordination statistics of a paracrystal. Δ_{ki} stands for Δ_{x_k} in equation (15)

to get information on these so-called coordination statistics. In an ideal paracrystal the correlation function $Q(\mathbf{x})$ is determined by these three coordination statistics. Let $H_k(\mathbf{x})$ be the coordination statistic of the cell edge \mathbf{a}_k ($k=1, 2, 3$). Then a special edge-vector $\mathbf{a}_k=\mathbf{y}$ has the probability $H_k(\mathbf{y})$. In the theory of paracrystals it is proposed that there shall be no correlation to the edge \mathbf{a}_k of the next cell. Hence to find the neighbouring edge $\mathbf{a}_k=\mathbf{z}$ it has the probability $H_k(\mathbf{z})$ and a special combination \mathbf{y}, \mathbf{z} of neighbouring edges has the probability $H_k(\mathbf{y}) H_k(\mathbf{z})$. If we wish to calculate the distance statistics between an atom and the neighbour of its neighbour in the direction k for a certain position $\mathbf{x}=\mathbf{y}+\mathbf{z}$ then we have to integrate over all \mathbf{y} values. Introducing this secondary condition we obtain

$$H_{2k}(\mathbf{x}) = \int H_k(\mathbf{y}) H_k(\mathbf{x}-\mathbf{y}) d\tau_{\mathbf{y}}$$

Comparing this with equation (6) we get

$$H_{2k} = \overbrace{H_k H_k} \quad (8)$$

and

$$H_{nk} = \overbrace{H_k H_k H_k \dots H_k}^{|n-1| \text{ times}} \quad (9)$$

Therefore one can find the entire distance statistics of the lattice with the help of convolution polynomials. Transforming this into Fourier space one obtains with the help of the convolution theorem a very simple expression for the so-called paracrystalline lattice factor $Z(\mathbf{b})$. It is given by the expression

$$Z(\mathbf{b}) = \prod_{k=1}^3 R_c \frac{1+F_k}{1-F_k}; \quad F_k(\mathbf{b}) = \mathcal{F}(H_k) \quad (10)$$

F_k is the Fourier transform of the coordination statistic $H_k(\mathbf{x})$. This paracrystalline lattice factor is the heart of the new theory. It gives rise to a background scattering

$$I_s = \prod_{k=1}^3 \frac{1-|F_k|}{1+|F_k|} \quad (11)$$

If the electron cloud of each paracrystalline lattice cell has another structure, then the next background component arises. It is given by

$$I_2 = N(\bar{f}_0^2 - \bar{f}_0^2) \quad (12)$$

$f_0(\mathbf{b})$ is the structure amplitude (equal to the Fourier transform of the electron density distribution of one lattice cell). If the single atoms or molecules within a lattice cell have the same shape but suffer frozen or thermal displacement, a third background component arises

$$I_1(\mathbf{b}) = N \bar{f}_0^2 (1 - D^2) \quad (13)$$

where

$$D(\mathbf{b}) = \mathcal{F}(H) \quad (14)$$

and H is the displacement statistic. For thermal vibrations D^2 is called the Debye factor.

In *Figure 14* the paracrystalline distance statistics of a two-dimensional paracrystalline lattice are calculated directly from a model (black blocks). The white blocks are calculated from the coordination statistics by means of equation (9). They agree within statistical error with the black blocks¹⁴.

The two coordination statistics here are for convenience straight line

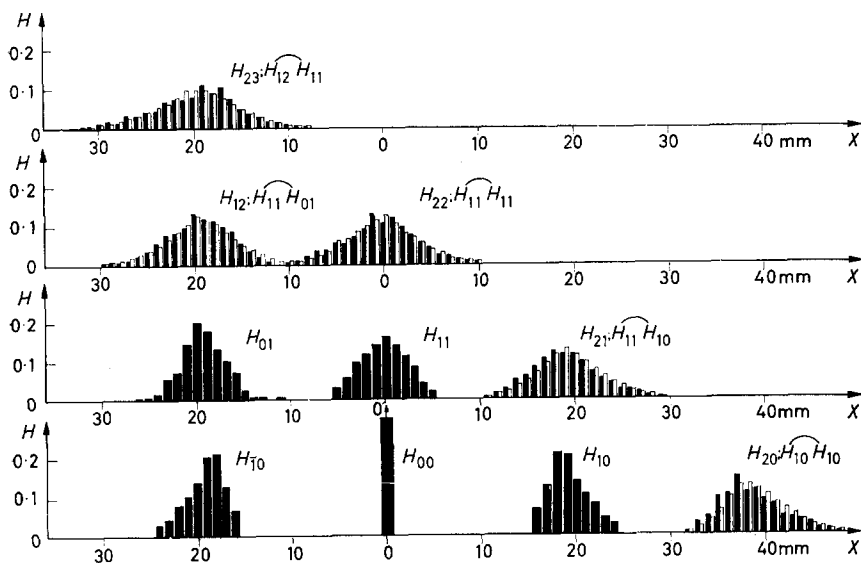


Figure 14—Distance statistics of a paracrystal. Black blocks directly calculated from *Figure 3*. White blocks calculated from the coordination statistics

functions parallel to each other. Hence the fluctuation tensors have only one principal axis unlike zero. *Figure 14* demonstrates the easy way in which the whole correlation function is determined from details of the two coordination statistics.

Figure 15 gives a schematic representation of one of the three k factors of equation (10) for a given coordination statistic $H_k(\mathbf{x})$. Each coordination statistic in the paracrystal gives rise to such a k factor. It consists of a family of planes which only near the zeropoint in Fourier space are very sharp and point-like. Here $|F_k| \simeq 1$. Their distance is reciprocal to a_k . With increasing $|\mathbf{b}|$ they are more and more broadened and merge near the ellipsoid $|F_k| = 0.3$ into one another. Outside this ellipsoid all the single families are so diffuse and merged into one another that the k factor reaches the value unity. Now we have entered the region of no reflections. Multiplying three such families of non-co-planar more or less diffuse planes one obtains the paracrystalline lattice-factor $Z(\mathbf{b})$ defined by equation (10). There are many possibilities for analysing such interesting functions.

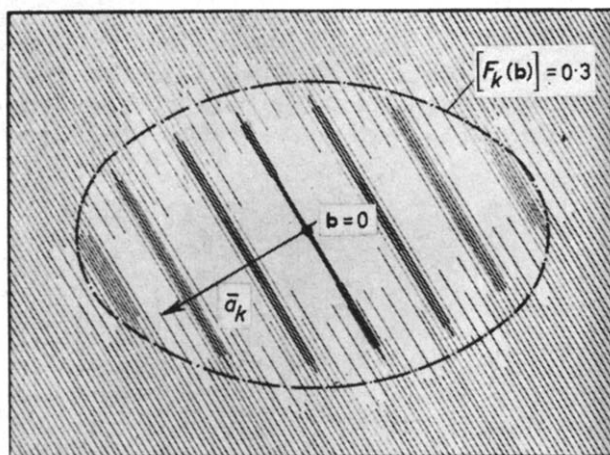


Figure 15—One k factor of the paracrystalline lattice factor $Z(b)$

Figure 16 gives an example of a one-dimensional paracrystal. It was constructed in the following way. We had two lottery boxes. In one lottery box we had a distance statistic which is the one-dimensional coordination statistic H_1 . We stuck a black needle on a white surface and the next needle

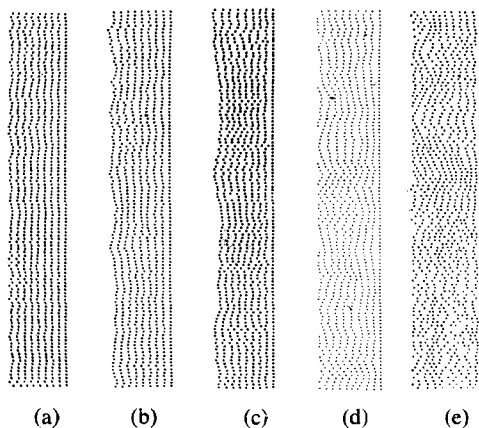


Figure 16, part 1—Five one-dimensional paracrystalline lattices, each consisting of about 100 individuals, all of which have the same statistical parameters^{1,5}

in a horizontal direction at a distance which we got from the lottery box. Then we picked out another label from the lottery box and stuck in the next needle. Step by step in this way we built up a one-dimensional paracrystal with nine points. With nine other needles another paracrystal was placed parallel to and below the first one and so on one paracrystal after

another. 100 paracrystals were built up from this one lottery box. To introduce distortions of the thermal kind we had another lottery box with quite another independent statistic. This is the thermal vibration statistic with plus and minus values. Now we took out labels from this next statistic and each needle got its one independent displacement from the

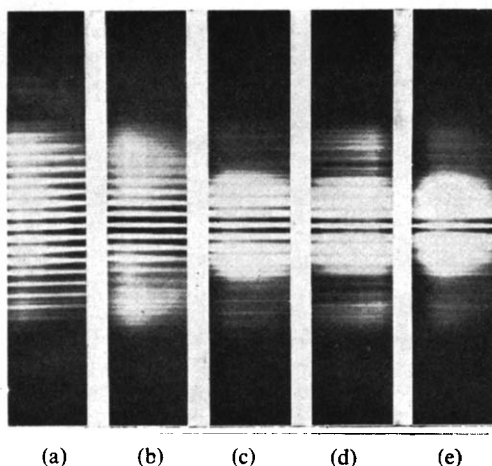


Figure 16, part 2—Single linear paracrystals and their Fraunhofer patterns

first position. A photograph of this model on Peruline plates with the size 2 cm × 2 cm was taken. Using a Fraunhofer apparatus with a slit orthogonal to the length of the single paracrystals one gets the diffraction pattern of Figure 16, part 2, which averages over all the 100 individual paracrystals with the same statistical parameters. The interesting thing is that by measuring only three different line widths one gets back all the information inserted into the models: the statistics of the paracrystal, the statistics of the thermal vibration and the mean size of the paracrystals¹⁵.

Table 2 gives the results. The column 'x-space' gives all the parameters we inserted into the models, the column 'b-space', those calculated from the intensity function. *L* is the averaged length of the paracrystals, *g_r* is the

Table 2. Analysis of one-dimensional paracrystalline lattices (after Bonart¹⁵)

| Model | x-space | | | | | | b-space | | |
|-------|-----------------------------|------------------------------|-------------------------------|-----------------------------|-----------------------------|------------------|-----------------------------|-----------------------------|------------------|
| | <i>g₁</i> (%) | <i>g₁₁</i> (%) | <i>g₁₁₁</i> (%) | <i>g_r</i> (%) | <i>g₁</i> (%) | <i>L</i> (mm) | <i>g_r</i> (%) | <i>g₁</i> (%) | <i>L</i> (mm) |
| a | 6.1 | 7.3 | 8.1 | 3.2 | 4.1 | 2.3 | 2.8 | 4.5 | 2.3 |
| b | 8.5 | 12.5 | 16.3 | — | 9.2 | 2.3 | — | 8.2 | 3.1 |
| c | 10.3 | 17.0 | 22.1 | — | 13.7 | 2.3 | — | 15.0 | 2.4 |
| d | 12.7 | 21.1 | 24.8 | 3.0 | 16.2 | 2.3 | — | (18.0) | ? |
| e | 25.0 | ? | ? | ? | ? | 2.3 | ? | ? | ? |
| f | 8.7 | 9.1 | 9.0 | 6.4 | 0 | 2.3 | 6.5 | 0 | 2.3 |
| g | 13.2 | 13.7 | ? | 9.0 | 0 | 2.3 | 9.2 | 0 | 2.3 |

relative distance fluctuation of the distortions of thermal vibrations and g_1 that of the paracrystalline distortions. The agreement between the x - and b -columns is satisfactory.

IV. PARACRYSTALLINE MACROLATTICES

The first macrolattice of the paracrystalline type we found was that of the β -feather-keratin of the seagull. *Figure 17* gives the small angle scattering pattern from the work of Bear and Rugo¹⁶. From the position of the reflections one gets details of the size of a macrolattice cell: 185 Å in the fibre direction and 34 Å in one lateral direction. A paracrystalline point structure and its Fraunhofer diffraction on the RHS of *Figure 17* proves how similar the two intensity functions are. The crystalline-like reflections along the meridian prove that the 185 Å cell edge can only change its direction but hardly changes its length at all. That means its coordination statistic has the shape of a disc orthogonal to the fibre direction. The lateral coordination statistic on the other hand has the shape of a globular cloud. The model has the same kind of statistical variability. So we see that such kinds of fibres even in colloidal or atomic dimensions have a new type of

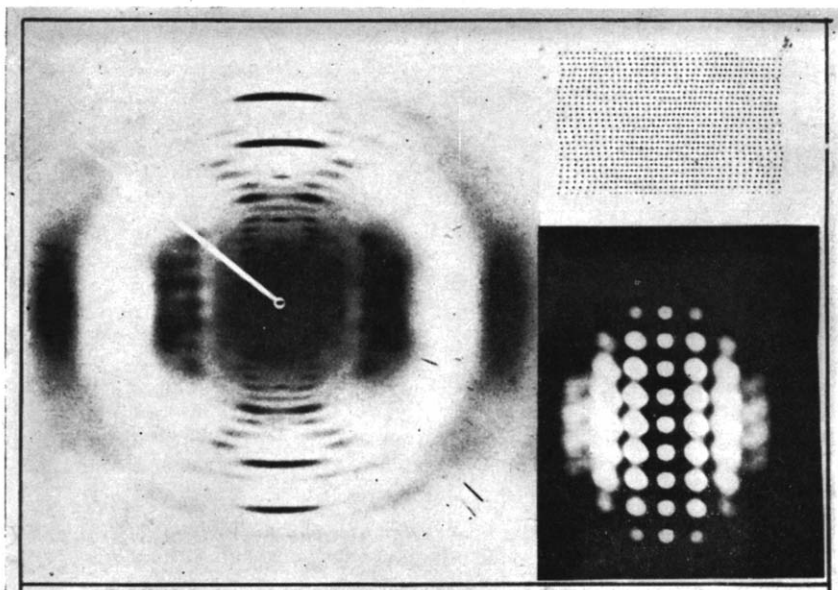


Figure 17—Small-angle diffraction of β -feather-keratin (after Bear and Rugo¹⁶) and a paracrystalline point structure with its Fraunhofer pattern

freedom which induces their fibrous behaviour in the macroscopic scale. A fibre can be defined mathematically from the special shape of its coordination statistics alone. The edge-vectors parallel to the fibre axis have only a very small relative fluctuation in their lengths, but a larger relative fluctuation of their direction. This is the consequence of the homopolar valence bonds. In the lateral direction there is a larger relative fluctuation

both in length and in direction. This is a consequence of hydrogen bonds or van der Waals forces. Such a structure can never be a crystal even in 100 Å dimensions. From the beginning it is a paracrystal and, hence, in the macroscopic scale, a fibre.

From the crystalline-like reflections along the meridian one can calculate directly the size of the paracrystal. One obtains a length of about 1 000 Å along the fibre and a thickness of about 130 Å (*Table 3*, p 369). From the orders of adjacent reflections which merge into one another one can calculate the tensors of the coordination statistics. In *Figure 17* wide-angle reflections appear which consist of about 12 or 16 small-angle macrolattice reflections.

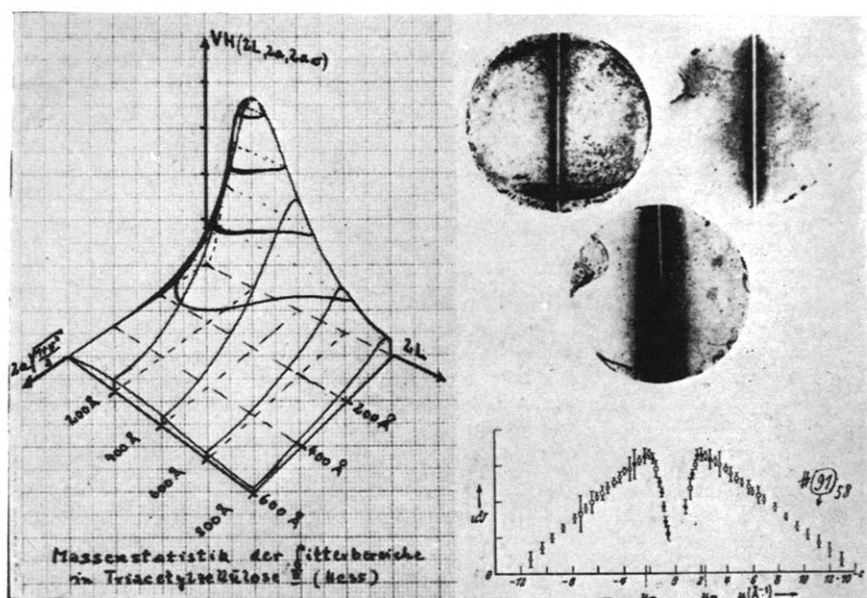


Figure 18—Small-angle scattering of triacetylcellulose II and the weight statistics VH of the lengths $2L$ and averaged thicknesses $2a\{(1+v^2)/2\}^{\frac{1}{2}}$ of the micelles

A fibre with a highly distorted macrolattice is the triacetylcellulose II of K. Hess (*Figure 18*). It produces a kind of continuous small-angle scattering without any reflection. Hence one can calculate the statistics of the length L and the mean diameter in the lateral direction of the particles (micelles). Here we have to deal with a highly dispersed and polydisperse system. Now the distances between the centres of the micelles fluctuate so greatly that there are no reflections. From theory, we know that here the relative distance fluctuation is greater than 35 per cent. If the mean relative distance fluctuation lies between 18 and 35 per cent one would get one reflection; if it is still smaller, two reflections or more (see equation 15). The macrolattice of the Hess triacetylcellulose II has such large distortions that we approach the domain of amorphous lattices.

Figure 19 gives the model of another type of macrolattice. Here the distance in the fibre direction is a constant. This coordination statistic is a point function. The lateral coordination statistic has a certain degree of freedom and such a small mean distance vector, that we have only black

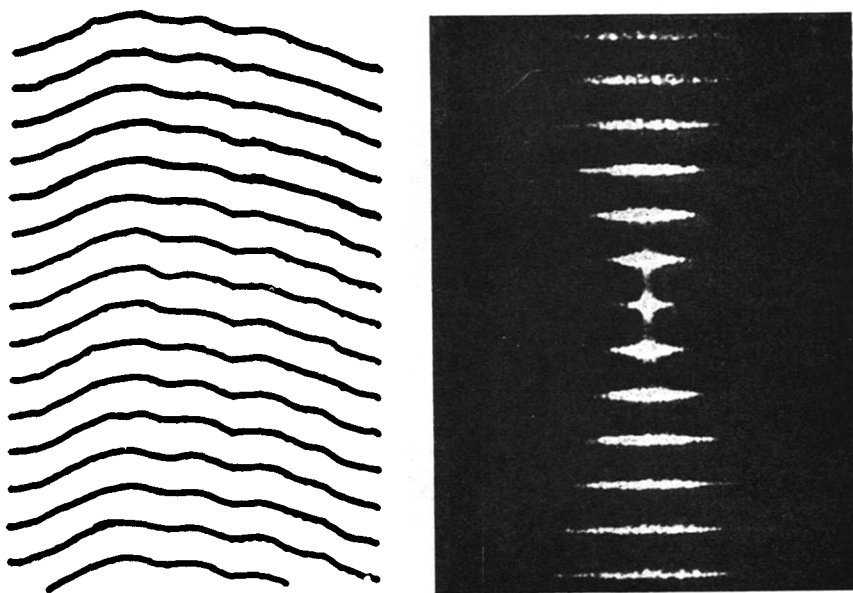


Figure 19—Paracrystalline layer lattice and its Fraunhofer pattern

lines with a statistical curvature. This so-called paracrystalline layer lattice produces a Fraunhofer diffraction pattern which is very similar to the small-angle scattering of the collagen of the tail of the Australian kangaroo (Figure 20). From the meridional distances one gets the fact that 655 Å is the macrolattice parameter in the fibre direction and from the number of the meridional reflections one can calculate that this cell edge is accurate within one per cent. This means that nature has the possibility of building up such 655 Å-macrolattice cells with an accuracy of ± 6 Å or better. Since in the horizontal direction the half-widths of the meridional reflections become larger with increasing $|b|$, the lateral cell edge must have freedom to change its direction. Hence there are layer lines orthogonal to the fibre axis with a paracrystalline curvature (see Figure 19). Nevertheless, the macrolattice of collagen has a higher order than that of β -keratin.

The macrolattices of stretched synthetic foils such as polyurethane or polyethylene give rise to only one meridional small-angle reflection (Figure 21), first observed by Hess and Kiessig¹⁷. We immediately see from equation (15) that the distortions are larger than 20 per cent. Therefore this macrolattice is more distorted than those of collagen or β -feather-keratin, but not so much as the triacetylcellulose II. If Δ_{kx_i} is the standard deviation of the coordination statistic H_k in the direction of the cell edge a_i , the number

of discrete reflections n_{ik} in the direction of a_i , which do not merge into neighbouring reflections in the direction a_k , is given by the simple relation (see *Figure 13*)

$$g_{ki} = \frac{\Delta_k x_i}{a_i} = \frac{0.35}{n_{ki}} \quad (15)$$

In this way some years ago we calculated the $\Delta_k x_i$ values of several coordination statistics for different man-made and natural fibres (*Table 3*).

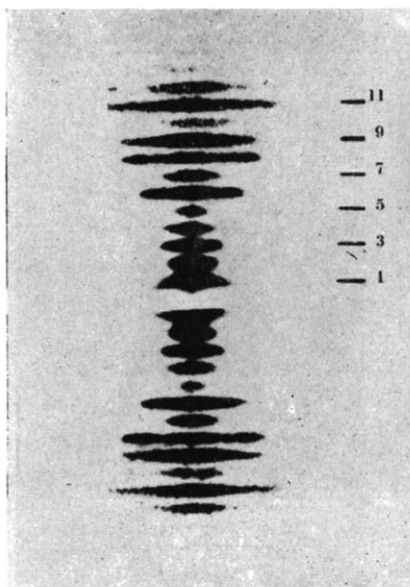


Figure 20—Low-angle diffraction lines from collagen (after Bear and Bolduan, 1951)

Cellulose in most cases has a very distorted macrolattice, so that one cannot calculate the principal axes $\Delta_k x_i$ of its coordination statistics by counting the number of the reflections because no reflections exist. Question marks denote that information is not available from small-angle patterns.

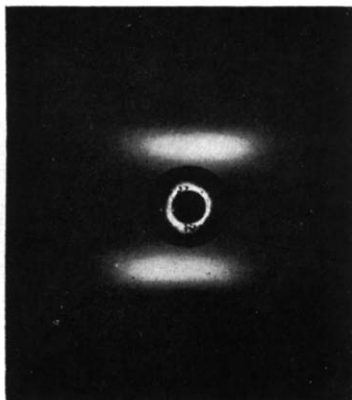


Figure 21—Small-angle diffraction of hot-stretched polyethylene

Table 3. Mean value \bar{a}_k of the edges of the cells of some paracrystalline macrolattices and their statistical fluctuations $\Delta_k a_i$ in the direction s_i and the mean sizes L_k of the macrolattices, calculated by the method of composite reflections (equation 15) and von Laue's method of undistorted reflections. s_1 , s_2 and s_3 denote the directions of the backbone linkage, fibre axis and secondary valence bond respectively

| \bar{A} | <i>Chymo- trypsin (moist)</i> | β -keratin dry | Collagen (untreated) | α -keratin | <i>Poly- urethane (stretched)</i> |
|----------------|---------------------------------------|-------------------------|-------------------------|-------------------|---|
| \bar{a}_1 | 67.8 | 34 | 110 | 83 | 20 |
| \bar{a}_2 | 49.6 | 185 | 655 | 198 | 70 |
| \bar{a}_3 | 66.5 | ? | ? | ? | ? |
| $\Delta_2 x_2$ | 1.0 | 1.4 | 6.0 | 1.8 | >16 |
| $\Delta_2 x_1$ | 1.0 | 3.7 | 30 | 5.2 | >17 |
| $\Delta_1 x_1$ | 1.5 | 2.5 | 2.5 | 5.0 | >6 |
| $\Delta_1 x_2$ | 1.5 | 1.8 | 2.1 | 2.9 | >15 |
| L_1 | ~500 | 130 | 880 | 160 | ? |
| L_2 | ~500 | 950 | 20 000 | 2 000 | ? |
| L_3 | ~500 | ? | ? | ? | ? |

V. PARACRYSTALS IN ATOMIC DIMENSIONS

The first people who discussed the possibilities of paracrystalline-like lattices in fibres were Meyer and Mark¹⁸. Figure 22 reproduces their picture of a possible arrangement of the chains in cellulose. If one introduces coordination statistics here one could define this structure quantitatively and calculate its diffraction pattern by means of equation (10).



Figure 22—Chain model of cellulose (after Meyer and Mark¹⁸)

The next very interesting paracrystal we found was at Chemstrand last year. Figure 23 gives the electron microscope picture and the electron diffraction pattern of a single 'crystal' of polyacrylonitrile (Lindenmeyer¹⁹). Its shape is similar to that of single polyethylene crystals, the long chains again orthogonal to the lamellae arranged in pseudo-hexagonal symmetry. The X-ray diagram (Figure 24) shows only some sharp equatorial reflections, but all the other reflections are very diffuse and scarcely observable. From equation (15) we see immediately that all three coordination statistics must be rod-like, the rod axes parallel to the chain molecules. The two-dimensional paracrystalline model of Figure 25(a) has rod-like coordination statistics, whose lengths $\Delta_2 x_2$ and $\Delta_1 x_1$ are about 20 per cent of the cell edges, while $\Delta_2 x_1 = \Delta_1 x_2 = 0$. This means that the lattice repeat distance in the direction of the polymer chain may fluctuate by as much as 20 per cent while the other two lattice distances are nearly constant. Its Fraunhofer pattern is of the same type as that of Figure 24. If one operates with a paracrystalline cell edge parallel to the chains in polyacrylonitrile and 14 Å

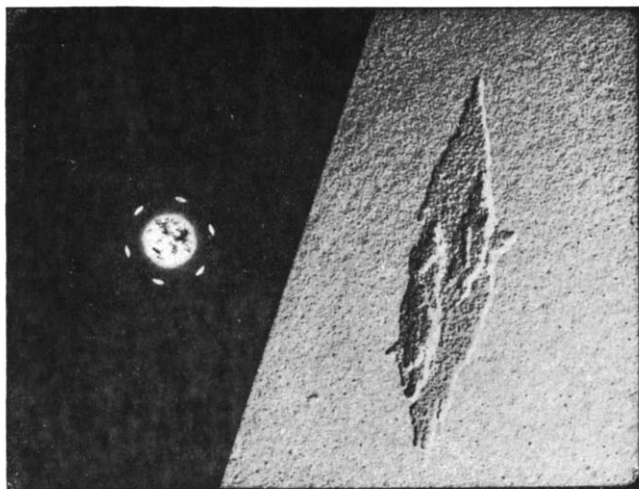


Figure 23—Single paracrystal of polyacrylonitrile and its electron diffraction (after Lindenmeyer¹⁹)

long, statistical fluctuations of 3 Å occur, which for all 3 cell edges are parallel to the chains. According to equation (15) the first layer line exists, though diffuse, while the second layer line is dissolved into the background. Since the rods are very thin, many crystalline-like reflections appear on the equator. Hence one must conclude that the lattice cells can change their lengths considerably parallel to the chains but not their lateral dimensions.

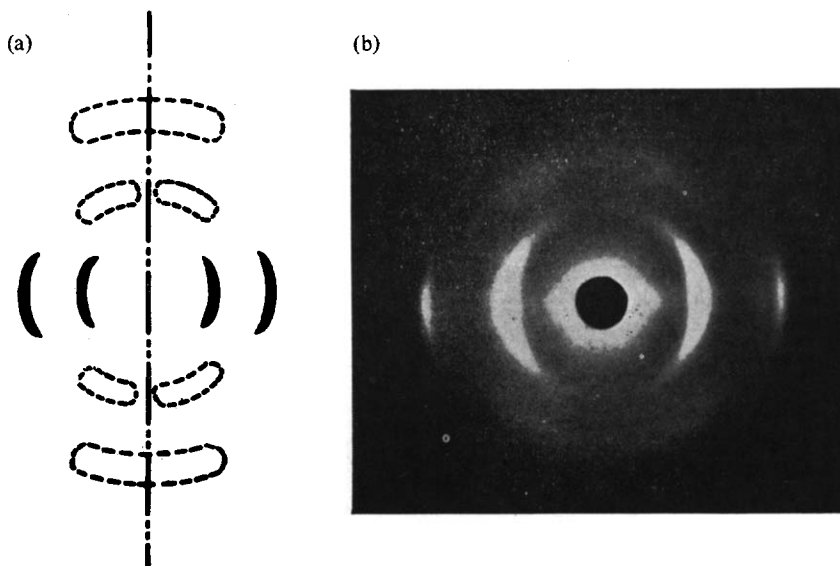


Figure 24—Schematic picture and X-ray pattern of the wide-angle diffraction of polyacrylonitrile (after Lindenmeyer¹⁹)

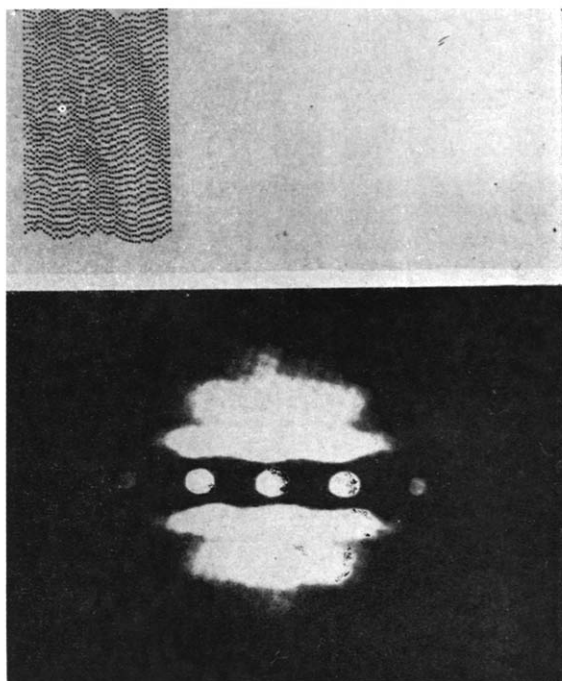


Figure 25(a)—Paracrystalline lattice with rodlike coordination statistics and its Fraunhofer pattern

The content can be drawn out without changing its lateral dimension. This gives interesting information as to what the structure can be. We thus get new statistical details which enable us to deduce how the chains are arranged in paracrystalline lattice cells. It can be proved that the results of Stefani²⁰ who discussed the existence of an isotactic and syndiotactic phase disagree with the paracrystalline nature of polyacrylonitrile.

Figure 25(b) gives the paracrystalline lattice factor $Z(\mathbf{b})$ along the meridian¹⁹ for different values of $g = \Delta_2 x_2 / \bar{a}_2$. Now we no longer have a

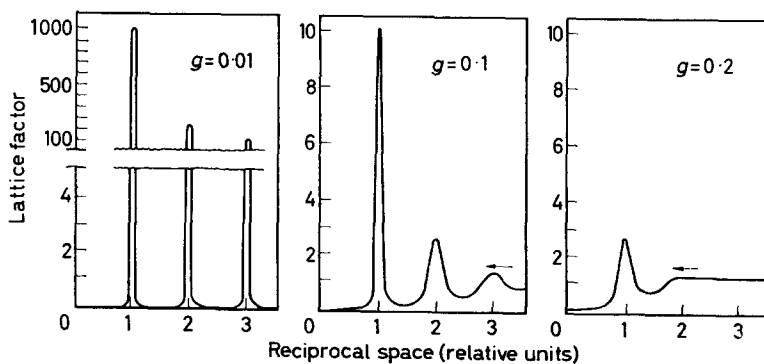


Figure 25(b)—Paracrystalline lattice factors for different relative distance fluctuations g (after Lindenmeyer¹⁹)

crystalline lattice factor but humps which are broadened. This means that the positions of the reflections are no longer those of conventional crystallography, but are shifted.

The next atomic paracrystal is the ammonia synthesis catalyst. We found a broadening of the wide-angle reflections similar to model (a) of

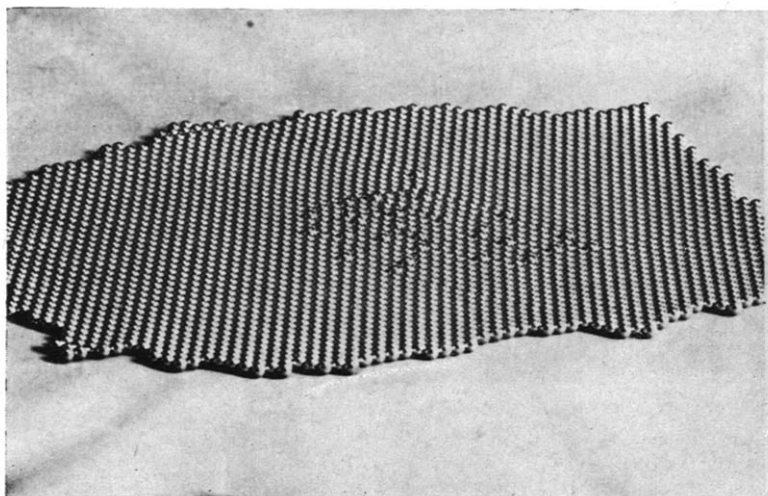


Figure 26—4 mm steel balls in crystalline arrangement with some 4.5 mm diameter steel balls in the central region

Figure 16, which yielded g values of several per cent. This catalyst consists of α -iron and a few per cent of alumina. The atomic volume of Al is about 40 per cent larger than that of Fe. *Figure 26* shows a model of a single ideal crystal which consists of 5 000 steel balls of 4 mm diameter all lying

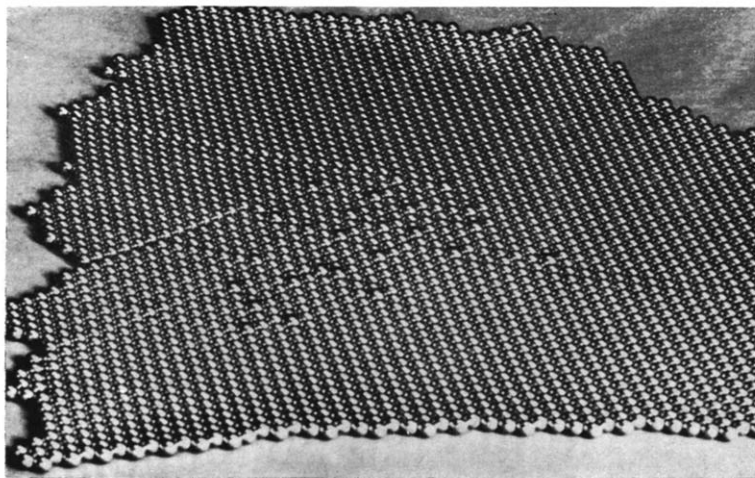


Figure 27—The same as *Figure 26* after a short time of shaking

on a drum. In the central region we have carefully replaced about 50 balls by larger steel balls with a diameter of 4.5 mm. This system is not in thermodynamic equilibrium, since the larger balls do not touch the drum. (D. Turnbull carried out similar work—private communication.) In *Figure*

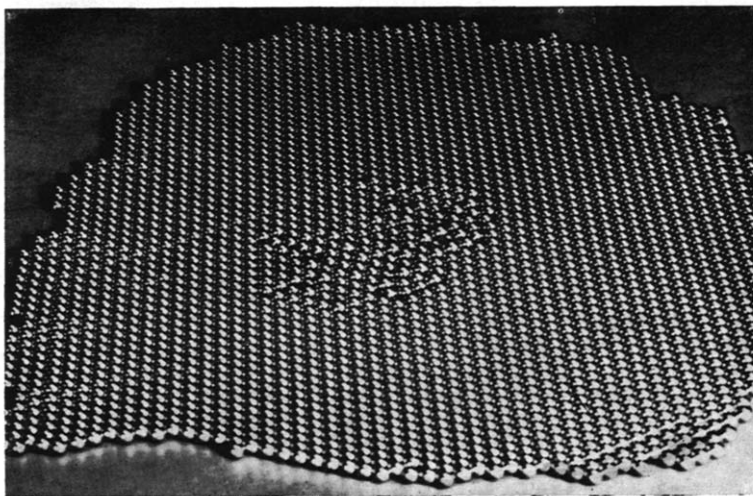


Figure 28—The same as *Figure 26* after a longer time of shaking

27 the system has been shaken smoothly for a short time. One sees that step dislocations travel out from the disturbance centre and the large balls begin to settle down.

After a longer time of shaking the larger balls finally obtain the space they need. But in the region where they lie the straight net planes become

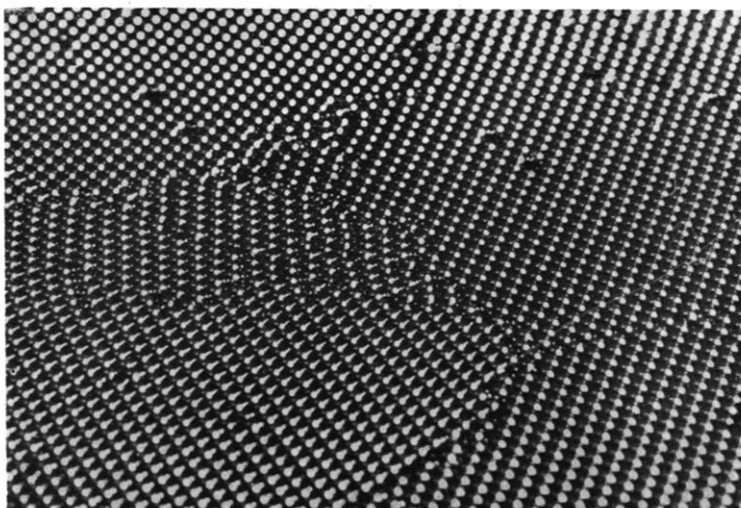


Figure 29—Two paracrystals and four crystalline mosaic blocks

curved rows (*Figure 28*). We now have a kind of paracrystal, embedded into a single crystal.

In *Figure 29* two small paracrystallites are surrounded by other crystals. Paracrystals arise only in regions where balls of different sizes are mixed. The same is applied in real mixed crystals where the atomic volumes of the respective components differ. Then paracrystalline structures are to be expected. To observe them with the help of X-ray patterns one must have high precision X-ray cameras. Otherwise one cannot detect the small effects of line broadening. (A High Precision Guinier–Jagodzinski Double Cylinder camera made by AEG—Berlin NW87, Sickingenstr. 71, was used. An ammonia synthesis catalyst with three per cent aluminium, for instance, gives a g value of 1.2 ± 0.2 per cent.)

VI. THE AMORPHOUS LATTICE

Figures 30(a) and *(b)* give schematic representations of a crystalline and an ideal paracrystalline lattice. Its lattice factor is given by equation (10). Here each lattice cell has the shape of a parallelepiped. In *Figure 30(c)* we

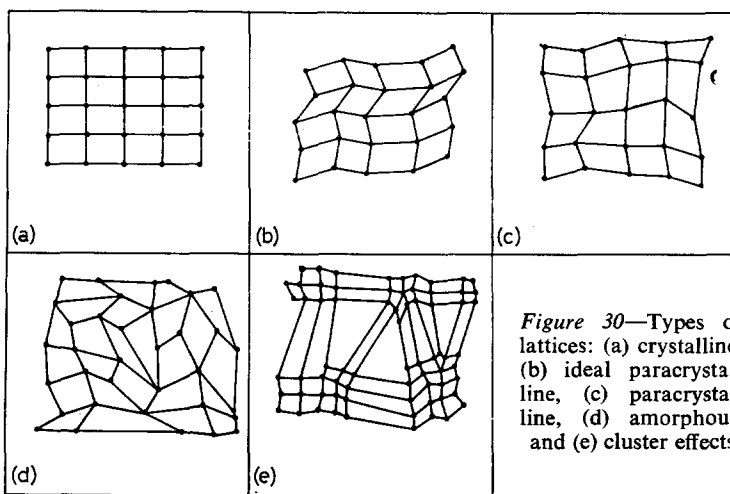


Figure 30—Types of lattices: (a) crystalline, (b) ideal paracrystalline, (c) paracrystalline, (d) amorphous, and (e) cluster effects

find a real paracrystal. Here there enters a correlation correction term not yet mentioned in equation (10). This is only a correction term calculated from the theory. In *Figure 30(d)* an amorphous lattice is given. In this it is no longer possible to find rows and columns where the single 'bricks' lie. Nevertheless it is a single 'lattice', because it has some homogeneous character, which statistically can well be defined by means of the Q function. The fifth structure of *Figure 30(e)* is no longer a lattice because here we meet with aggregation effects which lie beyond the statistical fluctuations. That means we now have clusters. These clusters can have an inner structure of crystalline, paracrystalline or amorphous type. Besides this we have a macrolattice whose bricks are the single clusters. This macrolattice can be of crystalline, paracrystalline or amorphous type, quite independent of the inner structure of the clusters. In natural fibrous systems Bear and Rugo¹⁶

pointed out that the more distortions there are in the microlattices, the less there are in the macrolattices and vice versa. The two statistical principals of order are competitors. For instance, with metals we find very fine crystalline lattices but macrolattices of the amorphous type.

Figure 31 gives some examples of such amorphous lattices, which are of interest in fibre work if we think of the two-dimensional models as cross sections orthogonal to the fibre axis. Then the Fraunhofer pattern of *Figure 31* relates to the situation around the equator. All three models have particles of the same polydispersity g_y of 30 per cent, but the packing

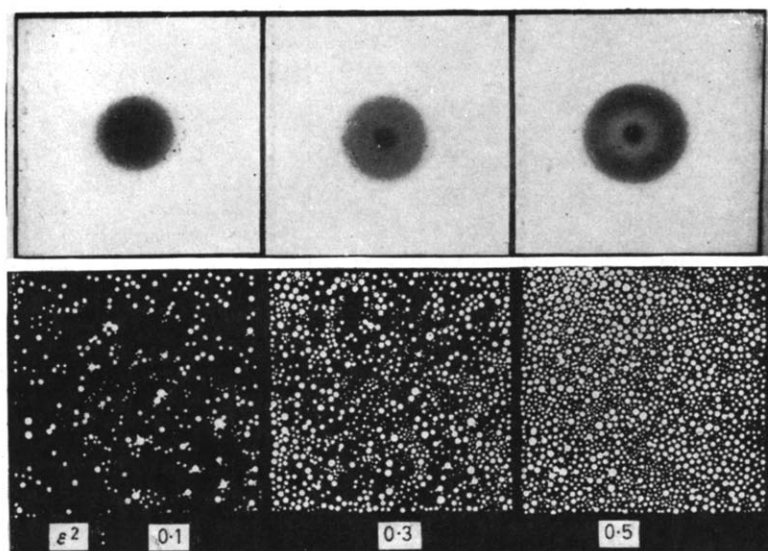


Figure 31—Polydisperse amorphous aggregations with constant polydispersity g_y and different packing density ϵ^2

density ϵ^2 varies from 0.1 to 0.5. If $g_y = \epsilon^2$ we have the intermediate case where the intensity goes monotonically down with increasing b but has a point of inflection where $dI/db = 0$. If $g_y > \epsilon^2$ we have the gaseous case with no reflection. If $g_y < \epsilon^2$ the liquid case with one or more 'liquid rings' results.

It is meaningless to say that on the RHS of *Figure 31* we have a liquid, on the LHS a gas, because the parameters g_y , ϵ^2 which describe the type of phenomenon have nothing directly to do with gases or liquids. The microphotometer curves of the Fraunhofer patterns of *Figure 31* can be seen in *Figure 32*. We clearly see the three different cases described above. Taking into account a so-called liquid correction term (Hosemann^{2,4} and Joerchel²¹) one can calculate from the intensity functions of *Figure 32* the polydispersity g_y , the packing density ϵ^2 and the mean diameter of the particles (right side of *Table 4*) which we have used in the models (left side

of Table 4). The examples of Table 4 show that we get reliable information with an accuracy of 3 to 10 per cent.

VII. STRUCTURE OF LINEAR POLYETHYLENE

Figure 21 is a reproduction of the small-angle X-ray pattern of hot-stretched linear polyethylene (Bonart and Hosemann²²). The position of the meridional 'Hess-Kiessig reflection' corresponds to a 120 Å distance along

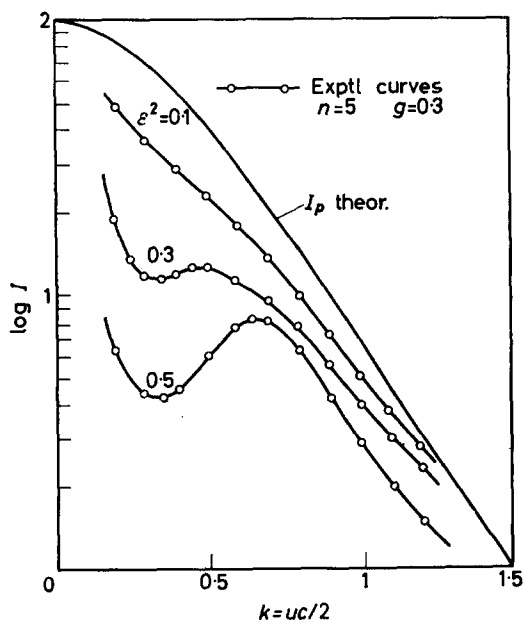


Figure 32 — Microphotometer curves of the Fraunhofer patterns of Figure 31, shifted in the vertical direction

the fibre axis which by heat treatment can be extended to 1000 Å or more (Mandelkern²³). It is interesting to note that no small-angle scattering occurs along the equator. Around the meridional reflections a background exists which we have investigated carefully. I shall deal with some of the results of our analysis.

If one transforms back the intensity function of Figure 21 one gets a Q function of the type of Figure 33(b). Guinier and Belbéoch²⁴ incorrectly equated this Q function to the density distribution $\rho(x)$ and published the structure of Figure 33(c). Analogous to Guinier-Preston zones in the centre there is a domain of higher density (+70). In the meridional direction one observes two domains of very low density (-10) and surrounding these a mean density near zero. This means there are three different phases similar to the case of metallic alloys of age-hardened (Al, Ag)-mixed crystals: clusters of Ag atoms are surrounded by a domain, enriched with Zn atoms, and outside this the ordinary mixed phase exists. In contrast to a spherical symmetry one now has in Figure 33 axial symmetry. Taking into account equations (4) and (5) one must remember that Q is the convolution square of ρ and hence that ρ can be



Figure 33(a)



Figure 33(b)

Figure 33—Hot-stretched polyethylene: (a) model, (b) folding square, (c) analysis of Guinier and Belbéoch²³

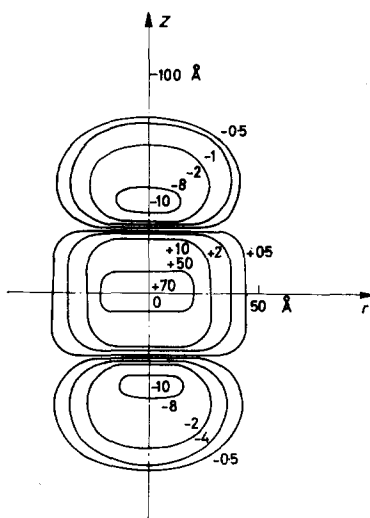


Figure 33(c)

quite different from Q (ρ is the folding root of Q). Figure 33(a) shows such a model of a folding root which has only two phases. Figure 33(b) is the folding square of Figure 33(a) produced by the folding machine (Figure 1).

Now we again have a paracrystalline-like lattice but in contrast to the paracrystalline layer model of Figure 19 the layer lines are not very long. Hence the particle size influences the Fraunhofer pattern. The distance fluctuations between single lamellae are about 30 per cent. Therefore according to equation (15) only one reflection appears on each side of the meridian. Figure 34 shows another similar model and its Fraunhofer pattern, which corresponds very closely to Figure 21. Hess and Kiessig¹⁷ published the model of Figure 35(a) for stretched polyethylene. It is incorrect, because the structure, smeared out in atomic dimensions

Table 4. Polydispersity g_y , packing density ϵ^2 and mean particle diameter y for different amorphous models after Joerchel²⁰

| Model No. | x-space | | | b-space | | |
|-----------|---------|-------|--------------|---------|-------|--------------|
| | y | g_y | ϵ^2 | y | g_y | ϵ^2 |
| 1a | 0.155 | 0.30 | 0.10 | 0.142 | 0.30 | 0.11 |
| 1b | 0.155 | 0.30 | 0.30 | 0.145 | 0.27 | 0.37 |
| 1c | 0.155 | 0.30 | 0.50 | 0.137 | 0.26 | 0.54 |
| 2a | 0.106 | 0.42 | 0.10 | 0.102 | 0.43 | 0.13 |
| 2b | 0.106 | 0.42 | 0.30 | 0.096 | 0.45 | 0.31 |
| 2c | 0.106 | 0.42 | 0.50 | 0.099 | 0.45 | 0.46 |
| 3a | 0.083 | 0.53 | 0.10 | 0.081 | 0.53 | 0.10 |
| 3b | 0.083 | 0.53 | 0.30 | 0.071 | 0.49 | 0.22 |
| 3c | 0.083 | 0.53 | 0.50 | 0.068 | 0.49 | 0.35 |
| 4a | 0.053 | 0.75 | 0.10 | 0.056 | 0.79 | 0.08 |
| 4b | 0.053 | 0.75 | 0.30 | 0.058 | 0.81 | 0.21 |
| 4c | 0.053 | 0.75 | 0.50 | 0.058 | 0.77 | 0.41 |

[Figure 35(b)] gives rise to a strong equatorial small-angle scattering which we have not observed in Figure 21.

Figure 36 is a model due to Statton and Geil²⁹ which is also incorrect for hot-stretched polyethylene because it produces a strong equatorial reflection which is not observable. Such structures can exist only in cold-stretched fibres where we have a strong equatorial interference effect [see Figure 37(d)].

Cold-stretched polyethylene loses its transparency and becomes white. Hence by cold-stretching inhomogeneities arise with sizes of optical wavelengths. Moreover, Figure 37(d) shows that these inhomogeneities go down to atomic dimensions. The Hess-Keissig reflections are relatively weak. After pressing together cold-stretched material in a lateral direction, one

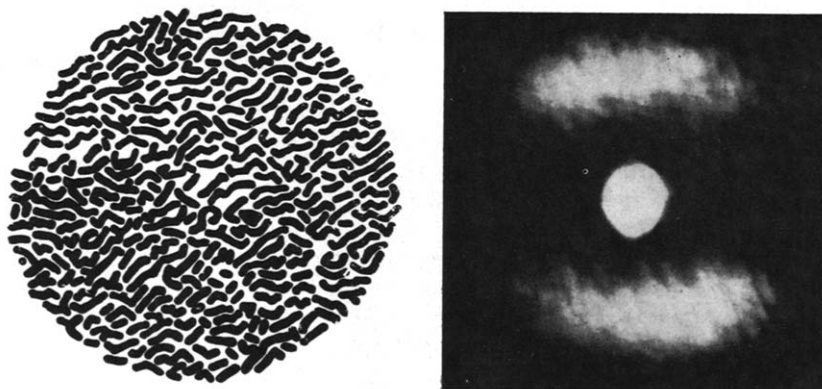


Figure 34—Hot-stretched polyethylene: (a) model, (b) Fraunhofer pattern

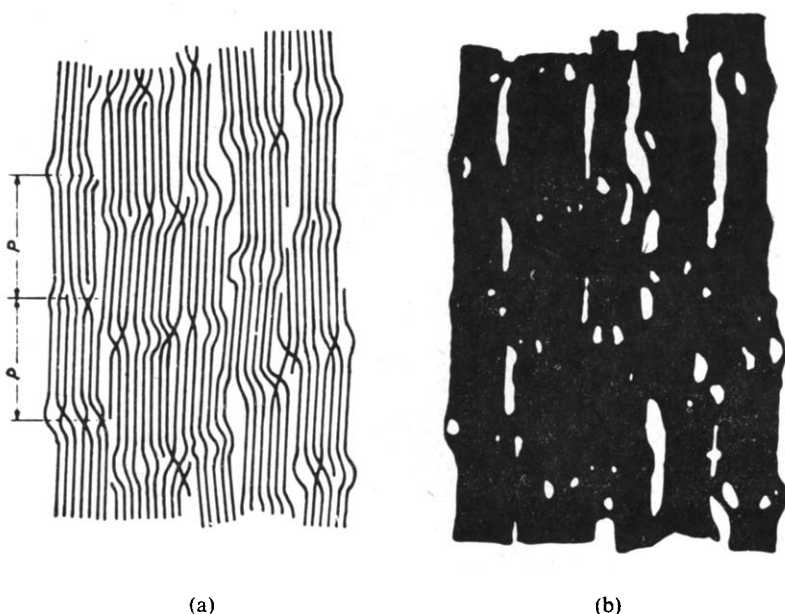


Figure 35—Model of stretched polyethylene (a) according to Hess and Kiessig¹⁶, (b) smeared out in atomic dimensions

gets a so-called four-point diagram [Figure 37(b), (c)] and at the same time the equatorial intensity at small angles disappears again [Figure 37(a)] and the optical transparency returns. This means that by pressing with the fingers one can alter atomic dimensions. Figure 38(c) shows schematically that in this case single ultrafibrils are pressed together to form a bulk structure with a paracrystalline hexagonal structure in the plane of pressure and stretching. Proof: The four-point diagram exists only if the X-rays are orthogonal to this plane [Figure 37(b), (c)] and do not exist if they run parallel to the direction of pressure [Figure 37(a)].

From the analysis of the intensive small-angle scattering [Figure 37(d)] of the cold-stretched fibre according to the theory of amorphous lattices (Figure 31) one gets direct information of the size distribution of the ultrafibrils which split off in cold-stretched material. In Figure 39 $\ln I$ along the equator is plotted against $|b|^2$. One gets the information that in the lateral direction as a result of cold-stretching the fibres must split up into ultrafibrils, the one of 100 Å diameter, the other of 200 Å diameter and the third of 400 Å. Using the Warren–Guinier approximation one can synthesize the $\ln I$ versus b^2 function from three Gaussian curves (Figure 40). It is interesting to know why 100, 200 and 400 Å ultrafibrils arise. We believe that there are working elements present of about 100 Å diameter. About 20% per cent of such elements are isolated, about 35% per cent cluster together to about four of them and 45% per cent to bundles of about 16 ultrafibrils [Figure 38(b)]. The rest $[(1 - \alpha) 100 \text{ per cent}]$ build up clusters with diameters larger than 400 Å.

One often finds in the literature the statement that the equatorial small-angle scattering arises from voids in the substances and that these voids



Figure 36—The model of stretched polyethylene after Statton and Geil²⁹

are holes like bubbles in a foam. The analysis of the intensity of the meridional reflection parallel to the equator (*Figure 39*) proves that this cannot be so. One gets from this interference a lateral size (see the black regions in the models of *Figures 33* and *34*) of 100 Å, which corresponds exactly to the diameter of the 'working elements' (= ultrafibrils) mentioned above. Hence, the 'voids' here are the intermediate spaces between the ultrafibrils and between the clusters of ultrafibrils. The next direct information of the existence of such 'working elements' one obtains from shearing experiments. *Figure 41(b)* shows a schematic drawing of what happens if one bends a stretched polyethylene sample by moving its ends in the direction of the arrows. The single ultrafibrils, or parts or clusters of them glide one along the other parallel to the macromolecular chains. Such shearing processes, in contrast to those of metals, we call 'shearing of the second kind'.

Although in metals shearing only arises if the distance of the sheared ends is small compared with the areas sheared and these lie parallel to the

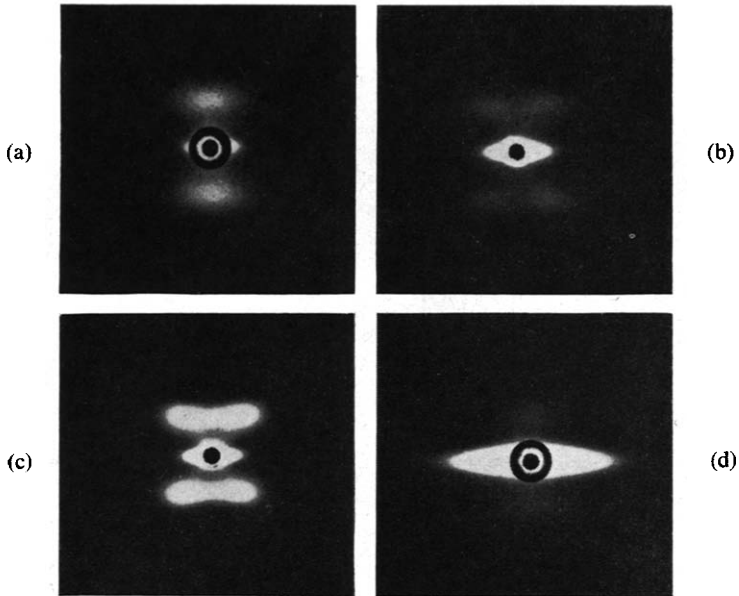


Figure 37—Small-angle diagrams of cold-stretched polyethylene: (a) laterally pressed parallel to the X-rays, (b) laterally pressed orthogonally to the X-rays, (c) ditto and annealed, (d) not pressed

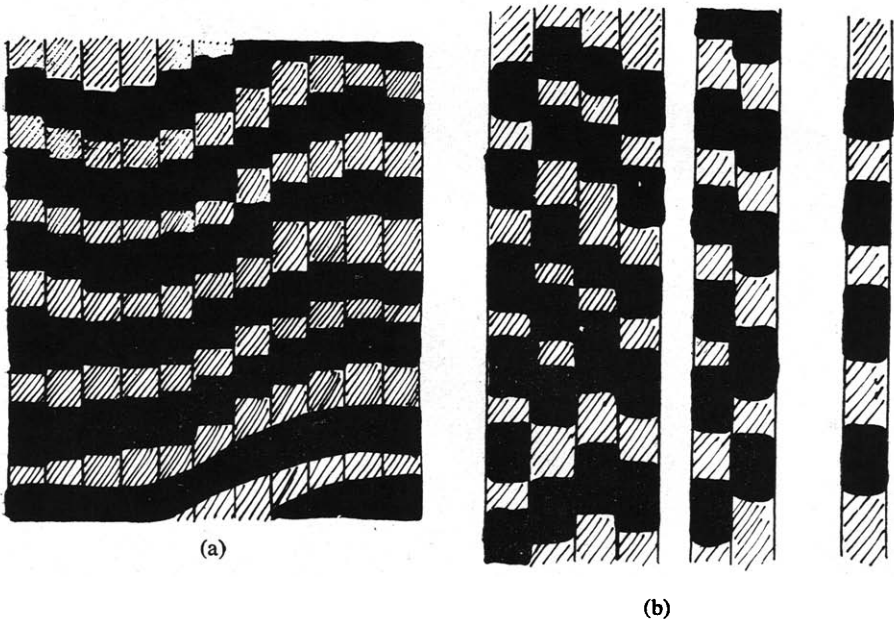


Figure 38. (See caption overleaf)

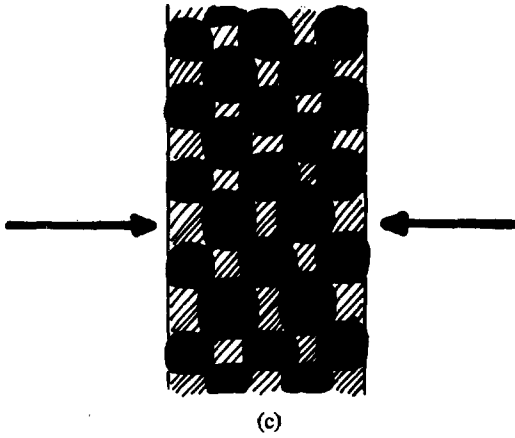


Figure 38—Paracrystalline macrolattices in stretched polyethylene: (a) heat treatment, (b) cold stretched, (c) ditto and laterally pressed.

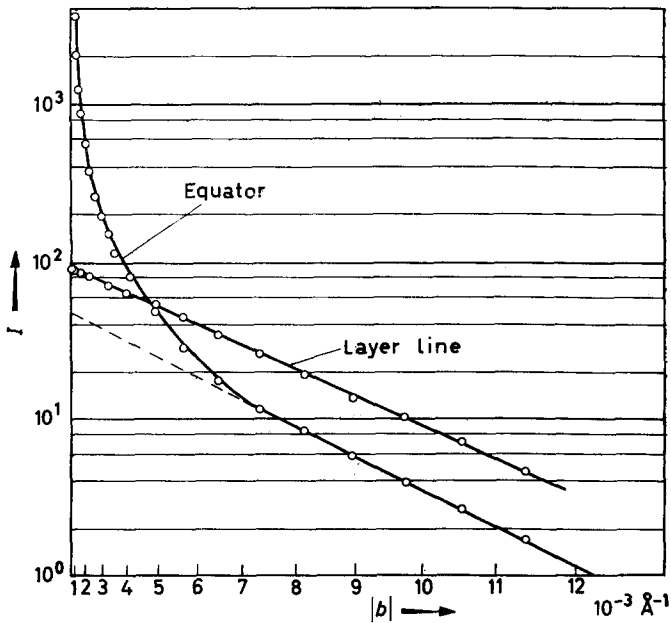


Figure 39—Small-angle intensity of cold-stretched polyethylene

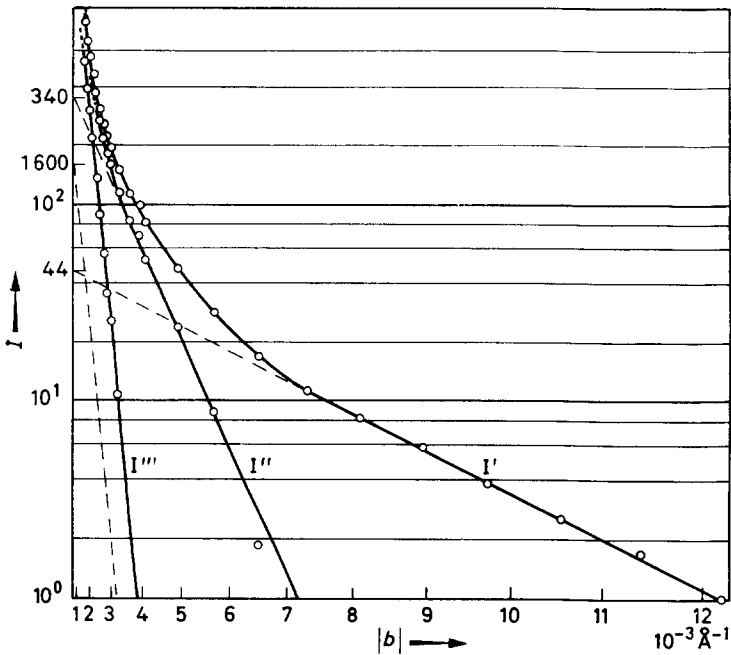


Figure 40—Gaussian analysis of Figure 39

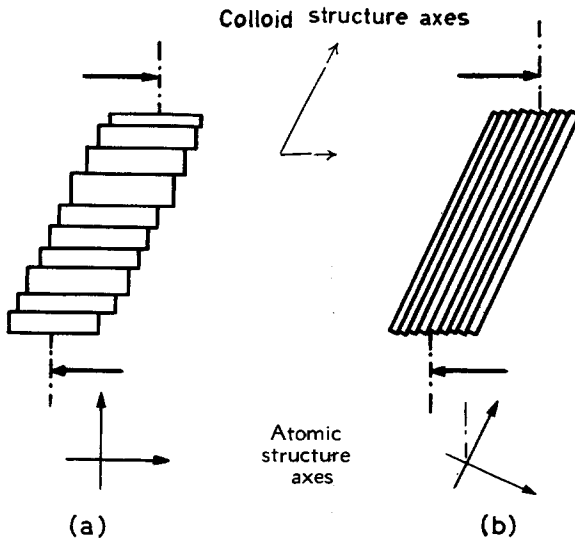


Figure 41—Types of shearing: (a) first kind (metals, etc., gliding planes parallel to the arrows), (b) second kind (high polymers, glide planes parallel to the chains)

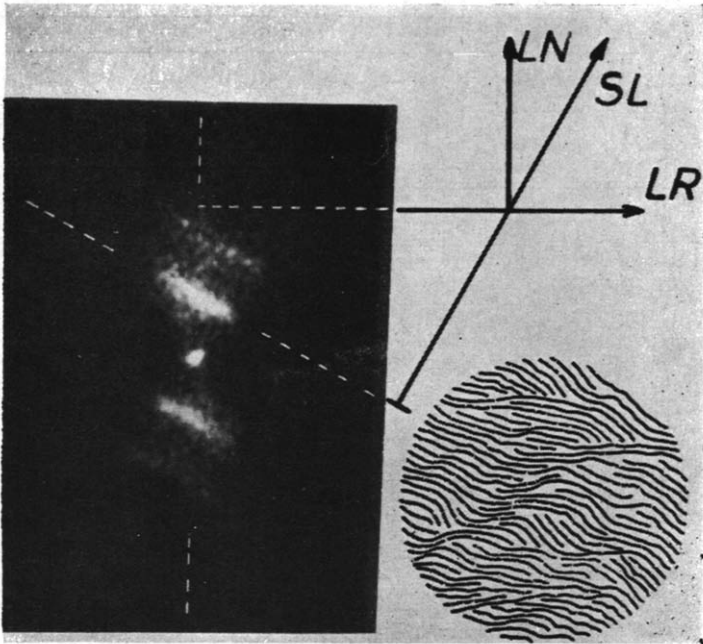


Figure 42—Paracrystalline layer lattice after shearing—LN old, SL new direction of the chains. LR old and new main direction of the layers

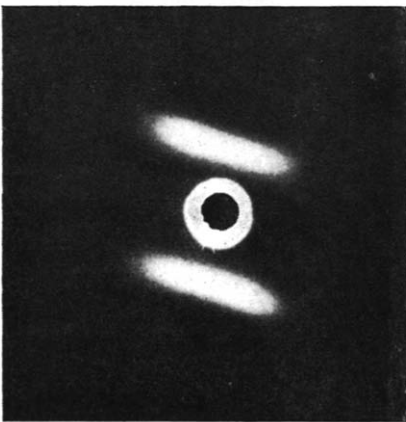


Figure 43(a)



Figure 43(b)

Figure 43—Small-angle diagrams of sheared polyethylene: (a) hot-stretched, (b) cold-stretched

arrows, the shearing of the second kind takes place also for long narrow strips and does not take place parallel to the arrows. In *Figure 41(b)* the mean edge vectors of the paracrystalline macrolattice cells are no longer orthogonal. Hence the small-angle pattern must be monoclinic. *Figure 42* gives a model and its Fraunhofer pattern, *Figure 43* the X-ray patterns of (a) hot- and (b) cold-stretched polyethylene after shearing.

Similar non-orthogonal small-angle patterns were found by Hendus²⁵ who cross-stretched a hot-stretched polyethylene (*Figure 44*).

By heat treatment of cold-stretched material it again becomes transparent and the intensity of the Hess-Kiessig reflection increases. From the analysis of the background around these reflections one then discovers that

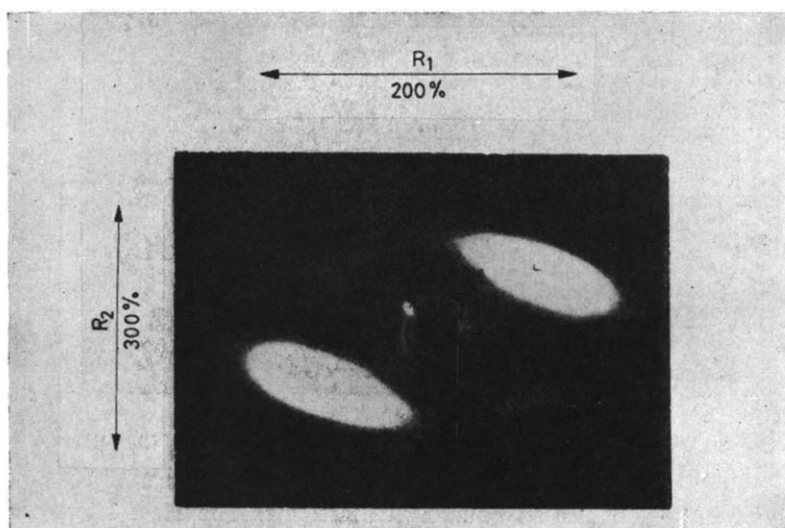


Figure 44—Hot-stretched polyethylene parallel to R_1 afterwards cross stretched parallel to R_2 (after Hendus²⁴)

correlations between the single ultrafibrils, which in the cold-stretched material are totally lost, return step by step. Paracrystalline layer lines are built up step by step with increasing order [*Figure 38(a)*]. Now the single crystalline-like layers resemble more and more the monocrystals described by Keller²⁶ and Fischer²⁷.

Besides crystalline-like wide-angle reflection, we find in such material a so-called 'amorphous halo' (*Figure 45*). This indicates that between the single crystalline regions there must be a high degree of freedom for the single chains. Taking all these facts together we get the following picture (*Figure 46*):

In certain colloidal domains, we always encounter paracrystalline layer lattices. The higher the lateral correlation between adjacent ultrafibrils, the larger the lateral size and the lower the paracrystalline curvature of these lamellae. Some of the chains must fold back at the surface of these layers. Otherwise one can never explain the hot-stretched diagram

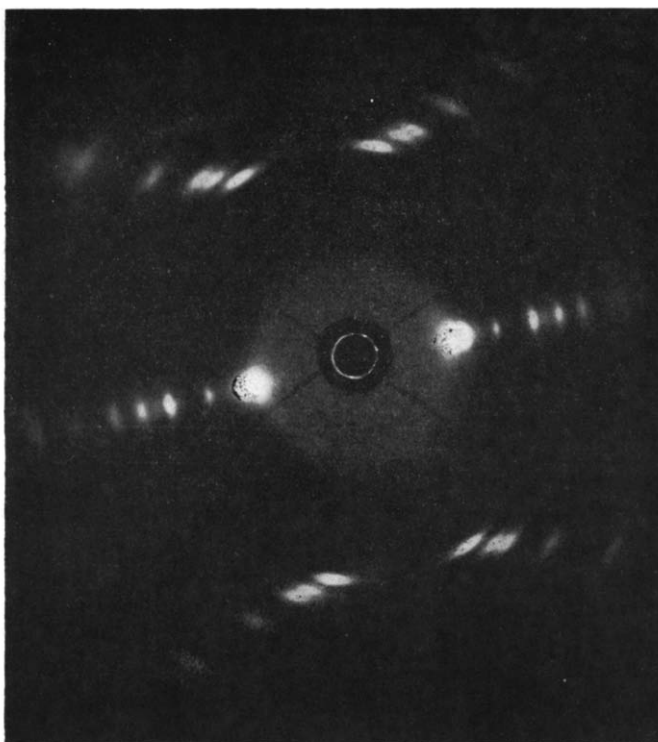


Figure 45—Wide-angle Bragg reflections and the 'amorphous halo' in hot-stretched polyethylene

of Figure 21 which has no equatorial scattering. The Hess-Kiessig and Statton models, which do not take into account this backfolding, always give rise to equatorial scattering and hence are incorrect. Thus, indirectly we can establish this backfolding in bulk material, which Fischer and Keller have proved directly for monocrystals. Let α be the amount of backfolding chains, β the portion of chains going straight through from one paracrystal to the next and γ the portion of largely disturbed chains in the amorphous phase. The nuclear magnetic resonance measurements prove directly the existence of these three phases (Hyndman and Origlio²⁸). Absolute intensity measurements of the amorphous halo in Figure 45 will give more information on the quantity of γ^* . The 'amorphous phase' thus consists of three different types of chains, S, LB and γ . It is thus problematical from the atomic point of view to speak of a 'phase'. On the left side of Figure 46 one can see what happens if one has a cold-stretched material. Then voids V appear and give rise to the glide planes of Figure 41(b). On the right side of Figure 46 we again have such shearing regions SH, which we found in our shearing experiments even for hot-treated material without voids. Here every 100 Å we meet boundaries of ultrafibrils, since

*Protons with low, medium or high mobility are in paracrystalline regions P and short back foldings SB, or in straight chains S and long back foldings LB, or in the much disturbed chains γ .

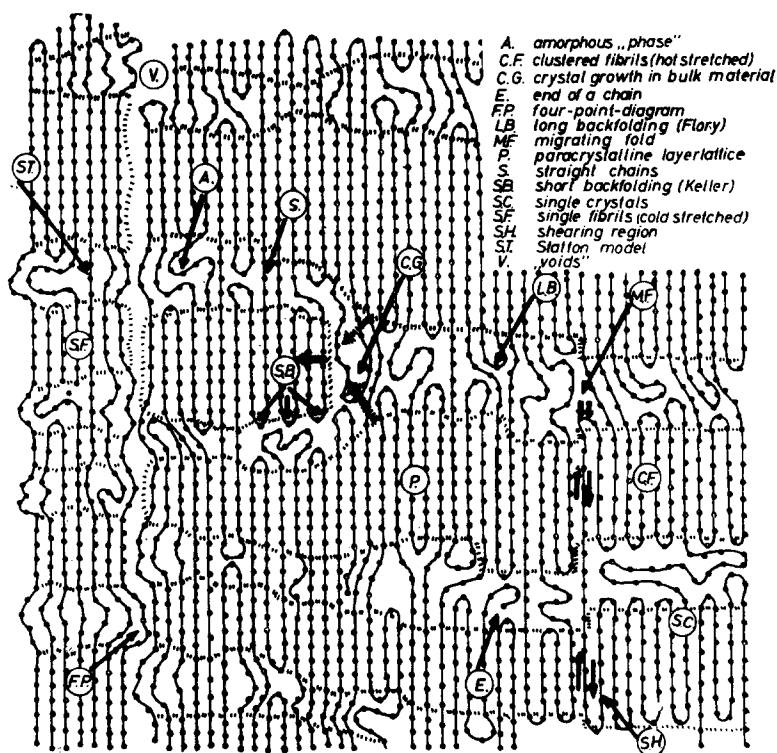


Figure 46—Model of the different types of macrolattices in stretched linear polyethylene

the chains like to build up families, working elements, or cybotactic groups which have this high degree of freedom between them, although certain correlations exist between the ultrafibrils which give rise to paracrystalline layers of considerable lateral size. Only after cold-stretching do the voids *V* exist. If one compresses the material then the four-point diagram [Figure 37(b) and (c)] emerges because the amorphous regions after cold-stretching have a larger lateral area (see the Statton model, Figure 36). The chains here have in some measure left the ultrafibrils and entered into the voids. If they are now pressed together they resist being pressed back. So the crystalline portion of one ultrafibril is forced to lie down near the amorphous region of the adjacent ultrafibril [Figure 38(c)] and therefore a hexagonal-like symmetry arises (lower left corner of Figure 46). In the centre of Figure 46 a domain *CG* exists where, we believe, crystallization can occur. The lateral end of one lamella is here. The chains on the right of this lamella belong to an amorphous region and hence have a higher mobility. With rising temperature the amorphous region will increase on the left side and destroy the crystalline region of the adjacent lamella. Then the surfaces of the adjacent lamellae above and below this region can grow and, hence, the mean distance between para-

crystalline layers statistically increases. Lowering the temperature, the converse process takes place and nucleation of new lamellae occurs.

On the right side of *Figure 46* the lateral correlation between adjacent ultrafibrils is so high that large paracrystalline domains exist. The back-folding now occurs with such great regularity and the lattice distortions inside the single lamellae are so small that we find here bundles of Keller crystals linked together by only a few straight chains. The above-defined quantity α here is very high, while β and γ are very small.

Thus one single atomic and colloidal model can explain all the different experimental observations, especially the growth of spherulites which to a considerable degree also reveal microfibrillar as lamellar features. More



Figure 47—Paracrystalline layer lattice on the sand near the mouth of the Tagliamento river in Italy

quantitative X-ray investigations following the lines mentioned above should help to prove the correctness of the paracrystalline model in greater detail.

The theory of paracrystalline structures is a little more complicated than that of conventional crystals. If, until this moment, we have discussed para-

crystalline structures in atomic or colloidal dimensions alone, it is important to realize that such structures also exist in macroscopic dimensions.

Figure 47 gives a picture of sand near the mouth of the Tagliamento river in Italy at low tide. Here one finds such structures illustrated. The distance between adjacent 'bricks' is not now in dimensions of Ångström units or microns but amounts to some centimetres. Nevertheless, the statistical problem here remains in principle the same as in the paracrystalline layer lattices of polyethylene. If I would give to a student the task of explaining quantitatively such a structure, I am sure he will encounter relatively serious difficulties. He will give me the mean length of the frozen waves in the sand but he will not give me a quantitative measure of their polydispersity and curvature. Using theories such as that of the paracrystal and of amorphous lattices, which take into account quantitatively statistical elements such as coordination statistics, partial correlations, etc., he will find the correct answer with relative ease. I believe this is a method of obtaining new statistical structure elements, which are of practical importance not only on the beach of the Tagliamento but which also explain many technological properties of man-made fibres.

*Fritz-Haber-Institut der Max-Planck Gesellschaft,
Faradayweg 4-6, Berlin-Dahlem, Germany*

DISCUSSION

Dr P. H. Hermans (Netherlands), Chairman: Would it be entirely meaningless to apply a procedure of dividing the diffraction picture into peaks and a background, for the hypothetical case when one has a substance consisting entirely of paracrystalline matter?

Professor R. Hosemann (Germany): The division of the X-ray pattern into peaks and a background is a first step in the analysis and never can be meaningless if one draws correct conclusions from the background- and peak-scattering. If, for instance, you have matter consisting of single paracrystallites and no amorphous regions, the background-scattering surely has nothing to do with an amorphous phase but depends alone on lattice distortions. The examples of paracrystals given above demonstrate that with the help of this division you can calculate the paracrystalline distortion (i.e. distortion of the second kind) as well as the displacement distortions (distortion of the first kind such as Frenkel displacement, thermal vibration, etc.) and furthermore you can analyse from the widths of a series of peaks not only these two different sorts of distortions but also the sizes of the crystallites or paracrystallites.

If a real amorphous phase exists, this produces another sort of background. After elimination of the distortion background as in Ruland's work one then gets information on the amorphous phase background.

Dr P. H. Hermans (Netherlands), Chairman: Ruland tried, in the case of polypropylene, to verify the procedure of drawing the background line by extending the observations of the diagram to very large angles and found the

same crystalline fraction and the same Debye factor included in the background independent of the angle of diffraction used.

You also mentioned that your paracrystalline distortions could be adequately described by a Debye factor.

Professor R. Hosemann (Germany): The method of Ruland is based on assuming an artificial Debye factor until, for one sample, the crystalline fraction calculated is independent of the angle of diffraction used. But one can prove that this artificial Debye factor depends on distortions of the first and second kinds, and is given by

$$D^2_{\text{apt}} = D^2 \cdot \prod_{k=1}^3 2|F_k| / (1 + |F_k|)$$

D^2 is defined by equation (14) and depends on the distortions of the first kind. F_k is defined by equation (10) and depends on the paracrystalline distortions, i.e. those of the second kind.

Professor L. Küchler (Germany): In connection with the questions just discussed, I wish to refer to some work by Herre and Reichert which has just been completed in our laboratory and which will shortly be published.

In the last 15 years the so-called crystalline fraction has usually been determined by X-rays. Until the work of Ruland already mentioned, the lattice imperfections about which Professor Hosemann has spoken have not been taken into account, at least as far as I am aware; I do not know of any other work.

Herre and Reichert have now endeavoured to take account of the lattice distortions in polyethylene exactly, and to determine from the scattering in as wide an angular range as possible—not as usually within a narrow range of angle—the crystalline fraction. Fundamentally, this is possible.

However, the errors are so large—in polyethylene the error in the crystalline fraction is estimated at ± 40 per cent—that the method is practically without significance. An attempt has also been made, of course, to use the X-ray method indirectly, that is to say, to use it to determine the density. But this means that the simple measurement of density is replaced by a somewhat complicated X-ray measurement, and I consider that this has no advantage.

Professor R. Hosemann (Germany): 40 per cent error is too large to allow analysis of atomic structure. It would be better to rely on simple density measurements. However, from *Table 1* it may be seen that Ruland (with polypropylene) had results of much higher accuracy. Perhaps the experimental technique can be improved for polyethylene.

Professor L. Küchler (Germany): The large error is not due to error in measurement, but is principally due to uncertainties in the atom form factor and in the incoherent scattering, and also to the not wholly correct simplification in the theoretical model (e.g. the assumption of anisotropic temperature scattering).

Professor F. H. Müller (Germany): In this connection I should like to make a point on thermal motion in crystalline partially crystallized polymers. Some experiments have been done in our institute by Dr Kilian, and he tried to obtain the thermal motion by a Debye factor D by measuring the wide angle scattering as a function of temperature in the range of -150° to 200°C (Figure 48). He found two regions of different behaviour. (In press.)

D is a linear function at higher temperatures, but at lower temperatures D becomes constant for branched polyethylene below -50°C , and for unbranched polyethylene below -70°C . Only at very low temperatures is there an effect of paracrystalline displacement. If you assume a distorted lattice, then by thermal motion you get a more symmetrical lattice at high enough temperatures. So at high temperatures you see only the thermal motion but you can measure the paracrystalline arrangement at low tem-

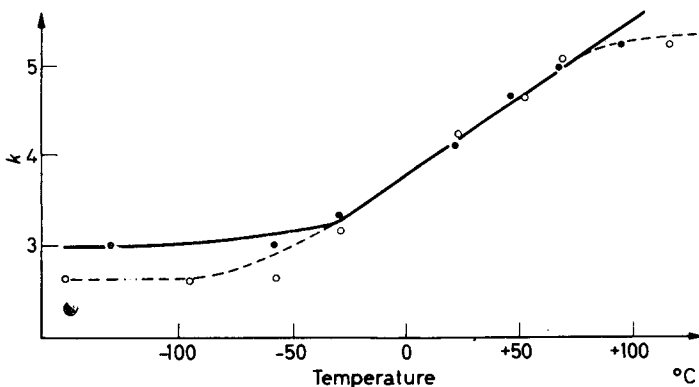


Figure 48— K^+ from the factor $\exp(-K+s^2)$ with $s=2/\lambda$ plotted as a function of temperature: ● branched, and ○ linear polyethylene (*Kolloidzshr. u. Z. f. Polym.* 1962, **183**, 1)

peratures only. You can estimate the respective paracrystalline fluctuations as four per cent for unbranched, and six per cent for branched polyethylene. Using one of your formulae and the number of undisturbed interferences you find six per cent and eight per cent as estimates. That is very fair agreement.

Professor R. Hosemann (Germany): According to Table 2 the thermal and paracrystalline distortions in polyethylene can be analysed even at room temperature. Using the high precision camera mentioned above, we obtained g values (defined by equation 15) between two and eight per cent. This seems to agree well with your results.

REFERENCES

- ¹ VON LAUE, M., FRIEDRICH, F. and KLIPPING, P. (1912). *S. B. bayer. Akad. Wiss. Math. Phys. Kl.* 303 and 363
- ² HOSEMAN, R. *Z. Phys.* 1950, **128**, 1 and 465
- ³ GUINIER, A. *Thesis*. 1939, Ser. A, No. 1854 and 2721 (Paris)
- ⁴ HOSEMAN, R. *Kolloidzshr.* 1950, **117**, 13 and **119**, 129
- ⁵ DEBYE, P. *Phys. Z.* 1930, **31**, 348

- ⁶ ZERNIKE, F. and PRINS, I. A. *Z. Phys.* 1927, **41**, 184
- ⁷ HOSEMANN, R. and BAGCHI, S. N. *Direct Analysis of Diffraction by Matter*. North-Holland: Amsterdam, 1962
- ⁸ EWALD, P. P. *Proc. phys. Soc., Lond.* 1940, **52**, 167
- ⁹ HERMANS, J. J. *Rec. Trav. chim. Pays-Bas*, 1944, **63**, 5
- ¹⁰ HOSEMANN, R. and BAGCHI, S. N. *Acta cryst., Camb.* 1952, **5**, 749
- ¹¹ HOSEMANN, R. and VOIGTLAENDER-TETZNER, G. *Z. Elektrochem.* 1959, **63**, 902
- ¹² RULAND, W. *Acta cryst., Camb.* 1961, **14**, 1180
- ¹³ HERMANS, P. H. and WEIDINGER, A. *J. Polym. Sci.* 1949, **4**, 135
- ¹⁴ HOSEMANN, R., SCHOKNECHT, G. and KAST, W. *Forschgs. Ber. 173*, Westdeutscher Verlag Köln-Opladen, 1956
- ¹⁵ BONART, R. *Z. Kristallogr.* 1957, **109**, 296 and 309
- ¹⁶ BEAR, R. S. and RUGO, H. J. *Ann. N.Y. Acad. Sci.* 1951, **53**, 627
- ¹⁷ HESS, K. and KIESSIG, H. *Naturwissenschaften*, 1943, **31**, 171
- ¹⁸ MEYER, K. H. and MARK, H. *Die Hochpolymeren Verbindungen*. Akademische Verlags-Gesellschaft: Leipzig, 1940
- ¹⁹ LINDENMEYER, P. H., HOLLAND, V. F., MITCHELL, S. B. and HUNTER, W. L. (1962). *J. Polym. Sci.* In press
- ²⁰ STEFANI, R., CHEVERETON, M., GARNIER, M. and EYRAUD, C. *C. R. Acad. Sci., Paris*, 1960, 2174
- ²¹ JOERCHERL, D. *Z. Naturf.* 1957, **125a**, 123 and 200
- ²² BONART, R. and HOSEMANN, R. *Makromol. Chem.* 1960, **34**, 105
- ²³ MANDELKERN, L., POSNER, A. S., DIORIO, A. F. and ROBERTS, P. E. *J. appl. Phys.* 1961, **32**, 1509
- ²⁴ GUINIER, A. and BELBÉOCH, B. *Makromol. Chem.* 1960, **31**, 1
- ²⁵ HENDUS, H. *Kolloidzshr.* 1959, **165**, 32
- ²⁶ KELLER, A. *Phil. Mag.* 1957, **2**, 1171
- ²⁷ FISCHER, E. W. *Z. Naturf.* 1957, **12a**, 753
- ²⁸ HYNDMAN, D. and ORIGLIO, G. F. *J. Polym. Sci.* 1959, **39**, 557
- ²⁹ STATTON, W. O. and GEIL, P. H. *J. appl. Polym. Sci.* 1960, **4**, 357

General

- BONART, R. and HOSEMANN, R. (1962). *Kolloidzshr.* In press
LINDENMEYER, P. H. (1961). *Report of Chemstrand Research Center, Durham, N.C.*

Polymer Single Crystals

A. KELLER

A brief survey is presented on polymer single crystals including some still unpublished material. After a short historical retrospect the basic facts on single crystals and chain folding, a new structural concept derived therefrom, are outlined. Subsequently problems concerning the structure of folds and the origin of chain folding are discussed, the latter point leading to various theories on chain folding. Structural consequences of chain folding such as sectorization and non-planar habits, which lead to the problem of fold packing, are next surveyed for the simplest monolayer crystals, followed by a brief description of observations on more complex multilayer crystals and on some new features of crystallization from concentrated solutions. Finally there is a short reference to the possibility of single crystals and chain folding occurring in the melt crystallized bulk, including oriented systems.

HISTORICAL RETROSPECT

THE FACT that chainlike—but not yet polymeric—molecules can crystallize in the form of macroscopic crystals has been common knowledge since long before the birth of modern polymer science. It is a common feature of all such long molecules that they consist of a number of consecutive identical units like a string of beads. The simplest of these are the paraffinoid substances with CH_2 groups as sub-units. The units terminating the molecules must necessarily differ from those in the interior. Such long molecules crystallize by the chains stacking in a parallel fashion which mostly results in platelike habits. The three-dimensionally periodic arrangement of the molecules within such crystals defines the lattice. The unit cell comprises at least one full molecule and because of the elongated nature of this building unit, is strongly anisodimensional. The longest dimension is equal or simply related to the length of the molecule, the other principal axes to the closest intermolecular distances. We denote this repeat unit as the true unit cell in contrast to a smaller three dimensional periodicity, the subcell, within the true unit cell itself (*Figure 1*). The existence of a subcell is the direct consequence of the beaded string nature of the molecule. In the crystal the 'beads' within one molecule are in a unique relation with respect to those in its neighbours, thus defining a three-dimensional repeat unit the exactly repeating sequence of which is confined to within the terminal groups of the molecules containing them. A complete crystal structure determination naturally requires the elucidation of the full content of the true unit cell. Nevertheless the subcell contains already a significant part of this information as the sub-units constitute a predominantly large portion of the molecule, and this will be increasingly so the larger the molecules. The existence of a subcell is immediately apparent from the diffraction patterns by the enhanced intensity of many of the reflections associated with it.

This paper was presented at a Polymer Science Conference, held in conjunction with the Second World Congress of Man-made Fibres, at the Connaught Rooms, Holborn, London W.C.2, 2nd and 3rd May 1962.

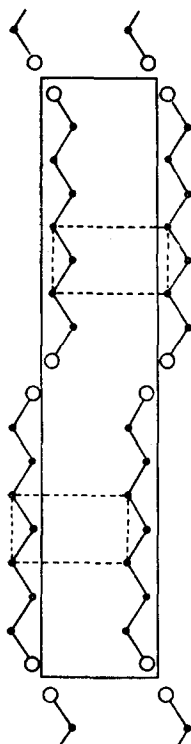


Figure 1—Diagrammatic illustration of the relation between the true unit cell and subcell. The drawing is a simplified two-dimensional representation of the arrangement of short paraffin chains in a crystal of vertical structure (see Keller³⁸). The small solid circles are CH₂ units, the large open circles are the terminal CH₃ groups. The large rectangle drawn with solid lines represents the true unit cell—which here contains two molecules—and the small dashed rectangles are subcells

Nevertheless there is a group of reflections, other than those from the subcell, which is expected to remain strong. These are reflections which correspond to the true cell periodicity along the chain direction. In oligomeric substances (paraffinoids, etc.) these are directly related to, and are thus measures of, the molecular lengths. For long molecules these periodicities will be large hence the corresponding reflections will be at small angles, requiring special low angle X-ray techniques for their detection.

In the pioneering days of polymer crystallography, crystallographers took the obvious route by examining molecules of increasing length—polyoxymethylenes in particular—synthesized at that time in Staudinger's laboratory. They found that while with increasing chain length the subcell reflections remained prominent, those due to the true spacings could not be directly recorded with the technical facilities of those days; their non-existence was inferred from the absence of the high orders accessible then. Existence of high orders presupposes high degree of regularity, which was taken for granted in a crystal at the time when imperfect lattices were not so prominent as they are today. On this basis the subcell was recognized as the true and only periodicity relevant to a polymer lattice. Next came the estimate of the size of the crystalline regions, based mainly on X-ray line broadening measurements with all its inherent pitfalls, from which it was concluded that the crystals were much shorter than the length of the molecule. This was followed by the necessity of considering also disordered amorphous regions on the basis of physical properties. These factors added together led to the familiar fringed micelle concept, which till recently has dominated our views on polymer crystals.

This development did not take place quite unopposed. In a paper¹ dated as early as 1930 and since practically forgotten it was deduced from high order reflections which (exceptionally as it appears) were present in the polyoxymethylene specimens in question that the true cell periodicities must have been larger than the one associated with the lattice based on the subcell, being in the range of 60 to 120Å. Ott attributed these spacings to the

long dimensions of the fully extended molecule. However, the molecules were believed to be of non-uniform length and in any case much longer than Ott's spacings from other evidence. As these large periodicities, manifesting themselves by their high orders, were not found again, this awkward point was bypassed at the time. Reports on large periodicities reappeared in the literature much later on with the advent of low angle X-ray techniques, and have since been recognized as typical of crystalline polymers. However, these have not been considered again in relation to the original problem but as something outside the scope of structural polymer crystallography proper. Structural crystallography was concerned exclusively with what we here term subcell structure. Admittedly the subcell structure accounts for nearly all the atoms in the structure and consequently is of prime importance. But as it turns out the minute amount of structural information which has remained beyond the scope of the classical approach holds the key to the understanding of ordering processes in polymers as opposed to those of non-polymeric chain molecules—a differentiation which is not apparent from the crystal structure studies proper. It is about these developments that I shall be concerned here. The new developments naturally do not displace the well established discipline of polymer crystallography as hitherto practised but widen its scope into a subject much more varied and comprehensive than it has been before.

THE BASIC FACTS ON SINGLE CRYSTALS AND CHAIN FOLDING

Paradoxically the new developments leading to the recognition of the unique mode of crystallization of polymeric chains commenced by the recognition of close similarities between the appearance of crystallization products in polymers and non-polymeric substances. It is to be remembered that on account of the fringed micelle model a crystalline polymer was expected to be quite featureless. The mere fact that discernible organizations became observable at all by microscopic techniques in itself represented a breach in the prevailing picture of randomly arranged unrelated micelles. On closer inspection these organizations were found to be quite unexpectedly distinct and regular. Morphologically they all had their counterparts amongst simple substances and there seemed to be no need to postulate any specific polymeric feature to account for their existence. Spherulites and their building units, sheaves and fibrils fall in this category (see reviews^{2,3}, which contain detailed references). This trend eventually culminated in the recognition of polymer single crystals. If we look back far enough we may see that this discovery should not have been such a surprise as it was. Crystals of polymerized formaldehyde were in fact seen as early as 1907⁴ and later again in 1929⁵ (see also Sauter⁶). However, no further attention was given to them during the period which followed characterized by the unconditional acceptance of the fringed micelle model which excluded the possibility of single crystals by implication. Single crystals were rediscovered again after stereoregular polymers with improved crystallization characteristics became available.

Unambiguously defined single crystals have been observed so far in

crystallization products from dilute solutions. (For references before 1959 see reviews ^{2,3}; some of the later ones will be quoted separately. When reference not quoted see above reviews.) There is a gradual accumulation of evidence, however, that morphologies reminiscent of single crystals also occur in the more concentrated systems and even in the bulk melt crystallized polymer. About these more will be said later. At first I shall deal with the simplest products obtained from dilute solution. The first systematic observations were made on linear polyethylene (*Figure 2*) but as research

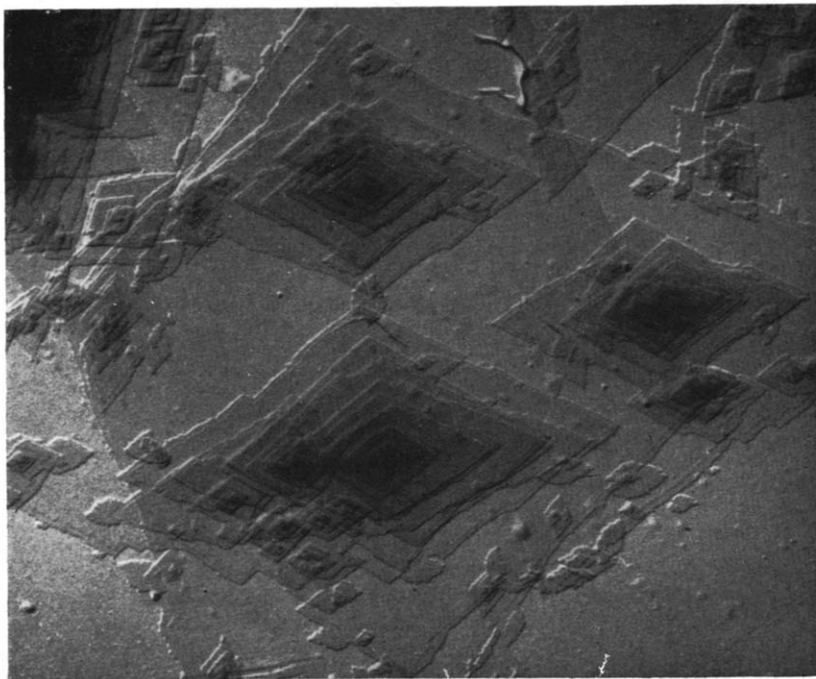


Figure 2—Typical solution-grown single crystal of polyethylene. Electron micrograph. Magnification $\times 12000$; reproduced without reduction (Keller²)

progressed single crystals were being detected in a number of other substances. Such are: polyoxymethylene (Geil⁷), polyoxyethylene (Keller, unpublished), polypropylene (Rånby, Morehead and Walter⁸), poly-4-methyl-pentene-1 (Keller, see ref. 3), polystyrene (Kargin *et al.*⁹), nylon 6 (Geil⁷), nylon 7, nylon 8, nylon 66 (all three in Holland^{8a}), polyacrylic acid (Miller *et al.*¹⁰), cellulose [Manley¹¹ (*Figure 3*), Rånby and Noe¹²], and this list is by no means complete. Thus the generality of the single crystal is beyond any reasonable doubt.

The standard method of producing crystals is to allow them to form in a supercooled solution when they appear in the form of a suspension which can be sedimented and examined by electron or optical microscopy. The basic properties of single crystals (as seen from *Figure 2*) are as follows. They consist of lamellae of uniform thickness in the range of 100 Å. The

crystals thicken via the screw dislocation growth mechanism which leads to a spiral terraced structure. In some instances the morphology is more of a flat ribbon or fibril character. It is, however, not clear whether these are distinct morphological forms or only degenerate or split versions of the basic lamellar morphology.

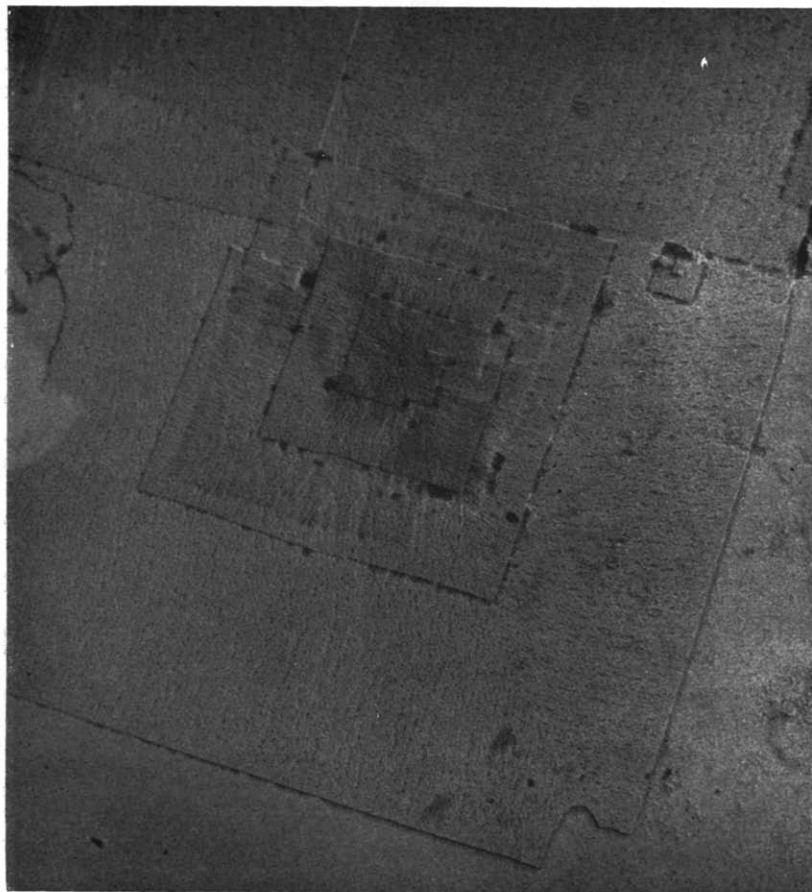


Figure 3—Single crystal of cellulose (Manley, private communication). Electron micrograph. Magnification $\times 20000$; reduced $\times 3/4$ on reproduction

Electron microscopy provides a means of assessing the molecular orientation within such crystals by diffraction patterns taken of individual crystals selected on the viewing screen. The diffraction pattern consists of spots arranged as expected from a single crystal (polyethylene in *Figure 4*). The sharpness of the spots is comparable with that of other simpler crystalline substances. Polymers, however, are affected by the electron beam which rapidly destroys the crystalline order usually by generating cross links. This beam sensitivity necessitates special precautions when diffraction effects are

to be recorded, but even so sets a limit to the exploitation of the full potentialities of electron optical techniques. Diffraction patterns like the one in *Figure 4* revealed that the long chains lie mainly along the shortest crystal direction, i.e. in lamellar habit they are normal or approximately so to the plane of the lamellae and in fibrillar development nearly perpendicular to the fibril axis. As the molecules are hundreds, thousands or even tens of thousands of Ångströms long it follows that they cannot be contained within a distance of 100 Å or so and stay straight. The only sensible alternative is to have the molecules fold back on themselves. This folding must be sharp so that the segments can return to their closest packing after having folded over. It is noteworthy that this suggestion had already been made as early as 1938 (Storks¹³) but then it passed unheeded. Accordingly the thickness of the layers (we shall restrict ourselves to the lamellar development in what follows) is equal or closely related to the fold length, which can be evaluated by direct measurements in shadowed electron micrographs. Another more accurate method of assessing the layer thickness



Figure 4—Electron diffraction pattern given by a polyethylene single crystal (Keller²)

and hence the fold length is by X-rays, as the regular sequence of the layers gives rise to diffraction effects in a number of orders. This latter fact substantiates the impression gained from the electron micrographs that the layers and hence the folds possess a high degree of uniformity.

It is worth reflecting that the tabular polymer crystals are closely analogous in appearance to crystals of long chain but non-polymeric substances. Thus the polyethylene single crystal in *Figure 2* is indistinguishable in appearance from that of a paraffin with a chain length corresponding to the fold period. The same applies to the diffraction pattern. The sublattice reflections are identical in both and the large spacings referred to are the exact counterparts of the reflections from the basal planes in paraffins where these define the long dimension of the true unit cell. Accordingly these large spacings in polyethylene also define the true unit cell, which, however, is not related to the length of the molecule as in paraffins but to that of the fold. In this way a previously unexpected continuity between

oligomers and polymers is becoming apparent—a point to which I shall return later.

The fold length in chain folded polymer crystals is not an invariant quantity, but is temperature dependent. We distinguish two types of temperature effect: (1) Temperature of crystallization, (2) Temperature to which the crystal already formed has been heated.

(1) In a given system the increase of crystallization temperature results in longer folds. A typical range of values for the best explored system namely polyethylene in xylene is 90 to 155 Å for crystallization temperatures between 50° and 90°C. This effect is strictly reproducible, and values from different laboratories agree closely. The fold length is a unique function of crystallization temperature and does not depend on the fold length in crystals already present. Thus a temperature change during crystallization produces a corresponding change in the growing crystal resulting in an upward or downward step in the layer thickness for a temperature increase or decrease respectively (Keller and Bassett¹⁴, Bassett and Keller¹⁵). These effects under (1) represent the most solidly established quantitative information we possess about chain folding.

(2) When crystals already formed are heated beyond the original crystallization temperature the layer thickness and the corresponding X-ray spacing increases while the overall molecular orientation may remain unchanged (Statton and Geil¹⁶, Statton¹⁷, Hirai *et al.*¹⁸). It is concluded that, astonishing as it may appear, the chains refold to a larger fold length. This increase of the fold length is at first rapid, in fact a large part of the change can take place within seconds, but continues apparently without limit with an ever decreasing rate. In a crystal with an initial fold length of about 100 Å the folds can increase up to at least 400 Å. The exact values depend on the initial fold length of the material (Baltá, Bassett and Keller, unpublished), and also on experimental circumstances such as rate of heating, the support or medium on or within which the material is kept (Statton¹⁷). There is evidence that at least part of these changes occur via an intermediate stage of melting (Fischer¹⁹, Fischer and Schmidt²⁰, and private communication).

We shall return to the structural implications of chain folding later. In this section only one further point will be made, required by the discussion which follows immediately: namely that folding is visualized to occur along the growing prism faces of the crystal.

THE STRUCTURE OF THE FOLD AND THE ORIGIN OF CHAIN FOLDING

When examining the chain folding hypothesis more closely, the first question to be raised is whether folding of the chains with the required abruptness is possible or not. Again the answer to this is readily available in the early literature: it was found in 1933 (Müller²¹) that large cyclic paraffin molecules pack in the same way as linear ones, which implies that the large rings must exist in a collapsed form in the crystal which in turn requires bending as sharp as postulated for chain folded polyethylene. Accordingly such sharp folds do exist, and experiments with models show that they can arise with unexpected facility. In principle, the structure of cyclic compounds should

reveal the exact fold configuration. In reality, however, these can have several subcell structures (Burbank and Keller; Newman, both unpublished), and the one directly relevant to the polyethylene problem has not yet been identified.

The possibility of a direct determination of the fold structure being still remote a *priori* geometric arguments need to be resorted to. For this purpose one may consider the diamond lattice (Frank, unpublished), which is a covalently bonded network of C atoms. Any non-closing sequence of C atoms in the diamond lattice corresponds to a possible chain configuration (subject to the restrictions imposed by the H atoms in the polyethylene chain). In this way proceeding from one C atom to the next the possible fold configurations can be mapped. Due allowance being made for the distortions required when going from the diamond to the polyethylene lattice (essentially due to the presence of hydrogens in the latter) the energetically most favoured fold configurations can be selected (Figure 5). It is found that the

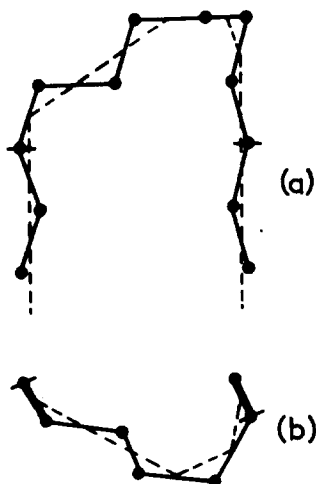


Figure 5—One of the simplest folded carbon-carbon paths in the diamond lattice as seen (a) normal to the plane of folding, (b) along the straight segment direction. In the actual polyethylene lattice a slight adjustment of the intersegment distance ($+0.24\text{\AA}$) and a considerable ($+50^\circ$ and -32°) twist of the stems is required to make this path correspond to a fold along (110). When considering also these adjustments the fold configuration illustrated here, containing four gauche bonds, emerges as the energetically most favourable one. In terms of surface free energy this would require a value of 100 to 150 erg cm^{-2} . (Frank, unpublished)

most likely candidate is asymmetrical both with respect to the planes parallel and perpendicular to the plane of folding, even in its undistorted configuration in the diamond lattice, a point to which I shall return later.

Accepting the geometric possibility of folding, obviously the question arises why should it occur in a crystallizing macromolecule. This enquiry has led to theories which will be outlined here only in the briefest possible way. Any theory would have to account for at least the reasons of a folded configuration, for the observed uniformity of the fold length and for its observed temperature dependence. There are two classes of theories: kinetic and equilibrium.

According to the kinetic theories (Lauritzen and Hoffman²², Price^{23,24}, Frank and Tosi²⁵) the thermodynamically most stable configuration would be the crystal consisting of completely extended chains, nevertheless in the actual structure the chains will have a folded configuration with a narrow

distribution of fold length because such will be favoured by the rate with which crystallization in the particular configuration in question can take place. In general any crystallization occurs via primary nucleation followed by growth. In polymers primary nucleation could take place intramolecularly by folding up of the same molecule. It can be shown that this would occur with a narrow distribution of fold lengths (Lauritzen and Hoffman²²). Further growth then could occur with the molecules folding up along the existing crystal faces. It is this latter growth process which really determines the fold height in the crystals formed (Price²³, Lauritzen and Hoffman²²). The experimental findings quoted above imply that the fold length is determined by the circumstances under which the deposition of the molecule occurs and is not observably influenced by the fold lengths already present at the crystal face where the new molecule deposits. It was not *a priori* obvious that a kinetic approach can account for this fact until it was recast in a form which now meets all the principal requirements (Frank and Tosi²⁵).

According to the equilibrium approach (Peterlin and Fischer²⁶) the state of maximum stability (lowest free energy) in a polymer crystal corresponds to a finite extension of the lattice along the chain direction, and this is the state towards which the system will tend in the actual crystal. This new stability criterion should be the consequence of the anisotropy of the force constants in a macromolecular lattice. Chain folding would be one way in which this criterion could be satisfied.

Both classes of theory should be amenable to quantitative experimental verification. The best test for this is the variation of the fold length with crystallization temperature which is best established in the dilute polyethylene-xylene system. Both classes account for the observed sign of this temperature dependence. For obtaining actual values certain parameters in the system need to be numerically defined. Thus both classes of theory require values for the surface free energies of the chain folded crystal. Information on the surface free energies of the side surfaces is available from independent evidence (Turnbull and Cormia²⁷) and those of the fold surfaces can be estimated *a priori* within broad limits (in the order of 70 to 150 erg/cm²). Both types of theory arrive at the correct magnitude of the fold height—with reasonable values for these parameters, although the kinetic theory only (Frank and Tosi²⁵) attempts to match the experimental fold height—temperature of crystallization curve which it does to a good approximation.

According to latest information values as low as 50 erg/cm² and less are being claimed for the fold surface free energies both on the basis of equilibrium (Peterlin, Fischer and Reinhold²⁸, 40 to 50Å) and on kinetic (Hoffman and Weeks, private communication) considerations. It takes a minimum of three gauche bonds to fold a chain back on itself, which on the basis of values for short hydrocarbons requires 45 erg/cm², which does not include distortions necessary to rotate the chain segments in their positions in the polyethylene lattice and the increase in free energy due to the defective packing of the methylene groups in the folds as compared with those in the straight segments. Including these the fold surface energies would come near 100 erg/cm² at the lowest estimate (Frank unpublished, see Figure 5). Accordingly 50 erg/cm² or even less would be too small.

As in the kinetic theories the fold length depends on the supercooling while in the equilibrium theory it is some function of the actual temperature, it might appear to be a simple matter to decide between them. However, the

true melting point of a crystal with an infinite fold length in the solvent (required for definition of supercooling) is uncertain to such an extent that it makes this test inapplicable at least in a straightforward manner. Nevertheless latest crystallization studies under pressure (Wunderlich, private communication) extended the hitherto realizable range of crystallization temperatures permitting a distinction to be made in favour of the kinetic approach, but whether to the complete exclusion of the equilibrium theory is not a straightforward matter to decide.

However, in addition to the fold height/crystallization temperature relationship in polyethylene crystallized from dilute solution, other phenomena are also being considered in arguments concerning the validity of the opposing theories. These refer to systems which are not yet defined with precision structurally, neither are they treated with any rigour theoretically. Nevertheless it may be justified to invoke them in search of qualitative criteria by which to distinguish between the theories in question. Such phenomena include the effect of annealing on the long spacings of both single crystals and the bulk. Both classes of theories are at least consistent about the increase of the fold length with temperature when the crystals already formed are heated subsequently. In the equilibrium case, however, this effect should be reversible: contraction of the fold is expected on cooling. Such reversibility has not been observed up to date; some claims to the contrary could not be substantiated. This in itself, however, does not settle the issue as according to the equilibrium approach the drive towards shorter fold lengths (or in general crystal thickness) should be smaller than in the reverse direction, hence the fact that such an effect is absent can at least be excused.

On the other hand there is one class of effects which, if confirmed, seems to lie beyond the scope of the kinetic approach. The morphological continuity between crystals of paraffins and polyethylene has already been mentioned. According to available indications it appears that oligomeric compounds might suddenly bend back on themselves beyond a certain length when forming a crystal. Experiments on polyethylene fractions (Keller and O'Connor²⁹) and more recently on oligomeric series of polyamides synthesized under controlled conditions (Zahn and Pieper³⁰, Kern *et al.*³¹) are strongly indicative of this kind of behaviour. It is found namely that the long spacings increase with the molecular length only up to the point where they are in the range of those of the corresponding polymer, remaining constant thereafter, responding to heat, recrystallization and swelling treatment roughly in the same way as the polymer does (for these latter aspects, Zahn and Pieper³⁰).

In all the work mentioned in this section the long spacings are being identified with the fold length or (in the short oligomer case) with the length of the molecule. However, the numerical identity of these lengths and the spacings measured directly cannot be guaranteed *a priori* without the knowledge of the molecular orientation with respect to the planes giving rise to the long spacings. Evidently great circumspection is needed when the exactness of the identification is of consequence. For example in some cases the spacings can decrease which, however, was found to be the consequence

of molecular re-arrangement (increase amount and/or regularity of stagger—see next section) at constant fold length (Baltá, Bassett and Keller, in preparation). In the oligomer work in particular the final confirmation of the key point mentioned above is still pending an account of some ambiguities along these lines (Baltá and Keller, unpublished).

The present situation as regards the theories perhaps could be summed up as follows. It is possible that there is a thermodynamic criterion for folded polymer crystallization, and if this is so it is certainly of great significance in itself. Nevertheless, equilibrium considerations do not usually govern crystal growth, and in polymers just as in general, kinetic factors are expected to influence the way crystals develop.

STRUCTURAL CONSEQUENCES OF CHAIN FOLDING IN SINGLE CRYSTALS

As already stated the chains are visualized as folding up along the growing prism faces of the crystals. Thus the folding direction will be different along the different crystal faces, and this difference will persist after the growth front has passed. Consequently the crystal will consist of structurally distinct sectors each based on a crystal face; there will be as many sectors as there are prism faces. Thus the unprecedented situation arises that different structures will be contained within the boundaries of what appears to be a single crystal. Different fold plane directions define different unit cells, i.e. structures. The packing of the straight segments in the interior of the lamellae, defined by the subcell, remains essentially unaffected by the fold plane direction (although by symmetry requirements some differences are in

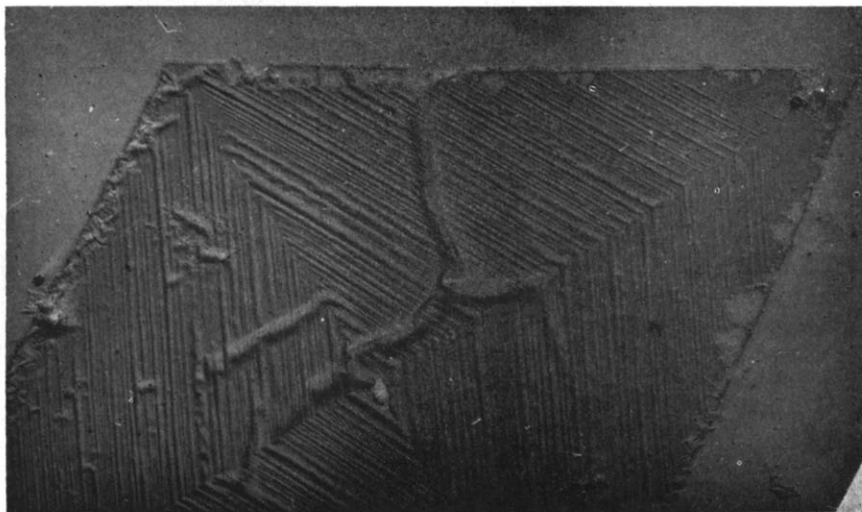


Figure 6—Electron micrograph revealing the existence of distinct sectors in a lozenge-shaped polyethylene crystal through morphological features (corrugations). Magnification $\times 2500$; reduced $\times 3/4$ on reproduction. (Bassett, Frank and Keller, in preparation)

principle to be expected and in fact some subtle differences in the diffraction patterns are found experimentally, Bassett, Frank and Keller³²; Keller, unpublished).

The existence of distinct sectors (or fold domains as termed in some recent literature, Reneker and Geil³³; Burbank³⁴) can make itself apparent in the morphology (e.g. Bassett, Frank and Keller³⁵; Keller and Bassett¹⁴). *Figures 6 and 7* are examples of monolayer crystals of polyethylene where the sectorization in the expected manner is apparent. The effects showing up

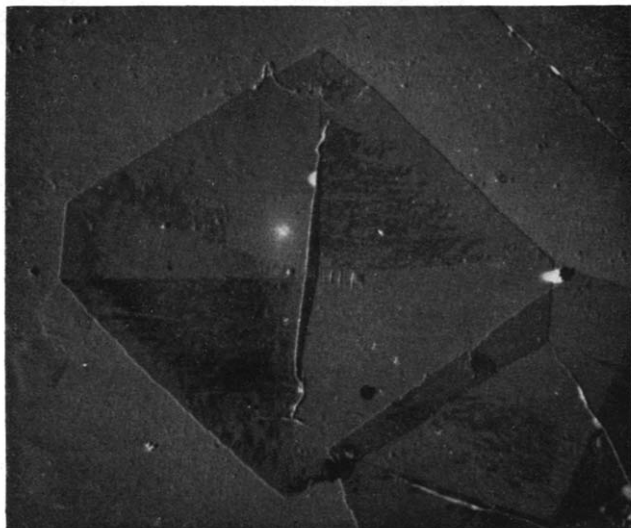


Figure 7—Electron micrograph revealing the existence of distinct sectors in a truncated lozenge-shaped polyethylene crystal through diffraction effects (Bragg extinction). Magnification $\times 4100$; reproduced without reduction (Bassett and Keller³⁶)

the distinctness of sectors are morphological features, like corrugations, changing direction along the sector boundaries (*Figure 6*) or diffraction effects arising from the fact that the different sectors may satisfy different diffraction conditions with respect to the direction of the electron beam in the microscope (*Figure 7*). In addition, different sectors may have different physical properties, e.g. may melt at lower temperatures as shown in *Figure 8* which represents a crystal in the melting region.

In general, the crystal lamellae are not planar, although they mostly become so on drying down, which is a necessary requirement for electron microscopy. The original non-planarity, however, makes itself apparent in various ways in flattened crystals. The central crease in *Figure 7* is one example. It is not possible to list all relevant observations at this place and in what follows I shall quote only the essentials of the final model as it stands today (Bassett and Keller³⁶, and to be published; earlier propositions leading up to it: Reneker and Geil³³; Niegisch and Swan³⁷). The simplest

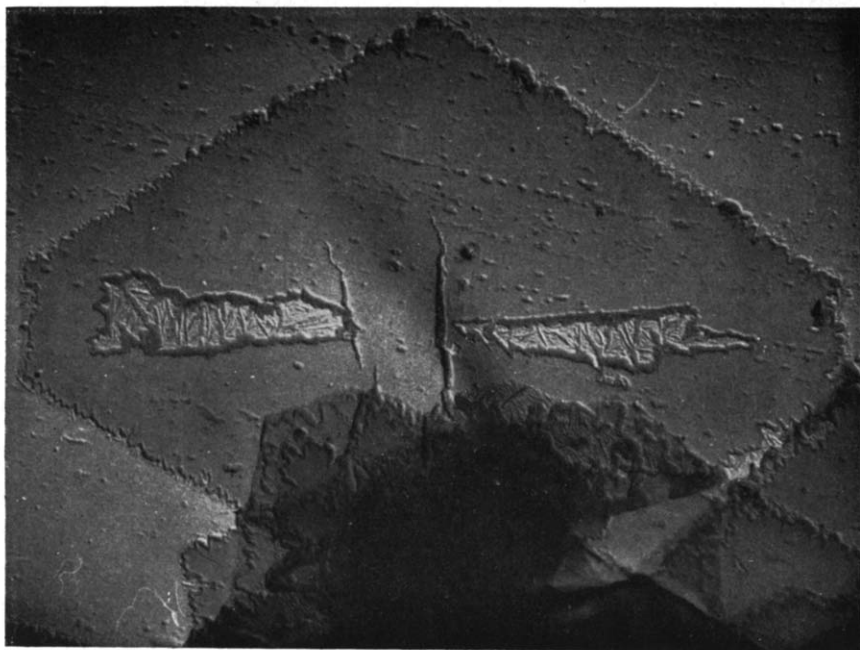


Figure 8—Electron micrograph of a polyethylene crystal near its melting point. The sectors bounded by the truncating faces melt before the rest of the crystal. Magnification $\times 6000$; reproduced without reduction. (Keller and Bassett¹⁴)

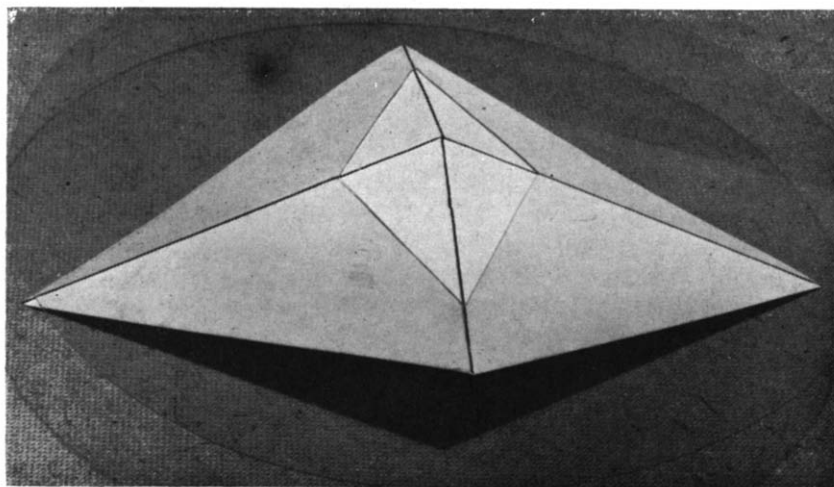


Figure 9—Model of a non flat-based hollow pyramid. This is the true three-dimensional configuration of some of the simplest monolayer polyethylene crystals. The transparent disc illustrates the relation of the pyramid to a flat base (plane perpendicular to the pyramid axis)

monolayer polyethylene crystal is a hollow, dished pyramid. The crystal sectors form the pyramid facets. The straight segment direction is assumed to be parallel to the pyramid axis. The pyramids are non flat based, i.e. pairs of basal planes lie at different heights as measured along the pyramid axis. A model for the simplest crystal shape in polyethylene (lozenge shape with $\{110\}$ prism faces only) is shown in *Figure 9*. More complicated habits show analogous but appropriately modified features. The transparent disc illustrates the intersection of a flat base with the pyramid. These intersections are crystallographic directions and define the geometry of the pyramid. Such directions can become structurally distinct (see *Figure 6*) either in the course of collapse on a substrate or during growth, and it is essentially from these that the present model has been derived.

The facets of the pyramids are clearly oblique to the directions of the straight segments. They are rational planes in the subcell, consequently can be defined by the subcell indices: (hkl) , where the subscripts refer to the subcell. Two of the indices (hk) , are defined by the direction of the line of intersection with the flat base, determining the direction of the steepest dip. The third index l , defines the magnitude of the dip. This latter cannot be determined directly from the electron microscope images but can be inferred from the change in diffraction conditions which arise when the pyramid facets lie down flat on the substrate in the course of specimen preparation in crystals which collapse via such a mechanism. Such diffraction information can be obtained both from aggregates of collapsed crystals by X-rays, and from individual crystals and sectors thereof by means of rotating stage experiments under the electron microscope. In addition under favourable circumstances direct measurements of these angles in uncollapsed pyramids by light optical methods has just become possible in certain favourable circumstances (see below; Bassett, Frank and Keller, to be published).



Figure 10—Dark field optical micrograph of a monolayer polyethylene crystal while floating in suspension. The pyramidal nature of the crystal is revealed. Magnification $\times 800$; reproduced without reduction. (Bassett, Frank and Keller, in preparation)

Until recently all information as regards three-dimensional shape of the crystals was inferred from crystals collapsed in some way on a substrate. The true three-dimensional character of the crystals became directly apparent only when examined while floating in the liquid, which is only

possible in the light microscope under specially favourable conditions. Photographs as *Figure 10* directly confirm the pyramidal habit while ones like *Figure 11* reveal that they can also grow in a corrugated or half-corrugated half pyramidal form (Bassett, Frank and Keller, in preparation). These corrugated crystals are really variants of the pyramidal model where the direction of slope of the oblique facets alternates instead of being uniform within a sector, the essential point being the particular obliquity rather than the uniformity of the pyramid.

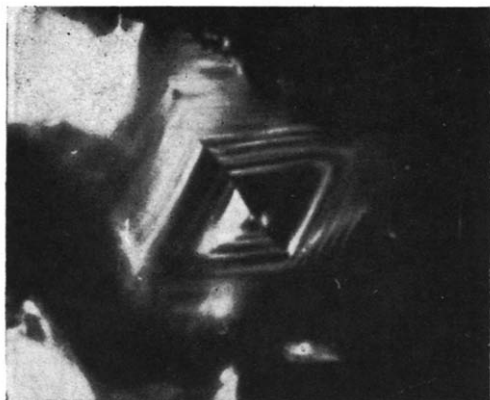


Figure 11—Dark field optical micrograph of a monolayer polyethylene crystal while floating in suspension. This crystal is pyramidal in the centre, but corrugated outside. Magnification $\times 800$; reproduced without reduction. (Bassett, Frank and Keller, in preparation)

The obliquity of the facets is directly related to the crystal structure; and what follows will be an illustration how the study of structure in the sense of conventional structural crystallography and that of morphology merges in these investigations. The model in *Figure 9* with the postulate that the ribbons of molecules are parallel to the prism faces in each sector, with the straight segments along the pyramid axis, requires that the folds should be staggered within the ribbon [*Figure 12(a)*] and that consecutive ribbons should stack in a staggered fashion [*Figure 12(b)*]. These staggerings must allow the atoms in adjacent straight segments to remain in register as required by the crystal structure, which means that the subcell is to be preserved. All the various observed or inferred oblique facets can be accounted for by a suitable adjustment of the obliquity of the ribbons and the staggering between them while still preserving the subcell, the displacement of adjacent folds being either equal to the carbon-carbon repeat or to a small multiple of it.

The quantitative assessment on polyethylene crystals reveals that the $(hk)_s$ indices of the oblique facets are either $(31)_s$ or occasionally some other direction close to $(31)_s$. Thus the direction of steepest dip is either identical or at any rate is within a narrow range in all the pyramids. The l_s index, however, can vary largely. So far the distinct cases of $l_s = 2$ and 4 have been identified which represent widely differing inclinations of the pyramid facets. In terms of staggering the near constancy of $(hk)_s$ and variability of l_s means that there is a relation between staggering within and between ribbons, the ratio of the two being approximately a constant (Bassett, Frank and Keller, in preparation).

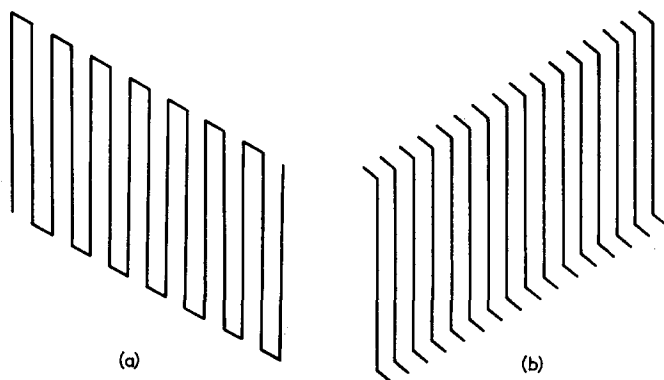


Figure 12—Sketch illustrating the principles of fold staggering leading to pyramidal and corrugated crystals. (a) A ribbon of a folded molecule seen normal to the ribbon plane. (b) Stacking of consecutive ribbons, seen along the ribbons. The folds are drawn asymmetric both with respect to the plane perpendicular to the ribbon (a) and with respect to the plane of the ribbons (b)

The type of staggering required by the polyethylene crystals implies that the folds are likely to be asymmetrical both with respect to the ribbon plane and to the plane perpendicular to the ribbon, the diagrams in *Figures 12(a)* and (b) having been drawn accordingly. Such asymmetries are implied in principle through the reduction of lattice symmetry when the folds are introduced along one diagonal ($\langle 110 \rangle$) of an originally orthorhombic cell, but as mentioned earlier they have in fact emerged in concrete structural terms from the examination of the possible fold configurations via the diamond lattice (Frank, unpublished) (*Figure 5*). In order to account for the observed staggerings quantitatively an exact knowledge of the fold structure would be needed, and further subtleties would have to be invoked which I cannot touch upon in this brief review.

These staggered structures have their counterparts amongst paraffins, where they can manifest themselves in analogous oblique facets, however, without sectorization (Keller³⁸). In paraffinoid substances it is the packing requirement of the terminal group which leads to staggering, while in polymers the fold plays the same part extending the analogy pursued here still further.

In crystals of simple substances the development of crystal faces does not affect the internal structure, and changes in the habit during growth can arise without leaving their mark in the crystal interior. This is not so in a polymer crystal. Each prism face has its associated sector which is structurally distinct by virtue of the direction of the fold plane. Accordingly crystals with differing prism faces are different structurally, consequently there are as many different structures as there are habits. Further any change of habit during growth implies a change of structure. Thus in contrast to crystals of

simple substances in polymers external habit and internal structure are closely linked. Naturally the sectors forming the crystals have to join. In view of the fact that the basal planes are oblique with respect to the straight segment direction—which is to be kept identical over the whole layer—and that this obliquity is different in the different sectors, there are only certain restricted planes along which smooth joining can occur. Even a slight violation of the exact joining requirement, such as might occur accidentally during growth would lead to only partial joining with parts of the edges remaining exposed. Such exposed edges will be favoured sites for further growth leading to overlapping layers and localized spiral terraces. This will be particularly frequent in crystals with serrated faces. Here each tiny prism face has an associated micro-sector which is the facet of a corresponding micro-pyramid. The whole crystal layer will be puckered in a complex way with a multitude of domain boundaries within, each with its particular joining requirement. The joining problem becomes even more acute when the habit changes during growth, in which case newly formed sectors have to join not only their neighbours in the same phase of growth but also the preceding sector behind the growth front (*Figure 13*). The variety of intriguing problems arising in this way is practically inexhaustible (see Bassett and Keller¹⁵, Geil and Reneker³⁹).

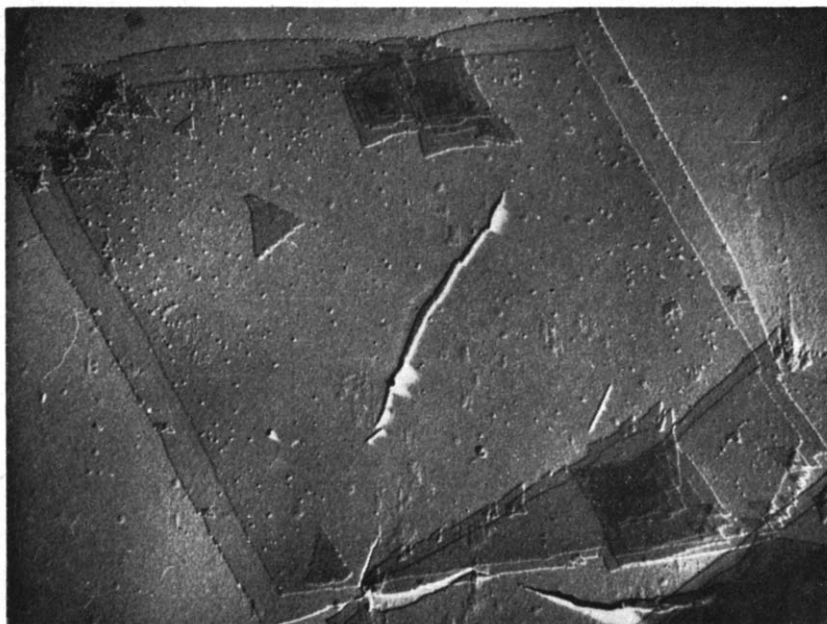


Figure 13—Crystal of polyethylene which has changed its habit during growth. Most of the crystal grew as a truncated lozenge, but owing to a change in growth temperature it continued to grow with faces which define true lozenges only. Complex growth features arise where these latter faces join the truncating faces formed during the earlier stages of growth. Electron micrograph. Magnification $\times 6300$; reproduced without reduction. (Keller and Bassett¹⁴, and Bassett and Keller¹⁵)

So far only the simplest monolayer development has been considered. Much less is known of how consecutive layers develop. Here further problems arise because of the pyramidal nature of the layers. If consecutive layers are concentric the pyramids could fit together not, however, without some inherent difficulties of how to account even for the simplest observed spirals (Bassett, Keller and Mitsuhashi⁴⁰) a point I cannot say more about at this place. In addition consecutive layers are often rotationally displaced



Figure 14—Multilayer polyethylene crystal where consecutive terraces are rotated with respect to each other always by the same amount in the same sense. Electron micrograph, replica, magnification $\times 6000$; reduced $\times 3/4$ on reproduction. (Bassett, Keller and Mitsuhashi, unpublished)

in some cases leading to quite spectacular formations (*Figure 14*) which are still unexplained. When the usual multilayer crystals are viewed sideways while still in the liquid, consecutive layers are often seen to be connected in the centre only, splaying otherwise (*Figure 15*) resembling in this view a radiating or sheafing structure (Mitsuhashi and Keller⁴¹). In other instances, however, concentric consecutive layers may be contiguous. We think the physical reason behind the splaying or contiguous sequence of layers lies in loose molecules which protrude from the lamellae. Accordingly we visualize the layer surfaces as 'hairy' which might either prevent consecutive layers from lying smoothly on each other, or on the contrary might tie them together, according to crystallization conditions. We find that higher crystallization temperature promotes connectedness.

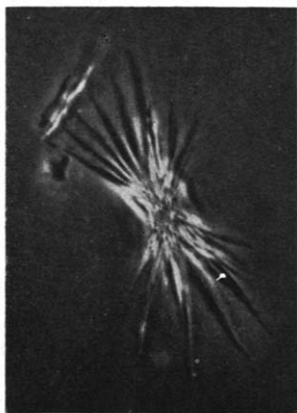


Figure 15—A simple multilayer polyethylene crystal seen edgewise while in suspension. Optical micrograph. Phase contrast illumination. Magnification $\times 410$; reproduced without reduction. (Mitsuhashi and Keller⁴¹)

SINGLE CRYSTAL-LIKE STRUCTURES FROM CONCENTRATED SOLUTION

The discussion has so far referred to crystals from dilute solution. Increase of concentration enhances the multilayer character of the crystals. Lower temperatures of crystallization yield complicated splaying aggregates of monolayers which when viewed from the side even more resemble sheaflike fibrillar aggregates such as were associated with spherulite development in the earlier literature on polymer morphology (*Figure 16*) (Bassett, Keller and Mitsuhashi⁴⁰). The present observations that such sheaves can represent one view of multilayer single crystals is clearly relevant to questions concerning spherulite morphology. This point is even more apparent with crystallization from concentrated solution at higher temperatures (polyethylene from xylene above 75°C beyond about 0.3 per cent) when increasingly more compact objects arise (Bassett, Keller and Mitsuhashi⁴⁰). These can be so deceptively different when viewed from different directions that it is difficult to believe that the images seen belong to the same object. Only a detailed exploration from different viewing directions could give even an approximate idea of what these objects really correspond to. The remarkable point is that the same object can reveal practically all the characteristic aspects usually

associated with spherulite growth yet retain from one range of viewing directions the characteristics of single crystals even if in a thick, compact version (*Figures 19, 20 and 21*). We termed these objects 'axialites' as they appear to consist of a lamellar structure splaying about an axis, which corresponds to one of the crystal diagonals. In this case the splaying units

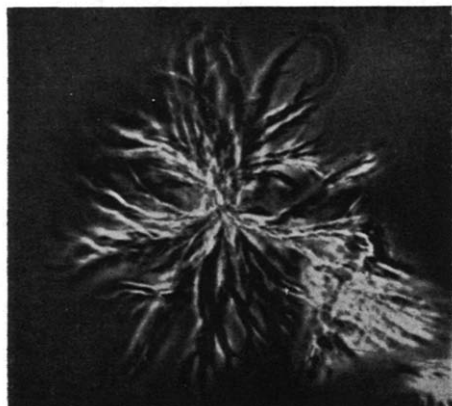


Figure 16—A complex multi-layer polyethylene crystal grown from a more concentrated solution than the one in *Figure 15* seen edgewise while in suspension. Optical micrograph. Phase contrast illumination. Magnification $\times 500$; reproduced without reduction. (Bassett, Keller and Mitsuhashi⁴⁰)

are not the ~ 100 Å monolayers any longer but are much thicker aggregates formed by them. There is evidence that even within such a contiguous stack of monolayers increased cohesion exists between a certain number of layers. To illustrate this briefly let us imagine that one could fix the layer forming the top surface of a stack and take away one layer after another starting from the bottom end of the stack. [Experiments equivalent to this—involving selective dissolution of layers where the top layer is being bonded to a carbon film—have in fact been carried out (Bassett⁴², Bassett, Keller and Mitsuhashi⁴⁰)]. It will be found that after the number of layers in the stack is reduced to a particular value further layers cannot be detached while the top surface is held fixed. This means that connectedness must exist between the remaining layers of the stack and the fixed top surface. It is found that the range of this connectedness increases with concentration and at a given concentration with the temperature of crystallization while the identity of the ~ 100 Å layers forming the stack remains apparent. We attribute this cohesion to tie molecules which may run through several chain folded layers thus tying a packet of them together.

Axialites were successfully grown from concentration as high as could be achieved experimentally which was up to beyond 30 per cent corresponding more to the plasticized bulk than to a solution. Here they tend to adhere together and resemble spherulites from an increasing range of viewing directions, still preserving the splaying lamellar appearance consisting of packets of chain folded layers.

These latest experiments indicate that chain folded crystallization is not restricted to dilute solutions. The characteristic structural features of chain

folded crystallization can be recognized in crystallization products even from very concentrated solutions, the layers being increasingly held together presumably by tie molecules running through several lamellae. It is this latter feature which we believe represents the link between crystallization from dilute and condensed systems.

The importance of interlamellar linkages became apparent quite unexpectedly in the course of the study of radiation damage in polyethylene (Salovey and Keller⁴³). As already stated ionizing radiation amongst others crosslinks the polyethylene chains which eventually leads to the destruction of crystallinity—a process which makes the electron microscopy of these objects particularly difficult. Long before crystallinity is affected, however, the crosslinks already reduce solubility by the formation of a connected network. It was found that the effectiveness of a given dose in reducing the solubility is largely dependent on the conditions of crystallization. In material crystallized from solution large variability was found (between 0 and 70 per cent insolubility for a given radiation dose) which correlates well with the state of aggregation of the lamellae established morphologically, increased insolubility being associated with a more compact aggregation of the lamellae. It follows that the crosslinks which are effective in reducing solubility are those between the different lamellae, and thus must link the bent parts of the molecule. Lamellae can only be linked if they are in close contact with each other which is automatically ensured when they are tied molecularly. These ideas were confirmed in two ways: (a) by reducing the radiation induced insolubility of compact aggregates by tearing the lamellae apart with ultrasonic radiation beforehand (Salovey and Keller⁴³); (b) by promoting the insolubility in loosely packed lamellar aggregates by means of compacting them first mechanically, e.g. by fast filtration (Salovey⁴⁴).

INDICATIONS OF SINGLE CRYSTALS FROM THE MELT

While single crystals comparable in definition and distinctness with those observed from solution have not been seen in the interior of melt crystallized specimens morphological features reminiscent of chain folded lamellae are becoming increasingly apparent. Admittedly they are necessarily observed under special conditions which makes the generality of the individual findings subject to argument. This, however, is the essence of the problem; we simply do not possess means to examine the submicroscopic morphology of the undisturbed interior of a bulk polymer comparable with those used in the study of products crystallized from solution. For obvious reasons morphologies arising during crystallization of thin molten layers are most amenable to examination. Such studies revealed a class of objects termed 'hedrites' which can show either clearly developed single crystal-like faces or splaying sheaf-like features or more frequently a mixture of the two (Geil⁴⁵, Leugering⁴⁶) (*Figure 17*). It appears that these are in the same class as the axialites obtained from concentrated solution but restricted in their three-dimensional developments.

In thicker melt crystallized objects it is the surface which is the most readily amenable to direct morphological examination and these very often

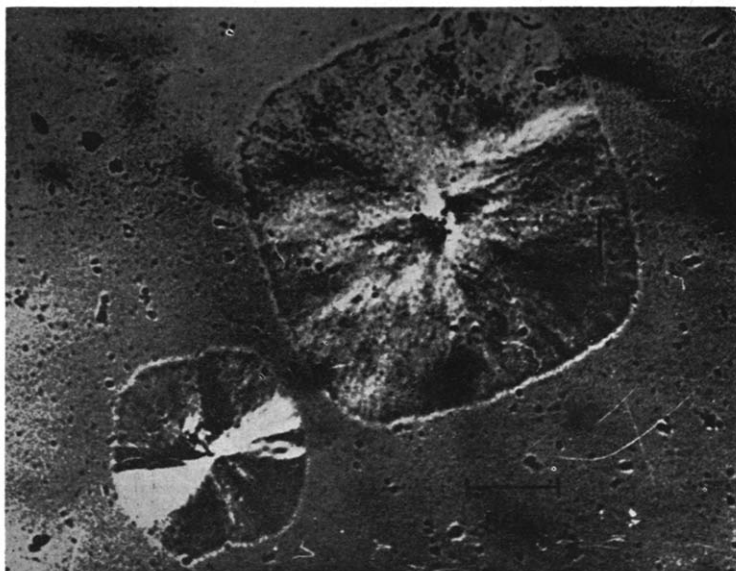


Figure 17—Polyoxyethylene 'hedrites' Partly polygonal, partly sheaflike objects formed from thin melt films. Optical micrographs. Cross polaroids plus first order red plate. Magnification $\times 250$; reproduced without reduction (Geil⁴⁷)

reveal lamellar structures. These in turn can be oriented in a periodically varying manner with respect to the plane of the surface, which corresponds to the by now familiar banded development of the spherulite (Figure 18) which accordingly should possess such a lamellar morphology. Spiral growth terraces can also be seen on some of these surface structures (Geil⁴⁵). It may appear that this in itself might settle the issue if it could be assured that surfaces are representative of the interior, which cannot be safely assumed *a priori* (Sella and Trillat⁴⁹). Nevertheless lamellar structures could be made visible along fracture surfaces (Geil⁴⁵, Fischer¹⁹), but here again the generality of such findings particularly in view of the danger of artefacts cannot be fully guaranteed. In addition to morphological evidence the low angle X-ray effects revealing large spacings must also be kept in mind. Such large spacings of 100 to 300 Å are well established in the bulk but have so far been essentially still unaccounted for. They are similarly present in single crystal preparations where they are convincingly attributed to chain folding as already discussed. It would not be logical to assume that similar effects in related systems are due to quite unrelated causes. Indeed late experiments on the effect of annealing on the long spacings showed close resemblance between the behaviour of unoriented melt and solution crystallized polyethylene (Fischer and Schmidt²⁰, and private communication.) These authors in fact conclude that the two structures must be basically identical and hence folded. Also correlation between the variation of long spacings on heating and the thickness of lamellae on the specimen surface

has been found (Geil, private communication). On the other hand thermodynamic and also structural arguments are being advanced against chain folded crystallization and single crystal type morphologies within the bulk (Chiang and Flory⁵⁰, Mandelkern *et al.*⁵¹). It appears nevertheless that the picture of lamellar chain folded crystallization in the bulk is gradually gaining ground. Also some theoretical foundations for it are being laid (Hoffman

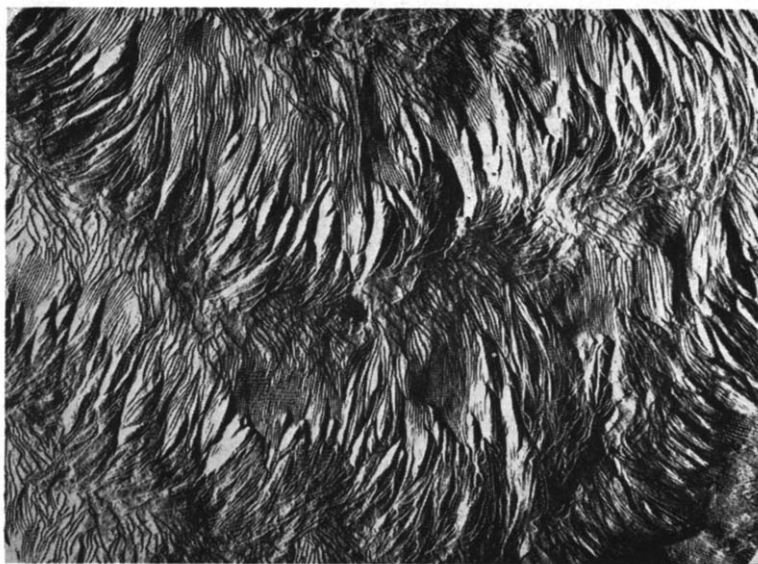


Figure 18—Surface of a melt-grown film of polyethylene which under the polarizing microscope reveals banded spherulites. Electron micrograph, replica. Magnification $\times 22000$; reproduced without reduction. (Fischer⁴⁸)

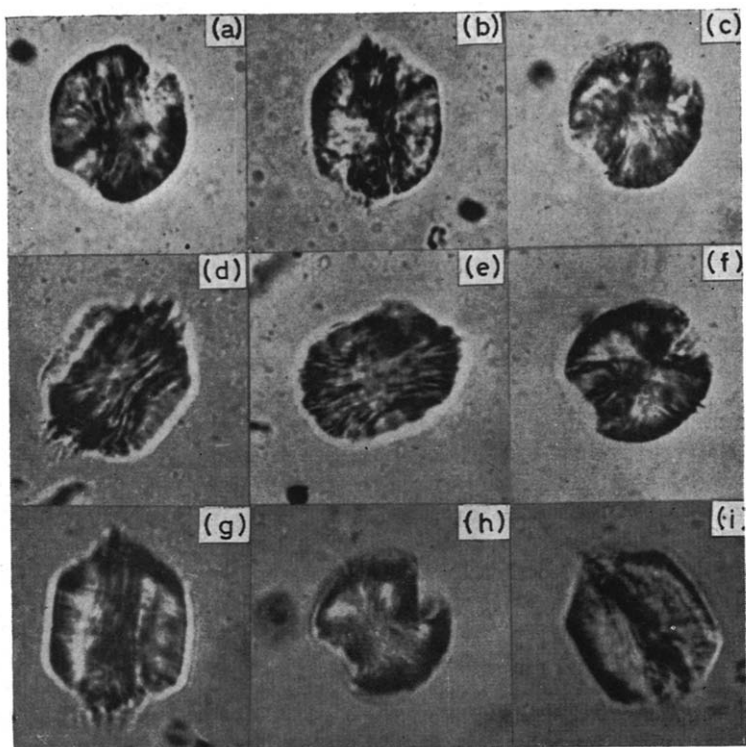
and Lauritzen⁵²). We feel therefore that chain folded lamellae with appropriate number of molecular ties between them may correspond to the real situation (Bassett, Keller and Mitsuhashi⁴⁰). The number of chains passing through layers as compared to those which fold back would determine whether the overall character of the crystallization is chain folded or not. Thus the issue is likely to be more a matter of degree than of principle. At any rate until individual lamellae which are thin compared with the length of the molecules can be distinguished folded structures must at least form a significant part of the material.

SOME REMARKS ON ORIENTED SYSTEMS

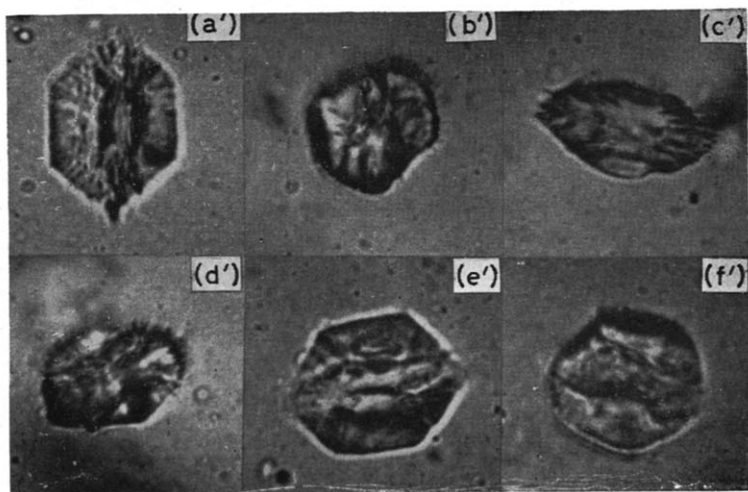
Little has been said so far about deformation of the morphological entities under external orienting influence and about the morphology of the drawn fibre. Bypassing at this place the numerous intriguing effects encountered during the intermediate stages of deformation, eventually in the course of drawing the molecules become parallel to the draw direction. Contrary to

the generally accepted views we have no real evidence that the chains are straight. In fact the draw ratio of the usual fibre is much lower than would correspond to full extension if the molecules were originally folded. The diffraction evidence only tells us that most of the molecule is along the draw direction in the same way as it informs us that the molecules are about normal to the basal plane of the single crystal. As in the latter the wide angle reflections do not reveal the fold, neither can we expect this in the case of a drawn fibre. In single crystal diffraction patterns the folds make themselves apparent via the low angle reflections due to large spacings along the chain direction. The corresponding diffraction effects are present also in the fibre and without any preconceived knowledge to the contrary there is no reason to assume that their origin is different (Bassett and Keller⁵³). These low angle reflections in fibres are often split along layer lines (so-called four-point diagram). This must be due to a staggering of some periodicity along the chain. We know that the folds are staggered in the single crystals giving rise to the pyramidal habit. If this staggering of folds pertains also in the fibre the four-point diagram would be accounted for. The analogy can be taken even further: when single crystals are heated the fold length increases, so does the larger periodicity in the fibre. In addition certain characteristic disorientation processes occur involving a rotation of the overall chain direction away from the fibre axis which is revealed by the wide angle (subcell) reflections. Now the same type of disorientations can be observed also in the single crystals which have never been extended. All this amounts to the fact that as far as the X-ray reflections are concerned—wide and low angle—drawn fibres and single crystals are indistinguishable in their qualitative behaviour, both as originally prepared and as heated. This suggests that there is a feature common to both which might be the folded configuration. Naturally in the fibre the folds could not be confined to lamellae otherwise its strength would be unaccounted for. In line with the suggestions made here earlier a number of molecules could run through several fold layers tying the whole system together. These tie molecules could be of two types: those incorporated in this form during crystallization as discussed in connection with unoriented systems and those which have been folded originally but have been fully or partially pulled out on drawing. The number of the latter is expected to increase with elongation. Significant differences found recently (Fischer and Schmidt²⁰, and private communication) in the annealing behaviour of highly drawn polyethylene (mostly $16\times$ elongation, which is much higher than that in the fibres encountered usually in practice) as compared with the undrawn bulk—differences attributed by these authors to a departure from the folded structure postulated for the unoriented material—could be attributed to this factor.

This type of picture (folded molecules together with straight or partially straight tie molecules) has also been arrived at by Bonart and Hosemann⁵⁴, and by Hosemann⁵⁵, by considering the possible origin of low-angle diffraction effects in fibres from the viewpoint of their generalized diffraction theory. The proportion of folded and extended molecules, or rather parts of molecules remains an open question and the closing remarks of the previous section pertain here also. It follows from the foregoing that this would be a



(A)



(B)

Figure 21—Details of (A) Figure 19, (B) Figure 20. The corresponding pictures are lettered in the stereograms. Mounting convention: Each photograph when viewed up the page represents the view when observed inwards on the stereogram. Magnification $\times 600$; reproduced without reduction. (Bassett, Keller and Mitsuhashi⁴⁰)

variable quantity characteristic of each individual system which would have to be assessed in each case when such a system is characterized.

As will have been noticed this review could only be kept reasonably up-to-date by quoting a substantial amount of still unpublished material. My thanks are due to all those mentioned in the text who informed me of their results in advance of the written publication.

*H. H. Wills Physics Laboratory,
University of Bristol*

DISCUSSION

Professor R. Brill (Germany): I should just like to mention that there is direct X-ray evidence for the fact that in polyamide fibres sheets are formed before the fibre is fully extended. In the extension of a bristle of a polyamide the cross section narrows at a certain point and two shoulders glide along the fibre in opposite directions. Between the shoulders the fibre is in a completely extended state, at the shoulder there is a transition state between the extended and the original state. In this transition state the orientation of molecules or crystallites starts. If one makes an X-ray diagram of that portion one sees that layers are present which are oriented parallel to the direction of extension, the layers or lamellae containing the hydrogen bonds between neighbouring polyamide molecules. The X-ray diagrams of the fully extended fibre in the neighbourhood of the shoulder show that the molecular layers, by further extension, have been rotated in such a way that the axis of the molecules is now parallel to the fibre. If here also the layers consist of folded molecules, by further extension an unfolding should take place by which the layers are just rotated into the direction of the fibre axis.

Dr A. Keller (U.K.): It is now well known that in the initial stages of drawing it is possible to obtain an orientation where the molecules are oriented perpendicular to the draw direction. This has been interpreted as resulting from the alignment of larger scale morphological units within which the molecules are oriented perpendicular to the direction which becomes parallel to that of drawing, the orientation of the molecules with respect to these units remaining unaffected at these low elongations (~50 per cent elongation). Also if filaments solidify under slight tension only, as e.g. when polyamide melts are allowed to drip out freely from a spinnerette head, solidification occurs in mid air, and the molecules are oriented perpendicular to the filament axis. This can be interpreted by visualizing the larger scale units, referred to above, actually forming in an aligned array along the filament axis during crystallization, the molecules within these units being perpendicular to the alignment direction. These larger units are probably those which are responsible for the radiating structure of the spherulites, and the postulated molecular orientation within them would be consistent with the tangential orientation known to exist within

the spherulites. Thus the perpendicular orientations referred to here could be visualized as resulting from the alignment of spherulite radii. According to the foregoing this alignment could arise either through deformation of existing spherulites on slight elongation or through some slight orienting influence during crystallization. In the latter case it is possible to elongate the solid filaments thus formed further, up to 300 per cent at elevated temperatures, in such a way that the perpendicular orientation is maintained or even improved. This can be visualized as a sliding past of the larger scale units without the molecular orientation within them being affected. (For details, see Keller⁵⁶).

Naturally, at large enough elongations the molecules do become aligned in the draw direction. As mentioned by Professor Brill usually a particular set of planes align first. These are invariably the planes which are parallel to the spherulite radii in undrawn specimens. In the perpendicular orientations quoted above these planes are parallel to the filament or draw direction, which is naturally required if such orientations are to be identified with those along the spherulite radii. On further drawing the molecules gradually align in the draw direction while these planes maintain this parallel orientation. If the initial stage of perpendicular orientation is missed, which mostly happens unless special care is taken, this preferential plane orientation alone becomes apparent.

Finally, I would like to quote an experiment related to the above observations on perpendicular orientations which also illustrate more concretely the part played by the texture in deformation processes. We (Bassett, Keller and Mitsuhashi⁴⁰) embedded polyethylene 'axialites' as in *Figures 19 to 21* in rubber by mixing the suspension with rubber solution and allowing it to dry. The 'axialites' could thus be stretched together with the rubber. The axialites could be classed in two groups: those where the planes of the lamellae were (a) predominantly parallel, (b) predominantly perpendicular to the stretching direction. Case (a) was by far the more frequent for obvious geometric reasons and also because some turning of the 'axialites' in this direction might have occurred. It was observed that such 'axialites' could draw out into streaks three to four times their original length. It could be concluded from the birefringence that the molecules were perpendicular to the long direction of the streak. We interpret this as the result of the chain folded lamellae slipping past each other without their internal structure being essentially affected. In case (b) the 'axialites' elongated in an accordion fashion with essentially unaltered molecular orientation as judged from the birefringence. This would be due to the layers being pulled apart. Thus the deformations observed in this experiment have one feature in common: they involve the displacement of otherwise essentially unaltered lamellae only. One would expect this to be an important feature also in the deformation of the bulk material.

Professor F. R. Eirich (U.S.A.), Chairman: I might relate very briefly that chain folding apparently occurs not only when a polymer molecule grows on its own crystal, but also when it lies down on a heterogeneous inter-

face. The chains seem to fold also and they show very similar relations as Dr Keller has mentioned, namely the fold thickness increases with temperature, and the fold thickness is related to crystal dimensions. So we might enter into a different phase of studying the adsorption of high molecular weight substances by transferring some of the things we have learned from Dr Keller to the study of high polymers at interfaces.

Professor R. Hosemann (Germany): The amorphous ring in polyethylene gives direct information of such folding back. It is interesting to note that if we are hot stretching polyethylene by 3 000 per cent, this amorphous ring can totally disappear if stretching is sufficiently slow. If we wait for one or two months it comes back step by step.

Dr B. Buchdahl (U.S.A.): I should like to ask Dr Keller if the calculations that he referred to by Professor Frank now permit an estimate of the surface energy?

Dr A. Keller (U.K.): I cannot enlarge on the point made in my talk at this place as this is a big and complex subject. I can only state that an estimate of 90 to 160 erg/cm² for the fold surface energies is probably a reasonable one.

Professor F. C. Frank (U.K.): *A priori* I do not think you can make very close estimates. The kind of value you have mentioned, 90 to 160, is about as good an *a priori* estimate as I should like to make.

Professor H. A. Stuart (Germany): I should like to say that the new thermodynamic theory of finite thickness of polyethylene crystals by Reinhold, Peterlin and Fischer leads to values for the surface energy between 30 and 50 erg/cm². In this theory which will be published in the *Journal of Chemical Physics* the free energy of a polyethylene crystal is calculated regarding the periodical lattice potential and its diminution by torsional vibrations of the chains. There is a minimum of the free energy which shifts and flattens with increasing temperature. Considering the run of the minimum as a function of temperature there is good agreement with the experimental long period of polyethylene between 40° and 110°C. Above 110°C this minimum disappears, which means that there is no longer a stable finite thickness in the crystal. So we understand the enormous increase of the period when approaching the melting point and the growth of the period with the time of annealing. We shall soon see, I hope, whether this thermodynamic effect or kinetic reasons lead to the periodic structure of polymer crystals.

REFERENCES

- ¹ OTT, E. *Z. phys. Chem. B*, 1930, **9**, 378
- ² KELLER, A. *Growth and Perfection of Crystals*, p 499. Wiley: New York, 1958
- ³ KELLER, A. *Makromol. Chem.* 1959, **34**, 1
- ⁴ AUERBACH and BARSCHALL. *Arb. Gesundh. Amt. Berl.* 1907, **27**, 183 (quoted by SAUTER⁵)
- ⁵ SCHWEITZER, O. *Freiburg. wiss. Ges. [Publ.]* 1929

- ⁶ SAUTER, E. Z. *phys. Chem. B*, 1932, **18**, 417
- ⁷ GEIL, P. H. *J. Polym. Sci.* 1960, **44**, 449
- ⁸ RANBY, B. G., MOREHEAD, F. F. and WALTER, N. M. *J. Polym. Sci.* 1960, **44**, 1961
- ⁹ KARGIN, V. A., BAKEER, N. F., LI, LI-SHEN and OCHAPOVSKAYA, T. S. *Vysokomol. Soed.* 1960, **2**, 1280
- ^{9a} HOLLAND, V. Paper to Electron Microscopists Society of America, Milwaukee, 1962
- ¹⁰ MILLER, M. L., BOTT, M. C. and RAUHUT, C. E. *J. Colloid Sci.* 1960, **15**, 83
- ¹¹ MANLEY, R. St *J. Nature, Lond.* 1961, **189**, 390
- ¹² RANBY, B. G. and NOE, R. W. *J. Polym. Sci.* 1961, **51**, 337
- ¹³ STORKS, K. H. *J. Amer. chem. Soc.* 1938, **60**, 1753
- ¹⁴ KELLER, A. and BASSETT, D. C. *Proc. Roy. Microscop. Soc.* 1960, **79**, 243
- ¹⁵ BASSETT, D. C. and KELLER, A. *Phil. Mag.* 1962. In press
- ¹⁶ STATTON, W. O. and GEIL, P. H. *J. appl. Polym. Sci.* 1960, **3**, 357
- ¹⁷ STATTON, W. O. *J. appl. Phys.* 1961, **32**, 2332
- ¹⁸ HIRAI, N., YAMASHITA, Y., MITSUHATA, T. and TAMURA, Y. Report of the Research Laboratory for Surface Science, Okayama University, 1961, **2**, 1
- ¹⁹ FISCHER, E. W. *Ann. N.Y. Acad. Sci.* 1960, **89**, 620
- ²⁰ FISCHER, E. W. and SCHMIDT, G. F. Presented at the meeting 'Kunststoffe and Kautschuk', Bad Nauheim, 1962
- ²¹ MÜLLER, A. *Helv. chim. Acta*, 1933, **16**, 155
- ²² LAURITZEN, J. I. and HOFFMAN, J. D. *J. Res. Nat. Bur. Stand.* 1960, **64A**, 73
- ²³ PRICE, F. P. *J. Polym. Sci.* 1960, **38**, 139
- ²⁴ PRICE, F. P. *J. chem. Phys.* 1961, **35**, 1884
- ²⁵ FRANK, F. C. and TOSI, M. P. *Proc. Roy. Soc. A*, 1960, **263**, 323
- ²⁶ PETERLIN, A. and FISCHER, E. W. *Z. Phys.* 1960, **159**, 272
- ²⁷ TURNBULL, D. and CORMIA, R. L. *J. chem. Phys.* 1961, **34**, 820
- ²⁸ PETERLIN, A., FISCHER, E. W. and REINHOLD, C. *J. Polym. Sci.* 1962. In press
- ²⁹ KELLER, A. and O'CONNOR, A. *Polymer, Lond.* 1960, **1**, 163
- ³⁰ ZAHN, H. and PIEPER, W. *Kolloidzshr.* 1962, **180**, 97
- ³¹ KERN, W., DAVIDOVITS, J., RAUTEKUS, K. J. and SCHMIDT, G. F. *Makromol. Chem.* 1961, **43**, 106
- ³² BASSETT, D. C., FRANK, F. C. and KELLER, A. *Nature, Lond.* 1959, **181**, 810
- ³³ RENEKER, D. H. and GEIL, P. H. *J. appl. Phys.* 1960, **31**, 1916
- ³⁴ BURBANK, R. D. *Bell Syst. tech. J.* 1960, **39**, 1627
- ³⁵ BASSETT, D. C., FRANK, F. C. and KELLER, A. *Proceedings of the European Regional Conference on Electron Microscopy, Delft*, 1960, Vol. I, p 244
- ³⁶ BASSETT, D. C. and KELLER, A. *Phil. Mag.* 1961, **6**, 344
- ³⁷ NIEGISH, W. D. and SWAN, P. R. *J. appl. Phys.* 1960, **31**, 1906
- ³⁸ KELLER, A. *Phil. Mag.* 1961, **6**, 329
- ³⁹ GEIL, P. H. and RENEKER, D. H. 1961, **51**, 569
- ⁴⁰ BASSETT, D. C., KELLER, A. and MITSUHASHI, S. *J. Polym. Sci.* 1962. In press
- ⁴¹ MITSUHASHI, S. and KELLER, A. *Polymer, Lond.* 1961, **2**, 109
- ⁴² BASSETT, D. C. *Phil. Mag.* 1961, **6**, 1053
- ⁴³ SALOVEY, R. and KELLER, A. *Bell Syst. tech. J.* 1961, **15**, 1397 and 1409
- ⁴⁴ SALOVEY, R. *J. Polym. Sci.* 1961, **51**, S1
- ⁴⁵ GEIL, P. H. *J. Polym. Sci.* 1960, **47**, 65
- ⁴⁶ LEUGERING, H. J. *Kolloidzshr.* 1960, **172**, 184
- ⁴⁷ GEIL, P. H. *Growth and Perfection of Crystals*, p 584. Wiley: New York, 1958
- ⁴⁸ FISCHER, E. W. *Z. Naturforsch.* 1957, **12a**, 753
- ⁴⁹ SELLA, C. and TRILLAT, J. J. *C.R. Acad. Sci., Paris*, 1959, **248**, 410
- ⁵⁰ CHIANG, R. and FLORY, P. J. Meeting of Division of Polymer Chemistry, American Chemical Society, New York, 1960, Vol. I, p 81
- ⁵¹ MANDELKERN, L., POSNER, A. S., DIORIO, A. F. and ROBERTS, D. F. *J. appl. Phys.* 1961, **32**, 1509
- ⁵² HOFFMAN, J. D. and LAURITZEN, J. I. *J. Res. Nat. Bur. Stand.* 1961, **65A**, 297
- ⁵³ BASSETT, D. C. and KELLER, A. *J. Polym. Sci.* 1959, **40**, 545
- ⁵⁴ BONART, R. and HOSEMAN, R. *Makromol. Chem.* 1960, **39**, 105
- ⁵⁵ HOSEMAN, R. *Polymer, Lond.* 1962, **3**, 349
- ⁵⁶ KELLER, A. *J. Polym. Sci.* 1956, **21**, 363

Stereoregular Polymers and Polymerization

F. DANUSSO

The historical development is traced of processes leading to the stereoregular polymerization of various substances with a view to indicating lines of interest for further exploratory work. Principal subdivisions of the text include: types of steric arrangements experimentally obtained, general considerations on the mechanism of stereospecific polymerization, some properties of stereoregular polymers, and future developments and applications.

EIGHT years have elapsed since a group of chemists of the Industrial Chemistry Institute of the Polytechnic of Milan, under the guidance of Professor Natta, for the first time succeeded in synthesizing and characterizing α -olefine stereoregular polymers employing stereospecific procedures of outstanding possibilities¹.

Only eight years have elapsed since that beginning, but we now find it already impossible to summarize in a short discussion all the results and consequences of that start and the subsequent development of the field of synthetic stereoregular polymers.

The reasons for the success of this new branch of industrial and macromolecular chemistry reside, as is now fairly well known, on the one hand, in the scientific interest of stereospecific syntheses and properties of numerous new polymers of regular structure; and on the other hand, in the accompanying industrial interest in the development of procedures, which from simple widely available and cheap monomers lead to versatile polymers rich in practical applications, such as resins, plastic materials, fibres and rubber.

FIRST DISCOVERIES AND ENSUING DEVELOPMENTS

The first synthetic stereoregular polymers prepared and clearly characterized were polymers of alkyl or aryl monosubstituted ethylenes (such as propylene, butene-1, styrene)¹.

The arrangement existing in the new polymers revealed itself to the discoverers through the presence in the products of a phase of high crystallinity. Never before had this been observed in polymers obtained by the previously available methods of polymerization from the same or analogous monomers.

The crystallinity was a simple external manifestation of a regular arrangement that soon after was shown to be of extremely fine structure, on a molecular scale, and which at first sight seemed to be of almost impossible realization when applying the concepts then available on growth mechanisms of polymeric chains.

This paper was presented at a Polymer Science Conference, held in conjunction with the Second World Congress of Man-made Fibres, at the Connaught Rooms, Holborn, London W.C.2, 2nd and 3rd May 1962.

Actually the stereospecific catalysts used, now frequently called 'Ziegler-Natta catalysts', have been developed from similar metalorganic catalysts which, through Professor Ziegler's brilliant achievements with ethylene², have proved capable of producing polyethylenes having a considerable degree of macromolecular linearity.

However, the high linearity obtained with a monomer such as ethylene, having two planes of molecular symmetry, did not allow the expectation of success with monomers, such as vinyl monomers, having a single plane of molecular symmetry.

The results obtained by Professor Natta with selected metalorganic catalysts were indeed surprising, having led to the synthesis of macromolecules which, besides being linear, have a regular structure relative to each centre of steric isomerism (tertiary carbon atom) possessed by each structural unit along the macromolecular chain.

After the first results many scientists quite soon understood the importance of attaining a control of factors of steric nature in macromolecular syntheses. Such a control created a new dimension in research and held out promising openings towards entire classes of new polymers having in all cases some interesting characteristics.

The application of the same Ziegler-Natta catalysts, either of classical formulation or modified, soon led to the preparation of new polymers of butadiene and isoprene with a steric structure completely ordered: four pure stereoisomers of polybutadiene and at least two of polyisoprene. These last two reproduced the structure of gutta percha and natural rubber.

These important results were subsequently followed by others. New catalytic systems were selected from the primitive ones and the stereospecific syntheses were extended to more complex hydrocarbon monomers, to entire homologous series of these, and to monomers containing polar groups, such as vinyl ethers, acrylates and methacrylates, aldehydes, ketones, ketenes and different cyclic compounds.

In some cases these polymers even possessed complex stereoregularities, based on more than one centre of steric isomerism of the units. Stereoregularity was also obtained and identified in various copolymers.

Work done on possible developments of the Ziegler-Natta catalysts stimulated considerable research in various directions which, however, do not always appear to be entirely independent.

The results of previous polymerization processes were reconsidered and carefully re-examined from the point of view of the steric structure of obtainable products. Thus, it has been found that certain crystallizable polyvinylethers previously obtained³ were stereoregular⁴, and that certain polystyrenes⁵ could undergo some crystallization and accordingly were stereoregular to a noticeable extent^{6, 7}.

Finally, it has been acknowledged that polymerizations of conventional type, such as cationic, anionic and later on even radical polymerizations, if carried out under particular conditions and with certain monomers, could be endowed with some stereospecificity (as was inferred from the appre-

cial crystallizability of previously known, radical polyvinylchlorides and polyacrylonitriles). A large volume of research work has been carried out recently in this direction and the results, at times satisfactory and at times uncertain, occupy a noteworthy space in the present macromolecular bibliography.

TYPES OF STERIC ARRANGEMENTS
EXPERIMENTALLY OBTAINED

(a) *General concepts on tactic polymers*

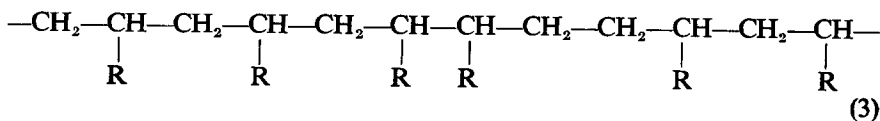
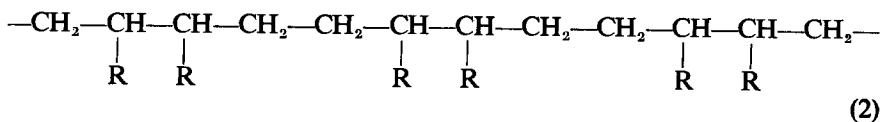
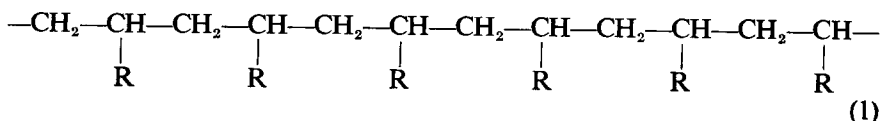
The notions of the usual stereochemistry, though useful in a general way, when applied to stereoregular polymers have always caused some difficulties in the classification and understanding of the obtainable stereostructures.

It has therefore been found suitable to establish a nomenclature which should answer not only to formal needs, but also to a desirable clarity on basic concepts⁸. This nomenclature has created the bases for extensions to cases of macromolecular steric isomerism more complex than those first observed, and which are in the course of further development.

It has been noticed that the ordered arrangements of a macromolecular chain can be conveniently treated in general terms of isomerism. That is any regular chain has a privileged structure among those of the possible isomeric chains. The privilege lies in the fact that the structure is built according to a very simple, non-statistical rule which imposes the intrinsic structure of the base units and their mode of enchainment, or one of these factors.

The possible isomerism may be classed in three types: positional, structural or steric. Any ordered arrangement can consequently be defined or distinguished with reference to each type of isomerism.

Let us examine, for example, the following three segments of polyvinyl chains:

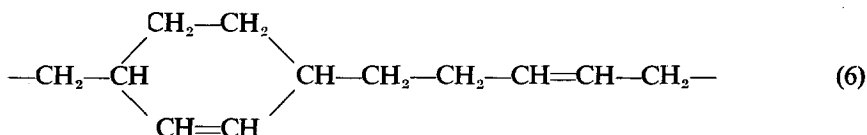
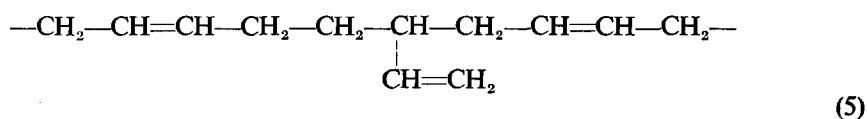
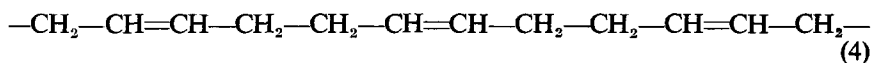


Neglecting for the moment any other difference, the structures of these segments differ in isomerism of position of the R substituents along the main chain. Even intuitively we recognize as 'positionally' regular the structures (1) and (2) with respect to structure (3). Actually the first two

structures possess regular enchainments of the units, respectively of the head-to-tail and head-to-head/tail-to-tail types. When observing these two regular segments we may notice that a 'repetitive rule' of the orientation of the unit is applied in the former, and an 'alternating rule' between two orientations is applied in the latter*.

Essentially identical considerations as those on the positional isomerism can be made in regard to structural and steric isomerisms.

The following three examples of polybutadiene segments differ at least in structural isomerism:



The first segment appears to be 'structurally' regular with respect to the other two, by virtue of a simple repetitive rule.

As to ordered arrangements based on steric isomerism it is convenient to lay special emphasis on the more interesting case in practice of linear chains (or macromolecules) which are already 'positionally' and 'structurally' ordered. As a matter of fact, it can be understood that for a stereospecific synthesis it is necessary to reach such mechanism requirements that the polymer obtained also proves to be ordered with respect to any other isomerism.

In this case, as is known, the arrangement of the steric structure leads to polymers which have been called 'tactic polymers'. Their steric regularity is called 'tacticity' and the ordering rule 'taxis'.

On the basis of examples drawn from experience, it may be of some interest to discuss here some types of tacticity definitely already achieved.

(b) Centres of steric isomerism and monotactic polymers

Steric isomerism among chains (or segments of chains) of the same composition, and consequently every tacticity, originates from 'sites' or 'centres' of steric isomerism contained in the base unit (and not necessarily

*Incidentally it can be remarked that the alternating rule of structure (2) can be equally related to a repetitive rule, provided a double repeating unit is considered with regard to that of structure (1). The choice of an alternating rule for structure (2), however, appears to be more convenient because it is referred to the same repeating unit as for structure (1), which is also the smallest distinguishable (and in addition corresponds to the monomeric unit). In this sense it may also be said that structure (1) possesses the 'finest' positional arrangement.

contained in the monomer). Hitherto it has been agreed to consider only centres situated on the main chain.

The 'stereocentre' of more simple consideration is the double bond of the ethylenic type. This may be inserted in the main chain in such a way that the holding unit intrinsically assumes a *cis* or *trans* structure.

Figure 1 shows, for instance, the two possible structures of a 1,4-enchainment butadiene unit (the representation fixes the end groups in an arbitrary conformation).

The taxis obtained up to now and recognized for this type of stereoisomerism is solely repetitive and gives rise to '*cis*-tacticity' or to '*trans*-tacticity', that is to polymers which are '*cis*-tactic' or '*trans*-tactic' respectively.

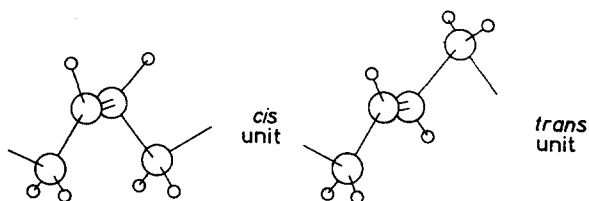


Figure 1

Another important site of steric isomerism, more frequently occurring than the preceding one, is the 'carbon atom differently disubstituted on the main chain' (hydrogen being also counted as a substituent). No simple denomination has been given to it yet, though it does deserve one. We shall call it here 'D.D. atom' for the sake of brevity (D.D. for 'differently disubstituted', in the sense expressed above).

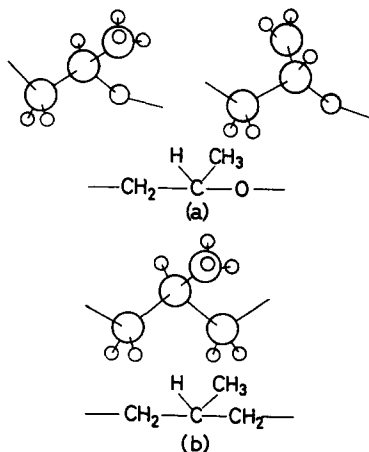


Figure 2

This stereocentre appears to be of a more general type than the 'asymmetric carbon atom' of conventional stereochemistry: in some instances it clearly shows itself to be an asymmetric carbon atom, but in others it seems to shun such a definition.

In *Figure 2* we find two typical examples: in the first (a) are represented the two possible steric structures of the unit which can be obtained from propylene oxide; in the second (b) the structure of a polypropylene chain is represented in correspondence with one of the tertiary carbon atoms. The 'D.D. atom' in the first example can be immediately recognized as asymmetric and its configuration is easily assignable in the limits of the unit, that is in its immediate neighbourhood. In the second example, on the contrary, the steric configuration is not easily assignable, or it could be so in a strictly formal way, only considering every detail of the structure of the entire molecule.

Of greater interest for the macromolecular chemist is the fact that such differences are not essential for the consideration of ordered steric arrangement. The formal difficulties are easily overcome if one refers to the configurations of 'D.D. atoms', in their succession along a chain, as they are recorded by a hypothetical observer who is supposed to proceed along the bonds constituting the principal chain (*Figure 3*) and meet and overtake these atoms one after the other. The direction in which the observer

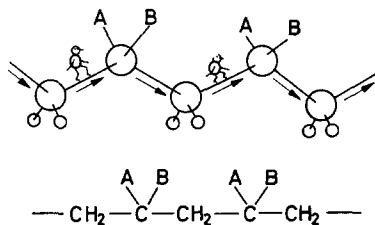


Figure 3

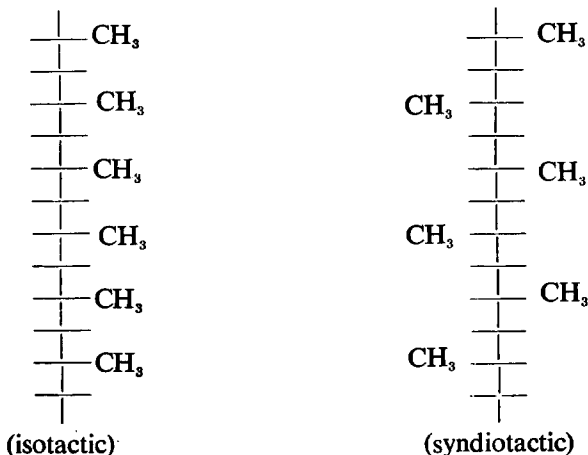
proceeds is unimportant provided that he does not change it.

The device of the hypothetical observer, which is common to various well known rules of physics, is very useful here, particularly when considering complex cases.

The taxes realized up to now with the site of the 'D.D. atom' are both the repetitive one, and the alternating one, which give rise to 'isotacticity' and 'syndiotacticity' respectively. In an 'isotactic' polymer, the hypothetical observer meets the 'D.D. atoms' all of them having the same disposition of the substituents (the remainder of the chain included); in a 'syndiotactic' polymer he finds them with dispositions alternating between the two possibilities.

The representation of the two structures may be made easily and without ambiguity following the so-called 'Fisher's projection', well known to chemists. This projection is nothing else than the visualization on a plane of the succession of the configurations of the 'D.D. atoms' met by the hypothetical observer mentioned above.

For example, the two tactic structures of polypropylene realized up to now, isotactic¹ and syndiotactic⁹, can be as shown below:



The isotactic polymers prepared up to the present time (fully or partially stereoregular) are very numerous, mostly of vinylic hydrocarbon and non-hydrocarbon types; others are of the vinylidenic, acetalic, epoxidic, etc. types. On the other hand, only a few cases of syndiotactic polymers are known; among these polypropylene, polybutadiene (with 1,2-enchainment) and certain polymers from partially stereospecific, radical polymerization (e.g. polyvinylchloride, polyacrylonitrile, polymethylmethacrylate and polyisopropylacrylate).

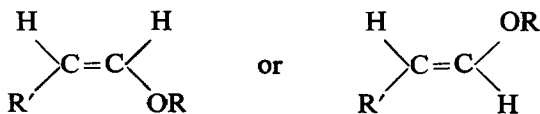
The repetitive taxis appears therefore to be the one greatly predominant.

Up to now it has not been found necessary to consider steric isomerism centres different from the ethylenic double bond and from the 'D.D. atom' on the main chain. Some particular cyclic structures might be treated as ulterior stereocentres but, as we shall see presently, their consideration has so far been led back to that of a pair of 'D.D. atoms'.

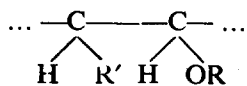
(c) *Polytactic polymers*

Besides tactic polymers based on a single centre of steric isomerism, therefore 'monotactic', there have long been prepared 'ditactic' and, more recently, 'tritactic' polymers.

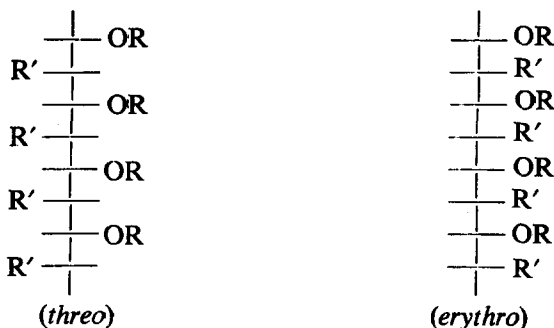
A first interesting example is that of the 'di-isotactic' polymers obtained from alkenylethers¹⁰:



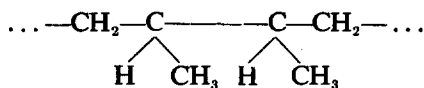
giving the unit



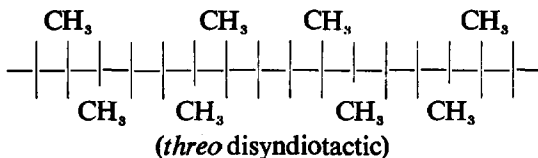
The two polymeric structures so far prepared, both recognizable as diisotactic (that is independently isotactic with regard to each of the two 'D.D. atoms') are of *threo* type and *erythro* type respectively, as follows:



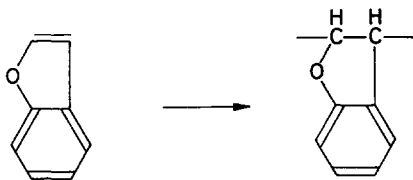
Another peculiar case of ditacticity is that of a crystallizable alternating copolymer obtained from *cis*-butene-2 and ethylene¹¹, whose repeating unit is



It might actually be considered a polypropylene with a 'positional' head-to-head/tail-to-tail arrangement and results to be a 'disyndiotactic' polymer, according to the following structure



An important example of ditacticity from a cyclic structure has been revealed by certain polymers prepared from benzofuran¹²:

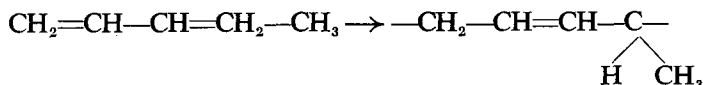


Here the ditacticity arises from the opening of a double bond of the cyclic monomer and might be treated in terms of monotacticity from *cis* or *trans* configurations relative to the cycle, taken as a new type of stereocentre; but it can be more conveniently treated as ditacticity deriving from a pair of 'D.D. atoms' on the principal chain. Actually there are four

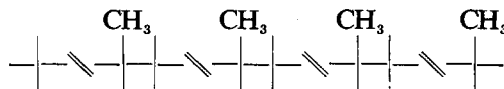
theoretical cases of steric isomerism of the whole unit, the two 'D.D. atoms' being also asymmetric atoms, each of them capable of assuming one of the two possible steric configurations.

Optically active polymers were also prepared in this case¹², when using catalysts with asymmetric atomic groups, by a method I shall mention presently.

A significant example of ditacticity based on two stereocentres of different types has been realized¹³ with a polymer from pentadiene-1,3

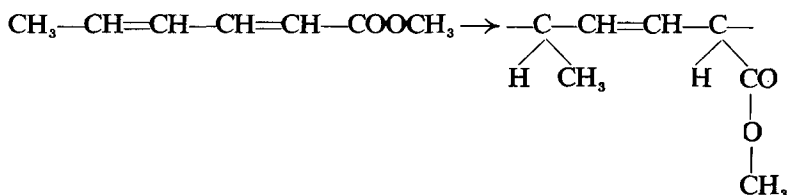


The polymeric structure is *trans*-tactic relative to the ethylenic double bond and isotactic with respect to the 'D.D. atom', and can be represented by the following intuitive projection, derived from a Fisher's projection

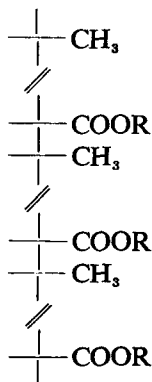


Here the 'D.D. atom' is also asymmetric and can be oriented in uncompensated configurations by suitable asymmetric catalysis, thus yielding optically active polymers¹⁴.

Finally, the example of the first tritactic polymer obtained can be mentioned here, deriving from methyl sorbate¹⁵



An ethylenic double bond and two 'D.D. atoms' are in this unit as stereocentres. The tritactic structure recognized up to date is that of *trans-erythro*-di-isotactic polymethylsorbate.



Also this polymer is optically active when produced by an asymmetric synthesis¹⁶.

GENERAL CONSIDERATIONS ON THE MECHANISM OF
STEREOSPECIFIC POLYMERIZATION

Since the beginning, the mechanism of stereospecific polymerizations has been the object of intense research and theoretical speculation. Here we shall limit ourselves to some considerations of a general character.

There is no doubt that in the stereospecific polymerizations yet known the stereoregularity of the polymer is obtained through a regulation of the structure and of the manner of enchainment of every new monomeric unit entering into the chain, a regulation which takes place in the elementary repetitive reaction of chain growth.

We must admit that the mechanism of such a regulation is so far in no way known with certainty in each particular detail. We know suitable catalysts, or catalyst-monomer couples, or particular operating conditions of conventional types of polymerization which produce stereoregularity in a more or less high degree. In some more important cases we know considerable details of the kinetic and chemical mechanism of the regulating reaction. The ultimate reasons, however, why the centres of steric isomerism range themselves in given configurations along the polymeric chain can be perceived by intuition, but cannot be described particularly without introducing structuralistic or mechanistic hypotheses having up to now the value of pure, and in some instances even arbitrary, speculation.

For an accurate study of this complex matter some important considerations should be borne in mind.

Nowadays, quite properly investigations of the stereospecific mechanisms must, for obvious heuristic reasons, be conducted on a great variety of polymerizations having any degree of stereospecificity. It is clear, however, that the investigations acquire depth of meaning if they are made to converge on types of reaction capable of producing polymers endowed with substantial, practically complete, tacticity and capable of transforming in such polymers wide classes of monomeric compounds.

Even today there is no doubt, as there was at the beginning of these investigations, that these two attributes are possessed to high degree by the syntheses with metalorganic catalysts, among which the Ziegler-Natta catalysts have the highest importance. The results obtained by the latter have facilitated remarkable progress in the mastery of macromolecular chemistry.

In the first place they have made clear a decisive superiority of ionic polymerizations over radical ones in the realization of positional, structural and steric arrangements in the polymers.

In particular they have pushed researchers to pay closer attention to the nature of the ionic couple responsible for the polymerization, and to develop the possibilities offered by secondary electrostatic couples, preferably constituting bonds having only a partially heteropolar component.

Among these apparently the most important are the coordination bonds obtainable in metalorganic complexes, owing to consideration of which the term 'coordination polymerization' was introduced for the Ziegler-Natta processes¹⁷.

The kinetic and chemical mechanisms of this reaction have been parti-

cularly studied in some specific cases and above all in its application to olefine monomers¹⁸.

Up to a few years ago we could distinguish, in ionic polymerization, purely the two cases of cationic and anionic polymerization, whose characteristics were substantially influenced by the presence in the system of an ion, respectively positive or negative, which grew by attacking monomer molecules and was only generically assisted by a counterion whose role was of hardly any relevance.

The first systematic work on the influence of steric and polar factors on coordination polymerization, carried out on a wide series of arylethylenic monomers¹⁹, has led to realization that, in this case, even if the chain grows on an end of negative character, the attack of the monomer double bond takes place by force of the metalorganic counterion, that is by force of a positive electrophilic centre.

These results have given useful evidence of the aptitude of the counterion to determine or predetermine the stereospecific addition. Various subsequent results, and other research work now in progress, have further confirmed that today the most important cases of stereospecific coordination polymerization appear to be principally due to a counterionic attack, or to a predominant intervention of the counterion in the elementary addition mechanism.

The application of this simple concept to subsequent experiments has yielded new satisfactory results, among them the asymmetric synthesis of polytactic stereoregular polymers, which have been found to be endowed with optical activity^{12, 16}. Their structure, containing stereocentres consisting of asymmetric carbon atoms in chain (for example polysorbates, polypentadienes and polybenzofurans), was unbalanced with regard to the statistical equivalence of the two possible configurations (impressed by the various catalytic centres contained in a single catalyst) through insertion of an asymmetric counterion in a stereospecific metalorganic catalyst of normal type.

Thus, a synthesis of a reiterative asymmetric type was carried out in the laboratory, simulating certain natural processes of enzymic catalysis.

Today in the light of the above considerations and with reference to the classical case of a Ziegler-Natta catalysis, the mechanism of a stereospecific polymerization is, at least in principle, easily conceivable as comprising: (a) a previous coordination of the monomer molecule to the catalytic counterion (in the cases of heterogeneous catalysis possibly constituting an active surface); and (b) the insertion of the resulting monomeric unit in the previously formed chain, which also adheres to the catalytic centre by virtue of a bond of coordinated type.

The stereospecificity is evidently imposed during the first stage by local, characteristic conditions, whose geometric and energetic details remain comprehensibly difficult to specify and individualize. Thus it is easy to suppose that the tacticities realized up to now are principally those based on a repetitive rule.

The alternating rule, actually realized in more than one case, is more difficult to understand. An explanation perhaps valid in some particular

circumstances (a typical one: radical polymerization) is based on the repelling action that the substituent of the last unit in the chain may exert on the substituent of the entering monomeric unit. On the other hand in the cases in which the alternating arrangement is impressed by a catalyst, the situation appears generally to be more complex. Furthermore it cannot always be excluded that, under the appearance of an alternating rule, a repetitive mechanism is hidden.

Before concluding this topic, it is interesting to point out that the considerations developed above on the role of the counterion lead if generalized to envisaging theoretically four possible cases of ionic polymerization²⁰. In fact for each case of formally cationic and anionic polymerization (that is with the growth of a chain end respectively positive or negative) we may have the two subsidiary cases of ionic or counterionic attack.

Hitherto three of these cases have been experimentally ascertained: the cationic and anionic ones 'by ionic attack' (conventional cationic and anionic polymerizations) and the anionic 'by counterionic attack' (for example: Ziegler-Natta polymerization of olefinic monomers). Not yet experimentally recognized for certain is the fourth case of cationic polymerization 'by counterionic attack'; to this there is no contradiction on theoretical grounds and it has probably already been realized in some cases.

SOME PROPERTIES OF STEREOREGULAR POLYMERS

Consideration of the properties of highly stereoregular polymers has theoretical and practical importance.

On the one hand, the highly stereoregular polymers are nowadays relatively numerous, and their number will increase more and more with the progress of studies; depending on the monomeric structure, they can assume a great variety of properties and therefore they offer an exceptional casuistry both for research and for application.

On the other hand, in the various cases in which their molecular structure may be entirely characterized, there is both the hope and the possibility to establish clear general relationships between structure and consequent properties, with a remarkable widening of the corresponding important chapter of macromolecular chemistry.

The fundamental element for comprehension of the properties of polymeric materials is the macromolecular conformation, and we shall preferably dwell on this aspect when describing some of the properties of tactic polymers.

It is intuitive that if a macromolecular chain has an ordered structure, it should have the possibility to assume, under favourable conditions, ordered conformations.

Actually, the essential geometry of a macromolecule depends on the bond distances between the atoms constituting the main chain and on the valency angles, and the various conformations which the molecule can assume are originated by all the possible internal rotations of parts of the molecule with respect to others around the valency bonds. An important role is played in such conformations by the properties of the lateral substituents, which

with their bulk, conformations and interactions, create hindrances to the possible conformations of the main chain itself.

Therefore, generally speaking, the possible conformations of a macromolecule will be disordered. But, if the structural mode of insertion of all the substituents to the main chain is ordered, which happens in tactic polymers, it must also be theoretically expected that the macromolecule will also admit particular conformations of ordered type, that is characterized by a well determined value of an identity period along a chain axis within which all (or almost all) the distances among atoms or atomic groups constituting the macromolecule assume fixed and constant values.

It can be easily understood that the substantial attainment of an ordered conformation in each single macromolecule is a first necessary, even if not sufficient, condition in order to reach crystallinity. Actually, a macromolecule in such an ordered conformation should become in a sense 'stiff' and find a condition which might be called 'monodimensional crystallinity'.

It is interesting to note that such a state of the macromolecule appears to be fairly independent of interactions with other macromolecules when examined from the point of view of its internal energy. In fact, it has been demonstrated in various cases already that the energetically most stable conformation of an isolated stereoregular macromolecule (supposed to be endowed with a periodicity along an axis), calculated theoretically (even if with unavoidable hypotheses) only on the basis of intramolecular interactions, corresponds to the conformation experimentally determined for the same macromolecule when inserted in the crystalline lattice of the polymer²¹.

In order to reach a real crystallinity, that is an ordered arrangement on a 'three-dimensional' scale, a further condition is obviously necessary: equal macromolecules, in ordered conformations of the same type (even enantiomorphous), must pack together with a sufficient energy to obtain a stable crystalline lattice, with a three-dimensionally periodic structure, leading to a minimum value of the free energy of the system.

Although in principle a stereoregular polymer should not be prevented from satisfying any condition for the attainment of crystallinity, in practice it has been found that not all the tactic polymers are crystallizable, owing probably to non-thermodynamic reasons.

Significant examples are found²² in *Table 1*, in which there is a list of isotactic polymers of substituted styrenes divided into two columns: those in the first column can be crystallized easily, whereas those in the second have not yet been crystallized, even if they proved by different methods to be equally tactic.

Table 1 shows that the para substituents allow crystallinity only if the substituent is of very small size; otherwise the polymer is not crystallizable. Substitutions in the meta positions do not follow simple rules. The ortho substitutions, if they do not hinder polymerization, generally give crystallizable polymers. The double substitutions appear to be favourable to crystallinity, even if meta or para positions are involved.

Some of the non-crystallizable polymers of *Table 1* show in the infra-red (i.r.) spectrum characteristic bands, which can be attributed to a helical shape of the chain. For these the hypothesis may be accepted that the chains,

even if they can assume substantially ordered conformations, cannot effect the packing which causes the three-dimensional crystalline arrangement, possibly because of hindrances due to lateral substituents.

Table 1. Crystallizability of isotactic polymers of nuclear substituted styrenes

| Crystallizable polymers from: | Non-crystallizable polymers from: |
|--|---|
| Styrene | |
| <i>o</i> -Methylstyrene <i>m</i> -Methylstyrene | (<i>p</i> -Methylstyrene)* <i>p</i> -Ethylstyrene <i>p</i> -Isopropylstyrene |
| <i>o</i> -Fluorostyrene <i>p</i> -Fluorostyrene | <i>m</i> -Fluorostyrene <i>m</i> -Chlorostyrene <i>p</i> -Chlorostyrene <i>p</i> -Bromostyrene |
| 1-Vinylnaphthalene | 2-Vinylnaphthalene 4-Vinylbiphenyl 9-Vinylphenanthrene |
| 2,4-Dimethylstyrene 2,5-Dimethylstyrene 3,4-Dimethylstyrene 3,5-Dimethylstyrene 2-Methyl-4-fluorostyrene | |

*Crystallizable following S. Murahashi *et al.*²².

Thus, in general, polymers which by i.r. examination appear 'crystalline' (in the meaning technicians give to this word) may on the contrary appear non-crystalline by X-ray examination.

In other cases, by i.r. analysis, bands are not observed which can be surely attributed to ordered conformations; but a suitable chemical transformation of the side groups of the non-crystallizable polymer confirmed the presence of isotacticity through the crystallizability of the polymer obtained by the transformation. This applies, for instance, to poly-*p*-chlorostyrene which, when obtained by Ziegler-Natta polymerization, cannot in practice be crystallized; but when hydrogenated in the nucleus and therefore dehydrochlorinated, can be transformed into isotactic crystalline polyvinylcyclohexane²⁴.

The molecular conformation reached by tactic polymers in the crystalline state proved to be predominantly of the helicoidal type (actual or generalized). In fact such a conformation, by admitting the validity of the so-called 'equivalence principle' was demonstrated to be really necessary for all the isotactic polymers of the vinyl type²⁵.

Figure 4 shows, for instance, the conformations of a chain of isotactic²⁶ and syndiotactic⁹ polypropylene. In this case the syndiotactic chain is also helix-shaped. But in Figure 5, in which the conformations of isotactic²⁷ and syndiotactic²⁸ polybutadiene are compared, it can be observed that the syndiotactic polymer assumes a conformation with an almost planar main chain.

The ternary helix conformation is very frequent, but other types of helices can occur.

In this sense the influence of the substituent appears to be determining. In fact the helix is ternary if the substituent has a certain bulk, larger, for instance, than in hydrogen, fluorine, hydroxyl, but not beyond a certain limit (be it, for instance, a methyl, ethyl, propyl, phenyl or methoxyl group).

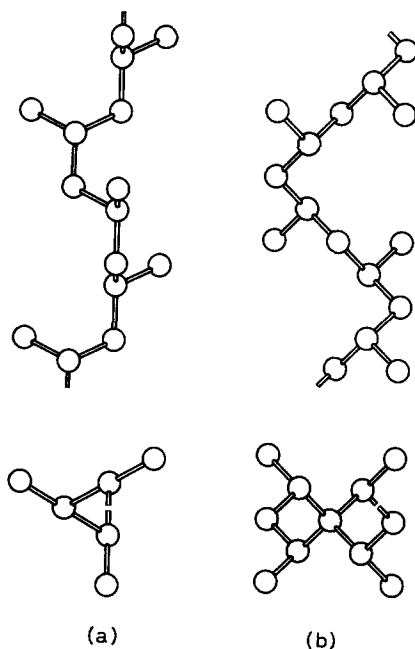


Figure 4

With substituents of a greater encumbrance, or even branched, the helix pitch increases. This happens, for instance, when the substituent is an isopropyl, isobutyl, isopropoxyl or *o*-methylphenyl group.

Figure 6 shows typical examples of helicoidal conformations of different pitch²⁹.

Obviously, particular energetic interactions among substituents can even be a cause of the increase of the pitch of the helix.

Simple or complex helicoidal conformations occur also with polytactic polymers. Figure 7 shows the conformation of the chain of the *threo* and *erythro* di-isotactic polymers of 1-deuteriopropylene, both shaped as a simple ternary helix³⁰. Figure 8, on the contrary, shows the chain of the *threo*-di-isotactic poly-methylisobutoxyethylene, which has the helix conformation with seven monomeric units in two pitches³¹.

A different pitch of the helix can also differentiate two polymorphous modifications of one polymer. Thus, isotactic polybutene-1 has a stable modification in the shape of a ternary helix, and a metastable modification for which a quaternary helix can be postulated³².

Always considering the topic of polymorphism, it is interesting to point out that the field of tactic polymers has revealed an extraordinary tendency

Figure 5

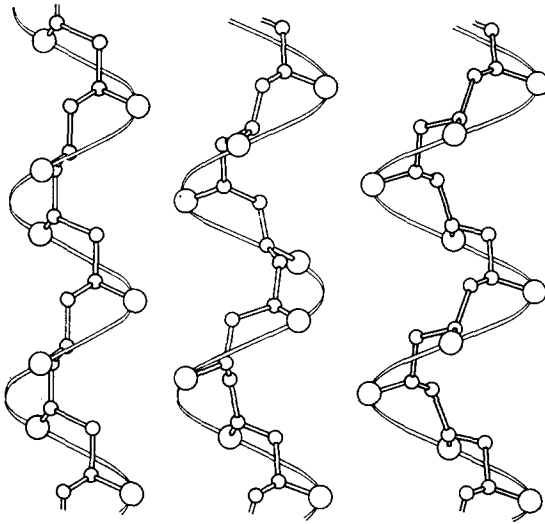
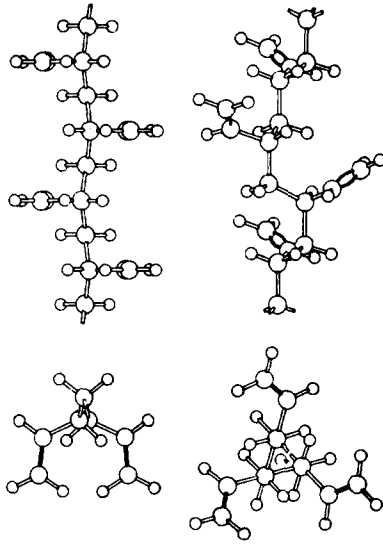
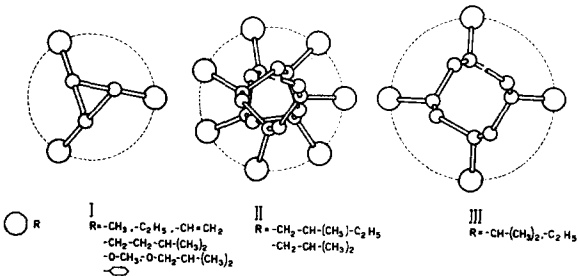


Figure 6



of the crystallizable polymers to appear in polymorphous modifications, so that today one is unlikely to find polymers showing only one crystalline structure.

Thus, for instance, isotactic polypropylene has at least three modifications, in addition to one of smectic type³³; isotactic polybutene-1 has also three

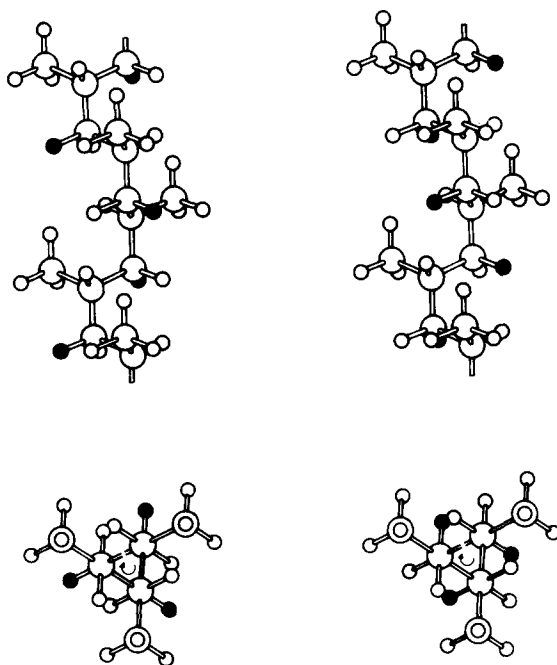


Figure 7

modifications^{32,34} and isotactic polybutene-1 has at least two modifications³⁵. At times they are difficult to prepare. For instance, hitherto it was thought that isotactic polybutene-1 had a melting temperature of about 80°C, while it probably yields a stable modification, melting above 110°C³⁵.

Modifications with a density lower than that of the corresponding atactic polymer, as with isotactic polyvinylcyclopropane³⁶, have also been observed in tactic polymers.

Among the polymorphic modifications of one polymer, one is generally stable and the others are metastable. So far, with *trans*-tactic polybutadiene only, two stable modifications were recognized for certain; they can be transformed one into the other, following a solid-solid thermodynamic transition²⁹.

Figure 9 shows the dilatometric curve of a sample of *trans*-tactic polybutadiene, in which the transition can be observed taking place at 76°C from a higher density modification into a second one having a much lower density and melting at 146°C³⁷.

By studying stereoregular copolymers, new concepts on isomorphism could be introduced. Thus, in various cases already, it has been observed that certain copolymers, prepared by using stereospecific catalysts, are crystallizable in the entire range of compositions.

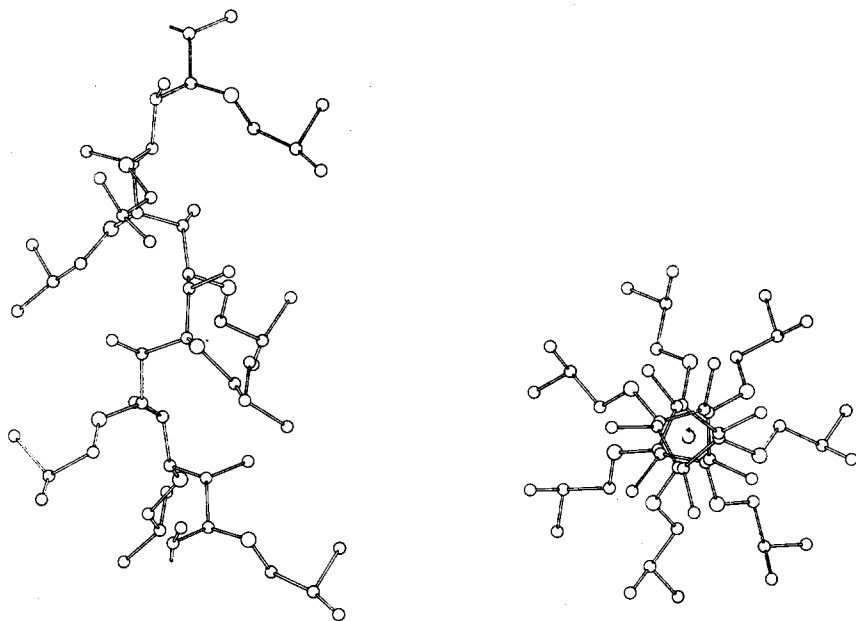
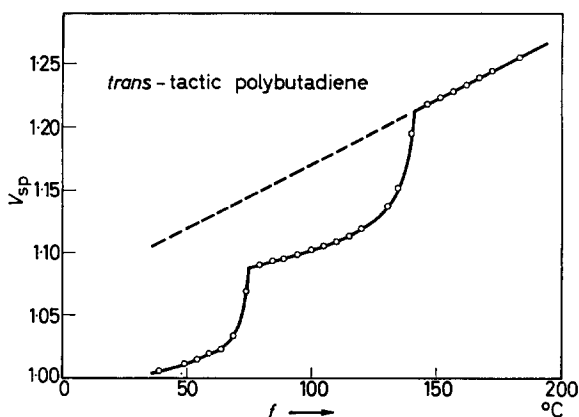


Figure 8

In Figure 10 the dependence of the melting temperature on the composition is reported for isotactic styrene-*p*-fluorostyrene copolymers³⁸. In this case, the crystallinity is present at any composition by virtue of a phenomenon which may be identified with isomorphism, and may be called 'monomeric unit isomorphism': the co-monomeric units of different type,

Figure 9
440

but of fairly similar structure, allow the mixed chains to crystallize in a single three-dimensional lattice. The compositions on the left of the diagram have ternary helix shape, while those on the right have quaternary helix shape.

In addition cases have been observed of 'isomorphism of chains', in which chains of different polymers or copolymers can pack together in a single crystalline lattice, with formation of solid solutions³⁹.

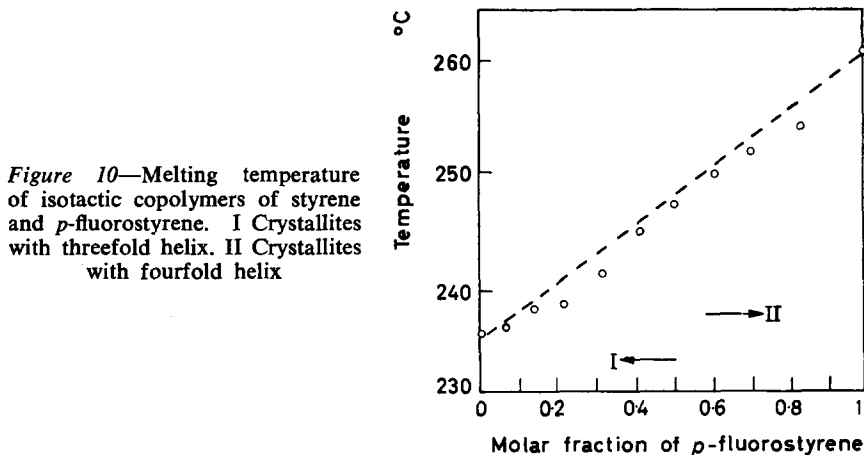


Figure 10—Melting temperature of isotactic copolymers of styrene and *p*-fluorostyrene. I Crystallites with threefold helix. II Crystallites with fourfold helix

By raising the temperature of a stereoregular polymer whose molecules are in ordered conformations with which we have so far dealt, the articulate macromolecules of the polymer progressively acquire degrees of freedom and therefore a tendency to more and more disordered conformations. If, in particular, the polymer was in the crystalline state, it undergoes melting and becomes amorphous.

Analogous phenomena occur if the polymer is dissolved in a solvent.

The defects thus created in the originally ordered conformations can be thought of as due to the appearance here and there in the chains of free 'joints' or 'folds', that allow establishment of a universe of conformations in the whole of the molecules of the polymer. The polymer will become intrinsically mobile and will assume physical, mechanical and rheologic properties peculiar to the macromolecular amorphous or solution state.

Also the topic of the molecular conformation of stereo-ordered polymers in the amorphous state or in solution, has always been the object of particular attention for many scientists.

At the beginning, the apparently strong tendency of the stereo-ordered macromolecules to assume regular conformations led one to believe that, even if they lost the peculiar packing of the crystalline solid state, they had to maintain a relatively stiff conformation even in the amorphous or solution state.

The study of the properties of the stereoregular polymers in solution, carried out for the first time on isotactic polystyrene⁴⁰ and subsequently

on some other polymers, soon showed that the average molecular dimensions of an isotactic polymer in solution are not very different from those of a corresponding atactic polymer. This has indicated that the 'joints' or 'folds' arising in respect of the primitive ordered conformations should be numerous also in the tactic macromolecules.

The observations on tactic polymers in solution, which furnish much analogous information on the pure amorphous state, are nowadays rather extensive, but the solvents used have usually been 'good' solvents. A broader research with 'bad' solvents might now be opportune, because most probably it will point out that, under thermodynamic conditions very near to precipitation, the stereoregular macromolecules should tend to become stiffer, foreshadowing a transition to the ordered, solid state.

Actually it is known that the swelling of crystallizable polymers in the metastable amorphous state in suitable non-solvent liquids causes rapid crystallization of the polymers themselves.

Fairly fundamental research on the thermodynamic fusion quantities of the stereo-ordered polymers, such as enthalpy and entropy of fusion, was carried out, but unfortunately it did not yet give a clearly significant contribution to the solution of these problems⁴¹.

Anyway, from the above considerations, it is possible, in principle, to conclude that the macromolecule of a tactic polymer in the amorphous or solution state nowadays can be reasonably conceived as being constituted by segments of chain conformed in a way essentially similar to that of the solid state, that is in an ordered conformation, interposed by 'joints' or 'folds', on the nature of which⁴² there is at the moment an active interest in research.

A further interesting aspect of the conformations of stereoregular polymers, whose ordered conformations are helicoidal, is that of the internal distribution of enantiomorphous conformations.

Frequently, in the crystalline lattices of these polymers, two adjacent chains have not identical, but rather enantiomorphous conformations. By neglecting other possible differences, in the case of helicoidal chains the two facing conformations are a left-handed and a right-handed helix. An example of this situation can be seen in *Figure 11* for the elementary unit cell of isotactic polybutene-1, in which the two types of enantiomorphous chains are indicated with A and B⁴³.

From the calculations carried out up to now of the conformational potential energy as a function of the successive internal rotation angles of an isolated regular chain, it has been deduced that the transformation of a helicoidal ordered conformation into its enantiomorphous one generally comprises a very limited potential barrier⁴⁴. With it, when the polymer passes into the amorphous or solution state, it must be expected that the various chain segments, which maintain an ordered conformation, can almost indifferently assume a given helicoidal conformation, or its enantiomorphous conformation. An equal probability of the two conformations should cause the chains to assume not only in different macromolecules, but also in different segments of a single macromolecule, mixed conformations of about 1 : 1 of each.

An interesting indication of this situation was obtained by preparing isotactic polymers of branched alpha-olefines, which are optically active due to an asymmetric carbon atom in their molecule⁴⁵. The polymers obtained have in various cases a much higher optical activity than that of the monomer.

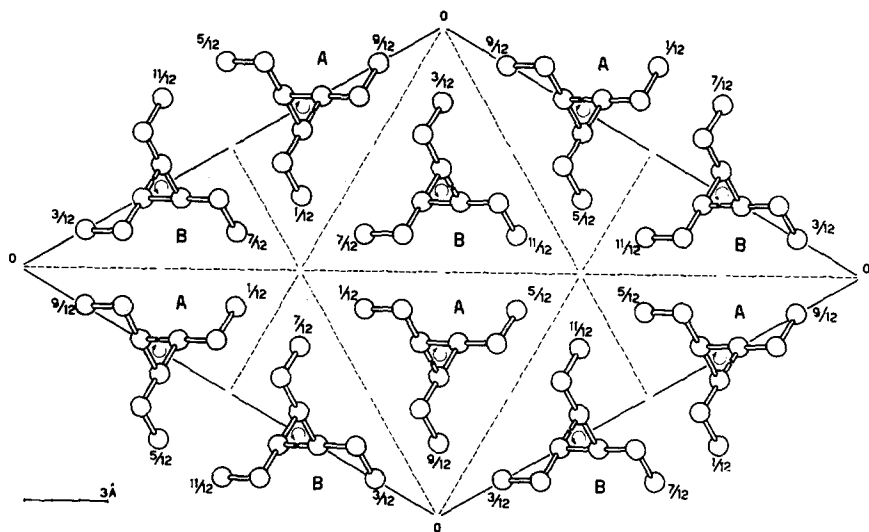


Figure 11

This phenomenon can be explained by the fact that the asymmetric carbon atoms, which are adjacent to the main chain and unbalanced in their two possible configurations, preferentially stabilize one of the two enantiomorphous helicoidal conformations of the polymeric chain (a phenomenon analogous to that observed in polyaminoacids with asymmetric and antipodic carbon atoms in the chain). As a consequence a conformational asymmetry is created in the polymer, which is the cause of the marked increase of the optical activity. This last should originate not so much from the helicoidal shape of the chain as from the lack of balance of the conformational isomerism of the monomeric units, with relation to their mode of insertion in the chain. In fact, the marked optical activity measured in the polymer is of the same order as that which can be calculated in model substances with low molecular weight, supposing their molecule stabilized in one of the possible conformations⁴⁶.

FUTURE DEVELOPMENTS AND APPLICATIONS

Even if impossible to examine here further peculiarities of stereoregular polymers and polymerization, it is at once understandable that macromolecular scientists expect many and ever more numerous developments in this field.

The refining of the conditions of stereospecificity of the reactions will no

doubt allow the preparation of many new polymers endowed with high degrees of steric purity. Similarly, the refining of the methods of characterization of the products will also facilitate notable developments in the study of the relations between properties and structure. From various points of view this will be simplified by the opportunity to operate on ever more numerous polymers having well known molecular structure. In other words no particular limit can be seen to a steadily increasing scientific interest in this field, engaging an ever-increasing number of workers.

Next to the scientific interest there are now other important interests of a practical nature and it is convenient to say a few words on them.

It cannot be doubted that if the scientific interest finds no foreseeable limit today, the practical interest is always firmly anchored to economic aspects.

Therefore it is obvious that industrial action polarizes at first exclusively on polymers derived from monomers of greater economic convenience; and immediately afterwards on those which by a suitable intensification of research can be expected to be advantageously obtained in the very near future. Still later we may have the eventual consideration of polymers producible from costly monomers, but for this it will be necessary to consider whether the quality will compensate for the greater cost of production.

Today industrial interest is still mainly centred on polymers derived from particularly cheap and plentiful monomers and therefore limited to monomers of a relatively simple molecular structure.

The balance of the bulk of industrial results finds the following polymers in the most advanced positions at present: the very versatile isotactic polypropylene, for the production of plastic materials, fibres and films; the *cis*-tactic polybutadiene and polyisoprene, for the preparation of rubber having a wide field of application and good characteristics; the ethylene-propylene copolymers possibly in the form of ter-polymers with special dienes, which can also be used for the production of cheap rubber with satisfactory properties.

Some other polymers are at present the object of advanced applied research, but for them the interest of industrial production in the proper sense is still to be seen. Among them we find the isotactic poly-butene-1 and polystyrene, and also the isotactic polymers of some aliphatic olefines with a branched substituent.

For other stereoregular polymers, a possible practical development rests with future research, and on this question it is relatively difficult to make any forecast.

The highly stereoregular polymers which have had up to now a positive success are hydrocarbon polymers. Research, however, has prepared several stereoregular polymers of monomers containing hetero-atoms (above all oxygen), of varying chemical nature (ethers, esters, aldehydes, ketones and ketenes). For some of these, there is no serious reason to exclude early development, limited perhaps to special applications. For many others there is a widespread feeling that there may be serious obstacles due particularly to poor thermal stability.

It is interesting to recall that still today the properties of the crystalline state appear to be of fundamental importance for the application of the stereoregular polymers.

Crystallinity attended by high melting temperatures may lead to good mechanical resistance and good dimensional stability, high hardness and elastic modulus, in polymers which can be employed as plastics and construction materials.

Furthermore, high melting temperature and high regularity of the molecular structure may involve high tenacity and orientability under stretching in materials suitable for fibres and films. For these materials the hydrocarbon stereoregular polymers have further demonstrated that the high interactions of a polar character are not indispensable in polymeric chains, as normally occurs in fibres previously developed. The high steric purity should also allow elimination of unfavourable effects due to relatively high glass transition temperature or to solubility of the crystalline polymer in common solvents.

Even in the application to rubber, the crystallizability of stereoregular polymers, even if requiring stretching lower temperatures, appears to be useful for aspects which today might still seem secondary but are probably fundamental. It cannot in fact be overlooked that natural rubber, whose characteristics are undoubtedly considered to be very good, is a stereoregular polymer, just like a number of other interesting natural polymers.

*Istituto di Chimica Industriale del Politecnico,
Piazza Leonardo da Vinci 32,
Milan, Italy*

DISCUSSION

Dr J. Corbiere (France): You have said that the regulation is of special interest for cheap monomers and cheap polymers, but your remarks refer mainly to hydrocarbon monomers. There are other polymers which are cheap and which I suppose would be of interest to have in stereoregular forms, such as polyacrylonitrile or polyvinyl alcohol. You have not spoken about these. Is it because the monomers are too difficult to polymerize with stereoregulation, or is there some other reason?

Professor F. Danusso (Italy): I have spoken about fully stereoregular polymers of the greatest industrial importance. It is possible that other stereoregular polymers can be employed with success for special applications, but so far we have not seen any application on a commercial scale of the polymers you have mentioned (as yet stereoregular only to some extent).

In my lecture the attention was mainly focused on hydrocarbon polymers from particularly cheap monomers, with which it is possible to reach substantially stereoregular polymers, among which some are largely recognized today as new materials and have become industrially important. As for the polymers you have mentioned, although these are endowed in particular cases with some degree of stereoregularity, they constitute improved rather than new materials.

Dr C. W. Bunn (U.K.): You mentioned a number of polymers which did not crystallize, or have not yet been crystallized, although I gather the evidence is that they have a stereoregular character. What is the reason for this?

Professor F. Danusso (Italy): Some of these polymers show infra-red bands which must refer to an ordered molecular conformation, but we must assume that the polymers cannot effect the packing necessary for three-dimensional ordering. For others it has been impossible to recognize significant infra-red bands. Thus, there are two cases for non-crystallizable polymers:

- (a) the polymer has difficulty in packing, although it has an ordered conformation;
- (b) the polymer cannot easily achieve an ordered conformation in single macromolecules.

Dr C. W. Bunn (U.K.): If the molecule itself is stereoregular why can it not take up an ordered configuration?

Professor F. Danusso (Italy): It is difficult to answer this question with certainty. Perhaps the polymer is formed in a disordered state and it cannot easily reach an ordered state, but in principle this is possible.

Dr C. W. Bunn (U.K.): One of the substances which does not crystallize is a fluorostyrene, is it not?

Professor F. Danusso (Italy): Isotactic polymers of ortho- and para-fluorostyrene crystallize, but isotactic polymers of meta-fluorostyrene do not.

Dr C. W. Bunn (U.K.): A fluorine atom is not very much bigger than a hydrogen atom, yet the unsubstituted styrene crystallizes well.

Professor F. Danusso (Italy): Yes, but there are evidently particular interactions, perhaps hydrogen bonding, which prevent crystallization.

Dr M. Gordon (U.K.): Could Professor Danusso enlarge a little on the role of the counterion in the stereospecific polymerization reaction?

Professor F. Danusso (Italy): I think that the view of the counterion at the moment is the opposite of that which was held originally. I think that in many cases there is a very clear role of the counterion, independent of the nature of the ion. In other cases there is a specific contribution by the ion also. In some cases it is difficult to think that the ion has any relevance in the first stage of the reaction. There are cases in which you can see, for instance, a copolymerization which proceeds as two independent simultaneous homopolymerizations. To have this it is necessary that the counterion shall attack the two monomers and that it is the only reagent attacking monomer molecules. The ion then does not play any role in kinetic and mechanical control. Other cases are possible in which a more concerted mechanism can be devised.

REFERENCES

- ¹ NATTA, G. *Atti Accad. Lincei, Mem.* 1955, **8**, 4
- NATTA, G., PINO, P., CORRADINI, P., DANUSSO, F., MANTICA, E., MAZZANTI, G. and MORAGLIO, G. *J. Amer. chem. Soc.* 1955, **77**, 1708
- ² ZIEGLER, K. *Angew. Chem.* 1955, **67**, 426
- ³ SCHILDKNECHT, C. E., GROSS, S. T., DAVIDSON, H. R., LAMBERT, I. M. and ZOISS, A. O. *Industr. Engng Chem. (Industr.)*, 1948, **40**, 2104

- ⁴ NATTA, G., BASSI, I. W. and CORRADINI, P. *Makromol. Chem.* 1955, **18-19**, 455
- ⁵ MORTON, A. A. *Industr. Engng Chem. (Industr.)*, 1950, **42**, 1488
- ⁶ WILLIAMS, J. L. R., VAN DEN BERGHE, J., DULMAGE, W. J. and DUNHAM, K. R. *J. Amer. chem. Soc.* 1956, **78**, 1260; 1957, **79**, 1716
- ⁷ NATTA, G. and DANUSSO, F. *Chim. e Industr.* 1958, **40**, 445
- ⁸ NATTA, G. and DANUSSO, F. *J. Polym. Sci.* 1959, **34**, 3
- NATTA, G., FARINA, M. and PERALDO, M. *J. Polym. Sci.* 1960, **43**, Issue N.142
- HUGGINS, M. L., NATTA, G., DESREUX, V. and MARK, H. *J. Polym. Sci.* 1962, **56**, 153
- ⁹ NATTA, G. *Makromol. Chem.* 1960, **35**, 111
- NATTA, G., PASQUON, I., CORRADINI, P., PERALDO, M., PEGORARO, M. and ZAMBELLI, A. *R. C. Accad. Lincei*, VIII, 1960, **28**, 539
- ¹⁰ NATTA, G., FARINA, M., PERALDO, M., CORRADINI, P., BRESSAN, G. and GANIS, P. *R. C. Accad. Lincei*, VIII, 1960, **28**, 442
- ¹¹ NATTA, G., DALL'ASTA, G., MAZZANTI, G., PASQUON, I., VALVASSORI, A. and ZAMBELLI, A. *J. Amer. chem. Soc.* 1961, **83**, 3343
- ¹² NATTA, G., FARINA, M., PERALDO, M. and BRESSAN, G. *Makromol. Chem.* 1961, **43**, 68
- NATTA, G., FARINA, M., PERALDO, M. and BRESSAN, G. *Chim. e Industr.* 1961, **43**, 161
- ¹³ NATTA, G., PORRI, L., CORRADINI, P., ZANINI, G. and CIAMPELLI, F. *R. C. Accad. Lincei*, VIII, 1960, **29**, 257
- ¹⁴ NATTA, G., PORRI, L., CARBONARO, A. and LUGLI, G. *Chim. e Industr.* 1961, **43**, 529
- ¹⁵ NATTA, G., FARINA, M., CORRADINI, P., PERALDO, M., DONATI, M. and GANIS, P. *Chim. e Industr.* 1960, **42**, 1361
- ¹⁶ NATTA, G., FARINA, M., DONATI, M. and PERALDO, M. *Chim. e Industr.* 1960, **42**, 1363
- ¹⁷ See for example: NATTA, G. *Experientia*, Suppl. VII, 1957, 21
- NATTA, G., DANUSSO, F. and PASQUON, I. *Coll. Czech. Chem. Commun.* 1957, **22**, 191
- ¹⁸ See for example: NATTA, G. and PASQUON, I. *Advances in Catalysis*, Vol. XI, p 1. Academic Press: New York, 1959
- ¹⁹ See for example: NATTA, G., DANUSSO, F. and SIANESI, D. *Makromol. Chem.* 1959, **30**, 238
- DANUSSO, F. and SIANESI, D. *Chim. e Industr.* 1962, **44**, 474
- DANUSSO, F. *Chim. e Industr.* 1962, **44**, 611
- ²⁰ DANUSSO, F. *Makromol. Chem.* 1960, **35A**, 116
- ²¹ NATTA, G. and CORRADINI, P. *J. Polym. Sci.* 1959, **39**, 29
- NATTA, G. and CORRADINI, P. *Nuovo Cim. Suppl.* 1960, **15**, 9
- LIQUORI, A. M. Lecture at the Summer School on Advanced Inorganic Chemistry, Varenna, 1959 (book by Accademia Nazionale Lincei: Roma)
- NATTA, G., CORRADINI, P. and GANIS, P. *Makromol. Chem.* 1960, **39**, 238
- LIQUORI, A. M. Lecture at Summer Course of Macromolecular Chemistry, Varenna, 1961 (book by Consiglio Nazionale Ricerche: Roma)
- ²² See for example: NATTA, G., DANUSSO, F. and SIANESI, D. *Makromol. Chem.* 1958, **28**, 253
- ²³ MURAHASHI, S., NOZAKURA, S. and TADOKORO, H. *Bull. chem. Soc. Japan*, 1959, **32**, 534
- ²⁴ NATTA, G. and SIANESI, D. *R. C. Accad. Lincei*, VIII, 1959, **26**, 418
- NATTA, G. *Makromol. Chem.* 1960, **35**, 93
- ²⁵ NATTA, G. Lecture held at the 133rd National Meeting of the American Chemical Society, San Francisco, 13 to 18 April 1958
- ²⁶ NATTA, G., CORRADINI, P. and CESARI, M. *R. C. Accad. Lincei*, VIII, 1957, **22**, 11
- ²⁷ NATTA, G. and CORRADINI, P. *R. C. Accad. Lincei*, VIII, 1955, **19**, 229
- ²⁸ NATTA, G. and CORRADINI, P. *J. Polym. Sci.* 1956, **20**, 251
- ²⁹ See for example: NATTA, G. and CORRADINI, P. *Nuovo Cim. Suppl.* 1960, **15**, 9
- ³⁰ NATTA, G., FARINA, M. and PERALDO, M. *R. C. Accad. Lincei*, VIII, 1958, **25**, 424
- ³¹ NATTA, G. *Makromol. Chem.* 1960, **35**, 94

-
- ³² NATTA, G., CORRADINI, P. and BASSI, I. W. *R. C. Accad. Lincei*, VIII, 1955, **19**, 404
- ³³ NATTA, G., PERALDO, M. and CORRADINI, P. *R. C. Accad. Lincei*, VIII, 1959, **26**, 14
- ³⁴ ZANNETTI, R., MANARESI, P. and BUZZONI, G. *Chim. e Industr.* 1961, **43**, 735
- ³⁵ DANUSSO, F. and GIANOTTI, G. Unpublished results
- ³⁶ DANUSSO, F. and FASSI, R. Unpublished results
- ³⁷ MORAGLIO, G. Unpublished results
- ³⁸ SIANESI, D., PAJARO, G. and DANUSSO, F. *Chim. e Industr.* 1959, **41**, 1176
NATTA, G. *Makromol. Chem.* 1960, **35**, 93
- ³⁹ NATTA, G., CORRADINI, P., SIANESI, D. and MORERO, D. *J. Polym. Sci.* 1961, **51**, 527
- ⁴⁰ DANUSSO, F. and MORAGLIO, G. *J. Polym. Sci.* 1957, **24**, 161
- ⁴¹ See for example: DANUSSO, F. Lecture at the Summer Course of Macromolecular Chemistry, Varenna 1961 (book by Consiglio Nazionale Ricerche: Roma)
- ⁴² LIFSON, S. *J. chem. Phys.* 1958, **29**, 80; 1959, **30**, 965
BIRSTEIN, T. M. and PTITSYN, O. B. *Zh. fiz. Khim.* 1954, **28**, 213
CORRADINI, P. and ALLEGRA, G. *R. C. Accad. Lincei*, VIII, 1961, **30**, 516
- ⁴³ NATTA, G., CORRADINI, P. and BASSI, I. W. *Nuovo Cim. Suppl.* 1960, **15**, 52
- ⁴⁴ CORRADINI, P. and ALLEGRA, G. *R. C. Accad. Lincei*, VIII, 1961, **30**, 516
- ⁴⁵ PINO, P., LORENZI, G. P. and LARDICCI, L. *Chim. e Industr.* 1960, **42**, 711
PINO, P. and LORENZI, G. P. *J. Amer. chem. Soc.* 1960, **82**, 4745
- ⁴⁶ PINO, P. Lecture at the Summer Course of Macromolecular Chemistry, Varenna 1961 (book by Consiglio Nazionale Ricerche: Roma)

Polymerization in the Solid State

M. MAGAT

Following a brief description of early investigations of processes of polymerization, the author discusses mechanisms likely to operate in the solid state and deals with the polymerizability of various monomers, factors determining whether a monomer may be polymerized in the solid state, the mechanism of solid state polymerization, activation energy and polymerization at very low temperatures, influence of 'texture' of solid, and stereospecificity of polymers.

I. HISTORICAL INTRODUCTION

WHILE bimolecular reactions of inorganic compounds in the solid state have been the subject of many investigations over a long period, the study of the reactions of organic substances under the same conditions have only recently begun. The reason for this is that, in view of the bulkiness of organic molecules it seemed unlikely that the movement of molecules in the middle of a lattice could take place with sufficient speed. In particular the possibility of polymerization in the solid state involving the displacement of a large number of molecules appeared *a priori* to be impossible. Nevertheless in 1933 Letort¹ in France and Travers² in England reported that acetaldehyde polymerized spontaneously 'on crystallization', or more exactly on fusion³ of the crystals of this substance.

It was not until 1954 that research on polymerization in the solid state was opened by a series of publications by Mesrobian, Adler, Ballantine, Dienes and co-workers^{4, 5} on the polymerization of crystalline acrylamide initiated by ionizing radiation. These authors found the ideal method for the initiation of such polymerizations, that is to say for the production *in situ* of radicals and eventually of ions which may catalyse them; since even if it possible in certain cases, as Bamford, Jenkins and Ward⁶ have since shown, to produce radicals by a photochemical route, this method of initiation is usually prevented by the optical inhomogeneity of the medium.

The work of Mesrobian and co-workers was followed in 1956 by the work of Lawton, Grubb and Balwit⁷ who showed that the polymerization of hexamethylcyclotrisiloxane by ionizing radiation was not only possible in the solid state but occurred only in the solid state. In 1959 Bensasson^{8, 9} on the one hand and Sobue and Tabata¹⁰ on the other showed that polymerizations in the solid state were not limited to solid monomers at ambient temperatures and above, but can also be carried out at low temperatures. They showed that acrylonitrile polymerizes 10 or 20 times more rapidly in the solid state than at several degrees above the melting point.

II. EXPERIMENTAL RESULTS CONCERNING THE POLYMERIZABILITY OF VARIOUS MONOMERS

We have gathered in the *Tables 1 to 4* the monomers whose polymerization in the solid state has been studied to date. This list is considerably longer than that which we published two years ago. We have indicated for each

monomer its melting point, the range of temperatures studied, the existence or otherwise of a post-effect, the type of initiation used and the ratio of the rates above and below the melting point (V_s/V_l).

It is striking that the number of monomers polymerizable in the solid state is very large, and that monomers of widely varying types are represen-

Table 1. Vinyl and divinyl monomers

| Monomers | M. pt (°C) | Tempera- ture of irradiation | Poly- meri- zation | Post- effect | Initiation | $\frac{V_s}{V_l}$ | $E_{sol.}^\dagger$ kcal/ mol | Refer- ences |
|-----------------------------------|---------------|------------------------------------|--------------------------|-----------------|---------------|-------------------|------------------------------------|-----------------|
| Styrene | -30 | -196 | - | + | γ | | | |
| α -Methylstyrene | -23 | -78 to -51 | + | + | γ | ≥ 1 | 9.2 | 11, 12, 13 |
| 2-4-Dimethyl- styrene | | -196, -78 | - | - | γ | 0 | — | 12 |
| Vinyl acetate | -159 | -80 | + | ? | γ | ? | ~ 1 | 13 |
| Vinyl carbazole | +64 | -196 | + | ? | γ | ~ 1 | 0 | 14 |
| Vinyl toluene | | 20 to 6.0; 70.9P (1) | + | + | γ | ≤ 1 | ~ 12 | 15 |
| Vinyl chloride | -138 | — | + | + | γ | — | ? | 16 |
| Vinylidene chloride | -80 | -196 to -138 | - | - | γ | 0 | ? | 5 |
| Vinyl stearate | +34 | -196 | - | - | γ | 0 | ? | 17 |
| Butadiene | | +34 | + | ? | γ, e^- | < 1 | ~ 1.5 | 18, 19 |
| Isoprene | | -196 | + | ? | γ | ? | ? | 20, 21 |
| Vinylpyrrolidone | +13.5 | -196 | + | ? | γ | ? | ? | 20 |
| Vinyl caprolactane | ? | +7 | + | ? | γ | ~ 1 | — | 22 |
| <i>n</i> -Succylvinylimide | ? | ? | —* | ? | γ | ≤ 1 | — | 23 |
| <i>n</i> -Vinylphthalyl- imide | ? | ? | -† | ? | γ | ≤ 1 | — | 23 |
| Vinyl octadecyl ether | +30 | ? | -† | ? | γ | ≤ 1 | — | 23 |
| Hexadecene | +4.2 | +10, +50 (1) | + | ? | γ | > 1 | ? | 24 |
| Isobutylene | -141 | -196, -77, 0, +20 (1) | + | ? | γ | ~ 2 | small | 25 |
| ρ -Vinylacetanilide | +148 | -196, -80 (1) | + | ? | γ | ~ 1 | ? | 26 |
| 1-Carboxybuta- diene | | +110 | + | ? | thermal | ? | ? | 27 |
| | | ? | + | ? | thermal | ? | ? | 27 |

*Polymerized very rapidly in the molten state.

†Explosive polymerization on dissolving.

ted. One even finds monomers such as acetone and trioxan whose polymerization in the liquid state has never been described as far as we know. Certain of these polymerizations proceed very rapidly: explosive polymerizations have been observed with formaldehyde and acetaldehyde, while others are very slow, as is the post-polymerization of acrylamide^{27, 49}.

III. FACTORS DETERMINING WHETHER A MONOMER MAY BE POLYMERIZED IN THE SOLID STATE

On the basis of *Tables 1* and *4*, let us try to deduce the conditions which determine whether or not a monomer may be polymerized in the solid state.

POLYMERIZATION IN THE SOLID STATE

Table 2. Acrylic monomers

| Monomer | M.pt (°C) | Temperature of irradiation | Polymerization | Post-effect | Initiation | $\frac{V_s}{V_l}$ | $E_{sol.} \dagger$ kcal/mole | References |
|-----------------------|--------------|-----------------------------------|----------------|-------------|----------------|-------------------|---------------------------------|-------------------------|
| Acrylic acid | +12 | ? | + | ? | γ | — | ? | 5 |
| Methacrylic acid | +16 | 0 | + | | u.v., γ | ? | ? | 6, 27 |
| Acrylamide | +85 | 0 to +60 | + | + | $\gamma, C(=)$ | | ?(+) | 4, 5, 28, 29, 30, 31 |
| Methacrylamide | +16 | ? | + | ? | γ | <1(?) | ? | 5, 32 |
| Acrylonitrile | -83 | -196 to -135 -135 to -83 | + + (?) | - | γ | | 0 | 8, 10, 17 |
| Methacrylonitrile | -40 | -196; -78 | + | + | γ | ≥ 1 | 1.5 | 8, 14, 17 |
| Methylacrylate | | -196; -78 | - | - | γ | ? | ? | 12, 33 |
| Methylmethacrylate | -50 | -196; -78 | - | - | γ | 0 | ?(++) | 12, 16 |
| Octadecylmethacrylate | +17 | -10; +30 (l) | + | ? | $\gamma; u.v.$ | 0 | ?—(++) | 12, 16 |
| Cetylmethacrylate | ? | ? | + | ? | γ | $\sim 1 \dagger$ | <0 | 34 |

(+) Shows a post-effect.

(++) Polymerizes rapidly in a glass formed by adding liquid paraffin.

(=) Azobis-isobutyronitrile.

† This monomer shows a maximum rate of polymerization at the melting point.

Two factors may be envisaged: the crystalline structure and the mechanism of polymerization.

(a) Crystalline structure

Unfortunately the exact crystalline structure of most of the monomers studied is not known. In view of the diversity of monomers polymerizable in the solid state it might be thought that this factor can play only a secondary role. This conclusion would be false since Morawetz²⁸ has shown that the different salts of acrylic and methacrylic acids which all possess the same polymerizable group, but have different structures, polymerize at very different rates. The same holds true for the different hydrates of calcium acrylate and even for the anhydrous crystals prepared from different hydrates²². It is nevertheless possible that these variations result not from different structures but from the different distances between double bonds, a factor which, according to Schmidt⁵⁰ determines the possibility of photochemical reactions between unsaturated compounds in the crystalline state. It should be pointed out that in other cases (polymerization of methylmethacrylate as a solid solution of monomer in liquid Paraffin^{12, 16}) an increase in intermolecular distance does not impede the reaction.

While waiting for the determination of crystalline structure of monomers, which is actually being carried out in several laboratories, it thus appears difficult to relate the possibility of polymerization in the solid state to crystalline structure.

It should be pointed out, however, in those cases where polymerization proceeds in the solid state and where the crystalline structure has been

Table 3. Various monomers

| Monomer | M. pt (°C) | Temperature of irradiation | Poly- meri- zation | Post- effect | Initiation | $\frac{V_s}{V_i}$ | $E_{sol.} \dagger$ kcal/mole | Refer- ences |
|----------------------------------|---------------|-------------------------------|--------------------------|-----------------|-----------------------|-------------------|---------------------------------|-------------------|
| Formaldehyde | -118 | -196 to -160 | + | + | γ | ≥ 1 | 2.2 | 14, 35, 36, 37 |
| Acetaldehyde | -123 | -160 to -118 | + | + | γ | ≥ 1 | ? | 36 |
| | | -196 to -150 | — ^(?) | — | γ | | 0 ^(?) | |
| Acetone | -95 | -196; -136 | + | ? | $\gamma, Mg \ddagger$ | ≥ 1 | ? | 38, 39 |
| Chloracetone | -44.5 | -78 | + | ? | γ | ? | ? | 39 |
| Bromacetone | -54 | -78; 0 (l) | + | ? | γ | ≥ 1 | ? | 39 |
| Trioxan | +64 | +30 to +80 | + | + | γ | ≥ 1 | ? | 39, 40, 41 |
| β -Propiolactone | -33.4 | -196 to -132 | + | —? | γ | — | 0.08 | 40, 42 |
| | | -132 to -70 | + | + | γ | ≥ 1 | 6.3 | 40, 42 |
| | | -70 to -33 | + | + | γ | ≥ 1 | -12.6 | 40, 42 |
| Diketene | -6.5 | -196 to -130 | + | +? | γ | ≥ 1 | 0.11 | 40, 43 |
| | | -130 to -6.5 | + | +? | γ | ≥ 1 | -2.4 | 40, 43 |
| 3-3-Bis-chloro- methyloxetane | +17 | -78 to +16.4 | + | + | γ | ≥ 1 | 3 | 40, 44 |
| Hexamethyl-cyclo- trisiloxane | +64 | +0 to +64 | + | ? | γ | ≥ 1 | 9.6 | 7, 45 |
| Cyanuric chloride | +146 | +16; +100 | + | ? | γ | ? | ? | 46 |
| Triphosphonitrilic chloride | +113 | +20; -70 | — | — | γ | ? | ? | 47 |
| Acetonitrile | -41 | -78; +20 (l) | + | ? | $\gamma, Mg \ddagger$ | ≥ 1 | ? | 48 |

*Explosive under certain conditions.

†Glassy deposit of a mixture of solvent and monomer followed by a rise in temperature.

‡No opening of the ring.

determined, that the polymer chain is already ordered in the crystal. This is so for acrylamide⁴, acetaldehyde⁵¹, trioxan⁵² and diketene⁵³.

(b) Mechanism of polymerization

We shall see later that the determination of the polymerization mechanism in the solid state presents problems which have not so far been completely resolved. Radical and cationic mechanisms would seem to be the most probable. But it is remarkable that several monomers which polymerize by radical and anionic mechanisms (vinyl chloride, vinylidene chloride, methylmethacrylate and methacrylate) cannot be polymerized in the solid state. This is not a general rule as several exceptions are known: acrylonitrile, methacrylonitrile, acrylamide, methacrylamide and acrylic and methacrylic acids. But for several of these monomers there are strong indications that solid state polymerizations occur by a radical

POLYMERIZATION IN THE SOLID STATE

Table 4. Post-polymerization of salts of acrylic and methacrylic acids^{27, 28}

| Monomer | T°C | Time for 10% conversion | Remarks |
|-----------------------------|-----|---|------------------------------|
| K ⁺ acrylate | 35 | 9800 | — |
| Na ⁺ | 150 | 35000 | — |
| Li ⁺ | 150 | 12000 | — |
| | | % conversion after 2.5 × 10 ⁶ sec | — |
| K ⁺ methacrylate | 153 | 3.5 | — |
| Na ⁺ | 153 | 7.5 | — |
| Li ⁺ | 153 | 0.0 | — |
| Ca ²⁺ acrylate | 50 | 18 | crystalline dihydrate |
| | 50 | 0 | crystalline mono- hydrate |
| | 100 | 6.3 | dehydrated mono- hydrate |
| | 100 | 46 | dehydrated dihydrate |

mechanism. The case of vinyl chloride is particularly interesting since it is known from other sources that the polar chlorides favour cationic rather than anionic polymerization; hence this monomer would be its own inhibitor.

However, these conclusions are only provisional and it must be recognized that it is impossible actually to predict whether a monomer will polymerize in the solid state or not.

IV. MECHANISM OF SOLID STATE POLYMERIZATION

In the initiation of solid state polymerizations by ionizing radiation, the establishment of the mechanism poses a very difficult problem, since most of the methods used to elucidate the mechanism in the liquid phase are not usable or give ambiguous results.

(a) Inhibition by radical scavengers

If it is accepted that however much the scavenger may diffuse, the diffusion of the growing chain is suppressed in the solid, the scavenger can react only either with radicals formed on adjacent sites, or with chains which in the course of their growth come into contact with the scavenger. To be efficient, the scavenger must therefore; (i) be present in fairly high concentrations; (ii) 'syncrystallize' with the monomer. But here the apparent inhibiting effect may result from lattice distortion, i.e. an effect which is not specific. Thus while the addition of five per cent of benzoquinone reduces by half the rate of polymerization of solid acrylonitrile, the addition of the same quantity of toluene produces an effect at least as great¹².

For methylmethacrylate mixed with liquid paraffin, Chapiro showed that the presence of oxygen inhibited the reaction, resulting in a fairly long induction period, indicating a radical polymerization in this case.

(b) Copolymerization

The study of copolymerization runs into the same difficulty of 'syncrystallization'. While Okamura and Hayashi have succeeded in copoly-

merizing in the solid state β -propiolactone with diketene and γ -butyrolactone^{52, 53} it has only been possible to prepare the copolymers of acrylamide with methacrylamide²⁹ and acrylamide with acrylonitrile⁵⁴ in the solid state.

(c) *Order of reaction*

The only order of reaction that can be determined experimentally is the order with respect to the intensity of the ionizing radiation. It is known that if a quasi-stationary state is established for bimolecular chain termination, which predominates in liquid phase polymerizations by radical mechanisms, this order α is $\frac{1}{2}$. If the termination is monomolecular (as for ionic polymerizations) $\alpha = 1$.

In the solid state, because of the absence of diffusion the bimolecular termination coefficient cannot occur, or occurs only very slowly. The stationary state cannot be reached, and one cannot expect to find an order of $\frac{1}{2}$ for polymerizations proceeding by a radical mechanism. In the absence of a quasi-stationary state, a value of $0.5 < \alpha < 1$ observed for vinylcarbazole¹⁵ and for formaldehyde³⁶ is at the very most an indication of an important radical contribution. The value $\alpha = 1$ found³⁶ for acetaldehyde at 131°C neither contradicts, nor demonstrates an ionic mechanism.

(d) *Photopolymerization*

The possibility of initiating polymerization by irradiating the monomer with ultra-violet (u.v.) light is undoubtedly an indication in favour of a radical mechanism, but it should not be forgotten that the ionization potential can be considerably lowered by transition from the gaseous to the condensed state. Thus Leach, Muller and Vermeil⁵⁵ have detected ionization of isopentane, methylpentane and isobutylene as liquids on irradiation with radiation whose energy was about 1 eV lower than their ionization potential in the gaseous state. For solid anthracene, the lowering of the ionization potential amounts⁵⁶ to ~ 3 eV.

Initiation by the photochemical decomposition of a chemical catalyst, which can in general be produced by wavelengths sufficiently long to avoid the danger of ionization, indicates a radical mechanism. On the other hand, a negative result does not necessarily mean an ionic mechanism because of the effect of 'syncrystallization'.

(e) *Electron paramagnetic resonance*

Numerous attempts have been made to define the mechanism from the results of electron paramagnetic resonance (e.p.r.). It is evident that by itself a signal resulting from radicals cannot be considered as an indication of a radical mechanism: radicals are always formed' on irradiation of molecular solids by γ -rays. However, if an initial signal is observed to change in the course of time into the signal characteristic of a growing chain⁸, which is recognized as a result of other work, it is only possible to conclude that a 'primary' radical can add a molecule of monomer. Such additions, giving chains of greater or lesser length, could very well constitute a secondary mechanism responsible for a small fraction of the total conversion.

Only if the behaviour of the radicals observed by e.p.r. is strictly parallel to that of the polymerization can it be supposed that the latter proceeds by a radical mechanism.

Thus, in quenched crystals of acrylonitrile, Bensasson, Dworkin and Marz¹⁹ observed the appearance, after irradiation, of a 'primary' radical ($\text{CH}_2-\dot{\text{C}}\text{H}$), which remained unchanged during reheating to -135°C . Below

$\begin{array}{c} \text{CN} \\ | \\ \text{CH} \end{array}$

this temperature a post-polymerization^{8, 12} is not observed. Above this temperature, which corresponds to the start of a pre-transition (this occurs at -114°C and is first order), the signal changes into that of a growing chain

$\begin{array}{c} \text{H} \\ | \\ \text{CH}_2-\dot{\text{C}} \\ | \\ \text{CH} \end{array}$

and the post-polymerization becomes observable.

With formaldehyde⁵⁷, the change of the primary signal into the signal of a growing chain was observed over a period of time above -196°C , while differential thermometry indicated a heating of the sample, i.e. the existence of a polymerization. The explosive polymerization which cannot occur if there is radical recombination does not occur above this temperature. Thus it seems that these two monomers polymerize in the solid state by means of a radical mechanism.

The situation is not always so simple. Thus the post-polymerization of acrylamide continues over a period of months, and throughout this period radicals can be observed by e.p.r.; but while the number of these radicals remains constant, the rate of the post-polymerization decreases with time according to the relation²⁷

$$\% \text{ conversion} = A \log (1 + Bt)$$

One cannot conclude from this discrepancy that the mechanism is ionic, since an absolutely analogous situation was observed by Bamford and Jenkins⁵⁸ for the radical polymerization of liquid acrylonitrile, which leads to the hypothesis of 'trapping' or occlusion of radicals.

(f) Comparison with the polymerization mechanism in the liquid state

Where polymerization in the liquid state can only proceed by a single mechanism, it could be considered that this mechanism is valid also in the solid state. Thus it is known from other sources that isobutylene, *n*-hexadecene, hexamethylcyclotrisiloxane, β -propiolactone, diketene, bis-chloro-3,3-oxetane and trioxan polymerize in the liquid state only in the presence of cationic catalysts. It is therefore not unreasonable to think that the polymerization in the solid state proceeds by the same mechanism.

It is most important to distinguish between the cationic polymerizations induced by ionizing radiation in the liquid and in the solid states. Ionic polymerization in the liquid state leads usually to polymers of very low molecular weight, probably because of the short lifetime of the ions. In the solid state, on the other hand, at least for cyclic monomers, high molecular weights are obtained and a post-polymerization period may last several hours. It must be assumed, therefore, that in solids the electrons are trapped in deep traps and may on being released from the trap give thermo-

luminescence. Russian workers⁵⁹ have found that this untrapping occurs in the region of a phase change. In order that an important post-effect can exist near the melting point, thermoluminescence must occur over a very narrow temperature interval. Such a thermoluminescence could not be observed by Kieffer and Deroulede⁶⁰ for trioxan. Other monomers are being studied.

It must be concluded that both radical and ionic mechanisms of polymerization can occur for polymerization in the solid state and that the mechanism must be determined for each case. Only a profound study by various methods can achieve a discrimination, which is not always too sure.

V. ACTIVATION ENERGY AND POLYMERIZATION AT VERY LOW TEMPERATURES

On examining the large amount of data concerning the variation of rate of polymerization as a function of temperature, it is possible in general to distinguish two types of polymerization, which sometimes occur with the same monomer.

(1) The polymerization proceeds rapidly in the region of the melting point or in a region existing between transition and melting points. The overall energy of activation calculated by the conventional method is fairly high: 6.3 kcal for β -propiolactone, 9.6 kcal for hexamethylcyclotrisiloxane, 9 kcal for styrene, ~ 12 for vinylcarbazole, 18.4 for trioxan and ~ 23 kcal for acrylamide. This leads to the conclusion that (a) the Arrhenius factor of the propagation reaction must be very high; in other words the pre-orientation of the molecules in the crystal reduces the steric factor very considerably; (b) a certain mobility of the molecules is indispensable since only a fraction of this activation energy is necessary for the chemical act itself. A study by nuclear magnetic resonance (n.m.r.) would undoubtedly help to clarify this point.

(2) The polymerization sometimes proceeds slowly (acrylonitrile, vinyl acetate, β -propiolactone, diketene, acetaldehyde) at very low temperatures and its rate is independent of temperature. The case of formaldehyde, for which the reaction proceeds rapidly at a very low temperature and has an appreciable activation energy (2.8 kcal), constitutes an exception.

The experimental technique for this polymerization is in general rather delicate. The sample after irradiation at say -196°C must be heated and melted before the degree of conversion can be determined. During this period of heating, rapid as it may be, the sample remains at higher temperatures and, during this period, a post-polymerization can occur. Nevertheless Amagi and Chapiro¹² with styrene, Chachaty with acetaldehyde³⁶, Bensasson¹⁷ and Amagi and Chapiro¹² with acrylonitrile, have determined the rate of post-polymerization as a function of temperature and so have been able to calculate the fraction of polymer formed during the period of heating. As an example, according to Bensasson¹⁷, of the 4.6 per cent of the monomer converted during irradiation at -196°C followed by heating and melting, only 0.18 per cent was formed during the heating period if the rate of post-

polymerization observed between -196°C and -90°C is extrapolated to the range -90°C to -83°C (m.pt). Two hypotheses can be suggested.

(i) 4.4 per cent of monomer has been converted into polymer between -90° and -83°C (the extrapolation used not being applicable) and during melting, this hypothesis would explain the absence of an activation energy between -196° and -130°C as well as the non-appearance of a signal characteristic of the growing chain on e.p.r. It can be objected that this hypothesis postulates an abnormally high rate of conversion at the melting point, for which there is no indication from other work on acrylonitrile. Further it does not explain the rapid polymerization of diketene and propiolactone for which the rate of polymerization starts to decrease with temperature some 30° to 40° below the melting point.

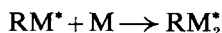
(ii) The conversion takes place efficiently at very low temperatures between -130° and -196°C . How then can the absence of an activation energy be explained? Semenov⁶¹ has put forward the following interesting suggestion based on the theory of energy chains due to Christiansen. This gives the following scheme :



where B^* is an excited molecule which has absorbed all or an important part of the heat of reaction. It is known that these energy chains have never been observed in the gaseous or liquid phases. The reason for this is that because of the steric factor reaction (2) does not occur at the first collision. B^* suffers 1 000 to 10 000 collisions before it is able to react and becomes deactivated. This is not so in the solid phase if the molecules of A are ordered in such a way that the steric factor is unity. Certain of the active centres C (ions or radicals) formed by the radiation may possess sufficient energy to carry out, immediately after their formation, the reaction



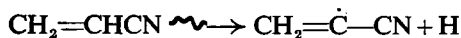
RM^* contains all the heat of reaction (3) which makes possible the reaction



and so on. The growth of chains will be very rapid and will not require any activation energy.

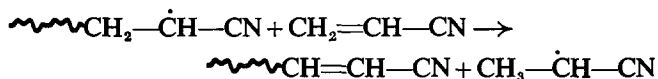
There are also active centres created by the radiation, but not possessing sufficient energy, which will be responsible for the post-effect.

With acrylonitrile, for example, the radicals observed on e.p.r. (responsible for the post-polymerization) correspond to $\text{CH}_3-\dot{\text{C}}\text{H}-\text{CN}$ and result from the sequence of reactions :



It might be thought that the primary radicals $\text{CH}_2-\dot{\text{C}}-\text{CN}$ are formed with sufficient energy to initiate an energy chain and disappear. It must,

however, be assumed that the polymer chains formed by this rapid process possess a termination reaction which might be, for example,



since, as has been noted above, the radicals of growing chains do not appear on e.p.r. between -196°C and -135°C . These transfer reactions have actually been observed at low temperatures⁵⁷.

It should be noted that, in order to explain certain peculiarities of the polymerization of formaldehyde, Chachaty³⁶ has been led to formulate a similar hypothesis to that of Semenov, that is to say that the local temperature in the immediate vicinity of the growing chain is considerably higher than, and almost independent of, the average temperature of the medium.

VI. INFLUENCE OF THE 'TEXTURE' OF THE SOLID

The quantitative results concerning polymerization in the solid state obtained in different laboratories sometimes show considerable discrepancies even for apparently identical experimental conditions. The reason for this is very often the difference of 'texture' of the solid—dimensions of crystals, their defects, etc. If the solid monomer possesses a transition point, there is in addition the further difference of 'annealing'. In such crystals which are rapidly cooled below the transition point the high temperature phase is sometimes 'frozen' at the low temperature. During heating this 'frozen' phase first changes to the 'low temperature' phase and then the whole crystal undergoes transition to the 'high temperature' phase at the transition point. In the absence of sufficient annealing, the rate and even the course of the reaction depend on the rates of cooling and crystallization which are difficult to control.

Let us now consider these questions in greater detail.

(a) *Influence of size and 'quality' of crystals*

The role of defects is a double one: (i) It is known from other evidence⁶² that the number of 'frozen' radicals depends on the 'quality' of the crystal. The slower the crystallization, i.e. the smaller the number of defects, the smaller is the number of radicals which escape immediate recombination (in the 'cage') and hence the smaller the number of centres capable of initiating polymerization.

(ii) It is reasonable to assume that in certain cases at least, the defects and the edges of the crystals stop polymerization. In other cases, by contrast, the defects (dislocations) favour the mobility of monomer molecules and hence accelerate the polymerization.

An increase of the rate of polymerization in large crystals has been observed, for example, by Chachaty³⁶ for acetaldehyde, by Okamura and Hayashi³³ for trioxan, by the same authors and by Chapiro and Penczek⁶³ for bis-chloromethyl-3,3-oxetane. It does not result from the increase in the

number of initiating centres since it corresponds exactly to the increase in average molecular weight.

By contrast, the rate of post-polymerization is smaller in large monocrystals of acrylamide than in small crystals⁵⁶, although this result is not confirmed²⁹.

(b) *Effects of impurities*

Crystal defects can also be introduced by the addition of impurities if these form a mixed crystal with the monomer. In other cases, the impurities are occluded in the crystal and produce a plasticization, that is to say that they act in the same way as an increase in temperature. The effect of impurities is therefore very complex and may depend on their concentration: thus, the addition of increasing quantities of benzene to vinylcarbazole produces first a diminution and then an increase in the rate of polymerization¹⁵. The addition of propionamide to acrylamide (the only case where the formation of mixed crystals with an impurity has been well established) increases the rate of polymerization, which corresponds to the accelerating role of defects for this particular polymerization; but it decreases the molecular weight probably by a transfer reaction⁶⁴. It is similar for the addition of ferric chloride to hexadecene²⁵. As previously mentioned, methylmethacrylate only polymerizes in the presence of liquid paraffin with which it forms a glass.

If, on the other hand, a very regular structure is necessary in order that the reaction should proceed rapidly, the introduction of 'syncrystallizable' impurities results in a decrease in the rate of polymerization. This is so for mixed crystals of β -propiolactone with ketene and γ -butyrolactone⁵³.

In other cases, the effect of the additive depends on its nature, but since it is known neither if there is effective formation of mixed crystals, nor if the dimensions of the crystal are altered, any discussion would appear to be premature.

(c) *Effect of polymer already formed. Conversion limit*

We are sure of one 'impurity' which is present in the interior of the crystal: this is the polymer already formed. The presence of polymer can therefore influence the rate of polymerization. Actually, except for acrylamide where a conversion of 100 per cent has been achieved⁶⁵, conversion in the solid state is never complete. While for certain monomers (vinyl carbazole¹⁵, formaldehyde³⁶, acetaldehyde³⁶, trioxan⁵³, 2,4-dimethylstyrene¹³) the conversion limit is of the order of 50 per cent, for others it is appreciably lower: 15 per cent for β -propiolactone⁵³ and bis-chloromethyl-3,3-oxetane, 5 per cent for styrene and 11 per cent for acrylonitrile irradiated¹⁷ at -196°C . Even so for the last monomer, a very brutal quenching (microcrystals?) enables this limit to be exceeded three or four times¹⁶ and an increase in the temperature of irradiation to -90°C enables it to reach 22 per cent.

What causes this limitation on conversion? Several factors would appear to play a part. In certain cases (trioxan⁵² and acetaldehyde³⁶) the existence of the conversion limit would appear to result from radiolytic degradation of the polymer formed.

Table 5. Maximum degree of conversion

| Monomer | T°C | % |
|-------------------------------------|-------|-------|
| Acrylamide | 27 | 100 |
| Vinyl carbazole | 20 | 50 |
| 2,4-Dimethylstyrene | -78 | 60 |
| Formaldehyde | -196 | 45 |
| | -131 | 23 |
| Acetaldehyde | -196 | 60¶ |
| | -131 | 20† |
| Trioxan | +55 | 35* |
| β-Propiolactone | | 50† |
| Diketene | -78 | 15.5 |
| 3,3-Bis-(chloromethyl)- oxetane† | -78 | 11 |
| | +11.2 | 15‡ |
| | | 7 |
| Acrylonitrile | -196 | 4.4 |
| | -196 | 11.0¶ |
| | -90 | 22.0 |
| Styrene | -78 | 5(?) |

*During irradiation.

†During post-polymerization.

‡Large crystals.

||Small crystals.

¶Including post-effect.

In other cases, the influence of the polymer already formed on the rate of polymerization appears to result from the perturbation of the crystal of monomer by the included polymer. The mechanism of these perturbations and their consequences can be very diverse.

With acrylamide, where it is known that polymerization takes place at the boundary between the crystalline phase and the amorphous polymerized phase⁶⁶, the presence of polymer can only accelerate the polymerization which can reach 100 per cent. Such an acceleration has been actually observed⁶⁵. It is probable that the situation may be the same for vinyl carbazole¹⁵ and for 2,4-dimethylstyrene¹³. The influence of the polymer formed is thus analogous to that of additives forming mixed crystals with these monomers.

The situation is the reverse if the polymerization propagates along certain preferred planes, i.e. if the polymer is stereoscopic. In this case, the presence of increasing quantities of polymer must lead first to a decrease in the molecular weight and then to a stopping of the polymerization. It is probably this which occurs for polyacrylonitrile formed at a low temperature. Although for this polymer the proof of syndiotacticity can only be indirect: in fact Tabata and Sobue⁶⁷ showed that the number of C=N—C linkages formed on heating the polymer, all other conditions being equal, was greater for the polymer formed in the solid state than for that polymerized in the liquid phase (however, see below).

It should be pointed out that always, with acrylonitrile, when once a conversion limit has been reached, if the mixture of polymer and monomer is melted, refrozen and then irradiated, once again a certain amount of polymer is formed^{12, 17}. The reason for this appears to be, according to a suggestion of Chachaty³⁶ the insolubility of polymer in the monomer. In

the molten state, the polymer separates and in reality a pure crystal of monomer is irradiated. By contrast, if the same experiment is carried out with formaldehyde or acetaldehyde, for the former the explosive reaction is suppressed and for the latter the polymerization is stopped. In these two cases no separation of polymer and monomer is observed on melting³⁶.

Finally for β -propiolactone and bis-chloromethyl-3,3-oxetane, the polymer chains have a tendency to aggregate and squeeze out the remaining monomer whose crystal structure becomes less perfect³². Very pertinent steric reasons have been put forward by Letort and Richard³¹.

VII. STEREOSPECIFICITY OF POLYMERS

One of the reasons which spurred on the study of polymerizations in the solid state was the hope that the crystalline structure would impose a stereospecific structure on the polymers so formed. For a long time this hope turned out to be false. Polyacrylamide, polyacetaldehyde and several other acrylic polymers formed under these conditions were amorphous, and Adler^{66,68} and other workers⁵¹ concluded that it was impossible to impose stereospecificity on a polymer using the crystalline lattice of the monomer. This opinion has proved to be too pessimistic. Morawetz²⁸ has reported that polymethacrylic acid produced in the solid state at 0°C and then methylated had a fourfold greater probability of having two successive centres of asymmetry than methylmethacrylate polymerized in the liquid phase.

We have referred earlier to the results of Tabata and Sobue⁶⁷ concerning the syndiotacticity of polyacrylonitrile formed in the solid state. It should be added that these results are contested by other authors¹⁷.

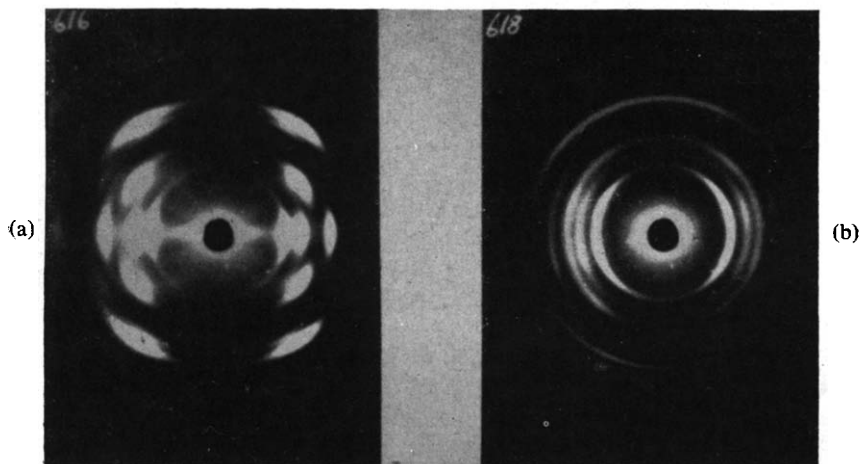


Figure 1—X-ray diffraction diagrams of polydiketene: (a) from large crystalline state monomer at -78°C , (b) from sudden-cooled crystalline state monomer at -78°C

The most spectacular results have been obtained by Okamura, Hayashi and Kitanishi⁵² on the polymers resulting from the solid state polymerization of certain cyclic monomers. For β -propiolactone, diketene, bis-



Figure 2

chloromethyl-3,3-oxetane and above all for trioxan, the melting points of the polymer obtained from large crystals of monomer were higher than those of polymers formed from microcrystals. An X-ray study showed that the crystalline structure was much better developed in the former. *Figure 1*, taken from the work of these authors, enables a comparison to be made between the X-ray diagrams of polydiketene prepared at -78°C from large and small crystals of monomer. Poly- β -propiolactone forms fibrils parallel to the longer axis of the crystal.

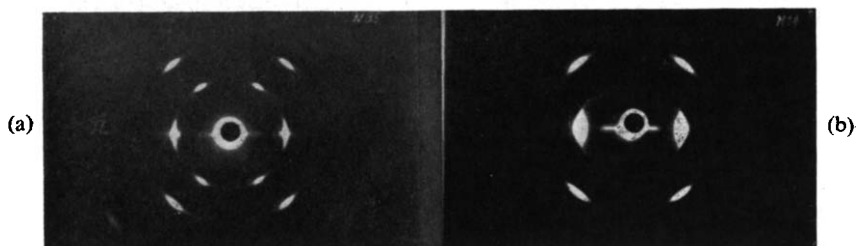


Figure 3—X-ray diffraction diagrams of: (a) polytrioxan from large crystalline state monomer at 30°C , (b) polyoxymethylene fibre stretched

With polytrioxan, the fibres obtained are the same length as the single crystal of monomer (*Figure 2*)⁵². The crystallinity of these fibres is appreciably greater than that of fibres drawn from normal polyoxymethylene as can be seen from *Figure 3*, and the melting point is about 10° higher.

VIII. CONCLUSION

We think we have shown that the study of polymerization in the solid state is only at the beginning. While the amount of experimental data is fairly

large, much information about, in particular, the crystal structure of monomers, the existence and significance of transition points, the formation of mixed crystals, the influence of different additives on the 'texture' of solid monomers, etc. is lacking. The absence of this information makes it impossible to coordinate the data logically or even to classify it simply. All that one can say is that probably two modes of polymerization are involved, the one requiring an appreciable activation energy, and the other little or none, but a perfect pre-arrangement of molecules.

Meanwhile one can say, especially after the spectacular success reported by the Japanese workers, that this field of research opens new and exciting possibilities, in particular in the subject which interests us at this Congress—since, for the first time the hope appears of being able to produce textile fibres in a single operation.

*Laboratoire de Chimie Physique,
11 Rue Pierre Curie,
Paris V^e, France*

DISCUSSION

Dr C. H. Bamford (U.K.): I should like to make some remarks about the polymerization of acrylic and methacrylic acids initiated by ultra-violet light. Professor Magat has referred to this briefly. The work is essentially a study of the polymerization of single crystals of these substances and it has been done by Dr Ward, Dr Eastmond and myself in our laboratories. The most interesting and striking phenomenon is the effect of pressure on these reactions. If one applies to the crystals quite a small stress such as may be obtained by squeezing them between quartz plates, the pressure being of the order of five atmospheres (which is very small) the photochemical polymerization may be slowed down very considerably. This is so at about 10° below the melting point of the acid; on removing the pressure, reaction may start again, either after an induction period, or directly. This is not only true of the direct photochemical reaction but also of the after-effect which occurs with methacrylic acid. Pressure is applied and the light turned off at the same moment; there is then no development of the normal after-effect, but on removing the pressure the after-effect starts. Obviously pressure has a large effect and the reaction is very structure-sensitive.

We believe that the results can be interpreted in terms of dislocations in the crystal and the movement of dislocations under the influence of stress. It is known that in some types of crystal, dislocations can be quite mobile under comparatively low stresses. We have to make some assumptions about the interactions of polymer molecules and dislocations. Dislocations appear to present particularly favourable sites for polymerization; they move away from the growing chains on the application of stress, so the reaction is retarded.

The second point about this kind of technique is that it provides a useful tool for investigating solid state polymerizations. As Professor Magat implied, one has the feeling that there are not many experimental variables to play with in this kind of work, and it is useful to have an additional one.

In the absence of pressure, the conversion/time curves are of the type often encountered in solid state reactions. There is a short induction period at the beginning followed by a gradually accelerating reaction. Finally the reaction slows down as 100 per cent conversion is reached. In this type of system one can hardly talk about orders of reaction or energies of activation in the absence of a complete kinetic analysis, which we have not been able to obtain. It seems likely that these polymerizations fall into Professor Magat's first group, and we believe that they can be explained in terms of comparatively well-understood solid state phenomena together with the idea of occlusion taken over from the liquid state, without having to invoke any special concepts about solid state polymerization.

Dr J. Corbiere (France): You have just said that polymerization processes other than radical processes are not known in some cases in the liquid state and that therefore in these systems polymerization in the solid state must also be a radical process. But I think that this reasoning is open to criticism since you have indicated certain instances of substances which are not known to polymerize in the liquid state by any process but which polymerize in the solid state.

You have not spoken of the degree of polymerization which is extremely important, especially for us in the textile industry. Have you some information on this subject, particularly for acrylonitrile which you seem to have studied particularly?

Professor M. Magat (France): I did not mean to imply that all polymerizations in the solid state take place by a radical process. I said that in the case where there is a single known mechanism in the liquid state it is probably the same mechanism as that in the solid state. Now, there are monomers which we have not been able to polymerize in the liquid state. This applies to acetone, chloroacetone, bromoacetone, etc. The reason is very simple: they form unstable polymers which decompose at ambient or even lower temperatures. If they are polymerized in the solid state, this is done at a very low temperature and a polymer is obtained which cannot be obtained from a liquid if an appreciably higher temperature is used. This is one of the reasons why certain polymerizations have been observed only in the solid state. Another explanation, by Kargin, is based on thermodynamics but I do not wish to dwell on this point here.

The second question concerns acrylonitrile, trioxan, formaldehyde and acetaldehyde. The molecular weights obtained from polymerizations in the solid state are fairly high, at least as high as if the polymerization were done in the liquid state. With styrene, on the contrary, molecular weights are appreciably lower and are in the neighbourhood of those observed in the ionic polymerization of styrene.

As far as Dr Bamford's results are concerned, this is a very interesting contribution; evidently all the variables which one can introduce can help in understanding these things.

Now, I would emphasize a general difficulty which we meet in this field. With rare exceptions the crystal structures of the monomers are not known. Those of acetaldehyde, diketene and acrylamide have been worked out

and acrylonitrile is being studied. In many cases we do not know whether the solid monomers have transition points; we do not know what kind of defects and diffusion mechanisms are involved. To enable us to proceed further and to predict to some extent the cases in which one can polymerize in the solid state, it will be necessary to have all this information.

Professor M. Baccaredda (Italy): Do you believe that there is a close relation between the conditions for polymerization in the solid state and between the crystalline structures of the monomer and of the polymer?

Professor M. Magat (France): Are we concerned with the possibility of polymerization or with the product obtained?

Professor M. Baccaredda (Italy): With the possibility of polymerization.

Professor M. Magat (France): There is probably a correlation in cases where a stereoscopic polymer is obtained, but not in cases like acrylamide or vinyl carbazole where, obviously, a large activation energy is needed and where any molecule in the neighbourhood of the reacting centre of the end of the growing chain can add on. I think that the exact structure is of secondary importance, the distance between the double bonds being the only important factor.

Professor D. C. Pepper (Eire): I have two questions I should like to ask the lecturer. One is a qualitative one. All the examples referred to quoted initiation within the crystal through the influence of radiation; are there any examples of initiation of a reaction within the crystal but from the surface, say from a dissolved initiator outside the crystal?

The other question is: a number of activation energies were quoted for the propagation reaction. Could we know how these are derived? One can presumably get an overall activation energy but how does one separate out the propagation reaction?

Professor M. Magat (France): I will take the last question first. The only propagation activation energy I have given is the one for formaldehyde, which was deduced assuming that the explosion which occurs in formaldehyde on irradiation at low temperatures can be explained by Semenov's theory of thermal explosions, which seems to be so. In this case, it is possible to calculate the activation energy of propagation.

In other cases, I have given only the overall activation energy, but since the activation energy for the initiation is nil, this overall energy is the difference between the activation energy of propagation and of termination.

Professor D. C. Pepper (Eire): Is it not possible to get what might be called a pseudo-activation energy for initiation in that the efficiency of the absorption processes is temperature dependent?

Professor M. Magat (France): No, the absorption processes are at least in first approximation temperature independent.

Concerning the utilization of other means of initiation than radiation, I could not quote all the results, of course, but you will find some in the printed paper.

Polymerization in the solid state was initiated photochemically by Bamford and co-workers, by ionic catalysts by Professor Kern, by mechanical means in Russia; also in Russia, Kargin and co-workers deposited on a glass wall a film of some metals (or salts) which they covered by a film of monomer, presumably in a glassy state. On warming, but still far below the melting point of the monomer, polymerization occurs.

Dr G. C. Eastmond (U.K.): With regard to the temperature dependence of initiation we have found that the production of radicals from crystalline methacrylic acid by ultraviolet light is very temperature dependent. This might suggest that there is some temperature dependence on photo-initiation in this case.

Professor M. Magat (France): If I had another hour I could tell you that the situation is even more complicated even for our gamma radiations. The presence of defects plays a very important role in the concentration of trapped radicals. If one irradiates, for instance, cyclohexane rapidly cooled to -196°C one obtains very irreproducible radical concentrations between two and four per 100eV. If the crystal is annealed below its transition temperature one obtains a fairly reproducible radical concentration of 1.2 to 1.4 radicals per 100eV. Defects thus play a double role; on the one hand they increase the number of possible reactive species, but on the other hand they may favour or disfavour the propagation. Close to the melting point the number of defects increases very rapidly with temperature. What the contribution of this is to the overall activation energy, I do not know.

Professor M. Letort (France): I wish to call attention to a point which appears to us very important in reactions in the solid state. I refer specifically to the formation of polyacetaldehyde by fusion of the crystal. We have shown that it is really on fusion of the crystal that this polymer is formed. We have examined the crystallography, the crystalline structure of the monomer in order to explain, independently of thermodynamic reasons, the great ease of reaction during melting of the crystal. We have found the pre-formed macromolecule, so to speak, in the crystal; that is to say the monomer molecules need only small displacements with respect to each other to form polymer-like chains in the crystal.

This suggests that the polarity of the molecule may be greater in the crystal than in the liquid or gaseous state, but we cannot be certain of this, for we are at the limit of experimental accuracy.

I present these suggestions for discussion.

Dr R. Mahommed (U.K.): One of the most striking things about trioxan is that the crystals are extremely flexible and you can almost bend them double without their snapping. We have heard Dr Bamford's remarks about the effects of pressure on acrylic acid. I wonder whether anything has been done on the effect of the sort of yields that you had in the final slide of polymerizing trioxan under extreme degree of strain.

Professor M. Magat (France): Not so far as I know.

Dr A. Parisot (France): Has the solid state polymerization of glucose crystals been tried?

Professor M. Magat (France): I believe not. Glucose would probably be destroyed under polymerization conditions.

Professor R. Hosemann (Germany): In this account of Dr Bamford's, the great influence of pressure on the things which happen is in very nice agreement with our observations on high polymers. With polyethylene, pressing it only with a very small force, we were able to prove that wide dislocations totally disappear in atomic dimensions. I would propose, following what Professor Magat said, that there must be possibilities for more precise electron density distribution measurements and for finding the texture and the crystallinity of such mono-crystals. We have nice new methods and many things could be done.

Professor W. Kern (Germany): May I add a few words at the end of the discussion about the polymerization of trioxan. One of the differences between the polymerization of trioxan at normal temperatures with cationic initiators and polymerization at very low temperatures in the solid state is the great discrepancy in molecular weight. One obtains relatively low molecular weights on polymerizing trioxan at normal temperatures, if no special care is taken, while Professor Magat has stated that very high molecular weights are obtained by radiation polymerization at very low temperatures.

This question has greatly interested us, and we have undertaken research in recent years to find out how it might be explained.

Cationic polymerization of trioxan at normal temperatures is extraordinarily sensitive to traces of water. When traces of water are excluded, one obtains molecular weights of 200 000 to 300 000 from dissolved trioxan at normal temperatures, that is to say very high molecular weights.

I suspect—and would like Professor Magat's opinion on this—that low temperature polymerization of trioxan, in the crystalline state, gives such a high molecular weight because water does not crystallize out with the trioxan, i.e. that it is a particularly highly purified trioxan which Professor Magat has polymerized. I grant, of course, that it has not yet been shown that this polymerization is cationic at low temperatures.

Professor M. Magat (France): I am very sorry, I cannot answer the questions completely. In the first place I have never personally worked on trioxan. Secondly, the polymerization of trioxan takes place rather rapidly in a temperature range of only 35° to 50°C. At lower temperatures it does not occur.

I know that the influence of water on radiation polymerization has been examined in different places, with results which are apparently rather contradictory, but very little has been published.

REFERENCES

- ¹ LETORT, M. *C.R. Acad. Sci., Paris*, 1933, **202**, 767
- ² TRAVERS, W. M. *Trans. Faraday Soc.* 1936, **32**, 246
- ³ LETORT, M. and RICHARD, A. *J. C. R. Acad. Sci., Paris*, 1955, **240**, 86
- ⁴ RESTAINO, A. J., MESROBIAN, R. B., BALLANTINE, D. S. and DIENES, G. J. *Ric Sci.* 1955, **25A**, 178
- ⁵ MESROBIAN, R. B., ANDER, P., BALLANTINE, D. S. and DIENES, G. J. *J. chem. Phys.* 1954, **22**, 565; *J. Amer. chem. Soc.* 1956, **78**, 2939
- ⁶ BAMFORD, C. H., JENKINS, A. D. and WARD, J. C. *J. Polym. Sci.* 1960, **48**, 37
- ⁷ LAWTON, E. J., GRUBB, W. T. and BALWIT, J. S. *J. Polym. Sci.* 1956, **19**, 445
- ⁸ BENSASSON, R. and MARX, R. *J. Polym. Sci.* 1960, **48**, 53
- ⁹ BENSASSON, R. *J. Chim. phys.* 1959, **55**, 796
- ¹⁰ TABATA, Y. and SOBUE, H. *J. Polym. Sci.* 1960, **43**, 459
- ¹¹ CHAPIRO, A. and STANETT, V. *J. Chim. phys.* 1960, **57**, 35
- ¹² AMAGI, Y. and CHAPIRO, A. In press
- ¹³ CHEN, C. S. Communication to the International Symposium, Montreal 1961. *J. Polym. Sci.* In press
- ¹⁴ GOLDANSKI, V. and ENIKOLOPIAN, —?— after SEMENOV, N. N. IUPAC Congress, Montreal 1961
- ¹⁵ CHAPIRO, A. and HARDY, G. *J. Chim. phys.* In press
- ¹⁶ CHAPIRO, A. Private communication
- ¹⁷ BENSASSON, R. Private communication
- ¹⁸ BURLANT, W. and ADICOFF, A. *J. Polym. Sci.* 1958, **27**, 269
- ¹⁹ BENSASSON, R., DWORKIN, A. and MARZ, R. *J. Chim. phys.* In press
- ²⁰ GROSMANGIN, J. Private communication
- ²¹ TABATA, Y., SOBUE, H. and ODA, E. *J. phys. Chem.* 1961, **65**, 1645
- ²² CHAPIRO, A., MELE, A. and BRONES, W. Private communication subsequent to 4/5/62
- ²³ HARDY, G. Private communication subsequent to 4/5/62
- ²⁴ PORT, S. and WITNAUER, L. P. *J. Polym. Sci.* 1958, **33**, 95
- ²⁵ COLLINSON, E., DANTON, F. S. and WALKER, D. C. *Trans. Faraday Soc.* 1961, **57**, 1732
- ²⁶ HOFFMAN, A. S. *J. Polym. Sci.* 1959, **34**, 241
- ²⁷ MORAWETZ, H. International Symposium on Macromolecular Chemistry, Montreal 1961
- ²⁸ MORAWETZ, H. in DE BOER, J. H. *Reactivity of Solids*, pp 144 ff. —?—?—?—? Amsterdam, 1960
- ²⁹ ZURAKOWSKA-ORSZAG, J. Private communication subsequent to 4/5/62
- ³⁰ HENGLEIN, A. and SCHULTZ, R. *Z. Naturf.* 1954, **96**, 617
- ³¹ SCHULZ, R., RENNER, G., HENGLEIN, A. and KERN, W. *Makromol. Chem.* 1954, **12**, 20
- ³² ZURAKOWSKA-ORSZAG, J. Congrès de l'Agence Internationale, Varsovie, 1959
- ³³ TABATA, Y., ODA, E. and SOBUE, H. *J. Polym. Sci.* 1960, **45**, 469
- ³⁴ ADLER, G. —? —? —? —? —? —?
- ³⁵ CHACHATY, C., MAGAT, M. and TER MINASSIAN, L. *J. Polym. Sci.* 1960, **48**, 139
- ³⁶ CHACHATY, C. *Thèses, Paris*, 1962
- ³⁷ TSUDA, Y. *J. Polym. Sci.* 1961, **49**, 369
- ³⁸ KARGIN, V. A., KABANOV, V. A. and ZUEOV, V. P. *Dokl. Akad. Nauk S.S.S.R.* 1960, **134**, 1098
- ³⁹ OKAMURA, S., HAYASHI, K. and MORI, S. *Isotopes and Radiation, Japan*, 1961, **4**, 70
- ⁴⁰ HAYASHI, K. and OKAMURA, S. *Makromol. Chem.* 1961, **47**, 230
- ⁴¹ SACK, H. Private communication
- ⁴² OKAMURA, S., HAYASHI, K., KITANISHI, Y. and NISHII, M. *Isotopes and Radiation, Japan*, 1960, **3**, 510
- ⁴³ OKAMURA, S., KITANISHI, Y. and HAYSASHI, K. *Isotopes and Radiation, Japan*, 1959, **3**, 346
- ⁴⁴ OKAMURA, S., HAYASHI, K. and WATANABE, H. *Isotopes and Radiation, Japan*, 1961, **4**, 473

POLYMERIZATION IN THE SOLID STATE

- ⁴⁵ BURLANT, W. and TAYLOR, C. *J. Polym. Sci.* 1959, **41**, 547
- ⁴⁶ OKAMURA, S., HAYASHI, K. and NISHII, M. *Isotopes and Radiation, Japan*, 1959, **4**, 69
- ⁴⁷ SPINDLER, M. W. and VALE, R. L. *Makromol. Chem.* 1961, **43**, 231
- ⁴⁸ OKAMURA, S., HAYASHI, K. and NAKAMURA, Y. *Isotopes and Radiation, Japan*, 1959, **4**, 69
- ⁴⁹ MORAWETZ, H. and FADNER, T. A. *Makromol. Chem.* 1959, **34**, 162
- ⁵⁰ SCHMIDT, G. M. J. IUPAC Congress, Montreal 1961
- ⁵¹ LETORT, M. and RICHARD, A. *J. Chim. phys.* 1960, **56**, 752
- ⁵² OKAMURA, S., HAYASHI, K. and KITANISHI, Y. Communication to the International Symposium on Macromolecular Chemistry, Montreal 1961
- ⁵³ OKAMURA, S., HAYASHI, K. *J. Chim. phys.* In press
- ⁵⁴ BERNAS, A. and BODARD, M. Private communication subsequent to 4/5/62
- ⁵⁵ LEACH, S., MULLER, F. and VERMEIL, C. Private communication
- ⁵⁶ KALLMAN, H. Private communication
- ⁵⁷ CHACHATY, C. and MARX, R. *J. Chim. phys.* In press
- ⁵⁸ BAMFORD, C. H. and JENKINS, A. D. *Proc. Roy. Soc. A*, 1952, **216**, 515; 1955, **228**, 220
- ⁵⁹ NIKOLSKY, V. G. and BOUBEN, N. YA. *Dokl. Akad. Nauk S.S.S.R.* 1960, **134** (1), 134
- ⁶⁰ KIEFFER, F. and DEROULEDE, A. Private communication
- ⁶¹ SEMENOFF, N. N. IUPAC Congress, Montreal 1961
- ⁶² SZWARC, H. Private communication
- ⁶³ CHAPIRO, A. and PENCZEK, S. *J. Chim. phys.* In press
- ⁶⁴ FADNER, T. H. and MORAWETZ, H. *J. Polym. Sci.* 1960, **45**, 475
- ⁶⁵ BAYSAL, B., ADLER, G., BALLANTINE, D. S. and COLOMBO, P. *J. Polym. Sci.* 1960, **44**, 117
- ⁶⁶ ADLER, G. and REAMS, W. *J. chem. Phys.* 1960, **32**, 1698
- ⁶⁷ TABATA, Y. and SOBUE, H. *Isotopes Congress, Kyoto 1961*
- ⁶⁸ ADLER, G. *J. chem. Phys.* 1959, **31**, 848

OKAMURA, S., HAYASHI, K. and NAKAMURA, Y. *Isotopes and Radiation, Japan*, 1959, **3**, 416

The Molecular Properties of Polymers

S. CLAESSON

The molecular properties of polymer molecules in solution are discussed briefly. The dimensions of chain molecules and the importance of chain stiffness and internal viscosity are mentioned and different ways of measuring these properties are reviewed. Because of the importance of sharp fractions for measurement some recently developed fractionation procedures are also included in the discussion. The effect of charge on the molecular dimensions of polyelectrolytes and the use of that property for transforming chemical into mechanical energy by means of Kuhn's synthetic muscle are mentioned finally as a typical macromolecular property not to be found among small molecules.

THE study of the properties of individual polymer molecules in solution has always been a challenge to the physical chemist because of its fundamental importance for the understanding of molecular behaviour in general and because of its application to the thermodynamics of solutions. It has of course also been extremely important for the understanding of the properties of polymers in general and the volume of work in this field has therefore increased rapidly with the enormous development of polymer technology. Even now, the work on molecular properties is small in comparison with the fantastic amount of work being done on the synthesis of new polymers and on the study of their properties as solids and fibres. The general interest in molecular properties down to the smallest details is, however, increasing very rapidly—an obvious fact, if one looks in any modern journal of polymer chemistry.

In fact I think that we are now in a state of rapid transition, when the more classical description of chain molecules based on the fundamental work of Staudinger, Meyer, Kuhn, Huggins, Flory, Debye, Mark, and many, many others will still remain the solid ground but when new and extremely detailed information of quite new types is being added at an increasing rate.

The reason for this is twofold. First the now classical treatment of chain molecules has reached such a degree of completion and perfection that new approaches are necessary for further progress. Secondly and perhaps even more relevant the polymers of today are so highly sophisticated that an extremely detailed knowledge is necessary in order to understand their behaviour completely. Of particular importance in this connection has been the studies of tacticity by Natta, Ziegler and many others. That has required completely new approaches to the old problem of polymer conformation or shape.

It is also interesting to note how rapidly the methods developed in other branches of chemistry for a study of conformation are now being assimilated

This paper was presented at a Polymer Science Conference, held in conjunction with the Second World Congress of Man-made Fibres, at the Connaught Rooms, Holborn, London W.C.2, 2nd and 3rd May 1962.

by the polymer chemists. This is particularly evident for methods which have earlier been used in protein chemistry.

The classical model for a polymer is the statistical chain molecule (Figure 1). One of the first and basic problems here was the calculation of

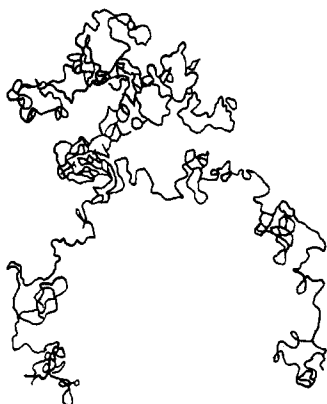


Figure 1—A statistical chain molecule

the chain dimensions, for instance the end-to-end distance for different types of chain behaviour. A typical example of our knowledge in such classical areas can be mentioned. The end-to-end distance of a freely jointed chain consisting of beads of (excluded) volume, v , has been calculated long ago for two and three dimensions which have physical reality corresponding to the shape when the chain is lying flat on a surface or moving around in a solution. Let l be the r.m.s. link length and t the number of links. But it has also been calculated exactly for four and five dimensions and approximate expressions are known for higher numbers of dimensions. [equations (1) to (5), after von Frankenberg and Hughes¹].

q -dimensional excluded volume in random flight chains

$$\langle r_2^2 \rangle = tl^2 [1 + (v/2\pi) (t/l^3)] \quad t^{\frac{1}{2}} \gg 1 \quad (1)$$

$$\langle r_3^2 \rangle = tl^2 [1 + (2/\pi) (3/2\pi)^{\frac{1}{2}} (vt^{\frac{1}{2}}/l^3)] \quad t^{\frac{1}{3}} \gg 1 \quad (2)$$

$$\langle r_4^2 \rangle = tl^2 [1 + (3/2\pi)^{\frac{1}{2}} (2/\pi)^2 (v \ln t/l^3)] \quad \ln t \gg 1 \quad (3)$$

$$\langle r_5^2 \rangle = tl^2 [1 + (5/2\pi)^{5/2} (4/\pi) (v/l^3)] \quad t^{\frac{1}{5}} \gg 1 \quad (4)$$

$$\langle r_q^2 \rangle = tl^2 [1 + 0 (t^{-a})] \quad a > 0, q \geq 6, t^{\frac{1}{q}} \gg 1 \quad (5)$$

That does not mean, however, that all is finalized in these classical areas. In particular, the experimental accuracy still leaves much to be desired and is frequently much lower than expected by most people. A typical example is the following.

One of the most useful parameters in polymer chemistry is the intrinsic viscosity introduced by Staudinger long ago (Figure 2). It is closely related to the dimensions of the polymer chain. It is easily measured and the Staudinger relation ($[\eta] = K \cdot M^a$) is used both as a convenient measure of

molecular weights and as an estimate of chain dimensions as the exponent α increases with increasing chain extensions. Last year two very extensive and thorough investigations on the viscosity of cellulose in the new and useful solvent cadoxen (cadmium ethylenediamine hydroxide) were published. The values of α reported were very different indeed, one gave the value 1.00 the other the value 0.77. This discrepancy is certainly not due to errors in the viscosity measurements but due to uncertainties in the molecular weights of the samples used.

This brings up one of the main difficulties in much polymer research, the difficulty of getting sharp fractions for the measurements. As is well known most polymer samples have a fairly broad distribution in molecular weights (*Figure 3*). Therefore, only average molecular weights can be determined and different averages will be obtained with different methods.

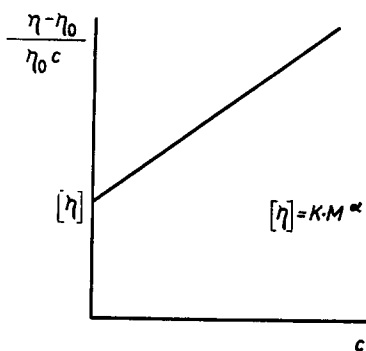


Figure 2—Intrinsic viscosity

It is customary to determine the weight average and the number average for a sample and use their ratio as a measure of heterogeneity. This ratio should be unity for a perfectly sharp fraction; it is two for the distribution obtained by random degradation of an infinitely long chain. The possibility of obtaining sharp fractions has improved tremendously in recent years. It can be shown that by the use of anionic polymerization and 'living' polymers, a Poisson distribution of molecular weights can be obtained^{2,3}. Such distributions are for all practical purposes completely monodispersed and values for M_w/M_n as low as 1.02 have been reported. It must be remembered, however, that a low value of M_w/M_n does not guarantee that

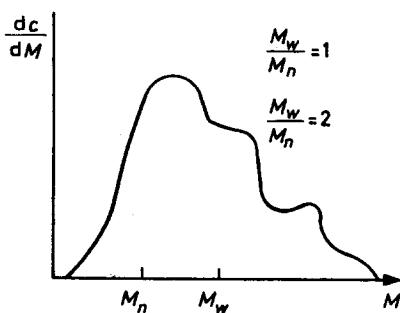


Figure 3—Broad distribution of molecular weights

the sample is particularly sharp (*Figure 4*). For instance a sample consisting of equal parts by weight of three fractions of molecular weights of 400 000, 500 000 and 600 000 will have a value for $M_w/M_n = 1.03$. Furthermore, the present limitations in experimental accuracy for molecular weight determinations make it rather difficult to determine M_w/M_n with precision when their difference is only a few per cent.

There is no doubt, however, that the possibility of synthesizing sharp polymer fractions gives us quite new means for studying small changes in configuration between different types of polymers, e.g. between linear and branched polymers. Such work is now in progress in many places. The preparation of such samples is, however, far from being easy, rigorous purity of all reagents must be maintained during the polymerization process. Even trace impurities will destroy the distribution completely, especially at higher molecular weights.

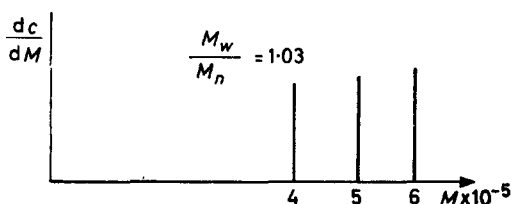


Figure 4— M_w/M_n for mixture of fractions

Frequently, however, the possibility of using that kind of preparation does not exist and then there is an urgent need for effective fractionation procedures. Here effort has been great but progress rather limited during recent years and only a few cases deserve mentioning.

Polymers which can be handled above their crystallization temperature like polyethylenes have been fractionated quite successfully by modifications of the original Desreux technique⁴. The sample is precipitated on to a powdered support and extracted successively with a solvent while raising the temperature. Some typical curves⁵ are shown in *Figure 5*. For materials which crystallize the method is much less successful.

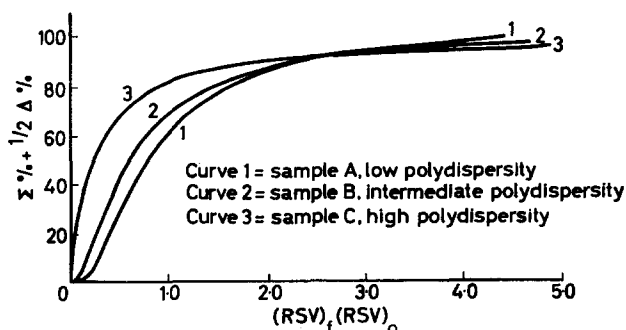


Figure 5—Normalized distribution curves for linear polyethylenes of varying degrees of polydispersity

Another column method of promise, particularly for smaller molecules (obtained for instance in degradation studies) is gel filtration. If a solution is passed through a column packed with small swollen gel particles, big molecules are excluded from the gel and emerge without retardation while smaller molecules which can diffuse into the gel particles move more slowly through the column. With increasing molecular weight the procedure becomes progressively more difficult but for moderate molecular weights it is still quite useful⁶.

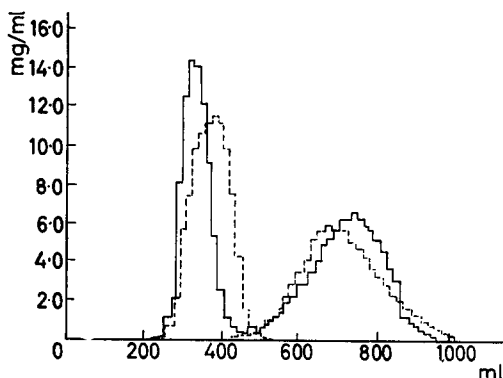


Figure 6—Gel filtration of a mixture of two dextran samples. The dotted lines are for the individual samples

The more widespread use of the well-known density gradient column will also certainly lead to much new information. It is very simple but also extremely sensitive. It can be used both for particles and for molecules (in the latter case the gradient is used in an ultracentrifuge) (Figure 7). They will come to rest at a level where the density of the column is the same as their own density. In this way it is for instance quite simple to distinguish between copolymers of different composition, or between linear and branched polymers and even between sodium chloride crystals with and

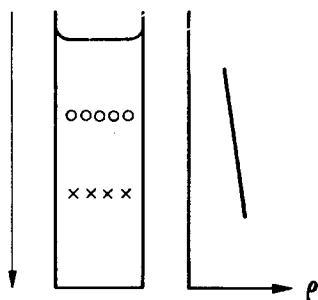


Figure 7—Particles of different density sedimenting in a density gradient will come to rest at different levels

without F centres (Figure 8). Meselson, Stahl and Vinograd have separated deoxyribonucleic acid containing ^{14}N and ^{15}N in this way⁷.

However, there is no doubt that there is still room for new and better separation methods in polymer chemistry which can be used preparatively or for determinations of molecular weight distributions.

Most physical methods developed for such purposes have been only moderately successful (ultracentrifugation, electrophoresis, adsorption chromatography, etc.). The reason is that they all depend on a variation

in mobility or frictional factor with molecular weight. However, the mobility also varies strongly with concentration and that leads in turn to very large changes in relative concentration during the separation process (*Figure 9*).

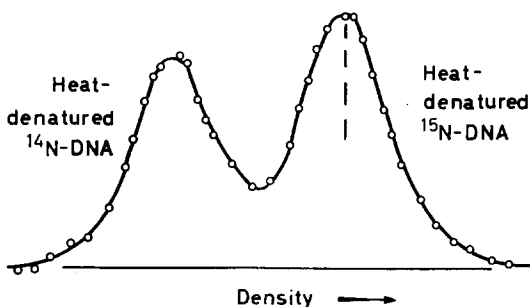


Figure 8—Separation of DNA containing ^{14}N and ^{15}N by ultracentrifugation in a density gradient

These effects are usually called Johnston-Ogston effects in sedimentation, adsorption displacement in frontal analysis chromatography and boundary anomalies in electrophoresis. They are often quite large and difficult to correct for theoretically except when the experiments can be performed at such low concentrations that the effects become negligible. The same diffi-

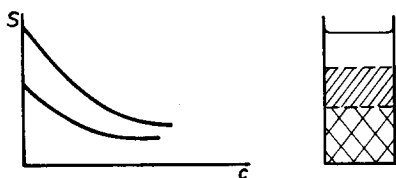


Figure 9—Concentration dependent sedimentation will lead to concentration jumps of *all* components occurring at a boundary

culties prevail also in equilibrium methods due to the large deviations from ideal thermodynamic behaviour for polymer solutions. However, some preliminary experiments in our laboratory and also in Mainz⁸ seem to indicate that the free boundary thermal diffusion may sometimes be used with advantage (*Figure 10*).

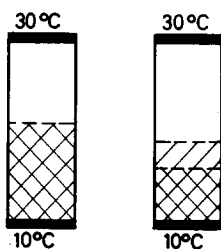


Figure 10—In a solution in a temperature gradient molecules of different weights will move with different rates towards the cold bottom of the cell

The use of physical methods for measuring frictional factors is, however, of very great importance for the determination of molecular dimensions. One can then use either the translational or the rotational friction factor

(*Figure 11*). Almost all our knowledge of molecular dimensions in solution is in fact based on deductions from these two frictional factors plus information from light scattering data. In general one may say that the agreement between data obtained by these three methods is fairly good as long as one is primarily interested in the main dimensions of the molecules.

If we now look at a chain molecule more in detail it is obvious that a chain of limited flexibility or whose links have restricted mobility will have larger extensions than a freely jointed chain of the same linear dimension. It is customary to describe this situation in a way originally developed by Kuhn (*Figure 12*). The real molecule is approximated by a chain of the same length but consisting of longer chain elements which are freely jointed. The length of these Kuhn chain elements will obviously increase with increasing stiffness of the real molecule. It can also be seen from *Table 1*.

In a more detailed discussion of these phenomena it is obviously necessary to distinguish between the extension of a molecule and its rigidity. A molecule can be extended due to valence angle restrictions and still be quite

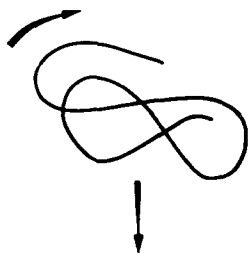


Figure 11—Rotation and translation of a molecule

flexible. We are thus directly led to a concept which has been called the internal viscosity of the molecule by Kuhn. It is a measure of the way a molecule will respond to forces which tend to deform it. Studies of such molecular properties have become increasingly important during recent years. Much pioneering work in this field has been done by Sadron and his co-workers Cerf, Benoit and others in Strasbourg.

The internal viscosity will influence many different kinds of measure-

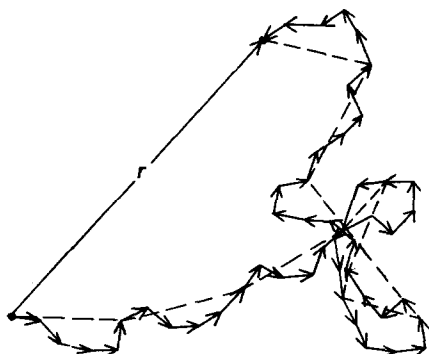


Figure 12—Illustration of the Kuhn statistical chain element

ments but it is particularly predominant when the molecule is brought to rotate and deform in a solution subject to shearing forces. This happens when one measures the viscosity of a polymer solution for instance in a

Table 1. Length of the Kuhn chain element (in Ångström units) for various molecules of different stiffness

| Polymer | Solvent | Am |
|------------------------|---------|------|
| Polystyrene | Benzene | 33 |
| Cellulose | Cadoxen | 70 |
| Cellulose acetate | Acetone | 114 |
| Cellulose trinitrate | Acetone | 193 |
| Hydroxyethyl cellulose | Water | 182 |

capillary viscometer (Figure 13). If the rate of flow through the capillary is increased the deforming forces on the molecule will increase and at the same time the relative importance of the interaction between the molecules will decrease. This will show up in two ways, the viscosity will decrease and

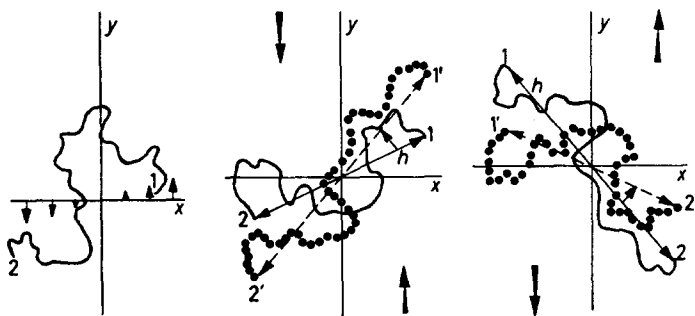


Figure 13—A flexible molecule in a velocity gradient

the concentration dependence of the viscosity will also decrease. In fact, as seen from Figure 14, the concentration dependence disappears even before the viscosity reaches its minimum value⁹. This type of behaviour has also been predicted by Simha in his theoretical studies of such effects. It should here be observed that a molecule will be more easily deformed if the viscosity of the solvent is high. At the present time, however, no adequate theory covers this effect satisfactorily which is seen from Figure 15.

This so-called non-Newtonian behaviour of the viscosity of polymer molecules in solution will certainly continue to be of very great interest for a long time as it is strongly dependent both on the extension of the polymer chains and their internal viscosity. Moreover, the striking difference in behaviour between rigid particles and flexible chains offers new means for studying conformational changes of macromolecules in solution. At present the theories for non-Newtonian behaviour are in a stage of rapid development.

To get more insight into these phenomena it is highly desirable to study the rotation of the molecules directly. That has led to renewed and increased

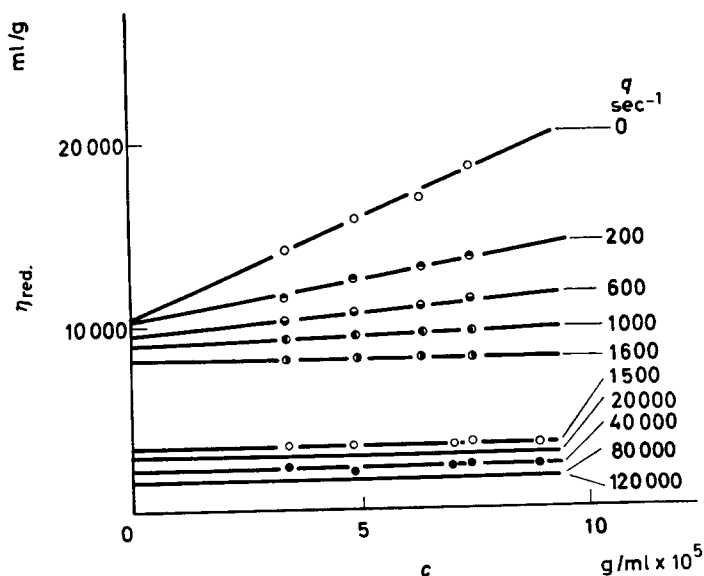


Figure 14—Reduced viscosity measured at various velocity gradients for a high molecular cellulose nitrate ($DP \sim 10^4$)

interest in the rotational properties of macromolecules. There are several ways in which they can be studied directly.

One of these goes back to Perrin. If the molecule contains chemical groups which can fluoresce, that is re-emit absorbed light after a very short (and known!) time interval, the depolarization of the fluorescence gives information about the rotation. This method has been used extensively by

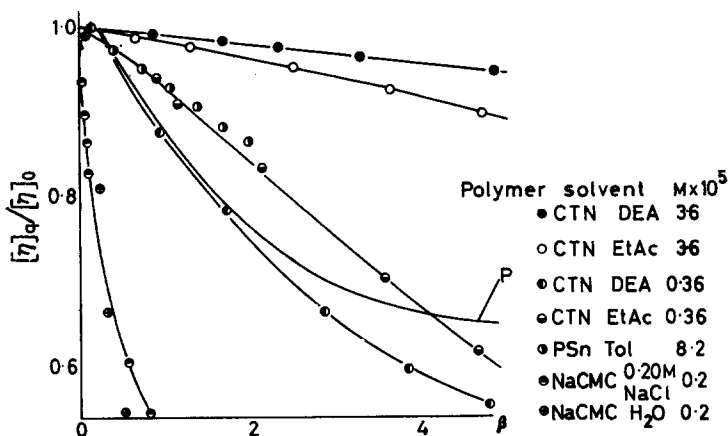


Figure 15—The relative intrinsic viscosity versus velocity gradient relationship for molecules of different internal viscosity (cellulose trinitrate, polystyrene and sodium carboxymethyl cellulose in diethyl adipate, ethyl acetate, toluene and water plus salt): P is theoretical curve according to Peterlin: the values are plotted against

$$\beta = \eta_0[\eta] \cdot M \cdot q / RT$$

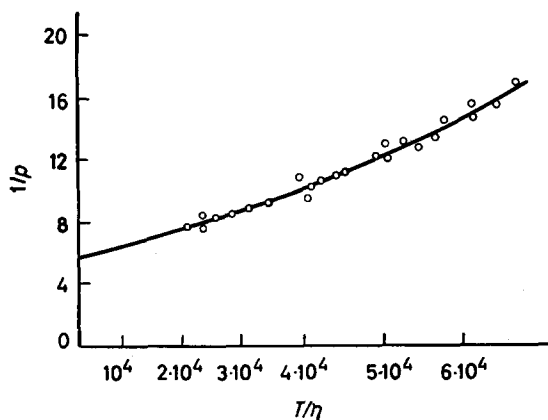


Figure 16—The depolarization of fluorescence for polyethylene-imine combined with 1 - dimethylamino-naphthalene-5-sulphonic acid chloride as a function of temperature/viscosity

Weber in Sheffield for proteins and by the Strasbourg school for polymers. It is now getting widespread use^{10,11} (Figures 16 and 17).

Another method is based upon orientation of the macromolecules in an electric field. The disappearance of the orientation due to the rotary motion of the molecules is followed by measuring the birefringence of the system. The theory for this kind of dynamic double refraction was developed by Peterlin and Stuart for the case of a sinusoidally varying field and later

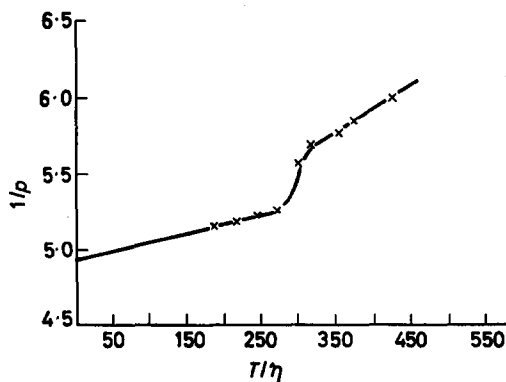


Figure 17—Depolarization of fluorescence for fumarase combined with substrate showing transition point

Benoit, Tinoco and O'Konski have considered the birefringence produced by rectangular pulses on dilute solutions of rigid macromolecules. From such measurements the dipole moment as well as the rotary diffusion coefficient can be determined. Unlike values obtained from hydrodynamic experiments the rotary diffusion coefficients do not depend upon explicit assumptions about the shape of an asymmetric molecule. Table 2 gives some typical values for the rotary diffusion coefficient of poly- γ -benzyl-L-

Table 2. Rotary diffusion coefficient of poly- γ -benzyl-L-glutamate, mol. wt 350000, as a function of concentration

| | | | | | |
|----------------------------|------|------|------|------|-------|
| c (g/l.) | 3.75 | 1.35 | 0.50 | 0.15 | (0) |
| θ sec ⁻¹ | 280 | 700 | 820 | 1010 | (980) |

glutamate of molecular weight 350 000. This molecule is rodlike and the rotary diffusion coefficient is highly concentration dependent indicating large interaction among the long dipolar rods. For a stiff rod the length can be calculated from the value at infinite dilution. It becomes 2 700 Å. From light scattering a corresponding value of 2 000 Å has been obtained. This might indicate a slight flexibility of the molecule as that would lower the rotary diffusion coefficient.

There is no doubt that the increasing use of methods for the study of molecular rotation will lead to much deeper understanding of the properties of polymer molecules, both their shape and their internal viscosity.

Another method for a similar purpose is the study of light scattering of solutions under shear. As light scattering is a very powerful method for the study of molecular configurations such a procedure is highly attractive. Pioneering work has been done by Heller. Unfortunately the method is subject to great experimental difficulties but when they have been overcome it will certainly be extremely useful.

A completely different way of studying small changes in molecular conformation is the use of optical rotatory dispersion or the variation in optical activity with wavelength. It has proved very useful for proteins and polypeptides and an excellent review article has recently been published by Urnes and Doty¹². It has also been used with advantage for the study of tacticity by Pino in Italy and others.

Figure 18 illustrates the large differences in optical rotation for polypeptide chains when they have a helical structure or when they are in the shape of

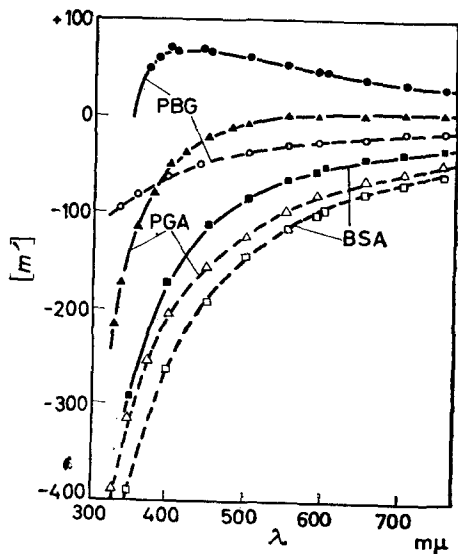


Figure 18—Optical rotatory dispersion for polypeptide chains

random coils¹³. The rotations for the helical forms are more positive than for the disordered forms. From theories developed by Moffit and others very valuable information can be obtained about the structure of the molecules from such data. It is also interesting to note that extremely small

changes in conformation can be observed by the use of optical rotation. *Figure 19* is a typical example of this where one can follow the transition from random coil to helical configuration for polypeptide chains of different degrees of polymerization as the temperature of the solution is varied (*Figure 19*, after Zimm and Bragg¹⁴). In this particular case the helical structure is the stable one at higher temperatures.

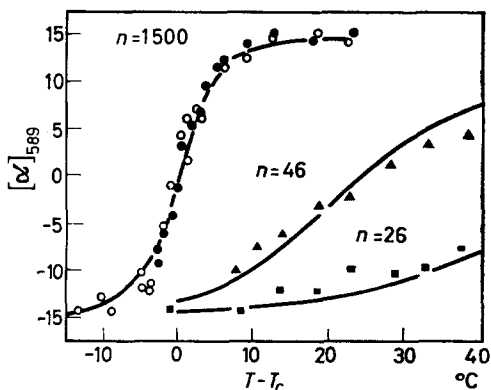
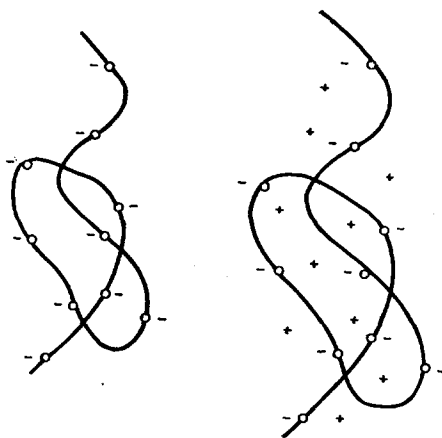


Figure 19—Optical rotation as a function of temperature for polypeptide chains

Lately Szent-Gyorgui, Kascha and Platt¹⁵ started some interesting discussions as to how the properties of a molecule change with its size. For instance molecules which contain between 5 and 50 atoms have a number of properties which could not have been anticipated from a knowledge of diatomics and triatomics alone. Such properties are for instance optical rotation, internal conversion of excitation energy, and strong electronic absorption in the visible region. If one moves one step farther and asks similar questions about macromolecules the most obvious



Figures 20 and 21—Polyelectrolyte molecules in solutions of different concentrations

new property is the large variation in size and shape with changes in the composition of the surrounding medium. This is well known in good and bad solvents where there are large differences in chain dimensions. The effect is, however, most pronounced in polyelectrolytes where a change in degree of ionization will cause very great changes in molecular dimensions. For a large polyelectrolyte molecule at infinite dilution this effect is due to the electrostatic repulsion between the charges (*Figure 20*). However, when the solution becomes more concentrated the swelling equilibrium which will be established is primarily due to the Donnan osmotic force, owing to the rather high ion concentration inside the molecule (*Figure 21*).

In this connection it is therefore of great importance that Kuhn and co-workers¹⁶ have used this phenomenon to construct an artificial muscle, that is a means of producing mechanical energy from different forms of chemical energy with high polymer systems. One of the models they studied was a cross-laminated system of alternate layers of polyvinylalcohol (non-contractile) and polyacrylic acid (contractile) (*Figure 22*). For such a one-dimensional pH-sensitive system they have been able to prove thermodynamically and experimentally that the free chemical energy expended

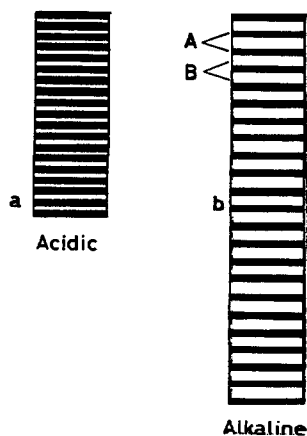


Figure 22—Artificial muscle according to Kuhn

for a chemically induced stretching of the system is exactly equal to the mechanical energy associated with the contraction. The situation is analogous when the dimensions are changed by addition of ions such as Ca^{2+} or Cu^{2+} and also for redox systems such as polyvinylalcohol and polyallylalloxan where a redox change without change in ionization will cause a contraction.

Finally, one could ask why make so many intricate measurements? Would it not be better to look at the molecules in an electron microscope? The answer is obvious; in the electron microscope we have to look at the molecules in a dry state. Fundamental information about molecular dimensions can be obtained but finer details in conformation and internal viscosity cannot be observed. It is not easy to make good electron micrographs of chain molecules as the thickness of the chain is not much greater

than the resolving power of the microscope. Recently, however, it has become possible to photograph individual chain molecules successfully if particular care is taken in the preparation of the specimen. Hall and Doty have obtained beautiful pictures of some polypeptides in this way and I will end by showing a photograph (*Figure 23*) of a cellulose molecule

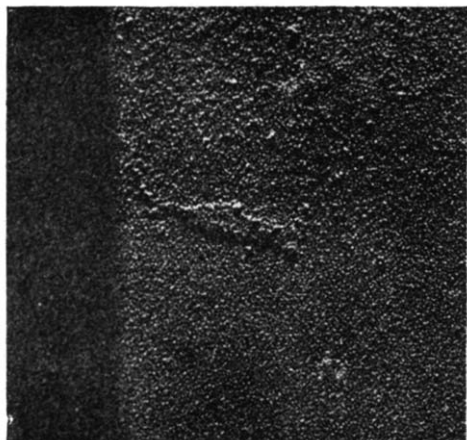


Figure 23—Electron micrograph of a hydroxyethyl cellulose molecule. The big shadow to the left is from a polystyrene sphere outside the picture used for calibration

(substituted with about one hydroxyethyl group per glucose unit) which has been obtained in my laboratory by Mr Gellerstedt¹⁷. From such photographs the length of the molecules can be measured with good accuracy and it is comforting to know that these values agree well (normally to better than ten per cent) with values obtained by the methods discussed earlier.

*Fysikalisk-Kemiska Institutionen,
Uppsala Universitet, Sweden*

DISCUSSION

Professor G. Gee (U.K.), Chairman: One of the problems which concerns us all a great deal, a preliminary one in a way, is that of fractionation, and I was interested in the comments which Professor Claesson made about the technique of filtration through a gel. I wonder if he has anything he would like to add to that. How far is the actual choice of the gel important? Have you any practical advice you can give us?

Professor S. Claesson (Sweden): I have not been working much in this area myself, but a lot of work is going on in Uppsala in this field, because the most common gel which you can get today for this purpose is a cross-linked dextran manufactured by Pharmacia. The trouble is that when you are going up in molecular weight, you must have fairly large meshes in your gel, and then your gel becomes very soft, and it may become a little difficult to work with, so I doubt if you can go up to very high molecular weight in this way. However, we have had very great success with this method in separating degradation products from big molecules. It is ideally

suiting for that particular kind of work. Also, I think that this technique is better developed for water solutions at present than for organic samples. It has given excellent service in protein chemistry.

Professor G. Gee (U.K.), Chairman: You presented it essentially as mainly a filtration technique, rather implying that there would be no interaction between the nature of the gel and the nature of the polymer. Is that borne out essentially?

Professor S. Claesson (Sweden): It is to a reasonable extent. It has been found at least for smaller molecules, that you get approximately the result that can be calculated from the ratio between the volume of the full vessel and the interstitial volume. However, in some cases weak absorption forces are mixed in with gel filtration.

Dr H. L. Vosters (Netherlands): You were asking for new methods. I wonder if you could get information from measuring the dielectric constant as a function of wavelength, for example, or temperature. Could Professor Claesson say something about that?

Professor S. Claesson (Sweden): I think that that is a very useful technique which has often been tried quite successfully, for example, by O'Konski and co-workers, when they have been looking for molecular motion. However, for a study of, say, molecular weight distribution, I think it would be much less successful.

Professor F. Danusso (Italy): I think it would be interesting to mention here the concept of micro-molecular transitions. We have determined the density/temperature dependence for polystyrene solutions. The curve has a singular point. The precise form is not yet known on account of the high accuracy required in the density measurements. Benoit and his colleagues in Strasbourg have found a peak in the molecular dimensions of polystyrene in a similar temperature region (about 50°C). The same seems to be true for the second virial coefficient. I think it would be interesting in connection with these phenomena, to speak about a transition of the polymer in a molecularly dispersed phase. I think that these transitions are different from helix coil transitions, being on a finer scale.

Professor S. Claesson (Sweden): Yes, I agree with you that these effects are very important, and I also agree that there are certainly transitions which are much less dramatic, for instance, than between a helical and a statistical coil. We have such a transition of course as a continuous one when we mix a good and a bad solvent or vice versa, but then it is happening slowly over an extended region. Here you have given some facts which tend to prove that you can also sometimes get such changes over a fairly narrow temperature region. But these were, I suppose, moderately concentrated solutions, were they not? How high were the concentrations?

Professor F. Danusso (Italy): 0.2, 0.3 per cent.

Professor J. Furukawa (Japan): You mentioned the free-boundary thermal diffusion method. What was the significance of the free boundary in this method?

Professor S. Claesson (Sweden): Thermal diffusion can be performed in two ways which are analogous to sedimentation equilibrium and sedimenta-

tion velocity experiments. You have a cell which is hot at the top and cold at the bottom, and you fill it at the start with your solution all the way up without a boundary. Then, as time goes on, you will get a concentration redistribution until you reach equilibrium with a higher concentration at the bottom of the cell than at the top. That would correspond exactly to equilibrium centrifugation when you are spinning a centrifuge at such a rate that at equilibrium you have a higher concentration at the bottom than the top. From this you can calculate the molecular weight, in the case of sedimentation, but you know very well that if you have several components present, equilibrium sedimentation is not particularly selective. The same is true for this ordinary type of thermal diffusion. However, if thermal diffusion is started with a free boundary in the middle of the cell and a fairly strong thermal gradient is used, the downward motion of the molecules will cause the boundary to move down and if several components are present the original boundary will be resolved into several boundaries moving with different rates. This can be observed by optical means as several peaks in exactly the same way as for velocity sedimentation when you are running a centrifuge at high speed (Claesson and Norberg, unpublished). Therefore free-boundary thermal diffusion has a much higher analytical resolving power than ordinary thermal diffusion for mixtures of several components.

Professor J. Furukawa (Japan): Is there any indication that this method could be scaled up for preparative purposes?

Professor S. Claesson (Sweden): It is a difficult question to answer, and you know people working on new separation methods are always much more hopeful than they ought to be really. But I think that the possibilities are about the same as in electrophoresis.

REFERENCES

- ¹ VON FRANKENBERG, C. and HUGHES, R. E. *J. chem Phys.* 1961, **35**, 503
- ² SZWARC, M. *Fortschr. Hochpolymer Forsch.* 1960, **2**, 275
- ³ MCCORMICK, H. W. *J. Polym. Sci.* 1959, **36**, 341
- ⁴ DESREUX, V. *Rec. Trav. chim. Pays-Bas*, 1949, **68**, 789
- ⁵ FRANCIS, P. S., COOKE, R. C. and ELLIOTT, J. H. *J. Polym. Sci.* 1958, **31**, 453
- ⁶ GRANATH, K. and FLODIN, P. *Makromol. Chem.* 1961, **48**, 160
- ⁷ MESELSON, M. and STAHL, F. *Proc. Nat. Acad. Sci., Wash.* 1958, **44**, 671
- ⁸ MEYERHOFF, G., LUTJE, H. and RAUCH, B. *Makromol. Chem.* 1961, **44**, 489
- ⁹ CLAESSION, S. and LOHMANDER, U. *Makromol. Chem.* 1961, **44**, 461
- ¹⁰ WAHL, P. H. *J. Polym. Sci.* 1958, **29**, 375
- ¹¹ MASSEY, V. *Biochem. J.* 1953, **53**, 67
- ¹² URNES, P. and DOTY, P. *Advances in Protein Chemistry*, p 681, 1962
- ¹³ URNES, P., IMAHORI, K. and DOTY, P. *Proc. Nat. Acad. Sci., Wash.* 1961, **47**, 1635
- ¹⁴ ZIMM, B. and BRAGG, J. K. *J. chem. Phys.* 1959, **31**, 526
- ¹⁵ PLATT, J. *J. theor. Biol.* 1961, **1**, 342
- ¹⁶ KUHN, W. *et al. Fortschr. Hochpolymer Forsch.* 1960, **1**, 540
- ¹⁷ GELLERSTEDT, N. *Ark. Kemi*, in press

Ionic Polymerization of Polar Monomers

JUNJI FURUKAWA

The polymerization of two classes of polar monomers (vinyl compounds which yield polymers having polar groups in side chains; oxygen-containing compounds having heteroatoms in the main chain) is considered, with special reference to the mechanism of their stereoregular chain propagations and to the role of polymerization catalysts. Principal aspects are: anionic polymerization of acrylic compounds, polymerization of aldehydes and ketones, polymerization of alkylene oxides, cyclic ethers of more than three ring members, stereoregulation in cationic polymerizations.

POLYMERIZATIONS of the so-called polar monomers have long been studied by a great number of researchers, and a large technical literature exists concerning the polymerization processes as well as the physical properties of the resulting high polymers. The most familiar polar monomers are such vinyl compounds as vinyl acetate, vinyl ethers, vinyl halides and acrylic esters, which afford high polymers having polar groups in side chains. There is another class of polar monomers, which give the polymers containing heteroatoms in the main chain. Included in this latter class of polar monomers are those oxygen-containing compounds like aldehydes, ketones and cyclic ethers such as alkylene oxide, oxacyclobutane and tetrahydrofuran. The present paper concerns the polymerizations of these two classes of polar monomers, with special reference to the mechanism of their stereoregular chain propagations and to the role of polymerization catalysts.

The polar monomers of our concern are listed in *Tables 1* and *2*, where the structures of the resulting high polymers are also represented in comparison with those of the corresponding non-polar polymers (or rather the reference olefine polymers).

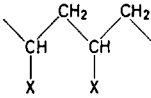
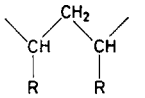
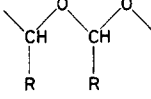
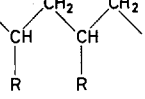
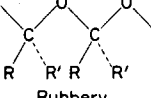
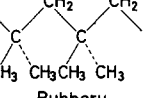
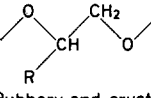
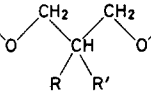
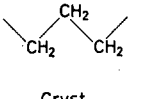
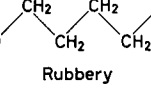
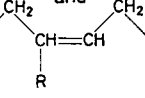
High polymerizations of aldehydes and cyclic ethers have been accomplished only lately by using ionic catalysts. Vinyl and acrylic compounds have received attention again from the viewpoint of stereoregular polymerization, the results being fine success in obtaining stereospecific polymers by use of ionic initiators. Ionic polymerization is thus attractive in high polymerization and stereoregular polymerization of polar monomers.

Clearly, ionic polymerizations are classified into two types according to the nature of the carrier ions of growing polymer chains. One is the cationic polymerization in which the growing chains carry a positively charged ionic centre while the other which is called anionic polymerization is just the ionic counterpart of cationic polymerization. A few typical catalysts for ionic polymerizations are given in *Table 3*.

In anionic polymerizations alkali and alkali-earth metals and their alkyl or alkoxy derivatives are used principally as polymerization catalysts.

This paper was presented at a Polymer Science Conference, held in conjunction with the Second World Congress of Man-made Fibres, at the Connaught Rooms, Holborn, London W.C.2, 2nd and 3rd May 1962.

Table 1

| Polar monomers | Polymer | Reference olefine polymer |
|---|---|---|
| $\begin{array}{c} \text{CH}_2=\text{CH} \\ \\ \text{X} \end{array}$ <p>Acrylic compds. Vinyl ethers</p> |  <p>Amorph. and cryst.</p> |  <p>Amorph. and cryst.</p> |
| $\begin{array}{c} \text{CH}=\text{O} \\ \\ \text{R} \end{array}$ <p>Aldehydes</p> |  <p>Rubbery and cryst.</p> |  <p>Rubbery and cryst.</p> |
| $\begin{array}{c} \text{R}' \\ \\ \text{C}=\text{O} \\ \\ \text{R} \end{array}$ <p>Ketones</p> |  <p>Rubbery</p> |  <p>Rubbery</p> |
| $\begin{array}{c} \text{RCH}-\text{CH}_2 \\ \diagdown \quad / \\ \text{O} \end{array}$ <p>Oxyrane</p> |  <p>Rubbery and cryst.</p> | |
| $\begin{array}{c} \text{R} \\ \\ \text{C}-\text{CH}_2 \\ / \quad \\ \text{R}' \quad \text{CH}_2-\text{O} \end{array}$ <p>Oxetane</p> |  <p>Cryst.</p> |  <p>Cryst.</p> |
| $\begin{array}{c} \text{CH}_2-\text{CH}_2 \\ \quad \\ \text{CH}_2 \quad \text{CH}_2 \\ \\ \text{O} \end{array}$ <p>Tetra-hydrofuran</p> |  <p>Rubbery</p> |  <p>Rubbery</p> |

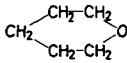
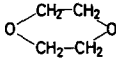
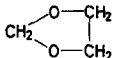
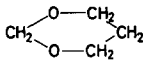
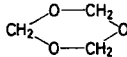
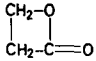
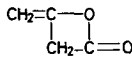
These catalysts are all believed to form active carbanions or alkoxyl anions on reacting with vinyl monomers, aldehydes and cyclic ethers. In the polymerization of alkylene oxides, we have found that the catalytic activity of metal alkyls is much enhanced when they are treated with an equimolar amount of water, whereby alkyl metal oxides are formed and are more efficient catalysts. Here, it is also noteworthy that in all these cases counter cations exert significant stereoregulating action on the propagation steps by pairing with the growing chain ends or by coordinating to the monomers to be attacked. The counter cations are not necessarily simple metallic cations but can exist also in associated or complex form of $M_I^+ - Z - M_{II}$, e.g. $\text{Li}^+ \dots \text{RM}$ and $\text{Zn}^+ - \text{O} - \text{ZnR}$. The significance of the counter-ion complexes in stereoregular polymerizations will be emphasized later.

In cationic polymerizations selection of catalysts seems to be of great importance for obtaining high polymers, inasmuch as cationic polymerizations are liable to be accompanied by undesirable side reactions such as

IONIC POLYMERIZATION OF POLAR MONOMERS

termination and isomerization. Many Lewis acids are used as effective cationic catalysts. Among others, a partly-hydrolysed alkylaluminium has been found to be an excellent catalyst for cationic homopolymerization of four- and five-membered cyclic ethers, e.g. oxetane and tetrahydrofuran. The

Table 2

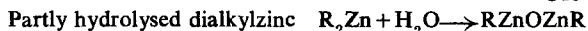
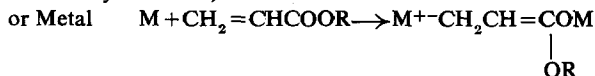
| | |
|---|---|
| Cyclic ether | |
|  | Tetrahydropyran (copolymer with oxetane) |
|  | 1,4-Dioxan (copolymer with oxetane) |
| Cyclic acetal | |
|  | 1,3-Dioxolane |
|  | 1,3-Dioxan |
|  | Trioxan |
| Cyclic ester | |
|  | β -Propiolactone |
|  | Diketene |

problems of co-catalysts and counter-ion effects in cationic polymerization will be dealt with in the forthcoming sections.

In connection with the problem of stereoregulation in ionic polymerizations, we would like to point out that four different modes are conceivable for ionic chain growth, as shown in *Table 4*.

Table 3. Ionic catalysts

Anionic polymerization



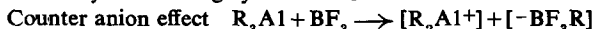
Cationic polymerization



Partly hydrolysed alkyl aluminium and co-catalyst

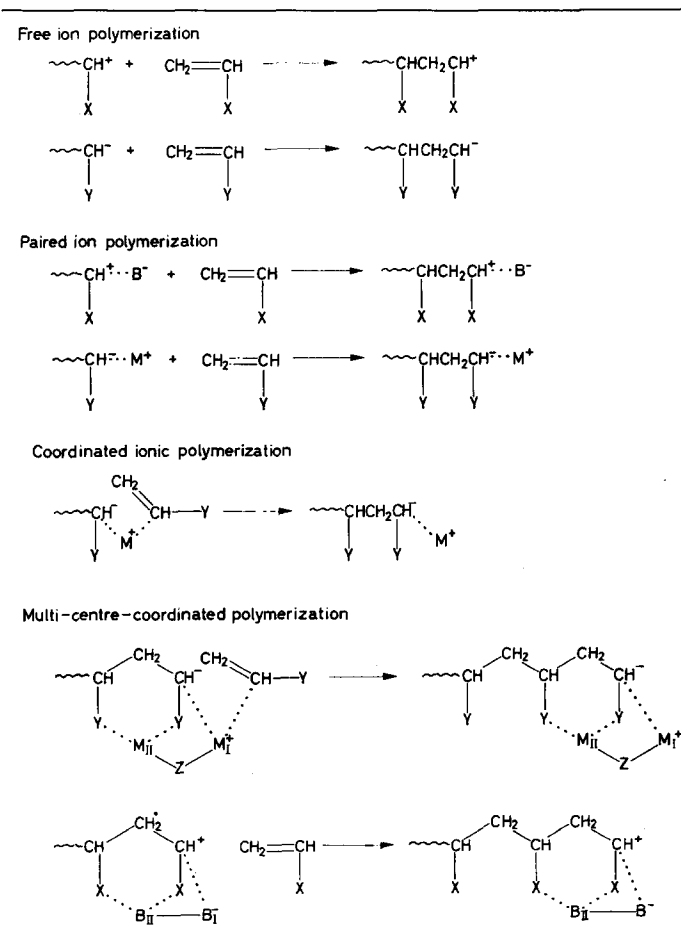


Co-catalyst small ring cyclic ether effective



Apparently, stereoregulation is possible in all of these four cases. In the free-ion and paired-ion polymerizations the reaction must be performed at extremely low temperatures, whereas in coordinated and multi-centre-coordinated polymerizations stereoregulation is possible even at elevated temperatures. Here, multi-centre-coordinated polymerization means a polymerization such that in the transition state of the propagation

Table 4



step, the polar groups of monomer as well as those neighbouring to the ionic centre of growing polymer are coordinated to more than one active centre of complex or associated catalyst. Such a multi-centred coordination will suffice to restrict the free rotation of chain ends and monomers in the chain propagation step.

IONIC POLYMERIZATION OF POLAR MONOMERS

ANIONIC POLYMERIZATION OF ACRYLIC COMPOUNDS
 Acrylic esters are typical monomers which undergo anionic polymerization to give stereoregular polymers. Extensive work has already been accomplished for methyl methacrylate¹⁻⁵ and butyl acrylate^{6,7}, and their crystalline polymers have been obtained by using alkyllithium and Grignard reagent as catalyst. Our efforts have been directed to obtaining further information on the catalysts to be used for acrylic and related monomers.

We found that some 'ate-complex' type compounds such as lithium aluminium hydride and calcium zinc tetraethyl exhibit an excellent catalytic and stereoregulating activity toward acrylic⁸ and methacrylic⁹ esters. These catalysts contain two metallic centres thus enabling multi-centred coordination. Other combinations of lithium, calcium, barium or strontium with metal alkyls have been known to possess a similar ability, as shown in Table 5. Some of these combinations afford stereoregular polymer even at room temperature.

Table 5. Examples of excellent catalysts of ate-complex type

| <i>Ate-complex</i> | <i>Solvent</i> | <i>Polymer</i> |
|---|----------------|----------------|
| LiAlH ₄ | ether, toluene | isotactic |
| LiBH ₄ | ether | isotactic |
| LiAlH ₄ -ZnEt ₂ , -CdEt ₂ , -AlEt ₃ | ether, toluene | isotactic |
| Ca-, Sr-, Ba-ZnEt ₂ | ether, toluene | isotactic |
| LiR-AlEt ₃ | ether, toluene | syndiotactic |

Radical type initiators are known to give crystalline (syndiotactic but not isotactic) polymers at extremely low temperatures only¹. Lithium or alkyllithium is a stereoregulating catalyst only when it is used in a non-polar solvent at low temperatures¹. On the contrary, ate-complex type catalysts do not necessitate any special condition to obtain isotactic polymers.

Alkyllithium and alkylmagnesium halide are known to be associated to some extent and such an association seems to contribute to the stereo-

Table 6. Properties of polyalkyl acrylates†

| <i>Catalyst</i> | <i>Polyalkyl acrylate</i> | | | | |
|-----------------------------------|---------------------------|---|---|---|---|
| | CH ₃ | <i>n</i> -C ₄ H ₉ | <i>i</i> -C ₄ H ₉ | <i>s</i> -C ₄ H ₉ | <i>t</i> -C ₄ H ₉ |
| AIBN | A | A | A | A | A |
| <i>n</i> -Bu ₃ B-BPO | — | A | A | A | A |
| <i>n</i> -BuLi | A | A | A | A | C |
| PhMgBr | — | A | — | C | C |
| <i>n</i> -BuLi·Et ₃ Al | — | — | — | — | C |
| <i>n</i> -BuLi·Et ₂ Cd | — | A* | C | C | C |
| Ca·ZnEt ₄ | A | A* | C | C | C |
| Sr·ZnEt ₄ | A | A* | C | C | C |

†A, amorphous; C, crystalline; A*, its i.r. spectrum differed from that of the authentic amorphous polymer.

regulation. But, generally speaking, the regulating ability is higher in complex catalysts than in associated catalysts. *Table 6* shows this trend.

The stereoregular polymerizations of a wide variety of acrylic compounds have been investigated by us from a viewpoint of steric hindrance of substituents in monomer. All the acrylic esters studied are represented in *Figure 1*, where the group α , which is attached to the key carbon, denotes hydrogen, methyl or chlorine and the group γ is methyl, ethyl, *n*-propyl, isopropyl, *n*-butyl, isobutyl, sec-butyl or *t*-butyl; silyl and benzyl esters being used as special examples. For the sake of comparison, the oxygen atom at the β position of acrylates has been replaced by sulphur and carbon atoms. These replacements led to the use of thiolacrylates¹⁰ and vinyl ketones¹¹, respectively, as special cases of acrylates.

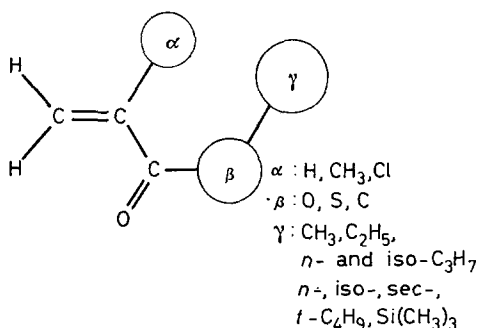


Figure 1

In the acrylic esters of ordinary alcohols the presence of bulky alkyl groups in the γ position seems to favour the polymer crystallinity, as is evidenced by the variation of solubility of the polymers obtained (*Table 7*).

The effective bulkiness of the γ position can be supposed to be larger in the cases of branched alkyl groups such as isopropyl, secondary butyl,

Table 7. Solubility and melting point of polyacrylic esters*
(Catalyst: SrZnEt₄)

| <i>Solvent</i> | CH ₃ | <i>n</i> -C ₄ H ₉ | <i>i</i> -C ₄ H ₉ | <i>s</i> -C ₄ H ₉ | <i>t</i> -C ₄ H ₉ |
|----------------------|-----------------|---|---|---|---|
| Acetone (cold) | sol. | sol. | swell | insol. | — |
| Dimethylformamide | sol. | sol. | sol. | insol. | — |
| Dioxan | sol. | sol. | sol. | insol. | insol. |
| Acetone (hot) | | | | swell | insol. |
| 3-Heptanone | sol. | sol. | sol. | swell | swell |
| Toluene | sol. | sol. | sol. | sol. | insol. |
| Carbon tetrachloride | sol. | sol. | sol. | sol. | swell |
| Chloroform | sol. | sol. | sol. | sol. | sol. |
| M.pt (°C) | — | 43–47 | 72–81 | 125–130 | 198–200 |
| Density (obs.) | | | 1.05 | 1.05 | 1.03 |
| Density (calc.) | | | 1.24 | 1.06 | 1.04 |
| Helix—type | — | — | 3 ₁ isotact | 3 ₁ isotact | 3 ₁ isotact |

*Sol., soluble; insol., insoluble.

and especially tertiary butyl than in normal butyl and isobutyl groups and, indeed, even benzyl and silyl groups.

It is also to be noticed that crystallinity depends not only upon regularity in polymer structure but also upon steric hindrance of groups in the crystallization process. In a detailed study the structural regularity was examined⁸ by means of the crystallinity of hydrolysed polymer as shown in *Table 8*.

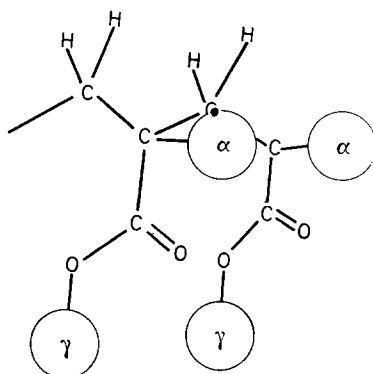
Table 8. Polyacrylic acids obtained by hydrolysis of polyacrylic esters

| Alkyl group | Acrylate polymer | | Hydrolysed polymer crystallinity* |
|---|---------------------|----------------|-----------------------------------|
| | Catalyst | Crystallinity* | |
| <i>n</i> -C ₄ H ₉ | AIBN | A | A |
| <i>t</i> -C ₄ H ₉ | AIBN | A | A |
| CH ₃ | SrZnEt ₄ | A | C |
| <i>n</i> -C ₄ H ₉ | SrZnEt ₄ | A | C |
| <i>i</i> -C ₄ H ₉ | SrZnEt ₄ | C | C |
| <i>t</i> -C ₄ H ₉ | Li | C | C |

*A, amorphous; C, crystalline.

Here polyacrylates of methyl and *n*-butyl alcohols were found to be essentially stereoregular despite the lack of crystallinity. Bulky groups in alcohol seem to be favourable for crystallization, perhaps because intramolecular interaction of neighbouring bulky groups restricts their free rotation around the carbon-carbon bonds in a polymer main chain. In other words, the polymer chain bearing bulkier side groups may be the more rigid during the crystallization process. Possible structures of the crystallized polyacrylates are proposed in *Figures 2* and *3*. *Figure 2* corresponds to the planar zig-zag structure while *Figure 3* represents the spiral form.

Figure 2



These planar zig-zag and spiral structures of the crystallized state may also be possible at the stage of polymerization, if the geometry of the polar groups located in the vicinity of the growing chain end is fixed by their coordination on to a bi-centred catalyst. Illustrated in *Figure 4* is a possible conformation of the growing polymer chain end coordinated to a metallic

centre of catalyst through the end and penultimate groups. For the spiral polymer structure, one may also conceive a coordination of polymer chain to catalyst through the end group and its nearest polar group of the same phase (see *Figure 3*).

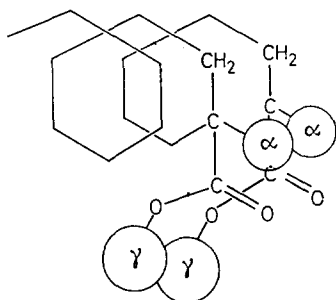


Figure 3

Substituents in the α position also exert serious influence upon crystallinity. Methacrylates afforded no crystalline polymer except for the case of the methyl ester, that is, the case of the smallest bulkiness of the γ position. Ionic polymerization of α -chloroacrylates was also practicable, but stereoregulation was unsuccessful in contrast to the case of α -chlorothiol acrylates.

Thiolacrylate¹⁰ and thiolmethacrylate¹² were studied to examine the effect of group in β position and similar effect of bulky alkyl group of thioalcohol. The influence seems to be rather more profound than in acrylic esters of

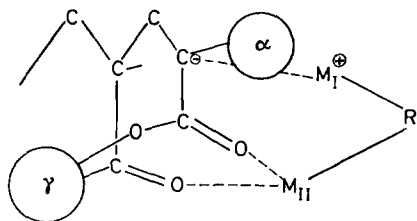


Figure 4

ordinary alcohol. Besides isopropyl, sec-butyl and *t*-butyl esters, both *n*-propyl and *n*-butyl esters were found to give crystalline polymers as well. Even the α -chloroacrylic ester of sec-butyl thiol can undergo stereoregular polymerization. However, the reason for enhancement in stereoregulation of this case is not known yet. It is difficult to decide at the present stage whether it has resulted from the larger radius of sulphur atom and accordingly the larger interaction of mercapto groups or from the weaker electronegativity of sulphur and accordingly the stronger coordinating property of carbonyl group.

Vinyl ketone¹¹ can be regarded as the extreme case where the β atom is carbon. Recently, isopropyl vinyl ketone has been reported to give crystalline polymer, and even methyl vinyl ketone has been converted to stereoregular polymer in our laboratory.

IONIC POLYMERIZATION OF POLAR MONOMERS

POLYMERIZATION OF ALDEHYDES AND KETONES

High polymers of acetaldehyde and higher aliphatic aldehydes are attainable by either cationic or anionic polymerization, where the stereoregularity of the polymers is much affected by the ionic character of the catalysts used. Table 9 is a list of excellent catalysts discovered for the acetaldehyde polymerization in our laboratory¹³⁻¹⁵.

Table 9. Metal compound catalysts for polymerization of acetaldehyde

| Metal compound | Assumed active species | Polymer | Ref. |
|--|---|-------------|------|
| RM | CH ₃ (R)CHOM | Crystalline | 14 |
| ROM | ROM | Crystalline | 14 |
| (RO) _m M + H ₂ O | (RO) _{m-1} M—O—M(OR) _{m-1} | Stereoblock | 15 |
| γ-Al ₂ O ₃ | $\begin{array}{c} \text{—Al—O—Al—} \\ \qquad \quad \\ \text{O} \qquad \quad \text{O} \\ \qquad \quad \end{array}$ | Atactic | 13 |

Since metal alkyls are amenable to react with aldehydes to give rise to metal alkoxides, it is very likely that the alkoxides are real active species. Indeed, several alkoxides were shown to have initiating ability. γ-Alumina itself also has catalytic activity, but it affords atactic polymer alone. Partly hydrolysed alkoxide is found to be another type of catalyst which affords stereoblock polymer consisting of isotactic and atactic blocks. Acetone was reported to be polymerized by the molecular ray method¹⁶ at low temperatures or by γ-irradiation¹⁷.

Polyacetaldehyde and polyacetone are interesting materials but are far from being put to practical use on account of very poor stability even when improved by the addition of stabilizer or by end-group modification.

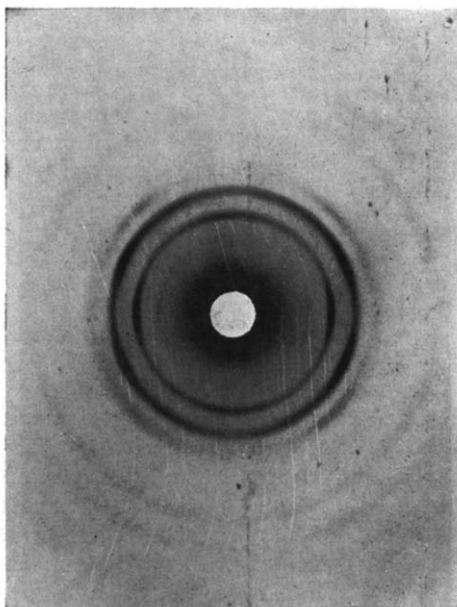
Table 10. Crystalline acetone block polymer

| |
|---|
| Polymerization |
| by Al(C ₂ H ₅) ₃ -TiCl ₃ -Salt, Salt: CaCl ₂ , CH ₃ COONa, (CH ₃ COO) ₂ Mg at -78°C under propylene atmosphere |
| Polymer |
| m.pt: 58° to 60°C |
| analysis: 83.7% acetone (C 65.0, H 10.5, O 24.4 per cent) |
| hydrolysis: acetone (m.pt of 2,4-dinitrohydrazone 127°C) |
| infra-red: ν _{COO} =1 148, 1 113, 1 062 cm ⁻¹ |
| X-ray analysis: a=b=14.65 Å, c=10.22 Å, N=28 |
| space group P ₄ |

We succeeded in the preparation of crystalline polymer of acetone or acetaldehyde blocked by poly-α-olefine¹⁸. Crystalline polyacetone of comparative stability was prepared under the atmosphere of α-olefine (propylene) by using a modified Ziegler catalyst consisting of triethylaluminium, titanium tri- or tetra-chloride and a metal salt such as calcium chloride, sodium acetate or magnesium acetate. The last component is essential for

the acetone polymerization. Without these salts there occurred the polymerization of propylene only. Elemental and infra-red analyses indicated the polymer to be polyacetone having 14 per cent of polypropylene blocks. It is highly crystalline and melts at 58° to 60°C. It is quite stable

Figure 5—X-ray fibre diagram of crystalline polymer of acetone



and no appreciable decomposition is observed even at 200°C. The analytical data are given in *Table 10*. *Figure 5* shows the X-ray fibre diagram. Block copolymer of acetaldehyde and propylene was also prepared by a similar procedure.

POLYMERIZATION OF ALKYLENE OXIDES

Propylene oxide is an interesting material; its low molecular weight block copolymer with ethylene oxide is now commercially available as the prepolymer for urethane rubber and its high polymer promises the appearance of a new rubber. The high polymerization has been possible with the use of suitable catalysts, one of which is diethylzinc activated by a controlled amount of water or alcohol. When diethylzinc is treated with water or alcohol, the compounds of *Table 11* are assumed to be produced.

Probably, ethylzinc hydroxide and ethylzinc alkoxide exist in the associated form. These compounds have zinc-oxygen-zinc linkage as a common structure which is suggested to play an important role in the propagation. The alkoxyl or alkyl anion attached to a metallic centre of the catalyst is assumed to initiate the polymerization by acting on the monomer coordinated at another zinc atom of the catalyst (*Figure 6*). This assumption is partly supported by the results of our recent investigation adopting a special alcohol like 9,10-dimethylolanthracene as co-catalyst. That is, poly-

IONIC POLYMERIZATION OF POLAR MONOMERS

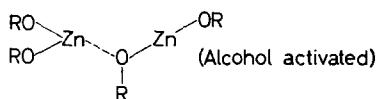
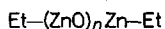
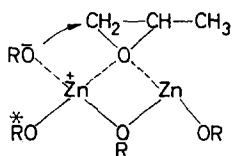


Figure 6—Modified alkylzinc catalyst



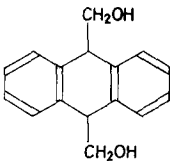
propylene oxide and poly- β -propiolactone prepared by use of dialkylzinc and the alcohol has been proved by u.v. analysis to contain the same alkoxy fragment as does the co-catalyst alcohol (Table 12).

It was also found that an alkoxy group in the catalyst plays an influential role on stereoregulation in propylene oxide polymerization, as is shown in Table 13. Apart from isobutanol, the use of lower alcohols seems to favour the stereoregulation.

Table 11

| | |
|--|--|
| Et ₂ Zn—H ₂ O system | |
| EtZnOH | |
| EtZnOZnEt | |
| Et(ZnO) _n ZnEt | |
| Et ₂ Zn—ROH system | |
| EtZnOR | |
| ROZnOR | |
| | |

Table 12

| | |
|---|--|
| Catalyst system | |
|  | + ZnBu ₂ |
| Polymer | |
| Poly(propylene oxide) : | Fluorescent polymers having 258 m μ absorption |
| Poly(β -propiolactone) : | Greenish fluorescent polymer having 262 m μ absorption |

We have succeeded in the preparation of optically active polymer from DL-propylene oxide by asymmetric induction, using optically active alcohols as co-catalyst (see Table 14).

It is interesting to note that the $[\alpha]_D$ of the obtained polymer changes in sign in different solvents, in agreement with Price's experimental findings concerning optically active poly(propylene oxide) prepared from the optically active monomer.

How then would asymmetric induction take place? It may be brought about either through direct stereoregulation by an alkoxy group in the catalyst or through indirect regulation due to the successive interaction

Table 13. Crystalline fraction in polypropylene oxide prepared by the system of dibutyl-zinc and alcohols

| (Monomer, 0.05 mole Solvent, 3.5 ml toluene Catalyst, 0.0023 mole Bu ₂ Zn Co-catalyst, 0.0046 mole alcohol Polymerization, room temperature) | | |
|---|-------------------|--------------------------|
| Alcohol | Polymer yield (%) | Crystalline fraction (%) |
| CH ₃ OH | 68 | 9.2 |
| C ₂ H ₅ OH | 51 | 5.3 |
| <i>n</i> -C ₃ H ₇ OH | 85 | 2.8 |
| <i>i</i> -C ₃ H ₇ OH | trace | — |
| <i>n</i> -C ₄ H ₉ OH | 93 | 1.6 |
| <i>i</i> -C ₄ H ₉ OH | 33 | 15.1 |
| <i>s</i> -C ₄ H ₉ OH | trace | — |
| <i>t</i> -C ₄ H ₉ OH | nil | — |

between the monomer and the penultimate unit in a growing polymer chain. In the latter case the first induction should be effected, of course, by the alkoxy group of the catalyst. This problem imposed on asymmetric induction is very important to establish the mechanism of stereoregulation.

IONIC POLYMERIZATION OF POLAR MONOMERS

Figure 7 illustrates possible arrangements of monomer units in polymerizations of propylene oxide and aldehydes. Both cases are similar in that the key atom for stereoregularity exists in monomer but not in chain end. Here direct asymmetric induction caused by catalyst alcohol seems

Table 14. Asymmetric induction in polymerization of propylene oxide

| Activator | Solvent for polymer | η_{sp}/C | $[\alpha]_D$ of polymer | |
|-------------|---------------------|---------------|-------------------------|---------------|
| | | | in benzene | in chloroform |
| (+) Borneol | Toluene | 5.63 | -5.9° | +7.4° |
| (+) Borneol | Hexane | 3.30 | -4.9° | +6.1° |
| (+) Borneol | Benzene | 3.65 | -3.7° | +2.5° |
| (-) Menthol | Benzene | 0.59 | -3.6° | +4.2° |

Polymerization: Propylene oxide, 0.5 mole; solvent, 30 to 35 ml; at 80°C; at conversion, 17 to 30%.
 Catalyst: Diethylzinc, 0.025 mole; Alcohol, 0.05 mole.
 Polymer: Crystalline fraction, ca. 10 per cent except for (-) menthol (2.7 per cent).
 Optical rotation: Measured in 1 to 3 per cent solutions at 10° to 15°C.

more probable, because the adjacent asymmetric centre in the growing chain is too far apart from the key atom to regulate the polymer structure by selecting one of the two enantiomeric monomer molecules.

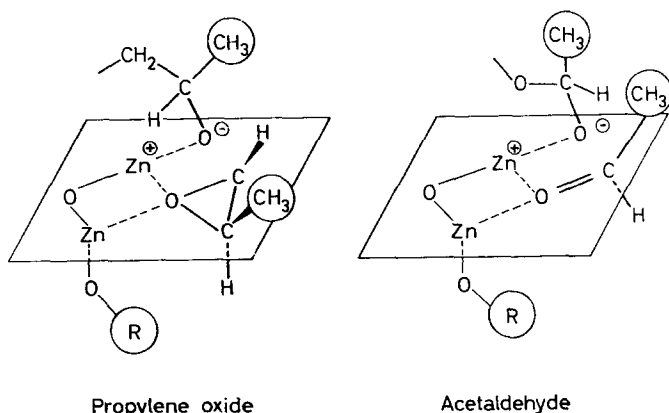


Figure 7—Stereoregular polymerization of propylene oxide and acetaldehyde

CATIONIC POLYMERIZATION OF CYCLIC ETHERS OF MORE THAN THREE RING MEMBERS

The polymerizability of cyclic ethers decreases as the ring size becomes larger. The polymerizations of oxacyclobutane and its derivatives are possible only with cationic catalyst. The cationic polymerization of tetrahydrofuran (THF), a five-membered cyclic ether, was enabled by finding suitable catalytic systems consisting of Lewis acid and co-catalyst. Six-membered cyclic ethers, for instance, tetrahydropyran and 1,4-dioxan, are rather stable and reluctant to polymerize. In our laboratory, a lot of work has been done on the polymerizations of four-, five- and six-membered cyclic ethers. Some new catalytic systems were discovered, and new co-

JUNJI FURUKAWA

Table 15. Polymerization of 3,3-bis(chloromethyl)oxacyclobutane by Lewis acid-co-catalyst systems
(Monomer, 0.025 mole; CH₂Cl₂, 20 ml)

| Co-catalyst* | (mole) | Temp. (°C) | Time (h) | Conversion (%) |
|--|---------|---------------|-------------|-------------------|
| Lewis acid: BF ₃ ·(C ₂ H ₅) ₂ O, 0.00125 mole | | | | |
| None | 0 | -78 | 96 | 0 |
| PO | 0.00250 | -78 | 48 | 95.6 |
| ECH | 0.00250 | -78 | 24 | 95.8 |
| Lewis acid: SnCl ₄ , 0.00250 mole | | | | |
| None | 0 | 0 | 96 | 0† |
| ECH | 0.00250 | 0 | 24 | 91.7 |
| Lewis acid: AlCl ₃ , 0.00250 mole | | | | |
| None | 0 | 0 | 48 | 0 |
| ECH | 0.00250 | 0 | 48 | 91.9 |

*PO Propylene oxide; ECH Epichlorohydrin.

†No polymer but an addition product of the monomer and SnCl₄ was produced.

polymers of two cyclic ethers of different ring size, including six-membered cyclic ethers, were prepared.

In cationic polymerization, the effects of co-catalysts such as water and hydrogen halides have been widely known. Meerwein¹⁹ succeeded in the

Table 16. Polymerization of tetrahydrofuran by Lewis acid-co-catalyst systems¹⁰

| (Bulk polymerization, at 0°C Lewis acid, 1 mole % for monomer) | | | | |
|--|-----------------------|------------------------------------|-------------------|---------------------|
| Co-catalyst | Mole % for monomer | Polymeri- zation time (days) | Conversion (%) | η _{sp} /C† |
| Lewis acid: BF ₃ ·(C ₂ H ₅) ₂ O | | | | |
| No co-catalyst | | 7 | 3.8 | 0.51 |
| 3,3-Bis(chloromethyl)- oxacyclobutane | 1 | 1 | 17.9 | 0.51 |
| β-Propiolactone | 1 | 7 | 13.6 | 0.48 |
| Diketene | { 1 | 1 | 24.9 | 0.28 |
| | { 1 | 2 | 84.5 | |
| Trioxan | 1 | 7 | 6.7 | |
| α-Methylstyrene-ethyl bromide | 1 | 7 | 5.7 | |
| Isoprene | 1 | 7 | 6.9 | |
| Phenylisocyanate | { 1 | 7 | 5.9 | |
| | { 2 | 7 | 9.7 | |
| Acetonitrile | 1 | 7 | 6.1 | |
| Propylene oxide‡ | 1 | 7 | 78.1 | |
| Acetic anhydride‡ | 1 | 7 | 8.6 | |
| Lewis acid: FeCl ₃ | | | | |
| No co-catalyst | | 7 | 0 | |
| 3,3-Bis(chloromethyl)- oxacyclobutane | 1 | 7 | 5.9 | |

*All the products were resinous solids.

†Measured on a solution of 0.2 g polymer in 100 ml benzene at 30°C.

‡Meerwein's co-catalyst.

IONIC POLYMERIZATION OF POLAR MONOMERS

THF polymerization by using suitable co-catalysts like α -haloethers, benzotrichloride, orthoesters, acid chlorides, acid anhydrides, alkylene oxides and hydrogen halides together with Lewis acid as the catalyst. These co-catalysts are rather basic toward Lewis acid, and transform the Lewis acid into the active species of Brönsted acid type which affords proton or carbonium ion and induces cationic polymerization.

Table 17. Polymerization of 3,3-bis(chloromethyl)oxacyclobutane
Activation of triethylaluminium catalyst;
Monomer, 0.025 mole
Hexane, 10 ml
Polymerization, at 0°C

| Al(C ₂ H ₅) ₃ (mole) | Additions (mole) | Polymerization time (h) | Conversion (%) |
|---|------------------------------------|----------------------------|-------------------|
| 0.00125 | None | 48 | 2.5 |
| 0.000625 | H ₂ O | 1 | 64.4 |
| 0.00125 | ECH* | 48 | ca. 100 |
| 0.00125 | ClCH ₂ OCH ₃ | 48 | 24.1 |

*Epichlorohydrin.

The acceleration of the Lewis acid induced polymerization of 3,3-bis(chloromethyl)oxacyclobutane (BCMO) by alkylene oxide was also observed in our laboratory. The results are shown in Table 15. Moreover, in the THF polymerization, we found other new co-catalysts whose functions were assumed to be of the same character as those of some Meerwein co-catalysts.

Table 18. Polymerization of tetrahydrofuran by Al(C₂H₅)₃-co-catalyst systems¹⁹

| (Monomer, 0.25 mole Al(C ₂ H ₅) ₃ , co-catalyst, each 0.0025 mole Bulk polymerization, at 0°C for 1 day) | | |
|--|-------------------|-----------------|
| Co-catalyst | Conversion (%) | η_{sp}/C^* |
| None | 0 | — |
| Epichlorohydrin | 24.7 | 3.49 |
| Propylene oxide | 25.8 | 3.49 |
| Acetyl chloride | 5.3 | 0.33 |
| Chloromethyl ether | 4.1 | — |

*Measured on a solution of 0.2 g of polymer in 100 ml of benzene at 30°C.

Table 16 shows the effects of these co-catalysts in the THF polymerization with Lewis acid catalyst. It is interesting to note that in the series of three-, four- and five-membered cyclic ethers, the ring-opening polymerization by Lewis acid catalyst is accelerated by the addition of a homologue of smaller ring size, i.e. the BCMO polymerization is co-catalysed by alkylene oxide and the THF polymerization is accelerated by alkylene oxide and by BCMO.

Trialkylaluminium can also be used for polymerization of higher cyclic ethers. However, it seems to act as a Lewis acid in contrast to the case of the polymerization of alkylene oxide catalysed by diethylzinc. It was found that the activity of triethylaluminium was much enhanced by the

presence of co-catalyst, such as epichlorohydrin, propylene oxide and chloromethyl ether.

Table 17 shows the effect of the co-catalysts on the BCMO polymerization with triethylaluminium.

According to the literature²⁰⁻²², BCMO is successfully polymerized by triethylaluminium without any co-catalyst only at an elevated temperature. Our triethylaluminium-co-catalyst systems are much more active than triethylaluminium alone and can even induce the low-temperature polymerization of THF (see Table 18).

Table 19. Charge density on aluminium

| | |
|---|-------------------------------|
| Et_3Al | +0.3882 |
| $\text{Et}_2\text{Al}-\text{O}-\text{AlEt}_2$ | +0.5385 |
| $\text{Et}_2\text{Al}-\text{O}-\text{Al}-\text{OAlEt}_2$ | +0.5579 (for the Al in sides) |
| $\begin{array}{c} \text{Et} \\ \\ \text{EtOAl}-\text{O}-\text{Al}-\text{OEt} \end{array}$ | +0.6723 (for the central Al) |
| $\begin{array}{c} \text{Et} \quad \text{Et} \\ \quad \\ \text{(EtO)}_2\text{Al}-\text{O}-\text{Al}(\text{OEt})_2 \end{array}$ | +0.7838 |
| $(\text{EtO})_2\text{Al}-\text{O}-\text{Al}(\text{OEt})_2$ | +1.0186 |
| $(\text{EtO})_3\text{Al}$ | +1.0517 |

The catalytic activity of triethylaluminium was found to be predominantly enhanced by addition of water. Here, water does not seem to have acted as a simple co-catalyst, because it reacts immediately with triethylaluminium evolving ethane gas as follows:

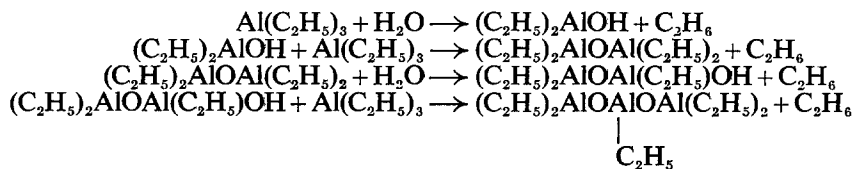


Table 20. Polymerization of tetrahydrofuran by $\text{Al}(\text{C}_2\text{H}_5)_3$ - H_2O -co-catalyst systems

Monomer, 0.125 mole
 $\text{Al}(\text{C}_2\text{H}_5)_3$, H_2O , each 0.00315 mole
 Bulk polymerization, at 0°C for 2 days

| Co-catalyst | Mole ratio to $\text{Al}(\text{C}_2\text{H}_5)_3$ - H_2O | Conversion (%) | η_{sp}/C^* |
|------------------------|--|----------------|-----------------|
| None | | 0 | — |
| Epichlorohydrin | 0.5 | 96.6 | 1.39 |
| Propylene oxide | 2.0 | 32.9 | 0.56 |
| Diketene | 2.0 | 44.5 | 1.06 |
| β -Propiolactone | 2.0 | 99.0 | 0.19 |
| Acetyl chloride | 2.0 | 64.4 | 0.61 |
| Chloromethyl ether | 2.0 | ca. 100 | 0.15 |

*Measured on a solution of 0.2 g polymer in 100 ml benzene at 30°C.

IONIC POLYMERIZATION OF POLAR MONOMERS

In fact the optimum amount of water in this case is much larger than that in the usual cationic polymerizations. Thus, the reaction product may be regarded as a mixture of the species involving carbon-aluminium and oxygen-aluminium bonds. Hereafter, the mixture will be referred to as

Table 21. Polymerization of 3,3-bis(chloromethyl)oxacyclobutane by $\text{Al}(\text{C}_2\text{H}_5)_3\text{-H}_2\text{O}$ -co-catalyst systems

| Monomer, 0.025 mole $\text{Al}(\text{C}_2\text{H}_5)_3$, H_2O , each 0.00125 mole (5 mole %) Co-catalyst, 0.00125 mole CH_2Cl_2 , 20 ml Polymerization, at -78°C for 2 days | |
|--|----------------|
| Co-catalyst | Conversion (%) |
| None* | 0 |
| Epichlorohydrin | <i>ca.</i> 100 |
| Propylene oxide | 60.7 |
| β -Propiolactone | 42.7 |
| Acetyl chloride | 4.6 |
| Chloromethyl ether | small |

*At 0°C , the reaction product of $\text{Al}(\text{C}_2\text{H}_5)_3$ and water without co-catalyst polymerized BCMO at a quantitative conversion.

ethylaluminium oxide. By replacement of the carbon-aluminium bond by an oxygen-aluminium bond, the electronegativity of aluminium is increased, and hence the catalytic activity is enhanced (*Table 19*).

Since water is consumed as above, the newly produced ethylaluminium oxide may well be activated by another co-catalyst. In fact, ethylaluminium oxide itself was inactive for the THF polymerization at 0°C , whereas it turned very active when a co-catalyst was added (*Table 20*). For the BCMO polymerization, several systems of ethylaluminium oxide and co-catalysts were active enough even at -78°C (*Table 21*).

The copolymerization of BCMO with THF was studied, using stannic tetrachloride or the complex compounds of boron fluoride. The formation of copolymer was fully substantiated from the solubility characteristics and infra-red spectra. The copolymers obtained from the monomer mixtures

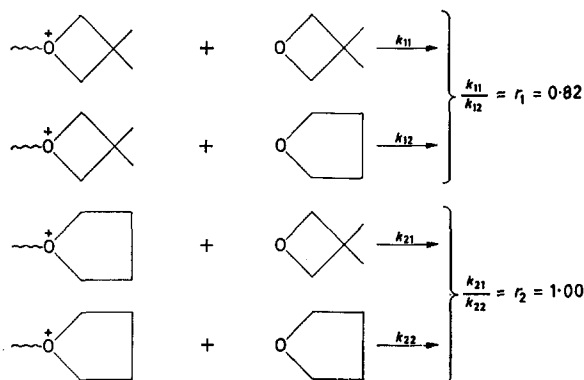
Table 22. Copolymers of THP and 1,4-dioxan with BCMO

| | |
|---------------------------|---|
| BCMO-THP copolymer | |
| Monomer | 1:1 |
| Catalyst | 5 mole % $\text{BF}_3 \cdot (\text{C}_2\text{H}_5)_2\text{O}$ |
| Polymerization | 0°C . 7 days in CH_2Cl_2 , 81.7% conversion |
| Polymer | chloroform-soluble waxy, 33.5 mole % THP units |
| BCMO-1,4-Dioxan copolymer | |
| Monomer | 1:1 |
| Catalyst | 5 mole % $\text{BF}_3 \cdot (\text{C}_2\text{H}_5)_2\text{O}$ |
| Polymerization | 20°C . 3 days, 68.1% conversion |
| Polymer | chloroform-insoluble resinous, 19.5 mole % 1,4-dioxan units |

containing more than 80 mole % BCMO were resinous solids while those from the mixtures less than 80 mole % BCMO were rubbery materials. From a set of copolymerization data obtained by using various monomer compositions, the monomer reactivity ratios were determined. The results were as follows:

$$r_1(\text{BCMO}) = 0.82 \pm 0.05$$

$$r_2(\text{THF}) = 1.00 \pm 0.05$$



Both of these ratios take values near unity, which means that the propagation rate of the copolymerization depends mostly upon the nature of oxonium ring structures at growing chain ends but not on that of the monomers.

The copolymerizations of BCMO with tetrahydropyran (THP) as well as 1,4-dioxan were conducted under similar conditions. The product of the former copolymerization was waxy whereas that of the latter was resinous. Elemental analysis indicated that either copolymer resulting from an equimolar mixture of THP or 1,4-dioxan with BCMO contained more than 50 mole % BCMO units (see *Table 22*).

STEREOREGULATION IN CATIONIC POLYMERIZATION

Although a considerable literature exists on anionic stereoregular polymerization, we have as yet very few examples of the stereoregular polymerization which proceeds by a cationic mechanism. The situation might be attributable to the difficulty of coordination of monomers on to the anionic counter ions of cationic catalysts.

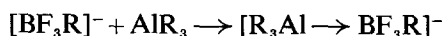
Vinyl ethers are a unique class of monomers which give isotactic polymers by the action of boron fluoride etherate at low temperatures²³. Recently, it has been reported that vinyl ethers can be polymerized to crystalline polymers even at elevated temperatures if suitable catalysts such as alkyl-aluminium sesquihalides²⁴, the aluminium sulphate-sulphuric acid system²⁵ and the Ziegler type catalysts²⁶ are used. Nakano *et al.*²⁷ found several excellent catalysts of the type of Lewis acid-Lewis base combination.

Furthermore, they made systematic analysis of the stereoregulating activity of various known catalysts and gave a hypothetical explanation of the stereoregulating action of those catalysts in the vinyl ether polymerizations.

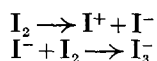
Here we will also attempt to give an interpretation to the mechanism of stereoregular polymerization of vinyl ethers in terms of the multi-centred coordination. It is our feeling that also in cationic polymerizations the coordination of polymer chains and monomers on to the catalyst would be possible if the complex counter anions have electrically positive centres. Let us take the boron fluoride etherate anion for example. There the boron atom would still have a positive formal charge on account of the large difference in electronegativity between fluorine and boron. Coordination of alkylaluminium, for instance, to the boron atom would then be probable, giving eventually cation and coordinated counter anion.



The central metal in the counter anions of this type still carries a positive charge. Therefore, further coordination of alkylaluminium on to the anions is conceivable so far as the coordination number of the central atom is sufficiently large.



The result is the formation of a complex counter anion enabling our multi-centre-coordinated polymerization (see *Table 3*). The whole process of the complex anion formation bears some resemblance to the complex iodide ion formation:



The formal charges localized on the central metals in anions and molecules may be estimated by properly accumulating Pauling's percentage ionic

Table 23. Charge density and stereoregulating property

| No. | Catalyst system | R.A. | Anion | e_A | Molecule | e_M | $e_A - e_M$ |
|-----|--------------------------|------|------------------|--------|--------------|--------|-------------|
| 1 | $R_3Al + BF_3$ | ++ | RBF_3^- | +0.629 | R_3Al | +0.388 | +0.241 |
| 2 | $R_3Al + VCl_4$ | ++ | $RVCl_4^-$ | +0.454 | R_3Al | +0.388 | +0.066 |
| 3 | $R_3Al + TiCl_4$ | ++ | $RTiCl_4^-$ | +0.521 | R_3Al | +0.388 | +0.133 |
| 4 | $R_3Al + SnCl_4$ | + | $RSnCl_4^-$ | +0.273 | R_3Al | +0.388 | -0.115 |
| 5 | $R_3Al + SbCl_5$ | + | $RSbCl_5^-$ | +0.265 | R_3Al | +0.388 | -0.123 |
| 6 | $Et_2AlCl + H_2O$ | + | $Et_2ClAlOH^-$ | +0.384 | Et_2AlCl | +0.506 | -0.122 |
| 7 | $EtAlCl_2 + H_2O$ | + | $EtCl_2AlOH^-$ | +0.474 | $EtAlCl_2$ | +0.624 | -0.146 |
| 8 | $BF_3 \cdot OR_2 + H_2O$ | + | F_3BOH^- | +0.746 | BF_3OR_2 | +0.870 | -0.136 |
| 9 | $CH_3TiCl_3 + H_2O$ | - | $CH_3Cl_3TiOH^-$ | +0.579 | CH_3TiCl_3 | +0.722 | -0.143 |
| 10 | $TiCl_4 + H_2O$ | - | Cl_4TiOH^- | +0.660 | $TiCl_4$ | +0.820 | -0.160 |
| 11 | $AlCl_3 + H_2O$ | - | Cl_3AlOH^- | +0.572 | $AlCl_3$ | +0.741 | -0.169 |
| 12 | $VCl_4 + H_2O$ | - | Cl_4VOH^- | +0.587 | VCl_4 | +0.761 | -0.174 |
| 13 | $SnCl_4 + H_2O$ | - | Cl_4SnOH^- | +0.219 | $SnCl_4$ | +0.402 | -0.183 |
| 14 | $VOCl_3 + H_2O$ | - | $HOVOCl_3^-$ | +0.786 | $VOCl_3$ | +0.971 | -0.186 |

Table 24

| No. | Catalyst system | R.A. | Most probable structure |
|-----|---|------|--|
| 1 | $\text{Al}_2(\text{SO}_4)_3 - \text{H}_2\text{SO}_4$ | ++ | |
| 2 | $\text{Et}_3\text{Al} - \text{H}_2\text{SO}_4$ | ++ | $\text{Et}_3\text{Al} + \text{H}_2\text{SO}_4 \rightarrow \text{Al}_2(\text{SO}_4)_2 + \text{C}_2\text{H}_6$ $\xrightarrow{\text{H}_2\text{SO}_4}$ The same complex as in No.1. |
| 3 | $\text{CrO}_3 - \text{H}_2\text{O}$ | ++ | |
| 4 | $\text{Cr}_2\text{O}_2\text{Cl}_2 - \text{H}_2\text{O}$ | ++ | |
| 5 | $\text{TiCl}_2(\text{OR})_2 - \text{H}_2\text{O}$ | ++ | $\text{TiCl}_2(\text{OR})_2 \xrightarrow{\text{H}_2\text{O}}$ |

characters of the relevant σ -bonds. We have calculated these charges for a number of catalyst systems. For the sake of convenience, let us take the difference in central charge between anions and molecules as a rough measure for the ease of the complex anion formation between them. Then, a good parallelism is observed between charge difference and stereo-regulating ability of the catalyst systems, as is shown in Table 23.

It should be noted here that the negative sign attached to the values of the charge difference does not imply a charge transfer in the reverse direction. Our argument is concisely as follows. Other things being equal,

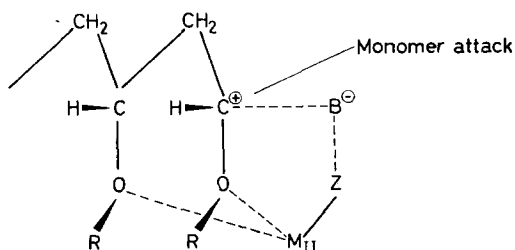


Figure 8

the relative ease of the complex anion formation due to charge migration from molecule to anion would be measured by the relative magnitudes of charge difference indicated with inclusion of positive or negative sign.

There are several other catalytic systems found to be more efficient than those listed in *Table 23*. These efficient catalysts seem to form metallic centres for multi-centre coordination through the formation of oxygen linkages. Probable structures for these cases are given in *Table 24*.

On the basis of the above consideration, we propose the following multi-centre mechanism for the cationic stereoregular polymerization of vinyl ethers: Two neighbouring ether oxygens which are linked to the polymer chain in the vicinity of the positively charged chain end are coordinated on to a metal centre of the complex anion. Monomer molecules approach the growing chain only from the opposite side of the chain, producing thus isotactic polymer exclusively (see *Figure 8*).

*Department of Synthetic Chemistry,
University of Kyoto, Japan*

DISCUSSION

Professor F. Danusso (Italy): We have seen that you have distinguished the polymers as crystalline, as stereoblock polymers and as atactic polymers. Which of the polymers you described as crystalline can be considered as highly stereoregular polymers?

Professor J. Furukawa (Japan): We obtained a mixture of polymers; one is atactic while the other is crystalline and sometimes stereoblock. Only when we used special catalysts such as partly hydrolysed aluminium alkoxide or hydroxide, did we obtain a stereoblock polymer. In other cases, without the special catalyst, stereoblock polymers cannot be obtained, and we obtained the mixture of atactic and crystalline polymers which can be separated by extraction. However, the stereoblock polymerization is a special case, by using a special catalyst such as partly hydrolysed aluminium alkoxide.

Professor F. Danusso (Italy): I should like to know which polymers from polar monomers can be considered fully stereoregular?

Professor J. Furukawa (Japan): I think the polymers of acrylates are stereoregular. We have had very crystallizable polymers but in the polymerization of alkylene oxides we have not obtained fully crystalline polymers; in general we can separate the atactic and crystalline polymers.

Professor F. Danusso (Italy): Are the crystalline polymers the stereoblock?

Professor J. Furukawa (Japan): I am not sure, but I think that the polymers of alkylene oxides are not a mixture of stereoblock and crystalline polymers but a blend of crystalline and atactic polymers. We have no evidence, however.

Professor H. A. Dieu (Belgium): I should like to know if you have ever published or studied the infra-red spectrum of your polytetrahydrofuran?

Professor J. Furukawa (Japan): It is not yet published but I am now studying the i.r. spectrum of polytetrahydrofuran.

Professor H. A. Dieu (Belgium): Do you find some double bonds or carbonyl groups?

Professor J. Furukawa (Japan): No, we have not found them.

Dr O. E. Lohuizen (Netherlands): Can you explain the difference in properties between the polyacetone you described and the polyacetone described by Kargin in Russia? Of course, I understand that you described a copolymer of acetone and propylene.

Professor J. Furukawa (Japan): It is not a random copolymer, but a block copolymer of acetone and propylene.

Dr O. E. Lohuizen (Netherlands): But in that case there must be a sequence of acetone units. If so, I cannot understand your high thermal stability. You mentioned 'stable up to 200°C'.

Professor J. Furukawa (Japan): Yes, that is right.

Dr O. E. Lohuizen (Netherlands): Are you certain you have sequences of acetone units?

Professor J. Furukawa (Japan): Yes, I am. Most of the polymer might be conventional polyacetone which is very unstable; we can obtain only the block copolymer, whose composition was calculated by analysis to be more than 70 or 80 per cent acetone units. The other part is polypropylene block.

Dr O. E. Lohuizen (Netherlands): When you speak about thermal stability up to 200° do you mean a thermal stability under dry nitrogen?

Professor J. Furukawa (Japan): The thermal stability was measured between two sheets of plate glass.

Dr K. Butler (U.K.): I would like to ask Professor Furukawa two questions about his hydrolysis experiments on the polyalkyl acrylates. I believe from your table that you were able to obtain crystalline polyacrylic acid from some samples of the acrylic esters which were atactic or not crystalline. Could you explain that please? Secondly, did you notice any differences in the rates of hydrolysis of the esters depending on the degrees of crystallinity?

Professor J. Furukawa (Japan): The rate of hydrolysis is much higher in isotactic polymers, and the more regular the polymer, the greater is the rate of hydrolysis.

Dr K. Butler (U.K.): But is this in solution? If you have the polymer in solution is the rate still higher?

Professor J. Furukawa (Japan): Still higher, yes; the detailed data may be published in the near future.

Dr K. Butler (U.K.): On the other question, perhaps I was misreading your table, but I thought that you did have atactic or non-crystalline polyacrylic acid as a result of hydrolysis. You had crystalline polyacrylic acid from atactic acrylic ester. Do you think that there is some change in the conformation of the chain?

Professor J. Furukawa (Japan): I have mentioned in my lecture that apparently the amorphous polymer is essentially not atactic but stereoregular, and when it is hydrolysed the polyacrylic acid formed exhibits very high crystallinity, and therefore the rubbery appearance and uncrystallizable nature of polyacrylate esters may be related with a certain cause other than tacticity.

REFERENCES

- ¹ FOX, T. G. *J. Amer. chem. Soc.* 1958, **80**, 1768; *J. Polym. Sci.* 1958, **31**, 173
- ² GLUSKER, D. L. *J. Polym. Sci.* 1961, **49**, 297 and 315
- ³ Rohm and Haas Co., *Belgian Patent No. 566 713* (1958); *Australian Patent No. 1 030 562* (1958)
- ⁴ GOODE, W. E. *J. Polym. Sci.* 1960, **46**, 317; 1961, **47**, 75
- ⁵ NISHIOKA, A. and WATANABE, H. *J. Polym. Sci.* 1960, **48**, 241
- ⁶ MILLER, M. L. *J. Amer. chem. Soc.* 1958, **80**, 4115; *J. Polym. Sci.* 1959, **38**, 63
- ⁷ GARRET, B. S., GOODE, W. E. and GRATCH, S. *J. Amer. chem. Soc.* 1959, **81**, 1007
- ⁸ MAKIMOTO, T., TSURUTA, T. and FURUKAWA, J. *Makromol. Chem.* 1960, **42**, 165; 1961, **50**, 116
- ⁹ KAWASAKI, A., FURUKAWA, J., TSURUTA, T., INQUE, S. and ITO, K. *Makromol. Chem.* 1960, **36**, 260
- ¹⁰ NAKAYAMA, Y., KAWASAKI, A., TSURUTA, T. and FURUKAWA, J. *Makromol. Chem.* 1961, **43**, 76; 1961, **49**, 112, 136 and 153
- ¹¹ FUJIO, R., TSURUTA, T. and FURUKAWA, J. *Makromol. Chem.* In press
- ¹² NAKAYAMA, Y., TSURUTA, T. and FURUKAWA, J. *Makromol. Chem.* In press
- ¹³ FURUKAWA, J., SAEGUSA, T., TSURUTA, T., KAWASAKI, A. and TATANO, T. *Makromol. Chem.* 1959, **33**, 32; *J. Polym. Sci.* 1959, **36**, 546
- ¹⁴ FURUKAWA, J., SAEGUSA, T., FUJII, H., KAWASAKI, A., IMAI, H. and FUJII, Y. *Makromol. Chem.* 1960, **37**, 149; 1961, **44-46**, 398
- ¹⁵ FURUKAWA, J., SAEGUSA, T., FUJII, H. and KAWASAKI, A. *Makromol. Chem.* 1960, **40**, 226
- ¹⁶ KARGIN, V. A., KABANOV, V. A., ZUBOV, V. P. and PAPISOV, I. M. *Dokl. Akad. Nauk S.S.S.R.* 1960, **134**, 1098
- ¹⁷ OKAMURA, S., HAYASHI, K., MORI, K. and NAKAMURA, Y. Read at the Tenth Annual Meeting of High Polymer Society, Japan, May 1961
- ¹⁸ FURUKAWA, J., SAEGUSA, T., TSURUTA, T., OHTA, S. and WASAI, G. *Makromol. Chem.* In press
- ¹⁹ MEERWEIN, H., DELFS, D. and MORSHEL, H. *Angew. Chem.* 1960, **72**, 927
- ²⁰ KAMBARA, S. and HATANO, M. *J. Polym. Sci.* 1959, **32**, 275
- ²¹ GODDU, R. F. *U.S. Patent No. 2 895 922* (1959)
- ²² HUDY, R. A. *U.S. Patent No. 2 895 924* (1959)
- ²³ SCHILDKNECHT, C. E. *et al. Industr. Engng Chem. (Industr.)* 1948, **40**, 2104
- ²⁴ *Japanese Patent Appl. Pub. 442* (1961)
- ²⁵ *British Patent No. 846 690* (1960)
YAMAOKA, H., HIGASHIMURA, T. and OKAMURA, S. *Chem. High Polymer, Japan*, 1961, **18**, 561
- ²⁶ *Japanese Patent Appl. Pub. 4 988* (1960)
- ²⁷ NAKANO, S., IWASAKI, K. and FUKUTANI, H. Read at the Tenth Annual Meeting of High Polymer Society, Japan, May 1961

The Sub-microscopic Morphology of Cellulose

R. D. PRESTON

The nature of the microfibrillar component of plant cell walls is discussed and its association with other paracrystalline components commented upon. Cellulose microfibrils are shown to consist of a central crystalline core which is probably composed of chains of β -1,4-linked glucose residues only. This is surrounded by a 'cortex' containing a mixture of chains including non-glucose chains. The mutual arrangement of the chains in the crystalline core is shown to be variable. It is recalled that the microfibrils in elongated cells pass helically round the cell. Most cells possess at least two such helically constructed wall layers, differing in pitch and giving the 'crossed fibrillar structure' shown most beautifully in some marine algae. In these latter plants the microfibrils frequently pass over from one wall lamella to the next forming an inter-lamella linkage which may also occur in higher plant fibres. These seaweeds (and some fungi) also show the phenomenon of spiral growth as a consequence of their helical structure. When the cells are prevented from twisting during growth—as they probably are in higher plant fibres—distortions are produced in the wall structure.

It is perhaps natural, when one and the same material is of importance in widely different fields of enquiry, that circumstances should arise in which even the name given to it should carry different connotations in the different contexts. So long as the implications involved are fully realized no harm is done; but when the material so named is taken in one field to have the structure and the properties implied in another field, then serious errors might follow. This seems to be a danger with cellulose.

The word *cellulose* was coined by the botanist Payen in 1844 to define the basic component of plant cell walls generally. This was a substance with certain characteristic staining reactions and it was not until much later that its structure was examined. The word is still used by botanists in precisely this sense and to them it is immaterial whether the plant is a flowering plant, a fern or a seaweed. The fibre technologist, however, consciously or unconsciously applies a restriction to this broad definition; to him the word cellulose refers solely to a structural component which can be isolated by certain standard chemical processes from the relatively small number of plants—almost exclusively flowering plants—which are usable commercially. This latter use of the word tends to hide the fact that celluloses as defined in this way vary significantly both in chemical composition and in structure. Structural determinations by physical methods have served, if anything, only further to confuse the issue. X-ray diffraction analysis, largely of ramie fibres but to a less extent also of other plant fibres and of wood and cotton and even of seaweeds, has been interpreted in terms of a crystal lattice containing long molecular chains of β , D-glucose residues

This paper was presented at a Polymer Science Conference, held in conjunction with the Second World Congress of Man-made Fibres, at the Connaught Rooms, Holborn, London W.C.2, 2nd and 3rd May 1962.

only, with the implication that the amorphous or paracrystalline cellulose associated with the crystallites is similarly constituted. This constituted a new, and more strictly selective definition. Examination of celluloses in the electron microscope has now revealed that, at this level, cellulosic bodies invariably contain long thin threads called *microfibrils*, ranging in diameter from less than 100 Å to more than 200 Å, which with some plant species (the seaweeds *Valonia*, *Cladophora* and *Chaetomorpha* for instance) have been shown to give electron diagrams typical of cellulose. The microfibrils therefore came to be regarded as cellulosic and have been looked upon as the naturally produced morphological unit of this substance, constituting yet another definition.

Only if the substance extractable from plants by standard methods consists solely of microfibrils, gives the X-ray diagram characteristic of the cellulose of crystallographers and on hydrolysis yields glucose only do all these definitions coincide. In fact, however, remarkably few so-called celluloses fall into this category and these—derived from a small group of seaweeds—are so different from all other celluloses that they can hardly be regarded as typical. It is the purpose of this article to survey the microfibrils derived from a wide variety of plants in order to assess the kind and the degree of the variability of this morphological unit. In order to avoid confusion in terms the definitions proposed by Myers, Preston and Ripley¹ will be employed; the term *cellulose* will be used for all those microfibrils which can be extracted from cell walls more or less intact, which then give X-ray diagrams with arcs, however broad, with spacings characteristic of cellulose and which hydrolyse to give glucose together with other sugars. Those few celluloses which hydrolyse to give no sugar other than glucose are then called *eucellulose*.

THE CHEMICAL NATURE OF CELLULOSE MICROFIBRILS

In isolating microfibrils for chemical investigation the technique of choice is clearly the one yielding clean microfibrils with a minimum weight loss. A satisfactory method has been found in a slight modification of the method of Jermyn and Isherwood². In their method, non-cellulosic wall constituents are progressively removed by boiling in water, chlorination (giving so-called holocellulose) and treatment with 4N caustic potash, leaving a residue which is called α -cellulose. Cronshaw *et al.*³ modified this treatment by postponing the chlorination until after the caustic potash treatment, a modification which still produces an α -cellulose consisting of equally clean microfibrils while, as shown by Dennis⁴, involving a markedly lower weight loss.

The sugars present in the resulting microfibrils and in the various extracts, as determined by paper partition chromatography of the hydrolysates, are presented in *Table 1* for a variety of celluloses. Of the plants so far examined only a small clearly defined group of seaweeds yields a cellulose which hydrolyses to give no detectable sign of sugars other than glucose and is therefore to be classed as eucellulose. These are *Valonia* on the one hand and *Cladophora* and *Chaetomorpha* on the other, members of two rather closely related families. They have other distinguishing features, to be discussed later, which give them a unique place among the celluloses.

THE SUB-MICROSCOPIC MORPHOLOGY OF CELLULOSE

All other celluloses so far examined contain sugars other than glucose in greater or lesser degree, reaching 50 per cent by weight of the cellulose in species like the red alga *Rhodymenia palmata*. The difficulty in obtaining chemically pure cellulose has long been recognized, but only with the advent of electron microscopy could it be shown that this is because the non-glucose sugars form an integral part of the cellulose complex. It remains to determine the spatial distribution of these sugars within the microfibrils.

Table 1. Composition of celluloses from various sources

| Source | Composition | Source | Composition |
|---|-------------|-------------------------------|---------------|
| <i>Valonia ventricosa</i> | S* Glucose | <i>Laminaria digitata</i> and | S Glucose |
| <i>Cladophora rupestris</i> | S Glucose | <i>L. saccharina</i> | M Uronic acid |
| <i>Chaetomorpha melagonium</i> | S Glucose | <i>Ptilota plumosa</i> | S Glucose |
| <i>Enteromorpha</i> sp. | W Arabinose | | W Galactose |
| | S Glucose | | W Xylose |
| | M Xylose | <i>Griffithsia flosculosa</i> | S Glucose |
| <i>Ulva lactuca</i> | M Rhamnose | | W Galactose |
| | S Glucose | | W Xylose |
| | S Xylose | <i>Rhodymenia palmata</i> | S Glucose |
| <i>Halidrys siliquosa</i> and all Fucales | S Glucose | | S Xylose |
| | W Xylose | <i>Porphyra</i> sp. | S Mannose |
| | W Fucose | | |

*S, M, W refer to the intensity of the spot on the chromatogram. S=strong; M=medium; W=weak.

Provided that amorphous incrusting substances and non-cellulosic crystalline materials (xylan, alginic acid, etc.) have been removed, all celluloses so far examined give an X-ray diffraction diagram either identical with that of the *Valonia* group or rather closely resembling it and, though some of the deviations are significant, there is undoubtedly a common pattern of structure. All members of the Red Algae, for instance, even when the cellulose contains 50 per cent xylose, are indistinguishable in this respect from higher plants. This has been interpreted as implying that the glucose polymer—eucellulose—is crystalline and that the xylose-containing chains lie outside the crystallite; in terms of the microfibrillar structure this means that the crystalline region should form a central core of eucellulose surrounded by a paracrystalline cortex containing xylose residues (Preston⁵; Preston and Cronshaw⁶) (Figure 1). This has been verified by a method which takes advantage of an earlier observation by Rånby⁷. When cellulose is refluxed with 2.5N sulphuric acid at 100°C for 24 hours and washed on a filter then, as the washings approach pH3, the cellulose suddenly becomes colloidal and washes through the filter. The dispersed phase consists of short rods (Figure 2) (Rånby⁷; Mukherjee and Woods⁸) which still yield an X-ray diagram of the original cellulose (Mukherjee and Woods⁸). It could be that these rods consist of short lengths of the crystalline core of the microfibrils and, if they do, then they should yield glucose only on hydrolysis. It has now been shown that this is so, even with microfibrils containing 50 per cent xylose (Table 2) (Dennis and Preston⁹) and that, moreover, the non-glucose sugars present in the microfibrils can be recovered from the acid extract. This seems to verify the structure presented diagrammatically in Figure 1.

The picture is not, however, always quite so clear in a quantitative sense. If the crystalline core of a microfibril is b Å wide and b/n Å thick then it contains $b^2/33n$ chains. In order completely to cover this with a single layer, of, say, xylan chains, the number required would be approximately $2b(5.4n + 6.1)/33n$. The ratio surface chains/body chains, would then be

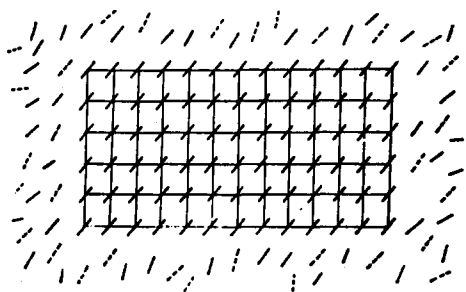


Figure 1—Diagrammatic representation of the transverse section of a cellulose microfibril about 100 Å wide and about 50 Å thick. The solid strokes represent the planes of the glucose residues in the cellulose chain molecule and the broken strokes the planes of other sugars or sugar derivatives in non-cellulosic molecular chains. The area joined into a lattice represents the solid central core

$2(5.4n + 6.1)/b$. Taking for wood cellulose $b = 60$ Å, $n = 2$ (see p 515) then in such a microfibril 37 per cent of the chains would be xylan chains; for the broader microfibrils of *Valonia*, etc., $b = 200$ Å, $n = 2$ leads to a value of 14 per cent. There is therefore seldom the quantity of xylose residues associated with the microfibrils to allow a complete surface of xylan chains; the paracrystalline cortex must therefore contain glucose chains in addition to xylose chains, or mixed gluco-xylan chains.

It is not clear, indeed, that the surface will be uniform. Celluloses vary considerably in resistance to chemical attack and this may be associated with the nature of the microfibril surface. Most higher plant celluloses,

Table 2. Analysis of celluloses

| Source of cellulose | Holocellulose | | After 4% KOH | | Acid from colloidal | | Colloidal cellulose | |
|---------------------|---------------|----|--------------|----|---------------------|----|---------------------|----|
| Elm wood | Glucose | S* | Glucose | S* | Glucose | S* | Glucose | S* |
| | Xylose | M | Xylose | W | Xylose | S | | |
| Pine wood | Glucose | S | Glucose | S | Glucose | S | Glucose | S |
| | Mannose | M | Mannose | M | Mannose | S | Mannose | T |
| | Xylose | M | Xylose | W | Xylose | S | | |
| | | | | | Galactose | W | | |
| <i>Rhodymenia</i> | Glucose | S | Glucose | S | Glucose | W | Glucose | S |
| | Xylose | S | Xylose | S | Xylose | S | Xylose | T |
| <i>Ulva</i> | Glucose | S | Glucose | S | Glucose | S | Glucose | S |
| | Xylose | W | Xylose | W | Xylose | M | | |
| | Rhamnose | T | Rhamnose | T | Rhamnose | W | | |
| | Uronic A | W | Uronic A | W | Uronic A | W | | |
| <i>Laminaria</i> | Glucose | S | Glucose | S | Glucose | S | Glucose | S |
| | Uronic A | M | Uronic A | W | | | | |

*Refers to the strength of spot on the chromatogram. S=strong; M=moderate; W=weak; T=trace.

including delignified wood cellulose, will dissolve in 72 per cent sulphuric acid. Untreated *Valonia* cell walls (which contain about 80 per cent cellulose) are known not to be soluble in sulphuric acid less than about 110 per cent, not to swell in cuprammonium solution and not to stain with iodine and sulphuric acid. After boiling in water and chlorinating, however, this cellulose behaves normally. Even when extracted in this way other celluloses

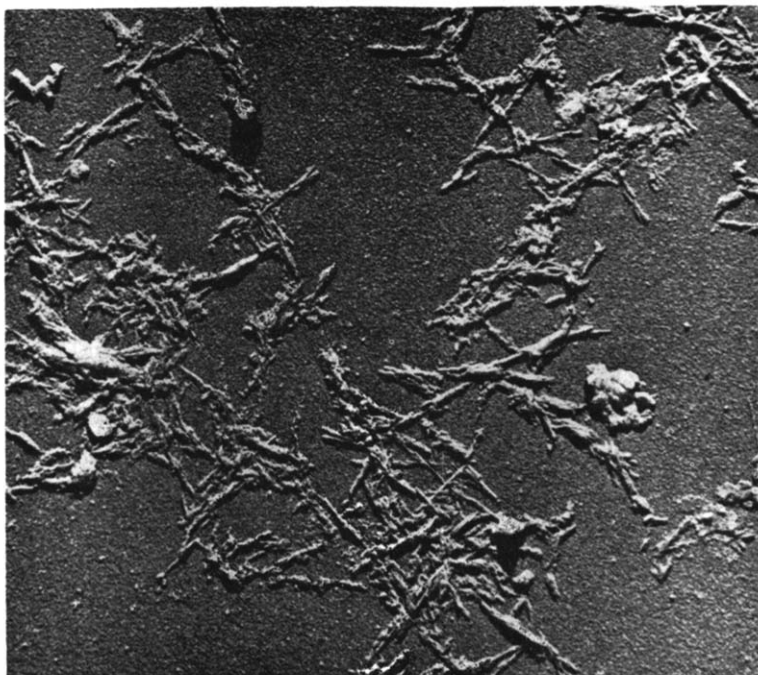


Figure 2—Electron micrograph of colloidal cellulose from elm wood. Magnification: 21000 \times , reproduced without reduction; shadowed Pd-Au. (Photo by Dr D. T. Dennis)

are still difficult to digest in sulphuric acid—the celluloses extracted from *Ulva lactuca* and from *Enteromorpha* are cases in point. These effects may clearly be due to the protective action of a non-cellulosic coating over the microfibril.

On the other hand some algal celluloses, though not markedly less crystalline than the cellulose of fibre plants, are very much more sensitive to alkali. Fibre celluloses commonly mercerize completely in around 20 per cent caustic soda. The cellulose of some brown seaweeds, on the other hand, become mercerized in 14 per cent caustic soda and red algal celluloses in solutions as weak as 10 per cent (Frei and Preston¹⁰). This seems to suggest some sophisticated differences in structure of these various celluloses.

THE PHYSICAL ORGANIZATION OF CELLULOSE
MICROFIBRILS

Cellulose microfibrils range in size over rather narrow limits. They are so long that ends are observed only under special circumstances (e.g. in the extra cellular cellulose of *Acetobacter xylinum*¹¹ and in cell wall layers in process of deposition¹²). In width they range from about 80 Å (*Nitella opaca*¹³; some woods¹⁴) through 100 Å (some seaweeds³, some woods¹⁴, cotton and other fibres) to between 200 and 300 Å (*Valonia* etc.^{12, 14, 15}). They are commonly about half as thick (Preston¹⁵) and are possibly elliptical in section.

The range of width of the crystalline region—the crystallites or micelles—is somewhat greater, whether judged by the width of high-angle arcs on the X-ray diagram or by the low angle scattering. In the primary walls of,



Figure 3—Electron micrograph of softwood cellulose microfibrils stained with Ag⁺, unshadowed. Magnification: ca. 25 000 ×, reproduced without reduction

for instance, conifer cambium these cannot be much more than 20 to 30 Å wide¹⁶ although the microfibrils are about 100 Å wide. In the similar microfibrils of plant fibres the micelles are 50 to 60 Å wide (Hengstenberg and Mark¹⁷). In these two cases more than 50 per cent of the material in the microfibrils is non-crystalline in the sense that it will not give coherent

diffraction of X-rays; the constituent chains, that is to say, are not regularly spaced. This material is made in large part of glucose residues (p 514). In the microfibrils of *Valonia*, *Cladophora* and *Chaetomorpha* the width of the crystallites is not noticeably less than that of the microfibrils (Preston and Ripley¹⁸). Moreover the cellulose content of the wall (Preston and Cronshaw⁶) is closely similar to the content of crystalline material present (Preston *et al.*¹⁹). The non-crystalline content of these microfibrils, which contains no detectable sugar residues other than glucose residues, must therefore be small and these microfibrils may well be, to a close approximation, single crystals.

Two types of observation suggest that the organization of a microfibril is not uniform along its length. In microfibrils of wood cellulose which have been immersed for a short time in silver nitrate and well washed, the silver is not taken up uniformly. *Figure 3*⁵ demonstrates that the microfibrils become opaque over short lengths, separated by lengths which have taken up little or no silver. This may well mean that over the opaque regions the crystallite core is interrupted or at least reduced in thickness. *Chaetomorpha* microfibrils do not show this phenomenon⁵ but they, like other microfibrils, when subjected to even such a mild treatment as boiling in water show the appearance illustrated in *Figure 4*. Short lengths of the microfibril are missing, though the shadow is continuous. These deletions must presumably represent regions of weakness.



Figure 4—Electron micrograph of cellulose microfibrils in the green seaweed *Chaetomorpha melagonium*. Magnification: 20 400 \times , reproduced without reduction; shadowed Pd-Au

Although the crystalline core has been shown to be eucellulose in some cases—and is probably so in all—its structure is not precisely the same in all plants. Four crystalline modifications of cellulose are recognized: cellulose I, formerly called native cellulose and typical of vegetable fibres, with a unit cell $a=8.35 \text{ \AA}$, $b=10.3 \text{ \AA}$, $c=7.9 \text{ \AA}$, $\beta=84^\circ$; cellulose II, mercerized cellulose, produced when cellulose I is dispersed and reprecipitated, with a unit cell $a=8.14 \text{ \AA}$, $b=10.3 \text{ \AA}$, $c=9.14 \text{ \AA}$, $\beta=62^\circ$; cellulose III which will not be discussed here; and cellulose IV, produced by heating cellulose II at 290°C in glycerine, with an almost tetragonal unit cell. It was suggested some years ago that cellulose II occurs naturally in many seaweeds (Nicolai and Preston²⁰) but this has been shown to be due to coincidence between the arcs on the X-ray diagram of cellulose II and those of clay minerals only recently known to be present (Frei and Preston²¹). There still remains, however, the seaweed, *Halicystis* described originally by Sisson²² as containing cellulose II, in which the presence of this substance has more recently been confirmed²³. The microfibrils of this plant contain equal quantities of glucose and xylose residues, the latter forming a β -1,3-linked xylan, and both the cellulose and the xylan are crystalline. In all other cellulose-containing seaweeds so far examined the structural polysaccharide is either cellulose I or a modification approaching cellulose IV (Frei and Preston, unpublished).

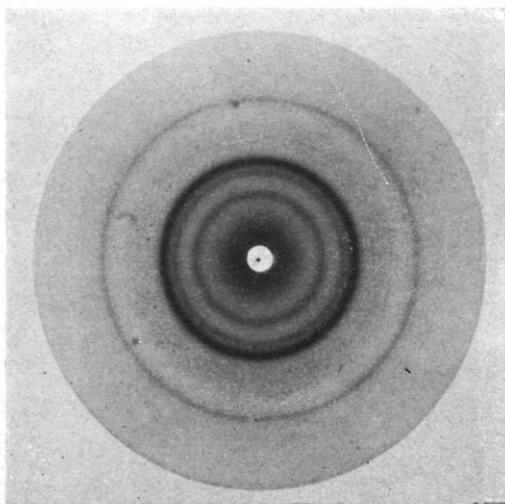


Figure 5—X-ray diagram of a pellet of the cellulose in the green seaweed *Acrosiphonia centralis*. Note the single innermost ring, replacing the two clearly spaced rings of cellulose I. (Photo by Dr Eva Frei)

The discovery by Kubo²⁴ of a naturally occurring cellulose with an almost tetragonal unit cell ($a=8.05 \text{ \AA}$, $b=10.3 \text{ \AA}$, $c=7.98 \text{ \AA}$, $\beta=89^\circ$) resembling that of cellulose IV, in Coltsfoot (*Tussilago farfara*) [mistranslated in the English edition of Meyer (1942) as *hoof* cellulose], has been commonly overlooked. This odd structure has now been confirmed (Frei and Preston, unpublished). In the X-ray diagram of this modification the (101) planes (6.1 \AA in cellulose I) and the (10 $\bar{1}$) planes (5.4 in cellulose I) reflect together.

Many seaweeds, green, brown and red contain normal cellulose I but in others the 101 spacing is low and the $10\bar{1}$ high so that the reflections approach each other. In still others the two reflections are fused (*Figure 5*). This is often observed in higher plants, where the fusion is due to a broadening of each arc consequent upon low crystallinity. This is not the case in the seaweeds. It is quite clear that in these plants the structure of the so-called cellulose I is within limits variable. Differences between the cellulose I of higher plants and that of *Valonia* have already been recorded and a wide survey of cellulose structure in higher plants is clearly desirable. There are reasons to think that the unit cell of Meyer and Misch²⁵ is in error in some respects; the true unit cell is probably twice as big as they suggested, and as illustrated in *Figure 6*, which would mean that the disposition of the cellulose chains cannot be precisely as shown. The fact that in *Valonia* cellulose, at least, the seventh layer line on the electron diffraction diagram is weak or absent (Balashov and Preston²⁶) suggests that the central chain in the Meyer and Misch unit cell is displaced along the b axis by an amount less than $b/4$ and, in any case, there is no clear reason why this chain should be antiparallel. There are indeed reasons to think it is not⁵.

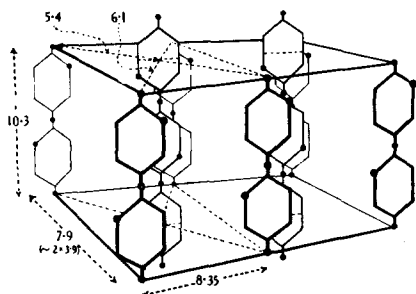


Figure 6—Two unit cells of cellulose I, side by side, after Meyer and Misch. The hexagons represent β -D-glucose residues (the solid circle is oxygen); distances in Å

The microfibrils in many cell walls are organized in specific orientations with respect to a cell axis, and their common orientation can therefore be determined by X-ray diffraction analysis and by electron microscopy. This will be discussed later. The point is to be made here, however, that, in some cases at least, the non-cellulosic wall polysaccharides are also crystalline and the constituent molecular chains are then oriented along the same direction as are the microfibrils. When samples of the red algae *Rhodymenia palmata* (flat, membranous fronds) after treatment with four per cent alkali are dried down on glass, the cells become flattened on the glass surface and therefore the microfibrils lie flat. An X-ray diagram taken with the beam parallel to the flattened faces shows reflections from the xylan and cellulose as distinct arcs (*Figure 7*). Under these circumstances the xylan is oriented with the cellulose and the difficulty encountered in producing the same effect by similar treatment of extracted xylan alone shows that this cannot be an artefact induced by drying down (Dennis⁴). It seems probable that xylan and cellulose may be similarly oriented in wood and fibre cellulose though here, since the cellulose content (*ca.* 50 per cent) is so much higher than in *Rhodymenia* (7 per cent), the cellulose

diagram is so intense as to swamp any xylan diagram which may be present. The long spacings often recorded in X-ray diagrams of celluloses may well come from this source.

An even more striking example is presented by alginic acid (Frei and Preston²¹), and the seaweed *Chorda filum* is particularly informative. In some cells of the cortex (the bulk of this filiform plant) the cellulose microfibrils are arranged helically and correspondingly the diagram is a four-point diagram. In addition to the arcs corresponding to typical cellulose I,

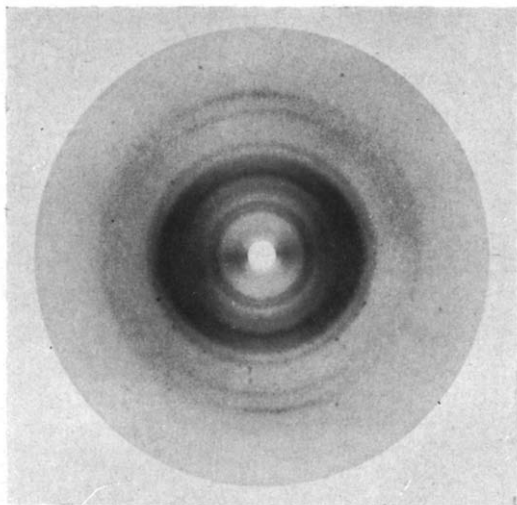


Figure 7—X-ray diagram of *Rhodymenia* cellulose (after extraction by 4 per cent caustic potash). Specimen flattened, beam parallel to flattened face. Note that all the arcs, referring to xylan as well as cellulose, are accentuated either on the equator or the meridian. (Photo by Dr D. T. Dennis)

this diagram contains arcs due to a crystalline alginate as can be verified by removing the latter. When the fresh plant is treated with dilute hydrochloric acid the alginate is converted to alginic acid with a much higher degree of crystallinity and the X-ray diagram then demonstrates most beautifully the parallel arrangement of alginic acid and cellulose. It is quite certain that here—and in many other seaweeds—the alginic acid compounds are crystalline in the plant and that they occur in close association with the cellulose. It has been shown, moreover, that the alginates, like cellulose, are crystalline even in material which has never been allowed to dry and which is exposed to the X-ray beam at 98 per cent r.h.

THE MUTUAL ORGANIZATION OF CELLULOSE MICROFIBRILS

It is now well documented that in the elongated cells of higher plants the cellulose microfibrils are specifically oriented, passing round the cell in a helix in such a way that the angle between the helical winding and cell length (θ) is related both to the breadth and to the length of the cell; the regression line with the length, L , takes the form $L = a + b \cot \theta$ where a and b are constants²⁷. Certainly in some fibres such as ramie the microfibrils lie almost longitudinally, and in the vessel elements of angiosperm wood almost

transversely, but these may be regarded as the limiting cases of helical organization. This particular arrangement of the microfibrils is known to be definitive for the mechanical properties of fibrous cells²⁸. Moreover, the 'crossed fibrillar' structure, first discovered in seaweeds³², is now known to be ubiquitous in fibres. In these cells it takes a form in which alternate wall layers carry microfibrils lying alternately in a flat and a steep helix. Conifer tracheids represent the prototype of this structure; the wall corresponds to three coaxial cylinders, the outer and inner both thin and the central one thick. The microfibrils of the outer and inner cylinders run in flattish helices (θ lying in the range, say, 50° to 90°) and in the central cylinder in steep helices (θ between 0° and 40° , say)²⁹. The range of structures found in conifer wood by Wardrop is illustrated in *Figure 8* and may be taken as typical of all fibrous cells though some fibres such as

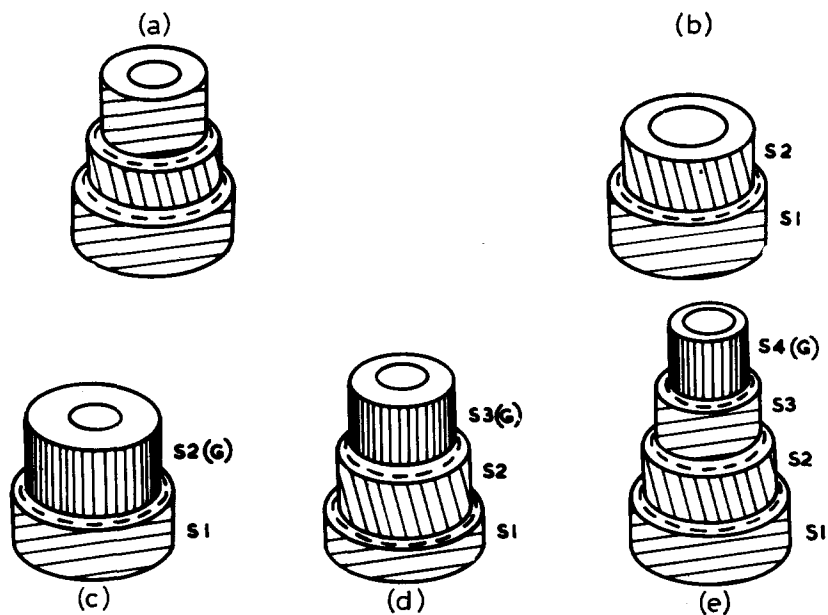


Figure 8—Diagrammatic representation of the structure of the secondary walls of softwood tracheids, dissected to show individual layers. Oblique lines represent the general run of the cellulose microfibrils (by courtesy of Dr A. B. Wardrop). (a) Normal three-layered structure of secondary wall, (b) Two-layered structure of secondary wall in compression wood tracheid, (c) (d) (e) Two-, three- and four-layered structures as observed in tension wood fibres

bamboo are still more complicated³⁰. The close proximity of the microfibrils, possibly together with the close association between the microfibril surface and the incrusting substances, sometimes gives the wall lamellae a smooth appearance in electron micrographs suggesting an aggregation into ribbons. This should not be allowed to obscure the fact that the microfibrils are nevertheless individual units which can be seen in the electron microscope even after the mildest treatment (*Figure 9*)³¹.

Crossed microfibrillar structure has now been demonstrated in many higher plant cells other than fibres in some fungi and in many algae, though nowhere does it occur with more precise expression than in the group of algae in which it was originally found^{12,32}. In this group, members of which range in size and form from the globules of *Valonia*, as large as a hen's egg, to the almost microscopically narrow filaments of *Chaeto-*

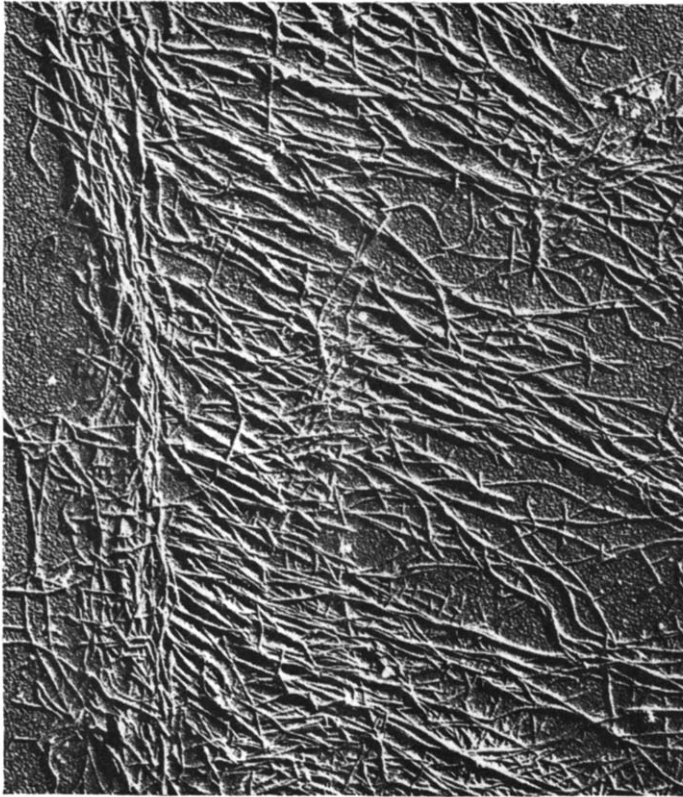


Figure 9—Electron micrograph of a longitudinal section through the layer S1 of a delignified tracheid of *Pinus radiata*. Magnification: 22500 \times , reproduced without reduction; shadowed Pd-Au

morpha, wall lamellae with microfibrils in one orientation alternate repeatedly with microfibrils in another direction (Figure 10). With all of them the microfibrils are exceptionally straight and well aligned. The wall of a *Valonia* vesicle was conceived by Astbury and Preston as possessing two sets of microfibrils, lying in two sets of lamellae, one of them running in a flat, and the other in a steep left-hand helix round the vesicle. It is now known that there is present a third type of lamella with microfibrils lying in a moderately flat right-hand helix (Cronshaw and Preston³²). This third lamella is not regularly present so that the whole structure is an interrupted

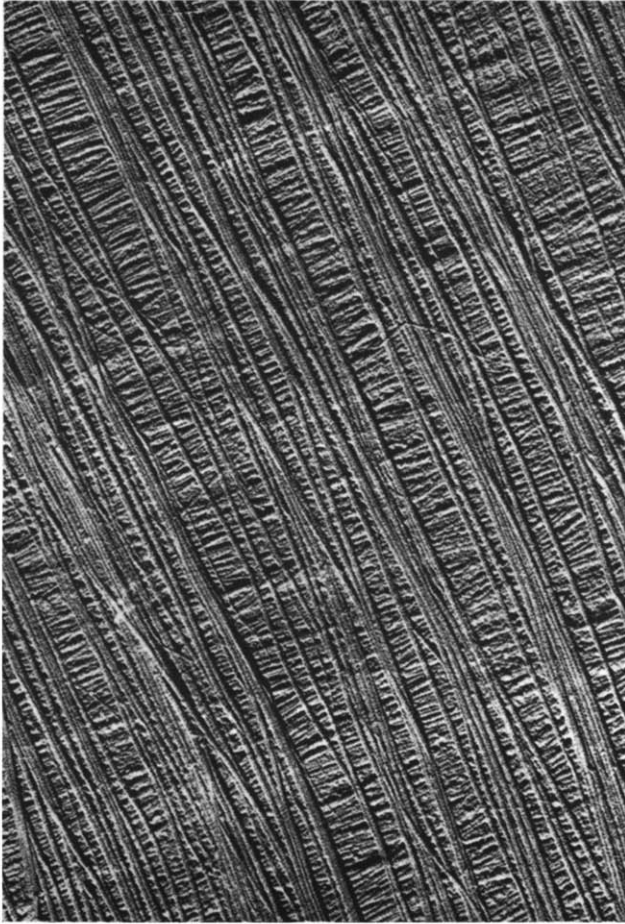


Figure 10—Electron micrograph of inner wall lamellae of cells of the green seaweed *Cladophora rupestris*, viewed from outside. Magnification: 24000 \times , reproduced without reduction; shadowed Pd-Au. Cell axis vertical

two-lamella repeat rather than a three-lamella repeat. The filamentous seaweeds *Cladophora* and *Chaetomorpha* are similarly organized, differing from each other and from *Valonia* both in the signs of the helices and in the abundance of the third type of lamella but with close geometrical relationships¹² (Figure 11).

The cells of these seaweeds though often small, are large enough that observations can readily be made upon them which are for technical reasons much more difficult with the much narrower fibrous cells of higher plants. This is important, since the wall structure of these plants is so similar to that of the fibrous cells that the observations made give pointers toward the kind of things which might be looked for in higher plants. It is known, for instance, that the individual lamellae in the walls of the seaweeds are not clearly separable over their whole area¹². Microfibrils can be seen to pass smoothly from one lamella to the next, with a consequent change in direction (Figure 12), or even to the next-but-one or next-but-many. If this were true in wood fibres, for instance, it might conceivably be of importance in paper-making. It is further known that, while the two (or three) helices do alternate almost exactly through the wall, the helical angle slowly

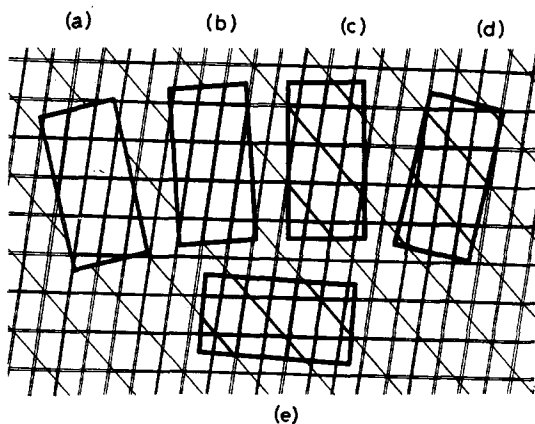


Figure 11—Diagram representing the relationships between the structure of the wall in *Chaetomorpha*, *Cladophora* and *Valonia*. The two major orientations of microfibrils correspond to the two sets of double lines. The third orientation is represented by single lines. The longer edge of each rectangle is taken parallel to the axis of the corresponding cell. (a) *Chaetomorpha melagonium*. (b) *Cladophora rupestris*. (c) *Chaetomorpha princeps*. (d) *Cladophora prolifera*. (e) *Valonia ventricosa*

changes on passing from the inside to the outside of the wall; the steep helix becomes flatter and the flat helix steeper (Frei and Preston³³). There is some evidence that similar changes are to be found in some fibres (Preston and Singh³⁰). If this phenomenon were found to be universal then it might be important in detailed considerations of the effect of stress on fibres.

It is known, moreover, that the helical organization of the walls of the seaweeds *Cladophora* and *Chaetomorpha* carries with it the consequence that as each constituent cell elongates it, and therefore the whole filament, twists about its own axis in the so-called *spiral growth* (Frei and Preston³³). If this twisting is artificially prevented then internal stresses are set up

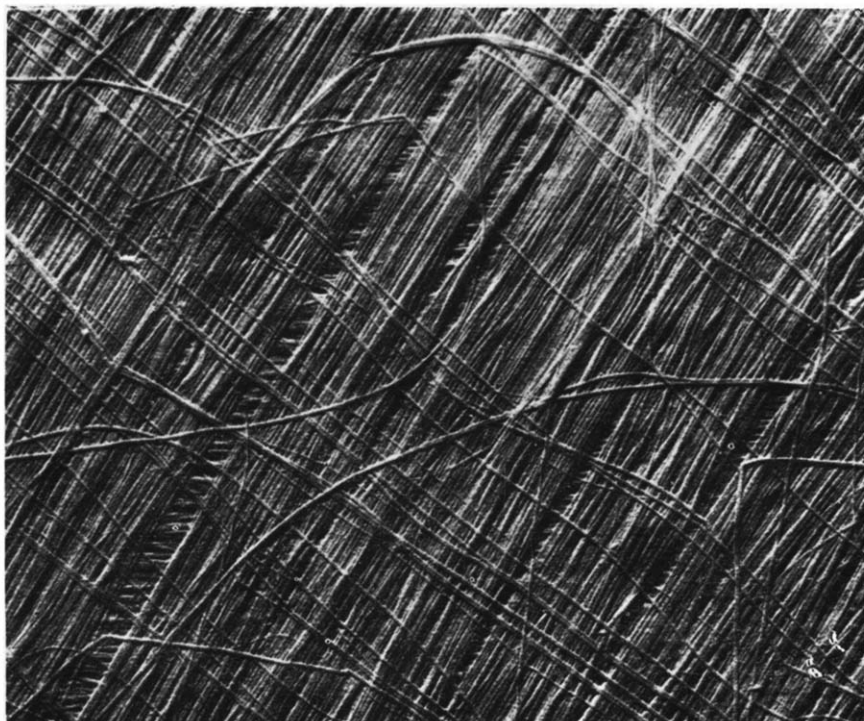


Figure 12—Electron micrograph of wall lamellae of cells of the green seaweed *Chaetomorpha princeps*. Magnification: 21 000 \times , reproduced without reduction; shadowed Pd—Au. Note the microfibril curved through about 90°, incorporated in wall at both ends. All the disoriented microfibrils shown are similarly incorporated

which lead to marked aberrations in structure. There seems to be no reason why any cell with helically organized walls should not show similar growth phenomena and indeed such a process has already been invoked in a semi-quantitative explanation of spiral grain in timber³⁴. In that case, one might expect internal stresses to be set up in any fibre which undergoes extension during development while being held firmly against twisting, and these stresses could have consequences which need to be taken into account.

If there is a moral to this tale of cellulose it is therefore this. The fibre scientist must accept his cellulose in the form presented to him in the plant and his endeavours are limited by its morphology. It is, however, within his power to select from the wide variety available a form of cellulose which

will readily give him the solution to a problem he perhaps cannot even investigate with fibres. He must then ask himself if he can safely transfer his solution to the cellulose of commerce, and the answer may be far to seek. At the least, however, on the way he will learn a great deal more about cellulose than fibres alone can teach him.

*The Astbury Department of Biophysics,
The University of Leeds, Leeds 2*

DISCUSSION

Professor H. Hopff (Switzerland), Chairman: May I thank you very much Professor Preston for this very interesting contribution to our knowledge of the morphology and the structure of cellulose. You have shown us that the term 'cellulose' can mean different things, and that there are in existence several kinds of cellulose which differ in their hydrolysis products. Do you mean that the xylose and the other sugars you find in cellulose are constituents of the long chain, or are the glucoses only in the core of the microfibrils?

Professor R. D. Preston (U.K.): I am not sure myself where the xylan chains are, but I think they are in the cortex, not in the crystalline core, so that the eucellulose is always the same.

Dr P. H. Hermans (Netherlands): Would you add something on the way in which one single microfibril grows; in particular, if it grows by lateral apposition or whether it grows from the end?

Professor R. D. Preston (U.K.): I think it grows from the end. There are several lines of evidence which suggest this—some of which I am sure you already know. Ross Colvin, in Canada, working with the extracellular cellulose of *Acetobacter xylinum* has very good electron micrographs showing that when you take a culture which has no cellulose in it, and take repeated strippings, in a few seconds you can see tiny little bits of things, and then a few seconds later these get longer and longer and longer, suggesting end synthesis. The diagrams which I have shown you, showing microfibrils interweaving, I think also mean that these microfibrils must be synthesized from the ends, just as starch is synthesized from the ends.

Dr P. H. Hermans (Netherlands): Would that mean that there is an enzyme on the top of the fibril which has a kind of template of the three-dimensional structure of the cellulose cell which is pushed forward by the fibril?

Professor R. D. Preston (U.K.): If microfibrils grow by end synthesis, then at first sight there must be an enzyme at the end and it must either push out the microfibrils or it itself must walk backwards. I think there is a way round this. In these plants *Chaetomorpha* and *Cladophora*, we can take off the innermost layer which is just being deposited and we can see what the cellulose was like at the precise moment we killed it. Here there is a series of granules in the form of cytoplasm with it too. The granules are arranged in cubic (?) symmetry and out of them apparently come the microfibrils, some going one way and some going the

other way. So it looks to us now as though the whole surface is an enzyme complex, and any part of it can be stimulated to make a microfibril by the presence of an end so that, when the end comes up against a particle, that particle continues the synthesis; the microfibril then meanders past to the next particle and so this microfibril travels through this complex of cubically arranged granules, being oriented, I presume, by their particular orientation. This is a very loose picture, but this is what we actually see, in this static picture, of this newly laid-down cellulose and this is how we interpret it at the moment.

Professor H. Hopff (Switzerland), Chairman: Undoubtedly you have examined the bacterial celluloses, for instance that from *Bacterium xylinum*. Are these eucellulose? Or are they composed of the glucose only?

Professor R. D. Preston (U.K.): I have not examined these myself. They are said to be eucellulose.

REFERENCES

- ¹ MYERS, A., PRESTON, R. D. and RIPLEY, G. W. *Proc. Roy. Soc. B*, 1956, **144**, 450
- ² JERMYN, M. A. and ISHERWOOD, F. A. *Biochem. J.* 1956, **64**, 123
- ³ CRONSHAW, J., MYERS, A. and PRESTON, R. D. *Biochim. biophys. Acta*, 1958, **27**, 89
- ⁴ DENNIS, D. T. 'The fine structure of cellulose microfibrils'. *Ph.D. Thesis*, University of Leeds, 1962
- ⁵ PRESTON, R. D. *Int. Rev. Cytology* (Ed. Bourne and Danielli) (Academic Press: New York) 1959, **8**, 33
- ⁶ PRESTON, R. D. and CRONSHAW, J. *Nature, Lond.* 1958, **181**, 248
- ⁷ RANBY, B. G. *Acta chem. Scand.* 1949, **3**, 649
RANBY, B. G. *Disc. Faraday Soc.* 1951, **11**, 158
- ⁸ MUKHERJEE, S. M. and WOODS, H. J. *Biochim. biophys. Acta*, 1953, **10**, 499
- ⁹ DENNIS, D. T. and PRESTON, R. D. *Nature, Lond.* 1961, **191**, 667
- ¹⁰ FREI, EVA and PRESTON, R. D. *Nature, Lond.* 1961, **192**, 939
- ¹¹ COLVIN, J. R., BAYLEY, S. T. and BEER, M. *Biochim. biophys. Acta*, 1957, **23**, 652
- ¹² FREI, EVA and PRESTON, R. D. *Proc. Roy. Soc. B*, 1961, **154**, 70
- ¹³ PROBINE, M. C. and PRESTON, R. D. *J. exp. Bot.* 1961, **12**, 261
- ¹⁴ HODGE, A. J. and WARDROP, A. B. *Austral. J. sci. Res. B*, 1950, **3**, 265
WARDROP, A. B. *Austral. Pulp & Paper Ind. Tech. Ass. Proc.* 1954, **8**, 6
- ¹⁵ PRESTON, R. D. *Disc. Faraday Soc.* 1951, **11**, 165
- ¹⁶ PRESTON, R. D. and WARDROP, A. B. *Biochim. biophys. Acta*, 1949, **3**, 549
- ¹⁷ HENGSTENBERG, J. and MARK, H. Z. *Kristallogr.* 1928, **69**, 271
- ¹⁸ PRESTON, R. D. and RIPLEY, G. W. *Nature, Lond.* 1954, **174**, 76
- ¹⁹ PRESTON, R. D., HERMANS, P. H. and WEIDINGER, A. *J. exp. Bot.* 1950, **1**, 344
- ²⁰ NICOLAI, M. F. E. and PRESTON, R. D. *Proc. Roy. Soc. B*, 1952, **140**, 244
- ²¹ FREI, EVA and PRESTON, R. D. To be published
- ²² SISSON, W. A. *Science*, 1938, **87**, 350; *Contr. Boyce-Thompson Inst.* 1941-2, **12**, 31
- ²³ ROELOFSON, P. A., DALITZ, V. C. and WIJNMAN, C. F. *Biochim. biophys. Acta*, 1953, **11**, 344
FREI, EVA and PRESTON, R. D. *Nature, Lond.* 1961, **192**, 939
- ²⁴ KUBO, T. Z. *phys. Chem. B*, 1939, **43**, 79
- ²⁵ MEYER, K. H. and MISCH, L. *Helv. chim. Acta*, 1937, **20**, 232
- ²⁶ BALASHOV, V. and PRESTON, R. D. *Nature, Lond.* 1955, **176**, 64
- ²⁷ PRESTON, R. D. *Proc. Roy. Soc. B*, 1946, **133**, 377
- ²⁸ SPARK, L. C., DARNBOROUGH, G. and PRESTON, R. D. *J. Text. Inst.* 1958, **49**, T 309
- ¹ PRESTON, R. D. 'Mechanical properties of cell walls' in *Encyclopedia of Plant Physiology*, Vol. II

- ²⁹ WARDROP, A. B. and PRESTON, R. D. *Nature, Lond.* 1947, **160**, 911
PRESTON, R. D. and WARDROP, A. B. *Biochim. biophys. Acta*, 1949, **3**, 585
- ²⁰ PRESTON, R. D. and SINGH, K. *J. exp. Bot.* 1950, **1**, 214; **3**, 162
- ³¹ FREI, EVA, PRESTON, R. D. and RIPLEY, G. W. *J. exp. Bot.* 1957, **8**, 139
- ³² ASTBURY, W. T. and PRESTON, R. D. *Proc. Roy. Soc. B*, 1937, **122**, 76
CRONSHAW, J. and PRESTON, R. D. *Proc. Roy. Soc. B*, 1958, **148**, 137
- ³³ FREI, EVA and PRESTON, R. D. *Proc. Roy. Soc. B*, 1961, **155**, 55
- ³⁴ PRESTON, R. D. *Forestry*, 1949, **23**, 48

Mechanical Relaxation in Some Oxide Polymers

B. E. READ

The shear modulus and damping have been measured at a frequency of about 1 c/s and at temperatures down to -190°C for polyethylene oxide, polypropylene oxide and polyacetaldehyde. Five different samples of polyethylene oxide have been investigated, ranging in molecular weight from about 4×10^3 up to 5×10^6 . The sample of highest molecular weight exhibits a loss peak at about -57°C . As the molecular weight decreases the temperature of maximum loss initially increases, passes through a maximum in the molecular weight region of 10^4 , and then decreases. After annealing the samples, the loss peaks move to higher temperatures and broaden slightly and the magnitudes of the relaxations show a small reduction. The reverse effect is observed when water or dioxan is added to the polymer. The relaxations are attributed to the motions of chain segments in the disordered regions of the polymer, and it is suggested that these regions may be subjected to strains induced by the ordered regions of the polymer. Polypropylene oxide and polyacetaldehyde exhibit loss peaks at about -62°C and -19°C , respectively, both of which are attributed to relaxation processes related to the respective glass transitions. The results are discussed and compared briefly with data on other related polymers.

IN A recent publication we reported on a study of molecular motions in polymethylene oxide ($([-\text{CH}_2-\text{O}-]_n)$) by dielectric and dynamic mechanical methods¹. The purpose of the present paper is to present and discuss some low frequency mechanical data on the related oxide polymers polyethylene oxide ($([-\text{CH}_2-\text{CH}_2-\text{O}-]_n)$), polypropylene oxide ($([-\text{CH}(\text{CH}_3)-\text{CH}_2-\text{O}-]_n)$) and polyacetaldehyde ($([-\text{CH}(\text{CH}_3)-\text{O}-]_n)$). The relaxation behaviour of polyethylene oxide has been found to depend significantly on the molecular weight of the polymer, its state of annealing and the presence of absorbed liquids such as water and dioxan. Partially crystalline and amorphous samples of polypropylene oxide and an elastomeric sample of polyacetaldehyde have also been studied.

EXPERIMENTAL

The logarithmic decrement (Δ) and the real and imaginary shear moduli, G' and G'' respectively, were determined from -190°C up to room temperature. For one sample of polyethylene oxide (Polyox FC 118) the measurements were extended up to the melting point of the polymer (66°C). The measurements were made with a torsion pendulum operating at a frequency of about 1 c/s¹.

Five samples of polyethylene oxide have been studied. They were obtained from the Union Carbide Chemicals Co. (U.S.A.) and are designated, in order of decreasing molecular weight, Polyox FC 118, Polyox FC 2 075, Polyox 2 464, Carbowax 20M and Carbowax 4 000. Strips of each polymer were moulded under pressure. The moulding temperature for the three

highest molecular weight samples was 90°C. The two samples of lower molecular weight were moulded at temperatures a few degrees above their melting points. The densities and estimated molecular weights² of the specimens are listed in *Table 1*. Samples were annealed by heating to 55°C

Table 1. Summary of data

| Polymer | Density (g/ml) | Estimated molecular weight* (wt av.) | $T_{\Delta, \max.}$ (°C) | $T_{G'', \max.}$ (°C) | Frequency (c/s) | $\langle Q^{-1} \rangle_{av.}^{-1}$ kcal/mole | β |
|--|----------------|--------------------------------------|--------------------------|-----------------------|-----------------|---|---------|
| <u>Polyethylene oxide</u> | | | | | | | |
| Polyox FC 118 | | 5×10 ⁶ | | | | | |
| Unannealed | 1.208 | 5×10 ⁶ | -56 | -59 | 0.34 | 34 | 0.27 |
| Annealed | 1.214 | 5×10 ⁶ | -50 | -52 | 0.75 | | |
| + Water (3%) | | 5×10 ⁶ | -59 | -61 | 0.44 | | |
| Dried | 1.2.8 | 5×10 ⁶ | -55 | -56 | 0.40 | | |
| + Dioxan (7%) | | 5×10 ⁶ | -66 | -71 | 0.50 | 32 | 0.33 |
| Polyox FC 2075 | | 8×10 ⁵ | | | | | |
| Unannealed | 1.216 | 8×10 ⁵ | -54 | -57 | 0.44 | 36 | 0.35 |
| Annealed | 1.222 | 8×10 ⁵ | -39 | -50 | 0.96 | | |
| Polyox 2464 | | 2×10 ⁵ | | | | | |
| Unannealed | 1.223 | 2×10 ⁵ | -41 | -48 | 0.86 | | |
| Annealed | 1.228 | 2×10 ⁵ | -38 | -44 | 1.01 | | |
| Carbowax 20M | | 1.5×10 ⁵ | | | | | |
| Unannealed | 1.196 | →2.0×10 ⁴ | -16 | -24 | 0.68 | 33 | 0.22 |
| Annealed | 1.216 | →2.0×10 ⁴ | + 2 | - 9 | 1.29 | | |
| Carbowax 4000 | | 4×10 ⁵ | | | | | |
| Unannealed | 1.222 | 4×10 ⁵ | -32 | -37 | 1.7 | | |
| <u>Polypropylene oxide</u> | | | | | | | |
| <u>Amorphous (sulphur vulcanizate)</u> | | | | | | | |
| Partially crystalline | 1.045 | | -62 | -65 | 0.24 | | |
| | 1.057 | | -62 | -65 | 0.32 | 28 | 0.50 |
| <u>Polyacetaldehyde</u> | | | | | | | |
| | 1.071 | 1.5×10 ⁵ † | -19 | -29 | 0.58 | | |

*The molecular weights quoted for the polyethylene oxide samples are to be regarded as approximate. They were suggested to us in a private communication with the Union Carbide Chemicals Company (U.S.A.)².

† Calculated from intrinsic viscosity measurements using the viscosity/molecular weight relationship of Bovey and Wands²⁰.

in sealed tubes under nitrogen for periods of about one week and slowly cooling to room temperature. In order to study the effect of absorbed water, a moulded specimen of Polyox FC 118 was placed over a beaker of water in an evacuated desiccator for four days after which 3 per cent by weight of water had been absorbed. After completing measurements on this sample below room temperature it was pumped under high vacuum for three days until its weight remained constant and a further run was then carried out. Although this drying procedure was not generally adopted it indicated that the specimen before wetting had contained only about 0.25 per cent of moisture. In order to investigate the effect of absorbed dioxan, a sample of Polyox FC 118 was immersed in dioxan at room temperature for 15 h after which approximately 7 per cent by weight of dioxan had been absorbed.

The partially crystalline sample was obtained from the polymerization of propylene oxide in dioxan solution using zinc diethyl and water as catalyst. For the mechanical measurements a strip was moulded at 90°C under pressure. The amorphous sample was prepared by a zinc diethyl-water catalysed polymerization of the monomer containing 10 per cent

of butadiene monoxide which rendered the product vulcanizable. The polymer was subsequently vulcanized with 2 per cent sulphur.

The polyacetaldehyde specimen was prepared in this laboratory by bulk polymerizing acetaldehyde using zinc diethyl as catalyst³. In order to stabilize the polymer the end groups were esterified by heating at 50°C in a pyridine-acetic anhydride solution. A small tough fraction of the polymer (thought to be the crystalline fraction³) was insoluble in the esterification mixture and was consequently separated. After esterification, the product was precipitated in water, and twice redissolved in acetone and precipitated with water. The polymer was then dried in a vacuum desiccator at room temperature and finally moulded into rubberlike strips at 60°C.

RESULTS

The variation of G' , Δ and G'' with temperature for the five unannealed samples of polyethylene oxide is shown in *Figure 1*. For all samples G' is seen to decrease with increasing temperature over the entire temperature.

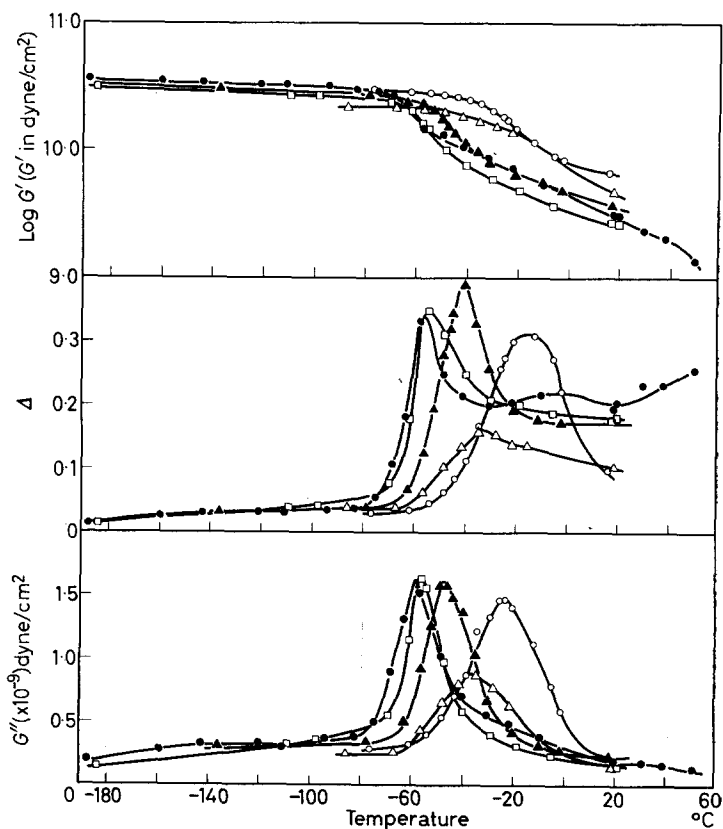


Figure 1—Variation of G' , G'' and the logarithmic decrement (Δ) with temperature for Polyox FC 118 (\bullet), Polyox FC 2075 (\square), Polyox 2464 (\blacktriangle), Carbowax 20M (\odot) and Carbowax 4000 (\triangle)

range investigated, but shows the largest changes in the relaxation regions where loss peaks are also observed. The Δ versus T curves are broad but exhibit well defined maxima at temperatures denoted by $T_{\Delta, \max.}$ in Table 1. The corresponding maxima in the G'' curves, shown as $T_{G'', \max.}$ in Table 1, occur at somewhat lower temperatures than $T_{\Delta, \max.}$ and coincide with the inflection points of the G' curves. Between $T_{\Delta, \max.}$ and room temperature the Δ values are fairly high on account of the low magnitude of G' in this region ($\Delta \approx \pi G''/G'$). The G'' peaks, which in all cases are more symmetrical than the corresponding Δ loss peaks, are slightly broadened in this high temperature region. As the molecular weight decreases, the G'' peaks

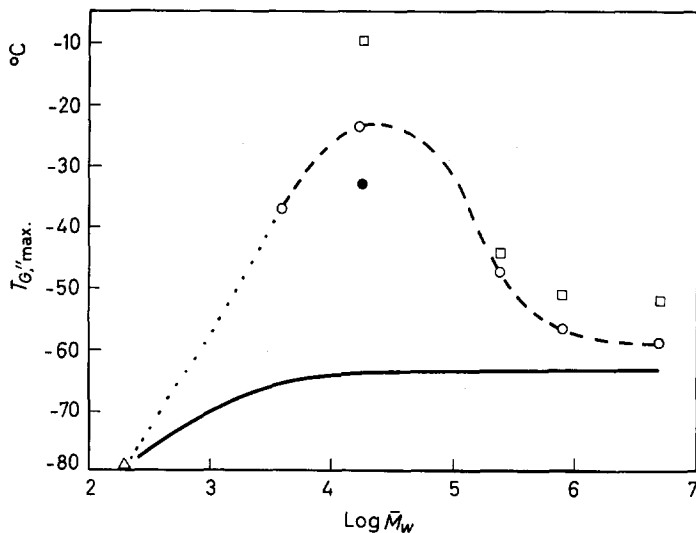


Figure 2—Plot of $T_{G'', \max.}$ versus $\log \bar{M}_w$ for unannealed (○) and annealed (□) polyethylene oxide. \bar{M}_w is the estimated weight average molecular weight. Filled circle (●) derived from McCrum's data⁴ on Carbowax 20M. The triangle (Δ) represents $T_{e'', \max.}$ estimated from the dielectric data of Koizumi and Hanai¹⁵. The solid line represents schematically the predicted dependence of $T_{G'', \max.}$ on molecular weight in the absence of crystallinity

broaden slightly and decrease in height, this effect being most marked with the three samples of lower molecular weight.

The variation of the loss peak temperature with molecular weight is illustrated in Figure 2 where $T_{G'', \max.}$ is plotted against $\log \bar{M}_w$. At the highest molecular weight (Polyox FC 118) $T_{G'', \max.}$ has an apparently limiting low value of -59°C . As the molecular weight decreases $T_{G'', \max.}$ increases, appears to reach a maximum value of about -24°C in the molecular weight region of 10^4 and subsequently decreases. The filled circle shown in Figure 2 is the value of $T_{G'', \max.}$ calculated from the data of McCrum⁴ on Carbowax 20M. It is seen to lie some 9°C below our own value.

After annealing, an increase in density was observed for all samples (see

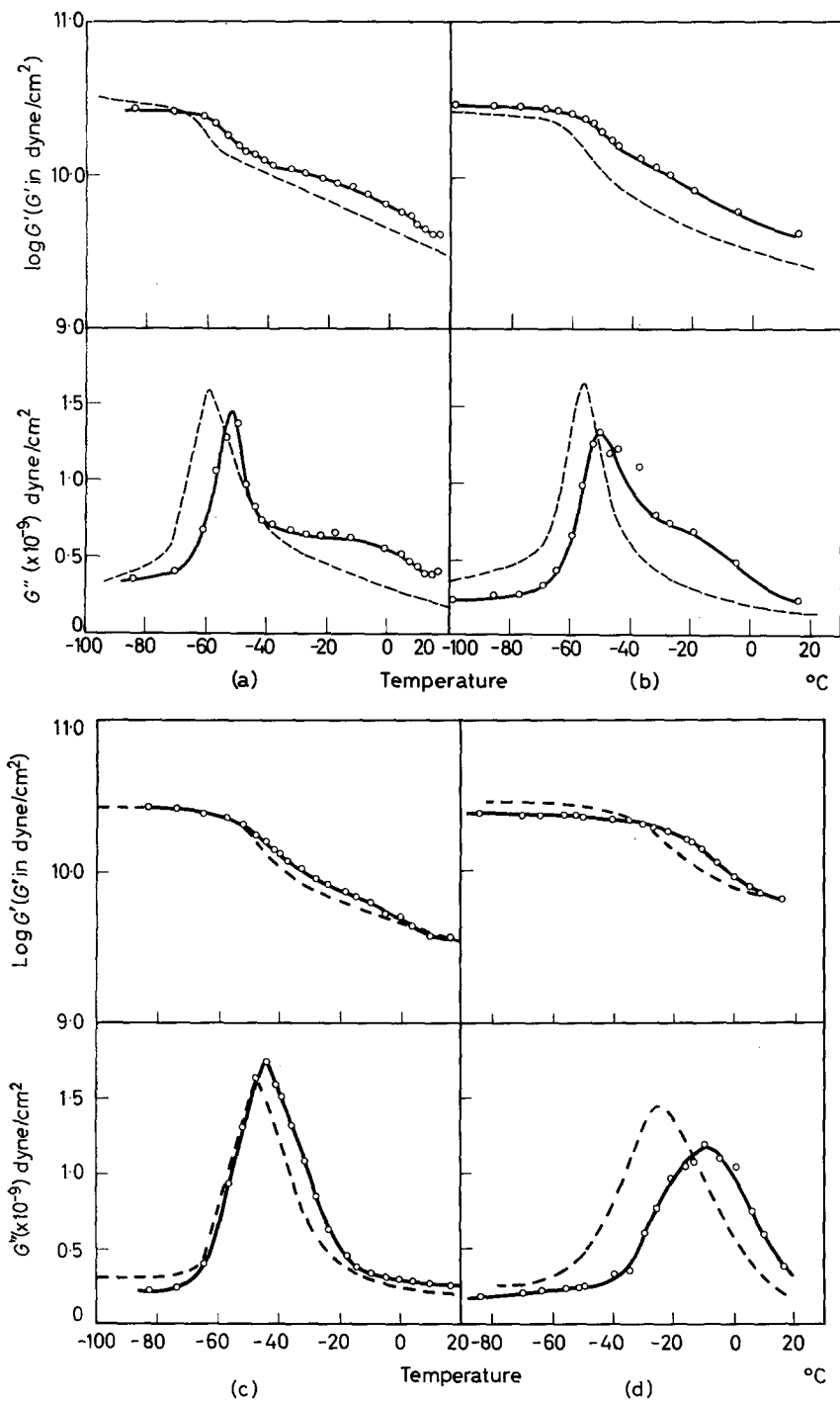


Figure 3—Plots of G' and G'' versus temperature for annealed polyethylene oxide (O): (a) Polyox FC 118, (b) Polyox FC 2075, (c) Polyox 2464, (d) Carbowax 20M. Broken lines show the data for the unannealed samples for comparison

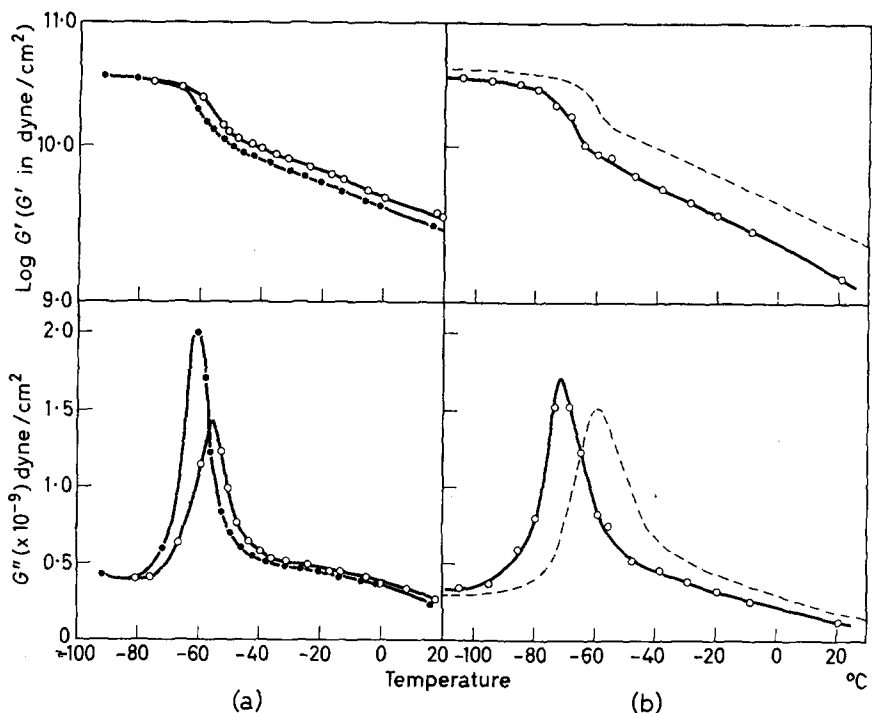


Figure 4—(a) G' and G'' versus temperature for Polyox FC 118 containing 3 per cent water (●) and after drying (○); (b) Data for Polyox FC 118 before (broken curve) and after full line adding 7 per cent dioxan

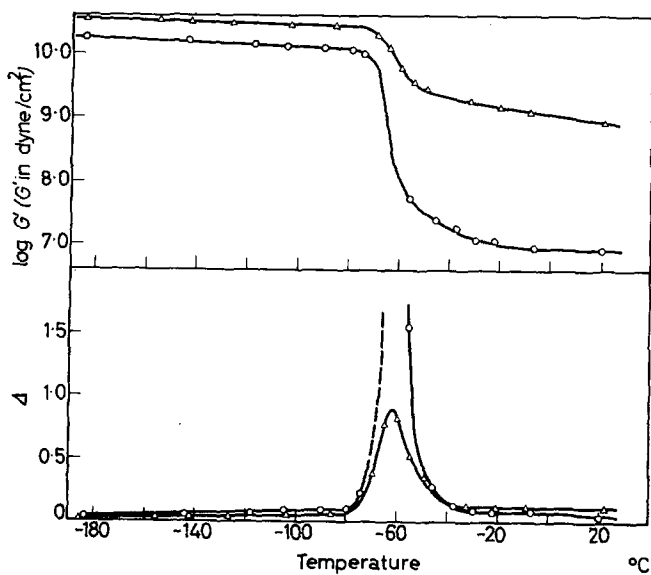


Figure 5—Plots of G' and Δ against temperature for amorphous (○) and partially crystalline (Δ) polypropylene oxide

Table 1). Plots of G' and G'' versus temperature for the annealed specimens are compared with those for the unannealed samples in *Figure 3*. In all cases annealing is seen to shift the loss maxima to higher temperatures, as shown also in *Table 1* and *Figure 2*. Generally the magnitude of the relaxation, determined by the incremental change in G' and the height of the loss peak, is decreased slightly. The loss peak for Polyox 2464 is considerably broadened, whilst the G'' curves for Polyox FC 118 and FC 2075 exhibit shoulders between the main loss peak and room temperature.

The effects due to absorbed water and dioxan are shown in *Figure 4* and *Table 1*. Both liquids cause the loss peaks to move to lower temperatures and cause a slight increase in the magnitude of the relaxation.

The data for both the partially crystalline and amorphous polypropylene oxide are shown in *Figure 5* and *Table 1*. Both samples exhibit a single relaxation below room temperature and, within experimental error, the loss peak temperature is the same for both samples. The magnitude of the relaxation is much larger, however, for the amorphous polymer.

The results for polyacetaldehyde are illustrated in *Figure 6* and *Table 1*. This polymer also shows a single relaxation region below room temperature.

Activation energies

In a recent paper⁵ it was shown that an average activation energy ($\langle Q^{-1} \rangle_{av.}^{-1}$) for relaxation may be estimated from the area beneath a plot

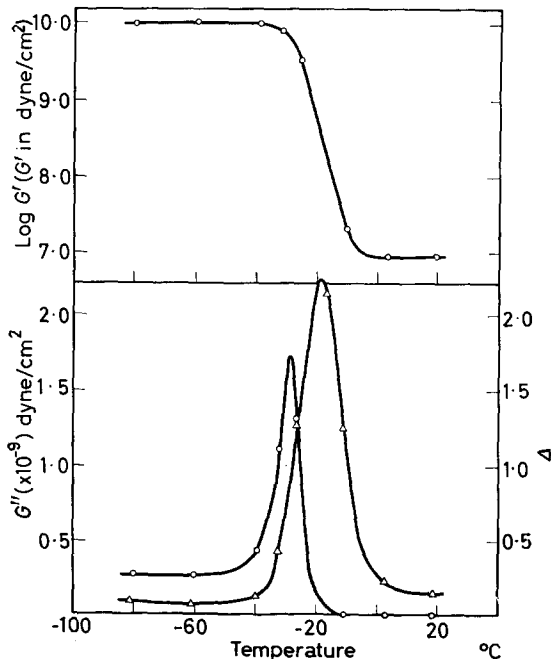


Figure 6— G' , $\Delta(\Delta)$ and G'' (\circ) against temperature for polyacetaldehyde

of G'' against $1/T$ at constant frequency

$$\begin{aligned} \langle Q^{-1} \rangle_{av.}^{-1} &= 1 / \int_0^\infty \int_0^\infty \Phi(\tau_0, Q) Q^{-1} d\tau_0 dQ \\ &= \frac{(G'_\infty - G'_0) R \Pi}{2 \int_0^\infty G'' d(1/T)} \end{aligned} \quad (1)$$

where G'_∞ and G'_0 are the infinite frequency and zero frequency moduli, respectively, determined from a frequency dispersion at constant temperature. Both G'_∞ and G'_0 are assumed to be independent of temperature. $\Phi(\tau_0, Q)$ is a normalized distribution function giving the fraction of relaxation processes have activation energies between Q and $Q+dQ$ and, *in addition*, relaxation times between τ_0 and $\tau_0+d\tau_0$ at infinite temperature. In the present application we may, to a good approximation, replace $(G'_\infty - G'_0)$ by the total modulus drop from -190°C to 20°C (at constant frequency) and graphically integrate the loss curves between the same temperature limits. Activation energies deduced in this way for several of the unannealed samples are presented in *Table 1*.

Distribution of relaxation times

From the general shape of the loss curves it is clear that an extremely broad non-symmetrical distribution of relaxation times would be required to describe the behaviour over the entire temperature range. In the vicinity

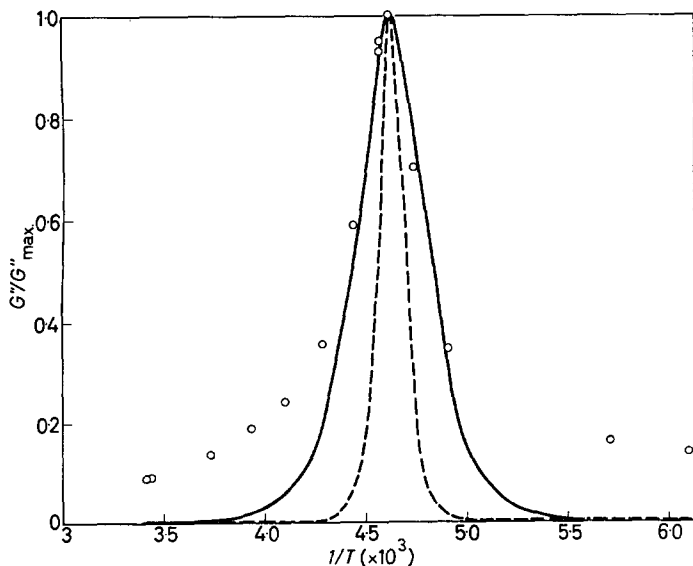


Figure 7—Theoretical curves of G''/G''_{\max} against $1/T$ for two values of the distribution parameter β : $\beta=1$ (broken curve), $\beta=0.35$ (full line). Experimental point for Polyox FC 2075 (O)

of the loss maxima, however, the loss peaks are relatively sharp and symmetrical and we may attempt to analyse them by the empirical Fuoss-Kirkwood equation⁶

$$G''/G''_{\max.} = \operatorname{sech} \beta \ln \omega \tau \quad (2)$$

where β is a parameter which is equal to unity for a single relaxation time and for a distribution lies between zero and unity. ω is the experimental frequency and the relaxation time $\tau = \tau_0 \exp(Q/RT)$. β may be obtained from the following equation relating the width of a G'' versus $1/T$ curve to Q ⁵

$$\beta = 2.63/Q (T_2^{-1} - T_{\max.}^{-1}) \quad (3)$$

where T_2 is the temperature at which $G'' = \frac{1}{2}G''_{\max.}$ and Q is given in cal/mole. Values of β , calculated from equation (3) using Q values determined as above, are given in *Table 1*. Plots of equation (3) for $\beta = 1$ and $\beta = 0.35$ respectively are shown in *Figure 7* together with the experimental points for Polyox FC 2 075. It is observed that the experimental curve is much broader than would be obtained for a single relaxation time. The curve for $\beta = 0.35$ fits the data reasonably well in the vicinity of the maximum but does not provide a good overall fit.

DISCUSSION

Polyethylene oxide

Polyethylene oxide is a highly crystalline polymer in which the fundamental unit cell is monoclinic and consists of two polymer chain segments probably present in the form of parallel helices⁷. The unit cells form crystalline aggregates which make up the radial arms of polymer spherulites⁷. The measured densities of the samples (*Table 1*) are considerably lower than the value of 1.33 g/ml estimated from the unit cell dimensions for a completely crystalline material. Although the low densities may partly be due to the presence of voids⁷, it is probable that the polymer contains 'disordered' regions which may be regarded either as a separate amorphous phase or as crystalline lattice defects⁸. When considering high degrees of crystallinity, the lattice defect hypothesis seems more appropriate and, furthermore, it is unlikely that a normal amorphous phase could exist unaffected by the large amount of crystallinity. However, in the absence of a precise knowledge of the physical structure of the polymer we refer generally to the existence within the material of disordered regions, the fraction of which is indicated by the density.

The loss peak temperatures of the four higher molecular weight unannealed polyethylene oxide samples (*Table 1*) correlate with the temperatures of dielectric loss maxima observed at higher frequencies in this laboratory⁹. In addition, the activation energies of about 30 to 35 kcal/mole compare well with values obtained from the temperature dependence of the average dielectric relaxation time. Thus similar mechanisms probably give rise to both the mechanical and the dielectric relaxations.

Since the proportion of disordered polymer generally decreases with annealing, the small decrease in the relaxation magnitudes after annealing

is consistent with a mechanism involving segmental motions in the disordered regions of the polymer. The effects of both water and dioxan in increasing the relaxation magnitude and moving the relaxations to lower temperatures support this conclusion. Both liquids may preferentially enter and plasticize the less dense disordered regions as in the case of polyoxymethylene¹. Also since water and dioxan are each potential solvents for the polymer they would tend partially to break down the crystallinity and plasticize the resulting disordered regions. The possibility that the loss mechanism arises entirely from small quantities of absorbed moisture has been considered, but this seems unlikely since the estimated 0.25 per cent of moisture normally present would probably have a negligible effect when compared with that produced by the 3 per cent of absorbed water. Unfortunately our present experimental set-up does not allow measurements to be made in a completely moisture-free atmosphere, and experiments under these conditions would be desirable. The suggestion that the relaxation process occurs in the disordered regions has received additional support from the dilatometric observation of a glass transition temperature at about -67°C for a quenched sample of Polyox FC 118¹⁰. Glass transitions determined dilatometrically usually occur some 10° to 15°C below low frequency mechanical loss peaks. The fairly high activation energies are also consistent with relaxation processes related to the glass transitions.

If the proposed mechanism is essentially correct, then the increase of $T_{G''_{\max}}$ after annealing shows that the heat treatment has in some way restricted molecular motions in the disordered regions. It is tentatively suggested that this restriction results from the existence within the disordered regions of strains induced by the ordered crystallites and therefore enhanced by annealing. In discussing the possible nature of the proposed strains it is convenient to distinguish between orientational strains in which the volume remains constant, and compressional (or dilatational) strains which involve volume changes. For example, when orientational strains are produced in natural rubber by simple extension, the loss peak associated with the glass-rubber transition broadens but its position remains unchanged¹¹. On the other hand, by analogy with dielectric behaviour¹², the loss peaks would be expected to shift to higher temperatures if the volume is decreased by an increase in external pressure. Also the peaks have been seen to move to lower temperatures when the volume is increased by the addition of liquid plasticizers. In fact much evidence exists to suggest that mechanical relaxation times are largely determined by the free volume available to the moving segments. We may thus suggest that the increase in $T_{G''_{\max}}$ (and $T_{\Delta_{\max}}$) upon annealing may be related to compressional strains induced in the disordered regions by expansion of the crystalline aggregates, and that the broadening observed in the case of Polyox 2 464 may be due to induced orientation.

The shoulders which appear after annealing on the high temperature side of the loss peaks for Polyox FC 118 and Polyox 2 075 are perhaps suggestive of a crystalline mechanism similar to the so-called α -mechanism in polyethylene¹³. Unfortunately there is little evidence for such a hypothesis. However, since the loss peak for Carbowax 20M lies in the

temperature region where this crystalline mechanism might be operative, the possibility of overlapping mechanisms due to both disordered and crystalline regions in this polymer cannot be excluded. In this connection it should be noted that crystalline peaks also move to higher temperatures after annealing owing to an increase in crystallite size¹³.

The dependence of $T_{G'',\max}$ (and $T_{\Delta,\max}$) on molecular weight appears at first sight surprising. In the absence of crystallinity $T_{G'',\max}$ would be expected to increase with molecular weight toward an asymptotic limit in the molecular weight region of 5 000 \rightarrow 10 000 (300 \rightarrow 600 chain atoms). Such a trend has been observed for the glass transition temperature of polystyrene and has been attributed to the plasticizing effect of chain ends at low molecular weights¹⁴. The packing around chain ends is inevitably looser than along the main chains which leads to an increase in free volume. The predicted molecular weight dependence of $T_{G'',\max}$ in the absence of crystallinity is represented qualitatively by the full line in *Figure 2*. The point shown at a molecular weight of 194 was derived from the dielectric data of Koizumi and Hanai¹⁵ on supercooled (amorphous) tetraethylene glycol. The maxima of ϵ'' (dielectric loss factor) versus T curves determined in the frequency range 10^3 c/s to 5×10^4 c/s were extrapolated to a frequency of 0.5 c/s. This comparison with dielectric data assumes a correlation with mechanical data at low molecular weights which is in fact found in the higher molecular weight range. The high values of $T_{G'',\max}$ in the intermediate molecular weight region are most likely due to crystallinity. As the molecular weight decreases from a value of 5×10^6 the chains are able to pack more easily together, the proportion of disordered material decreases, and the strains induced in the disordered regions increase. Hence the magnitude of the loss decreases, the loss peaks broaden slightly and shift to higher temperatures. Below molecular weights of about 10^4 the additional chain end effect causes $T_{G'',\max}$ to decrease with a further reduction in molecular weight. The fact that $T_{G'',\max}$ for Carbowax 20M (-33°C) derived from McCrum's data⁴ is 9°C lower than our value could perhaps be due to differences in molecular weight between different batches of this material or to different moulding conditions (for example, a faster rate of cooling). According to the above discussion $T_{G'',\max}$ should depend on annealing and molecular weight largely through its dependence on density. Although a general trend with density is found, the density of Carbowax 20M appears low. Density measurements in this material are probably unreliable on account of small holes which were often visible in moulded samples, although care was taken to select an apparently homogeneous sample. It should be emphasized that the interpretation suggested for the effect of molecular weight is somewhat tentative, particularly in view of the possibility, mentioned above, of the existence of a crystalline mechanism in the samples of lower molecular weight.

In comparing the loss peak temperature of polyethylene oxide with that of related polymers, it is preferable to consider the $T_{\Delta,\max}$ value for the very high molecular weight Polyox FC 118. At high molecular weights the effects of crystallinity and chain ends are probably at a minimum and possibly negligible. McCrum⁴ has compared the $T_{\Delta,\max}$ value of -27°C

(1 c/s) which he observed for Carbowax 20M with loss peaks exhibited by polytrimethylene oxide¹⁶ ($[-\text{CH}_2-\text{CH}_2-\text{CH}_2-\text{O}-]_n$) at -45°C (100 c/s), polytetramethylene oxide¹⁶ ($[-\text{CH}_2-\text{CH}_2-\text{CH}_2-\text{CH}_2-\text{O}-]_n$) at -55°C (100 c/s), and a very small peak (labelled β) in polymethylene oxide ($[-\text{CH}_2-\text{O}-]_n$) at about -13°C (1 c/s)⁴. Though tentative, this comparison would indicate that the loss peak temperature increases as the proportion of oxygen in the main chain increases. However, in view of the large variation of $T_{\Delta, \text{max.}}$ with molecular weight for polyethylene oxide this conclusion is not necessarily valid. For example, from the data on the high molecular weight Polyox FC 118 sample we estimate, in conjunction with the dielectric data, a $T_{\Delta, \text{max.}}$ value of -50°C at 100 c/s which is intermediate between the values for polytrimethylene oxide and polytetramethylene oxide*. Also we consider that the predominant peak shown by polymethylene oxide at -60°C (100 c/s), which McCrum labels the γ peak⁴, should be involved in the comparison rather than the small β peak which we were unable to detect¹. Both polytrimethylene oxide and polytetramethylene oxide exhibit additional peaks at -110°C (100 c/s) which have been attributed by Willbourn¹⁶ to $[-\text{CH}^2-]_n$ segments containing a minimum of three $-\text{CH}_2-$ units. The fact that polyethylene oxide and polymethylene oxide do not show peaks in this temperature region lends support to this view.

Polypropylene oxide and polyacetaldehyde

Stereoregular polypropylene oxide crystallizes with an orthorhombic unit cell¹⁷. Two planar zig-zag molecules lie parallel to the c axis. From the unit cell dimensions we estimate a theoretical crystalline density of 1.154 g/ml. From the densities of amorphous polypropylene oxide (1.002 g/ml)¹⁰ and the partially crystalline sample used in this study the latter sample is estimated to contain 39 per cent by weight of crystalline material. Since the loss maximum temperatures for both the amorphous and crystalline samples coincide, the loss peaks for both samples are undoubtedly related to the glass transition in this polymer. Also the disordered regions of the partially crystalline sample, at this relatively low degree of crystallinity, probably resemble a normal amorphous phase.

The close proximity of the loss peaks for the high molecular weight polyethylene oxide (-57°C , 0.34 c/s) and polypropylene oxide (-62°C , 0.3 c/s) suggests that the methyl substituents in the latter polymer do not have much influence on molecular mobility. This may be partly due to the effect of oxygen atoms in spacing apart the methyl substituents. For example, in the planar chain configuration, successive CH_3 groups occur on opposite sides of the chain axis. A similar conclusion results from a comparison of the position of the loss peak in polypropylene oxide with that shown by its isomer polytrimethylene oxide¹⁶ (-45°C , 100 c/s).

The large modulus change accompanying the relaxation in polyacetaldehyde is also indicative of processes related to the glass transition in this material. The value of $T_{\Delta, \text{max.}}$ (-19°C , 0.58 c/s) compares well with

*Since $T_{\Delta, \text{max.}}$ for polytrimethylene oxide and polytetramethylene oxide could also depend on molecular weight, this comparison is tentative.

a value of approximately $+10^{\circ}\text{C}$ (100 c/s) very recently reported for this polymer by Weissmehl and Schmieder¹⁸. From the position of our low frequency loss peak we would estimate a glass-transition temperature of about -30°C . Comparison of $T_{\Delta, \text{max}}$ in this polymer with that shown by polymethylene oxide (-76°C , 0.43 c/s) and also with that of its isomer polyethylene oxide (-57°C , 0.34 c/s) indicates that the occurrence of methyl substituents on alternate carbon atoms sterically hinders molecular motions. It is interesting to note that the polyacetaldehyde loss maximum lies fairly close to that observed for polypropylene¹⁹ (-4.7°C , 1 c/s) which also has $-\text{CH}_3$ substituents on alternate carbon atoms.

The positions of the loss peaks in polypropylene oxide and polyacetaldehyde could, of course, depend on molecular weight. However, amorphous samples of both polymers were studied, the polypropylene oxide being an infinitely crosslinked network, and the polyacetaldehyde having a molecular weight (Table 1) much higher than the usually critical value of about 10^4 .

The author wishes to thank Dr F. E. Bailey of Union Carbide Chemicals Co. for supplying the polyethylene oxide samples and Dr G. Allen of Manchester University for the polypropylene oxide specimens. Thanks are also due to Mr G. O'Neill for preparing the polyacetaldehyde and to Mrs J. Hawkins for help with the experimental work. The work described above has been carried out as part of the research programme of the National Physical Laboratory and is published by permission of the Director of the Laboratory.

Basic Physics Division,
National Physical Laboratory,
Teddington, Middlesex

(Received December 1961)

REFERENCES

- ¹ READ, B. E. and WILLIAMS, G. *Polymer, Lond.* 1961, **2**, 239
- ² BAILEY, F. E. Private communication
- ³ FURUKAWA, J., SAEGUSA, T. and FUJII, H. *Makromol. Chem.* 1961, **44-46**, 398
- ⁴ MCCRUM, N. G. *J. Polym. Sci.* 1961, **54**, 561
- ⁵ READ, B. E. and WILLIAMS, G. *Trans. Faraday Soc.* 1961, **57**, 1979
- ⁶ FUOSS, R. M. and KIRKWOOD, J. G. *J. Amer. chem. Soc.* 1941, **63**, 378 and 385; *J. chem. Phys.* 1941, **9**, 327
- ⁷ SMITH, K. L. and CLEVE, R. V. *Industr. Engng Chem. (Industr.)*, 1958, **50**, 12
- ⁸ STUART, H. A. *Ann. N.Y. Acad. Sci.* 1959, **83**, 23
- ⁹ WILLIAMS, G. To be published
- ¹⁰ ALLEN, G. Private communication
- ¹¹ MASON, P. 'The physical properties of polymers', p 262. *S.C.I. Monograph No. 5*, London, 1959
- ¹² O'REILLY, J. M. Abstracts of IUPAC Conference on Macromolecular Chemistry, Montreal, Canada, 1961
- ¹³ NIELSEN, L. E. *J. Polym. Sci.* 1960, **42**, 357
- ¹⁴ FOX, T. G and FLORY, P. J. *J. appl. Phys.* 1950, **21**, 581; *J. Polym. Sci.* 1954, **14**, 315
- ¹⁵ KOIZUMI, N. and HANAI, T. *J. phys. Chem.* 1956, **60**, 1496
- ¹⁶ WILLBOURN, A. H. *Trans. Faraday Soc.* 1958, **54**, 717

- ¹⁷ STANLEY, E. and LITT, M. *J. Polym. Sci.* 1960, **43**, 453
¹⁸ WEISSERMEL, K. and SCHMIEDER, W. *Makromol. Chem.* 1962, **51**, 39
¹⁹ NEWMAN, S. and COX, W. P. *J. Polym. Sci.* 1960, **46**, 29
²⁰ BOVEY, F. and WANDS, R. C. *J. Polym. Sci.* 1954, **14**, 113

The Melting Point of Polyethylene Terephthalate

G. W. TAYLOR

The thermodynamic relation between heat, entropy of fusion and melting point is used to calculate the melting point of polyethylene terephthalate from the melting points of several series of oligomers. The success of the method depends on the assumption that the heat and entropy of fusion per repeat unit are constant, in a series of oligomers, and it is shown that, in the series of linear diol oligomers higher than dimer, this assumption is approximately justified. This finding is in accord with crystallographic data.

THE problem of the melting points of members of homologous series, and the limiting melting point of the member of infinite chain length, has occupied considerable attention for many years. King and Garner¹, summarizing their work on the melting points of members of homologous series containing methylene as repeat unit, showed experimentally in the even-membered linear aliphatic saturated hydrocarbons, that if the number of methylene units was ten or more, there was a constant increment in each of the heat and entropy of fusion as methylene units were added to the chain. That is to say, the melting point of a high member of the series could be calculated from a relationship of the form

$$T_m = (H_0 + nH_1) / (S_0 + nS_1) \quad (1)$$

where T_m denotes the melting point of the member with n methylene units, H_0 is the heat of fusion of (hypothetical) zeromer, S_0 is the entropy of fusion of zeromer, H_1 is the heat of fusion per methylene unit, S_1 is the entropy of fusion per methylene unit and n is the number of methylene units in the molecule.

H_1 and S_1 were determined from the known melting points and heats of fusion for a number of oligomers.

The melting point, T_∞ , of the member of infinite chain length is readily obtained from expression (1). Thus

$$T_\infty = H_1 / S_1$$

For the hydrocarbon containing an infinite number of methylene units (polymethylene), King and Garner¹ calculated a melting point of about 135°C, very close to the actual melting point of polymethylene, 136.5°C².

Garner and his co-workers showed experimentally that expression (1) could be used to calculate the melting point of a high polymer. In the present work, it is assumed that expression (1) holds for oligomeric series related to polyethylene terephthalate, and it is used to calculate the melting point of the polymer from the melting points of the members of several series of low oligomers.

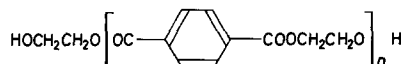
The actual melting point of polyethylene terephthalate is still open to dispute. Let us define the melting point as that temperature at which a perfect crystal is in equilibrium with a liquid phase. It is well known that high polymers are not completely crystalline, and hence the individual crystallites are probably imperfect; but by a process of slow annealing, most of these can be obtained as nearly perfect crystals. The melting point of the nearest perfect crystals so obtained is thus closest to the 'true' melting point as defined above. By several cycles of slow annealing, Hartley³ raised the melting point of polyethylene terephthalate from the 'usual' value of 264°C⁴ to 278°C.

The melting point of polyethylene terephthalate is here calculated from the following series of oligomers: (i) the linear diols, (ii) benzyl ester-ended oligomers, and (iii) phenyl ester-ended oligomers. The values so obtained are compared with the value obtained by Hartley, and possible reasons for the discrepancies among the values are briefly discussed.

I. LINEAR DIOL OLIGOMERS

The melting points of a series of linear diol oligomers have been determined by Zahn and Krzikalla⁵.

Table 1. Melting points of linear diol oligomers



I

| <i>n</i> | <i>M. pt.</i> , °C | <i>M. pt.</i> , °A |
|----------|--------------------|--------------------|
| 1 | 109.5 | 383 |
| 2 | 169 | 442 |
| 3 | 201 | 474 |
| 4 | 218.5 | 492 |

The melting points in Table 1 allow the following equations to be set up:

$$H_0 + H_1 = 383 (S_0 + S_1) \quad (2)$$

$$H_0 + 2H_1 = 442 (S_0 + 2S_1) \quad (3)$$

$$H_0 + 3H_1 = 474 (S_0 + 3S_1) \quad (4)$$

$$H_0 + 4H_1 = 492 (S_0 + 4S_1) \quad (5)$$

We require

$$H_1/S_1 = T_\infty$$

Equations (2) to (5) solved simultaneously give $T_\infty = 571^\circ$ (298°C). Solved in two groups of three, corresponding to extrapolating the melting points of monomer, dimer and trimer, and those of dimer, trimer and tetramer, the equations give the following values of T_∞ :

$$(2) \text{ to } (4), T_\infty = 581^\circ$$

$$(3) \text{ to } (5), T_\infty = 557^\circ$$

These findings are summarized in *Table 2*.

Table 2. Melting point of polyethylene terephthalate predicted from diol oligomers

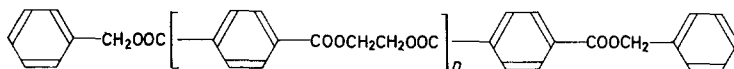
| Oligomers used | Predicted m. pt. ($^{\circ}\text{C}$) |
|-------------------------|---|
| All four | 298 |
| Monomer, dimer, trimer | 308 |
| Dimer, trimer, tetramer | 284 |

It is seen that the series dimer, trimer, tetramer predicts a polymer melting point of 284°C , a value close to Hartley's experimental value of 278°C . The discrepancy between any of the calculated values and the experimental value may be due to any of the following causes: (a) the experimental value is incorrect, (b) the oligomeric melting points are incorrect and (c) the assumptions made in setting up equations (2) to (5) do not hold. The latter two causes are now considered.

II. BENZYL ESTER-ENDED OLIGOMERS

The melting points of the benzyl ester-ended oligomers have been determined by Zahn and Seidel⁶, and are given in *Table 3*.

Table 3. Melting points of benzyl ester-ended oligomers



II

| n | M. pt., $^{\circ}\text{C}$ | M. pt., $^{\circ}\text{A}$ |
|-----|----------------------------|----------------------------|
| 3 | 202 | 475 |
| 4 | 220 | 493 |
| 5 | 235 | 508 |

The melting points in *Table 3* predict a polyethylene terephthalate melting point of 400°C . This deviates widely from Hartley's value of 278°C . The following exercise shows that small errors in the oligomeric melting points can give rise to a large discrepancy between the calculated polymeric melting point and the experimental value.

The twenty seven possible melting points, obtainable by varying each of the oligomeric melting points by $\pm 1^{\circ}$, range between -52°A and infinity. This wide range arises because, as the oligomeric melting points are relatively close together, the variation of $\pm 1^{\circ}$ gives rise to disproportionately large changes in the differences between successive melting points within the oligomeric series; and this is reflected mathematically in the set of three equations from which T_{∞} is derived. Indeed, certain combinations of oligomeric melting points result in a constant increment in melting point per chain segment as the series is ascended, and in this case, the value of T_{∞} is infinity.

The above result shows that in using the melting points of the diol oligomers to calculate T_{∞} , part of the discrepancy between the two calcu-

lated values of T_{∞} (308° and 284°C) and the experimental value (278°C) may well be due to small errors in the oligomeric melting points. However, part is probably due to physical differences between monomer and dimer, and higher oligomers. These differences are now considered.

III. CRYSTAL STRUCTURES OF THE LINEAR DIOL OLIGOMERS

The crystal structures of the linear diol oligomers have been investigated by Zahn and Krzikalla⁵ using X-ray photography. The authors concluded that, while the structures of all the oligomers and of polyethylene terephthalate itself showed similarities, the structures of the monomer and dimer could not be classed as the same as that of polyethylene terephthalate. On the other hand, the principal reflections for trimer and tetramer were much the same as those for polyethylene terephthalate. It is concluded that the crystal structures of oligomers higher than dimer are much like that of the high polymer, whereas those of monomer and dimer show some dissimilarity. It is not surprising, therefore, that the melting points of dimer, trimer and tetramer predict a more 'realistic' value for the melting point of polyethylene terephthalate than do those of monomer, dimer and trimer.

IV. NATURE OF THE LINEAR DIOL ZEROMER

If $n=0$ in the formula for the linear diol oligomers, the formula of zeromer is obtained.

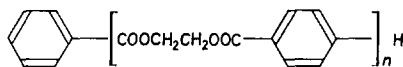


Linear diol zeromer thus appears to be ethylene glycol itself. Though it is tempting, it is probably not profitable, to press the comparison between zeromer and glycol too far. Let it be observed that the predicted melting point is -36°C ; this is close (on the absolute scale) to the actual value (-13°C).

V. THE PHENYL-ENDED OLIGOMERS

Yet a third oligomeric series from which the melting point of polyethylene terephthalate can be calculated is that of the phenyl-ended oligomers. The melting point data are given in *Table 4*.

Table 4. Melting-points of the phenyl-ended oligomers



III

| n | $M. pt., ^{\circ}\text{C}$ | $M. pt., ^{\circ}\text{A}$ |
|-----|----------------------------|----------------------------|
| 0 | 5.5 | 278.7 |
| 1 | 73.5 | 346.7 |
| 2 | 114.5 | 387.7 |

The dimer has been prepared and characterized by Allan, Iengar and Ritchie⁷.

The data in *Table 4* predict the melting point of (phenyl-ended) polyethylene terephthalate to be 279°C. This is remarkably close to the experimental value of 278°C obtained by Hartley³. The coincidence may be due to mathematics—the differences between successive melting points in the oligomeric series are relatively high—but physical reasons may be partly responsible also. However, there is only a superficial resemblance between the crystal structure of benzene and that of polyethylene terephthalate!

CONCLUSIONS

If it is assumed that the heat and entropy of fusion per repeat unit are constant for polyethylene terephthalate diol oligomers corresponding to dimer and higher, then the melting point of polyethylene terephthalate itself can be calculated with a fair degree of accuracy from the melting points of dimer, trimer and tetramer. The series monomer, dimer, trimer gives a less satisfactory value probably because the crystal structure of monomer (and to some extent, dimer) differs from that of the higher oligomers, and polyethylene terephthalate itself.

The author thanks Dr C. W. Bunn and various of his colleagues for valuable discussions. He is particularly indebted to Mr P. L. Goldsmith for mathematical assistance.

*I.C.I. Ltd, Fibres Division,
Hookstone Road,
Harrogate, Yorkshire*

(Received February 1962)

REFERENCES

- ¹ KING, A. M. and GARNER, W. E. *J. chem. Soc.* **1936**, 1368
- ² MANDELKERN, L., HELLMANN, M., BROWN, D. W., ROBERTS, D. E. and QUINN, F. A. *J. Amer. chem. Soc.* **1953**, **75**, 4093
- ³ HARTLEY, F. D. Private communication
- ⁴ HILL, R. and WALKER, E. E. *J. Polym. Sci.* **1948**, **3**, 609
- ⁵ ZAHN, H. and KRZIKALLA, R. *Makromol. Chem.* **1957**, **23**, 31
- ⁶ ZAHN, H. and SEIDEL, B. *Makromol. Chem.* **1959**, **29**, 70
- ⁷ ALLAN, R. J. P., IENGAR, H. V. R. and RITCHIE, P. D. *J. chem. Soc.* **1957**, 2107

X-ray Measurements of the Elastic Modulus of Cellulose Crystals

J. MANN* and L. ROLDAN-GONZALEZ†

Measurements have been made of the increase in length of molecular chains in crystalline regions which occurs when Fortisan H fibres are stressed. Results at different relative humidities suggest that the behaviour of the fibres towards stress can be approximately represented by a series model in which crystalline and amorphous regions alternate along the length of the fibre. The apparent moduli of crystalline material calculated on the basis of such a model lie in the range 7 to 9×10^{11} dyne/cm². This is larger than the theoretical modulus calculated from force constant data but smaller than elastic moduli which have been reported for cellulose fibres.

CALCULATIONS of the elastic moduli of polymer crystals have been made by Treloar¹ by treating an isolated molecule and considering the changes in bond lengths and in bond angles which would be caused by the application of stress. The changes in these quantities were calculated from the appropriate force constants derived from spectroscopic data.

The modulus calculated for the cellulose crystal was 5.65×10^{11} dyne/cm² which is lower than moduli which have been reported^{2,3} for cellulose fibres. Treloar tentatively assigned this discrepancy to the neglect of secondary forces in the theoretical treatment.

Measurements by an X-ray diffraction method of the deformation of chains in crystalline regions of Terylene have been made by Dulmage and Contois⁴. The crystal modulus which they derived from their results using the assumption that the average stress on crystalline regions was equal to the average stress on the fibre is in fair agreement with the value calculated by Treloar¹.

In the present paper results of similar measurements on Fortisan H fibres are given. The position of the 040 reflection has been measured with and without load on the fibres. The crystallographic 040 planes are perpendicular to the chain axes of the molecules and the 040 spacing gives a measure of the length of the repeating unit of the chain.

EXPERIMENTAL

X-ray measurements

A conventional fibre-type X-ray camera with a specially designed sample holder was used. The collimator was of the slit type with dimensions 0.25 mm × 5 mm and length 100 mm. Unfiltered Cu K radiation was used.

A bundle of parallel fibres was fixed horizontally in the sample holder, the fibre axes being set at the Bragg angle for the 040 reflection with respect to the incident beam. The ends of the fibre bundle were secured in screw clips which contained rubber sheet to prevent damage to the fibres. One

*Present address: Carrington Research Laboratory, Shell Chemical Co. Ltd, Urmston, Manchester, England.

†Present address: Central Research Laboratory, Allied Chemical Corporation, Morristown, New Jersey.

of these clips was fixed rigidly whereas the other clip could slide freely in the fibre direction in a groove cut into a metal support. The latter clip was fixed to a metal hook from which a length of cord passed over a pulley to a hanging weight located beneath the camera platform. For measurements on the unstrained fibre a small weight was placed on the cord to ensure that the sample was taut.

Photographic plates (Ilford Special Contrast) were used to record the reflections in order to avoid the changes in dimension which occur with changes in relative humidity with the more usual X-ray film.

The 040 reflections from stressed and unstressed fibres were recorded side by side on the same photographic plate, a metal screen being used to cover one half of the plate. As a check on possible changes in specimen-film distance aluminium powder was distributed on the surfaces of the fibres in the bundle and all measurements were made relative to the 111 aluminium reflection using a recording microdensitometer.

The X-ray camera and weights were placed in a polythene bag to allow the relative humidity of the atmosphere around the fibres to be controlled. This was achieved by placing trays of the appropriate agent inside the bag. Phosphorus pentoxide was used for measurements on dry fibres, a saturated solution of sodium nitrite for measurements at ~64 per cent r.h. and a saturated solution of potassium nitrate for measurements at ~93 per cent r.h. The temperature was constant to within $\pm 2^\circ\text{C}$.

Samples

The Fortisan H was in the form of an 1 100 denier continuous filament yarn which contained a small amount of twist (1.06 turn/cm). No purification was carried out.

Measurement of yarn cross sections

The cross section of the Fortisan yarn was determined by taking a 50 cm length of yarn adjacent to the length used in the X-ray measurements. This was weighed in equilibrium with an atmosphere of 65 per cent r.h. and the cross section determined from the density value given by Hermans⁵. The cross section of the dry yarn was obtained using the water-sorption values of Jeffries⁶ and the density data of Hermans⁵. The cross section of the yarn at 93 per cent r.h. was obtained using the water-sorption values of Jeffries and the swelling curve for a highly oriented regenerated cellulose given by Hermans⁵.

Results

The percentage extensions of cellulose chains under different conditions are shown in column 2 of *Table 1*. These extensions were calculated from the equation

$$\% \text{Ext.} = 100 \times \cot \theta \times \cos^2 2\theta \times \Delta a / 2r$$

where Δa is the measured shift of the 040 reflection on the photographic plate, θ is the Bragg angle for the 040 reflection and r is the specimen-film

distance. The extensions recorded were completely recoverable on removing the load and were found to be reproducible between successive loading cycles.

The errors quoted in *Table 1* for the measured extensions are about ten per cent and represent the experimental error in measuring Δa . The main reason for these rather large errors lies in the width of the X-ray reflections relative to the small displacement being measured, which were of the order of 0.5 mm.

DISCUSSION

In attempting to calculate moduli from the observed extensions of chains in crystalline regions it is necessary to know the stress supported by these chains and hence the way in which the total stress in the fibre is distributed between crystalline and amorphous material. Two limiting models can be postulated to represent the behaviour of fibres towards stress and the real behaviour of a given fibre should lie somewhere between the two extremes.

The first model is a series model in which crystalline and amorphous regions alternate along the length of the fibre. In this model the stresses on crystalline and amorphous regions would be the same and equal to the total stress on the fibre. The stress on crystalline regions would be independent of the relative moduli of crystalline and amorphous material.

The second model is a parallel model in which crystalline and amorphous material extend the full length of the fibre and are arranged in parallel with one another. In this model the stress falling on crystalline regions would depend on the relative moduli of crystalline and amorphous material and would be larger, the larger the ratio of the modulus of crystalline material to the modulus of amorphous material. It would only equal the stress on the fibre when the moduli of crystalline and amorphous material were equal.

The effect of water on the fibres provides a possible method of testing whether their behaviour towards stress approximates to either of the limiting models. It is known that the absorption of water reduces the modulus of Fortisan H and this is presumably due to the lowering of the modulus of amorphous material produced by the swelling action of the water. With the series model such a lowering of the modulus of amorphous material would cause no change in the stress supported by crystalline regions and hence no change in the percentage extension of chains in crystalline regions. With the parallel model, however, absorption of water would lead to an increase in the stress falling on crystalline regions and hence to an increase in the percentage extension of chains in crystalline regions.

The data in the second column of *Table 1* show the percentage extensions of chains in crystalline regions for the same bundle of fibres under the same load at 0 per cent and 93 per cent r.h. It can be seen that the extension does not increase when water is absorbed and it may be concluded that Fortisan H fibres do not behave in the way expected for a parallel model. Although there appears to be a *decrease* in extension for a given stress on the fibre with increasing relative humidity, the difference between the results at 0 per cent and 93 per cent r.h. is not much greater than the

experimental error, and it may be concluded that the series model provides a reasonable approximation to the behaviour of Fortisan H fibres.

Table 1

| % r.h. | % Ext. Δd | Fibre cross section at r.h. stated $\text{cm}^2 \times 10^{-4}$ | Stress on fibres dyne/cm^2 $\times 10^9$ | Modulus (Assump- tion 1) dyne/cm^2 $\times 10^{11}$ | Cross section of dry fibre $\text{cm}^2 \times 10^{-4}$ | Stress on dry fibre dyne/cm^2 $\times 10^9$ | Modulus (Assump- tion 2) dyne/cm^2 $\times 10^{11}$ |
|-----------|----------------------|--|---|--|---|--|--|
| 0 | 0.77 | 7.40 | 5.46 | 7.1 ± 0.7 | 7.40 | 5.46 | 7.1 ± 0.7 |
| 64 | 0.67 | 8.14 | 4.86 | 7.2 ± 0.7 | 7.40 | 5.35 | 8.0 ± 0.7 |
| 93 | 0.61 | 8.90 | 4.54 | 7.4 ± 0.7 | 7.40 | 5.46 | 8.9 ± 0.7 |

Two methods have been used to calculate the apparent moduli of crystalline regions from the measured extensions on the basis of the series model. In the first it is assumed that the average stress on crystalline regions is equal to the stress on the fibre; the resulting apparent moduli are independent of relative humidity as shown in the fifth column of *Table 1*. This assumption is the same as that used by Dulmage and Contois⁴ in their work on Terylene.

With cellulose, however, absorption of water leads to a significant increase in cross-sectional area of the fibres and hence for a given load to a lower stress on the fibres and a lower assumed stress on crystalline material. It is difficult to see how the stress on crystalline material can be reduced when water is absorbed if we accept the argument that this results in a decreased modulus of amorphous material. For this reason the moduli shown in the last column of *Table 1* have been calculated using a different assumption. This is that the stress on crystalline regions is equal to the stress on the dry fibre, i.e. the cross-sectional area used in the calculations at all relative humidities is that of the dry fibre. In many ways this assumption seems more reasonable, since the important quantity determining stress is presumably the total number of polymer chains available to bear stress and not the cross-sectional area of the fibres. The apparent moduli calculated on this assumption show a variation with relative humidity, though the difference between the value at 0 per cent and 93 per cent r.h. is not much greater than the experimental error.

Despite the experimental error in the measurements and the different assumptions which can be made in calculating apparent moduli on the basis of a series model, it can be stated that the apparent modulus of crystalline regions of Fortisan H fibres lies in the range 7 to 9×10^{11} dyne/cm². This is greater than the value of 5.65×10^{11} dyne/cm² calculated by Treloar¹ and supports the suggestion which he made that the calculated modulus is likely to be low because of the neglect of secondary forces between chains.

The apparent modulus is similar to the moduli for unstressed flax and hemp at 65 per cent r.h., reported by De Vries², i.e. 7.4 and 8.3×10^{11} dyne/cm² respectively, but lower than the values he found for strained

fibres of these materials (9.3 and 10.3×10^{11} dyne/cm²) and lower than the value reported by Meyer and Lotmar³ for bone dry flax, 11×10^{11} dyne/cm².

It is difficult to see how the real modulus of crystalline cellulose can be lower than the modulus of any cellulose fibre and it would seem desirable therefore that further work on fibre moduli and on apparent crystal moduli of cellulose should be carried out.

The authors would like to thank Dr L. R. G. Treloar for suggesting the problem and for helpful advice and discussions.

*British Rayon Research Association,
Heald Green Laboratories,
Manchester 22*

(Received September 1961)

REFERENCES

- ¹ TRELOAR, L. R. G. *Polymer, Lond.* 1960, **1**, 95, 279, 290
- ² DE VRIES, H. 'On the elastic and optical properties of cellulose fibres'. *Thesis*, Delft, 1953
- ³ MEYER, K. H. and LOTMAR, W. *Helv. chim. Acta*, 1937, **20**, 232
- ⁴ DULMAGE, W. J. and CONTOIS, L. E. *J. Polym. Sci.* 1958, **28**, 275
- ⁵ HERMANS, P. H. *Contributions to the Physics of Cellulose Fibres*. Elsevier: Amsterdam and New York, 1946
- ⁶ JEFFRIES, R. J. *Text. Inst.* 1960, **51**, T339

*The Gelation of Aqueous Solutions of Polymethacrylic Acid**

J. ELIASSAF† and A. SILBERBERG

The dependence of rigidity and viscosity on concentration and temperature of aqueous solutions of polymethacrylic acid was measured in a specially designed viscoelastometer. The solutions show no rigidity up to a certain critical concentration range (depending on the degree of polymerization) of about one per cent in which the rigidity rises sharply with concentration and so does the viscosity. This is considered to be due to a gel network formed by intermolecular hydrogen bonding. While at low polymer concentrations intramolecular bonding prevails, the likelihood of intermolecular bonding increases with concentration until (in the critical concentration range) a gel network is formed. Above 47°C the solution separates into two layers, a concentrated gel and a dilute sol. The critical concentration for phase separation coincides with that for gelation. This is attributed to a contribution to the chemical potential of the solute due to changes in rigidity with concentration.

MUCH study has been devoted to the gelation of biocolloidal systems such as gelatin¹. The complicated structure of biocolloids does not enable us to determine unequivocally the forces that are operative during gelation, and a quantitative approach is often hampered by the fact that gelation is not reversible. The study of synthetic water-soluble polymers, in particular of polyelectrolytes, may enable us to get a more clear-cut relationship between viscoelastic properties and chemical constitution.

We have reported previously² that concentrated solutions of polymethacrylic acid (PMA) in water form thermoreversible gels. The detailed study of the viscoelastic properties as well as the related phase separation (see below) is the object of the present investigation.

The viscoelastic properties have been studied by viscometry in an Ostwald viscometer³. With that method no meaningful results can be obtained in solutions that display negative thixotropy². However, it is just in these solutions that gelation occurs. In order to study the viscoelastic properties without subjecting the system to large shear forces which might change the magnitude of these properties we had to devise a special viscoelastometer to enable us to investigate the solutions at an extremely low rate of shear. We have only investigated the properties of the solutions 'at rest' and have not studied the phenomenon of negative thixotropy. The present study is confined to PMA solutions at their natural pH with no other material added.

In discussing our results we shall use the knowledge gained from previous hydrodynamic and thermodynamic studies of PMA in dilute solutions⁴.

*This paper represents part of a thesis submitted by J. ELIASSAF to the Hebrew University in partial fulfillment of the requirements for the Ph.D. degree. Parts of it were presented by A. SILBERBERG at the Symposium on Macromolecular Chemistry, Prague, September 1957.

†Present address: The Negev Institute for Arid Zone Research, P.O.B. 79, Beer Sheva, Israel.

EXPERIMENTAL

The preparation and characterization of the PMA fractions has already been described⁴. Besides the sample of DP 3 500, used for dilute solution study, we have investigated samples of DP 2 250, 6 900 and 10 300.

When designing the viscoelastometer we had to bear in mind the following points: (a) the instrument should be sensitive enough to determine small moduli of rigidity (about 10 dyne/cm); (b) it should determine viscosity as well as rigidity; (c) the measurements should be carried out at the lowest rates of shear possible—to avoid the effect of negative thixotropy and (d) emptying of the viscoelastometer due to the Weissenberg effect should be avoided. These requirements were met in a special viscoelastometer built by Silberberg and Frei which has already in part been described elsewhere⁵. It consists of two concentric cylinders made of stainless steel. The outer one is stationary while the inner is suspended from a torsion wire and is caused to execute an oscillatory movement by means of an alternating magnetic field of low frequency (0.2 to 5.0 c/s). The movement of the inner cylinder is converted into an electrical signal by an optical lever. Lissajous figures are produced on an oscilloscope, the *X* and *Y* directions being respectively the axis of torque and the inner cylinder displacement. At resonance the axes of the figure are parallel to the *X* and *Y* directions corresponding to a phase difference $\pi/2$. Assuming that the behaviour of the system at the frequency under consideration is adequately described by a single modulus of rigidity *G* (which comprises the rigidity of the torsion wire and that of the PMA solution) and a single coefficient of viscosity η , one finds

$$G = A\omega_0^2; \quad \eta = A \tan \delta (\omega_0^2 - \omega^2)/\omega$$

$$A = (I\Delta r)/(2r^2l_{\text{eff}})$$

where ω_0 is the resonance frequency, *I* is the moment of inertia of the inner cylinder assembly, *r* is the radius of the inner cylinder, Δr is the gap between the cylinders, l_{eff} is the effective length of the cylinder surface according to a design by Mooney and Ewart⁶ and δ is the phase angle between the two oscillations when the angular frequency of the oscillator is ω . When it is desired to measure viscosity, a capacitance (*C*)-resistance (*R*) coupling circuit is introduced between the oscillator and the *X* deflection plate of the oscilloscope. If the *RC* product is so adjusted that the axes of the Lissajous figure are again parallel to the *X* and *Y* directions

$$\eta = ARC (\omega_0^2 - \omega^2)$$

Since $r=0.9$ cm, $\Delta r=0.1$ cm, and the maximal amplitude of vibrations was 0.009 radian, the rate of shear of the solution in the gap was between 0.005 and 0.14 sec⁻¹, according to the frequency used. By means of circulating thermostat fluid through the outer cylinder a desired temperature could be maintained within $\pm 0.5^\circ\text{C}$.

Although *A* can be computed theoretically from the geometry of the instrument, we considered a calibration by means of paraffin oils of known viscosity to be more reliable.

THE GELATION OF AQUEOUS SOLUTIONS OF POLYMETHACRYLIC ACID

The PMA solution to be measured was carefully poured into the instrument and allowed to relax overnight from the effect of negative thixotropy. It was then measured, first at 30°, then at 20°, 10° and finally at 40° and 47.5°C. (During preliminary investigation we found that at 47.5°C the rigidity decreases with time while at 30°C it is constant for at least 24 hours after relaxation.) Two identical solutions were measured by this procedure and the values obtained were identical within experimental error.

RESULTS

Rigidity

We found that up to a certain concentration (depending on the degree of polymerization) the solution had no detectable rigidity, but above it the rigidity increased sharply over a concentration range of about one per cent. This range will be referred to henceforth as the critical concentration range (CCR). We could not extend the measurements to higher concentrations because these involved rigid gels which could not be poured into the apparatus. Within the CCR the rigidity increases with temperature between 30° and 47.5°C. *Figure 1* shows the concentration dependence of the rigidity of DP 3 500 at 30° and 47.5°C. (The data for other temperatures have been omitted to avoid overcrowding.) *Figure 2* shows the temperature dependence of the rigidity of an 8.15 per cent solution (DP 3 500). The simplest expression for the concentration dependence of the modulus of rigidity in the CCR (at given degree of polymerization and temperature) was found to be

$$\log G = ac + b$$

where a and b are empirical constants and c is the concentration of the

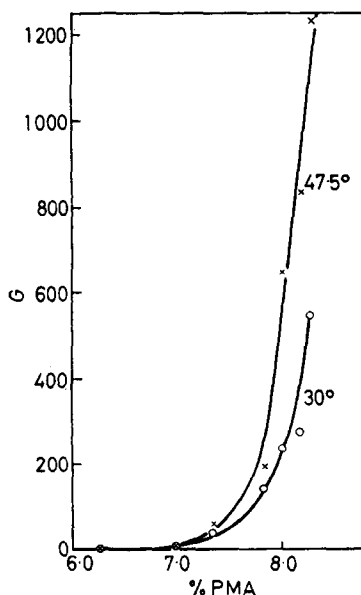


Figure 1—Concentration dependence of modulus of rigidity (dyne/cm) of PMA solutions (DP 3 500) at 30° and 47.5°C

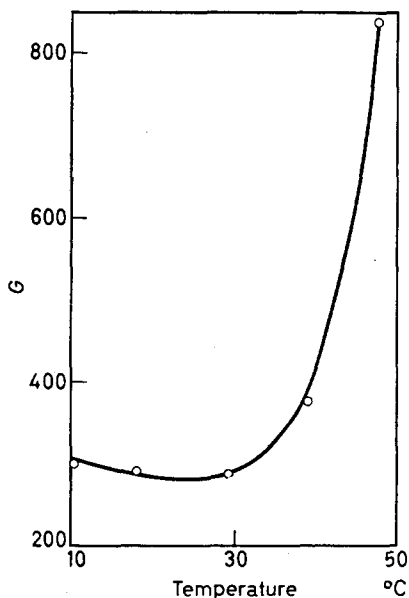
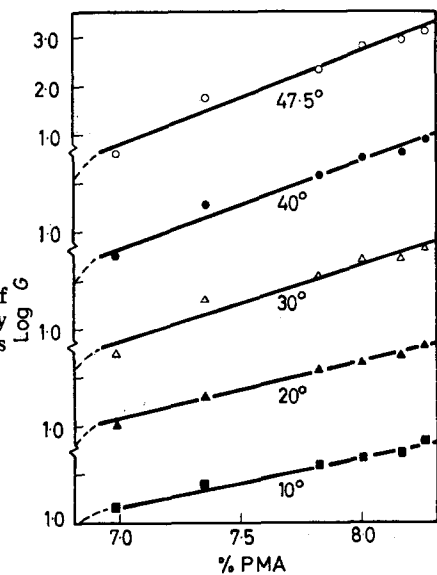


Figure 2—Temperature dependence of modulus of rigidity (dyne/cm) of 8.15 per cent PMA solution (DP 3 500)

Figure 3—Concentration dependence of the logarithm of the modulus of rigidity of PMA solutions (DP 3 500) at various temperatures



polymer as a weight percentage. Figure 3 shows the plot of $\log G$ against c at different temperatures for DP 3 500. (The dashes below seven per cent indicate that the line must be even steeper in that region as at 6.25 per cent G is zero.) All the values for a and b of the four samples at different temperatures are given in Table 1. It should be noticed that the more rigid the solution measured the higher is the resonance frequency at which the modulus of rigidity was determined. In the formula given above

THE GELATION OF AQUEOUS SOLUTIONS OF POLYMETHACRYLIC ACID

Table 1. Values of a and b in equation, $\log G=ac+b$ at different temperatures and for different degrees of polymerization

| <i>Temp. °C</i> | 10 | 20 | 30 | 40 | 47.5 |
|-----------------|------|-----------|------|------|------|
| | | DP 2 250 | | | |
| <i>a</i> | 1.16 | 1.44 | 1.65 | 1.88 | 1.72 |
| <i>b</i> | 8.2 | 10.4 | 12.8 | 14.9 | 13.2 |
| | | DP 3 500 | | | |
| <i>a</i> | 1.03 | 1.24 | 1.59 | 1.79 | 1.87 |
| <i>b</i> | 5.8 | 7.6 | 10.3 | 11.8 | 12.2 |
| | | DP 6 900 | | | |
| <i>a</i> | — | 2.68 | 3.07 | 3.39 | 3.36 |
| <i>b</i> | — | 16.8 | 19.5 | 21.7 | 21.4 |
| | | DP 10 300 | | | |
| <i>a</i> | 2.95 | 2.90 | 2.87 | 2.80 | 2.88 |
| <i>b</i> | 16.1 | 15.9 | 15.5 | 15.0 | 15.4 |

we have assumed that G does not vary with frequency (between 0.2 and 5.0 c/s). This assumption could not be tested in our viscoelastometer.

We could determine the concentration dependence of the rigidity only in the CCR as we could not pour more rigid solutions into the instrument. However, we know from inspection that solutions of higher concentration (say 10 to 20 per cent for DP 3 500) are soft gels (like gelatin) which do not have the high rigidity predicted by our formula. At higher concentrations the increase of rigidity must be more moderate than in the CCR. As G is zero below the CCR it seems to be established that dG/dc (the increase of rigidity with concentration) is largest in the CCR. The importance of this fact will be pointed out in the discussion.

Viscosity

Below the CCR the viscosity is Newtonian within the range of shear rates measured and *decreases* with increase of temperature. In the CCR (i) there is a tremendous increase in viscosity, (ii) the viscosity *increases* with temperature and (iii) the viscosity is non-Newtonian even at the low rates of shear at which our measurements were made. This is summarized for DP 3 500 in *Figure 4* in which we have plotted $\log \eta$ (poise) against c . The great changes in viscosity that take place in the CCR are also brought out in *Table 2*. *Figure 5* shows the temperature dependence of the viscosity of the sample whose rigidity dependence is given in *Figure 3*. Since in the CCR the viscosity is non-Newtonian no exact meaning can be attached

Table 2. Temperature dependence of (a) the intrinsic viscosity in 0.02N hydrochloric acid⁴; (b) the reduced specific viscosity of 6.25 per cent (below the CCR) and (c) the reduced specific viscosity of 8.00 per cent (in the CCR) of PMA DP 3 500. (All values in cm³/g)

| <i>Temp. °C</i> | (a) | (b) | (c) |
|-----------------|-----|-----|--------|
| 10 | 50 | 735 | 7 440 |
| 30 | 36 | 455 | 14 700 |
| 47.5 | 25 | 259 | 38 800 |

to the actual values of the viscosity measured. However, an increase in viscosity happened to coincide with an increase in rigidity and therefore with an increase of frequency ω_0 at which it was measured. Hence our conclusions are true whatever the exact dependence of viscosity on rate of shear may be.

It should be noted here that by means of viscometry in an Ostwald viscometer³ (i.e. at higher rates of shear) it was also found that PMA solutions are Newtonian up to a certain concentration and that the temperature dependence of viscosity is inverted when the solution becomes non-Newtonian.

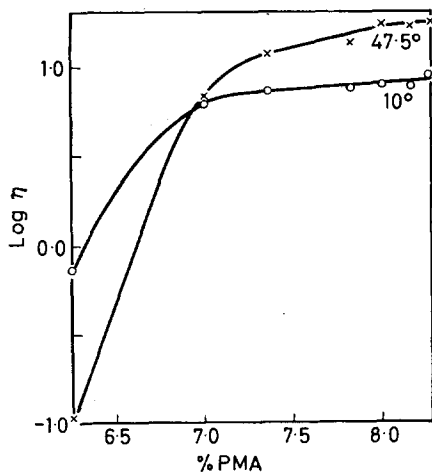


Figure 4—Concentration dependence of the logarithm of the coefficient of viscosity (poise) of PMA solutions (DP 3500) at 10° and 47.5°C. (The results at intermediate temperatures have been omitted for the sake of clarity)

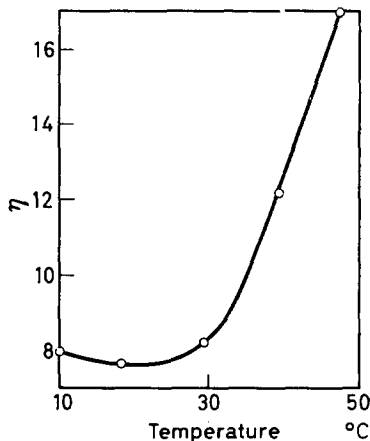
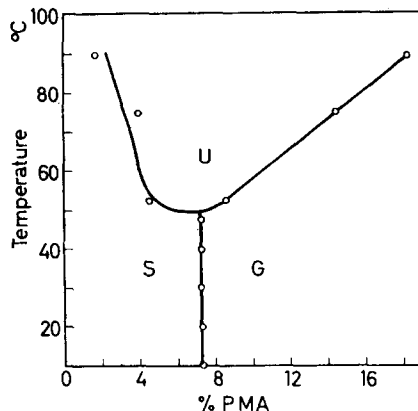


Figure 5—Temperature dependence of coefficient of viscosity (poise) of 8.15 per cent PMA solution (DP 3500)

Phase separation

In addition to viscoelastic properties we have investigated the phase diagram of PMA solutions. When a concentrated solution of PMA is warmed it coagulates like albumin and after sufficient time phase separation occurs—a dilute sol is formed above a concentrated gel. The phase separation is completely reversible. In order to obtain the full phase diagram, PMA solutions of known concentration were sealed into ampoules and kept in an oven at the desired temperature ($\pm 1^\circ$). The two layers were separated by decantation and the concentration of each was determined by titration of the polyacid. In order to obtain reproducible results the solutions had to be kept in the oven for three weeks. The phase diagram obtained for DP 6900 is given in Figure 6. It displays the asymmetry typical of polymer solutions⁷. In the diagram we have also marked the concentrations at which the rigidity is 500 dyne/cm. (The choice is arbitrary—any other rigidity means a slight shift of that line.) We see that within

Figure 6—Phase diagram of PMA solutions (DP 6 900). In region S the solution is a sol, in region G it is a gel and in region U a gel and a sol coexist



experimental error the critical concentration for phase separation is identical with the critical concentration range of gelation. (The phase diagram of DP 3 500 was also studied and found to have the same features.) The phase diagram therefore consists of three regions: a region S in which the solution is a sol, a region G in which it is a gel and an unstable region U in which the solution separates into two layers. (The phase separation of PMA solutions has been studied by means of nephelometry³, but only part of the diagram was obtained by that method.)

DISCUSSION

Since PMA is a weak acid it is only slightly ionized in concentrated solutions. (The pH of the solutions in the CCR was found to be about 3.6.) In discussing the gelation phenomena we shall treat the PMA molecule as essentially undissociated and neglect electrostatic effects. The viscometric and thermodynamic study of undissociated PMA⁴ has indicated that the molecule is intramolecularly bonded in dilute solutions. Now intramolecular bonding in dilute solutions should correspond to agglomeration (e.g. gelation) in concentrated solutions⁸. Variations in intrinsic viscosity should correspond to variations in agglomeration.

In discussing our results we shall accept the postulate that gel formation is due to a three-dimensional network of the solute¹. In thermoreversible systems like the one investigated here the polymer molecules must be held together by secondary forces only. Hydrogen bridges between carboxyl groups are the most likely bonds so that we shall assume that these are responsible for forming the gel network. We shall also accept the postulate that gel elasticity is rubberlike elasticity.

A probable explanation of the viscoelastic properties as well as phase separation is the following. In dilute solutions (well below the CCR) each PMA molecule exists in its isolated state and bonding tendency is satisfied intramolecularly. With increasing concentration the likelihood of two carboxyl groups of different molecules meeting and forming intermolecular bonds becomes greater (while the possibility of intramolecular bonding remains unchanged). The CCR is the range in which, for purely geometrical

reasons, the likelihood of intermolecular bonding has become so great that a coherent network necessary for gelation is formed.

This model enables us to find a connection between the CCR of PMA of a given degree of polymerization and its intrinsic viscosity. As a rough approximation let the CCR be that in which the space of the solution is filled with hydrodynamic equivalent spheres⁹ each of volume v , so that

$$v = (4\pi/3) (r^2/2)^{3/2}$$

where $(r^2)^{1/2}$ is the root-mean-square (r.m.s.) end-to-end distance of the molecule. According to our assumption we have at the critical concentration $1/v$ molecules the weight of each being M/N_A (M being the molecular weight of the PMA fraction and N_A Avogadro's number). Using the connection between $(r^2)^{1/2}$ and the intrinsic viscosity $[\eta]$ ⁹ we find the critical concentration c to be

$$c = 1/v = 6\Phi/(N_A\pi[\eta])$$

where Φ is Flory's constant. In *Figure 7* we have plotted the calculated connection between the intrinsic viscosity and the CCR as well as c' the concentrations (of the four degrees of polymerization investigated) at which the solution was found to have a modulus of rigidity of 500 dyne/cm. We see that whereas the line $c'/[\eta]$ is straight, as required by the theory, it does not pass through the origin. Moreover, c' is about four times larger than c , indicating that the hydrodynamic equivalent spheres must interpenetrate to a marked degree to permit the intermolecular bonding necessary for gelation. The degree of interpenetration varies with the degree of polymerization.

It follows from the kinetic theory of rubber elasticity that a solution having a modulus of rigidity of 500 dyne/cm at 30°C contains 1.97×10^{-8} moles of bonds per cm^3 . In *Table 3* we have computed from c' : (a) the fraction of carboxyl groups (two for each bond) that are linked to the gel network and (b) the fraction of polymer chains linked to the network. We

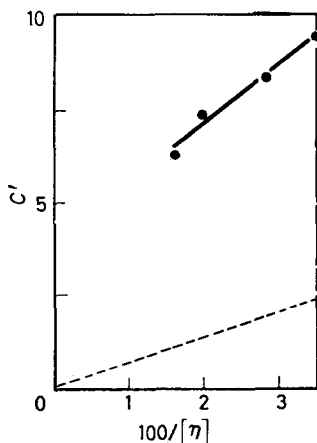


Figure 7—Calculated and experimental dependence of the CCR on the intrinsic viscosity of the PMA fraction

THE GELATION OF AQUEOUS SOLUTIONS OF POLYMETHACRYLIC ACID

Table 3. Concentration c' of the PMA solution whose rigidity at 30°C is 500 dyne/cm; (a) the fraction of 'efficient' carboxyl groups, and (b) the fraction of 'efficient' polymer chains in that solution

| <i>DP</i> | c' | (a) | (b) |
|-----------|------|----------------------|-------|
| 2 250 | 9.35 | 3.6×10^{-5} | 0.041 |
| 3 500 | 8.26 | 4.1×10^{-5} | 0.070 |
| 6 900 | 7.30 | 4.6×10^{-5} | 0.160 |
| 10 300 | 6.34 | 5.3×10^{-5} | 0.225 |

see that in the CCR only a minute fraction of the carboxyl groups takes part in the gel network while the majority of the carboxyl groups must satisfy its bonding tendency either by intermolecular bonding or by forming 'wasted' intermolecular bonds. We also see that the fraction of efficient bonds increases with molecular weight and so does the fraction of the efficient polymer chains. This is quite reasonable since *ceteris paribus* the likelihood of two efficient bonds occurring on one polymer chain is increased with the number of carboxyl groups present on that chain.

The kinetic theory of rubber elasticity predicts an increase in gel rigidity with temperature. However, the increase found in PMA gels is about ten times that accounted for by the kinetic theory. To be consistent we have to infer that the number of effective network bonds increases with temperature.

The decrease of intrinsic viscosity of PMA with temperature⁴ indicates increased carboxyl-carboxyl bonding (at the expense of carboxyl-water bonding) which in dilute solutions must be satisfied intramolecularly, while in concentrated solutions it may cause enhanced agglomeration with temperature⁸. In the CCR, part of the intermolecular bonds formed by increase in temperature will be 'effective' in contributing to the network rigidity.

It was pointed out by Lodge¹⁰ that the viscosity of a polymer solution may be due not only to hydrodynamic resistance but also to a temporary network structure. In PMA solutions at concentrations below the CCR the hydrodynamic resistance is apparently the main cause of viscosity. The enhanced coiling is the reason for diminished viscosity with increasing temperature. With the formation of the gel network another energy dissipation factor becomes dominant. If a network bond is broken while the gel is under deformation, the deformation energy cannot be recovered but is dissipated. We assume that the lifetime of a carboxyl-carboxyl bond is of the order of magnitude of the time of deformation. This explains the non-Newtonian behaviour even at the low rates of shear used by us. The probability of a bond breakage occurring also increases with the total number of network bonds and therefore with concentration and temperature. The increase of viscosity with concentration within the CCR and the close similarity of temperature dependence of rigidity and viscosity is readily understood.

The fact that PMA solutions separate into two layers with rising temperature is in agreement with the negative entropy of dilution and negative heat

of dilution derived from light scattering data⁴. We still have to explain the coincidence of the critical concentration for phase separation with that for gelation. To do this we wish to point out that in a gel the free energy of dilution consists of two parts, a contribution due to changes in elasticity of the network, and the ordinary term due to mixing¹¹. In PMA solutions below the CCR the chemical potential of the polymer is given by the well known expression

$$\mu_u - \mu_u^0 = RT (v_u/v_1)/(\ln v_2)/x - (1 - 1/x)(1 - v_2) + \chi_1(1 - v_2)^2$$

But in the CCR we have to add another term to account for the changes in elastic free energy with concentration. We do not have at present either the theoretical or the experimental knowledge for a quantitative formulation of that term in PMA solutions where dilution involves breaking of bonds. The kinetic theory of rubber elasticity states that the elastic free energy is proportional to the number of network bonds and hence to the modulus of rigidity¹². It is therefore most likely that the contribution of elasticity to the chemical potential contains the expression dG/dc (the increase in rigidity with concentration). We have already given our reasons for assuming that dG/dc is largest in the CCR from which it follows that the elastic contribution to the chemical potential should be a maximum in the CCR. The osmotic term and the elastic term of the chemical potential combine in such a way that at sufficiently high temperatures the chemical potential curve becomes binodal in the CCR and phase separation occurs.

*Weizmann Institute of Science,
Rehovot, Israel*

(Received February 1962)

REFERENCES

- ¹ FERRY, J. D. *Advances in Protein Chemistry*, Vol. IV, pp 1-88. Academic Press: New York, 1948
- ² ELIASSAF, J., SILBERBERG, A. and KATCHALSKY, A. *Nature, Lond.* 1955, **176**, 1119
- ³ LIPATOV, YU. S., ZUBOV, P. I. and ANDRYUSHCHENKO, E. A. *Colloid J., Moscow*, 1959, **21**, 577
- ⁴ SILBERBERG, A., ELIASSAF, J. and KATCHALSKY, A. *J. Polym. Sci.* 1957, **23**, 259
- ⁵ SILBERBERG, A. and FREI, E. *Bull. Res. Council. Israel*, 1955, **5**, 83
- ⁶ MOONEY, M. and EWART, R. H. *Physics*, 1934, **5**, 350
- ⁷ SHULTZ, A. R. and FLORY, P. J. *J. Amer. chem. Soc.* 1952, **74**, 4760
- ⁸ ALFREY, T., BARTOVICS, A. and MARK, H. J. *J. Amer. chem. Soc.* 1942, **64**, 1557
- ⁹ FLORY, P. J. *Principles of Polymer Chemistry*, pp 605-611. Cornell University Press: New York, 1953
- ¹⁰ LODGE, A. S. *Trans. Faraday Soc.* 1956, **52**, 120
- ¹¹ FLORY, P. J. *Principles of Polymer Chemistry*, p 577. Cornell University Press: New York, 1953
- ¹² FLORY, P. J. *Principles of Polymer Chemistry*, pp 469-470. Cornell University Press: New York, 1953

Dilute Solution Properties of Tactic Polymethyl Methacrylates I—Intrinsic Viscosities of Isotactic Fractions*

SONJA KRAUSE and ELIZABETH COHN-GINSBERG

Intrinsic viscosities in acetone and in benzene solution were obtained on fractions of isotactic polymethyl methacrylate having $\overline{M}_w/\overline{M}_n \approx 1.4$. The intrinsic viscosities in both solvents were higher than those of fractions of conventional free-radically initiated polymethyl methacrylate having comparable molecular weight. These data indicate that the isotactic molecules are more extended in solution than molecules of conventional polymethyl methacrylate. This conclusion is confirmed by data on the r.m.s. end-to-end distance of two of the fractions in acetone as determined from light scattering measurements.

THERE have not been many published investigations of the dilute solution properties of stereospecifically polymerized polymer fractions. In those cases which have been investigated, isotactic polypropylene¹⁻⁴, isotactic polystyrene⁵⁻⁹, and isotactic and syndiotactic polymethyl methacrylate¹⁰, only very small differences were found between the dilute solution properties of the tactic and conventionally polymerized polymer fractions. Specifically, no differences at all were found in the intrinsic viscosity/molecular weight relationships in thermodynamically good solvents^{1, 2, 5, 7-10}. Small changes, however, have been found in the second virial coefficient of isotactic polystyrene in toluene solution^{7, 8} at 30°, and an 8° difference was found between the theta temperature of isotactic and that of conventional polypropylene in diphenyl ether³. Although Krigbaum *et al.*⁹ found that the molecular dimensions of isotactic polystyrene were the same as those of atactic polystyrene in *p*-chlorotoluene solution, they used other data to calculate that in a theta solvent these dimensions would be about 30 per cent greater for the isotactic polymer.

The work of Tsvetkov and co-workers¹⁰ on isotactic and syndiotactic polymethyl methacrylate fractions was done in benzene, a very good solvent for the polymer. Although they reported no differences between the intrinsic viscosity/molecular weight relationship of the two polymer configurations, their data do indicate small but significant differences. On a log/log plot of intrinsic viscosity versus molecular weight in their paper, all the points for the isotactic fractions lie above those for the syndiotactic fractions, and, furthermore, all the points for the isotactic fractions lie above the straight line which represents the intrinsic viscosity/molecular weight relationship for fractions of conventionally polymerized, free-radically initiated polymethyl methacrylate¹¹. Such a difference, greater than that found for either poly-

*Presented at the meeting of the American Physical Society at Monterey, California, 21 to 23 March 1961.

propylene or polystyrene is to be expected for polymethyl methacrylate, since this polymer is already unusual in exhibiting a very large difference in glass temperature between the isotactic polymer¹⁴, $T_g = 45^\circ$, and the conventional polymer, $T_g = 104^\circ$. No perceptible difference in glass temperature has been found between isotactic and conventional samples either for polypropylene¹⁵ or for polystyrene⁵.

If the very slight differences in the intrinsic viscosity/molecular weight relationships for isotactic and conventional polymethyl methacrylate which can be discerned in Tsvetkov's data are assumed to be real, then much greater differences should be observed in solvents which are thermodynamically poorer than benzene for the conventional polymer. The present work shows such differences, well outside of experimental error, for fractions of isotactic polymethyl methacrylate in acetone solution.

EXPERIMENTAL

The sample of isotactic polymethyl methacrylate that was used for this work was made by R. P. Fellmann of our laboratories from 125 ml freshly distilled, uninhibited Rohm and Haas monomer in toluene solution (1380 ml) at -70° using 0.025 mole of freshly prepared 9-fluorenyllithium¹⁶ as initiator. The mixture, which had become quite viscous by the time the last of the methyl methacrylate had been added, was held at -70° overnight, 5 ml of methanol was added, and the mixture was warmed to room temperature. The polymer was isolated by precipitation into ten volumes of petroleum ether at room temperature, and was then dried overnight under vacuum. A quantitative yield of polymer was obtained. The finely divided polymer was washed by stirring in a 90-10 water-methanol mixture containing 5 per cent hydrochloric acid, was then stirred in a similar mixture without the acid, and was finally washed with deionized water. The polymer was characterized as isotactic from its infra-red spectrum^{17, 18}, having a J value¹⁶ of 33. Samples of isotactic polymethyl methacrylate generally have J values¹⁶ between 25 and 35, the most isotactic samples having the lowest J values. The number average molecular weight of the sample, as determined from the intensity of the absorption at $304\text{ m}\mu$ of the fluorenyl end-group on each polymer chain¹⁹, was 2.92×10^4 . The intrinsic viscosity in acetone at 30° was 0.505 ± 0.005 dl/g, which would correspond to a viscosity average molecular weight of 3.09×10^5 , assuming the intrinsic viscosity/molecular weight relationship obtained for fractions of conventional polymethyl methacrylate in this solvent²⁰

$$[\eta] = 7.7 \times 10^{-5} M^{0.70} \quad (1)$$

where $[\eta]$ is the intrinsic viscosity in decilitres per gramme.

There were two fractionations of this sample, both at 40.0° , using reagent grade benzene as the solvent and *n*-hexane (Skellysolve B) as the nonsolvent. The first fractionation was meant to be a trial fractionation, to find out whether isotactic polymethyl methacrylate could be fractionated so far below its melting point¹⁴, 160° . An attempt was first made to remove the lowest molecular weight molecules by precipitating 33 g of sample from benzene solution using a large excess of methanol, in which low molecular weight

conventional polymethyl methacrylate is soluble. A part of the 22.5 g of recovered precipitate, $\overline{M}_n = 4.53 \times 10^4$ by osmometry, $\overline{M}_w = 4.4 \times 10^5$, was then fractionated from 0.5 per cent solution in benzene into 15 fractions. The success of this fractionation led directly to the second fractionation. This time, without first removing low molecular weight material, 56 g of sample was fractionated from 0.5 per cent solution in benzene. The highest molecular weight fractions were obtained after a great deal of sub-fractionation from 0.1 per cent solution in benzene and recombination of sub-fractions. It appears pointless to give here our complete flow diagram for the fractionation, since our only object was to obtain a few good fractions. Subfractionations were performed on the basis of number average molecular weights and single point intrinsic viscosities of the fractions.

Reagent grade acetone and benzene were used for the viscosity and osmotic pressure measurements without further purification. For light scattering, reagent grade acetone was distilled through a packed column and a centre cut of constant boiling point was collected in each distillation. The n_D^{25} of the cuts used in the light scattering was 1.35583 ± 0.00005 ; the limits of error refer to variations between batches.

Intrinsic viscosities were obtained at 30° using Cannon-Ubbelohde semi-micro viscometers with solvent flow times above 100 sec so that no kinetic energy corrections were necessary. No shear corrections were necessary because of the low values of all the intrinsic viscosities obtained. At least three concentrations were run for each intrinsic viscosity determination.

The osmotic pressure measurements were obtained in the modified Schulz-Wagner osmometer, and analysed by the method discussed by Fox *et al.*²¹.

The refractive index increments of the unfractionated polymer and of one large fraction in acetone solution were measured at 436 m μ and at 546 m μ using a Brice-Phoenix differential refractometer. At room temperature (near 25°) values of 0.136 and 0.134 were found at these two wavelengths, respectively, in perfect agreement with the values previously reported for conventional polymethyl methacrylate from this laboratory²⁰.

Light scattering data were obtained at 436 m μ and 546 m μ on a Brice-Phoenix light scattering photometer at scattering angles from 30° to 135°. All solvents and polymer stock solutions were clarified by pressure filtration through sintered glass ultrafine filters. Runs were always made by adding polymer stock solution to solvent in the light scattering cell; five concentrations were run for each sample. The instrument calibration factor, k , for acetone was obtained as follows: first the instrument calibration factor for butanone and toluene was found from the 90° scattering of a 0.5 per cent solution of the Cornell polystyrene light scattering standard²² using the values for the turbidity, τ , at 437 m μ and at 546 m μ given by Doty and Steiner²²

$$k = \tau / (16\pi/3)(I_{90}) \quad (2)$$

where I_{90} is the intensity of the light scattered by the 0.5 per cent solution of the standard over and above that scattered by the solvent. Values of k

were found for both wavelengths in each solvent. The two values of k found for each wavelength were then plotted against the refractive index of solvent at that wavelength, and the values of k for acetone were read off the graph. The refractive indices of the solvents at 436 $m\mu$ and 546 $m\mu$ were calculated from the measured n_D^{25} and the known dispersion of each solvent.

For determination of weight average molecular weight, the light scattering data were first extrapolated to zero angle and then to infinite dilution, making the usual corrections for polarization and scattering volume for each intensity first.

For determination of the radius of gyration, $(\overline{s^2})^\dagger$, or the mean square end-to-end distance, $(\overline{r^2})^\ddagger$, of the polymer coil, where

$$\overline{r^2} = 6\overline{s^2} \quad (3)$$

for Gaussian coils, the light scattering data were first extrapolated to infinite dilution at each scattering angle, and then to zero scattering angle, again making the usual corrections for polarization and scattering volume first. The mean square radius of gyration of the sample was determined in the usual manner from the initial slope and the intercept of the curve in which the infinite dilution data are extrapolated to zero scattering angle²³.

RESULTS

Table 1 shows the dilute solution data for the fractions from both of the fractionations of the sample of isotactic polymethyl methacrylate that were used for this work.

Table 1. Data on fractions of isotactic polymethyl methacrylate

| $\overline{M}_n \times 10^{-3}$ * | $\overline{M}_w \times 10^{-3}$ | | $\overline{M}_w / \overline{M}_n$ | Acetone† | | Benzene‡ | |
|-----------------------------------|---------------------------------|------------|-----------------------------------|-------------------|---------------------------------|-------------------|---------------------------------|
| | 436 $m\mu$ | 546 $m\mu$ | | $[\eta]$ (dl/g) | $\overline{M}_v \times 10^{-3}$ | $[\eta]$ (dl/g) | $\overline{M}_v \times 10^{-3}$ |
| 2.70 | 6.34 | 7.06 | 2.5 | 1.05 | 8.72 | 1.53 ₅ | 7.6 |
| 1.42 | 2.00 | 1.92 | 1.4 | 0.48 ₂ | 2.88 | 0.62 ₆ | 2.35 |
| 0.86 ₄ | 1.34 | 1.16 | 1.4 | 0.293 | 1.42 | 0.42 | 1.38 |
| 0.68 ₃ | 1.02 | 0.96 | 1.4 | 0.290 | 1.41 | — | — |
| 7.45 | 12.8 | 11.3 | 1.6 | 1.45 | 13.7 | 2.53 | 14.7 |
| 3.89 | 5.36 | 5.34 | 1.4 | 0.87 ₅ | 6.7 | 1.31 | 6.1 |
| 0.445 | 0.541 | 0.538 | 1.2 | 0.203 | 0.57 | — | — |

*Determined by end-group analysis.

† \overline{M}_v calculated from equation (1).

‡ \overline{M}_v calculated from equation (5).

In Table 1 the intrinsic viscosities of the isotactic fractions are higher than those expected for fractions of conventional polymethyl methacrylate having the same molecular weights. In other words, as shown in Table 1, the weight average molecular weights of these fractions are less than their viscosity average molecular weights, if these are calculated from the intrinsic viscosity/molecular weight relationships previously obtained for conventional polymethyl methacrylate fractions. This is also indicated in Figures 1 and 2, which include the data used to obtain the $[\eta]/M$ relation-

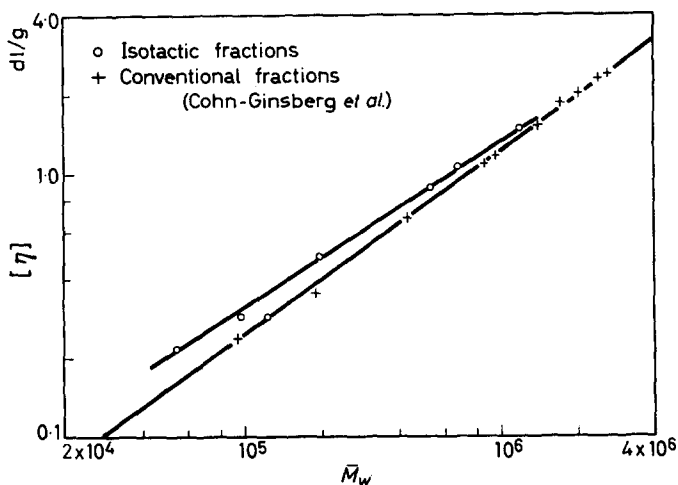


Figure 1—Log/log plot of intrinsic viscosity versus weight average molecular weight of fractions of polymethyl methacrylate in acetone at 30°

ships for conventional polymethyl methacrylate. These data are shown in order to indicate the experimental error to be expected for such fractions. In Figure 1, one of the points for the isotactic polymethyl methacrylate fractions falls very close to the conventional $[\eta]/M$ relationship. We suspect that the intrinsic viscosity for this fraction is in error, since we had to work with samples that had been used and then recovered from solution several times. It is possible that some polymer was lost or permanently altered or

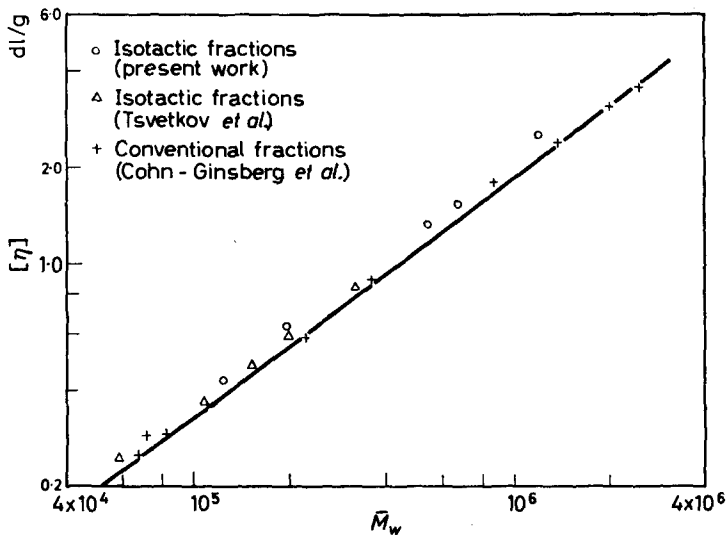


Figure 2—Log/log plot of intrinsic viscosity versus weight average molecular weight of fractions of polymethyl methacrylate in benzene

that an impurity was collected somewhere in these processes. The other six fractions appear to lie on a straight line which can be represented by the formula

$$[\eta] = 2.30 \times 10^{-4} M^{0.63} \quad (4)$$

In *Figure 2*, data for our fractions of isotactic polymethyl methacrylate are shown together with the data for Tsvetkov's fractions¹⁰. The data for all the isotactic fractions are consistent; all these points fall above the line representing the intrinsic viscosity/molecular weight relationship for conventional polymethyl methacrylate fractions in benzene solution²⁰ at 30°

$$[\eta] = 5.2 \times 10^{-5} M^{0.76} \quad (5)$$

Since the data for the isotactic fractions in benzene solution are very close to those of the conventional fractions, no new intrinsic viscosity/molecular weight relationship was derived for the isotactic fractions in benzene.

DISCUSSION

The data for isotactic polymethyl methacrylate fractions in acetone and in benzene solution indicate that the molecules of isotactic polymethyl methacrylate are more expanded in solution than are those of conventional polymethyl methacrylate. This is shown more explicitly by the $(\bar{r}^2)^{\frac{1}{2}}$ determined by light scattering for two of the fractions as shown in *Table 2*.

Table 2

| \bar{M}_w (average) of fraction | $(\bar{r}^2)^{\frac{1}{2}}$ exptl | | $(\bar{r}^2)^{\frac{1}{2}}$ calc. |
|--------------------------------------|-----------------------------------|-------------|-----------------------------------|
| 12.0×10^6 | 436 m μ | 546 m μ | 890 |
| 5.35×10^6 | 700 | 820 | 550 |

These two values of $(\bar{r}^2)^{\frac{1}{2}}$ are compared with values calculated from the equation

$$(\bar{r}^2)^{\frac{1}{2}} = 0.20 M^{0.60} \quad (6)$$

which was calculated from data of Cohn-Ginsberg *et al.*²⁰ on fractions of conventional polymethyl methacrylate in the molecular weight range from 8.7×10^5 to 2.5×10^6 , that is, more or less in the range of our isotactic fractions. These calculated values are much smaller than those found experimentally for the fractions. This discrepancy cannot have anything to do with molecular weight distribution, since the fractions on which equation (6) is based had \bar{M}_w/\bar{M}_n equal to 1.2 to 1.4, not very different from our isotactic fractions.

The difference in dilute solution properties of isotactic and conventional polymethyl methacrylate could be associated either with an effect of configuration upon the unperturbed end-to-end distance or with a difference in their interaction with solvent, or with both of these effects. An unequivocal answer will not be available until measurements in a theta solvent at the theta temperature have been completed for both configurations. However,

enough data are already available from the measurements reported in this paper to allow us to make some good guesses with very few additional assumptions.

If, following Flory and Fox²⁴, a plot is made of $[\eta]^{\frac{1}{3}}/\bar{M}_w^{\frac{1}{3}}$ versus $M/[\eta]$, the intercept at vanishing $M/[\eta]$ should be equal to $K^{\frac{2}{3}}$, where K is defined by

$$K = \phi(\bar{r}_0^2/M)^{3/2} = [\eta]/M^{\frac{1}{2}}\alpha^3 \quad (7)$$

where ϕ is a universal constant, \bar{r}_0^2 is the unperturbed end-to-end distance of the polymer fraction of molecular weight M , and α is the expansion factor for this fraction in the solvent in which the intrinsic viscosity is measured.

Figure 3— $[\eta]^{\frac{1}{3}}/\bar{M}_w^{\frac{1}{3}}$ versus $\bar{M}_w/[\eta]$ for fractions of polymethyl methacrylate in acetone at 30°

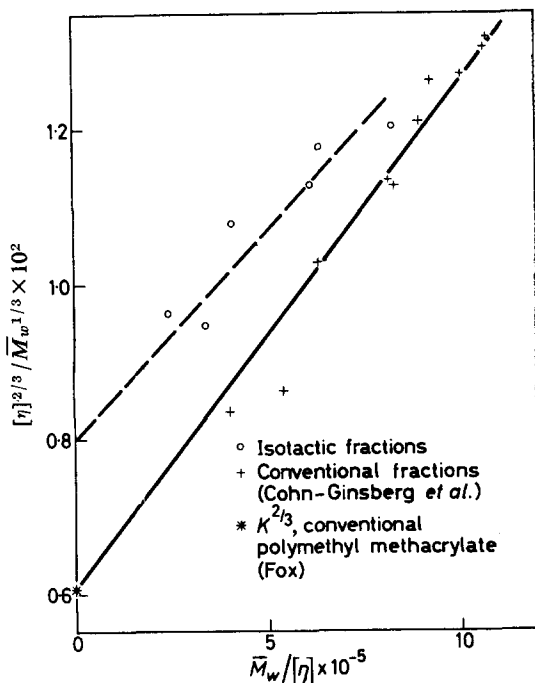


Figure 3 shows the data for the isotactic fractions (except for the most polydisperse fraction) in acetone solution plotted in this way. Also in Figure 3 are the data of Cohn-Ginsberg *et al.*²⁰ for fractions of conventional polymethyl methacrylate in acetone. The solid line in Figure 3 is drawn through the points for conventional polymethyl methacrylate fractions in such a way that its intercept at $M/[\eta]=0$ corresponds to the value of $K=4.8 \times 10^{-4}$ found for such fractions by Fox²⁵. All the data for the isotactic polymethyl methacrylate fractions in acetone lie above those for conventional polymethyl methacrylate. It is certainly presumptuous to draw a straight line through the points for the isotactic fractions, either the dashed line that has been drawn on Figure 3, or any other. However, it should be safe to say that if a straight line can be drawn at

all, that is, if the molecules of isotactic polymethyl methacrylate obey the general dilute solution statistics of polymers, then this straight line will intersect the ordinate of *Figure 3* above the intersection point for the line drawn for the conventional fractions. The dashed line has been drawn to represent the data reasonably well and to give an order of magnitude for K for the isotactic fractions, namely, $K = 7 \times 10^{-4}$. Using equation (7) with a value of 2.1×10^{21} for ϕ , this gives $(\bar{r}^2/M)^{\frac{1}{2}} = 7 \times 10^{-9}$, a value somewhat lower than that for polystyrene²⁶, 7.4×10^{-9} , and higher than that for conventional polymethyl methacrylate²⁵, 6.1×10^{-9} .

It is possible to get another order of magnitude approximation for $(\bar{r}_0^2/M)^{\frac{1}{2}}$ for the isotactic polymer by using the estimated value of K from *Figure 3* in equation (7) in a somewhat different manner. The far right hand side of equation (7) contains the expansion factor for the molecules, α ; therefore, equation (7) can be used to calculate this expansion factor for these fractions for which $[\eta]$ in acetone was measured. And then, since

$$\bar{r}^2 = \bar{r}_0^2 \alpha^2 \quad (8)$$

knowledge of α allows calculation of \bar{r}_0^2 for the two fractions for which \bar{r}^2 was measured. $(\bar{r}_0^2/M)^{\frac{1}{2}}$ for these two fractions is then 8.1×10^{-9} and 8.7×10^{-9} . These values are slightly higher than the value calculated from K alone, probably because the measured values of \bar{r}^2 are somewhat higher averages than the weight average, which is the average that should be used in this calculation. In spite of the fact that we know the \bar{M}_w/\bar{M}_n of our fractions, we did not attempt to correct our values of the mean square end-to-end distance for polydispersity.

Our thanks to Mr R. P. Fellmann who synthesized our polymer sample, to Mrs Eleanor Cherry who did both of the fractionations of the sample and also determined all of the number average molecular weights by end-group analysis, and to Mr John Begley who obtained most of the intrinsic viscosities.

(Received February 1962)

Rohm and Haas Co.,
Research Laboratories,
Bristol, Pa, U.S.A.

REFERENCES

- ¹ DANUSSO, F. and MORAGLIO, G. *Makromol. Chem.* 1958, **28**, 250
- ² KINSINGER, J. B. and HUGHES, R. E. *J. phys. Chem.* 1959, **63**, 2002
- ³ KINSINGER, J. B. and WESSLING, R. A. *J. Amer. chem. Soc.* 1959, **81**, 2908
- ⁴ PARRINI, P., SEBASTIANO, F. and MESSINA, G. *Makromol. Chem.* 1960, **38**, 27
- ⁵ NATTA, G., DANUSSO, F. and MORAGLIO, G. *Makromol. Chem.* 1956, **20**, 37
- ⁶ PEAKER, F. W. *J. Polym. Sci.* 1956, **22**, 25
- ⁷ DANUSSO, F. and MORAGLIO, G. *J. Polym. Sci.* 1957, **24**, 161
- ⁸ TROSSARELLI, L., CAMPI, E. and SAINI, G. *J. Polym. Sci.* 1959, **35**, 205
- ⁹ KRIGBAUM, W. R., CARPENTER, D. K. and NEWMAN, S. *J. phys. Chem.* 1958, **62**, 1586
- ¹⁰ TSVETKOV, V. N., SKAZKA, V. S. and KRIVORUCHKO, N. M. *Vysokomol. Soedineniya*, 1960, **2**, 1045

- ¹¹ We prefer *not* to call the conventional polymethyl methacrylate 'atactic' since it is now known that such samples contain mostly syndiotactic placements^{12,13}
- ¹² FOX, T. G., GOODE, W. E., GRATCH, S., HUGGETT, C. M., KINCAID, J. F., SPELL, A. and STROUPE, J. D. *J. Polym. Sci.* 1958, **31**, 173
- ¹³ BOVEY, F. A. and TIERS, G. V. D. *J. Polym. Sci.* 1960, **44**, 173
- ¹⁴ FOX, T. G., GARRETT, B. S., GOODE, W. E., GRATCH, S., KINCAID, J. F., SPELL, A. and STROUPE, J. D. *J. Amer. chem. Soc.* 1958, **80**, 1768
- ¹⁵ NATTA, G., DANUSSO, F. and MORAGLIO, G. *Atti Accad. Lincei, R.C. Sci. Fis. Mat. e Nat.* 1958, **24**, 254
- ¹⁶ GOODE, W. E., OWENS, F. H., FELLMANN, R. P., SNYDER, W. H. and MOORE, J. E. *J. Polym. Sci.* 1960, **46**, 317
- ¹⁷ SPELL, A. In preparation
- ¹⁸ BAUMAN, U., SCHREIBER, H. and TESSMAR, K. *Makromol. Chem.* 1959, **36**, 81
- ¹⁹ GLUSKER, D. L., STILES, E. and YONCOSKIE, B. *J. Polym. Sci.* 1961, **49**, 297
- ²⁰ COHN-GINSBERG, E., FOX, T. G. and MASON, H. F. *Polymer, Lond.* 1962, **3**, 97
- ²¹ FOX, T. G., KINSINGER, J. B., MASON, H. F. and SCHUELE, E. M. *Polymer, Lond.* 1962, **3**, 71
- ²² DOTY, P. and STEINER, R. F. *J. chem. Phys.* 1950, **18**, 1211
- ²³ DEBYE, P. *J. phys. Chem.* 1947, **51**, 18
- ²⁴ FLORY, P. J. and FOX, T. G., Jr, *J. Polym. Sci.* 1950, **5**, 745
- ²⁵ FOX, T. G. *Polymer, Lond.* 1962, **3**, 111
- ²⁶ FLORY, P. J. *Principles of Polymer Chemistry*, Chap. XIV. Cornell University Press: New York, 1953

The Effect of Temperature, Conversion and Solvent on the Stereospecificity of the Free Radical Polymerization of Methyl Methacrylate

T. G. FOX and H. W. SCHNECKO*

High resolution n.m.r. spectra are readily obtained at room temperature on ten per cent solutions of polymethyl methacrylate in chloroform. For polymers prepared by free radical polymerization, the tacticity parameter β (the probability that neighbouring asymmetric carbon atoms in the chain are in syndiotactic placement) computed accurately (± 2 per cent) from the relative areas of the α -methyl magnetic resonance peaks, is observed to obey Bernoulli trial statistics (as reported by others), to increase from 0.64 to 0.86 as the temperature chosen for polymerization ranges from 250° to -40°, and to be unaffected by other polymerization variables such as the initiator, the conversion, the molecular weight of the product, and the presence of any of a variety of solvents. Accordingly, the reaction producing an isotactic placement occurs with an Arrhenius factor 1.65-fold greater, and an activation energy 1.07 kcal larger, than the corresponding variables for the competing syndiotactic addition, a result somewhat different from that found in Bovey's pioneering investigation. Speculations on correlations between sequence length distributions and the diffraction pattern and solubility of partially crystalline polymers are included.

HIGH resolution nuclear magnetic resonance (n.m.r.) spectra of polymer solutions have been used¹⁻⁵ to determine the stereochemical structure of certain vinyl polymers. Employing this technique to determine the dependence of the structure of polymethyl methacrylate (PMMA) on the temperature of polymerization, and considering the polymerization to consist of two independent competing reactions producing, respectively, isotactic and syndiotactic stereochemical placements of nearest neighbours in the chain⁶⁻¹⁰, Bovey found³ the syndiotactic addition favoured by an activation energy lower by 775 cal than isotactic addition, with no difference in the frequency factors. In his work two factors require further clarification: (a) his low temperature polymerization (-78°C) was achieved in solution whereas the other samples were prepared in bulk; (b) his polymerizations at different temperatures differ greatly in the conversion (1.7 to 100 per cent). The probability[†] α of an isotactic placement or of a syndiotactic placement $\beta = 1 - \alpha$ in these polymers may^{2, 8, 11} or may not⁴ be affected by the variation in the reaction medium with conversion or with solvent. Finally it is of interest to demonstrate the utility of the Varian A-60 n.m.r. spectrometer for such measurements, and to establish the precision with which this structural parameter can be measured.

*Present address: Universität Mainz, Mainz, Germany.

†We use the symbol α originally proposed by Coleman¹, which is identical with σ employed later by Bovey².

In order to study these points, free radical polymers of methyl methacrylate were prepared in bulk to low conversion (less than ten per cent) at temperatures ranging from -40° to 250° . Moreover polymerizations were carried out with two different initiators, to conversions at 60° ranging from 1 to 84 per cent, to different molecular weights (from 10^5 to 10^6), and in ten different solvents. The n.m.r. spectra were used to characterize the stereostructure, and the applicability of infra-red (i.r.) spectra for this purpose^{4, 8, 11, 12} was explored.

EXPERIMENTAL

Bulk polymerizations

Methyl methacrylate (MMA) from the Monomer Polymer Laboratories, Borden Chemical Company, was destabilized (washed with ten per cent sodium monohydrogen sulphite, 1N caustic soda, water), dried, distilled, degassed and sealed in ampoules under vacuum, and polymerized in constant temperature baths. Afterwards, the polymer was precipitated in methanol and reprecipitated from benzene solution. The polymerizations carried out from -40° to 0° were initiated with benzoin photosensitized by ultra-violet (u.v.) light. The initiators were recrystallized before use. Azobisisobutyronitrile (AIBN) was used as the initiator between 30° and 150° ; in most of these experiments 0.5 per cent dodecyl mercaptan was added. In order to detect any effect of the initiator on the structure of the polymers, one polymerization at 100° (M 127) with benzoin activated by u.v. light was carried out. In a thermal polymerization at 250° some polymer (< 10 per cent of the yield) was formed on heating before the desired polymerization temperature was reached, consequently the observed α value (0.36) may be slightly low. Attempts to eliminate the prepolymerization by addition of diphenylpicrylhydrazine (1.4×10^{-3} per cent) in the presence of AIBN were successful, but in this case α was even lower (0.33).

Solution polymerization

Polymerizations of solutions of the monomer 20 per cent by volume in each of nine freshly distilled solvents were made at 60° with AIBN as initiator, to conversions not in excess of 20 per cent. A similar polymerization in nitromethane was made at 100° , and another at -40° in ethyl acetate solution with benzoin at a monomer concentration of 50 per cent.

The n.m.r. spectra

The spectra were taken with the Varian A-60 spectrometer at room temperature (30°) with polymer ($10 \text{ g}/100\text{cm}^3$) dissolved in ethanol-free chloroform. The solutions were introduced into precision tubes, degassed and sealed on a vacuum line. One per cent tetramethylsilane was used as an internal reference standard. For evaluation of the areas the heterotactic h (9.0 τ), and syndiotactic s (9.14 τ) α -CH₃ triad peaks² were used; in addition to these the isotactic, i-peak (8.8 τ) was utilized only with the samples polymerized at high temperature. Spectra of two polymers made at -40° were also taken with a sweep width of 250 c/s, instead of the usual 500 c/s; in this case the tubes were heated to 120° before inserting

THE FREE RADICAL POLYMERIZATION OF METHYL METHACRYLATE

into the probe. In order to obtain high accuracy (*ca.* 2 to 5 per cent in the areas, cf. *Tables 1* and *2*) the method of Brace¹³, i.e. approximation by triangles, was applied and the areas measured with a planimeter. The ratio of the peak heights was found to be related to the ratio of the

Table 1. Values of α determined for polymethyl methacrylate prepared to various conversions in bulk polymerizations at 60°C with AIBN*

| Sample designation | Dodecyl mercaptan (%) | Conversion (%) | $M_w \times 10^{-5}$ | P_h/P_s | α | J value ¹¹ |
|--------------------|-----------------------|----------------|----------------------|-----------|----------|-------------------------|
| M 128 | 0.5 | 1 | 1.45 | 0.620 | 0.24 | 93 |
| M 153 | | 5 | 10.6 | 0.663 | 0.25 | |
| M 134 | 0.5 | 5 | 1.59 | 0.690 | 0.26 | 94 |
| M 133 | 0.5 | 10 | 1.40 | 0.625 | 0.24 | 88 |
| M 102 | | 12 | 9.35 | 0.710 | 0.26 | 84 |
| M 136 | 0.5 | 20 | 1.59 | 0.620 | 0.24 | 89 |
| M 138 | 0.5 | 39 | 1.45 | 0.574 | 0.22 | 90 |
| M 139 | 0.5 | 56 | 1.41 | 0.649 | 0.24 | 81 |
| M 137 | 0.5 | 84 | 1.51 | 0.622 | 0.24 | 90 |
| | | | | | 0.243 ± | 0.01 |

*From 2×10^{-3} to 2×10^{-2} per cent.

Table 2. Stereoregularity of PMMA prepared to low conversion (< 20 per cent) in 20 per cent (V/V) solutions with (2 to 6×10^{-2} per cent) AIBN

| Sample designation | Polym. temp. (°C) | Solvent | P_h/P_s | α | |
|--------------------|-------------------|---------------|-----------|----------|------------------|
| | | | | Obsd | Calc. by eq. (3) |
| M 214 | 100 | Nitromethane | 0.738 | 0.27 | 0.27 |
| M 215 | 60 | Nitromethane | 0.618 | 0.24 | 0.25 |
| M 212 | 60 | Ethanol | 0.666 | 0.25 | 0.25 |
| M 209 | 60 | Acetonitrile | 0.665 | 0.25 | 0.25 |
| M 207 | 60 | Acetone | 0.660 | 0.25 | 0.25 |
| M 205 | 60 | Chloroform | 0.629 | 0.24 | 0.25 |
| M 215 | 60 | Nitromethane | 0.618 | 0.24 | 0.25 |
| M 211 | 60 | Toluene | 0.603 | 0.23 | 0.25 |
| M 204 | 60 | Benzene | 0.591 | 0.23 | 0.25 |
| M 210 | 60 | 2-Octanone | 0.591 | 0.23 | 0.25 |
| M 206 | 60 | 2-Butanone | 0.583 | 0.23 | 0.25 |
| M 216* | -40 | Ethyl acetate | 0.318 | 0.14 | 0.14 |

*In 50 (V/V) per cent solution with 2 per cent benzoin.

corresponding areas; thus, if fast evaluation of α is desired, it is not necessary to measure areas once the relationship is established¹⁴.

The i.r. spectra

The i.r. spectra were scanned from cast films in a Perkin Elmer 21 instrument according to the method of Spell given by Goode *et al.*¹¹. The characteristic ' J value' as defined by these workers was calculated from the intensity ratios of the 9.3 – 10.1μ and 6.75 – 7.20μ bands.

Molecular weights

Values of M_w were calculated from the measured values of the intrinsic viscosities (dl/g) in benzene at 30°, employing the relation¹⁵

$$[\eta] = 5.12 \times 10^{-5} M_w^{0.76}; M_w \geq 35\,000 \quad (1)$$

RESULTS

The n.m.r. spectra

Some characteristic n.m.r. spectra of PMMA taken with the Varian A-60 spectrometer are shown in *Figure 1*. In addition to the spectra of the least [*Figure 1(a)*] and most [*Figure 1(b)*] syndiotactic polymers obtained

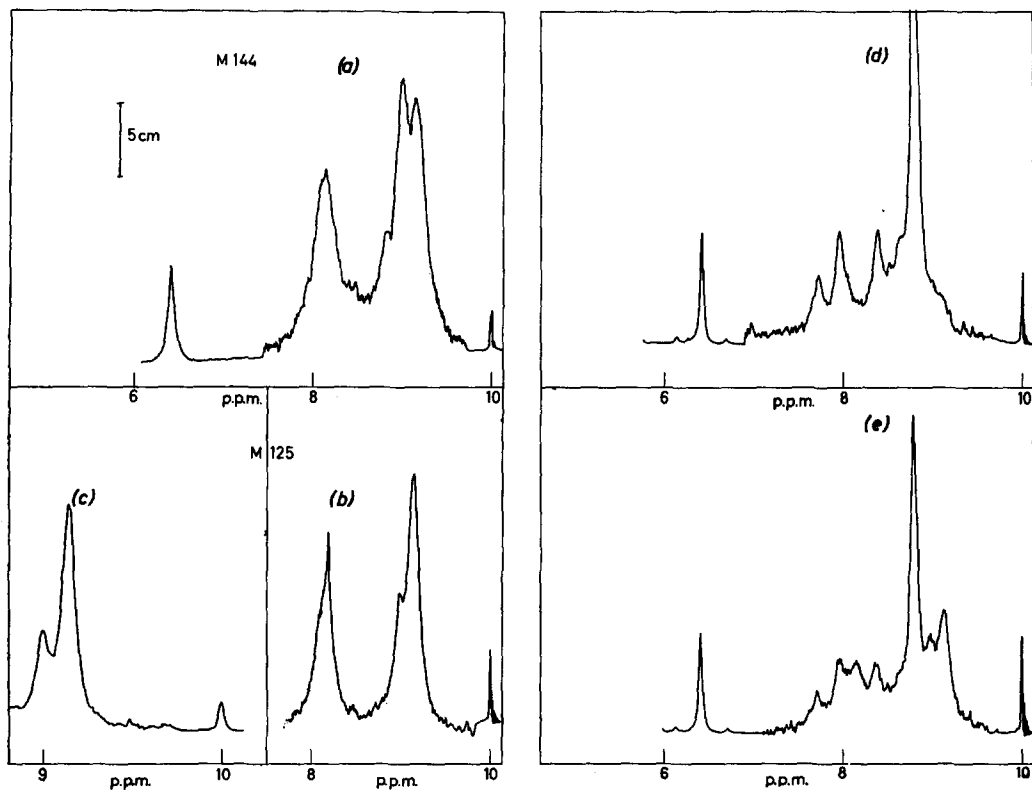


Figure 1—The n.m.r. spectra of 10 per cent chloroform solutions at room temperature of polymer prepared in free radical polymerizations (a) at 250° (Sample M 144, $\alpha=0.36$) and (b and c) at -40° (Sample M 125, $\alpha=0.14$). Spectra (d) of an isotactic polymer ($\alpha\sim 1$) and (e) of a stereoblock copolymer ($\alpha\sim 0.62$, estimated from methylene peaks) prepared in anionic polymerization are included for comparison. Spectra obtained with the Varian A-60 spectrometer having a frequency response of 0.4 c/s, r.f. field 0.15 Mc/s, sweep width 500 c/s (calibrated¹⁶ in τ), spectrum amplitude 2.5, 25, 2.5. Sample (c) same as (b) but preheated and observed with a sweep time of 100 sec, sweep width 250 c/s, spectrum amplitude 1.6

by free radical polymerization, spectra of a highly isotactic [Figure 1(d)]* and of a stereoblock PMMA [Figure 1(e)]* are included for comparison purposes. Although the older instrument, the Varian 4300, at peak performance is capable of even higher resolution, the improved stability and ease of operation of the present apparatus so markedly reduces the effort needed to obtain good data that the precision achieved is often actually better.

Thus, for the present measurements at room temperature on ten per cent solutions the resolution is excellent and reproducible; all spectra of Table 2 were scanned twice with indistinguishable results. Even higher resolution can be obtained by preheating the sample tubes and immediately afterwards scanning with an expanded scale; a spectrum obtained in this way is shown in Figure 1(c).

In order to evaluate the amount of stereoregularity from the α -methyl peaks it is not necessary—and usually not possible—to estimate with the desired precision all three areas P_i , P_h , P_s as described in the literature^{2,3}. From the ratio of the larger areas P_h/P_s for the polymer of interest here α is easily calculated by the relation

$$\alpha/(1-\alpha) = 0.5P_h/P_s \quad (2)$$

For the polymers prepared at high temperatures, values of α determined from the equation $\alpha/(1-\alpha) = [P_i/P_s]^{1/2}$ were in agreement with the corresponding values of α obtained with equation (2), thus demonstrating the applicability here of Bernoulli trial statistics^{2,7}.

It is obvious from Figure 1 that under the conditions we employed the different methylene peaks (8.2τ) are generally not suitable for evaluation of the microstructure of the present samples of PMMA, in contrast to n.m.r. results for other polymers¹⁷. The detection of isotactic portions in the more syndiotactic polymers by means of the methylene peak is complicated by three factors: (a) the general broadening of proton resonance signals in the polymer chain where motions are evidently much more restricted than in side groups (hence, the peak is broad and low in the case of the high molecular weight polymers, but becomes higher and sharper with decreasing molecular weight); (b) the presence of only two protons in the methylene group in contrast to the three protons of the α -methyl group; (c) the splitting of the signal in the isotactic form into four peaks. Thus for PMMA with $\alpha < 0.35$, such as studied here, it is impossible to measure these areas. Only in one case, that of the stereoblock copolymer [Figure 1(e)], was it possible to make an estimation of α from such data.

The dependence of α on polymerization variables

The data in Table 1 indicate that for polymers prepared at 60° there is, within the error of the measurements (± 0.01 in α), no influence on α by the

*We are indebted to Dr W. E. Goode of the Rohm and Haas Company who kindly supplied these samples. The isotactic and stereoblock polymers, respectively, were prepared with phenyl magnesium bromide at 0° and with butyl magnesium chloride at -60°, by procedures described¹¹ for the preparation of Type II and Type III polymethyl methacrylate, except for the use of 'Esso octane'—a mixture of aliphatic and (20 per cent) aromatic hydrocarbons—as the polymerization medium, from which the polymer precipitated as formed. Dr Goode reports that the samples exhibited respectively, i.r. J values of 34 and 64, glass temperatures of 48° and 82°, melting points of 140° to 150° and of 130° to 140°, essentially identical number average molecular weights of 44 000, and ratios of viscosity average to number average chain lengths of 2.9 and 12.6.

degree of conversion, by the initiator, by the presence of mercaptan, or by the chain length.

The results in *Table 2* indicate that the stereochemical structure of the polymers prepared in solution polymerizations is, within the precision of the present data, independent of the solvent used and not measurably different from that of the polymers obtained in bulk polymerizations at the same temperature.

Data on bulk polymerizations of MMA between 250° and -40° at low conversions are shown in *Table 3*. From the Arrhenius plot of

Table 3. Values of α determined on polymethyl methacrylate prepared in bulk polymerization at various temperatures

| Sample designation | Polym. temp. (°C) | Initiator conc. (%) A=AIBN B=Benzoin | Polym. time (h) | Conversion % | P_h/P_s | α ($\pm 2\%$) | J value | $M_w \times 10^{-4}$ |
|--------------------|-------------------|--|-----------------|--------------|-----------|------------------------|---------|----------------------|
| M 144 | 250 | — | 0.2 | 6 | 1.100 | 0.36 | 78 | |
| M 131* | 150 | 2.3×10^{-3} A | 0.25 | 15 | 0.990 | 0.33 | 78 | 1.05 |
| M 130 | 150 | 2.3×10^{-3} A | 0.75 | 30 | 0.990 | 0.33 | 79 | 11.0 |
| M 127* | 100 | 4.4×10^{-3} B | 0.25 | 7 | 0.742 | 0.27 | | |
| M 129* | 95 | 2.3×10^{-3} A | 2 | 18 | 0.728 | 0.27 | 84 | 1.45 |
| M 128* | 60 | 2.3×10^{-3} A | 2.5 | 1 | 0.620 | 0.24 | 93 | |
| M 133* | 60 | 7.0×10^{-3} A | 4 | 10 | 0.625 | 0.24 | 88 | 1.40 |
| M 132* | 30 | 7.0×10^{-3} A | 4 | 1 | 0.560 | 0.22 | | |
| M 118 | 0 | 0.1 B | 1 | 10 | 0.486 | 0.20 | 104 | |
| M 120 | -20 | 0.1 B | 2 | 5 | 0.420 | 0.17 | 109 | |
| M 122 | -20 | 0.4 B | 3 | 19 | 0.455 | 0.18 | 92 | |
| M 123 | -20 | 0.4 B | 6 | 34 | 0.443 | 0.18 | 100 | |
| M 126 | -40 | 0.4 B | 3 | 4 | 0.312 | 0.14 | 94 | 1.02 |
| M 125 | -40 | 0.4 B | 8 | 25 | 0.326 | 0.14 | 102 | |

*Made in presence of 0.5 per cent dodecyl mercaptan.

$\ln \{\alpha/(1-\alpha)\}$ versus $1/T$, where $\ln \{\alpha/(1-\alpha)\}$ is readily derived from equation (2), we find the difference in activation enthalpies between the syndiotactic and isotactic propagation step

$$\Delta(\Delta H_p^\ddagger) = (1.07 \pm 0.05) \text{ kcal}$$

a value about 50 per cent larger than Bovey's. For the entropy difference we have

$$\Delta(\Delta S_p^\ddagger) = (0.99 \pm 0.10) \text{ e.u.}$$

contrary to Bovey's value of nil. Alternatively, the modified Arrhenius equation can thus be written

$$\alpha/(1-\alpha) = k_i/k_s = 1.65 \exp(-1070/RT) \quad (3)$$

where k_i and k_s are the rate constants for the addition of monomer to form in the chain isotactic and syndiotactic placements, respectively. It can be seen from *Figure 2(b)* that Bovey's data, except for the point obtained on his polymer prepared at -70° in ethyl acetate, show little deviation from the present results. We found no difference (*Table 2*) in the stereostructure obtained at -40° in bulk or in ethyl acetate.

Infra-red absorption

A correlation (*Figure 3*) observed between the i.r. absorption and the stereostructure of these polymers may be expressed by the approximate empirical relation $\alpha = 1 - J/120$ applicable at least in this range of α (0.1 to 0.4). Thus in principle it would be possible, as suggested earlier⁸

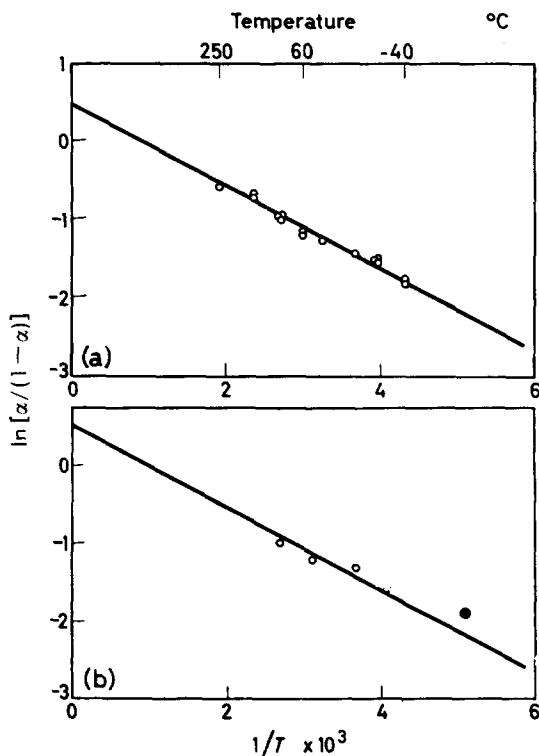


Figure 2— $\ln [\alpha / (1 - \alpha)]$ versus $1/T$ for polymethyl methacrylate prepared in free radical polymerization at temperature T , with α determined from the proton magnetic resonance peaks of the α -methyl groups: (a) present data on bulk polymerization carried to low conversion, and (b) comparison of present results (straight line) with earlier data² on polymers prepared to various conversions in bulk, \circ , or in ethyl acetate, \bullet

and illustrated recently^{4,12}, to employ i.r. data to determine the stereoregularity. Unfortunately, as illustrated by the scatter of the data in Figure 3, the determination is not as reproducible as desired. An attempt to increase the accuracy by the use of other bands^{4,12} gave no significant improvement, and it is believed that development of improved methods for the preparation of films more uniform in thickness would be essential for this method.

DISCUSSION

General implications

The applicability of equation (3) in the free radical polymerization of a typical olefin, methyl methacrylate, indicates that the stereospecificity in such polymerizations is consistent with a difference in the free energy of formation⁶⁻¹⁰ of an intermediate complex formed between the initially planar free radical and the approaching monomer, depending on which configuration relative to the penultimate unit the radical assumes in the process. The evidence (Tables 1 and 2) indicates that the free energy difference is insensitive to other parameters describing the reaction medium, such as the dielectric constant, viscosity, and the thermodynamic interaction between polymer and its surroundings. These findings (Table 2) weigh against the hypothesis¹⁸ that the stereospecific sequences in the polymer are predetermined by the presence of regions of ordered arrangement of monomer units relative to each other in the liquid.

These results demonstrate further the important finding, postulated earlier⁶⁻¹⁰, that for polymers prepared by a free radical technique a full description of the stereochemical arrangements of the units in the chain is given by Bernoulli trial statistics, requiring a single parameter α , which for a given homopolymer is sensitive only to the polymerization temperature. For example, the fraction of units in isotactic sequences of N units is $F_1^N = N\beta^2\alpha^N$, while the similar result for syndiotactic sequences is $F_s^N = N\alpha^2\beta^N$. (In contrast, the chain length distribution for such polymers is given by a simple relation only for low conversions, since it depends on three ratios of rate constants and on the concentrations of initiator, monomer and additives, all of which may vary in complex fashion with extent of

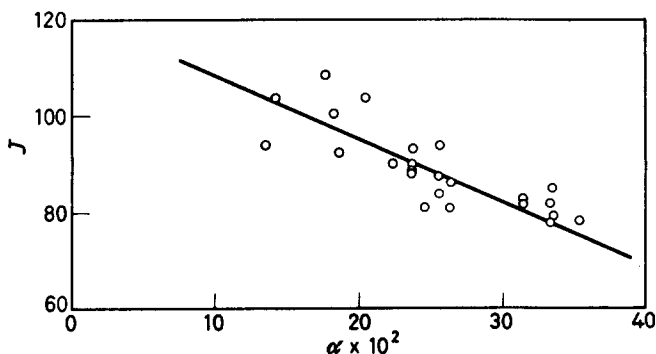


Figure 3—Infra-red J values versus α determined for the present polymethyl methacrylate prepared in free radical polymerizations

reaction and with temperature.) It should be a general objective, therefore, to devise and employ methods to measure α (including the use of high resolution n.m.r. when practicable) for such homopolymers, and subsequently to determine the relation between α and specific chemical and physical properties⁸. An example of the latter is provided by Coleman's treatment⁷ of the dependence of the melting point on α . As further examples, approximate considerations of two problems of interest are given below.

Before presenting these, we note that the small magnitude of the exponent in equation (3) would appear to render impracticable any attempt to determine α from exact kinetic measurement of the dependence of the propagation rate constant ($k_p = k_i + k_s$) on temperature. This is possible, in principle, from measurements of the curvature in plots of $\ln k_p$ versus $1/T$, since the slope at a given temperature is proportional to $E_T = \alpha(E_i - E_s) + E_s$, where E_i and E_s are the activation energies for the isotactic and syndiotactic additions, respectively. Since E_T would decrease only ca. 140 calories between 100° and -40° , measurement at these extremes to ca. ± 10 calories (i.e. to ca. 1 per cent) would be required to yield a significant measure of α . In view of the uncertain variations over this range in the effective initiation and termination rate constants, this is a virtual impossibility.

Sequence distribution and crystallinity

It has been observed that polymers of methyl methacrylate prepared by

free radical means at 0° or lower are crystallizable, while polymers prepared at higher temperatures are not⁸. The fraction f_N of polymer present in syndiotactic blocks of length $\geq N$, calculated by the expression $f_N = \beta^{N+1} (1 + \alpha N)$ given earlier⁸, is plotted for various values of N versus the polymerization temperature in *Figure 4*. If it is assumed that *ca.* 5 per cent to 20 per cent of the sample must be in the crystalline phase before the diffraction pattern will be sufficiently developed to constitute clear evidence of crystalline order, and that the crystallites contain all of the material in blocks longer than a certain threshold length, it follows from *Figure 4* that the threshold length must lie between 10 and 20 monomer units. If one crystallite dimension was limited by this length it would be small indeed ($< 50\text{\AA}$), and would be expected to yield relatively diffuse crystalline diffraction rings, such as are observed for crystalline samples of syndiotactic polymethyl methacrylate^{8,11}

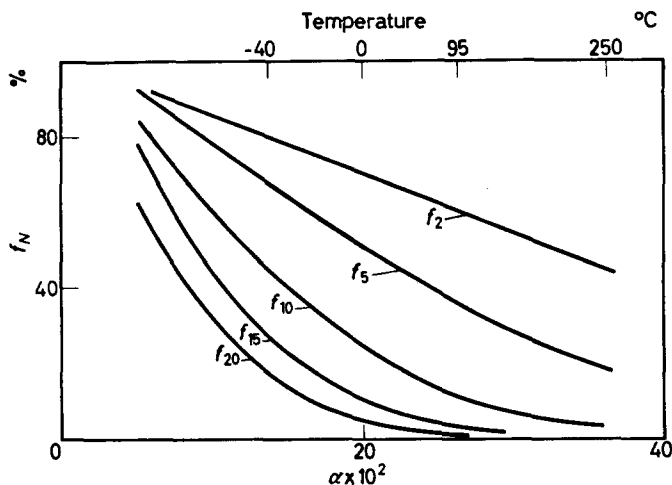


Figure 4— f_N versus N computed for various values of α (see text), where f_N is the weight fraction of polymer in syndiotactic blocks of length $\geq N$

For polymers whose placements obey Bernoulli trial statistics the presence of only a small fraction (e.g. 5 per cent) of syndiotactic blocks greater than the postulated threshold length may be sufficient to insolubilize the greater portion of the sample. Thus, if only those chains containing *no* syndiotactic sequences of length $\geq N^*$ are completely soluble when the polymer is crystallized from solution, then for a homogeneous polymer of degree of polymerization P the weight fraction of soluble polymer is

$$w_{\text{sol}} = (1 - \beta^{N^*})^{(P - N^* + 1)}$$

When $\beta = 0.8$ and $N^* = 20$ this corresponds to 20 per cent, 10 per cent and 0.3 per cent sol fractions for molecular weights of 10^4 , 2×10^4 , and 5×10^4 , respectively. The latter high molecular weight polymer on crystallization from solution would be essentially completely insolubilized, but highly swollen, since the major portion would still be amorphous. Such behaviour

has been noted^{8, 11, 19}. Both the degree of crystallinity and the fraction of polymer insolubilized are expected to increase rapidly for a given molecular weight as the tacticity parameter β increases from 0.8 toward 1.0. In a heterogeneous polymer with $\beta \sim 0.8$, it should be possible by fractional crystallization and/or extraction to separate a portion of soluble low molecular weight polymer, in greater amount the lower the average degree of polymerization of the sample.

The authors are indebted to Drs A. A. Bothner-By and B. Shapiro for helpful discussions and for instructions and assistance in the use of the Varian A-60 spectrometer.

Mellon Institute,
Pittsburgh, Pa

(Received February 1962)

REFERENCES

- ¹ BOVEY, F. A., TIERS, G. V. D. and FILIPOVICH, G. J. *Polym. Sci.* 1959, **38**, 73
- ² BOVEY, F. A. and TIERS, G. V. D. *J. Polym. Sci.* 1960, **44**, 173; cf. JOHNSEN, U. and TESSMAR, K. *Kolloidzshr.* 1960, **168**, 160
- ³ BOVEY, F. A. *J. Polym. Sci.* 1960, **46**, 59
- ⁴ NISHOIKA, A., WATANABE, J., ABE, K. and SONO, Y. *J. Polym. Sci.* 1960, **48**, 241
- ⁵ BYWATER, S., BROWNSTEIN, S. and WORSFIELD, D. J. *Makromol. Chem.* 1960, **48**, 127
- ⁶ HUGGINS, M. L. *J. Amer. chem. Soc.* 1944, **66**, 1991
- ⁷ COLEMAN, B. D. *J. Polym. Sci.* 1958, **31**, 155
- ⁸ FOX, T. G., GOODE, W. E., GRATCH, S., HUGGETT, C. H., KINCAID, J. F., SPELL, A. and STROUPE, J. D. *J. Polym. Sci.* 1958, **31**, 173
- ⁹ HUGHES, R. E. Abstracts of papers, 133rd Meeting of American Chemical Society, San Francisco, California, April 1958, p 10R
- ¹⁰ FORDHAM, J. W. L. *J. Polym. Sci.* 1959, **39**, 321
- ¹¹ GOODE, W. E., OWENS, F. H., FELLMAN, R. P., SNYDER, W. H. and MOORE, J. E. *J. Polym. Sci.* 1960, **46**, 317
- ¹² BAUMANN, U., SCHREIBER, H. and TESSMAR, K. *Makromol. Chem.* 1960, **36**, 81
- ¹³ PECSOK, R. L. *Principles and Practice of Gas Chromatography*, p 145. Wiley: New York, 1959
- ¹⁴ MILLER, W. L., BREY, W. S. and BUTLER, G. B. *J. Polym. Sci.* 1961, **54**, 329; cf. ROBERTS, J. D. *An Introduction to the Analysis of Spin-Spin Splitting in High-Resolution Nuclear Magnetic Resonance*, p 6. Benjamin: New York, 1961
- ¹⁵ COHN-GINSBERG, E. S., FOX, T. G. and MASON, H. F. *Polymer, Lond.* 1962, **3**, 97
- ¹⁶ TIERS, G. V. D. *J. phys. Chem.* 1958, **62**, 1151
- ¹⁷ JOHNSEN, U. *J. Polym. Sci.* 1961, **54**, 56
- ¹⁸ SEMENOV, N. N. *J. Polym. Sci.* 1961, **55**, 563; NORTH, A. M. *Vysokomol. Soedin-eniya*, 1961, **3**, 1874
- ¹⁹ WATANABE, W. H., RYAN, C. F., FLEISCHER, Jr, P. C. and GARRETT, B. S. *J. phys. Chem.* 1961, **65**, 896

Tracer Studies of 2-Cyano-2-propylazoformamide I—Use of the Compound as a Sensitizer for the Polymerization of Styrene

J. C. BEVINGTON and ABDUL WAHID

2-Cyano-2-propylazoformamide, labelled in its methyl groups with carbon-14, has been used to sensitize the polymerization of styrene at 100°C. From the rates at which labelled initiator fragments become incorporated in polymer, it has been deduced that the velocity constant for dissociation of the azo compound into available radicals is $1.08 \times 10^{-5} \text{ sec}^{-1}$ and that the transfer constant for transfer to initiator is 0.17.

THIS paper is the first of a series concerned with 2-cyano-2-propylazoformamide, $(\text{CH}_3)_2\text{C}(\text{CN}) \cdot \text{N}:\text{N} \cdot \text{CO} \cdot \text{NH}_2$. Unsymmetrical azo compounds, such as this, are likely to be of value in studies of geminate recombination of radicals and of the cage effect during dissociations in solution. The azo compound used here is of particular interest since it is a source of 2-cyano-2-propyl radicals which can be generated in pairs by the dissociation of azoisobutyronitrile. It can be used conveniently as an initiator for radical polymerizations at temperatures in the region of 100°C.

The azo compound is easily prepared and labelled with carbon-14 in the methyl groups. The labelled material has been used for measurement of rates of initiation by 2-cyano-2-propyl radicals in the polymerization of styrene, and also for assessing the importance of transfer to initiator.

EXPERIMENTAL

The compound $(\text{CH}_3)_2\text{C}(\text{CN}) \cdot \text{NH} \cdot \text{NH} \cdot \text{CO} \cdot \text{NH}_2$ was prepared by the condensation of acetone, semicarbazide and hydrogen cyanide; it was oxidized to the azo compound using potassium permanganate. The product was extracted with ether and recrystallized from benzene to give yellow crystals (m. pt 81° to 82°C). A labelled specimen of the azo compound was prepared starting with 1,3- ^{14}C -acetone; the specific activity of the product, determined by gas counting, was 51.7 $\mu\text{c/g}$. For presentation of results, specific activities are quoted in $\mu\text{c/g}$ of carbon in the material being assayed.

Polymerizations were performed in sealed dilatometers at 100°C using mixtures of styrene and benzene and the initiator at concentrations up to 0.7 g/l. Reaction mixtures were degassed before the dilatometers were sealed. For calculation of rates of polymerization, 18.67 per cent contraction of styrene at 100°C was taken as equivalent to 100 per cent polymerization, and the density of the monomer as 0.832 g/cm³. The reactions were allowed

to proceed to five per cent conversion. Polymers were recovered by precipitation in methanol from benzene solutions; tests showed that this procedure was adequate for removal of all traces of uncombined initiator from polymers.

RESULTS

In the polymerizations of styrene at 100°C using 2-cyano-2-propylazoforamide as thermal sensitizer, there were no inhibition periods; steady rates were rapidly reached and were maintained through the reactions. There were no systematic differences between the rates of polymerizations involving labelled and unlabelled samples of initiator. From the results in *Table 1*, it can be deduced that the order of the polymerization with respect to initiator is close to 0.5 and with respect to monomer a little over unity.

If the azo compound is labelled in its methyl groups, the rate (R_e) at which 2-cyano-2-propyl groups enter polymer can be calculated from the observed rate of polymerization and the specific activities of the initiator and the polymer. The number (n) of styrene units in a polymer for each incorporated group is given by

$$\frac{\text{specific activity of polymer}}{\text{specific activity of labelled group}} = \frac{4}{8n}$$

unless n is rather small. If the specific activity of the azo compound (labelled in its methyl groups only) is c $\mu\text{C/g}$ of carbon, that of the 2-cyano-2-propyl group is $5c/4$. The number n is equal also to (rate of polymerization)/ R_e and so

$$R_e = 8sR_p/5c$$

where s is the specific activity of the polymer, and R_p is the rate of polymerization. Values of R_e for reactions involving various concentrations of monomer and initiator are included in *Table 1*.

Table 1. Experiments with labelled initiator

| [styrene] (mole/l.) | 10^3 [initiator] (mole/l.) | $10^5 R_p$ (mole l^{-1} sec $^{-1}$) | 10^2 (spec. act. polymer) ($\mu\text{C/g}$ of carbon) | $10^8 R_e$ (mole l^{-1} sec $^{-1}$) |
|------------------------|---------------------------------|--|---|--|
| 1 | 1.2 | 0.7 | 10.08 | 0.97 |
| 1 | 2.2 | 1.0 | 17.94 | 2.34 |
| 1 | 3.6 | 1.3 | 23.11 | 3.94 |
| 1 | 4.6 | 1.6 | 26.44 | 5.60 |
| 2 | 1.2 | 1.6 | 6.33 | 1.34 |
| 2 | 2.2 | 2.2 | 9.19 | 2.67 |
| 2 | 3.6 | 2.5 | 11.19 | 3.71 |
| 2 | 4.6 | 3.5 | 12.97 | 6.02 |
| 3 | 1.2 | 3.0 | 3.67 | 1.45 |
| 4 | 1.2 | 3.5 | 2.37 | 1.10 |
| 4 | 2.2 | 4.9 | 3.66 | 2.38 |
| 4 | 4.6 | 6.7 | 6.72 | 5.98 |
| 8 | 1.2 | 8.8 | 1.20 | 1.40 |
| 8 | 3.6 | 12.4 | 3.36 | 5.52 |
| 8 | 4.6 | 17.5 | 2.83 | 6.58 |

Specific activity of initiator = 120.6 $\mu\text{C/g}$ of carbon.

Polymerizations involving the labelled initiator at 1.2×10^{-3} mole/l. and styrene at various concentrations were performed at 100°C using di-*t*-butyl peroxide as a second unlabelled initiator. The derived values of R_e are plotted against $R_p/[M]$ in *Figure 1*.

DISCUSSION

The kinetic characteristics of the polymerization of styrene sensitized by 2-cyano-2-propylazoformamide are normal; the value of the order with respect to initiator indicates that there is mutual termination of reaction chains.

Initiator fragments enter polymer by three processes, viz.:

- (a) initiation by attachment of primary radicals to molecules of monomer (rate, R_i)
- (b) transfer to initiator
- (c) primary radical termination by combination of polymer and primary radicals.

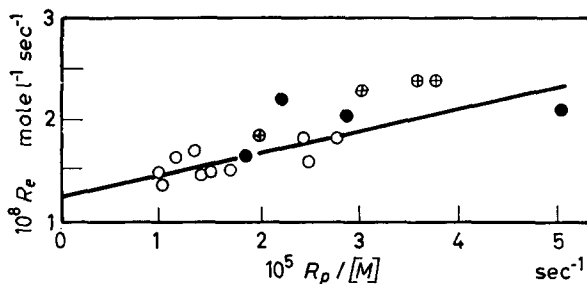


Figure 1—Rate of incorporation of 2-cyano-2-propyl groups plotted against $R_p/[\text{monomer}]$ for polymerizations involving a fixed concentration of azo initiator and various concentrations of di-*t*-butyl peroxide. Concentrations (mole/l.) of styrene: \times 2.3; \circ 3.0; \bullet 4.6

R_e , determined by the tracer technique in this work, is the sum of the rates of these processes for the 2-cyano-2-propyl group. It is probable that primary radical termination can be neglected for the concentrations of monomer and initiator used here, especially as the reaction temperature is quite high so that the importance of this type of termination relative to initiation is decreased¹. The importance of transfer to initiator can be assessed from the results of experiments in which the concentration of the labelled initiator is fixed and that of a second unlabelled initiator is varied². In a set of experiments of this type, the rate of initiation by the labelled initiator is fixed; the differences between the rates of the various polymerizations are caused by differences between the stationary concentrations of growing radicals and these are responsible for differences between the frequencies of transfer to initiator.

For experiments with mixtures of initiators and in which the labelled initiator is unsymmetrical in structure and has only one part labelled

$$R_e = R_i + k_x [\text{labelled initiator}] R_p / k_p [\text{monomer}],$$

where k_x is the velocity constant for reaction of polymer radicals with the molecules of initiator; this velocity constant may be composite corresponding to the various possible types of transfer to initiator. From the slope of the line in *Figure 1*, it is deduced that k_x/k_p is 0.17; from the intercept, the rate of initiation due to initiator at 1.2 mole/l. is 1.30×10^{-8} mole l⁻¹ sec⁻¹. The value of k_x/k_p has been used to calculate values of R_i from those for R_e in *Table 1*. The values of $(R_e - R_i)$ are significant; for the experiments with styrene at 1 mole/l., they range from 0.14×10^{-8} mole l⁻¹ sec⁻¹ for the reaction involving the lowest concentration of initiator to 1.25×10^{-8} mole l⁻¹ sec⁻¹ for that with the highest concentration.

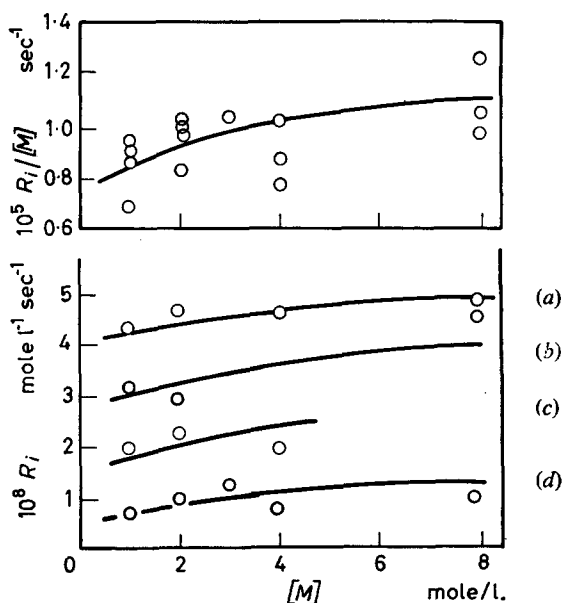


Figure 2—Plots of rate of initiation (R_i) by 2-cyano-2-propyl radicals and $R_i/[\text{initiator}]$ against concentration of monomer. Concentrations (mole/l.) of initiator: a 4.6×10^{-3} ; b 3.6×10^{-3} ; c 2.2×10^{-3} ; d 1.2×10^{-3}

In *Figure 2*, R_i is plotted against concentration of monomer for the various concentrations of initiator; the dependence of $R_i/[\text{initiator}]$ upon the concentration of monomer also is shown. Evidently, the rate of initiation for a given value of $[\text{initiator}]$ does not vary much over the range of monomer concentrations examined. It is concluded that in styrene at 8 mole/l. almost all the available 2-cyano-2-propyl radicals are incorporated

in polymer, and that therefore the velocity constant for the dissociation of the azo compound to available radicals is $1.08 \times 10^{-5} \text{ sec}^{-1}$ at 100°C . If the other radicals produced by dissociation of the azo compound initiate with an efficiency equal to that for the 2-cyano-2-propyl radicals, then the total rate of initiation, $R_{i, \text{total}}$, is given by

$$R_{i, \text{total}} = 2.16 \times 10^{-5} [\text{initiator}] \text{ mole l}^{-1} \text{ sec}^{-1} \text{ for monomer at 8 mole/l.}$$

For a polymerization involving mutual termination of growing centres

$$R_i = 2 k_t R_p^2 / k_p^2 [\text{monomer}]^2$$

In the relationships $R_{i, \text{total}} = K [\text{initiator}]$ and $R_p^2 = K' [\text{initiator}]$, the average values of K are 1.72×10^{-5} , 1.92×10^{-5} , 1.77×10^{-5} and $2.21 \times 10^{-5} \text{ sec}^{-1}$ for monomer concentrations of 1, 2, 4 and 8 mole/l. respectively, and the corresponding values of K' are 0.5×10^{-7} , 2×10^{-7} , 10×10^{-7} and $57 \times 10^{-7} \text{ mole l}^{-1} \text{ sec}^{-2}$. The derived values for k_t/k_p^2 are 172, 192, 142 and 124 $\text{mole l}^{-1} \text{ sec}$. In these calculations, the contributions of the direct initiation, which is responsible for the unsensitized polymerizations, are ignored since the rates of the unsensitized polymerizations were small compared with those recorded here. The derived values of k_t/k_p^2 are reasonable, however, indicating that there are no substantial errors in the derivation of the total rates of initiation in these systems.

We thank Mr S. C. Goadby of Messrs Whiffen and Sons Ltd for information on the preparation of the azo compound.

*Department of Chemistry,
University of Birmingham.*

(Received February 1962)

REFERENCES

- ¹ ALLEN, J. K. and BEVINGTON, J. C. *Trans. Faraday Soc.* 1960, **56**, 1762
- ² BEVINGTON, J. C. and LEWIS, T. D. *Polymer, Lond.* 1961, **1**, 1

Ceiling Temperature and Low Temperature Polymerization

D. HEIKENS and H. GEELEN

From the different temperature gradients of the Gibbs free energies of liquid monomer, crystalline monomer and polymer, conclusions are drawn about the possibility of polymerization of monomer in the different physical states. The ceiling temperature, below which polymerization is feasible, depends on the physical state of the monomer. In general crystallization does not favour polymerization. The picture is not substantially changed by spontaneous mixing of monomer and polymer. The ceiling temperature is then replaced by temperatures of definite intermediate monomer/polymer composition.

SOMETIMES the possibility of polymerization of liquid monomers at low temperatures is discussed in terms of the Gibbs free energy $G = H - TS$. As for certain cases the change in enthalpy upon polymerization is positive or zero, the change in entropy should be positive for spontaneous polymerization to occur. The entropy of liquid monomer is generally larger than that of the polymer so polymerization seems impossible. Then it is proposed that the liquid monomers under consideration should be crystallized so as to lower the entropy and make polymerization possible¹.

Further, a molecular picture is used: in a monomer crystal the molecules stay in an ordered array, ready to polymerize into a polymeric chain^{1,2}. However, as is well known from general principles, a reaction can occur spontaneously if the product (polymer) has a lower free energy than the initial system (monomer). Now at room temperature certain liquid monomers may have lower free energies G than the corresponding polymers and thus they cannot polymerize at this temperature. As the free energy will not change by crystallization of the liquid monomer at the melting point, crystallization alone cannot make polymerization possible. Indeed, the lower entropy S resulting from crystallization is fully compensated for by the loss in enthalpy H .

The problem can be solved by considering that

$$(\partial G / \partial T)_p = -S \quad (1)$$

This relation shows that G will increase with decreasing temperature for both polymer and monomer. As the entropies of the liquid monomers being considered are assumed to be higher than those of their polymers, it may be possible to find low temperatures for which $G_{\text{monomer}} > G_{\text{polymer}}$. The limiting temperature below which polymerization is possible is the well known ceiling temperature T_c , see *Figure 1*. Thus it is not crystallization but a sufficient decrease of temperature which makes polymerization possible.

A complication may arise from the fact that upon cooling certain mono-

mers the freezing point T_f is reached which may be higher than the ceiling temperature, see *Figure 2*. When this happens the G/T line of the polymer will never cross the G/T line of the solid monomer (indicated by s in *Figure 2*) unless at a much lower temperature depending on the S values of polymer and solid monomer.

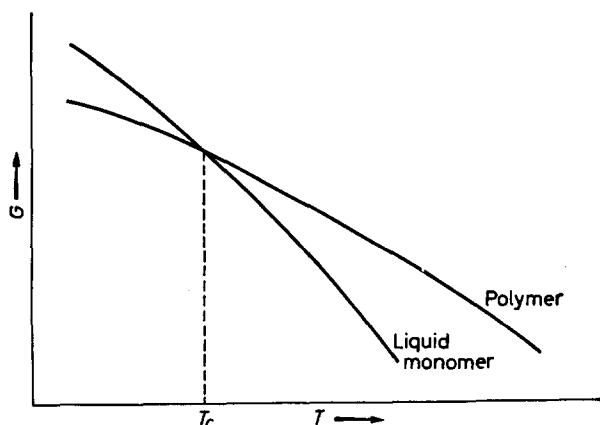


Figure 1—Dependence of Gibbs free energy $G=H-TS$ on T for polymer and liquid monomer. T_c denotes ceiling temperature

So, here, crystallization minimizes the possibility of polymerization. There remains, however, the possibility of polymerization in the under-cooled liquid or glassy state, with values of G indicated by the broken line (*Figure 2*) for temperatures $T < T_c$. In such cases, when heated slowly, a deeply cooled monomer in the glassy state will at a certain temperature crystallize with measurable velocity and reach G values represented by

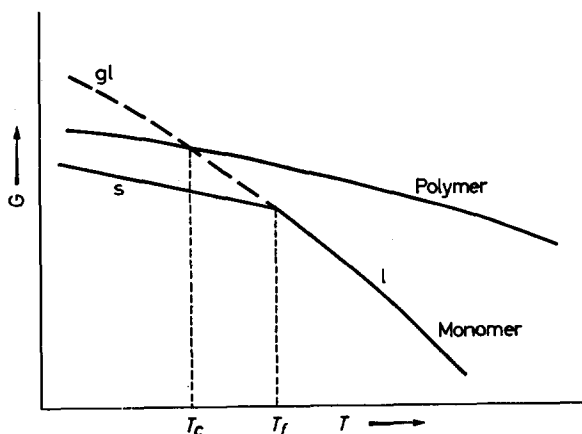


Figure 2—Dependence on temperature of Gibbs free energy of monomer in the liquid (l), solid (s) or glassy (gl) state and of polymer. T_f denotes fusion temperature of monomer. T_c denotes ceiling temperature

the full line of the solid monomer. If, however, sufficient initiator is embedded in the glass, the monomer will polymerize before it can crystallize. This case seems to be met by the polymerization of liquid acetone, which has been described as polymerizing precisely in the way indicated here¹. Again not the crystalline but the (undercooled) liquid monomer with its high free energy G will polymerize.

If in another case the G/T line of the polymer crosses the G/T line of the monomer at a temperature T_c above the freezing point T_f , then both liquid and crystalline monomer can polymerize below the ceiling temperature T_c . Perhaps this case is met by acrylamide in the crystalline state after irradiation at low temperatures³.

One might expect that true polymerization in the crystallized state with its low enthalpy H should exhibit a high activation energy as compared with that for polymerization in the liquid state. Indeed it has been found that acrylamide polymerizes in the crystalline state with an activation energy of 25 kcal, which is high as compared with 7 to 10 kcal for normal vinyl polymerization in the liquid state³ and with -2.47 kcal for isobutylene⁴ between -20° and 120°C .

It should be remarked that the general ideas given will be somewhat changed by the possibility of spontaneous mixing of polymer and liquid monomer which results in a free energy of mixing. Such facts will blur the simple picture somewhat, replacing the ceiling temperature T_c by temperatures of definite intermediate monomer/polymer composition (see *Figure 3*). The shape of the composition/temperature curve will be such that a relatively narrow temperature range will remain, above which virtually no polymer will be present in equilibrium with the monomer⁵.

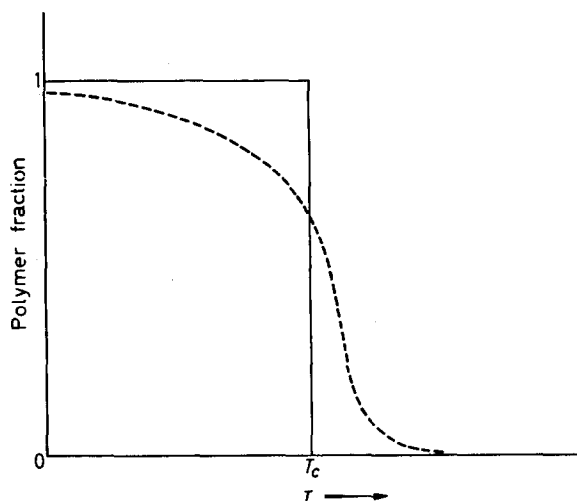


Figure 3—Polymer/monomer composition as a function of temperature. Full line, polymer does not mix with monomer; broken line, polymer and monomer give solutions in the temperature range considered

A possible complication may also arise from partial demixing in different phases.

However, all these possibilities do not facilitate general conclusions on trends.

It should be added that it is dangerous to forecast much about differences in polymerization velocities between crystals and liquids. This will depend strongly on crystal and liquid structure and on the manner of the polymerization⁶.

*Department of Chemical Engineering,
Laboratory for Polymer Chemistry,
Technical University of Eindhoven*

(Received March 1962)

REFERENCES

- ¹ KARGIN, V. A., KABANOV, V. A., ZUBOV, V. P. and PAPISOV, I. M. *Internat. chem. Engng*, 1961, **1**, 17
KARGIN, V. A., KABANOV, V. A., ZUBOV, V. P. and PAPISOV, I. M. *Dokl. Akad. Nauk S.S.S.R.* 1960, **134**, No. 5, 1098
- ² LETORT, M. and PETRY, J. *J. Chim. phys.* 1951, **48**, 594
- ³ FADNER, T. A. and MORAWETZ, H. *J. Polym. Sci.* 1960, **45**, 475
- ⁴ SEMENOV, N. N. *J. Polym. Sci.* 1961, **55**, 563
- ⁵ FLORY, P. J. *Principles of Polymer Chemistry*, p 514. Cornell University Press: New York, 1953
- ⁶ BAMFORD, C. H., EASTMOND, G. C. and WARD, J. C. *Nature, Lond.* 1961, **192**, 1036

Solution and Diffusion in Silicone Rubber *I—A Comparison with Natural Rubber*

R. M. BARRER, J. A. BARRIE and N. K. RAMAN

The diffusion and solubility of n- and iso-butane and of n- and neo-pentane has been studied in the range 30° to 70°C, in polydimethylsiloxane rubbers. The solubilities are very similar to those in natural rubbers and show comparable agreement with the statistical theory of polymer penetrant mixtures. Diffusion coefficients are at least an order of magnitude greater in silicone than in natural rubbers. The very low energy of activation, E_D , of about 4 kcal/mole is almost invariant among the hydrocarbons studied and is the same as for self-diffusion and viscous flow in this rubber. The low value of E_D means that permeabilities of the hydrocarbons increase as the temperature falls. Because diffusion in silicones is less dependent upon molecular size and shape of penetrant than in natural rubber, the silicones are less selective though much more permeable separation barriers.

THE Si—O linkage of the backbone chain of polysiloxanes is the structural feature to which their ease of segmental rotation has been attributed^{1, 2}. The resultant chain flexibility should be reflected in the diffusion properties of penetrants in silicone rubber and, in fact, these rubbers are known to be very permeable^{3, 4}. Solution and diffusion of the isomeric butanes and pentanes in natural rubber was studied earlier⁵, and it was of interest to compare the transport properties of the same hydrocarbons in these two elastomers, in order to measure and interpret the role of chain flexibility. The results are discussed in the present paper.

EXPERIMENTAL

Rubber and gas samples

Polydimethylsiloxane rubber was supplied in sheets approximately 15 cm × 15 cm × 0.2 cm by Imperial Chemical Industries Ltd. The samples contained either 0.1 mole per cent or 1 mole per cent of vinyl groups respectively and were crosslinked with 2,4-dichlorobenzoyl peroxide followed by an oven cure of one hour at 150°C. Prior to use the rubber samples were extracted with boiling acetone for three hours, dried in an oven at 50°C and finally outgassed thoroughly under high vacuum. The densities of the samples were determined by the water displacement method.

The hydrocarbons, *n*- and iso-butane and *n*- and neo-pentane, were Research Grade products supplied by the National Chemical Laboratories, Teddington. They required no further purification.

Apparatus

The solubilities of the hydrocarbons in the rubber were measured in a volumetric sorption system identical with that of Barrer, Barrie and Slater⁶.

The diffusion cell used in the measurement of steady state permeation and time-lag data was also similar but for the modification adopted by Barrie and Platt⁷. In this the membrane was first clamped between a pair of circular stainless steel discs joined together by a set of screws. When the membrane was introduced directly between the faces of the diffusion cell then on tightening the latter pronounced bulging of the membrane resulted. A second set of screws was therefore threaded through the top plate only, until they came in contact with the bottom plate. These served to maintain the distance of separation between the two plates once the unit as a whole was inserted between the faces of the diffusion cell.

RESULTS AND DISCUSSIONS

Solubility

Three sheets of unfilled rubber designated A, B and C were used. Samples A and B were prepared from the same stock and contained respectively 0.1 and 1 mole per cent of vinyl groups. Rubber C was prepared from a separate stock used in the fabrication of the filled sheets and contained 0.1 mole per cent of vinyl groups.

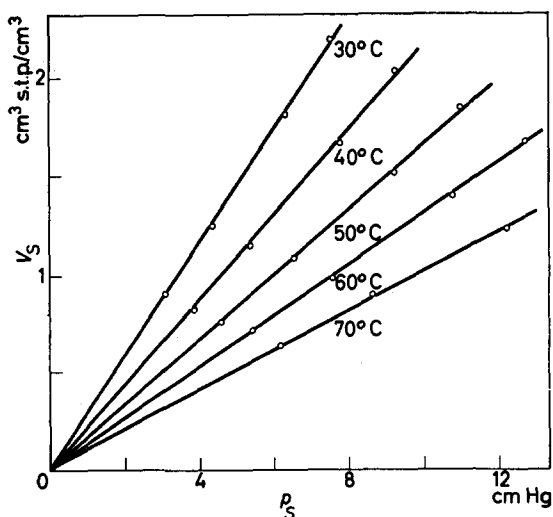


Figure 1—Typical Henry's law isotherms, *n*-butane: rubber B

Sorption isotherms were determined at temperatures of 30°, 40°, 50°, 60° and 70°C for all vapours and rubbers. Henry's law was obeyed in each case (Figure 1) and hysteresis effects were absent. From the slopes of the isotherms the solubility coefficients expressed as cm³ s.t.p. per 1 cm³ of polymer per 1 cm of mercury were calculated and are recorded in Table 1. These values are similar to those* obtained by Aitken and Barrer with natural rubbers⁵. If anything the solubility is slightly greater in the silicones.

*Aitken and Barrer used the solubility σ^s related to $\sigma^s=76\sigma$.

SOLUTION AND DIFFUSION IN SILICONE RUBBER—I

 Table 1. Solubility coefficient, σ (cm³ s.t.p./cm³/cm Hg)

| Substance | 30°C | 40°C | 50°C | 60°C | 70°C |
|--|-------|-------|-------|-------|-------|
| Rubber A | | | | | |
| <i>n</i> -C ₄ H ₁₀ | 0.281 | 0.214 | 0.165 | 0.120 | 0.100 |
| iso-C ₄ H ₁₀ | 0.186 | 0.145 | 0.109 | 0.087 | 0.069 |
| <i>n</i> -C ₅ H ₁₂ | 0.819 | 0.589 | 0.432 | 0.315 | 0.243 |
| neo-C ₅ H ₁₂ | 0.322 | 0.243 | 0.187 | 0.144 | 0.113 |
| Rubber B | | | | | |
| <i>n</i> -C ₄ H ₁₀ | 0.288 | 0.218 | 0.163 | 0.128 | 0.101 |
| iso-C ₄ H ₁₀ | 0.198 | 0.150 | 0.115 | 0.092 | 0.074 |
| <i>n</i> -C ₅ H ₁₂ | 0.839 | 0.597 | 0.437 | 0.320 | 0.247 |
| neo-C ₅ H ₁₂ | 0.339 | 0.253 | 0.194 | 0.147 | 0.116 |
| Rubber C | | | | | |
| <i>n</i> -C ₄ H ₁₀ | 0.295 | 0.227 | 0.171 | 0.135 | 0.107 |
| iso-C ₄ H ₁₀ | 0.199 | 0.153 | 0.119 | 0.093 | 0.070 |
| <i>n</i> -C ₅ H ₁₂ | 0.836 | 0.585 | 0.436 | 0.324 | 0.246 |
| neo-C ₅ H ₁₂ | 0.364 | 0.269 | 0.209 | 0.158 | 0.129 |

As with natural rubber the solubilities of the hydrocarbons decrease exponentially with increasing temperature. Standard partial molar free energies, heats and entropies of solution were calculated from the relations:

$$\overline{\Delta G^0} = -RT \ln \sigma^0$$

$$\overline{\Delta H^0} = RT^2 \partial \ln \sigma^0 / \partial T$$

and

$$\overline{\Delta S^0} = (\overline{\Delta H^0} - \overline{\Delta G^0}) / T$$

respectively and are shown in *Table 2*. These results resemble closely the corresponding data obtained with natural rubber and in both cases *n*-pentane exhibits the greatest value of $\overline{\Delta H^0}$. Presumably the linear addition of a CH₂ group to a hydrocarbon will increase $\overline{\Delta H^0}$ by a fixed amount whereas with non-linear addition the effective contribution to $\overline{\Delta H^0}$ will be less as a result of screening and steric effects. $\overline{\Delta S^0}$ is also greatest for *n*-pentane so that the increase in solubility on the linear addition of a CH₂ group is a result of additional contributions to both $\overline{\Delta H^0}$ and $\overline{\Delta S^0}$.

In *Table 3* are given free energies, heats and entropies of dilution, which refer to the transfer of liquid hydrocarbon to hydrocarbon-rubber mixture with a hydrocarbon weight fraction of 0.01. As for natural rubber $\overline{\Delta S}$ values are large and positive whilst $\overline{\Delta H}$ values are small and positive except for *n*-butane. In *Table 4* are values of $\overline{\Delta S}$ calculated from Flory's equation⁸

$$\overline{\Delta S} = -R [\ln(1 - v_r) + v_r]$$

where v_r is the volume fraction of rubber corresponding to a weight fraction of 0.01. The agreement between these and the experimental values is good except for *n*-butane which gives lower values than the other hydrocarbons in all three silicone rubbers. The values of $\overline{\Delta H}$ in *Table 4* were calculated from the Hildebrand-Scott equation⁹ using a value of 53.3 for the cohesive

Table 2. Standard free energies, heats and entropies of solution at 50°C

| Substance | Rubber A | | | Rubber B | | | Rubber C | | |
|--|-------------------------------------|-------------------------------------|---|-------------------------------------|-------------------------------------|---|-------------------------------------|-------------------------------------|---|
| | $\overline{\Delta G^0}$ cal/mole | $\overline{\Delta H^0}$ cal/mole | $\overline{\Delta S^0}$ cal/mole deg. | $\overline{\Delta G^0}$ cal/mole | $\overline{\Delta H^0}$ cal/mole | $\overline{\Delta S^0}$ cal/mole deg. | $\overline{\Delta G^0}$ cal/mole | $\overline{\Delta H^0}$ cal/mole | $\overline{\Delta S^0}$ cal/mole deg. |
| <i>n</i> -C ₄ H ₁₀ | -1 624 | -5 270 | -11.3 | -1 618 | -5 361 | -11.6 | -1 649 | -5 045 | -10.5 |
| iso-C ₄ H ₁₀ | -1 361 | -5 186 | -11.84 | -1 394 | -5 305 | -12.1 | -1 415 | -5 144 | -11.5 |
| <i>n</i> -C ₃ H ₁₂ | -2 243 | -6 258 | -12.4 | -2 252 | -6 257 | -12.4 | -2 250 | -6 326 | -12.6 |
| neo-C ₃ H ₁₂ | -1 706 | -5 361 | -11.3 | -1 730 | -5 500 | -11.7 | -7 778 | -5 397 | -11.2 |

Table 3. Free energies, heats and entropies of dilution at 50°C

| Substance | Rubber A | | | Rubber B | | | Rubber C | | |
|--|------------------------|------------------------|---|------------------------|------------------------|---|------------------------|------------------------|---|
| | ΔG cal/mole | ΔH cal/mole | $\overline{\Delta S}$ cal/mole deg. | ΔG cal/mole | ΔH cal/mole | $\overline{\Delta S}$ cal/mole deg. | ΔG cal/mole | ΔH cal/mole | $\overline{\Delta S}$ cal/mole deg. |
| <i>n</i> -C ₄ H ₁₀ | -1 895 | -339 | 4.8 | -1 885 | -497 | 4.3 | -1 913 | -350 | 4.8 |
| iso-C ₄ H ₁₀ | -1 750 | 92 | 5.7 | -1 774 | 160 | 5.9 | -1 787 | 146 | 6.0 |
| <i>n</i> -C ₃ H ₁₂ | -1 824 | 83 | 5.9 | -1 825 | 110 | 6.0 | -1 826 | 120 | 6.2 |
| neo-C ₃ H ₁₂ | -1 812 | 181 | 6.2 | -1 816 | 56 | 5.8 | -1 829 | 177 | 6.4 |

energy density of silicone rubber¹⁰. Again reasonable agreement is obtained between theory and experiment with all the hydrocarbons except *n*-butane.

Table 4. Theoretical heats and entropies of dilution and the interaction parameter χ

| Substance | $\overline{\Delta S}$ cal mole ⁻¹ deg ⁻¹ | $\overline{\Delta H}$ cal mole ⁻¹ | χ |
|--|---|---|--------|
| <i>n</i> -C ₄ H ₁₀ | 6.05 | 148 | 0.061 |
| iso-C ₄ H ₁₀ | 5.96 | 310 | 0.220 |
| <i>n</i> -C ₅ H ₁₂ | 6.24 | 57 | 0.298 |
| neo-C ₅ H ₁₂ | 6.12 | 148 | 0.176 |

Values of the interaction parameter obtained from the Flory-Huggins equation⁸ are small and as for natural rubber are less than 0.5 which would indicate that the hydrocarbons are solvents for uncrosslinked silicone rubber.

Silicone rubbers thus differ but little from natural rubber in their solution behaviour towards the isomeric butanes and pentanes and for both rubbers thermodynamic functions calculated from concentrated polymer solution theory compare favourably with the experimental values.

Permeation results

The permeability \overline{P} is defined as the amount of gas in cm³ at s.t.p. passing per second in the steady state through 1 cm² of a membrane 1 cm thick and across which exists a pressure difference of 1 cm of mercury. \overline{P} was measured as a function of ingoing pressure in the range 0 to 6 cm of mercury for all three rubbers at temperatures of 30°, 40°, 50°, 60° and 70°C. Compared with the ingoing pressure, the outgoing pressure was always effectively zero.

With all membranes \overline{P} decreased slightly the higher the ingoing pressure, behaviour which may have been due to effective reduction of the diffusion area by contact with the supporting gauze of the diffusion cell especially at the higher ingoing pressures. To minimize this effect the ingoing pressure was kept as low as possible without decreasing the accuracy of the measurements. The values of \overline{P} recorded in Table 5 are then effectively equal to permeabilities at zero concentration.

As with the solubility the difference in degree of crosslinking between rubbers A and B has little significant effect on the permeability. However, there is a decided difference in permeability between these and rubber C which is not reflected to the same extent in the solubility data. This difference may be attributed to the fact that rubber C was prepared from a different stock which, if it were of a lower average molecular weight, would contain a proportionately larger number of end groups, the presence of which would facilitate the diffusion process.

The permeabilities are about 25 to 40 times larger than the corresponding values for natural rubber. (For comparison with \overline{P} measured by Aitken and Barrer⁵ the values of \overline{P} in Table 5 are to be multiplied by a factor of 10 since these workers referred \overline{P} to 1 mm thickness of membrane.)

Table 5. Permeability coefficients $\bar{P} \times 10^6$

| Substance | 30°C | 40°C | 50°C | 60°C | 70°C |
|--|-------|-------|-------|-------|-------|
| Rubber A | | | | | |
| <i>n</i> -C ₄ H ₁₀ | 1.53 | 1.46 | 1.40 | 1.35 | 1.29 |
| iso-C ₄ H ₁₀ | 0.896 | 0.868 | 0.841 | 0.818 | 0.795 |
| <i>n</i> -C ₅ H ₁₂ | 3.67 | 3.33 | 2.99 | 2.67 | 2.48 |
| neo-C ₅ H ₁₂ | 0.910 | 0.867 | 0.807 | 0.766 | 0.723 |
| Rubber B | | | | | |
| <i>n</i> -C ₄ H ₁₀ | 1.62 | 1.52 | 1.38 | 1.26 | 1.53 |
| iso-C ₄ H ₁₀ | 0.856 | 0.836 | 0.818 | 0.800 | 0.771 |
| <i>n</i> -C ₅ H ₁₂ | 3.95 | 3.51 | 3.12 | 2.80 | 2.51 |
| neo-C ₅ H ₁₂ | 0.944 | 0.910 | 0.847 | 0.809 | 0.773 |
| Rubber C | | | | | |
| <i>n</i> -C ₄ H ₁₀ | 2.05 | 1.96 | 1.87 | 1.79 | 1.71 |
| iso-C ₄ H ₁₀ | 1.14 | 1.12 | 1.09 | 1.06 | 1.05 |
| <i>n</i> -C ₅ H ₁₂ | 5.41 | 4.73 | 4.17 | 3.70 | 3.29 |
| neo-C ₅ H ₁₂ | 1.33 | 1.27 | 1.22 | 1.17 | 1.13 |

Diffusion coefficients

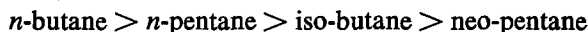
Steady-state and transient-state diffusion coefficients were calculated respectively from the relationships:

$$D_s = \bar{P} / \sigma$$

and

$$D_L = l^2 / 6L$$

where l is the thickness of the membrane and L the time lag¹¹. The values of D_s and D_L for all three rubbers are given in Table 6. With natural rubber the order of decreasing D_s at any given temperature was



which is also observed with rubbers B and C. A significant feature is that the diffusion coefficients for the silicone rubber are greater by an order of

Table 6. Steady-state and transient-state diffusion coefficients $\times 10^6$ (cm² sec⁻¹)

| Substance | 30°C | | 40°C | | 50°C | | 60°C | | 70°C | |
|--|-------|-------|-------|-------|-------|-------|-------|-------|-------|-------|
| | D_s | D_L | D_s | D_L | D_s | D_L | D_s | D_L | D_s | D_L |
| Rubber A | | | | | | | | | | |
| <i>n</i> -C ₄ H ₁₀ | 5.44 | 5.23 | 6.83 | 6.51 | 8.49 | 8.02 | 10.7 | 9.64 | 12.9 | 11.89 |
| iso-C ₄ H ₁₀ | 4.81 | 3.83 | 5.98 | 4.75 | 7.71 | 5.78 | 9.40 | 6.97 | 11.5 | 8.38 |
| <i>n</i> -C ₅ H ₁₂ | 4.48 | 4.36 | 5.65 | 5.58 | 6.92 | 7.03 | 8.48 | 8.78 | 10.2 | 10.9 |
| neo-C ₅ H ₁₂ | 2.83 | 2.49 | 3.53 | 3.06 | 4.32 | 3.72 | 5.32 | 4.43 | 6.40 | 5.95 |
| Rubber B | | | | | | | | | | |
| <i>n</i> -C ₄ H ₁₀ | 6.53 | 5.13 | 8.09 | 5.89 | 9.42 | 6.78 | 11.7 | 8.17 | 14.2 | 9.68 |
| iso-C ₄ H ₁₀ | 4.32 | 3.77 | 5.57 | 4.79 | 7.11 | 6.03 | 8.71 | 7.44 | 10.5 | 9.17 |
| <i>n</i> -C ₅ H ₁₂ | 4.71 | 4.38 | 5.87 | 5.58 | 7.14 | 6.83 | 8.75 | 8.22 | 10.2 | 9.98 |
| neo-C ₅ H ₁₂ | 2.78 | 2.62 | 3.50 | 3.11 | 4.36 | 3.77 | 5.50 | 4.64 | 6.66 | 5.68 |
| Rubber C | | | | | | | | | | |
| <i>n</i> -C ₄ H ₁₀ | 6.96 | 6.52 | 8.62 | 7.94 | 10.9 | 10.2 | 13.2 | 12.2 | 16.0 | 15.3 |
| iso-C ₄ H ₁₀ | 5.71 | 5.11 | 7.32 | 6.45 | 9.15 | 8.02 | 11.4 | 9.82 | 13.7 | 12.0 |
| <i>n</i> -C ₅ H ₁₂ | 6.47 | 5.31 | 8.09 | 6.71 | 9.56 | 8.35 | 11.4 | 10.3 | 13.4 | 12.6 |
| neo-C ₅ H ₁₂ | 3.66 | 2.79 | 4.74 | 3.56 | 5.84 | 4.48 | 7.4 | 5.58 | 8.76 | 6.90 |

magnitude or more. The relatively high permeabilities of silicone rubbers to gases and vapours are to be attributed to large diffusion coefficients since the solubilities of the hydrocarbons are similar in both rubbers. It is also noted that the spread in the values of D for the four hydrocarbons is less with the silicone rubber indicating that the addition of a CH_2 group to the penetrant does not have such a marked effect as with natural rubber.

Agreement between steady-state and transient-state diffusion coefficients is not particularly good and in general D_s values tend to be greater than the corresponding D_L values. This feature has also been observed with the hydrocarbons in natural rubber^{5, 12} but in these studies the differences between D_L and D_s were much less. On the other hand, larger differences between D_s and D_L were observed for diffusion of benzene in filled natural rubber and in partly crystalline polythene¹³.

Temperature dependence of D and \bar{P}

Plots of $\log D_s$ versus $1/T$ exhibited only very slight curvature so that both E_D and D_0 in the Arrhenius equation $D_s = D_0 \exp(-E_D/RT)$, were regarded as temperature independent in the range investigated. Values of these parameters are given in *Table 7*. From self-diffusion studies with polydimethylsiloxanes containing from one to nine dimethylsiloxane groups the

Table 7. Values of E_D (cal mole⁻¹) and D_0 (cm² sec⁻¹)

| Substance | Rubber A | | Rubber B | | Rubber C | |
|--|----------|-------|----------|-------|----------|-------|
| | E_D | D_0 | E_D | D_0 | E_D | D_0 |
| <i>n</i> -C ₄ H ₁₀ | 4 200 | 49 | 3 800 | 131 | 4 300 | 82 |
| iso-C ₄ H ₁₀ | 4 000 | 17 | 4 500 | 131 | 4 400 | 89 |
| <i>n</i> -C ₅ H ₁₂ | 4 300 | 64 | 3 900 | 43 | 3 700 | 105 |
| neo-C ₅ H ₁₂ | 4 200 | 24 | 4 000 | 72 | 4 500 | 93 |

apparent energy of activation for self-diffusion was obtained as a function of chain length¹⁴. A limiting value of approximately 4 kcal was approached as the length of the chain was increased, in good agreement with the values of *Table 7*. Moreover, the same energy of activation (4 kcal) has recently been established for viscous flow of a dimethylsiloxane rubber¹⁵. The identity of E among these several rate processes provides excellent support of the zone theory¹⁶ of diffusion of the hydrocarbons in silicone rubber. According to this theory the energy of activation is distributed over a zone of rubber segments within which is contained the penetrant molecule. The activation energy is available through local thermal energy fluctuations, and unit acts of penetrant diffusion or of self-diffusion or viscous flow of polymer are then the similar results of the more vigorous Brownian motions of the polymer segments in the zones of activation.

The high permeabilities of these rubbers can now be traced to extremely low energies of activation for diffusion, a reflection of the comparative ease of segmental motions in these rubbers. The values of E_D for natural rubber are from two to three times as large, indicating a much higher internal viscosity.

In *Figure 2* the results for both the natural⁵ and silicone rubbers are plotted as $\log D_0$ versus E_D/T . The points for silicone rubber lie above and

apart from the mean curve through the points for natural rubber and it is also seen that the spread in both D_0 and E_D is very much less than for the natural rubber. Thus penetrant size and shape are less important factors in determining E_D and D_0 for silicone than for natural rubber. According to the zone theory of diffusion the zone of activation is larger the larger E_D/T . On this basis diffusion in silicone rubber requires the cooperative movement of a smaller number of polymer segments than in natural rubber, presumably the outcome of the greater chain flexibility.

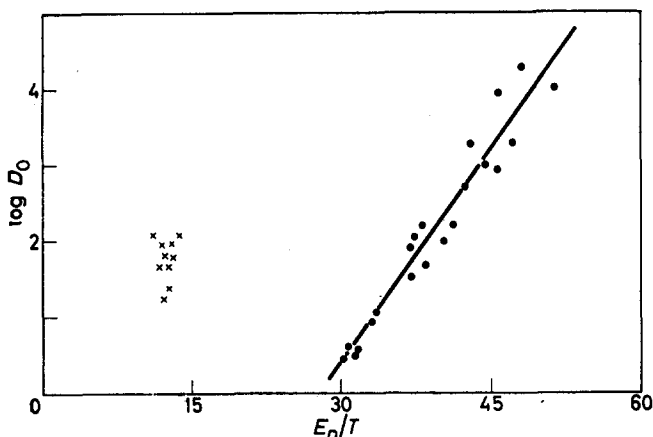


Figure 2—Log D_0 versus E_D/T . ●—natural rubber; ×—silicone rubber

The low energies of activation for diffusion lead to another interesting difference between the temperature coefficients of permeation for the two rubbers. For both systems plots of $\log \bar{P}$ versus $1/T$ are linear but whereas the permeability decreases with increasing temperature for silicone rubber, a corresponding increase is observed for natural rubber. This distinction arises because of the relative magnitudes of ΔH^0 and E_D in the two systems, since if $\bar{P} = \bar{P}_0 \exp(-E_P/RT)$ then $E_P = E_D + \Delta H^0$.

Gas separation factors

In Table 8 are shown ratios of the steady-state permeabilities for each pair of isomers in rubber C. Values for natural rubber are given in parentheses. The natural rubber shows higher fractionation factors, being more sensitive to penetrant shape and size. However, this advantage could

Table 8. Separation factors for silicone and natural rubbers

| Temperature | 30°C | 40°C | 50°C | 60°C |
|---------------------------|-------|-------|-------|-------|
| $\bar{P}_{n-C_4H_{10}}$ | 1.8 | 1.7 | 1.7 | 1.7 |
| $\bar{P}_{iso-C_4H_{10}}$ | (2.3) | (2.2) | (2.2) | (2.1) |
| $\bar{P}_{n-C_5H_{12}}$ | 4.1 | 3.7 | 3.4 | 3.2 |
| $\bar{P}_{neo-C_5H_{12}}$ | (8.7) | (7.8) | (6.5) | (5.4) |

()—values for natural rubber.

be more than offset by the much greater permeation rate through the silicone barriers. The difference between the separation factors becomes less the higher the temperature, the natural rubber chains presumably becoming proportionately more flexible.

CONCLUSION

This comparison of the solution and diffusion data for the hydrocarbon vapours in silicone and natural rubber has indicated the following main features:

(a) Both rubbers are similar as solvent media towards the paraffins studied.

(b) The relative ease of segmental rotation about the Si-O linkage is reflected in low energies of activation for diffusion in silicone rubber. As a result diffusion coefficients and permeabilities of the hydrocarbons are an order of magnitude greater than in natural rubber.

(c) The standard partial molar heat of solution $\bar{\Delta}H^\circ$ is numerically larger than E_D for silicone rubber and smaller for natural rubber. As a result permeabilities decrease with increasing temperature for the former and increase for the latter.

(d) Diffusion in silicone rubber is less sensitive to size and shape of the penetrant molecule, and thus silicone rubber is less selective than natural rubber as a separation medium.

One of us (N.K.R.) is indebted to I.C.I. (Plastics) for a scholarship which enabled him to take part in the work described in this and in the following paper (Part II).

*Physical Chemistry Laboratories,
Chemistry Dept, Imperial College,
South Kensington, London, S.W.7*

(Received March 1962)

REFERENCES

- ¹ ROTH, W. L. and HARKER, D. *Acta. cryst.*, Camb. 1948, **1**, 34
- ² SCOTT, D. W. *J. Amer. chem. Soc.* 1946, **68**, 1877
- ³ KAMMERMEYER, K. *Industr. Engng Chem. (Industr.)*, 1957, **49**, 1685
- ⁴ REITLINGER, S. A., MASLENNIKOVA, A. A. and TARKHO, I. S. *Soviet phys.-tech. Phys.* 1956, **1**, 2467 (English translation)
- ⁵ AITKEN, A. and BARRER, R. M. *Trans. Faraday Soc.* 1955, **51**, 116
- ⁶ BARRER, R. M., BARRIE, J. A. and SLATER, J. J. *Polym. Sci.* 1958, **28**, 177
- ⁷ BARRIE, J. A. and PLATT, B. J. *Polym. Sci.* 1961, **49**, 479
- ⁸ FLORY, P. J. *Principles of Polymer Chemistry*. Cornell University Press: New York, 1953
- ⁹ HILDEBRAND, J. H. and SCOTT, R. L. *Solubility of Non-electrolytes*. Reinhold: New York, 1950
- ¹⁰ BURRELL, H. *Interchemical Reviews*, 1955, **14**, 3
- ¹¹ BARRER, R. M. *Trans. Faraday Soc.* 1939, **35**, 629
- ¹² BARRIE, J. A. and PLATT, B. J. *Polym. Sci.* 1961, **54**, 261
- ¹³ BARRER, R. M. and FERGUSSON, R. R. *Trans. Faraday Soc.* 1958, **54**, 989
- ¹⁴ MCCALL, D. W., ANDERSON, E. W. and HUGGINS, C. M. *J. chem. Phys.* 1961, **34**, 804
- ¹⁵ GARDNER, J. C. *Ph.D. Thesis*, University of Manchester, 1961
- ¹⁶ BARRER, R. M. *Trans. Faraday Soc.* 1942, **38**, 322; 1943, **38**, 48

Solution and Diffusion in Silicone Rubber

II—The Influence of Fillers

R. M. BARRER, J. A. BARRIE and N. K. RAMAN

An investigation has been made of the effect of a high area silica filler upon the solubility and diffusion of some C₄ and C₅ paraffins in silicone rubbers. The membranes studied contained by weight 0, 10, 20, 30 and 40 parts of filler per 100 parts of polymer. The solubilities have been discussed in terms of two reference models: the first in which silica and rubber phases act independently as sorbents; and the second in which the filler is regarded as completely wetted by polymer and is thus a non-sorbent. Diffusion and permeation have also been considered in terms of the models, assuming with the first model an immobile sorbed layer on the porous silica. It has been found that, although some aspects of the behaviour can be explained, the results are not fully in agreement with either model, and that the behaviour of the heterogeneous membrane is complex.

THE interpretation of the physical properties of heterogeneous media (in which a phase A is dispersed in a continuum of phase B) in terms of the properties of pure A and B, is an outstanding problem of great importance in such related fields as mass flow, heat flow, electrical conduction, dielectric constant and magnetic permeability¹. Diffusion in filled rubbers or in semicrystalline polymers is clearly in this category, although relatively few extensive diffusion studies^{2-4, 6} have so far been made in such media. Accordingly, in order to investigate more fully the role of filler in silicone rubbers of known⁵ diffusion characteristics, a study was made of solubility and permeation of hydrocarbon penetrants in various silica-filled rubbers.

EXPERIMENTAL

Materials

The filled silicone rubbers used were of the same type as described in Part I⁵, and contained respectively 10, 20, 30 and 40 parts by weight of Santocel CS, a relatively porous amorphous form of silica, to 100 parts of polymer. All the filled rubbers had 0.1 mole per cent of vinyl groups and were crosslinked using di-*t*-butyl peroxide. The hydrocarbons used as diffusants were *n*- and iso-butane and *n*- and neo-pentane of Research Grade, supplied by the National Chemical Laboratories.

Apparatus

The apparatus and diffusion cells have been briefly described in Part I.

Volume fraction of filler

For the silica filler a ET surface area of 114 m²/g was obtained with nitrogen at 90°K indicating an appreciable internal surface consistent with

a porous material. The high pressure region of an oxygen isotherm at 77°K is shown in *Figure 1*; hysteresis was not detected above $p/p_0 \sim 0.8$. With a desorption loop of this nature it is not possible to separate with any degree of certainty inter-particle from intra-particle capillary sorption. For a rough estimate of the porosity it was assumed that intra-particle desorption commenced at 75 cm³ s.t.p. per gramme which corresponds to 0.089 cm³ of liquid oxygen per gramme of powder. With a density of 2.22 for silica, an average density of 1.85 was obtained for the powder.

Another procedure adopted was to pump rapidly from a known weight of the powder for a short time to remove all air without causing appreciable loss of water from the intra-particle capillaries. Water was then admitted to the evacuated bulb, the volume of which was known, and the volume of displaced water obtained. The average of three measurements, in one of which outgassing was carried out at 0°C, gave a density of 1.66 ± 0.03 g/cm³. Initially the capillaries are not likely to be completely filled with water and the above value may be somewhat high. As a check on the procedure, a sample was thoroughly outgassed at 100°C and a density of 2.22 was obtained in good agreement with literature values for non-porous silica.

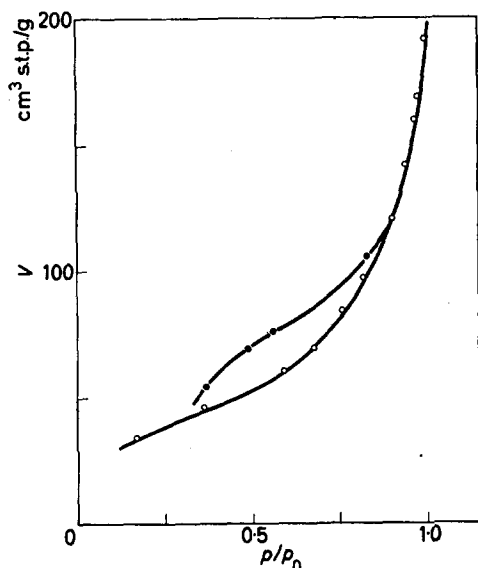


Figure 1—Oxygen isotherm at 77°K for silica filler. ○—sorption; ●—desorption

Assuming additivity of volumes of filler and rubber phases, and with densities of 1.66 and 0.974 for the filler and polymer respectively, values of λ_f , the volume fraction of filler, were calculated as given in *Table 1*. Sheets D, E, F and G contained respectively 10, 20, 30 and 40 parts filler

Table 1. Volume fraction of filler, λ_f

| C | D | E | F | G |
|---|-------|-------|-------|-------|
| 0 | 0.056 | 0.106 | 0.149 | 0.191 |

per 100 parts of rubber stock. For a comparison with unfilled rubber, sheet C was used (Part I), as this and all filled sheets were made from a common gum stock.

RESULTS AND DISCUSSION

Sorption of hydrocarbons by filler

To further the analysis of the sorption and diffusion results the sorption of hydrocarbons on the bulk filler was measured at 30°C and 50°C. Some typical sorption isotherms are shown in *Figure 2*. The *n*-butane and neo-

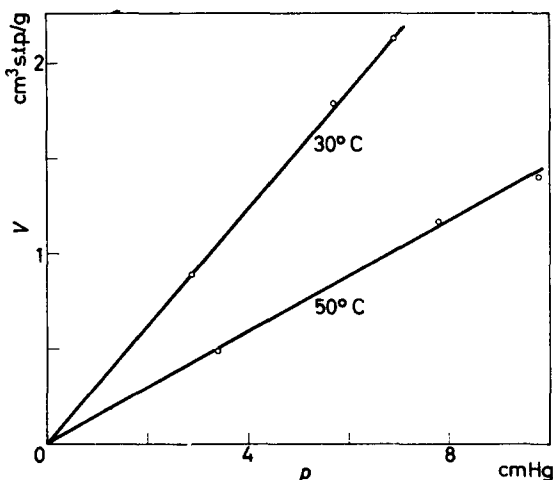


Figure 2—Sorption isotherms for *n*-pentane on silica filler

pentane isotherms exhibited some curvature at the higher pressures. Sorption coefficients σ_f (cm^3 s.t.p. per 1 cm^3 of filler per cm of mercury) were calculated from the initial linear regions of the isotherms. Values of σ_f at 30°C and 50°C are given in *Table 2* along with the standard partial molar heat of sorption $\overline{\Delta H}_f^\circ$. The sorption coefficients and heats of sorption are comparable with the corresponding data for the unfilled rubber.

Table 2. Sorption coefficient σ_f and $\overline{\Delta H}_f^\circ$

| Substance | 30°C | 50°C | $\overline{\Delta H}_f^\circ$ cal/mole |
|--|-------|-------|---|
| <i>n</i> -C ₄ H ₁₀ | 0.216 | 0.102 | -7 300 |
| <i>n</i> -C ₄ H ₁₀ | 0.535 | 0.242 | -7 700 |
| neo-C ₅ H ₁₂ | 0.343 | 0.165 | -7 100 |

Solution in filled rubber

As with the unfilled rubber Henry's law sorption isotherms were obtained with all rubbers at temperatures of 30°, 40°, 50°, 60° and 70°C (*Figure 3*).

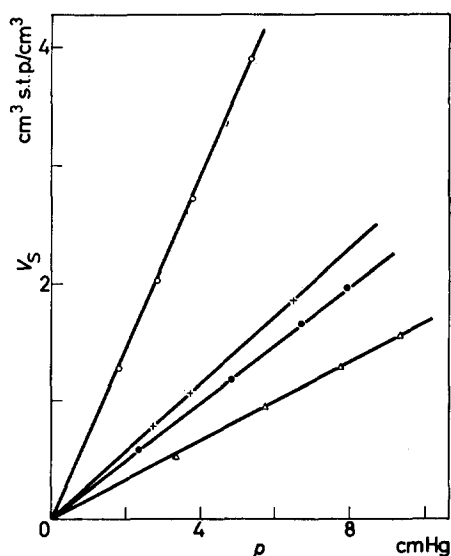


Figure 3—Henry's law isotherms for rubber F. \circ —*n*-pentane, \bullet —*n*-butane, \times —neo-pentane, \triangle —iso-butane

To compare the results for the filled and unfilled rubber a percentage difference in solubility was defined by

$$\nabla\sigma = (1 - \sigma/\sigma_r) 100$$

where σ and σ_r denote respectively the solubilities in filled and unfilled rubber. The values of $\nabla\sigma$ are given in *Table 3* and are accurate to within ± 3 .

Table 3. Percentage difference in solubility, $\nabla\sigma$

| Substance | 30°C | 40°C | 50°C | 60°C | 70°C |
|--|------|------|------|------|------|
| Rubber D ($\lambda_f = 0.056$) | | | | | |
| <i>n</i> -C ₄ H ₁₀ | 6.1 | 8.8 | 7.0 | 7.4 | 9.4 |
| iso-C ₄ H ₁₀ | 6.0 | 7.8 | 8.4 | 9.0 | — |
| <i>n</i> -C ₅ H ₁₂ | 3.2 | 1.5 | 4.4 | 5.6 | 6.9 |
| neo-C ₅ H ₁₂ | 12.3 | 13.0 | 13.4 | 10.8 | 14.0 |
| Rubber E ($\lambda_f = 0.106$) | | | | | |
| <i>n</i> -C ₄ H ₁₀ | 9.8 | 10.6 | 8.8 | 9.7 | 10.3 |
| iso-C ₄ H ₁₀ | 8.6 | 8.5 | 8.5 | 6.5 | 10.4 |
| <i>n</i> -C ₅ H ₁₂ | 10.2 | 8.9 | 9.0 | 9.9 | 9.4 |
| neo-C ₅ H ₁₂ | 14.3 | 13.8 | 16.7 | 13.3 | 17.1 |
| Rubber F ($\lambda_f = 0.149$) | | | | | |
| <i>n</i> -C ₄ H ₁₀ | 16.3 | 19.4 | 17.6 | 18.6 | 18.7 |
| iso-C ₄ H ₁₀ | 15.6 | 17.0 | 16.8 | 16.1 | 18.2 |
| <i>n</i> -C ₅ H ₁₂ | 13.6 | 13.0 | 14.3 | 16.1 | 15.0 |
| neo-C ₅ H ₁₂ | 20.3 | 20.5 | 23.0 | 22.2 | 24.9 |
| Rubber G ($\lambda_f = 0.191$) | | | | | |
| <i>n</i> -C ₄ H ₁₀ | 17.6 | 16.3 | 19.3 | 19.3 | 20.0 |
| iso-C ₄ H ₁₀ | 14.4 | 13.7 | 16.5 | 16.4 | 18.3 |
| <i>n</i> -C ₅ H ₁₂ | 14.4 | 13.7 | 16.5 | 16.4 | 18.3 |
| neo-C ₅ H ₁₂ | 21.8 | 21.2 | 24.0 | 20.3 | 23.3 |

Before discussing these results it is of interest to consider the possible role of filler particles in the solution process. As one reference model the filler and rubber phases may be regarded as independent so that for the solubility of the filled rubber one can write

$$\sigma = \lambda_r \sigma_r + \lambda_f \sigma_f \quad (1)$$

where σ_r and σ_f denote respectively the solubility and sorption coefficient of unfilled rubber and of bulk filler. The volume fractions of the respective phases are λ_r and λ_f . If the polymer completely wets the filler surface to the exclusion of hydrocarbon then equation (1) can be reduced to a second reference model

$$\sigma = \lambda_r \sigma_r \quad (2)$$

Plots of the solubility σ versus λ_f are shown in *Figure 4* for several of the hydrocarbons and on the whole the results are seen to be best fitted by

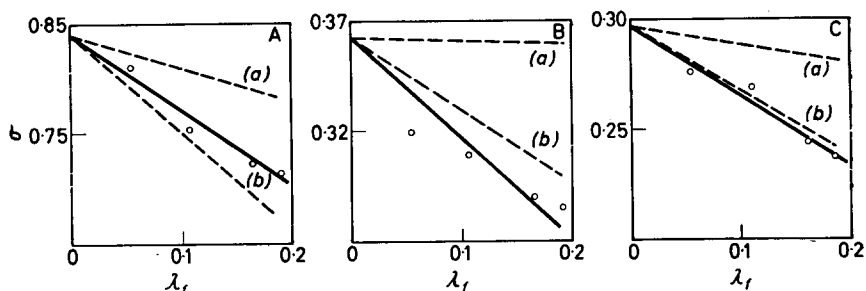


Figure 4—Solubility versus volume fraction of filler at 30°C. A—*n*-pentane, B—neo-pentane, C—*n*-butane, (a)—equation (1), (b)—equation (2)

equation (2). An examination of the data of *Table 3* leads to the same conclusion.

Thus using equations (1) and (2) the following expressions are obtained respectively for $\nabla\sigma$:

$$\nabla\sigma = (1 - \lambda_r) (1 - \sigma_f/\sigma_r) 100 \quad (3)$$

and

$$\nabla\sigma = (1 - \lambda_r) 100 \quad (4)$$

Reasonable numerical agreement is obtained with equation (4). There are, however, two other features worthy of examination. First, there is a tendency for $\nabla\sigma$ to increase with temperature which is consistent with the model on which equation (3) is based but not with that leading to equation (4). In *Table 4* are given values of $\nabla\sigma$ at 30°C and 50°C calculated using

Table 4. $\nabla\sigma$ from equation (3)

| Substance | Rubber D | | Rubber E | | Rubber F | | Rubber G | |
|--|----------|------|----------|------|----------|------|----------|------|
| | 30°C | 50°C | 30°C | 50°C | 30°C | 50°C | 30°C | 50°C |
| <i>n</i> -C ₄ H ₁₀ | 1.5 | 2.3 | 2.8 | 4.3 | 4.0 | 6.0 | 5.1 | 7.7 |
| <i>n</i> -C ₅ H ₁₂ | 2.0 | 2.5 | 3.8 | 4.7 | 5.4 | 6.7 | 6.9 | 8.5 |
| neo-C ₅ H ₁₂ | 0.32 | 1.2 | 0.6 | 2.2 | 0.9 | 3.1 | 1.1 | 4.0 |

equation (3). These values show the observed increase in $\nabla\sigma$ with temperature but the numerical agreement with experimental values of $\nabla\sigma$ is now very poor. However, this is not surprising as σ_j for the bulk filler is in all probability much higher than the sorption coefficient of the filler in the rubber since the filler must be at least partly wetted by the polymer.

Secondly, values of $\nabla\sigma$ for neo-pentane are in general somewhat larger than those for the other hydrocarbons and indeed are even slightly greater than values calculated from equation (4). However, this may be due to uncertainty in the density of the silica filler, taken as 1.66.

Permeation and diffusion in filled rubber

For steady-state and transient-state diffusion coefficients the order of the series, *n*-butane > *n*-pentane > iso-butane > neo-pentane was unaffected by the presence of filler. Plots of $\log D_s$ versus $1/T$ were linear and values of the activation energy for diffusion are given in Table 5. Within experimental error the filler does not appear to have any marked effect on E_D (cf. Part I, Table 7). Since the standard partial molar heat of solution was not significantly altered by the presence of filler the temperature coefficient of permeation was also unchanged and negative, so that permeability decreased with increasing temperature as for the unfilled rubber.

To facilitate a comparison of the results with those for unfilled rubber, percentage differences were defined for the permeability, steady- and transient-state diffusion coefficients in the same way as for the solubility. For example, the percentage difference in the permeability is given by

$$\nabla\bar{P} = (1 - \bar{P}/P_A) 100$$

where the subscript A denotes unfilled rubber, in this case rubber C.

Table 5. Activation energies for diffusion, E_D cal/mole

| Substance | Rubber D | Rubber E | Rubber F | Rubber G |
|--|----------|----------|----------|----------|
| <i>n</i> -C ₄ H ₁₀ | 4 000 | 3 700 | 3 400 | 3 700 |
| iso-C ₄ H ₁₀ | 4 100 | 4 300 | 3 900 | — |
| <i>n</i> -C ₅ H ₁₂ | 3 900 | 3 700 | 3 900 | 3 500 |
| neo-C ₅ H ₁₂ | 4 700 | 4 200 | 4 600 | 3 700 |

Values of the percentage differences $\nabla\bar{P}$, ∇D_s and ∇D_L are given in Table 6. The permeability differences are accurate to within ± 5 and the diffusion coefficient differences to within ± 8 . Inspection of the data reveals the following trends:

- Values of $\nabla\bar{P}$ are larger than those for the corresponding ∇D_s
- ∇D_L is usually larger than the corresponding ∇D_s
- $\nabla\bar{P}$ and ∇D_s increase slightly with temperature
- At a given temperature $\nabla\bar{P}$, and to a lesser extent ∇D_s and ∇D_L , increase with size of penetrant.

Role of filler in permeation

A dispersion of filler in a rubber matrix represents a complex heterogeneous medium for which an exact solution of the diffusion equation has

SOLUTION AND DIFFUSION IN SILICONE RUBBER—II

Table 6. Percentage differences in permeabilities and diffusion coefficients

| T°C | n-C ₄ H ₁₀ | | | iso-C ₄ H ₁₀ | | | n-C ₅ H ₁₂ | | | neo-C ₅ H ₁₂ | | |
|-----------------|----------------------------------|--------------|--------------|------------------------------------|--------------|--------------|----------------------------------|--------------|--------------|------------------------------------|--------------|--------------|
| | $\nabla \bar{P}$ | ∇D_S | ∇D_L | $\nabla \bar{P}$ | ∇D_S | ∇D_L | $\nabla \bar{P}$ | ∇D_S | ∇D_L | $\nabla \bar{P}$ | ∇D_S | ∇D_L |
| Rubber D | | | | | | | | | | | | |
| 30 | 12 | 6.0 | 20 | 15.0 | 7.0 | 28 | 19 | 16 | 16 | 31 | 21 | 13 |
| 40 | 14 | 8.0 | 26 | 16.0 | 9.0 | 36 | 21 | 20 | 18 | 30 | 20 | 19 |
| 50 | 16 | — | 34 | 16.0 | 9.0 | 42 | 22 | 19 | 20 | 30 | 19 | 24 |
| 60 | 18 | 4.0 | 38 | 22.0 | 15.0 | 36 | 22 | 18 | 22 | 29 | 20 | 30 |
| 70 | 20 | 7.0 | 37 | 25.0 | 13.0 | 35 | 25 | 19 | 23 | 29 | 17 | 32 |
| Rubber E | | | | | | | | | | | | |
| 30 | 29 | 22 | 23 | 35 | 29 | 31 | 37 | 30 | — | 42 | 32 | — |
| 40 | 32 | 24 | — | 37 | 31 | — | 38 | 34 | — | 42 | 33 | — |
| 50 | 34 | 28 | — | 37 | 31 | — | 37 | 31 | 31 | 42 | 31 | — |
| 60 | 37 | 30 | — | 37 | 33 | 39 | 37 | 30 | 36 | 42 | 34 | — |
| 70 | 38 | 31 | — | 39 | 32 | 41 | 37 | 30 | 41 | 47 | 36 | — |
| Rubber F | | | | | | | | | | | | |
| 30 | 35 | 23 | 32 | 36 | 24 | 47 | 40 | 30 | 43 | 46 | 33 | 33 |
| 40 | 40 | 25 | 35 | 39 | 26 | 43 | 40 | 30 | 38 | 47 | 33 | 40 |
| 50 | 41 | 28 | 37 | 41 | 29 | 43 | 42 | 33 | 39 | 46 | 31 | 45 |
| 60 | 43 | 31 | 41 | 43 | 32 | 47 | 44 | 34 | 48 | 47 | 32 | 51 |
| 70 | 47 | 35 | 47 | 39 | 33 | 52 | 45 | 36 | 48 | 48 | 31 | 53 |
| Rubber G | | | | | | | | | | | | |
| 30 | 40 | 26 | 32 | — | — | — | 41 | 31 | 40 | 46 | 31 | 40 |
| 40 | 43 | 32 | 34 | — | — | — | 41 | 32 | 48 | 49 | 35 | 39 |
| 50 | 46 | 30 | 45 | — | — | — | 43 | 31 | 53 | 50 | 35 | 46 |
| 60 | 46 | 33 | 44 | — | — | — | 44 | 33 | 60 | 53 | 41 | — |
| 70 | 47 | 34 | 52 | — | — | — | 46 | 33 | 61 | 55 | 41 | — |

not been given. Instead, it is usual to modify the corresponding equations for flow through homogeneous media by the introduction of suitable structure factors. This approach has had a reasonable degree of success in interpreting flow in semicrystalline polymers^{6, 3, 4}.

For the filled rubber one may write for the flux J per unit area of the geometrical cross section

$$J = -D_A \lambda_r \kappa \partial C_r / \partial x \quad (5)$$

where D_A is the diffusion coefficient in the rubber phase and is assumed equal to that for the unfilled rubber. The concentration of penetrant in the rubber phase is C_r , and λ_r , the volume fraction of rubber, is a measure of the geometrical cross section occupied by the rubber phase. It is assumed that surface or gas phase fluxes on or in the filler particles are absent. The structure factor κ allows for the fact that the average diffusion path length is increased by the presence of filler particles and the localized direction of flow is in general not normal to the geometrical cross section of the membrane. The experimentally measured steady-state flux per unit area is $-D_S \partial C / \partial x$ where C the concentration of penetrant is referred to unit volume of the filled rubber and can be expressed as

$$C = \lambda_r C_r + \lambda_f C_f \quad (6)$$

C_f is the concentration of penetrant referred to unit volume of filler. Since $C_f = \sigma_f \rho$ and $C_r = \sigma_r \rho$ it follows that

$$C = (\lambda_r + \lambda_f \sigma_f / \sigma_r) C_r \quad (7)$$

Equating the experimental flux with that of equation (5) one has

$$D_s = \kappa D_A \frac{\lambda_r}{\lambda_r + \lambda_j \sigma_j / \sigma_r} \quad (8)$$

which for zero sorption by filler can be reduced to

$$D_s = \kappa D_A \quad (9)$$

Equations (8) and (9) also hold for transient state flow, although in general the structure factor κ will be different because the possibility exists of part of the rubber phase not contributing to the steady state of flow. However, this fraction which may be termed 'dead volume' will contribute to the establishment of the steady state, in that equilibrium must be set up between it and the main flow space. The quantity $-D_A \partial C_r / \partial x$ represents the flux per unit area of unfilled rubber, and hence it follows that

$$\bar{P} = \kappa \lambda_r \bar{P}_A \quad (10)$$

irrespective of whether the gas is sorbed by the filler, provided that if sorption does occur the molecules are immobile on the filler surface.

Expressions for the percentage differences in permeabilities and diffusion coefficients follow and are respectively:

$$\nabla \bar{P} = (1 - \kappa \lambda_r) 100 \quad (11)$$

and

$$\nabla D_s = \left[1 - \frac{\kappa \lambda_r}{(\lambda_r + \lambda_j \sigma_j / \sigma_r)} \right] 100 \quad (12)$$

for immobile sorption by filler, and

$$\nabla D_s = (1 - \kappa) 100 \quad (13)$$

for zero sorption by filler.

The percentage differences in permeabilities and diffusion coefficients

It is clear from equations (11), (12) and (13) that as κ and λ_r are both less than unity $\nabla \bar{P}$ will in general be greater than ∇D_s , but as the ratio σ_j / σ_r approaches unity ∇D_s will equal $\nabla \bar{P}$ and for higher ratios will ultimately become larger than $\nabla \bar{P}$. However, even assuming independent sorption by filler and rubber phases the ratio σ_j / σ_r is less than unity for all hydrocarbons and rubbers investigated so that it is to be expected that $\nabla \bar{P}$ will be greater than ∇D_s .

The model does not allow for any differences between ∇D_s and ∇D_L . The fact that ∇D_L is in general larger than ∇D_s must be attributed to slightly different structure factors for the transient- and steady-state flows.

To consider the model on a more quantitative basis it is necessary to obtain an estimate of the structure factor κ . Several relationships have been presented relating the conductivity of heterogeneous conductors, consisting of dispersions of small particles in a medium of different conductivity,

to the conductivity of the homogeneous continuous phase⁷. These expressions are applicable to the corresponding diffusion problem. For the range of filler content covered by the silicone rubbers Rayleigh's expression⁸ for a dispersion of non-conducting spheres in a continuum may be regarded as sufficiently accurate. For the steady state of flow this can be expressed in the form

$$\kappa = \frac{1}{\lambda_r} \left[\frac{2 - 2\lambda_f - 0.394\lambda_f^{10/3}}{2 + \lambda_f - 0.394\lambda_f^{10/3}} \right] \quad (14)$$

Values of κ calculated from equation (14) at volume fractions corresponding to those of the rubber phase in the different rubbers are given in *Table 7*. The corresponding values of $(1 - \kappa) 100$ and $(1 - \kappa\lambda_r) 100$ are also included

Table 7. The structure factor from Rayleigh's equation

| Factor | Rubber D | Rubber E | Rubber F | Rubber G |
|-----------------------------|----------|----------|----------|----------|
| λ_r | 0.944 | 0.894 | 0.857 | 0.809 |
| κ | 0.972 | 0.949 | 0.931 | 0.913 |
| $(1 - \kappa) 100$ | 2.8 | 5.1 | 6.9 | 8.7 |
| $(1 - \kappa\lambda_r) 100$ | 8.2 | 15.2 | 20.8 | 26.1 |

and may be compared with the data of *Table 6*. The $\nabla\bar{P}$ values are definitely larger than the corresponding $(1 - \kappa\lambda_r) 100$. Similarly ∇D_s is larger than $(1 - \kappa) 100$ and more nearly equal to $(1 - \kappa\lambda_r) 100$. According to the model ∇D_s can in fact equal the latter factor if $\sigma_f = \sigma_r$. However, the solubility data are certainly not consistent with completely independent sorption by filler and rubber. Further, sorption by the filler cannot account for $\nabla\bar{P}$ values larger than $(1 - \kappa) 100$ since $\nabla\bar{P}$ is not affected by immobile sorption on the filler. For non-spherical particles lower structure factors are obtained, in fact for lamellar particles the structure factor κ may be reduced considerably⁹. Melikhova, Reitlinger and Kuzina¹⁰ found that mica or aluminium powder fillers were relatively more effective in reducing the flow of nitrogen through rubber vulcanizates. A lower structure factor for the silicone rubbers would in fact account for the differences between observed and calculated values of ∇D_s and $\nabla\bar{P}$.

If the trends in $\nabla\bar{P}$ and ∇D_s with temperature and size of penetrant are to be regarded as significant then the simple model must be modified. It is perhaps significant that exactly the same trends are present in the solubility data but to a less marked extent. This would suggest that the 'blind pore' volume associated with the filler is to a limited extent a function of the size of the penetrant molecule.

CONCLUSION

To a first approximation the results for filled rubber are consistent with little or no sorption of hydrocarbon by the filler particles. The influence of the filler in reducing the permeabilities and diffusion coefficients is greater than would be expected for a regular dispersion of non-conducting spheres, suggesting that a filled rubber is a considerably more complex

medium. Trends in the solubility and permeation results also indicate that the models discussed are over-simplified and that the existence of complex surface and gas phase flows within the filler particles cannot be ruled out.

*Physical Chemistry Laboratories,
Chemistry Department,
Imperial College, London, S.W.7*

(Received March 1962)

REFERENCES

- ¹ e.g. BARRER, R. M. and PETROPOULOS, J. H. *Brit. J. appl. Phys.* 1961, **12**, 691
- ² MICHAELS, A. S. and PARKER, R. B. *J. Polym. Sci.* 1959, **41**, 53
- ³ MICHAELS, A. S. and BIXLER, H. J. *J. Polym. Sci.* 1961, **50**, 393, 413
- ⁴ KLUTE, C. H. *J. appl. Polym. Sci.* 1959, **1**, 340; *J. Polym. Sci.* 1959, **41**, 307
- ⁵ BARRER, R. M., BARRIE, J. A. and RAMAN, N. K. *Polymer, Lond.* 1962, **3**, 595
- ⁶ BARRIE, J. A. and PLATT, B. *J. Polym. Sci.* 1961, **54**, 261
- ⁷ MEREDITH, R. E. and TOBIAS, C. W. *J. appl. Phys.* 1960, **31**, 1270
- ⁸ RAYLEIGH, Lord. *Phil. Mag.* 1892, **34**, 481
- ⁹ FRICKE, H. *Phys. Rev.* 1924, **24**, 575
- ¹⁰ MELIKHOVA, N. A., REITLINGER, S. A. and KUZINA, N. *Soviet Rubber Tech.* 1959, **18**, 344 (English translation)

Viscosity of Branched Styrene–Maleic Anhydride Copolymers

C. E. H. BAWN and M. B. HUGLIN

A 1:1 copolymer of styrene and maleic anhydride has been esterified to different extents with primary alcohols R.OH and the viscosity of the esters measured in benzene and dioxan at 25°C. The intrinsic viscosity decreases and the Huggins parameter k' increases respectively with the length of R for fully esterified copolymers and k' increases with the extent of esterification. The roles of benzene and dioxan as good solvents for the branches and the backbone respectively are discussed.

THE solution viscosity of a high polymer is a measure of the size of the dissolved molecule, and is thus directly related to the molecular weight and the chain structure. The latter is determined partly by the degree of branching and under appropriate conditions viscosity measurements may be used to estimate the degree of branching of the polymer. Thus Zimm and Stockmayer¹ expressed the diminution in size of the branched chain of the same molecular weight as the unbranched polymer by the factor g where

$$g = \bar{S}^2_{(\text{branched})} / \bar{S}^2_{(\text{linear})}$$

or

$$g^{\frac{3}{2}} = [\eta]_{(\text{branched})} / [\eta]_{(\text{linear})}$$

where \bar{S}^2 is the mean square radius of gyration. In later developments², $g^{\frac{3}{2}}$ was replaced by R^3 and the function R gave numbers of branches several times higher than g . Another function which has been used extensively as a qualitative measure of branching is the Huggins factor k' in the relationship

$$\eta_{sp.}/c = [\eta] + k' [\eta]^2 c$$

Much of the evidence supporting this viewpoint was derived from the observed dependence of k' on the experimental condition of polymerization³ and on graft copolymers⁴. Although no quantitative theory has been given for the variation of k' with degree of branching, a study has been made in the present work of the dependence of k' and other viscosity parameters on branching in a series of well-defined branched copolymers.

Branched polymers were synthesized by attaching side chains to a polymer backbone in a controlled manner such that both the number and nature of the branches are accurately predetermined. The alternating 1:1 copolymer of styrene and maleic anhydride proved an admirable starting system because the anhydride portion could be esterified readily with

primary alcohols to yield branches of the type $-\text{COO}(\text{CH}_2)_n\text{CH}_3$, in which n depended on the alcohol used and the degree of branching, *D.B.*, on the extent of esterification.

EXPERIMENTAL

Materials

Commercial maleic anhydride, refluxed with chloroform and filtered free from maleic acid, was crystallized three times from chloroform to yield white needles of m.pt 53.0°C and molecular weight 97.7. 99.5 per cent pure styrene was freed from inhibitor, purified in the usual manner and stored under vacuum at -78°C . Azo-bis-isobutyronitrile (AZDN), was crystallized three times from ethanol to give white needles of m.pt 102.5° to 103.2°C (decomp.). Acetone and petroleum ether were rigorously dried and distilled. Diazomethane was prepared as a solution in toluene by dissolving 0.5 g clean sodium in 30 ml ethylene glycol and adding 3 ml nitrosomethylurethane to the solution dropwise. The diazomethane evolved was swept by gaseous nitrogen into 80 ml toluene at -95°C .

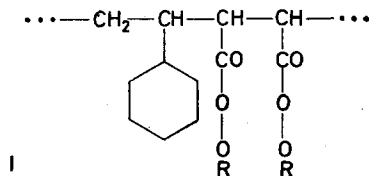
Normal propyl, butyl, amyl, octyl and undecyl alcohols and the branched ones 2-methyl propanol, 2-methyl butanol and 3-methyl, 5-dimethyl hexanol were dried over magnesium sulphate and distilled. Cetyl alcohol was crystallized from aqueous ethanol and octadecyl alcohol of high purity was kindly donated by Dr H. W. Douglas.

Copolymerization

10 ml of 0.042 per cent w/v AZDN in acetone, 0.0524 mole styrene and 0.0738 mole maleic anhydride made up to 30 ml with acetone were out-gassed and the flask sealed off. After $4\frac{1}{2}$ h at 50°C the reaction was quenched by chilling. The homogeneous solution was diluted to 100 ml with acetone and poured into 1 l. ice-cold petroleum ether when the copolymer settled as a fine white precipitate, which was redissolved, precipitated and dried to constant weight in a vacuum oven at 45°C . This reaction was performed in triplicate and the products were identical with respect to yield, composition and intrinsic viscosity. The molar ratio styrene/maleic anhydride in this copolymer (designated as MS in *Table I*) was 1.073 and it thus approximates to a 1:1 copolymer. All subsequent esterifications were performed on this compound.

Esterification

(a) *Fully esterified di-esters*—To produce copolymers bearing the alternating unit I from polymer MS, direct esterification with a large excess of pri-



mary alcohol and pure sulphuric acid as catalyst was employed: ca. 0.5 g 1:1 copolymer, 40 ml alcohol and 0.2 ml concentrated sulphuric acid were

VISCOSITY OF BRANCHED STYRENE-MALEIC ANHYDRIDE COPOLYMERS

Table 1

| Sample No. | Composition | D.B. | Solubility | k' | $[\eta]$ (dl/g) | | |
|------------|---|-------|---|--------|-----------------|-------|--------------|
| | | | | Dioxan | Benzene | | |
| MS | 1:1 copolymer | | v.s. acetone, s. dioxan i.s. petrol ether, benzene | 0.745 | 0.385*, 0.45† | 0.36 | 3.03*, 2.90† |
| DE 1 | dimethyl ester | ca. 1 | s. benzene, dioxan, i.s. methanol | 0.35 | | 3.05 | |
| DE 3 | di- <i>n</i> -propyl ester | " | " | 0.375 | | 1.82 | |
| DE 4 | di- <i>n</i> -butyl ester | " | " | 0.39 | | 1.57 | |
| DEB 4 | di-(2-methyl- <i>n</i> -propyl) ester | " | " | 0.38 | | 1.41 | |
| DE 5 | di- <i>n</i> -amyl ester | " | " | 0.41 | 0.24 | 1.36 | 2.15 |
| DEB 5 | di-(2-methyl- <i>n</i> -butyl) ester | " | " | 0.42 | 0.24 | 1.335 | 2.25 |
| DE 8 | di- <i>n</i> -octyl ester | " | " | 0.46 | 0.31 | 1.085 | 1.87 |
| DEB 9 | di-(3-methyl-5-dimethyl- <i>n</i> -hexyl) ester | " | " | 0.505 | | 0.75 | |
| DE 11† | di-undecyl ester | " | s. benzene, i.s. methanol | | 0.44 | | 0.34 |
| DE 16 | di-octyl ester | " | " | | 0.51 | | 1.79 |
| DE 18 | di-octadecyl ester | " | " | | 0.56 | | 1.70 |
| DE 1 | dimethyl ester | 0 | s. benzene, dioxan, i.s. methanol | 0.35 | | | |
| OM 1 | octylmethyl ester | 0.677 | " | 0.42 | | | |
| OM 2 | " | 0.746 | " | 0.42 | | | |
| OM 3 | " | 0.750 | " | 0.43 | | | |
| OM 4 | " | 0.889 | " | 0.45 | | | |
| OM 5 | " | 0.991 | " | 0.46 | | | |
| OD 1 | octadecyl half-ester | 0.540 | s. benzene, i.s. methanol | | 0.22 | | |
| OD 2 | " | 0.689 | " | | 0.45 | | |
| OD 3 | " | 0.765 | " | | 0.47 | | |
| OD 4 | " | 0.859 | " | | 0.49 | | |
| OD 5 | " | 0.895 | " | | 0.52 | | |
| DE 18 | di-octadecyl ester | 0.984 | s. benzene, dioxan, i.s. methanol | | 0.56 | | |

*In acetone. †In methyl ethyl ketone. s.—soluble, v.s.—very soluble, i.s.—insoluble. ‡Data unreliable because of superheating during esterification with resultant gelation and degradation.

heated for 72 h under air-refluxing. With cetyl and octadecyl alcohols, these solids were melted first in the flask to which MS and the catalyst were then added. After dissolving the reaction mixture in benzene and cooling, the di-esters were precipitated in a tenfold excess of methanol, washed free from alcohol R.OH and catalyst, redissolved, precipitated and dried at 45°C in a vacuum oven. With cetyl and octadecyl di-esters, unreacted alcohols were coprecipitated with the esters on pouring into methanol. They were removed by repeatedly boiling the precipitates with methanol and discarding the washings until they gave no trace of turbidity with water. These di-esters are referred to as compounds DE 1 to DE 18 in *Table 1*.

(b) *Partially esterified octadecyl acid-esters*—As the esterification of an anhydride to a di-ester proceeds via the formation of a half-ester, incomplete reaction of MS with octadecyl alcohol yields polymers bearing simultaneously both acid-ester and di-ester segments and *D.B.* may be formulated as

$$D.B. = \frac{\text{No. of octadecyl groups}}{\text{No. of octadecyl groups} + \text{No. of carboxyl groups}}$$

Using copolymer MS, octadecyl alcohol and sulphuric acid as in section (a) above and reaction times varying from 30 min to 50 h, a series of branched species of varying *D.B.* values was obtained. *D.B.* was evaluated by:

- (i) Titration to give no. of —COOH groups/g
 - (ii) Analysis of percentage of oxygen to give no. of pairs of oxygen atoms/g, i.e. total number of —COOC₁₈H₃₇ + —COOH groups/g.
- Subtraction (i) from (ii) yields the number of ester branches.

Benzene was used to extract the partially esterified product, which dissolved rapidly if *D.B.* was high but incompletely or with difficulty for polymers of low *D.B.* The extracts were treated subsequently as in section (a) to yield dry rubbery products. Dioxan would have extracted the product more completely but would have dissolved simultaneously any unreacted MS conceivably present after short reaction times. Furthermore, as the fully esterified di-octadecyl ester is insoluble in dioxan, only benzene was available as solvent for the complete range of these esters, which are designated as OD 1 to DE 18 in *Table 1*.

Because of this mode of extraction a partial fractionation was effected and no attempt was made to correlate *D.B.* with intrinsic viscosity $[\eta]$.

(c) *Octylmethyl esters*—With the intention of comparing *k'* with *D.B.* two unsatisfactory features of system (b) above become apparent, viz:

- (1) The base or unbranched polymer of this series is the di-acid, which is insoluble in benzene, thus rendering a comparison down to *D.B.* = 0 impossible.
- (2) The base polymer for these partial esters should more appositely be the fully esterified dimethyl ester, which is soluble in dioxan.

As the di-C₈ ester (unlike the di-C₁₈ one) is soluble in dioxan, a favourable system was devised in which octyl acid-esters were methylated. In

the resultant copolymers if the octyl groups be considered as the branches then

$$D.B. = \text{No. of octyl groups} / (\text{No. of octyl groups} + \text{No. of methyl groups})$$

Partially octylated esters were prepared similarly to the octadecyl compounds [section (b)] and then analysed to find the residual number of COOH groups/g. Solutions in benzene were methylated with an excess of diazomethane solution. Unreacted diazomethane was dispelled with acetic acid and the octylmethyl esters precipitated with methanol. The percentage of oxygen in these esters gave the total number of all ester groups/g. The number of carboxyl groups (subsequently methylated) being known, subtraction yielded the number of octyl groups/g and hence *D.B.* Octylmethyl esters are designated as DE 1 to OM 5 in *Table 1*.

Analysis

As maleic anhydride reacts as a monobasic acid its determination in a polymer is accomplished by adopting the method of Fritz and Lisicki⁵ for estimating acids and anhydrides in non-aqueous media. Bamford and Barb⁶ have applied this method to styrene-maleic anhydride copolymers and their procedure was used here both for determining the composition of MS and for estimating the concentration of carboxyl groups in the partially esterified copolymers.

Viscosity

Solution viscosities for each polymer within the concentration range 0.2 to 0.9 g/dl were measured at $25^\circ \pm 0.02^\circ\text{C}$ in an Ostwald viscometer, successive dilutions being made *in situ*. The long flow times (520 sec and 877 sec for benzene and dioxan respectively) and small intrinsic viscosities (generally between 1 and 2 dl/g) did not warrant kinetic energy or shear corrections, nor did calculation reveal them to be significant.

k' and $[\eta]$ were evaluated in the usual manner from

$$\eta_{sp.}/c = [\eta] + k'[\eta]^2c$$

The precision of the k' values is no better than ± 0.01 unit and they are accordingly reported to two significant figures only.

RESULTS

Analysis of the di-esters DE 1 to DE 18 to test completeness of esterification revealed that the dimethyl ester, prepared by reaction of the di-acid with diazomethane, was completely neutral. For the amyl, *n*-octyl and octadecyl di-esters reaction was 99.6, 98.9 and 98.9 per cent complete respectively and of similar magnitude for the others. *Figure 2* curve B demonstrates that for DE 18, where the effect would be greatest, these small differences are reflected in k' by a maximum of 0.01 unit.

Figure 1 shows the general increase in k' with increasing size of side chain when *D.B.* = 1. The values are uniformly higher in the poorer solvent,

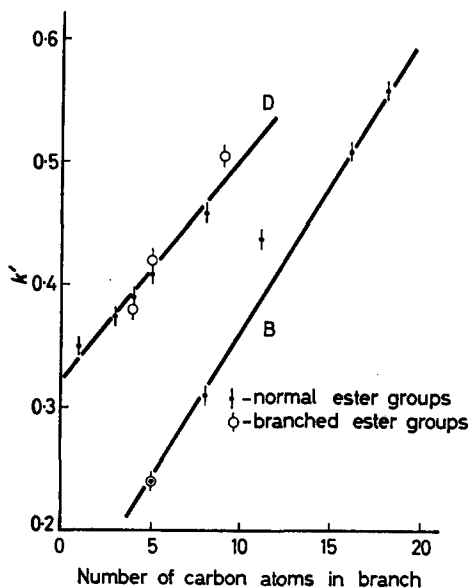


Figure 1—Variation of k' with length of side chain for fully esterified copolymers in dioxan [D] and benzene [B]

dioxan, than in the good one, benzene. The accompanying decrease in intrinsic viscosity with branch size (Figure 3) is more pronounced in the poorer solvent than in benzene and in both cases becomes less rapid after a branch size of about six carbon atoms is attained.

Although no experimental determinations of molecular weight or size have been made, a comparative estimate of the effect of increasing size of branch on the root-mean-square (r.m.s.) end-to-end dimensions $(\bar{r}_n^2)^{\frac{1}{2}}$ for polymers of $D.B.=1$ may be made as follows.

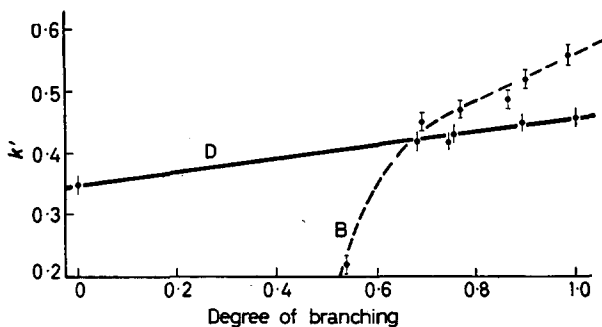


Figure 2—Variation of k' with degree of branching for octylmethyl esters in dioxan [D] and octadecyl half-esters in benzene [B]

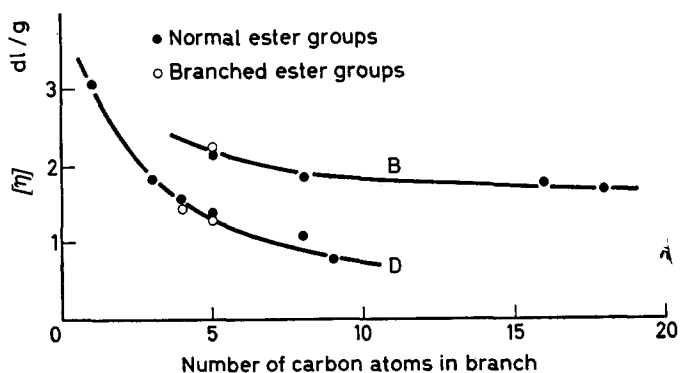
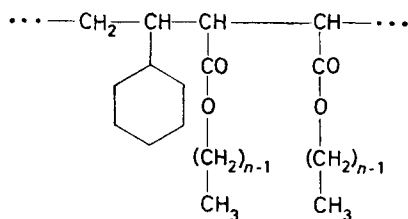


Figure 3—Dependence of intrinsic viscosity on length of side chain for fully esterified copolymers in dioxan [D] and benzene [B]

Consider the unbranched copolymer as the dimethyl ester (subscript 1) and the branched species (subscript n) as



Representing intrinsic viscosity, molecular weight and r.m.s. end-to-end length by $[\eta]$ cm³/g, M and $(\bar{r}_n^2)^{\frac{1}{2}}$ cm respectively, then as [styrene]/[maleic anhydride] in copolymer MS is 1.073

$$M_n = M_1 [1 + 28(n-1)/255.6]$$

If the radius of an 'equivalent hydrodynamic sphere' is proportional to $(\bar{r}_n^2)^{\frac{1}{2}}$ then

$$[\eta]_n = \Phi (\bar{r}_n^2)^{\frac{3}{2}} / M_n$$

where Φ is a constant of accepted value 2.2×10^{23} . Hence

$$(\Phi/M_1)^{\frac{1}{3}} (\bar{r}_n^2)^{\frac{1}{2}} = [1 + 28(n-1)/255.6]^{\frac{1}{3}} [\eta]_n^{\frac{1}{3}} \quad (1)$$

Taking $(\Phi/M_1)^{\frac{1}{3}}$ as a constant, the values of const. $(\bar{r}_n^2)^{\frac{1}{2}}$ may be computed from n and the measured $[\eta]_n$. It is seen from Figure 4 that in dioxan $(\bar{r}_n^2)^{\frac{1}{2}}$ decreases with n in a similar way to the fall in $[\eta]$, but that in the good solvent the mean size actually increases.

For the octylmethyl esters a linear relation exists between k' and $D.B.$ in the range $D.B. = 0.68$ to 0.99 (Figure 2, curve D). The fact that the line passes through the point corresponding to the dimethyl ester affords good

confirmation for regarding this as the unbranched compound. For a similar range in *D.B.* there is also a smooth increase in k' with *D.B.* for octadecyl acid-esters in benzene. However, when *D.B.* = 0.540, k' is also low. This must be attributed to the low branching rather than poor solubility which would have increased k' .

DISCUSSION

Whilst dioxan is a good solvent for the unbranched copolymer DE 1 ($k' = 0.35$, $[\eta] = 3.05$ dl/g), it is a poor one for the hydrocarbon side chains, e.g. for a dinonyl ester DEB 9 $k' = 0.505$, $[\eta] = 0.75$ dl/g and the most highly branched species DE 18 is insoluble in this solvent. Conversely, benzene is a poor solvent for the backbone and a good one for the side chains. Hence both the favourability of the solvent to the branches and their size n must be invoked in explaining the variations of $[\eta]$ and k' with n .

In dioxan, polymer-polymer (to the exclusion of polymer-solvent) and segment-segment interactions are enhanced as the side chains increase in length. The resulting coiling-up is reflected in the observed fall in $[\eta]$ and $(\Phi/M_1)^{\frac{1}{2}} (\bar{r}_n^2)^{\frac{1}{2}}$ with n and in the rise of k' , which is a qualitative measure of such interactions. In benzene, larger side chains might be anticipated to produce enhanced polymer-good solvent contacts and hence small k' values. However, this tendency is offset to some extent by the inter-segment interactions of the branches themselves, with the net result that k' increases with n . The magnitude of this counterbalancing is rather small as k' is uniformly less in benzene than in dioxan for any particular value of n , and also the fall in $[\eta]$ is less pronounced. Referring to equation (1) it is clear that in benzene the fall in $[\eta]_n^{\frac{1}{2}}$ with rise in $(n-1)^{\frac{1}{2}}$ is too slight to yield a resultant increase in the overall mean dimensions and $(\bar{r}_n^2)^{\frac{1}{2}}$ effectively increases with molecular weight.

Figure 2, curve D demonstrates that for the series of octylmethyl esters

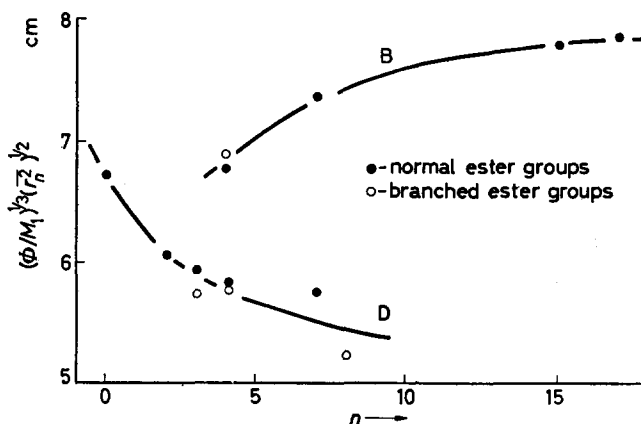


Figure 4—Effect of length of side chain on r.m.s. end-to-end distance of fully esterified copolymers in dioxan [D] and benzene [B]

k' increases by 0.11 unit for 100 per cent branching. Hence an experimentally significant change, i.e. 0.01 unit, reflects a 9 per cent increase in $D.B.$ and k' is a definite but insufficiently sensitive indicator of the presence of branching.

*Department of Inorganic, Physical and Industrial Chemistry,
The University of Liverpool*

(Received March 1962)

REFERENCES

- ¹ ZIMM, B. H. and STOCKMAYER, W. H. *J. chem. Phys.* 1949, **17**, 1301
- ² STOCKMAYER, W. H. and FIXMAN, M. *Ann. N.Y. Acad. Sci.* 1953, **57**, 334
- ³ ALFREY, T., BARTOVICS, A. and MARK, H. *J. Amer. chem. Soc.* 1943, **65**, 2319
- ⁴ JONES, M. H. *Canad. J. Chem.* 1956, **34**, 1027
- ⁵ FRITZ, J. S. and LISICKI, N. M. *Analyt. Chem.* 1951, **23**, 589
- ⁶ BAMFORD, C. H. and BARB, W. G. *Disc. Faraday Soc.* 1953, **14**, 208

*Effect of Heterogeneity in Molecular Weight on the Second Virial Coefficient of Polymers in Good Solvents**

EDWARD F. CASASSA

Recent theoretical treatments of the second virial coefficient A_2 for chain polymers in good solvents lead to rather complicated results, which because of mathematical difficulties have not so far been extended to the general case of solutes heterogeneous in molecular weight. Expressions in simple analytical form can be obtained, however, if three simple assumptions are made: for homogeneous polymers, A_2 varies as a power of molecular weight; interactions between two unlike solute species are given by the relation for rigid spheres of the equivalent radii determined by A_2 in the homogeneous cases; in heterogeneous polymers the dispersion of molecular weight is described by a Schulz distribution function or a sum of several such functions. For one special case, a solution of two polymer fractions differing only in molecular weight, results are in qualitative accord with both prior theory and experiment in indicating the existence of conditions under which A_2 passes through a maximum as a function of the relative proportions of the two components in the solute. It is also predicted that A_2 is increased by heterogeneity in comparison with the value for a sharp fraction of molecular weight corresponding to the appropriate average weight of the heterogeneous polymer.

SINCE synthetic high polymers are ordinarily heterogeneous in chain length to some degree, even after the most exacting fractionation procedures, interpretation of measurements of thermodynamic and hydrodynamic properties that depend on molecular weight is hampered by the difficulty that the effects of heterogeneity are not well understood even though, as is far from always the case, the nature of the weight distribution may be known precisely.

Because an exact treatment of the statistical thermodynamics of polymers in good solvents appears almost hopelessly difficult, various theories based on approximate molecular models have been developed¹⁻¹¹ for the molecular weight dependence of the second virial coefficient. For none of these treatments, however, has it so far proved feasible to carry the generalization for a distribution of molecular weights to the point of numerical computations: at most, in some cases, results for a mixture of two solute species are obtained without great difficulty³. Hence, experimental tests of the theories are somewhat ambiguous in that the idealized homogeneous systems dealt with theoretically may not be well enough approximated in practice. The problem of heterogeneity also arises directly in comparisons of virial coefficients obtained by the two most important experimental techniques, osmometry and light scattering; for the two measurements are not exactly equivalent, yielding, as they do, different averages over any distribution of species present¹¹⁻¹⁴.

*This work was supported in part by the Wright Air Development Division, Air Research and Development Command, United States Air Force, under Contract No. AF 33(616)-6968.

In view of these questions, we have investigated the effect of polydispersity on the virial coefficient by utilizing very simple assumptions that make it possible to obtain results in analytical form. We can make no claim for the adequacy of the most important of our simplifications (except a perhaps naïve one of some physical plausibility) and neither do we pretend to have alleviated the need for realizing developments based on the more sophisticated models.

Conveniently, the problem may be described under two heads. First, we require a means of expressing the thermodynamic interaction of two molecules unlike in chain length, though otherwise identical. A complete theory of the second virial coefficient would of course provide this as a general result; but for the immediate purpose, we pursue the more limited aim of expressing this interaction as a function of parameters, which may be purely empirical, determined by the interaction in the common solvent, between pairs of like molecules of the two species. In other words, we seek a basis for some way of relating given virial coefficients for homogeneous systems to obtain coefficients for interaction of unlike species. At this stage results can be applied to the idealized case of two perfectly sharp polymer fractions. Finally, if it is possible to sum (or integrate) over a molecular weight distribution, virial coefficients can be computed for polydisperse systems. Although molecular weight distributions produced in polymerization reactions or by fractionation procedures sometimes assume fairly uncomplicated forms, or can be expressed in approximate ways, the double integrations of expressions for bimolecular interactions over the distribution appear quite impossible analytically for any of the earlier statistical thermodynamic theories cited above except in poor solvents as the virial coefficient approaches zero. But in this limit, rigorous theory can be applied¹⁵ just as easily.

INTERACTION OF POLYMER CHAINS OF DIFFERENT LENGTH

We assume at the outset that the second virial coefficient A_2 in a solution of a homogeneous polymer of degree of polymerization n is given by

$$A_2 = B_0 n^{-a} \quad (1)$$

where B_0 and a are constants characteristic of the polymer-solvent pair at a particular temperature, but independent of the molecular weight of the polymer. This expression has little theoretical basis for molecular weights of ordinary magnitude* but does in fact conform, well within the limits of experimental error, to virtually all reliable light scattering and osmotic pressure data for polymer fractions in good solvents over wide ranges of molecular weight. Theoretical expressions of unrelated functional form might of course fit the experimental results equally well. Thus we can best regard equation (1) merely as a representation of experimental fact without seeking any other justification. The relation is useful because it

*Some of the theoretical models indicate that at high molecular weights, A_2 may become asymptotically proportional to $z^2/n^{1/2}$, z being the factor by which the chain molecule is expanded beyond random flight dimensions by the intramolecular volume exclusion effect in good solvents. If, in this the limit, z depends on a power of n , the form of equation (1) is obtained^{15, 17}.

contributes to making the ensuing mathematical operations extremely simple; and while the analytical forms that result may be of slight interest, the validity of conclusions, *in quantitative numerical terms*, will be no less, for this assumption at least, than if we were to make a purely numerical analysis based on experimental results directly, so long as we can avoid difficulties with mathematical convergence.

In order to proceed toward the treatment of a molecular weight distribution by expressing the virial coefficient for interaction of unlike polymer molecules in terms of B_0 and a , we make the speculative assumption that the form of averaging appropriate for hard spheres of different sizes is applicable. An elementary statistical mechanical calculation¹⁸ shows that for hard spheres of radii r_i and r_j and respective molar masses M_i and M_j , the interaction coefficient is given by

$$B_{ij} = 2\pi N_0 (r_i + r_j)^3 / 3M_i M_j \quad (2)$$

where N_0 is Avogadro's number. Thus, B_{ii} is the virial coefficient for a system of homogeneous spheres of radius r_i expressed in the units of volume/(mass)² customarily used in studies of macromolecular substances. It follows that

$$(B_{ij} M_i M_j)^{1/3} = \frac{1}{2} [(B_{ii} M_i^2)^{1/3} + (B_{jj} M_j^2)^{1/3}] \quad (3)$$

Applying this relation to polymers by equating B_{ii} to $B_0 n_i^{-a}$ and noting that M_i is proportional to n_i , we obtain the equation

$$(B_{ij} n_i n_j)^{1/3} = \frac{1}{2} B_0^{1/3} [n_i^{(2-a)/3} + n_j^{(2-a)/3}] \quad (4)$$

which can then be substituted in the general expressions for the virial coefficients for heterogeneous systems: for the osmotic pressure¹²

$$A_2^{(II)} = \sum_i \sum_j B_{ij} w_i w_j \quad (5)$$

and for Rayleigh scattering^{12,13}

$$\begin{aligned} A_2^{(R)} &= \sum_i \sum_j B_{ij} M_i w_i M_j w_j / (\sum_i M_i w_i)^2 \\ &= \sum_i \sum_j B_{ij} n_i w_i n_j w_j / \langle n \rangle^2 \end{aligned} \quad (6)$$

where w_i , w_j are weight fractions of species in the solute (hence $\sum w_i = 1$) and $\langle n \rangle$ is $\sum n_i w_i$, the weight average degree of polymerization.

MIXTURES OF TWO POLYMER SPECIES

Before undertaking the summations in equations (5) and (6) we can use the results so far advanced to discuss the behaviour of a ternary solution containing two homogeneous fractions of the same polymer. From equation (5) it is evident that $A_2^{(II)}$ for such a system, as a function of either of the weight fractions w determining the composition, is described by a parabola. Similarly $A_2^{(R)}$ is a more complicated quotient of quadratic expressions in w ; and thus $A_2^{(R)}$ and $A_2^{(II)}$ are alike only for w equal to zero and to unity (and at one other point for some values of the three B_{ij}).

As one result of the statistical theory of Flory and Krigbaum^{2,7} in which the interaction of two chains of different length is considered explicitly, it is predicted that under certain conditions—certain magnitudes of the thermodynamic parameters characterizing interactions between two chain segments, and of the molecular weights of the two species—the values of both $A_2^{(M)}$ and $A_2^{(R)}$ pass through a maximum with variation of w . It is very easy to show from the general equations (5) and (6) that the necessary and sufficient condition for the appearance of a maximum is simply that the cross-coefficient B_{ij} with $i \neq j$ be the largest of the three parameters¹⁴. If we designate the higher molecular weight component as 4 and the lower as 2, we thus require that $B_{24} > B_{22}$ since all theories and experiments agree in having $B_{22} > B_{44}$. The appearance of a minimum A_2 requires that $B_{24} < B_{44}$, but neither theory nor experiment so far indicates this as a possibility.

In the scheme developed here, equation (4) gives

$$B_{24}/B_{22} = (1/8\gamma)[1 + \gamma^{(2-a)/3}]^3 \quad (7)$$

where γ is the molecular weight ratio n_4/n_2 . For $0 < a < 1$, B_{24}/B_{22} initially decreases from unity as γ increases and then increases, approaching $\gamma^{1-a}/8$ asymptotically. When a is zero the ratio is never less than unity; and for $a=1$, it decreases monotonically to approach the limit $1/8$. As a becomes smaller the critical γ for $B_{24} > B_{22}$ decreases. These points are illustrated in Figure 1. Empirically, $1/4$ is a typical value of a for

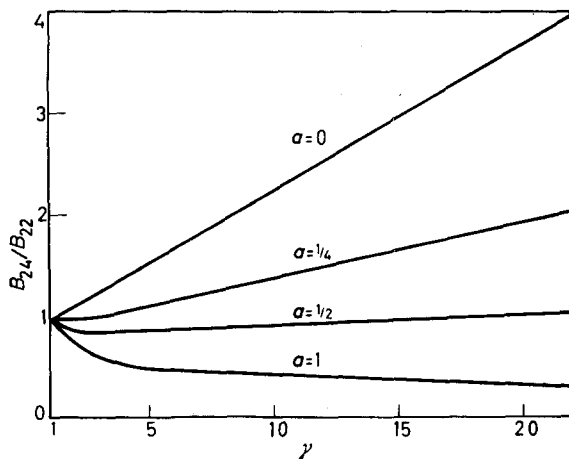


Figure 1— B_{24}/B_{22} from equation (7) as a function of γ at constant a

systems in very good solvents. Roughly, the magnitude of a seems to parallel the solvent power and is seldom found to be much larger than this¹⁹⁻²¹.

From equation (4) we also get

$$B_{24}/B_{44} = (1/8\gamma^{1-a})[1 + \gamma^{(2-a)/3}]^3 \quad (8)$$

As this ratio is always greater than unity over the meaningful range of a , no minimum in A_2 is allowed.

Experimentally, the maximum in A_2 has been found as expected in some systems and not in others; but the possible comparisons with equation (7) are at the moment very limited, only few sufficiently reliable results having been published. The best work is probably that of Krigbaum and Flory¹⁹ whose experimental results for two systems (polyisobutene-cyclohexane and polystyrene-toluene) are given in *Table 1*. In the last column, values of B_{24}/B_{22} as required by the Flory-Krigbaum² theory are also listed. These were calculated entirely from the theory* and the thermodynamic constants obtained independently of the A_2 measurements by interpretation of intrinsic viscosity data according to the method of Flory and Fox²². Another procedure of forcing B_{22} and B_{44} to fit the experimental data and retaining the theory only in combining these coefficients to obtain B_{24} sometimes leads to physically meaningless results unless a constant appearing in the theory is altered. These modifications are discussed elsewhere^{14,23}, but here only the original treatment as described by Krigbaum and Flory¹⁹ is considered. For the first two systems in *Table 1*, the Flory-Krigbaum theory correctly predicts a maximum A_2 , but it gives values of B_{24}/B_{22} apparently somewhat too low while the present treatment seems to exaggerate the magnitude of the ratio. Studies of systems of mixed fractions of polymethyl methacrylate in good solvents have given contradictory results, as indicated in the tabulation. In one study of a polymethyl methacrylate-butanone system, the experimental data indicated the occurrence of a maximum in A_2 to be impossible¹⁷ but in another similar investigation²⁴ a maximum was found, although there may be some question as to the magnitude of experimental error. Finally, measurements on ternary solutions of polymethyl methacrylate in acetone have given equivocal results^{14,25}. In all these last three cases both the Flory-Krigbaum theory and our treatment demand that $B_{24} > B_{22}$, our theory always giving by far the larger B_{24}/B_{22} ratio.

We digress briefly at this point from the main course of the argument to observe that equation (1) can be regarded as a generalization of the hard sphere relation. For matter of uniform density the radius is proportional to the cube root of the mass so that B_{ii} is proportional to M^{-1} . Thus a is unity and, according to equations (7) and (8), B_{24} for hard spheres is always intermediate between B_{22} and B_{44} . If a polymer molecule is regarded as an impenetrable sphere of size determined by a random-flight dimension (e.g. the radius of gyration) proportional to $n^{1/2}$, the virial coefficient varies with $n^{-1/2}$ and, depending on γ , B_{24} may be either larger than B_{22} or intermediate between B_{22} and B_{44} . For a real polymer chain, the excluded volume effect causes the radius of gyration to increase more rapidly than $n^{1/2}$ and a should be less than 0.5, as it is actually found to be. Equation (1) and the more specific hard sphere relation agree in giving a virial coefficient that becomes infinite as n approaches zero. On the other hand, all the statistical theories, both approximate¹⁻¹⁰ and rigorous^{16,26}, assume the form of a

*Equations (24) to (26) below were used in the calculations together with an approximate closed form given by Orofino and Flory³ for the function $F(X)$ in equation (24).

Table I. Second virial coefficients in solutions of mixtures of two polymer fractions

| System and method | $M_2 \times 10^{-3}$ | γ | a | Experimental ^(a) | | | B_{34}/B_{22} (Flory-Krigbaum theory) | B_{34}/B_{22} (Eq. 7) |
|--|----------------------|----------|---|-----------------------------|----------------------|---------------------|--|----------------------------|
| | | | | $B_{22} \times 10^4$ | $B_{44} \times 10^4$ | B_{34}/B_{22} | | |
| Polystyrene-toluene (II ^(b) , 30°C) ¹⁹ | 0.614 | 9.80 | 0.22 ^(d) (0.22) ¹⁹ | 4.98 | 3.26 | 1.28 | 1.08 | 1.48 |
| Polyisobutene-cyclohexane (II, 30°C) ¹⁹ | 0.814 | 8.85 | 0.16 (0.14) ¹⁹ | 7.26 | 5.38 | 1.14 | 1.10 | 1.56 |
| PMMA ^c -butanone (R ^(b) , 25°C) ¹⁷ | 1.26 | 21.0 | 0.33 (0.24) ¹⁷ | 2.93 | 1.08 | 0.58 | 1.14 | 1.68 |
| PMMA-butaneone (R, 25°C) ²⁴ | 3.8 | 8.32 | 0.21 | 2.13 | 1.29 | 1.34 | 1.18 | 1.41 |
| PMMA-acetone (II, 25°C) ^{(e), 25} | 0.86 | 12.2 | 0.24 (0.22) ^{(f), 20} | 3.10 | 1.42 | 0.99 | 1.08 | 1.27 |
| PMMA-acetone (R, 25°C) ^{(e), 25} | 0.92 | 12.8 | 0.085 (0.22) ^{(f), 21} | 1.92 | 1.45 | 1.04 ^(m) | 1.08 | 2.20 |

(a) Most of the listed coefficients are least-squares parameters [for equations (5) and (6)]. (b) II denotes osmotic pressure; R, light scattering. (c) Polymethyl methacrylate. (d) Values of a were calculated from A_2 for the two fractions in question; more extensive measurements give the results in parentheses. The former were used in determining B_{34}/B_{22} from equation (7). (e) The same fractions were used in osmotic and light scattering measurements. (f) From measurements at 30°C. (g) Another analysis²⁴ of the same data gives $B_{34}/B_{22} < 1$.

constant multiplied by a series $1 + O(n^{1/2})$ in integral powers of $n^{1/2}$. This discrepancy is trivial, however, in regard to molecular weight inasmuch as we can require $n \gg 1$ to be a condition for physical significance*.

This assumption appears to be implicit in all the statistical derivations.

THE VIRIAL COEFFICIENT FOR HETEROGENEOUS POLYMERS

In calculating the virial coefficient for systems with a distribution of molecular weights we adopt the familiar distribution function first applied to polymers by Schulz²⁷:

$$f(n) = y^{Z+1} n^Z e^{-yn} / \Gamma(Z+1) \tag{9}$$

$$y = (Z+1) / \langle n \rangle$$

where $f(n) dn$ is the weight fraction of the solute with n within the differential increment dn , and $\Gamma(x)$ denotes the gamma function. The value of Z increases with decreasing heterogeneity: the limit of infinite sharpness is characterized by $Z = \infty$ while $Z = 1$ corresponds to the 'most probable' distribution obtained in the polyester type of condensation and also in free-radical polymerizations carried to low degrees of conversion in the presence of a chain transfer agent²⁸.

We substitute equation (9) into the integral expressions corresponding to the sums of equations (5) and (6)

$$A_2^{(II)} = \int_0^\infty \int_0^\infty B(m, n) f(m) f(n) dm dn \tag{10}$$

$$A_2^{(B)} = \langle n \rangle^{-2} \int_0^\infty \int_0^\infty B(m, n) mf(m) nf(n) dm dn \tag{11}$$

and let $B(m, n)$ be given by

$$B(m, n)mn = (B_0/8)[m^{(2-a)/3} + n^{(2-a)/3}]^3 \tag{12}$$

in accordance with equation (4). The definite integrals resulting reduce to various combinations of the single standard form

$$\int_0^\infty u^{t-1} e^{-ku} du = \Gamma(t) / k^t$$

For the osmotic pressure we obtain finally

$$A_2^{(II)} = \frac{B_0 y^{3(Z+1)}}{4[\Gamma(Z+1)]^2} \times \iint [m^{Z+1-a} n^{Z-1} + 3m^{(3Z+1-2a)/3} n^{(3Z-1-a)/3}] e^{-y(m+n)} dm dn$$

$$= B_0 y^a \phi^{(II)} / 4[\Gamma(Z+1)]^2 \tag{13}$$

where

$$\phi^{(II)} = \Gamma(Z+2-a)\Gamma(Z) + 3\Gamma[(3Z+4-2a)/3]\Gamma[(3Z+2-a)/3] \tag{14}$$

*The double integrals following [e.g. equations (10), (11)] with equation (1) and the form of molecular weight distribution we adopt, remain convergent even though we integrate over the entire range $0 \leq n \leq \infty$. The fractional contribution to the integrals from the range $0 \leq n \leq n_0$ is of the order of $(n_0 / \langle n \rangle)^{2-a+\delta}$ where $\delta > 0$.

Since the number average degree of polymerization n_N is given by

$$n_N^{-1} = \int \{f(n)/n\} dn = y/Z$$

the ratio of $A_2^{(II)}$ to the virial coefficient B_{NN} of the homogeneous polymer with degree of polymerization n_N is

$$A_2^{(II)}/B_{NN} = Z^a \phi^{(II)} / 4[\Gamma(Z+1)]^2 \quad (15)$$

For light scattering, the analogous relations are:

$$A_2^{(R)} = B_0 y^a \phi^{(R)} / 4[\Gamma(Z+2)]^2$$

$$\phi^{(R)} = \Gamma(Z+3-a)\Gamma(Z+1) + 3\Gamma[(3Z+7-2a)/3]\Gamma[(3Z+5-a)/3] \quad (16)$$

and

$$A_2^{(R)}/B_{WW} = (Z+1)^a \phi^{(R)} / 4[\Gamma(Z+2)]^2 \quad (17)$$

where B_{WW} refers to a homogeneous polymer with $n = \langle n \rangle$. The ratio of the two virial coefficients for one polymer is obviously

$$A_2^{(II)}/A_2^{(R)} = (Z+1)^2 \phi^{(II)} / \phi^{(R)} \quad (18)$$

Finally the ratio of equation (15) to equation (17)

$$A_2^{(II)}B_{WW}/B_{NN}A_2^{(R)} = [Z/(Z+1)]^a A_2^{(II)}/A_2^{(R)} \quad (19)$$

is of interest since it represents the comparison obtained by superimposing osmotic and scattering data plotted against n_N and $\langle n \rangle$ respectively.

The expressions just derived for heterogeneous polymers have the property that for any given distribution, characterized by Z , the form of the relation between the virial coefficient and average molecular weight is still that of equation (1) for a single species: thus double logarithmic plots of $A_2^{(II)}$ versus n for a sharp fraction and of $A_2^{(II)}$ and $A_2^{(R)}$ versus n_N or $\langle n \rangle$ are all predicted to be straight lines of the same slope, $-a$. The ratios defined by equations (15) and (17) to (19) for $a=1/4$ are shown as functions

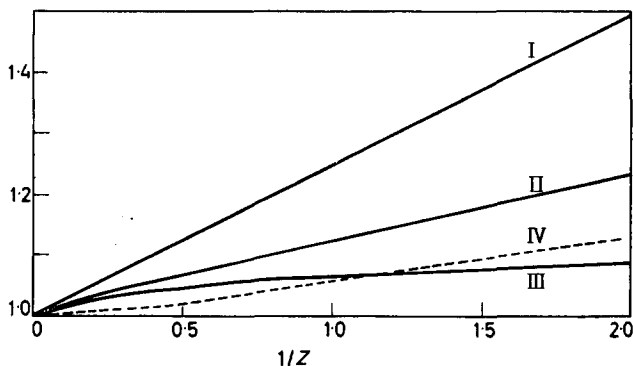


Figure 2—Effect of polymer heterogeneity on the second virial coefficient. The ordinate represents the ratios given by equations (15) and (17) to (19) with $a=1/4$: $A_2^{(II)}/A_2^{(R)}$ for curve I, $A_2^{(II)}/B_{NN}$ for curve II, $A_2^{(R)}/B_{WW}$ for curve III, $A_2^{(II)}B_{WW}/A_2^{(R)}B_{NN}$ for curve IV

of Z in *Figure 2*. All are seen to increase from unity with increasing heterogeneity. As Z approaches zero, $\phi^{(II)}$ becomes infinite—because of the divergence of the integral $\Gamma(0)$ —and all the ratios become infinite except $A_2^{(R)}/B_{ww}$ which attains its maximum value of 1.13. The most pronounced effect is on $A_2^{(II)}/A_2^{(R)}$ for the same polymer; in comparison, divergences between virial coefficients for heterogeneous samples and for sharp fractions of molecular weight corresponding to the appropriate average are less marked. Numerical values of the ratios for $Z=1$ and $a=1/4$ are listed in the second column of *Table 2*. These values indicate that comparison of virial coefficients from osmotic pressure and light scattering measurements

Table 2. Calculated effect of polymer heterogeneity on virial coefficients for the most probable distribution ($Z=1$)

| Ratio | B_{ij} from equation (4) | B_{ij} from equations (1), (28) | | B_{ij} from equations (1), (29) | |
|--------------------------------------|-------------------------------|--------------------------------------|---------|--------------------------------------|------------------|
| | $a=1/4$ | $a=1/3$ | $a=1/4$ | $a=1/4$ $v=0$ | $a=1/4$ $v=1$ |
| $A_2^{(II)}/A_2^{(R)}$ | 1.255 | 1.190 | 1.138 | 1.143 | 1.455 |
| $A_2^{(II)}/B_{NN}$ | 1.127 | 0.885 | 0.909 | 0.919 | 1.608 |
| $A_2^{(R)}/B_{ww}$ | 1.068 | 0.937 | 0.950 | 0.956 | 1.315 |
| $A_2^{(II)}/B_{ww}/A_2^{(R)}/B_{NN}$ | 1.055 | 0.945 | 0.957 | 0.961 | 1.223 |

on the same normally heterogeneous polymer sample may reveal a significant effect due to polydispersity; but since the experimental error in determination of $A_2^{(II)}$ is perhaps five per cent at best, one could scarcely expect on the basis of this theory to discover an experimentally significant difference in comparing $A_2^{(II)}$ as a function of n_N with $A_2^{(R)}$ as a function of $\langle n \rangle$ obtained by independent measurements on different series of polymers. In view of these results it appears that by reasonably good fractionation one can hope to eliminate the effects of heterogeneity for all practical purposes to the extent that a solution of a single polymer fraction can be considered as a binary system.

MIXTURES OF HETEROGENEOUS POLYMERS

The unexplained disagreements between experiment and theory for mixtures of two fractions of the same polymer prompt a question as to whether the expected maximum in A_2 could have been vitiated if the individual fractions were in fact rather heterogeneous. For polymethyl methacrylate in particular it has been recognized that good fractionation is difficult to attain^{21, 29-31}. To investigate this problem we again use the Schulz distribution assuming that polymers 2 and 4 each exhibit a distribution in molecular weight characterized by Z_2 and Z_4 in the distribution functions $f_2(n)$, $f_4(n)$ given by equation (9). Thus we describe the composite distribution by

$$\Phi(n) = f_2(n)w_2 + f_4(n)w_4$$

where, as above, $w_2 + w_4 = 1$ and

$$\int \Phi(n) dn = 1$$

as is required.

The virial coefficient for the osmotic pressure is thus

$$A_2^{(II)} = \int \int B(m, n) \Phi(m) \Phi(n) dm dn$$

$$= \langle B_{22}^{(II)} \rangle w_2^2 + 2 \langle B_{24}^{(II)} \rangle w_2 w_4 + \langle B_{44}^{(II)} \rangle w_4^2 \quad (20)$$

where

$$\langle B_{ij}^{(II)} \rangle = \int \int B(m, n) f_i(m) f_j(n) dm dn$$

As before, we assume equation (12) for $B(m, n)$. The coefficients $B_{22}^{(II)}$ and $B_{44}^{(II)}$ are then given directly by equations (10) and (13). The remaining one $B_{24}^{(II)}$ is readily derived in similar fashion; but the general result for $Z_2 \neq Z_4$ and $y_2 \neq y_4$ is more cumbersome

$$\langle B_{24}^{(II)} \rangle = \frac{B_0 \langle n_2 \rangle^{-a}}{8\xi} \frac{(Z_2 + 1)(Z_4 + 1)}{\Gamma(Z_2 + 1)\Gamma(Z_4 + 1)} \left\{ \frac{\Gamma(Z_2 + 2 - a)\Gamma(Z_4)}{(Z_2 + 1)^{2-a}} \right.$$

$$+ \frac{3\Gamma[(3Z_2 + 4 - 2a)/3]\Gamma[(3Z_4 + 2 - a)/3]\xi^{\xi^{(2-a)/3}}}{[(Z_2 + 1)^{2/3}(Z_4 + 1)^{1/3}]^{2-a}}$$

$$\left. + \frac{3\Gamma[3Z_2 + 2 - a]\Gamma[3Z_4 + 4 - 2a]\xi^{2(2-a)/3}}{[(Z_2 + 1)^{1/3}(Z_4 + 1)^{2/3}]^{2-a}} + \frac{\Gamma(Z_2)\Gamma(Z_4 + 2 - a)\xi^{2-a}}{(Z_4 + 1)^{2-a}} \right\}$$

where $\xi = \langle n_4 \rangle / \langle n_2 \rangle$, the ratio of the weight average molecular weights $\langle n_2 \rangle$, $\langle n_4 \rangle$, replaces γ used above in discussion of a binary solute. In the simpler case in which $Z_2 = Z_4 = Z$, this expression is reduced to

$$\langle B_{24}^{(II)} \rangle / \langle B_{22}^{(II)} \rangle = (2\xi\phi^{(II)})^{-1} \{ (1 + \xi^{2-a})\Gamma(Z)\Gamma(Z + 2 - a)$$

$$+ 3(\xi^{(2-a)/3} + \xi^{2(2-a)/3})\Gamma[(3Z + 2 - a)/3]\Gamma[(3Z + 4 - 2a)/3] \} \quad (21)$$

where $\phi^{(II)}$ is defined by equation (14).

For light scattering, the virial coefficient for the mixture of two polymers is given by

$$A_2^{(R)} n_w^2 = \langle B_{22}^{(R)} \rangle \langle n_2 \rangle^2 w_2^2 + 2 \langle B_{24}^{(R)} \rangle \langle n_2 \rangle w_2 \langle n_4 \rangle w_4 + \langle B_{44}^{(R)} \rangle \langle n_4 \rangle^2 w_4^2$$

Equation (11) gives $\langle B_{22}^{(R)} \rangle$ and $\langle B_{44}^{(R)} \rangle$, and the other coefficient is

$$\langle B_{24}^{(R)} \rangle = (\langle n_2 \rangle \langle n_4 \rangle)^{-1} \int \int B(m, n) m f_2(m) n f_4(n) dm dn$$

$$= \frac{B/8\xi \langle n_2 \rangle^a}{\Gamma(Z_2 + 1)\Gamma(Z_4 + 1)} \left\{ \frac{\Gamma(Z_2 + 3 - a)\Gamma(Z_4 + 1)}{(Z_2 + 1)^{2-a}} \right.$$

$$+ \frac{3\Gamma[3Z_2 + 7 - 2a]\Gamma[(3Z_4 + 5 - a)/3]\xi^{\xi^{(2-a)/3}}}{[(Z_2 + 1)^{2/3}(Z_4 + 1)^{1/3}]^{2-a}}$$

$$+ \frac{3\Gamma[(3Z_2 + 5 - a)/3]\Gamma[(3Z_4 + 7 - 2a)/3]\xi^{2(2-a)/3}}{[(Z_2 + 1)^{1/3}(Z_4 + 1)^{2/3}]^{2-a}}$$

$$\left. + \frac{\Gamma(Z_2 + 1)\Gamma(Z_4 + 3 - a)\xi^{2-a}}{(Z_4 + 1)^{2-a}} \right\} \quad (22)$$

When $Z_2 = Z_4$, this becomes

$$\begin{aligned} \langle B_{24}^{(R)} \rangle / \langle B_{22}^{(R)} \rangle &= (2\xi\phi^{(R)})^{-1} \{ (1 + \xi^{2-a})\Gamma(Z+3-a)\Gamma(Z+1) \\ &+ 3(\xi^{2-a}/3 + \xi^{2(2-a)/3})\Gamma[(3Z+5-a)/3]\Gamma[(3Z+7-2a)/3] \} \end{aligned} \quad (23)$$

with $\phi^{(R)}$ given by equation (16).

It is apparent from equations (21) and (23) that the ratios $\langle B_{24}^{(II)} \rangle / \langle B_{22}^{(II)} \rangle$ and $\langle B_{24}^{(R)} \rangle / \langle B_{22}^{(R)} \rangle$ both increase as Z decreases, with the effect somewhat more marked for osmotic pressure. When Z is unity and a one fourth, the apparent B_{24}/B_{22} for the osmotic pressure is increased by factors of 1.02, 1.07, 1.16 and 1.20 respectively for ξ equal to 2, 5, 10 and 20: the corresponding values for light scattering are 1.01, 1.03, 1.09 and 1.11. It is predicted then that the effect that leads to a maximum in A_2 as a function of composition for a binary solute is enhanced rather than suppressed by an equal degree of heterogeneity in the two components. As heterogeneity increases in this way, the critical molecular weight ratio ξ for appearance of the maximum decreases; thus at fixed $\langle n_2 \rangle$ and $\langle n_4 \rangle$ a heterogeneous system may give a maximum A_2 for particular values of $\langle n_2 \rangle$ and $\langle n_4 \rangle$ for which a strictly two-component solution would not.

The situation is different if we consider the possibility that Z_2 is not the same as Z_4 . An increase in the heterogeneity of polymer 4 relative to that of polymer 2 increases the ratio $\langle B_{24}^{(II)} \rangle / \langle B_{22}^{(II)} \rangle$ at a fixed value of the number average molecular weight ratio

$$\varepsilon + \xi[Z_4(Z_2 + 1)/Z_2(Z_4 + 1)]$$

while a decrease has the opposite effect. In particular, therefore, $\langle B_{24}^{(II)} \rangle / \langle B_{22}^{(II)} \rangle$ is greater when $Z_4 < Z_2$ than the value given by equation (21) for the same ε and $Z = Z_2$, and does not decrease to unity when ε is unity. Conversely, when Z_4 is infinite, $\langle B_{24}^{(II)} \rangle / \langle B_{22}^{(II)} \rangle$ at finite Z_2 is smaller than the B_{24}/B_{22} ratio for homogeneous polymers and again does not become unity for $\varepsilon = 1$. [When one Z is infinite, B_{24} is easily got from the integrals given above, in equations (20) and (22), by using a delta function to describe the distribution of the homogeneous component.] The same qualitative relations hold with regard to $\langle B_{24}^{(R)} \rangle / \langle B_{22}^{(R)} \rangle$, the comparisons being made at a given value of ξ . Consequently a maximum A_2 predicted for a mixture of two homogeneous fractions at a particular value of γ would not appear in a real system if in fact fractionation were inadequate and Z_2 happened to be sufficiently less than Z_4 . Calculations for the case $Z_2 = 1$, $Z_4 = \infty$, $a = 1/4$, $\varepsilon = 10$ (*i.e.* $\xi = 5$), give $\langle B_{24}^{(II)} \rangle / \langle B_{22}^{(II)} \rangle = 1.22$ and $B_{24}^{(R)}/B_{22}^{(R)} = 1.04$ as compared with B_{24}/B_{22} equal to 1.13 and 1.41 for mixed homogeneous fractions with γ of 5 and 10 respectively.

The generalization of this development for a mixture of two heterogeneous polymers to more complex molecular weight distributions is at once obvious. The assumption of the Schulz distribution is therefore scarcely restrictive since almost any distribution could be described reasonably well as a combination of several heterogeneous polymers each characterized by an appropriate value of Z and $\langle n \rangle$.

OTHER FORMS FOR B_{ij}

In choosing the rigid sphere relation for combining second virial coefficients of homogeneous systems to obtain the interaction coefficient B_{ij} for unlike components, we have made perhaps the simplest possible assumption suggested by a physical model. Aside from this tenuous justification, the treatment is arbitrary and acceptable only to the degree in which it may be found to agree with experiments or with developments of greater rigour. Unfortunately the exact statistical treatment of polymer solutions has been worked out only for systems near the theta point, the limit of vanishing A_2 , where equation (1) is not valid*.

Among the approximate theories, that of Flory and Krigbaum³ (see also ref. 4) includes the calculation of B_{ij} for molecules of dissimilar size. In their model the polymer molecule is represented as a spherically symmetrical cloud of chain segments with a gaussian density distribution normalized so that the radius of gyration agrees with that of the real polymer chain. The interaction (interpenetration) of two such spheres is then treated according to standard statistical mechanical technique to obtain B_{ij} . The result may be written in the form:

$$B_{ij} = \frac{N_0 \beta n_i n_j}{2M_i M_j} F(X_{ij}) \quad (24)$$

$$\left(\frac{X_{ij}}{n_i n_j}\right)^{2/3} = \frac{2(X_{ii}/n_i^2)^{2/3}(X_{jj}/n_j^2)^{2/3}}{(X_{ii}/n_i^2)^{2/3} + (X_{jj}/n_j^2)^{2/3}} \quad (25)$$

$$X_{ii} = (\beta n_i^{1/2} / \alpha^3) (9/2\pi b_0^2)^{3/2} \quad (26)$$

where n_i is now the number of segments or steps of r.m.s. length b_0 in the equivalent unperturbed chain representing a polymer molecule of weight M_i , and α_i is the linear factor by which the radius of the chain in a good solvent is expanded by intramolecular interactions characterized by the volume of mutual exclusion β for a pair of segments. The function $F(X)$ expressing the molecular weight dependence of A_2 cannot be written exactly in closed form; however, it is unity for $X=0$ and decreases monotonically to approach zero as X becomes infinite. In terms of parameters of the assumed chain model, the molecular radius of gyration is given by

$$\langle R_i^2 \rangle = n_i b_0^2 \alpha_i^2 / 6$$

Putting this into equation (26) and thence into equation (25) we obtain an effective radius for interaction of two unlike molecules defined by

$$\langle R_{ij}^2 \rangle \equiv \left(\frac{n_i n_j}{X_{ij}}\right)^{2/3} \frac{3\beta^{2/3}}{4\pi} = \frac{1}{2} (\langle R_i^2 \rangle + \langle R_j^2 \rangle)$$

which may be compared with the simple mean

$$r_{ij} = (r_i + r_j) / 2$$

of the radii r_i , r_j , of hard spheres implied by equation (2).

*The exact and the approximate statistical theories agree in form in having $\partial \log A_2 / \partial \log n$ proportional to $n^{1/2}$ in the neighbourhood of the theta point.

As a consequence of the form of the Flory-Krigbaum result, it is not possible to express B_{ij} directly as a function of B_{ii} , B_{jj} , and molecular weights, as in equation (3), except in the limit as $\beta n^{1/2}$ becomes very large^{5,7} and even then only in approximation. The limiting relation is

$$F(X) \sim 4(\ln X)^{3/2} / 3\pi^{1/2} X$$

but over a finite range of X for sufficiently large X this is equivalent to $F(X)$ proportional to $1/X$. Then we can write

$$(B_{ij}n_i n_j)^{2/3} = \frac{1}{2} [(B_{ii}n_i^2)^{2/3} + (B_{jj}n_j^2)^{2/3}] \quad (27)$$

which is analogous to equation (3) for hard spheres except for the exponents $2/3$ in place of $1/3$. If the definition of X (equation 26) is accepted literally though, the limiting form of $F(X)$ is not realized in a physically attainable range of the variable, at least not for uncharged macromolecules. Since the Flory-Krigbaum theory and our theory are in accord qualitatively to the extent of predicting $B_{24} > B_{22}$ for two fractions under some conditions, it would be of interest to make a quantitative comparison of results for more complicated molecular weight distributions. Unfortunately, however, it does not seem possible to carry out analytically the integrations required after combining the Schulz distribution function with even the fairly simple form for B_{ij} given by equations (1) and (27).

In addition to the schemes already discussed one might choose to obtain B_{ij} in various arbitrary ways from values of B_{ii} and B_{jj} . Use of the geometric mean

$$B_{ij} = (B_{ii}B_{jj})^{1/2} \quad (28)$$

for example, has been proposed³². Another completely arbitrary but tractable form is given by

$$B_{ij}(n_i n_j)^\nu = \frac{1}{2} (B_{ii}n_i^{2\nu} + B_{jj}n_j^{2\nu}) \quad (29)$$

which for $\nu=0$ reduces to the ordinary arithmetic mean. With B_{ii} and B_{jj} positive, B_{ij} is always intermediate in value for both the geometric and arithmetic averages, the latter being the greater of the two. These rules, therefore, would never allow the appearance of a maximum in the composition dependence of A_2 for mixtures of two polymers; hence they are untenable in view of experience. When ν is not zero, equation (29) does, under some conditions, yield a maximum.

In combination with the B_{ii} of equation (1) and the Schulz distribution, equations (28) and (29) both lead to simple expressions for $A_2^{(1)}$ and $A_2^{(R)}$ in terms of gamma functions. For comparison with the theory based on hard sphere interactions, some numerical values calculated in this way are listed in *Table 2* for Z unity. For both light scattering and osmotic pressure, the effect of heterogeneity as determined by the last relation vanishes for ν approximately 0.5, in the sense that then $A_2^{(1)}/B_{NN}$ and $A_2^{(R)}/B_{ww}$ become unity.

We are indebted to Mr R. E. Kerwin for the numerical computations required in this work.

*Mellon Institute,
Pittsburgh, Pa, U.S.A.*

(Received March 1962)

REFERENCES

- ¹ FLORY, P. J. *J. chem. Phys.* 1945, **13**, 453
- ² FLORY, P. J. *J. chem. Phys.* 1949, **17**, 1347
- ³ FLORY, P. J. and KRIGBAUM, W. R. *J. chem. Phys.* 1950, **18**, 1086
- ⁴ ISIHARA, A. and KOYAMA, R. *J. chem. Phys.* 1956, **25**, 712
- ⁵ OROFINO, T. A. and FLORY, P. J. *J. chem. Phys.* 1957, **26**, 1067
- ⁶ KOYAMA, R. *J. chem. Phys.* 1957, **27**, 234
- ⁷ CASASSA, E. F. and MARKOVITZ, H. *J. chem. Phys.* 1958, **29**, 493
- ⁸ CASASSA, E. F. *J. chem. Phys.* 1959, **31**, 800
- ⁹ PITTSYN, O. B. and ÉIZNER, YU. E. *Vysokomol. Soedineniya*, 1959, No. 1, 1200
- ¹⁰ KRIGBAUM, W. R., CARPENTER, D. K., KANEKO, M. and ROIG, A. *J. chem. Phys.* 1960, **33**, 921
- ¹¹ SCATCHARD, G. J. *Amer. chem. Soc.* 1946, **68**, 2315
- ¹² KIRKWOOD, J. G. and GOLDBERG, R. J. *J. chem. Phys.* 1950, **18**, 54
- ¹³ STOCKMAYER, W. H. *J. chem. Phys.* 1950, **18**, 58
- ¹⁴ CASASSA, E. F. *Polymer, Lond.* 1960, **1**, 169
- ¹⁵ YAMAKAWA, H. and KURATA, M. *J. chem. Phys.* 1960, **32**, 1852
- ¹⁶ ALBRECHT, A. C. *J. chem. Phys.* 1957, **27**, 1002
- ¹⁷ CASASSA, E. F. and STOCKMAYER, W. H. *Polymer, Lond.* 1962, **3**, 53
- ¹⁸ HIRSCHFELDER, J. O., CURTISS, C. F. and BIRD, R. B. *Molecular Theory of Gases and Liquids*, Chapter 3. Wiley: New York, 1954
- ¹⁹ KRIGBAUM, W. R. and FLORY, P. J. *J. Amer. chem. Soc.* 1953, **75**, 1775
- ²⁰ FOX, T. G., KINSINGER, J. B., MASON, H. F. and SCHUELE, E. M. *Polymer, Lond.* 1962, **3**, 71
- ²¹ COHN-GINSBERG, E., FOX, T. G. and MASON, H. F. *Polymer, Lond.* 1962, **3**, 97
- ²² FLORY, P. J. and FOX, T. G. *J. Amer. chem. Soc.* 1951, **73**, 1901
- ²³ STOCKMAYER, W. H. *J. Polym. Sci.* 1955, **15**, 595
- ²⁴ VARADIAH, V. V. and RAO, V. S. *J. Polym. Sci.* 1961, **50**, 31
- ²⁵ CHIEN, J.-Y., SHIH, L.-H. and YU, S.-C. *J. Polym. Sci.* 1958, **29**, 117
- ²⁶ ZIMM, B. H. *J. chem. Phys.* 1946, **14**, 164
- ²⁷ SCHULZ, G. V. *Z. phys. Chem. B*, 1939, **43**, 25
- ²⁸ FLORY, P. J. *Principles of Polymer Chemistry*, Chapter 8. Cornell University Press: Ithaca, 1953
- ²⁹ BISCHOFF, J. and DESREUX, V. *Bull. Soc. chim. Belg.* 1952, **61**, 10
- ³⁰ MEYERHOFF, G. and SCHULZ, G. V. *Makromol. Chem.* 1952, **7**, 297
- ³¹ BISCHOFF, J. and DESREUX, V. *J. Polym. Sci.* 1957, **10**, 437
- ³² BLUM, J. J. and MORALES, M. F. *J. chem. Phys.* 1950, **18**, 153

Heterogeneous Radical Polymerization of Ethylene

B. L. ERUSSALIMSKY, S. G. LYUBETZKY, W. W. MAZUREK, S. YA. FRENKEL
and L. G. SHALTYKO

In the course of investigating the polymerization of ethylene initiated by azoisobutyronitrile in the presence of small amounts of benzene at 100 to 600 atm and at 70°C several unusual features were found, connected with an unusual polymerization mechanism. The polymerization was carried at a temperature below the melting point of polymer. For this reason the polymer precipitated during the process as a crystalline solid phase containing 'living' chains, the presence of which was proved experimentally. A kinetic scheme and equations are given for the dependence of degree and rate of polymerization on the time; they agree with experimental results. A statistical treatment of the molecular weight distribution of the polyethylene obtained under such conditions confirms the kinetic scheme given.

HETEROGENEOUS radical polymerization accompanied by transition of growing macroradicals from the liquid or gaseous phase into the solid phase has long attracted the attention of various investigators¹⁻³ and has been most thoroughly studied by Bamford *et al.* for acrylonitrile and other monomers⁴⁻⁷. The radical polymerization of ethylene below the melting point of the polymer with the formation of a solid phase—one of the most interesting examples of such processes—has not hitherto been studied in detail. In this field only the investigations of Laird *et al.*⁸ and of Kodama *et al.*⁹ are known, and these are not concerned with the problem of the phase state. Here we report the results of the polymerization of ethylene initiated by azoisobutyronitrile (AIBN) at 70°C and at 100 to 600 atm in the presence or absence of benzene. Unusual kinetic results obtained in the course of our investigation are connected not only with the heterogeneity of the process in the sense mentioned above, but also with the homogeneity of the monomer-solvent-initiator system under the conditions of the experiments.

As we have shown, the initial stage of the polymerization is characterized by the usual laws of homogeneous radical processes. But even at relatively low conversions substantial deviations appear in the dependence of polymerization rate and number average degree of polymerization on the monomer and solvent concentrations. These apparent anomalies result from the essential role in the polymerization of 'living' chains, transferred to the solid phase at the very beginning of the process. Chain propagation to the living macroradicals and the absence of termination by radicals in the solid phase lead to a continuous increase of the molecular weight of polymer with conversion*.

*The properties of the polymer obtained under such conditions are similar to those of Ziegler-polyethylene (density 0.95 to 0.96, m.pt 130°C, mol. wt up to 2×10^5)⁹.

EXPERIMENTAL

The ethylene contained 99.3 per cent of ethylene, 0.5 per cent of ethane and up to 0.0002 per cent of oxygen. Benzene and AIBN were purified as usual and had properties corresponding to the published data. The polymerization was carried out in an autoclave equipped with stirrer and thermostat. The initiator solution was placed in the de-aerated autoclave and the necessary pressure was applied simultaneously with temperature

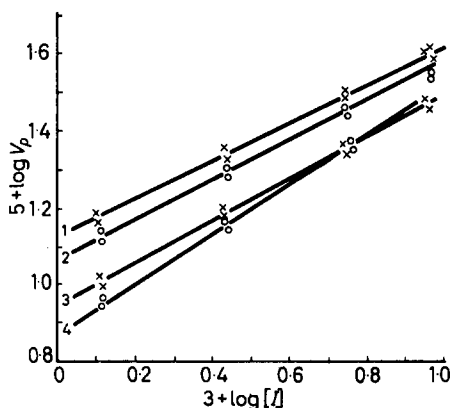


Figure 1—Influence of initiator concentration on initial rate of ethylene polymerization. Pressure 500 atm; temperature 70°C; benzene concentration (mole l⁻¹): 1—0.14, 2—0.07, 3—0.28, 4—no benzene. Duration of polymerization—1 h

control. The temperature was held to within $\pm 0.2^\circ\text{C}$. All experiments were carried out at an ethylene pressure constant to within ± 2 to 5 atm. The molecular weights of polyethylene obtained were measured viscometrically (in decalin at 135°) being calculated from the equation¹¹

$$[\eta] = 3.873 \times 10^{-4} \bar{M}_n^{0.738}$$

Fractionation of the polymers was carried out by precipitation with benzyl alcohol from tetralin solution in the temperature range¹² 156° to 20°C.

KINETICS OF THE HETEROGENEOUS POLYMERIZATION OF ETHYLENE

The main results obtained for the initial stage of ethylene polymerization are given in *Figures 1* and *2*¹³. The diagrams show a linear logarithmic relation between polymerization rate and initiator concentration for $[I]=0.001$ to 0.01 and $[\text{benzene}]=0$ to 0.28 mole l⁻¹. This indicates homogeneous distribution of the initiator in the monomer and in the homogeneous system solvent-monomer. As appears from these data, a definite optimum of the solvent concentration exists in relation both to the rate and to the degree of polymerization. This is due to the growth of living polymer chains in the solid phase. It seems probable that under such conditions a small quantity of the solvent influences only the diffusion rate of ethylene in the solid phase without giving rise to a marked increase of the mobility of the growing macroradicals.

The above facts are very similar to the phenomena established by Bamford and Jenkins in their investigation of the influence of DMF concentration on the polymerization of acrylonitrile⁵.

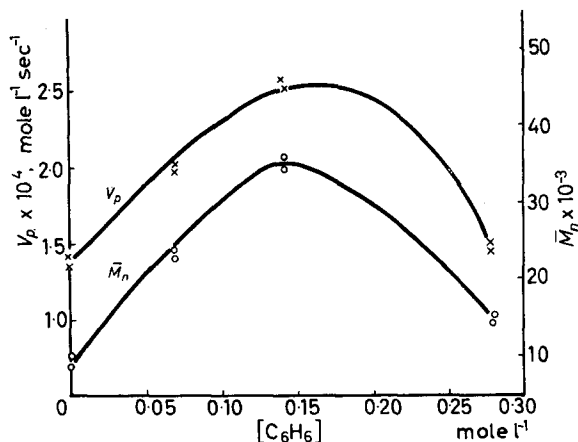


Figure 2—Influence of benzene concentration on polymerization rate and molecular weight of polymer. Pressure 500 atm; temperature 70°C; initiator concentration 2.75×10^{-3} mole l^{-1} . Duration of polymerization—1 h

The dependence of the initial polymerization rate and the molecular weight of the polymer on the monomer concentration changes abruptly in character above 300 to 400 atm (Figures 3 and 4). At 100 to 300 atm the polymerization rate is first order in $[M]$, and $1/\bar{P}$ varies linearly with $1/[M]$. Above 300 atm the relation of the above-mentioned quantities to the monomer concentration changes abruptly. Similar relations are valid for the fugacity of ethylene¹³.

The above results were obtained at relatively low conversions of monomer. At greater extents of heterogeneous polymerization the role of living macroradicals increases. For these conditions the following relations

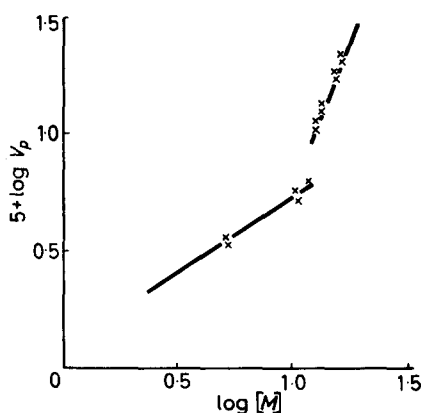
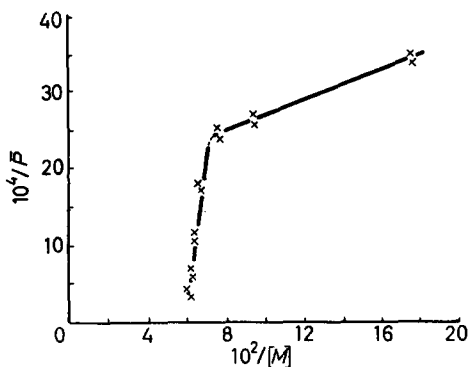


Figure 3—Influence of ethylene concentration on initial rate of polymerization at 70°C. Concentration (mole l^{-1}): benzene—0.14, initiator— 2.75×10^{-3} . Duration of polymerization—1 h

have been established. Continuation of the polymerization for a period exceeding the time necessary for practically complete decomposition of the initiator leads to a continuous increase of polymer molecular weight as well as a constant rate of polymerization (Figure 5). Apparently under such

conditions the termination of living polymer chains in the solid phase is possible only by free radicals from the gaseous phase. For this reason after the initiator is consumed the process becomes kinetically one in which there is no termination. A somewhat slow increase of molecular weight near the beginning of the process results from a continuous addition of a low molecular weight fraction to the polymer at this period.

Figure 4—Influence of ethylene concentration on degree of polymerization at 70°C. Concentration (mole l⁻¹): benzene—0.14, initiator— 2.75×10^{-3} . Duration of polymerization—1 h



The presence of living polymer chains in the solid phase was confirmed by direct experiments. After 4 to 10 hours of polymerization at 70°C and 500 atm the temperature was rapidly lowered to 20°; the decrease of the pressure was compensated by addition of fresh ethylene and the reaction mixture remained under these conditions for several hours. It was shown that during this additional time both yield and molecular weight of polymer increased markedly (*Table 1*). This phenomenon cannot be ascribed to the presence

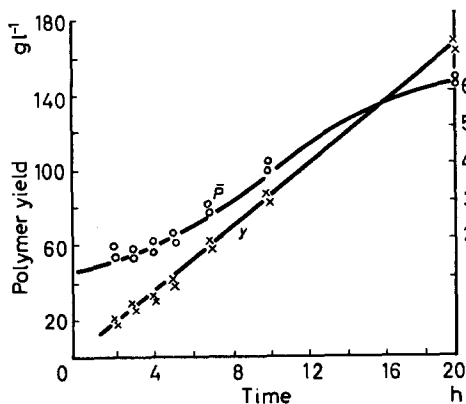


Figure 5—Influence of duration of reaction on degree of polymerization and on polymer yield. Concentration (mole l⁻¹): initiator— 1.35×10^{-3} , benzene—0.14

of the undecomposed initiator, because AIBN is quite stable at 20°.

The presence of an active solid phase also allows us to explain the change in character of the dependence of both degree and rate of polymerization on the monomer concentration. The break in the curve (*Figure 4*) corresponds to the monomer concentration at which the formation of macroradicals having

HETEROGENEOUS RADICAL POLYMERIZATION OF ETHYLENE

a relatively high degree of polymerization occurs even in the initial stages of the process.

For this reason the aggregation of the growing chains leading to the accumulation of living polymer, acquires a decisive importance even at the

Table 1. Polymerization of ethylene by living macroradicals
 $[C_2H_4] = 0.14$, $[I] = 1.3 \times 10^{-3}$ mole l^{-1}

| Duration of polymerization (h) at | | Polymer | |
|-----------------------------------|--------------|-----------|----------|
| 70°, 500 atm | 20°, 500 atm | Weight, g | $[\eta]$ |
| 4 | 0 | 125 | 1.10 |
| 4 | 4 | 145 | 1.45 |
| 4 | 7 | 156 | 1.70 |
| 7 | 0 | 246 | 1.60 |
| 7 | 7 | 280 | 2.00 |
| 10 | 0 | 335 | 2.05 |
| 10 | 10 | 381 | 2.40 |

very beginning of the polymerization. This can be expressed as a functional relation of the following general type

$$k_a = f(\bar{P}) = f(\psi[M])$$

where I denotes initiator, $R\cdot$ is the radical of the gaseous phase, $R_a\cdot$ is a \bar{P}_n is the number average degree of polymerization, and $[M]$ is the monomer concentration. Hence the dependence of the rate of polymerization on the monomer concentration (or fugacity) may exceed first order.

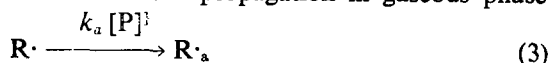
The above mechanism of heterogeneous polymerization of ethylene can be represented by the following scheme from which the characteristic kinetic features of the overall process may be deduced*.



Decomposition of initiator



Chain propagation in gaseous phase



Transition of radical into solid phase



Chain propagation in solid phase

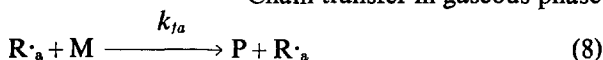
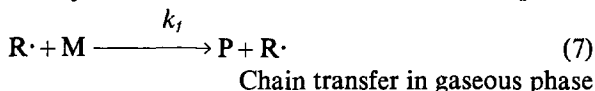


Chain termination in gaseous phase



*This scheme differs from one considered earlier¹⁴ in that it takes account of chain transfer in the solid phase. This gives better agreement between calculated and experimental data.

Chain termination by interaction of radicals from different phases



Chain transfer in solid phase

where I denotes initiator, $\text{R}\cdot$ is the radical of the gaseous phase, $\text{R}\cdot_a$ is a radical in the solid phase, M is monomer, P is dead polymer molecule, k_d is the rate constant of initiator decomposition, k_p is the rate constant of chain propagation in the gaseous phase, k_t is the rate constant of chain termination in the gaseous phase, k_{ta} is the rate constant of chain termination in the solid phase, k_f is the rate constant of chain transfer to monomer in the gaseous phase, and k_{fa} is the rate constant of chain transfer to monomer in the solid phase. Let us consider some specific features of this scheme.

(a) The polymerization process begins as an ordinary homogeneous polymerization in the gaseous phase. Colliding polymer molecules and radicals aggregate into particles, which remain in a suspended state. Gradually the aggregation begins to play a minor part in the process of radical transition as compared with the trapping of radicals by the surface of the polymer particles. Thus the rate of transition of the radicals into the solid phase depends on their concentration in the gaseous phase as well as on the surface area of the solid phase. The latter is proportional to the polymer concentration to the two-thirds power. This holds if the average size of the polymer molecules does not change with time. Actually during the polymerization in which the living radicals participate the average size of the polymer molecules increases. As a first approximation we assume that the change of the surface due to the growth of the degree of polymerization can be included in k_a as a constant factor.

(b) Chain termination takes place both in the gaseous phase and by the interaction of a radical on the solid phase surface with a radical from the gaseous phase. Termination by interaction of two radicals of the solid phase does not take place. This is one of the most important features of heterogeneous polymerization with the precipitation of polymer as a solid phase, insoluble and not swelling in the reaction medium.

Adopting the quasi-stationary conditions we can write on the basis of the equations (1) to (6):

$$d[\text{R}\cdot]/dt = 2k_d[\text{I}] - k_t[\text{R}\cdot]^2 - k_a[\text{R}\cdot][\text{P}]^{2/3} - k_{ta}[\text{R}\cdot_a][\text{R}\cdot] = 0 \quad (9)$$

$$d[\text{R}\cdot_a]/dt = k_a[\text{R}\cdot][\text{P}]^{2/3} - k_{ta}[\text{R}\cdot_a][\text{R}\cdot] = 0 \quad (10)$$

from which
$$[\text{R}\cdot_a] = (k_a/k_{ta})[\text{P}]^{2/3} \quad (11)$$

Substituting (11) into (9) we obtain

$$[\text{R}\cdot] = \left[-k_a[\text{P}]^{2/3} + \{k_a^2[\text{P}]^{4/3} + 2k_a k_t [\text{I}]\}^{1/2} \right] / k_t \quad (12)$$

Substituting (11) and (12) for $[\text{R}\cdot_a]$ and $[\text{R}\cdot]$ into the rate equation

$$-d[\text{M}]/dt = k_p[\text{M}][\text{R}\cdot] + k_{pa}[\text{M}][\text{R}\cdot_a] \quad (13)$$

we obtain

$$-\frac{d[M]}{dt} = [M] \left\{ k_p \frac{-k_a[P]^{2/3} + \{k_a^2[P]^{4/3} + 2k_a k_t [I]\}^{1/2}}{k_t} + \frac{k_{pa} k_a [P]^{2/3}}{k_{ta}} \right\} \quad (14)$$

[P] (the number of polymer molecules per unit volume) can be expressed in terms of the initiator concentration thus

$$[P] = n\{[I]_0 - [I]\} \quad (15)$$

where $[I]_0$ is initial concentration of initiator and $[I]$ the concentration at the time considered; n is the coefficient of proportionality which takes into account the type of termination, chain transfer, and also the efficiency of initiation. Since the initiator decomposition takes place unimolecularly

$$[I] = [I]_0 e^{-k_d t}$$

Then

$$[P] = n[I]_0(1 - e^{-k_d t}) \quad (16)$$

Substituting the above value for [P] in equation (14) and assuming that n can be included in k_a we obtain the equation for the rate of polymerization in its most general form

$$-\frac{d[M]}{dt} = [M] \left\{ (k_p/k_t) (-k_a [I]_0^{2/3} (1 - e^{-k_d t})^{2/3} + \{k_a^2 [I]_0^{4/3} (1 - e^{-k_d t})^{4/3} + 2k_a k_t [I]_0 e^{-k_d t}\}^{1/2}) + (k_{pa} k_a / k_{ta}) [I]_0^{2/3} (1 - e^{-k_d t})^{2/3} \right\} \quad (17)$$

At the very beginning of the process, i.e. when $t \rightarrow 0$, equation (17) may be transformed into

$$-\frac{d[M]}{dt} = \sqrt{2k_p k_a^{1/2}} [M] [I]_0^{1/2} / k_t^{1/2} \quad (18)$$

which is the ordinary equation for the rate of a homogeneous polymerization. For the power of $[I]_0$ we have obtained values near 0.5 (for one hour of reaction time).

When the process has progressed so far that the initiator concentration tends to zero, equation (17) is transformed into

$$-\frac{d[M]}{dt} = (k_{pa} k_a / k_{ta}) [M] [I]_0^{2/3} \quad (19)$$

This means that after the initiator is consumed the polymerization rate should remain constant, its value being proportional to the initial concentration of initiator to the two-thirds power. Under such conditions the polymerization reaction depends on the living chains, occurring as a process without chain termination.

Equation (17) can be greatly simplified if we assume that the rate constants of propagation and termination change in an equal proportion after the radicals pass into the solid phase, i.e.

$$k_{pa} / k_p = k_{ta} / k_t \quad (20)$$

This assumption, which seems doubtful at first sight, results from our idea that both chain propagation and chain termination in this system occur at the

interface. The adsorbed radical is equally accessible for both monomer molecules and radicals from the gaseous phase. We do not believe this assumption to be valid for all cases of the heterogeneous polymerization. It seems applicable only to those systems in which the precipitating polymer crystallizes. On the contrary, with swelling and mobile structures allowance should be made for coiling and occlusion of trapped radicals. This results in a sharp difference in the accessibility of the active end for the monomer molecule (growth) and for the polymer radical (termination)⁷.

Since from (20) $(k_{pa}/k_{ia}) = (k_p/k_t)$ equation (17) may be transformed into

$$-d[M]/dt = (k_p/k_t)[M] \{k_a^2[I]_0^{4/3}(1 - e^{-k_a t})^{4/3} + 2k_a k_t [I]_0 e^{-k_a t}\}^{1/2} \quad (21)$$

On the basis of the mechanism proposed the time dependence of the mean polymerization degree \bar{P} can be deduced. It is assumed that the termination occurs by combination*:

$$\begin{aligned} \bar{P} &= \frac{-d[M]/dt}{V_t + V_f} = \frac{k_p[R\cdot][M] + k_{pa}[R\cdot_s][M]}{\frac{1}{2}k_t[R\cdot]^2 + \frac{1}{2}k_{ta}[R\cdot][R\cdot_s] + k_f[R\cdot][M] + k_{fa}[R\cdot_s][M]} \quad (22) \\ \frac{1}{\bar{P}} &= \frac{1}{2} \cdot \frac{k_t[R\cdot] + k_{ta}[R\cdot_s]}{k_p[R\cdot] + k_{pa}[R\cdot_s]} \cdot \frac{[R\cdot]}{[M]} + \frac{k_f[R\cdot] + k_{fa}[R\cdot_s]}{k_p[R\cdot] + k_{pa}[R\cdot_s]} \\ &= \frac{1}{2} \cdot \frac{(k_t/k_{ta})[R\cdot] + [R\cdot_s]}{(k_p/k_{pa})[R\cdot] + [R\cdot_s]} \cdot \frac{[R\cdot]}{[M]} \cdot \frac{k_{ia}}{k_{pa}} + \frac{(k_f/k_{fa})[R\cdot] + [R\cdot_s]}{(k_p/k_{pa})[R\cdot] + [R\cdot_s]} \cdot \frac{k_{fa}}{k_{pa}} \quad (23) \end{aligned}$$

It may be supposed that the above assumption (20) can also be extended to the chain transfer:

$$k_t/k_{ta} = k_p/k_{pa} = k_f/k_{fa} \quad (24)$$

when equation (23) becomes

$$\frac{1}{\bar{P}} = \frac{k_t[R\cdot]}{2k_p[M]} + \frac{k_i}{k_p} \quad (25)$$

Substituting for $[R\cdot]$ from (12) into equation (25) and taking into account (16) we obtain

$$\frac{1}{\bar{P}} = (1/2k_p[M]) \{k_a^2[I]_0^{4/3}(1 - e^{-k_a t})^{4/3} + 2k_a k_t [I]_0 e^{-k_a t}\}^{1/2} - k_a [I]_0^{2/3} (1 - e^{-k_a t})^{2/3} + k_f/k_p \quad (26)$$

Initially, i.e. as $t \rightarrow 0$

$$\frac{1}{\bar{P}} \rightarrow \left\{ \frac{(k_a k_t [I]_0)^{1/2}}{\sqrt{2} k_p [M]} + \frac{k_f}{k_p} \right\} \quad (26a)$$

This equation corresponds to ordinary homogeneous polymerization. At high conversions the first term of equation (26) tends to zero and

$$1/\bar{P} \rightarrow k_f/k_p \quad (26b)$$

When the initiator is consumed the polymerization proceeds without termination and the degree of polymerization then depends only on chain transfer and tends to the limiting value k_p/k_f .

*We suppose termination to occur by combination on account of the low content of terminal double bonds (0.01 per 1000 C atoms), as is shown by the infra-red spectra¹⁴.

HETEROGENEOUS RADICAL POLYMERIZATION OF ETHYLENE

The general relations expressed by the above equations agree well with experimental observations on the heterogeneous polymerization of ethylene¹³. The validity of the assumptions made can be proved by calculations on the basis of the experimental data.

In equation (21) the values of k_p , k_t and k_a are unknown. The value of k_d (the rate constant of the AIBN decomposition at 70°C) is calculated from the data of Overberger *et al.*¹⁷. Using the experimental data for the initial reaction period (reaction time, 1 h) the value of k_p^2/k_t may be obtained from equation (18) and is found to be 3.0×10^{-4} mole⁻¹ l. sec⁻¹. Using the experimental value of the rate at three hours reaction time the value of k_a^2/k_t may be calculated from equation (21) and proves to be 8.2×10^{-4} mole⁻¹ l. sec⁻¹. From these values the dependence of the rate of polymerization on time has been calculated (Figure 6, Table 2). As Figure 6 shows,

Table 2. Dependence of rate and degree of polymerization on the reaction time. Conditions of polymerization: pressure 500 atm, temperature 70°C

| Duration of reaction (h) | Polymerization rate 10 ⁴ V mole l ⁻¹ sec ⁻¹ | | Exptl data 10 ⁴ / \bar{P} | Calcd from (26) 10 ⁴ / \bar{P}_0 | Transfer constant to monomer 10 ⁴ C _M |
|--------------------------|--|-----------------|--|---|---|
| | Exptl data | Calcd from (21) | | | |
| 1 | | | | | |
| 2 | 0.90-0.95 | 0.88 | 5.6-6.6 | 3.2 | 2.4-3.4 |
| 3 | 0.84-0.89 | 0.87 | 5.9-6.2 | 2.5 | 2.4-3.7 |
| 4 | 0.78-0.85 | 0.87 | 5.3-5.8 | 2.2 | 3.1-3.6 |
| 5 | 0.93-0.95 | 0.87 | 4.6-4.8 | 1.6 | 3.0-3.2 |
| 7 | 0.85-0.89 | 0.88 | 3.5-4.0 | 1.2 | 2.3-2.8 |
| 10 | 0.83-0.85 | 0.89 | 2.5-2.8 | 0.6 | 1.9-2.2 |
| 20 | 0.83-0.85 | 0.90 | 1.8-2.0 | 0.08 | 1.7-1.9 |

Mean 2.7×10^{-4}

satisfactory agreement exists between the theoretical curve and the rate data obtained for the period 1 to 20 hours. For calculating the change of the degree of polymerization with time the values of k_a^2/k_t and k_p^2/k_t ,

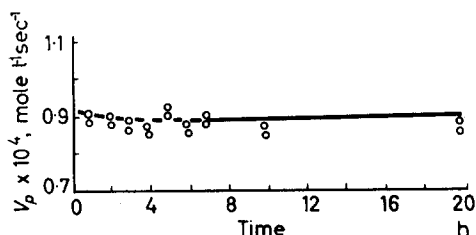


Figure 6—Influence of duration of reaction on rate of polymerization at 500 atm and 70°C. Initial concentration of the initiator— 1.35×10^{-3} , benzene concentration— 0.14 mole l⁻¹. (o experimental points, — theoretical curve, calculated from equation 21)

calculated from equations (18) and (21) have been used. Equation (26) can be written in the form

$$1/\bar{P} = 1/\bar{P}_0 + C_M \quad (27)$$

The calculated values of $1/\bar{P}_0$ are given in Table 2 (column 5). The last column of the table presents the difference between the experimental

values of $1/\bar{P}$ and the calculated ones of $1/\bar{P}_0$. This difference is equal to the transfer constant to monomer C_M . The mean value of C_M , 2.7×10^{-4} , agrees satisfactorily with the value 5.0×10^{-4} obtained from the investigation of the homogeneous polymerization of ethylene in benzene solution at 70°C and at pressures up to 100 atm¹⁸.

The value of $1/\bar{P}$, calculated with $C_M = 2.7 \times 10^{-4}$ agrees satisfactorily with the experimental data (Figure 7).

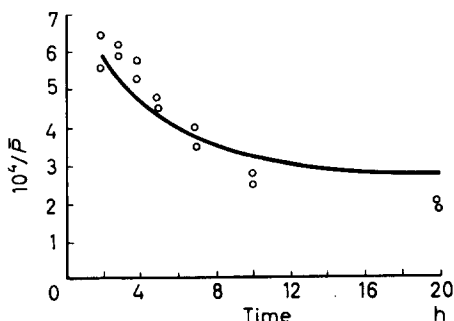


Figure 7—Influence of duration of reaction on degree of polymerization at 500 atm and 70°C . Initial concentration of initiator— 1.35×10^{-3} , benzene concentration— 0.14 mole l^{-1} . (○ experimental points, — theoretical curve, calculated from equation 26)

One of the consequences of the calculated dependence of the reaction rate on time is the conclusion that when the reaction time is great, the rate should be proportional to the initial concentration of the initiator to the two-thirds power (equation 19). The experimental results listed in Table 3 and Figure 8 give a direct confirmation of this conclusion. The mean value for the power of the initial concentration of the initiator is 0.65 ± 0.03 .

Table 3. Dependence of rate of polymerization on initial concentration of initiator (500 atm, 70°C , $t = 10 \text{ h}$)

| | | | | | | |
|---|-------|-------|------|------|------|------|
| Initial conc. of initiator $[I]_0 \times 10^3 \text{ mole l}^{-1}$ | 13.50 | 13.50 | 6.75 | 6.75 | 3.38 | 3.38 |
| Rate of polymerization $V_p \times 10^5 \text{ mole l}^{-1} \text{ sec}^{-1}$ | 8.20 | 8.30 | 5.45 | 5.33 | 3.36 | 3.44 |

STATISTICAL ASPECTS

We shall now consider some statistical aspects of the problem¹⁹. Imagine an active surface F growing under some arbitrary law during polymerization. With every chain growing on this surface we can associate some effective surface element ΔF such that any collision of a free radical from the gaseous phase with this element leads to chain termination. It follows immediately that a special steady-state condition for such a system will be

$$\Delta F \cdot [R_2^*] = \frac{1}{2}F \quad (28)$$

where $[R_2^*]$ is the surface concentration of growing chains. If this condition is fulfilled, every pair of collisions with the active surface consists on an average of a termination followed by reactivation (trapping of a new free

radical) or vice versa. In other words such a sequence of events may be considered as a two-step transference reaction.

After initial formation of the active surface and establishment of the steady-state condition (28), a continuous change in the relative concentrations of free (in colloidal sense) and trapped radicals ($[R^*]$ and $[R_a^*]$ respectively) begins. This change is due to reaction (3) and continuous growth of the active surface. If at low conversion the overall concentration of free radicals is constant (the case may be easily generalized to take into account a decrease in this concentration with time) because of this change in relative concentrations, the overall termination rate attains its maximum at $[R_a^*] = [R^*]$ and then gradually falls. The fact that from this moment $[R^*]$ becomes less than $[R_a^*]$ shows that some fraction of trapped chains will begin to grow without termination. On account of further changes in the

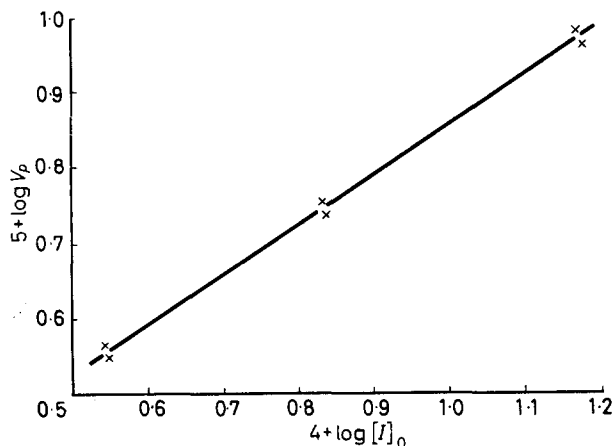


Figure 8—Influence of initial concentration of initiator on polymerization rate. Pressure—500 atm, temperature—70°C, benzene concentration—0.14 mole l^{-1} , duration of polymerization—10 h

relative concentrations of radicals and exhaustion of initiator this fraction will increase at high conversions until eventually the whole process becomes an uninterrupted growth of living chains.

Sufficient evidence has already been presented to substantiate such a sequence of events. Here we shall investigate the form of the number distribution of molecular weights $q_n(M)$ in this kind of process.

As may be shown by trivial calculations, in any n -phase system where initiation takes place in one phase only and the growth proceeds progressively in all phases with the possibility of both intra- and inter-phase termination, the number of maxima in the distribution equals n in the case of disproportionation and $\frac{1}{2}n(n+1)$ for combination. It follows that in the case under consideration the number of maxima will be at least two. One must add to these an additional maximum necessarily appearing in the later stages of polymerization when the growth of living chains begins.

Thus the resulting molecular weight distribution will consist of at least two equilibrium distributions of dead chains and one distribution of living chains, of which the latter may be arbitrarily wide due to the continuous creation of living chains in any stage of the process. The detailed calculation of the real shape and its changes with conversion would involve great labour, but we can predict qualitatively these changes with sufficient precision to check them experimentally.

First we shall discuss the partial distribution arising in the pre-stationary period resulting from growth and mutual termination of chains exclusively in the gaseous phase. This distribution, which we shall denote $S(M)$, must be of the usual form for homogeneous distributions, i.e.

$$S(M) = \alpha e^{-\alpha M} \quad (29)$$

for disproportionation, or

$$S(M) = \alpha^2 M e^{-\alpha M} \quad (30)$$

for combination. Here the statistical parameter for the gaseous phase is

$$\alpha = \frac{\text{overall termination rate}}{\text{propagation rate} \times \text{mol. wt of monomeric unit}}$$

Now the essential point is that on formation of the active surface, the probability of mutual collisions between free (in the colloidal sense) radicals will become considerably smaller than the probability of their impact with the active surface. In a first approximation one may put it equal to zero*. Then the partial distribution $S(M)$, once formed, will remain unaltered during the whole polymerization process.

After the active surface is formed, the whole system changes in the following manner. The growing chains, still beginning their growth in the gaseous phase, are distributed before being trapped according to the law (29) (though with a new value of α), but now one must include in the overall termination rate the rate of collisions with the surface or, alternatively, the rate of trapping, because every collision is effective. Moreover, on account of the above-mentioned assumption of the relative probabilities of mutual collisions and trapping, the overall termination rate for the gaseous phase becomes equal to the rate of trapping. The trapped chains continue to grow steadily on the active surface and in the steady state the molecular weight distribution of these 'appendix' chains will also be of the form

$$f^*(M) = \beta e^{-\beta M} \quad (31)$$

where the star shows that the distribution describes the growing chains only and the new parameter β is given by

$$\beta = \frac{\text{termination rate on surface of solid phase}}{\text{propagation rate on surface} \times \text{mol. wt of monomeric unit}}$$

Now we can use the inversion principle of statistics and assume that the resulting molecular weight distribution of whole growing chains will

*This may be proved easily by direct calculation using the laws of the kinetic theory of gases (or liquids).

be the same as if the 'appendix' chains had grown separately and then reacted with the chains formed in the gaseous phase. Using the theorem of the multiplication of probabilities we obtain the resulting distribution

$$P^*(M) = \int_0^M S^*(\xi) f^*(M - \xi) d\xi \quad (32)$$

Integration yields

$$P^*(M) = \frac{\alpha\beta}{\alpha - \beta} \left\{ e^{-\beta M} - e^{-\alpha M} \right\} \quad (33)$$

For termination by disproportionation the resulting distribution of dead chains $P(M)$ will be identical with $P^*(M)$ given in (33), but for combination one must repeat the operation (32), i.e. put

$$P(M) = \int_0^M P^*(\xi) S^*(M - \xi) d\xi \quad (34)$$

which gives after integration

$$P(M) = \left\{ \alpha / (\alpha - \beta) \right\} P^*(M) - \left\{ \beta / (\alpha - \beta) \right\} S(M) \quad (35)$$

Thus the overall distribution at an arbitrary stage of polymerization must include: a distribution of the form (29) or (30); a distribution of the form (33) or (35), and a certain distribution of living chains.

It should be mentioned that a fourth, additional, maximum could occur owing to the disproportionation of free radicals of the gaseous phase with radicals growing on the surface. In the present case, however, when termination by combination predominates this maximum will not exist.

We now consider the manner in which the distribution changes during polymerization. It is quite sufficient for this purpose to consider only the distribution of 'appendix' chains (31), and to assume that the only variable in the formula for β is the concentration of free radicals formed in the gaseous phase $[R^*]$. As already mentioned a special transition period is attained when $[R^*] = [R^*]_0$. If the steady state conditions are still fulfilled, i.e. $[R^*] + [R^*]_0 = \text{constant}$, and if in the beginning of the transition period $\beta = \beta_0$ while $[R^*] = [R^*]_0$, then the distribution of hypothetical chains formed in a disproportionation process of 'appendix' chains only would be

$$\begin{aligned} f(M) &= \int_{[R^*]_0}^0 \beta_0 [R^*] e^{-\beta_0 [R^*] M} d[R^*] \\ &= \frac{1}{\beta_0 M^2} \left\{ \beta_0 [R^*]_0 M e^{-\beta_0 [R^*]_0 M} + (e^{-\beta_0 [R^*]_0 M} - 1) \right\} \end{aligned} \quad (36)$$

One should apply this operation to equation (33), but this would lead to unnecessary complexity as we are not trying to obtain strict numerical results.

As follows immediately from (36) (and the same obviously will hold for strict computation), the maximum of the distribution will migrate during the

transition period towards zero. It may even be possible that the maximum will disappear according to the prediction of the classical paper by Herington and Robertson²⁰. This migration may blur the maximum of the distributions (33) or (35). After the transition distribution (or its more precise analogue) is attained, there remains only the growth of living chains. Nothing can be said in advance about the shape of this last partial distribution, except that the distribution will grow and migrate towards still higher molecular weights. If the transfer reaction (8) is absent the width of the distribution must remain constant.

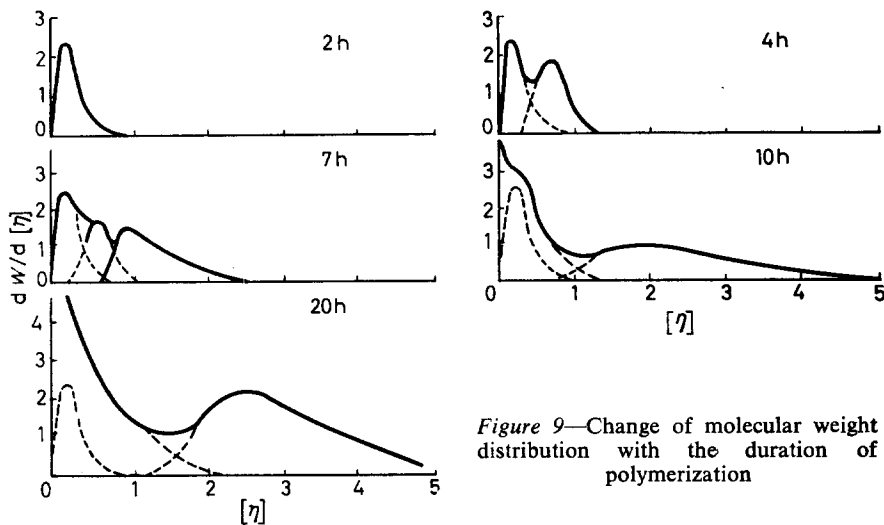


Figure 9—Change of molecular weight distribution with the duration of polymerization

To check these considerations several fractionations were carried out on five samples differing only in conversion. The results of these are presented as intrinsic viscosity/frequency curves (weight distributions) in Figure 9*.

For the sake of convenience in the examination of partial distribution changes with conversion, we normalized to unity the first curve corresponding to 2h of the process. The remaining curves were normalized to $t/2$, where t is time of polymerization (one must bear in mind that the conversion in our system is proportional to the time of polymerization, see Figure 5).

We consider first the curves for two and four hours of polymerization. As can be seen, the initial maximum remains unchanged, though a second one, approximately of the same size, appears after four hours of the process. Two conclusions may be drawn from this. First, once formed in practice, the active surface adsorbs practically all chains beginning their growth in the gaseous phase and the area under the first maximum equals the weight of polymer entering into the formation of the initial solid phase. Secondly, the termination mechanism must be combination rather than disproportionation, because with the latter the low molecular weight maximum would grow, resulting from accumulation of chains formed in the gaseous phase only.

*We preferred this way of representation because intrinsic viscosity data are obtained experimentally and not subjected to uncertainties arising from application of the Mark-Houwink formula to an excessively wide range of molecular weights.

The frequency curve for seven hours when resolved reveals three maxima, the first one being unchanged, whereas the second above has split into two. One of these seems to be that associated with living chains and the other we ascribe to dead chains formed on the active surface.

Probably some living chains were present at even earlier stages of the process, for in the diagram corresponding to seven hours the height of the curve at $[\eta] = 0.7$ is somewhat lower than that for four hours (the precision of fractionation is sufficient to allow this conclusion).

The overall shape of the distribution changes drastically when we turn to the diagram for ten hours reaction time. In accordance with the predictions made above, the first maximum is blurred on account of the change in the second partial distribution accompanying the exhaustion of free radicals from the gaseous phase. A similar picture is obtained for twenty hours of polymerization. In this case a wide maximum due to living chains is quite distinct. The accumulation of relatively low molecular weight chains has become still greater; this may be due in part to the transfer reaction (8).

The precision of reconstruction of the frequency curve at this late stage of the process is insufficient to warrant conclusions about the numerical value of the transfer constant. Nevertheless, the relative value of this constant presented earlier (2.7×10^{-4}) is sufficiently large to explain the additional accumulation of low molecular weight fractions. The mechanism involving migration of the second partial distribution may still take place even at this stage of process.

To conclude, we point out that the distribution derived from purely statistical considerations checks well with fractionation and kinetic data.

A P P E N D I X

The purely statistical method of examining the polymerization process used above may be of general value, and when applied to simpler systems leads to quantitative results. As an example we shall present the purely statistical derivation of Beasley's molecular weight distribution²¹ for high pressure polyethylene. We begin with the general statement first formulated by Herington and Robertson²⁰ for the steady-state molecular weight distribution of growing chains

$$q^*(M) = \alpha(M) \exp \left[- \int_0^M \alpha(M) dM \right] \quad (37)$$

where $\alpha(M)$ is again the statistical parameter that depends in general on chain length. We use the inversion principle of statistics and denote by β the long branching parameter, in other words the probability of formation of a branch on a number average chain. From the statistical point of view there is no difference between a process in which the growing chains 'die' due to mutual termination and are then reactivated by transfer and a process in which branching and growth proceed simultaneously. We see in the latter case that the rate of propagation for one initial chain increases proportionately to the number of branches growing on this chain. Then the probability of formation of a new branch on a chain of molecular weight M is

$$\beta M / M_n^* \equiv \alpha_0 \beta M$$

where $M^* = 1/\alpha_0$ is the number average molecular weight of an initial unbranched chain, or of a branch, because both unbranched chains and separate branches are statistically equivalent. It follows from the inversion principle that the dependence of the statistical parameter on the molecular weight, resulting from the dependence of the effective rate of growth on the molecular weight, will be given by

$$\alpha(M) = \alpha_0 / (1 + \alpha_0 \beta M) \quad (38)$$

Substituting (38) in (37) and integrating we obtain immediately

$$q_n(M) = \alpha_0 / (1 + \alpha_0 \beta M)^{(1+1/\beta)} \quad (39)$$

which is Beasley's distribution.

The same statistical treatment is applicable to any kind of polymerization process when its topology and other physical features are known.

*Institute of High Molecular Compounds,
Leningrad, U.S.S.R.*

(Received March 1962)

REFERENCES

- ¹ CHAPIRO, A. *J. Chim. phys.* 1950, **47**, 747
- ² THOMAS, G. and PELLON, M. *J. Polym. Sci.* 1954, **13**, 329
- ³ DURUP, J. and MAGAT, M. *J. Polym. Sci.* 1955, **18**, 586
- ⁴ BAMFORD, C. H. and JENKINS, A. D. *Proc. Roy. Soc. A*, 1953, **216**, 515
- ⁵ BAMFORD, C. H. and JENKINS, A. D. *Proc. Roy. Soc. A*, 1955, **228**, 220
- ⁶ BAMFORD, C. H., JENKINS, A. D., SYMONS, M. C. and TOWNSEND, M. G. *J. Polym. Sci.* 1959, **34**, 181
- ⁷ BAMFORD, C. H. and JENKINS, A. D. *J. Chim. phys.* 1959, **56**, 798
- ⁸ LAIRD, R., MORELL, A. and SEED, L. *Disc. Faraday Soc.* 1956, **22**, 126
- ⁹ KODAMA, S., MATSUSHIMA, Y., UEYESHI, A. and SHIMIDZU, T. *J. Polym. Sci.* 1959, **41**, 89
- ¹⁰ LYUBETZKY, S. G., DOLGOPLOSK, B. A. and ERUSSALIMSKY, B. L. *Vysokomol. Soedineniya*, 1961, **3**, 1000
- ¹¹ UEBERREITER, K., ORTHMAN, H. and SORGE, H. *Makromol. Chem.* 1952, **8**, 21
- ¹² ALLEN, P. W. *Techniques of Polymer Characterization*. Butterworths: London, 1959
- ¹³ LYUBETZKY, S. G., DOLGOPLOSK, B. A. and ERUSSALIMSKY, B. L. *Vysokomol. Soedineniya*, 1962, **4**, 533
- ¹⁴ LYUBETZKY, S. G. and MAZUREK, W. W. *Vysokomol. Soedineniya*, 1962, **4**, 1027
- ¹⁵ BAMFORD, C. H., BARB, W. G., JENKINS, A. D. and ONYON, P. F. *The Kinetics of Vinyl Polymerization by Radical Mechanisms*. Butterworths: London, 1958
- ¹⁶ GOLDENBERG, A. L. and LYUBETZKY, S. G. *Vysokomol. Soedineniya*, In press
- ¹⁷ OVERBERGER, C. G., O'SHAUGHNESSY, M. T. and SHALIT, H. *J. Amer. chem. Soc.* 1949, **71**, 2661
- ¹⁸ LYUBETZKY, S. G., DOLGOPLOSK, B. A. and ERUSSALIMSKY, B. L. *Vysokomol. Soedineniya*, 1961, **3**, 734
- ¹⁹ FRENKEL, S. YA., SHALTYKO, L. G. and LYUBETZKY, S. G. *Abstracts of the Ninth Conference of the Institute of High Molecular Compounds*, p 10. Academy of Sciences of the U.S.S.R.: Leningrad, 1962
- ²⁰ HERINGTON, E. F. and ROBERTSON, A. *Trans. Faraday Soc.* 1942, **38**, 490
- ²¹ BEASLEY, J. K. *J. Amer. chem. Soc.* 1953, **75**, 6123

Crystallization Kinetics Study of Nylon 6

J. H. MAGILL

Spherulite growth rates in undried nylon 6 have been measured over the crystallization range 90° to 185°C using a cine-camera technique. Crystallization rate constants determined by a depolarized light intensity method cover a much wider region (140° to 204°C) than previously presented in the literature. Measurements were made on both dried and undried polymer. A maximum in the rate of crystallization occurs about 140°C. Below 190°C, nucleation of spherulites is simultaneous in time, while above this temperature spherulites form sporadically. Molecular parameters governing the crystallization behaviour have been calculated using the plausible concept of two-dimensional surface nucleation on a primary three-dimensional nucleus.

DESPITE the considerable effort devoted to the study of crystallization processes in high polymers of technological interest during the past decade, nylon 6 has received belated attention. Only recently has the effect of melt conditions on the spherulite crystallization behaviour of this polymer been examined in detail^{1, 2} although the structural aspects of fibres and films have been studied closely^{3, 4}. With the exception of a paper on the kinetics of spherulite growth using a cine-camera technique⁵, other published work has been concerned with rate measurements in a very limited temperature range near the melting temperature. Dilatometric^{2, 6} and density balance methods⁷⁻⁹ have been used but these techniques are inadequate for following the fast crystallization rates usually encountered at large degrees of supercooling.

A light depolarization method^{10, 11} developed recently by the author has proved more versatile than these conventional procedures. In the present study it has been applied to both dried and undried nylon 6. Spherulite growth rates obtained using cine-photography are also presented. Although spherulite growth and spherulite nucleation can be studied separately by this method, no bulk nucleation rates were measured.

EXPERIMENTAL

The kinetics of crystallization of unstabilized nylon 6 were measured by:

- (1) Cine-camera technique for following spherulite growth rates.
 - (2) Depolarized light intensity method for rate constant determinations.
- (1) *Spherulite growth rates*

Microtomed 50 μ sections of polymer (R.V. 73, \bar{M}_n 24 700) mounted in MS 550 silicone oil between $\frac{5}{8}$ in. diameter, No. 1 glass cover slips, were melted for 30 minutes at 270° \pm 3°C on a Gallenkamp hot plate and then rapidly transferred to the Köfler hot stage mounted on the polarizing microscope and maintained within \pm 0.5°C of the desired crystallization temperature.

Rapid equilibration of the molten sample to the crystallization temperature was facilitated by a thin film of silicone oil intermediate between the sample and hot stage. The growth of spherulites was followed with a Paillard-Bolex H16 Reflex camera suitably mounted and connected to the ocular tube of the microscope. The camera was previously focused on a crystallized specimen representative of the thickness of the crystallizing samples. When necessary, minor adjustments were made with the microscope fine-focus as the spherulite crystallization was observed through the reflex viewfinder.

Kodak Panatomic X film was used for all photomicrography. A 125 W mercury arc lamp was employed as a light source. All films were projected at $\times 1\,230$ total magnification. The system was calibrated by photographing and projecting large spherulites of known dimensions. At least three growth rate determinations were made for each crystallization temperature. Good agreement of results was found within and between different samples.

(2) Measurements of rate constants

Sections 100μ of polymers (R.V. 70.8, \overline{M}_n 24 100 and R.V. 73, \overline{M}_n 24 700) were mounted between cover slips, melted and crystallized as described previously. The cine-camera was replaced by a photomultiplier-millivolt recording system which measured the rate of depolarization of light by the sample crystallizing on the Köfler hot stage. The mercury arc lamp was replaced by a 24 V stabilized tungsten light source. Details of this apparatus are given in earlier publications^{10, 11}. Several measurements were made at each crystallization temperature. Rate determinations were also carried out after drying similar polymer sections for three hours at 10^{-2} mm of mercury at 160°C .

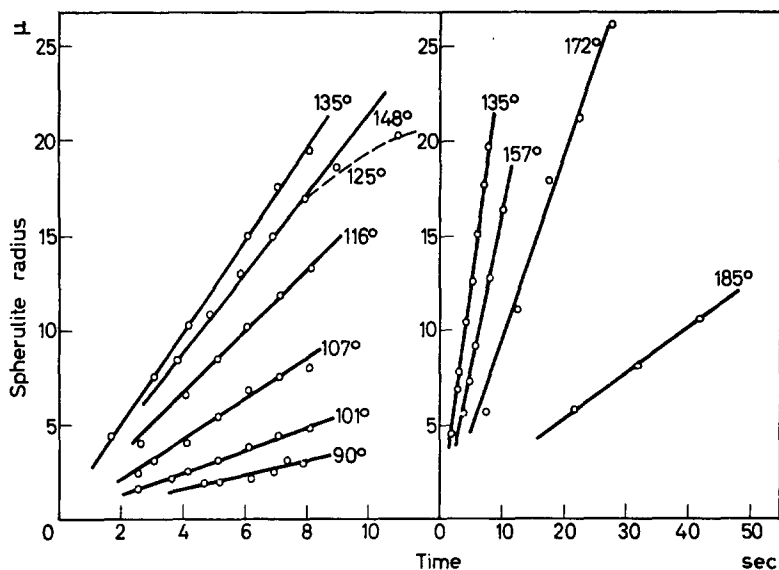


Figure 1—Spherulite radius versus time for different isothermal crystallizations

RESULTS

Rate of growth of spherulites

Typical plots of the spherulite growth rate versus time, are shown in *Figure 1*. As spherulites approach each other, the growth rate along the impinging direction ceases to be linear with time (dashed line *Figure 1*). The rate of generation of spherulite nuclei was simultaneous in time over the crystallization range examined (90° to 185°C). Measurements were not possible below 90°C because polymer films were partially quenched on cooling from the melt temperature and the very small spherulites gave insufficient light for photographic purposes.

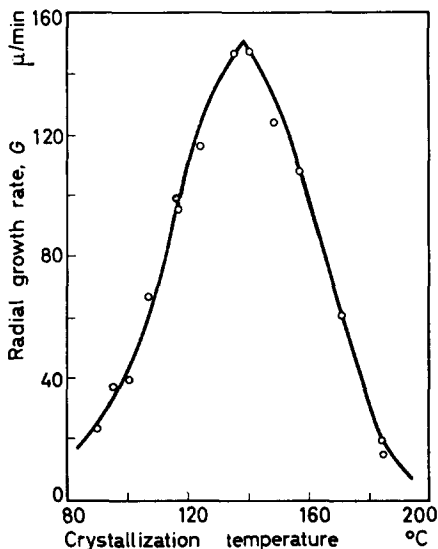


Figure 2—Spherulite growth rate, G , of nylon 6 versus crystallization temperature

The radial growth rates, G (microns/minute), are plotted as a function of crystallization temperature in *Figure 2*. A maximum in the growth rate occurs at a crystallization temperature of about 138°C. Growth rate/temperature variables are presented in *Figure 3*.

Light depolarization rate constants and Avrami parameters

For the primary crystallization process sigmoidal shaped depolarized light intensity versus time curves were obtained. Representative graphs of these isotherms were transformed to fit the Avrami equation

$$\theta = \exp(-kt^n)$$

by putting $\theta = (I_c - I_t)/(I_c - I_0)$ where θ is the fraction of unchanged material remaining after time t seconds, k is the rate constant and n is a parameter dependent on the form of the bulk nucleation. I_0 , I_t and I_c are the light intensities corresponding to the initial, intermediate and final stages of the crystallization process. Transformed isotherms versus time are plotted logarithmically in *Figure 4* for the undried polymer. Theoretical straight lines corresponding to nucleation which is simultaneous in time (slope $n=3$),

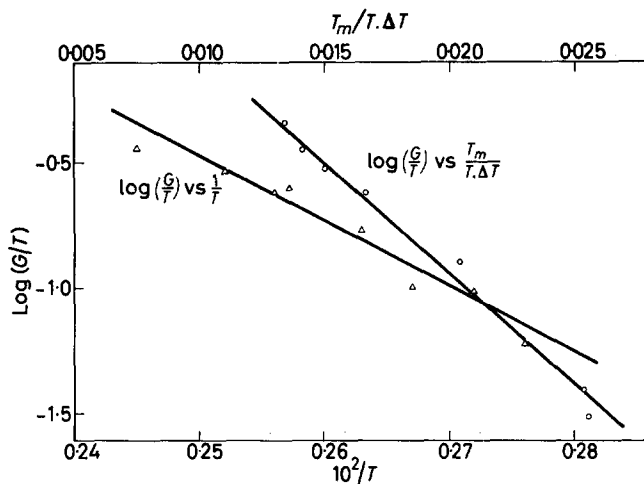


Figure 3—Plot of $\log(G/T)$ versus temperature variables for spherulite growth in nylon 6

and sporadic (slope $n=4$) in time are fitted to these plots. Below 190°C approximately spherulite nuclei are generated simultaneously. Rate constants were calculated directly from the half-times of crystallization, $t_{1/2}$, and the appropriate value of n using the Avrami equation. These results for the

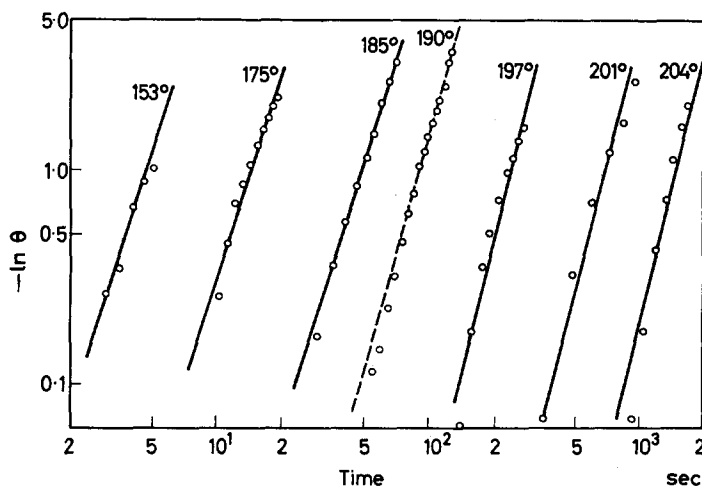


Figure 4—Avrami crystallization isotherms for undried nylon 6 polymer chip

dried and undried nylon 6 are illustrated in Figure 5. Some $t_{1/2}$ values are plotted in Figure 6 together with literature values at the higher crystallization temperatures⁸. The rates approach a maximum about 140°C .

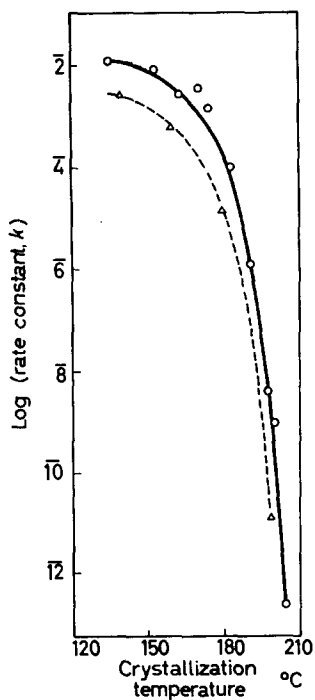
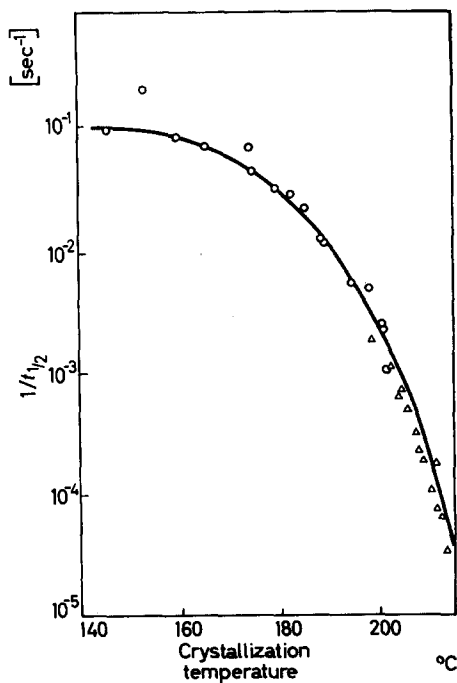


Figure 5—Rate constant versus crystallization temperature for (Δ) dried and (\circ) undried nylon 6 (R.V. 70-8)

Figure 6—Reciprocal of half-times of crystallization versus crystallization temperature: (\circ) this work, (Δ) data of ref. 7



DISCUSSION

Spherulite model

The growth of a nylon 6 spherulite has been assumed to occur by lateral accretion of molecular segments at the faces of the growing fibrils which radiate outwards from the initial three-dimensional sheaf-like nucleus. Three-dimensional space in spherulites is filled by fibrillar branching which probably arises, and is perpetuated, through defects at the growing fibril faces. Only positively birefringent spherulites have been grown¹ in nylon 6, and in these spherulites the molecular chains are probably disposed at a large angle to the spherulite radius as in nylon 6.6 positively birefringent spherulites²¹. This concept of spherulite growth requires the molecules in the melt to have or to adopt a well-defined conformation to gain admission to the fibril crystal face. Should the addition occur by a fold-mechanism then the fibril width would be a function of the crystallization temperature in accordance with the observation of the increase in fold height of single crystals¹⁴ as the crystallization temperature is raised. Although microscope observations show that the fibrillar-like structures in nylon 6 spherulites are coarser the higher the crystallization temperature, these structures require further investigation. The ultimate fibrils should be resolved and measured by electron microscopy and the temperature dependence of their width established.

Nucleation and growth of spherulites

The simultaneous nucleation of spherulites observed from the cine-camera films concurs with that deduced by Avrami analysis of the rate measurements for crystallization temperatures below 190°C. Above this temperature spherulites are formed sporadically in time as instanced by Avrami $n=4$. Rybníkář found a similar nucleation parameter in his dilatometric studies at temperatures 193° to 213°C. In both respects, results agree with earlier microscope observations¹ on the melting and crystallization behaviour of nylon 6. The melt conditions (270°C for half an hour) employed in the present work are the outcome of these earlier investigations and are preferable to the shorter melt conditions (300°C for 30 seconds) of Burnett and McDevit⁵ since inadequate fusion causes a high incidence of heterogeneously nucleated spherulites¹. The higher growth rates obtained by these authors can be accounted for because the isothermal rate of spherulite growth has been found to increase with lowering of the melt temperature¹⁵ and melt time. The observed differences in the rates do not merit consideration on a \overline{M}_n basis because of the proximity of both polymers (\overline{M}_n 27 400 and 24 700) in this respect.

Rate constants found for the dried polymer are less than the undried presumably because of the plasticizing action of the moisture:

Molecular growth rate parameters

In the crystallization region just below T_m , the rate of growth of spherulites from the melt is principally determined by T the crystallization temperature, σ_s the interfacial free energy and T_m the thermodynamic melting point. The spherulite growth and crystallization rates for nylon 6 have a dependence on the first power of the supercooling (*Figures 3 and 7*) implying that the growth occurs by a two-dimensional nucleation

mechanism involving surface nucleation^{5, 6}. Assuming that such a mechanism is operative at a cylindrical fibril surface of the growing spherulite, E_D is the activation energy for transport of molecular segments across the melt/crystal interface and σ_s were calculated from the spherulite growth rate data. These molecular parameters were obtained from the spherulite growth rate equation⁵:

$$\log \frac{G}{T} = \log G_0 - \frac{A}{T} - B \frac{T_m}{T\Delta T} \quad (1)$$

where $A = E_D/2.3k$, $B = \pi|\sigma_s|^2/2.3k\Delta h\mu$ and $\Delta T = T_m - T$.

Values of A and B were computed from the G/T results of Figure 2 which were 'least squared' to this equation using a melting temperature, T_m , of 227°C. This value which is 5°C lower than that used in previous

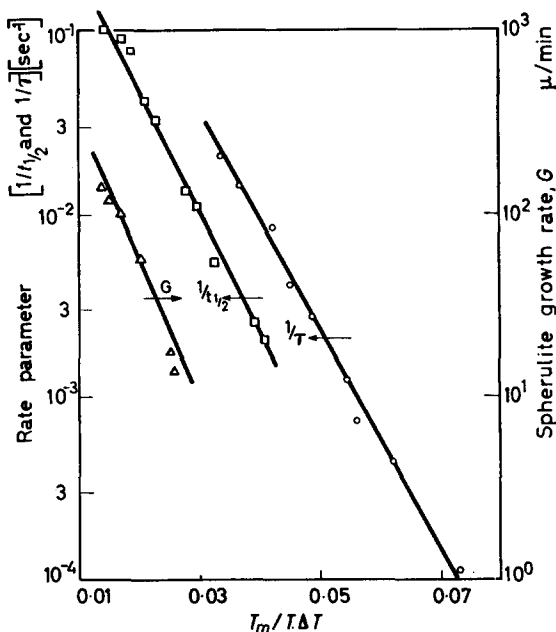


Figure 7—Growth parameters $1/t_{1/2}$, $1/\tau$ and G versus temperature variables for nylon 6: (Δ , \square) this work, (\circ) data of ref. 1

work, was deemed adequate because the $\log G/T$ versus $T_m/T\Delta T$ was linear (Figure 3) for the experimental data on the RHS of the maximum T_{max} . Below this maximum, the $\log G/T$ versus $1/T$ plot though not entirely linear but concave downwards as T_{max} is approached, was acceptable. The density at T_m assumed unity (literature value⁷ is 0.99 approximately) gave a molar volume of 226 cm³ per mole of polymer repeat units. $\Delta h\mu$, the heat of fusion per unit volume of repeating units, was derived using Dole and Wunderlich's value¹² of 45 cal/g for the heat of fusion for a drawn nylon 6 yarn. The interplanar or monolayer thickness of the surface nucleus¹³, l , was taken to be 4.2Å and k is Boltzmann's

constant. The parameters relating to the spherulite growth of nylon 6, calculated using these data, are presented in *Table 1* with Burnett and McDevit's results

Table 1

| Source | T_m °C | $\Delta H\mu$ kcal/mole repeat units | $\Delta h\mu$ erg/cm ³ of repeat units |
|-------------|----------|--|---|
| This work | 227 | 10.18 | $18.8_5 \times 10^8$ |
| Reference 5 | 232 | 4.3 | 8×10^8 |

| A | E_D kcal/mole repeat units | B | σ_s erg/cm ² | $\sigma_G/\Delta H\mu$ |
|-------|------------------------------------|-----|-----------------------------------|------------------------|
| 3 931 | 18.0 | 165 | 27.4 | 0.35 |
| 3 884 | 17.9 | 182 | 18.1 | 0.51 |

The ratio $\sigma_G/\Delta H\mu$ relates the surface area per mole of repeat units one molecule thick to the heat of fusion per mole of repeat units.

The magnitudes of E_D and σ_s , although proportional to the slope of the $\log G/T$ versus $1/T$ and $\log G/T$ versus $T_m/T\Delta T$ plots respectively, are not directly calculable from these gradients. Except at measurements near T_m and at very low degrees of supercooling the influences of these two temperature variables are inseparable. For this reason, calculations were made by the least squares method. However, the magnitude of σ_s is higher than previously found because $\Delta h\mu$ was derived using Dole's value¹² of 45 cal/g for the heat of fusion. This was preferred to Allen's value¹⁶ of 19 cal/g previously used⁵ since the crystalline perfection within a spherulite is probably at least equal to that of a drawn fibre. A value for $\Delta H\mu$, 12.1 kcal/mole, comparable with the heat of fusion in this paper is given by Hirai¹⁸ in his theoretical treatment of Burnett and McDevit's spherulite growth results⁵ on an absolute rate theory.

The observed maximum in *Figure 2* depends on $\Delta h\mu$, E_D and the nucleation parameters and is predicted by equation (1). The term $T_m/T\Delta T$ preponderates at the higher temperatures whilst the $1/T$ term becomes increasingly predominant as the crystallization temperature T is lowered. Near T_m and at T_g (the glass transition temperature) the growth rate becomes imperceptible. Assuming a symmetrical distribution about $T_{max.}$, the latter will be the mean of T_m and T_g . This empiricism is realized experimentally for several polymers, e.g. nylon 6, isotactic polypropylene, polyethylene terephthalate and polyethylene succinate.

From the rate constant results a lower value of E_D (15.4 kcal/mole repeat units) was obtained using the equation

$$E_D = \frac{2 T_{max.} - T}{(T_m - T_{max.})^2} \times 2.3k_B \times T_m \quad (2)$$

which was established by differentiating equation (1) with respect to T , equating to zero, and substituting the maximum growth rate temperature $T_{max.} = 138^\circ\text{C}$, $T_m = 227^\circ\text{C}$ and $B = 165$. Assuming that the depolarized

light intensity rates depended primarily on the overall growth rates of spherulites, the data were analysed as described by Rybníkář⁷. The $\log k$ versus $T_m/T\Delta T$ plot was made using $T_m=230^\circ\text{C}$. From Dole's value¹² for the heat of fusion and the gradient of this graph, σ_s was found to be 21.2 erg/cm^2 . The activation energy, E_D , was calculated to be $12.8 \text{ kcal/mole repeat units}$ from equation (2). Bearing in mind this approximate procedure which normally leads to low values, reasonable agreement has been obtained between these parameters and those calculated directly from the spherulite growth measurements and from crystallization rate determinations using density techniques. Rybníkář's experiments⁷ gave $\sigma_s=16.7 \text{ erg/cm}^2$ and E_D s in the range 5 to 25 kcal/mole repeat units. The correspondence of some literature $t_{\frac{1}{2}}$ values⁸ in the crystallization range 193° to 213°C with those presented in this paper is also encouraging (Figure 6).

Almost identical temperature dependence is found for the overall crystallization rate which is proportional to $(1/t_{\frac{1}{2}})$ and the spherulite growth rate (G) presented in this paper. The rate of nucleation¹, represented by the reciprocal of the induction time $(1/\tau)$ for the appearance of a birefringent sheaf, follows a similar pattern and is also illustrated in Figure 7. Similar unpublished relationships have been noted for isotactic polypropylene. From these results it would appear that for a particular polymer such rate processes are controlled by the same mechanism.

Superficially, the appreciably higher rates of spherulite growth in nylon 6.6 over nylon 6 at equal degrees of supercooling cannot readily be accounted for by the variables in the growth equation (1). The tentative proposal²⁰ that nylon 6 molecules pack in an antiparallel fashion to facilitate H-bonding could impose a restriction on the rate of growth when compared with nylon 6.6 where both parallel and antiparallel arrangements are equally possible from symmetry considerations. The extent of 'order in the melts' of both polymers also merits further investigation in this respect¹. More detailed examination of positively birefringent spherulites in both polymers with low angle X-ray and electron microscopy techniques should be informative concerning the mechanism and mode of spherulite growth. However, the value of $\sigma_G/\Delta H\mu$ of 0.35 obtained for nylon 6 in this work, suggests that the segmental crystallization of nylon 6 polymer appears analogous to the crystallization process occurring in low molecular weight materials¹⁹ in agreement with the findings of other investigators⁵.

The author thanks Mr C. Mumford for assistance with the experimental work. He also expresses indebtedness to Mr D. M. Ellis for least squares computations and to Dr T. R. White for helpful discussion.

Research Department,
British Nylon Spinners Limited,
Pontypool, Mon.

(Received March 1962)

REFERENCES

- MAGILL, J. H. *Polymer, Lond.* 1962, **3**, 43
- RYBNÍKÁŘ, F. *Chem. Listy*, 1961, **11/36**, No. 4, 217
- ZIABICKI, A. *Kolloidzshr.* 1959, **167**, No. 2, 132

- ⁴ HENDUS, H., SCHNEIDER, K., SCHNELL, G. and WOLF, K. A. *B.A.S.F.* 1960 festival volume, prepared in honour of the president's 60th birthday, pp 291-319
- ⁵ BURNETT, B. B. and McDEVIT, W. F. *J. appl. Phys.* 1957, **28**, 1101
- ⁶ ČEFELIN, P., CHMELÍR, M. and WICHTERLE, O. *Coll. Trav. chim. Tchécosl.* 1960, **25**, 1267
- ⁷ RYBNIKÁŘ, F. *Coll. Trav. chim. Tchécosl.* 1961, **26**, 937
- ⁸ RYBNIKÁŘ, F. *Chem. Listy*, 1961, **11**, No. 3, 157
- ⁹ MAGILL, J. H. To be published
- ¹⁰ MAGILL, J. H. *Polymer, Lond.* 1961, **2**, 221
- ¹¹ MAGILL, J. H. *Polymer, Lond.* 1962, **3**, 35
- ¹² DOLE, M. and WUNDERLICH, B. *Makromol. Chem.* 1959, **34**, 29
- ¹³ RYBNIKÁŘ, F. and BURDA, J. *Faserforschung u. Textiltechnik*, 1954, **12**, 324
- ¹⁴ KELLER, A. and O'CONNOR, A. *Disc. Faraday Soc.* 1958, **25**, 114
- ¹⁵ McLAREN, J. V. To be published
- ¹⁶ FLORY, P. J. and McINTYRE, A. D. *J. Polym. Sci.* 1955, **18**, 592
- ¹⁷ ALLEN, P. W. *Research, Lond.* 1952, **5**, 492
- ¹⁸ HIRAI, N. *J. Polym. Sci.* 1960, **42**, 213
- ¹⁹ TURNBULL, D. and FISHER, J. C. *J. chem. Phys.* 1949, **17**, 71
- ²⁰ HOLMES, D. R., BUNN, C. W. and SMITH, D. J. *J. Polym. Sci.* 1955, **17**, 159
- ²¹ MANN, J. and ROLDAN, L. *Brit. J. appl. Phys.* 1961, **12**, 261

Contributions to Polymer

Papers accepted for future issues of
POLYMER include the following:

- Some Properties of Poly-(2-vinylpyridine) in Solution*—A. J. HYDE and R. B. TAYLOR
- The Dependence of the Viscosity on the Concentration of Sodium Carboxymethylcellulose in Aqueous Solutions*—D. A. I. GORING and G. SITARAMAIAH
- Radiochemical Investigation of Polymer Unsaturation. Reaction of Butyl Rubber with Radiochlorine*—I. C. MCNEILL
- The Low Frequency Dielectric Relaxation of Polyoxymethylene (Delrin) using a Direct Current Technique*—G. WILLIAMS
- Viscosity/Temperature Relationships for Dilute Solutions of High Polymers*—R. J. FORT, R. J. HUTCHINSON, W. R. MOORE and Miss M. MURPHY
- Rubber Elasticity in a Highly Crosslinked Epoxy System*—D. KATZ and A. V. TOBOLSKY
- Infra-red Spectra and Chain Arrangements in Some Polyamides, Polypeptides and Fibrous Proteins*—E. M. BRADBURY and A. ELLIOTT
- The Crystallization of Polyethylene, Part I*—W. BANKS, M. GORDON, R.-J. ROE and A. SHARPLES
- The Radiation Chemistry of Some Polyamides. An Electron Spin Resonance Study*—C. T. GRAVES and M. G. ORMEROD
- Proton Magnetic Relaxation in Polyamides*—D. W. MCCALL and E. W. ANDERSON
- Intermolecular Forces and Chain Flexibilities IV—Internal Pressures of Polyethylene Glycol in the Region of Its Melting Point*—G. ALLEN and D. SIMS
- The Crystallization of Poly(decamethylene terephthalate)*—A. SHARPLES and F. L. SWINTON
- Stress Relaxation of Vulcanized Rubbers I—Theoretical Study*—S. BAXTER and H. A. VODDEN
- Stress Relaxation of Vulcanized Rubbers II—Mathematical Analysis of Observations*—L. A. EDELSTEIN, H. A. VODDEN and M. A. A. WILSON
- Stress Relaxation of Vulcanized Rubbers III—Experimental Study*—S. BAXTER and M. A. A. WILSON
- A Kinetic Study of the Isothermal Spherulitic Crystallization of Poly-(hexamethylene adipamide)*—J. V. McLAREN
- The Influence of Particle Size and Distortions upon the X-ray Diffraction Patterns of Polymers*—R. BONART, R. HOSEMANN and R. L. McCULLOUGH
- Shear Modulus in Relation to Crystallinity in Polymethylene and its Copolymers*—J. B. JACKSON, P. J. FLORY, R. CHAING and M. J. RICHARDSON
- Crystallization and Melting of Copolymers of Polymethylene*—M. J. RICHARDSON, P. J. FLORY and J. B. JACKSON

- The Constant Pressure Dynamic Osmometer*—I. C. McNEILL
The Crystallization of Polyethylene after Partial Melting—W. BANKS,
M. GORDON and A. SHARPLES
The Diffusion and Clustering of Water Vapour in Polymers—J. A. BARRIE
and B. PLATT
Solid State Polymerization of β -Propiolactone—G. DAVID, J. VAN DER
PARREN, F. PROVOOST and A. LIGOTTI
The Glass Transition Temperature of Polymeric Sulphur—A. V. TOBOLSKY,
W. MACKNIGHT, R. B. BEEVERS and V. D. GUPTA
Aminolysis of Polyethylene Terephthalate—H. ZAHN and H. PFEIFER
New Transition in Polystyrene—G. MORAGLIO and others
*The Radiation Chemistry of Some Polysiloxanes: An Electron Spin
Resonance Study*—M. G. ORMEROD and A. CHARLESBY

CONTRIBUTIONS should be addressed to the Editors, *Polymer*, 4-5 Bell Yard,
London, W.C.2.

Authors are solely responsible for the factual accuracy of their papers. All papers will be read by one or more referees, whose names will not normally be disclosed to authors. On acceptance for publication papers are subject to editorial amendment.

If any tables or illustrations have been published elsewhere, the editors must be informed so that they can obtain the necessary permission from the original publishers.

All communications should be expressed in clear and direct English, using the minimum number of words consistent with clarity. Papers in other languages can only be accepted in very exceptional circumstances.

A leaflet of instructions to contributors is available on application to the editorial office.

Classified Contents

- Acetylation of ethylamine-treated cotton, 187
- Action of ethylamine on cellulose, I—Acetylation of ethylamine-treated cotton, 187
- II—Solvent extraction of ethylamine-treated bacterial cellulose: changes in the hydroxyl-absorption region of the infra-red spectrum, 195
- III—The formation of cellulose III and its infra-red spectrum between 1500 and 650 cm^{-1} , 211
- Birefringence, treatment of static and dynamic, in linear amorphous polymers by an extension of the molecular theory of viscoelasticity, 143
- Butyllithium-initiated polymerization of methyl methacrylate, 175
- Carbonization of polymers, I—Thermogravimetric analysis, 1
- Ceiling temperature and low temperature polymerization, 591
- Cellulose, action of ethylamine on, 187, 195, 211
- sub-microscopic morphology of, 511
- Cellulose crystals, X-ray measurements of the elastic modulus of, 549
- Comparison of solution and diffusion in silicone rubber with natural rubber, 595
- Crystallinity in high polymers, especially fibres, 349
- Crystallization kinetics study of nylon 6, 655
- Degradation of polyethylene terephthalate by methylamine—A study by infra-red and X-ray methods, 17
- Development of an elution chromatography technique for *cis*-1,4-polybutadiene, 153
- Die hochpolymeren organischen Verbindungen—Kautschuk und Cellulose*, review of, 243
- Dilute solution properties of tactic polymethyl methacrylates I—Intrinsic viscosities of isotactic fractions, 565
- Effect of heterogeneity in molecular weight on the second virial coefficient of polymers in good solvents, 625
- Effect of temperature, conversion and solvent on the stereospecificity of the free radical polymerization of methyl methacrylate, 575
- Ethylene, heterogeneous radical polymerization of, 639
- Formation of cellulose III and its infra-red spectrum between 1500 and 650 cm^{-1} , 211
- Formation of nuclei in crystallizing polymers, 250
- Gelation of aqueous solutions of polymethacrylic acid, 555
- Glass Reinforced Plastics*, review of, 243
- Heterogeneous radical polymerization of ethylene, 639
- Hexene-1 polysulphone, solution properties of, 129
- Influence of fillers [in solution and diffusion in silicone rubber], 605
- Interference microscopy of solution-grown polyethylene single crystals, 247
- Intrinsic viscosities of isotactic fractions [of polymethyl methacrylates], 565
- Intrinsic viscosity/temperature relationships for conventional polymethyl methacrylate, 111
- Ionic polymerization of polar monomers, 487
- Ionic polymerization, reactivity of the growing ion in, 167
- Isotactic polypropylene, crystallization of, 35
- Kinetic study of the benzene-induced crystallization of polyethylene terephthalate, 27
- Kinetics of the polycondensation of 12-hydroxystearic acid, 257
- Lexan, thermodynamic functions of, 316
- Light scattering and viscometric properties of solutions of conventional polymethyl methacrylate, 97
- Mechanical relaxation in some oxide polymers, 529
- Melting behaviour and spherulitic crystallization of polycaproamide (nylon 6), 43
- Melting point of polyethylene terephthalate, 543

- Methyl methacrylate, butyllithium-initiated polymerization of, 175
- the effect of temperature, conversion and solvent on the stereospecificity of the free radical polymerization of, 575
- Methylmethacrylate and polymethylmethacrylate, thermodynamic functions of, 317
- Molecular motion in polymethylmethacrylate by proton spin-lattice relaxation, 336
- Molecular motion in polypropylene by proton spin-lattice relaxation, 339
- Molecular properties of polymers, 471
- New technique for following rapid rates of crystallization II—Isotactic polypropylene, 35
- Nylon 6, crystallization kinetics study of, 655
- melting behaviour and spherulitic crystallization of, 43
- Osmotic and viscometric properties of solutions of conventional polymethyl methacrylate, 71
- Penton, thermodynamic functions of, 271
- Polybutadiene, development of an elution chromatography technique for *cis*-1,4-, 153
- cis*- and *trans*-1,4-Polybutadiene, thermodynamic functions of, 297
- Polyisobutene, study of the thermodynamic properties and phase equilibria of solutions of, in *n*-pentane, 215
- Polyisobutene systems, shear viscosities of,—a study of polymer entanglement, 11
- Polycaproamide, melting behaviour and spherulitic crystallization of, 43
- Polyethylene, thermodynamic functions of, 277
- Polyethylene single crystals, interference microscopy of solution-grown, 247
- Polyethylene terephthalate, degradation of, by methylamine—A study by infra-red and X-ray methods, 17
- kinetic study of the benzene-induced crystallization of, 27
- melting point of, 543
- Polymer entanglement, a study of, 11
- Polymer single crystals, 393
- Polymeric Materials*, review of, 245
- Polymerization in the solid state, 449
- Polymerization of epoxides, part IV (1)—Polymerization of propylene oxide and ethylene oxide with ferric chloride catalyst, 231
- Polymerization of propylene oxide and ethylene oxide with ferric chloride catalyst, 231
- Polymethacrylic acid, gelation of aqueous solutions of, 555
- Polymethyl methacrylate, conventional, osmotic and viscometric properties of solutions of, 71
- light scattering and viscometric properties of solutions of, 97
- Intrinsic viscosity/temperature relationships for, 111
- molecular motion in, by proton spin-lattice relaxation, 336
- thermodynamic properties of dilute solutions of, in butanone and in nitroethane, 53
- Polymethyl methacrylates, intrinsic viscosities of isotactic fractions of, 565
- Polyoxymethylene, thermodynamic functions of, 263
- Polypropylene, molecular motion in, by proton spin-lattice relaxation, 339
- Polysulphones, thermodynamic functions of, 310
- Properties of dilute polymer solutions, I—Osmotic and viscometric properties of solutions of conventional polymethyl methacrylate, 71
- II—Light scattering and viscometric properties of solutions of conventional polymethyl methacrylate, 97
- III—Intrinsic viscosity/temperature relationships for conventional polymethyl methacrylate, 111
- Radiation-induced solid state polymerization, 323
- Reactivity of the growing ion in ionic polymerization, 167
- Reactivity ratio in styrene maleic anhydride copolymerization, 335
- Second virial coefficient, effect of heterogeneity in molecular weight on the, of polymers in good solvents, 625
- Shear viscosities of polyisobutene systems—A study of polymer entanglement, 11
- Single crystals from polyamide salts, 252
- Solution and diffusion in silicone rubber, I—Comparison with natural rubber, 595
- II—the influence of fillers, 605
- Solution properties of olefin polysulphones, I—Hexene-1 polysulphone, 129
- Solvent extraction of ethylamine-treated bacterial cellulose: changes in the hydroxyl-absorption region of the infra-red spectrum, 195
- Spherulitic crystallization, melting behaviour and, of polycaproamide (Nylon 6), 43

- Stereoregular polymers and polymerization, 423
- Stereospecific poly- α -olefins, thermodynamic functions of, 286
- Study by infra-red and X-ray methods of degradation of polyethylene terephthalate by methylamine, 17
- Study of the thermodynamic properties and phase equilibria of solutions of polyisobutene in *n*-pentane, 215
- Styrene maleic anhydride copolymerization, reactivity ratio in, 335
- Styrene-maleic anhydride copolymers, viscosity of branched, 615
- Styrene, use of 2-cyano-2-propylazofornamide as a sensitizer for the polymerization of, 585
- Sub-microscopic morphology of cellulose, 511
- Thermodynamic functions of linear high polymers, parts I to VIII, 263, 271, 277, 286, 297, 310, 316, 317
- Thermodynamic properties of dilute solutions of polymethyl methacrylate in butanone and in nitroethane, 53
- Thermogravimetric analysis and the pyrolysis of polymers, 1
- Tracer studies of 2-cyano-2-propylazofornamide I—Use of the compound as a sensitizer for the polymerization of styrene, 585
- Treatment of static and dynamic birefringence in linear amorphous polymers by an extension of the molecular theory of viscoelasticity, 143
- Use of 2-cyano-2-propylazofornamide as a sensitizer for the polymerization of styrene, 585
- Viscosity of branched styrene-maleic anhydride copolymers, 615
- X-ray measurements of the elastic modulus of cellulose crystals, 549

Author Index

- ABDUL WAHID: *See* BEVINGTON, J. C. and ABDUL WAHID
- BAKER, C. H., BROWN, W. B., GEE, G., ROWLINSON, J. S., STUBLEY, D. and YEADON, R. E.: A study of the thermodynamic properties and phase equilibria of solutions of polyisobutene in *n*-pentane, 215
- BARRER, R. M., BARRIE, J. A. and RAMAN, N. K.: Solution and diffusion in silicone rubber I—A comparison with natural rubber, 595
- — — — II—The influence of fillers, 605
- BARRIE, J. A.: *See* BARRER, R. M., BARRIE, J. A. and RAMAN, N. K.
- BAWN, C. E. H. and HUGLIN, M. B.: The kinetics of the polycondensation of 12-hydroxystearic acid, 257
- — — — Viscosity of branched styrene-maleic anhydride copolymers, 615
- BEVINGTON, J. C. and ABDUL WAHID: Tracer studies of 2-cyano-2-propylazoformamide I—Use of the compound as a sensitizer for the polymerization of styrene, 585
- BROWN, W. B.: *See* BAKER, C. H., BROWN, W. B., GEE, G., ROWLINSON, J. S., STUBLEY, D. and YEADON, R. E.
- BYWATER, S.: *See* WILES, D. M. and BYWATER, S.
- CASASSA, E. F.: Effect of heterogeneity in molecular weight on the second virial coefficient of polymers in good solvents, 625
- — — — and STOCKMAYER, W. H.: Thermodynamic properties of dilute solutions of polymethyl methacrylate in butanone and in nitroethane, 53
- CLAESSON, S.: The molecular properties of polymers, 471
- COHN-GINSBERG, ELIZABETH: *See* KRAUSE, SONJA, and COHN-GINSBERG, ELIZABETH
- — — — FOX, T. G and MASON, H. F.: Properties of dilute polymer solutions II—Light scattering and viscometric properties of solutions of conventional polymethyl methacrylate, 97
- DAINTON, F. S., EVANS, D. M., HOARE, F. E. and MELIA, T. P.: Thermodynamic functions of linear high polymers, I—Polyoxymethylene, 263
- — — — II—Penton, 271
- — — — III—Polyethylene, 277
- — — — IV—Stereospecific poly- α -olefins, 286
- — — — V—*cis*- and *trans*-1,4-polybutadiene, 297
- — — — VI—Polysulphones, 310
- — — — VII—Lexan, 316
- — — — VIII—Methylmethacrylate and polymethylmethacrylate, 317
- DANUSSO, F.: Stereoregular polymers and polymerization, 423
- ELIASSAF, J. and SILBERBERG, A.: The gelation of aqueous solutions of polymethacrylic acid, 555
- ENDE, H. A.: *See* IVIN, K. J., ENDE, H. A. and MEYERHOFF, G.
- ERUSSALIMSKY, B. L., LYUBETZKY, S. G., MAZUREK, W. W., FRENKEL, S. YA. and SHALTYKO, L. G.: Heterogeneous radical polymerization of ethylene, 639
- EVANS, D. M.: *See* DAINTON, F. S., EVANS, D. M., HOARE, F. E. and MELIA, T. P.
- FARROW, G., RAVENS, D. A. S. and WARD, I. M.: The degradation of polyethylene terephthalate by methylamine—A study by infra-red and X-ray methods, 17
- FOX, T. G: Properties of dilute polymer solutions III—Intrinsic viscosity/temperature relationships for conventional polymethyl methacrylate, 111
- — — — *See* COHN-GINSBERG, E., FOX, T. G and MASON, H. F.
- — — — and SCHNECKO, H. W.: The effect of temperature, conversion and solvent on the stereospecificity of the free radical polymerization of methyl methacrylate, 575
- — — — KINSINGER, J. B., MASON, H. F. and SCHUELE, E. M.: Properties of dilute polymer solutions I—Osmotic and viscometric properties of solutions of conventional polymethyl methacrylate, 71
- FRENKEL, S. YA.: *See* ERUSSALIMSKY, B. L., LYUBETZKY, S. G., MAZUREK, W. W., FRENKEL, S. YA. and SHALTYKO, L. G.
- FUKUI, K.: *See* HIGASHIMURA, T., IMANISHI, Y., YONEZAWA, T., FUKUI, K. and OKAMURA, S.
- FURUKAWA, J.: *See* JUNJI FURUKAWA

- GARRATT, P. G.: Radiation-induced solid state polymerization—a review, 323
- GEE, G.: See BAKER, C. H., BROWN, W. B., GEE, G., ROWLINSON, J. S., STUBLEY, D. and YEADON, R. E.
- HIGGINSON, W. C. E. and JACKSON, J. B.: Polymerization of epoxides, part IV (1)—Polymerization of propylene oxide and ethylene oxide with ferric chloride catalyst, 231
- GEELLEN, H.: See HEIKENS, D. and GEELLEN, H.
- GILBERT, J. B., KIPLING, J. J., MCENANEY, B. and SHERWOOD, J. N.: Carbonization of polymers I—thermogravimetric analysis, 1
- HARRIS, P. H.: See MAGILL, J. H. and HARRIS, P. H.
- HEIKENS, D. and GEELLEN, H.: Ceiling temperature and low temperature polymerization, 591
- HIGASHIMURA, T., IMANISHI, Y., YONEZAWA, T., FUKUI, K. and OKAMURA, S.: The reactivity of the growing ion in ionic polymerization, 167
- HIGGINSON, W. C. E.: See GEE, G., HIGGINSON, W. C. E. and JACKSON, J. B.
- HOARE, F. E.: See DAINTON, F. S., EVANS, D. M., HOARE, F. E. and MELIA, T. P.
- HOSEMANN, R.: Crystallinity in high polymers, especially fibres, 349
- HUGLIN, M. B.: The reactivity ratio in styrene maleic anhydride copolymerization, 335
- See BAWN, C. E. H. and HUGLIN, M. B.
- HULME, J. M. and MCLEOD, L. A.: Development of an elution chromatography technique for *cis*-1,4-polybutadiene, 153
- IMANISHI, Y.: See HIGASHIMURA, T., IMANISHI, Y., YONEZAWA, T., FUKUI, K. and OKAMURA, S.
- IVIN, K. J., ENDE, H. A. and MEYERHOFF, G.: The solution properties of olefin polysulphones I—Hexane-1 polysulphone 129
- JACKSON, J. B.: See GEE, G., HIGGINSON, W. C. E. and JACKSON, J. B.
- JENNINGS, B. E.: review of *Polymeric Materials*, 245
- JOHNSON, J. F.: See PORTER, R. S. and JOHNSON, J. F.
- JUNJI FURUKAWA: Ionic polymerization of polar monomers, 487
- KELLER, A.: Polymer single crystals, 393
- KINSINGER, J. B.: See FOX, T. G., KINSINGER, J. B., MASON, H. F. and SCHUELE, E. M.
- KIPLING, J. J.: See GILBERT, J. B., KIPLING, J. J., MCENANEY, B. and SHERWOOD, J. N.
- KRAUSE, SONJA, and COHN-GINSBERG, ELIZABETH: Dilute solution properties of tactic polymethyl methacrylates I—Intrinsic viscosities of isotactic fractions, 565
- LYUBETZKY, S. G.: See ERUSSALIMSKY, B. L., LYUBETZKY, S. G., MAZUREK, W. W., FRENKEL, S. YA. and SHALTYKO, L. G.
- MCENANEY, B.: See GILBERT, J. B., KIPLING, J. J., MCENANEY, B. and SHERWOOD, J. N.
- MCLEOD, L. A.: See HULME, J. M. and MCLEOD, L. A.
- MAGAT, M.: Polymerization in the solid state, 449
- MAGILL, J. H.: A new technique for following rapid rates of crystallization II—Isotactic polypropylene, 35
- Melting behaviour and spherulitic crystallization of polycapromide (nylon 6), 43
- Crystallization kinetics study of nylon 6, 655
- and HARRIS, P. H.: Single crystals from polyamide salts, 252
- MANN, J. and ROLDAN-GONZALEZ, L.: X-ray measurements of the elastic modulus of cellulose crystals, 549
- MANSFIELD, P.: See POWLES, J. G. and MANSFIELD, P.
- MASON, H. F.: See COHN-GINSBERG, E., FOX, T. G. and MASON, H. F.
- See FOX, T. G., KINSINGER, J. B., MASON, H. F. and SCHUELE, E. M.
- MAZUREK, W. W.: See ERUSSALIMSKY, B. L., LYUBETZKY, S. G., MAZUREK, W. W., FRENKEL, S. YA. and SHALTYKO, L. G.
- MELIA, T. P.: See DAINTON, F. S., EVANS, D. M., HOARE, F. E. and MELIA, T. P.
- MEYERHOFF, G.: See IVIN, K. J., ENDE, H. A. and MEYERHOFF, G.
- NEVELL, T. P. and ZERONIAN, S. H.: The action of ethylamine on cellulose, part I—The acetylation of ethylamine-treated cotton, 187
- OKAMURA, S.: See HIGASHIMURA, T., IMANISHI, Y., YONEZAWA, T., FUKUI, K. and OKAMURA, S.
- PORTER, R. S. and JOHNSON, J. F.: Shear viscosities of polyisobutene systems—A study of polymer entanglement, 11

- POWLES, J. G. and MANSFIELD, P.: Molecular motion in polymethylmethacrylate by proton spin-lattice relaxation, 336
- —: Molecular motion in polypropylene by proton spin-lattice relaxation, 339
- PRESTON, R. D.: The sub-microscopic morphology of cellulose, 511
- RAMAN, N. K.: See BARRER, R. M., BARRIE, J. A. and RAMAN, N. K.
- RAVENS, D. A. S.: See FARROW, G., RAVENS, D. A. S. and WARD, I. M.
- READ, B. E.: A treatment of static and dynamic birefringence in linear amorphous polymers by an extension of the molecular theory of viscoelasticity, 143
- Mechanical relaxation in some oxide polymers, 529
- ROBINSON, C.: review of *Die hochpolymeren organischen Verbindungen—Kautschuk und Cellulose*, 243
- ROLDAN-GONZALEZ, L.: See MANN, J. and ROLDAN-GONZALEZ, L.
- ROWLINSON, J. S.: See BAKER, C. H., BROWN, W. B., GEE, G., ROWLINSON, J. S., STUBLEY, D. and YEADON, R. E.
- SCHNECKO, H. W.: See FOX, T. G. and SCHNECKO, H. W.
- SCHUELE, E. M.: See FOX, T. G., KINSINGER, J. B., MASON, H. F. and SCHUELE, E. M.
- SHALTYKO, L. G.: See ERUSSALIMSKY, B. L., LYUBETSKY, S. G., MAZUREK, W. W., FRENKEL, S. YA. and SHALTYKO, L. G.
- SHARPLES, A.: The formation of nuclei in crystallizing polymers, 250
- SHELDON, R. P.: A kinetic study of the benzene-induced crystallization of polyethylene terephthalate, 27
- SHERWOOD, J. N.: See GILBERT, J. B., KIPLING, J. J., MCENANEY, B. and SHERWOOD, J. N.
- SILBERBERG, A.: See ELIASSAF, J. and SILBERBERG, A.
- SPEDDING, H.: The action of ethylamine on cellulose, part II—Solvent extraction of ethylamine-treated bacterial cellulose: changes in the hydroxyl-absorption region of the infra-red spectrum, 195
- The action of ethylamine on cellulose, part III—The formation of cellulose III and its infra-red spectrum between 1500 and 650 cm^{-1} , 211
- STOCKMAYER, W. H.: See CASASSA, E. F. and STOCKMAYER, W. H.
- STUBLEY, D.: See BAKER, C. H., BROWN, W. B., GEE, G., ROWLINSON, J. S., STUBLEY, D. and YEADON, R. E.
- SULLIVAN, P.: See WUNDERLICH, B. and SULLIVAN, P.
- TAYLOR, G. W.: The melting point of polyethylene terephthalate, 543
- TURNER, A. G.: review of *Glass Reinforced Plastics*, 243
- WARD, I. M.: See FARROW, G., RAVENS, D. A. S. and WARD, I. M.
- WILES, D. M. and BYWATER, S.: The butyllithium-initiated polymerization of methyl methacrylate, 175
- WUNDERLICH, B. and SULLIVAN, P.: Interference microscopy of solution-grown polyethylene single crystals, 247
- YEADON, R. E.: See BAKER, C. H., BROWN, W. B., GEE, G., ROWLINSON, J. S., STUBLEY, D. and YEADON, R. E.
- YONEZAWA, T.: See HIGASHIMURA, T., IMANISHI, Y., YONEZAWA, T., FUKUI, K. and OKAMURA, S.
- ZERONIAN, S. H.: See NEVELL, T. P. and ZERONIAN, S. H.